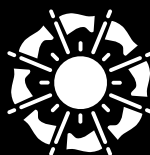


SPIE. PHOTONICS
WEST
OPTO



INTERNATIONAL
YEAR OF LIGHT
2015



2015 TECHNICAL SUMMARIES.

WWW.SPIE.ORG/PW

The Moscone Center
San Francisco, California, USA

Conferences & Courses
7-12 February 2015

Photonics West Exhibition
10-12 February 2015
BIOS EXPO
7-8 February 2015



SPIE. PHOTONICS WEST OPTO

The Moscone Center
San Francisco, California, USA

DATES

Conferences & Courses:
7-12 February 2015

SYMPOSIUM CHAIRS:



David L. Andrews
Univ. of East Anglia
(United Kingdom)



Alexei L. Glebov
OptiGrate Corp. (USA)

SYMPOSIUM CO-CHAIRS:



Jean Emmanuel Broquin
IMEP-LAHC (France)



Shibin Jiang
AdValue Photonics,
Inc. (USA)

Contents

9357:	Physics and Simulation of Optoelectronic Devices XXIII	3
9358:	Physics, Simulation, and Photonic Engineering of Photovoltaic Devices IV	21
9359:	Optical Components and Materials XII	33
9360:	Organic Photonic Materials and Devices XVII	52
9361:	Ultrafast Phenomena and Nanophotonics XIX	64
9362:	Terahertz, RF, Millimeter, and Submillimeter-Wave Technology and Applications VIII	82
9363:	Gallium Nitride Materials and Devices X	94
9364:	Oxide-based Materials and Devices VI	121
9365:	Integrated Optics: Devices, Materials, and Technologies XIX	141
9366:	Smart Photonic and Optoelectronic Integrated Circuits XVII	155
9367:	Silicon Photonics X	162
9368:	Optical Interconnects XV	177
9369:	Photonic Instrumentation Engineering II	187
9370:	Quantum Sensing and Nanophotonic Devices XII	195
9371:	Photonic and Phononic Properties of Engineered Nanostructures V	227
9372:	High Contrast Metastructures IV	246
9373:	Quantum Dots and Nanostructures: Synthesis, Characterization, and Modeling XII	254
9374:	Advanced Fabrication Technologies for Micro/Nano Optics and Photonics VIII	261
9375:	MOEMS and Miniaturized Systems XIV	275
9376:	Emerging Digital Micromirror Device Based Systems and Applications VII	285
9377:	Advances in Photonics of Quantum Computing, Memory, and Communication VIII	291
9378:	Slow Light, Fast Light, and Opto-Atomic Precision Metrology VIII	300
9379:	Complex Light and Optical Forces IX	310
9380:	Laser Refrigeration of Solids VIII	318
9381:	Vertical-Cavity Surface-Emitting Lasers XIX	325
9382:	Novel In-Plane Semiconductor Lasers XIV	333
9383:	Light-Emitting Diodes: Materials, Devices, and Applications for Solid State Lighting XIX	351
9384:	Emerging Liquid Crystal Technologies X	365
9385:	Advances in Display Technologies V	376
9386:	Practical Holography XXIX: Materials and Applications	383
9387:	Broadband Access Communication Technologies IX	392
9388:	Optical Metro Networks and Short-Haul Systems VII	401
9389:	Next-Generation Optical Communication: Components, Sub-Systems, and Systems IV	408
9390:	Next-Generation Optical Networks for Data Centers and Short-Reach Links II	415

SPIE is the international society for optics and photonics, a not-for-profit organization founded in 1955 to advanced light-based technologies. The Society serves nearly 225,000 constituents from approximately 150 countries, offering conferences, continuing education, books, journals, and a digital library in support of interdisciplinary information exchange, professional growth, and patent precedent. SPIE provided \$3.4 million in support of education and outreach programs in 2014.

**Click on the Conference Title
to be sent to that page**

Conference 9357: Physics and Simulation of Optoelectronic Devices XXIII

Monday - Thursday 9-12 February 2015

Part of Proceedings of SPIE Vol. 9357 Physics and Simulation of Optoelectronic Devices XXIII

9357-1, Session 1

Chaos in VCSEL light polarization dynamics (*Invited Paper*)

Marc Sciamanna, Supélec (France); Martin Virte, Supélec (France) and Vrije Univ. Brussel (Belgium); Emeric Mercier, Supélec (France); Hugo Thienpont, Krassimir Panajotov, Vrije Univ. Brussel (Belgium)

Vertical-Cavity Surface-Emitting Lasers (VCSELs) have found numerous applications e.g. in optical communications, sensing and metrology. Moreover, their intriguing polarization properties have gathered the interest of the laser physics and nonlinear dynamics communities since more than twenty years [1].

A recent major breakthrough is the report of polarization chaos in a free-running VCSEL [2] by simply varying the driving injection current, i.e. without the need for additional modulation or light injection. We will review the underlying physics and discuss the onset of bifurcations on both linearly and elliptically polarized eigenstates.

The achievement of such a low-cost integrated chaotic light source motivates its application in e.g. chaos secure communications or random number generation. We report on the successful extraction of a random bit sequence at bit rate exceeding 100 Gb/s [3]. The random bit sequence is achieved by sampling the VCSEL chaotic polarization dynamics at 20 GS/s and post-processing the digitized output with bit extraction and a single comparison. The successful randomness at high sampling rate is explained by the fast growth rate of the Shannon entropy which itself results from the fast divergence of trajectories in our VCSEL chaotic attractor.

[1] M. Sciamanna, "Mode competition driving laser nonlinear dynamics" in *Nonlinear Dynamics: from Quantum Dots to Cryptography*, ed. Kathy Lüdge, WILEY-VCH (2012).

[2] M. Virte, K. Panajotov, H. Thienpont, M. Sciamanna, *Nat. Photon.* 7, 60-65 (2013).

[3] M. Virte, E. Mercier, H. Thienpont, K. Panajotov, M. Sciamanna, *Opt. Express* 22, 17271-17280 (2014).

9357-2, Session 1

Free space ranging based on a chaotic long-wavelength VCSEL with optical feedback

Ana Quirce, Vrije Univ. Brussel (Belgium); Pablo Perez, Angel Valle, Luis Pesquera, Univ. de Cantabria (Spain); Ignacio Esquivias, Univ. Politécnica de Madrid (Spain); Krassimir Panajotov, Hugo Thienpont, Vrije Univ. Brussel (Belgium)

Chaotic Lidar systems (CLIDAR) are used for high-resolution ranging. They are based on the correlation of the chaotic signal waveform with the signal that is reflected back from the target. CLIDAR has the following advantages with respect to pseudorandom code modulation CW LIDAR [1]: i) high range resolution benefiting from the broadbandwidth of optical chaos ii) It does not need expensive high-speed code generation and modulation electronics. iii) it has not the ambiguity caused by the limited length of pseudorandom codes.

We report a novel CLIDAR system based on the autocorrelation of the signal obtained by the coherent superposition of the chaotic signal waveform and the signal that is reflected back from the target. A simplified set-up with just one detector is required in contrast to the two detectors used in standard

CLIDAR systems [1]. Our experimental results are obtained with a chaotic 1550-nm vertical-cavity surface-emitting laser (VCSEL) subject to optical feedback. We obtain an autocorrelation function with several sharp minima. The position of the target can be obtained from the location of these minima. Preliminary experiments show a distance to the target of 137 cm with a 3 cm spatial resolution. These results are checked using a Time-of-Flight technique with pulses obtained by gain-switching the VCSEL without optical feedback. A theoretical analysis of our CLIDAR system will also be presented.

[1] F. Y. Lin, J. M. Liu, "Chaotic Lidar", *IEEE J. Selected Topics in Quantum Electron.*, vol. 10, no. 5, 2004.

9357-3, Session 1

Optothermally induced excitabilities and instabilities in quantum dot lasers

Bryan Kelleher, Tyndall National Institute (Ireland) and Cork Institute of Technology (Ireland); Boguslaw Tykalewicz, David Goulding, Stephen P. Hegarty, Tyndall National Institute (Ireland); Guillaume Huyet, Tyndall National Institute (Ireland) and National Research Univ. of Information Technologies, Mechanics and Optics (Russian Federation); Thomas Erneux, Univ. Libre de Bruxelles (Belgium); Evgeny A. Viktorov, National Research Univ. of Information Technologies, Mechanics and Optics (Russian Federation) and Univ. Libre de Bruxelles (Belgium)

Relaxation oscillation resonances in Quantum Dot lasers (QDLs) are typically strongly damped resulting in more stable output dynamics and, in particular, greatly enhanced stability against external forcing like injection and feedback. We show here that slow optothermal relaxations may significantly affect the output power in QDLs leading to excitable dynamics and the formation of sustainable low frequency pulsations. For free-running QDLs we reveal the role of a homoclinic bifurcation from a cavity mode. For the injection problem we show that Type II excitability, mediated by a Hopf bifurcation as in the Fitzhugh-Nagumo model, arises in this system. For both configurations we demonstrate experimentally and theoretically new regimes where square-wave like pulsations are observed. Statistical analyses of these pulses show that there are regions of noise-induced pulsations and also regions of periodic square-wave emission. The experimental findings are well reproduced by a standard model supplemented with a new equation describing optothermal effects. In the injection case we prove that the noise-induced pulsation region is an excitable region. In fact, the behavior is just like that of the famous Fitzhugh-Nagumo model. Standard rate equation modeling of the system predicts a phase-locked bistability at moderate to high injection strengths, consistent with the Class A like characteristics of these devices. However, thermal effects cause a change in the material refractive index, which in turn changes the wavelength and hence the detuning. In the nominally bistable region this breaks the hysteresis cycle and one instead obtains a fast-slow limit cycle resulting in square-wave emission.

9357-4, Session 1

Spectral phase aberration and its influence on pulse compression in an actively modulated ultrafast laser system

Ke Wang, Ping Qiu, Shenzhen Univ. (China)

**Conference 9357: Physics and Simulation of
 Optoelectronic Devices XXIII**

Coherent Raman Scattering (CRS) microscopy allows label-free imaging of biological samples with endogenous image contrast based on vibrational spectroscopy and thus has aroused widespread research interest. An important technical challenge in CRS microscopy is the requirement of two synchronized picosecond excitation sources for chemical specificity. We have developed a novel ultrashort laser system based on the active modulation technique and have demonstrated its successful application in both CRS microscopy and spectroscopy. In such actively modulated laser systems, quadratic temporal phase modulation was naturally considered as the “ideal” modulation. However, it is unknown that whether a quadratic temporal phase modulation (equivalently, a linear chirp) translates into a quadratic spectral phase modulation, which can be easily eliminated using compressors. Here we study this phase transfer both analytically and numerically. Our results indicate that depending on the pulse shape, non-quadratic spectral phase aberration arises even if the temporal phase modulation is quadratic. Consequently, there is observable difference between the compressed pulses with a flat spectral phase and with quadratic spectral phase compensation only. However, both analytical and numerical analyses show that as quadratic temporal phase modulation increases, non-quadratic spectral phase modulation decreases, and pulse compression with quadratic spectral phase tends to that with a flat spectral phase.

9357-5, Session 2

**Coupled simulation of carrier transport
 and electrodynamics: the EMC/FDTD/MD
 technique** *(Invited Paper)*

Irena Knezevic, Univ. of Wisconsin-Madison (United States)

Conductive materials (semiconductors, semimetals, and metals) and their nanostructures are used for a variety of electronic, optoelectronic, and plasmonic applications. In these systems, carriers of charge (electrons and holes) interact with the applied electromagnetic fields, lattice vibrations, other charge carriers and charged impurities, and various structural defects. In order to understand the response of conductive materials to high-frequency electrical or optical excitations, where the fields might vary considerably over the scale of the carrier mean free path, one must fully account for the interplay between carrier transport and electrodynamics.

In this talk, I will present our recent work on developing a self-consistent coupled simulation of semiclassical carrier transport with full-wave electrodynamics. Carrier transport is described by the ensemble Monte Carlo (EMC) technique, a stochastic solution to the Boltzmann transport equation. During the simulation, an ensemble of carriers exhibit periods of free flight under the influence of the local electromagnetic fields, interrupted by scattering events. Full-wave electrodynamics is described by the finite-difference time-domain (FDTD) technique, a well-known grid-based explicit numerical approach to solving Maxwell's curl equations. In realistic materials, two charge carriers or carriers and ions can be found at distances smaller than the grid-cell size; in order to capture these short-range interactions, the molecular dynamics (MD) technique is employed. I will discuss the challenges and necessary conditions for a successful coupling of the constituent techniques into a self-consistent EMC/FDTD/MD solver, and show examples of ac transport in doped silicon and in graphene on a substrate with charged impurity clusters.

9357-6, Session 2

**Large-area gate-tunable terahertz
 plasmonic metasurfaces employing
 graphene anti-dot array structures**

Peter Q. Liu, Federico Valmorra, Curdin Maissen, Giacomo Scalari, Jérôme Faist, ETH Zürich (Switzerland)

A set of periodic square-lattice graphene anti-dot array structures of different dimensions are implemented using standard photolithography

on large-area monolayer graphene grown with chemical vapor deposition (CVD) and transferred onto SiO₂/Si substrate, and subsequently investigated with systematic transmission spectroscopy characterizations. The transmission extinction spectra of various graphene anti-dot array structures reveal multiple distinct resonances in the terahertz frequency range (3-10 THz) which arise from the engineered band-structures of the deep sub-wavelength graphene surface plasmon polariton (SPP) modes associated with such periodically modulated graphene sheet, analogous to the formation of photonic band-structures in two-dimensional photonic crystals. Both the frequencies and the strengths of the observed SPP resonances are readily tuned as expected with the carrier density electrostatically controlled by the Si substrate as the back-gate. Full-wave simulation results show excellent agreement with the experimental observations, and further shine light on the symmetry-based requirements on the specific SPP modes that couple to the incident free-space propagating electromagnetic waves. The SPP band-structures of such graphene anti-dot arrays exhibit high engineering flexibility through combined tuning of the lattice constant, the size and the shape of the removed dots as well as the carrier density. Furthermore, the operating frequency range can be extended into mid-infrared by scaling down the characteristic dimensions of the structures from currently a few micrometers to hundreds of nanometers. Therefore, such graphene-based anti-dot array structures can be employed as versatile tunable plasmonic metasurfaces or other types of building blocks in the terahertz to mid-infrared frequency range for various applications.

9357-7, Session 2

**Metal germanides for group IV based mid-
 infrared plasmonics**

Justin W. Cleary, Air Force Research Lab. (United States); Nima Nader, Solid State Scientific Corp. (United States); William Streyer, Univ. of Illinois at Urbana-Champaign (United States); Shiva R. Vangala, Solid State Scientific Corp. (United States); Daniel M. Wasserman, Univ. of Illinois at Urbana-Champaign (United States); Richard Soref, Univ. of Massachusetts Boston (United States)

Metal germanides are investigated in order to enable a group IV based plasmonics technology. Metal germanide compositions were formed by electron beam evaporation of Ge and metal (Ni, Pd, Pt, Ta, and Ti) and annealing in a nitrogen purged furnace. Infrared (IR) ellipsometry is used to determine the IR complex permittivity and associate with stoichiometry which is determined via x-ray diffraction. Basic plasmonic characteristics such as propagation loss and mode confinement are determined analytically for each stoichiometry. Scanning electron microscopy and x-ray photoelectron spectroscopy (while sputtering) are used to characterize the surface quality and depth profiles respectively. 1D grating structures of metal germanides on etched undoped silicon were fabricated. Resonant absorption observed in long-wave infrared reflection spectra agree with theory, and indicate coupling to surface plasmon polaritons. By annealing and forming stoichiometries that are less metallic the plasmon mode confinement becomes increasingly tight with little degradation observed experimental in-coupling efficiency. Example numerical simulations of a dielectric-conductor-dielectric ribbon waveguide structure are shown. Practical operation in the 3 to 20 micron wavelength range is predicted. Group IV plasmonics is compatible with group IV photonics enabling a synergistic on-chip “convergence” of these two technologies in conjunction with Si CMOS foundries. These results may be utilized for capabilities in chemical-biological sensing, enhanced detection, signal processing, and communications.

9357-9, Session 3

Modeling of optical amplifier waveguide based on silicon nanostructures and rare earth ions doped silica matrix gain media by a Finite difference time domain method: comparison of achievable gain with Er³⁺ or Nd³⁺ ions doped waveguide.

Julien C. Cardin, Ctr. de Recherche sur les Ions, les Matériaux et la Photonique (France); Alexandre Fafin, Ecole Nationale Supérieure d'Ingenieurs de Caen et Ctr. de Recherche (France); Christian Dufour, Ctr. de Recherche sur les Ions, les Matériaux et la Photonique (France); Fabrice Gourbilleau, ENSICAEN (France)

Since some decades, optical properties of rare earth ions incorporated in a Silicon-rich Silicon Oxide waveguide have been investigated experimentally by many groups. However, theoretical modelling of such a system, describing simultaneously electromagnetic properties and physical properties on a time scale of up to steady state have not been carried out satisfactorily. A new algorithm based on auxiliary differential equations and finite-difference time-domain method (ADE-FDTD method) is presented so that the steady state of rare earth ions and silicon nanostructures electronic levels populations along with the electromagnetic field can be fully described. This algorithm is stable and applicable to a wide range of optical gain materials in which large differences of characteristic lifetimes are present. A comparative study of waveguide amplifiers whose active layer contains silicon nanostructures acting as sensitizer of either neodymium ions (Nd³⁺) or erbium ions (Er³⁺) has been carried out by means of our method. We investigate the steady state regime of both rare earth ions and silicon nanostructures levels populations as well as the electromagnetic field for different pumping powers ranging from 1 to 10000 mW/mm². Moreover, the achievable gain has been estimated in this pumping range. The Nd³⁺-doped waveguide shows a higher gross gain per unit length at 1064 nm (up to 30 dB/cm) than the one with Er³⁺-doped active layer at 1532 nm (up to 2 dB/cm). Taking into account the experimental background losses we demonstrate that a significant positive net gain can only be achieved with the Nd³⁺-doped waveguide.

9357-10, Session 3

Valley-selective optical pumping scheme in compound semiconductors

Tetsuya Sakamoto, The Univ. of Tokyo (Japan); Yuhsuke Yasutake, The Univ. of Tokyo (Japan) and Japan Science and Technology Agency (Japan); Susumu Fukatsu, The Univ. of Tokyo (Japan)

An efficient solar cell requires the ability to control the absorption characteristics of semiconductors. It is generally taken for granted that electron-hole pairs once generated eventually relax towards their band extrema regardless of excitation energy. But this is wholly unfounded. On the other hand, prompt charge separation is an issue just as important to solar cells. In this regard, the use of indirect-valley is of benefit as it obviates the need for potential engineering. As such, the ability to bring electrons to a "sweet spot" in terms of energy and k-space simultaneously is of great significance from, not just solar cells but the fundamental and technological viewpoints. Here we develop a new optical pumping scheme for semiconductors, which enables otherwise unattainable selective population of remote valleys simply by light pumping. All is needed is to choose the appropriate excitation energy to sort out one specific group of the conduction and valence band valleys in k-space. The choice of energy is determined from the 30(34)-band k.p perturbation calculation. Our scheme also features (i) controlled relaxation

using asymmetric k-dispersion, and (ii) orders-of-magnitude resonantly enhanced absorption even for indirect valleys by taking advantage of a van Hove singularity, i.e., off-peak resonance. In fact, excitation at 2.91eV(HH) and 3.19eV(SO) allows substantial selective excitation of L-valley in GaAs, as with Ge. Such an off-peak pumping is an added advantage for thin film devices, and the valley-selective optical pumping allows one to gain insight into intervalley processes involving spins and the complicated mechanism of photoluminescence excitation.

9357-11, Session 3

Photo-modulated reflection and temperature-dependent photoluminescence studies of Ga(AsBi) bulk and quantum well structures

Nils Rosemann, Jan Kuhnert, Peter Ludewig, Lukas Nattermann, Kerstin Volz, Sangam Chatterjee, Philipps- Univ. Marburg (Germany)

Bismuth-containing structures based on GaAs are promising candidates for semiconductor lasers operating at telecom wavelength. The desired wavelength of 1550nm is reached by an incorporation of about 10% Bi, due to the large band gap reduction of about 60meV per percentage of Bi. In contrast to the incorporation of In or N, the incorporation of Bi influences the valence bands rather than the conduction bands and thus reduces the band gap. To quantify the influence of bismuth concentration, we investigated multiple Ga(AsBi)/GaAs bulk samples with different Bi concentrations by room temperature photo-modulated reflection spectroscopy. This sensitive technique gives rise to additional near band edge states that occur only for high Bi-concentrations. Furthermore, a set of multiple-quantum-well structures is investigated using the same technique to characterize confinement effects. [1]

In addition to the band gap shift, the spin orbit coupling is increased and the split-of valence band is shifted significantly, [2] inhibiting hole-related Auger recombination processes. The rather large covalent radius of Bi, on the other hand, induces significant disorder effects in such alloys. To quantify these, we investigated the same set of samples by temperature-dependent absolute photoluminescence spectroscopy using an integrating sphere mounted inside a closed-cycle cryostat. The temperature dependence of the luminescence is then used to quantify disorder.

[1] P. Ludewig et al., J. Cryst. Growth, 370, 95-99 (2013)

[2] K. Alberi et al., Appl. Phys. Lett, 91, 051909, (2007)

9357-13, Session 4

Impact of alloy fluctuation effects on the optoelectronic properties of InAlN and InGaN materials and devices (Invited Paper)

Eoin P. O'Reilly, Stefan Schulz, Tyndall National Institute (Ireland); Miguel A. Caro, Aalto Univ. (Finland)

We address the impact of random alloy fluctuations on bulk and quantum well (QW) InGaN and InAlN systems, applying atomistic models ranging from density functional theory (DFT) up to tight-binding (TB) theory. We show by first principle calculations that In-related localized states are formed both in the conduction and the valence bands of InAlN for low In compositions, and that these localized states dominate the evolution of the band structure with increasing In composition. Based on the DFT calculations, we have developed an atomistic TB model which is combined with our recently developed local polarization theory to include local fluctuation effects explicitly. Our TB results are in very good agreement with recent experimental and theoretical data on the composition dependence of the energy gap in InGaN and InAlN alloys. Surprisingly, we find a band-

**Conference 9357: Physics and Simulation of
 Optoelectronic Devices XXIII**

edge optical polarization switching from TM- to TE-mode occurring at approximately 15-18% InN in InAlN; from a linear interpolation of the crystal field splitting energies such a switching should occur for ~90% InN. Next we discuss the impact of alloy and well width fluctuations on the properties of polar and non-polar InGaN QWs. We show that random alloy fluctuations lead to a strong hole wave function localization (on the nm scale) for both polar and non-polar QWs. Our theoretical finding of strongly localized states is consistent with the experimentally observed low temperature inhomogeneous luminescence line width in InGaN QWs. Finally, we discuss the consequences of these localisation effects on the properties of III-N optoelectronic devices.

9357-14, Session 4

Dual-wavelength GaInNAs semiconductor quantum-well distributed feedback laser

 Xiao Sun, Alcatel-Lucent Shanghai Bell Co. Ltd. (China);
 Qingjiang Chang, Alcatel-Lucent Shanghai Bell Co. Ltd.
 (China) and Alcatel-Lucent Shanghai Bell (China)

Incorporation of N into GaInAs results in a huge reduction of the material band-gap and this has been successfully modelled using a Band Anti-Crossing (BAC) model in which the N acts as a defect in the GaInAs conduction band mixing with it and pushing it downwards. The N defect levels also alter the effective mass of the conduction band. Compositional fluctuations of N in GaInNAs result in Quantum Dot (QD)-like fluctuations in the Conduction Band Edge. The QD-like fluctuations have significant inhomogeneous broadening due to the local differences in N. We model the laser using a rate equation model containing the energies of the QW ground state and an inhomogeneous array of QD states including: the electron population dynamics in the QW and QD distribution, the holes in the QW level, non-radiative carrier losses and spontaneous and stimulated radiative emissions.

At low nitrogen composition (N=1%), due to small density of states (DOS) of the QD-like fluctuations, the electron density is insufficient to reach the lasing threshold of the QD system. In this case these fluctuations act like defect-related non-radiative centers. At high N composition (N=2%), the QD DOS increases allowing lasing directly from the QD fluctuations to form new lasing centers. Simultaneous lasing arises from the QW and the QD fluctuations for high current injection. While as the QD DOS further increases, only QD lasing occurs whereas a short pulse with a pulse-width of 15 ps is generated from the QW confined level.

9357-15, Session 4

Modeling Extreme-ultraviolet emission from laser-produced plasma using particle-in-cell method

 Po-Yen Lai, Shih-Hung Chen, National Central Univ.
 (Taiwan)

Effective generation of EUV light source from laser-produced plasma has been widely studied due to the practical importance of high-volume-production semiconductor devices with the 22-nm half-pitch size. The proposed light source using 13.5±2% nm and 6.X nm radiations from multi-charged ions of tin (Sn) and the rare-earth elements gadolinium (Gd), respectively. The plasma-based system of both tin and gadolinium includes various multi-time-scale physical mechanisms is too complicated to be theoretically analyzed. Therefore, computer simulation becomes indispensable to optimize the experimental conditions and comprehend the complex physical mechanisms. To estimate the EUV radiation from laser-produced plasma, many researchers simulated plasma dynamics using hydrodynamics model due to efficient computation. However, the hydrodynamic model can not only be used to simulate the interactions between electromagnetic fields and charged particles but also collision processes between charged particles. The collision model has to be included

in the simulation for studying the laser heating, energy transport and ultrafast electron motions in the dense plasma. In order to simulate above kinetic phenomena, PIC simulation is a better numerical approach with least approximations.

In this work, we develop a relativistic collisional PIC code to simulate dynamics of dense plasmas. The PIC model presents the convergent results due to mitigation of self-heating effect and numerical thermalization. The ionization model based on electron-ion collision is coupled with our PIC code to determine the ion populations of different charge states. Finally, the EUV emission can be estimated according to the weighted oscillator strengths of multi-charged ions.

9357-16, Session 4

Phonon absorption induced thermal bistability in PECVD grown silicon nitride waveguide

 Tingyi Gu, Columbia Univ. (United States); Mingbin Yu,
 Dim-Lee Kwong, A*STAR Institute of Microelectronics
 (Singapore); Chee Wei Wong, Columbia Univ. (United
 States)

The wavelength selective linear absorption in communication C-band is investigated in CMOS-processed PECVD silicon nitride rings. In the overcoupled region, the linear absorption loss lowers the on-resonance transmission of a ring resonator and increases its overall quality factor. Both the linear absorption and ring quality factor are maximized near 1520 nm. The direct heating by phonon absorption leads to thermal optical bistable switching in PECVD silicon nitride based microring resonators. We calibrate the linear absorption rate in the microring resonator by measuring its transmission lineshape at different laser power levels, consistent with coupled mode theory calculations.

9357-17, Session 5

Mid-infrared sensing with plasmonic germanium antennas (*Invited Paper*)

 Paolo Biagioni, Emilie Sakat, Politecnico di Milano (Italy);
 Leonetta Baldassarre, Istituto Italiano di Tecnologia (Italy);
 Eugenio Calandrini, Univ. degli Studi di Roma La Sapienza
 (Italy); Antonio Samarelli, Kevin Gallacher, Univ. of
 Glasgow (United Kingdom); Jacopo Frigerio, Politecnico
 di Milano (Italy); Giovanni Isella, Lab. for Epitaxial
 Nanostructures on Silicon and Spintronics (Italy); Douglas
 J. Paul, Univ. of Glasgow (United Kingdom); Michele
 Ortolani, Univ. degli Studi di Roma La Sapienza (Italy)

The quest for novel plasmonic materials has been a lively area of research over the last few years. In the mid-infrared (mid-IR) spectral region, in particular, localized plasmon resonances in nanoparticles and nanoantennas hold promise for enhanced IR spectroscopies targeting the unique vibrational fingerprints of molecules, with key applications in biology, medicine, and security. We introduce a novel all-semiconductor group-IV material platform for mid-IR plasmonics based on heavily-doped Ge [doping density $n \sim 2.5 \cdot 10^{19} \text{ cm}^{-3}$] epitaxially grown on standard Si(100) wafers. We experimentally obtain plasma frequencies up to around 1000 cm^{-1} and we fabricate antenna arrays by electron beam lithography and reactive ion etching techniques.

Antennas supporting localized plasmon resonances in the 400-900 cm^{-1} range are demonstrated, both in the form of single-wire antennas and of double-wire gap antennas, with strong spectral signatures both in transmission and in reflection measurements. The antenna arrays are applied to the detection of a thin (< 40 nm) polydimethylsiloxane (PDMS) layer and of a micrometer-sized droplet of chloroethyl methyl sulfide (CEMS),

**Conference 9357: Physics and Simulation of
 Optoelectronic Devices XXIII**

a transparent liquid that can be used to fabricate rudimentary explosive devices. By careful analysis of the sensing results and comparison with numerical simulations, we demonstrate an enhancement of one to two orders of magnitude for the fingerprint signal generated by the material located in the hot spots of the antennas.

This novel material platform, thanks to its high quality and full CMOS compatibility, points towards the possibility for efficient, cost-effective and integrated mid-IR devices for the detection of gases and molecules.

9357-18, Session 5

Nonlinear plasmonic scattering and its application to superresolution microscopy
(Invited Paper)

Shi-Wei Chu, Hsueh-Yu Wu, Yen-Ta Huang, Hsuan Lee, Kuan-Yu Li, Po-Hsuan Lee, Po-Ting Shen, National Taiwan Univ. (Taiwan); Ryosuke Oketani, Yasuo Yonemaru, Satoshi Kawata, Osaka Univ. (Japan); Chih-Wei Chang, National Taiwan Univ. (Taiwan); Kung-Hsuan Lin, Academia Sinica (Taiwan); Katsumasa Fujita, Osaka Univ. (Japan)

During the past decade, the diffraction limit of resolution was beautifully overcome by manipulating the on/off switching of fluorophores, or by saturation of fluorescence emission, resulting in resolution below 100 nm. Nevertheless, fluorescence exhibits intrinsic photobleaching issues. The on/off switching techniques require repeated excitation of a single fluorophore while the saturation techniques need strong incident power, both leading to faster bleaching of labeling. Therefore, it will be more than desirable to develop superresolution imaging modality based on an alternative contrast agent without bleaching, such as scattering.

The study of surface plasmon resonance (SPR) has recently attracted extensive interest because it provides light manipulation capability for photonic integrated circuits, nano laser, biosensing, and near-field superresolution imaging applications. It is known that scattering is greatly enhanced in SPR structures, but neither saturation, nor switching of scattering from SPR structures has been reported. In this report, we feature the first observation of interesting nonlinearities of SPR scattering, including saturation, reverse saturation, and all-optical switching, in an isolated plasmonic nanostructure. These nonlinear behaviors are successfully applied to imaging, and bring the spatial resolution down to $\lambda/8$, which is enough to resolve the wavelength of surface plasmon polariton in nanoscale optoelectronic devices. Potential applications range from biomedical imaging and functional plasmonic nanostructures. We also anticipate our demonstration to be a stimulating example in finding more exotic contrast agents for improving optical resolution.

9357-19, Session 5

Propagation characteristics of multilayered subwavelength gratings composed of metallic nanoparticles

Joaquim Junior Isidio de Lima, Juarez Caetano da Silva, Vitaly Felix Rodriguez-Esquerre, Univ. Federal da Bahia (Brazil)

The absorption and reflection characteristics of multilayered nanoplasmonic gratings with sub-wavelength sizes are analyzed in detail by using an efficient finite element method. The multilayered structures are composed by several layers of nanoparticles of metals such as silver, gold, aluminum embedded in dielectric such as amorphous silicon over a metallic substrate. The propagation characteristics for several geometrical configurations are obtained and a broadband reflection or absorption covering the near infrared wavelengths has been observed. The proposed nanoplasmonic structures have a great potential for applications in photovoltaic cells or

polarizers by improving their reflection or absorption efficiency. Peaks of reflection or absorption larger than 80% were obtained and their performance over the near infrared can be improved by adequately tuning their geometrical parameters, the refractive index and thickness of the layers as well as the nanoparticles shape and size.

9357-20, Session 5

Effects of surface plasmon localization and grating shape on the light emission enhancement in quantum-well emitters

Toufik Sadi, Jani Oksanen, Jukka J. Tulkki, Aalto Univ. (Finland)

In recent years, experimental work has shown that significant luminescence enhancement can be obtained from quantum-well (QW) light-emitting diodes (LEDs) by using metallic grating, which diffracts efficiently optical modes and resonances trapped in these structures and converts surface plasmon (SP) modes into radiative modes. We employ a powerful simulation tool to provide a deep insight into the physics of plasmonic enhancement and present guidelines on how to optimize light-extraction in III-nitride LED structures incorporating an emitting InGaN QW located in the vicinity of a grating silver surface. The model uses first-principle theory, coupling the dyadic Green's function formalism for solving Maxwell's equations to fluctuational electrodynamics, and employs a recursive and transparent solution method allowing the fields to be written in a closed form.

We demonstrate the significant effect of surface plasmon localization and the type of the periodic grating on light-extraction efficiency by simulating structures with different grating shapes (including 2D and 3D rectangular, triangular and modulated gratings) and filling ratios. Careful optimization of the grating features shows that the maximum enhancement ratio more than doubles (reaching a factor of around 5 to 6 as compared to the flat semiconductor structure) and the plasmonic losses can be significantly reduced, as compared to the simple rectangular grating with a 50% filling ratio.

9357-21, Session 6

Impact of the carrier relaxation paths on two-state operation in quantum dot lasers

Grigori S. Sokolovskii, Vladislav V. Dudelev, Ioffe Physical-Technical Institute (Russian Federation); Ekaterina D. Kolykhalova, Ioffe Physical-Technical Institute (Russian Federation) and St. Petersburg State Electrotechnical Univ. (Russian Federation); Ksenya K. Soboleva, Saint-Petersburg State Polytechnical Univ. (Russian Federation); Anton G. Deryagin, Innokenty I. Novikov, Mikhail V. Maximov, Ioffe Physical-Technical Institute (Russian Federation); Alexey E. Zhukov, St. Petersburg Academic Univ. (Russian Federation); Victor M. Ustinov, Vladimir I. Kuchinskii, Ioffe Physical-Technical Institute (Russian Federation); Wilson Sibbett, Univ. of St. Andrews (United Kingdom); Edik U. Rafailov, Aston Univ. (United Kingdom); Evgeny A. Viktorov, National Research Univ. of Information Technologies, Mechanics and Optics (Russian Federation) and Univ. Libre de Bruxelles (Belgium); Thomas Erneux, Univ. Libre de Bruxelles (Belgium)

Simultaneous two-state lasing at ground (GS) and excited state (ES) in quantum dot (QD) lasers is attractive for multiple technological applications. We demonstrate that the carrier relaxation pathways in QD materials play an important role in the formation of the two state QD lasing, and distinguish three different regimes of operation depending on pumping.

**Conference 9357: Physics and Simulation of
 Optoelectronic Devices XXIII**

We study InGaAs QD laser with 2.5mm-long cavity operating simultaneously at ground (GS) and excited (ES) states in the whole range of 30ns-pulsed electrical pumping.

There are merely two carrier relaxation pathways from the wetting layer (WL) in QD materials: the cascade-like (WL-ES-GS) and the direct-capture (WL-GS).

For the low ($I < 0.68A$) or the high ($I > 1.2A$) ranges of the pump current, either the cascade-like pathway or the direct capture pathway is dominant. The current increase leads to the ES intensity increase, and to the GS intensity decrease (or saturation) for range ($I < 0.68A$), what is typical for the cascade-like pathway. Both the GS and ES intensities steadily increase for current range ($I > 1.2A$), what proves the dominance of the direct-capture pathway. The relaxation oscillations are not pronounced for these ranges of the pump current as characteristic for QD lasers.

For the mediate current range ($0.68A < I < 1.2A$), the interplay between both relaxation pathways leads to the excitation of pronounced relaxation oscillations with significant deviation of their frequency from the initial value during the pulse. The oscillations appear simultaneously at GS and ES, but can be either inphase or antiphase depending on the temperature conditions.

9357-22, Session 6

Influence of Inhomogeneous Broadening on the Dynamics of Quantum Dot Lasers

Cheng Wang, Institut National des Sciences Appliquées de Rennes (France); Mariangela Gioannini, Ivo Montrosset, Politecnico di Torino (Italy); Jacky Even, Institut National des Sciences Appliquées de Rennes (France); Frédéric Grillot, Télécom ParisTech (France) and Ecole Nationale Supérieure des Télécommunications (France)

Quantum-dot (QD) lasers are promising laser sources for optical communication networks. However, the modulation performance of QD lasers is still far away with what is expected from an ideal QD laser. One of the crucial limitations is the inhomogeneous broadening due to the dot size dispersion. This work investigates the effects of inhomogeneous broadening on dynamic performances employing a multi-population rate equation model [1]. The numerical model takes into account carrier populations in the barrier, wetting layer (WL), the GS, first and second excited states of the dot. Besides, the QD ensemble is divided into multiple groups and the dot size dispersion is characterized by a Gaussian distribution [2]. At lasing threshold, it is found that the linewidth enhancement factor at the energy center of the GS increases with the broadened gain. The intensity modulation response of the QD laser is obtained numerically. As in the experiment, the resonance frequency (f_R) and damping factor (γ) is extracted through the conventional modulation transfer function [3]. It is shown that the fitted K-factor ($\gamma = Kf_R^2 + \gamma_0$) firstly increases with the inhomogeneous broadening. Once the broadening reaches the GS-ES energy separation, the K-factor experiences a sharp decrease to a low value, and then increases slowly with the broadening. In addition, both the differential gain and the gain compression extracted from the K-factor formula decrease with the broadening below the GS-ES energy separation, while it slightly increases beyond. Inhomogeneous broadening impacts on the large-signal chirp and the eye diagram will be discussed as well.

9357-23, Session 6

Ultrafast excitable switching between two lasing states in quantum dot lasers

Bryan Kelleher, Tyndall National Institute (Ireland) and Cork Institute of Technology (Ireland); Boguslaw Tykalewicz, David Goulding, Stephen P. Hegarty, Tyndall National Institute (Ireland); Guillaume Huyet, Tyndall

National Institute (Ireland) and National Research Univ. of Information Technologies, Mechanics and Optics (Russian Federation); Evgeny A. Viktorov, National Research Univ. of Information Technologies, Mechanics and Optics (Russian Federation) and Univ. Libre de Bruxelles (Belgium)

The unique carrier processes in quantum dot lasers mean that lasing can be achieved at the ground state (GS) transition wavelength or at the excited state (ES) transmission wavelength or indeed simultaneously at both wavelengths. The details depend on the device characteristics and control parameters such as the pumping current and temperature. When the lasing is from the ES only one can induce all-optical switching between the two states via optical injection into the GS. The high damping of the relaxation oscillations in these devices allows for very fast switching times, with sub-nanosecond transitions easily obtained. Such ultrafast switching times – vastly superior to those obtained with conventional semiconductor lasers – make these devices very attractive for all-optical switching applications. The interplay of the two states leads to a new excitable regime. Near the boundary of stable locking for the injected GS, deep GS intensity dropouts are observed. Analyses of the statistics show that these are noise-induced. Further, each dropout in the GS coincides with a burst in the ES output. The shape and depth of the ES antiphase excitable dynamics suggests a new mechanism for the phenomenon reveal the role of intradot processes. Experimental electric field measurements allow for a resolution of the phase of the slave laser. Detailed numerical simulations using a model tailored for quantum dot devices support the findings and help identify the physical mechanism responsible for the phenomenon.

9357-25, Session 7

How small can one make a semiconductor laser? (Invited Paper)

Jacob B. Khurgin, Johns Hopkins Univ. (United States)

Recently semiconductor lasers based on metal dielectric structures promising sub-wavelength operation have generated a lot of interest. Yet it is not clear exactly how small semiconductor laser can be made without sacrificing performance. In this talk recent experimental and theoretical results will be reviewed and a theory outlining the fundamental limits of how small can the nano-laser actually be will be presented. Comparison with state of the art semiconductor lasers, such as VCSEL's in terms of threshold, efficiency, linewidth and modulation speed will be made.

9357-26, Session 7

Purcell effect of very small metallic cavity (Invited Paper)

Yong-Hee Lee, Jung H. Shin, Jung-Hwan Song, KAIST (Korea, Republic of)

We report the direct measurement of a record-large Purcell factor over 100 from Er atoms in a very small metallic cavity. An ensemble of Er atoms is deterministically placed at the anti-node of a low-quality factor very small nano-metallic cavity. The straightforward confirmation of strong Purcell enhancement is attributed to the the very small modal volume of the metallic nano-cavity and the long intrinsic radiation lifetime of Er atoms. We show that the properly-designed metallic cavity can be made to have an extraction efficient better than the quantum efficiency of Er atoms embedded in SiO₂ thanks to the low-Q nature of the metallic resonator that radiates electromagnetic energy in just one or two optical cycles.

9357-27, Session 7

Theory of an optically-driven quantum-dot phonon laser *(Invited Paper)*

Julia Kabuss, Andreas Knorr, Technische Univ. Berlin (Germany)

Recent technological progress in nanophononics has enabled the design of an acoustic counterpart to optical cavities. Such a phonon cavity device constitutes a basis for phonon lasers, where the concept of stimulated emission into a single cavity mode can be generalized also to phononic systems. As a coherent and nonequilibrium phonon source an optically pumped quantum dot that is coupled to a high-Q acoustic cavity is proposed. In a full quantum theory approach it is shown that this system can be operated as a phonon laser exhibiting truly Poissonian phonon statistics within a well defined pumping regime. For an analysis of the operational limits of this quantum dot phonon laser, the theory is further supported by an effective analytic and also semiclassical treatment, revealing strong similarities to the typical incoherently pumped single atom laser.

9357-28, Session 7

Rate equation analysis of high-speed nanolasers

William Hayenga, Mercedeh Khajavikhan, CREOL, The College of Optics and Photonics, Univ. of Central Florida (United States)

Here we provide a theoretical rate equation model that properly describes the dynamics of the recently developed nanolaser structures. By taking into account the Purcell effect that is known to drastically affect the spontaneous emission rate of such sub-wavelength cavities, we appropriately modify the corresponding rates of stimulated emission and absorption. Other effects arising from the confinement factor, spontaneous emission coupling factor, gain suppression, and mode volume are also considered in our equations. In particular, we investigate the effect an enhanced Purcell factor has in relaxing the limitations caused by non-radiative recombination processes on the performance of nanolasers. This model is then used to predict the onset of lasing in such nanolaser systems. These predictions are in excellent agreement with previously reported experimental results. The small signal response of these nanolasers is also investigated in detail using the above rate equation model. Our simulations indicate that nanoscale metallic coaxial lasers can exhibit a large modulation bandwidth in excess of 200 GHz. We show that the small volume involved and the associated low quality factor of the mode are key factors behind these anticipated high bandwidths. Our theory emphasizes the importance of optimizing the cavity parameters with respect to other more global factors that emerge as the cavity size drops into the sub-wavelength scale. Our model can be used to design and further tailor the performance of this newly emerging class of nanolasers.

9357-29, Session 7

Superradiance and super-thermal photon emission from quantum-dot microcavity lasers

Christopher Gies, Univ. Bremen (Germany); Heinrich A. Leymann, Alexander Foerster, Jan Wiersig, Univ. of Magdeburg (Germany); Sven Höfling, Univ. of St. Andrews (United Kingdom); Marc Assmann, Manfred Bayer, Technische Univ. Dortmund (Germany); Frank Jahnke, Univ. Bremen (Germany)

Superradiance is typically understood as an enhanced cooperative emission from a gas of atoms. In semiconductor systems, superradiant effects play a small role because fast scattering and dephasing destroy the inter-emitter coupling. For few-quantum-dot (QD) systems with weak dephasing, photon bunching and the appearance of super- and sub-radiant emission regimes has been theoretically discussed in [1].

In a collaboration between theory and experiment, we demonstrate superradiance in a typical quantum-dot micropillar laser (VCSEL). High time-resolution streak-camera measurements in single-photon-counting mode [2] provide access to photon autocorrelations on a ps time scale. At low pumping, excitation is converted into the formation of a coherent superradiant phase throughout the active material. Evidence is a phase-correlated photon emission that leads to a giant photon bunching with $g^{(2)}$ far exceeding the thermal limit. Furthermore, correlations between the emitters form at the expense of reduced photon output, causing a pronounced jump in the input/output curve. Typical laser models attribute the characteristic jump to the beta factor of a device. Our demonstration of "superradiant excitation trapping" puts a new perspective on this procedure relevant for common nanolaser devices [3].

The results are fully explained by a microscopic semiconductor laser model that accounts for QD-QD superradiant coupling and semiconductor properties of the gain material, such as multi-excitonic states, electron-hole correlations, and inhomogeneous broadening.

[1] V.V. Temnov and U.Woggon, Optics Express 17, 5774 (2009); A. Auffeves et al., New Journal of Physics 13, 093020 (2011)

[2] J. Wiersig et al., Nature 460, 245 (2009)

[3] W.W. Chow, F. Jahnke, and C. Gies, Emission properties of nanolasers during transition to lasing, Light: Science and Applications (2014), accepted for publication

9357-30, Session 8

Quantum optics in many-body physics: Superradiance, quantum feedback, and optomechanical quantum nonlinearities *(Invited Paper)*

Alexander Carmele, Andreas Knorr, Technische Univ. Berlin (Germany)

It is up to now still a challenge to compute quantum optical effects and signatures in quantum many body systems. Both sides require a microscopical treatment, including higher order quantum correlations for photons, electrons, and phonons. We discuss in this contribution tools to identify theoretically quantum optical features in many-body systems such as the cluster expansion method, inductive equation of motions, and the derivation of effective Hamiltonians in the adiabatic regime. We illustrate these approaches in discussing these approaches for superradiant coupled quantum dots, strong coupling of optomechanics to an ensemble of Rydberg atoms, and quantum optical feedback setups with an external mirror.

9357-31, Session 8

Theoretical and experimental considerations on threshold limitations of the SPASER *(Invited Paper)*

Günter Kewes, Rogelio Rodriguez-Oliveros, Kathrin Höfer, Alexander Kuhlicke, Humboldt-Univ. zu Berlin (Germany); Kurt Busch, Humboldt-Univ. zu Berlin (Germany) and Max-Born Institut (Germany); Oliver Benson, Humboldt-Univ. zu Berlin (Germany)

Nanoscope sources of coherent electromagnetic fields are essential

elements for nanoplasmonics, metamaterials, and quantum plasmonics. A surface plasmon laser (spaser) might be such a source. Recently, first spaser devices have been characterized and theoretical work has addressed fundamental and device-specific spaser properties. However, several questions remain to be answered, among them the issue of the rather high spaser threshold. A complete description of a spaser requires a full quantum-mechanical treatment. Here, we restrict ourselves to the still quite challenging goal of developing a fully electromagnetic semi-classical rate-equation approach. This allows for a quantitative investigation of the input-output characteristics, notably the quantitative determination of the spasing thresholds. Our model is based on the eigenfrequencies and quality factors for the different multi-polar resonances of a metal sphere as well as the radiative and non-radiative rates. All these quantities are obtained analytically from the full Maxwell equations via Mie theory. Therefore, we drop the widely used quasi-static approximation of the electromagnetic field. This allows for precise incorporation of realistic gain relaxation rates that so far have been massively underestimated. We obtain a quantitative understanding of the threshold characteristics that limit efficient spaser devices. Specifically, our model highlights the significance of emitter-free spacing layers between the gain material and the metal with regards to the spasing threshold. In addition, we show that our model can be extended to complex plasmonic nanostructures using the recently introduced concept of quasi-normal modes.

9357-32, Session 8

Theory of deterministic and robust entanglement of nitrogen-vacancy centers via low-Q photonic-crystal cavities

Julia Kabuss, Technische Univ. Berlin (Germany); Janik Wolters, Oliver Benson, Humboldt-Univ. zu Berlin (Germany); Andreas Knorr, Technische Univ. Berlin (Germany)

With respect to solid state quantum platforms, the negatively charged nitrogen vacancy (NV) defect center in diamond constitutes one of the most promising candidates for future solid state quantum technology. Further, recent technological progress has enabled the integration of NV centers into hybrid photonic crystal cavities [J. Wolters et al., APL (2010)]. Here, we theoretically explore the feasibility of a two-qubit gate on such a quantum platform by studying a deterministic, robust and fast entanglement scheme [A. Imamoglu, PRL (1999)] using a set of realistic parameters (cavity quality factors, radiative dephasing and spectral diffusion). The entanglement operation is considered for two radiatively coupled NV-centers, each represented by a Λ -type level structure via the coupling to a single cavity mode and two external laser fields. Via the exchange of a virtual photon, the NV centers are effectively coupled, inducing a population swap within the lower states manifold. Even, if considering dephasing as well as realistic quality factors ($Q=9800$), the maximal concurrence reaches $c=0.6$, indicating significant entanglement. We solve the dynamics of the full set of operator correlations using an equation of motion approach that generates reliable results beyond an approximative treatment [J. Wolters et al., PRA(R) (2014)]. Further, we compare our numerics and a newly developed effective treatment to previous models of similar systems. We find, that a significant entanglement between two medium distant NV centers can be achieved via an effective adiabatic population transfer process. A remarkable quality of the explored entanglement scheme is its tolerance against typical experimental imperfections. Our calculations suggest robustness against cavity loss, spectral diffusion and radiative dephasing.

9357-33, Session 8

Non-classical light from single and coupled quantum dots in semiconductor nanowires

Milad Khoshnagar, Univ. of Waterloo (Canada); Tobias Huber, Univ. of Innsbruck (Austria); Dan Dalacu, National

Research Council Canada (Canada); Ana Predojevic, Univ. of Innsbruck (Austria); Philip J. Poole, National Research Council Canada (Canada); Gregor Weihs, Univ. of Innsbruck (Austria); Amir H. Majedi, Univ. of Waterloo (Canada)

The clean and bright photoluminescence spectrum of quantum dots embedded inside defect-free wurtzite nanowires offers them as promising emitters of single photons. Here we first report on the demonstration of entangled photon pair generation from the biexciton-exciton cascade of a single InAsP quantum dot epitaxially grown inside a bottom-up InP nanowire. The nanowire is 200 nm-thick at the bottom and slightly tapered at the top in order to waveguide the single photons and efficiently deliver them into the collection optics. The measured entanglement is 250 ps durable and approximately 8-fold shorter than the exciton lifetime (2 ns) due to the nonzero fine structure splitting (18 meV) of the quantum dot. We further advance the study by developing coupled InAsP quantum dots embedded in similar photonic nanowires. The deterministic nature of growth process allows for controllable size of individual dots and their interdot spacing. The photoluminescence spectra exhibit two sets of resonances attributed to the multiexcitons localized in the coupled dots. We observe a clear signature of quantum coupling by performing time-correlation experiment on certain pairs of resonances picked up from different sets. These quantum correlations are size dependent and vanish once the quantum dots are adequately separated (15 nm) and excitons are no longer coupled via their Coulomb interactions. In addition, cross-correlation patterns evidence several cascade recombinations that can be exploited for creating multiphotons regulated in time. Above observations serve as prototypical studies toward realizing multiphoton states required for the scalable quantum computing and communication.

9357-34, Session 8

Photon pairs from a biexciton cascade with feedback-controlled polarization entanglement

Sven M. Hein, Franz Schulze, Technische Univ. Berlin (Germany); Alexander Carmele, Technische Univ. Berlin (Austria); Andreas Knorr, Technische Univ. Berlin (Germany)

Entangled photon pairs are essential for quantum information processing applications, e.g. quantum computing and quantum cryptography. Especially for integrated quantum circuits, a solid-state based source of photon pairs on demand with tunable entanglement is needed. The decay of a biexciton in a quantum dot provides such a source. However, due to the fine structure splitting of the involved exciton levels, the maximally achievable polarization entanglement is usually strongly reduced.

We propose to use a time-delayed quantum-coherent feedback mechanism to increase and control photon entanglement, which can be implemented e.g. using a lens-mirror setup or a waveguide. We show that by tuning the time delay, we have control over the amount of entanglement in the photon pair and can even counteract the adverse effects of fine-structure splitting to a large extent.

In order to include the feedback, we propose a fully coherent, measurement free approach. We model the feedback by coupling the biexciton cascade to a structured reservoir. As in many cases of time-delayed feedback control, the effects are strongest when the delay time matches a timescale inherent to the system that is to be controlled. In our case, this timescale is given by the fine-structure splitting.

Our results can be explained by an interference of original and reflected light, which can be used to shape the spectrum in order to control the amount of entanglement.

We report on substantial enhancements of entanglement, and also discuss to what extent this mechanism is stable against deteriorating effects, such as inhomogeneous broadening.

9357-35, Session 9

Passive cavity laser and tilted wave laser for coherently-coupled bars and stacks

Nikolay N. Ledentsov, Vitaly A. Shchukin, VI Systems GmbH (Germany); Mikhail V. Maximov, Nikita Y. Gordeev, Nikolay A. Kalyuzhnyi, Sergey A. Mintairov, Alexey S. Payusov, Yuri M. Shernyakov, Ioffe Physical-Technical Institute (Russian Federation)

Semiconductor diode gain chips with ultralarge output apertures are applied in external cavity lasers as a large beam spot size facilitates efficient back coupling of light even at small reflectivity of the mirror necessary for high efficiency operation. We address thick (10-30 μm) and ultrabroad (>1000 μm) waveguides that may serve as enabler for direct diode high-power high-brightness coherent source of light. Two design concepts based on selection of a single high-order vertical mode by chip design and a single lateral mode by multistripe chip and external mirrors are addressed.

(i) Passive cavity laser extends an idea of placing the active media outside the passive cavity waveguide [1], namely in a clad, wherein the high order mode having the slowest decay inside the clad has the highest modal gain, and an ultralow n-doping of the passive waveguide reduces the free carrier absorption modal losses.

(ii) Tilted wave laser [2] utilizes coupling of a thin active waveguide supporting a single vertical mode and a thick passive waveguide resulting in a single vertical mode of the coupled structure having the maximum modal gain. Prototypes show a wall plug efficiency of ~55% and two vertical beam emission with 2-degree divergence each.

Ultrathick and ultrabroad waveguides provide a unique advantage of lateral coherent coupling of neighboring stripes at a large pitch size of >10 μm [3]. In this work we study pitch sizes up to 400 μm .

With the proposed approach we address multiple possible application fields from projection displays and LIDARs to material processing.

[1] V. A. Shchukin, et al. SPIE Proc. 8255, 8255-54 (2012).

[2] N. N. Ledentsov, et al., SPIE Proc. 8965, 8965-25 (2014).

[3] N. Yu. Gordeev, et al. SPIE Proc. 6889, 6889OW (2008).

9357-37, Session 9

Nonlinear conversion efficiency of InAs/InP nanostructured Fabry-Perot lasers

Heming Huang, Télécom ParisTech (France); Kevin Schires, Télécom ParisTech (France) and Telecom ParisTech (France); Mohamed-Essghair Chaibi, Télécom ParisTech (France); Philip J. Poole, National Research Council Canada (Canada); Didier Erasme, Frédéric Grillot, Télécom ParisTech (France)

Nondegenerate four-wave mixing (NDFWM) is a nonlinear effect arising from the third-order optical susceptibility. In semiconductor medium, NDFWM is supported both from interband (carrier density modulation) and intraband mechanisms (spectral hole burning and carrier heating). In the literature, NDFWM in bulk and quantum well semiconductor materials has been extensively studied for wavelength conversion in wavelength division multiplexed (WDM) systems and to produce high repetition-rate self-pulsating signals. Owing to their ultrafast carrier dynamics, large inhomogeneous broadening and higher nonlinear susceptibility, nanostructured lasers are good candidates for exalting nonlinearities in semiconductor materials without requiring a very long cavity length. Most studies have been conducted with travelling wave semiconductor optical amplifiers (SOA) and little is known on FWM generation with nanostructured lasers. We report on how injection-locking an InAs/InP nanostructured Fabry-Perot (FP) laser leads to an efficient signal conversion for a large pump-probe detuning from 50 GHz up to 3.5 THz. Due to the

reduced amplified spontaneous emission, an excellent signal-to-noise ratio (SNR) is demonstrated with respect to the SOA counterparts. Locking the pump signal at different wavelengths within the gain curve shows a different symmetry between up and down conversion. When the FP longitudinal mode is locked at wavelengths shorter than the gain peak, the asymmetry proves not to be predominant as opposed to the situation arising at longer wavelengths. From the measured normalized conversion efficiency (NCE) and SNR, the role of linewidth enhancement factor is discussed and the extracted nonlinear susceptibility is compared to InAs/InP SOAs.

9357-38, Session 9

Transition from absolute to convective instabilities in a swept source laser

Bryan Kelleher, Tyndall National Institute (Ireland) and Cork Institute of Technology (Ireland); Svetlana Slepneva, Ben O'Shaughnessy, David Goulding, Tyndall National Institute (Ireland); Andrei G. Vladimirov, Weierstrass-Institut für Angewandte Analysis und Stochastik (Germany); Stephen P. Hegarty, Tyndall National Institute (Ireland); Guillaume Huyet, Tyndall National Institute (Ireland) and National Research Univ. of Information Technologies, Mechanics and Optics (Russian Federation)

Fourier domain mode locked lasers (FDMLs) are novel frequency swept lasers, typically used in Optical Coherence Tomography. They are also rich sources of non-linear dynamics. An FDML consists of a semiconductor optical amplifier in a long fiber ring cavity with an intracavity tunable filter modulated at the cavity roundtrip frequency so that the system contains an entire sweep and lasing does not have to continually begin from amplified spontaneous emission. There is a sweep direction asymmetry induced by the non-zero phase amplitude coupling in semiconductor lasers. The asymmetry is manifest in both phase and intensity. The decreasing frequency part of the sweep is characterized by a form of mode-hopping between discrete, stable chirped-frequency solutions while for the increasing frequency part, the output is chaotic. Using a delayed homodyne technique we demonstrate that the frequency and phase evolution during the transition (the "hop") between chirped modes is non-monotonic but rather jumps back and forth in a complicated manner. Conversely, during the chaotic part of the sweep, the frequency evolution is very smooth meaning that, somewhat surprisingly, the chaotic part of the sweep may be better for some applications. Each mode-hop is mediated by a sub-critical modulational instability. By varying the mismatch between the filter sweep period and the cavity roundtrip time, this instability can be transformed from an absolute instability for a small mismatch to a convective instability when the mismatch is made larger. Numerical modelling using a set of delay differential equations is in excellent agreement with experiment.

9357-76, Session 9

Nitride-on-silicon microdisks resonators for deep-UV laser emission at room-temperature

Julien Sellés, Guillaume Cassabois, Thierry Guillet, Christelle Brimont, Univ. Montpellier 2 (France); Philippe Boucaud, Xavier Checoury, I. Roland, Y. Zeng, Institut d'Électronique Fondamentale (France); Meletios Mexis, Fabrice Semond, Ctr. de Recherche sur l'Hétéro-Epitaxie et ses Applications (France); Bruno Gayral, Commissariat à l'Énergie Atomique (France)

Deep ultra-violet semiconductor lasers have numerous applications for optical storage, biochemistry or optical interconnects. UV-emitting ridge lasers usually embed nitride heterostructures grown on complex buffer

**Conference 9357: Physics and Simulation of
 Optoelectronic Devices XXIII**

layers or expensive substrates – an approach that cannot be extended to nanophotonics and microlasers. We demonstrate here the first deep ultra-violet microlaser operating at 275nm at room temperature under optical pumping. It is based on binary GaN/AlN thin quantum wells (QWs) grown on a silicon substrate and embedded in microdisk resonators. Those QWs indeed combine UV-C emission with a good emission efficiency even at room temperature thanks to the huge band offset between GaN and AlN. They form the active layer of state-of-the-art microdisk resonators, which electromagnetic modes, the so-called Whispering-Gallery Modes (WGMs), present a low modal volume and a high quality factor ($Q=6000$). This active layer can form freestanding membranes and is further compatible with future developments of nitride nanophotonic platforms on silicon.

9357-39, Session 10

Simulation of solid-state dye solar cells based on organic and perovskite sensitizers (Invited Paper)

Aldo Di Carlo, Desirée Gentilini, Univ. degli Studi di Roma “Tor Vergata” (Italy); Alessio Gagliardi, Technische Univ. München (Germany)

The Dye-sensitized Solar Cell (DSC) represents an important photovoltaic (PV) technology based on solution processes and organic or hybrid organic/inorganic energy harvesting materials. A milestone on DSC's development was represented by the replacement of liquid electrolyte with organic semiconductor as hole transporter material in the solid-state Dye Solar Cells (ssDSC). Recently the introduction of hybrid Perovskites as sensitizer and charge transport material has further boosted the development of this PV technology leading to certified efficiency above 17%.

This contribution reports on the effort made to develop a consistent simulation model to describe both ssDSCs and Perovskite Solar Cells (PSCs). The model, based on drift-diffusion equations, uses Gaussian density of states and hopping mobility for transport in the organic materials and is able to simulate IV-characteristics, external quantum efficiency, as well as, electric field and carrier density profiles of the PV cell. Particular emphasis is given to the simulation of transport in Spiro Ometad, a widely used hole transporter materials used in both ssDSC and PSCs.

A detailed discussion will be devoted to the influence of charged trap states at the interface between TiO₂ and hole transport material. The analysis is performed by simulating in a multiscale framework charge transport inside the mesoporous active layer. The morphology of the TiO₂ is obtained from experimental measurements and inserted into a finite element DD simulator. This casts light on the effects induced by electrons trapped at the interface and also on the effect of ionic additives in screening trapped charges.

9357-40, Session 10

Surface photo-voltage properties near grain boundaries in Cu₂ZnSn(S,Se)₄ thin-films solar cells

Gee Yeong Kim, Ju Ri Kim, William Jo, Trang T. Nguyen, Hae-Young Shin, Seokhyun Yoon, Ewha Womans Univ. (Korea, Republic of); Dae-Ho Son, Dae-Hwan Kim, Jin-Kyu Kang, Daegu Gyeongbuk Institute of Science & Technology (Korea, Republic of)

Cu₂ZnSn(S,Se)₄ (CZTSSe) and its related compounds are promising for thin-film solar cells. We confirmed the grain boundary and work function properties of CZTSSe thin-films by Kelvin probe force microscopy and conductive atomic force microscopy under illumination. The high efficiency of CZTSSe thin-films showed positive potential at GBs, it induced negative band bending near GB and thus GBs acting as photo generated electron-hole carrier separation region. The work function of CZTSSe indicates single

peak around 4.7 eV in higher efficiency film. For this studies we can confirm the cause and effect for improving device properties.

9357-42, Session 11

Modes analysis in random structures varying the disorder magnitude

Carlo Molardi, Univ. degli Studi di Parma (Italy); Houkun Liang, Xia Yu, Singapore Institute of Manufacturing Technology (Singapore); Annamaria Cucinotta, Stefano Selleri, Univ. degli Studi di Parma (Italy); Ying Zhang, Singapore Institute of Manufacturing Technology (Singapore)

In a traditional laser the light amplification is obtained by a cavity that partially traps the light into an active material which provides an optical gain. In a random laser the light is localized into the material through the multiple scattering effect caused by the presence of a disordered scatterers pattern. Experiments show that the emission spectra of these devices are characterized by a high number of narrow peaks, which can be explained by physical phenomena like coherent backscattering and Anderson localization. To deep understand random laser spectra it is crucial to understand the nature of the passive random pattern without gain. In this contribution the relation between the disorder degree, evaluated in test random structures, and their mode spectra has been investigated. A set of 1D and 2D structures, suitable to work in Mid-IR region around 10 μm, has been considered with different realization of random patterns, varying important parameters such as the amount of the disorder and the density of the scatterers over the structure. The statistic of the disorder has been analyzed using the Fourier analysis while the mode spectra has been investigated with the help of a FEM software, additional parameters like the Q-Factor and the Mean Free Path have been calculated. A clear and sufficiently general definition of disorder has been developed to measure the amount of randomness in these structures and a formulation which describes the mode spectral properties has been proposed. Simulations are in good agreement with this formulation.

9357-43, Session 11

Compact polarization beam splitter for silicon-based slot waveguides based on an asymmetrical multimode interference coupler

Yin Xu, Jinbiao Xiao, Xiaohan Sun, Southeast Univ. (China)

A compact polarization beam splitter (PBS) for silicon-based slot waveguides is proposed based on a multimode interference coupler, where an asymmetrical multimode waveguide (AMW), cut by a right angle at one corner, is employed to efficiently separate the TE and TM modes. With the unique modal properties of the slot waveguides and corresponding optimized designs, the input TE mode can almost pass through the AMW and then enter into the bar port, while a mirror image is formed at the cross port for the input TM mode due to the self-imaging effect. Meanwhile, tapered waveguide structures and S-bend are incorporated into the designed PBS for further enhancing the performance. According to the numerical results, a PBS with an AMW of 2.3μm in length is achieved, where the extinction ratios are 16.6 and 20.9dB, respectively, for TE and TM modes, and the insertion losses are 1.37 and 0.81dB, respectively, at the wavelength of 1.55μm. For keeping extinction ratios over 15 and 20dB for TE and TM modes, the bandwidths are around 59 and 73nm, respectively, both covering the entire C-band. In addition, field evolution along the propagation distance through the PBS is also demonstrated.

9357-44, Session 11

Simulating the linear and nonlinear response of 1D nanostructures with a B-spline modal method

Patrick Bouchon, ONERA (France); Paul Chevalier, ONERA (France) and Lab. de Photonique et de Nanostructures (France); Sébastien Héron, ONERA (France) and LPN/CNRS (France); Fabrice Pardo, Lab. de Photonique et de Nanostructures (France); Riad Haïdar, ONERA (France)

Focusing the light onto nanostructures thanks to spherical lenses is a first step to enhance the field, and is widely used in applications, in particular for enhancing non-linear effects like the second harmonic generation.

Nonetheless, the electromagnetic response of such nanostructures, which have subwavelength patterns, to a focused beam can not be described by the simple ray tracing formalism. Here, we present a method to compute the response to a focused beam, based on the B-spline modal method (P. Bouchon et al., J. Opt. Soc. Am., 27, 696 (2010)), which is known to be fast thanks to a non-uniform mesh and sparse matrices. The eigenmodes are computed in each layer for both polarizations in conical mounting, and are then combined for the computation of scattering matrices. The simulation of a gaussian focused beam is obtained thanks to a truncated decomposition on plane waves computed on a single period, which limits the computation burden (P. Chevalier et al., J. Opt. Soc. Am., 31, 1692 (2014)).

Eventually, we develop a formalism to compute the second harmonic field under the undepleted pump approximation. The nonlinear polarization induced by a fundamental plane wave or a focused beam generates a source term at the doubled frequency. The latter is divided into a finite number of sub-sources and the second harmonic field is subsequently computed by integration of these sub-sources contributions (S. Heron, manuscript in preparation).

9357-50, Session PWed

Graphene-based metamaterial structures with single and multiple tunable transparency windows

Jun Ding, Bayaner Arigong, Han Ren, Mi Zhou, Jin Shao, Yuankun Lin, Hualiang Zhang, Univ. of North Texas (United States)

Novel graphene-based tunable plasmonic complementary metamaterials featuring single and multiple transparency windows are numerically studied in this paper. The proposed structures consist of a graphene layer perforated with a quadrupole slot structure and a dolmen-like slot structure printed on a substrate. Specifically, the graphene-based quadrupole slot structure can achieve a single transparency window without breaking the structure symmetry, which is different from conventional electromagnetically induced transparency (EIT) systems or EIT-like systems usually requiring symmetry breaking. Further investigations have revealed that the single transparency window in the proposed quadrupole slot structure is more likely originated from the quantum effect of Autler-Townes splitting (ATS) other than EIT. Next, for the proposed graphene-based dolmen-like slot structure, which is formed by introducing a dipole slot to the quadrupole slot structure, an additional transmission dip could occur in the transmission spectrum. Thus, a multiple-transparency-window system can be achieved based on graphene (for the first time for graphene-based devices). More importantly, the transparency windows for both the quadrupole slot and the dolmen-like slot structures can be actively controlled over a broad frequency range by varying the Fermi energy levels of the graphene layer through electrical gating. The proposed complementary metamaterial structures with tunable single and multiple transparency windows could find potential applications in many areas such as multiple-wavelength slow-light devices, active plasmonic switching, and optical sensing.

9357-51, Session PWed

Tunable graphene-based dual-frequency cross polarization converters

Jun Ding, Bayaner Arigong, Han Ren, Jin Shao, Mi Zhou, Yuankun Lin, Hualiang Zhang, Univ. of North Texas (United States)

The capability of manipulating the polarization of electromagnetic waves and light is of practical importance in many optical applications. Especially, polarization converters have been deemed as key elements in sensor applications and coherent optical systems. Metamaterial-based polarization converters have attracted considerable attention. They are realized through the excitation of the localized surface plasmon from the nanoscale particles or slots. However, in order to work at different frequencies, the polarization converters based on non-tunable materials need to be adjusted by carefully re-optimizing the geometrical dimensions due to the reliance on resonances. In this paper, we proposed a novel tunable cross-polarization converter (CPC) based on graphene that can work at two different frequencies. The CPC is composed of a single layer Graphene drilled with L-shaped nanoslots, and a dielectric spacer backed by a gold ground plane to suppress the transmission, which is likely to convert a linear polarization completely to its orthogonal state in a reflection mode. The normal incident wave at these two working frequencies can be rotated to its orthogonal directions. This phenomenon can be explained by the simultaneous excitation of both eigenmodes that are characterized as the results of the localized surface plasmon resonances. Furthermore, by merely varying the Fermi energy of the graphene through electrical gating, both working frequencies can be tuned within a large frequency range, which suggests numerous potential applications at mid-IR frequencies.

9357-52, Session PWed

Cavity-mode properties of semiconductor lasers operating in strong-feedback regime

Qin Zou, Télécom SudParis (France) and Institut Mines-Télécom (France)

This paper investigates the modal properties of semiconductor lasers operating in the strong-feedback regime. Analytical expressions are developed based on an iterative travelling-wave model, which enable a complete and quantitative description of a compound cavity mode in its steady state. We provide additional information about the physical inside into a compound laser system, such as a bifurcation diagram of the compound cavity modes for full variation range (from 0 to 1) of the external reflection coefficient and a more general shape for the diagram of photon density versus mode phase - this latter will reduce to the classical «ellipse» in the weak-feedback regime. We show that in the strong-feedback regime, a feedback laser is characterized by a small mode number and a high density of photons. This behavior confirms previous experimental observations, showing that beyond the coherence-collapse regime, the compound laser system could be re-stabilized, and that as a result power-enhanced low-noise stable laser operation with quasi-uniform pulsation is possible with external-mirror reflectivity close to 1. Moreover, we show that for a compound system operating in the strong-feedback regime, an anti-reflection treatment of a laser can significantly reduce its current threshold, and that in the absence of this treatment excitation of a minimum-linewidth mode with higher output power would be possible inside such a system. Finally, we show that in the weak-feedback regime except for a phase shift the iterative travelling-wave model will reduce to the Lang-Kobayashi model in cases where the product of the feedback rate and the internal round-trip time is much less than unity (that would mean in situations of as-cleaved lasers).

9357-53, Session PWed

Multichannel high-current-sensitivity all-fiber current sensor

Junzhen Jiang, Fujian Normal Univ. (China); Hao Zhang, Fujian Jiangxia Univ. (China); Baocheng Lin, Zhangting Huang, Yishen Qiu, Fujian Normal Univ. (China)

All-fiber current sensor (AFCS) have been intensively studied in the past three decades. Fiber in AFCS is not only a sensitive element but a signal carrier. The advantages of AFCSs include immunity against electromagnetic interferences, electrical isolation, absence of saturation effects, lightweight, and compact size. And it has more flexible configuration, easier fabrication and lower cost than other optical current sensors. However, there are still a major problem hinder the applications of AFCSs---the current sensitivity of AFCSs is very low.

Very recently, we reported a novel all-fiber current sensor using ordinary silica fiber based on the fiber loop architecture to improve current sensitivity. The sensor employs a fiber solenoid as a current sensor head, which improves the current sensitivity via allowing optical signals to traverse the sensor head repeatedly to improve current sensitivity. However, we adopted a single-channel system, which is capable of measuring the current only at one point. In order to improve the efficiency of the sensor and reduce cost, we want a sensor to synchronous monitor the currents at many different points. To achieve it, we present in this Letter the idea of multichannel all-fiber current sensor based on the principle of time-division multiplexing. [????? In order to improve the efficiency of the sensor and reduce cost, we present a multichannel all-fiber current sensor based on the principle of time-division multiplexing in the paper.] To illustrate the principle, we study the typical dual-channel all-fiber current sensor in our experiment. It shows that the currents at two different points can be measured simultaneously.

9357-54, Session PWed

Polarization-dependent photocurrent in MoS2 phototransistor

Jiu Li, Wentao Yu, Saisai Chu, Hong Yang, Peking Univ. (China); Kebin Shi, Qihuang Gong, Peking Univ. (China) and Collaborative Innovation Ctr. of Quantum Matter (China)

Monolayer or few-layer molybdenum disulfide (MoS₂) has attracted increasing interests in studying light-induced electronic effect due to its prominent photo-responsivity at visible spectral range, fast photo-switching rate and high channel mobility. However, the atomically thin layers make the interaction between light and matter much weaker than that in bulk state, hampering its application in two-dimensional material optoelectronics. One of recent efforts was to utilize resonantly enhanced localized surface plasmon for boosting light-matter interaction in MoS₂ thin layer phototransistor. Randomly deposited metallic nano-particles were previously reported to modify surface of a back-gated MoS₂ transistor for increasing light absorption cross-section of the phototransistor. Wavelength-dependent photocurrent enhancement was observed. In this paper, we report on a back-gated multilayer MoS₂ field-effect-transistor (FET), whose surface is decorated with oriented gold nanobar array, of which the size of a single nanobar is 60nm:60nm:120nm. With these oriented nanostructures, photocurrent of the MoS₂ FET could be successfully manipulated by a linear polarized incident 633nm laser, which fell into the resonance band of nanobar structure. We find that the drain-source current follows \cos^2 relationship with respect to the incident polarization angle. We attribute the polarization modulation effect to the localized enhancement nature of gold nanobar layer, where the plasmon enhancement occurs only when the polarization of incident laser parallels to the longitudinal axis of nanobars and when the incident wavelength matches the resonance absorption of nanobars simultaneously. Our results indicate a promising application

of polarization-dependent plasmonic manipulation in two-dimension semiconductor materials and devices.

9357-55, Session PWed

Nano scale confinement using dielectric waveguides at the mid-infrared region

Rania Gamal, The American Univ. in Cairo (Egypt) and Zewail City of Science and Technology (Egypt); Sarah A. Shafaay, The American Univ. in Cairo (Egypt); Yehea Ismail, The American Univ. in Cairo (Egypt) and Zewail City of Science and Technology (Egypt); Mohamed A. Swillam, The American Univ. in Cairo (Egypt)

The mid-infrared (MIR) region is one of the most thriving spectral regions as it contains the vibrational resonances of several molecules of interest, as well as the absorption bands for hot bodies. In this work, we propose a novel dielectric waveguide that confines the light in a nanoscale air gap. This dielectric waveguide is a suitable candidate for on-chip sensing. Detailed dispersion analysis of this 3D waveguide is also provided. The effect of the refractive index change in the gap is studied and shows very high sensitivity and causes significant changes in the modal parameters. We also show that these waveguide modes exhibit plasmonic-like characteristics at the MIR region with controllable plasma frequency, without the inclusion of any metals. This waveguide is also utilized in various on-chip applications with nanoscale confinement at the MIR region

9357-56, Session PWed

Designing plasmonic slot waveguide networks using a semi-analytical approach

Mohamed A. Swillam, The American Univ. in Cairo (Egypt); Amr S. Helmy, Univ. of Toronto (Canada)

A semi-analytical approach for efficient modeling of arbitrary plasmonic slot waveguide networks is proposed, examined and its efficacy is assessed. The model is simple and suitable for arbitrary scale networks of plasmonic junctions. The model utilizes waveguide impedances of plasmonic slot waveguides to estimate the transmission and reflection at each junction. This efficient and accurate methodology enables full analysis of a complete network of plasmonic slot waveguides without the need for any full wave analysis, which renders it resource efficient. As such it allows for fast design optimization. The performance predictions obtained using our approach for a range of network topologies match well those obtained using FDTD simulations. Examples of various plasmonic networks with different and interesting functionalities will be discussed.

9357-57, Session PWed

Automatic modulation format recognition for the next-generation optical communication networks using artificial neural networks

Latifa Guesmi, Hraghi Abir, Mourad Menif, SUP'COM (Tunisia)

The rapid growth of capacity demand on wavelength division multiplexing (WDM) system has caused considerable interest in alternative modulation format that can increase the capacity of communication system. Moreover, optical networks are nowadays becoming more heterogeneous, supporting a plethora of services with different modulation formats. Therefore, in recent years, to enable a real-time information about the signal modulation format,

**Conference 9357: Physics and Simulation of
 Optoelectronic Devices XXIII**

much interest by academic and military research institutes has focused around the research and development of automatic modulation format recognition (AMFR) algorithms.

In this paper, we present a new implementation of AMFR technique, where we propose the use of artificial neural network (ANN) in conjunction with the features of linear optical sampling (LOS) of the detected signal at high bit rates using direct detection and coherent detection. The use of LOS method for this purpose mainly driven by the increase of bit rates, enables the measurement of eye diagrams.

In order to investigate the validity of the proposed technique, numerical simulation have been performed for commonly-used modulation format at various data rate, namely 10 Gbps NRZ-OOK, 40 Gbps NRZ-DQPSK, 100 Gbps RZ-DP-QPSK, 160 Gbps DP-16QAM and 1 Tbps WDM-Nyquist RZ-DP-QPSK.

The efficiency of this technique is demonstrated under different transmission impairments such as chromatic dispersion (CD), differential group delay (DGD) and accumulated Amplified Spontaneous Emission (ASE). This technique allows us the estimation of the optical signal to-noise ratio (OSNR) in the range of 10-30 dB, chromatic dispersion (CD) in the range of -500 to 500 ps/nm and differential group delay (DGD) in the range of 0-15 ps.

The results of numerical simulation demonstrate successful recognition of all modulation formats from a known bit rates with a higher estimation accuracy.

9357-58, Session PWed

High Q/V hybrid photonic-plasmonic crystal nanowire cavity at telecommunication wavelengths

Chih-Kai Chiang, Yi-Cheng Chung, National Taiwan Ocean Univ. (Taiwan); Pi-Ju Cheng, Academia Sinica (Taiwan); Chien-Wei Wu, National Taiwan Ocean Univ. (Taiwan); Chung-Hao Tien, National Chiao Tung University (Taiwan); Tzy-Rong Lin, National Taiwan Ocean Univ. (Taiwan)

We have analyzed a hybrid photonic-plasmonic crystal nanocavity consisting of a silicon grating nanowire adjacent to a metal surface with a gain gap between. The hybrid plasmonic cavity modes are highly confined in the gap due to the coupling of photonic crystal cavity modes and surface plasmonic gap modes. Using the finite-element method, we numerically solve guided modes of the hybrid plasmonic waveguide at a wavelength of 1.55 μm . The modal characteristics such as waveguide confinement factors and modal losses of the fundamental hybrid plasmonic modes are explored as a function of the groove depth at various gap heights. After that, we show the band structure of the hybrid crystal modes, corresponding to a wide band gap of 17.8 THz. To effectively trap the optical modes, we introduce a single defect into the hybrid crystal. At a deep sub-wavelength defect length as small as 180 nm, the cavity modes exhibits a high quality factor of 566.5 nm and a ultrasmall mode volume of $0.00186 (\lambda/n)^3$ at the resonance wavelength of 1.55 μm . In comparison to the conventional photonic crystal nanowire cavity in the absence of metal surface, the figure of merit Q/V is enormously enhanced around 15 times. The proposed nanocavities open up the opportunities for various applications with strong light-matter interaction such as nanolasers and biosensors.

9357-59, Session PWed

High efficiency and broadband superconducting nanowire single photon detector with a composite optical structure

Min Gu, Lin Kang, Labao Zhang, Tao Jia, Chao Wan,

Ruiying Xu, Xiaozhong Yang, Peiheng Wu, Nanjing Univ. (China)

We theoretically proposed a kind of superconducting nanowire single photon detector (SNSPD) with a composite optical structure, which is composed of a phase grating and optical cavity, to enhance the detecting efficiency and response bandwidth. The numerical simulation by FDTD method shows that the photon absorption of composite optical structure SNSPDs can be enhanced greatly by adjusting the structure parameters of phase grating and optical cavity at multiple frequency bands. The absorption of superconducting nanowires is up to 70%, 72%, 60.73%, 61.7%, 41.2% and 46.5% at the wavelength of 684 nm, 850 nm, 732 nm, 924 nm, 1256 nm and 1426 nm, respectively. Meanwhile, by using composite optical structure, the total filling factor of superconducting nanowires is reduced to only 0.25, which decreases kinetic inductance of SNSPDs and improves its count rates.

9357-60, Session PWed

Investigation of degraded efficiency in blue InGaN multiple-quantum well light-emitting diodes

Yen-Kuang Kuo, National Changhua Univ. of Education (Taiwan); Jih-Yuan Chang, Kuang-Ming Junior High School (Taiwan)

The III-N light-emitting diodes (LEDs) have been widely utilized in several applications. For solid-state lighting, the development of high efficiency and high power LEDs is desired. In this demand, the major feature that needs to be solved might be the efficiency droop. However, the physical origin of efficiency droop remains debatable at present even though numerous explanations were proposed in recent years. An overall solution is hence still a lack. It is believed that heating is not the major cause of efficiency droop due to the fact that the efficiency droop occurs in both pulsed and continuous wave conditions as well as that the efficiency droop becomes severer with the decrease of ambient temperature. Various mechanisms, such as the carrier delocalization, Auger recombination, insufficient hole injection, carrier leakage, and polarization effect have been demonstrated to be relevant to the efficiency droop in III-N LEDs. In this study, degraded efficiency in blue InGaN LEDs is investigated numerically with the APSYS simulation program. It is depicted that the joint effects of polarization-induced electric field, current crowding, Auger recombination and SRH recombination are responsible for the degraded efficiency. Among them, the SRH recombination due to the poor crystalline quality is the main cause of reduced peak efficiency, while the Auger recombination is the major factor contributing to efficiency droop. It is shown that the strong built-in polarization field and the crowded current flow will result in the nonuniform carrier distribution, and thus enlarge the Auger losses and efficiency droop.

9357-62, Session PWed

Parity-time symmetry breaking in surface-plasmon waveguides

Youngsun Choi, Jong Kyun Hong, Seok-Ho Song, Hanyang Univ. (Korea, Republic of)

One of the postulates of quantum mechanics is that Hamiltonians are Hermitian operators, which is justified by the need for real eigenvalue spectra. Some years ago, Bender and co-authors pointed out that a whole class of PT-symmetric Hamiltonians also possess real spectra, despite being non-Hermitian[This has initiated a remarkable surge of research activity, much of it focusing on the ability of such Hamiltonians to undergo spontaneous PT-symmetry breaking transitions between real and complex (conjugate-pair) eigenvalue. It was realized that such Hamiltonians can be studied using optical waveguides and waveguide lattices, where PT-

symmetric non-Hermiticity may be implemented with spatially balanced gain and loss.

Here we evaluate PT-symmetry breaking behaviors of double-electrode surface-plasmon polaritons (SPP) waveguide structures, composing a directional coupler with two double-electrode SPP slab-waveguides. We propose that double-electrode SPP waveguide coupler can be an excellent optical system to investigate further physics on PT-symmetry breaking phenomena.

9357-63, Session PWed

Analysis of microwave frequency combs generated by semiconductor lasers under hybrid optical injections

Yu-Shan Juan, Cheng-Ting Lin, Yi-Hua Wu, Yuan Ze Univ. (Taiwan)

Microwave frequency combs utilizing hybrid optical injections schemes by varying the operational parameters, injection strength, repetition frequency, and detuning frequency are demonstrated and characterized. The dynamical hybrid optical injections is realized by both optical pulse injection and optical cw injection to the slave laser simultaneously under the condition of zero detuning frequency between two injecting source lasers. For pure pulse injection case, the amplitude variation of ± 34.57 dB in a 30 GHz range is obtained. By further applying the injection strength of the cw injection to the pulses injected semiconductor laser, the amplitude variation of ± 2.96 dB in a 30 GHz range in microwave frequency combs are observed when operating the cw injection system in a stable locking state. In addition, the bandwidth enhancement to about 30 GHz is also observed and the bandwidth enhancement of 11.8 times is achieved. In order to examine the microwave frequency comb precisely, each operational parameters of the hybrid optical injections schemes are analyzed. The amplitude variation of microwave frequency combs is also strongly influenced by operating the cw injection system in different states. Comparing to the cw injection system operated in period-one states, the amplitude variation is reduced when operated in the stable locking states. Moreover, the bandwidth broadening in microwave frequency comb is expected when the cw injection system operating in a stable locking state. In this paper, strongly improve the amplitude variation of the microwave frequency combs generated utilizing hybrid injections scheme compared to single injection case are obtained and compared.

9357-64, Session PWed

Investigation of the influence of unwanted micro lenses caused by semiconductor processing excursions on optical behavior of CMOS photodiodes

Andrea Kraxner, Jong Mun Park, Rainer Minixhofer, ams AG (Austria)

The net spectral sensitivity of photodetectors done with CMOS photodiodes is one of the most important performance parameters. For today's Sensor Systems on Chip (SSOC) the specification limits of these parameters caused by the variability in the intrinsic diode or the covering back end of line (BEOL) stack is of utmost interest. In this work, one source of variability, the influence of nanoscale particles caused by processing excursions during BEOL processing on top of the photodiode active region is investigated. The particles are located inside the BEOL and lead to an increased surface roughness and a deviation from planar conditions. The observed particle density varies across the semiconductor wafer from regions with almost zero fill factor to regions up to about 50% fill factor. To investigate the influence of the particles and their varying density on the photodiode performance, wafer level optical responsivity measurements are done on regions with different fill factors and the results are compared. In addition to

the measurements the effect of the particles is simulated with a simplified model based on a modified transfer matrix method (MTMM) [1]. The simulation and measurements are in very good agreement with each other and lead to the conclusion that even though some decrease of sensitivity is observed, the overall system variability is reduced by the presence of particles.

[1] Yin, G. and Merschjann, C. and Schmid, M., "The effect of surface roughness on the determination of optical constants of CuInSe₂ and CuGaSe₂ thin films", Journal of Applied Physics, 113, 213510 (2013), DOI: <http://dx.doi.org/10.1063/1.4809550>

9357-65, Session PWed

Numerical simulation of the transverse coincidence distribution of SPDC light

Robert Elsner, Dirk Puhlmann, Axel Heuer, Ralf Menzel, Univ. Potsdam (Germany)

Spontaneous parametric down conversion (SPDC) is a source of entangled photon pairs. In our setup we focus on a pump photon that is split into a signal and an idler photon due to a nonlinear interaction inside a crystal. For type II phase matching, the signal and idler photons are orthogonally polarized and can be separated at a polarizing beam splitter. We present a numerical simulation of the transverse coincidence distribution of the generated SPDC light. The model consists of a preparation stage and a measurement stage. The preparation stage is composed of two independent 4f-correlators for both the signal and the idler modes with the crystal situated at the input planes of both correlators. By inserting appropriate amplitude masks into the correlators, the near- and far-field mode distributions can be manipulated freely. The measurement stage encompasses two single-photon detectors which can be placed either in the near-field or far-field of the preparation stage. The simulation includes effects due to anisotropy, length and orientation of the nonlinear crystal. The numerical model thus allows for a detailed quantitative comparison of experimental data with simulation data. The simulation is compared with an optimized rerun of a recent experiment by Menzel et al. which exhibited an apparent violation of duality [1]. We experimentally improved the apparent violation $D^2 + V^2 = 1.42$ where V is the interference fringe visibility and D is the which-way distinguishability at a double slit. The numerical simulation excellently agrees with experimental data while predicting a maximum violation of 1.43.

[1] "Wave-particle dualism and complementarity unraveled by a different mode" PNAS, Vol. 109, No. 24, 9314-9319 (2012)

9357-66, Session PWed

Enhancement of figure of merit of a SPR based fiber optic sensor using tin oxide as an intermediate layer

Satyendra K. Mishra, Anisha Pathak, Banshi D. Gupta, Indian Institute of Technology Delhi (India)

The excitation of collective metallic electrons at metal-dielectric interface by evanescent field of guided waves in optical fiber gives rise to the phenomena of surface plasmon resonance (SPR). The sensor technology based on SPR has a great potential for detection and analysis of chemical and biochemical substances in many areas including medicine, biotechnology, food quality and environment. The performance of SPR based sensors is defined in terms of sensitivity (shift in the resonance wavelength per unit change in the refractive index of the sensing medium), full width at half maximum (FWHM) of SPR curve and figure of merit (FOM) which is defined as the ratio of sensitivity to FWHM. Higher is the value of FOM, better is the sensor. Here we report a novel design of a SPR based fiber optic sensor and analyze it in terms of FOM. The probe consists of coatings of tin oxide (SnO₂) followed by 40 nm thick metal

(Ag, Al or Cu) layer over an unclad core of the fiber with NA=0.36 and core diameter=600 μ m. Simulations were performed for various thicknesses of SnO₂ layer using geometrical optics and matrix method. The maximum value of FOM was obtained for 50 nm thickness. The values of FOM determined for three metals Ag, Al and Cu are 42, 39 and 46 respectively. Thus the combination of SnO₂ and copper layers gives best performance of the sensor. Similar calculations were performed for TiO₂ and ZnO and it was found that SnO₂ shows best performance in terms of FOM.

9357-67, Session PWed

Circuit-level simulation of transistor lasers and its application to modelling of microwave photonic links

Stavros Iezekiel, Andreas Christou, Univ. of Cyprus (Cyprus)

The transistor laser is an HBT-based device in which lasing occurs in the base region; stimulated emission occurs at the expense of current gain. Compared to conventional laser diodes, transistor lasers promise improved performance in terms of larger bandwidth, increased damping, reduced RIN and reduced nonlinear distortion.

Small-signal, large-signal and noise equivalent circuit models of a transistor laser are used to investigate the suitability of this relatively new device for analog microwave photonic links. The models are a composite of well-established equivalent circuits of hetero-junction bipolar transistors and circuit representations of the rate equations.

The three-terminal nature of the device enables transistor-based circuit design techniques to be applied to optoelectronic transmitter design. To this end, we investigate the application of balanced microwave amplifier topologies in which 90 degree hybrid couplers are applied to both ports of the transistor laser and to a pair of photodiodes. This topology enables low-noise links to be realized with reduced intermodulation distortion and improved RF impedance matching compared to conventional microwave photonic links. Equivalent circuit models are used to verify the link gain, noise figure and spurious-free dynamic range and to investigate the effect of passive impedance matching on these figures of merit.

9357-68, Session PWed

Constant-loss taper for mode conversion

Alexandre Horth, McGill Univ. (Canada); Raman Kashyap, Ecole Polytechnique de Montréal (Canada); Nathaniel Quitarioro, McGill Univ. (Canada)

The large index of refraction contrast between silicon and its oxide enables high-density integrated photonics but also raises coupling problems between integrated waveguides and standard fiber optics due to their large mode area mismatch. In order to achieve reasonable coupling between these two types of waveguide, mode conversion is required. Such a mode conversion can be achieved through tapered waveguide: tapering a waveguide reduces the effective index of its fundamental mode, which, by lowering the index contrast between the core and the cladding, results in expanding the mode area. Here the mode conversion efficiency of a linear, parabolic, and our novel constant-loss taper (CLT) is investigated. The CLT's shape is initially derived using coupled-mode theory on 1D slabs of silicon embedded in silicon dioxide. These slabs are connected together in a staircase fashion in order to form a 2D taper. An iterative technique is employed in order to evenly distribute the taper's loss along its length. Using 2D finite-difference time-domain simulations (FDTD), the fundamental mode conversion efficiency of a linear, parabolic and CLT is shown to be 72%, 80% and 90%, respectively for a 4.45 μ m long taper. The formalism developed for 2D tapers is then generalized to 3D tapers, specifically the mode conversion process from a 4.9 μ m mode field diameter fiber to a Si waveguide with height and width of 450 and 220nm is investigated using eigenmode expansion and 3D FDTD.

9357-69, Session PWed

Numerical full vectorial modeling method for calculating dispersion characteristics of single-mode high-contrast arbitrary radial refractive index profile optical fibers

Raushan Mussina, Hadi Baghsiahi, F. Aníbal Fernández, David R. Selviah, Univ. College London (United Kingdom)

The Galerkin method has advantages in terms of accuracy and speed for the analysis of circularly symmetric optical fibers with arbitrary refractive index profiles. The authors have previously shown that when combined with simple basis functions such as orthogonal Laguerre-Gauss polynomials, this method enables the first three derivatives of the propagation coefficient to be obtained analytically by repeated differentiation of the matrix equation (with respect to wavelength) resulting from the Galerkin method to find the first and higher order dispersion characteristics (group delay, β_g , chromatic dispersion, D, and dispersion slope) of single mode or multimode weakly guiding optical fibers having arbitrary radial refractive index profiles. In this paper, this approach is substantially expanded to enable high index contrast single mode optical fibers of arbitrary radial refractive index to be analyzed. The full-vectorial Helmholtz wave equation is solved using the Galerkin method with Laguerre-Gauss basis functions followed by repeated differentiation of the matrix equation to find the derivatives of the propagation coefficient required for the calculation of the first and higher order dispersion characteristics. As for the earlier scalar approach, this full vectorial approach avoids the approximation errors inherent in numerical differentiation, giving better accuracy and, at the same time, significantly reduced computational time and unlike the earlier scalar approach is no longer restricted to weakly guiding optical fibers so opening the possibility of using it to analyze silicon photonic waveguides, for example. The paper provides simulation results to validate the approach and compares the simulation results with available published data.

9357-70, Session PWed

A Complete theoretical description of the first-order delta-sigma modulation for analog-to-binary conversion

Azad Siahmakoun, Erin Reeves, Rose-Hulman Institute of Technology (United States); Pablo A. Costanzo Caso, Ctr. de Investigaciones Ópticas (Argentina)

A novel photonic analog-to-binary converter based on the first-order asynchronous delta-sigma modulation (ADSM) has been theoretically investigated and experimentally demonstrated (the results from a fiber-optic prototype system will be presented in a separate paper in this conference). The principles of operation for the proposed first-order ADSM are mathematically modeled and simulated. The all optical system is capable of producing NRZ type binary output for oversampling rates of 300 Gb/s and frequency bandwidth of 30 GHz at 8 effective number of bits (ENOB).

Asynchronous delta-sigma modulation is a straightforward approach to A/D conversion because in this case an external clocking is not required and demodulation can be simply performed via a low-pass filtering process. The modeling concept behind the photonic first-order ADSM is described by a closed-loop system with linear filter and non-linear single-bit quantizer. To improve signal-to-noise ratio and thus system ENOB, a non-interferometric optical implementation has been constructed. The ADSM is comprised of three photonic devices: an inverted output photonic leaky integrator, bistable quantizer, and positive corrective feedback. The hysteretic quantizer is described by symmetrically-coupled two semiconductor optical-amplifiers (SOA) where quantum-confined Stark Effect and nonlinear absorption provide the bistable behavior of the device. The photonic integrator which is a recirculating loop performs the oversampling of an analog input using the cross-gain modulation in an SOA. We will show that the photonic ADSM produces an inverted non-return-to-zero (NRZ) pulse-density modulated

output describing an input analog signal. The potential implementation of the integrated photonic version will also be discussed.

9357-72, Session PWed

Controllable harmonic generation by double couplings of ordinary rays-involved second-order processes

Yiqiang Qin, Nanjing Univ. (China)

For quasi-phase-matching (QPM) technique, much research has been done for purpose of obtaining efficient frequency conversion where the largest nonlinear coefficient (corresponding to $ee-e$ process) is used. However, these crystals do have other considerable nonlinear coefficients. In these cases, QPM parametric interactions such as $oo-e$, $oe-o$ and $eo-e$ process can be realized efficiently. From the viewpoint of coupling, the conventional harmonic generation with largest nonlinear coefficient should be treated as a particular case, the coupling of second-order parametric interactions based on different nonlinear second-order processes could be considered as a more general situation.

We concentrate on the cascading third harmonic generation (THG) with domain engineered micro-structures. To investigate the QPM nonlinear interactions by coupling of non- $ee-e$ processes, we select cascaded $o1e1-o2$ (SHG) and $o1o2-e3$ (SFG) processes for THG as an example. $o1e1-o2$ process generates y -polarized second harmonic (SH) using both ordinary and extraordinary components of the fundamental, while $o1o2-e3$ process utilizes the remaining ordinary fundamental and the produced SH to generate z -polarized third harmonic (TH). In this way, not only SHG is coupled with SFG process but also the polarization has a strong coupling with the ratio of nonlinear coefficients, resulting in more flexibility in dynamic tuning of the harmonic conversion.

It is noted that the coupled equations have a symmetrical form. We concentrate on the relationship between the maximum TH conversion efficiency and the ratio of coupling coefficients t , as well as the angle between the incident fundamental polarization and the z -axis of the crystal. The conversion efficiencies can be solved analytically. The two solutions are valid in different domains, which are separated by a continuous boundary. Generally, the coupled wave equations in nonlinear optics are difficult to solve analytically, especially for the multiple parametric processes. It's surprising to get such complete analytical results in current configuration.

9357-73, Session PWed

Simulation of the influence of the passivation layer on the plasmonic filter for IR image sensors

Hong-Kun Lyu, Hui-Sup Cho, Daegu Gyeongbuk Institute of Science & Technology (Korea, Republic of); Sung-Hyun Jo, Jang-Kyoo Shin, Kyungpook National Univ. (Korea, Republic of)

Since subwavelength metal gratings on proper condition and structure show the characteristics of extraordinary optical transmission (EOT), many researchers are expecting that it has potentialities as plasmonic color filters (PCFs). The PCFs has various filtering characteristics as the shape and size of the subwavelength metallic holes and the optical characteristics of the materials associated with the used metal layers and insulator layers. In this work, we investigated the optical transmission properties of subwavelength metallic apertures for IR image sensor using a commercial computer simulation tool utilizing finite-difference time-domain (FDTD) method as several thicknesses and the ratios of the hole diameter to the pattern period. Applied gold (Au) for the metal film and the dispersion information associated with Au was derived from the Lorentz-Drude model. As a result, optical transmission properties was influenced by the thickness of metallic apertures and especially it was highly influenced by existence or not of the

passivation layer. For the near IR band of 900nm wavelength it is proper condition that the period of the hole array is 425nm, the hole diameter is half of the period of the hole and the thickness of the metal is 200nm. The complete structure is composed of a quartz passivation layer and a gold (filled hole) layer on the Quartz substrate. We expects that a near IR optical filter could be realized by a simple insulator/metal/insulator structure using this results. In the further work, we will fabricate the near IR optical filter and investigate the optical properties.

9357-74, Session PWed

Optoelectronic properties of graphene on silicon substrate: effect of defects in graphene

Brahmanandam Javvaji, Indian Institute of Science (India); A. Ghan, National Institute of Technology, Karnataka (India); D. Roy Mahapatra, Gopalkrishna M. Hegde, Indian Institute of Science (India); R. Rahman, National Institute of Technology, Karnataka (India)

Engineering the electronic energy band structure in graphene based nanostructures has several potential applications. The most common and efficient way to create a bandgap in graphene is by placing it on a suitable substrate. Interaction of antibonding valance electrons in graphene with substrate affects the bandstructure of graphene. As a result of this bandgap may open up. In this paper we model and analyze the optoelectronic characteristics like optical conductivity and optical bandgap of graphene on silicon substrate wherein various different inter-band transitions are possible under the excitation of incident electromagnetic radiation. Several defects like structures, including Stone-Walls, octagonal and higher-order defects are observed when a graphene sheet is exfoliated from graphite. Existence of defect may cause change in the bonding interactions with the substrate. As a result the optoelectronic characteristics may get altered. Molecular dynamics simulations are performed to obtain the equilibrium geometry of graphene with defects placed on silicon substrate. The interactions between the atoms are modeled using Tersoff inter-atomic potential. Noose-Hoover thermostat is employed to control the temperature of the system at 300K. Electronic band structure of the equilibrated system is estimated by density functional theory based calculations. Inter-band transitions and the resulting optical conductivity are obtained using the Fermi distributions functions and Pauli's exclusion principle. From the inter-band transitions, the optical bandgap of the G-Si system is estimated and results are compared for pristine graphene and graphene with defects. This study is useful in understanding graphene based design of realistic photodetectors, photodiodes and quantum information processing.

9357-75, Session PWed

Modeling and measurements of optical properties in InAs/GaSb superlattice structures

Julien Imbert, III-V Lab. (France) and ONERA (France); Virginie Trinite, III-V Lab. (France); Sophie Derelle, ONERA (France); Mathieu Carras, III-V Lab. (France); Riad Haidar, Julien Jaeck, ONERA (France); Borge Vinter, Univ. de Nice Sophia Antipolis (France); Jean-Baptiste Rodriguez, Philippe Christol, Institut d'Electronique du Sud (France)

An 18-band $k.p$ formalism has been developed to determine the band structure and wave functions of InAs/GaSb type II superlattices (T2SL). First bandgap results are in good agreement with bandgaps measured for symmetrical superlattices. In order to validate the input parameters of our model, we developed a tool to simulate the absorption coefficient and compare results with measurements performed on superlattice samples

**Conference 9357: Physics and Simulation of
 Optoelectronic Devices XXIII**

at cryogenic temperature. Thus we are able to calculate theoretical optical and electrical properties of InAs/GaSb T2SL as the effective mass, the absorption coefficient and the free carrier concentration. The IES team manufactures different T2SL structures with a different InAs to GaSb thickness ratio R , but the same cut-off wavelength of $5\ \mu\text{m}$ at 77K. We compare these properties for these structures in order to investigate the influence of this ratio R .

References

B. Vinter, "Auger recombination in narrow-gap semiconductor superlattices", Phys. Rev. B 66, 045324 (2002).

G. Bastard, "Wave mechanics applied to semiconductor heterostructure", Les éditions de la physique (1988).

R. Talaat, J. B. Rodriguez, M. Delmas, and P. Christol, "Influence of the period thickness and composition on the electro-optical properties of type-II InAs/GaSb midwave infrared superlattice photodetectors" J. Phys. D: Appl. Phys. 47,015101 (2014).

9357-45, Session 12

Coupled semiconductor laser network topologies for efficient synchronization

Michail Bourmpos, Apostolos Argyris, Dimitris Syvridis, National and Kapodistrian Univ. of Athens (Greece)

The potential of conventional semiconductor lasers (SLs) to generate complex chaotic and broadband dynamics urged investigations in applications oriented to security. Latest theoretical and experimental works have demonstrated the capability of joint behavior or even synchrony of mutually coupled arrays of SLs in various configurations that mimic diverse network architectures with interacting nodes. In this work, two multi-SL topologies with at least fifty nodes, based on mutually coupled semiconductor lasers and representing a star-type and a mesh-type network, are compared in terms of their synchrony potential and their sensitivity towards critical SLs' parameters. The coupling topology determines the types of dynamics of the emitted optical signals which are always associated with the coupling conditions and the discrepancies of the SLs' parameters. The number of coupling elements and the detuning in their fundamental properties have been assessed to be decisive in the final dynamical map of the network. De-synchronization events are almost always observed in both topologies, even in highly correlated emitted signals. Occurrences and duration of these events can be partially or entirely harnessed by appropriate control on SLs' discrepancies. Multi-nodal networks with inherent non-linearities due to interactions may contribute to a better understanding of synchrony conditions in large scale networks. Additionally, this type of investigation will provide preliminary guidelines on building experimentally large scale networks of coupled SLs under various coupling matrices that could support optical sensing or cryptographic applications.

9357-46, Session 12

Fiber-optic analog-to-binary conversion

Azad Siahmakoun, Rose-Hulman Institute of Technology (United States) and Innovative Photonics Technologies LLC (United States); Erin Reeves, Rose-Hulman Institute of Technology (United States)

A novel photonic analog-to-binary converter based on the first-order asynchronous delta-sigma modulation (ADSM) has been theoretically investigated and experimentally demonstrated. For this purpose, a fiber-optic prototype ADSM is constructed and its performance characteristics are compared to the theoretical predictions. An ADSM is a straightforward approach to A/D conversion since an external clocking is not required in this case. The photonic first-order ADSM is comprised of a closed-loop system with a linear filter and a non-linear single-bit quantizer. The linear

filter is a leaky integrator designed as a unidirectional recirculating-loop that performs the oversampling of an analog input using the cross-gain modulation in an SOA. The integrator incorporates a bandpass filter to produce an accumulating output at a wavelength, λ_{2} , that is different from that of the analog input (λ_{1}). This technique provides a non-interferometric optical implementation that helps to improve the system SNR and ENOB. A non-linear single-bit quantizer (bistable quantizer) is constructed by symmetrically-coupled two SOAs in which the quantum-confined Stark Effect and nonlinear absorption provide the bistable hysteresis like behavior. This photonic quantizer converts the oversampled signal to an inverted NRZ pulse-density modulated output. Furthermore, part of this binary stream is used as positive corrective feedback to the input analog signal. That is, for maximum input value, minimal corrective feedback is applied whereas maximum feedback is added to a minimum input.

The fiber-optic prototype ADSM system achieves a sampling frequency of 13.8 Mb/s, an SNR of 37.95 dB, SFDR of 23.21 dB, and ENOB of 6 within the 6.9 MHz band of interest for a 3 MHz input.

9357-47, Session 12

On-chip generation and in-plane transmission of indistinguishable photons

Sokratis Kalliakos, Toshiba Research Europe Ltd. (United Kingdom); Yarden Brody, Andre Schwagmann, Univ. of Cambridge (United Kingdom) and Toshiba Research Europe Ltd. (United Kingdom); Anthony J. Bennett, Martin B. Ward, David J. P. Ellis, Joanna Skiba-Szymanska, Toshiba Research Europe Ltd. (United Kingdom); Ian Farrer, Jonathan P. Griffiths, Geb A. C. Jones, David A. Ritchie, Univ. of Cambridge (United Kingdom); Andrew J. Shields, Toshiba Research Europe Ltd. (United Kingdom)

Since its proposal, the use of single photons as flying qubits for quantum computing using linear optics has triggered a lot of scientific interest. In the core of most applications in quantum information processing lies the two-photon interference, in which two photons impinging on a different side of a 50/50 beamsplitter leave from the same exit. For successful interference, along with the perfect spatial overlap of photon wave functions at the beamsplitter, photons need to be indistinguishable in the spectral, temporal and polarization degrees of freedom.

For on-chip quantum information processing, the integration of the quantum emitter in the photonic quantum circuit is highly desired. Here, we report the on-chip generation of indistinguishable photons and their transmission along the semiconductor chip. Single photons are emitted by the excitonic recombination from a single InAs quantum dot, which is embedded in the waveguide region of a photonic crystal waveguide. Coupling of the quantum dot with the propagation mode of the waveguide allows for the efficient in-plane light transmission. We demonstrate the indistinguishability of the in-plane photons by performing two-photon interference with photons collected from the exit of the photonic crystal waveguide. Under continuous wave optical excitation, the interference visibility is measured to be 0.40 ± 0.04 , limited by the temporal resolution of our single-photon detectors. Our results are in excellent agreement with our theoretical model, in which all the parameters were determined experimentally. The possibility for enhanced interference visibility using resonant excitation schemes is also discussed.

9357-48, Session 12

Comparison of photonic integrated circuits for millimeter-wave signal generation between dual wavelength sources for optical heterodyning and pulsed mode locked lasers

Guillermo Carpintero del Barrio, Carlos Gordón Gallegos, Robinson C. Guzmán Martínez, Univ. Carlos III de Madrid (Spain); Frédéric Van Dijk, Gaël Kervella, III-V Lab. (France); Martyn J. Fice, Katarzyna Balakier, Cyril C. Renaud, Univ. College London (United Kingdom); Xaveer J. M. Leijtsens, Technische Univ. Eindhoven (Netherlands)

The paper will present the current advances in the development of photonic sources for the generation of millimeter wave signals for wireless communications, using Photonic Integrated Circuit techniques. We demonstrate different photonic integrated sources, designed to implement either time domain or frequency photonic signal generation technique. These two are the most promising, in conjunction with high frequency diodes.

For the time domain technique, based on short optical pulses, we demonstrate the short pulse generation (below 1 ps pulsewidths) of monolithic mode locked laser diodes (MMLLD) devices, using monolithic multimode interference reflectors. For the frequency domain technique, also known as optical heterodyne, we show a dual wavelength laser source based on monolithic integration of two DFB lasers, with a wide frequency tuning range. In addition, we also present the results from different schemes to implement an integrated optical frequency comb generator.

9357-49, Session 12

Ultra-high sensitivity optical biosensor based on Vernier effect in triangular ring resonators (TRRs) with surface plasmon resonance (SPR)

Tae-Ryong Kim, Jun Li, Hong-Seung Kim, Chung-Ang Univ. (Korea, Republic of); Geum-Yoon Oh, Korea Electronics Technology Institute (Korea, Republic of); Doo-Gun Kim, Korea Photonics Technology Institute (Korea, Republic of); Young Wan Choi, Chung-Ang Univ. (Korea, Republic of)

We propose a novel sensor structure that achieves ultra-high sensitivity, in which the Vernier effect and SPR effect are applied on triangular ring resonators (TRRs). The sensitivity of the sensor structure is enhanced by surface plasmon resonance (SPR) phenomenon of a thin gold film deposition at a total internal reflection (TIR) mirror and with Vernier effect in InP-based structure.

For achieving high sensitivity, we apply two designs on a TRR sensor. First, cascaded double triangular ring structures act as filter and sensor to induce the Vernier effect. Double TRRs are designed to have free spectral ranges (FSRs) that equal to 2.4 nm and 2.3 nm, respectively. Overall transmission is explained by the multiplication of transmission of each TRR. Because of mismatch in FSRs, the output transmission signal looks like envelope signal. The envelope signal has a large periodicity compared to FSR of single resonator. According to calculation, the sensitivity is enhanced from 472.5 nm/RIU to 7162.1 nm/RIU about one order of magnitude with respect to a single TRR sensor (enhanced factor $M = 15$). Second, the high sensitivity is also achieved by the deposition of thin gold film on the sidewall of resonator. The gold film deposition, at the sidewall of TRR, makes a SPR and enhances the sensitivity of TRR sensor. For the TRR with gold film, the sensitivity is significantly increased from 500 nm/RIU to 4200 nm/RIU compared to TRR without gold film.

We confirmed that the sensitivity of the TRR structure combining double TRR to make Vernier effect and deposition of SPR region is much higher than a single TRR sensor.

Conference 9358: Physics, Simulation, and Photonic Engineering of Photovoltaic Devices IV

Tuesday - Thursday 10-12 February 2015

Part of Proceedings of SPIE Vol. 9358 Physics, Simulation, and Photonic Engineering of Photovoltaic Devices IV

9358-1, Session 1

Light-trapping in ultra-thin solar cells: a new paradigm based on multi-resonant absorption (*Invited Paper*)

Stéphane Collin, Nicolas Vandamme, Clément Colin, Inès Massiot, Andrea Cattoni, Nathalie Bardou, Aristide Lemaitre, Lab. de Photonique et de Nanostructures (France); Jean-François Guillemoles, Institut de Recherche et Développement sur l'Énergie Photovoltaïque (France)

Introduction: Conventional light trapping in solar cells is based on anti-reflection coatings deposited on an optically thick absorber layer, and light scattering to increase the optical path close to the semiconductor bandgap. An upper limit for the optical path enhancement has been derived by E. Yablonovitch for optically thick but weakly absorbing media: $F=4n^2/50$. This approach has been extended to the sub-wavelength regime by considering grating coupling to guided modes in very thin layers. The $4n^2$ limit can be overcome in particular cases, but the spectrally averaged absorption is still very low.

Approach and results: We argue that infinite optical path enhancement ($F=\infty$) can be reached for any resonant mode in the critical coupling regime (absorption=100%), in contradiction with the conventional upper limit. We propose a new paradigm for light trapping in nanometer-thick absorbers. It aims at reaching nearly perfect optical absorption on a broad spectral range, with a number of resonant modes in periodical structures. We focus on very thin semiconductor absorbers (25nm), and use metal nanostructure arrays with sub-wavelength period, $d=200$ nm (to avoid diffraction losses). The goal of multi-resonant absorption seems unrealistic due to the small number of modes in such tiny unit cells ($25 \times 200 \times 200 \text{ nm}^3$). Indeed, we demonstrate theoretically and experimentally:

- Novel resonance modes in deep sub-wavelength structures (nanoscale Fabry-Perot resonators),
- Multi-resonant absorption in a 25 nm-thick GaAs semiconductor layer with metal nanostructure arrays, independent of incidence angle,
- Nearly-total absorption (~100%) at each resonance wavelength (critical coupling regime),
- Three-fold enhancement of the density of optical modes (DOS) on a broad spectral range (500-800 nm) as compared to bulk media,
- Very low metal (parasitic) absorption over the entire absorption spectrum (<13%) despite the use of metal nanostructures for DOS enhancement.

Conclusion: These results leads to broadband, highly efficient absorption in ultrathin GaAs layers (figure 1). They exceed recent previous theoretical predictions for the upper limit of broadband light coupling [3]. They could allow a drastic reduction of the absorber thickness in thin-film photovoltaics. It is also a key step in the development of new concepts for high-efficiency solar cells (hot-carriers, intermediate-band, up- and down-conversion,...), since all these concepts require strong optical confinement in very thin absorbers.

9358-2, Session 1

Exploring the effective absorption length of Si nanohole array for photovoltaic by plasmonic enhanced Raman scattering

Zingway Pei, Thiyagu Subramani, Devi Parvathy, National Chung Hsing Univ. (Taiwan)

Either nanowire or nanohole array for semiconductor were proved to be an efficient nanostructure to harvest solar light. However, for Si, the length of nanostructure about several micrometers is required to have acceptable absorption. Although this length already far less than the bulk Si in which hundred micrometers are required, the micrometers length still not feasible for Si nanostructure. High density nanostructures will cause extensive surface recombination that reduces the power conversion efficiency. Therefore, explore the dependence of light absorption to the length of Si nanostructure is very important to design an efficient solar cell. In this work, the Si nanohole array was fabricated in several depths from 110 to 960 nm. The total reflection was less than 1% at visible regime for 960 nm depth hole. The Ag nanoparticles were put at the bottom of the nanohole to explore the light absorption by plasmonic enhanced Raman scattering. A chemical, pNTP, was cover Ag nanoparticle as the prober for the plasmonic effect. As the laser light incident to the Ag nanoparticle, the surface plasmonic effect will enhance the Raman scattering of the pNTP. The enhanced Raman signal obtained from pNTP indicates the incident light could penetrate into the bottom of the Si nanohole array without significant absorption. The experiment result indicate the Raman signal decay fast after the depth of nanohole exceed 240 nm. This result indicate, the length of Si nanostructure may not need micrometers length to harvest incident solar light. This finding pave a bright route for design of Si solar cell with nanostructures.

9358-3, Session 1

Sufficient condition for perfect antireflection by optical resonance at dielectric interface

Ken X. Wang, Zongfu Yu, Sunil Sandhu, Victor Liu, Shanhui Fan, Stanford Univ. (United States)

Antireflection is important for many devices such as solar cells. A new approach was recently proposed by Prof. A. Polman's group [Spinelli, et al, Nat. Commun. 3, 692, 2012]: one places arrays of nanostructures at the air-dielectric interface and uses the Mie resonances to minimize reflection. This approach has a few advantages: first, it can be easily achieved without inducing much surface recombination; second, the resonances might additionally provide light-trapping functionalities. In this talk, we present a theoretical analysis of resonant antireflection and rigorously derive a sufficient condition for complete antireflection. The condition has two parts and their physical origins are as follows: first, the periodicity of the array needs to be carefully chosen in order to suppress backward diffraction; second, the resonance needs to radiate in a balanced fashion to air and to the dielectric side by reciprocity (in particular, if the periodicity is smaller than the wavelength in the dielectric, the resonance needs to radiate equally to air and to the dielectric, which is contrary to the claim that the antireflection effect is attributed to the tendency of the resonance to radiate dominantly into the dielectric). We validate the theoretical results using electromagnetic simulations, for both high-Q and low-Q resonances. The formalism we develop is general and can be used to study other effects such as reflection enhancement. It is interesting to note that, the condition for perfect antireflection happens to be optimal for light trapping. Thus, our theory is useful for understanding simultaneous antireflection and light trapping.

9358-4, Session 1

Optimal subwavelength light trapping textures for photovoltaics

Vidya Ganapati, Univ. of California, Berkeley (United States); Owen D. Miller, Massachusetts Institute of Technology (United States); Eli Yablonovitch, Univ. of California, Berkeley (United States)

Light trapping in solar cells allows for increased current and voltage, as well as reduced materials cost. It is known that in geometrical optics, a maximum $4n^2$ absorption enhancement factor can be achieved by randomly texturing the surface of the solar cell, where n is the material refractive index. This ray-optics absorption enhancement limit was proven only for solar cell thicknesses much greater than the optical wavelength. In sub-wavelength thin films, the maximum absorption enhancement and the exact surface texture that achieves this maximum is unknown. We use adjoint-based shape optimization in order to solve for the optimal nanoscale texture for light trapping in sub-wavelength thin films, using electromagnetic finite-difference time-domain methods to evaluate the textures. We demonstrate that we cannot exceed the $4n^2$ limit for high index absorber materials for isotropic illumination, and there is no particular preference for the texture. However, for collimated illumination, we exceed $4n^2$, as expected, and in that case, we show convergence to a particular texture.

9358-5, Session 2

Advanced light trapping approaches in thin-film silicon solar cells (Invited Paper)

Arno H. M. Smets, Fai Tong Si, Rudi Santbergen, Hairen Tan, Olindo Isabella, Miro Zeman, Technische Univ. Delft (Netherlands)

Thin-film silicon (TF Si) solar cell technology can deliver low-cost solar electricity. A drawback of this technology is a relatively low stabilized efficiency of modules that varies between 6 to 12.2%. In order to stay competitive with other PV technologies TF Si solar cells have to demonstrate 20% efficiency. This goal requires intensive R&D activities and breakthroughs on the material-, interface-, and device level. Light trapping plays an important role in increasing the performance of TF Si solar cells by enhancing absorption in the absorber layers, especially in the wavelength regions of low absorption. In today's TF Si solar cells light trapping techniques are based on scattering of light at randomly textured rough interfaces, the employment of highly reflective metal layers at the back contact and refractive-index matching layers at the front side. Although the conventional anti-reflection coatings and surface textures eliminate most of the reflection losses, the supporting layers in TF Si solar cells, such as TCO, doped layers and back reflector, are still responsible for significant parasitic absorption losses.

In order to approach and overcome the theoretical absorption enhancement limit in TF Si solar cells several advanced light trapping approaches have been studied and introduced recently such as:

- i) scattering at modulated surface textures,
- ii) plasmonic scattering using metal nanoparticles,
- iii) triple and quadruple-junction solar cells.
- iv) intermediate reflector layers
- v) transparent non silicon based doped layers.

In this contribution I will discuss the recent progress made on these advanced light trapping in the Photovoltaic Devices and Materials group at the Delft University of Technology. Modulated surface textures are created by novel glass and TCO texturing processing. This approach relaxes the competition between textured surfaces and ability to process device grade PV material. State-of-the-art light trapping, fill factor and open circuit voltages are obtained for single, double and triple junctions based on silicon alloys. State-of-the-art plasmonic back reflectors have been manufactured

for amorphous and nanocrystalline silicon solar cells. The reasons why these plasmonic reflectors do not outperform the current conventional back reflectors will be discussed. The route to 20% efficient TF Si PV devices will be discussed using silicon based triple and quadruple junctions, including the important role of intermediate reflector layers. Finally, new materials to replace the doped layers will be presented to reduce the parasitic absorption losses of these devices.

9358-6, Session 2

Nanofrustum hexagonal array solar cells for ultrathin crystalline silicon devices

Yunae Cho, Dong-Wook Kim, Minji Gwon, Eunah Kim, Ewha Womans Univ. (Korea, Republic of); Joondong Kim, Incheon National Univ. (Korea, Republic of); Hyeong-Ho Park, KANC (Korea, Republic of)

Nanostructure at the surface provides a novel strategy to enhance broadband light absorption, as well as conventional light trapping techniques such as surface texturing and anti-reflection coating. Although recent optical simulation studies have suggested potential of nanostructures for high efficient solar cells, there have been few reports to demonstrate the high performance compared with conventional solar cells.

In this study, we achieved a very large photocurrent of 36.96 mA/cm², one of the largest photocurrents recorded for nanostructured cells, for 4-in-diameter 500- μ m-thick c-Si solar cells having hexagonal nanoconical frustum array surface patterns. The samples were prepared using an ultraviolet (UV) nanoimprint lithography technique. Optical simulations of patterned solar cells showed significantly enhanced optical absorption; optical gain was maintained, as the absorber thickness was reduced to 10 μ m. The expected photocurrent of the 10- μ m-thick cell slightly exceeded the Lambertian limit. Graded refractive index of nanopatterned structures effectively reduced the optical reflectance and the periodic patterns also worked as a refractive diffraction grating enlarging the optical path length of light in the thin absorber. These results suggest nanopatterned structures as strong candidates for ultrathin c-Si solar cell applications.

9358-7, Session 2

Design of nano-pattern reflectors for thin-film solar cells based on three-dimensional optical and electrical modeling

Hui-Hsin Hsiao, Hung-Chun Chang, Yuh-Renn Wu, National Taiwan Univ. (Taiwan)

Thin film solar cells offer the benefits of reduced materials and fabrication costs and are attractive candidates for light-weight, and flexible devices. To achieve efficient absorption of the solar spectrum with thin semiconductor volumes, many researches focus on improving light trapping schemes, which are frequently realized by random or periodic textures. In this research, we propose a new type photonic-plasmonic nanostructure called anti-ring array comprised of a nanodome centered inside a nanohole, as the back reflector geometry. Then, a 120-nm-thick silver film and a 160-nm-thick AZO layer are deposited above the nano-patterned glass substrate. The a-Si:H layer with thickness 180 nm and ITO layer with thickness 50 nm are deposited accordingly. Our in-house developed three-dimensional (3-D) finite-difference time-domain (FDTD) program is used to calculate the absorption within the a-Si:H layer. Next, the optical generation rate is obtained by weighting the FDTD results according to the AM 1.5 solar spectrum. In addition, a 3-D Poisson and drift-diffusion solver is implemented to simulate the dynamics of optical-generated carriers transport within the device. Our model predicts an optimized 9.81 % efficiency where $J_{sc} = 15.09$ (mA/cm²), $V_{oc} = 0.94$ (V), and $FF = 68.84$ % for 700 nm period. With the help of our 3D models, we systematically studied the optical and electronic effect of the anti-ring structure as the back reflector for thin-film solar cells. For the optical optimization, we found the key factor relies on the design with the

**Conference 9358: Physics, Simulation, and Photonic
 Engineering of Photovoltaic Devices IV**

resonances of the focusing effect and the Fabry-Perot modes overlapped. For the electronic property, the topography of the nano-pattern has a significant influence on the potential profiles, where a high aspect-ratio pattern may result in an extensive effective flat-band region due to the metallic shell shadowing effect. Meanwhile, the enlarging low-field flat-band region facilitates the radiative and non-radiative recombinations to happen and degrades the photocurrent collecting efficiency.

9358-8, Session 2

Angle selective light management in photovoltaics using self assembled anodized aluminum oxide nanopatterns

Brian Roberts, Pei-Cheng Ku, Univ. of Michigan (United States)

Thin film photovoltaic (PV) technologies have the potential to reduce solar energy costs, though thin active layers are inefficient absorbers. Light management structures can improve absorption within optically thin layers, as well as enabling new functionality such as semitransparency for building integrated PVs. We propose and investigate two nanostructured approaches for angle selective light management in PV window coatings, allowing high absorption of direct sunlight from an elevated angle without sacrificing transparency in the normal direction. The proposed nanostructures can be self-assembled over large areas by electrochemical anodization of aluminum into nanoporous aluminum oxide films.

The first nanostructured approach for angle selective light management exploits the localized surface plasmon resonance properties of vertical metal nanorods, which can be fabricated by electroplating metal into the nanopores of an anodized aluminum oxide (AAO) film. Normally incident light, polarized along the short axis of the nanorods, interacts with a short-wave plasmon resonance only, with longer wavelengths transmitted. Angled light polarized along the nanorods' long axis interacts with a redshifted plasmon resonance, scattering this light back to an accompanying PV.

In the second approach, the scattering properties of AAO itself are investigated. Anodization of aluminum at high voltage results in an array of high aspect ratio nanopores with horizontal feature sizes on the order of the visible wavelengths. Normally incident light is transmitted across the film, while angled light probes the structure and undergoes coherent multiple scattering. Experimental data and numerical simulations are presented demonstrating the potential for angle selective semitransparent PVs.

9358-9, Session 3

Impact of photon recycling and luminescent coupling in III-V photovoltaic devices (Invited Paper)

Alexandre W. Walker, Oliver Höhn, Daniel M. Neves, Frank Dimroth, Fraunhofer-Institut für Solare Energiesysteme (Germany)

Photon recycling in III-V semiconductor solar cells is essential in reaching open circuit voltages larger than 1.06 V under AM1.5g illumination conditions. Without these effects, modeling tools cannot predict the experimentally observed high device performance. A sophisticated model has been developed to fully account for the optoelectronic performance of thin film GaAs solar cells, and is used to explore the design and material parameter constraints which produce world record solar cell devices. The initial major constraint is the dominance of radiative versus non-radiative recombination rates. Once the cell is radiatively dominated, the thickness of the active region becomes the major constraint, albeit coupled to the efficiency of the back mirror in reflecting the incident light and the photoluminescence. A breakdown of the origin in open circuit voltage enhancement is given for these various constraints. A further boost in voltage is also possible using a selective angular filter on the top surface

such as a multi-dielectric stack. The extendibility of the model to multi-junction solar cells is briefly discussed, before studying the luminescent coupling between series connected sub-cells in a GaInP/GaAs tandem cell. The behaviour of the individual sub-cells for various designs is explored, along with the overall device performance under concentrated illumination.

9358-10, Session 3

Multi-junction-solar-cell designs and characterizations based on detailed-balance principle and luminescence yields (Invited Paper)

Hidefumi Akiyama, The Univ. of Tokyo (Japan)

We developed a straightforward and potentially standard method of accessing the balance sheets of energy and carriers as well as respective subcell photovoltaic properties in multi-junction tandem solar cells by measuring absolute electroluminescence quantum yields.

This method was indeed applied to a InGaP/GaAs/Ge 3-junction solar cell for satellite use, and subcell I-V characteristics, internal luminescence yields were evaluated. Moreover, the derived balance sheets of energy and carriers revealed respective subcell contributions of radiative and nonradiative recombination losses, junction loss, thermalization loss, and luminescent coupling. These results provide detailed diagnosis and valuable feedback to fabrications.

We calculated conversion-efficiency limit and optimized bandgap energy in 1-, 2-, 3-, 4-, and 5-junction tandem solar cells the 1-sun and 100-sun conditions, including finite values of sub-cell internal luminescence quantum yields to account for realistic material qualities in sub-cells. With reference to the measured internal luminescence quantum yields, the theoretical results provide realistic targets of efficiency limits and improved design principles of practical tandem solar cells, which are useful for realistic designs of tandem solar cells.

9358-11, Session 3

Light management of quantum wells in thin GaAs solar cells with coherent back reflection

Wei Wang, Akhil Mehrotra, Alexandre Freundlich, Univ. of Houston (United States)

Thin GaAs solar cells offer cost reduction through reuse of substrates compared to conventional technologies, whose total thickness less than 2um also provide photon-recycling through back reflection. Conventional bi-layer ARCs gives thin GaAs (i.e. 0.5 um) as high as 13 % reflection loss (when there is perfect back reflector) instead of 3.8% reflection loss in ideal thick devices, due to limited absorption inside SCs.

QWs also provide a way to improve current in SCs. Yet increasing the number of QWs (hence the thickness of QW region) trades off a reduction of Voc. By using back mirror, further improvement of current can be achieved without sacrificing Voc. Here is this work, InGaAs/GaAs QWs has been calculated. Total thickness of QWs is generally less than 100nm, contributing to weak absorption below its bandgap, hence optimization of ARC is required for higher quantum efficiency. Due to use of coherent back reflection, light oscillation are generated in thin SC devices. Hence accurate positioning of QWs in i-region is essential for maximum utilization (absorption) of below bandgap photons. In order to take maximum advantage of back reflection, here a novel design has been discussed where QWs are located at constructive coupling areas in i-region. Optimized QW position is found to be 150nm from GaAs surface, and optimized gap between QWs is 100nm. For less than 100nm InGaAs QW under AM1.5G spectrum between 870 to 1030 nm, integrated absorption is improved from 22% to 26% in back mirror condition, compared to 17% absorption in no mirror condition.

9358-12, Session 3

Impact of light management on photovoltaic characteristics of GaAs solar cells with selective filter

Mu-Min Hung, National Chiao Tung Univ. (Taiwan); Chung-Yu Hong, Arima Photovoltaic & Optical Corp. (Taiwan); Tung-Ting Yang, Yi-Chin Wang, Peichen Yu, National Chiao Tung Univ. (Taiwan)

In detailed balance model, the efficiency of single-junction solar cells can be potentially as high as 33.5% under AM 1.5G illumination. However the best state-of-the-art devices are still far lower than those figures, even the electronic quality is nearly perfect. Therefore the efficiency gap should stem from the light management inside solar cells. Recently, Alta device, Inc. has successfully fabricated a thin-film GaAs single junction solar cell with conversion efficiency of 28.8%, under 1 sun illumination, which aggregates the loss of backward emission into substrate. This factor can be highly relevant to the cell's performance, especially open-circuit voltage (Voc), and maximizing Voc is generally considered as the last mile to approach ultra-high efficiency limit.

In this work, we try to quantify the Voc enhancement in GaAs solar cells by reducing emission loss. The simulation tools are RCWA simulation and photon recycling model NREL developed recently. The top structures we simulate here are different cutoff wavelength thin film selective filter of alternate TiO₂ and SiO₂. After our calculation, the cutoff wavelength of 840 nm can make the biggest Voc enhancement 46.4meV compared with bare one, and the structure also has excellent anti-reflection ability for maintaining high Jsc. Our results also show that using this way to enhance Voc is especially suitable for cells with ordinary material quality. Therefore, the requests of ideal top structures for solar cells' use are not only near-perfect anti-reflection, but the ability to minimize the emission loss.

9358-13, Session 4

Five-volt photonic power converter (Invited Paper)

Christopher E. Valdivia, Matthew M. Wilkins, Univ. of Ottawa (Canada); Boussairi Bouzazi, Abdelatif Jaouad, Vincent Aimez, Richard Arès, Univ. de Sherbrooke (Canada); Denis P. Masson, Azastra Opto Inc. (Canada); Simon Fafard, Azastra Opto Inc. (Canada) and Univ. de Sherbrooke (Canada); Karin Hinzer, Univ. of Ottawa (Canada)

The high-efficiency conversion of photonic power into electrical power is of broad-range applicability to many industries due to its electrical isolation from the surrounding environment and immunity to electromagnetic interference which affects the performance and reliability of sensitive electronics. In such a system, a laser launches up to several watts of photonic power through a multimode fiber for distances of up to several kilometers. A phototransducer absorbs and converts this power back to electrical power for use by remote devices. The photonic power typically uses near-infrared light due to the low loss of optical fibers and the availability of high-powered lasers in this wavelength range. However, electronic devices typically require a voltage of 5 V, at least 4x higher than the photovoltage produced by these photons.

In this research, we have designed and fabricated a photovoltaic phototransducer capable of converting infrared laser light to electrical power having a voltage of >5 V at realistically achievable efficiencies of >60%. Optoelectronic simulation and device optimization has been carried out using Synopsys Sentaurus commercial software. Growth and fabrication of designed devices were completed by industrial partner, Azastra Opto, utilizing fully-lattice matched materials grown on GaAs substrates, leveraging prior experience on III-V multi-junction solar cells. Early

measurements of these devices have shown good agreement with simulated internal quantum efficiency and also open-circuit voltages in excess of 5 V even under conditions of very low current. We will present calibrated quantum efficiency and current-voltage behavior, showing device operation with ≥ 1 W of near-infrared light.

9358-14, Session 4

Origami photovoltaics

Chih-Wei Chien, Kyusang Lee, Stephen R. Forrest, Max Shtein, Pei-Cheng Ku, Univ. of Michigan (United States)

The key metric to benchmark any solar energy technology is the cost in terms of dollars per watt (\$/Wp) or levelized cost of electricity (LCOE). Reducing the \$/Wp requires lowering the materials cost, e.g. by using the concentrated photovoltaics (CPV) technology. However, the CPV technology requires a costly tracking system. A parabolic trough with one axis tracking can cost more than \$200/m². Furthermore, one cannot directly apply the CPV tracking system to a flat panel system to reduce the materials cost. To this end, we have proposed and demonstrated an origami PV panel that combined advantages of both the flat panel and CPV systems. The origami PV consists of an array of origami concentrator and origami tracking. Standard CAD tools were used for the design and fabrication of the array to allow scalability to large-scale manufacturing. Origami structures can be made with simple folding without the need for any external mold. With GaAs cells, we have measured the concentration factor to be 6.1 under AM1.5 and the angle dependence is about the same as a regular flat panel.

9358-15, Session 4

Demonstration of a 5x5 cm² self-tracking solar concentrator

Volker Zagolla, Eric J. Tremblay, Christophe Moser, Ecole Polytechnique Fédérale de Lausanne (Switzerland)

Solar concentration is using optics in order to minimize the amount of expensive photovoltaic cell material needed. For concentration factors higher than approximately 4, tracking the sun's position is needed to keep the focal spot on the solar cell. Based on recent developments using a waveguide slab to concentrate sunlight we propose and demonstrate a light responsive, self-tracking solar concentrator. Using a phase change material acting at the focal spot, it is possible to maintain efficient coupling into the waveguide, up to an angular range of +/- 20 degrees. The system uses the unused infrared part of the solar spectrum as energy for the phase change actuator to achieve its high acceptance angle. With a spectrally matched custom silicon solar cell attached to the waveguide slab, in which light is coupled, the visible part of the solar spectrum can be efficiently converted to electricity. A proof-of-concept single lens device was demonstrated in our previous work. Here we extend the principle to a 3x3 lens array demonstration device. The current demonstration device features an acceptance angle of +/- 16 degrees and an effective concentration factor of up to 20x.

9358-16, Session 5

Monolithic integration of GaAsPN dilute-nitride compounds on silicon substrates: toward the III-V/Si tandem solar cell (Invited Paper)

Olivier Durand, Samy Almosni, Yanping Wang, Charles Cornet, Antoine Létoublon, Christophe Levallois, Alain Rolland, Jacky Even, Nicolas Bertru, Alain Le Corre, Institut National des Sciences Appliquées de Rennes (France);

**Conference 9358: Physics, Simulation, and Photonic
Engineering of Photovoltaic Devices IV**

Pierre Rale, Laurent Lombez, Jean-François Guillemoles, Institut de Recherche et Développement sur l'Energie Photovoltaïque (France); Anne Ponchet, Ctr. d'Elaboration de Matériaux et d'Etudes Structurales (France)

GaAsPN semiconductors are promising material for the elaboration of high efficiencies tandem solar cells on silicon substrates. GaAsPN diluted nitride alloy is studied as the top junction material due to its perfect lattice matching with the Si substrate and its ideal bandgap energy allowing a perfect current matching with the Si bottom cell. We review our recent progress in materials development of the GaAsPN alloy and our recent studies of all the different building blocks toward the elaboration of a PIN solar cell. A lattice matched (with a GaP(001) substrate) 100 nm-thick GaAsPN alloy has been grown by MBE. After a post-growth annealing step, this alloy displays a strong absorption around 1.8-1.9 eV, and efficient photoluminescence at room temperature suitable for the elaboration of the targeted solar cell top junction. An early stage GaAsPN PIN solar cell prototype have been grown on a GaP (001) substrate. The quantum efficiency and the I-V curve show that carriers have been extracted from the GaAsPN alloy absorber, with an open-circuit voltage around 1 eV, while however displaying a low short circuit current meaning that the GaAsPN structural properties needs an optimization. Considering all the pathways for improvement, the >2% efficiency obtained under AM1.5G is however promising, therefore validating our approach for obtaining a lattice-matched dual junction solar cell on silicon substrate. This work was supported by the French ANR, project MENHIRS (grant N°ANR-2011-PRGE-007-0).

9358-17, Session 5

Time-resolved PL and TEM studies of MOVPE-grown bulk dilute nitride and bismide quantum well heterostructure

Yongkun Sin, Zachary Lingley, Miles Brodie, William T. Lotshaw, Steven C. Moss, The Aerospace Corp. (United States); Tae Wan Kim, Yingxin Guan, Kamran Forghani, Luke J. Mawst, Thomas F. Kuech, Univ. of Wisconsin-Madison (United States)

Among several approaches proposed to achieve high-efficiency III-V multi-junction solar cells, the most promising one is to incorporate a bottom junction consisting of a 1 - 1.25 eV material. Several groups have studied MBE- and MOVPE-grown 1 - 1.25 eV bulk (In)GaAsN(Sb) dilute-nitride lattice matched to GaAs substrates, but it is a challenge to grow dilute-nitrides without introducing a number of localized states. Localized states originating from random distributions of nitrogen sites in dilute-nitrides behave as highly efficient traps, leading to short minority carrier lifetimes. As our group previously reported, carrier dynamics studies are indispensable in the optimization of dilute-nitride materials growth to achieve improved solar cell performance. Also, bismide QW heterostructures have recently received a great deal of attention for solar cell and laser applications because theoretical studies have predicted reduction in nonradiative recombination in Bi-containing materials.

We employed time-resolved PL techniques to study carrier dynamics in MOVPE-grown bulk (In)GaAsN(Sb) materials nominally lattice matched to GaAs substrates. Our present samples showed a significantly less background C doping density compared to our previous samples. Carrier lifetimes were measured from dilute-nitride samples with low C doping density at various temperatures between 10K and RT. We compared carrier lifetimes measured from (In)GaAsN(Sb) DH samples grown on GaAs substrates with different orientations - (100) and (311)B. Carrier lifetimes were also measured from as-grown and annealed bismide QW structures consisting of GaAsBi(P) wells and GaAsP barriers. Lastly, TEM cross sections were prepared from both dilute-nitride and bismide samples for defect and composition analysis using a high-resolution TEM.

9358-18, Session 5

Stacked GaAs(Sb)(N)-capped InAs/GaAs quantum dots for enhanced solar cell efficiency

Antonio D. Utrilla, Jose María M. Ulloa, Žarko Gacevic, Univ. Politécnica de Madrid (Spain); Daniel F. Reyes, David González, Teresa Ben, Univ. de Cádiz (Spain); Alvaro Guzmán, Adrian Hierro, Univ. Politécnica de Madrid (Spain)

Different approaches have arisen aiming to exceed the Shockley-Queisser efficiency limit. Particularly, stacking QD layers allows exploiting their unique properties for intermediate-band solar cells (IBSCs) or tandem cells in which the tunability of QD properties through the capping layer (CL) could be very useful.

The beneficial impact of GaAsSb CLs on InAs/GaAs QDs has recently been reported to improve IBSCs characteristics. On the other hand, using GaAsN compensates the accumulated strain allowing the stacking of a larger number of QD layers. Therefore, using a GaAsSbN CL could, in principle, take advantage of both approaches, as well as from the independent control of the QD-CL conduction and valence band offsets, which would allow designs that facilitate carrier extraction.

We have studied the impact of using GaAs(Sb)(N) CLs on the photocurrent characteristics of stacked InAs/GaAs-QDs embedded in the intrinsic region of a p-i-n junction. A comparative analysis among samples using GaAsSbN and both ternary counterparts has been carried out. Moreover, since GaAsSbN growth conditions are found to be critical, different growth approaches are analyzed as well as the effect of using a thin spacer in order to electronically couple the periodic QD-CL structure.

The impact of using a type-II band alignment will be also discussed, as well as the effect of rapid thermal annealing, which seems to depend on the CL material.

Finally, the samples are structurally characterized by transmission electron microscopy, as well as by X-ray diffraction measurements, and critical parameters like the overall strain are correlated with their optoelectronic properties.

9358-19, Session 5

Characterization of regrown interfaces in a nipi solar cell

Michael A. Slocum, David V. Forbes, Seth M. Hubbard, Rochester Institute of Technology (United States)

The nipi solar cell utilizes epitaxial regrowth contacts to ensure carrier selective contacts to the alternating n and p-type doped layers, forming selectively ohmic and rectifying contacts. Significant development work has been completed in recent years to improve experimental results reaching a record efficiency of 9.14% under one sun AMO conditions with no anti-reflection coating. However, defects or traps formed in the rectifying contact during the epitaxial regrowth process result in injected current that contributes directly to dark current. As a result detailed characterization of the epitaxial regrowth interface is required to understand and minimize the formation of interface traps. Electron beam induced current (EBIC) measurements have been taken on diodes formed by epitaxial regrowth to characterize the impact the epitaxial regrowth process on diffusion length. Further characterization has been completed by using a scanning electron microscope technique used to visualize dislocations and stacking faults in the regrown layer. As a result an increased understanding has been gained of the impact of processing and regrowth conditions on the regrowth crystal quality. Additionally concentration measurements have been completed to characterize the trap states impact on efficiency as higher concentration results in state filling and a recovery in open circuit voltage.

9358-20, Session 6

Investigation on carrier collection in InAs quantum dots solar cell

Yushuai Dai, Stephen J. Polly, Staffan Hellström, Rochester Institute of Technology (United States); Paul J. Roland, The Univ. of Toledo (United States); David V. Forbes, Rochester Institute of Technology (United States); Randy J. Ellingson, The Univ. of Toledo (United States); Seth M. Hubbard, Rochester Institute of Technology (United States)

InAs quantum dot (QD) has been attractive in high conversion efficiency solar cell applications, due to its extended absorption to infrared spectrum and as a promising material for the intermediate band solar cell (IBSC). To realize the concept of IBSC, it is essential to enhance sequential absorption process, which competes with thermal escape and tunneling process at room temperature. However, suppressing thermal and tunneling rate of carrier inside QDs is usually associated with increasing carrier traps and recombination probability during carrier transportation. Conversion efficiency of a quantum dot solar cell (QDSC) is determined by photo-excited carrier collection from the absorption of both bulk material and embedded QDs, which depends on solar cell design and operating conditions (temperature, light intensity, etc). In this study, three InAs/GaAs QDSCs with increasing QD local electric field value of 5 kV/cm, 15 kV/cm and 50 kV/cm were measured via time-resolved photoluminescence at 15K. Using laser excitation wavelength of 800 nm, the lifetime the ground state of QD is 2.1 ± 0.1 ns, 1.3 ± 0.1 ns, and 1.4 ± 0.1 ns, respectively. Temperature and electric field dependent carrier lifetime of the QDSCs will be discussed. Two laser excitation wavelengths (above GaAs band and resonant to transition of bounded level of QD) will be used to detect carrier capture process. Relevant external quantum efficiency will be showed to characterize carrier collection from both bulk material and QDs. Finally, based on carrier dynamics in QDSCs, simulation results will help to optimize solar cell design under different operating conditions.

9358-21, Session 6

Optoelectronic characterization of polycrystalline solar cells using time-resolved biased luminescence techniques

Gilbert El Hajje, Daniel Ory, Myriam Paire, Jean-François Guillemoles, Laurent Lombez, Electricité de France (France) and Institut de Recherche et Développement sur l'Energie Photovoltaïque (France)

This study aims to provide an innovative insight on polycrystalline solar cells characterization. Accurate and complete information on the material's performance is achieved by probing micrometric fluctuations of its charge carriers' transport properties which might influence the global device's performance[1][2].

Under different excitation wavelengths, maps of time-resolved photoluminescence emission allowed a micrometric resolution of the minority carriers' lifetime.

Results on microcrystalline Cu(In,Ga)Se₂ solar cells absorbers[3] exhibited an initial fast decay followed by a slower one. Short decay lifetimes varying between 0.4 ns and 1.8 ns, were found to be linked to recombination centers, whereas longer decay lifetimes fluctuating between 3ns and 8ns, were associated with the presence of shallow emission traps.

Unambiguous treatment of the lifetime results[4], allowed accurate calculations of the surface recombination velocity and access to bulk properties.

Combination of the lifetime maps, with micrometric maps of the external quantum efficiency led to the evaluation of the spatial fluctuations of carrier diffusion length[5] and mobility.

So far, these results characterized the solar cell operation at open-circuit voltage.

In order to expand this study to any solar cell operating point, the authors developed a new theoretical understanding on time-resolved luminescence (TRL) emission combined with voltage-bias (V_{bias}) application: A promising solar cell characterization technique on which few comprehensive theories appear to exist.

The theoretical work matches with the experimental data, and provides evidence and a quantification of the influence of V_{bias} on two key quantities: TRL intensity and the minority carriers' lifetime within the solar cell's bulk and surface.

[1] U. Rau and J. H. Werner, "Radiative efficiency limits of solar cells with lateral band-gap fluctuations," Applied Physics Letters, vol. 84, p. 3735, Apr. 2004.

[2] J. H. Werner, J. Mattheis, and U. Rau, "Efficiency limitations of polycrystalline thin film solar cells: case of Cu(In,Ga)Se₂," Thin Solid Films, vol. 480481, pp. 399-409, June 2005.

[3] R. K. Ahrenkiel, B. M. Keyes, D. L. Levi, K. Emery, T. L. Chu, and S. S. Chu, "Spatial uniformity of minority carrier lifetime in polycrystalline CdTe solar cells", Applied Physics Letters 64, 2879 (1994)

[4] M. Paire, et al.. Appl. Phys. Lett. 98, 264102 (2011)

[5] L. Lombez et al., Thin Solid Films (2014), and J. Appl. Phys (2014) in press

9358-22, Session 6

Numerical modeling of radiation effects in triple-junction solar cell

Alexandre I. Fedoseyev, CFD Research Corp. (United States); Seth M. Hubbard, Rochester Institute of Technology (United States); Ashok Raman, CFD Research Corp. (United States); David V. Forbes, Rochester Institute of Technology (United States); Alexandre Freundlich, Univ. of Houston (United States)

Physics based approach that limits the use of DLTS experiments for trap data is proposed for simulation of space radiation effects in triple-junction solar cells. This approach has been implemented in a CFDRC 3D TCAD simulator, NanoTCAD and tested on a model of a triple-junction photovoltaic cell, that has calibrated the various physical parameters to match experimental data (dark and light JV). The model and simulation results are validated by experimentally measured characteristics of the original and irradiated PV cell. The proposed model demonstrated a good match of simulations with experiments.

9358-23, Session 6

Transient lateral photovoltaic effect in patterned ferromagnetic metal-oxide-semiconductor films

Farkhad G. Aliev, Isidoro Martinez, Juanpedro Cascales, Univ. Autónoma de Madrid (Spain)

The time dependent transient lateral photovoltaic effect (T-LPE) has been studied with microsecond time resolution and with chopping frequencies in the kHz range, in lithographically patterned 21 nm thick, 5, 10 and 20 micron wide and 1500 micron long Co lines grown over naturally passivated p-type Si (100). We have observed a nearly linear dependence of the LPE transient response with the laser spot position. An unusual T-LPE dynamic response with a sign change in the laser-off stage has also been corroborated by numerical simulations. A qualitative explanation suggests a modification of the drift-diffusion model by including the influence of a local inductance. In addition, influence of anisotropic magnetoresistance of the Co line structure

**Conference 9358: Physics, Simulation, and Photonic
Engineering of Photovoltaic Devices IV**

on dynamic response on T-LPE has been investigated. Specifically, we have experimentally investigated influence of the angle between external magnetic field and drift direction of the photogenerated carriers on T-LPE. We have observed notable dependence of both T-LPE and on the magnetic field, compatible with anisotropic magnetoresistance value. These findings indicate that the microstructuring of the ferromagnetic line based position sensitive detectors (PSD) could improve their space-time resolution and add capability of magnetic field fine tuning of the PSD characteristics.

9358-24, Session 7

Impacts of contacts and interdot coupling on the photovoltaic performance of quantum dot arrays

Aude Berbezier, Urs Aeberhard, Forschungszentrum Jülich GmbH (Germany)

In various concepts for next generation solar cells, nanostructures provide the specific physical properties required to reach beyond current efficiency limitations. Among these nanostructures, quantum dots may be especially useful due to their easily tunable optoelectronic characteristics, and quantum dot based solar cells are thus promising candidates for the implementation of novel concepts aiming to increase photovoltaic solar energy conversion efficiency.

However, the physical mechanisms of carrier generation and recombination coupled to quantum transport at the nanoscale cannot be described consistently using standard semiclassical theories [1]. One needs to resort to advanced quantum kinetic theories such as the nonequilibrium Green's function (NEGF) formalism, which is ideally suited for the study of open quantum systems under arbitrary nonequilibrium conditions [2].

Using an effective mesoscopic model based on NEGF [3], we investigate the influence of system size and configuration, especially the strength of interdot coupling and dot-contact hybridization, on the radiative rates and consequently on the ultimate performance of photovoltaic devices with selectively contacted quantum dot arrays as the active medium.

We examine the photovoltaic performance in terms of the spectral response and the radiative dark current due to carrier injection under applied bias voltage. Photogeneration and radiative recombination processes are described via corresponding self-energies for the electron-photon interaction, including both stimulated and spontaneous terms. This provides a description of optical transitions based on the same electronic structure as used for the transport simulation. Our results enable a comprehensive assessment of the impact of structural design parameters on the photovoltaic performance.

[1] U. Aeberhard, IEEE J. Sel. Topics in Quantum Electron. 19, 4000411 (2013).

[2] U. Aeberhard, J. Comput. Electron. 10, 394 (2011), 10.1007/s10825-011-0375-6.

[3] U. Aeberhard, Opt. Comput. Electron. 4, 133 (2012).

9358-47, Session 7

Radiative dark current in optically-thin III-V photovoltaic devices

Roger E. Welsler, Magnolia Optical Technologies, Inc. (United States); Rao Tatavarti, MicroLink Devices, Inc. (United States)

High-voltage GaAs and InGaAs quantum well devices have been demonstrated in a thin-film format, utilizing structures that employ advanced band gap engineering to suppress non-radiative recombination and expose the limiting radiative component of the diode current. The dark diode characteristics of these high-voltage III-V photovoltaic devices are compared to the radiative dark current calculated from a generalized detailed balance model specifically adapted for optically-thin absorber

structures. The potential impact of light trapping (and other mechanisms such as hot carrier effects) as a means to suppress radiative recombination will also be explored.

Thin (30 nm) GaAs well devices fabricated via epitaxial lift-off have achieved one-sun open circuit voltages in excess of 1.12 V, while multiple InGaAs quantum well structures with an open circuit voltage of 1.05 V have been demonstrated. The underlying dark diode characteristics have been assessed by measured the short circuit current and open circuit voltage at varying light intensities. Detailed balance calculations employing the measured external quantum efficiency from these devices suggest that radiative recombination is indeed limiting the underlying diode dark current. While increasing the optical path length can be an effective means of reducing radiative recombination in thicker absorber structures, calculations suggest that light trapping has a only minimal impact on the radiative dark current in optically-thin absorbers, and that other mechanisms should be explored for suppressing radiative recombination in nano-enhanced absorber structures.

9358-26, Session 8

Improved photovoltaic performance of hybrid organic/silicon-nanowire heterojunction solar cells via interface engineering

Yi-Chun Lai, Yu-Fan Chang, Peichen Yu, Hsin-Fei Meng, Gou-Chung Chi, National Chiao Tung Univ. (Taiwan)

According to many reports, the interface treatment plays a significant role in device characteristics due to the interface defect density. If interface treated well, we can suppress the recombination of carriers which is the problem we need to be solved. Herein, we introduce the widely used organic materials for hole blocking layers (HBL) which is also used for electron transport layers on organic light emitting diodes. BCP, Alq₃, PBD and OXD-7 have been used as an effective electron-injection and hole-blocking layer at cathode interface in organic devices. First, hole-blocking materials suppress the saturation current via a lower home energy level which can block holes transport and decrease the recombination of minority carriers. Second, hole-blocking materials also increased the built-in potential. The highest power conversion efficiency reaches a 12.86 %, which is largely ascribed to the modified the transport of interface and suppressed saturation current that boost the open-circuit voltage and fill factor.

Due to the high cost of vacuum evaporation process, we use the blade-coating process to coat the HBL materials on the rear surface of silicon. The blade-coating process is controllable, rapid and low-cost. By using the coating speed and concentration of organic material we can easily control the thickness of HBL. The thickness of HBL which we use blade-coating process is ultra-thin, less than 2 nm and uniform.

The best hybrid heterojunction solar cell demonstrates a PCE of 12.8% which major enhancement results from an improved Voc from 0.52 to 0.55 V, and a FF from 61.8 to 72.52. From the analysis of dark current density-voltage, we can find the saturation current decreased which lead the open-circuit voltage increased. And from the analysis of capacitance-voltage we can find the built-in potential increase via the insertion of organic material. For the simulation, we simulated the electrical characteristics depends on different defect density of state. And we found that in the absence of interface defects, a projected efficiency of 14 % is obtained. The interface carrier recombination plays an important role to influence the photovoltaic performance of hybrid organic/silicon-nanowire heterojunction solar cells.

In conclusion, surface treatment of hybrid heterojunction solar cell via an intermediate HBL is demonstrated, which achieves power conversion efficiency of 12.86%. HBL materials suppress the recombination of minority carriers and increase the built-in potential. This low-cost, simple, low temperature fabrication and solution process for hybrid heterojunction solar cells is promising for photovoltaics. These learnings point toward future directions for versatile interface engineering techniques for the attainment of highly efficient hybrid photovoltaics.

9358-27, Session 8

Optimization of the fabricated silicon nanowires for energy-harvesting applications

Sara H. Abel Razek Mohamed, Nageh K. Allam, Mohamed A. Swillam, The American Univ. in Cairo (Egypt)

The vertically aligned Silicon nanowires are fabricated with optimized dimensions for energy applications. These nanowires are single crystalline with nanoscale diameter and micro scale length. These nanowires are fabricated in arrays for ultra wide band of absorption over all the visible domain. Unlike bulk silicon, the experimental measurements of these nanowires demonstrate maximum light absorption over ultra wide range of incident angles. Hence, these nanowires are considered as excellent candidate for cheap energy harvesting without antireflection coatings.

Our experimental measurements have been also verified through electromagnetic simulations using finite difference time domain simulations. The I-V characteristics of solar cell using these Nanowires are also presented and discussed.

9358-28, Session 8

Simulation of exciton diffusion in carbon nanotube-based photovoltaics

Amirhossein Davoody, Irena Knezevic, Univ. of Wisconsin-Madison (United States)

Semiconducting carbon nanotubes (s-CNTs) are versatile materials with strong optical absorptivity, tunable near-infrared bandgaps, ultrafast exciton and charge transport, and excellent chemical stability, which are all desirable properties for the light absorbing material in photovoltaics. However, one major remaining issue that limits the efficiency of CNT-based photovoltaics is the process of excitonic energy transfer in the CNT-based light absorbing layer. Here, we show a Monte Carlo simulation of exciton diffusion process in a composite film of s-CNTs.

We use the tight-binding single-particle wavefunctions as a basis to solve the Bethe-Salpeter equation and calculate the excitonic energies and wavefunctions. The intratube exciton transport is wavelike, with phonons and other impurities acting as scattering sources. The intertube excitonic energy transfer happens via a hopping mechanism, which originates in the Coulomb coupling between electrons on the two s-CNTs. We use the Su-Schrieffer-Heeger model Hamiltonian to calculate the exciton-phonon interaction and study the intratube exciton diffusion coefficient in different types of s-CNTs. Our study shows that inelastic phonon scattering processes are important in the exciton transfer process between CNTs of different chirality. We study the dependence of the intertube exciton diffusion coefficient on the chirality and relative orientation of s-CNTs. Moreover, the effect of surrounding impurities on the exciton localization and intertube exciton transfer process is discussed.

9358-29, Session 8

High-efficiency photoelectrochemical water splitting using InGaN/GaN nanowires grown directly on Si

Bandar M. Alotaibi, Shizhao Fan, Zetian Mi, McGill Univ. (Canada)

The application of photoelectrochemical (PEC) cells for direct conversion of solar energy to hydrogen is one of the viable approaches to overcome future fuel shortage. Critical to this technology development is the exploitation of semiconductor electrodes that can lead to high efficiency and stability. In this context, we have investigated the use of InGaN/GaN nanowire arrays

as the photoelectrodes in a PEC cell, which can exhibit stable hydrogen production. The absorbed photon conversion efficiency can reach as high as ~ 80% in the ultraviolet and visible wavelength range.

Catalyst-free InGaN/GaN nanowire arrays were grown directly on Si substrate by plasma-assisted molecular beam epitaxy. The nanowires are vertically aligned to the substrate with a high degree of size uniformity. With the use of double-band InGaN/GaN core/shell nanowire photoanode in acidic solution, the current densities were measured to be ~ 23 mA/cm² and ~ 11 mA/cm² under an anodic bias (1 V vs. Ag/AgCl) using AM1.5 G and 375 nm long-pass filters for a 300 W xenon lamp, respectively. The maximum incident photon-to-current efficiency (IPCE) is 27.6% at 350 nm where both GaN and InGaN were activated. At 380 nm where only InGaN is excited, the IPCE value is 15.7%. We have further investigated the use of InGaN nanowires as photocathode, which can exhibit IPCE of ~ 65% and ~ 45% at wavelengths of 350 nm and 408 nm, respectively.

The development of InGaN nanowire photoanode and photocathode with further improved efficiency is being investigated and will be reported.

9358-42, Session PWed

Hybrid multi-junction silicon solar cell simulation

Robert LaFleur, Ronald A. Coutu Jr., Air Force Institute of Technology (United States)

Photon absorption is a primary cause of limited solar cell performance. A proposed solution is investigated in this paper through modeling and simulation of a hybrid multi-junction silicon (HMJ-Si) solar cell. HMJ-Si cells, which are stacked silicon solar cells with an insulating air gap between them, are designed with front and rear metal grating geometries that exploit interference patterns for enhanced light management. Interference patterns were investigated in MATLAB® by using the Rayleigh-Sommerfeld formula to model 31 distinct wavelengths from 800-1100nm. Also incorporated in the model were plane wave tilts from -0.005 to 0.005 radians to account for the maximum angle of light subtended by the sun. The exploration of various grating geometries showed that contact widths of 400µm spaced 900µm apart provided an optimal destructive interference pattern while maintaining a 69.2% throughput. This contact grating was selected for finite-difference time-domain (FDTD) analysis using Lumerical® FDTD Solutions. The resulting far-field projection verified that the destructive interference pattern reaches the bottom cell with negligible fringing effects. Further analysis of the data lead to a nominal bottom cell front contact width of 200µm spaced 1100µm apart.

9358-43, Session PWed

The durability of the dye-sensitized solar cell with silicon resin

Hyun Chul Ki, Seon Hoon Kim, Doo-Gun Kim, Tae Un Kim, Haengyun Jung, Korea Photonics Technology Institute (Korea, Republic of); Jae-Man Yoon, TKHT Co., LTD (Korea, Republic of)

Dye-Sensitized solar cell (DSSC) is expected to be one of the next-generation photovoltaics because of its environment-friendly and low-cost properties. However, commercialization of DSSC is difficult because of the electrolyte leakage. We propose a new Ultraviolet (UV) and Thermal curable base on silicon resin. The resin aimed at sealing of DSSC and gives a promising resolution for sealing of practical DSSC. Furthermore, the optimized resin was fabricated into solar cells, which exhibited best durability by retaining 80% of the initial photoelectric conversion efficiency after 1,000 hours tracking test at 80°

9358-44, Session PWed

Density-controlled ZnO/TiO₂ nanocomposite photoanode for improving dye-sensitized solar cells performance

Jimmy Yao, Chih-Min Lin, Shizhuo Yin, The Pennsylvania State Univ. (United States)

Dye-sensitized solar cell (DSSC) via ZnO/TiO₂ nanocomposite photoanode with density-controlled ability is presented in this paper. This nanocomposite photoanode is composed of TiO₂ nanoparticles dispersed into the density-controlled vertically aligned ZnO-TiO₂ core-shell nanorod arrays. The density-controlled ZnO-TiO₂ core-shell nanorod arrays were synthesized directly on fluorine-doped tin oxide (FTO) substrates by using an innovative two-step wet chemical route. First, the density-controlled ZnO nanorod arrays were formed by applying ZnO hydrothermal process from the TiO₂ seed layer. Secondly, the ZnO-TiO₂ core-shell nanorod arrays were formed by deposited a TiO₂ shell layer from sol-gel process. The major advantages of density-controlled ZnO/TiO₂ nanocomposite photoanode include (1) providing a better diffusion path from ZnO nanorod arrays and (2) reducing the recombination loss by introducing an energy barrier layer TiO₂ conformal shell coating. To validate the advantages of density-controlled ZnO/TiO₂ nanocomposite photoanode, DSSCs based on ZnO/TiO₂ nanocomposite photoanode were fabricated, in which N719 dye was used. The average dimensions of the ZnO nanorod arrays were 20 μm and 650 nm for the length and the diameter, respectively, while the designate spacing between each nanorod is around 5 μm. The performance of solar cell was tested by using a standard AM 1.5 solar simulator from Newport Corporation. The experimental result confirmed that an open-circuit voltage, 0.93 V, was achieved, which was much higher than the conventional thin film structure for the same thickness. Thus, density-controlled ZnO/TiO₂ nanocomposite photoanode could indeed improve the performance of DSSC by offering a better electron diffusion path.

9358-45, Session PWed

Continuous and time-resolved photoluminescence as a probing tool for the growth of Cu(In,Ga)Se₂

Matthieu Moret, Yoann Robin, Bernard Gil, Olivier Briot, Univ. Montpellier 2 (France)

Copper Indium Gallium diSelenide (Cu(In,Ga)Se₂, CIGS) is a promising material for cost efficient solar cells. efficiencies above 20% have already been demonstrated in laboratory, and large area CIGS solar panels are already on the market.

However it is still an interesting issue to find efficient characterization techniques that can be used to validate the quality of the different layers at any step of the process, without having to process a complete cell and measure its electrical properties. In this work, we have deposited CIS and CIGS onto Mo coated soda lime glass by co-evaporation, using the so-called three step deposition process. The process parameters were varied to obtain different stoichiometries and different crystalline qualities.

Then, photoluminescence (PL) and time resolved photoluminescence (TRPL) measurements were made on the samples, to determine both the spectral and time dependence of the luminescence. The samples were then processed by depositing CdS buffer layer and ZnO transparent electrode in order to make solar cells, and the cells electrical properties were measured. We correlated the optical data with the cell properties, such as the open circuit voltage (Voc). A clear correlation is obtained, demonstrating that PL and TRPL can be used as a tool for optimizing the deposition parameters. This opens an interesting perspective for in-line characterization of CIGS during solar cell processing.

9358-46, Session PWed

Laser-assisted manufacturing of micro-optical volume elements for improving the amount of light absorbed by solar cells in photovoltaic modules

Gerhard Peharz, Ladislav Kuna, Claude Leiner, JOANNEUM RESEARCH Forschungsgesellschaft mbH (Austria)

The predominant type of solar cells used today are made of crystalline Silicon which have screen printed electrodes. In particular the illuminated sides of the cells are covered with a pattern comprising of 100 μm metal-grid lines with a spacing of about 2 mm. Consequently about 5% of the solar cell (156x156 mm²) area is covered with grid lines which accordingly reduces the amount of light absorbed.

Volume optics consisting of diffractive micro-structures is fabricated in the solar cell encapsulation by the use of a femtosecond laser micromachining. The optical properties of a standard encapsulation material (Ethylene-vinyl acetate (EVA)) used for photovoltaic modules are changed by means of the interaction between focused laser beam and material. Test samples comprising of a sandwich structure of glass - metal grid - EVA - glass are manufactured in order to test the optical performance of volume optics. In particular the optical transmission of test samples is measured with and without volume optics within the EVA. First results clearly show that the optical shadowing of metal grid lines can be decreased by applying a new approach. Moreover the impact of the incidence angle of light is investigated experimentally. It is found that up to an incidence angle of 20° the volume optical elements enable an increase in optical transmission. In addition the optical performance is investigated by applying coupled wave-optical and ray-tracing simulations, which show, that the optical shadowing of solar cell grid lines can be reduced by up to 40% when optimizing the diffractive volume optics.

9358-30, Session 9

Extreme broadband photocurrent spectroscopy on InAs quantum dot solar cells

Ryo Tamaki, Yasushi Shoji, Shunya Naitoh, Yoshitaka Okada, Kenjiro Miyano, The Univ. of Tokyo (Japan)

In intermediate band solar cell (IBSC), the gain in photocurrent can be achieved via two-step photon absorption while preserving the output voltage as of the host material. Quantum dot solar cell (QDSC) is a promising candidate to realize IBSC because zero-dimensional quantized states are suitable for efficient intersubband transitions and quasi-Fermi level separation between the IB and conduction band (CB). Recently, lots of theoretical and experimental studies have been performed to evaluate and understand the two-step photon absorption processes. Here, we have investigated the IB to CB transition by applying extreme broadband photocurrent spectroscopy extended to mid-infrared (IR) region. InAs QDSCs are fabricated by molecular beam epitaxy (MBE) on n-GaAs(001) substrates. Multi-stacked self-assembled InAs QD arrays are embedded in the i-region of p-i-n host single junction solar cells. In Si-doped InAs QDSCs, displacement photocurrent is observed at the short-circuit condition at low temperature by illuminating only with the sub-bandgap IR photons, which cannot excite interband transitions hence cannot create photo-carriers in QDs. The mid-IR photo-response is obtained only in Si-doped QDs but not without doping. Furthermore, the obtained mid-IR spectra are similar to photocurrent enhancement spectra of the IB to CB transition on two-step photon absorption. Therefore, we ascribe the mid-IR photocurrent to the intersubband transition of thermal equilibrium carriers in QDs.

9358-31, Session 9

Characterization of a novel AlAsSb/InAlAs heterojunction emitter design for InAs/AlAsSb quantum-dot intermediate-band solar cell

Zachary S. Bittner, Staffan Hellström, Rochester Institute of Technology (United States); Ramesh Babu Laghumavarapu, Diana L. Huffaker, Univ. of California, Los Angeles (United States); Seth M. Hubbard, Rochester Institute of Technology (United States)

The intermediate band solar cell is a novel approach for breaking the Shockley Queisser single junction efficiency limit using a single electrical junction by introducing an intermediate band of states between valence and conduction bands of a host material in order to efficiently capture a larger portion of the solar spectrum. Epitaxial quantum dots are one potential way of establishing an intermediate band in a host material. In previous work, InAs quantum dots (QD) were grown in an AlAs_{0.56}Sb_{0.44}/GaAs matrix in the unintentionally doped (uid) region of an In_{0.52}Al_{0.48}As solar cell, establishing a variety of optical transitions both into and out of the QDs in order to demonstrate sequential absorption, where one photon is absorbed, promoting an electron from the valence band into the QD, and a second photon is absorbed in order to promote the trapped electron from a QD state into the host conduction band. Photoreflectance provided evidence of both interband optical transitions into the QD and an intraband transition from QD to AlAs_{0.56}Sb_{0.44} conduction band and broadband infrared (IR) biased spectral responsivity provided evidence of sequential absorption, however the 15 nm AlAs_{0.56}Sb_{0.44} barrier impeded carrier transport through the InAlAs solar cell, limiting short circuit current density to 1.76 mA/cm² and heavily degraded open circuit voltage and fill factor. For this study, a new sample set was grown with an AlAs_{0.56}Sb_{0.44} emitter in order to remove the injection barrier present in previous samples. A comprehensive study of electrical and optical characteristics of the new devices will be presented.

9358-32, Session 9

Suppression of thermal carrier escape and enhanced two-step photon absorption in quantum-dot intermediate-band solar cells with a high-potential barrier

Shigeo Asahi, Haruyuki Teranishi, Naofumi Kasamatsu, Tomoyuki Kada, Toshiyuki Kaizu, Takashi Kita, Kobe Univ. (Japan)

We investigated the effects of an increase in the barrier height on the enhancement of the efficiency of two-step photo-excitation in quantum dot intermediate-band solar cells (QD-IBSCs). We fabricated solar cell (SC) devices incorporating a dot-in-well (DWELL) structure of InAs/GaAs sandwiched by Al_{0.3}Ga_{0.7}As, and conventional InAs/GaAs QD-IBSCs as a reference. We measured temperature dependence of integrated photoluminescence (PL) intensity for these SC devices. The thermal activation energies obtained from the Arrhenius plots of the integrated PL intensities are 390 meV for reference QD-IBSC and 630 meV for DWELL-IBSC, respectively. This substantial increase of the activation energy revealed that a high potential barrier of Al_{0.3}Ga_{0.7}As was formed in DWELL-IBSC. The external quantum efficiency (EQE) of QD-IBSC shows apparent signals in the sub-bandgap region, which arises from thermal carrier escape from the intermediate levels. Conversely, the EQE for DWELL-IBSC was dramatically eliminated in the energy region smaller than the bandgap of the barrier. This result indicates that the high potential barrier of Al_{0.3}Ga_{0.7}As effectively suppressed thermal electron escape. Next, we examined increase of EQE-signal for DWELL-IBSC using a two-color photo-excitation system; DWELL-IBSC was additionally illuminated by a continuous

wave infrared (IR) laser light with a wavelength of 1300 nm which enables to excite electrons in the intermediate levels toward the conduction band. When exciting electrons in the intermediate levels by the IR light, the two-step photon absorption has been obviously occurred in the DWELL-IBSC at room temperature. This demonstrates a gain of photo-carrier generation in IBSC with the high potential barrier.

9358-33, Session 9

Investigation of carrier collection and open-circuit voltage of multi-quantum well solar cells by luminescence

Amaury Delamarre, Hiromasa Fujii, Kentaroh Watanabe, The Univ. of Tokyo (Japan); Laurent Lombez, Institut de Recherche et Développement sur l'Energie Photovoltaïque (France); Jean-François Guillemoles, The Univ. of Tokyo (Japan) and Institut de Recherche et Développement sur l'Energie Photovoltaïque (France); Yoshiaki Nakano, Masakazu Sugiyama, The Univ. of Tokyo (Japan)

Multi-Quantum well solar cells (MQWSC) have been shown to present several advantages, among which are low dark currents and tunable bandgaps. They are especially suited for implementation in multi-junction cells, and are highly promising as 3rd generation photovoltaics technologies (Intermediate Band Solar Cells (IBSC) or Hot Carrier Solar Cells (HCSC)).

Such applications require high concentration ratio, which arises the issue of collection efficiency. Whereas it is usually considered that collection in MQW is very close to unity at one sun, it has been shown to not be the case under high concentration at the maximum power point. We propose in this work to take advantage of the luminescence spectral variation to investigate the depth collection efficiency.

In order to validate the model, a series of strain compensated InGaAs/GaAsP MQW solar cells with intentional variation of the MQW doping concentration are grown. This has the effect of switching the space charge region position and width as well as the electric field intensity. Recording the luminescence spectra at various illumination intensities and applied voltages, we show that the in-depth carrier concentration profile and thus collection efficiencies can be probed. Standard electrical measurements (EQE, IV curve in the dark and under illumination) are shown to be consistent with these results.

Regarding their use as HCSC or IBSC, the luminescence of MQW solar cells has been mainly used so far for investigating the quasi-Fermi level splitting and the temperature. Our results improve our understanding by adding information on carrier transport. This enable us to clarify the relationship between open-circuit voltage and quasi-Fermi level splitting.

9358-34, Session 10

Hot carriers at elevated temperatures in InAs/AlAsSb quantum wells: an interesting system for practical hot-carrier solar cells (Invited Paper)

Jinfeng Tang, Vincent R. Whiteside, Hamidreza Esmailpour, Sangeetha Vijayaragunathan, Michael B. Santos, Ian R. Sellers, The Univ. of Oklahoma (United States)

Hot carrier solar cells, in which high-energy photogenerated carriers are extracted prior to thermalization, have long been predicted as a route to increasing the efficiency of single-gap solar cells. Recently, there have been a number of interesting experimental demonstrations of hot-carrier effects in several low-dimensional systems. Here we present experimental evidence of robust hot-carrier effects in InAs/AlAsSb quantum wells. This system has several important potential advantages (amongst others) for

**Conference 9358: Physics, Simulation, and Photonic
Engineering of Photovoltaic Devices IV**

use in practical hot-carrier solar cells: 1. The ground-state transition can be tuned to an optimum position (for hot carrier applications) within the solar spectrum, 2. The strong decoupling of the quantum well from the continuum facilitates the absorption of multiple energies across the solar spectrum in the InAs, promoting hot-carrier absorption directly in the quantum well, and 3. The valence band offset in this system can be controlled such that degeneracy is achieved. This increases the spatial diffusion, and therefore, the mobility of holes. Data will be presented that show that these properties result in increased hot-carrier populations at elevated temperatures; which is attributed to inhibited electron relaxation, and therefore a longer radiative recombination lifetime due to the spatial diffusion of holes at increasing temperature.

9358-35, Session 10

A metallic hot carrier photovoltaic cell

James A. R. Dimmock, Sharp Labs. of Europe Ltd. (United Kingdom) and Imperial College London (United Kingdom); Matthias Kauer, Sharp Labs. of Europe Ltd. (United Kingdom); Paul Stavrinou, Nicholas J. Ekins-Daukes, Imperial College London (United Kingdom)

Hot carrier solar cells offer a method to overcome the fundamental loss mechanism of carrier thermalisation, inherent in current photovoltaic devices, however current incarnations of hot carrier solar cells suffer from disadvantages such as low absorption of incident light and the inability to use light of the full solar spectrum.

In order to overcome these losses we have investigated a metallic version of the hot carrier solar cell, with absorption in a thin metallic layer, followed by extraction into a semiconductor. Thin metallic layers, with optimized dielectric coatings, are shown to have high absorption over a broad range of wavelengths, giving rise to a high absorbed energy density in the metallic layers. This absorbed energy acts to heat the electron distribution in the metal, from which electrons can be extracted. We will contrast this device with the Internal Photoemission (IPE) cell, which extracts non-thermal electrons, and show that high device efficiencies are possible with the Metallic Hot Carrier cell.

We have designed and fabricated devices using this concept in a prototype metal/GaAs architecture, exploring optimum structural and fabrication conditions, characterizing the devices under laser illumination, with laser wavelengths both above and below the GaAs energy gap. Current-voltage characteristics of these cells will be presented, demonstrating absorption of light in a thin metal film followed by extraction of carriers.

9358-36, Session 10

Below band edge light recovery with plasmonics

Scott K. Cushing, Jiangtian Li, Alan D. Bristow, Nianqiang Wu, West Virginia Univ. (United States)

The easily tunable absorption and scattering cross section of localized surface plasmon resonance (LSPR) make it ideal for aiding photoconversion. For above band edge light, scattering and light trapping can be used to increase absorption in thin semiconductor films. Below the band edge, plasmonic hot electrons can transfer to the semiconductor directly or resonant energy transfer can non-radiatively induce charge separation. In this presentation we explore the mechanisms and efficiency of below bandgap energy recovery with plasmonics. Metal-semiconductor nanostructures with varying energy alignment, insulating barrier thickness, and spectral overlap are systematically varied to differentiate the two transfer mechanisms. Transient absorption spectroscopy and action spectrum analysis are applied to track plasmonic charge creation and transfer, linking short and long time scale behavior. The efficiency and losses for both mechanisms are revealed, providing guidelines for optimal below bandgap light enhancement.

9358-37, Session 10

Molecular-plasmonics and hot electrons: merging photovoltaics and thermoelectrics

Ahmet A. Yanik, Golam I. Hossain, Univ. of California, Santa Cruz (United States)

Ultrafast hot electron dynamics in plasmonic devices have recently attracted much interest. Novel physical phenomena related to hot electron generation are proposed and observed in photovoltaic applications. However, efficiencies of these devices are extremely low. In this letter, we introduce a bottom-up approach for hot electron dynamics and current generation. Our approach merging photovoltaics and thermoelectrics at a fundamental level enabled us to design a novel nanophotonic-engine enabling efficient creation of photocurrent for solar harvesting applications.

9358-38, Session 11

Rare-earths-doped materials for up-conversion (*Invited Paper*)

Anne-Laure Joudrier, Institut de Recherche et Développement sur l'Energie Photovoltaïque (France); Nicolas Vandamme, Lab. de Photonique et de Nanostructures (France); Laurent Lombez, Institut de Recherche et Développement sur l'Energie Photovoltaïque (France); Stéphane Collin, Lab. de Photonique et de Nanostructures (France); Gérard P. Aka, Ecole Nationale Supérieure de Chimie de Paris (France); Jean-François Guillemoles, Institut de Recherche et Développement sur l'Energie Photovoltaïque (France)

The main limit to the solar cell efficiency is the incompatibility between the incident solar spectrum and the absorption of the cell. To improve the light/electricity conversion, it is necessary to adapt the solar light to the spectral sensitivity of the cell. Three phenomena may be exploited: down-shifting, up- and down- conversion. In this work, we focus only on up-conversion. In the last years, studies were mainly focused on oxides (Y2O3) and fluorides (NaYF4), doped with Er³⁺ and Yb³⁺.

To overcome the limitation of the up-conversion efficiency of these materials, a plasmonic structure using erbium doped yttrium fluoride thin layer was elaborated. The confinement of the incident photon and the resonance tuned at the absorption frequency of the ion allows the increase of the absorption of the Er³⁺. Properties of these samples which exhibit an up-conversion visible with naked eyes were characterized using a confocal microscope. The broadband resonance is independent to light polarization and can be tuned by design specific structure. The measurement of the enhancement factor of structures associated with the plasmonic resonator has been performed. A total average enhancement factor up to x35 was achieved with maximal values close to x100 for some frequencies, as compared to the same layer deposited on a bare glass substrate.

Nevertheless, other materials like sesquioxides, such as Lu2O3 or Sc2O3, doped with rare earths, also present interesting properties for up-conversion. Up-conversion results obtained with different sesquioxides will be presented and compared with the "usual" materials.

9358-39, Session 11

Radiative cooling for solar cells

Linxiao Zhu, Aaswath P. Raman, Ken X. Wang, Marc A. Anoma, Shanhui Fan, Stanford Univ. (United States)

Standard solar cells heat up under sunlight. The increased temperature of a solar cell due to this heating has adverse consequences on both its

efficiency and its long-term reliability.

In this work, we exploit new developments in the use of nanophotonic structures to control thermal radiation, to propose a radiative cooling scheme that can drastically reduce the operating temperature of a solar cell under sunlight. The Earth's atmosphere has a transparency window between 8-13 microns, which coincides with peak wavelengths of thermal emission from terrestrial bodies. Solar cells typically have little thermal radiation. Exploiting the Earth's transparency window, we propose photonic structures to be placed on the front surface of the solar cell. Such photonic structures allow full sunlight transmission, but have very strong thermal remission in the transparency window. By combining electromagnetic and thermal simulations, we show that such photonic structures can result in very significant cooling of solar cells under direct sunlight by radiating its heat to outer space. For an example case of a bare crystalline silicon solar cell, we show that a photonic structure consisting of microscale silica pyramids can passively lower its operating temperature by 17.6 K, approaching the cooling performance of an ideal scheme for radiative cooling of solar cells. We also show that the benefit of radiative cooling persists even in the presence of significant convection and conduction, and in the presence of parasitic solar absorption in the cooling layer, provided that we design the cooling layer to be sufficiently thin.

9358-40, Session 11

Thermally-enhanced photoluminescence for efficient photovoltaics

Assaf Manor, Leopoldo L. Martin, Carmel Rotschild, Technion-Israel Institute of Technology (Israel)

The Shockley-Queisser (SQ) efficiency limit for single-junction solar-cells is caused, to a great extent, by the inherent heat dissipation accompanying the quantum process of electro-chemical potential generation. Concepts such as solar thermo-photovoltaics (STPV) and thermo-photonics aim to harness this dissipated heat, yet exceeding the SQ limit has not been achieved due to high operating temperatures. Here, we experimentally study endothermic photoluminescence (PL), which has mainly been studied in the framework of optical refrigeration. In optical cooling, a narrow-line pump at the absorption tail of a PL material leads to endothermic PL at shorter wavelengths, thereby extracting heat. The same mechanism may be utilized at high temperatures for photonic heat-pumping, that is, the generation of high-energy photons in rates that are orders of magnitude higher than thermal emission, at similar temperatures. However, at low-temperature refrigeration, the thermal population is negligible with respect to the PL excitation, where at high temperatures the endothermic PL and thermal emission compete for dominance. This leads to the inherent abrupt transition of PL to thermal emission, characterized by the vanishing of the PL chemical-potential and the transition from a photon-number conserving emission to non-conserving thermal emission.

Relying on these observations, we propose and theoretically study a highly efficient solar-energy converter, wherein solar radiation is absorbed by a low-bandgap PL material. The dissipated heat is emitted by endothermic PL, and harvested by a higher-bandgap photovoltaic cell. While such device operates at much lower temperatures than STPV, the theoretical efficiencies approach 70%, bringing its realization into reach.

9358-41, Session 11

GaSb thermophotovoltaics: current challenges and solutions

Nassim Rahimi, Virginia Polytechnic Institute and State Univ. (United States); Andrew A. Aragon, Darryl M. Shima, Orlando S. Romero, Thomas J. Rotter, Tito L. Busani, Olga Lavrova, Ganesh Balakrishnan, The Univ. of New Mexico (United States); Luke F. Lester, Virginia Polytechnic Institute and State Univ. (United States)

Thermophotovoltaic (TPV) cells are intended to generate electricity from the thermal sources such as waste heat and combustion. GaSb with a bandgap of 0.72 eV is a material of choice because of its ability to be grown lattice matched with ternary and quaternary materials covering bandgaps from 0.5 to 0.7 eV. To fabricate TPVs, Molecular Beam Epitaxy (MBE) and ion implantation have been chosen to make TPV cells with high yield and low defect density. However, there are challenges related to each fabrication method. MBE-grown GaSb TPVs demonstrate shunt defects that tend to short the device as the area increases. The origin of these defects has been identified using SEM, TEM and EDX. These defects are classified into two categories, one originated from poor quality substrate and the other initiated during MBE growth. This work presents a detailed study of these defects' formation and solutions to suppress them. Ion-implanted GaSb TPVs were fabricated using Be and Te into n-type and p-type GaSb substrates, respectively. Implant damage removal was accomplished by Rapid Thermal Annealing (RTA) process, although GaSb poses unique challenges during RTA due to the high temperature required to recover the crystal lattice and the possibility of Sb evaporation. Different ion doses and energies were tried to minimize the crystal damage and different RTA process recipes were investigated to maximize the crystal structure recovery after implant. The GaSb and GaInAsSb TPV devices fabricated using MBE and ion implantation will be discussed and their electrical and optical characteristics compared.

Conference 9359: Optical Components and Materials XII

Monday - Wednesday 9-11 February 2015

Part of Proceedings of SPIE Vol. 9359 Optical Components and Materials XII

9359-1, Session 1

Two-dimensional semiconductors for ultrafast photonic applications (*Invited Paper*)

Jun Wang, Shanghai Institute of Optics and Fine Mechanics (China)

Owing to the specific two-dimensional (2D) confinement of electron motion and the absence of interlayer perturbation, 2D semiconductors possess unique optoelectronic properties and has become a research hot-spot in recent years. Whereas the electronic and luminescent properties of 2D transition metal dichalcogenide (TMDC) nanosheets, say, MoS₂, MoSe₂, WS₂, etc., have been generating much research interest, the ultrafast nonlinear optical (NLO) properties remain largely unexplored. Realized that the sizable and thickness-dependent bandgap offers TMDCs a huge potential in the development of photonic devices with high performance and unique functions, we studied extensively the ultrafast NLO property of a range of TMDC nanosheets. 2D TMDC nanosheets with high-quality layered nanosheets were prepared using liquid-phase exfoliation technique. Ultrafast saturable absorption, two-photon absorption, ultrafast nonlinear photoluminescence were observed from the 2D nanostructures. The exciting results open up the door to 2D photonic nano-devices, such as optical switches, pulse shaping devices, mode-lockers, optical limiters, etc., capable of ultrafast response and broadband tunability.

9359-2, Session 1

Widely tunable soliton self-frequency shift and dispersive wave generation in a highly nonlinear fiber

Dinghuan Deng, Tonglei Cheng, Xiaojie Xue, Tuan H. Tong, Takenobu Suzuki, Yasutake Ohishi, Toyota Technological Institute (Japan)

Widely wavelength tunable soliton self-frequency shift (SSFS) and dispersive wave were experimentally demonstrated in a highly nonlinear fiber (HNLF). By pumping with a mode-locked sub-100 fs Er-doped fiber laser, SSFS from 1.58 μm to 2.07 μm was achieved in the 1-meter long HNLF with zero dispersion wavelength of 1.535 μm . The maximum output spectrum (full width at half maximum, FWHM) around 2 μm is 143 nm. The Pulse widths of SSFS and dispersive wave were measured by an intensity autocorrelator with different filters. Although the pulse width of SSFS in longer wavelength was measured to be about a few picoseconds, the large FWHM of SSFS spectrum shows that soliton with sub-50 fs pulse width could be achieved if the giant chirp pulse is efficiently re-compressed to be transforms limited. The generated solitons can be used as a seed laser for Tm-doped fiber amplifier to replace the mode-locked Tm-doped fiber laser oscillator near 2 μm , because the ultrashort pulse generation in this wavelength is very difficult for the relatively high dispersion of the silica fibers. Dispersive wave determined by phase matching condition of the soliton and the fiber dispersion was also observed during the soliton self-frequency shift generation. The minimum pulse width of the dispersive wave measured by the intensity autocorrelator was 50 fs.

9359-3, Session 1

Raman gain of SiC as a potential medium for Raman lasers

Larry D. Merkle, Jun Zhang, U.S. Army Research Lab. (United States); Graham S. Allen, Jay W. Dawson, Lawrence Livermore National Lab. (United States); Mark Dubinskii, U.S. Army Research Lab. (United States)

Solid-state Raman lasers exhibit considerable promise for laser power scaling with nearly diffraction-limited output via beam combining. Unlike parametric nonlinear OPO/OPA frequency shifting, Raman shifting may lead to significant heat deposition with power scaling. Therefore, in the search for Raman gain media amenable to significant power scaling materials with high thermal conductivity (e.g., diamond) are of major interest. In that regard, scalable materials like silicon carbide (SiC), with its copper-like thermal conductivity at room temperature, are viewed as potential diamond replacements and, thus, are the most promising candidates. While thermal conductivity of single-crystalline SiC is reasonably well studied, to the best of our knowledge, there is no data on Raman gain coefficient of this material. Therefore, measuring it would be of great practical value.

We have studied the 4H polytype, as it has a larger band gap than some other common polytypes, potentially making it useful at shorter wavelengths. Our polarized spontaneous Raman studies confirm the identity of our sample's polytype as 4H and preclude any significant admixture of other polytypes. The Raman gain of 4H SiC over the range 750-820 cm^{-1} was measured using a pump-probe technique around 1030 nm. For the sample geometry available for this experiment, we find one significant peak, at 777 cm^{-1} having a Raman gain coefficient of 0.46 cm^2/GW and a linewidth of 2 cm^{-1} . Despite this modest gain coefficient, estimates of the material's losses together with simple modeling indicate that Raman lasing should be possible with pulsed pumping at 1064-nm.

9359-4, Session 1

Ultra-long fiber Raman lasers: design considerations

Igor Koltchanov, Dimitar Kroushkov, André Richter, VPIphotonics GmbH (Germany)

In frame of the European Marie Currie project GRIFFON [<http://astonishgriffon.net/>] the usage of a green approach in terms of reduced power consumption and maintenance costs is envisioned for long-span fiber networks. This shall be accomplished by coherent transmission in unrepeated links (100km - 350km) utilizing ultra-long fiber Raman laser (URFL)-based distributed amplification, multi-level modulation formats, and adapted Digital Signal Processing (DSP) algorithms.

The URFL uses a cascaded 2-order pumping scheme where two -1365nm pumps illuminate the fiber. The URFL oscillates at -1450nm whereas amplification is provided by stimulated Raman scattering (SRS) of the 1365nm pumps and the optical feedback - realized by two FBGs at the fiber ends reflecting at 1450nm. The light field at 1450nm provides amplification for signal waves in the 1550nm range due to SRS.

In this work we present URFL design studies intended to characterize and optimize the power and noise characteristics of the fiber links. We use a bidirectional fiber model describing propagation of the signal, pump and noise powers along the fiber length. From the numerical solution we evaluate the on/off Raman gain and its bandwidth, the signal excursion over the fiber length, OSNR spectra, and the accumulated nonlinearities. To achieve best performance for these characteristics the laser design is optimized with respect to the forward/backward pump powers and

wavelengths, input/output signal powers, reflectivity profile of the FBGs and other parameters.

9359-5, Session 2

Design of nanomaterials for advanced energy storage (*Invited Paper*)

Cengiz Sinan Ozkan, Univ. of California, Riverside (United States)

Graphene is a one atom thick two-dimensional material that exhibits exceptional physical and electronic properties, and offers alternatives for applications in energy storage devices, nanoelectronics, spintronics, biosensors, and medicine. I will describe innovative approaches for the synthesis of hierarchical three dimensional graphene hybrid materials which possess characteristics including ultra large surface area, mechanical durability and high conductivity which are appealing to diverse energy storage systems. Rapid charging and discharging supercapacitors are promising alternative energy storage systems for applications such as portable electronics and electric vehicles. Integration of pseudocapacitive metal oxides with structured nanomaterials has received a lot of attention recently due to their superior electrochemical performance. In order to realize high energy density supercapacitors, we developed a scalable method to fabricate graphene/MWNT/RuO₂ nanoparticle hybrid systems. Excellent capacitance retention and high charge-discharge cycles have been demonstrated. Next, I will talk about three-dimensional cone-shape carbon nanotube clusters decorated with amorphous silicon for lithium ion battery anodes. An innovative silicon decorated cone-shape CNT clusters (SCCC) is prepared by depositing amorphous silicon onto CCC via magnetron sputtering. The seamless connection between silicon decorated CNT cones and graphene facilitates the charge transfer in the system and provides a binder-free technique for fabricating lithium ion batteries. Very high reversible capacity and excellent cycling stability has been demonstrated. Such multi-scale engineered materials could have wide range implications to facilitate new technological innovations in energy storage.

9359-6, Session 2

Third harmonic generation and multiphoton fluorescence in graphene using a compact femtosecond 1.56 μm laser

Antti Säynätjoki, Lasse Karvonen, Juha Riikonen, Wonjae Kim, Joonas Mäkinen, Aalto Univ. (Finland); Seyed Soroush Mehravar, Robert A. Norwood, The Univ. of Arizona (United States); Nasser Peyghambarian, The Univ. of Arizona (United States) and Aalto Univ. (Finland); Harri Lipsanen, Aalto Univ. School of Science and Technology (Finland); Khanh Q. Kieu, The Univ. of Arizona (United States)

Graphene has unique electrical and optical properties. Its zero bandgap and linear energy dispersion of electrons give rise to broadband efficient absorption that can be utilized in detectors and saturable absorbers [1,2]. At the same time, these properties provide an intriguing platform for studies of quantum relativistic phenomena [3]. Graphene has also been shown to exhibit a high third-order nonlinearity [4-6]. The deposition of graphene and other 2D materials typically involves a transfer process. This technique can be applied to the hybrid integration of 2D materials with e.g. photonic chips, where the optical nonlinearity can be utilized in all-optical data processing for telecommunications and other applications. Therefore, it is particularly important to study the nonlinear optical properties of graphene at telecommunications wavelengths.

In this work, we perform multiphoton microscopy at 1.56 μm wavelength for the characterization of graphene, employing an erbium doped fiber laser

described in Ref.[7]. We find that multiphoton microscopy is an excellent method for rapid imaging of graphene; the measurement is orders of magnitude faster than Raman mapping, which is the conventional method of identifying graphene.[8] High contrast over the substrate is achieved for graphene on glass as well as for graphene on oxidized silicon. We will discuss the generated light intensity as a function of layer number and laser power, as well as the spectral properties of the signal. We will also discuss the effects of femtosecond laser radiation on graphene.

[1] Sun, Z.; Hasan, T.; Torrisi, F.; Popa, D.; Privitera, G.; Wang, F.; Bonaccorso, F.; Basko, D. M.; Ferrari, A. C., ACS Nano 2010, 4, 803-810.

[2] X. Gan, R.-J. Shiu, Y. Gao, I. Meric, T. F. Heinz, K. Shepard, J. Hone, S. Assefa, D. Englund, Nature Photonics 7, 883-887 (2013)

[3] Ishikawa, K. L., Phys. Rev. B 2010, 82, 201402(R).

[4] N. Kumar, J. Kumar, C. Gerstenkorn, R. Wang, H.-Y. Chiu, A. L. Smirl, and H. Zhao, Phys. Rev. B 87, 121406(R) (2013).

[5] S.-Y. Hong, J. I. Dadap, N. Petrone, P.-C. Yeh, J. Hone, and R. M. Osgood, Jr., Phys. Rev. X 3, 021014 (2013).

[6] C. H. Lui, K. F. Mak, J. Shan, and T. F. Heinz, Phys. Rev. Lett. 105, 127404 (2010).

[7] Kieu, K.; Jones, J.; Peyghambarian, N. IEEE Photonics Technol. Lett. 22, 1521 (2010).

[8] A. Säynätjoki, L. Karvonen, J. Riikonen, W. Kim, S. Mehravar, R. Norwood, N. Peyghambarian, H. Lipsanen, and K. Kieu, ACS Nano, 7, 8441 (2013).

9359-7, Session 2

Amorphous chalcogenide layers and nanocomposites for direct surface patterning

Sandor Molnar, Roland Bohdan, Istvan Csarnovics, The Univ. of Debrecen (Hungary); Julia E. Burunkova, National Research Univ. of Information Technologies, Mechanics and Optics (Russian Federation); Sandor J. Kokenyesi, The Univ. of Debrecen (Hungary)

Homogeneous, 200 - 3000 nm thick layers of chalcogenide glasses as well as nanocomposite structures, containing gold nanoparticles have been produced and used for in situ surface relief fabrication by optical (CV and femtosecond laser) or e-beam, ion-beam recording. Investigations were focused on the formation of giant (height modulation from nanometers up to micrometers) geometrical reliefs and elements (dots and microlenses, lines and diffractive elements) applicable in the 0.5 - 10 micrometer spectral range. The recording is based on the irradiation-stimulated mass-transport, without any additional processing. Comparison was made with optical recording due to the stimulated mass-transport in polymer nanocomposites. The selection of the materials from As(Ge)-S(Se) systems with optimum recording parameters was done. Essential changes in the character of the process and enhancement of the optical recording was observed in the layers with gold nanoparticles. The mechanisms of the under laying photo-physical and mass-transport processes, are connected with excitation of non-equilibrium electron-hole pairs in these amorphous semiconductors, generation of defects, charge and mass transport in the gradients of optical, electrical and stress fields. The role of the photo-thermal effects was analyzed due to the possible influence on the efficiency of relief formation or erasing. These materials can be used in micro-nanolithography for fabrication of prototype holographic diffractive gratings, lens matrixes, couplers to waveguides and may be combined in integrated optical sensors.

9359-8, Session 2

Spectral analysis based on compressive sensing in nanophotonic structures

Zhu Wang, Zongfu Yu, Univ. of Wisconsin-Madison (United States)

**Conference 9359:
 Optical Components and Materials XII**

A method of spectral sensing based on compressive sensing is shown to have the potential to achieve high resolution in a compact device size. The random bases used in compressive sensing are created by the optical response of a set of different nano-photonics structures, such as photonic crystal slabs. The complex interferences in these nanostructures offer diverse spectral features suitable for compressive sensing, as it can create diverse spectral features with both broad and narrow line shapes. Also, the enormous degrees of freedom in choosing the spatial parameters of the nanostructures allow us to create virtually unlimited number of different response functions.

Simulation shows that using the interference patterns generated by 400 different photonic crystal slabs by varying hole radius and lattice constants as random bases, a wide range of signal types represented by N=1001 unknowns in the spectral range from 1450nm to 1550nm can be recovered, such as two close sharp spikes, a Lorentz signal with a 30nm bandwidth and a sharp peak, a combination of 5 Lorentzian lines or 5 Gaussian lines. Also, the resolution can be achieved as high as 0.1nm, and noise tolerance is 40dB.

As these proposed nanostructures can be readily integrated on a chip with little requirement for optical alignment, it can be potentially implemented in a very compact dimension to be used in low-cost applications.

9359-9, Session 2

Optical properties of MgF2 nano-composite films dispersed with noble metal nanoparticles synthesized by sol-gel method

Moriaki Wakaki, Nobuaki Soujima, Takehisa Shibuya, Tokai Univ. (Japan)

Porous MgF2 films synthesized by a sol-gel method exhibit the lowest refractive index among the dielectric optical materials and are the most useful materials for the anti-reflection coatings. On the other hand, surface plasmon resonance (SPR) absorptions of noble metal nanoparticles in various solid matrices have been extensively studied. New functional materials like a SERS (Surface Enhanced Raman Spectroscopy) tips are expected by synthesizing composite materials between porous MgF2 film featured by the network of MgF2 nanoparticles and noble metal nanoparticles introduced within the network. Fundamental physical properties including morphology and optical properties are characterized for these materials to make clear the potential of the composite system.

In this study, composite materials of MgF2 films dispersed with noble metal nanoparticles were prepared using the sol-gel technique with various annealing temperatures and densities of noble metal nanoparticles. The structural morphology was analyzed by an X-ray diffractometer (XRD) and a scanning electron microscope (SEM). The size and shape distributions of the metal nanoparticles were observed using a transmission electron microscope (TEM). The optical properties of fabricated composite films were characterized by UV-Vis-NIR and FT-IR spectrophotometers. The absorption spectra due to the surface plasmon resonance (SPR) of the metal nanoparticles were analyzed using the dielectric function considering an effective medium approximation, typically Maxwell-Garnett model. The Raman scattering spectra were also studied to check the enhancement effect of MgF2 vibration modes by the surface enhanced Raman spectrum (SERS) at the interface between MgF2 and Ag or Au nanoparticles embedded in the film.

9359-10, Session 3

Apodized reflective volume Bragg grating for high-resolution spectroscopy

Sergiy Mokhov, Daniel Ott, CREOL, The College of Optics and Photonics, Univ. of Central Florida (United States); Vadim Smirnov, OptiGrate Corp. (United States); Ivan B.

Divliansky, Boris Y. Zeldovich, Leonid B. Glebov, CREOL, The College of Optics and Photonics, Univ. of Central Florida (United States)

Uniform volume Bragg gratings (VBGs) are widely used in spectroscopic applications as narrow band optical filters due to low optical losses and wide aperture enabling high power applications. Main quantitative characteristics of such elements are signal-to-noise ratio (SNR), which is determined in this case as a ratio of intensity in maximum of transmission to intensity out of the filter's band (spectral contrast), and spectral range in which it is achieved. The highest SNR for uniform VBGs was demonstrated with sequential reflections from several VBGs resulting. It is known from the coupled wave theory and fiber Bragg grating experiments that apodization of refractive index modulation (RIM) spatial profiles, where RIM is minimized at the ends of a grating, demonstrates higher SNR. In this work we propose a new method of smooth apodization in a spatial profile of RIM that simultaneously provides constant average refractive index along direction of beam propagation. This method is based on sequential recording two VBGs with slightly different resonant Bragg wavelengths and the same modulation amplitudes. As result, a moiré pattern is recorded that actually is a VBG with slow envelope sinusoidal spatial modulation of RIM. A comprehensive model of such complex VBGs is elaborated. An experimental characterization procedure for determination of exact location of zero RIM zones is developed. As result, we were able to fabricate an apodized VBG with a single sinusoidal semi-period profile of RIM. Our experimental measurements of reflection spectra show extremely high SNR and are in good agreement with theoretical predictions.

9359-11, Session 3

Reflection type CMY color filters incorporating a aluminum-coated nanoporous anodic aluminum oxide cavity

Wenjing Yue, Vivek R. Shrestha, Chul-Soon Park, Sang-Shin Lee, Yang Li, Cong Wang, Nam-Young Kim, Eun-Soo Kim, Kwangwoon Univ. (Korea, Republic of)

Structural color filters have been receiving tremendous attention in the recent days due to their applications in various applications like displays, image sensors, security tags etc. One of the popular structure used in realization of color filters is an etalon based on metal-dielectric-metal multilayers, whose resonance wavelength may be tailored by varying the thickness of dielectric cavity. For the general practice of realizing an reflection type etalon filter using a pure metal film, the suppression ratio of achieved reflection spectrum is very low as the level of reflection dip is proved to be extremely sensitive to the thickness of metal layer. It is highly desirable for the reflection type color filters to have less sensitivity to the metal thickness for the practical applications.

In this paper, cyan, magenta and yellow (CMY) reflection type etalon color filters incorporating a aluminum-coated nanoporous anodic aluminum oxide (AAO) template attached to a thick aluminum substrate, was proposed. As the interpore distance of AAO template is fixed to be 100 nm, which is much smaller than the visible light wavelength, the cavity and coated metal film behaves as a homogeneous layer with an effective index. Finally, the reflection dip for proposed CMY filters was centered at 617, 530 and 437 nm when the cavity length of AAO is 250, 310 and 150 nm, respectively. The suppression ratio is ~76%, and with increasing the metal thickness from 10 to 30 nm the ratio for the case of using pure metal layer is dramatically decreased from 0.96 to 0.08, while for the proposed structure it is slowly decreased from 0.89 to 0.63.

9359-12, Session 3

bending strength measurements at different materials used for IR-cut filters in mobile camera devices

Volker Dietrich, Franca Kerz, Peter Hartmann, SCHOTT AG (Germany)

Digital cameras are present everywhere in our daily life. Science, business or private life cannot be imagined without digital images. The quality of an image is often rated by its color rendering. In order to obtain a correct color recognition, a near infrared cut (IRC-) filter must be used to alter the sensitivity of imaging sensor. Increasing requirements related to color balance and larger angle of incidence (AOI) enforced the use of new materials as the e.g. BG6X series which substitutes coated interference filters on D263 thin glass.

Although optical properties are the major design criteria devices have to withstand numerous environmental conditions during use and manufacturing – as e.g. temperature change, humidity, mechanical shock as well as mechanical stress. The new materials show different behavior with respect to all these aspects. They are usually more sensitive against these requirements to a larger or smaller extent. Bending strength is one of the properties which needs to be considered.

Especially for mobile phone camera applications customers ask for reliable strength data. As bending strength of a glass component depends not only upon the material itself but mainly on the surface treatment and test conditions a single number for the strength might be misleading if the conditions of the test and the samples are not described precisely. Therefore Schott started investigations upon the bending strength data of various IRC-filters materials. Different test methods were used to obtain statistical relevant data.

In this presentation the measurement approaches will be described and results will be presented.

9359-13, Session 3

Acousto-Optic Tunable Filter for imaging applications with high performance in the IR region

Stefano Valle, Jon D. Ward, Gooch & Housego plc (United Kingdom); Christopher N. Pannell, Gooch & Housego plc (United States); Nigel P. Johnson, Univ. of Glasgow (United Kingdom)

Acousto-Optic Tunable Filters with large acceptance angles are the components of choice for imaging applications in the visible and NIR region. However large aperture AOTFs in the wavelength range beyond 2 μ m are impractical due to the λ^2 dependency on acoustic field intensity to achieve peak diffraction efficiency.

A potential solution to reduce the RF power requirement for full diffraction efficiency is to realize a resonant acoustic cavity, and “recycle” the phonons. This configuration could provide a potential advantage factor of at least 4. We explain why the tuning characteristics make this concept particularly applicable at long wavelengths.

Because of the presence of standing waves, when the cavity is not in resonance, a feedback signal from the acoustic transducer influences the electrical matching and the power delivered to the device is mostly reflected back (VSWR > 25). Therefore a novel RF driver is required in order to maintain resonance. The resonance is also affected by the temperature of the device, thus a temperature control/compensation mechanism with high accuracy is required.

We present the preliminary results of a prototype AOTF, which are in good agreement with the predicted characteristics. An advantage factor of about four has been measured. A new optimised AOTF and driver have been designed and we present an overview of the anticipated performance.

9359-14, Session 3

Angle insensitive thin-film color filters based on an etalon structure incorporating a top dielectric layer

Chul-Soon Park, Vivek R. Shrestha, Sang-Shin Lee, Eun-Soo Kim, Kwangwoon Univ. (Korea, Republic of); Duk Yong Choi, The Australian National Univ. (Australia)

Recently, there have been increased interests in nano-structural color filters due to their diverse applications in display/imaging devices, organic solar cells, etc. However, the angular sensitivity in structural color filters results in a significant change in color reproduction, prohibiting their practical applications since the center wavelength is shifted and its efficiency is degraded for oblique incidence.

In this work, we have proposed and demonstrated highly angle insensitive thin-film red, green and blue (RGB) color filters based on a Ag-TiO₂-Ag etalon structure combined with a top TiO₂ layer. In order to de-escalate the angle dependence, we not only incorporate a high index material as the cavity but also introduce a top dielectric layer atop the etalon structure. By means of a top dielectric layer, we could achieve enhanced transmission and angle-invariant characteristics. The effect of thickness of a top layer and the states of incident polarization by using the optical admittances at different incident angles were also analyzed. The filters have a transmission as high as 68.5% at the center wavelengths of 635, 545 and 442 nm for RGB colors, respectively. With regard to the angular dependence, the relative center wavelength shift ($\Delta\lambda/\lambda$) and peak transmission variation of the filters were below -0.040 and -6.5% for 70° oblique incidences with p-polarization. Featuring a highly angle insensitive property, it is expected that those filters can be easily utilized as a RGB tri-color pixel for many applications such as image sensors, LCD and OLED devices.

9359-15, Session 4

Linear and nonlinear optical properties of chalcogenide microstructured optical fibers (Invited Paper)

Johann Trolès, Univ. de Rennes 1 (France); Laurent Brilland, PERFOS (France); Celine Caillaud, Univ. de Rennes 1 (France); Gilles Renversez, Univ. of Aix Marseille (France); David Mechin, PERFOS (France); Jean-Luc Adam, Univ. de Rennes 1 (France)

Chalcogenide glasses are known for their large transparency in the mid-infrared and their high linear refractive index (>2). They present also a high non-linear coefficient (n_2), 100 to 1000 times larger than for silica, depending on the composition. We have developed a casting method to prepare the microstructured chalcogenide preform. This method allows optical losses as low as 0.4 dB/m at 1.55 μ m and less than 0.05 dB/m in the mid IR. Our group has prepared various chalcogenide MOFs operating in the IR range in order to associate the high non-linear properties of these glasses and the original MOF properties. For example, small core fibers have been drawn to enhance the non linearities for telecom applications such as signal regeneration and generation of supercontinuum sources. On another hand, in the 3-12 μ m window, single mode fibers and exposed core fibers have been realized for Gaussian beams propagation and sensors applications respectively.

9359-16, Session 4

Design and performance of Multi-Core Fiber (MCF) optimized towards communications and sensing applications

Judith Hankey, Tristram Read, Mark D. Hill, Peter Maton, Fibercore Ltd. (United Kingdom)

Multi-Core Fibers (MCF) are gaining particular interest for applications in communications [1] and sensing [2]. Data transfer through MCF has the potential to break through the limits of current transmission systems by improving the spectral efficiency. Similarly, in space limited environments such as data centers and super-computers, MCF technology offers benefits in terms of miniaturization.

The use of MCF technology has also demonstrated advantages for shape sensing measurements in applications such as structural health monitoring and minimally invasive surgery. Nevertheless, some key parameters still need to be considered when designing the ideal MCF for use in communications and sensing applications.

In this paper, Fibercore will introduce its MCF manufacturing platform that was developed in order to realize fully customisable MCF. The results of the 7-core MCF developed and optimized for shape sensing will be presented.

Such MCF has been produced by using a sonic drill to position the core holes in the cladding glass. Cross-talk between core and bending loss have been minimised by implementing high numerical aperture cores of 0.20. Additionally, the high level of Ge doping also allows Fiber Bragg Gratings (FBGs) to be written into each core without the need for hydrogen loading. Finally, in order to enable distinction between any potential twist and the strain in the fiber from the bend under measurement controlled, a permanent twist has been introduced in the fiber by spinning it whilst it is being drawn.

References:

1. Sakaguchi et al. - <http://dx.doi.org/10.1364/OFC.2011.PDPB6> (2011)
2. Duncan et al. - Proc. SPIE 65301S (2007)

9359-17, Session 4

Opportunities for designing microstructured optical fibers for efficient femtosecond laser grating inscription

Tigran Baghdasaryan, Thomas Geernaert, Hugo Thienpont, Francis Berghmans, Vrije Univ. Brussel (Belgium)

Microstructured optical fibers (MOFs) are a major achievement in the field of optical fiber technology. Owing to their unprecedented design flexibility, MOFs have found numerous applications in various fields of photonics. By adapting the parameters of the holey cladding, MOFs with tailored dispersion properties, large mode area, endlessly single mode operation and high non-linear response can be designed and fabricated.

This paper deals with designing MOFs with a specific microstructure that would allow increasing the efficiency with which fiber gratings can be photo-inscribed in a MOF. The air holes are usually impeding the delivery of optical power to the core region, which results in a lower grating writing efficiency. This problem is exacerbated when using IR femtosecond laser sources for the inscription, as the induced refractive index changes stem from a highly non-linear multi-photon absorption process and are hence very dependent on the optical intensity that actually reaches the MOF core.

In this paper first we study regular hexagonal lattice MOFs to find a range of lattice parameters that would facilitate femtosecond grating inscription, considering the non-linear nature of the index change. To assess the influence of the microstructured cladding on the transverse delivery of light to the core region we introduce a figure of merit to which we refer as 'transverse coupling efficiency' (TCE). We also evaluate the index changes that would be obtained when implementing a special type of holey structure

that acts as a transversely focusing microstructure - known as Mikaelian lens - in the cladding of the MOF.

9359-18, Session 4

The role of highly non-linear index change mechanism during femtosecond grating writing in microstructured optical fibers

Tigran Baghdasaryan, Thomas Geernaert, Hugo Thienpont, Francis Berghmans, Vrije Univ. Brussel (Belgium)

New methods for fiber Bragg grating inscription in optical fibers use femtosecond laser sources, which can induce refractive index changes even in non-photosensitive fibers and which allow achieving gratings that remain stable at high temperatures. The index change takes place as a result of a highly non-linear multi-photon absorption process. Although such gratings were successfully inscribed in conventional fibers, there are still challenges involved when attempting to fabricate femtosecond gratings in microstructured optical fibers (MOFs). The air holes are usually impeding the delivery of optical power to the core region, which results in a lower grating writing efficiency.

In this paper we report on our numerical computations that aim to estimate the influence of the MOF's holey cladding on the induced index change during interferometric grating inscription with an infrared (IR) femtosecond laser source. For high power femtosecond laser pulses at 800 nm the refractive index change in silica stems from a highly non-linear five photon absorption process. Using empirical data on refractive index changes from literature and intensity distribution data from our transverse coupling simulations we propose an approach to reconstruct the non-linear refractive index modification in the MOF core region. We then study the influence of the MOF angular orientation on the induced index change and we model the impact of MOF tapering as a possible way to increase the grating writing efficiency.

9359-19, Session 4

Advances in Chalcogenide glasses and Optical fibers (*Invited Paper*)

Younes Messaddeq, Sandra H. Messaddeq, Univ. Laval (Canada); Mohammed El-Amraoui, Univ. de Laval (Canada); Jean-Philippe Bérubé, Univ. Laval (Canada); Réal Vallée, Univ. de Laval (Canada)

The main issues and greatest challenges for the development of new photonic glasses are related to several aspects, from their synthesis to their shaping and integration into photonic devices. Nowadays, although the Holy Grail of glass science still remains the reduction of the intrinsic losses of infrared glasses to their theoretical limits, two new drivers have arisen in recent years for the exploration and development of new technologies related to glass science: i) the photonic band-gap effect and ii) the production of nanostructured materials. Based on these aspects, we will discuss on the development of chalcogenide glasses and their impact on various fields of application.

Also, we will present the Photoinduced surface relief structures generated in a variety of chalcogenide glasses (like As₂S₃, GeGaAsS and GeS). The macroscopic surface structures can be inscribed by irradiation with a focused beam of femtosecond Ti:sapphire laser (1kHz, 100 fs, 800 nm). By appropriately controlling the irradiation condition of fs-laser two distinct types of fs-LIPSS [so-called low-spatial-frequency LIPSS (LSFL) with period of 180 nm and high-spatial-frequency LIPSS (HSFL)] with period of 720 nm with different spatial orientations were identified. Increasing the energy we increase temperature accumulation and induce the micro-explosion process creating nanovoids with 300 nm of diameter.

However, to date a complete description of the underlying microscopic mechanism has not been produced. Much experimental has been performed

**Conference 9359:
 Optical Components and Materials XII**

to clarify the formation of surface relief, where volumetric internal pressure, interaction among dipoles, anisotropic diffusion, or optical gradient forces was considered as the driving force for deformation.

This phenomenon is potentially useful for technologies such as active optical devices, nanofabrication, and optical actuators.

9359-20, Session 5

Hybrid Reflection Type Metasurface Design for Optical Needle Field Generation

Shiyi Wang, Qiwen Zhan, Univ. of Dayton (United States)

We design a reflection type metal-insulator-metal (MIM) metasurface composed of hybrid optical antennas to create a radially polarized vectorial beam with amplitude and phase modulations and demonstrate its application in optical needle field generation. Behaving as local quarter-wave-plates (QWP), the MIM metasurface is designed to convert circularly polarized incident into local linear polarization, and thus overall radial polarization with corresponding binary phases and desired normalized amplitude ranging from 0.07 to 1. For the MIM structure, a glass spacer layer is sandwiched between an optically thick gold layer and an antenna-based metasurface top layer, which provides the function of finely engineering the reflection vectorial light. To obtain enough degrees of freedom, the optical-antenna-based layer comprises periodic arrangements of double metallic nano-bars with perpendicular placement and single nano-bars respectively for different modulation requirements. Both types of antennas are able to introduce $\pi/2$ retardation while reaching the desired phase and amplitude modulation range. Through carefully adjusting the antennas' geometry and array parameters, the gap-surface plasmon resonances can be shifted to facilitate the manipulation of the properties of the reflected vectorial optical fields. Working at 1064 nm wavelength, the particular vectorial light output can be further tightly focused by a high numerical aperture objective to produce a longitudinally polarized flat-top field along the longitudinal direction, the so-called optical needle field. The proposed example illustrates that metasurface as a new class of compact optical components based on nano-scaled structures is a very attractive candidate in the designing of optical devices with compound functions for vectorial light generation.

9359-21, Session 5

Hot carrier generation in SWIR-active plasmonic TCO-Si heterostructures

Joshua D. Caldwell, Alexander J. Giles, Heungsoo Kim, María González, Sharka M. Prokes, Orest J. Glembocki, Antti J. Makinen, U.S. Naval Research Lab. (United States)

We report the demonstration of a Schottky diode -based architecture, comprising a transparent conductive oxide (TCO) film/ Si junction which by hot carrier generation is suitable for sensor applications in short wave infrared (SWIR). By adjusting the dielectric function and the microstructure of the TCO films, including indium-tin-oxide (ITO), aluminum-zinc-oxide (AZO), we show that it is possible to tune the surface plasmon resonance (SPR) of the TCO films, and consequently, to tune the response of the diode device across the SWIR band (1-3 microns). We will discuss the critical role of controlling the hot carrier generation following SPR excitation in the TCO element and charge extraction across the oxide-silicon contact. For the latter, we will highlight the interface fabrication process, involving the use of hydrogenated amorphous silicon passivation layer in between the TCO film and the Si substrate, leading to the optimized Schottky barrier structure for hot carrier harvesting.

9359-22, Session 5

Various surface plasmon polariton waveguide with gap

Dong Hun Lee, Myung-Hyun Lee, Sungkyunkwan Univ. (Korea, Republic of)

We investigate characteristics of various surface plasmon polariton waveguides with a gap (G-SPP-Ws) to control a guided input surface plasmon polariton (SPP) with interaction of an applied force in the gap at a telecommunication wavelength of 1.55 μm . Mode size and normalized transmission (NT) of the output SPPs, resulted from the propagation losses in the SPP-Ws and the coupling losses in the gaps are characterized in 28 μm -long G-SPP-Ws with the 8 μm -long gap and the 20 nm thickness of metal strips. A metal in insulator-metal-insulator waveguides (IMI-Ws) is designed with gold. A low-loss polymer is used for 30 μm -thick upper and lower cladding layers. The lowest NT of the G-SPP-W is about -0.04 dB. The metal strip structure of the lowest NT G-SPP-W is composed of an input 2 μm -wide and 10 μm -long tapered IMI-W and an output 2 μm -wide and 10 μm -long reverse tapered IMI-W with the 6 μm -wide gap. The excited input SPP propagates, jumps over the gap with the coupling loss of less than 0.04 dB and propagates again with the very low propagation loss of less than 0.00024 dB/ μm . The output SPP characteristics in the G-SPP-W can be properly controlled by controlling the guided SPP with interaction of an applied force in the gap. The G-SPP-W has a possibility of new plasmonic modulation applications.

9359-23, Session 5

Enhanced Solar Absorption in Thin Film Photovoltaic Cells via Embedded Silica-Coated Silver Nanoparticles

Sam Aminfar, The Univ. of Texas at Austin (United States); Richard Harrison, Sandia National Labs. (United States); Adela Ben-Yakar, The Univ. of Texas at Austin (United States)

Thin film photovoltaic solar cells offer significant advantages in flexibility and manufacturing costs over conventional crystalline silicon cells, but at the cost of lower device efficiency. The thinness of these cells inhibits capture and conversion of near-bandgap photons. Plasmonic nanostructures have the potential to dramatically improve the performance of thin film photovoltaics by selectively enhancing the absorption of near-band gap light by scattering photons laterally. However, the use of conventional metal plasmonic particles has only enabled a minimum performance improvement to-date. Here, we consider silver core nanoparticles coated with a thin silica shell (Ag@SiO₂) to overcome two limiting drawbacks of conventional metal plasmonic particles. First, embedding plasmonic nanoparticles in silicon tends to red-shift the plasmonic response beyond silicon's bandgap. A thin silica coating blue-shifts the response of embedded nanoparticles to within silicon's bandgap without the need to reduce the particle's size, thereby maintaining a high scattering-to-absorption ratio. Second, the silica shell insulates the metal particle from charges recombining at its surface. We have created an optical simulation of Ag@SiO₂ nanoparticles embedded in one micron of microcrystalline silicon using extended Mie theory and Fresnel equations. These simulations have shown a potential absorption increase of 27%, resulting in a 36% enhancement in device efficiency. We have also chemically synthesized Ag@SiO₂ nanoparticles of uniform size using seeded-growth citrate reduction and modified Stober processes. Spectrometry of PECVD-deposited silicon thin films embedded with these nanoparticles has demonstrated an absorption enhancement of up to 38% in the 600-1000 nm spectrum.

**Conference 9359:
 Optical Components and Materials XII**

9359-24, Session 5

super focusing using plasmonic lens based on super oscillation effect

Mahmoud El Maklizi, Mostafa Hendawy, Mohamed A. Swillam, The American Univ. in Cairo (Egypt)

A novel plasmonic is proposed for super-focusing. This lens contains two slits surrounded by finite metal corrugations for enhanced focusing. This simple surface has the super-focusing capabilities in both near and far field light in a hot-spot with FWHM much smaller than half the wavelength of the incident light. The structure is suitable for one dimensional and two dimensional focusing applications. The lens is optimized to maximize the super oscillation of the field near the hot spot. The proposed structure lends itself to various applications including subwavelength imaging and nanolithography.

9359-25, Session 6

Latest advance on fused fiber components for power scaling of fiber lasers (Invited Paper)

Baishi Wang, Vytran LLC (United States)

Power scaling of fiber lasers has been realized either coherently or incoherently. Fused fiber component plays a pivotal role in implementation of these laser systems, especially in all-fiber configuration. In this paper, we review latest advance of such fiber components including large fiber count combiners and output coupling devices with an emphasis on the optical fundamentals, fabrication methods using graphite filament based glass processing technology, and how these devices can enable power scaling of laser systems. In addition, we will provide some application examples of laser systems using such fiber components.

9359-26, Session 6

Characterization of multimode polymer optical fiber coupler development using lapping technique and load force

Latifah S. Supian, Univ. Kebangsaan Malaysia (Malaysia) and National Defence Univ. of Malaysia (Malaysia); Mohd Syuhani Ab Rahman, Norhana Arsad, Univ. Kebangsaan Malaysia (Malaysia)

A multimode polymer optical fiber coupler fabricated using geometrical blocks that have matching refractive index material and lapping technique is characterized. The aim is to provide a considerable explanation on the characteristics in splitting ratio, excess loss and insertion loss when different bending radii due to radii of circular blocks is applied to the couplers with the existence of load F. Other factors that contribute to the characterization of the coupler include fiber diameters and forces exerted upon the two fibers that are lapped together forming the coupler developed. The performance of the directional coupler is studied on the dependency of the fibers' coupling lengths and distances between the two fibers' cores which is related to the amount of force exertion. The fibers are initially etched at the middle sections. Both the fibers are then attached to geometrical blocks with certain radii and the middle tapered sections are then brought into closed proximity and they are lapped to each other. The different radii of circular blocks are used to investigate the effect of macro-bending of the fibers which will help the transfer of energy from primary fiber to the secondary fiber. A particular amount of load F is mounted on the other side of the geometrical blocks to provide some force or stress onto the fibers

which leads to certain coupling length between the fibers. The coupler is characterized when the force is given in order to see the behavior of the coupling when different bending radii, coupling length and force are varied. Coupling ratio as high as 60:40 is achieved based on the experiments done.

9359-27, Session 6

High signal-to-noise acoustic sensor using phase shift gratings interrogated by the Pound Drever Hall technique

Peter Kung, QPS Photonics Inc. (Canada); Maria I. Comanici, McGill Univ. (Canada)

Optical fiber is made of glass, an insulator, and thus it is immune to strong electromagnetic interference. Therefore, fiber optics is a technology ideally suitable for sensing of partial discharge (PD) in both transformers and generators. Extensive development efforts have been used to find a cost effective solution for detecting partial discharge, which generates acoustic emission, with signals ranging from 30 kHz to 200 kHz. The requirement is similar to fiber optics Hydro Phone, but requires higher frequencies. There are several keys to success: there must be at least 60 dB signal-to-noise ratio (SNR) performance, which will ensure not only PD detection but later on provide diagnostics and also the ability to locate the origin of the events. Defects that are stationary would gradually degrade the insulation and result in total breakdown. Transformers currently need urgent attention: most of them are oil filled and are at least 30 to 50 years old, close to the end of life. In this context, an issue to be addressed is the safety of the personnel working close to the assets and collateral damage that could be caused by a tank explosion (with fire spilling over the whole facility). This paper will describe the latest achievement in fiber optics PD sensor technology: the use of phase shifted fiber gratings with a very high speed interrogation method that uses the Pound-Drever-Hall technique. More importantly, this is based on a technology that could be automated, easy to install, and, eventually, available at affordable prices.

9359-28, Session 6

Fiber Bragg grating based sensors in conventional double clad large mode area fibers

Alexander Nieborowsky, Benjamin Weigand, Photonik-Zentrum Kaiserslautern e.V. (Germany); Jürgen Bartschke, Xiton Photonics GmbH (Germany); René Beigang, Johannes A. L'huillier, Photonik-Zentrum Kaiserslautern e.V. (Germany)

Fiber Bragg Gratings (FBGs) in photosensitized single mode fibers became one of the most commonly used devices in optical sensing. Applied tensile strain as well as temperature changes result in a shift of the reflected Bragg wavelength. In practice it is difficult to distinguish between the two effects solely by interpretation of the reflected wavelength shift. Hence it is desirable to produce FBGs being more sensitive to only one of the quantities to be measured. We report on the fabrication of sensors based on FBGs in conventional large mode area (LMA) fibers. Strain coefficients of LMA fibers are one order of magnitude smaller than the coefficients of their single mode counterparts. This leads to a lower sensitivity to tensile forces while retaining the sensitivity to temperature changes. By using a commercial quintupled Nd:YVO4 laser (IMPRESS 213, Xiton Photonics GmbH), emitting at a wavelength of 213 nm, it is possible to write FBGs in conventional double clad LMA fibers with up to 50 µm core diameter. Time consuming hydrogen loading, as well as expensive doping of the LMA fiber are redundant and standard passive LMA fibers can be used. The produced FBGs are characterized with respect to their Bragg wavelength shift by applying temperature changes as well as tensile strain. Fibers with different diameters are investigated and operating ranges of strain sensors identified.

**Conference 9359:
 Optical Components and Materials XII**

The ease of coupling with light sources into fibers with large diameter as well as their comparatively elevated robustness makes them promising sensor solutions for harsh environments.

9359-30, Session 7

Advances in laser development based on fully-crystalline double-clad fibers (*Invited Paper*)

Mark Dubinskii, U.S. Army Research Lab. (United States)

Fully crystalline channel waveguide lasers are very promising as efficient and compact sources for many laser applications requiring significant power scaling with nearly diffraction-limited beam quality. In a double-clad implementation they are direct analogs of conventional (glass-based) laser fibers with the same ability to provide tight confinement of high NA pump light along the entire length of the gain medium while maintaining propagation of only fundamental laser mode in the low NA doped core. Compared to conventional fibers, fully crystalline double-clad fibers (FCDCFs) are best suitable for laser power scaling due to their ~10 times higher thermal conductivity as well as an order of magnitude higher absorption and emission cross sections of common rare-earth dopants. In addition, doped YAG cores have an extremely low SBS gain coefficient versus that of silica glass. Due to all these beneficial features, FCDCF lasers (FCDCFLs) can be scaled to tens of kilowatts of power out of single aperture even in the most demanding, ultra-narrowband, single longitudinal mode laser designs. This overview presents our research efforts toward FCDCFLs in comparison with other existing efforts. We report our results based on recent experiments with resonantly-pumped Er-doped and Yb-doped cores, including single-mode, Er:YAG channel waveguide laser with diffraction limited output and nearly quantum defect limited efficiency. We also show that crystalline-core fibers with glass cladding, though they presents a major technological simplification, are a major deviation from the FCDCF concept and do not possess the thermal efficiency required for multi-kW power scaling out of single aperture.

9359-31, Session 7

UV-visible absorption and luminescence properties of Yb:CALGO laser crystal

Anael Jaffres, Suchinder K. Sharma, Pascal Loiseau, IRCP Chimie Paristech (France); Bruno Viana, Ecole Nationale Supérieure de Chimie de Paris (France); Jean Louis Doualan, Ctr. de Recherche sur les Ions, les Matériaux et la Photonique (France); Richard Moncorge, Ctr. de Recherche sur les Ions, les Matériaux et la Photonique, Univ. de Caen (France)

Yb:CALGO is now recognized to exhibit outstanding properties for the production of high-power and ultra-short laser pulses. Very recently this crystal has also been integrated in a thin-disk geometry. These experiments clearly demonstrate the interest of Yb:CALGO in classical bulk or thin-disk configurations for high power laser systems. UV-visible absorption bands can be also observed in Yb³⁺-doped oxide materials due to O₂-Yb³⁺ ligand-to-metal charge transfer (LMCT) transitions. These electric dipole allowed transitions are very intense with cross sections of about two orders of magnitude larger than the near infrared ones. Because of the existence of these bands, it was shown that optically pumped Yb-doped materials experienced changes of ionic polarizabilities responsible for pseudo-nonlinear changes of refractive indices, and that these refractive index variations could be used advantageously for laser clean-up and self-organization of high power laser systems. Most of these LMCT absorption bands have been registered only via excited-state absorption (ESA) experiments, and their position determined by shifting the obtained ESA bands by the energy of the pumped Yb³⁺ emitting state, i.e. around 10200

cm⁻¹ which is about the energy of the Yb³⁺ zero-line transition in most of most of the Yb-doped materials. The ESA band are observed in Yb:CALGO and LMCT absorption band in Yb:CALGO extends between about 200 and 280 nm. From the position and the intensity of these bands, it is then possible to calculate optical parameters of the CaGaAlO₄ material.

9359-32, Session 7

Investigation of Yb-Tm energy transfer constant in highly-doped tellurite glasses

Stefano Taccheo, Swansea Univ. (United Kingdom); Daniel Milanese, Politecnico di Torino (Italy); Hrvoje Gebavi, Swansea Univ. (United Kingdom) and Institut Ruder Bošković (Croatia)

We will present investigation on the energy transfer rate between Yb and Tm ions in highly-doped tellurite glasses.

We prepared an extensive set of Tm-doped, Yb-doped and Yb-Tm-doped tellurite glasses samples and we will present our results on a precise determination of the energy transfer constant between Tm and Yb. In addition we will review the full set of parameters (lifetimes and cross relaxations) needed for properly modelling the system

9359-33, Session 7

Down- and up-conversion emissions in Er-doped transparent fluorotellurite glass-ceramics (*Invited Paper*)

Adrian Miguel, Univ. del País Vasco (Spain); Roberta Morea, Jose A. Gonzalo, Consejo Superior de Investigaciones Científicas (Spain); Joaquín Fernández, Univ. del País Vasco (Spain) and Ctr. de Fisica de Materiales (Spain); Rolindes Balda, Univ. del País Vasco (Spain) and Ctr. de Fisica de Materiales (Sudan)

In this work, we report the near infrared and upconversion emissions of Er³⁺-doped transparent fluorotellurite glass-ceramics obtained by heat treatment of the precursor Er-doped TeO₂-ZnO-ZnF₂ glass. The comparison between the fluorescence properties of Er-doped glass and glass-ceramics confirms the presence of Er³⁺ ions in a crystalline environment in the glass-ceramic samples. The 4I_{13/2}->4I_{15/2} transition in the glass-ceramic samples presents a more resolved and narrower emission band, whereas the 4I_{13/2} decay which is single exponential in the glass sample can be described by two single exponential functions in the glass-ceramic samples. This suggests that a fraction of Er³⁺ ions are forming nanocrystals while the rest remain in a glass environment. Upconversion emission due to (2H_{11/2,4S_{3/2}})->4I_{15/2} and 4F_{9/2}->4I_{15/2} transitions has been observed under excitation at 801 nm in the glass and glass-ceramic samples. However, for glass-ceramics, new emission bands due to electronic transitions from 2H_{9/2} and 4F_{3/2,5/2} levels to the ground state are observed. Moreover, the intensity of the 4F_{9/2}->4I_{15/2} transition is strongly dependent on the heat treatment. The temporal evolution of the red emission together with the excitation upconversion spectra suggest that energy transfer processes are responsible for the enhancement of the red emission. Structural analysis showed that the nanocrystals nucleated in the glass-ceramic samples are homogeneously distributed in the glass matrix with a typical size of about 45 nm, and contain Er and F but not Te or Zn.

9359-34, Session 7

Modelling of photodarkening in Yb-doped fibre lasers

Stefano Taccheo, Swansea Univ. (United Kingdom)

In this paper we present a complete rate-equation system able to model highly-doped Yb-fiber lasers for cw lasers. All effects of Photodarkening are included in the rate equation system: dependence on doping level, concentration, as well as impact on lifetime. Data from a series of lasers with different doping concentrations and inversion level have been used to validate the model.

The model suggest that Yb-doped laser with doping level in excess of 0.1 %wt can be affected by PD. The model shows the effect of PD on laser threshold and slope efficiency.

9359-35, Session 8

Rare-earth-ion-doped waveguide lasers on a silicon chip (*Invited Paper*)

Markus Pollnau, KTH Royal Institute of Technology (Sweden)

Rare-earth-ion-doped materials are of high interest as amplifiers and lasers in integrated optics. Their longer excited-state lifetimes and the weaker refractive-index change accompanied with rare-earth-ion excitation compared to electron-hole pairs in III-V semiconductors provide spatially and temporally stable optical gain, allowing for high-speed amplification and narrow-linewidth lasers. Amorphous Al₂O₃ deposited onto thermally oxidized silicon wafers offers the advantage of integration with silicon photonics and electronics. Layer deposition by RF reactive co-sputtering and micro-structuring by chlorine-based reactive-ion etching provide low-loss channel waveguides. With erbium doping, we improved the gain to 2 dB/cm at 1533 nm and a gain bandwidth of 80 nm. The gain is limited by migration-accelerated energy-transfer upconversion and a fast quenching process. Since stimulated emission is even faster than this quenching process, lasers are only affected in terms of their threshold, allowing us to demonstrate diode-pumped micro-ring, distributed-feedback (DFB), and distributed-Bragg-reflector (DBR) lasers in Al₂O₃:Er³⁺ and Al₂O₃:Yb³⁺ on a silicon chip. Surface-relief Bragg gratings were patterned by laser-interference lithography. Monolithic DFB and DBR cavities with Q-factors of 1.35×10^6 were realized. In an Er-doped DFB laser, single-longitudinal-mode operation at 1545 nm was achieved with a linewidth of 1.7 kHz, corresponding to a laser Q-factor of 1.14×10^{11} . Yb-doped DFB and DBR lasers were demonstrated at 1020 nm with output powers of 55 mW and a slope efficiency of 67% versus launched pump power. A dual-phase-shift, dual-wavelength laser was achieved and a stable microwave signal at -15 GHz was created via the heterodyne photo-detection of the two laser wavelengths.

9359-36, Session 8

Optical and magnetic studies of InGaN nanorods doped with ytterbium

Wojciech M. Jadwisieniczak, Jingzhou Wang, Ohio Univ. (United States); Kiran Dasari, Univ. of Puerto Rico (United States); Venkata R. Thota, Ohio Univ. (United States); Ratnakar Palai, Univ. of Puerto Rico (United States); Eric A. Stinaff, Ohio Univ. (United States)

Nanorods of in situ ytterbium (Yb) doped (~5%) InGaN have been grown on (0001) sapphire substrates without any buffer layer by plasma assisted molecular beam epitaxy (MBE). We report on the structural (XRD, SEM, HRTEM), optical (PL, PL kinetics and PLE), and magnetic (SQUID) properties

of undoped InGaN and InGaN:Yb epitaxial nanorods. The structural and microstructural studies reveal the nanorods are of c-axis orientation with high crystalline nature. PL studies shows the dominance of single excitonic peak for InGaN and InGaN:Yb samples in green to orange-red spectral range dependent on the In content and material homogeneity which can be effectively tuned by Yb-doping. The PL excitonic peaks of InGaN:Yb nanorods show red shift, narrowing of line width, and weakly temperature dependence compared to InGaN films with the same In content. The PL temperature dependent and PL kinetics studies suggest that the exciton localization energy, due to In content fluctuation, in undoped InGaN is smaller than in Yb-doped InGaN:Yb nanorods. We believe that the observed changes could be related to the rare earth (Yb) gettering effect. The PLE studies investigated in 400 - 800 nm spectral range confirm that Yb³⁺ ions are optically active and can be excited via resonant excitation or electron-hole pair generation/recombination processes. Our results demonstrate an alternative way to solve the long standing issue of developing high quality InGaN materials with high In content. Furthermore, magnetic hysteresis loop measurements demonstrate the existence of ferromagnetism in InGaN:Yb nanorods. The temperature variation of magnetization reveals the non-zero magnetization at 300 K. Collected structural, optical and magnetic results will be analyzed in the frame of formation and presence of rare earth structural isovalent (RESI) traps model. Finally, the prospect of using rare earth dopants for improving p-type conductivity in InGaN material will be discussed.

9359-37, Session 8

Comparison of photodarkening in 1030 nm and 1070 nm Yb-doped fibre lasers

Riccardo Piccoli, Swansea Univ. (United Kingdom) and Univ. of Pavia (Italy); Hrvoje Gebavi, Swansea Univ. (United Kingdom) and Institut Ruder Bošković (Croatia); Maurizio Ferrari, Istituto di Fotonica e Nanotecnologie (Italy); Stefano Taccheo, Swansea Univ. (United Kingdom)

In this paper we present an extensive investigation of photodarkening in Yb-doped fibre lasers. Several lasers with different inversion and fibre doping levels have been fabricated and tested, lasing both 1030 nm and 1070 nm. Comparison on impact of Photodarkening in the two type of lasers will be presented.

The investigation shows that impact of Photodarkening is related to the emission and absorption cross section and lasers that can compensate an extra loss by minimal change of inversion level will suffer less degradation due to Photodarkening. The work also confirm that losses in fibre lasers in the 1 micron - 1.1 micron wavelength interval are of the order of 1/20 of the loss value at 633 nm

9359-38, Session 8

Upconversion against direct emission in Er³⁺-Tm³⁺-codoped tellurite-glass containing gold nanoparticles

Victor A. Garcia Rivera, Otávio de Brito Silva, Univ. de São Paulo (Brazil); Mohammed El-Amraoui, Yannick Ledemi, Ctr. d'Optique, Photonique et Laser (Canada); Younes Messaddeq, Univ. Laval (Canada); Euclides Marega Jr., Univ. de São Paulo (Brazil)

Gold nanoparticle embedded in Er³⁺-Tm³⁺-codoped tellurite glass are able produce two effects on the emission properties these glasses: (i) quenching on direct emission under excitation by a 405 nm laser diode, or (ii) enhancement on upconversion emission under excitation by a 976 nm laser diode in these glasses. Both effects were investigated from the luminescence decay dynamics of Er³⁺-Tm³⁺ ions. Glasses of 74TeO₂-5ZnO-15Na₂O-5GeO₂-1Er₂O₃:0.5Tm₂O₃ (mol%) nominal composition and

**Conference 9359:
 Optical Components and Materials XII**

containing 0.25 mol% of Au added in the form of chloride (AuCl_3) were prepared by the traditional melt-casting technique. The formation of gold nanoparticle was subsequently produced by heat treatment at 300 °C. The localized surface plasmon resonance (LSPR) band of gold nanoparticles at around 580 nm resulted in the quenching/enhancement of Er^{3+} - Tm^{3+} emission for the Er^{3+} ($4S_{3/2} \rightarrow 4I_{15/2}$) transition (green colour, 542 nm) under excitation 405/976 nm. The lifetime of the $4S_{3/2}$ was monitored at 542 nm (away from LSPR), where was verified an energy transfer processes or local field enhancement to quenching or enhancement, respectively, in the intensity emission Er^{3+} - Tm^{3+} ions. A tendency of the lifetime to decrease gradually with heat treatment holding time was observed. The results are interpreted in terms of (i) an ion-to-nanoparticle excitation energy transfer operating via LSPR in the gold nanoparticle to quenching luminescence, and (ii) local field enhancement operating via LSPR nanoparticle-to-ion. Besides, a complete description of photon-plasmon interactions of noble metal nanoparticles with the Er^{3+} and Tm^{3+} ions is provided. These hybrid materials can be utilized for various photonic and optoelectronic applications, here as infrared to visible light converters or emitting green light.

9359-39, Session 8

The REPUSIL process and the capability of fluorine doping for the adjustment of optical and thermochemical properties in silica materials

Kay Schuster, Stephan Grimm, André Kalide, Frank Fröhlich, Jan Dellith, Anka Schwuchow, Matthias Jäger, Hartmut Bartelt, Institut für Photonische Technologien e.V. (Germany)

The demand on tailored silica materials for fiber optic applications regarding the optical as well as thermochemical properties has been increased during the past years. In particular this takes place in connection with the requirements on the fibers for high power fiber lasers.

Here we report on the advancement of the powder based process (REPUSIL) for high performance silica materials concerning the Fluorine doping/codoping. As with Aluminum/Ytterbium doped silica the Fluorine incorporation in the REPUSIL process allows the fabrication of doped bulk materials/preforms for the fiber processing.

The recently achieved maximum Fluorine concentration of 1.5 mol% SiF_4 corresponds to a refractive index decrease of -7.5×10^{-3} . Simultaneously, the T_g of the doped material is reduced by about 200 K compared to pure silica. Both, the refractive index decrease and the reduction of the glass transition temperature are outstanding tools for the fine tuning of fiber properties of passive transport fibers, as these fibers have to be adjusted to highly doped (mainly Al/Yb or Al/Tm) active systems.

Moreover, the fluorine doping is also eminently suitable for the direct refractive index adjustment in active doped silica glass materials (e.g. Al/Yb or Al/Tm). The index matching with pure silica is possible to date up to 3 mol% Al_2O_3 and 0.1 mol% Yb_2O_3 . The Fluorine codoping of Al/Yb silica glass also allows the reduction of parasitic formation of Yb^{2+} . The additional influence on the blue shift of the UV transmission will also be discussed.

9359-41, Session 9

Polarization-independent light-dispersing device based on diffractive optics

Jun Amako, Toyo Univ. (Japan); Eiichi Fujii, Seiko Epson Corp. (Japan)

We report a light-dispersing device consisting of two transmission gratings and a waveplate, bearing in mind the spectroscopic applications of this device. The gratings separate two orthogonal polarization components

of light incident at the Bragg angle. The waveplate, which is sandwiched between the gratings, functions as a polarization converter for oblique light incidence. If these optical parts are suitably integrated, the resulting device efficiently diffracts unpolarized light with high spectral resolution. For a proof of concept, we chose a wavelength range between 630 and 730 nm and designed a device using coupled-wave theories and Mueller matrix analysis. Surface-relief gratings with a 400-nm period were formed on fused silica substrates using laser interference lithography and a waveplate that functions at 58-degree incidence was fabricated by combining two crystalline quartz phase retarders. They were assembled within a tolerance of alignment errors. Irradiating a 633-nm laser on the device, ~80% of the incident power was coupled to the first-order diffraction, regardless of the polarization. Using white light, the transmittance was measured to be less than 5% for TE and TM polarizations. The spectral range for the device, which provides a minimum diffraction efficiency of 80%, was estimated at 89 nm, ranging from 638 to 727 nm. From the characterization of this optical device, we validated the proposed polarization-independent, light-dispersing scheme. The novelty of our scheme is use of two gratings, rather than a single one. This frees us from the dilemma of choosing either a large dispersion power or low polarization dependence.

9359-42, Session 9

Optical performance of random anti-reflection structures on curved surfaces

Courtney D. Taylor, Menelaos K. Poutous, Kevin J. Major, Rajendra Joshi, The Univ. of North Carolina at Charlotte (United States); Lynda E. Busse, Jesse A. Frantz, Jasbinger S. Sanghera, U.S. Naval Research Lab. (United States); Ishwar D. Aggarwal, The Univ. of North Carolina at Charlotte (United States)

Random anti-reflection structured surfaces (rARSS) have been reported to improve transmittance of optical-grade fused silica planar substrates to values greater than 99%. These textures are achieved using reactive-ion etching techniques and often result in transmitted spectra with no measurable interference effects (fringes) for a wide range of wavelengths. The inductively-coupled reactive ion plasma (ICP-RIE) used in the fabrication process to etch the rARSS is anisotropic, and thus well-suited for planar components. The improvement in spectral transmission has been found to be independent of optical incidence angles, for values from 0° to ±30°. Qualifying and quantifying the rARSS performance on curved substrates, such as concave and convex lenses, is required to optimize the fabrication of a desirable AR effect on optical-power elements. In this work, rARSS was fabricated on fused silica plano-convex and plano-concave lenses, using an optimized ICP-RIE process, to maximize optical transmission in the range from 500 nm to 1100 nm. Results are presented from optical transmission tests of matched sets of varying curvature lenses with rARSS at a wavelength of 633nm. The transmission was measured as a function of radial distance from the apex of each lens, and shows the anisotropic dependence of the etch process. The transmittance profiles between the different sphericity of the tested lenses as well as the matched sets of concave and convex surfaces are compared. The measured angle-of-incidence dependence of planar silica versus silica lenses with rARSS is also presented.

9359-43, Session 9

ALD-tuned nanobeam cavity on titanium dioxide platform operating in the visible

Arijit Bera, Markus Häyrinen, Matthieu Roussey, Markku Kuittinen, Seppo K. Honkanen, Univ. of Eastern Finland (Finland)

Photonic crystal nanobeam cavity has emerged as an alternative to the 2D photonic crystal cavity, owing to its higher Q-factor, smaller mode volume

**Conference 9359:
Optical Components and Materials XII**

and smaller device footprint. It is possible to achieve strong light-matter interaction and strong coupling with quantum emitters in the cavity region, leading to potential applications in nonlinear optics, on-chip bio-sensing, cavity-QED etc. Since most of the solid state active emitters operate in the visible and because of the water absorption peak in the near-IR, it is important to find a platform operating in the visible. Owing to its broadband transparency, high Kerr coefficient and negligible two-photon absorption, TiO₂ shows the promise in these aspects. Here, we have realized a nanobeam cavity on TiO₂ platform operating in the visible. We have adopted an ALD-assisted fabrication methodology, where a 300 nm-thin film of amorphous TiO₂ is deposited on an oxidized silicon substrate by ALD. The nanobeam is patterned by e-beam lithography using HSQ as a resist, followed by reactive ion etching. Finally, a 20 nm re-coating of TiO₂ is done by ALD to reach the hole radii precisely and to reduce sidewall roughness induced propagation loss. The sample is characterized by in and out coupling light with lensed fibers at both ends of the sample. A photonic band-gap is found with an extinction ratio of 15 dB and a resonance peak at around 725 nm.

9359-44, Session 9

A graphene-based microfiber in-line polarizer with stereo rod-microfiber-air structure

Fei Xu, Nanjing Univ. (China)

To increase the interaction between lightwave and graphene, more and more attention is paid to combine the advantages of graphene and microfiber. In this paper, we present a simple and effective wrapping-on-a-rod technique for the fabrication of a graphene-based microfiber in-line polarizer.

A monolayer graphene sheet grown by chemical vapor deposition was mechanically transferred onto the surface of a Teflon-coating micro-rod. Then, a microfiber (~ 3 μm in diameter) was wrapped on the graphene sheet supported by the rod. Distance (tens of micrometers in separation) was kept between different turns of the microfiber in order to prevent mutual coupling which may cause negative effect on the results.

The polarization mechanism rises from graphene only interacting with the in-plane electric field of electromagnetic waves in microfiber waveguide. Without complex and expensive micromachining facility, our device has a compact 3D geometry and standard input/output ends. A broadband polarizer is capable of achieving an extinction ratio high as ~ 10 dB/turn. By employing a two-turn coil structure, extinction ratio as high as ~ 20dB is obtained over 400nm bandwidth around telecommunication wavelength. Similar results are expected by using RGB fibers in the visible and endless single mode photonic crystal fibers throughout visible to NIR.

The compact size, high efficiency and broadband operation enable the graphene-based microfiber in-line polarizer possessing great potentials for optical communication application and make it a candidate for future lab-on-a-rod devices.

9359-45, Session 9

Wide-angle structural color filter featuring high-efficient transmission and high-excitation purity

Vivek R. Shrestha, Sang-Shin Lee, Eun-Soo Kim, Kwangwoon Univ. (Korea, Republic of); Duk Yong Choi, The Australian National Univ. (Australia)

Nanophotonic structural color filters have received enormous attention in view of their prominent applications such as display and imaging devices, colorful decoration, anti-counterfeiting, automobile, textiles, etc. They have been considered an attractive replacement for current colorant pigmentation in the display technologies, in view of its increased

efficiencies, ease of fabrication and eco-friendliness. However angular dependency of such filters poses a detrimental barrier for practically developing high performance display and sensing devices. In order for the filter devices to prove their appreciable feasibility in display or imaging applications, apart from the improvement of the performance in terms of transmission or reflection efficiencies and angle independence, the hue and saturation properties of the produced color should improved and stable with change in angle.

In this work, we report on a wide-angle transmissive structural color filter, fabricated in a large area of 76.2 x 25.4 mm², by taking advantage of triple stacked etalon resonators in dielectric films, each of which is composed of a high-index cavity in hydrogenated amorphous silicon sandwiched with a pair of SiO₂ films, which enables both a high transmission above 80%, a high excitation purity of 0.93 and non-iridescence over a wide-angle 160°, showing no significant change in the center wavelength, dominant wavelength and excitation purity, implying no change in hue and saturation of the output color. Besides, a very low dependence on polarization was obtained for over a wide-angle 160°. The proposed structure may find its potential applications to large display and image sensor systems.

9359-46, Session 10

Through silicon via developments for silicon photomultiplier sensors

Carl Jackson, Kevin O'Neill, Liam A. Wall, Brian McGarvey, Deborah Herbert, SensL (Ireland)

Packaging has a significant impact on the performance characteristics of SiPM sensors, also impacting reliability and yield. SensL have recently developed and tested a SMT through silicon via (TSV) package that provides high reliability from having no wire bonds, high reproducibility, long service life, high yield and large operating temperature range (- 40oC to 95oC). Additionally, the TSV package has minimal deadspace and so allows close packing when creating sensor arrays. Sensor arrays created with TSV SiPM will be shown to achieve the highest fill factor possible as compared to other packaging technologies.

To create the new wafer scale package, the silicon wafer is first attached to glass and thinned to <0.10mm. Contact vias are etched, filled and then solder balls are attached. The final parts are provided on tape and reel and are reflow solderable using industry standard printed circuit board assembly techniques.

The TSV parts have full compatibility with magnetic resonance imaging systems as will be demonstrated by showing the results of TSV samples in a 3 Tesla MRI.

The PDE of a TSV packaged sensor is significantly improved over other package types, particularly in the UV and blue region. The PDE curve of the TSV package will be compared to epoxy, clear MLP and bare die. The TSV package will be shown to have the highest package PDE approaching that of bare die. Additionally full performance characterization of this new SiPM package will be presented for multiple sensor sizes.

9359-47, Session 10

Fully-CMOS analog and digital SiPMs

Yu Zou, Federica A. Villa, Danilo Bronzi, Politecnico di Milano (Italy); Simone Tisa, Micro Photon Devices S.r.l. (Italy); Alberto Tosi, Franco Zappa, Politecnico di Milano (Italy)

Silicon Photomultipliers (SiPMs) are emerging single photon detectors used in many applications requiring large active area, photon-number resolving capability and immunity to magnetic fields.

We present three families of analog SiPM fabricated in a reliable and cost-effective fully standard planar CMOS technology with a total photosensitive area of 1x1 mm². These three families have different active areas with fill-

**Conference 9359:
Optical Components and Materials XII**

factors (21%, 58.3%, 73.7%) comparable to those of commercial SiPM, which are developed in vertical custom technologies. The peak photon detection efficiency in the near-UV tops at 38% (fill-factor included) comparable to commercial custom-process ones and dark count rate density is just a little higher than the best-in-class commercial analog SiPMs.

We propose a SPICE model for simulating the working behavior of analog SiPMs, and we compare the response of analog SiPMs with different readout electronics.

Thanks to the CMOS processing, these new SiPMs can be integrated together with active components and electronics both within the microcell and on-chip, in order to act at the microcell level or to perform global pre-processing.

We also report CMOS digital SiPMs in the same standard CMOS technology, based on microcells with digitalized processing, all integrated on-chip. This CMOS digital SiPMs has four 32x1 cells (128 microcells), each consisting of SPAD, active quenching circuit with adjustable dead time, digital control (to switch off noisy SPADs and readout position of detected photons), and fast trigger output signal. The achieved fill-factor is still very good 20%.

9359-49, Session 10

Ultra-low noise and exceptional uniformity of SensL C-series SiPM sensors

Carl Jackson, Kevin O'Neill, Brian McGarvey, Liam A. Wall, Deborah Herbert, SensL (Ireland)

Advances in SiPM production have resulted in the newly released C-Series Silicon Photomultiplier (SiPM) sensors. Both the dark current and uniformity of the C-Series SiPM has been improved. The dark count of the C-Series sensors has been lowered through the reduction of damage during semiconductor processing. The breakdown voltage and optical uniformity has been improved through process optimization to minimize breakdown voltage variation.

With these process improvements ultra-low noise with typical dark count rates of 70kHz/mm² are achieved simultaneously with breakdown voltage uniformity of ± 250 mV. The SiPM are fabricated in a shallow P-on-N junction optimized for the detection of shorter wavelength photons, with a peak PDE of >40% at 420nm and extending to 300nm. C-Series sensors also feature the Fast Output whose characteristics are a ~300ps rise time and ~600ps FWHM, and leads to excellent timing capabilities. Results from end-of-line wafer level test, package level product qualification and application specific measurements will be presented. The benefits of the C-Series properties will be demonstrated by showing energy resolution and CRT (Coincidence Resolving Time) results, relevant to PET and radiation detection applications.

SensL C-Series sensors are a commercially proven technology that is fabricated in a high-volume CMOS foundry to a custom SensL process, and packaged as a reflow solderable surface mount device. This paper will show the exceptional uniformity achievable from the CMOS processing, both electrical and optical, as well as results on a range of reliability testing to integrated circuit standards.

9359-50, Session 10

Effect of multi-input injection locking on hysteresis width and switching time in single-mode Fabry-Perot laser diode for short pulse controlled switching

Bikash Nakarmi, Yonghyub Won, KAIST (Korea, Republic of)

Optical switch, which is one of the important units of optical signal processing is of widely concern in present optical research work. Various components such as semiconductor optical amplifier, Fabry-Perot laser

diode, erbium doped fiber, and others have been widely analyzed. Among various components, single mode Fabry-Perot laser diode (SMFP-LD) has advantages of less power consumption and cheap in price, hence SMFP-LDs can be used for demonstration of different logic units, switches and others. We focused on analyzing the effect of multi-input injection on hysteresis width and rising falling time at the output of SMFP-LDs with respect to wavelength detuning. These analyzed results are used in different stages of proposed novel short pulse controlled all-optical 1x2 switch using SMFP-LDs. The basic principle involved for the demonstration of short pulse controlled 1x2 switch is the optical bistability property of injection locking phenomena. The proposed scheme consists of two units; control unit, which generates the control signal according to the short input pulses applied and switching unit which switch input data at output ports either Port 1 or Port 2. The control unit consist of Set Reset latch, hence short input pulses are sufficient to switch input data to respective output ports rather than requiring logic high or low control pulses thorough out the switching period. The pulse duration of 280 ps at input ports are sufficient enough to generate control signals which switch 10 Gbps input data at output ports according to the output of SR latch used in control unit.

9359-51, Session 10

Monolithically-integrated quantum dot optical gain modulator with semiconductor optical amplifier for 10-Gb/s photonic transmission

Naokatsu Yamamoto, Kouichi Akahane, Toshimasa Umezawa, Tsutsuya Kawanishi, National Institute of Information and Communications Technology (Japan)

Short-range interconnection and/or data center networks require high capacity and a large number of channels for the numerous connections. Solutions for meeting these requirements involve the use of alternative wavebands to increase the usable optical frequency range. We recently proposed the use of the T and O bands (Thousand band: 1000–1260 nm, Original band: 1260–1360 nm) as the alternative wavebands because large optical frequency resources (>60 THz) can be easily employed. Additionally, a simple and compact Gb/s-order high-speed optical modulator is a critical photonic device for short-range communications. Therefore, we focused on the use of self-assembled quantum dots (QDs) as a three-dimensional confined structure for developing an optical modulator that acts as a high-functional photonic device because the QD structure is highly suitable for realizing broadband optical gain media in the T+O band.

In this paper, we used the high-quality broadband QD optical gain to develop a monolithically integrated QD optical gain modulator (QD-OGM) device with a semiconductor optical amplifier (QD-SOA) for Gb/s-order high-speed optical data generation in the 1.3- μ m waveband. Insertion loss of the device can be compensated through the SOA, and an optical gain change as high as -7 dB can be obtained in the OGM section. Furthermore, we successfully demonstrated a 10-Gb/s clear eye opening using the QD-OGM/SOA device with a clock-data recovery sequence at the receiver end. These results suggest that the monolithic QD-OGM/SOA is attractive for increasing the number of wavelength channels for smart short-range communications.

9359-53, Session PWed

Development of a long-gauge fiber-optics-distributed vibration sensor

Peter Kung, QPS Photonics Inc. (Canada); Maria I. Comanici, McGill Univ. (Canada)

Recently, we found that by terminating a long length of fiber of up to several kilometers with an in-fiber cavity structure, the entire structure can detect vibrations over a frequency range from 5 Hz to 100 Hz. We want to

**Conference 9359:
Optical Components and Materials XII**

determine whether the structure (including packaging) can be optimized to detect vibrations at even higher frequencies. The structure can be used as a distributed vibration sensor mounted on large motors and other rotating machines to capture the entire frequency spectrum of the associated vibration signals, and therefore, replace the many accelerometers, which add to the maintenance cost. This will replace the many accelerometers used for maintenance. Similarly, it will help detect in-slot vibrations inside an air cooled generator which causes intermittent contact leading to sparking under high voltages. However, that will require the sensor to detect frequencies associated with vibration sparking, ranging from 6 kHz to 15 kHz. Then, at even higher frequencies, the structure can be useful to detect acoustic vibrations (30 kHz to 150 kHz) associated with partial discharge (PD) in generators and transformers. Detecting lower frequencies in the range 2 Hz to 200 Hz makes the sensor suitable for Seismic studies and falls well into the vibrations associated with rotating machines. Another application of interest is corrosion detection in large re-enforced concrete structures by inserting the sensor along a long hole drilled around structures showing signs of corrosion. The frequency response for the proposed long gage vibration sensor depends on packaging

9359-54, Session PWed

Diffraction gratings as humidity sensors

Sergio Calixto-Carrera, Ctr. de Investigaciones en Óptica, A.C. (Mexico); Miguel V. Andrés, Univ. de Valencia (Spain)

Control and measurement of humidity is important in diverse areas and industries like automotive, food processing, semiconductors, textiles and more. Here we describe the results of using relief gelatin gratings to measure relative humidity (RH). Gelatin is composed of a complex chain of amino acids. When water molecules are absorbed by gelatin they attach to the polar groups of the chains. The absorption (desorption) of water molecules by gelatin film causes the swelling (shrink) of the film. Hardening of gelatin can be made by light. Hardened gelatin does not swell as much as unhardened gelatin when water molecules are absorbed. Low frequency gratings were made by recording a sinusoidal interference pattern (15 l/mm) with dichromated gelatin. Crests in the light pattern hardened the gelatin and after development a sinusoidal spatial relief distribution of hardened and unhardened material was present. When gratings were immersed in an atmosphere with changing RH, water molecules were absorbed by the gelatin gratings. Valleys in the profile swelled more than crests because they were less hardened. Thus, optical path difference between the light that passed through the valleys and the one that passed through the crests changed. This change in optical path affected the diffraction efficiency. In this way, by measuring first order intensity when RH changes, we can use gelatin gratings as RH sensors. Simple measuring arrangements can be foreseen. So far we have tested the gratings in the range of 20% to 50% RH.

9359-55, Session PWed

Fabry-Pérot fiber interferometer formed by fusion splicing and chemical etching

Hsuan Chen, Chin-Ping Yu, National Sun Yat-Sen Univ. (Taiwan)

Fabry-Pérot fiber interferometers (FPFIs) have been widely employed in optical sensors owing to their simple structures, compact sizes, high sensitivities, and immunity to electromagnetic interference. The FPFIs are usually formed by introducing an air cavity along an optical fiber by using laser micromatching or fusion splicing different kinds of fibers. In this paper we propose a simple FPFI sensor formed by fusion splicing and chemical etching. We first used the grinding technology to create an inclination on the endface of a single-mode fiber (SMF). The surface-inclined SMF was then spliced to another cleaved SMF by a fusion splicer with specific discharge parameters to create an air gap between the two fibers. To enlarge the air gap size, the splicing point was immersed into a 15% HF solution for 90 minutes. After cleaning by DI water, the sample was

connected to a light source and an OSA through a 3-dB circulator to obtain the reflective interference spectrum. Very clear interference spectrum can be observed, and the air cavity length is about 8.3 μ m, which is deduced from the measured free spectrum range (FSR). We then measured the temperature sensitivity of our fabricated FPFI. As the ambient temperature was increased, the interference spectrum shifted toward longer wavelength region linearly. The experimental results indicate that the proposed FPFI possesses a temperature sensitivity of 525pm/°C in the temperature range of 28.5°C-58.5°C. The proposed all-fiber FPFI sensor has a very high potential for other sensing applications due to its simple structure and flexibility in design.

9359-56, Session PWed

Flattened supercontinuum generation in tellurite-phosphate and chalcogenide-tellurite hybrid microstructured optical fibers with tailored chromatic dispersion profiles

Tuan H. Tong, Hiroyasu Kawashima, Koji Asano, Zhongchao Duan, Tonglei Cheng, Dinghuan Deng, Toyota Technological Institute (Japan); Morio Matsumoto, Tezuka Hiroshige, Furukawa Denshi Co., Ltd. (Japan); Takenobu Suzuki, Yasutake Ohishi, Xiaojie Xue, Toyota Technological Institute (Japan)

We report here the flattened supercontinuum (SC) generated in tellurite-phosphate and chalcogenide-tellurite hybrid microstructured optical fibers (HMOFs) whose chromatic dispersion profiles were controlled with high freedom due to a large refractive index difference (Δn) between core and cladding materials. It was theoretically shown that the tellurite-phosphate HMOFs whose dispersion profiles were near-zero and flattened with three zero-dispersion wavelengths (ZDWs) over a wide wavelength range from 1000 to 4000 nm were beneficial to obtain a broad and flattened SC spectrum. By using a large Δn of 0.49, the tellurite-phosphate HMOF which had flattened dispersion and 3 ZDWs was successfully fabricated. When the fabricated tellurite-phosphate HMOF of 20-cm long was pumped at 1550 nm under a low pump power of 12.5 mW, an SC spectrum extended from -800 to 2400 nm (-1600 nm bandwidth) where a ± 2.5 -dB spectral flatness in the wavelength ranges from 890 to 1425 nm and from 1875 to 2400 nm was observed. In addition, a flattened SC spectrum of ± 3.0 -dB over a broad wavelength range from 950 to 3350 nm was demonstrated by using 1-cm long chalcogenide-tellurite HMOF pumped at 2300 nm under a pump power of 200 mW.

9359-57, Session PWed

Experimental research on the multi-order acousto-optic diffraction based on Raman-Nath diffraction

Huadong Gu, Suzhou Institute of Biomedical Engineering and Technology (China) and Jiangsu Key Lab. of Medical Optics (China); Zhongxing Shao, Suzhou Institute of Biomedical Engineering and Technology (China); Chenqi Zheng, Suzhou Institute of Biomedical Engineering and Technology (China) and Jiangsu Key Lab. Medical Optics (China); Ruitao Chen, Jie Yang, Suzhou Institute of Biomedical Engineering and Technology (China) and Jiangsu Key Lab. of Medical Optics (China); Zetong Gu, Suzhou Institute of Biomedical Engineering and Technology (China)

**Conference 9359:
Optical Components and Materials XII**

In this paper, the experimental investigation on the interaction length for getting the optimum diffraction of the multi-order acousto-optic diffraction is presented. Based on these results, the feasibility of acousto-optic Q-switch taking H₂O or TeO₂ as medium respectively for ultraviolet and visible lasers are discussed.

The fact that the optimum interaction length tightly relies on the frequency of the sound and does not relate to the wavelength and power of the light is found in the experiment. The interaction length will become longer as the frequency of the ultrasound becomes higher. The interaction length is about 8mm when the acoustic frequency is at about 9MHz and becomes about 4mm at 6MHz. A Q-switch that works with pure water is designed and a total diffractive efficiency of about 98% was obtained under the condition that the acoustic frequency is 9MHz and the acoustic power is 3.4W.

An acousto-optic Q-switch made of TeO₂, in terms of Raman-Nath diffraction is designed. With a cooling system on the device, a total diffractive efficiency of about 75% is obtained under the condition that the acoustic frequency is 10MHz and the acoustic power is 10W. The first-order diffractive angle is 1.4 mrad. The loss by one path of the device is tested by a Nd:YAG/KTP laser with pulse width of 20ms and energy per pulse of 400mJ. The loss is about 5% on the best condition. Then the modulated pulse width is measured as about 200ns on the condition that the acoustic frequency is 11MHz, the acoustic power is 6W and the repetition frequency is 10kHz.

9359-58, Session PWed

Luminescence of (Mg,Zn)Al₂O₄:Tb mixed spinel thin films prepared by spin-coating

Robin E. Kroon, Univ. of the Free State (South Africa); Wael A. I. Tabaza, Univ. of the Free State (South Africa) and Islamic Univ. (Palestinian Territory, Occupied); H. C. Swart, Univ. of the Free State (South Africa)

MgAl₂O₄ and ZnAl₂O₄ both have the spinel structure similar lattice constants, but the bandgap of MgAl₂O₄ is double that of ZnAl₂O₄, making it interesting to consider the mixed spinel (Mg_xZn_{1-x})Al₂O₄ as a possible host for luminescent ions. Prior to preparing thin films, the Mg:Zn ratio and Tb concentration were optimized for green luminescence from the 5D₄ - 7F₅ transition of Tb³⁺ ions using nanocrystalline samples prepared by combustion synthesis. Thin films with x = 0.75 and 0.5 mol% Tb were spin-coated on Si(100) substrates using a solution of the nitrates of Mg, Zn, Al and Tb in ethanol, with ethylene glycol as complexing agent. Samples about 200 nm thick were obtained by sequentially depositing 10 layers at 3000 rpm for 30 s. Samples were annealed for 1 h in air before measuring their luminescence properties. For the sample annealed at 600 °C, x-ray diffraction showed the thin film had a strong (111) texture. Atomic force microscopy revealed an rms roughness of 1 nm and Auger electron spectroscopy depth profiles showed a uniform layer with a sharp interface at the Si substrate. With an increase in annealing temperature up to 1000 °C, the luminescence increased while the surface became slightly rougher and the layer-substrate interface less sharp. Annealing the samples at 1200 °C resulted in diffusion of Si through the layer and the formation of an additional phase. While the green Tb emission was slightly reduced, blue emission from the 5D₃ level of Tb³⁺ was greatly enhanced in these samples.

9359-59, Session PWed

Optical properties and size distribution of the nanocolloids made of rare-earth ion-doped NaYF₄

Darayas N. Patel, Oakwood Univ. (United States); Sergey S. Sarkisov, SSS Optical Technologies, LLC (United States); Ashley Lewis, Donald Wright III, Danielle Lewis, Maucus Valentine, Oakwood Univ. (United States)

In this paper we investigate optical properties and size distribution of the nanocolloids made of trivalent rare-earth ion doped fluorides: holmium and ytterbium, thulium and ytterbium, and erbium and ytterbium co-doped NaYF₄. These materials were synthesized by using simple co-precipitation synthetic method. The initially prepared micro-crystals had very weak or no visible upconversion fluorescence signals when being pumped with a 980-nm laser. The fluorescence intensity significantly increased after the crystals were annealed at a temperature of 400C - 600C undergoing the transition from cubic alpha to hexagonal beta phase of the fluoride host. Nano-colloids of the crystals were made in polar solvents using the laser ablation and ball milling methods. Size analyses of the prepared nanocolloids were conducted using a dynamic light scatterometer and atomic force microscope. The nano-colloids were filled in holey PCFs and their fluorescent properties were studied and the feasibility of new a type of fiber amplifier/laser was evaluated.

9359-60, Session PWed

Activation of in-situ dopants in GeSn by rapid thermal anneal

Birendra R. Dutt, APIC Corp. (United States); Elizabeth H. Edwards, PhotonIC Corp. (United States); Colleen K. Shang, James S. Harris, Stanford Univ. (United States); Yi-Chiau Huang, Yihwan Kim, Applied Materials, Inc. (United States)

Si-compatible optical devices are desired to replace metal wires with optical links, since silicon (Si) is the dominant CMOS technology. A key missing component of the Si photonics platform is an efficient, electrically injected laser diode, owing to the indirect bandgap of Si. Germanium (Ge), another group IV (and therefore silicon-process-compatible) material, is being investigated owing to its pseudodirect band gap behavior. Heavily n-doping Ge by implantation techniques has allowed a lasing demonstration, albeit with threshold currents on the magnitude of hundreds of kA/cm². The alloying of Ge with a second group-IV element, tin (Sn) and the use of in-situ doping to avoid the lattice damage inherent to implantation could yield lower lasing threshold voltages.

In this study, we show that using in-situ doping of phosphorus during the low-temperature epitaxial growth of GeSn on Si substrates, dopant concentrations exceeding 5e19cm⁻² with activation greater than ~30% (measured by SIMS and SRP) can be achieved in both blanket and heterostructured films. This is despite a high concentration of fully-crystal-incorporated Sn (measured by RBS). Further, we investigate the effects of rapid thermal anneals on the active phosphorus dopant concentration of GeSn.

9359-61, Session PWed

Application of photo-doping phenomenon in amorphous chalcogenide GeS₂ film to optical devices

Yoshihisa Murakami, National Univ. Corp. Tsukuba Univ. of Technology (Japan); Katsuya Arai, Moriaki Wakaki, Takehisa Shibuya, Tokai Univ. (Japan); Toshihiro Shintaku, Tokyo Polytechnic Univ. (Japan)

Photodoping phenomenon is observed when a double-layer consisting of amorphous chalcogenide film (As₂S₃, GeS₂, GeSe₂ etc.) and metal (Ag, Cu etc.) film is illuminated by light. The metal diffuses abnormally into the amorphous chalcogenide layer. Amorphous chalcogenide films of GeS₂ with an Ag over layer exhibited large increase of refractive index through the abnormal doping of Ag by irradiating the light around the absorption edge of the GeS₂ chalcogenide. In this study, the quantitative characterization of photodoping phenomena was carried out for amorphous GeS₂ films using Ag as a doping metal to obtain the basic information for

**Conference 9359:
Optical Components and Materials XII**

fabrication of photonic devices. Especially, quantum efficiency to reach the saturation of the doping was derived using the laser diodes at several wavelengths. We aimed the application of this effect for the optical devices and fabricated various micro doped patterns by using a laser beam to study the feasibility for devices. Mask less patterning using the refractive index modification caused by the selective doping of Ag into an amorphous chalcogenide GeS₂ film are possible by manipulating a laser beam. Various types of light waveguides were fabricated by manipulating a laser beam and characterized. In addition, the feasibility to fabricate various types of holograms like gratings by using the two-beam interference through the holographic recording was examined.

9359-62, Session PWed

Optical and electronic properties of Si ion implantation of silver atoms

Yevheniia Chernukha, Vasyl S. Stashchuk, National Taras Shevchenko Univ. of Kyiv (Ukraine)

This work is devoted to providing appropriate modification of Si⁺ surface structure and their investigations. The article's main problem is analyzing information about optical properties of obtained samples with chemically pure Si. Ion implantation of Si was made by silver's atoms with energy 75 keV. The dose of ions should be D₁ = 10¹⁶ ion/sm², D₂ = 10¹⁵ ion/sm² and D₃ = 10¹⁴ ion/sm² for effective modification of samples structure. The samples' surface were explored in wide spectral range $\lambda = 0,23 - 2,8\text{nm}$ ($h\nu = 0,44 - 5,39\text{ eV}$) by the Beatty's spectral ellipsometry method. While an experiment was carried out ellipsometry parameters Ψ and Δ were measured near the principle angle of incidence. The dispersive dependences of optical conductivity $\sigma(\text{hv})$, reflection coefficient $R(\text{hv})$ and permittivity $\epsilon(\text{hv})$ were calculated using those ellipsometry parameters. The angular dependence of ellipsometric parameters were investigated using the serial ellipsometer LEF-3M-1 with the working wavelength 632,8 nm and a range of angles of incidence changes 65-80°. With increasing of the radiation dose observed a general shift of the bands in the direction lower energies. High intensity irradiation silver ions lead to a significant increase in surface roughness of single-crystal silicon, creating a large number of vacancies maybe forms a further area at the bottom of the conduction band of silicon.

9359-63, Session PWed

Nonlinear electro-optic tuning of plasmonic nano-filter

Rehab K. Abd-Allah, The American Univ. in Cairo (Egypt); Yehea Ismail, Zewail City of Science and Technology (Egypt); Mohamed A. Swillam, The American Univ. in Cairo (Egypt)

Efficient, easy and accurate tuning techniques to the behavior of a plasmonic nano-filter are investigated. The proposed filter supports both blue and red shift in the resonance wavelength. By varying the refractive index with a very small change (in the order of 10^{-3}), the resonance wavelength can be controlled efficiently. Using Pockels material, an electrical tuning to the response of the filter is demonstrated. The resonance wavelength is blue shifted up to 47nm by applying an external voltage. In addition, the behavior of the proposed filter can be controlled optically using Kerr material. By controlling the intensity of the input light, a red shift in the resonance wavelength up to 80nm is achieved. A new approach of multi-stage electro-optic controlling is introduced for the first time. By cascading two stages and filling the first stage with pockels material and the second stage with kerr material, the output response of the second stage can be controlled by controlling the output response of the first stage electrically. Due to the sharp response of the proposed filter, 60nm shift in the resonance wavelength per 10 voltages is achieved. This nano-filter has compact size, low loss, sharp response and wide range of tunability which is highly demandable in many biological and sensing applications.

9359-64, Session PWed

Ultra-flat and broad gain bandwidth of optical parametric amplification in highly-nonlinear tellurite hybrid microstructured optical fibers

Lei Cheng, Toyota Technological Institute (Japan); Tuan H. Tong, TTI (Japan); Xiaojie Xue, Dinghuan Deng, Takenobu Suzuki, Yasutake Ohishi, Toyota Technological Institute (Japan)

Fiber optical parametric amplifiers (FOPAs) with flat and broad gain bandwidth are very promising for all-optical signal processing applications, such as switching, signal generation, optical sampling, broadband wavelength conversion, wavelength division multiplexing (WDM) and optical time division multiplexing (OTDM). However, most of the former researches on FOPAs are based on silica fibers and its low nonlinearity requires the fiber length of several kilometers to obtain practical FOPA gain. Recently much attention has been given to non-silica materials with high refractive index and high nonlinearity, such as tellurite and chalcogenide glasses. In the paper, the parametric gains with different pump wavelengths and powers are simulated in the tellurite hybrid microstructured optical fibers (HMOFs). The cores of the HMOFs are made from TeO₂-Li₂O-WO₃-MoO₃-Nb₂O₅ glass and the claddings are made from TeO₂-ZnO-Na₂O-P₂O₅ glass. The non-degenerated four-wave mixing (FWM) is investigated with different pump wavelengths and pump powers in the HMOFs with different chromatic dispersions. An ultra-flat gain bandwidth of $\lambda = 658\text{ nm}$ with $\pm 0.01\text{ dB}$ gain fluctuation is achieved by 1.25 W dual-pumping, and a broad gain bandwidth of $\lambda = 524\text{ nm}$ at 60-dB signal gain with gain ripples is obtained by 3.0 W dual-pumping from 25 cm tellurite HMOF.

9359-65, Session PWed

Requirements for gain/oscillation in Yb³⁺/Er³⁺-codoped microring resonators

Juan A. Valles, Univ. de Zaragoza (Spain); Ramona M. G?l?us, Technical Univ. of Cluj Napoca (Romania)

Due to their fabrication scalability, functionalization and easiness in sensor interrogation microring resonators (MRR) with chip-integrated linear access waveguides have emerged as promising candidates for scalable and multiplexable sensing platforms. The near-infrared spectral range and, in particular, the 1.5- μm wavelength band is already employed in several biological and chemical sensing tasks. If gain is incorporated inside the ring, the filtering and amplifying/oscillating functionalities are combined and the sensing potentialities become enhanced.

We developed a detailed model of the performance of a highly Yb³⁺/Er³⁺-codoped phosphate glass MRR that considers the intensity rates of both pump and signal powers at resonance and affected by their interaction with the dopant ions through absorption/emission processes. Due to the high dopant concentrations considered, the microscopic statistical formalism based on the statistical average of the excitation probability of the Er³⁺ is used to describe energy-transfer inter-atomic mechanisms. In this paper this model is used to analyze the optimized design of an Yb³⁺/Er³⁺-codoped phosphate glass MRR side-coupled to two straight waveguides for pump and signal input/output, in order to determine the practical requirements to achieve amplification and oscillation. In particular, the influence of the configuration symmetry and the decisive performance dependences on rare earth ions concentration and couplers' additional loss, are fully discussed.

9359-66, Session PWed

Yb³⁺-doped TeO₂-WO₃-ZrO₂ glasses for high-power laser applications

Venkataiah G., Sri Venkateswara Univ. Tirupati (India); Babu P., Government Degree College Satyavedu (India); Inocencio Rafael Martín Benenzuela, Victor Lavín della Ventura, Univ. de La Laguna (Spain); Chalicheemalapalli K. Jayasankar, Sri Venkateswara Univ. (India); Venkata Krishnaiah, Ecole Polytechnique de Montréal (Canada)

In recent years, extensive research work is going on Yb³⁺-doped laser glasses which are suitable for high-power diode-pumped solid-state lasers, ultrafast lasers and tunable lasers around 1 μm region. Yb³⁺-doped TeO₂-WO₃-ZrO₂ based optical quality glasses with high refractive indices (2.08–2.21) have been prepared and investigated their physical, spectroscopic and gain properties through absorption, fluorescence and decay curves. The inter-molecular distance is found to decrease from 34.5 to 8.9 Å with the increase in Yb³⁺ ion concentration. The stimulated emission cross-section for the 2F_{5/2} → 2F_{7/2} transition has been calculated by applying McCumber theory. The decay curves, measured by exciting at 915 nm and monitoring at 980 nm, are found to be single exponential for all the concentrations of Yb³⁺ ions. The experimental lifetime of the 2F_{5/2} emitting level of the Yb³⁺ ions has been evaluated and are found to be 0.35, 0.39, 0.42, 0.40, 0.36 and 0.29 ms for 0.05, 0.1, 0.5, 1.0, 2.0 and 3.0 mol % of Yb³⁺ ion concentrations, respectively. The lifetime of the 2F_{5/2} level is found to increase up to 0.5 mol % and then decreases for higher concentrations of Yb³⁺ ions. The increase in lifetime is due to re-absorption of emitted energy by Yb³⁺ ions. The decrease in lifetime at higher Yb³⁺ ions concentration is due to energy migration among Yb³⁺ ions and then transfer to traps. Systematic analysis of the results suggests that the present tellurite based glasses doped with Yb³⁺ ions are useful as high power laser gain media.

9359-67, Session PWed

Optical characterization of Er³⁺ ions doped zincfluorophosphate glasses

Sreedhar V.B., Vijaya N., Sri Venkateswara Univ. (India); Krishna M. Nutakki, Akkineni Nage Swara Rao College (India); Chalicheemalapalli K. Jayasankar, Sri Venkateswara Univ. (India)

Er³⁺-doped P₂O₅-K₂O-ZnF₂-Al₂O₃-Er₂O₃ glasses have been prepared by conventional melt- quenching technique and are characterized through Raman, visible and near-infrared (NIR) emission spectra and decay rate measurements. In the frame work of well known Judd-Ofelt (JO) theory to the absorption spectrum of 1.0 mol % of Er₂O₃ doped glass, the intensity parameters (J₂=8.23, J₄=1.04 and J₆=1.91, J₁₀₋₂₀ cm²) and radiative properties for the important luminescent levels of Er³⁺ ions have been predicted. The studied glasses exhibit intense green and weak red emissions under 378 nm excitation and an intense NIR emission has been observed at 1.53 μm with the maximum full width at half maximum (FWHM = 53 nm for 2.0 mol% of Er₂O₃) under 980 nm laser diode excitation. The absorption (4.32 × 10⁻²¹ cm²) and emission cross-section (5.19 × 10⁻²¹ cm²) for 4I_{13/2} → 4I_{15/2} have been derived from McCumber theory and compared with the other reported glass systems. Lifetime for the 4I_{13/2} level of Er³⁺ ion is found to decrease from 7.17 to 1.42 ms with increase in concentration of Er³⁺ ions from 0.01 to 2.0 mol % due to non-radiative processes. The results indicate that the glasses may be suitable for the development of optical amplifier in the 1.53 μm optical region.

9359-68, Session PWed

Optical properties of Pr³⁺-, Ce³⁺-, and Eu³⁺-doped KPb₂Cl₅

EiEi Brown, Uwe H. Hömmerich, Hampton Univ. (United States); Althea G. Bluiett, Elizabeth City State Univ. (United States); Sudhir B. Trivedi, Brimrose Corp. of America (United States)

The luminescent properties of rare-earth doped solids have been under intense exploration for a wide range of applications ranging from displays and lasers to scintillators. Potassium lead chloride (KPb₂Cl₅) materials have recently emerged as new non-hygroscopic laser hosts with low maximum phonon energies (~208 cm⁻¹), which lead to small non-radiative decay rates for trivalent rare earth dopants. In this work, the material purification, crystal growth, and spectroscopic properties of Pr³⁺-, Ce³⁺-, and Eu³⁺-doped KPb₂Cl₅ (KPC) were investigated for possible applications in infrared lasers and radiation detectors. The studied materials were synthesized through careful purification of starting materials including multi-pass zone-refinement and chlorination. The growth of the purified materials was then carried out through vertical or horizontal Bridgman technique. The trivalent praseodymium ion (Pr³⁺) offers a large number of laser transitions in the visible and infrared (IR) spectral regions. Using ~1.45 μm and 1.9 μm pumping, IR emissions at ~1.6, ~2.4, and ~4.5 μm were observed from Pr: KPC corresponding to the 4f-4f transitions of 3F₄/3F₃ → 3H₄, 3F₂/3H₆ → 3H₄, and 3H₅ → 3H₄, respectively. Under Xenon flash lamp excitation, preliminary spectroscopic results showed Pr³⁺ 5d-4f emission centered ~385 nm accompanied by weak Pr³⁺ 4f-4f emission ~480-680 nm in Pr:KPC. In addition, allowed 5d-4f emission centered at ~375 nm was also observed in Ce:KPC. Detailed spectroscopic results including time-resolved excitation and emission, temperature dependent emission studies as well as decay dynamics of the investigated crystals will be presented at the conference.

9359-69, Session PWed

Chirped long-period grating for dispersion minimization

Krishna C. Patra, Sambalpur Univ. (India)

Modern communication system requires high bandwidth and with less distortion. Fiber-Bragg Gratings attracted much of the attraction in last decade for its applications as sensors, filters. In contrast to FBG, Long Period Fiber Grating (LPG) is being developed by undulation in the refractive index in GeO₂ doped core by using ultraviolet light. LPG can be used for various purposes such as design of bio-sensors, filters and for dispersion compensating device. Although LPGs in tapered fibers have been fabricated for sensor applications, the procedure to analyze and obtain the transmission characteristics of such gratings is not reported in literature. We have developed the procedure for numerical solution of the multiple coupled mode equations for such gratings. For a given grating period the phase matching condition can be satisfied for a given mode at different wavelengths or at one wavelength to different modes as it propagates through the grating inside the fiber. The coupled mode equations for amplitudes of modes have been solved numerically and it is observed that in the numerical solution process a correction for the change in effective indices of the coupled modes along the grating length needs to be applied. In the LPG in a tapered fiber the coupling coefficient and phase matched wavelength for mode coupling to each cladding mode changes along the length. This behavior is similar to that of a slightly apodized chirped grating and can be used to manage dispersion.

9359-70, Session PWed

Nonlinear optical properties of single crystal cadmium magnesium telluride

David Lombardo, Shekhar Guha, Air Force Research Lab. (United States)

The third-order nonlinear susceptibility of crystalline and poly-crystalline Cadmium Magnesium Telluride (CdMgTe) was studied using a spatially resolved Irradiance Scan method including picosecond and nanosecond laser pulsewidths at 532nm. The samples were placed in a loosely focused beam and a series of individual laser pulses at different energies were collected. The transmitted beam was re-imaged to a CCD with a microscope objective providing a detailed objective function for numerical simulations. The nonlinear transmission results were modeling by way of a split-step nonlinear beam propagation method including diffraction, nonlinear absorption and refraction, and carrier effects. The angular dependence of the third order susceptibility with respect to the electric field is also presented along with laser induced damage thresholds.

9359-71, Session PWed

Optical thermal sensing based on neodymium-doped materials with excitation and emission within the first biological window

Kagola Upendra Kumar, Wesley Queiroz Santos, Carlos Jacinto da Silva, Univ. Federal de Alagoas (Brazil)

Owing to the presence of suitable Thermally Coupled Levels ($\sim 4F5/2/2H9/2$ and $4F3/2$), Nd³⁺ is promising in applications in optical thermometry by using its near infrared emissions. This temperature measuring technique utilizes the intensity ratio of photoluminescence spectra emitting from the same doped ions in neighboring energy levels to reduce the environment interference and improve the sensitivity. Nd³⁺ has large absorption cross-section at 800 nm, so the lasers centered around this wavelength were usually used to excite the Nd³⁺ doped sensing medium. Since Nd³⁺ ions possess both photoluminescence excitation and emission bands in the highest biological transparency spectral region of tissue or water, they are particularly suitable for use in in vitro and in vivo nano-thermometry. Also this technique can be very convenient for temperature measures in high-demanding working environment. Numerous studies have focused attention on Nd³⁺-doped glasses and glass ceramics as high sensitive optical temperature measuring material, for e.g., phosphate, tellurite, and Strontium Barium Niobate glass ceramics. In the present work, we applied the fluorescence intensity ratio (FIR) method to explore the possibility of thermal sensing using Nd³⁺ doped commercial glasses. Comparative analyses were performed to see what FIR lines are more suitable for temperature measurements and in which temperature ranges.

9359-72, Session PWed

Assessment of fiber optic sensors for ageing monitoring of industrial liquid coolants

Christos Riziotis, National Hellenic Research Foundation (Greece); Alexandros El Sachat, National Hellenic Research Foundation (Greece) and Institut Català de Nanotecnologia (Spain); Christos Markos, National Hellenic Research Foundation (Greece) and DTU Fotonik (Denmark); Anastasia Meristoudi, National Hellenic Research Foundation (Greece); Aggelos Papadopoulos,

Kleemann S.A. (Greece)

Lately the demand for in situ and real time monitoring of industrial assets and processes has been dramatically increased. Although numerous sensing techniques have been proposed, only a small fraction can operate efficiently under harsh industrial environments. In this work the operational properties of a proposed photonic based chemical sensing scheme, capable to monitor the ageing process and the quality characteristics of coolants and lubricants in industrial heavy machinery for metal finishing processes is presented. The full spectroscopic characterization of different coolant liquids revealed that the ageing process is connected closely to the acidity/ pH value of coolants, despite the fact that the ageing process is quite complicated, affected by a number of environmental parameters such as the temperature, humidity and development of hazardous biological content as for example fungi. Efficient and low cost optical fiber sensors based on pH sensitive thin overlayers, are proposed and employed for the ageing monitoring. Active sol-gel based materials produced with various pH indicators like cresol red, bromophenol blue and chorophenol red in tetraethylorthosilicate (TEOS), were used for the production of those thin film sensitive layers deposited on polymer's and silica's large core and highly multimoded optical fibers. The optical characteristics, sensing performance and environmental robustness of those optical sensors are presented, extracting useful conclusions towards their use in industrial applications.

9359-73, Session PWed

Azobenzene-based surfaces for liquid crystal alignment

Amalya Minasyan, Tigran V. Galstian, Univ. Laval (Canada)

One of the most important applications of liquid crystals (LC) is their use in display devices such as TVs monitors, cellphones, etc. The mechanical rubbing is the most commonly used method to align the LC molecules near the surface, but it has several drawbacks due to the mechanical contact. Those problems incite the search for alternative methods of alignment of LCs. Among them, the method of photo alignment shows the largest industrial prospects. One of the used mechanisms of such alignment is the photo induced reorientation of azobenzene molecules. In our approach we generate a reorientation of azobenzene molecules thanks to a thin command layer, which is cast on the glass surface. This reorientation is achieved by irradiating the surface with linearly polarized light. The homogeneous alignment of the molecules of nematic liquid crystal achieves when putting them in contact with this command layer of azobenzene by fabricating the sandwich-like cell. By irradiating the cell with the polarized laser beam through a rough glass it is possible to create the defects on the surface leading the cell to become scattering when an electric field is applied to the cell. Polarized microscopic and polarimetric studies were done to characterize the samples.

9359-75, Session PWed

Spectroscopic investigation and optical properties of Eu³⁺ ions in fluorophosphate glasses

Kiran Kumar K., Basavapoornima Ch, Vijaya N., Chalicheemalapalli K. Jayasankar, Sri Venkateswara Univ. (India); Venkata Krishnaiah, Ecole Polytechnique de Montréal (Canada)

Eu³⁺-doped (PKaCaLF:P2O5 - K2O - Al2O3 - CaF2 - LiF) glasses were prepared by melt quenching technique. The structural and optical studies are characterized through Raman, FTIR, absorption, photoluminescence and decay time measurements. The Judd-Ofelt parameters have been obtained from the absorption spectrum and are found to be $\Omega_2 = 5.21 \times 10^{-20} \text{ cm}^2$, $\Omega_4 = 8.11 \times 10^{-20} \text{ cm}^2$ and $\Omega_6 = 1.03 \times 10^{-20} \text{ cm}^2$. These parameters were used to calculate the spontaneous emission probability, radiative

lifetime, branching ratio and stimulated emission cross-section. The relative luminescence intensity ratio, $R(2/1)$ has been evaluated and are found to be 3.25 which indicates moderate asymmetric nature around Eu^{3+} ions. The luminescence decay of 5D0 level exhibit single exponential nature and the lifetimes (~ 2.50 ms) are found to be almost constant with increasing Eu^{3+} ion concentration. This trend confirms that the probability for non-radiative energy transfer between the Eu^{3+} ions in the present system is negligible. The chromaticity color coordinates ($x = 0.63$, $y = 0.31$) are in the reddish orange region and hence the present glasses can be used as red luminescent materials. The analysis of the results indicates the potentiality of the PKACaLF glasses for the development of optical display devices.

9359-76, Session PWed

Chalcogenide amorphous nanoparticles doped poly(methyl methacrylate) with high nonlinearity for optical waveguide

Xiaojie Xue, Tonglei Cheng, Takenobu Suzuki, Yasutake Ohishi, Toyota Technological Institute (Japan)

Nonlinear optical polymers show promising potential applications in photonics, for example electro-optical devices. Poly(methyl methacrylate) (PMMA) is widely used in optical waveguides, integrated optics and optical fibers. However, PMMA have not been used for nonlinear optical waveguides since it has a low nonlinear refractive index. We successfully prepared chalcogenide amorphous nanoparticles doped PMMA that had a high nonlinearity. The As₃S₇ bulk glass was dissolved in propylamine to form a cluster solution. Then the As₃S₇/propylamine solution was added into methyl methacrylate (MMA) containing photoinitiator Irgacure 184 about 0.5 wt%. After well mixed the As₃S₇ nanoparticle doped MMA was transparent. Under the irradiation of 365 nm UV light As₃S₇ doped PMMA was obtained with yellow color. The refractive index of As₃S₇ doped PMMA was higher than non-doped PMMA that was prepared by the same procedure without adding As₃S₇/propylamine cluster solution. The nonlinear optical susceptibility and nonlinear refractive index of As₃S₇ nanoparticles doped PMMA were investigated. An optical waveguide based on the As₃S₇ nanoparticles doped PMMA of high nonlinearity was fabricated.

9359-77, Session PWed

Multi-wavelength fiber laser based on liquid crystal filter

Hyun Ji Lee, Myoung Ock Ko, Moon Deock Kim, Jong-Hyun Kim, Min Yong Jeon, Chungnam National Univ. (Korea, Republic of)

Liquid crystals (LCs) are widely used for various applications such as electronic imaging, displays, and optoelectronics. In general, Fabry-Perot filters with LC have been developed for use in wavelength-division-multiplexing communication systems as they can be used as wavelength-tunable elements.

In this presentation, we report a multi-wavelength fiber laser using a device based on a nematic LC Fabry-Perot filter. The device consists of glass substrates, indium tin oxide (ITO) layers as the electrodes, dielectric layers as highly reflective surfaces, polyimide layers as the planar alignment layers, and a LC layer.

The thickness of the device is about 50 μm . The laser comprises two semiconductor optical amplifiers (SOAs), a polarization controller, two optical isolators, an optical output coupler, and a nematic liquid crystal Fabry-Perot filter. There are several lasing modes for the multi-wavelength fiber laser.

9359-78, Session PWed

Intense highly-efficient solid-state yellow light source based on rare-earth-doped luminescent concentrator

Juna Sathian, Neil M. Alford, Mark Oxborrow, Imperial College London (United Kingdom)

Highly efficient, low-cost, solid-state sources of intense yellow light are still not available. This deficit impedes a host of potential applications: compact video projectors without hazardous mercury arc lamps, vascular laser surgery and beauty therapies (e.g. wrinkle removal), photo-chemical reactors for drug manufacture, optically-pumped organic MASERs etc. Though developed as flat-panel light collectors for solar cells, luminescent concentrators (LCs) can compete successfully against lasers as light sources in applications requiring high optical power yet only modest light intensity (luminance). LCs offer higher wall-plug efficiencies, greater mechanical ruggedness and lower fabrication costs. In comparison: both conventional flash-lamp-pumped pulsed (Rhodamine 6G) liquid dye lasers, and CW (diode-pumped) solid-state lasers (such as Topica's SodiumStar) offer wall-plug efficiencies of around 2%; both require precise optical alignment; neither can be regarded as low-cost. Rare-earth-doped materials show promise as LCs due to their large Stokes shifts, reduced reabsorption losses, and capability to operate at high dissipated power densities. We report here, the realization of an LC-based light source, capable of continuously outputting ~ 50 W of yellow light through a 1.6-by-1.6 mm square aperture, with substantially higher wall-plug efficiency than any laser. It is based on an air-cooled strip of Cerium (Ce^{3+}) - doped Yttrium Aluminum Garnet (YAG) sandwiched between commercially-available arrays of royal blue (460 nm) Indium Gallium Nitride (InGaN) pump diodes. The outputted light is centered around 575 nm with a full-width-half-maximum (FWHM) ~ 76 nm. Our prototype device works well and we believe that it has significant potential in the applications named above.

9359-79, Session PWed

Packaging of phosphor-converted white light-emitting diodes for solid-state lighting

Chun-Chin Tsai, Cheng-Feng Yue, Far East Univ. (Taiwan); Yu-Chun Lee, Lextar Electronics Corp. (Taiwan); Kai-Jo Fu, Shanghai Univ. of Finance and Economics (China); Wood-Hi Cheng, National Sun Yat-sen Univ. (Taiwan)

For both high conversion efficiency and thermal stability, glass-based phosphor-converted white light-emitting diodes (GBPC-WLEDs) were packaged for optic characterization study. $\text{Y;Ce}^{3+}\text{:YAG}$, $\text{G;Tb}^{3+}\text{:YAG}$, $\text{R;CaAlCISiN}_3\text{:Eu}^{2+}$ was doped into such low melting temperature glass to improve the illumination and process characteristics comparing with GBPC-WLEDs and PC-WLEDs. Using 30% less phosphor amount, the optic characterization results were color coordinates (x , y) = (0.37, 0.30), quantum efficacy (Q.E) = 66.48%, color rendering index (CRI) = 86.8, correlated color temperature (CCT) = 4059 K, as color coordinates Standard Deviation Value x (STDEV x) was lower than 3×10^{-3} through the same thermal stability tests. In addition to high optic quality and low manufacture cost, such better thermal stability of glass phosphor layer may be beneficial to the many applications where the LEDs with high-power and high reliability are demanded.

9359-80, Session PWed

Measurement of refractive index distribution of photochromic materials by scanning focused refractive index microscopy

Teng-Qian Sun, Qing Ye, Xiao-Wan Wang, Jin Wang, Zhi-Chao Deng, Jian-Chun Mei, Wen-Yuan Zhou, Chun-Ping Zhang, Jianguo Tian, Nankai Univ. (China)

The improved scanning focused refractive-index microscopy (SFRIM) technique is applied to the quantitative study of photochromic materials. The refractive index (RI) distribution of methyl red sample is obtained in a reflection mode. Compared with the widely-used Z-scan method, our method provides detailed information of RI distribution rather than the mean values of the sample. The RI accuracy is 0.002, and the RI resolution is about 0.0002. The central spatial resolution of SFRIM achieves , smaller than the size of the focal spot. This technique reveals the relationship between the intensity distribution of the exciting light and the RI profile of the sample, and is furthermore an effective approach in the study of light-induced and thermal-induced index changes of methyl red. The experimental results shows that SFRIM is a promising technique in many application fields, such as optical waveguides, photosensitive materials, photochromic materials, and RI imaging in biomedical fields.

Conference 9360: Organic Photonic Materials and Devices XVII

Monday - Wednesday 9-11 February 2015

Part of Proceedings of SPIE Vol. 9360 Organic Photonic Materials and Devices XVII

9360-1, Session 1

Biopolymers in optoelectronics (*Keynote Presentation*)

James G. Grote, Air Force Research Lab. (United States); Fahima Ouchen, Univ. of Dayton Research Institute (United States); Emily M. Heckman, Air Force Research Lab. (United States); Larry R. Dalton, Univ. of Washington (United States)

No Abstract Available

9360-2, Session 1

Rare earth-DNA materials for application in electronics (*Invited Paper*)

Ileana Rau, Maria Mihaly, Cosmina Lazar, Aurelia Meghea, François Kajzar, Univ. Politehnica of Bucharest (Romania)

In the last decade an important research effort was done in materials science in order to find eco-friendly materials for different applications. A particular attention has attracted the deoxyribonucleic acid (DNA). This is mainly due to its versatility, biodegradability and abundance. It originates also from renewable resources and can be extracted from the waste produced by the food processing industry. However to provide to DNA properties necessary for practical applications it has to be functionalized with active molecules. In this respect several rare earth metals were tested in order to complex DNA by sol - gel method. The obtained new materials were characterized by spectral methods in solutions as well as in thin films. The obtained results will be presented and discussed. They show that the DNA - rare-earth complexes are potentially very promising materials for applications in electronics.

Acknowledgement

The work of Cosmina Lazar is funded by the Sectorial Operational Programme Human Resources Development 2007-2013 of the Ministry of European Funds through the Financial Agreement POSDRU/159/1.5/S/132397.

9360-3, Session 1

Iridescent organisms from nature: inspiration for reflective materials (*Invited Paper*)

Evelien De Meulenaere, Dimitri D. Deheyn, Scripps Institution of Oceanography, Univ. of California, San Diego (United States)

Many organisms use vision or photosensing to interact with others, either to avoid them, push them away, or attract them using sometimes amazing displays. From an optical sense, organisms have therefore evolved to develop properties to blend in or stand off their surrounding environment. These properties can include light production (bioluminescence) or iridescence (coloration), both of which involving (but not exclusively) specific proteins that can produce or scatter light. We will present our current research on iridescent nudibranchs (Mollusks) that appear to have reflectin-like proteins. Such proteins are usually found only in mollusks cephalopods where they are involved in the mechanisms of camouflage. Here, in the more basal nudibranchs, the reflectin-like proteins seem to be

involved in making bright colors, sometimes in association with pigments. We will present the possible mechanisms by which color is generated through the reflectin-like proteins, while also addressing the molecular and proteomic aspects of the protein, as well as applications to make organic reflective and colorful materials.

9360-4, Session 2

Measuring the coherence of organic light sources (*Invited Paper*)

Ifor D. W. Samuel, Guohua Xie, Mingzhou Chen, Yue Wang, Shuyu Zhang, Guy L. Whitworth, Fei Chen, Michael Mazilu, Kishan Dholakia, Univ. of St. Andrews (United Kingdom); Thomas F. Krauss, The Univ. of York (United Kingdom); Graham A. Turnbull, Univ. of St. Andrews (United Kingdom)

Organic semiconductors are now well established as compact and convenient light sources for displays and lighting. However, can they also exhibit significant coherence? There are very few studies of coherence of these sources, and it is highly relevant to shaping light emission from such sources to make "structured light." We report measurements of the spatial coherence of organic light-emitting diodes (OLEDs) and lasers. We also explore the effect of wavelength scale microstructure on the coherence of light emission from OLEDs.

9360-5, Session 2

From gold nanoparticles to luminescent hybrid nano-objects (*Invited Paper*)

Frederic Lerouge, Ecole Normale Supérieure de Lyon (France); Julien R. G. Navarro, Ecole Normale Supérieure de Lyon (France) and Dept. of Materials and Environmental Chemistry (Sweden); Delphine Manchon, Emmanuel Cottancin, Jean Lermé, Institut Lumière Matière (France); Cyrille Monnereau, Chantal Andraud, Guillaume Micouin, Ecole Normale Supérieure de Lyon (France); Patrice L. Baldeck, Ecole Normale Supérieure de Lyon (France) and Univ. Joseph Fourier (France); Stéphane Parola, Univ. Claude Bernard Lyon 1 (France)

One of the main goals in nano-material science lies in the design and synthesis of objects with shape and size finding their applications in many domains. In this context, gold based nanometric systems are the subject of numerous studies, in particular regarding the impact of their morphologies on their physico chemical properties such as the SPR (surface Plasmon resonance). The effects of these gold nanostructures on the photophysics of nearby molecules are very interesting, as exemplified by Surface-Enhanced Raman Scattering. A tempting objective is to find ways of optimizing metal nanostructures in such a way that specific molecular photonic signals are enhanced, as this opens perspectives for ultrasensitive detection in various applications.

In this communication we will describe the design, modeling and characterization of nanomaterials combining gold nanoparticles of different shape and size with chromophores. Two types of architecture will be presented. First we will consider nanocapsules entrapping organic chromophores¹, the final objects presenting very interesting luminescent properties². In a second part, we will describe hybrid particles with

**Conference 9360:
 Organic Photonic Materials and Devices XVII**

chromophores surrounding the gold core presenting either a spherical geometry or a sharp structure known as bipyramid³. Finally, the influence of the size and morphology of the gold part on the luminescent properties of the final objects will be discussed^{4, 5}.

- [1] F. Lux, F. Lerouge, J. Bosson et al. *Nanotechnology*, 2009, 20, 355603.
- [2] S. Zaiba, F. Lerouge, A.M. Gabudean, et al. *Nanoletters*, 2011, 11, 2043
- [3] JRG Navarro, D. Manchon, F. Lerouge, et al. *Nanotechnology*, 2012, 145707.
- [4] J.R.G. Navarro, F. Lerouge, C. Cepraga, et al *Biomaterials*, 2013, 34, 8344.
- [5] JRG Navarro, F. Lerouge, G. Micoin, et al. *Nanoscale*, 2014, 6, 5138 .

9360-6, Session 2

Low-threshold lasing from organic and polymeric microdisk printed by room temperature atmosphere ink-jet technique

Cong Chen, Soichiro Ryu, Hiroaki Yoshioka, Kyushu Univ. (Japan); Kei Yasui, Nissan Chemical Industries, Ltd. (Japan); Yuji Oki, Kyushu Univ. (Japan)

Many research works on microcavities including microdisks have progressively conducted, because they have various potential applications owing to their high storage of optical power near specific resonant frequencies leading to high quality factor (Q-factor), supporting of whispering-gallery modes (WGMs). Previously, most microdisks were fabricated by the “subtractive method” such as the lithography method with process including (i) photolithography to create a disk, (ii) etching of substrate and (iii) heat reflow to improve surface inhomogeneity. In our present study, we fabricated a microdisk by the “additive method” using ink-jet printing method, which consists of only two steps, (i) fabrication of a clad pedestal and core disk by the ink-jet technique and (ii) etching of the clad pedestal. Then we demonstrated a WGM lasing with a low threshold by LDS798 dye-doped organic and polymeric microdisk with a diameter of 75 μm. The WGM lasing by the pumping of a SHG Q-switched Nd:YAG laser was achieved with comb shape spectra at the wavelength of around 800 nm. Then a longitudinal mode width of 1.55 nm was obtained, and it is agreed with the theoretical longitudinal mode width. Furthermore, the input-output characteristics were evaluated, and a lasing threshold of 2.80 μJ/mm² was obtained at the wavelength of 806.8 nm by determination of the onset of a superlinear output. This low threshold from the ink-jet printed microdisk is comparable to that of microdisks fabricated by “subtractive method”.

9360-7, Session 2

Amplified spontaneous emission and lasing from a fluorene-based copolymer

Pradeep Chandran, Mathew Sebastian, C. P. Vallabhan, Cochin Univ. of Science & Technology (India); P. Radhakrishnan, Cochin Univ. of Science and Technology (India); V. P. N. Nampoori, Cochin Univ. of Science & Technology (India)

Organic conjugated polymers have attracted much interest due to their potential as active medium in optoelectronic applications such as light emitting diodes, electroluminescent displays, field effect transistors and solar cells. Due to their chemical tunability, they have become attractive materials in photonic applications. Spectral narrowing has been observed in conjugated polymers in various geometries such as waveguides, microcavity, micro-ring, and distributed feedback resonators and photonic bandgap structures. Conjugated polymers based on fluorene are of great interest as photonic materials because they exhibit high quantum yield, large stimulated emission cross-section and chemically tunable emission wavelengths. Poly(9,9-dioctylfluorene) (PFO) is a prototypical main-chain liquid-crystalline homopolymer that emits in the blue and exhibits polymorphic behaviour, with striking implications for its photophysical

properties. PFO and some of its derivatives such as F8BT, F8DP, PDHF, PF3Cz, 2C6BPF, PBSDFHS/PDHFPPV, PEHSAF, CPDHFPPV and certain oligofluorenes functionalized with hexyl chains have been studied for lasing due to high photoluminescence quantum yield.

PFN is used as an cathode interfacial layer/ electron injection layer in organic and polymer light emitting devices and solar cells. Here we report the observed amplified spontaneous emission (ASE) and laser emission from a fluorene based copolymer, PFN [poly(9,9-bis(3'-(N,N-dimethylamino)propyl)-2,7-fluorene)-alt-2,7-(9,9-dioctylfluorene)] in solution form in cuvette cavity, under optical pumping from third harmonic frequency of Nd:YAG laser (355 nm, 7 ns, 10 Hz). The polymer solution exhibits ASE which is verified by spectral narrowing and superlinear response of output energy versus input energy. Additionally mode structure has been observed using an air filled external cavity by introducing a quartz plate in the lasing path adjacent to the cuvette.

9360-8, Session 2

Blue phosphorescent organic light-emitting devices with a ten-fold improved operational lifetime

Jaesang Lee, Yifan Zhang, Stephen R. Forrest, Univ. of Michigan (United States)

Development of long-lived blue phosphorescent organic light-emitting devices (PHOLEDs) has long been a technological hurdle impeding the implementation of phosphorescence in full color displays and lighting. The challenge primarily stems from the intrinsic degradation mechanism inherent to PHOLEDs; i.e. energetically driven triplet-polaron annihilation (TPA) creates highly excited, “hot” polaron states in the emissive layer (EML), which in blue PHOLEDs can briefly obtain energies > 6 eV. These hot polarons have the opportunity to cleave relatively weak chemical bonds of molecules via thermal dissipation, ultimately leading to a permanent loss in luminance. In this work, we demonstrate a systematic approach to reduce TPA reactions, and thereby increase the operational lifetime of blue PHOLEDs by two strategies: modifying the conventional EML structure and stacking optically and electrically optimized devices that feature the modified EML design. As a result, we achieve a 10-fold improvement in lifetime of blue PHOLEDs compared with conventional devices, to T80 = 616±10 hrs (measured) and T50 = 3,500 hrs (extrapolated) at an initial luminance of LO = 1000 cd/m². These devices with chromaticity coordinates of [0.15, 0.29] also show an improved external quantum efficiency as high as 18.0±0.2 %. If operated at luminance levels required for mobile display applications, the blue PHOLED lifetime in this work is comparable to that of commercial green PHOLEDs. Our results confirm that the mitigation of TPA is a key to extending PHOLED lifetime while maintaining high efficiency at high brightness.

9360-9, Session 3

Nanopatterning of photoanodes for efficient light harvesting in solid-state solar cells

Jongbeom Na, Younghoon Kim, Chihyun Park, Jeonghun Kim, Eunkyong Kim, Yonsei Univ. (Korea, Republic of)

The development of nanostructured semiconductor films such as TiO₂ and ZnO is very important for highly effective photoanodes applied in light harvesting cells. Nanopatterned photoanodes were explored to optimize light dispersing and trapping for light harvesting in solid state solar cells. Mesoporous inorganic oxide film used for solid state dye-sensitized solar cells (ssDSSCs) with solid-state polymerized poly(3,4-ethylenedioxythiophene) (PEDOT) was patterned by nanoimprinting methods to give well-arrayed nanopatterns of photoelectrode. In this presentation, we report multi-layers of nanopatterned mesoporous TiO₂

films prepared from universal nanopatterning method at low cost using readily available pastes and elastomeric nanostamps. As prepared TiO₂ photoelectrodes with nanopatterned multi-layers were applied in I²-free solid-state DSSCs having highly conductive PEDOT as a hole-transporting material (HTM). The light harvesting efficiency of ssDSSCs was dramatically enhanced by multi-reflection of incoming lights at the nanopatterned layers. The optimum layer number and thickness of the nanopatterned photoanode will be discussed along with possible application of such multi-nanopatterned photoanode in other photovoltaic cells.

9360-10, Session 3

Comparing optical properties of different species of diatoms

Christian Maibohm, Søren M. M. Friis, Karsten Rottwitt, DTU Fotonik (Denmark); Yanyan Su, Univ. of Copenhagen (Denmark)

Diatoms are single cellular algae encapsulated in an external wall of micro-structured porous silica called the frustule. Diatoms are present in all water environments and contribute with 20-25 % of the global primary production of oxygen by photosynthesis. The appearance of the frustule is very species dependent with huge variety in size, shape, and micro-structure. We have experimentally investigated optical properties of frustules of several species of diatoms to further understand light harvesting properties together with common traits, effects and differences between the different frustules. We have observed, when incident light interacts with the micro-structured frustule it is multiple diffracted giving rise to wavelength dependent multiple focal points and other optical effects. Experimental results have been simulated and well confirmed by free space FFT propagation routine analysis software. The software allows us to directly import experimental images and use them as basis for simulation and allows us to extract the influence of the different elements of the frustule. The information could be used both for predicting optical properties of diatoms and by changing frustule parameters, maybe by altering growth conditions of the diatoms tailor their optical properties.

9360-11, Session 3

Optical properties of organotin sulfide clusters

Nils Rosemann, Jens Eußner, Stefanie Dehnen, Sangam Chatterjee, Philipps-Univ. Marburg (Germany)

Chalcogenide clusters and complexes in combination with various different ligands offer a large variety of structural and physical properties. By changing the elemental combinations and structures within the inorganic cores and/or the nature of the organic ligands, their properties can be tuned to fit the desired purpose, e.g., optimized light harvesting in organic solar cells[1]. To identify the impact of different ligands, we study a series of three different organotin sulfide complexes, based on the same Sn₂S₂ core but with different functional groups R1 or R2, with or without attachment of further metal complexes. The first structure consists of two (R1Sn-Cl) fragments that are bridged by 2 μ-S ligands. The other two have a central {R1₂Sn(μ-S)₂} unit that is terminated by two {Au(PPh₃)(μ-S)} groups. These units point away from the central Sn₂S₂ ring and show a trans arrangement of Cl-Sn1-S2-Au1 in case of the second structure (comprising R1) but a cis arrangement in the third structure (comprising R2).

All compounds have been investigated in respect to their absorption and luminescence in solution and in solid state phase. In solution they all show similar absorption and luminescence spectra, with absorption edge towards the UV-range. In solid state, however, they exhibit totally different morphologies, as they form crystals with clean facets and diameters of several 100 μm, in case of the first structure. The second structure on the other hand forms no clean crystal but a more thin film like phase, while the third structure forms needles. In addition to this structural changes

the optical properties change drastically, e.g., disabling optical activity or changing from optical activity to dichroism.

[1] Kershaw S.V., et al.; Chem. Soc. Rev, 2013, 42, 3033-3087

9360-12, Session 3

Electro-optic diffraction switches mediated with imidazolium ions for high bistability

Chihyun Park, Seogjae Seo, Haijin Shin, Jongbeom Na, Eunkyong Kim, Yonsei Univ. (Korea, Republic of)

Diffraction switches were explored by using reversible electrodeposition of metals in contact to imidazolium ion media. The switches showed large reflectance change and high diffraction efficiency in a pattern through a metal-deposited state and a highly transparent state, upon the applied potential. While the transparent state was quite stable and remained the state when the electrical power was turned off, the reflective state of the switches was unstable. Interestingly, the bistability at the diffractive state of this switchable devices was highly dependent on the media. By using imidazolium based media, we were able to stabilize metallic films and remained diffractive when the electrical power was turned off. Preparation and effect of composition on the bistability of an electro-optic diffraction switches will be discussed.

9360-13, Session 4

Nonlinear chromophores with NIR properties for applications in biology and defense (Keynote Presentation)

Chantal Andraud, Ecole Normale Supérieure de Lyon (France)

Two-photon excited luminescence, and photodynamic therapy are becoming promising tools for biological applications like imaging, diagnostic or even therapy. In this context, we designed chromophores, with excellent quantum yield of luminescence, or exhibiting enhanced efficiency for singlet oxygen generation, and featuring optimized biphotonic cross-section (1-3).

The use of laser sources in the NIR range (1100 -1660 nm) in optical telecommunications has stimulated the design of new systems for optical power limiting. We present properties of heptamethine cyanines and those of aza-bodipy derivatives for this type of applications; properties will be discussed on the basis of 2PA and of excited states properties (4).

(1) Bourdolle, Brustlein A. S., Fauquier T., Grichine A., Duperray A., Baldeck P. L., Andraud C., Bresselet S., Maury O. *Angew. Chem. Int. Ed.* 2012, 51, 1

(2) a) Lanoe P. H., Gallavardin T. Dupin A., Maury O.; Baldeck P. L., Lindgren M., Monnereau C., Andraud C. *Org. Biomol. Chem.* 2012, 10, 6275-6278.

(3) (a) Massin J., Charaf-Eddin A., Appaix F., Bretonnière Y., Jacquemin D., van der Sanden B., Monnereau C., Andraud C. *Chem. Sci.* 2013, 4, 2833.

(4) (a) Bouit P.-A., Kamada K., Feneyrou P., Berginc G., Toupet L., Maury O., Andraud C. *Adv. Mat.* 2009, 21, 1151; (c) Bellier Q., Makarov N. S., Bouit P.-A., Rigaut S., Kamada K., Feynerou P., Berginc G., Perry J.W., Maury O., Andraud C. *Phys. Chem. Chem. Phys.*, 2012, 14, 15299; D. Château, Q. Bellier, F. Chaput, P. Feneyrou, G. Berginc, O. Maury, C. Andraud, S. Parola J. *Mater. Chem. C*, 2014, 2, 5105.

9360-14, Session 4

From nonlinear magneto-optics to organic magnetism (Invited Paper)

André P. Persoons, Katholieke Univ. Leuven (Belgium)

**Conference 9360:
 Organic Photonic Materials and Devices XVII**

A review is given on magneto-optical properties of π -conjugated polymers, in particular regioregular poly(3-alkyl)thiophenes. The recently developed materials based upon macrocycles of thiophenes showing very large Faraday rotation in solution will be discussed. Detailed calculation on the π -electron distribution in macrocycles of regioregular and regiodefect 10-ring thiophenes will be presented and related to persistent currents as previously shown to be present in mesoscopic rings of (not superconducting) metals. SQUID measurements on these macrocycles undertaken to investigate the possibility of fluctuating magnetic moments in these new molecular structures will be presented. These could be the cause of giant Faraday rotation observed, as well as the ferromagnetism observed in regioregular poly(3-alkyl)thiophenes at cryogenic temperatures. Possible correlations between magnetic properties of macrocycles of π -conjugated thiophene rings and chirality of the macrocycles will be highlighted.

Experimental results on Faraday rotation studies from thin films of various polythiophene derivatives with high degree of regioregularity, but with random alkyl sidechains and of different morphologies will be presented. Possible correlations of the Faraday rotation and the supramolecular organization within these thin films will be discussed as derived from toroidal structures

The simple model of a particle-on-a-ring will be presented will be used to highlight the magnetic properties of organic macrocycles and cyclic structures as related to the strong Faraday rotation observed in thin films of these polymers.

9360-15, Session 4

Hybrid molecule/nanowire systems with a hyperpolarizability that approaches the fundamental limit (*Invited Paper*)

Mark G. Kuzyk, Sean M. Mossman, Washington State Univ. (United States)

Device applications require materials that have both a large nonlinear optical response and low loss. Depending on the application, other considerations become important. For example, electro-optic switching applications have the additional requirement that the dielectric constant and refractive index match to insure that the electric control pulse and the optical wave stay in step so that the switching efficiency is optimized.

Most material limitations originate in the underlying microscopic composition, which is governed by quantum mechanics. We use general quantum principles to (1) derive several device figures of merit in terms of fundamental properties of a material to show which factors are responsible and (2) predict the ideal that is attainable in the best materials, known or unknown, based on the competition between quantum processes.

Finally, we show how a hybrid system made of a molecule attached to a nanowire provides flexibility in tuning the underlying parameters in a way that optimizes the nonlinear optical response. A specific target system is proposed that should be simple to make by combining nanotechnology techniques for growing quantum nanowires and synthetic chemistry to make the ideal molecule. When the two pieces are made to interact using known adsorption phenomena, the resulting hybrid quantum system is predicted to have a record intrinsic hyperpolarizability a few percent below the fundamental limit. Since such systems should follow simple scaling laws, a larger nonlinear response should result simply by making the system larger.

We will also discuss how the hybrid structure can be adjusted through small modifications in the synthetic and fabrication process to control other material properties that optimize the relevant figures of merit.

9360-16, Session 4

Triphenylmethyl- and triphenylsilyl-based molecular glasses for photonic applications

Martins A. Rutkis, Univ. of Latvia (Latvia); Kaspars Traskovskis, Riga Technical Univ. (Latvia)

Over the last two decades increased interest in the development of organic photonics and optoelectronics is driven by demand for new cost effective high performance materials which are easy to process. The key process in manufacturing organic photonic device is preparation of uniform thin films by thermal vacuum vapor deposition or solution based methods like spin coating. For the first one high equipment and processing cost is characteristic. Solution based thin film production processes are less demanding therefore became more and more popular among researchers in field of organic photonics. Nowadays polymers and polymer composites are most intensively employed in attempts to create devices via solution based technology. Among them there has also been increasing interest in so called "organic molecular glasses" as photonic thin film materials. Compared to polymeric systems, organic molecular glasses do not need complicated chemical synthesis or purification processes and has a well-defined structure.

Within last decade our attention is paid to develop organic materials for nonlinear optical and organic electroluminescent applications. During our research it came to our attention that the presence of triphenylmethyl and triphenylsilyl substitutes noticeably enhances amorphous phase formation of low molecular weight molecules. Exploiting this molecular motif large amount of glass forming structures with different active chromophores are synthesized at RTU. Thermal, optical, electrical and electrooptical properties of these compounds are intensively investigated at ISSP UL. In this contribution we would like to present our investigation results and discuss possible structure property relations within this new class of low molecular glasses.

9360-17, Session 5

Non-linear photobleaching for optical data storage (*Invited Paper*)

Kenneth D. Singer, Cory W. Christenson, Anuj Saini, Case Western Reserve Univ. (United States); Christopher J. Ryan, Folio Photonics LLC (United States); Guoqiang Zhang, Lei Zhu, Case Western Reserve Univ. (United States); Christoph Weder, Univ. de Fribourg (Switzerland); Eric Baer, Jie Shan, Case Western Reserve Univ. (United States)

A number of recent announcements on Blu-Ray disc libraries indicate new interest in optical data storage for enterprise archival storage due to its low latency, energy efficiency, and long lifetime. To this end, a move to a scalable, high capacity medium would propel this approach. A number of approaches to terabyte scale optical media are under consideration. We have reported optical data storage in 23 layers of a 75 μ m thick periodic bilayer polymeric film using a 405nm continuous wave (CW) diode laser. This film was produced using a low-cost multilayer polymer co-extrusion, having 300nm thick writing layers separated by 3 μ m thick buffer layers. Physical layers allows high density, low-crosstalk data storage, and the use of a CW laser promises a read/write system evolved from current Blu-Ray technology.

We report here on the investigation of the nonlinear photophysics during writing, which is based on photobleaching of organic fluorophores, such as 1,4-bis(4-cyano-4-octadecyloxystyryl)-2,5-dimethoxy-benzene (C18-RG). Spots are written by pulsing a 405nm diode laser from 20ns duration and up, using various intensities. We have recently found that, at short pulse durations, the bleaching process exhibits a well-defined fluence

**Conference 9360:
Organic Photonic Materials and Devices XVII**

threshold, characteristic of the material and other writing properties. This allows for use of these films for optical data storage with a CW laser and a one-photon writing process. We interpret our results using a model of thermally activated molecular transition rates. We describe these results as well as ongoing investigations of new active nonlinear dyes and metal nanoparticles.

9360-18, Session 5
Active tunable photonics and ultrafast nonlinear optics with nematic and blue phase liquid crystals (*Invited Paper*)

Iam Choon Khoo, The Pennsylvania State Univ. (United States)

A critical review of the nonlinear optical responses of nematic as well as Blue-Phase liquid crystals for all-optical switching with femtoseconds – microseconds response speed is presented. These liquid crystalline materials have been incorporated in a multitude of novel structures to enable dynamical all-optical control of light transmission, spectral reflection, polarization states, beam shape propagation direction and other characteristic. We will discuss the merits and limitation of using nematics, and new possibilities with Blue-phase liquid crystals.

Ref.

I. C. Khoo, "Nonlinear Optics of Liquid Crystalline Materials," Physics Report 471, pp:221-267 (2009); I. C. Khoo, "Nonlinear Optics, Active Plasmonic and Tunable Metamaterials with Liquid Crystals," Progress in Quantum Electronics, Volume 38, Issue 2, pp: 77-117 (2014); I. C. Khoo and S. Zhao, "Multiple Time Scales Optical Nonlinearities of Liquid Crystals for Optical-Terahertz-Microwave Applications," Progress in Electromagnetic Research PIER, Vol. 147, page 37-56, 2014

9360-19, Session 5
Time-resolved circular dichroism: What can we learn on conformational changes? (*Invited Paper*)

Francois Hache, Lab. d'Optique et Biosciences (France)

Time-resolved circular dichroism (CD) is a powerful technique to investigate the dynamics of conformational changes in molecules and in biomolecules. Starting from a pump-probe configuration, it consists in measuring the CD of the pump-excited molecules to gain information on the relevant timescales. Complementary experiments on short (picoseconds) or longer (microseconds) timescales have been set-up based on various polarization-sensitive measurements. However, in order for this technique to be quantitative, it must rely on a priori knowledge of the CD spectra before and after photoexcitation or on some simple models. In this talk, such issues will be discussed for several experimental studies : ultrarapid conformational changes in Binaphthol molecules or in the chromophore of Photoactive Yellow Protein on the one hand ; determination of thermodynamic and kinetic parameters in microsecond thermal denaturation of poly(Glutamic acid) on the other hand.

9360-20, Session 6
Quantum dot-based organic-inorganic hybrid materials with optoelectronic functions (*Invited Paper*)

Kwang-Sup Lee, Hannam Univ. (Korea, Republic of)

Harnessing the full potential of quantum dots (QDs) in optoelectronic devices require efficient mechanisms for transfer of energy or electrons

produced in the optically excited QDs. We propose semiconducting π -conjugated molecules as ligands to achieve energy or charge transfer. The hybridization of p-type π -conjugated molecules to the surface of n-type QDs can induce distinct luminescence and charge transport characteristics due to energy and/or charge transfer effects. QDs and π -conjugated molecule hybrids with controlled luminescent properties can be used for new active materials for light-emitting diodes in flexible displays. In addition, such hybrid systems with enhanced charge transfer efficiency can be used for nanoscale photovoltaic devices. Single molecule-based electronics using QDs and π -conjugated molecule hybrids with molecular-scale n-p or n-insulating (ins)-p heterojunction structures are new promising building blocks for nanoscale electronics and quantum device concepts.

The charge transfer and energy transfer efficiencies between the n-type QD and p-type π -conjugated molecules depends on the degree of their spatial proximity and spectral overlap respectively. Along these lines, we designed and synthesized hybrid nanoparticles consisting of a CdSe/ZnS QD as a core and π -conjugated polythiophenes as well as carbazole as a shell. The nanoscale PL and molecular optoelectronic properties of hybrids consisting of QDs and π -conjugated molecules could be tuned by their relative distance and the degree of spectral overlap. The novel properties of hybrids consisting of QDs attached to π -conjugated organic molecules can be used new scientific and application fields for molecular electronics and optoelectronics, including luminescent displays and energy harvesting cells.

9360-21, Session 6
Janus tectons: a versatile platform for self-assembling chromophores on sp²-carbon based substrates (*Invited Paper*)

André-Jean Attias, Ping Du, David Kreher, Fabrice Mathevet, Univ. Pierre et Marie Curie (France); Zheng Han, Vincent Bouchiat, Institut NÉEL (France); Fabrice Charra, Commissariat à l'Énergie Atomique (France)

In view of the demanding forthcoming applications in nanotechnology, it is of prime interest to create functions out-of the plane and fully exploit the room above the substrate. Accessing the third dimension is so a mandatory step for nanooptics/electronics. Previously we introduced the Janus-like 3D tecton concept. It consists of a dual-functionalized unit presenting two faces linked by a rigid spacer: one face (A) is designed for steering 2D self-assembly, the other one (B) is a functional molecule. The objective is to take advantage of the in-plane self assembly of building blocks lying on face A to control the positioning of out-of plane active unit B, linked to the base by a rigid pillar. Here we present a series of Janus tectons incorporating chromophores ranging from fluorescent dyes to photoswitchable molecules. We will present the optical properties in solution as well as the properties of the self-assembled functional monolayers on flat sp²-carbon based substrates like HOPG and graphene

9360-22, Session 6
Two-dimensional inorganic-organic perovskite hexagonal nanosheets: growth and mechanism

Suman Lata Shakya, G. Vijaya Prakash, Indian Institute of Technology Delhi (India)

In this era of novel technological materials, inorganic-organic (IO) materials has emerged as new class of materials for their application in photonic materials, miniaturized sensors, optoelectronic devices, non-linear optical apparatus by exploiting the properties of both constituents in a single entity [1]. Here we present the formation and growth mechanism of 2D IO perovskite structures from anisotropically grown PbO hexagonal nanosheets, in three steps: Fabrication of hexagonal PbO nanosheets by the versatile bottom-up electrochemical deposition technique, iodination

**Conference 9360:
 Organic Photonic Materials and Devices XVII**

of PbO into PbI₂, followed by conversion of PbI₂ into IO hybrid by the intercalation of organic moiety. A systematic and detailed structural study reveals that PbO nanosheet formation is more likely to result from an oriented attachment mechanism [2], in which the sheets form by the reduction in surface area that happens during aggregation of small nanoparticle that each has a net dipole moment, which tends to form a self-assembled structure. Intercalation of organic moiety into the PbI₂ layers yielded a self-assembled multiple quantum-wells system of one of the IO hybrid, i.e. (C₆H₉C₂H₄NH₃)₂PbI₄ (CHPI), sustaining the hexagonal shape. These nanosheets show the visible excitonic photoluminescence peak at 518 nm.

References:

[1] Shahab Ahmad, et al , ACS Appl. Mater. Interfaces, 6 (2014) 10238.

[2] Constanze Schliehe, et al, Science 329 (2010) 550.

9360-23, Session 6

The relationship between polymer waveguide optical interconnection end facet roughness and the optical input and output coupling losses

Hadi Baghsiahi, David R. Selviah, Univ. College London (United Kingdom); Kai Wang, Richard C. Pitwon, Seagate Technology LLC (United Kingdom)

This paper presents experimental results, analysis and discussion of the relationship between polymer waveguide end facet roughnesses and their optical input and output coupling losses when used as high bit rate interconnections on optical printed circuit board backplanes. Polymer waveguide end facets were cut with a dicing saw, a one flute router. The surface roughness across the waveguide core 2D surface area was measured using an atomic force microscope. The one flute router gave the best surface quality with a roughness of 183 nm and a measured combined input and output coupling losses of 1.8 ± 0.2 dB when used at an optimum rotation speed of 15000 rpm and a translation speed of 0.25 m/min. A number of measures of surface roughness were assessed and it was established that that the input and output coupling losses is non-linearly dependent on the RMS roughness, σ , and inversely non-linearly related to the calculated autocorrelation length, T , of the roughness. The paper shows that these measures of surface roughness gave more reproducible results compared to other statistical parameters. The paper shows, for the first time, that the measured waveguide optical insertion loss including both input and output coupling losses is directly linearly proportional to the ratio of the waveguide RMS roughness to its autocorrelation length. This ratio of RMS roughness to autocorrelation length, σ/T , is defined to be a figure of merit fully quantifying the roughness from which the optical input and output coupling losses can be determined. The paper also introduces a novel end facet treatment for cut polymer waveguides to reduce the roughness after cutting and so reduce the optical input and output coupling losses.

9360-24, Session 6

Optical waveguides using PDMS-metal oxide hybrid nanocomposites

Arash Hosseinzadeh, Christopher T. Middlebrook, Michael Mullins, Michigan Technological Univ. (United States)

Polymer based optical materials have gained attention in fabrication of optical passive and active components as a result of their excellent properties such as low loss, cost, and ease in fabrication. However, optical polymers have limited range of the refraction index tuning. Combining the advantages of polymeric and inorganic optical materials is a potential route to prepare nano-composites yielding a higher range of the refractive indices while enabling the formation of active devices. In this paper a new material is proposed based on polymer-metal oxide nanocomposites for

optical components. The polymer portion of the material consists of PDMS (Polydimethylsiloxane) that contains nano-particles of suspended titanium dioxide. A refractive index as high as 1.74 has been obtained with these composites. For PDMS-TiO₂ hybrids, the higher the ratio of titanium, the higher the refractive index of the composites are. To investigate the optical properties of the new material, multimode waveguides are fabricated using soft-lithography technique. Refraction indices of the core and cladding material are controlled by the ratio of titanium oxide. Attenuation rate of the waveguides are investigated in terms of the mixing rate of PDMS and TiO₂. The new material shows a higher range of the refraction index (real and imaginary parts) that can be utilized in future optical components fabrication.

9360-25, Session 7

Diketopyrrolopyrroles-porphyrins conjugates: from Ferrari to photodynamic therapy (Invited Paper)

Frederic Bolze, Valerie Heitz, Julie Schmitt, Univ. de Strasbourg (France); Barbara Ventura, Lucia Flamigni, Istituto per la Sintesi Organica e la Fotoreattività (Italy)

Two-photon Photodynamic Therapy (2P-PDT) is a promising therapeutical method for the treatment of various disease from age-related macular degeneration to cancer. Indeed, new sensitizers sensitive to two-photon absorption are required, classical sensitizers being engineered for one-photon excitation show generally low 2P-PDT efficiency. We will describe here the synthesis and characterization of water soluble new sensitizer based on diketopyrrolopyrroles-porphyrin conjugates. Their one and two-photon photo physical properties will be described and discussed. They present high two-photon absorption cross sections up to 4000 GM at 920 nm and efficient singlet oxygen generation, over 50% for singlet oxygen generation quantum yields. Preliminary confocal and two-photon microscopy, as well as two-photon induced phototoxicity on cell culture will also be presented.

9360-26, Session 7

Evaluation and improvement of thermal stability in poled electro-optic polymers using thermally-stimulated depolarization current measurement (Invited Paper)

Akira Otomo, Isao Aoki, Chiyumi Yamada, Toshiki Yamada, National Institute of Information and Communications Technology (Japan); Ryoma Ikemoto, Dai Taguchi, Takaaki Manaka, Mitsumasa Iwamoto, Tokyo Institute of Technology (Japan)

Electro-optic (EO) modulator is the key component for making the optical communication system faster in speed and larger in capacity. Performance of the EO modulator is determined by the modulation bandwidth and driving voltage. Since dielectric constant of the EO polymer in millimeter wave is small, the EO polymer modulator has large modulation bandwidth and can be operated at 100 GHz and more. Recently, EO chromophores that have large hyperpolarizability have been developed and poled EO polymers show large EO coefficient of more than 100 pm/V. Thus, the EO polymer modulator is expected to play a key role in next generation optical communication network. However, improving thermal stability is one of the important issues for making the EO polymer modulator practical. We have successfully developed thermally stable EO polymers that have high glass transition temperature (T_g) up to 180 °C. They show excellent thermal stability with the Telcordia thermal test. Thermal stability can be improved more but it takes a long time to evaluate stability of such stable polymers with the Telcordia test. We propose thermally stimulated depolarization

**Conference 9360:
 Organic Photonic Materials and Devices XVII**

current (TSDC) measurement as a fast and reliable evaluation method for thermal stability of the EO polymers. Analyzing the TSDC, we can estimate the activation energy and relaxation time of polarization at any temperature. We will discuss thermal stability of the high T_g polymers and the validity of TSDC method for evaluating thermal stability.

9360-27, Session 7

Understanding degradation phenomena in organic photovoltaic devices

Jagdish A. K., G. Pavan Kumar, Praveen C. Ramamurthy, D. Roy Mahapatra, Gopalkrishna M. Hegde, Indian Institute of Science (India)

The unique properties of conducting polymers open up new possibilities while reliability issues in organic electronic devices are yet to be addressed. Here we study the phenomena of rupturing of polymer and electrode films in a thin film polymer diode P3HT (Poly(3-hexylthiophene-2,5-diyl)) in a device structure Glass/ITO/P3HT/Al. Simultaneous presence of electric fields and thermally induced morphological changes arising due to polymer flow are considered. The morphological changes are localized because of the device geometry-induced localized joule heating. Our experiments show that these morphological changes and consequent spatial variation in the electric fields cause two distinct deformations – rupture sites or clamps where the polymer film ruptures in a flower-like pattern, and the free region between the rupture sites where only aluminium ruptures. Further, the stresses in aluminium and polymer are analytically modelled with suitable approximations, incorporating the spatial variation of electric fields at the rupture sites and thermal distributions. Stresses in the polymer film at the rupture sites, and in the aluminium film in the free regions, are evaluated. The results of the model support the experimental findings and quantitatively predict the conditions required for optimal function in terms of geometrical parameters (thickness of Al and polymer films), temperature, thermal gradient and voltage. Rupturing occurs due to bending stress in the Al and compressive stress in the polymer. It is of further interest to study these effects under various illumination conditions, in the context of photovoltaic devices.

9360-28, Session 7

Molecular organization and phase transition at the air-water interface investigated by second-harmonic generation

Emmanuel Benichou, Aurélie Bruyère, Emilie Forel, Oriane Bonhomme, Pierre-François Brevet, Univ. Claude Bernard Lyon 1 (France)

Second Harmonic Generation (SHG), the optical process whereby two photons at a fundamental frequency are converted into one photon at the harmonic frequency, has been shown to be an ideal tool to investigate molecular organization at the nanometer scale. This sensitivity arises from its cancellation in centrosymmetric media like liquids within the electric dipole approximation. We have therefore investigated the possibility to probe this organization in molecular films formed at the air-water by SHG experiments. We show, combining surface pressure measurements and SHG, that the non-linear optical signal is sensitive to the phase transition occurring in the molecular film. Polarization analysis of the nonlinear optical intensity provides further insights into the origin of the response and we present a nonlinear correlation method to monitor the presence of supramolecular assemblies at the air-water interface.

9360-29, Session 8

Structural origins of voc tunability in ternary blend solar cells (Keynote Presentation)

Petr P. Khlyabich, Yueh-Lin Loo, Princeton Univ. (United States)

Organic bulk-heterojunction solar cells based on polymer donors and fullerene acceptors have shown remarkable efficiency increase in the last decade, with record efficiencies of almost 10%. Among the numerous approaches, recently emerged ternary blend solar cells provide an inexpensive approach to further enhance the photovoltaic performance while preserving the simplicity of active layer fabrication from solution in a single processing step. Efficiency enhancement originates from the complementary absorption of the three components in the active layer of such devices. While it was previously believed that the open-circuit voltage (Voc) in such solar cells would be pinned by the lowest energy level of the highest occupied molecular orbitals between the two polymer donors, recent studies have shown this need not be the case. In fact, ternary blend solar cells whose active layer shows strong electronic interactions between constituents exhibit Voc that is tunable depending on the blend composition. Herein, we demonstrate that the tunability of the Voc in such devices is correlated with the morphology of the active layer. Our data, obtained from the grazing-incidence X-ray diffraction (GIXD) measurements of ternary blend films, indicate that strong compatibility between the constituents in the blend is necessary to tune device Voc. Poor physical interactions between the constituents in the active layers, on the other hand, lead to pinned Voc in devices, thus supporting the organic alloy model that was put forth previously.

9360-30, Session 8

Photophysics of organic semiconductors: from ensemble to the single-molecule level

Rebecca R. Grollman, Whitney E. B. Shepherd, Alexander Robertson, Keshab R. Paudel, Oregon State Univ. (United States); John E. Anthony, Univ. of Kentucky (United States); Oksana Ostroverkhova, Oregon State Univ. (United States)

We present photophysical properties of functionalized anthradithiophene (ADT) and pentacene (Pn) derivatives, from ensemble to the single molecule level. Fluorinated and/or cyano-substituted ADT and Pn molecules, functionalized with various side groups, were imaged in several hosts using single molecule fluorescence spectroscopy (SMFS) at 532 nm and 633 nm excitation, respectively, at room temperature in air. Fluorescence quantum yields ranged between ~0.7 and 0.9, depending on the molecule and the host. Photobleaching quantum yields of guest molecules strongly depended on the host matrix and improved by up to an order of magnitude in a polycrystalline benzothioiophene (BTBTB) host as compared to polymer hosts, due to reduced oxygen diffusion into BTBTB. Total numbers of photons emitted by the molecule N_{tot} ranged between 2 and ~10 x 10⁵, depending on the derivative and on the host, with best values comparable to those for standard fluorophores for SMFS. Molecular packing of guest molecules into host matrices was investigated by polarization-dependent SMFS, which revealed that the transition dipole moment of guest molecules embedded in the BTBTB matrix is oriented close to the surface normal of our films and is constrained to a small range of polar angles; such constraints were absent in the polymer films. Subtle differences in photophysics and molecular orientation of guest molecules with different side groups were also observed. Intermolecular interactions leading to FRET and/or exciplex formation between ADT and Pn molecules were also observed and quantified.

9360-31, Session 8

Towards multicolor photolithographic structuring of organic electroluminescent displays: influence of bilayer resist processing on p-i-n OLEDs

Simonas Krotkus, Technische Univ. Dresden (Germany); Robby Janneck, Shrujan Kalkura, Alexander A. Zakhidov, Fraunhofer-COMEDD (Germany); Daniel Kasemann, Simone Hofmann, Karl Leo, Sebastian Reineke, Technische Univ. Dresden (Germany)

For organic light-emitting diodes (OLEDs) to compete with liquid crystal displays, scalable RGB pixel patterning techniques such as photolithography or ink-jet printing must be implemented. However, structuring of organic thin film devices remains a challenging task. This is mainly due to the incompatibility of organic materials with wet processing steps of traditional photolithography. We propose [1] an alternative route to photolithographic patterning of organics based on orthogonal bilayer processing. Our approach consists of using a fluoropolymer film placed below a commercial imaging photoresist. The latter is used for a UV induced pattern transfer, while the former acts as a sacrificial layer enabling lift-off in hydrofluoroether (HFE) solvents. Recently, it has been shown by our group [2] that such bilayer processing allows successful structuring of efficient Ir(ppy)₂(acac) emitter based p-i-n OLEDs comprising doped organic films.

In this work, we focus on further steps required to achieve multicolor structuring of OLEDs using our bilayer resist approach. Firstly, we show that the green p-i-n phosphorescent OLED stack is undamaged after lift-off in HFEs, which is crucial in order to achieve RGB pixel array structured by means of lithography. Furthermore, we investigate the influence of both, double resist processing on Ir(ppy)₂(acac) OLEDs and exposure of the devices to ambient conditions, on the basis of the device's electrical, optical and lifetime parameters. We test and compare several different fluoropolymer/imaging resist systems. We show that, in general, the fluoropolymer provides a good protection from the PGMEA and TMAH based solvents due to the orthogonality of the materials. However, it doesn't form a good barrier for oxygen, which is known to degrade OLEDs. We conclude, that orthogonal bilayer processing is capable of enabling multicolor pixel patterning, provided that the exposure of the devices to ambient conditions is kept short.

[1] Kleemann, H. et al. Direct structuring of C60 thin film transistors by photo-lithography under ambient conditions. *Org. Electron.* 13, 506–513 (2012).

[2] Krotkus, S. et al. Photo-patterning of highly efficient state-of-the-art phosphorescent OLEDs using orthogonal hydrofluoroethers (submitted to *Adv. Opt. Mater.*)

9360-33, Session 8

Anisotropic singlet-exciton fission in single-crystalline perfluoropentacene

Kolja Kolata, Tobias Breuer, Gregor Witte, Sangam Chatterjee, Philipps-Univ. Marburg (Germany)

The optimum performance of conventional photovoltaic devices is constrained by the Shockley-Queisser limit. However, molecular semiconductors offer the possibility for carrier multiplication schemes such as singlet exciton fission,[1] which enable efficiencies beyond this boundary. If the energy level alignment in the molecules favor this configuration, one dipole-allowed singlet exciton may be converted into two triplet states. These are parity-forbidden for individual molecules, however, once excited they may contribute to charge extraction and hence increase the quantum efficiency, eventually even above unity.

We experimentally investigate the correlation between singlet-exciton fission and the molecular arrangement by time- and polarization-resolved

pump-probe measurements. By exploiting the specific epitaxial growth relations of the prototypical organic semiconductor perfluoropentacene (C22F14, PFP) on KCl(100) and NaF(100) substrates we can optically address all three crystal axes in a single crystal by linearly polarized light independently.[2] The spectral signatures are highly anisotropic caused by a strong uniaxial delocalization of the excitations which, in turn, leads to weakened molecular selection rules. The pronounced slip stacking of the molecules along the b-axis enhances the intermolecular coupling, accompanied by delocalization of singlet excitons and direct coupling to the correlated triplet pair.[3] These findings significantly enhance the fundamental understanding of the relation between molecular arrangement and electronic response laying the foundation for future high-performance organic electro-optical devices.

1. M. B. Smith and J. Michl, *Annu. Rev. Phys. Chem.* 64, 361 (2013)

2. T. Breuer and G. Witte, *Phys. Rev. B* 83, 155428 (2011)

3. K.Kolata et al., *ACS nano* 8, 7377 (2014)

9360-34, Session 9

High-speed 3D laser printing by two-photon induced chemistry: breaking the centimeter-scale limit (*Invited Paper*)

Pablo M. Romero, Nerea O. Otero, AIMEN - Asociación de Investigación Metalúrgica del Noroeste (Spain); Olivier Stephan, Univ. Joseph Fourier (France); Kevin J. Heggarty, Télécom Bretagne (France); Maria Farsari, Foundation for Research and Technology-Hellas (Greece); Boris Chichkov, Laser Zentrum Hannover e.V. (Germany); Patrice L. Baldeck, Univ. Joseph Fourier (France) and Ctr. National de la Recherche Scientifique (France)

In late 1990's, the research community on "nonlinear organic materials and applications" first demonstrated, and then developed the technique of 3D multiphoton lithography. The high intrinsic 3D resolution results from the highly localized two-photon absorption threshold. Most 3D objects have maximum sizes in the micron to millimeter ranges as they are fabricated with microscope optics, and pulsed laser oscillators.

In this conference, we report on the high-speed fabrication of centimeter scale 3D objects using a commercial laser marking machine based on a multiwatt picosecond laser. The machine has been modified to obtain 3D layer per layer fabrication at writing speeds up to m/sec with a laser-axis resolution in the tens to hundreds micron scales. The process has been optimized by an international network including experts in laser applications, diffraction optics, and material photochemistry. For the first time, we demonstrate that two-photon induced chemistry can not only be used for 3D micro-printing, but also for macro-scale printing. In addition, as photo-induced processes are intrinsically much faster than thermal-induced processes, we report that 3D laser printing by multiphoton induced chemistry has the potential to emerge as the fastest 3D laser printing technique for diverse materials such as polymers, ceramics, metals and biomaterials.

9360-35, Session 9

Peculiarities of carrier dynamics at PEN/C60 interfaces studied by time resolved photoluminescence

Nils Rosemann, Andrea Karthäuser, Robin Döring, Tobias Breuer, Gregor Witte, Sangam Chatterjee, Philipps-Univ. Marburg (Germany)

Heterostructures of pentacene (PEN) and fullerenes are model systems for organic photovoltaics, where PEN acts as a donor and the Buckminster

**Conference 9360:
Organic Photonic Materials and Devices XVII**

fullerene (C60) acts as an acceptor. The use of organic semiconductors offers the potential of a printing like process, and thus a low-cost fabrication that is also capable of a variety of shapes [1]. The efficiency of such solar cells is governed by three processes, the creation, separation and extraction of charge carriers. The creation of charge carriers in such PEN/C60-systems is mainly governed by light absorption of PEN and a corresponding HOMO-LUMO transition. Once created, the charge carriers are separated because of the electron acceptor function of the C60 [2]. It is self-evident that this separation strongly depends on the charge dynamics on the interface between PEN and C60. To study this dynamics, we performed time resolved luminescence measurements on samples of mono- and multilayers of C60 on top of mono- and multilayers of PEN. Besides a full separation of carriers, correlated states with a prominent transient behaviour are found. These states can be related to the interface and thus give rise to a better understanding of the charge carrier separation and potential improvement of the later.

[1] Dissanayake, DM Nanditha M., et al., Appl. Phys. Lett. 90, 253502 (2007)

[2] Gorodetsky, Alon A., et al., Chem. Mater. 21, 4090-4092, (2009)

9360-36, Session 9

Time-resolved spectroscopy of charge transfer phenomena in organic solar cells

Marina Gerhard, Philipps-Univ. Marburg (Germany); Andreas Arndt, Aina Quintilla, Karlsruher Institut für Technologie (Germany); Arash Rahimi-Iman, Philipps-Univ. Marburg (Germany); Uli Lemmer, Karlsruher Institut für Technologie (Germany); Martin Koch, Philipps-Univ. Marburg (Germany)

Geminate recombination of photo-generated excitons represents a considerable loss mechanism in polymer solar cells. We apply time-resolved photoluminescence (TRPL) to study the radiative recombination which accompanies the process of charge generation. Therefore, we use a NIR-streak camera, which is sensitive for both the photoluminescence (PL) from the initially excited singlet (S1) excitons and the weaker emission from charge transfer (CT) excitons. The latter are formed at internal interfaces when the polymer is blended with a fullerene acceptor. We draw a comparison between our results for two polymers, P3HT and PTB7 respectively, which were studied in blends with the fullerene derivative PCBM. In addition, pristine films were investigated, allowing for the identification of interfacial features in the blends. For both polymers, the PL of the singlet states was rapidly quenched in blends with PCBM. In P3HT, time constants of about 40 ps were recorded for the S1 decay and related to exciton diffusion, whereas the PL of PTB7 was almost completely quenched within the first 3 ps. The decay rates of the emissive CT excitons were 2-3 orders of magnitude smaller than those of the singlet state. However, due to their slower dynamics (~ 500 ps), they could be separated from the superimposed S1 emission. The CT decay times in blends with P3HT exhibited no significant temperature dependence, indicating that thermally driven dissociation of emissive excitons is unlikely. For blends with PTB7, however, a faster decay of the CT emission was obtained at room temperature.

9360-32, Session PWed

Comprehensive photo-physics investigation of novel Corroles

Sai Santosh Kumar Raavi, Indian Institute of Technology Hyderabad (India) and Nanyang Technological Univ. (Singapore) and Istituto Italiano di Tecnologia (Italy); Jun Yin, Nanyang Technological Univ. (Singapore); Giulia Grancini, Istituto Italiano di Tecnologia (Italy); Lingamallu Giribabu, Indian Institute of Chemical Technology (India);

Cesare Soci, Indian Institute of Chemical Technology (Singapore) and Nanyang Technological Univ. (Singapore); Soma Venogopal Rao, Univ. of Hyderabad (India)

Corroles are molecules very similar to porphyrins. They have same tetrapyrrolic construction and their spectra consist of the characteristic B, Q bands [1]. Corroles have recently been subjected to intense research activity due to their salient properties finding numerous applications, straddling from antitumor therapeutic properties to catalytic and important sensor applications, for light energy conversion and singlet oxygen generation. Corroles possess stronger fluorescence properties than their porphyrin counterparts opening up the potential for their utility in diverse areas such as cancer diagnosis. The spectral, electro-chemical, and photo-physical properties make these compounds promising building blocks to be used in dye sensitized solar cells (DSSC) with superior conversion efficiency [1]. Recently, we had synthesized four novel Corroles and examined their (a) applicability for solar cell applications and (b) studied third order nonlinear optical properties using picosecond (ps) and femtosecond (fs) pulses for photonics applications [2,3]. The investigation of photo-physical properties of Corroles (and similar molecules) is imperative for their potential use. Herein we present a comprehensive study of photo-physics in four Corroles: (a) Tetraphenyl Corrole (TPC) (b) Tetratolyl Corrole) (TTC) (c) Germanium substituted TTC (GeTTC) and (d) Phosphorous substituted TTC (PTTC) achieved using fs/nanosecond (ns) transient absorption techniques and time-resolved photoluminescence studies to understand the generation and lifetimes of the triplet states. All the measurements were performed in inert atmosphere to avoid interference of oxygen. Complete details of fs and ns transient absorption data and analysis of the obtained data will be presented. The transient absorption peaks are interpreted by using natural transition orbitals (NTOs), which provides a simple orbital picture of time dependent density functional theory (TDDFT) results. The corresponding dominant NTOs clearly show its significant intramolecular charge transfer and polaron absorption character of corrole molecules. Specifically, the central Ge atom in GeTTC or P atom in PTTC molecules can act as an electron donor for given optical transitions from the ground to excited states.

References

1. D. Walker, PhD Thesis, California Institute of Technology, Pasadena, California, 2011.
2. P.T. Anusha, D. Swain, S. Hamad, T. Shuvan Prashant, L. Giribabu, S. P. Tewari, S. Venugopal Rao, J. Phys. Chem. C, 116, 17828-17837 (2012).
3. S. Hamad, S.P. Tewari, L. Giribabu, S. Venugopal Rao, J. Porphyrins and Phthalocyanines, 16(1), 140-148, 2012.

9360-37, Session PWed

Directional solidification of C8-BTBT films induced by temperature gradients and its application for transistors

Ichiro Fujieda, Naoki Iizuka, Yosuke Onishi, Ritsumeikan Univ. (Japan)

Because charge transport in a single crystal is anisotropic in nature, directional growth of single crystals would enhance device performance and reduce its variation among devices. For an organic thin film, a method based on a temperature gradient would offer advantages in throughput and cleanliness. In experiments, a temperature gradient was established in a spin-coated film of 2,7-dioctyl [1]benzothieno[3,2-b]benzothiophene (C8-BTBT) by two methods. First, a sample was placed on a metal plate bridging two heat stages. When one of the heat stages was cooled, the material started to solidify from the colder region. The melt-solid interface proceeded along the temperature gradient. Cracks were formed perpendicular to the solidification direction. Second, a line-shaped region on the film was continuously exposed to the light from a halogen lamp. After the heat stage was cooled, cracks similar to the first experiment were observed, indicating that the melt-solid interface moved laterally. We fabricated top-contact, bottom-gate transistors with these films. Despite

**Conference 9360:
Organic Photonic Materials and Devices XVII**

the cracks, field-effect mobility of the transistors fabricated with these films was close to $6\text{cm}^2/\text{Vs}$ and $4\text{cm}^2/\text{Vs}$ in the first and second experiment, respectively. Elimination of cracks would improve charge transport and reduce performance variation among devices. It should be noted that the intense light from the halogen lamp did not damage the C8-BTBT films. The vast knowledge on laser annealing is now available for directional growth of this type of materials. The associated cost would be much smaller because an organic thin film melts at a low temperature.

9360-38, Session PWed

Fabrication of Au nanoparticle monolayer embedded in the photoactive layer using oxygen plasma to improve the efficiency of organic solar cell

Sun-Joo Park, Kwan-Yong Lee, Do-Hyun Kim, Cheolsang Yoon, Hyoungjun Jeon, Kangtaek Lee, Young-Joo Kim, Yonsei Univ. (Korea, Republic of)

Metal nanoparticles (NPs) have been known as plasmonic sources to improve relatively low optical absorption in the organic photovoltaic devices. Based on our simulation, it was confirmed that Au NPs monolayer inside the photoactive layer can improve the power conversion efficiency (PCE) by a localized surface plasmonic resonance (LSPR) effect. To realize this novel structure of photoactive layer with Au NP monolayer in the central region, we tried the alternative spin-coating processes with a half thickness of photoactive layer and NP monolayer. However, there were two fabrication difficulties; 1) the resolving of bottom half layer(L1) during the deposition of top half layer(L2), and 2) the non-uniform deposition of Au NPs dissolved in ethanol on L1 layer due to its hydrophobic property. To solve these two difficulties, we introduced the O₂ plasma treatment on the L1 layer to produce the hydrophilic property as well as to make a barrier layer on L1 to prevent the dissolving of L1 during the deposition of L2 layer. Thus the novel structure of Au nanoparticle monolayer embedded in the photoactive layer at the central position was fabricated successfully with careful control of O₂ plasma conditions such as 60sec treatment with the power of 50W, and its microstructure was confirmed by SEM measurement. Actually, the optical absorption was improved in the range of 550-750nm wavelength, which confirms the LSPR effect of Au NPs in the photoactive layer. In addition, the J_{sc} characteristics resulted in the 15% improvement from 10.92mA to 12.47mA with the increase of PCE.

9360-39, Session PWed

Symmetry breaking and birth of chirality in molecular film at the air/water interface: an approach with nonlinear optics

Aurélie Bruyère, Emmanuel Benichou, Univ. Claude Bernard Lyon 1 (France); Pierre-François Brevet, Institut Lumière Matière (France)

Chirality is an important issue in chemistry, biology and material science. This symmetry property can be observed at different scales, from the molecular to the supramolecular level. Recently, it has been shown that achiral amphiphilic dyes can form chiral molecular aggregates at the air/water interface during the monolayer compression. The exact mechanism of chirality formation, spontaneous or compression-induced, is still an open question. To give an insight into the origin of this induced chirality, we report examples of chiral aggregation and non-aggregated molecules at the air/water interface. The first example is given by achiral molecules known to form chiral Langmuir-Schaefer film. The second example reports studies of binaphthyls, chiral molecules.

The chirality of the Langmuir monolayer at different surface densities was measured in-situ at the air/water interface using the Surface Second Harmonic Generation (SSHG), which has proven in the past to be a powerful

surface sensitive tool. Indeed, this technique, based on the conversion of two photons at a fundamental frequency ω into one photon at the harmonic frequency 2ω , is surface sensitive at interfaces between two centrosymmetric media. Hence, the approach is non-invasive and can be used to investigate both structure and dynamics at such surfaces and interfaces. Its combination with a Langmuir trough allows non-linear optical studies with a precise control of the average surface density of amphiphilic compounds spread at the liquid surface.

9360-40, Session PWed

Optical absorption and photoluminescence properties of perylene single-crystals

Andre Rinn, Andre Pick, Gregor Witte, Sangam Chatterjee, Philipps-Univ. Marburg (Germany)

We investigate the optical properties of the prototypical organic semiconductor perylene, used, e.g., as a blue-emitting dopant in light-emitting diode. It crystallizes in two different phases [1]: the alpha phase with a monomeric herringbone structure containing two molecules in its primitive unit cell, whereas the beta phase features double that number with a dimeric herringbone configuration. An ensemble of single-crystals is grown in silicon oil exhibiting excellent structural quality. The lateral dimensions allow for addressing individual crystallites which feature atomically flat surface without molecular steps, yet they are thin enough to enable transmission experiments. We perform polarization-resolved linear absorption spectroscopy in an achromatic microscopy setup featuring 0.45 numerical aperture all-reflective optics at temperatures of 10K. These reveal pronounced crystal-related resonance at energies below the single-molecule HOMO-LUMO gap which we determine in the vapor phase. The alpha phase shows a significantly more complex response than the beta phase. This is attributed to the larger unit cell containing twice as many molecules. The polarization resolved response in both cases, however goes beyond the standard Davydov-splitting of the exciton [2]. In addition to this commonly expected coupling between neighboring molecules, we observe both longitudinal and transversal exciton-polariton modes. The Davydov-coupling is manifested by the shift of the lowest energy transitions to higher energies due to coupling of the two parallel dimers in the larger unit cell of the α phase. Time-resolved photoluminescence data are acquired using a streak camera and show indications of excimer formation [3].

[1] A. Camerman and J. Trotter, Proc. Roy. Soc. A, 279,129 (1964)

[2] M. A. Bayoumi et al., Pure Appl. Chem. 11, 371 (1965)

[3] H. Auweter et al., Chem. Phys. Lett. 85, 325 (1982).

9360-41, Session PWed

Optical tweezers-based probe of charge transfer in organic semiconductors at microscopic scales

Rebecca R. Grollman, Jacob Busche, Oksana Ostroverkhova, Oregon State Univ. (United States)

We present a novel non-contact technique to study exciton dissociation and intermolecular charge transfer depending on the local environment, which has a potential to achieve elementary charge resolution. Micron-sized silica spheres were coated with organic semiconductor molecules or their donor-acceptor (D/A) blends and suspended in liquids with dielectric constants ranging between 2 and 80. The coated spheres were trapped using optical tweezers, and the surface charge was measured by analyzing Brownian motion of the trapped sphere in the presence of an applied AC electric field. Surface charge of <10 elementary charges was obtained on spheres coated with functionalized anthradithiophene (ADT) derivatives in water and in toluene. This measurement was combined with fluorescence imaging of the trapped sphere and in-situ measurement of electric field-dependent fluorescence to monitor Frenkel and/or charge transfer exciton

Conference 9360:
Organic Photonic Materials and Devices XVII

dissociation in the organic semiconductor coating. Feasibility of such measurements using spheres coated with functionalized ADT and pentacene derivatives as well as their D/A blends was demonstrated. Simultaneous measurements of surface charge and fluorescence from the coated spheres enable us to probe exciton dissociation followed by charge exchange with the environment, depending on the applied electric field, dielectric constant of the environment, and the properties of the acceptor molecules in the environment.

9360-42, Session PWed

Analysis of light scattering in SI-POFs by using side illumination technique

Iñaki Bikandi, Univ. del País Vasco (Spain)

One of the issues that affects the performance of plastic optical fibers (POFs) is the light scattering caused by the presence of inhomogeneities in the polymer, which is responsible for the optical energy loss and for the mode coupling in POFs. The aim of this work is to compare two different methods for measuring light scattered in step index polymer optical fibers (SI-POF) by using the side illumination technique. On the one hand, scattered intensity, as well as near and far field patterns at single wavelength have been measured by varying the launching conditions: position of the excitation spot in the fiber and incidence angle. On the other hand, we have measured the spectral distribution of the scattered light in SI-POFs by exciting the fiber with a supercontinuum source. A theoretical model based on Mie theory has been used to analyze the obtained experimental results. From this analysis, the size and position of the most influential scattering centers in step-index POFs can be estimated. The results obtained employing both methods have been compared, resuming the advantages and drawbacks of each one for characterizing the optical quality on SI-POFs.

9360-43, Session PWed

Charge separation in OPV bulk heterojunctions

Andrew B. Matheson, Arvydas Ruseckas, Ifor D. W. Samuel, Univ. of St. Andrews (United Kingdom)

Here we use polarization sensitive transient absorption to study the dynamics of photogenerated holes in two different photovoltaic blends (P3HT:PC60BM and PTB7:PC70BM) over a wide time range from femtoseconds to 1 nanosecond. In P3HT:PC60BM, kinetics following charge generation show no dependence on excitation energy and an initial fast depolarization of the hole polaron signal following electron transfer, followed by a much slower depolarization on a timescale of several nanoseconds [1].

In a PTB7:PC70BM blend we observe a time dependent charge recombination rate, consistent with a charge mobility which rapidly decreases. We therefore conclude that the efficient separation of polaron pairs is due to initial high polaron mobility, as opposed to excess energy.

[1] Matheson et al. J.Phys. Chem Lett. 2013, 4, 4166-4171

9360-45, Session PWed

Thermally-induced third-order optical nonlinearity of Aniline blue diammonium salt investigated by Z-scan technique for nonlinear optical applications

Poornesh P, Manipal Univ. (India); Pramodini S. Sandhya, Manipal Institute of Technology (India)

We present the results of thermally induced third-order optical nonlinearity and optical limiting performance of an organic dye Aniline blue diammonium salt. Single beam Z-scan technique was used to determine the sign and magnitude of the absorptive and refractive nonlinearities. Continuous wave (CW) He-Ne laser operating at 633nm was used as source of excitation. The nonlinear refractive index n_2 , the nonlinear absorption coefficient β_{eff} and the third-order optical susceptibility $\chi^{(3)}$ were found to be of the order 10^{-5} esu, 10^{-3} cm/W and 10^{-7} esu respectively. The observed large third-order optical nonlinearity in the dye is due to the presence high π -electron density in the backbone of the molecular structure. Self-diffraction rings pattern were observed in the dye and it is due to the refractive index change and thermal lensing. The dye exhibits good optical power limiting characteristics at the experimental wavelength 633nm. Optical power limiting and clamping studies were carried out at various input power levels. Optical clamping of about - 3mw and limiting threshold of 5-mw was observed. The nonlinear optical studies indicate that the dye investigated here materialize as a promising candidate for nonlinear optical devices applications such optical power limiters.

9360-46, Session PWed

Effect of acid dopants in gellan gum gel polymer electrolytes and the performance in an electrochemical double-layer capacitor

Y. N. Sudhakar, M. Selvakumar, Manipal Institute of Technology (India)

A proton-conducting biodegradable gellan gum gel polymer electrolytes (GPEs) has been prepared by using three different dopants such as ortho-phosphoric ($\text{o-H}_3\text{PO}_4$), sulfuric (H_2SO_4) and hydrochloric acids (HCl). The GPEs were cross-linked using borax. The polymeric gels were characterized by spectroscopic, thermal, ionic conductivities and dielectric measurements. Proton conductivity was in the range of 2.1×10^{-2} to 4.7×10^{-3} S cm⁻¹ and activation energies were between 0.34 meV and 0.49 meV, at different temperatures. The H_3PO_4 doped GPE exhibited thermal stability at varying temperature. The polymer electrolyte with the highest ionic conductivity applied to fabricate symmetrical supercapacitor (DSSC) and its shows the highest specific capacitance of 146 F/g at 2 mVs⁻¹.

9360-47, Session PWed

Preparation and properties of graphene sheets coupled with magnetic nanoparticles

Yi-Seul Han, Hannam Univ. (Korea, Republic of); Kyung Eun Lee, KAIST (Korea, Republic of); Sung-Hyun Kim, Hannam Univ. (Korea, Republic of); Sang-Ouk Kim, KAIST (Korea, Republic of); Ji-Hwan Park, Kwang-Sup Lee, Hannam Univ. (Korea, Republic of)

The pioneering experiments in graphite exfoliated-graphene sheets by Geim et al established its potential to surpass and substitute many best performing electronic and photonic alternatives. The chemical and electronic properties of graphene can be modulated by effective coupling of this material with other nanomaterials. A successful functionalization strategy would be one that would leave the graphene surface unperturbed and preserves its much valued electronic properties. We present the design and application of pyrene based ligands which couple nanomaterials to graphene surface through π - π stacking. We have successfully developed novel synthetic routes of the pyrene-dopamine systems tethered to γ -Fe₂O₃. Iron oxide intercalated graphene composites are highly desirable materials for energy storage. In this presentation, we will report design, synthesis and properties on various optoelectronic and magnetic organic-inorganic hybrid systems.

9360-48, Session PWed

Growth, characterization and molecular hyperpolarizabilities of 1-(5-chlorothiophen-2-yl)-3-(2,3-dimethoxyphenyl)prop-2-en-1-one single crystal: a superior NLO organic material

Ashwatha N. Prabhu, Vyasa Upadhyaya, Manipal Institute of Technology (India)

A novel superior characteristic nonlinear optical (NLO) organic material, 1-(5-chlorothiophen-2-yl)-3-(2,3-dimethoxyphenyl)prop-2-en-1-one [CTDMP], has been synthesized and grown as a good-quality single crystal by the slow evaporation solution growth technique. The grown crystals were characterized by FT-IR, single-crystal X-ray diffraction (XRD), differential scanning calorimetry and UV-Visible spectroscopy. Single beam Z-scan technique was employed to study the third order NLO properties of the material. The nonlinear refractive index is found to be of the order of 10⁻¹¹ cm² W⁻¹ [1]. The magnitude of third order susceptibility is of the order of 10⁻¹³ esu. The observed increase in the third order nonlinearity in these molecules clearly indicates the electronic origin. The compounds exhibit good optical limiting at 532 nm, is due to the substituted strong electron donor. The mechanical property of the grown crystals was studied using Vicker's micro hardness tester and the load dependence hardness was observed. CTDMP belongs to the monoclinic crystal system with space group P2₁/c [2]. The morphology of CTDMP single crystal was indexed using the XRD data as input to the morphology indexing computer program (WinXMorph). To support the observed variation in the experimental NLO property the static second and third order NLO hyperpolarizabilities of the chalcone derivative was computed using semiempirical MOPAC 2012 computer program.

[1] A.N. Prabhu, V. Upadhyaya, A. Jayarama, K. Subrahmanya Bhat "Synthesis, growth and characterization of p conjugated organic nonlinear optical chalcone derivative" Materials Chemistry and Physics 138 (2013) 179e185.

[2] A. N. Prabhu, A. Jayarama, Ravish Sankolli, T. N. Guru Row and V. Upadhyaya "(2E)-1-(5-Chlorothiophen-2-yl)-3-(2,3-dimethoxyphenyl)prop-2-en-1-one", Acta Crystallogr. E67(2011) 2665.

9360-49, Session PWed

Growth and characterization of a new nonlinear optical organic crystal: 2,4,6-trimethylacetanilide

Vyasa Upadhyaya, Manipal Institute of Technology (India); Sharada G. Prabhu, NMAM Institute of Technology (India)

A new nonlinear optical organic material, 2,4,6-trimethylacetanilide (246TMAA), also known as N-[2,4,6-trimethylphenyl]acetamide, has been synthesized and grown as a single crystal by the slow evaporation technique by organic solvents. The grown crystals have been characterized by morphology study. The crystals are prismatic. Surface examination shows granular dendritic pattern in optical micrograph. The Scanning Electron Micrograph shows the layered growth of the crystal. The Differential Scanning Calorimeter plot shows no phase change until melting point (219°C). The density of the crystals is 1.1g/cc and the crystals are soft. The crystals are transparent in the visible region and in the ultra-violet region till 280 nm. 246TMAA crystallizes with 2 molecules in a monoclinic unit cell in the non-centrosymmetric point group m, space group Pn [1]. Refractive indices of this optically biaxial crystal along the three crystallo-physical axes have been measured at 633 nm. The optical second harmonic generation efficiency of the crystal at 1064 nm is about half that of the urea crystal, measured by powder method using Nd:YAG laser. The results show that the 246TMAA crystal can efficiently be used for up-conversion of infrared radiation into visible green light.

[1] V. Upadhyaya et al, Acta. Cryst. E58 (2002) o997.

Conference 9361: Ultrafast Phenomena and Nanophotonics XIX

Sunday - Wednesday 8-11 February 2015

Part of Proceedings of SPIE Vol. 9361 Ultrafast Phenomena and Nanophotonics XIX

9361-1, Session 1

Ultrafast plasmon dynamics in graphene *(Invited Paper)*

Francisco Javier García de Abajo, ICFO - Institut de Ciències Fotòniques (Spain)

Plasmons in graphene feature several advantages with respect to more conventional materials, including a large electro-optical tunability and extreme optical-field enhancement, which are suitable building blocks to produce complete optical absorption, extreme light modulation, and ultra sensitive response down to the single-molecule level. We will explore plasmons in graphene and graphene related materials, including the ultrafast dynamics that rule their decay into other excitations, as well as their transient evolution during high optical pumping.

9361-2, Session 1

Imaging carrier transport in one-dimensional nanoscale devices using femtosecond photocurrent microscopy *(Invited Paper)*

Yeong Hwan Ahn, Ajou Univ. (Korea, Republic of)

Investigation of carrier dynamics with an ultrashort time scale is one of the primary steps necessary for developing high-speed electronic devices. Femtosecond photocurrent microscopy enables a direct visualization of ultrafast carrier motions in nanoscale devices, such as Si nanowire (NW) and carbon nanotube (CNT) field-effect transistors. Here, we focus on transit times of ultrashort carriers that are generated near one metal electrode and subsequently transported toward the opposite electrode based on drift and diffusion motions. We measured the transit times for the devices with different channel lengths (1 – 10 μ m) and found that the transit time of CNT devices is much shorter than that of Si NWs, because of the higher CNT mobility. We observed drift-like motion in Si NWs, in which the average velocity did not change noticeably with changes in the channel length. More importantly, the carrier dynamics have been measured for various working conditions that strongly modify the electronic band structures of NWs. In particular, gate-dependent measurements reveal that the carrier velocity changes linearly with the applied gate bias in accordance with changes in the electric field strength in the Schottky barrier. We also found that the localized potential imposed by the electrodes results in the tailoring of electrical pulse shape. Based on these results, it will be possible to design novel devices in which we create ultrafast carrier pulses and simultaneously control their dynamics.

9361-3, Session 1

Q-switched fiber laser based on carbon nano wall saturable absorber

Soichiro Omi, IHI Corp. (Japan) and Kyushu Univ. (Japan); Norihito Kawaguchi, IHI Corp. (Japan); Yuji Oki, Kyushu Univ. (Japan)

Carbon nano materials such as carbon nano tube (CNT) and graphene have been reported as good saturation absorption for passive mode-locked laser in previous study. CNT and graphene has short relaxation time compared to semiconductor saturable absorber. Especially graphene has high response speed compared to CNT, and has no absorption peak, due to the unique

band structure. But monolayer graphene has only 2.3% absorption. If we want to get more high absorption, multi-layered graphene was one of a solution to this request.

But, it has been pointed out that depression of modulation depth due to the increase in a number of layers of graphene.

We propose new material, called carbon nanowall (CNW), as saturable absorber. CNW is vertically aligned nanographite sheets on Si substrate synthesized by plasma-enhanced chemical vapor deposition technique.

This structure is expected that has high absorption and modulation depth.

In this study, we report an optical characteristic of CNW saturable absorber and Q-switched laser operation using this saturable absorber. A polyimide thin film, with incorporated carbon nanowall, coated by spin-coating method, is used as saturable absorber. Linear absorption spectrum of carbon nano-walls was observed without absorption peak wavelength range from 1000 to 2000nm. Modulation depth of carbon nanowall saturable absorber was measured with wavelength of about 1560nm. Q-switch laser operation with carbon nanowall saturable absorber and erbium-doped optical fiber was demonstrated.

9361-4, Session 1

Efficient Auger scattering in Landau-quantized graphene

Florian Wendler, Technische Univ. Berlin (Germany); Martin Mittendorff, Stephan F. Winnerl, Manfred Helm, Helmholtz-Zentrum Dresden-Rossendorf e. V. (Germany); Andreas Knorr, Ermin Malic, Technische Univ. Berlin (Germany)

We present theoretical and experimental investigations of the ultrafast carrier dynamics in Landau-quantized graphene. The calculations are based on microscopic modeling of the carrier-light, carrier-carrier, and carrier-phonon interactions within the framework of the density matrix theory. Experimentally, the carrier dynamics is accessed by differential transmission spectroscopy with circularly polarized light.

Landau-quantized graphene obeys specific selection rules for circularly polarized light allowing to selectively address single Landau level transitions. We explore the relaxation dynamics in the three energetically lowest Landau levels by microscopic modeling and by measuring differential transmission spectra for all four possible combinations of pump and probe pulse polarization. This reveals a broken electron-hole symmetry accompanied by an unexpected sign of one of the four experimental signatures. While the former can be explained by a finite doping of the system, the latter is a direct consequence of strong Auger scattering in the system. Both theoretical modeling as well as experimental measurements reflect well this behavior and are in excellent agreement.

Furthermore, Auger scattering bridging valence and conduction Landau levels gives rise to a change of the charge carrier density. Our microscopic calculations reveal the occurrence of a significant carrier multiplication under certain experimentally controllable conditions.

9361-5, Session 1

Optical nonlinearities in few-layer gallium selenide

Lasse Karvonen, Antti Säynätjoki, Aalto Univ. (Finland); Seyed Soroush Mehravar, College of Optical Sciences, The Univ. of Arizona (United States); Raul D. Rodriguez, Susanne Hartmann, Dietrich R. T. Zahn, Technische Univ.

**Conference 9361:
Ultrafast Phenomena and Nanophotonics XIX**

Chemnitz (Germany); Seppo K. Honkanen, Univ. of Eastern Finland (Finland); Robert A. Norwood, College of Optical Sciences, The Univ. of Arizona (United States); Nasser N. Peyghambarian, College of Optical Sciences, The Univ. of Arizona (United States) and Aalto Univ. (Finland) and Univ. of Eastern Finland (Finland); Khanh Q. Kieu, College of Optical Sciences, The Univ. of Arizona (United States); Harri Lipsanen, Juha Rikonen, Aalto Univ. School of Science and Technology (Finland)

Graphene is an interesting layered material, but its zero band-gap induces strong optical absorption, which limits its applicability in photonics, particularly in integrated optics. Therefore the research field of non-graphene layered photonic semiconductors is now growing rapidly. Bulk gallium selenide (GaSe) is a well-known material for nonlinear optics and GaSe crystals have been used for second-harmonic generation (SHG) at near- and mid-infrared (IR) wavelengths. GaSe is a layered semiconductor with a band-gap of 2.1 eV and therefore transparent at near IR wavelengths. The optical nonlinearities of GaSe flakes with different numbers of layers were investigated using multiphoton microscopy at an excitation wavelength of 1560 nm, relevant for telecommunications. Strong second- and third-harmonic generation (THG) were observed in few-layer GaSe flakes. The SHG and THG signals showed clear contrast for different numbers of GaSe layers; even fourth-harmonic generation was detected from a ~40-nm-thick flake. Second-, third-, and fourth-harmonic generation was confirmed by spectral analysis. The third-order optical nonlinearity coefficient $\chi^{(3)}$ was estimated to be on the order of 10^{-8} esu. Strong nonlinear characteristics reported here for few-layer flakes demonstrate that GaSe is an intriguing material for all-optical signal processing, even as few atomic layer films. These results can contribute to the development of GaSe thin-layer flakes for next generation nonlinear photonics applications satisfying the continuous need for device miniaturization and integration.

9361-6, Session 2

Pulse shaping of the intense few-cycle terahertz pulses for nonlinear spectroscopy (*Invited Paper*)

Masaya Nagai, Osaka Univ. (Japan)

The carrier-envelope phase (CEP) of few-cycle pulses strongly affects nonlinear optical phenomena such as high harmonic generation in gases. It has been developed to stabilize and control CEP of extremely short pulses at visible, mid-infrared and near-infrared frequencies, but usually require large complicated equipment. Intense few-cycle terahertz (THz) pulses can be generated with inherently locked CEP and field amplitude exceeding 1 MV/cm, enabling materials analysis by various forms of nonlinear THz spectroscopy. Although CEP is also fundamental to THz pulses, practical control has been missing. Here we propose a simple passive component for controlling CEP of few-cycle THz pulses. It is based on the THz pulse propagating with group velocity different from the phase velocity. This technique also applies to a new achromatic wave plate available for few-cycle THz pulses. Using these components, we perform nonlinear spectroscopy of various materials, such as a semiconductor. This THz pulse-shaping technique will facilitate phase-sensitive nonlinear spectroscopy and coherent control in condensed matter.

9361-7, Session 2

Elucidating photodynamics with ultrafast pulse sequences: pump-repump, multidimensional spectroscopy, and beyond (*Invited Paper*)

Patrick Nürnbergger, Ruhr-Univ. Bochum (Germany) and

Julius-Maximilians-Univ. Würzburg (Germany); Stefan Ruetzel, Tobias Brixner, Julius-Maximilians-Univ. Würzburg (Germany)

We demonstrate how diverse femtosecond spectroscopy approaches coalesce to a comprehensive understanding of the photochemical reaction pathways of a molecule. Two ring-open forms of the merocyanine 6-8-dinitro-BIPS coexist in solution, differing by a cis/trans configuration of a double bond. Pump-probe transient absorption spectroscopy shows that both isomers may undergo a photo-induced ring closure, whereas coherent two-dimensional (2D) electronic spectra directly visualize that cis/trans isomerization among the isomers is a negligible reaction channel.

Via pump-repump-probe spectroscopy, the photodynamics accessible by further excitation are explored and the formation of a radical cation species is identified. By combining the benefits of pump-repump-probe with coherent 2D spectroscopy, we then introduce coherent triggered-exchange 2D (TE2D) electronic spectroscopy, so that reactants can be connected with products formed by the repump pulse after the pump sequence but before the probe event. This approach unveils that only one of the isomers is the reactant from which the radical cation is formed. TE2D electronic spectroscopy thus is a versatile tool for analyzing excited states and associated reaction pathways, with the information from where the reaction started intrinsically preserved.

Further studies employing third-order three-dimensional (3D) spectroscopy on the similar compound 6-nitro-BIPS directly visualize the photochemical connectivity between molecular species and disclose coherent molecular motion involved in the photochemical reaction. Hence, 3D spectroscopy not only provides an intuitive picture for which reactants can be turned into which products, but also exposes the reactive molecular modes connecting them.

9361-8, Session 2

Detection of dark-state relaxation through twodimensional nanooptical spectroscopy

Markus Krecik, Sven M. Hein, Technische Univ. Berlin (Germany); Mario Schoth, TU Berlin (Germany); Marten Richter, Technische Univ. Berlin (Germany)

Nanoplasmonic structures are nowadays capable of manipulation and concentration of light on a subwavelength scale. Apart from electric field enhancements, field gradients over few nanometers can be created, opening a possibility to observe dipole-forbidden transitions.

On the other hand, coherent multidimensional spectroscopy allows, beside other applications, for analysis of coupling and population-transfer processes between energy levels.

Thus it can be used for studying relaxation processes in nanostructures and molecules, important for the understanding of new nanotechnological devices or biological processes like photosynthesis. An important relaxation process is the exciton-phonon interaction in nanostructures. Herein, non-secular relaxation processes convert different coherences into each other. Usually, they are neglected in the secular approximation since energy-conserving secular processes dominate the relaxation.

Through the combination of coherent spectroscopy and nanoplasmonics, we provide a way for detection and study of non-secular processes. For this purpose, a quantum emitter is placed in a plasmonic structure. Depending on the polarization of the exciting pulse, electric field gradients are created. Thus optical selection rules can be lifted on demand and excitation of dipole-forbidden states become allowed. Multidimensional spectroscopy with an appropriate choice of non-gradient and gradient-enforcing pulses yields only a signal upon the occurrence of non-secular relaxation.

Potential applications for the detection scheme include structures like dye, photosynthetic pigments etc. We illustrate the protocol on a spherical CdSe quantum dot with photoelectron detection as a measurement technique.

9361-9, Session 2

Signatures of Förster and Dexter transfer processes in coupled nanostructures for linear and two-dimensional coherent optical spectroscopy

Judith F. Specht, Marten Richter, Technische Univ. Berlin (Germany)

In Coulomb coupled quantum systems, two different mechanisms of resonance energy transfer between nanostructures arise: Förster and Dexter interaction. We show that the signals obtained by linear and two dimensional coherent spectroscopy reveal the nature of the exciton transfer processes occurring between two coupled quantum emitters.

Both Förster and Dexter processes transfer the excitation energy from an initially excited donor to an acceptor and thus cause a delocalization of the excitonic states of the coupled system. However, the underlying mechanisms differ strongly: Förster transfer describes a purely dipole-dipole mediated exciton transfer between two nanostructures. For semiconductor quantum dots, it can either transfer or flip the spin state of the excited electron. Dexter transfer denotes an exchange of electrons between the nanostructures and therefore requires an electronic wave function overlap.

According to the selection rules for electronic transitions, the polarizations of the exciting laser pulses determine the possible excitation pathways in a specific material system. Since Förster energy transfer in quantum dots depends on the interband dipole orientations, spin preserving and spin flipping Förster coupling strengths can be controlled by varying the mutual orientation of the two quantum emitters. In contrast to Förster coupling, Dexter coupled biexcitonic states are not limited by the optical selection rules. The variety of excitation and coupling characteristics determines the optical signatures.

We show that spectroscopic signals thus allow to deduce the type of excitation transfer processes and the underlying selection rules.

9361-10, Session 3

Excitonic dark states in single atomic layer of tungsten disulfide (*Invited Paper*)

Ziliang Ye, Ting Cao, Kevin O'Brien, Hanyu Zhu, Univ. of California, Berkeley (United States); Xiaobo Yin, Univ. of Colorado at Boulder (United States); Yuan Wang, Steven G. Louie, Xiang Zhang, Univ. of California, Berkeley (United States)

Recently, transition metal dichalcogenide monolayer shows promising potentials for semiconducting optoelectronic devices. One example is tungsten disulfide (WS₂). When thinned down to a monolayer, WS₂ transforms from an indirect band gap to a direct band gap semiconductor, enabling an intense light-matter interaction. Nevertheless, the fundamental band gap size is still under heated debate. The observed optical resonance was initially considered to be band-to-band transitions. Nevertheless, first-principle calculations predicted a much larger quasiparticle band gap size and an optical response that is dominated by excitonic effects. Here, we measure the two-photon excitation spectrum and discover a series of excitonic dark states in single-layer WS₂, which has a very unusual non-hydrogenic energy series. Together with GW-BSE theory, these strong excitonic dark states prove the excitons are Wannier excitons with extraordinarily large binding energy (-0.7 eV).

If electrons and holes in semiconductors interact through Coulomb potential, the electron-hole pair forms a series of excitonic Rydberg-like states with definite parity. Incident photons can excite the electronic system from the ground state to one of these excitonic states. In addition to energy conservation, the selection rule also depends on the symmetry of the final state: one-photon transitions can only reach excitonic states with even parity, while two-photon transitions reach states with odd parity. Owing to

the direct band gap in TMDC monolayer, the excited exciton relaxes to the lowest exciton and induces luminescence. By measuring the two-photon-induced-luminescence while scanning the excitation laser energy, we obtain a complete two-photon excitation spectrum.

9361-11, Session 3

Environmental effects in relaxation pathways of 1D and 2D nanostructures (*Invited Paper*)

Libai Huang, Purdue Univ. (United States)

I will present our recent work on transient absorption microscopy (TAM) as a novel tool to image carrier and phonon dynamics in single nanostructures with simultaneously high spatial (~200 nm) and temporal resolution (~200 fs). We have applied TAM to probe environmentally-dependent energy relaxation pathways in single-walled carbon nanotubes and graphene. We observed that the hot phonon effect occurs at much lower excitation intensity for suspended graphene compared to substrate-supported graphene. These results show the importance of the environment in controlling the properties of graphene. We have successfully demonstrated structure-specific transient absorption imaging of single-walled carbon nanotubes as a way to investigate intrinsic relaxation pathways in these important materials.

We have also initiated an investigation into exciton dynamics in novel 2D atomically thin crystals. Exciton dynamics for the monolayer and few-layer MoS₂ 2D crystals were found to be remarkably different from those of the bulk. Fast trapping of excitons by surface trap states was observed in monolayer and few-layer structures, pointing to the importance of controlling surface properties in atomically thin crystals such as MoS₂ in addition to controlling their dimensions.

9361-12, Session 3

Ultrafast carrier dynamics in atomically thin WS₂ layers in the low- and high-density regime

Claudia Ruppert, Technische Univ. Dortmund (Germany) and Columbia Univ. (United States); Alexey Chernikov, Heather M. Hill, Albert Rigosi, Tony F. Heinz, Columbia Univ. (United States)

We perform white light pump-probe measurements to study the carrier dynamics of mechanically exfoliated mono- and bilayer WS₂ with femtosecond temporal and high spectral resolution. The transient change of the absorbance of the tightly bound A exciton reveals dynamics on the picosecond timescale. A line-shape analysis allows for separation of the pump induced bleaching, line shift and broadening of the exciton resonance. At very high excitation densities we see complete bleaching and unusually large red shifts of the exciton resonance related to many-body interactions and screening.

9361-13, Session 3

Excitonic effect in single atomic layers of transition metal dichalcogenides (*Invited Paper*)

Jie Shan, The Pennsylvania State Univ. (United States)

One of the most distinctive features of electrons in two-dimensional (2D) semiconductors is the significantly reduced dielectric screening of Coulomb interactions. An important consequence of strong Coulomb interactions

**Conference 9361:
 Ultrafast Phenomena and Nanophotonics XIX**

is the formation of tightly bound excitons. Such tightly bound excitons are expected to not only dominate the optical response, but also play a defining role in the optoelectronic processes, such as photoconduction and photocurrent generation in 2D semiconductors. In this talk, we will present recent optical studies on single atomic layers of MoS₂ and WSe₂. Similar to graphene, these materials are built up of van der Waals bonded layers and as such can be separated into stable units of atomic thickness. Using the combined linear absorption and two-photon photoluminescence excitation spectroscopy, we determine the exciton binding energy in single layer WSe₂ to be 0.37eV, which is about an order of magnitude larger than that in III-V semiconductor quantum wells and renders the exciton excited states observable even at room temperature. The exciton excitation spectrum distinctly differs from the simple 2D hydrogenic model. Furthermore, trions, quasi-particles of two electrons and a hole (for a negative trion) have been observed in doped MoS₂ monolayers with a binding energy comparable to room temperature. These results reveal significantly reduced and nonlocal dielectric screening of Coulomb interactions in 2D semiconductors. The observed large exciton binding energy will also have a significant impact on next-generation photonics and optoelectronics applications based on 2D atomic crystals.

9361-14, Session 3

Continuously-tunable ultrastrong light-matter interaction

Curdin Maissen, Giacomo Scalari, Mattias Beck, Jérôme Faist, ETH Zürich (Switzerland)

A SRR unit cell, originally developed as homogeneous THz-metamaterial films, acts as a sub-wavelength resonator for THz radiation. The lowest frequency mode which is a LC-resonance, confines the electric field within a strongly sub wavelength volume $V_{\text{eff}} = (\lambda/2)^3 / 10^6$, where $\lambda = 600 \mu\text{m}$ is the free space wavelength corresponding to the LC-resonance. We couple this confined radiation to the cyclotron transition of a 2DEG which is embedded in a GaAs/AlGaAs quantum well. The coupling strength is given as $\kappa = E_{\text{vac}} d \sqrt{N_e}$, where E_{vac} is the SRR's vacuum electric field, d the electric dipole moment of the cyclotron transition and N_e the number of electrons coupling to the SRR mode. By gating the 2DEG, we can continuously vary the carrier density in the 2DEG, increasing the coupling strength in a controlled way and observing the emergence of the polaritonic branches.

At low carrier concentrations, we observe a transmission peak at the bare LC-mode frequency. The transmission amplitude decreases significantly and the peak frequency red shifts with increasing the carrier density. Only at higher electron densities, a second peak, corresponding to the upper polariton, starts to appear. At the highest density achievable, the transmission amplitudes for both polaritonic peaks reach similar values. In this situation from the measured vacuum Rabi splitting of 220 GHz, we estimate a carrier density of $2.9 \times 10^{11} \text{ cm}^{-2}$ in good agreement with simulations.

Ultrastrong light matter coupling and the control thereof is of importance for basic quantum optics research as well as from the THz-technology point of view. Our system presents a route towards implementing the control over THz radiation in microstructures.

9361-15, Session 4

Relaxation dynamics in single-crystalline perfluoropentacene

Kolja Kolata, Tobias Breuer, Gregor Witte, Sangam Chatterjee, Philipps-Univ. Marburg (Germany)

The optimum performance of conventional photovoltaic devices is constrained by the Shockley-Queisser limit. However, molecular semiconductors offer the possibility for carrier multiplication schemes such as singlet exciton fission [1]. Here, one dipole-allowed singlet exciton may be

converted into two triplet states. These are parity-forbidden for individual molecules, however, once excited they may contribute to charge extraction and hence increase the quantum efficiency, eventually even above unity.

Recently, we experimentally investigated the correlation between singlet-exciton fission and the molecular arrangement the prototypical organic semiconductor perfluoropentacene (C₂₂F₁₄). [2] We exploited its specific epitaxial growth relations on various transparent crystalline substrates allowing us to address all three crystal axes time- and polarization-resolved pump-probe measurements in transmission geometry. The spectral signatures are highly anisotropic caused by a strong uniaxial delocalization of the excitations which, in turn, leads to weakened molecular selection rules. A pronounced slip stacking of the molecules enhances the intermolecular coupling, accompanied by delocalization of singlet excitons and direct coupling to the correlated triplet pair. These excitations decay into triplets which are more strongly localized. In turn, these lift the coupling between the slip-stacked molecules and a more single-molecule-like response is found for higher-energy absorption channels.

1. M. B. Smith and J. Michl, *Annu. Rev. Phys. Chem.* 64, 361 (2013)
2. K. Kolata et al., *ACS nano* 8, 7377 (2014)

9361-16, Session 4

Effect of the Zn coordination complex on the excited-state and two-photon absorption spectra of a novel salicylidene compound

Marcelo G. Vivas, Univ. Federal de Alfenas (Brazil); Jose Germino, Cristina Barboza, Univ. Estadual de Campinas (Brazil); Leonardo De Boni, Univ. de São Paulo (Brazil); Tereza Atvarz, Univ. Estadual de Campinas (Brazil); Cleber R. Mendonça, Univ. de São Paulo (Brazil)

Recently, there has been an increasing interest in searching on the synthesis and optical response characterization of small molecules, in special, those containing organometallic and coordination compounds since these materials play an important role in the development of optoelectronic and photonics devices such as ion selective field effect transistor (ISFET), optical sensors, optical power limiting, all optical switching, holography, photodynamic therapy and so on. For example, Zn (II) complexes with azomethanes (Schiff bases), benzothiazoles among other heterocycles has been used in several kind of applications, from biology to physics. In all these cases, the chelatogenic cycle possess the metal-oxygen-nitrogen chain, which acts as a bridge that performs the intramolecular charge transfer (ICT) between the π -conjugated arms. This important outcome contributes to the increases of the molecular hyperpolarizability of these compounds potentiating their optical features.

In this present work, we have investigated two salicylidene compounds, the first one (KG15) containing two arms based on the phenol-imine group connected by an aromatic ring and the other (KG15/Zn) that has a Zn (II) complex forming a chelatogenic group (metal-oxygen-nitrogen group) in its molecular structure connecting two π -conjugated arms (phenol-imine). Here shown that the Zn (II) coordination complex acts as a bridge that allows the ICT between the arms of molecule, which generate a cooperative effect that increase strongly the hyperpolarizability of organic molecules. To prove that, we studied the influence of Zn (II) on the excited state absorption and two-photon absorption spectra employing the white-light pump-probe and open-aperture Z-scan techniques, respectively, by using an amplified femtosecond laser system (160 fs) operating at low repetition rate (1 kHz). Our outcome shows that the Zn coordination complex modify completely the ESA dynamics and the 2PA spectrum of salicylidene compound causing a great improve in their optical properties due preferentially the intramolecular charge transfer between the arms of molecule provided by the Zn atom.

Financial support from FAPESP (Fundação de Amparo à Pesquisa do Estado de São Paulo), FAPEMIG (Fundação de Amparo à Pesquisa do Estado de Minas Gerais), CNPq (Conselho Nacional de Desenvolvimento Científico

**Conference 9361:
Ultrafast Phenomena and Nanophotonics XIX**

e Tecnológico), Coordenação de Aperfeiçoamento de Pessoal de Nível Superior (CAPES) are acknowledged.

9361-17, Session 4

A spectroscopic ruler for intermediate-zone FRET measurements

Garth A. Jones, David L. Andrews, Univ. of East Anglia (United Kingdom)

It is well known that Förster Resonance Energy Transfer (FRET) has an inverse sixth dependence on the rate of transfer as a function of the distance between the chromophores. However, the unified theory of electronic energy transfer, derived from quantum electrodynamics, also predicts an R⁻⁴ dependence on the distance between the chromophores. This intermediate-zone term becomes especially important when the distance between the chromophores is approximately equal to the reduced wavelength of the mediating photon. In previous theoretical studies we have suggested that inclusion of the intermediate term, through rate equation and quantum dynamical calculations, may be important for describing the exciton diffusion process in some circumstances.[1,2] In particular when the distance between the chromophores exceeds 5 nm.

In this paper, we focus of the role of the intermediate-zone coupling contribution to distance measurements between chromophores, made through the application of spectroscopic ruler techniques. One of the major assumptions made in employing these experimental techniques is that the dependence is valid. In this work, we reformulate the spectroscopic ruler technique for intermediate distances to include the inverse fourth term, and compare this reformulation to experimental FRET results from the literature.

1) M. P. E. Lock, D. L. Andrews and G. A. Jones; J. Chem. Phys., 140, 044103, 2014

2) J. E. Frost and G. A. Jones, New J. Phys., submitted.

9361-18, Session 4

Polyethylene terephthalate: nonlinear optical material for compression of ultra-high-power laser pulses

Efim A. Khazanov, Sergey Y. Mironov, Vladislav Ginzburg, Ekaterina I. Gacheva, Dmitry E. Silin, Andrey A. Shaykin, Institute of Applied Physics (Russian Federation); Gérard A. Mourou, Ecole Polytechnique (France)

An increase of laser pulse peak power over 1PW is possible through additional pulse compression due to spectrum broadening as a result of the phase self-modulation and subsequent spectrum phase correction. However it faces difficulties connected with fabrication of elements having an aperture over 10cm and thickness less than 1mm. We study possibilities to solve this problem by using a transparent plastic – polyethylene terephthalate.

The r.m.s. deviation of the optical thickness of the sample with an aperture of 250x250mm and thickness 0.7mm was 0.73µm. In the 100mm-aperture, the r.m.s. deviation was only 0.3µm. The energy losses in the sample are due to the Fresnel reflection only. The radiation depolarization was below 0.01%, i.e. negligible in practice.

The nonlinear properties of polyethylene terephthalate were examined using 70fs pulse at beam intensity 1.3TW/cm². A spectrometer was placed immediately behind the studied sample. The spectra of the radiation that has passed through the silica sample 1.75mm thick and the polyethylene terephthalate sample 0.7mm thick have the same topology, and the spectrum broadening in these samples differs only insignificantly. Consequently, cubic nonlinearity of polyethylene terephthalate is approximately twice that of silica. It is important that no visible damage of the plastic sample was observed in the course of the experiments with a

peak intensity exceeding 1TW/cm².

Taking into consideration almost unlimited aperture, submillimeter thickness and low cost of polyethylene terephthalate, the obtained results demonstrate that it is a prospective material to be used for spectrum broadening and subsequent compression of petawatt laser pulses.

9361-19, Session 4

Chirp scanning technique to determine the non-degenerate two-photon absorption

Renato Juliano Martins, Instituto de Física de São Carlos (Brazil); Cleber R. Mendonça, Univ. de São Paulo (Brazil)

In this work we introduce a technique which allows retrieving the non-degenerate two photon absorption of materials. Such method is based on shaped femtosecond laser pulses, and it was demonstrated using the conjugated polymer Poly[(9,9-dioctyl-2,7-divinylene-fluorenylene)-alt-co-(9,10-anthracene)] (ADS108ge), a light emitter copolymer with high emission centered at 530 nm. In last decades, pulse shaping has been widely used to control the excitation, and consequently emission, of several materials. As the excitation source we used a chirped pulsed amplified (CPA) system, delivering pulses with 35 fs (bandwidth of approximately 30 nm) at 780 nm and repetition rate of 1 KHz. The spectral phase of the pulse is manipulated by using a spatial light modulator (SLM) with 640 pixels, controlled by a specially designed computer. Initially we determined the phase mask that leads to the Fourier Transform limited pulse. Subsequently we apply a linear chirp to the pulse and measure the sample's fluorescence as a function of features of the phase mask that leads to the linear chirp. In this way we can control the interference of pair of photons that excite the material. The obtained results carry information about the non-degenerate two-photon band of the sample. By using an appropriate simulation, we are able to determine the center and width of the two-photon band.

9361-201, Session PLEN

Ultrafast coherent charge transfer in solar cells and artificial light harvesting systems: toward movies of electronic motion

Christoph Lienau, Institute of Physics, Carl von Ossietzky Univ. Oldenburg (Germany) and Ctr. of Interface Science, Carl von Ossietzky Univ. Oldenburg (Germany)

The efficient conversion of (sun-)light into electrical or chemical energy is one of the most fundamental and relevant challenges in current energy research. Our ability to construct artificial molecular or nanostructured devices that can harvest and exploit sunlight inevitably relies on an in-depth understanding of the elementary microscopic principles that govern the underlying light conversion processes.

Generally, these processes happen on an exceedingly short femtosecond time scale, making real time studies of the light-driven dynamics particularly important. To elucidate these dynamics, we have recently combined coherent femtosecond spectroscopy and first-principles quantum dynamics simulations [1,2] and have used this approach to explore the primary photoinduced electronic charge transfer in two prototypical structures: (i) a carotene-porphyrin-fullerene triad, an elementary component for an artificial light harvesting system [2] and (ii) a polymer:fullerene blend as a model for an organic solar cell [1].

Surprisingly, our experimental and theoretical results provide strong evidence that in both systems, at room temperature, the driving mechanism of the primary step within the current generation cycle is a quantum-correlated wavelike motion of electrons and nuclei on a timescale of few tens of femtoseconds. Our results suggest that the strong coupling between electronic and vibrational degrees of freedom is of key importance for the dynamics and yield of the charge separation process. In my talk, I will present our most recent findings and their implications for the

**Conference 9361:
 Ultrafast Phenomena and Nanophotonics XIX**

light-to-current conversion in solar cells. In an outlook, I will discuss new opportunities to probe such dynamics at a single nanostructure level.

[1] S. M. Falke et al., Coherent ultrafast charge transfer in an organic photovoltaic blend. *Science* 344, 6187 (2014).

[2] C. A. Rozzi et al. Quantum coherence controls the charge separation in a prototypical artificial light harvesting system. *Nature Comm.* 4, 1602 (2013).

9361-20, Session 5

controlling femtosecond dynamics on the nanometer scale (*Keynote Presentation*)

Nicolo Accanto, Lukasz Piatkowski, Jan Renger, ICFO - Institut de Ciències Fotòniques (Spain); Niek F. van Hulst, ICFO - Institut de Ciències Fotòniques (Andorra) and Institució Catalana de Recerca i Estudis Avançats (Spain)

The ultrafast coherent control of light localization in resonant plasmonic nanostructures is intricately related to the

phase response of the involved plasmon resonances. In this work, we exploit the second harmonic signal generated by single optical nanoantennas subject to broadband phase-controlled femtosecond pulses to study and tailor the coherent resonance response. Our results reveal that both the spectral phase and the amplitude components associated with the plasmon resonance of arbitrary individual nanoantennas can be accurately determined.

Next we design coupled plasmonic structures to achieve welldefined ultrafast and phase-stable field dynamics in a predetermined nanoscale hotspot. We present two examples of the application of such structures: control of the spectral amplitude and phase of a pulse in the near field, and ultrafast switching of mutually coherent hotspots. This simple, reproducible and scalable approach transforms ultrafast plasmonics into a straightforward tool for use in fields as diverse as room temperature quantum optics, nanoscale solid-state physics, and quantum biology.

9361-21, Session 5

Enhancement mechanisms for second-harmonic generation from metal nanostructures (*Invited Paper*)

Martti Kauranen, Robert Czaplicki, Jouni Mäkitalo, Kalle O. Koskinen, Tampere Univ. of Technology (Finland); Joonas Lehtolahti, Janne Laukkanen, Markku Kuittinen, Univ. of Eastern Finland (Finland)

The optical properties of metal nanoparticles depend on their plasmon resonances. The resonances give rise to strong local fields (hot spots) near the particles, which can enhance optical interactions. This is particularly important for nonlinear optical effects, which scale with a high power of the optical field. In this Paper, we summarize our recent results on second-harmonic generation (SHG) from metal nanostructures.

SHG requires non-centrosymmetric structures and is also otherwise extremely sensitive to the sample symmetry. Symmetry-breaking defects support their own hot spots, which can play a disproportionate role in the SHG response. Such effects can also be interpreted in terms of multipolar (magnetic, quadrupolar) contributions to the effective nonlinear response. Improvements in sample quality, however, have allowed the dipole limit of the effective response to be reached, opening the possibility for nanostructures with engineered nonlinear properties.

We have subsequently shown how subtle details of nanoparticle arrays can have a strong influence on SHG. These effects arise from diffractive coupling between the particles. Furthermore, by combining SHG-active particles with SHG-passive particles, we have enhanced the SHG response through lattice interactions between the two types of particles.

It is presently assumed that the nonlinear responses are strongly dependent on having the fundamental wavelength close to the plasmon resonance wavelength. While this is correct for a given sample geometry, we have shown that the resonant conditions are not sufficient, because the detailed local-field distributions, which depend on geometry, can favor or suppress selected nonlinear signals.

9361-22, Session 5

Second-harmonic generation with double resonant hybrid plasmonic/dielectric antennas

Heiko Linnenbank, Stefan Linden, Rheinische Friedrich-Wilhelms-Univ. Bonn (Germany)

Excitation of particle plasmons with ultrashort light pulses can give rise to a spatiotemporal concentration of the electromagnetic field in the vicinity of a metallic nanostructure. The intensity in these "hot spots" can exceed the incident intensity by orders of magnitude. By carefully varying the geometry of the metallic nanostructures it is possible to create metallic nanostructures with multiple plasmonic resonances and to tune these plasmonic resonance frequencies.

In several studies it has been shown that the excitation of plasmonic resonances in gold nanostructures with ultrashort light pulses can give rise to large second and third harmonic signals. Here, we demonstrate that the second harmonic generation efficiency of metallic nanostructures can be increased by depositing a dielectric material with a large second order nonlinear coefficient in the hot spots of the structures. By varying the geometry of the nanostructures and by performing nonlinear spectroscopy we rule out that the enhancement of the second harmonic signal is due to a trivial shift of the plasmonic resonance frequency caused by the incorporation of the dielectric material. Furthermore, we have performed nonlinear experiments with double-resonant metallic nanostructures that exhibit plasmonic resonances at both the frequency of the pump light and the generated second harmonic light. Compared to metallic nanostructures which are only resonant to the pump light, the double-resonant structures give rise to larger second harmonic signals. Moreover, they also allow to control the polarisation properties of the generated light.

9361-23, Session 5

Nano-scale characterization of gold nanostructures using polarized nonlinear microscopy

Naveen K. Balla, Institut Fresnel Equipe MOSAIC (France); Carolina Rendon, Institut Fresnel (France) and Ctr. National de la Recherche Scientifique (France); Esteban B. Ureña, ICFO - Institut de Ciències Fotòniques (Spain); Pawel Karpinski, Wroclaw Univ. of Technology (Poland); Julien Dubboiset, Institut Fresnel (France); Patrick Ferrand, Hervé Rigneault, Institut Fresnel (France) and Ctr. National de la Recherche Scientifique (France); Romain Quidant, ICFO - Institut de Ciències Fotòniques (Spain); Sophie Brasselet, Institut Fresnel (France) and Ctr. National de la Recherche Scientifique (France)

The effects of the shape of a nanostructure on its nonlinear response to polarized light are not well understood. Here we present a study on polarized second harmonic generation (SHG) and four wave mixing (FWM) microscopy of specially designed gold nanostructures which sheds some light on these questions. We have used gold nanoparticles whose shapes resemble two dimensional projections of spherical harmonics of orders of symmetry 2, 3, 4 and 5. Though these nanostructures are small in size as

**Conference 9361:
 Ultrafast Phenomena and Nanophotonics XIX**

compared to the excitation point spread function (PSF) of our nonlinear optical microscope, they respond differently in SHG and FWM to varying incident polarizations. Each polarized excitation modulation gives rise to a particular, if not unique, SHG/FWM image modulation from the nanoparticle which shows sub-resolution features that can be associated to their specific symmetry and wavelength resonance. The results of this analysis emphasize two main effects. First, the SHG image response of nanostructures can be represented as resulting from the coherent superposition of spatially distributed nonlinear induced dipoles, which couple specifically to incident polarization directions. Second, the spatial nature of the SHG polarization responses is governed by the symmetry of the nanostructure which can be revealed by directly extracting symmetry information from such responses. While working in the far field, our method is thus a powerful tool to probe the spatial behavior of nanostructures at the nano-scale.

9361-24, Session 6

Nano-focused ultrafast spectroscopy and imaging reaching the single quantum level
(Invited Paper)

Markus B. Raschke, Univ. of Colorado at Boulder (United States)

The near-field tip-antenna enhanced signal transduction with femtosecond laser pulses allows for spatio- spectral and spatio-temporal imaging and quantum coherent control with the perspective to reach the single electronic or vibrational quantum level. Combining plasmonic and optical antenna concepts with ultrafast and shaped laser pulses allows for the precise control of an optical excitation on femtosecond time and nanometer length scales. I will discuss concepts describing the induced near-field light-matter interaction in terms of impedance matching to a quantum system. I will extend into questions concerning the competition of radiative and nonradiative decay of the metallic nanostructure against preserving and manipulating the quantum coherence of the coherent excitation. Specific examples from our lab include adiabatic nano-focusing on a tip for nano-spectroscopy, spatio-temporal superfocusing, and optical control at the 10 nm-10 fs level. We demonstrate reaching the quantum regime at the tunneling limit. We furthermore demonstrate the optical antenna coupled ultrafast free-induction decay in near-field infrared nano- spectroscopy of vibrational resonances and both their tip-enhanced decoherence as well as the observations of long-lived intrinsic coherences for small molecular ensembles.

9361-25, Session 6

An electrically-driven plasmon nanosource
(Invited Paper)

Elizabeth Boer-Duchemin, Univ. Paris-Sud 11 (France); Tao Wang, National Univ. of Singapore (Singapore); Eric Le Moal, Gérald Dujardin, Univ. Paris-Sud 11 (France)

Surface plasmons are extensively studied for their ability to confine electromagnetic fields in sub-wavelength volumes and for their use in miniaturized waveguides. Their ultrafast properties are also beginning to be explored in detail. Using the inelastic tunneling electrons of a scanning tunneling microscope is a unique, local, low energy, and electrical method for exciting both localized and propagating surface plasmons on metal films and nanostructures. These STM-excited plasmons have a spectrum that is broadband in nature. This polychromatic spectrum, the ability to precisely position the excitation source and the absence of any excitation background light are all essential properties for many types of experiments.

In our setup, the STM is coupled to an inverted optical microscope and the resulting emitted light is collected through the glass substrate. Recently, we have used this technique to perform a type of “Young’s double-slit” experiment for plasmons and investigate the coherence of surface plasmon polaritons (SPP). When the excitation source is equidistant from two holes

in an opaque gold film, the spatial coherence of the STM-plasmon source may be studied and the effective STM-source size estimated (<200 nm). On the other hand, when the plasmon wave excited by the STM tip on the gold film no longer propagates the same distance before reaching each hole, the temporal coherence of the STM-excited SPPs is probed.

This local STM-plasmon source may also be used to selectively excite the local modes of variously-shaped particles, as well as the modes of other more sophisticated structures such as nano-antennae.

9361-26, Session 6

Single photon detector with high-polarization extinction ratio
(Invited Paper)

Lixing You, Shanghai Institute of Microsystem and Information Technology (China)

Light has a few key parameters, like the wavelength, intensity, phase and polarization. Many applications have been realized based on the detection of wavelength, intensity and phase of light. However, polarization is a parameter which is unpopular for applications. There are a few demonstrated applications based on the detection of the polarization, such as polarized sunglasses, polarization imaging and polarization-coding quantum key distribution. Since most of the optical detectors are area detector, which is insensitive to the polarization of the light. To realize the polarization-sensitive detection, a popular way is to add a polarizing filter to an optical detector or adopt a bulk polarization controller. For the ultrasensitive detection, single photon detector will be the sole choice. However, there is no polarization sensitive semiconducting single photon detector demonstrated.

In the past ten years, a new type of single photon detector based on superconducting meandered nanowire has been demonstrated to have better performance beyond the traditional semiconducting single photon detectors in near infrared wavelengths. Due to its natural nanowire structure, superconducting nanowire single photon detector (SNSPD) is polarization sensitive. However, all the previous studies were focused on realizing a polarization insensitive SNSPD, since it may have more prospective applications. In this talk, we will present our work on studying SNSPD in an opposite way — how to realize a polarization sensitive SNSPD. We systematically discussed the relation of polarization extinction ratio (PER) on SNSPD structure parameters (linewidth, space etc). SNSPD with the detection efficiency of 13% and PER of 22 has been successfully demonstrated.

9361-27, Session 6

Far-field super resolution microscopy based on the nonlinear response of photothermal excitation

Omer Tzang, Ori Cheshnovsky, Tel Aviv Univ. (Israel)

Far field Super resolution (SR) microscopy has developed in the last two decades into an important tool in life sciences. It relies on the ability to control the emission of label fluorescent molecules. We introduce a new far field label free SR method, based on thermo reflectance (TR) opt to material science. It relies on the ability to photo-excite a temperature spatial distribution inside the diffraction limited spot by an ultra-short pump pulse. A second probe pulse probes the temperature variations by reflectance changes. Spatial resolution within the diffraction limited spot is enhanced due to nonlinearities in thermal properties of the matter. Two examples are presented: First, the nonlinear change of thermo-reflectance of VO₂ upon phase transition at -340K. In this case, nano particles are imaged by the probe laser, using a modulated pump beam at $\omega = 2.6$ kHz, and a lock in amplifier. Resolution is enhanced when the pump energy is tuned slightly above phase transition. In the case of silicon, we extract the nonlinear components by demodulating the TR intensity at the corresponding harmonic frequencies ($2\omega, 3\omega, \dots$) with a lock-in amplifier, similarly to SAX

**Conference 9361:
 Ultrafast Phenomena and Nanophotonics XIX**

fluorescence microscopy. At 80 mJ/cm², harmonic frequencies are discernible in the TR signal. We demonstrate enhancement of at least x4 better than the diffraction limit and show the applicability to SR optical imaging of VO₂ and Silicon nano structures. Our approach can be extended to include additional materials and to exploit other physical properties which depend on temperature such as luminescence and Raman shift.

9361-28, Session 7

Cooperative atomic motion probed by femtosecond electron diffraction (*Invited Paper*)

Jure Demsar, Technische Univ. Ilmenau (Germany); Maximilian Eichberger, Technische Univ. Ilmenau (Germany) and Univ. Konstanz (Germany)

Intertwined electronic and lattice orders are common to strongly correlated materials. Here, femtosecond time-resolved optical [1,2] and diffraction techniques [3-6] recently contributed many important insights into the origin of their ground states by tracking their dynamics following excitation with femtosecond light pulses. Recently, several studies of structural dynamics in quasi-two-dimensional charge density wave systems were performed using femtosecond electron diffraction in transmission [3-5]. It was demonstrated that tracking the time evolution of the lattice and super-lattice peak intensities with sub-picosecond electron pulses enables direct access to the dynamics of the order parameter. It was shown that light-excitation and the ensuing changes in the electronic distribution result in changes in the atomic potential, driving the coherent cooperative atomic motion towards the high temperature non-modulated state [3-6]. This process, which takes place on a fraction of a period of the corresponding amplitude mode (100 fs timescale), is accompanied by a rapid sub-picosecond energy transfer to the lattice via electron-phonon and phonon-phonon scattering. Both processes, the coherent order parameter dynamics and the incoherent energy redistribution among different subsystems, affect the diffraction pattern. Here we show, that by simultaneous tracking the dynamics of intensities of super-lattice peaks, lattice peaks and that of the incoherent background for multiple diffraction orders, this being one of the main advantages of femtosecond electron diffraction against time-resolved X-ray methods, the two processes can be effectively disentangled.

[1] H. Schaefer et al., Phys. Rev. Lett. 105, 066402 (2010); H. Schaefer et al., Phys. Rev. B 89, 045106 (2014).

[2] M. Porer et al., Nature Mat. (2014); K.W. Kim, et al., Nature Mat. 11, 497 (2012).

[3] M. Eichberger, et al., Nature 468, 799 (2010).

[4] N. Erasmus, et al., Phys. Rev. Lett. 109, 167402 (2012).

[5] K. Haupt et al., submitted

[6] T. Huber et al., Phys. Rev. Lett. 113, 026401 (2014).

9361-29, Session 7

Terahertz field acceleration, angular tuning, and kinetic energy tailoring of ultrashort electron pulses

Shawn R. Greig, Abdulhakem Y. Elezzabi, Univ. of Alberta (Canada)

The influence of terahertz (THz) electric fields on ponderomotively accelerated, surface plasmon generated, ultrashort electron pulses is investigated. In the absence of any terahertz electric field, ultrashort electron pulses are generated through multi-photon absorption of a 800 nm optical pulse used to excite a surface plasmon (SP) at the Ag-Vacuum interface on a silica prism (Kretschmann configuration). Electrons are subsequently accelerated away from the prism by the ponderomotive potential of the SP field, achieving electron pulses with broadband kinetic

energy spectrums. However, through application of ultrafast THz electric fields, tailoring of the kinetic energy, as well as the angular directivity of the accelerated electron pulse can be realized. Utilizing a single THz electric field pulse, kinetic energies up to 1.56 keV can be achieved. Simultaneously, by varying the THz field strength, the angular distribution of the electrons can be controlled through manipulation of the electrons' nanoscale trajectories. Introduction of a second THz electric field allows for further tailoring of the energy spectrum by controlling the temporal acceleration profile that each electron experiences. This configuration leads to kinetic energies approaching 2.2 keV. Notably, we also observe that the kinetic energy spectrum's dependence on the carrier envelope phase of the excitation pulse is maintained in the presence of a THz electric field.

9361-30, Session 7

Plasmoemission: Emission of photoelectrons from a plasmonic field (*Invited Paper*)

Frank J. Meyer zu Heringdorf, Univ. Duisburg-Essen (Germany)

Observing surface plasmon polaritons (SPPs) in a photoemission electron microscope (PEEM) is possible via a nonlinear photoemission process, if ultra-short laser pulses (<20fs) of a suitable wavelength are directed onto the surface of a plasmonic material. Spatial control over the excitation location of SPPs is possible by appropriately structuring the surface beforehand with focused ion beams. We study the development and interaction of SPPs in time and space by means of a direct conceptual visualization of the SPPs in a "normal incidence geometry" in PEEM. This experimental setup provides us with direct access to the phase-velocity of SPPs in time-resolved experiments, and allows the studying of transient wave phenomena that exist only few femtoseconds during interaction of the ultrashort SPP pulses.

In focusing structures for SPPs we find an unexpected time-signature of the nonlinear photoemission signal at the focus point. By separating the fs laser pulses from the SPP pulses in time, it can be demonstrated that the electron emission from the focus point must be explained by emission of electrons from the SPP. The energy distribution of these "plasmoelectrons" shows that the SPP fields are sufficiently high to make nonlinear photoemission pathways of higher orders the dominant contribution to the PEEM signal.

9361-31, Session 7

Ultrafast low-energy electron diffraction (ULEED) driven by nanotip cathodes (*Invited Paper*)

Claus Ropers, Univ. Göttingen (Germany)

Ultrafast electron diffraction is among the most powerful and direct techniques to study structural dynamics in materials on sub-picosecond timescales. In the past years, a variety of experimental schemes was developed to investigate laser-driven phase transitions with electron pulses at kinetic energies of tens to hundreds of keV. In contrast, low-energy electron diffraction (LEED), a widely applied technique to characterize the atomic-scale structure and symmetry of surfaces, has not yet been established with ultrashort temporal resolution. Electron pulses at low electron energies experience particularly severe velocity dispersion and space charge broadening in the propagation from the source to the sample. Laser-triggered photoemission from sharp metal tips presents unique possibilities to minimize such detrimental effects on electron pulse quality.

We recently demonstrated a first implementation of Ultrafast Low-Energy Electron Diffraction (ULEED) based on the generation of electron pulses from nanoscale needle cathodes. Compared to planar cathodes, nanoscopic emitters offer specific advantages of enhanced electron extraction fields and reduced effective source sizes. Such features are used to achieve a

**Conference 9361:
 Ultrafast Phenomena and Nanophotonics XIX**

temporal resolution of few picoseconds at typical LEED energies. Employing a laser-pump/electron-probe scheme, the structural dynamics of an ultrathin polymer layer on freestanding monolayer graphene is investigated in a transmission geometry. Specifically, the relaxation of a stripe-shaped superstructure of poly(methyl methacrylate) (PMMA) on the graphene substrate is investigated after optical excitation. We identify a sequence of processes, which is interpreted in terms of interlayer energy transfer, loss of superstructure order and the formation of an expanded amorphous phase.

9361-32, Session 7

Classical electron trajectories and birth time in polar-asymmetric two-color laser fields

Aram Gragossian, The Univ. of New Mexico (United States); Denis V. Seletskiy, Univ. Konstanz (Germany); Mansoor Sheik-Bahae, The Univ. of New Mexico (United States)

The generation of high harmonics in rare gases follows a non-perturbative mechanism, with its main features captured by a classical three-step model. In this picture, electrons are liberated in a tunnel ionization process and accelerated every half cycle of the driving laser pulse. Depending on their birth time, a fraction of these electrons can acquire sufficient kinetic energy to trigger high-energy photon emission upon recombination with the parent ion. If this process is driven by asymmetric electric fields, for example by mixing a weak second harmonic field with the fundamental, the change of polar asymmetry will modify the electron trajectories and harmonic generation will be modulated due to the interference of long and short trajectories. We have extended the three-step model to calculate spectra for different polar asymmetries. The extended three-step model explains the results of experiments for both weak and strong polar asymmetries. In the case of 1% second harmonic injection, harmonics are maximized at different relative phases. In the case of 10% injection, the asymmetry is so large that the harmonics are generated once per cycle and they all peak at $m\pi$. This model also provides more information about contributions of long and short trajectories at different harmonic orders. In the plateau region long harmonics are mainly responsible for harmonic generation. In the cut-off region however, short trajectories dominate the harmonic generation process.

9361-33, Session 8

Fully quantized spaser physics: towards exact modeling of mesoscopic CQED systems

(Invited Paper)

Michael Gegg, Technische Univ. Berlin (Germany) and Freie Univ. Berlin (Germany); T. Sverre Theuerholz, Andreas Knorr, Marten Richter, Technische Univ. Berlin (Germany)

Nanoplasmonics includes applications like local amplification of light and its localization below the diffraction limit through plasmonic nanoantennas and surface plasmon polaritons. In this respect, a nanostructure generating plasmons of different statistics is crucial for future devices.

For instance, a spaser, a device for generating coherent plasmons, was proposed by Bergman and Stockman and recently experimentally realized by Noginov et al.. A spaser consists of externally pumped quantum emitters (e.g. quantum dots or organic dyes) located close to a metal nanoparticle.

In order to understand the different operating regimes in the single plasmon, coherent and thermal limit of the spaser structure, a theoretical analysis of the plasmon and exciton statistics is crucial. We use a density matrix method, which allows to calculate numerically exact dynamics of the full density matrix from small numbers of identical quantum emitters identically coupled to the plasmon mode of the metal nanoparticle up to

large emitter numbers (hundreds). Our approach allows full access to any observable and the full plasmon and exciton probability distributions.

The calculated probability distributions give a direct characterization of the underlying physics for the different operating regimes. We will analyze the quantum statistics in dependence of the number of quantum emitters and other the system parameters below and above the spasing transition.

The analysis will give hints how to design nanoplasmonic emitters for different applications.

9361-34, Session 8

Bandwidth-energy limits in photonic and plasmonic modulators *(Invited Paper)*

Juejun Hu, Hongtao Lin, Okechukwu A. Ogbuu, Univ. of Delaware (United States); Jifeng Liu, Dartmouth College (United States); Lin Zhang, Jurgen Michel, Massachusetts Institute of Technology (United States)

In this talk, we will first review our prior work that quantitatively defines the trade-off between modulation speed and power consumption in electro-optic modulators. A formally simple, analytical energy-bandwidth limit was derived for electro-optic modulators based on intra-cavity index modulation. Here we further extend the analysis to photonic and plasmonic devices based on other modulation principles besides Pockels effects, such as free-carrier dispersion or electro-absorption in semiconductors (for example, the Franz-Keldysh effect and the quantum confined Stark effect). We show that our model allows quantitative performance comparison between devices operating on different modulation mechanisms. The potential of using complex cavity modulation schemes and plasmonic confinement effects to overcome the apparent limit will also be discussed.

9361-35, Session 8

Long-range hybrid plasmonic modes in asymmetric structures *(Invited Paper)*

Amr S. Helmy, Charles Lin, Wen Ma, Univ. of Toronto (Canada)

A novel approach that enables long range hybrid plasmonic modes to be supported in asymmetric structures will be discussed. Examining the modal behavior of an asymmetric hybrid plasmonic waveguide (AHPW) reveals that field symmetry on either side of the metal is the only necessary condition for plasmonic structures to support long range propagation. In this talk we shall demonstrate that this field symmetry condition can be satisfied irrespective of asymmetry in the waveguide structure, material, or even field profile. This versatility in the choice of parameters allows for long range hybrid plasmonic modes to be achieved in generic structures, which are based on materials and dimensions conducive to their realization using conventional SOI technology amongst others. This design methodology can significantly alleviate the propagation loss-mode area trade-off that is characteristic of this class of waveguides by providing a radically improved attenuation - confinement performance. Altering the existing limitations of these performance metrics (mode area and propagation losses) can have significant implications on the attainable nonlinear optical effects in nanoscale waveguides. In this talk, implications on the nonlinear and ultrafast phenomena in this class of waveguides will also be discussed. The utility of these waveguide designs is demonstrated when combined with 2D materials to realize optoelectronic components such as filters, modulators and switches with record footprint, performance and insertion losses.

9361-36, Session 8

Bloch oscillations and Anderson localization in plasmonic waveguide arrays *(Invited Paper)*

Stefan Linden, Rheinische Friedrich-Wilhelms-Univ. Bonn (Germany)

Light passing through discrete periodic structures can show interesting dynamics resembling quantum mechanical condensed matter phenomena. By mapping the time-dependent probability distribution of an electronic wave packet to the spatial light intensity distribution in the corresponding photonic structure, the quantum mechanical evolution can be visualized directly in a coherent, yet classical wave environment. Based on this approach, several groups have recently observed the optical analogues of discrete diffraction, Bloch oscillations, Zener tunnelling, and Anderson localization in different dielectric waveguide structures.

In this presentation, we show that these ideas can be extended to the field of plasmonics. In particular, we will report on the observation of discrete diffraction, Bloch oscillations, and Anderson localization of plasmons in arrays of evanescently coupled dielectric-loaded surface plasmon polariton waveguides. The samples have been fabricated by a negative-tone gray-scale electron beam lithography process that enables us to precisely control all geometrical sample parameters with high precision. The complete spatial distribution of the surface plasmon polariton intensity inside of a given waveguide array was directly monitored by leakage radiation microscopy.

9361-37, Session 8

Routing of deep-subwavelength optical beams without reflection and diffraction using infinitely anisotropic metamaterials *(Invited Paper)*

Peter B. Catrysse, Shanhui Fan, Stanford Univ. (United States)

Media that are described by extreme electromagnetic parameters, such as very large/small permittivity/permeability, have generated significant fundamental and applied interest in recent years. Notable examples include epsilon-near-zero, ultra-low refractive-index, and ultra-high refractive-index materials. Many photonic structures, such as waveguides, lenses, and photonic band gap materials, benefit greatly from the large index contrast provided by such media. In this paper, I discuss recent work on media with infinite anisotropy, i.e., infinite permittivity (permeability) in one direction and finite in the other directions. As an illustration of the unusual optical behaviors that result from infinite anisotropy, I describe efficient light transport in deep-subwavelength apertures filled with infinitely anisotropic media. I then point out some of the opportunities that exist for controlling light at the nano-scale using infinitely anisotropic media by themselves. First, I show that a single medium with infinite anisotropy enables diffraction-free propagation of deep-subwavelength beams. Next, I demonstrate interfaces between two infinitely anisotropic media that are impedance-matched for complete deep-subwavelength beams and enable reflection-free routing with zero bend radius that is entirely free from diffraction effects even when deep-subwavelength information is encoded on the beams. These behaviors indicate an unprecedented possibility to use media with infinite anisotropy to manipulate beams with deep-subwavelength features, including complete images. To illustrate physical realizability, I demonstrate a metamaterial design using existing materials in a planar geometry, which can be implemented using well-established nanofabrication techniques. This approach provides a path to deep-subwavelength routing of information-carrying beams and far-field imaging unencumbered by diffraction and reflection.

9361-38, Session 8

Ultrafast silicon nanoplasmonic grid-gate transistor

Shawn R. Greig, Abdulhakem Y. Elezzabi, Univ. of Alberta (Canada)

We present the detailed investigation of a silicon nanoplasmonic waveguide based grid-gate transistor. The device consists of a Si core, upper and lower Cu claddings, and a W grid embedded in the Si. An 84 fs 1.55 μm optical pulse excites a nanoplasmonic mode at the upper Cu-Si interface that decays towards the W grid. Electrons generated through two-photon absorption in the Si core are accelerated/decelerated in the ponderomotive potential due to the high spatial gradient of the nanoplasmonic field. As the acceleration and deceleration are not equal, the electrons experience an increase or decrease of kinetic energy as they are directed towards the W grid. Application of a negative potential to the grid introduces an effective energy barrier that the electrons must pass through to reach the bottom Cu electrode. Altering the strength of the applied grid potential directly modulates the energy barrier and thus the number of electrons passing through it. Electrons that possess energy above the barrier height can pass through to reach the bottom Cu electrode, generating a net current flow. Varying the nanoplasmonic field strength and applied grid potential results in triode-like behavior. The device can achieve a pulsed current output of 11.7 mA/ μm within 150 fs, in a compact footprint compatible with complementary-metal-oxide-semiconductor technology.

9361-39, Session 9

Quantum-optical spectroscopy on dropletions *(Invited Paper)*

Mackillo Kira, Martin Mootz, Stephan W. Koch, Philipps-Univ. Marburg (Germany); Andrew Almand-Hunter, Hebin Li, Steven Cundiff, JILA (United States)

Quantum spectroscopy [1,2] excites desired many-body quasiparticles by tailoring the quantum-optical fluctuations of an ultrafast laser pulse. We establish an experimentally robust quantum spectroscopy with present-day laser setups by projecting [3] high-quality classical measurements. The unprecedented capabilities of the method are demonstrated with our high-precision characterization of biexcitons [4] and discovery of a new quasiparticle – the dropletion [5] – in GaAs quantum wells. A dropletion is created when four or more electrons and holes form a tiny correlation bubble via the attractive Coulomb interaction. Dropletion's electron-hole pairs are in a liquid-like state, however, it has quantized energy bands [6] and it couples strongly only to quantum light due to its microscopic size.

[1] M. Kira and S.W. Koch, Quantum-optical spectroscopy of semiconductors, *Phys. Rev. A* 73, 013813 (2006).

[2] M. Kira and S.W. Koch, *Semiconductor quantum optics*, (Cambridge University Press, 2011).

[3] M. Kira, S.W. Koch, R.P. Smith, A.E. Hunter, and S.T. Cundiff, Quantum spectroscopy with Schrödinger-cat states, *Nature Physics* 7, 799-804 (2011).

[4] M. Mootz, M. Kira, S.W. Koch, A.E. Almand-Hunter, and S.T. Cundiff, Characterizing biexciton coherences with quantum spectroscopy, *Phys. Rev. B* 89, 155301 (2014).

[5] A.E. Hunter, H. Li, S.T. Cundiff, M. Mootz, M. Kira, and S.W. Koch, Quantum droplets of electrons and holes, *Nature* 506, 471 (2014).

[6] M. Mootz, M. Kira, and S.W. Koch, Pair-excitation energetics of highly correlated many-body states, *New J. Phys.* 15, 093040 (2013).

9361-40, Session 9

Quantum droplets of electrons and holes (Invited Paper)

Steven Cundiff, JILA (United States)

To develop an understanding of complex many-body systems, it is useful to identify quasiparticles. I will present evidence for a new quasiparticle in optically excited semiconductor quantum wells. This quasiparticle consists of equal numbers of electrons and holes that lack pair-wise correlations, and thus are not excitonic, but rather have a correlation function that is similar to a liquid. The quasiparticles are small enough so that quantum size effects are important, thus it is designated as a quantum droplet.

Evidence for the quantum droplet is present in a measurement of the absorption spectrum of a weak probe pulse after excitation by a strong pump pulse. In the absence of the pump, an absorption resonance is observed that corresponds to the creation of a 1s exciton consisting of a heavy-hole and an electron. As the pump-power is increased, a new resonance appears below the exciton. Initially this resonance is due to biexcitons. However, as the pump power is increased this resonance shifts to lower energy, whereas the exciton energy shifts to higher energy. This behavior is inconsistent with that expected for the biexciton, but are consistent with it being due to the formation of successive quantum droplets with increasing numbers of electrons and holes.

To verify the assignment, the technique of projecting the quantum optical response is used [1]. The projections reveals stepwise evolution with pump-power, as expected for the quantum droplets [2].

[1] M. Kira, et al., Nature Phys. 7, 799 (2011).

[2] A.E. Almand-Hunter, et al., Nature 506, 471 (2014).

9361-42, Session 9

Ultrafast biexciton dynamics in single CdSe/ZnSe quantum dots

Denis V. Seletskiy, Christopher Hinz, Johannes Haase, Christian Traum, Florian Werschler, Stefan Lohner, Alfred Leitenstorfer, Univ. Konstanz (Germany)

II-VI semiconductor quantum dots with high confinement potentials and large Coulomb correlation energies provide promising systems for quantum optical experiments. Here we report on two-color femtosecond pump-probe measurements on a single self-assembled CdSe/ZnSe quantum dot. The charge carrier dynamics of the system was spectro-temporally investigated across both the trion line and the biexcitonic emission lines. In addition to the bleaching and stimulated emission at the trion resonance, we observe an induced absorption into the biexciton states, switched on by the Coulomb renormalization of the X- ground state due to the excitation by the pump.

9361-43, Session 10

Transducing electron and photons in electrically-contacted optical gap antennas (Invited Paper)

Alexandre Bouhelier, Ctr. National de la Recherche Scientifique (France)

Molecular-scale gaps are essential for engineering the response of advanced plasmonics devices. Trapping and sensing at the nanoscale, enhancing weak nonlinear optical processes, or accessing the quantum regime are recently emerging because electromagnetic fields can be confined to extremely small gaps. We describe a new method for nanoscale information processing based on a reversible transduction between electron and a photon using optical gap antennas. Our concept provides a novel approach

where the light source and the detector are integrated into a single metallic superstructure. At the core of the device is an atomic-scale tunnel gap whereby optical rectification or inelastic tunneling can reciprocally mix photons and electrons. The fabrication of such gap remains challenging by standard top-down approaches. Instead, we rely on the controlled electromigration of contacted gold antennas to create molecular-scale gap. Electromigration produce failing points stochastically distributed at current-crowding structural defects placed along the contacts. This is drastically hampering a subsequent structuration of the electromagnetic response of the gap. To pre-determine the location of the tunneling gap and engineer its optical response with parasitic elements, we developed an innovative imaging technique to identify the position of the gap before it is formed. Our approach relies at evaluated second-order nonlinear properties of the nanowire antenna and correlate them to its electron transport characteristics. The change of the antenna morphology during the electromigration process is spatially followed by recording the second harmonic generation (SHG), two-photon luminescence (TPL), and the differential conductance $\partial i/\partial v$ dictating the electronic transport. Local defects along the nanowire are generating enhanced nonlinear responses that are correlated with a reduced conductance. We found that the location of the largest conductance minima is always leading to the formation of a gap (Fig. 1). We will show evidence for light emission from an electron-fed optical antenna and demonstrate that the same device can rectify optical radiation into an electrical current.

The research leading to these results has received funding from the European Research Council under the European Community's Seventh Framework Program FP7/2007–2013 Grant Agreement no 306772.

9361-44, Session 10

Ultrafast acousto-magneto-plasmonics (Invited Paper)

Vasily V. Temnov, Univ. du Maine (France) and Centre National de la Recherche Scientifique (France)

Nano-optical experiments appear to be particularly useful to study metallic nanostructures. In this talk I will review [1] some recent experiments in the magneto-plasmonic metal-ferromagnet multilayer structures. Applying various experimental pump-probe techniques we were able to monitor and understand ultrafast dynamics in gold-cobalt bilayer structures excited by femtosecond laser pulses. Energy transport of superdiffusive hot electrons, exotic electron-phonon relaxation pathways at metal-ferromagnet interfaces, excitation and the non-linear propagation of ultrashort acoustic pulses, generation of coherent magnons illustrate the richness of electron-phonon-magnon interactions in hybrid metallic nanostructures.

[1] V.V. Temnov, Nature Photonics 6, 728 (2012)

9361-45, Session 10

Active and passive optical modulation via Bi:YIG based magnetoplasmonic waveguides

Curtis J. Firby, Abdulkhem Y. Elezzabi, Univ. of Alberta (Canada)

A novel method for manipulation of plasmonic modes involves the use of magneto-optical materials. Incorporation of a static magnetic field over these materials can induce phenomenon such as TE-TM mode coupling via the Faraday effect and nonreciprocal phase shifts. Here, our fully vectorial finite-difference-time-domain (FDTD) simulations demonstrate the incorporation of magneto-optical effects into plasmonic waveguides constructed with layers of bismuth-substituted-yttrium-iron-garnets. Investigations with a static magnetic field applied transverse to the propagation direction can induce nonreciprocal phase shifts between the forward and backward propagating mode. Since plasmonic systems naturally incorporate metal layers, they provide a convenient platform for

**Conference 9361:
 Ultrafast Phenomena and Nanophotonics XIX**

studying the transient switching dynamics. This can be practically realized by applying a current pulse through the metal film which will generate a transient magnetic pulse, and hence a transient magnetization response from the material. The Landau-Lifshitz model of magnetization dynamics was combined with the fully vectorial FDTD solution of Maxwell's equations to study this phenomenon. We examine the effects of nanosecond Gaussian magnetic field transients on the system to develop a series of plasmonic modulators. Such devices will have integral applications in hybrid electronic-nanoplasmonic circuitry.

9361-46, Session 10

Interfacial effects in plasmonic resonant energy and charge transfer

Scott K. Cushing, Jiangtian Li, Alan D. Bristow, Nianqiang Wu, West Virginia Univ. (United States)

Plasmonics has proven a powerful tool for increasing photoconversion at energies below the bandgap in solar energy and optoelectronics. The optical energy absorbed by the plasmon is transferred to the semiconductor by hot electrons overcoming the interfacial Schottky barrier or through resonant energy transfer nonradiatively exciting interband transitions. However, these models only account for the dynamics of the plasmon and not the effect of the interface with the semiconductor. In this presentation we will therefore study the transfer dynamics from a femtosecond to nanosecond time scale, focusing on how the interface controls both initial energy transfer and subsequent back transfer. On short time scales, we will discuss the importance of the coherence of the plasmon for resonant energy transfer and the effects of Schottky barrier height for hot electron transfer. The interplay between the two mechanisms through dephasing of the plasmon and the effect on transfer efficiency will be established. On long time scales, the balance between prolonged charge separation with increasing interfacial barrier height and initial transfer yield will be discussed. The results presented extend beyond the initial stages of the plasmon to the time scales required for efficient charge extraction, providing valuable insight for below bandgap enhancement with plasmonics.

9361-47, Session 10

Reverse design of a bull's eye structure for oblique illumination and wider angular transmission efficiency

Akira Yamada, Mitsuhiro Terakawa, Keio Univ. (Japan)

Extraordinary optical transmission (EOT) of light through a bull's eye structure has been receiving much attention. Since conventional bull's eye structures are designed for normally incident light, its transmission efficiency dramatically drops when incident angle θ is varied. Many design methods have been proposed for normally incident light, but a method for oblique incidence has not been considered up to date. Here, we propose a novel design method of a bull's eye structure enabling to design (1) transmission peaks to a specified angle, (2) with wider angular transmission efficiency. By using finite-difference time-domain (FDTD) method, we calculated the optical near-field pattern around a single subwavelength aperture in an obliquely illuminated gold film. The interference of the scattered waves and incident light forms an asymmetric ripple-like pattern around the aperture. By determining the groove geometry based on this pattern, a bull's eye structure with transmission peaks at oblique incident angles was successfully designed. Structures designed up to $\theta = 20^\circ$ showed transmission efficiency comparable to the structure designed for $\theta = 0^\circ$, except with transmission peaks shifted towards the desired angle. Moreover, by combining groove patterns of two different bull's eye structures designed for different angles (e.g. $\theta = 10^\circ, 20^\circ$) we designed a structure, which has its transmission peak at the desired angle (e.g. $\theta = 15^\circ$), but a wider angular transmission efficiency. Our novel design method enables the shift of transmission peaks and the broadening of angular transmission

efficiency, which overcomes the angular limitations of conventional bull's eye structures.

9361-48, Session 11

Higgs amplitude mode in s-wave superconductors revealed by terahertz pump-terahertz probe spectroscopy (Invited Paper)

Ryusuke Matsunaga, Ryo Shimano, The Univ. of Tokyo (Japan)

By using the THz pump-THz probe spectroscopy, we have investigated ultrafast nonequilibrium dynamics of s-wave superconductors NbTiN. After an instantaneous excitation with intense monocycle THz pulse, a transient oscillation of the superconducting order parameter is observed in the transmission of the THz probe pulse, which is referred to as the Higgs amplitude mode. Although the Higgs mode does not have a charge, an electric dipole, nor a spin and therefore it does not couple to the electromagnetic field, we revealed that the Higgs mode does indeed appear by shaking the BCS ground state with the nonadiabatic perturbation as theoretically anticipated. We also discovered that the Higgs mode can be resonantly excited by sub-gap multi-cycle THz pulses in the nonlinear response regime. This resonance between the THz light and the Higgs mode results in an efficient third-order harmonics generation. These results shed new light on the ultrafast control of macroscopic quantum condensates by optical means as well as THz nonlinear optics using superconductors.

9361-49, Session 11

Nanoscale charge-order dynamics in stripe-phase nickelates probed via ultrafast THz spectroscopy

Giacomo Coslovich, Sascha Behl, Bernhard Huber, Lawrence Berkeley National Lab. (United States); Takao Sasagawa, Tokyo Institute of Technology (Japan); Wei-Sheng Lee, Zhi-Xun Shen, Stanford Univ. (United States); Hans A. Bechtel, Michael C. Martin, Robert A. Kaindl, Lawrence Berkeley National Lab. (United States)

The dynamics of low-energy excitations and charge transport at the nanoscale is of critical importance for a wealth of applications, ranging from quasi 1D conduction in nanostructured materials to charge ordering in complex compounds. However the relevant cause-effect relations between real-space charge organization and the low-energy excitations remain hidden in time-averaged studies. The complex layered material $\text{La}_{1.75}\text{Sr}_{0.25}\text{NiO}_4$ represents an ideal model system to investigate such physics, since at low temperatures electrons organize in quasi 1D atomic-scale rivers of charge, called stripes.

Here we report ultrafast optical pump-THz probe spectroscopy of this model stripe-ordered system at temperatures below the charge and spin ordering transitions ($T_{CO} \approx 110$ K and $T_{SO} \approx 90$ K respectively). Ultrafast experiments in the multi-THz spectral range (up to ≈ 17 THz) show strong THz reflectivity variations around the phonon bending mode frequency (centered at 11 THz). This phonon mode exhibits a splitting at low temperatures directly related to the formation of the stripe order at the nanoscale, while the background conductivity is reminiscent of the opening of the mid-IR pseudogap due to charge localization. The transient THz probe therefore captures both the electronic and structural dynamics relevant to the charge and spin ordering in a single pulse of light. The results reveal the interplay between the charge localization dynamics and the phonon bending mode folding, providing insight in the symmetry breaking dynamics of nanoscale charge order.

9361-50, Session 11

Control of intra-excitonic scattering in semiconductor quantum wells by an external magnetic field

Harald Schneider, Jayeeta Bhattacharyya, Sabine Zybell, Faina Esser, Helmholtz-Zentrum Dresden-Rossendorf e. V. (Germany); Manfred Helm, Helmholtz-Zentrum Dresden-Rossendorf e. V. (Germany) and Technische Univ. Dresden (Germany); Lukas Schneebeil, Christoph N. Böttge, Benjamin Breddermann, Mackillo Kira, Stephan W. Koch, Philipps-Univ. Marburg (Germany)

We report on the internal dynamics of excitons in high-quality GaAs quantum wells and on the control of intra-excitonic transitions by an external magnetic field. The free-electron laser FELBE in Dresden is ideally suited for selective excitation of intra-excitonic transitions, since it provides intense, spectrally narrow transform-limited terahertz pulses in a unique continuous pulse train, which also allows us to use a synchroscan streak camera system [1]. Subsequent to the production of excitons by pulsed interband excitation, we resonantly pump the 1s-2p intra-excitonic transition which is located at around 2 THz. Coulomb-mediated transfer from the optically “dark” 2p to the radiative 2s state and relaxation into the fundamental 1s state is investigated by time-resolved photoluminescence involving the 1s and 2s excitonic levels [2]. In particular, applying an external magnetic field strongly affects the observed behavior. Detailed analysis of the experimental behavior based on a newly developed microscopic theory allows us to demonstrate the remarkable impact of magnetic fields on the Coulomb and terahertz interactions in the excitonic system, which occurs as a consequence of magnetically induced changes of excitonic orbitals and energetic detuning of excitonic levels [3]. As an interesting application, we also discuss the possibility of observing terahertz gain induced by intra-excitonic transitions.

[1] J. Bhattacharyya et al., Rev. Sci. Instrum. 82, 103107 (2011)

[2] W. D. Rice et al., Phys. Rev. Lett. 110, 137404 (2013)

[3] J. Bhattacharyya et al., Phys. Rev. B 89, 125313 (2014)

9361-51, Session 11

Broadband transient THz conductivity of the transition-metal dichalcogenide MoS₂

Jan H. Buss, Ryan P. Smith, Giacomo Coslovich, Robert A. Kaindl, Lawrence Berkeley National Lab. (United States)

Transition metal dichalcogenides are of great interest due to a multitude of physical properties linked to their layered structure, broadband absorption across the visible, and an electronic structure governed by strong spin-orbit coupling. Understanding their basic excitations and charge dynamics is also of importance to novel opto-electronic, catalytic and photovoltaic applications. In particular, semiconducting molybdenum disulfide (MoS₂) exhibits a crossover from a -1.3 eV indirect to a -1.9 eV direct bandgap as it varies from bulk to the monolayer limit. While visible light couples strongly to carriers and excitons at the direct gap, momentum-indirect optical excitations involve weak, phonon-assisted coupling that renders them poorly accessible by visible photons.

We report ultrafast optical-pump THz-probe studies of MoS₂ that access transient conductivity dynamics of optically “dark” carriers excited at its indirect bandgap. Broadband terahertz pulses were employed as a contactless probe of the ground state conductive properties and transient photoresponse up to 7 THz. In equilibrium, we observe a Drude-like conductivity corresponding to $\sim 5 \times 10^{16}$ cm⁻³ background carriers, with 3 THz scattering rate indicating ~ 350 cm²/Vs mobility. Near-IR excitation with ~ 60 μ J/cm² fluence results in generation of indirect e-h pairs between the highest, zone-center valence band and conduction band minimum along Gamma-K. The THz response builds up quickly on a fs timescale and is

characterized by suppressed fields signifying increased conductivity of transient charge pairs, along with broadband dielectric function changes. We will discuss the spectra and ensuing dynamics over a 100 ps timescale, along with ongoing studies to access many-particle and vibrational coupling beyond 10 THz.

9361-52, Session 11

Time-resolved observation of excitonic dynamics under coherent terahertz excitation in GaAs quantum wells

Kento Uchida, Kyoto Univ. (Japan); Hideki Hirori, Kyoto Univ. (Japan) and Japan Science and Technology Agency-CREST (Japan); Takao Aoki, Waseda Univ. (Japan) and Japan Science and Technology Agency-CREST (Japan); Christian Wolpert, Kyoto Univ. (Japan) and Japan Science and Technology Agency-CREST (Japan); Yu Mukai, Kyoto Univ. (Japan); Koichiro Tanaka, Kyoto Univ. (Japan) and Japan Science and Technology Agency-CREST (Japan); Toshimitsu Mochizuki, Changsu Kim, Masahiro Yoshita, Hidehumi Akiyama, The Univ. of Tokyo (Japan); Loren N. Pfeiffer, Kenneth W. West, Princeton Univ. (United States)

The resonant excitation of excitonic transitions in semiconductors with time-dependent terahertz (THz) electric fields leads to intriguing nonlinear effects [1], such as Rabi splitting and bandgap modulation. These effects manifest as energy shifts of the optical excitonic absorption which show different quantitative responses to the external field amplitude. However, so far, due to the lack of phase stable, intense, narrowband THz pulses with frequency tunability, the nonlinear behavior of excitons under a THz electric field has been elusive. In this study, we developed a novel narrow-bandwidth intense THz pulse with frequency tunability by using tilted-pump-pulse-front scheme [2], which has the maximum peak field amplitude of 10 kV/cm and bandwidth of 50 GHz. By performing THz pump and optical probe experiments on GaAs QWs we observed that the incident THz pulse induces a strong spectral modulation of the 1s heavy-hole exciton peak due to Rabi splitting. For elevated THz electric fields an additional net blueshift can be observed. Our measurement allows us to compare the excitonic peak shift with electric field strength in time domain precisely, strongly indicating that the amount of excitonic blue shift is much larger than the ponderomotive energy. This finding is in stark contrast to the theoretical prediction of bandgap shifts due to the dynamical Franz-Keldysh effect [3].

[1] M. Wagner et al., Phys. Rev. Lett. 105, 167401 (2010).

[2] H. Hirori et al., Appl. Phys. Lett. 98, 091106 (2011).

[3] K. B. Nordstrom et al., Phys. Rev. Lett. 81, 457 (1998).

9361-53, Session 11

Accurate simulation of terahertz transmission through doped silicon junctions

Chih-Yu Jen, Christiaan Richter, Rochester Institute of Technology (United States)

At SPIE 2014 we presented results demonstrating the ability of transmission mode terahertz time domain spectroscopy (THz-TDS) to detect doping profile differences and deviations in silicon. This capability is potentially useful for quality control in the semiconductor and photovoltaic industry. In this presentation we will share subsequent experimental results revealing that terahertz interactions with both electrons and holes are strong enough to recognize both n- and p-type doping profile changes. We also show that the relatively long wavelength (~ 1 mm) of THz radiation allows this approach to be compatible with surface treatments like for instance the

**Conference 9361:
 Ultrafast Phenomena and Nanophotonics XIX**

texturing (scattering layer) typically used in the solar industry. Next we demonstrate the accuracy with which current terahertz optical models can simulate the power spectrum of terahertz radiation transmitted through junctions with known doping profiles (as determined with SIMS). We show that current optical models predict the terahertz transmission and absorption in silicon junctions well.

9361-54, Session 12

Manipulation of the valley degree of freedom in MoS2 transistors (*Invited Paper*)

Kin Fai Mak, The Pennsylvania State Univ. (United States)

Two-dimensional atomic layers of molybdenum disulfide (MoS₂) have attracted much recent attention due to their unique electronic properties. In addition to charge and spin, electrons in MoS₂ monolayers possess a new valley degree of freedom (DOF) that has finite Berry curvatures. As a result, optical control of the valley DOF is allowed. In the first part of the talk, we will discuss the generation of valley-polarized carriers in monolayer MoS₂ by pumping with circularly polarized light. By analyzing the resultant photoluminescence handedness, we have observed long-lived valley polarization in the system. The finite Berry curvatures associated with each valley also have profound consequences on the electrical properties of the material. A well-known example is the valley Hall effect, a Hall effect in the absence of a magnetic field whose sign depends on the valley index. By optically injecting valley-polarized carriers in monolayer MoS₂ transistors, we observe a finite anomalous Hall effect whose sign depends on the incident photon handedness. We will discuss the dependence of the anomalous Hall conductivity on photon helicity, photon energy, doping levels and crystal symmetry, and will compare these observations with theoretical predictions. Finally, possibilities of using the valley DOF as an information carrier in next-generation electronics and optoelectronics will also be discussed.

9361-55, Session 12

Ultrafast element-specific magnetization dynamics of complex magnetic materials on a table top (*Invited Paper*)

Stefan Mathias, Technische Univ. Kaiserslautern (Germany); Chan La-O-Vorakiat, Univ. of Colorado (United States) and National Institute of Standards and Technology (United States); Justin M. Shaw, National Institute of Standards and Technology (United States); Emrah Turgut, Patrik Grychtol, Univ. of Colorado (United States) and National Institute of Standards and Technology (United States); Roman Adam, Denis Rudolf, Forschungszentrum Jülich GmbH (Germany) and JARA-FIT (Germany); Hans T. Nembach, Thomas J. Silva, National Institute of Standards and Technology (United States); Martin Aeschlimann, Technische Univ. Kaiserslautern (Germany); Claus M. Schneider, Forschungszentrum Jülich GmbH (Germany) and JARA-FIT (Germany); Henry C. Kapteyn, Margaret M. Murnane, Univ. of Colorado (United States) and National Institute of Standards and Technology (United States)

X-rays represent one of the most powerful tools for understanding complex materials at the nanoscale, uncovering important information related to all electronic, magnetic, structural, and chemical properties of a solid. Rapid progress in ultrafast X-ray science worldwide, both in high-harmonic and X-ray free electron laser sources, has now paved the way for a completely new generation of experiments investigating ultrafast magnetic processes with ultrahigh time-resolution and element-specificity.

Here, we use extreme ultraviolet pulses from high-harmonic generation as a probe of ultrafast, optically driven, spin dynamics in a ferromagnetic alloys and multilayer structures [1,2]. With the new experimental capabilities of ultrahigh time-resolution, combined with element-specific simultaneous probing, we are able to disentangle important microscopic processes that drive magnetization dynamics on femtosecond timescales. We elucidate the role of exchange interaction on magnetization dynamics in strongly exchange-coupled alloys [3], and the role of photo-induced superdiffusive spin currents in magnetic multilayer stacks [4,5].

[1] La-O-Vorakiat, C. et al., Phys Rev Lett 103, 257402 (2009).

[2] Mathias, S. et al., Journal of Electron Spectroscopy and Related Phenomena 164-170 (2013).

[3] Mathias, S. et al., PNAS 109, 4792-4797 (2012).

[4] Rudolf, D. et al., Nat Commun 3, 1037-6 (2012).

[5] Turgut, E. et al., Phys Rev Lett 110, 197201 (2013).

9361-56, Session 12

Nonlinear magnetization dynamics in HoFeO3 induced by strong terahertz magnetic field

Yu Mukai, Hideki Hirori, Takafumi Yamamoto, Hiroshi Kageyama, Koichiro Tanaka, Kyoto Univ. (Japan)

The ultra-intense single-cycle THz pulses have opened up the new research field of nonlinear THz optics and are enabling comprehensive control over electronic or structural dynamics [1]. However, the study of nonlinear dynamics is limited to the electric excitations and nonlinear dynamics of the magnetism has been inaccessible so far because of the limited magnetic field strength and relatively small dipole moment of magnetic excitations. Here, for the first time, we report on the nonlinear magnetization dynamics of a HoFeO₃ crystal excited by the terahertz magnetic field and measured by means of Kerr rotation optical microscopy. To realize the extremely high magnetic field inside the crystal, we fabricated split ring resonators (SRR) on the crystal surface and irradiate the intense THz pulse generated by using the tilted-pulse-front technique with LiNbO₃ crystal [2]. The incident THz electric field induces a circulating current that in turn generates a magnetic field, which is enhanced at the SRR resonance frequency [3]. As an increase of the magnetic field, the amplitude and frequency of Kerr rotation signal relevant to the antiferromagnetic resonance mode becomes saturated and redshifted, respectively. Our simulation using Landau-Lifshitz-Gilbert equation based on the two-lattice model reproduces these behaviors, and implies that the magnetic field enhanced by SRR is strong enough to drive the spin motion into nonlinear dynamics regime.

[1] T. Kampfrath et al., Nature Photon. 7, 680 (2013).

[2] H. Hirori et al., Appl. Phys. Lett. 98, 091106 (2011).

[3] Y. Mukai et al., Appl. Phys. Lett. 105, 022410 (2014).

9361-57, Session 12

Simultaneous excitation of the magnetic and electronic systems in a ferromagnetic cobalt by ultra intense [λ]³ THz bullet

Mostafa Shalaby, Carlo Vicario, Paul Scherrer Institut (Switzerland); Yan Luning, Univ. Pierre et Marie Curie (France); Christoph P. Hauri, Paul Scherrer Institut (Switzerland)

The speed of magnetization reversal is a key feature in magnetic data storage. Magnetic fields from intense THz pulses have been recently shown to induce fractional magnetization dynamics (~0.005) on the picosecond

**Conference 9361:
 Ultrafast Phenomena and Nanophotonics XIX**

scale. In this work, we significantly up-scaled the excitation intensities targeting total magnetic flip in a thin Cobalt film. We observed strong change in the material dielectric response driven by the THz electric field. The magnetic field-induced precessions persisted in the range of excitation used. While the magnetic precessions lasted only during the THz excitation (sub-ps), the electric field effect is found to last over long time scale (>20 ps) after the excitation pulse has finished. Such an effect may eventually turn out to be the bottleneck for THz-induced magnetic switching.

The excitation comes from a low frequency ≈ 3 THz laser. The THz source is based on small aperture organic (DSTMS) crystal. We used a new concept of THz wave front correction and manipulation to bring the THz to the ultimately minimal length (diffraction limit) and time (single optical cycle) scales. The center frequency of our trigger was 3.2 THz and the spot size was ~ 100 nm. The maximum electric and magnetic fields were 5 GV/m and 17 T, respectively. Such fields are order of magnitude higher than any reported THz fields from a laser-based system and surpassing the performance of large scale accelerator facilities.

9361-58, Session 12

Novel nanoring structure for light-induced generation of ultrashort magnetic pulses

Guillaume G. Vienne, A*STAR - Data Storage Institute (Singapore) and Nanyang Technological Univ. (Singapore); Xiaoye Chen, Ying Shi Teh, Ying Jye Ng, Nyap Oon Chia, Ching Pin Ooi, A*STAR - Data Storage Institute (Singapore)

In 1820 Seebeck observed the deflection of a compass needle when heating one of the junctions in a closed loop of two dissimilar metals or semiconductors with a lamp. The origin of what was then coined thermomagnetism is now known as the Seebeck effect, and Oersted pointed out that it is in fact thermoelectric in nature. Recently, it was proposed that a nanoscale version of this structure, composed of one quadrant of nickel and three quadrants of gold, can generate intense magnetic pulses under illumination by ultrashort laser pulses. We show that it is possible to modify this structure to obtain a light distribution at plasmonic resonance which is more efficient at generating the magnetic field. We propose to use four sectors of two thermoelectric materials with a carefully chosen layout to drive the current along the nanoring by two electromotive forces instead of one. With the example of nickel and gold, we show that the magnitude of the generated magnetic field can be increased by more than 50% compared to the original structure. Beyond the larger magnetic field, another advantage of this design is the reduced risk of melting due to the more even distribution of heat along the nanoring. In this scheme the magnetic field indirectly originates from the Seebeck effect but this structure also leads to an enhancement of the magneto-optical Kerr effect.

9361-59, Session 13

Nonlinear semiconducting metamaterials at terahertz frequencies (Invited Paper)

Richard D. Averitt, Univ. of California, San Diego (United States)

Metamaterials provide a route for creating new functional devices through the judicious design of subwavelength elements that are fashioned into various two- or three-dimensional arrays. This idea has proven particularly fruitful at terahertz frequencies with regards to creating dynamic filters, phase and amplitude modulators, and detectors. Further, metamaterials extend to the nonlinear regime, with a typical approach being the incorporation of a nonlinear element within the electric field-enhanced capacitive region of a split ring resonator (SRR). Coinciding with advances in generating intense terahertz electromagnetic pulses (approaching 1MV/cm), this enables exploration of nonlinear metamaterial devices in the far-infrared. We present our recent efforts in this area, with a focus on obtaining enhanced nonlinear responses using semiconductors as the resonant

subwavelength elements. We have patterned doped thin films of InAs into arrays of disks that exhibit a plasmonic response at terahertz frequencies. Further, the plasmonic response exhibits nonlinear damping as a function of the incident terahertz field strength. This arises primarily from field-induced scattering of carriers from the Γ valley to the lower mobility L valley. In addition, we have incorporated InAs plasmonic disks into various absorber geometries, which enable the creation of terahertz saturable absorbers and optical limiters.

9361-60, Session 13

Terahertz monopole resonators using planar plasmonic metamaterials (Invited Paper)

Joong-Wook Lee, Chonnam National Univ. (Korea, Republic of)

We first present a new phenomenon: the quarter-wavelength resonance of an electromagnetic field in planar plasmonic metamaterials consisting of asymmetrically coupled air-slot arrays, which is essential for a monopole resonator. The anti-nodal electric field intensity of the quarter-wavelength fundamental mode is formed by strong charge concentrations at the sharp metallic edges of the crossing position of the air-slots, and the nodal point of the electric field intensity naturally occurs at the other end of the air-slot. By tuning the structural asymmetry, the quarter-wavelength resonances were successfully split from the half-wavelength resonance, experimentally and numerically.

9361-61, Session 13

High-Q fully-switchable THz superconducting complementary metasurfaces

Giacomo Scalari, ETH Zürich (Switzerland); Sara Cibella, Istituto di Fotonica e Nanotecnologie (Italy); Curdin Maissen, ETH Zürich (Switzerland); Roberto Leoni, Istituto di Fotonica e Nanotecnologie (Italy); Mattias Beck, Jérôme Faist, ETH Zürich (Switzerland)

High degree of control of THz radiation is desired in a number of applications, from fundamental research to applied science. Metamaterials are known for their flexibility and their scalability making them powerful elements for the control of THz beams and also strongly subwavelength resonators for light-matter coupling experiments. We present a new metasurface realized with superconducting Niobium which displays switching behavior as a function of the temperature. The metasurface is based on the complementary metamaterial concept and acts as a narrow bandpass filter and/or resonator with a high quality factor. The 100 nm Nb film is deposited by dc-magnetron sputtering on Si GaAs, then the metasurface is defined by direct writing with Ebeam lithography and the niobium is selectively removed by dry reactive ion etching. The design of the metasurface is aimed to provide high quality factor together with a pronounced switching behavior. Thanks to the large difference of inductance created by the superconducting regime via the kinetic inductance of the Cooper pairs, the metasurface behavior is radically different above and below T_c . For temperatures below 5 K a narrow and pronounced transmission peak is observed at the frequency of 270 GHz, with a quality factor $Q=34$. Above 8 K, no resonance is visible anymore. Experimental results are in very good agreement with FE simulations based on surface impedance measurements of an unpatterned Nb film. This fully switchable metasurface can be employed as a narrow band filter and as an high Q cavity with switching behavior for light-matter coupling experiments.

9361-62, Session 13

Sensitive detection of microorganisms using terahertz metamaterials and plasmonic devices

SaeJune Park, Yeong Hwan Ahn, Ajou Univ. (Korea, Republic of)

We demonstrate that THz metamaterials (split-ring resonators) and plasmonic devices (slot antenna and bow-tie antenna) can work as efficient sensors for detecting microorganisms such as molds, yeasts and bacteria. A clear shift in the resonant frequency is observed following the deposition of microorganisms, and arises due to the change in the effective dielectric constant in a gap area of the metamaterials and plasmonic structures. Strong field localization and enhancement in the gap area enables us to detect the microorganisms with high sensitivity. The resonant frequency shift is higher for the larger dielectric constants, which was confirmed by the dielectric constant measurements of individual fungi and bacteria. In addition, our THz metamaterials and plasmonic sensors can be used in aqueous conditions as well as in ambient conditions, because it is highly sensitive to the substances located near the surface. THz metamaterial and plasmonic sensing is a universal method because it is based on the dielectric sensing, while a selective detection is also possible by functionalizing the substrates with antibodies specific to the target substances. Finally, the sensitivity has been studied as a function of substrate dielectric constant, gap size and metal film thickness to optimize the microbial sensors. Our experimental findings are in a good agreement with the results of finite-difference time-domain simulations.

9361-63, Session 13

High-power and broadband terahertz generation through large-area plasmonic photoconductive emitters

Nezh T. Yardimci, Univ. of California, Los Angeles (United States)

Large area photoconductive emitters are one of the most promising sources of high power and broadband terahertz radiation since they can accommodate relatively high optical pump power levels without suffering from the carrier screening effect and thermal breakdown. By illuminating the active area and applying an external bias electric field, electron-hole pairs are generated and accelerated in opposite directions. A time-varying dipole moment is induced by the acceleration and separation of the photocarriers, generating terahertz radiation. However, the acceleration and transport velocity of the photocarriers are limited by carrier scattering in the photo-absorbing substrate lattice, limiting the magnitude of the induced dipole moment. Thus, even though these devices have great promise for high power terahertz radiation generation, the optical-to-terahertz conversion efficiency of conventional large area photoconductive emitters is limited by their weak effective dipole moment. In order to increase the optical-to-terahertz conversion efficiency of large area photoconductive emitters, we present a novel design that incorporates plasmonic contact electrodes within the device active area. As a result, the induced dipole moment improves remarkably by drifting the majority of the photocarriers to the plasmonic contact electrode, greatly enhancing the optical-to-terahertz conversion efficiency. We demonstrate up to 3.6 mW of pulsed terahertz radiation at an optical pump power of 150 mW, exhibiting two-orders of magnitude higher optical-to-terahertz conversion efficiencies compared with conventional large area photoconductive emitters.

9361-64, Session 14

Experimentally determining the true coupled rate equation for charge dynamics in semiconductor heterostructures (*Invited Paper*)

Alan D. Bristow, Scott K. Cushing, Tess R. Senty, West Virginia Univ. (United States)

Heterostructured semiconductor devices are wide ranging in their application and are reliant on the engineering and control of charge transport across the interfaces. For example photocatalysis requires the charge excitation, separation and migration to occur from an absorbing semiconductor to the reaction site. Similar is true in photovoltaics or photodetectors. In order to rationally design useful heterostructures, transient absorption has been employed to characterize the lifetimes of charge dynamics such as radiative recombination, Shockley-Read-Hall effects, Auger scattering and charge transfer between charge donors and charge acceptor regions. For the most part these dynamics are fit to a multi-exponential with each exponential being assigned to a single process during the transient. However, the transient is usually a non-exponential solution to a coupled rate-equation model. Unfortunately, the true underlying rate equation is difficult to guess and fit from the transient data alone, hence the popularity of multi-exponential fits. Predictions of donor-to-acceptor transfer times vary over several orders of magnitude. Here we present an inversion analysis technique for transforming the transient back into the rate equation without fitting, unambiguously giving the lifetime versus carrier density even if the decay is non-exponential. Consequently, we determine regimes that are dominated by Auger and linear scattering rates, as well as trapping effects and transfer rates. Experimentally we apply the method to CdSe-TiO₂ nanoparticles and nanorod samples and find that trap-based Auger-scattering can dominate and that for all materials at low enough excitation density that their decay is indeed linear. Finally we predict transfer rates across the heterostructure interface.

9361-65, Session 14

Optical control of patterns and polariton flow in semiconductor microcavities (*Invited Paper*)

Stefan Schumacher, Univ. Paderborn (Germany)

With long-lived coherences and strong nonlinearities, polaritons in semiconductor quantum-well microcavities have recently proven an ideal playground for nonlinear optical physics. Recent studies have focussed both on direct resonant excitation of polaritons and on off-resonant excitation of coherent polariton condensates through an exciton reservoir. The interest in polaritons is fueled both by an interest in fundamental physics as well as by their promise for future applications.

In my presentation I will discuss our recent work in the area of self-organization and pattern formation of coherently driven polariton systems. In particular the spinor character of the polariton quantum fluid distinguishes the patterns formed from patterns previously studied in other systems. Apart from being of fundamental interest, this also opens up new possibilities to optically control the patterns. In the second part I will discuss off-resonant excitation of polariton condensates with spatially structured excitation profiles. In this scenario the spatial shape of the exciton reservoir density can be re-configured by changing the optical excitation profile which can be used to control the flow of the polaritons in the two-dimensional plane.

**Conference 9361:
Ultrafast Phenomena and Nanophotonics XIX**

9361-66, Session 14

Time-domain calculations of shift currents in bulk GaAs

Reinold Podzinski, Univ. Paderborn (Germany); Huynh T. Duc, Vietnamese Academy of Science and Technology (Viet Nam); Torsten Meier, Univ. Paderborn (Germany)

We experimentally and theoretically investigate shift currents optically induced in semiconductors. The studies were performed for (110)-oriented bulk GaAs samples using 150 fs excitation laser pulses at normal incidence and at room temperature. In this configuration shift currents may be induced in either of the two in-plane directions [001] and [1-10]. The currents were detected by time-resolved measurement of the simultaneously emitted THz radiation using a standard electro-optic sampling setup. To account for different excitation energies the carrier frequency of the laser pulses has been varied. The shift currents were analyzed using a microscopic theory that combines k.p band structure calculations with multisubband Bloch equations. Our numerical solutions of the multisubband Bloch equations provide a detailed and transparent description of the dynamics of the material excitations in terms of interband and intersubband polarizations/coherences and occupations. The resulting shift currents originate from off-resonant excitations involving energetically higher conduction and lower valence bands, respectively.

9361-67, Session 14

Ultrafast optical control over the exciton polariton propagation in CdZnTe

Jan Lohrenz, Stefan Melzer, Claudia Ruppert, Technische Univ. Dortmund (Germany); Matthias Reichelt, Torsten Meier, Univ. Paderborn (Germany); Markus Betz, Technische Univ. Dortmund (Germany)

We analyze the influence of optically injected charge carriers on the light propagation on the lower exciton polariton branch in CdZnTe bulk crystals at cryogenic temperatures. Pumping with 800 nm pulses relies on two-photon absorption and yields a rather uniform excitation profile throughout the ~200 μm thick semiconductor slab. Remarkably, we observe transmissivity changes of up to ~80% in a ~10 nm spectral window close to the exciton resonance. These features persist on a ~10ps timescale and can be explained taking into account the free induction decay of the exciton in combination with an excitation induced dephasing and shift of the resonance.

9361-68, Session 15

Investigation of coupled optical parametric oscillators for novel applications (Invited Paper)

Yujie J. Ding, Lehigh Univ. (United States)

During this presentation, we review the progress made by us on the coupled optical parametric oscillators and their applications. In a conventional optical parametric oscillator, a pump beam generates a pair of signal and idler waves in a nonlinear medium being placed in an optical resonator. In our novel scheme, each pump wave generates a pair of signals and a pair of idlers from a composite consisting alternating nonlinear plates. These signal twins (also idler twins) exhibit ultrastability, i.e. their relative phase difference and frequency separation are insensitive to the temperature fluctuation and the phase variation of the pump beam. As a result, these twins can be used to realize variety of the applications. For example, when using them for THz generation, the THz output power is greatly enhanced compared with that generated by the pair of signal and idler waves in the conventional optical parametric oscillator. Moreover, the linewidth and

noise of the THz output are greatly reduced using the twins. These coupled parametric processes can be also used to compensate for the effect induced by the atmospheric turbulence which makes images lose their original resolutions and generates additional noises for the electromagnetic waves propagating through atmosphere. Other applications include quantum communications and imaging.

9361-69, Session 15

Intense THz radiation from laser plasma with controllable waveform and polarization (Invited Paper)

Peng Liu, Ya Bai, Liwei Song, Ruxin Li, Zhizhan Xu, Shanghai Institute of Optics and Fine Mechanics (China)

Waveform and polarization controlled Terahertz (THz) radiation is of great importance due to its potential application in THz sensing and coherent control of quantum systems. We demonstrated a scheme of generating waveform-controlled THz radiation from air plasma produced when carrier-envelope-phase (CEP) stabilized few-cycle laser pulses undergo filamentation in ambient air. We launched CEP-stabilized 10 fs laser pulses at 1.8 micron (about 1.7 optical cycles) into air and found that the generated THz waveform can be controlled by varying the filament length and the CEP of driving laser pulses. Calculations using the photocurrent model and including the propagation effects well reproduce the experimental results, and the origins of various phase shifts in the filament are elucidated.

By changing the polarization state of the home-built optical parameter amplifier output beams to be circular, the spectrum is expanded to supercontinuum (1300nm-2100nm) with an extremely high transmittance (> 65%). Elliptically polarized THz waves are generated from air plasma induced by the circularly polarized few-cycle pulses. Our results reveal that electric field asymmetry in rotating directions of the circularly polarized few-cycle laser pulses produces the enhanced broadband transient currents, and the phase difference of perpendicular laser field components is partially inherited in the generation process of THz emission. The ellipticity of the THz emission and its major axis direction are optically controlled by the duration and CEP of the laser pulses.

9361-70, Session 15

Temporal characterization of full attosecond pulse by THz streaking

Fernando Ardana Lamas, Paul Scherrer Institut (Switzerland) and Ecole Polytechnique Fédérale de Lausanne (Switzerland); Christian Erny, Paul Scherrer Institute (Switzerland) and Ecole Polytechnique Fédérale de Lausanne (Switzerland); Andrey Stepanov, Paul Scherrer Institut (Switzerland); Ishkhan Gorgisyan, Paul Scherrer Institut (Switzerland) and Ecole Polytechnique Fédérale de Lausanne (Switzerland); Pavle Juranic, Paul Scherrer Institut (Switzerland); Christoph P. Hauri, Paul Scherrer Institut (Switzerland) and Ecole Polytechnique Fédérale de Lausanne (Switzerland)

We present a scheme for a complete temporal characterization of an entire attosecond pulse train (APT) in one single shot. The technique is based on an all-optical streak camera, which is commonly used for isolated attosecond pulse characterization using a near infrared streak field. Here we demonstrate that streaking with a strong THz transient increases the temporal window of the attosecond streak camera from a few hundred attoseconds to approximately 100 fs. This makes it suitable to measure a complete APT of up to 100 fs in duration.

The measured APT is generated by high-order harmonic generation using a 50 fs, 800 nm laser in a pulsed Ar target. The THz source is based on

Conference 9361:
Ultrafast Phenomena and Nanophotonics XIX

optical rectification in LiNbO₃ using the tilted pulse front technique and is intrinsically synchronized to the HHG drive laser. The generated THz pulses are centred at around 0.3 THz and have a pulse length of 2 ps. The produced THz field is strong enough to induce a strong energy shift of the photo-electrons produced by the APT by up to 6 eV. We finally discuss the streaking scheme's capability for single shot APT measurements.

9361-71, Session 15

Split ring resonator based THz-driven electron streak camera featuring femtosecond resolution

Justyna Fabiańska, Univ. Bern (Switzerland); Günther H. Kassier, Max-Planck-Institut für Struktur und Dynamik der Materie (Germany); Thomas Feurer, Univ. Bern (Switzerland)

In the past decade, modified streak cameras have been applied in the field of ultrafast electron diffraction (UED) to characterize the electron bunch length. While initial experiments relied on single-shot operation to obtain sub-picosecond pulse duration measurements [1], Kassier et al. demonstrated a low-jitter streak camera suitable for accumulation mode measurements with a temporal resolution of 150 fs [2]. Further improvements towards a better temporal resolution may prove to be difficult mostly due to limitations of the maximum voltage that can be applied to the GaAs photo-switches. That is, a temporal resolution in the 10-100 fs regime seems to be conceivable with current proven technologies. A few-femtosecond resolution, however, is out of reach for both relativistic and sub-relativistic electron energy regimes.

Here, we propose a route to accomplish temporal electron bunch characterization with the potential capability of achieving few-femtosecond temporal resolution for high-energy electron pulses (10-100 kV range) as well as relativistic electrons in the MeV range. Since electrons and THz pulses are generated from the same laser system, synchronization between the two is inherently guaranteed. To generate the streaking field we use a THz split-ring resonator which is designed to feature a resonant response and a moderate field enhancement in order to alleviate the demands on the driving laser. We show through combined electromagnetic field simulations (COMSOL) and electron trajectory simulations (ASTRA) that such scheme is well adapted to measure ultrashort electron bunches with femtosecond resolution, even on a single-shot basis.

Conference 9362: Terahertz, RF, Millimeter, and Submillimeter-Wave Technology and Applications VIII

Tuesday - Thursday 10-12 February 2015

Part of Proceedings of SPIE Vol. 9362 Terahertz, RF, Millimeter, and Submillimeter-Wave Technology and Applications VIII

9362-1, Session 1

Intra-operative terahertz probe for detection of breast cancer

Alessia Portieri, TeraView Ltd. (United Kingdom)

A Terahertz intra operative scanning probe has been developed by TeraView Ltd. for medical use. The probe is capable of acquiring THz images during breast surgery to distinguish between benign and malignant breast tissue, thus assisting in obtaining complete surgical excision of tumors.

Initial ex-vivo tests have been carried out using the system located in Guys and St Thomas's Hospital in London.

Initial findings of this study are discussed in this paper.

9362-2, Session 1

Numerical studies of supercontinuum generation based on quasi-continuous wave pumping

Tonghui Liu, Dongfang Jia, Ying Liu, Zhaoying Wang, Tianxin Yang, Tianjin Univ. (China)

Spectral broadening and the generation of supercontinuum are inherent features of nonlinear optics, and have been studied intensively for many years. Supercontinuum generation has been found numerous applications in such various fields as spectroscopy, pulse compression, and the design of tunable ultrafast femtosecond laser sources. Generally, supercontinuum is mainly generated by ultra-short pulse. Nanoseconds pulse laser has a high efficiency and low Calorific value, which is an ideal pump for supercontinuum generation. In this paper, supercontinuum generation based on nanoseconds pulse is investigated numerically. Firstly, we introduced the nonlinear Schrödinger (NLS) equation to deduce the temporal and spectral evolution of pulse broadening in the fiber. Secondly, with different types of pulses, including Ultra-Gaussian, quasi-rectangle pulses, we investigated the generation of new frequency and spectral broadening by numerical methods. Comparisons of broadening ratios with pulses in different types, peak powers and nonlinear coefficients are made in the following parts of paper. In addition, after changing the length of fiber from 0.5km to 2.0km, broadening process of nanoseconds pulse in the fiber is demonstrated in the paper. It is found that the Self-phase modulation (SPM) and Raman effects play main roles in the spectral broadening and generation of supercontinuum. Thus, to enhance the nonlinear effects of fiber by increasing the peak power of pulses would improve the generation of supercontinuum, which is going to be proved in our experiments.

9362-3, Session 1

Incoherent sub-terahertz radiation source with a photomixer array for active imaging in smoky environments

Naofumi Shimizu, Nippon Telegraph and Telephone Corp. (Japan); Ken Matsuyama, Hidetake Uchida, Tokyo Univ. of Science (Japan)

We propose a sub-terahertz (THz) illuminator suitable for use with a THz camera when exploring objects in and behind smoke at the scene of a fire. The illuminator contains a photomixer array and each photomixer generates

incoherent sub-THz waves from a single-mode laser light and optical noise using photomixing. Incoherency of the generated sub-THz waves enables us to raise their intensity by increasing the number of photomixers in operation, which makes it possible to realize very bright sub-THz illumination. Consequently, objects under search in or behind smoke can be illuminated clearly with the illuminator and visualized with the THz camera even though they are surrounded by thick and/or high-temperature smoke.

To verify our concept, we performed active imaging with coherent and incoherent sub-THz radiation from a photomixer array with reflection geometry in the 370-GHz band. In the imaging with coherent radiation, the shape of the target was degraded by the interference pattern of the illuminated sub-THz waves, although the contrast of the image was improved by increasing number of photomixers in operation. With incoherent radiation, the contrast of the image was improved without obscuring the shape of the target by increasing the number of photomixers. These results indicate that the use of incoherent sub-THz waves and an array of photomixers should enable a sub-THz illuminator with high brightness for active imaging. In the presentation, we'll also discuss the optimum frequency band, in which we can minimize the absorption of sub-THz waves by gases in smoke emitted by combustion.

9362-4, Session 1

Structured-surface-plasmon-inspired THz components and devices (*Invited Paper*)

Elliott R. Brown, Wright State Univ. (United States)

Structured-surface-plasmons (SSPs) have been broadly cited for interesting electromagnetic effects observed in the THz region. The prime example is extraordinary transmission (EOT) – a phenomenon whereby a much greater fraction of incident radiation passes through a periodic metallic pattern on a lossless substrate than predicted by geometric optics. Another interesting phenomenon is wave-impedance enhancement, which enables much improved coupling from free space to high-impedance semiconductor devices like Schottky diodes, and without the use of planar antennas. This presentation will emphasize the use of SSPs to make superior THz components and devices, such as substrate-based (single-crystal quartz) wire-grid polarizers having unprecedented levels of extinction ratio (> 60 dB).

9362-5, Session 2

Photoconductive materials for THz generation at 1550 nm: ErAs:GaAs- vs InGaAs-based materials

Matthieu Martin, Elliott R. Brown, Wright State Univ. (United States)

Since the 1990s the photoconductive material of choice for THz generation has been low-temperature grown GaAs (LTG-GaAs) thanks to its high mobility ($\sim 200 \text{ cm}^2/\text{V}\cdot\text{s}$), high dark resistivity ($10^7 \text{ }\Omega\cdot\text{cm}$), and fast carrier lifetime ($\sim 0.2 \text{ ps}$). However, due to the band gap energy of GaAs, the usual optical drive wavelength is around 800 nm where suitable lasers, both cw and pulsed, tend to be marginal in output power and rather expensive. Consequently, research has pushed towards the development of InGaAs-on-InP-based ultra-fast photoconductive materials operating at 1550-nm where cw and pulsed lasers are superior in all respects. Several such materials have been investigated during the past 15 years, but none have been able to fully compete with the well-established LTG-GaAs at 800 nm. Recently, we

**Conference 9362: Terahertz, RF, Millimeter, and
 Submillimeter-Wave Technology and Applications VIII**

discovered extrinsic photoconductivity in ErAs:GaAs at 1550 nm, allowing the efficient generation of both cw and pulsed THz waves. GaAs-based materials have major electrical advantages over InGaAs-based because of their superior dark resistivity and breakdown field. In this paper, we propose that 1550-nm-driven ErAs:GaAs is now a very promising alternative to InGaAs-based photoconductive material. We focus on the electrical and ultrafast photoconductive behavior, and compare the performance of ErAs:GaAs devices to those from state-of-the-art ultrafast InGaAs devices. We also present a study of the influence of the erbium concentration on the electrical and photoconductive behavior of the material and devices, such as the time-domain THz response.

9362-6, Session 2

A compact fiber-coupled terahertz sensor system for industrial automation applications

Alireza Zandieh, Daniel M. Hailu, TeTechS Inc. (Canada); Mohamed Missous, The Univ. of Manchester (United Kingdom); Daryoosh Saeedkia, TeTechS Inc. (Canada)

In this paper, we present a new portable, modular, compact, and low-cost continuous-wave (CW) terahertz (THz) sensor system operating at 800 nm wavelength for industrial automation applications. The system is based on terahertz photoconductive antenna photomixer technology capable of testing solid, powder, thin film, and liquid samples for material sensing and characterization applications. The THz sensor system is a single frequency THz sensor system with a selectable operation frequency. The fiber-coupled movable transmitter and receiver heads can be mounted around the object/sample/process under test.

The key components are the fiber-coupled THz transmitter and receiver modules, where the laser beam is directly coupled to the THz chip using optical fibers to provide stable and movable transmitter and receiver heads. A high power terahertz photoconductive antenna is used as the transmitter antenna chip. Using a hyper-hemispherical silicon lens at the transmitter module increases the THz signal to achieve 50 dB-Hz dynamic range at 1 THz. To achieve compactness by using small diameter lenses (1") and 50 mm effective focal length, and custom built collimating lens 10 mm in diameter. Antenna packaging has integrated silicon lens and fiber pigtail, making it alignment free. The outputs of the fiber lasers are combined and then is divided into two arms to drive the transmitter and receiver antennas. To achieve an all fiber system, fast scan optical delay module is implemented using two fiber stretchers to realize real-time THz signal. We use the system to find previously undetectable objects in industrial automation.

9362-7, Session 2

Terahertz wavefront assessment based on 2D electro-optic imaging

Harsono Cahyadi, Ryuji Ichikawa, Univ. of Tokushima (Japan); Jérôme Degert, Eric Freysz, Univ. Bordeaux 1 (France); Takeshi Yasui, Univ. of Tokushima (Japan); Emmanuel Abraham, Univ. Bordeaux 1 (France)

Terahertz (THz) radiation roughly covers the 0.1-10 THz frequency range and bridges the gap between optical and radio waves. This radiation can propagate through many non-conducting and non-polar materials providing a specific spectroscopic diagnosis. Contrary to optical beams, the wavelengths associated to the THz beams are not negligible compared to the size of the optical elements leading to diffraction and a possible deviation from the standard Gaussian beam propagation. However, due to the lack of effective THz cameras, it is still challenging to fully measure the spatial profile of a THz beam. In this communication, we propose a simple arrangement based on free-space collinear 2D electro-optic sampling in a ZnTe crystal for the characterization of THz wavefronts.

The THz beam is generated by optical rectification of amplified femtosecond laser pulses (800 nm, 1 mJ, 150 fs). By using a femtosecond IR probe pulse, the 2D THz field distribution in the ZnTe crystal is converted into a 2D optical intensity distribution recorded by a CMOS camera. By changing the time delay between both pulses, one can map the temporal evolution of the THz electric field in the crystal. This system makes it possible to characterize the THz wavefronts of plane or spherical waves. From the Fourier Transform of the temporal waveforms, one can also obtain the curvature of a broadband THz wave for every frequency within the 0.1-4 THz range. Perspectives include the development of a Shack-Hartmann sensor for an instantaneous characterization of the THz wavefront.

9362-8, Session 2

Terahertz plasmonic channel waveguide based on metallic rod arrays

Borwen You, National Taiwan Univ. (Taiwan) and National Cheng Kung Univ. (Taiwan); Wen-Jie Cheng, Ja-Yu Lu, National Cheng Kung Univ. (Taiwan)

A two dimensional metallic rod array (MRA) with a channelized defect is experimentally demonstrated to guide and localize terahertz field based on surface plasmon resonance. The guided terahertz field is found to be strongly localized and low loss transmitted in the channel of waveguide, and the evanescent field is quickly decayed to the MRAs closely adjacent to the channel. Several resonant dips are observed in the measured THz transmission spectrum, and the spectral-dip positions depend on the channel width and the rod period of the MRA waveguide. This result indicates the spectral dips are caused by resonance of the localized terahertz field bound at the channel walls, which are constructed by metallic rods and resemble surface plasmon polaritons (SPP) resonance. When the dielectric constant of the channel wall is changed, the spectral dip caused by SPP resonance obviously shifts. The MRA-based channel waveguide is potentially a miniature chip to manipulate terahertz field for molecular sensing and waveguide coupling, respectively, based on the resonance and guidance modes.

9362-9, Session 2

Terahertz photonic crystals based on two-dimensional rod array

Borwen You, National Taiwan Univ. (Taiwan); Wen-Jie Cheng, Ja-Yu Lu, National Cheng Kung Univ. (Taiwan)

A THz photonic crystal, constructed by two dimensional arranging metallic rods in a rectangular array, is experimentally demonstrated to capture terahertz photon in the spectral range of 1THz. According to the designed air-space among the rods, the coverage frequency of photonic band gap can be manipulated with the considerably high distinction. Assembling a movable metal cladding outside the metal rod array is able to dynamically control the forbidden band gap in terahertz frequency because the evanescent field around the photonic crystal structure is controllable via various air spaces. Furthermore, the uniformity of the air-space in photonic crystal is studied for the rod structure, constructed on a flexible polymer substrate, and found the attenuation ability at photonic band gaps is reduced while the substrate is mechanically bent.

9362-47, Session 2

**Glasses and ceramics for THz photonics
 (Invited Paper)**

S. K. Sundaram, New York State College of Ceramics at Alfred Univ. (United States)

**Conference 9362: Terahertz, RF, Millimeter, and
Submillimeter-Wave Technology and Applications VIII**

Glasses and ceramics are fairly transparent in the THz region, making them attractive for applications in active and passive THz photonics. We present composition-dependence of THz properties in selected glasses and ceramics, measured using the time-domain THz spectroscopy. In the case of glasses, a power-law relationship has been reported in the literature for frequencies $2\pi\nu \gg v_D/l$ where v_D is the Debye velocity of sound and l is the average correlation length: $n(\nu) = K\nu^{-\alpha}$, where n is the index of refraction, α is the absorption coefficient, ν is frequency, and the exponent $\alpha \approx 2$ for glassy materials. The coefficient K is described as: $K = (4\pi^2 q^2 N^2) / (c^3 v_D^3)$, where q is the amplitude of density of charge fluctuations N , $\nu = (n^2 + 2)/3$ is the local field correction, ρ is mass density, and c is the speed of light. Recently, we evaluated this relationship by systematically varying modifiers (alkali and alkaline earths) in silicate glasses. In the case of ceramics, we investigated the effect of non-stoichiometry on the THz absorption of fully dense optical ceramics of Y₃Al₅O₁₂ (YAG) and compare to that of undoped and 1 at% Nd³⁺ doped single-crystals. A set of twenty ceramic samples was prepared by solid-state sintering of Y₂O₃ and Al₂O₃ powder mixtures with compositions ranging from -0.62 to +0.96 mol% of Y₂O₃ on each side of the stoichiometric YAG composition. These samples exhibit a similar broad absorption band, which we assign to a 2-phonon difference process, and whose width and intensity depend upon composition. We will present our results and correlations.

9362-10, Session 3
Preliminary results of non-contact THz imaging of cornea (Invited Paper)

Shijun Sung, James Garritano, Neha Bajwa, Sophie Deng, Jean-Pierre Hubschman, Warren S. Grundfest M.D., Zachary D. Taylor, Univ. of California, Los Angeles (United States)

This talk presents a novel THz optical design that allows the acquisition of THz reflectivity maps of in vivo cornea without the need for a field flattening window and preliminary imaging results of in vivo rabbit cornea. The system's intended use is to sense small changes in corneal tissue water content (CTWC) that can be precursors for a host of diseases and pathologies. Unique beam optics allow the scanning of a curved surface at normal incidence while keeping the source detector and target stationary. Image sets and time lapse videos of normal, healthy cornea and a disease model cornea simulated by membrane stripping are presented and the role of the tear film discussed. The results represent the first in vivo corneal images ever presented using THz frequency illumination

9362-11, Session 3
Flexible waveguide-enabled single-channel terahertz endoscopic system

Pallavi Doradla, Univ. of Massachusetts Lowell (United States); Karim Alavi, Univ. of Massachusetts Medical School (United States); Cecil S. Joseph, Robert H. Giles, Univ. of Massachusetts Lowell (United States)

Colorectal cancer is the third most commonly diagnosed cancer in the world. The current standard of care for colorectal cancer is the conventional colonoscopy which relies exclusively on a physician's experience. The terahertz (THz) frequency range, located midway between the microwave and infrared region, is non-ionizing and has high sensitivity to water content. This study investigates the feasibility of a prototype terahertz endoscopic system in detecting colorectal cancers, thereby increasing the overall impact of terahertz imaging for in vivo cancer detection/screening applications.

We demonstrate the design and development of a single-channel prototype terahertz endoscopic system based on flexible metal-coated THz waveguides. A CO₂ pumped Far-Infrared molecular gas laser operating at 584 GHz was used for illuminating the tissue, while the reflected

signals were detected using a liquid Helium cooled silicon bolometer. The continuous-wave terahertz imaging system utilizes a single channel to transmit and collect the reflected terahertz signal from the sample. Using polarizers in the experiment both co-polarized and cross-polarized remittance from the samples were collected. Consequently, obtained cross- (co-) polarized terahertz images showed intrinsic contrast between cancerous and normal regions based on increased reflection from the tumor. The level of contrast observed using terahertz endoscopic imaging correlates well with the contrast levels observed in ex vivo terahertz reflectance studies of colon cancer. The data and results will be presented and discussed during SPIE conference.

9362-12, Session 3
A new scheme for ultra-intense terahertz pulse production and nonlinear THz science

Christoph P. Hauri, Carlo Vicario, Paul Scherrer Institut (Switzerland)

We present a novel concept for ultra-intense Terahertz generation by optical rectification of a powerful, mid-infrared laser pulse (30 mJ) in a large-size, mosaic patterned organic crystal. Our original scheme allows the production of single-cycle Terahertz pulses with energies at the mJ level covering the frequency range of 1-5 THz. Thanks to the collimated pump geometry the emitted THz radiation offers excellent pulse wavefront characteristics and outstanding focusing capabilities. The THz field strength reaches up to 50 MV/cm (16 Tesla), which is an order of magnitude beyond state of the art. The availability of such ultra-intense pulses opens a new era in Terahertz nonlinear optics with applications ranging from particle acceleration, biological applications to fundamental novel opportunities in condensed matter physics. Here, we show a full characterization of the THz radiation emitted from the patterned organic crystal structure and present a first intriguing experimental result on inducing a strong $\chi^{(3)}$ nonlinearity in a glass substrate by this ultra-intense Terahertz source.

9362-13, Session 3
Room-temperature zero-bias plasmonic THz detection by asymmetric dual-grating-gate HEMT

Takayuki Watanabe, Tetsuya Kawasaki, Akira Satou, Stephane A. Boubanga Tombet, Tetsuya Suemitsu, Tohoku Univ. (Japan); Guillaume Ducournau, Institut d'Electronique de Microélectronique et de Nanotechnologie (France); Dominique Coquillat, Wojciech Knap, Univ. Montpellier 2 (France); Hiroaki Minamide, Hiromasa Ito, RIKEN (Japan); Yahya M. Meziani, Univ. de Salamanca (Spain); Vyacheslav V. Popov, Institute of Radio Engineering and Electronics (Russian Federation); Taiichi Otsuji, Tohoku Univ. (Japan)

Plasmonic terahertz (THz) detectors based on field-effect-transistor structures are promising for THz wireless communications and have been actively researched. They utilize hydrodynamic nonlinearities in two-dimensional (2D) electron channels. Due to fast and sensitive response of plasmons even at room temperature, higher performance than existing THz detectors are expected. Especially, InP-based high-electron-mobility transistor (HEMT) with the so-called asymmetric dual-grating-gate (A-DGG) structure has been theoretically shown to exhibit enormous performance. The dual-grating-gate structure, which interdigitates two types of grating gates with lengths of submicrons, enables strong coupling between incident radiation and 2D plasmons. By applying a negative bias to either type of the gates, plasmonic cavities and almost depleted regions adjacent to them, which act as voltage readouts, are created in the channel simultaneously,

**Conference 9362: Terahertz, RF, Millimeter, and
 Submillimeter-Wave Technology and Applications VIII**

so that the photovoltage sums up for each unit cell. Furthermore, the asymmetry of the placement of those gates enables intense nonlinear rectification response even with zero drain-to-source bias.

9362-14, Session 3
Enhancing the low frequency THz resonances (1 THz) of organic molecules via electronegative atom substitution

Jyotirmayee Dash, CSIR Madras Complex (India); Shaumik Ray, CSIR-Madras Complex (India); Bala Pesala, CSIR Madras Complex (India)

Terahertz (THz) technology is an active area of research with various applications in non-intrusive imaging and spectroscopy. THz radiation mainly excites low frequency modes involving intra/intermolecular vibrations. Very few organic molecules have significant resonances below 1 THz. Understanding the origin of the low frequency THz modes in these molecules and their absence in other molecules with similar structures could be extremely important in the design and engineering of molecular systems which can show prominent low frequency THz resonances. These engineered molecules can be used as THz tags for anti-counterfeiting applications and as highly absorbing materials for THz radar frequencies.

Several organic molecules having signatures in the THz region have been studied to understand the reason behind the origin of these resonances. Analysis of these studies shows that low frequency THz resonances are commonly observed in molecules having higher molecular mass and weak intermolecular bonds such as hydrogen bonds. In this paper, we have explored the possibility of enhancing the strength of THz resonances below 1 THz through electronegative atom substitution. Acetanilide (C₈H₉NO) has been used as a model system for this study. THz-Time Domain Spectroscopy (TDS) results show that Acetanilide has a strong resonance at 1.73 THz with no significant resonance below 1 THz. Acetanilide can be converted to 2-Fluoroacetanilide by adding an electronegative atom, fluorine, resulting in a shift of resonance to 1.61 THz. However, by optimally choosing the position of the electronegative atom as in the case of 4-Fluoroacetanilide, a significant THz resonance below 1 THz (0.86 THz) is observed. The origin of these resonances can be understood by carrying out Density Functional Theory (DFT) simulations of full crystal structure. These studies show that adding electronegative atom to the organic molecules at an optimized position can result in significantly enhanced resonances below 1 THz.

9362-15, Session 4
Deep sub-wavelength structure empowered THz components (*Invited Paper*)

Jinghua Teng, A*STAR Institute of Materials Research and Engineering (Singapore)

To realize the full potentials of terahertz (THz) wave in applications such as molecular spectroscopy and imaging, it requires the development of high performance and compact THz sources, detectors and various components. The restrictions on materials and the different wavelength scale of THz as compared to its counterpart in optics put some challenges to the THz component fabrication. The emergence and intensive studies of metamaterials in the last decade have provided unique opportunities and dimensions for THz technology development. In this talk, I will introduce several of our recent work in using deep sub-wavelength structures to manipulate the THz wave. This includes the high efficiency continuous wave THz emitter using a nano-electrode incorporated photomixer [1], the THz polarizer with ultra-high extinction ratio by using a bi-layer sub-wavelength metal grating [2], broadband response with concurrent filed localization and optical tuning of THz transmission using InSb plasmonic response in the THz range [3, 4], MEMs based tunable THz metamaterials [5, 6], and the perfect

antireflection coating in THz range using ultra-thin sub-wavelength metal wire gratings [7].

References:

- [1] H. Tanoto, et al, Scientific Report, 3, 2824, 2013
- [2] L. Y. Deng, et al, Applied Physics Letters, 101, 011101, 2012
- [3] S. M. Hanham, et al, Advanced Materials, 24, OP226, 2012
- [4] L. Y. Deng, et al, Advanced Optical Materials, 1, 128, 2012
- [5] W. M. Zhu, et al, Advanced Materials, 23, 1792, 2011
- [6] W. M. Zhu, et al, Nature Communications, 3, 1274, 2012
- [7] L. Ding, et al, Advanced Optical Materials, 39, 630, 2014

9362-16, Session 4
Video rate imaging of narrow band THz radiation based on frequency upconversion

Patrick F. Tekavec, Microtech Instruments, Inc. (United States); Vladimir G. Kozlov, Microtech Instruments Inc. (United States); Ian McNee, Microtech Instruments, Inc. (United States); Igor E. Spektor, Sergey P. Lebedev, A. M. Prokhorov General Physics Institute (Russian Federation)

We demonstrate video rate THz imaging by detecting a frequency upconverted signal with a CMOS camera. A fiber laser pumped, double resonant optical parametric oscillator generates THz pulses via difference frequency generation in a quasi-phaseshifted gallium arsenide (QPM-GaAs) crystal located inside the OPO cavity. The output produced THz pulses centered at 1.5 THz, with an average power up to 1 mW, a linewidth of <100 GHz, and peak power of >2 W. By mixing the THz pulses with a portion of the fiber laser pump (1064 nm) in a second QPM-GaAs crystal, distinct sidebands are observed at 1058 nm and 1070 nm, corresponding to sum and difference frequency generation of the pump pulse with the THz pulse. By using a polarizer and long pass filter, the strong pump light can be removed, leaving a nearly background free signal at 1070 nm. For imaging, a Fourier imaging geometry is used, with the object illuminated by the THz beam located one focal length from the GaAs crystal. The spatial Fourier transform is upconverted with a large diameter pump beam, after which a second lens inverse transforms the upconverted spatial components, and the image is detected with a CMOS camera. We have obtained video rate images with spatial resolution of 1mm and field of view ca. 20 mm in diameter without any post processing of the data.

9362-17, Session 4
Novel method of generation of linear frequency modulation optical waveforms with swept range of over 200 GHz for lidar systems

Tianxin Yang, Yuchen Zhang, Tianhe Wang, Changren Qiu, Chunfeng Ge, Tianjin Univ. (China)

Light detection and ranging (lidar) is used for various applications such as remote sensing, altimetry and imaging. Since the average transmitted power is directly linked to the receiver Signal to Noise Ratio (SNR), it is desired to increase the pulse width while simultaneously maintaining adequate range resolution. This can be achieved by implementing the phase modulation or frequency modulation to the transmitted signal. Linear frequency modulation (LFM) signals have the characteristic that the instantaneous frequency increase (or decreases) linearly over the duration of the signal. The LFM waveforms can be generated by phase or frequency modulation of a carrier which can provided greater waveform flexibility since bandwidth and pulse width can be varied easily. However it is hard to generate

**Conference 9362: Terahertz, RF, Millimeter, and
 Submillimeter-Wave Technology and Applications VIII**

super-broadband optical chirped pulses with exactly linear frequency modulation for the implement of high range resolution in the optical domain. In this paper, a new method is proposed and designed to synthesize a linearly chirped continuous light waves during a flat top optical pulse with large frequency swept range by using optical intensity modulators, optical phase modulators and optical arrayed waveguide gratings (AWG). The optical phase modulators are driven by an ideal parabolic temporal signals which is formed by superposition of RF signals. The numerical simulations of the synthesized optical waveforms are made for different parameters, such as, the frequency and the electric power of the RF signals driving the phase modulator, the AWG parameters, and optical gating techniques by electric absorption modulators which can chop off the part of non-linear frequency components at the edges of the modulated light pulses. Then the chopped and linearly chirped light waveforms are multiplexed to generate a chirped and flat light waves.

9362-18, Session 4

Introduction of liquid crystal device into THz phase imaging

Ryota Ito, Takuya Takahashi, Michinori Honma, Toshiaki Nose, Akita Prefectural Univ. (Japan)

We investigate the terahertz phase imaging using liquid crystal (LC) device. Recently, there have been extensive efforts to measure the refractive indices and transmission losses of some LC materials in THz region. From these results, LC materials show relatively large refractive index anisotropy and they can have a potential application to some control devices similar to the display application. Furthermore, tunable LC THz phase shifter has been reported. In this study, an attempt was made to introduce the LC device into the THz phase imaging which was based on four-step phase-shifting algorithm. Four-step phase-shifting algorithm is one of the most effective methods of phase imaging and moving mirror is needed to introduce phase shift in standard measurements. In addition, we should prepare the two rays with common source, therefore experimental setup becomes complicated. While on the other hand, it is just needed to insert a LC phase shifter into the light pass when we adopt LC device. Furthermore, low-voltage application is enough to introduce the phase-shifting, hence it is not necessary to prepare the moving mirror. In this work, we fabricate the standard LC device which has sandwich cell structure. Quartz substrates and PEDOT/PSS electrode were used to keep THz wave transmittance high. High quality of LC molecular alignment was achieved using display technology. Measurements were made by using an optically pumped gas laser system which can generate continuous wave THz waves with an enough power for precise measurements.

9362-19, Session 5

Plasmonic photomixers for high-power continuous-wave terahertz generation
(Invited Paper)

Christopher W. Berry, Univ. of Michigan (United States); Mohammad R. Hashemi, Univ. of California, Los Angeles (United States) and Univ. of Michigan (United States); Sascha Preu, Technische Univ. Darmstadt (Germany); Hong Lu, Arthur C. Gossard, Univ. of California, Santa Barbara (United States); Mona Jarrahi, Univ. of California, Los Angeles (United States) and Univ. of Michigan (United States)

Utilizing plasmonic contact electrodes has proven to be very effective in enhancing the quantum efficiency of photoconductive terahertz sources and detectors. This is because of the unique capability of plasmonic electrodes in manipulating the intensity of an incident optical pump beam and focusing it tightly next to the device contact electrodes. By enhancing the number

of photocarriers in close proximity to the device contact electrodes, the number of the photocarriers drifted to the contact electrodes within a sub-picosecond timescale is increased and significantly higher quantum efficiency levels are achieved. Up to date, this unique capability of plasmonic electrodes has only been utilized to enhance the radiation power of photoconductive switches for broadband, pulsed terahertz generation. Here, we demonstrate the impact of plasmonic electrodes in enhancing the radiation power of photomixers for continuous-wave, frequency-tunable terahertz generation, for the first time. We present a 1550 nm plasmonic photomixer operating under pumping duty cycles below 10%, which offers significantly higher terahertz radiation power levels compared to previously demonstrated photomixers. The duty cycle of the optical pump is set to prevent thermal breakdown at high optical pump powers. The repetition rate of the optical pump can be specifically selected at a given pump duty cycle to control the spectral linewidth of the generated terahertz radiation. At an average optical pump power of 150 mW and pump duty cycle of 2%, we demonstrate up to 0.8 mW radiation power at 1 THz, within each continuous-wave radiation cycle.

9362-20, Session 5

Optical multi-coset sampling of GHz-band chirped signals

George C. Valley, George A. Sefler, Thomas J. Shaw, Stephen L. Smith, The Aerospace Corp. (United States)

Direct digitization of long wideband chirped RF signals in the GHz band requires power hungry ADCs and produces large data sets. Here we present an optical scheme to perform multi-coset sampling of such signals with reduced power consumption and smaller output data sets. In our scheme a repetitively pulsed femtosecond laser is temporally broadened by a dispersive fiber-optic component with chosen ps/nm dispersion, an RF signal is modulated on the optical field, and the field is directed to a wavelength-division demultiplexer and multiplexer (WDM) pair. The demultiplexed WDM channels are attenuated with a pseudo-random sequence and re-multiplexed to form a coset pattern that repeats at the laser repetition rate. The dispersion of the dispersive component and the WDM channel spacing determine the effective sampling rate of the coset. After detection with a photodiode, photocurrent is integrated for the duration of the dispersed optical pulse. Since the laser repetition rate is uncorrelated with the RF, each coset provides an independent measurement of the RF. Processing the multiple coset samples using orthogonal matching pursuit, experimental and numerical results show that the complete properties of the RF chirp pulse can be determined from the multiple coset samples: carrier frequency, chirp rate, start time, and pulse duration. Experimental results are presented showing recovery of a 20MHz chirp on a 13 microsecond pulse at a carrier of 2.473 GHz.

9362-21, Session 5

Optical and quasi-optical analysis of system components for a far-infrared space interferometer

Colm P. Bracken, Cr  idhe O'Sullivan, National Univ. of Ireland, Maynooth (Ireland); Giorgio Savini, Univ. College London (United Kingdom); Peter A. R. Ade, Cardiff Univ. (United Kingdom); J. Anthony Murphy, National Univ. of Ireland, Maynooth (Ireland); Enzo Pascale, Cardiff Univ. (United Kingdom); Locke D. Spencer, Univ. of Lethbridge (Canada); Roser Juanola-Parramon, Univ. College London (United Kingdom); Ian Walker, Cardiff Univ. (United Kingdom); Kjetil Dohlen, Aix Marseille Univ. (France); John F. Lightfoot, Science and Technology Facilities Council (United Kingdom); Martyn Jones, David D. Walker,

**Conference 9362: Terahertz, RF, Millimeter, and
 Submillimeter-Wave Technology and Applications VIII**

Alison McMillan, Glyndwr Univ. (United Kingdom); Nicola Baccichet, Univ. College London (United Kingdom); Anthony Donohoe, Neil A. Trappe, National Univ. of Ireland, Maynooth (Ireland)

Many important astrophysical processes occur at wavelengths that fall within the far-infrared band of the EM spectrum, and over distance scales that require sub-arc second spatial resolution. It is clear that in order to achieve sub-arc second resolution at these relatively long wavelengths (compared to optical/near-IR), which are strongly absorbed by the atmosphere, a space-based far-IR interferometer will be required. We present analysis of the optical system for a proposed spatial-spectral interferometer, discussing the challenges that arise when designing such a system and the simulation techniques employed that aim to resolve these issues. Many of these specific challenges relate to combining the beams from multiple telescopes where the wavelengths involved are relatively short (compared to radio interferometry), meaning that care must be taken with mirror surface quality, where surface form errors not only present potential degradation of the single system beams, but also serve to reduce fringe visibility when multiple telescope beams are combined. Also, the long baselines required for sub-arc second resolution present challenges when considering propagation of the relatively long wavelengths of the signal beam, where beam divergence becomes significant if the beam compression ratio of the telescopes is not carefully designed. Furthermore, detection of the extremely weak far-IR signals demands ultra-sensitive detectors and instruments capable of operating at maximum efficiency. Thus, as will be shown, care must be taken when designing each component of such a complex quasioptical system.

9362-22, Session 5

Antenna-coupled silicon-organic hybrid integrated photonic crystal modulator for broadband electromagnetic wave detection

Xingyu Zhang, The Univ. of Texas at Austin (United States); Amir Hosseini, Harish Subbaraman, Omega Optics, Inc. (United States); Shiyi Wang, Qiwen Zhan, Univ. of Dayton (United States); Jingdong Luo, Alex K. Y. Jen, Univ. of Washington (United States); Ray T. Chen, The Univ. of Texas at Austin (United States)

The detection and measurement of electromagnetic field (EMF) have attracted significant amounts of attention in recent years. Traditional electronic EMF sensors use large active conductive probes which perturb the field to be measured and make the devices bulky. In order to address these problems, integrated photonic EMF sensors have been developed, in which an optical signal is modulated by an RF signal collected by a miniaturized antenna. In this work, we design, fabricate and characterize a compact, broadband and highly sensitive integrated photonic EMF sensor based on a silicon-organic hybrid modulator driven by a bowtie antenna. Slow-light effects in the electro-optic (EO) polymer refilled silicon slot photonic crystal waveguide (PCW), together with broadband field enhancement provided by the bowtie antenna, are utilized to enhance the interaction of microwaves and optical waves, enabling a high EO modulation efficiency and thus a high sensitivity. The modulator is experimentally demonstrated with a very low V_{π} of 0.0282Vcm, corresponding to a record-large effective in-device EO coefficient of 1230pm/V. Modulation response up to 43GHz is measured, with a 3-dB bandwidth of 11GHz. The broadband bowtie of the device is measured with a central resonance frequency of 10GHz. The sensor is experimentally demonstrated with a minimum detectable electromagnetic power density of 8.4mW/m² at 8.4GHz, corresponding to a minimum detectable electric field of 2.5V/m and an ultra-high sensitivity of 0.000027V/m Hz^{-1/2} ever demonstrated. To the best of our knowledge, this is the first silicon-organic hybrid device and also the first PCW device used for EMF detection.

9362-23, Session 5

Integrated broadband bowtie antenna on transparent substrate

Xingyu Zhang, The Univ. of Texas at Austin (United States); Shiyi Wang, Univ. of Dayton (United States); Harish Subbaraman, Amir Hosseini, Omega Optics, Inc. (United States); Qiwen Zhan, Univ. of Dayton (United States); Ray T. Chen, The Univ. of Texas at Austin (United States)

A modified bowtie antenna integrated on a transparent glass substrate is demonstrated. This bowtie antenna is miniaturized with an area smaller than 1cm². The antenna is a conventional bowtie antenna with extension bars attached to the apex points, in order to obtain an extended near-field area with a uniformly enhanced local electric field under RF illumination. The bowtie antenna is optimized to cover a broad frequency bandwidth, with a central resonant frequency at ~10GHz. The electric field inside the feed gap is enhanced by 670 times compared to the incident electric field. The dependency of resonant frequency on bowtie geometry, such as arm length and flare angle is numerically computed and experimentally verified. In addition, the radiation pattern of the bowtie antenna is simulated and measured, and a large angular beam width similar to a typical dipole antenna is demonstrated. Furthermore, the difference of the bowtie antenna performance on glass substrate and silicon-on-insulator substrate is investigated.

This bowtie antenna has potential applications in microwave photonics, such as the detection and measurement of free-space electromagnetic waves. By integrating an optical phase modulator within the feed gap of the bowtie antenna, a photonic electromagnetic field sensor is formed. With the bowtie antenna as a receiver, a strongly enhanced electric field is confined in the feed gap, which directly modulates the optical waves. Utilizing this photonic sensor in one arm of an external Mach-Zehnder Interferometer (MZI) setup, an incident electromagnetic field as low as 2.5V/m is experimentally detected.

9362-24, Session 6

A multistandard and multiservice radio-over-fiber system for next-generation network

Sarra Rebhi, Rim Barrak, Mourad Menif, SUP'COM (Tunisia)

Next Generation Networks (NGN) based on Radio over Fiber (RoF) systems are deploying small cell concept to burst the network capacities and provide high data rates. Due to small cell range, and high mobility, traffic distribution between cells is disparate and requires multiple transmission techniques in the central office. In a recent work, we investigated high spectral efficiency multi-band RoF system using single wavelength carrying multi-services. The deployment of optical comb source raised system spectral efficiency. The aim of this work is to evaluate the RoF system performances in terms of EVM and cell coverage to meet NGN requirements.

The proposed architecture is based on an Optical Flat Comb Source (OFC) generating 16 wavelengths spaced by 12.5 GHz in order to deliver multi-service for 16 Remote Access Unit. The generated optical spectrum is demultiplexed and each optical carrier undergoes multi-band Single-Side Band (SSB) modulation using a Mach-Zehnder Interferometer (MZI). The target data are the WiFi (2.4 GHz and 5 GHz) and the mm-wave (60 GHz).

WiFi signals are multiplexed and then used to modulate the even optical wavelength λ_i by using a MZI modulator. The mm-wave services are generated at intermediate frequencies (IF1=8.32 GHz, IF2 = 10.48GHz, IF3=2.64GHz and IF4=4.8GHz). We assume that mm-wave services deploy multi modulation schemas (B-PSK, Q-PSK, 8-PSK and 16-QAM) with data rates up to 4 GHz. The IF mm-wave channels drive the MZI modulator in order to modulate the next optical wavelength λ_{i+1} using SSB modulation as described in Fig. 1. The modulated wavelengths are combined through a multiplexer with a shifted central frequency of approximately 6 GHz

**Conference 9362: Terahertz, RF, Millimeter, and
 Submillimeter-Wave Technology and Applications VIII**

and having 12.5 GHz bandwidth and transported to the RN where each wavelength is routed to the corresponding RAU through an Arrayed Wavelength Grating (AWG). In order to separate services, the incoming wavelength λ_i undergoes an AWG before converting them to RF signals.

9362-25, Session 6

Demonstration of high-resolution doping profile mapping using terahertz time domain spectroscopy with electrochemical anodization

Chih-Yu Jen, Gaurav Tulsyan, Christiaan Richter, Rochester Institute of Technology (United States)

At SPIE 2014 we presented results demonstrating the ability of transmission mode terahertz time domain spectroscopy (THz-TDS) to detect doping profile differences and deviations in silicon. Here we report follow up work demonstrating doping profile measurement by first precisely removing a thin layer (currently ~ 20 nm) from the junction by anodization followed by selective oxide etching. The anodization-etching step is followed by measuring the terahertz transmission using THz-TDS. The anodization and terahertz measurement steps are then alternated. The doping profile can then be reconstructed using the resultant dataset. In this presentation we share results obtained on phosphorus doped silicon wafers. We find good agreement between the measured transmitted terahertz spectra and the simulated terahertz spectra for all etching cycles when the doping profile used in the simulations agrees with SIMS analysis. We conclude that anodization combined with THz-TDS can potentially be a high resolution destructive doping profile mapping method.

9362-26, Session 6

Performance of microwave optoelectronic oscillators based on crystalline whispering-gallery mode resonators

Khalidoun Saleh, Guoping Lin, Souleymane Diallo, Romain Martinenghi, Yanne K. Chembo, FEMTO-ST (France)

Optoelectronic oscillators (OEOs) are expected to play a key role in the area of ultra-stable microwave generation in a near future. The original architectures used an optical fiber delay line as energy storage element but however, the constraints of size and power consumption optimization have led to novel configurations where this fiber delay line is replaced by a ultra-high Q whispering-gallery mode (WGM) resonator. We present here the stability performances of these oscillators, and discuss pathways for phase noise improvement.

9362-27, Session 6

High-performance PIN photodetector at 67GHz and beyond for radio-over-fiber applications

Toshimasa Umezawa, Naokatsu Yamamoto, Kouichi Akahane, Atsushi Kanno, Tetsuya Kawanishi, National Institute of Information and Communications Technology (Japan)

In radio over fiber applications, a definition of base band frequency is very important for long range wireless communications. Because a high base band frequency with a wide bandwidth has a big potential to increase data rates in the communications. Here the frequency and bandwidth are linked. In IEEE802.11ad standard for wireless communications, a base band of 60

GHz is already applied. On the other hand, the atmospheric attenuation dependence of a frequency has been well known. The low atmospheric attenuation at 30 to 90-GHz band is useful and can be extended to detect small signals. Therefore the base band signal quality in the frequency range has to be respected. A high speed photodetector (PD) can be used to obtain high quality signals in the millimeter wave region through OE conversion process. In particular, the high output power and linearity are important factors. The low output power and low output linearity lead to degraded signal to noise ratios and wave form distortions.

In this paper, we report that high performance photodetectors at 67 GHz and beyond, using a low carrier concentration of InGaAs absorption layer. The back illuminated PD structure with a 50 Ohm impedance matching resistor and GSG electrodes were designed. The high output power of +6.8 dBm at 67 GHz was successfully obtained at optical input power of +17 dBm (photo-current of 17 mA), without output saturations. In addition, the high frequency response up to 110 GHz will be discussed with a RF interface technology.

9362-43, Session PWed

Terahertz wave modulators using organic/inorganic hybrid structures

Joong-Wook Lee, Chonnam National Univ. (Korea, Republic of)

Using hybrid bilayer systems comprising a molecular organic semiconductor and silicon, we achieve optically controllable active terahertz (THz) modulators that exhibit extremely high modulation efficiencies. A modulation efficiency of 98% is achieved from thermally annealed C60/silicon bilayers, due to the rapid photo-induced electron transfer from the excited states of the silicon onto the C60 layer. Furthermore, we demonstrate the broadband modulation of THz waves. The cut-off condition of the system that is determined by the formation of efficient charge separation by the photo-excitation is highly variable, changing the system from insulating to metallic. The phenomenon enables an extremely high modulation bandwidth and rates of electromagnetic waves of interest. To deeply understand the underlying mechanisms, the characteristics measured in copper-phthalocyanine(CuPc)/silicon and pentacene/silicon bilayers showing a photo-induced hole transfer phenomenon are compared with those measured in the C60/silicon bilayers. The realization of near-perfect modulation efficiency in THz frequencies opens up the possibilities of utilizing active modulators for THz spectroscopy and communications.

9362-44, Session PWed

A distributed online optical power monitor based on optoelectronic oscillator

Han Chen, Southeast Univ. (China); Mingyu Xia, Southeast University (China); Mingming Sun, Xiaohan Sun, Southeast Univ. (China); Chun Cai, Xueming Sun, Shenzhen Academy of Metrology & Quality Inspection (China)

Dynamically reconfigurable transparent optical networks will require advanced optical performance monitoring (OPM) techniques to allow for real time control of compensation devices and facilitate network management operations, including reporting degradations for alarm correlation and fault localization. One of the key parameters to be monitored is the optical power, especially in WDM reconfigurable networks, where each channel may be routed through different paths and accumulate a different amount of noise.

We introduce a novel distributed online optical power monitoring method based on a tunable optoelectronic oscillator (OEO) incorporating a semiconductor optical amplifier (SOA). The photonic oscillator generates a set of regular oscillation frequencies range from 8.4GHz to 10.4GHz satisfying a certain single channel optical power condition in the WDM system and exhibits a good stability with SSB phase noises below -100dBc/

**Conference 9362: Terahertz, RF, Millimeter, and
 Submillimeter-Wave Technology and Applications VIII**

Hz@10KHz. The proposed optical power monitoring scheme, which is highly sensitive to the optical power perturbations, transforms the typical optical power detection to the visualized spectral components measurement of the generated RF signals. Therefore, we can obtain the distributed online optical power monitoring information by analyzing the spectral components and the corresponding intensity values. In this paper, the theoretical fundamentals of the design are explained and a prototype of two nodes distributed online optical power monitor with a dynamic measuring range of 6dB and an accuracy of 0.25dB is experimentally demonstrated.

9362-45, Session PWed

Numerical modeling of bi-directional dual-wavelength pumped L-band few-mode erbium doped fiber amplifiers

Changren Qiu, Tianxin Yang, Dongfang Jia, Tianjin Univ. (China)

Recent demonstrations of long-distance transmission over few-mode fibers (FMFs) clearly show the potential of mode-division multiplexing (MDM) to overcome the capacity limitation of single-mode fibers (SMFs), by modulating the signals on different modes of the FMF. For a MDM system, optical amplifiers for few-mode signals will be the key components. Currently, most of the studies on the optical amplifiers for MDM systems focus on few-mode erbium doped fiber amplifiers (FM-EDFAs). However, these FM-EDFAs all without exception operate in the conventional C-band transmission window (1530-1565nm). L-band amplification in few-mode erbium-doped fiber (FM-EDFs) has not been reported so far. In this paper, we extend the idea of L-band amplification from single-mode EDFs to FM-EDFs. It was argued that FM-EDFAs could offer advantages in terms of pump power efficiency (pump power required to achieve net gain), compared to multiple single-mode EDFAs. A comprehensive set of metrics for FM-EDFA should include: gain, noise figure and power conversion efficiency (PCE). The loss of FMFs are expected to be more than SMFs, so high gain is important, especially in L-band. One of the goals of MDM is to improve power consumption so high PCE is desired. It is known from research on single-mode EDFAs that backward pumping offers better power conversion efficiency while forward pump offers better noise figure. In this paper we present the first model for highly doped bi-directional dual-wavelength pumped L-band FM-EDFAs with an optimized length and provide pump configurations that yield the best trade-off between noise figure and PCE.

9362-46, Session PWed

A low-noise readout integrated circuit based on 0.18 um SiGe process for Nb5N6 microbolometer array

Chao Wan, Yufeng Pei, Nanjing Univ. (China); Chao Wang, Jie Ma, China Key System Integrated Circuit Co. Ltd. (China); Xuecou Tu, Lin Kang, Peiheng Wu, Nanjing Univ. (China)

Nb5N6 microbolometer is a good candidate for sensitive THz detectors due to its outstanding performance, such as high responsivity (~ 480 V/W @ 0.28 THz), low noise equivalent power (~ 2*10⁻¹¹ W/√Hz) and working at room temperature. However, the lack of a proper readout circuit limits the development of Nb5N6 microbolometer arrays with hundreds of pixels. We chose 0.18 μm SiGe process to design and fabricate a low noise readout integrated circuit for Nb5N6 microbolometer array, considering SiGe heterojunction bipolar transistors (HBT) shows better performance than regular bipolar junction transistors and FETs in terms of noise. This circuit is mainly consist of 3*3 amplifiers, which are designed in common emitter structure. The single amplifier gain can be set as ~ 15 or ~ 30 by adjusting the gain control bits, and the 9 amplifiers' gains show high uniformity with

variance ~ 2%. The bandwidth is 20 Hz ~ 1 MHz, and can be narrowed to ~ 10 kHz by adding off-chip capacitors, which can let the response signal pass without much harmonic distortion and noise. The input referred noise density is ~ 10 nV/√Hz, close to Nb5N6 microbolometer's noise density, so this circuit has little effect on the detector's NEP and supplies a promising way to promote Nb5N6 microbolometer's applications in real-time THz imaging systems with focal plane array.

9362-48, Session PWed

Thin-film sensing with phase delayed terahertz pulses

Tae-In Jeon, Hyeon Sang Bark, Jingshu Zha, Korea Maritime Univ. (Korea, Republic of); Eui Su Lee, Electronics and Telecommunications Research Institute (Korea, Republic of)

The highly sensitive terahertz (THz) measurement of a thin-film is studied using a two channels formed by inserting a single slit sheet in the parallel-plate waveguides (PPWGs). When a thin-film is applied to coat the upper surface of the channel, the phase difference between the coated upper and uncoated lower channels makes a single resonance frequency which is shifted as a result of the layer's properties, including length, thickness, and refractive index. Q-factors of the resonances are 31 and 23 for the only open upper and lower channels, respectively. The measured frequency tuning sensitivities (FTS) throughout the 20-mm layer length are 2.41 and -1.95 GHz/mm at the open upper and lower channels, respectively. The measured transmission spectra of thickness-dependent resonances, which are 0.7 to 2.8 μm in thickness with a fixed length of 5.0 mm are observed. When the upper channel is open and the lower channel is close, the resonance frequency shifts up to 42.7 GHz (FTS is 15.1 GHz/μm). When the lower channel is open and the upper channel is close, the resonance frequency shifts up to -45.0 GHz (FTS is -15.9 GHz/μm). The experimental results agree with those of theoretical simulations performed using the finite-difference time-domain (FDTD) method. This research demonstrates thin dielectric layer sensing using two-channel PPWG with a single slit sheet. This experimental scheme can be easily adapted to industrial and scientific applications, such as semiconductor and biological studies, as an independent sensor.

9362-49, Session PWed

Large loop antenna to enhance impedance matching characteristics for a terahertz photomixer

Han-Cheol Ryu, Sahmyook Univ. (Korea, Republic of); Eui Su Lee, Kyung Hyun Park, Electronics and Telecommunications Research Institute (Korea, Republic of)

We propose a large loop antenna to integrate with a terahertz (THz) photodiode (PD) type photomixer for optimum impedance matching. Proper impedance matching between the antenna and the PD is very important to increase the THz output power because optimization of the impedance matching characteristics is crucial to enhance a coupling efficiency from the THz PD to the integrated antenna. The PD type photomixer has complex impedance which varies according to the operating frequency. Usually the reactance component of the PD type photomixer is negative because it has capacitive characteristic. Thus the large loop antenna was proposed to control both resistance and reactance for the impedance matching optimization. The large square loop antenna which perimeter is one-wavelength has one-quarter wavelength sides. Radiation pattern of the large loop antenna is maximum normal to the plane of the loop, which is quite different from the small loop antenna. The resonant frequency was controlled by varying the perimeter of the antenna. The input

**Conference 9362: Terahertz, RF, Millimeter, and
 Submillimeter-Wave Technology and Applications VIII**

resistance and reactance of the antenna were changed by varying the width of the strip. The length and the width of the strip were controlled at the same time to optimize the impedance matching condition. The large loop antenna is less affected by the attached bias line than the dipole structure. The bias line was also designed in the consideration of the impedance matching between the antenna and the photomixer. At operating frequency band the proposed antenna was optimized to the complex conjugated impedance of the PD type photomixer.

9362-50, Session PWed

Yb-doped short pulse fiber laser for terahertz radiation

Moon Sik Kong, Min Hee Kim, Yong Seok Kwon, Chungnam National Univ. (Korea, Republic of); Sang-Pil Han, Namje Kim, Kyung Hyun Park, Electronics and Telecommunications Research Institute (Korea, Republic of); Han-Cheol Ryu, Sahmyook Univ. (Korea, Republic of); Min Yong Jeon, Chungnam National Univ. (Korea, Republic of)

Ultra short pulse lasers for time-domain THz spectroscopy have been developed by several research laboratories. The most common optical source for THz radiation is a mode-locked femtosecond Ti:sapphire laser operating around 800 nm. This kind of the solid state laser is bulky and robust. Therefore it is not convenient for in-field applications. It is desirable for intense, compact, and simple THz radiation sources which can be applied for sensing, imaging, and time-resolved THz spectroscopy. The mode-locked fiber laser is a good candidate compact and portable optical THz source. Most of the mode-locked fiber lasers are developed at 1550 nm band using Er-doped fiber. However, the output power of THz radiation is limited by the mode-locked fiber laser source at 1550 nm. In this presentation, we report an experimental demonstration of an Yb-doped short pulse fiber laser for time-domain terahertz spectroscopy. The Yb-doped fiber laser consists of a 20-cm long Yb-doped fiber as an gain medium, 15-m long single mode fiber, an optical isolator, a linear polarizer, two polarization controllers, and a 3 dB fiber coupler. Using the short pulsed Yb-doped fiber laser @ 1030 nm, the time-domain THz radiation can be generated by an all-fiber THz measurement system with LTG-InGaAs photomixing emitter and receiver modules.

9362-28, Session 7

Frequency tuning of THz quantum cascade lasers (Invited Paper)

Andriy Danylov, Alexander R. Light, Jerry Waldman, Univ. of Massachusetts Lowell (United States); Neal Erickson, Univ. of Massachusetts Amherst (United States); Xifeng Qian, Univ. of Massachusetts Lowell (United States)

Terahertz quantum cascade laser (TQCL) developed as a compact, coherent and continuous-wave solid state source has shown potential applications in astronomy, biological and medical science, non-destructive evaluation, and homeland security. Single mode, widely tunable THz lasers are particularly required in spectroscopic applications. Researchers have been working on the development of THz QCLs with broad tuning range using either distributed feedback lasers, which relies on the change of the waveguide refractive index, or external cavity. This paper introduces the continuously tunable THz radiation through side band generation of a previously demonstrated, free running, solid-nitrogen-cooled TQCL [1]. The 2.324 TQCL operates in a single longitudinal mode in continuous-wave (CW) was mixed with a swept synthesized microwave signal by a THz Schottky-diode-balanced mixer. Two frequency branches were observed at low and high frequency, characterized with a Fourier-transform spectrometer. At low frequency, the side band generates frequency from -50 GHz to +50 GHz. At

high frequency, it generates frequency from 70 GHz to 150 GHz. The total ± 100 GHz tuning range can be further expanded with higher frequency millimeter wave amplifier/multiplier source. The side band generates 1 μ W of output power with 200 μ W of driven power from the TQCL, showing a power conversion efficiency of 5 ? 10⁻³.

1. A. A. Danylov, A. R. Light, J. Waldman, N. R. Erickson, X. Qian, and W. D. Goodhue, "2.32 THz quantum cascade laser frequency-locked to the harmonic of a microwave synthesizer source", Opt. Express 20, 27908 (2012)

9362-29, Session 7

Development of portable terahertz scanner for imaging and spectroscopy using InP-related devices (Invited Paper)

Kyung Hyun Park, Electronics and Telecommunications Research Institute (Korea, Republic of)

Over the last 10 years, lots of the terahertz (THz) technologies have been progressively invented. Thanks to the continuous and intensive research on the THz technologies, the performances of the main building blocks of THz technologies are dramatically improved. Recently, commercially available THz spectrometer shows the potential of the THz techniques in the industry. However, a compact continuous-wave terahertz line-of-sight commercialized system is still not insufficient to examine the terahertz finger prints from the specimens without any limitations. Several types of our own developed dual mode lasers and broadband antenna-integrated photomixers show the possibility of the realization of compact and cost-effective THz spectrometer. THz line-scanner which can evaluate the quality of THz imaging and THz finger patterns has been proposed based on InP-related devices.

To evaluate THz image and finger patterns of specimen using handheld type THz instrument, the high-power tuneable continuous wave (CW) THz emitter platform and high-sensitivity THz receiver platform are prerequisite. Such THz emitter platform can be realized by combining the tuneable optical beating source and broadband photomixer. The evanescently-coupled photodiodes with high saturation current and semiconductor optical amplifier (SOA) integrated optical beating source are newly developed for the THz emitter platform. For the high-sensitivity THz receiver platform, we also developed arrayed system of photomixers and Schottky barrier diodes.

In this talk, our recent studies from material growth for THz device to the module for the high-performance THz platform for various industrial applications including the portable THz scanner will be briefly reviewed.

9362-30, Session 7

Multiple-angle approach for enhanced terahertz spectroscopic pattern recognition

Frank Ellrich, Daniel Molter, Soufiene Krimi, Joachim Jonuscheit, Georg von Freymann, Fraunhofer-Institut für Physikalische Messtechnik (Germany); Frank Platte, Christoph Fredebeul, Konstantinos Nalpantidis, IANUS Simulation GmbH (Germany); Daniel Hübsch, Tobais Würschmidt, Thorsten Sprenger, HÜBNER GmbH & Co KG (Germany)

Terahertz (THz) time-domain spectroscopy is a useful tool for identifying crystalline substances like explosives, drugs or chemicals even under concealments like paper or cardboard. Several layers of these covering materials can lead to multiple reflections of the THz beam so that the detected signal is overlaid by a number of echoes. In the frequency domain this leads to additional spectral features perturbing the THz fingerprint of the substance. Since the mentioned multi-reflections as a part of the

**Conference 9362: Terahertz, RF, Millimeter, and
 Submillimeter-Wave Technology and Applications VIII**

detected signal are inherently given by the sample setup it is not possible to suppress them in the measurement process itself. Just by combining our principal-component-analysis based pattern recognition algorithm with further chemometric tools we successfully improve the automatic identification algorithm. But there is still potential for further improvements by changing the detection method itself. Therefore, we investigate the dependency of the material absorption lines and the ones occurring from the Fourier transformation of the echoes on changing the incidence angle of the THz beam. The received measurement results confirm our previous numerical predictions: Changing the angle of incidence keeps the absorption lines of the substances fixed in frequency. Only the amplitudes are changing due to different effective path lengths in the absorbing samples. In contrast, the artificial bands in the extinction spectra strongly depend on the angle of incidence. This obviously different behavior is used to separate true absorption lines from the artificial bands. With such preprocessed data substance identification is much more efficient, leading to a reduction in false alarm rate.

9362-31, Session 7

**High-power photodetector modules for
 microwave photonic applications**

Kejia Li, Xiaojun Xie, Univ. of Virginia (United States);
 Efthymios Rouvalis, Sascha Fedderwitz, Andreas G.
 Steffan, Finisar Corp. (Germany); Qinglong Li, Zhanyu
 Yang, Andreas Beling, Joe C. Campbell, Univ. of Virginia
 (United States)

Photodiodes (PDs) with high RF output power and wide bandwidth are essential components in microwave photonic applications since they have the potential to improve the link gain, noise figure and spurious free dynamic range.

To achieve high output power, significant previous work on high-power photodetector chip technology has been published. However, only a limited number of module demonstrations have been reported. K. Sakai and et al. reported a TO-can package module with a 3 dB bandwidth of 8 GHz and 25 dBm RF output power at 5 GHz. E. Rouvalis and et al. demonstrated a hermetically packed photodetector module that achieved 17 dBm RF output power at 30 GHz and bandwidth of 30 GHz.

In this work, we report fully-packaged photodetector modules based on InGaAs/InP modified uni-traveling carrier photodiodes (MUTC-PDs). The MUTC-PDs with cliff layers were designed for high RF output power and high saturation current at high frequency. A high-impedance coplanar waveguide (CPW) transmission line was employed to compensate for the parasitic capacitance and to enhance the bandwidth. The devices were flip-chip bonded on AlN submounts for efficient heat dissipation. Modules using chips with active area diameters of 10 μm were developed. The modules showed typical dark currents of $\sim 0.2 \mu\text{A}$ at reverse bias up to 6V and a responsivity of 0.2 A/W at 1.55 μm wavelength. 3-dB bandwidth up to 50 GHz and output power of 13.5 dBm at 50 GHz were demonstrated.

9362-32, Session 7

**Wavelength-spacing tunable
 multiwavelength erbium-doped fiber laser
 using polarization-differential time delay
 for photonic microwave filter**

Soo Kyung Kim, Young Bo Shim, Sunduck Kim, Young-
 Geun Han, Hanyang Univ. (Korea, Republic of)

Recently, photonic microwave filters have attracted much research interest because of their many advantages, such as high bandwidth, low loss, and immunity to electromagnetic interference. One of promising techniques

to realize photonic microwave filters is to exploit the multiwavelength laser including an array of laser diodes with different center wavelengths, multi-wavelength fiber laser with tunable birefringent Sagnac loop, and etc. However, the free spectral range (FSR) of the photonic microwave filter cannot be tuned continuously because of the discrete tunability of the wavelength spacing of the multiwavelength laser.

We propose the photonic microwave filter based on continuous tunable wavelength-spacing multiwavelength erbium-doped fiber (EDF) laser. The wavelength spacing was continuously controlled by implementing the Lyot filter with a polarization differential delay line, while the mode competition of the EDF laser was mitigated by the NPR structure. By controlling the wavelength spacing of the multi-wavelength in a range from 0.12 to 0.28 nm, the FSR of the microwave filter was continuously tuned from 1.5 to 0.43 GHz.

9362-33, Session 7

**Recent developments in electroabsorption
 modulators at Acreo Swedish ICT**

Qin Wang, Andy Z. Zhang, Susanne Almqvist, Stephane
 Junique, Bertrand Noharet, Duncan Platt, Michael Salter,
 Jan Y. Andersson, Acreo Swedish ICT AB (Sweden)

Electroabsorption modulators (EAM) based on III-V semiconductor multiple quantum wells (MQW) can be used as a key component in a variety of optical communication systems. MQW EAMs have many advantages: low driving voltage, broad bandwidth, compact-size and monolithic or hybrid integration capabilities with other devices. In particular, either traveling-wave (TW) or surface normal (SN) configurations can be achieved by adapting the MQW structure design and device layout to the communication link's requirements.

The development of III-V semiconductor MQW EAMs has been one of the research areas at Acreo Swedish ICT AB (Acreo) since 2000. Nowadays, besides continuous improvements of the performance of both TW and SN MQW EAMs as general technique platform, various formats of EAMs and their 1 or 2 dimensional (1D/2D) arrays have been manufactured according to customized specifications for civil, defense and space applications.

Here we present three types of our EAMs in different optical communication links. One is a novel monolithic integration TW-EAMs for an analog optical transmitter/transceiver to achieve an integrated photonic mm-wave function for broadband connectivity. Another link is composed of an integrated EAM 1D array with a photonic beam-former as a Ku-band phased array antenna, which was developed in frame of EU FP7 project Sandra (Seamless Aeronautical Networking through integration of Data links, Radios, and Antennas). The third communication link addresses the use of MQW EAMs in free space optical links through biological tissue for transcutaneous communication.

9362-34, Session 8

**Compensating the carrier screening effect
 in plasmonic photoconductive terahertz
 sources**

Shang Hua Yang, Univ. of Michigan (United States) and
 Univ. of California Los Angeles (United States); Nezh T.
 Yardimci, Univ. of California, Los Angeles (United States);
 Mona Jarrahi, Univ. of California, Los Angeles (United
 States) and Univ. of Michigan (United States)

Terahertz spectroscopy systems have attracted extensive attention due to their unique applications in medical imaging, environmental monitoring, chemical sensing and security screening. However, the practical feasibility of many of these applications is constrained by the low radiation power, low efficiency and bulky nature of existing terahertz radiation sources.

**Conference 9362: Terahertz, RF, Millimeter, and
 Submillimeter-Wave Technology and Applications VIII**

Recently demonstrated plasmonic photoconductive terahertz sources have shown very promising performance for narrowband/broadband terahertz generation at room temperature. The high optical-to-terahertz conversion efficiency and radiation power of the plasmonic photoconductive terahertz sources offer a compact solution for portable terahertz systems. In spite of their great promise, the quantum efficiency and maximum radiation power of plasmonic photoconductive sources is still limited by the carrier screening effect at high optical pump power levels.

Here, we present a new design of plasmonic photoconductive terahertz sources incorporating two-dimensional plasmonic contact electrodes. The geometry of the contact electrodes is designed to achieve a uniform electric field distribution inside the device active area. It also allows increasing the device active area without a considerable impact on device parasitics, maintaining a high quantum efficiency and ultrafast operation simultaneously. As a result, the presented design of plasmonic photoconductive sources increases the maximum radiated terahertz power by mitigating the carrier screening effect at high optical pump powers.

9362-35, Session 8

Hydration kinetics of cement composites with varying water-cement ratio using terahertz spectroscopy

Shaumik Ray, CSIR-Madras Complex (India); Nirmala Devi, CSIR (India); Jyotirmayee Dash, CSIR Madras Complex (India); Saptarshi Sasmal, CSIR - Structural Engineering Research Ctr. (India); Bala Pesala, CSIR Madras Complex (India)

Ensuring the durability and protection of concrete structures from mechanical abrasion due to adverse environmental exposure and unforeseen loadings are major challenges in the civil engineering industry. When cement is mixed with water to form concrete, various reactions take place to harden the cement paste. This process is known as hydration. For achieving higher mechanical strength and improved durability of concrete, the water-cement ratio has to be optimized during the hydration process. Optimizing the formation of hydration products such as Calcium-Silicate-Hydrate (C-S-H) and Calcium Hydroxide (Ca(OH)₂) results in better performance of concrete. In addition, incorporation of materials such as silica fume and fly ash enhances the mechanical strength, combination of silica fume and amorphous nano-silica improves the plasticity and performance. Earlier compressive strength studies have demonstrated that a water-cement ratio of approximately 0.44 is the optimum level to achieve concrete with a moderate compressive strength. Though strength studies can help in determining the performance of concrete after the completion of the hydration process, a technique that can help to accurately track the hydration kinetics as well as quantify the hydration products is highly desirable.

In the earlier study by the present authors, it has been shown that THz spectroscopy is a useful tool in monitoring the reactions during the hydration process. In this paper, THz spectroscopy has been successfully employed to study the effect of varying water-cement ratio (0.3 - 0.6) on the hydration kinetics and to track the formation of the key hydration products, viz., C-S-H (responsible for providing strength to concrete) and Ca(OH)₂ (responsible for durability of concrete). This analysis can be vital in tracing and optimizing the hydration process to increase the C-S-H content and to reduce the formation of Ca(OH)₂. Further, this study will be useful to assess the influence of addition of foreign materials such as nano-silica, fly ash or other fillers for optimizing the concrete hydration process.

9362-36, Session 8

Design of hybrid optical delay line for automotive radar test system

Byung-Hee Son, Kwang-Jin Kim, Ye Li, Chung-Ang Univ.

(Korea, Republic of); Chang-In Park, Chung-Ang Univ (Korea, Republic of); Young Wan Choi, Chung-Ang Univ. (Korea, Republic of)

Recently, automotive radar that is mounted on the vehicle at various points (front, side, back) is studied as a key element for the next generation intelligent vehicles and intelligent transport system (ITS). Accordingly, the demand of automotive radar test system (RTS) is also increased. The coaxial cable is used to make the artificial delay time in the conventional RTS, however, the volume and power loss of the system are being larger when the delay distance is longer than 50 m. In addition, it has a low resolution because of narrow bandwidth (< 300 MHz). In the case of optical fiber, it has the advantages like light, small size, low loss and wide bandwidth compared with coaxial cable.

In this paper, hybrid optical delay line (HODL) which is demanded on automotive radar test system (RTS) is proposed and demonstrated. HODL is composed with coaxial cable in short delay time (< 32 nsec) and optical fiber in long delay time (≥ 32 nsec) which are considering the volume, loss and frequency characteristics. Because HODL is designed 1 GHz bandwidth at 4.2 GHz, frequency modulated continuous wave (FMCW) and ultra wideband (UWB) signal could be applied to this system. Experimental results show that the S21 is ± 0.5 dB in the optical transceiver and ± 1.7 dB in the whole system at 3.7 GHz - 4.7 GHz. The resolution of delay time is 1 ns and the delay flatness is ± 0.23 ns.

9362-37, Session 8

Broadband receiver-based distortion elimination in phase-modulated analog optical links using four-wave mixing

Amit Bhatia, Hong-fu Ting, Mark Foster, Johns Hopkins Univ. (United States)

We present a method for full distortion elimination in phase-modulated analog optical links using the nonlinear optical process of four-wave mixing (FWM). Phase-modulated analog optical links consist of a laser and phase modulator in the transmitter and an interferometer (or local oscillator) and a photodiode in the receiver. Since phase modulation is essentially a linear process, distortion is introduced in the receiver by the interferometric detection process. Aligning the interferometer at quadrature eliminates all even-order distortion products, but the odd-order distortion remains. Here we introduce a method for eliminating these odd-order distortion products in the receiver. A small portion of the phase-modulated signal is tapped and combined with an unmodulated CW laser to seed a cascaded FWM comb source. This process generates an array of lightwaves with integer multiples of the signal's phase modulation. By suitably scaling and combining these lightwaves with the original signal the overall transfer function of the interferometric receiver can be linearized (or given another tailored shape) through a Fourier synthesis approach. Here we present a proof-of-principle demonstration by combining a single lightwave from the generated comb with the original signal. We demonstrate the complete elimination of third-order distortion from the phase-modulated link leaving fifth-order distortion as the dominate source of distortion. We show an 18-dB improvement in link SFDR at a 1-Hz bandwidth (from 99-dB/Hz^{2/3} to 117-dB/Hz^{4/5}). By appropriately combining additional lightwaves from the generated comb, higher-order distortion products can be eliminated to produce an ideal linear (or custom shaped) transfer function.

9362-39, Session 9

Reconfigurable thermo-optic polymer switch based true-time-delay network utilizing imprinting and inkjet printing

Zeyu Pan, The Univ. of Texas at Austin (United States); Harish Subbaraman, Omega Optics, Inc. (United States);

**Conference 9362: Terahertz, RF, Millimeter, and
 Submillimeter-Wave Technology and Applications VIII**

Xingyu Zhang, Yi Zou, The Univ. of Texas at Austin (United States); Xiaochuan Xu, Omega Optics, Inc. (United States); Xiaohui Lin, The Univ. of Texas at Austin (United States); Qiaochu Li, Cheng Zhang, Tao Ling, L. Jay Guo, Univ. of Michigan (United States); Ray T. Chen, The Univ. of Texas at Austin (United States)

The most common methods for polymer optical device fabrication includes either using photolithography to define the pattern into a resist, and transferring the pattern to the optical polymer via high energy Reactive Ion Etching (RIE), or directly writing the pattern in a low-loss UV-curable polymer using lithography. Although these methods are straightforward, they are not a cost-effective due to complicated fabrication process and low throughput. Previously, we introduced a novel and an etch-less solution processing technique utilizing a combination of imprinting and ink-jet printing for developing polymer photonic devices. In this work, we further demonstrate the feasibility of developing large-area photonic systems. Specifically, a complete reconfigurable 4-bit true-time-delay unit, with dimensions of 25 mm × 18 mm, comprising of an array of five interconnected Thermo-Optic (TO) switches and polymer delay lines is developed. By controlling the ON/OFF states of the individual switches, true-time-delay behavior over a broad RF bandwidth is obtained. Due to the roll-to-roll (R2R) compatibility of the solution processing techniques employed, photonic system development over large areas at high-throughput, on rigid or flexible substrates, is possible which will lead to tremendous cost savings. Moreover, these devices can be integrated with other printed photonic and electronic components, such as light sources, modulators, antennas, etc on a single substrate, thus enabling an integrated system that can be conformably integrated on any platform.

9362-40, Session 9

**Fourier transform molecular
 rotational resonance spectroscopy for
 reprogrammable chemical sensing**

Brent J. Harris, Robin L. Pulliam, Justin L. Neill, Matt T. Muckle, Roger Reynolds, Brooks H. Pate, BrightSpec (United States)

Molecular rotational resonance (MRR) spectroscopy gives spectral signatures with high chemical selectivity. At room-temperature, the peak intensity of the MRR spectrum occurs in the 100 GHz - 1 THz frequency range. Advances in high-power sub-mm-wave light sources has made it possible to implement time-domain Fourier transform (FT) spectroscopy techniques that are similar to FT nuclear magnetic resonance (FT-NMR) measurements. In these measurements, the gas sample is excited by a short (200 ns) excitation pulse that creates a macroscopic sample polarization. The electric field of the subsequent transient molecular emission is detected using a heterodyne receiver and a high-speed digitizer. FT-MRR spectroscopy offers speed and sensitivity improvements over absorption spectroscopy. For chemical analysis, FT-MRR spectrometers combine the benefits of broad chemical coverage typical of gas chromatography - mass spectrometry (GC-MS) instruments and the direct measurement capabilities of infrared gas sensors all in a reprogrammable platform. Pulse sequence measurements can be implemented for advanced spectroscopic analysis. Trace level quantitation of volatile species at ppbv concentration can be performed on the time scale of a minute. In cases where the sample is a complex mixture, a double-resonance pulse sequence can be used to achieve chemical selectivity even in cases where spectral overlap occurs. These measurement capabilities are illustrated using the application of FT-MRR spectroscopy to residual solvent analysis of pharmaceutical products.

9362-41, Session 9

**Design and characterization of
 evanescently-coupled dual-photodiodes
 for 1.3 μm wavelength**

Eui Su Lee, Won-Hui Lee, Namje Kim, Jeong-Woo Park, Sang-Pil Han, Kyung Hyun Park, Electronics and Telecommunications Research Institute (Korea, Republic of)

The evanescently-coupled dual-photodiodes (EC dual-PDs) has been fabricated and used for the generation of continuous-wave (CW) terahertz (THz) field at a 1.3 μm wavelength. We designed a matching layer to evanescently couple the optical beam from the base waveguide to the active region so as to get a high responsivity, 0.36 A/W. Surface-illuminated structures such as p-i-n, uni-traveling carrier, and partially depleted absorber photodiodes, have demonstrated high-power operation. However, the tradeoff between quantum efficiency and transit time limits the responsivity for small devices that can operate at high frequencies. In case of side-illuminated photodiodes, although the responsivity and transit time can be decoupled and overcome this restriction, the saturation current can be limited by space charge screening at the input facet. But, EC dual-PDs that utilize to couple the optical beam evanescently from the base waveguide to the active region (absorber), can achieve several times higher saturation current than a side-illuminated approach. Therefore, we designed the tapered geometry of the matching layer to get the high saturation current and the high speed operation with the small active region (5x5, 5x7 μm). And we designed the dual-photodiodes having two absorption regions in parallel to overcome the saturation current limit inherent in a single photodiode, resulting in high power operation. We measured CW THz power at 300 GHz with various broadband and resonant antenna-integrated EC dual-PDs as emitting photomixer for the practical and cost effective purpose.

9362-42, Session 9

**Aluminum-doped zinc-oxide for radio
 frequency applications**

Seyma Canik, Mohammad Amin Nazirzadeh, Berk Berkan Turgut, Kagan Topalli, Ali Kemal Okyay, Bilkent Univ. (Turkey)

The progressive development of radio frequency (RF) systems drives an ever-increasing need for component miniaturization that could benefit significantly from the monolithic integration of components and antennas on the same substrate. Next generation RF designs are projected to have increased functionality, tunability and also low cost and simple fabrication which constitute a strong drive for utilizing new materials and exploiting their properties in RF components and systems. Zinc oxide (ZnO) is a very appealing material due to its optical, electrical and piezo-mechanical properties and Al-doped ZnO (AZO) is a promising candidate as a transparent conductor for optoelectronic RF applications.

In this work, AZO thin films are synthesized by atomic layer deposition (ALD) technology and electromagnetic properties are investigated in the RF range. Conductivity, efficiency and transmittance are analyzed in order to obtain new reconfiguration modalities. For RF performance characterization, S-parameter measurements are carried out with basic design where AZO layers are integrated with coplanar waveguide transmission lines in different configurations. Fused silica is used as a substrate to evaluate transparency. The tunability of the electromagnetic properties and transparency of AZO in the visible region, are investigated under optical and electrical stimuli.

Conference 9363: Gallium Nitride Materials and Devices X

Monday - Thursday 9-12 February 2015

Part of Proceedings of SPIE Vol. 9363 Gallium Nitride Materials and Devices X

9363-1, Session 1

Ammonothermal growth of polar and non-polar bulk GaN crystal (*Invited Paper*)

Yutaka Mikawa, Takayuki Ishinabe, Shinichiro Kawabata, Tae Mochiduki, Atsuhiko Kojima, Yuji Kagamitani, Hideo Fujisawa, Mitsubishi Chemical Corp. (Japan)

In recent years, high quality bulk GaN substrates are strongly demanded for both optoelectronic and power electric devices. Currently free standing GaN substrates are mostly grown by hydride vapor phase epitaxy. However the considerably high dislocation density is caused by the growth on non-native seeds. To solve this problem, various growth methods such as high nitrogen pressure solution, basic- and acidic-ammonothermal and Na-flux method have been studied by many researchers. We proposed an original ammonothermal method known as SCAAT (Super Critical Acidic Ammonia Technology) which enable to obtain strain free, high quality and large size bulk GaN crystals. SCAAT GaN crystals are grown under high pressure and high temperature super-critical ammonia.

To realize this technology, scalable and corrosion-resistant autoclave was newly designed, which can be operated under the severe conditions. By use of this autoclave as well as optimizing growth conditions and parameters, we have succeeded to grow high quality and large size bulk GaN crystals. One of the unique features of SCAAT is relatively high growth rate of more than a few hundred micrometers per day toward various crystal axes. This feature allowed us to grow polar, non-polar and semi-polar bulk GaN crystals by using various cutting angle seeds with excellent crystalline quality. For example, the x-ray rocking curve on (200) plane of m-plane GaN crystal showed less than 10 arcsec measured by germanium (440) symmetry 4-bounce monochromator.

9363-2, Session 1

High-purity and highly-transparent AlN bulk crystal growth for UVC LED application by HVPE (*Invited Paper*)

Yoshinao Kumagai, Tokyo Univ. of Agriculture and Technology (Japan); Toru Nagashima, Toru Kinoshita, Tokuyama Corp. (Japan); Rie Togashi, Tokyo Univ. of Agriculture and Technology (Japan); Reo Yamamoto, Tokuyama Corp. (Japan); Baxter Moody, HexaTech, Inc. (United States); Hisashi Murakami, Tokyo Univ. of Agriculture and Technology (Japan); Ramon Collazo, North Carolina State Univ. (United States); Akinori Koukitu, Tokyo Univ. of Agriculture and Technology (Japan); Zlatko Sitar, HexaTech Inc. (United States) and North Carolina State Univ. (United States)

For the fabrication of high performance AlGaIn-based UVC light emitting diodes (LEDs), AlN wafers with low dislocation densities and high transparency in the UVC range are essential. Currently, AlN bulk single crystals with low dislocation densities less than $1e4 / \text{cm}^2$ can be prepared by physical vapor transport (PVT). However, the grown crystals generally show poor optical transparency in the UVC range around 265 nm. On the other hand, growth of highly UVC transparent AlN layers at several 10 micrometer/hour is possible by hydride vapor phase epitaxy (HVPE), although AlN layers grown on foreign substrates contain high densities of dislocations above $1E7 / \text{cm}^2$. Therefore, our group examined HVPE growth of thick AlN layers on PVT-AlN wafers for the preparation of low dislocation

density AlN wafers with UVC transparency.

Thick HVPE-AlN layers were grown by supplying AlCl_3 and NH_3 precursors into the growth reactor using a H_2+N_2 carrier gas mixture at 1450°C with a growth rate of 25 micrometer/hour. Freestanding AlN wafers were then prepared from the HVPE-AlN layers by removing the PVT-AlN portions. The HVPE-AlN wafers inherited high structural quality such as low dislocation densities below $1E6 / \text{cm}^2$ from the PVT-AlN wafers, and showed UVC transparency with an optical transmission cutoff at the bandgap, which was attributed to low carbon impurity concentration. Influence of growth temperature, growth rate, growth procedure, and intentional impurity doping on the structural and optical properties of freestanding HVPE-AlN wafers will be presented.

9363-3, Session 1

Thermodynamic principle for AlN growth using Ga-Al flux and its growth mechanism (*Invited Paper*)

Hiroyuki Fukuyama, Tohoku Univ. (Japan)

Recently, we have studied the liquid phase epitaxy growth of AlN layer using Ga-Al fluxes, and have succeeded to grow high quality AlN layers on sapphire substrates 1)-4). The selective growth of AlN is well explained using the equilibrium phase relation between AlN-GaN phase and Ga-Al flux phase. The activities of the AlN-GaN system was measured using EMF method by K. T. Jacob et al 5). The activities of the Al-Ga system was evaluated using the phase diagram. The details of the thermodynamic principle of the LPE growth process will be presented together with its growth mechanism in the conference.

References

- [1] M. Adachi, K. Maeda, A. Tanaka, H. Kobatake, H. Fukuyama, *physica status solidi (a)*, 208, 7, 1494-1497, (2011).
- [2] M. Adachi, M. Sugiyama, A. Tanaka, H. Fukuyama, *Materials Transactions*, 53, 7, 1295-1300, (2012)
- [3] M. Adachi, M. Takasugi, D. Morikawa, K. Tsuda, A. Tanaka, H. Fukuyama, *Applied Physics Express*, 5, 101001-1-3, (2012)
- [4] M. Adachi, K. Tsuda, M. Sugiyama, J. Iida, A. Tanaka, H. Fukuyama, *Applied Physics Express*, 6, 091001-1-3, (2013)
- [5] K. T. Jacob, G. Rajitha, L. Rannesh, H. Fukuyama, Y. Waseda, *Acta Materialia*, 60, 59-66, (2012)

9363-4, Session 1

Ammonothermal growth of GaN on HVPE crystals prepared with the use of ammonothermal seeds

Robert Kucharski, Marcin Zajac, Malgorzata Iwinska, Romuald Stankiewicz, Ammono S.A. (Poland); Tomasz Sochacki, TopGaN sp. z o.o. (Poland) and Institute of High Pressure Physics (Poland); Jan L. Weyher, Institute of High Pressure Physics (Poland); Michal Bockowski, TopGaN sp. z o.o. (Poland) and Institute of High Pressure Physics (Poland)

Among the bulk GaN crystallization technologies, the combination of ammonothermal and HVPE method is regarded as the most optimal one, thanks to a promising synergy of high structural quality (extremely low

**Conference 9363:
Gallium Nitride Materials and Devices X**

dislocation density and high crystal curvature radius), purity and large growth rate. It was shown that the ammonothermally grown GaN crystals (A-GaN) can be successfully used as seeds for the HVPE growth [1], yielding crystals (A-HVPE-GaN) of low dislocation density (10^4 cm^{-2}) and satisfying structural properties. A very important issue is to study the results of application of such crystals as seeds in ammonothermal growth again. Such approach can be very helpful in seed multiplication stage and release of large size ammonothermal GaN substrates, even 4-inch diameter.

Two kinds of crystals were used in the ammonothermal growth as seeds. The first one were A-HVPE seeds mentioned above. Before the ammonothermal process, the first A-seed was removed. The second one were HVPE crystals obtained with the use of sapphire (Sap-HVPE). The growth conditions were adjusted in order to obtain crystals of electron concentration of the order of 10^{17} cm^{-3} . In this communication we will show and compare the results of structural properties of ammonothermal GaN crystals grown with the use of both types of seeds.

Obtained crystals (A-HVPE-A-GaN and Sap-HVPE-A-GaN) were studied with the use of X-ray diffraction technique (Panalytical X'Pert Pro MRD high resolution with a Cu K α 1 line source, slit width 0.1 mm x 0.1 mm and 2mm x 2mm for the incident beam and an open-detector mode for the diffracted beam) and defect selective etching (DSE). As expected, speaking about structural properties, the A-HVPE-A-GaN crystals outperform the Sap-HVPE-A-GaN ones. The full width of at half maximum (FWHM) of A-HVPE-A-GaN crystals is about 20 arcsec, while the crystal curvature radius is about 100 m. The dislocation density is kept at the order 10^4 cm^{-2} . For comparison, Sap-HVPE-A-GaN crystals have FWHM of 100 arcsec, curvature radius of few meters and dislocation density of $2 \times 10^7 \text{ cm}^{-2}$. Some optical properties of the studied crystals will also be shown.

To conclude, successful ammonothermal growth of GaN crystal was realized using A-HVPE seeds. They owe their outstanding structural properties to the ammonothermal seeds, previously adopted to HVPE growth. Consequently, a much more effective seed multiplication can be launched, using ammonothermal method.

[1] T. Sochacki et al., Appl. Phys. Express 6 (2013) 075504.

Acknowledgments:

The work was partially supported by the National Center for Research and Development through grant PBS No. 177589.

9363-5, Session 1

Current status of hydride vapor phase epitaxy on ammonothermally-grown GaN seeds

Michał Bockowski, Institute of High Pressure Physics (Poland)

It was shown that the ammonothermally grown GaN crystals (Am-GaN) can be successfully used as seeds for the Hydride Vapor Phase Epitaxy (HVPE). Crack-free and up to 2 mm thick HVPE-GaN layers are obtained. The free-standing (FS) HVPE-GaN crystals sliced from Am-GaN seeds show high structural as well as optical, electrical and thermal qualities.

Since the structural properties of the FS HVPE-GaN crystals are not different from the excellent structural properties of the Am-GaN seeds, the FS HVPE-GaN can be successfully used as a seed for the further HVPE-GaN growth. It is feasible to multiply the ammonothermally grown GaN by the HVPE technology. The FS HVPE-GaN crystals can also be used as seeds for the ammonothermal, as well as the High Nitrogen Pressure Solution (HNPS) growths.

In this paper the state of the art of the HVPE-GaN growth on the Am-GaN seed will be demonstrated. Particular attention will be paid to the growth rate and its influence on the structural quality of the HVPE-GaN layers. New directions in the development of the HVPE-GaN growth will be presented. The main goal for today is how to develop a method of doping by donors and acceptors. It seems that due to the high purity of the HVPE-GaN, the free carriers can be compensated at a very low level of doping. Thus, high-quality HVPE-GaN with a high resistivity should easily be obtained. On the

other hand, high-quality HVPE-GaN with a free carrier concentration of the order of $5 \times 10^{18} \text{ cm}^{-3}$ should also be fabricated.

9363-6, Session 2

Growth of GaN and related materials on large silicon substrates (Invited Paper)

Michael Heuken, AIXTRON SE (Germany) and RWTH Aachen Univ. (Germany)

Solid State Lighting (SSL) based on LED, solar energy harvesting and low loss energy saving power conversion based on new AlGaInN/GaN electronic devices require advanced, high yield and high throughput MOCVD production technology. To further improve the cost-of-ownership and to allow LED market penetration for SSL the proven multiwafer Planetary Reactor[®] as well as the Showerhead reactor family was recently extended. Simulation of temperature distribution and gas flow allows understanding the growth process as well as limiting technological factors.

Revolutionary as well as evolutionary steps have led to the introduction of the AIX G5 HT and Close Coupled Showerhead (CCS) reactors. Both exhibit high wafer capacity configurations with 56x2", 14x4", 8x150mm and 5x200mm for AIX G5 HT, and 75x2", 19x4" for showerhead reactors. The basic design rules and principles of MOCVD growth optimization and details of today's high brightness LED and HEMT technology on Silicon substrates will be explained, demonstrating uniformity data within the 1% range on 200 mm Si wafers which is suitable for mass production.

The Cost of Ownership (CoO) of MOCVD tools is influenced by wafer yield and also by the reduction of user interaction due to automation. This paper discusses the different developments in the field of MOCVD to facilitate further reduction of the production costs and simultaneously improving the device characteristics. In addition physics and technology of LED on Si for SSL as well as progress in HEMT on Si technology and recent market developments will be explained and discussed.

9363-7, Session 2

GaN on Si: new approaches for stress engineering and doping (Invited Paper)

Stephanie Fritze, LayTec AG (Germany) and Otto-von-Guericke-Univ. Magdeburg (Germany); Armin Dadgar, André Strittmatter, Alois J. Krost, Otto-von-Guericke-Univ. Magdeburg (Germany)

Nowadays, GaN based technology is omnipresent involving general lighting, high efficiency LED back lighted smart TVs, base stations for wireless communication and portable electronics, to cite a few. However, due to the permanent demand to cut costs, it is imperative to consider large Si substrates in place of sapphire and SiC.

The obstacles for GaN on Si are the resulting tensile strain upon cool down from layer growth, leading to wafer bow and cracking and a fairly high dislocation density originating from lattice mismatch. To combat these intractable problems, low temperature AlN interlayers have been introduced with some success, but revealing some limitations, especially in material quality. In order to achieve thicker crack-free material with higher crystalline quality, we developed compositionally graded AlGaIn interlayers. Using in-situ monitoring and multiple ex-situ characterization methods, such as x-ray diffraction, TEM, optical microscopy and SEM, the role of these AlGaIn interlayers can be strictly elucidated revealing a critical and unique role played by each and every single interlayer in the GaN stack.

Another critical step in GaN technology is the achievement of highly conductive GaN. Almost exclusively, n-type conductivity in GaN is obtained by using Si as a dopant. Unfortunately, high Si concentrations in GaN lead to detrimental tensile strain and degradation of the material quality, particularly beyond a critical doping level of about $2 \times 10^{19} \text{ cm}^{-3}$. Doping with Ge will be presented as highly promising alternative leading to smooth

**Conference 9363:
Gallium Nitride Materials and Devices X**

surfaces independent from the Ge doping level and without any additional stress. In addition Ge doped GaN allows an order of magnitude higher electron concentration compared to Si.

In this presentation, details of the AlGaIn interlayers in a thick GaN stack as well as doping with Ge will be discussed.

9363-8, Session 2

In-situ x-ray diffraction analysis for MOVPE growth of nitride semiconductors (*Invited Paper*)

Motoaki Iwaya, Taiji Yamamoto, Koji Ishihara, Tetsuya Takeuchi, Satoshi Kamiyama, Meijo Univ. (Japan); Isamu Akasaki, Meijo Univ. (Japan) and Nagoya Univ. (Japan)

Nowadays, high-brightness blue, green, and white light-emitting diodes (LEDs) and high-power violet and blue laser diodes based on group-III nitride semiconductors have been commercialized as a result of several breakthroughs such as the growth of high-crystallinity GaN on sapphire using a low-temperature deposited buffer layer and realization of conductivity control of nitrides. Optoelectronics in the visible-short wavelength region has been established via the use of nitrides. These devices are typically fabricated by metalorganic vapor phase epitaxy (MOVPE).

In device manufacturing, a key process is an in situ monitoring method for MOVPE. Such a method can be used to obtain information about some parameters during growth, such as the wafer bow, crystalline quality, and lattice constant. This information provides feedback about the growth condition and can be used to determine the growth mechanism. Therefore, in situ monitoring is expected to serve as a key technology to improve the device performance.

In this presentation, we investigated the application of a novel in situ X-ray diffraction monitoring method to determine the critical thickness in GaInN/GaN heterostructure system. We also investigated dislocation density dependence of the critical thickness in GaInN/GaN heterostructure. As a result, critical thickness of misfit dislocation in GaInN was significant depends on the dislocation density in the GaN underlying layer.

9363-9, Session 2

Green laser diodes: dependence of in-composition fluctuations on substrate polarity

Lucja Marona, Marcin Sarzynski, Grzegorz Staszczak, Institute of High Pressure Physics (Poland); Wojciech Zaleszczyk, Institute of Physics (Poland); Piotr Perlin, Tadek Suski, Institute of High Pressure Physics (Poland)

III-nitrides based optoelectronic devices suffer from a combination of In fluctuations and high-electric field, especially pronounced in the region of long wavelengths (blue-green). To look in more detail at this problem we compare structures grown in the same epitaxial conditions, but on different substrates.

The first substrate is c-plane GaN and the second one semipolar (20-21) plane. Due to the smaller built-in electric field in the structure grown on semipolar plane the blue shift of the emitted light should be smaller than in the polar structure, assuming similar scale of indium composition fluctuation.

Low/high laser pumping photoluminescence measurements are performed and we observe almost the same wavelength shift in both kinds of structures.

To shed some light on that problem we analyze the contribution of In-fluctuations to the observed blue shift in the samples with different polarity

types. At first we measure the emission peak position as a function of temperature looking for typical "s-shape" dependence confirming existence of indium fluctuations. The observed dependences of the emission as a function of temperature are similar in both, the semipolar and in the polar sample. In both cases we observe strong s-shape indicating existence of indium composition fluctuations. On the other hand, cathodoluminescence images show that in the case of semipolar sample the indium arrangement is much more uniform than in the polar sample. This result seems to be in a contradiction to the obtained similar blue shifts and similar "s shapes" for the samples with different polarities. Therefore, the further investigation of the problem is required.

9363-10, Session 3

Theoretical aspects in growth of In-rich InGaIn (*Invited Paper*)

Yoshihiro Kangawa, Koichi Kakimoto, Kyushu Univ. (Japan)

InxGa1-xN semiconductor alloy is a promising material for bright LEDs in visible range. Although the emission wavelength of the material can be controlled from ultraviolet to violet, blue, green, and amber regions by increasing the In composition, quantum efficiency of the devices rapidly degrades at wavelengths beyond the blue-green spectral range. This is because its crystalline quality becomes poor with increasing of In composition owing to the decomposition temperature, i.e., optimum growth temperature, of the material becomes low. A pressurized-reactor MOVPE (PR-MOVPE) would give us an answer to solve this problem, because the decomposition of the material is suppressed even at relatively high growth temperature. In the present work, we have developed a surface phase diagram of InN during PR-MOVPE by an ab initio based-approach to discuss the preferable growth conditions.

In 2001, we have proposed a new theoretical approach based on an ab initio calculation. This theoretical approach enables the investigation of the influence of growth conditions such as partial pressure and temperature on the surface stability. The theoretical approach is applied to the research on the incorporation of metastable cubic InN (c-InN) into wurtzite InN (h-InN) matrix during PR-MOVPE. It was found that the {1-1-1} facet formation causes the spontaneous formation of the c-InN islands. Moreover, the results suggest that the transition of the reconstructed structures on the surfaces influences on the growth form. To improve the phase purity of thin films, it is important to control surface reconstructions on the growth surfaces using the surface phase diagram.

9363-11, Session 3

Progress in GaInN growth by RF-MBE and development to optical device fabrication (*Invited Paper*)

Tomohiro Yamaguchi, Kogakuin Univ. (Japan); Tsutomu Araki, Ritsumeikan Univ. (Japan); Takeyoshi Onuma, Tokyo National College of Technology (Japan) and Kogakuin Univ. (Japan); Tohru Honda, Kogakuin Univ. (Japan); Yasushi Nanishi, Ritsumeikan Univ. (Japan)

As a recent progress in GaInN growth by RF-MBE, we mainly introduce the growth of thick films using DERI (droplet elimination by radical-beam irradiation) method. The DERI method is composed of the two series of growth steps; (1) an In-rich growth step (MRGP: Metal Rich Growth Process) and (2) a nitrogen radical beam irradiation step (DEP: Droplet Elimination Process). This method enables reproducible growth of high-quality films with a flat surface, since the appearance and elimination of excess metal on the growing surface can be simply monitored and controlled using in-situ RHEED and laser reflection. The unique growth mechanisms of DERI method are discussed. Structural, optical and electrical properties of thick GaInN films are also shown.

**Conference 9363:
Gallium Nitride Materials and Devices X**

In this presentation, we also present the recent research activities on the pn-GaN LEDs fabricated using the thick GaInN films grown by DERI method.

This work was partly supported by JSPS KAKENHI Grant Nos. #25706020, #26600090, #25420341 and #25390071, ALCA project of JST and Nanotechnology Platform Project (NIMS Nanofabrication Platform) sponsored by MEXT. The authors also thank to N. Ikeda, K. Oosato, L. Sang and M. Sumiya of NIMS for their help with the device fabrication.

9363-12, Session 3
High-density nitrogen plasma source for growing high In content InGaN by plasma-assisted MBE (*Invited Paper*)

Hiroki Kondo, Masaru Hori, Hiroshi Amano, Nagoya Univ. (Japan)

Plasma-assisted molecular beam epitaxy (PA-MBE) is one of important methods to grow high-quality GaN and InGaN films. However, the growth rate obtained by this technique is lower than that obtained by metal organic vapor phase epitaxy (MOVPE). In order to improve the growth rate of PA-MBE, a high-density radical source (HDRS) was developed in this study. According to vacuum ultraviolet absorption spectroscopy (VUVAS) measurement, nitrogen radical density generated employing the HDRS increased up to $3 \times 10^{12} \text{ cm}^{-3}$ with increasing nitrogen molecular (N_2) gas flow rate. This value is more than one order of magnitude higher than that obtained by the conventional inductively-coupled plasma source (ICP). Then, faster growth rate of $2.5 \mu\text{m/h}$ in GaN homoepitaxy was performed by the PA-MBE employing the HDRS. The growth rate of InGaN was also enhanced by this method. When III/V ratio was varied ranging from 1.0 to 1.67 at the growth of InGaN with 10%-In content, full width at half maximum (FWHM) of the X-ray omega rocking curve (XRC) for (0002)-plane diffraction of the epilayer was minimalized at the III/V ratio of 1.46. While such the FWHM value increased with increasing In content in the case using the ICP, that by the HDRS hardly changed even at the In content of 16%. Clear single emission peak around 470 nm from the epilayer was confirmed by photoluminescence at RT, indicating superior crystalline quality of the epilayer. These results indicate high potential of the HDRS to realize the high-rate growth of high quality and high-In content InGaN.

9363-13, Session 3
HVPE growth of AlXGa1-XN templates for UV-LED applications (*Invited Paper*)

Chi-Tsung Tsai, Jia-Hao Liang, Tsung-Yen Tsai, Ray-Hua Horng, National Chung Hsing Univ. (Taiwan); Dong-Sing Wu, National Chung Hsing Univ. (Taiwan) and Da-Yeh Univ. (Taiwan)

AlXGa1-XN compounds on the sapphire substrates were successfully obtained by the halide vapor phase epitaxy process (HVPE) at a growth temperature of 1100°C. The flow ratio ($R = [\text{HClAl}]/([\text{HClAl}] + [\text{HClGa}])$), which was defined by the individual HCl flow rates through Al and Ga metal sources, can be altered for the Al content control. The atomic percent of Al increases linearly with the R value by the determination of XPS, whereas the atomic percent of Ga increases abruptly below the R value of 0.33. The crystal structure belonged to AlGaN is only detected in samples as the R value exceeds 0.25. This result indicates that a sufficient Al concentration is certainly vital for the formation of AlXGa1-XN compounds. Furthermore, the low R value strongly enhances the formation probability of GaN instead of AlGaN. It can be found that the AlXGa1-XN prepared at a R value of 0.80 has the best crystallinity and the lowest surface roughness. Additionally, the CL spectrum shows that there is a principal emission band at 324.7 nm. The transmittance of the AlXGa1-XN is above 70% between the wavelength of 225 nm and 400 nm. As a result, the AlXGa1-XN can be applied to be a growth template for the ultraviolet light-emitting diodes. The effect of

the R value on the optical properties of AlXGa1-XN compounds is also systematically reported in this study.

9363-14, Session 3
Homoepitaxial HVPE-GaN growth in non-polar and semi-polar directions

Mikolaj Amilusik, Michal Bockowski, Institute of High Pressure Physics (Poland)

There is a huge interest in homoepitaxial growth of GaN crystals in other than the c direction. The seeds for the non-polar and semi-polar growth can be obtained from a thick bulk GaN crystal (grown in the c direction by the HVPE method) by slicing it in the appropriate crystallographic directions.

Crystals with different non-polar semi-polar surfaces have already been used as seeds for the HVPE processes. Two main observations were made. The first one was the lack of the stacking faults in the non-polar (10-10) layers. The second one involved the reduction of the threading dislocation density for crystals grown in the [20-2-1] direction. The TDD was reduced one order of magnitude (from $5 \cdot 10^6 \text{ cm}^{-2}$ to $5 \cdot 10^5 \text{ cm}^{-2}$).

In this work three crystallization processes, in the same experimental conditions (in sense of geometric configuration of the HVPE reactor, growth temperature and reagents flows) but using different carrier gases: N_2 , H_2 and a mixture of 50% H_2 and N_2 , are described. The growth rates, morphologies and structural properties of the new non-polar and semi-polar HVPE-GaN crystals are investigated. Oxygen and silicon contaminations of the new grown GaN are shown. The influence of the growth directions and the applied carrier gas on the quality and physical as well as chemical properties of GaN are analyzed and discussed in detail. X-ray, CL, and TEM methods are applied in order to examine the structural properties of the non-polar and semi-polar HVPE-GaN. A model of dislocation reduction for GaN grown in the [20-2-1] direction is proposed.

9363-15, Session 4
Optical properties and band structure of highly-doped gallium nitride (*Invited Paper*)

Ruediger Goldhahn, Karsten Lange, Martin Feneberg, Otto-von-Guericke-Univ. Magdeburg (Germany)

We present the absorption and emission features of c- and a-plane GaN from very low electron concentrations up to 10^{20} cm^{-3} . The studies are based on c-plane free-standing HVPE-grown GaN:Si and MOVPE-grown films (GaN:Ge and GaN:Si) on sapphire substrates. Hall measurements and high-resolution X-ray diffraction yielded the carrier concentrations, mobilities and the residual stress.

The dielectric functions (DF) were determined from 30 meV up to 10 eV, the high-energy data refer to synchrotron radiation (Berlin electron storage ring - BESSY II). The fit of the infrared DFs yielded the two coupled phonon-plasmon-modes. The extracted plasmon frequencies mirror the occupation of the conduction band and provide clear evidence for the anisotropic band dispersion.

The DFs in the visible into the ultraviolet undergo continuous changes with increasing electron density. While the free excitonic absorption and the formation of coupled exciton-phonon complexes (EPC) dominate at low and moderate electron densities around the band gap, exciton screening, the formation of the Mahan exciton, band filling, and band-gap renormalization become dominant effects at high densities. We present a model for describing the dependence of the characteristic absorption energies on the electron densities. Photoluminescence measurements made for comparison yielded then the Stokes shift.

Finally, the three main transitions between 6.5 and 10 eV related to critical points undergo an increasing red-shift accompanied by a decreasing absorption magnitude and an increasing broadening. The reduced refractive

**Conference 9363:
 Gallium Nitride Materials and Devices X**

index in the transparent regions is attributed to these effects as well as to the blue-shift of the absorption edge.

9363-16, Session 4

Off-resonant plasmonic enhancement of linear and multi-photon emission from InGaN-GaN quantum wells

Arup Neogi, Jie Lin, Univ. of North Texas (United States); Sergio Pereira, Univ. de Aveiro (Poland); Ian M. Watson, Univ. of Strathclyde (United Kingdom)

Resonant plasmon induced light enhancement suffers from dissipative effects, which reduces the internal quantum efficiency of light emission from semiconductor light emitters. Using metal nanoparticles with localized surface plasmon (LSP) energy lower than the emission energy of the quantum well, the absorption or scattering of photons by the metal nanoparticles can be avoided. By engineering the metal nanoparticles to strongly couple with the electrons/holes within the quantum wells, electrostatic image charge effect can be used to manipulate the carrier concentration around the metal nanoparticles and increase the radiative recombination rate compared to the non-radiative carrier recombination process.

The InGaN/GaN with inverted V-pits were grown using MOCVD technique and the metal nanoparticles such as Au, Pd and Ag were selectively introduced within these pits without any accumulation on the surface to manipulate the lateral carrier transport within the well. A five- eight fold enhancement in the photoluminescence emission (PL) was observed in the presence of Au- or Pd-nanoparticles whereas Ag nanoparticles resulted in quenching. The two-photon process induced by near-bandgap excitation by near-infrared light in the 710-750 nm wavelength range results in red-shifted defect bound emission from the band edge of the quantum well. This nonlinear emission can be enhanced by tuning the incident laser light closer to the LSP energy. A two-three fold enhancement is observed in the presence of the Au nanoparticles, whereas no change is observed due to Ag-nanoparticles. The physical origin of the enhancement is studied using time-resolved PL spectroscopy.

9363-17, Session 4

An electrical-pumped single-photon source with polarization control

Lei Zhang, Chu-Hsiang Teng, Pei-Cheng Ku, Hui Deng, Univ. of Michigan (United States)

We report electrically driven, site-controlled InGaN single-photon sources (SPSs) that emit light with pre-defined linear polarizations. Each SPS consists of an InGaN quantum dot (QD) in a free-standing GaN nanowire, etched from a c-plane InGaN/GaN single-quantum wafer. The location and cross-section of each SPS is precisely defined by electron-beam lithography. Electrically driven devices are made by applying an indium-tin-oxide (ITO) p-contact, Ti/Au bottom n-contact and spin-on-glass insulating layer. High current-injection efficiency is achieved by the high overlap between the current pathway and the QD active region. The electroluminescence (EL) spectrum of a single device at 5 V forward bias shows a dominant exciton peak at -3.1 eV, whose intensity linearly depends on the applied current. Single-photon emission is demonstrated by strong antibunching in the second-order correlation function of single QD's EL. Linearly polarization emission is achieved using QDs with elliptical cross-sections. Due to the strong piezo-electricity in InGaN QDs, the anisotropic strain distribution in an elliptical QD results in highly linearly polarized emission. The direction and degree of the EL polarization is defined by the long-axis orientation and the ellipticity of the QD's cross-section, respectively. Our device integrates for the first time both electrical pumping and site-control in III-N based quantum dots. It is also the first polarization-controlled III-N SPS. It represents an important progress towards efficient, scalable on-chip quantum information processing.

9363-18, Session 4

Temperature-dependent time-resolved photoluminescence measurements of (1-101)-oriented semi-polar AlGaIn/GaN MQWs

Daniel Rosales, Bernard Gil, Thierry Bretagnon, Univ. Montpellier 2 (France) and Lab. Charles Coulomb (France); Morteza Monavarian, Fan Zhang, Serdal Okur, Natalia Izyumskaya, Vitaliy Avrutin, Ümit Özgür, Hadis Morkoç, Virginia Commonwealth Univ. (United States)

We studied the temperature dependence and the recombination dynamics of the photoluminescence (PL) of (1-101)-oriented semi-polar Al_{0.2}Ga_{0.8}N/GaN multiple quantum wells (MQWs) grown on patterned 7°-off Si (001) substrates. The typical studied structures are made of five 1.5 nm thin GaN quantum well separated by 8.5 nm thick Ga_{0.8}Al_{0.2} barrier layer. The polarized low-temperature PL measurements reveal that radiative recombinations associated to annihilation of localized excitons exhibit an expected anisotropic behavior. With increasing temperature, the excitonic emission shows a red-energy shift characteristic of the thermal delocalization of carriers. The PL intensity at room temperature is reduced by an only one order of magnitude with respect to low temperature. We attribute this finding to a reasonably good crystalline quality leading to a low density of PL killing centers. The contributions of radiative and non-radiative recombination to the effective photoluminescence decay time are obtained in the traditional way by simultaneous processing of the evolutions of PL decay time and intensity with temperature. We find that the thermally activated non-radiative component saturate at a value of about 250 ps at room temperature. The radiative decay time exhibits a mixed behavior: it is roughly constant at 360 ps from 8K to temperatures ranging near 140-150K and then rapidly increases with a slope of 10 ps.K⁻¹. This behavior is indicative of coexistence of localized excitons and free excitons which relative proportion are statistically computed. We conclude that semi-polar AlGaIn/GaN MQWs structures are a promising approach for the production of low-cost UV operating devices.

9363-19, Session 4

Photoluminescence behavior of amber light emitting GaInN-GaN heterostructures

Huong Thi Ngo, Daniel Rosales, Bernard Gil, Pierre Valvin, Univ. Montpellier 2 (France) and Lab. Charles Coulomb (France); Benjamin Damilano, Kaddour Lekhal, Philippe De Mierry, Ctr. de Recherche sur l'Hétéro-Epitaxie et ses Applications (France)

Time-resolved photoluminescence spectra of amber/orange light emitting (Ga,In)N-based devices have been grown by metal-organic vapor phase epitaxy on c-plane sapphire for indium compositions ranging up to 23 percents. The temperature dependent time-resolved photoluminescence spectra collected through the 8K-300K range are found to exhibit behaviors that are found to be very similar to what is reported in literature in samples with different designs (well width, indium composition in the well layer). However, our quantum devices always exhibit a two-mode exponential decay with a long decay time about 4 to five times longer than the short one, which was not reported so far. The photoluminescence decay times are wavelength-dependent as always found for indium rich quantum well, a behavior that is interpreted in terms of carrier localization in indium-rich regions of the alloy active layers. The spectral dependence of the decay time, which were fitted using sigmoid function, give access to an average decay time, centered at a given energy, with a phenomenological broadening constant. The average splitting between characteristic energies for long and short decay times, the broadening constants both increase with the indium composition. Radiative and non-radiative recombination times are deduced in the whole temperature range. The average decay

**Conference 9363:
Gallium Nitride Materials and Devices X**

time increase exponentially with the product of the well width to indium composition. This quantity is found to be an excellent indicator of the device performance.

9363-20, Session 4

Identification of point defects in HVPE-grown GaN by steady-state and time-resolved photoluminescence

Michael A. Reshchikov, Denis O. Demchenko, Virginia Commonwealth Univ. (United States); Alexander S. Usikov, Nitride Crystals, Inc. (United States) and National Research Univ. of Information Technologies, Mechanics and Optics (Russian Federation); Heikki I. Helava, Yuri Makarov, Nitride Crystals, Inc. (United States)

Gallium nitride is a very promising material for high-power electronics. The hydride vapor phase epitaxy (HVPE) technique has several advantages for high-power electronics including fast growth rate, a very low density of dislocations, and a low concentration of point defects. Further improvement is hindered by a poor understanding of the majority of point defects in GaN. We have prepared a large number of undoped GaN films grown by HVPE and investigated them with steady-state and time-resolved photoluminescence (PL). The main PL bands in our HVPE GaN are the red luminescence (RL) band with a maximum at 1.8 eV and the green luminescence (GL) band with a maximum at about 2.4 eV. The latter can be easily recognized in time-resolved PL measurements due to its exponential decay even at low temperatures, with a characteristic lifetime of 1-2 ns. We attribute the GL band to transitions of electrons from the conduction band to the 0/+ level of the isolated carbon in nitrogen site. The yellow luminescence (YL) band, related to transitions via the -/0 level of the same defect, has a maximum at 2.1 eV and it is often obscured by another yellow luminescence band, which has a similar shape but peaks at about 2.2 eV. The 2.2 eV band is attributed to the carbon-oxygen complex. The 2.2 eV band is the dominant defect-related PL band in GaN grown by metal-organic vapor phase epitaxy.

9363-21, Session 4

Interface state trap density on characteristics of MOS-HEMT

Ming-Chun Tseng, Ming-Hsien Hung, Dong-Sing Wu, Ray-Hua Horng, National Chung Hsing Univ. (Taiwan)

In this study, we investigate the effect of chemical treatment on the properties of MOS capacitors and metal-oxide-semiconductor high electron mobility transistor (MOS-HEMT). The structure consist of Al₂O₃/u-GaN/AlN buffer/ Si substrate and Al₂O₃(10 nm)/u-AlGa_{0.5}N (25 nm)/u-GaN (2 μm)/AlN buffer/Si substrate for MOS capacitor and MOS-HEMT device, respectively. There are four chemical treatments, which consist of organic solvents, oxygen plasma, BCl₃ plasma, dilute acidic solvent, hydrofluoric acid and RCA-like clean process to remove the metal ions, organic contamination and native oxide. Four different chemical treatment recipes treat the surface of u-GaN before Al₂O₃ growth to reduce the interface state trap densities (D_{it}). D_{it} value is calculated from measurement of C-V curve with 1M Hz frequency.

The formation of interface state trap of u-GaN surface is modified by different chemical solution of varied chemical treatment recipe, which further influence the breakdown voltage (V_{bk}), on-resistance (R_{on}), threshold voltage (V_{th}) and drain current (I_d) of MOS-HEMT. The V_{th} of MOS-HEMT with organic solvents clean treatment is -10.02V. The MOS-HEMT after BCl₃ plasma and organic solvents clean treatment shows the lowest V_{th} of -8.15V. The electronic characteristics of MOS HEMT device with four different chemical treatment recipes are investigated in this article.

9363-22, Session 5

Structural characterization of low defect density III-Nitrides semipolar films and heterostructures by transmission electron microscopy (Invited Paper)

Philippe Vennéguès, Florian Tendille, Ctr. National de la Recherche Scientifique (France); Michel Khoury, Ctr. National de la Recherche Scientifique (France) and CEA-LETI (France); Jesus Zuniga-Perez, Lars Kappei, Julien Brault, Ctr. National de la Recherche Scientifique (France); Maxim Korytov, Nikolay Cherkashin, Ctr. d'Elaboration de Matériaux et d'Etudes Structurales (France); Guy Feuillet, CEA-LETI (France) and CRHEA (France); Philippe De Mierry, Ctr. de Recherche sur l'Hétéro-Epitaxie et ses Applications (France)

III-Nitrides films and heterostructures suffer from the presence of large densities of structural defects which are detrimental for the development of efficient devices. These defects result both from differences between III-Nitride films and foreign substrates (structure, chemistry, lattice parameters) and between different III-Nitrides (lattice parameters, growth conditions...). Transmission electron microscopy (TEM) is the technique of choice for studying crystalline defects. The understanding of the origin and behavior of structural defects may allow their management and the development of low defect density materials.

III-Nitrides are classically grown along the polar c-direction. In this case, internal electric fields play a major role in the properties of heterostructures. In order to eliminate or at least to reduce the influence of internal electric fields, growth along alternative directions with the c-direction in the growth plane (nonpolar) or inclined (semipolar) have been developed. Heteroepitaxial nonpolar and semipolar films contain large densities of basal plane stacking faults (BSF) and related partial dislocations and prismatic stacking faults.

In this presentation, results from multi-scale TEM studies of semipolar GaN films on patterned substrates will be presented. The understanding of the nucleation and propagation of defects allowed us to develop a 3 step growth process resulting in high quality GaN films with dislocation densities in the high 10⁷ cm⁻² range and BSF densities below 10² cm⁻¹.

These GaN films are then used as templates for InGa_{0.5}N/GaN and AlGa_{0.5}N/GaN heterostructures. TEM results about their structural characterizations will also be presented. The mechanisms of strain relaxation will be investigated.

9363-23, Session 5

Nanoscale structural analysis of nitride-based nanostructures: a multi-technique approach (Invited Paper)

Catherine Bougerol, Institut NÉEL (France) and CNRS (France); Jean Paul Barnes, Mark Beeler, Edith Bellet-Amalric, Bastien Bonef, Adeline Grenier, Pierre-Henri Jouneau, Miguel Lopez-Haro, Eva Monroy, Eric Robin, CEA Grenoble (France)

From the early studies of III-nitride semiconductors, numerous analyses have focused on the structural aspects, and especially the detailed investigations of extended defects. Nowadays, the development of nitride-based nanostructured materials in the domain of photonics or optoelectronics requires us to go a step further and to obtain quantitative information at the nanometer-scale of the structure, strain state, and/or composition. This is particularly true when extended to ternary or quaternary systems and in that case a multi-technique approach is necessary. Besides the combination of X-ray diffraction and electron microscopy to cover the macroscopic

**Conference 9363:
Gallium Nitride Materials and Devices X**

and microscopic scale, it is now possible to benefit from the versatility of transmission electron microscopes equipped with a new generation of detectors (High Resolution (Scanning)-Transmission (HR-(S)-TEM), quantitative Energy Dispersive X-ray Spectroscopy (EDX)) to perform on the same sample nano-scale compositional and spatial characterisation. The results can be combined with Atom Probe Tomography (APT) and/or Time of Flight SIMS (ToF-SIMS) data which add compositional analyses at the microscopic and macroscopic scales, but also provide a three-dimensional characterisation and the detection of doping elements, respectively. The capability of this multi-technique approach will be illustrated by our recent work on AlGaIn/GaN superlattices.

9363-24, Session 5

Stress related aspects of GaN technology physics

Ephraim Suhir, ERS Co. (United States)

Easy-to-use and physically meaningful analytical (mathematical) predictive models are developed for the evaluation of the lattice-misfit (LM) and thermal-mismatch (TM) stresses in bi-material (semiconductor, and particularly GaN film grown on a suitable substrate) assemblies. An elongated bi-material strip and a circular assembly are considered. Strength of materials analysis (SMA) model was developed and used to evaluate the LM and TM stresses in both elongated [1] and circular [2] assemblies, while a more sophisticated theory-of-elasticity (ToE) based approach was employed, in addition to the SMA model, in the case of a circular assembly. The considered stresses include the normal stress acting in the cross-sections of the semiconductor film and responsible for its fracture toughness and possible buckling, and the interfacial shearing stress responsible for the occurrence and growth of dislocations, for possible delaminations in the assembly and for the strength of an intermediate strain buffering material, if any. In the case of a circular assembly, the normal radial and normal circumferential (tangential) stresses acting in the GaN cross-sections have been determined. Since the interfacial stresses concentrate at the peripheral portions of the assembly, the role of the curvilinear edges on the magnitude and distribution of the induced stresses has been addressed. It has been shown that significant stress relief can be achieved, as has been predicted in our early publications [3, 4], by using properly engineered or porous substrates and that, unless such substrates are employed, the LM stresses are considerably higher than the TM stresses, even if a reasonably good lattice match takes place as, e.g., in the case of a GaN film fabricated on a SiC substrate, when the lattice-mismatch strain is only about 3%. This is true even when the temperature change from the semiconductor growth temperature to a low, operation or testing, temperature is significant, and the TM stresses are, therefore, the highest.

The numerical example is carried out, as an illustration, for a GaN film grown on a SiC substrate. Based on the calculated data, it is concluded that the SMA model is acceptable for understanding the physics of the state of stress and for assessing the LM stress level. The SMA model underestimates, however, the maximum interfacial shearing stress at the assembly end, and, because of its very nature, is unable to address the circumferential stresses. It is the ToE model should be used to assess these stresses and the role of the curvilinear boundary of a circular substrate.

The developed predictive models can be used, in addition to the routine finite-element analyses (FEA), for the assessment of the merits and shortcomings of a particular semiconductor crystal growth technology, as far as the expected LM and TM stresses are concerned, before the actual experimentation and/or fabrication efforts are considered and carried out. The models can be used particularly to determine, from the observed critical film thickness, the material, design and technological factors that might lead to elevated dislocation densities.

References

1. E. Suhir, Stresses in bi-material GaN assemblies, J. Appl. Physics, 110, 2011
2. E. Suhir, Lattice-misfit stresses in a circular bi-material GaN assembly, J. Appl. Mech., vol.80, January 2013
3. E. Suhir, "Stresses in bi-metal thermostats", J. of Appl. Mech., vol.55, No.4, 1986.

4. S. Luryi, E. Suhir, "New approach to the high quality epitaxial growth of lattice-mismatched materials", Appl. Phys. Letters, vol.49, No. 140, 1986

9363-25, Session 5

Highly-spatially-resolved cathodoluminescence of GaN/AlN quantum dots directly performed in a scanning transmission electron microscope

Gordon Schmidt, Christoph Berger, Sebastian Metzner, Peter Veit, Frank Bertram, Armin Dadgar, André Strittmatter, Jürgen Christen, Otto-von-Guericke-Univ. Magdeburg (Germany)

In semiconductor quantum dots (QD) carriers are confined into all three spatial dimensions leading to a delta-function density of states, increased exciton binding energy and stronger oscillator strength. Using heteroepitaxially Stranski-Krastanov growth mode the confinement in the order of the de-Broglie wavelength of the carriers can be realized for self-organized III-nitride semiconductor QDs. Hence, there is a great interest of QDs and their devices for applications like single-photon sources.

In this study we will present our results from nanoscale optical and structural characterization of a III-nitride based QD heterostructure which was grown by MOVPE. A 1 μm thick AlN layer grown on a c-plane sapphire substrate serves as template for the further growth process. Subsequent, a layer of GaN QD was intentionally grown capped by a 30 nm AlN layer.

The cross-section STEM image clearly shows the AlN/sapphire template and the GaN QD layer. Originating from the AlN/sapphire interface vertically running threading dislocations (TD) show up in the STEM images. We observe an overall formed GaN layer, which exhibits a higher layer thickness in the vicinity of these TDs. The comparison of the STEM images with the simultaneously recorded panchromatic CL mappings at 16 K exhibits a spot like emission located at the TD/GaN layer intersection. We observe sharp emission lines (FWHM <1.9 meV) between 220 nm and 300 nm originating from the GaN layer positions with higher thickness in the vicinity of TD ensemble. In the defect free GaN regions an emission at 215 nm can be seen.

9363-26, Session 5

Direct imaging of nitride-based microrod LED structures using nano-scale scanning transmission electron microscope cathodoluminescence

Marcus Müller, Benjamin Max, Christopher Karbaum, Gordon Schmidt, Peter Veit, Frank Bertram, Jürgen Christen, Otto-von-Guericke-Univ. Magdeburg (Germany); Martin Mandl, Tilman Schimpke, Martin Strassburg, OSRAM Opto Semiconductors GmbH (Germany)

The application of III-nitride microrods as light emitting devices (LED) offers many advantages like the high crystal quality and an increased effective light emitting area in comparison to conventional planar devices.

In this study, we correlate the structural and optical properties of single InGaIn/GaN core-shell microrod LED structures on a nanometer-scale using cathodoluminescence spectroscopy (CL) performed in a scanning transmission electron microscope (STEM).

The core-shell microrods were grown by MOVPE on a c-plane GaN/sapphire template covered with SiO₂-mask. Out of the mask openings, n-doped GaN microrod cores were grown under conditions favouring 3D growth. In a second growth step an InGaIn single QW encased by thin GaN and AlGaIn layers was deposited under 2D growth conditions.

To investigate the optical properties of the LED heterostructure on

**Conference 9363:
 Gallium Nitride Materials and Devices X**

nanometer-scale we performed a CL linescan across the whole microrod diameter. The CL linescan clearly resolves the emission of the individual layers. Starting in the microrod center, we observe only weak luminescence from the n-GaN core structure. The AlGaIn layer on top of the GaN core exhibits a CL at 3.65 eV. In contrast to the GaN core, the n-GaN shell on the AlGaIn layer shows an intense donor-bound exciton emission at 3.47 eV and donor-acceptor pair recombination at 3.26 eV. Here, the generated excess carriers are already able to diffuse to the InGaIn SQW resulting in an intense emission at 2.81 eV. Finally, the p-GaN cap layer exhibits an emission at 3.10 eV which can be attributed to the blue band luminescence.

9363-27, Session 6

A theoretical study of III-nitride nanowire arrays for emission and detection (*Invited Paper*)

Bernd Witzigmann, Univ. Kassel (Germany)

Tremendous progress has been made in the synthesis of III-nitride nanowire arrays. This builds a platform for various device concepts, such as light emitting diodes, solar cells or optoelectronic sensors. In this presentation, the performance of nanowire light emitters and detectors is analyzed with theoretical modeling.

Three aspects are considered for simulating nanowire arrays: first, light extraction or trapping by the solution of Maxwell's equations, including a complex dielectric constant and anisotropic dipole sources from spontaneous emission. Second, the carrier injection or extraction by a combination of semi-classical and quantum transport models. Third, the interaction of electromagnetic fields and the charge carriers. To first order, this is accomplished by local generation/recombination in the carrier balance. Higher order effects include photon reabsorption and spontaneous emission enhancement due to weak quantum electrodynamics. As a consequence, the internal quantum efficiency is coupled to the extraction efficiency (by spontaneous emission enhancement) and vice versa, the extraction efficiency depends on the internal quantum efficiency (by photon recycling). In contrast to thin film LEDs, these coupling effects cannot be neglected in the external efficiency of nanowire arrays. This is shown both in a general theoretical framework, also for the case of a radial junction nanowire array. As outlook, nanowire arrays as solar cells for hydrogen generation will be investigated. In contrast to planar structures, the wires serve as intrinsic optical concentrator element, and improve the areal efficiency due to their surface area enhancement. Some fundamental design aspects of a nanowire based solar fuel system are discussed.

9363-28, Session 6

Photocathode electron beam sources using GaN and InGaIn with NEA surface (*Invited Paper*)

Tomohiro Nishitani, Takuya Maekawa, Yoshio Honda, Masao Tabuchi, Nagoya Univ. (Japan); Takashi Meguro, Tokyo Univ. of Science (Japan); Hiroshi Amano, Nagoya Univ. (Japan)

Photocathodes using III-V semiconductors with a negative electron affinity surface (NEA-semiconductor photocathodes) have played important roles as highly spin-polarized electron sources in several fields of fundamental science. The key technology of NEA-semiconductor photocathodes is that NEA surface enables excited electrons in the conduction band to escape to vacuum. However, surface of NEA-semiconductor photocathodes is damaged by adsorption of the residual gas and back bombardment of ionized residual gas by photoelectrons.

The existing strategy for maintaining NEA state is extreme high vacuum below $1e-8$ Pa for decreasing residual gas. However, the essential solution for maintaining the NEA state for long time is improvement of a surface

potential structure of semiconductors.

Large surface band bending on p-semiconductors contributes to the long lifetime of NEA-semiconductor photocathodes. The potential depth of surface band bending is half the band gap energy because the Fermi level in p-doped semiconductors is pinned by the surface state. Therefore, p-semiconductors with wide band gap are suitable for large surface band bending.

A p-GaN and a p-InGaIn (In fraction = 0.12) semiconductor with a bulk structure were fabricated as a test samples for NEA-semiconductor photocathodes. Decay of quantum yield as the lifetime of NEA-semiconductor photocathodes using p-GaN and p-InGaIn in ultra-high vacuum were measured. NEA-semiconductor photocathodes using p-GaN and p-InGaIn achieved lifetimes that were 17times and 7times longer respectively than that using a p-GaAs with a bulk structure as the conventional NEA-semiconductor photocathode.

9363-29, Session 6

Ordered arrays of InGaIn/GaN dot-in-a-wire nanostructures as single-photon emitters (*Invited Paper*)

Snezana Lazic, Ekaterina Chernysheva, Univ. Autónoma de Madrid (Spain); Marko Gacevic, Noemi García-Lepetit, Univ. Politécnica de Madrid (Spain); Herko P. van der Meulen, Univ. Autónoma de Madrid (Spain); Marcus Müller, Frank Bertram, Otto-von-Guericke-Univ. Magdeburg (Germany); Almudena Torres-Pardo, José María González Calbet, Univ. Complutense de Madrid (Spain); Jürgen Christen, Otto-von-Guericke-Univ. Magdeburg (Germany); Enrique Calleja, Univ. Politécnica de Madrid (Spain); José Manuel Calleja, Univ. Autónoma de Madrid (Spain)

The quest for high efficiency single photon emitters operating at high temperatures and located at precise positions is essential for the development of solid state systems for quantum light applications. We demonstrate here highly efficient single-photon emission from InGaIn nano-disks embedded into two-dimensional ordered arrays of GaN nanowires (NWs). The structures were fabricated by molecular beam epitaxy on (0001) GaN-on-sapphire templates using nanohole masks prepared by colloidal lithography. Cathodoluminescence measurements reveal the spatial distribution of light emitted from a single NW heterostructure. The emission in the blue-green spectral region originating from the topmost part of InGaIn sections show intense and narrow excitonic lines in the in micro-photoluminescence spectra. These lines exhibit high degree of linear polarization with an average polarization ratio ~92%. Comparison of the emission intensity from the vertically aligned NW ensemble with horizontal individual NWs dispersed on a silicon substrate indicates a marked increase in the emission efficiency along the NW direction. Photon correlation measurements performed on these sharp excitonic lines show a pronounced photon antibunching with a $g(2)(0)$ values below 0.3. The antibunching rate increases linearly with the optical excitation power, extrapolating to the exciton decay rate of ~1 ns⁻¹ at vanishing pump power. This value is in agreement with the direct exciton lifetime measurements by time-resolved photoluminescence. Efficient, fast generation and strong linear polarization of antibunched photons as well as the possibility to control the spatial location of quantum emitters, render this system promising for the realization of arrays of site-controlled single-photon sources for on-chip quantum information management.

**Conference 9363:
 Gallium Nitride Materials and Devices X**

9363-30, Session 7

Prospects and problems for III-N solar cells: theoretical and experimental (*Invited Paper*)

Akihiko Yoshikawa, Chiba Univ. (Japan)

InGaN-based III-Ns are expected as a plausible material system for constructing high efficiency tandem solar cells covering almost whole solar spectrum. We have been developing InGaN digital-ternary alloy-based solar cells named as "SMART III-N solar cell". First, we performed comprehensive theoretical analyses of InGaN solar cells paying special attention how their realistic material properties affect cell performances, in particular their effects on defects-induced current components resulting in extremely higher forward current than the theoretical diffusion current. Concerning the defects-induced current, the recombination current through deep level point defects and simple Ohmic leakage current thorough extended defects were taken into account. Of course, some of other material properties and device parameters as well also greatly affect the current transport mechanism through the pn-junction. Anyway, it should be noted that the relative magnitude of each component current against the photocurrent density under operation is quite important. Simply in other words, the solar cell must be designed/fabricated so that any defects-induced current density level must be lower than the operating photocurrent density to expect high performance.

For the theoretical study, we have quite carefully derived experimental equations for several material properties dominating solar cell performances, such as the absorption coefficient and electron/hole mobilities, on the basis of many reported literatures so that they should be valid and/or plausible in whole composition range and in wide carrier concentration range at the same time.

Detailed results for the systematic theoretical study and an experimentally observed serious bottleneck will be discussed in the symposium.

9363-31, Session 7

Transport measurements in GaN nanowires (*Invited Paper*)

Norman A. Sanford, National Institute of Standards and Technology (United States)

Gallium nitride nanowires are technologically attractive for a variety of applications including sensors, solid-state lighting, nanomechanical oscillators, and scanned-probe tools. Recently, nanowires are finding applications in next-generation wireless communication networks. This span of functionality is enabled by several key features, namely, the wire-like morphology, the high surface area to volume ratio, GaN's high mechanical strength and chemical durability, and that nanowires can be nearly defect-free under certain growth conditions. However, the morphology itself greatly complicates direct measurements of free carrier concentration and mobility. In this talk I will survey our multifaceted approach to transport studies which includes dark conductivity and photoconductivity, Raman scattering, X-ray photoelectron spectroscopy, FET stability studies, scanning microwave microscopy, and various simulation efforts. Emerging work involving compositional analysis of nanowire heterostructures via laser-assisted atom probe tomography will also be briefly discussed.

9363-32, Session 7

Improved performance of GaN MSM photodetectors by ultrathin interfacial Hafnia layer

Burak Tekcan, Manoj Kumar, Ali K. Okyay, Bilkent Univ. (Turkey)

GaN with its superior electrical, optical and chemical properties is a significant material for many optoelectronic device applications. Specifically, GaN based UV photodetectors are greatly utilized for space and military purposes such as space communications and missile detection. However, device performance is limited by high density of dislocations at the surface that causes excess leakage current and reduced photo-responsivity. The attempts to increase responsivity using different techniques resulted in high responsivity while, on the other hand, devices suffered from slow response time. It is reported previously that the utilization of interfacial insulator layers passivate surface defects. We inserted ultrathin layer (1.5 nm) of HfO₂ using atomic layer deposition technique between GaN and contact metal. The HfO₂ interfacial layer not only enhances photo-responsivity, but also suppresses dark current. The dark current is decreased more than two orders of magnitude for 1.5-nm-thick HfO₂ and eight orders of magnitude for 5-nm-thick HfO₂ at 10V bias. The current transport mechanism is shown to be Fowler-Nordenheim tunneling. Moreover, responsivity values increased significantly (4.5 times) comparing with and without ultrathin HfO₂ layer.

9363-33, Session 7

Screening of the quantum confined stark-effect in AlN/GaN hetero-structures based on GaN nanowires with Germanium doping

Nils Rosemann, Philipps-Univ. Marburg (Germany); Pascal Hille, Jan Müßener, Justus-Liebig-Univ. Giessen (Germany); Pascal Becker, Philipps-Univ. Marburg (Germany); Maria de la Mata, Institut de Ciència de Materials de Barcelona (Spain); César Magén Domínguez, Instituto de Nanociencia de Aragon (Spain); Jordi Arbiol, Institut de Ciència de Materials de Barcelona (Spain) and Institució Catalana de Recerca i Estudis Avançats (Spain); Jörg Teubert, Jörg Schörmann, Martin H. Eickhoff, Justus-Liebig-Univ. Giessen (Germany); Sangam Chatterjee, Philipps-Univ. Marburg (Germany)

Nanowires (NWs) exhibit a low defect density due to the self-assembling growth. This makes them an ideal system to investigate the influence of doping on the crystal structure and the related optical properties. In addition to that they provide the ideal basement to grow hetero-structures inside the NWs. These AlN/GaN hetero-structures give rise to the analysis of carrier confinement effects. For high Al-content these structures exhibit a strong luminescence shift, in respect to bulk material, due to internal polarization-induced electric fields and resulting quantum-confined Stark effect(QCSE). This QCSE strongly depends on the hetero-structure geometry and doping. This QCSE can be temporally screened by optically excited carriers, giving rise to the overall strength of the QCSE. Previous studies investigated AlN/GaN hetero-structures based on GaN NWs in respect to the influence of Si- and Mg-doping on such NWs[1]. As a next step the doping was changed to germanium, which has a much larger covalent radius than Si or Mg. To determine the influence of the Ge-doping, we investigated a series of AlN/GaN hetero-structures embedded in GaN NWs, with different layer thicknesses and doping concentrations. Method of choice is time resolved photoluminescence spectroscopy using a standard streak-camera setup. Screening of the QCSE caused by free carriers provided by the Ge-doping was found accompanied by a drastic decrease in luminescence decay-time.

[1] F. Furtmayr et al., J. Appl. Phys. 104(7), 074309, (2008)

9363-34, Session 7

Optical properties of small GaN/ Al_{0.5}Ga_{0.5}N quantum dots grown on (11- 22) GaN templates

Julien Selles, Daniel Rosales, Bernard Gil, Guillaume Cassabois, Thierry Guillet, Univ. Montpellier 2 (France) and Lab. Charles Coulomb (France); Julien Brault, Benjamin Damilano, Philippe Vennéguès, Philippe De Mierry, Jean Massies, Ctr. de Recherche sur l'Hétéro-Epitaxie et ses Applications (France)

GaN-Al_{0.5}Ga_{0.5}N quantum dots deposited on the (11-22) plane have been grown by combining Molecular Beam Epitaxy and Metal Organic Vapor Phase Epitaxy. The (11-22) GaN oriented pseudo-substrates were realized by MOVPE starting from m-plane oriented sapphire substrates. This combination is interesting for the realization of ultraviolet operation light emitting diodes, lasers and single photon sources [1,3]. The growth of GaN dots was achieved by MBE using ammonia as nitrogen precursor. After the GaN deposition, a growth interruption without ammonia is done to trigger the dot formation [4]. The orientation of the growth plane dictates in-plane anisotropies which are effectively found leading to a transition from isolated dots to nano chains -oriented along the <1-100> direction- as evidenced from Atomic Force Microscopy features or optical properties: polarization rates and temperature dependent measurements of the radiative recombination process for instance [5]. We here restrict to small size isolated quantum dots and present innovative optical properties among which are micro-photoluminescence data versus pump power, polarization of the emitted photons at different temperatures. We also analyze the photoluminescence decay times and model our finding in the context of the effective mass approximation. The crystal field splitting is measured in Al_{0.5}Ga_{0.5}N polarized microphotoluminescence under high photo- injection conditions.

[1] J. Brault et al. J. Appl. Phys. 105, 033519 (2009).

[2] J. Brault et al. Semicond. Sci. Technol. 29, 084001 (2014).

[3] <http://iopscience.iop.org/0268-1242/labtalk-article/57816>.

[4] A. Kahouli et al. J. Appl. Phys. 110, 084318 (2011).

[5] D. Rosales et al. Phys. Rev. B 88, 125437 (2013).

9363-35, Session 8

Present and future of GaN power devices and their applications (Invited Paper)

Daisuke Ueda, Kyoto Institute of Technology (Japan)

GaN-based power devices maintain GHz operation capability, while required operation frequency is less than MHz in power electronics. Unconnectedly, "Wireless power transfer" technology has been developed, creating an expectation in application fields. Implementing the system with high frequency will make the system compact because it uses a resonance. GaN-based devices will be a key for the system. Focusing the application of DC-isolated gate driver, we developed DbM (Drive-by-Microwave) technology, which is a technological fusion of microwave and power electronics. In this paper, recently developed DbM systems, targeting the applications for inverter and matrix converter, will be introduced.

9363-36, Session 8

Direct comparison of GaN-based e-mode architectures (recessed MISHEMT and p-GaN HEMTs) processed on 200mm GaN- on-Si with Au-free technology (Invited Paper)

Denis Marcond, Marleen E. Van Hove, Dirk Wellekens, Niels Posthuma, Shuzhen You, Xuanwu Kang, Tian-Li Wu, Maarten Willems, Steve Stoffels, Stefaan Decoutere, IMEC (Belgium)

Gallium nitride transistors are going to dominate the power semiconductor market in the coming years. The natural form of GaN-based devices is a so-called normally-on or depletion mode (d-mode) device. Despite these type of devices can be used in power semiconductor systems by means of special drivers or in cascode package solution, yet the market demands for normally-off or enhancement mode (e-mode) devices. This is because e-mode devices are easier to use in circuit solutions and they do not need to be cascoded with a Si transistor to become normally-off. Yet, however, the performance of e-mode devices does not match the one of d-mode devices and, for this reason, d-mode devices in cascoded solution still represent an easy and attractive entry into the power semiconductor market, offering much better performance than the Si counterparts.

In this work, we directly compare and analyze the two most common approaches to obtain GaN-based e-mode devices: recessed gate MISHEMTs and p-GaN HEMTs. The first approach consists in recessing the AlGaN barrier below the gate to interrupt the 2DEG hereby obtaining normally-off operation. This critical step is then followed by two additional critical steps: the gate dielectric and gate metal deposition. The second approach, instead, consists in growing a p-type layer onto the AlGaN barrier to lift up the conduction band under the gate to obtain normally-off operation. In this case, the most critical steps consist in growing the p-GaN layer and controlling the recess of the p-GaN layer over the AlGaN barrier in the access areas. Both approaches have their pro's and con's as well as their critical process steps. In this work both the technological challenges and the device performance of both e-mode types are compared and discussed.

9363-37, Session 8

Enhancement of AlGaN/GaN high- electron mobility transistor off-state drain breakdown voltage via backside proton irradiation (Invited Paper)

Fan Ren, Univ. of Florida (United States)

Proton irradiations from the backside of the AlGaN/GaN high electron mobility transistors (HEMTs) were employed to enhance its off-state drain breakdown voltage. Via holes were fabricated directly under the active area of the HEMTs by etching through the Si substrate for the backside irradiations. The steep drop at the end of proton energy loss profile allows radiation-induced defects to be placed at precise locations within the AlGaN/GaN HEMT structure. Neither degradation of drain current nor enhancement of off-state drain voltage breakdown voltage was observed for the HEMTs irradiated with the proton energy of 225 or 275 keV, for which the defects were put in the GaN buffer. HEMTs with defects placed in the two dimensional electron gas (2DEG) channel region and the AlGaN barrier, using 330 or 340 keV irradiations, not only showed degradations on drain current and extrinsic transconductance but also demonstrated improvements of the off-state drain breakdown voltage. Finite element thermal simulation was also performed to estimate the maximal junction temperature. By filling up the via hole with plated copper, the maximal junction temperature reduced around 24°C as compared to the HEMT without the via hole.

9363-38, Session 8

GaN power switches based on cascode configuration *(Invited Paper)*

Yifeng Wu, Transphorm, Inc. (United States)

The GaN-on-Si platform boasts the advantage of superior performance, low cost and the potential for high volume production therefore is identified as a strong contender as future power semiconductor. For safety reasons power devices are normally off. Numerous reach efforts have been made to realize the enhancement-mode GaN FETs with great difficulty and much sacrifice.

A successful approach is to follow the Mother Nature to develop a depletion-mode high-voltage GaN HEMT and match it with a low-voltage enhancement-mode Si MOSFET to form a cascode structure. This can be simply construed as to use the DRAIN of common-SOURCE Si FET to drive the SOURCE of a common-GATE GaN HEMT. The combined device is normally-off having a gate threshold of the Si MOSFET and a blocking voltage equal to the GaN HEMT gate-drain breakdown voltage. Years of sustained effort has been made to obtain an AlGaIn/GaN epi film with high blocking voltage >1000V, sufficient mobility and charge density, as well as a robust device structure with adequate electric field management for a low dynamic on resistance. This enabled 600-V rated GaN switch products after passing the JEDEC qualification in 2013. Compared to the best Si counterparts, the 1st generation GaN switches show greatly improved figure of merits such as 4x reduction in $R_{on} \cdot Q_g$ and 20x improvement in $R_{on} \cdot Q_{rr}$. Extended high temperature operation life test showed no degradation after 3000hr at 175C. Intrinsic life time based on voltage acceleration tests exceeded 1E7 hours. Additional device and application data will be presented in the conference.

9363-39, Session 8

Trapping processes related to iron and carbon doping in AlGaIn/GaN power HEMTs

Matteo Meneghini, Davide Bisi, Isabella Rossetto, Carlo De Santi, Antonio Stocco, Fabiana Rampazzo, Gaudenzio Meneghesso, Enrico Zanoni, Univ. degli Studi di Padova (Italy)

HEMTs based on GaN offer high breakdown voltages and high operating temperatures; as a consequence, they are expected to find wide application in the power conversion field. Unfortunately, GaN is not a perfectly insulating material, due to its intrinsic n-type conductivity. The resistivity of GaN layers is usually increased through the use of acceptor (compensating) doping; this allows one to reduce the vertical leakage current components, and to improve the confinement of the carriers in the 2DEG. The most commonly adopted compensating species are iron and carbon. Nevertheless, the use of high acceptor concentrations may lead to a significant worsening in the dynamic performance of the devices (stronger dynamic R_{on} increase/current-collapse).

This paper reviews our recent results on the impact of iron and carbon compensation on the dynamic performance of GaN-based HEMTs; based on combined pulsed and transient characterization, we demonstrate that: (i) the use of Fe-doping may lead to a significant increase in current collapse, due to the presence of a trap level with activation energy equal to 0.6 eV. We discuss the properties of this trap, its physical origin and the correlation with device parameters; (ii) high levels of C-doping may favor dynamic R_{on} increase, mostly due to the presence of a trap located at $E_v + 0.8$ eV. We demonstrate that the effect of this trap can be significantly reduced through the use of a double heterostructure. Our results are compared to previous reports to provide a more detailed description of the traps related to iron and carbon.

9363-40, Session 9

Vertical power semiconductor electronic devices based on bulk GaN substrates *(Invited Paper)*

Isik C. Kizilyalli, Avogy, Inc. (United States)

Power electronics serves as the necessary interface between an electrical source and a load that can differ in frequency, amplitude, number of phases, and where voltages and currents can be converted from one form to another [1]. The building blocks comprising a power electronics system include power semiconductor devices, gate drivers, controller circuits and the like. To date, the power semiconductor components of this system have been well served by silicon based diodes and transistors (MOSFETs, IGBTs). While the performance of silicon-based power semiconductor devices have improved over the past several decades resulting in tremendous improvements in efficiency, size, weight, and power density of power electronic systems, these devices are rapidly approaching the fundamental material limits of silicon. This has resulted in a rapid expansion of efforts to develop wide-bandgap power semiconductor alternatives utilizing SiC [2] and GaN [3-8]. Desirable properties associated with GaN and related alloys and heterostructures include large bandgap energy which implies low intrinsic carrier concentrations useful for high temperature operation, favorable transport properties (large electron mobility and saturation velocity), a high breakdown field, and high thermal conductivity. SiC diodes have already been commercialized and they are increasing market share in applications that demand higher efficiency. There is great interest in developing GaN-based vertical power devices because the fundamental material based figure of merit (FOM) of GaN is significantly better than SiC.

In this presentation vertical PN diodes, Schottky diodes, and vertical transistors fabricated on pseudo bulk GaN substrates are discussed. The measured PN devices demonstrate breakdown voltages as high as 3700V with a differential specific on-resistance of $3m\Omega \cdot cm^2$. Furthermore, large area (16mm²) PN diodes with pulsed current of 400A and breakdown voltage exceeding 700V are demonstrated indicating the recent advances in the bulk GaN substrate technology. Contrary to common belief, GaN devices do possess avalanche capability. The temperature coefficient of the breakdown voltage is positive, indicating that the breakdown is indeed due to impact ionization and avalanche. Avalanche energy capability of 1000mJ is demonstrated for the 2600V diodes. This is an important property of the device for operation in inductive switching environments. Critical electric field, mobility, and hole minority carrier lifetime parameters for epitaxial GaN layers grown on bulk GaN are extracted from electrical measurements. The reverse recovery time of the vertical GaN PN diode measured by double pulse testing is not discernible. This is because the switching speed of the GaN diode is limited by capacitance rather than minority carrier storage and hence its switching performance exceeds that of the highest speed Si diode. Finally, fabricated vertical transistors with a breakdown voltage of 1500V and specific-on resistance of $2.2m\Omega \cdot cm^2$ will be discussed.

Acknowledgement: This work was partially supported by ONR N122-135-0058 and ARPA-E SWITCHES Program. Significant contributions of H. Nie, D. Disney, A. Edwards, M. Raj, B. Alvarez, O. Aktas, Q. Diduck, G. Ye, R. Brown, and T. Prunty are gratefully acknowledged.

References:

1. Power Electronic: A first course, N. Mohan, John Wiley & Sons, 2012.
2. J. Palmour, et al, Proc. of IEEE International Conference on Power Electronics, pp. 1006-1013, 2010.
3. J.W. Johnson, et al, IEEE Trans. Electron Devices, vol. 49, pp. 32-36, 2002.
4. Y. Uemoto, et al, IEDM Tech. Dig., pp. 861-864, 2007.
5. Y. Dora, et al, IEEE Electron Device Lett., vol. 27, no. 9, pp. 713-715, 2006.
6. Y. Hatakeyama, et al, IEEE Electron Device Lett., vol. 32, no. 12, pp. 1674-1676, 2011.
7. Y. Saitoh, et al, Applied Physics Express, 081001, pp. 1 - 3, 2010.
8. B. Lu and T. Palacios, IEEE Electron Device Lett., vol. 31, pp. 951-953, 2010.

9363-41, Session 9

High-breakdown-voltage and low-on-resistance GaN p-n junction diodes on free-standing GaN substrates (*Invited Paper*)

Yohei Otoki, Masatomo Shibata, Hitachi Metals (Japan); Kazuki Nomoto, Univ. of Notre Dame (United States); Akihisa Terano, Tomoyoshi Mishima, Hitachi, Ltd. (Japan); Naoki Kaneda, Hitachi Metals (Japan); Tohru Nakamura, Hosei Univ. (Japan)

Gallium Nitride (GaN) has supreme potential for ultra-high performance power switching devices compared with Si, GaAs and even with SiC, because it has excellent material properties such as high breakdown field and high electron saturation velocity. The properties appear at enormous figure of merits on Ron vs breakdown voltage relationship. A key issue to realize such devices is to acquire high quality material with low densities of dislocations, native defects and impurities to provide well controlled doping profiles. The high quality GaN substrates and epitaxial layers have been achieved by our VAS method^{1,2} and well matured MOCVD growth technology, respectively.

Using these materials together with optimized device structure design, we demonstrate the characteristics of GaN p-n junction diodes fabricated on free-standing GaN substrates with low specific on-resistance Ron and high breakdown voltage.

The breakdown voltage of the diodes with the field-plate (FP) structure was over 3 kV, and the leakage current was low, i.e., in the range below 10⁻⁴ A/cm². The specific on-resistance of the diodes of 600 μm diameter with the FP structure was 0.9 mohmcm². Baliga's figure of merit (VB²/Ron) of 10 GW/cm² is obtained³. Although a certain number of dislocations were included in the device, these excellent results indicate a definite availability of this material system for power-device applications.

- 1) Y. Oshima, et.al: Jpn. J. Appl. Phys. 42 (2003) L1.
- 2) T. Yoshida, et al.: J. Cryst. Growth 310 (2008) 5.
- 3) Y.Hatakeyama, at al.,Jpn. J. Appl. Phys. 52 (2013) 028007

9363-42, Session 9

Theoretical modelling of GaN inversion layer transport properties

Sara Shishehchi, Enrico Bellotti, Boston Univ. (United States)

The goal of this work is to investigate the transport properties of the inversion layers in GaN vertical channel MOSFET devices. Nitride material systems, due to their unique properties, are the desired materials in the new generation power electronic devices compared to the current silicon and silicon carbide devices. Among power electronic devices, nitride based MOSFETs are very important in power switching applications, however, majority of the current nitride power devices are planar (lateral), fabricated on sapphire or silicon substrates. These devices are normally-on devices that from the safety and reliability points of view, not desirable. Furthermore, these devices can hardly be designed to operate at high breakdown voltages due to the correspondence of breakdown voltage with the distance between the gate and the drain electrodes.

On the contrary, vertical channel normally-off devices are more reliable and offer a higher breakdown voltage. However, not much research has been performed on the properties of these structures. As an initial step of a more comprehensive research curriculum on power MOSFET devices, in this work we are presenting the transport properties of the inversion layer of a vertical channel normally-off nitride-based MOSFET. The transport model is based on the ensemble Monte Carlo method within a two-dimensional electron gas system. The electron energies and wave functions are calculated

self-consistently based on the Schrödinger and Poisson equations and the scattering rates are calculated by computing the appropriate matrix element using the numerical wave functions.

9363-43, Session 10

InGaN power laser chips in a novel 50W multi-die package (*Invited Paper*)

Andreas Loeffler, Christoph Eichler, Jens Mueller, Sven Gerhard, Bernhard Stojetz, Soenke Tautz, Jelena Ristic, Adrian Avramescu, Markus Horn, Thomas Hager, Christoph Walter, Thomas D. Dobbertin, Harald Koenig, Uwe Strauss, OSRAM Opto Semiconductors GmbH (Germany)

In this paper we report recent developments on high power blue laser chips. Reduction of internal losses as well as optimized thermal management had been essential to increase optical output power. Average performance of 3W optical output at junction temperatures of 130°C is demonstrated. The chips are suitable for use in a novel multi chip housing: For the first time up to 20 blue laser chips have been packaged into one compact housing resulting in the first InGaN laser device with optical output > 50W. The highly integrated package offers a unique small size. The outer dimensions of the package are 25.5mm x 35mm with an emitting surface of 16mm x 16.5mm. Therefore the complexity of optical alignment is dramatically reduced and only a single sheet multi lens array is required for beam collimation. Besides the unique technical performance the multi-die package offers significantly lower assembly costs because of the reduced complexity and assembly time. A further cost advantage is a reduced \$/W price in comparison to single TO solutions due to the special design and a doubled output power of the individual laser chips. This will speed up the integration rate of lasers into projectors. The butterfly package contains 4 copper bars with up to 5 multimode laser chips in series connection on each bar operating at 2.3A. The typical module wavelength is 450nm +/- 10nm. At a case temperature of 50°C a typical efficiency of 29% and an optical output power of 50W are achieved corresponding to an electrical power consumption of 165W. This new technology greatly simplifies the construction of professional laser projectors enabling projectors above 2000 lumens of brightness.

9363-44, Session 10

Internal optical waveguide loss in nitride laser diodes

Agata Bojarska, Szymon Stańczyk, Institute of High Pressure Physics (Poland); Robert Czernecki, Institute of High Pressure Physics (Poland) and TopGaN Ltd. (Poland); Alexandr Khachapuridze, Institute of High Pressure Physics (Poland); Piotr Perlin, Institute of High Pressure Physics (Poland) and TopGaN Ltd. (Poland)

Internal optical loss in semiconductor laser diodes is often associated with free carrier absorption (GaAs) or bound - holes absorption in p-type layers (GaN). As understanding of mechanisms responsible for optical loss is crucial in the structure optimization processes, we decided to verify the role of Mg doping in GaN devices.

We used two experimental methods to evaluate the optical losses in a series of nitride laser structures:

a shifting excitation spot (SES) method, which allows to measure unprocessed, cavity - free devices,

a classical Hakki-Paoli (HaPa) method performed on fully processed and mounted devices.

In case of SES method we investigated a pair of structures: one containing magnesium and second with no Mg doping.

In case of HaPa method we studied the pair of lasers one with high Mg

**Conference 9363:
Gallium Nitride Materials and Devices X**

content in the waveguide and the other with no Mg in the waveguide.

We also measured the losses using both methods in the function of temperature.

Both SES and HaPa method consistently indicate that the influence of Mg doping on optical losses do not exceed 2-3 cm⁻¹. Additionally, all measured losses do not change with temperature. We calculated the absorption due to free-holes plasma and found that it has very low (0.5-1 cm⁻¹) value. As by increasing temperature we convert most of bound holes into free (almost non-absorbing) hole-plasma, we believe that Mg related absorption should be strongly temperature dependent. Our results lead to conclusion that absorption on Mg is not the main cause of optical loss in nitride laser diodes.

9363-45, Session 10

Advances in single-mode and high-power AlGaInN laser diode technology for systems applications

Stephen P. Najda, Piotr Perlin, Tadek Suski, Lujca Marona, Michal Bockowski, Mike Leszczynski, Piotr Wisniewski, Robert Czernecki, TopGaN Ltd. (Poland); Robert Kucharski, Ammono Sp. z o.o. (Poland); Grzegorz Targowski, TopGaN Ltd. (Poland); Scott Watson, Anthony E. Kelly, Univ. of Glasgow (United Kingdom)

The latest advances in AlGaInN laser diode technology are reviewed for various system applications including display, defence, automotive, and communications. The AlGaInN material system allows for laser diodes to be fabricated over a very wide range of wavelengths from u.v., ~380nm, to the visible ~530nm, by tuning the indium content of the laser GaInN quantum well. Ridge waveguide laser diode structures are fabricated to achieve single mode operation with optical powers of >100mW with high reliability. Visible light communications at high frequency (up to 2.5 Gbit/s) using a directly modulated 422nm Gallium-nitride (GaN) blue laser diode with single longitudinal mode operation is reported.

High power operation of AlGaInN laser diodes is also reviewed. We demonstrate the operation of a single chip, high power AlGaInN laser diode 'mini-array' consisting of a 3 stripe common p-contact configuration at powers up to 2.5W cw in the visible wavelength range. Low defectivity and highly uniform GaN substrates allow arrays and bars of nitride lasers to be fabricated. Laser bars with up to 20 emitters have shown optical powers up to 4W cw at ~395nm with a common contact configuration. An alternative package configuration for AlGaInN laser arrays allows for each individual laser to be individually addressable allowing complex free-space and/or fibre optic system integration within a very small form-factor. TopGaN are developing a new range of high power laser array technology over the u.v.- visible spectrum together with new packaging solutions for optical integration.

9363-46, Session 10

Low-threshold deep UV lasers grown on sapphire substrates

Russell D. Dupuis, Xiao-Hang Li, Theeradetch Detchprohm, Yuh-Shiuan Liu, Tsung-Ting Kao, Shyh-Chiang Shen, Mahbub Satter, P. Douglas Yoder, Georgia Institute of Technology (United States); Shuo Wang, Yong Wei, Hongen Xie, Alex M. Fischer, Fernando A. Ponce, Arizona State Univ. (United States); Tim Wernicke, Christoph Reich, Martin Martens, Michael Kneissl, Technische Univ. Berlin (Germany)

The AlGaInN/AIN MQW laser structures were grown on 2-in. dia. c-plane sapphire substrates in a 3?2" AIXTRON low-pressure MOCVD reactor.

The laser structure consisted of an AlN "template" layer deposited on the sapphire substrate with a thickness of 3.5 ?m. Subsequently, an AlxGa1-xN grading waveguide layer, five periods of 2.0-nm-AlxGa1-xN / 4.8-nm-AlyGa1-yN MQWs designed for laser emission at ~250 nm and a thin Al0.83Ga0.17N cap layer for surface passivation and carrier confinement were grown on the AlN template layer sequentially. The Al composition of AlxGa1-xN QW layers in each sample was either 66% or 53%, corresponding to the Al composition of AlyGa1-yN quantum barrier (QB) layers of 83% or 76%, respectively. AlyGa1-yN instead of AlN was used for the QB layers because the larger bandgap of AlN QB layers can impede carrier transport in an electrically-driven device and AlyGa1-yN QB layers can contribute to better optical confinement in the MQW region because of higher refractive index. The 300K PL spectra excited by an ArF excimer laser for the 249 nm laser at various pumping power densities were measured and the threshold pumping power density was determined to be 90 kW/cm². The threshold for a similar AlGaIn MQW/AIn/sapphire laser bar emitting at 255.9nm was ~61 kW/cm². The threshold is comparable with the reported state-of-the-art optically-pumped AlGaIn MQW DUV lasers grown on bulk AlN substrates lasing at 266 nm with a threshold of 41 kW/cm² suggesting the relatively high quality of the active region and good optical confinement. Further results will be described.

9363-47, Session 10

352-nm AlGaIn laser diodes enabled by low-dislocation-density AlGaIn templates

Mary H. Crawford, Andrew A. Allerman, Michael L. Smith, Karen C. Cross, Sandia National Labs. (United States)

While InGaIn-based laser diodes are well developed down to ~370 nm, achieving shorter UV wavelengths requires higher Al-content AlGaIn alloys with increasing challenges in achieving p-type doping and low-defect, lattice-matched substrates. Given these challenges, very few groups have reported AlGaIn-based laser diodes at wavelengths shorter than 355 nm.[1, 2] A critical element in these reports is the epitaxial overgrowth of AlGaIn on patterned templates to reduce threading dislocation densities (TDDs), including AlGaIn overgrown on GaN (11-22) pyramids [2] and on etched trenches in GaN [1] or AlGaIn [3]. Here, we report a distinct approach of AlGaIn overgrowth of Al0.3Ga0.7N templates patterned with submicron-wide-mesas on a 2 micron pitch.[4] Overgrowth of these narrow features yields spatially-uniform TDDs of 2-3e8 cm⁻², eliminating the need to align laser diodes to lower-defect striped regions. The low-TDD AlGaIn templates yielded a 15x increase in electroluminescence from laser diode heterostructures compared to structures with TDDs of 3-4e9 cm⁻². Optical pumping of heterostructures employing GaN/AlGaIn MQWs, Al0.2Ga0.8N waveguides, a Al0.3Ga0.7N bottom cladding and etched facets on low-TDD AlGaIn templates yielded room-temperature lasing at 346 nm with a threshold of 50 kW/cm². We further applied this AlGaIn template approach to achieve room-temperature, pulsed-current operation of UV laser diodes with emission at 352 nm. Ridge-waveguide lasers with etched facets demonstrated threshold current densities of ~22 kA/cm² and were operated to peak output powers of > 5 mW per facet. Comparative performance of heterostructures with doped and undoped waveguides will be presented.

[1.] Iida, et al. Jpn. J. Appl. Phys. 43, L499 (2004).

[2.] Yoshida, et al. Jpn. J. Appl. Phys. 46, 5782 (2007), Yoshida, et al. APL 93, 241106 (2008).

[3.] Tsuzuki, et al. Phys. Stat. Sol. (a) 206, 1199 (2009).

[4.] Allerman, et al. J. Crystal Growth 388, 76 (2014).

9363-48, Session 10

Ultralow threshold electrically-injected AlGaIn nanowire ultraviolet lasers on Si

Kwai Hei Li, Xianhe Liu, Songrui Zhao, Qi Wang, Zetian Mi, McGill Univ. (Canada)

**Conference 9363:
Gallium Nitride Materials and Devices X**

Ultraviolet (UV) lasers are of paramount importance for applications in water purification, diagnosis and bio-agent detection. To date, however, the performance of UV lasers have been restricted by the high dislocation densities and large residual strain introduced during the growth of AlGaIn epitaxial layers. Here we report that, with the use of dislocation-free AlGaIn nanowires formed directly on Si substrate, electrically injected UV emission in the wavelength range of 319 to 335 nm can be readily achieved, which is the shortest wavelength range ever reported for electrically injected semiconductor lasers.

In this work, catalyst-free AlGaIn nanowire arrays are grown directly on Si substrate by radio frequency plasma-assisted molecular beam epitaxy. Our detailed calculation shows that such vertically aligned randomly distributed sub-wavelength scale nanowires array can sustain random lasing action. With optimization of the nanowire size and filling factor, a Q-factor of more than 20,000 can be achieved. Subsequently, electrically injected devices are developed by standard fabrication process, including surface passivation and planarization, contact metallization and rapid annealing process. The lasing characteristics of AlGaIn nanowires are investigated under continuous wave electrical injection. Various lasing peaks from 319 nm to 335 nm can be measured from such AlGaIn nanowire samples. The threshold is measured to be in the range of tens of A/cm² at cryogenic temperature, which is significantly smaller than the commonly reported GaN-based quantum well lasers. The measured linewidth is as narrow as 0.2 nm. Work is currently in progress to demonstrate ultralow threshold AlGaIn nanowire UV lasers at room-temperature.

9363-49, Session 10

Influence of the quantum well thickness on optical properties of blue-violet InGaIn laser diodes

Szymon Stańczyk, Anna Kafar, Lucja Marona, Ewa Grzanka, Szymon Grzanka, Alexandr Khachapuridze, Katarzyna Pieniak, Grzegorz Targowski, Tadek Suski, Piotr Perlin, Institute of High Pressure Physics (Poland)

In laser diode and light emitting diode structures grown on a c-plane GaN substrates the built-in polarization is one of the most important properties which greatly influence the optoelectrical parameters of the mentioned devices. The piezoelectric field, formed due to large lattice mismatch between GaN-based alloys, and spontaneous polarization, present due to electrical field in the intrinsic material, leads to band bending in the quantum wells (Quantum Confined Stark Effect - QCSE). This phenomenon causes the electrons to move to one side of the QW and holes to other side, therefore spatial separating the wave functions of electrons and holes, which results in the decrease of the probability of electron-hole recombination. By controlling the thickness of the QWs, the overlap of the electron and hole wave functions can be modified and therefore, the optoelectronic parameters of the devices can be improved.

Investigated structures were grown by metalorganic vapor phase epitaxy (MOVPE) on GaN substrates obtained by ammonothermal method and on sapphire substrates. The quantum wells thickness in examined structures varies from 3 nm to 1.5 nm. The structures were studied by cathodoluminescence, photoluminescence, electroluminescence and gain measurement using Hakki-Paoli technique. The investigation revealed that for the thinnest quantum well the gain saturates very quickly effectively preventing the device from lasing. For better understanding of influence of the thickness of the quantum wells on optoelectronic parameters we performed theoretical calculation of band diagrams of grown structures.

9363-50, Session 11

buried tunnel junction for micro-LEDs and VCSELs (Invited Paper)

Marco Malinverni, Denis Martin, Lorenzo Lugani, Lise

Lahourcade, Nicolas Grandjean, Ecole Polytechnique Fédérale de Lausanne (Switzerland)

GaN tunnel junction (TJ) is an attractive alternative to replace transparent conductive oxides (TCOs) in LEDs and VCSELs, as both excellent current spreading and current confinement could be achieved. The strongest advantage resides in the epitaxial lattice-match to the underlying material and the high transparency in the visible and near-UV range.

Attempts to achieve efficient TJs have been made either by metalorganic vapour phase epitaxy (MOVPE) or plasma-assisted molecular beam epitaxy (PA-MBE). A common solution is to introduce a thin InGaIn layer within the junction to improve the tunnelling thanks to a reduction of the bandgap combined to piezoelectric polarization field effects.

Here we report on the realization of GaN TJs, without InGaIn layers. The extremely high net acceptor concentration characteristic of NH₃-MBE grown p-type layers, and the lack of hydrogen passivation, allows the demonstration of state of the art current-voltage (I-V) characteristics (2 kA/cm² at 4.8V) in a n-p-n structure contacted with standard n-type Ti/Al/Ti/Au metal contacts only. The structure grown on Ga-polar freestanding (FS) GaN substrate showed remarkable electrical robustness sustaining cw current densities up to 20 kA/cm² at 8.8 V.

The current spreading capability is investigated on blue LEDs. Homogeneous light emission for low forward current densities (0.3 A/cm²) is obtained over a 600 μm wide circular mesa, confirming efficient current spreading and low leakage currents. Finally, we fabricated buried TJs exhibiting excellent current confinement and remarkably low leakage currents.

9363-51, Session 11

Status and future of GaN-based vertical-cavity surface-emitting lasers (Invited Paper)

Daniel F. Feezell, The Univ. of New Mexico (United States)

Vertical-cavity surface-emitting lasers (VCSELs) offer distinct advantages over conventional edge-emitting lasers, including lower power consumption, single-longitudinal-mode operation, circularly symmetric output beams, wafer-level testing, and the ability to form densely packed, two-dimensional arrays. High-performance GaN-based VCSELs are well suited for applications in high-density optical data storage, high-resolution printing, lighting, displays, projectors, miniature atomic clocks, and chemical/biological sensing. Thus far, the performance of these devices has been limited by challenges associated with the formation of high-reflectance distributed Bragg reflectors (DBRs), cavity-length control, lateral current spreading, mode confinement, and polarization-related electric fields. This talk will review approaches to overcome these challenges and discuss the state-of-the-art results in electrically injected GaN-based VCSELs. A particular focus will be on the development of nonpolar GaN-based VCSELs. Nonpolar orientations exhibit anisotropic optical gain within the quantum well plane and uniquely enable VCSELs with a well-defined and stable polarization state. Potential applications for these polarization-pinned VCSELs will be discussed. The talk will also provide a detailed description of a band-gap-selective photoelectrochemical (PEC) etching process for substrate removal and fine cavity length control on free-standing GaN substrates. Finally, the talk will speculate on future directions for GaN-based VCSELs, including approaches for increasing output powers, reducing threshold currents, and extending emission wavelengths.

9363-52, Session 11

GaN-based bipolar-cascade vertical-cavity surface-emitting laser

Joachim Piprek, NUSOD Institute LLC (United States)

In contrast to the success of GaN-based in-plane lasers in recent years, GaN-based vertical-cavity surface-emitting lasers (VCSELs) face significant

**Conference 9363:
Gallium Nitride Materials and Devices X**

challenges and reported output powers are still below 1mW. Using self-consistent electro-thermal-optical simulations based on previously published measurements, we analyze performance limiting mechanisms in GaN-VCSELs. One of the problems revealed is the strong non-uniformity of the carrier density distribution inside the thick multi-quantum well (MQW) active region. Only the p-side QWs deliver optical gain while the n-side QWs cause optical loss. As a solution, we propose the insertion of a tunnel junction into the MQW which enables the repeated use of carriers for light generation (carrier recycling) and leads to a more uniform gain distribution. Such bipolar cascade designs were demonstrated in the past for GaAs- and InP-based VCSELs. However, we keep the number of quantum wells constant and show that tunnel junction insertion doubles the output power despite enhanced absorption. Surprisingly, the simultaneous rise in device bias does not cause a proportional increase in self-heating. The thermal resistance is smaller than before.

9363-53, Session 11

All nitride confinement structures for deep UV microcavity lasers

Alexander Franke, Marc P. Hoffmann, Isaac S. Bryan, Zachary Bryan, Milena Bobea, James Tweedie, Felix Kaess, Ronny Kirste, North Carolina State Univ. (United States); Michael Gerhold, U.S. Army Research Office (United States); Ramon Collazo, Zlatko Sitar, North Carolina State Univ. (United States)

AlN and their ternary alloy AlGaIn provide the basis for the fabrication of ultra-low threshold UV vertical emitting lasers and novel inversion-less polariton lasers. These structures consist of two high reflecting distributed Bragg reflectors (DBRs) separated by a cavity structure that includes the gain medium. However, to fabricate highly reflecting AlN/AlGaIn-based DBRs, a trade-off between achieving a high refractive index contrast at low Al fractions and a low lattice mismatch at high Al concentration is mandatory. Our crack-free DBR structures provide a high refractive index contrast of 5% at the resonance wavelength as achieved by an Al content of 65% in AlGaIn. We report on MOCVD-grown highly reflecting Al_{0.65}Ga_{0.45}N/AlN DBRs and on a semi-microcavity structure. This structure consists of a bottom DBR and an active medium within a lambda-cavity operating in the UV at 270 nm. All structures were grown on strain optimized AlGaIn templates grown on c-sapphire substrates. Using 10.5 mirror pairs, a maximum reflectivity of 76% with a stop bandwidth of 7 nm was achieved. By increasing the number of layer pairs, the reflectivity increases further to 93% for 20.5 pairs and up to 97% for 25.5 pairs. The suitability of our structures for vertical laser applications was demonstrated by growing of a lambda-cavity including a 5 fold AlN/Al_{0.55}Ga_{0.45}N multiple quantum well on top of our DBRs. Spatially resolved PL investigations across the wafer reveal spectral resonance between the MQW emission peak and the reflectivity maximum across the complete two inch wafer.

9363-54, Session 11

Nitride superluminescent diodes with broadened emission spectra

Anna Kafar, Institute of High Pressure Physics (Poland); Marcin Sarzynski, Institute of High Pressure Physics (Poland) and TopGaN Ltd. (Poland); Szymon Stańczyk, Institute of High Pressure Physics (Poland); Lucja Marona, Institute of High Pressure Physics (Poland) and TopGaN Ltd. (Poland); Grzegorz Targowski, Irina Makarowa, TopGaN Ltd. (Poland); Przemek Wiśniewski, Institute of High Pressure Physics (Poland) and TopGaN Ltd. (Poland); Tadek Suski, Institute of High Pressure Physics (Poland);

Piotr Perlin, Institute of High Pressure Physics (Poland) and TopGaN Ltd. (Poland)

Superluminescent diodes meet the requirements of applications, which need light sources with low time coherence (wide emission spectra) and high spatial coherence (high beam quality). Still, nitride superluminescent diodes being based on wide-band gap material with the large electron density of states, suffer inherently from narrow optical gain spectra. This creates an unbreakable limit for the width of emission spectra and subsequently increases time coherence of this light source. In the present work we show an approach to increase the spectral width of the emission beyond the standard material limits. We use a special technique of substrate patterning, which enables us to spatially control the value of the active layer bandgap.

It is known that different indium incorporation occurs in substrates with different vicinal angles. Our method uses dry etching in order to produce a pattern on the substrate, with locally changing vicinal angle. The pattern is designed in a way, which provides a decrease of indium concentration along the waveguide, towards the front facet. The light generated in different regions of the chip has a different gain spectrum and, as a result, the final emission spectrum is broadened.

We prepared a substrate with flat and patterned regions on which we performed the epitaxial growth. The fabricated epitaxial structure was characterized by cathodoluminescence mapping in order to show the changes in local indium content. Based on this epiwafer, we fabricated superluminescent diodes having constant or variable indium concentration within their waveguides. Optical spectra of this devices will be demonstrated.

9363-76, Session PWed

Impact of the stripe geometry on the relaxation behavior of InGaIn/GaN MQW nanostripe arrays

Cory C. Lund, Stacia Keller, Tyler Wyland, Feng Wu, Silvia Chan, Carl Neufeld, Shuji Nakamura, Steven P. DenBaars, James S. Speck, Umesh K. Mishra, Univ. of California, Santa Barbara (United States)

Planar 7 and 23 period InGaIn/GaN MQWs were grown on GaN-on-sapphire then patterned into nanostripe arrays with height/width or aspect ratios of 0.5 and 1, respectively, using holographic lithography and dry etching. After processing, the samples were reloaded into the MOCVD chamber and a -100 nm thick GaN coalescence layer was deposited on top of the stripe arrays. The strain state in the stripe arrays with embedded MQWs was monitored at each process step by recording XRD (114) reciprocal space maps.

All as-grown MQWs were coherently strained, and relaxed perpendicular to the stripe direction after stripe processing. After re-growth of the GaN layer at 1080 °C, however, the 2 sample sets behaved differently. The 7 period MQW stripes with an aspect ratio of 0.5 maintained their relaxation perpendicular to the stripes, however their luminescence significantly declined. In contrast, the lattice constant of the 23 period MQW stripes with an aspect ratio of 1 assumed a somewhat smaller value, though the samples remained partially relaxed. In addition, the stripes maintained their strong luminescence. Transmission electron microscopy revealed dislocation formation for samples with an aspect ratio of 0.5 after GaN re-growth. The results illustrate the need for aspect ratios of 1 or larger to prevent defect formation in the nanostripes. The XRD, AFM, SEM, TEM, PL and CL results will be discussed in detail at the conference.

9363-77, Session PWed

Deep level transient spectroscopy on light-emitting diodes based on (In,Ga)N/GaN nanowire ensembles

Mattia Musolino, Paul-Drude-Institut für Festkörperelektronik (Germany); Matteo Meneghini, Laerte Scarpato, Carlo De Santi, Univ. degli Studi di Padova (Italy); Abbes Tahraoui, Lutz Geelhaar, Paul-Drude-Institut für Festkörperelektronik (Germany); Enrico Zanoni, Univ. degli Studi di Padova (Italy); Henning Riechert, Paul-Drude-Institut für Festkörperelektronik (Germany)

III-N nanowires (NWs) are an attractive alternative to conventional planar layers as the basis for light-emitting diodes (LEDs). In fact, the NW geometry enables the growth of (In,Ga)N/GaN heterostructures with high In content and without extended defects regardless of the substrate. Despite these conceptual advantages, the NW-LEDs so far reported exhibit often higher leakage currents and higher turn-on voltages than the planar LEDs. We found that these issues are mainly related to the p-type contact, and that they may be improved by optimizing the processing technology. We achieved significant improvements employing a thick indium tin oxide (ITO) contact instead of the commonly used Ni-based one. Nevertheless, also the NW-LEDs contacted with ITO exhibit abnormal leakage currents.

In this work, we investigate the mechanisms responsible for the anomalous leakage currents in the NW-LEDs by analyzing the current-voltage (I-V) characteristics in a temperature range between 83 and 403 K. The studied devices are (In,Ga)N/GaN LEDs based on self-induced NW ensembles grown by molecular beam epitaxy on Si substrates. The temperature-dependent I-V characterization reveals that temperatures higher than 240 K may activate a further conduction process, which is not present in the low temperature range. Deep level transient spectroscopy measurements show the presence of electron traps, which are activated in the same temperature interval. These results suggest that the leakage process might be related to trap-assisted tunneling, possibly produced by point defects at the interface between the p-type top contact and the tips of the NWs and/or on the sidewalls of the NWs.

9363-78, Session PWed

Band gaps and internal electric fields in short period nitride superlattices

Izabela Gorczyca, Kamila Skrobias, Tadek Suski, Institute of High Pressure Physics (Poland); Niels E. Christensen, Axel Svane, Aarhus Univ. (Denmark)

Nitride based quantum structures are building blocks for light emitting diodes and laser diodes. The electronic structures of short-period mIn(Ga)N/nGaN and mGaN/n(Ga)AlN polar, nonpolar and semipolar superlattices (SLs) are calculated for various, small numbers m of well- and n of barrier-monolayers.

The general trends in band gap behavior can be to a large extent explained by the composition (m,n), SL geometry and strength of the internal electric field present in polar and semipolar wurtzite structures. The above relations are discussed taking into account existing experimental results. The most interesting results are:

1. Exceptionally strong built-in electric fields present in polar mInN/nGaN SLs (from 1 to 11 MV/cm depending on n and m values) strongly influence valence- and conduction-band profiles; the band gaps are indirect in real space and small, vanishing for $n=m \geq 4$. Much larger band gaps are obtained in the absence of electric field, for nonpolar mInN/nGaN SLs. Semipolar SLs exhibit intermediate behavior.
2. Experimental photoluminescence data obtained for polar mInN/nGaN SLs are in a very good agreement with the band gaps obtained for polar mInGaN/nGaN SLs, suggesting that in real samples the well layer is not pure

InN, but consists of a ternary alloy (InGaN), the hypothesis recently confirmed experimentally.

3. Band gaps in mGaN/n(Ga)AlN SLs are much larger than in mIn(Ga)N/nGaN structures. The results for mGaN/nAlN agree well with experimental data. The internal electric field being much smaller in mGaN/n(Ga)AlN (from 1 to 7 MV/cm) has smaller influence on the band gap values than in mIn(Ga)N/nGaN SLs.

9363-79, Session PWed

Degradation of InGaN laser diode with negative characteristic temperature T₀

Agata Bojarska, Institute of High Pressure Physics (Poland); Irina Makarowa, TopGaN Ltd. (Poland); Przemek Wiśniewski, Robert Czernecki, Institute of High Pressure Physics (Poland) and TopGaN Ltd. (Poland); Tadek Suski, Institute of High Pressure Physics (Poland); Piotr Perlin, Institute of High Pressure Physics (Poland) and TopGaN Ltd. (Poland)

InGaN laser diodes degradation processes differ substantially from that characteristic for phosphide and arsenide lasers. Since the dislocation movements and multiplication processes are quite ineffective, the degradation seems to be related with point defects via nonradiative recombination processes. However, it is not clear which region of the laser diode is in fact responsible for degradation: quantum wells or maybe other layers.

In the present work we studied the degradation InGaN laser diode, emitting in the blue region of the spectrum, characterized by a large negative characteristic temperature T₀. Negative value of T₀ parameters means that for these devices the threshold current decreases with the increasing temperature. As the free holes concentration is strongly dependent on the temperature, we can quite easily tune the injection efficiency by varying the device temperature. Our study shows that the internal efficiency is governed by two processes: injection efficiency and thermal escape of carriers from the quantum wells. The degradation rate of the laser diode measured for various temperatures shows quite complex character, which can be fully accounted for when we assume the proportionality of this process to the carrier escape from quantum well and to standard thermal activation factor. We interpret the result as strong suggestions that the InGaN laser diode degradation process requires non-radiative recombination of carriers escaping from the quantum wells (recombination-assisted degradation). Additionally this results suggest that the nonradiative recombination occurs most likely outside of quantum well system.

9363-80, Session PWed

X-ray diffraction study of A- plane nonpolar InN epilayer grown by MOCVD

Matthieu Moret, Olivier Briot, Bernard Gil, Univ. Montpellier 2 (France)

Strong polarisation-induced electric fields in C-plane oriented nitrides reduce the performance of devices. Eliminating the polarization fields can be achieved by growing nitrides along non polar direction.

We have grown non polar A-plane oriented InN on R-plane (1102) nitridated sapphire substrate by MOCVD.

We have studied the structural anisotropy observed in these layers by analyzing High Resolution X-Ray Diffraction rocking curve (RC) experiments as a function of the in-plane beam orientation.

A-plane InN epilayer have a unique epitaxial relationship on R-Plane sapphire and show a strong structural anisotropy.

Full width at half maximum (FWHM) of the InN(1120) XRD RC values are contained between 44 and 81 Arcmin. FWHM is smaller when the diffraction

**Conference 9363:
 Gallium Nitride Materials and Devices X**

occurs along the [0001], and the largest FWHM values, of the (1120) RC, are obtained when the diffraction occurs along the [1100] in-plane direction.

Atomic Force Microscopy imaging revealed morphologies with well organized crystallites. The grains are structured along a unique crystallographic orientation of InN, leading to larger domains in this direction.

XRD reciprocal space mappings (RSM) were performed in assymetrical configuration on (1340) and (2202) diffraction plane. RSM are measured with a beam orientation corresponding to a maximal and a minimal width of the (1120) Rocking curves, respectively. A simple theoretical model is exposed to interpret the RSM.

We concluded that the dominant contribution to the anisotropy is due to the scattering coherence length anisotropy present in our samples.

9363-81, Session PWed

Metal organic vapour phase epitaxial growth of indium-rich InGaN alloys: continuous and time resolved photoluminescence properties

Olivier Briot, Matthieu Moret, Bernard Gil, Univ. Montpellier 2 (France)

We report the growth of indium-rich InGaN alloys by Metal-Organic Vapour Phase Epitaxy, using ammonia,

trimethylgallium and trimethylindium as precursors. The photoluminescence properties, both continuous and time resolved were studied versus sample temperature. The sample compositions were determined by x-ray diffraction experiments to be in the range 0 to 28 % Ga. The sample quality was assessed by rocking curve experiments, where full width at half maximum were found to be in the range of 3 to 30 arcmin, depending upon composition.

Compared to indium nitride, our alloy samples photoluminescence persists with temperature. The analysis of the photoluminescence data of these samples indicates the existence of two non radiative recombination channels : one with a thermal activation temperature of 77 K and another one with an activation temperature ranging from 300K for InN up to 640 K for In_{0.72}Ga_{0.28}N. The latter competes with the former at low temperatures whilst the former rules the optical properties at ambient conditions.

9363-82, Session PWed

Vertical excitation profile in diffusion injected multi-quantum well light emitting diode structure

Lauri J. Riuttanen, Pyyri Kivisaari, Olli Svensk, Aalto Univ. School of Science and Technology (Finland); Teemu Vasara, Pertti Mylly, Aalto University (Finland); Jani Oksanen, Sami Suihkonen, Aalto Univ. School of Science and Technology (Finland)

The conventional approach to inject charge carriers into the active region of a light-emitting diode (LED) is to sandwich the active region between p- and n-doped regions. This approach is used whether the active region is based on quantum wells (QWs) or nanowires. The conventional approach works well on QW structures, but the charge carrier injection into the nanowire array can be considered tedious due to the challenges in depositing the electrical contacts.

We have fabricated and characterized a III-nitride diffusion injected light-emitting diode (DILED) structure in which the active region is located outside the pn-junction. In the fabricated DILED both p- and n-type GaN layers, thus also the pn-junction, are located above the indium gallium nitride (InGaN) MQW stack, which need not to be etched for electrical

contact. When the pn-junction is biased, the charge carriers are injected into the MQW stack by bipolar diffusion of minority charge carriers.

This work provides the experimental demonstration that bipolar diffusion can transport electrons and holes into the active region located outside the pn-junction proving that it can be utilized for electrical excitation. In order to understand better the charge carrier spreading in the fabricated DILED structures, we study the light emission profile using spectral and subwavelength imaging.

The demonstrated structure is expected to help overcome some of the challenges related to current injection into conventional structures and with further optimization possibly challenging the conventional device structures in selected applications. In particular, it would enable a new way to inject current into nanowires and near surface structures as well as provide a new way to fabricate large-area devices with improved current spreading.

9363-83, Session PWed

Numerical analysis on the effect of electron blocking layer in 365-nm ultraviolet light-emitting diodes

Fang-Ming Chen, National Changhua Univ. of Education (Taiwan); Jih-Yuan Chang, Kuang-Ming Junior High School (Taiwan); Yen-Kuang Kuo, National Changhua Univ. of Education (Taiwan); Bing-Cheng Lin, Hao-Chung Kuo, National Chiao Tung Univ. (Taiwan)

The 365-nm ultraviolet light-emitting diodes (UV LEDs) are of special interest for medicine, biochemistry, sensing, and data storage applications. To enhance the device performance, various approaches including crystal quality enhancement, increasing p-doping efficiency, carrier confinement improvement, usage of non-polar or semi-polar substrate, improving light extraction efficiency, and decreasing self-heating have been reported. In order to resolve the issue of weak carrier confinement, the employment of an electron blocking layer (EBL) is usually believed to be necessary for blocking the electrons from overflowing to the p-side region. However, the large polarization field in conventional EBL might pull down the effective barrier height for electrons, which in turn largely reduces the capability of EBL in blocking electrons. Moreover, the low hole mobility, low p-type doping efficiency, and serious polarization effect in hetero-interfaces might further limit the hole injection efficiency. In this study, with the purpose of effectively reducing the electron leakage and enhancing the hole injection efficiency, the Al content, thickness, and p-doping concentrations of the EBL in 365-nm UV LED are investigated systematically. The UV LED structure used as a reference was grown on c-plane sapphire substrate by MOCVD, which had an emission peak wavelength of 365 nm at 100 A/cm². The energy band diagrams, distribution of electrons and holes in the active region, recombination rate in quantum wells, electron overflow, and electrostatic field are studied systematically by using the APSYS simulation program. Specifically, designs of AlGaIn/GaN superlattice EBL and Al-content-graded EBL are explored in detail.

9363-84, Session PWed

Carrier transport in the nonpolar and c-plane InGaIn quantum well by considering the indium fluctuation effects

Chen-Kuo Wu, Tsung-Jui Yang, National Taiwan Univ. (Taiwan); Claude Weisbuch, Univ. of California, Santa Barbara (United States) and Ecole Polytechnique (France); James S. Speck, Univ. of California, Santa Barbara (United States); Yuh-Renn Wu, National Taiwan Univ. (Taiwan)

The influence of indium fluctuation to the carrier transport and efficiency droop in the c-plane quantum well (QW) has been studied by our past work.

**Conference 9363:
Gallium Nitride Materials and Devices X**

In this paper, we further analyzed the influence of the indium fluctuation to the nonpolar InGaN QW LED. We simulate the structure with a fully three-dimensional Poisson and drift-diffusion solver and indium fluctuation generator developed by our lab and compared with the uniform QW LED, c-plane QW LED with indium fluctuation. The recent work from the Atom Probe Tomography (APT) has shown the random indium alloy fluctuation in the QW no matter it is c-plane QW or nonpolar plane QW. In our past research, we found that the indium fluctuation will strongly benefit the commercial c-plane LED. Because of the carrier localization, the strong band bending caused by the strain-induced polarization field will be screened. Therefore, the electron-hole overlap will be improved. Besides, the carrier will find a percolation way in the QW and lead to a relative good I-V curve when comparing to the uniform QW LED.

For a typical nonpolar LED, the polarization field will be minimized so there is no QCSE-induced triangular potential between the InGaN/GaN heterosurface. Without the strong band bending in the QW, the electron-hole overlap will be improved compared to the c-plane case. Therefore, if the crystal quality is good without too much defects, the radiative recombination is expected to be very good without considering indium fluctuation. Even with the published Auger coefficient C , the droop should be very weak. Our studies by including the indium fluctuation shows different trend. If we include the indium fluctuation model, we found the internal resistance in QW is smaller than the uniform case. The forward voltage is slightly smaller than uniform nonpolar plane case. The fluctuation of indium makes electron or hole crossing the barrier easier. When the indium fluctuation is included in studying the IQE, the IQE reach to the peak value earlier due to the carrier localization at the low current density to avoid the defect related nonradiative recombination. However, when the carrier density gets larger, the Auger recombination starts to affect nonradiative recombination and the droop effects start to happen. On the other hand, when considering the ideal QW nonpolar LEDs, there is almost no IQE droop when the current density is close to 200A/cm². Unlike the indium fluctuation case, the carrier is uniformly distributed in the QW with a much higher recombination rate and lower carrier density at the same current density. Therefore, the droop effect is improved. Unlike the c-plane QW LED that the indium fluctuation will improve the IQE performance of the device, the result shows that if the QCSE is not presented, the uniform QW is a more desirable structure for improving the device performance.

9363-85, Session PWed

Strain relaxation and In incorporation kinetics in high In-content InGaN layers synthesized by plasma-assisted molecular-beam epitaxy

Sirona Valdueza-Felip, Edith Bellet-Amalric, CEA Grenoble (France); Arantzazu Nuñez Cascajero, Univ. de Alcalá (Spain) and CEA-Grenoble (France); Yi Wang, Marie-Pierre Chauvat, Pierre Ruterana, Ecole Nationale Supérieure d'Ingenieurs de Caen et Ctr. de Recherche (France); Stephanie Pouget, CEA Grenoble (France); Katharina Lorenz, Eduardo Alves, Univ. Técnica de Lisboa (Portugal); Eva Monroy, CEA Grenoble (France)

In incorporation and strain relaxation kinetics in high-In-content In_{0.3}Ga_{0.7}N layers grown by plasma-assisted molecular-beam epitaxy on GaN-on-sapphire are reported. Best structural and morphological quality is obtained under In excess conditions, and at a growth temperature where InGaN decomposition is active. Under these growth conditions, both in-situ (RHEED) and the ex-situ (XRD) experiments point to an onset of strain relaxation at 40 nm, which stabilizes at an almost relaxed value after 350 nm. This relaxation is associated to the appearance of misfit dislocations, stacking faults, a tilt of the lattice towards [1-100] and surface roughening (rms=0.5-3 nm for 7-500 nm thick layers). Moreover, the inhomogeneous strain state along the growth axis perturbs the alloy composition. In atoms are excluded from the InGaN film under compressive stress (only 20% of In incorporates) in order to minimize the lattice mismatch between

the epitaxial layer and the substrate. The layer only reaches its nominal composition for thicknesses >350 nm. Optically, the composition gradient translates into a red shift of the emission/absorption, and an increase of the Stokes shift as a function of the layer thickness, confirmed by RBS, transmission and photoluminescence measurements.

InGaN junctions were fabricated using different p-layers: p-GaN, p-InGaN and a graded p-In_xGa_{1-x}N layer (x=0.35-0), and processed into devices showing rectifying current-voltage behaviour. The deficient hole collection efficiency present in p-GaN terminated structures kills the photocurrent coming from the InGaN layer. However, p-InGaN capped junctions present a flat photocurrent with a spectral cut-off red-shifted to 620 nm.

9363-86, Session PWed

Improved light extraction efficiency of GaN-based light-emitting diode by depositing novel optical layer with reflect index linear variation

Sheng-Wen Wang, Yu-Lin Tsai, Hao-Chung Kuo, Po-Tsung Lee, National Chiao Tung Univ. (Taiwan)

We demonstrate the GaN-base light emitting diode (LED) grown by metalorganic chemical vapor deposition (MOCVD) on c-plane sapphire substrate with novel anti-reflectance (AR) layer to improve light output power.

The novel AR-coating layer mix with SiO₂ and TiO₂, and each reflect index is 1.5 and 2.5, respectively. In this study, we compare with common AR-coating layer and novel AR-coating layer. For the former, we just mix with two kind of materials and fix the reflect index on 1.71 which between Indium Tin Oxide (ITO) layer and air. Besides, we simulate the light extraction efficiency by using Finite-difference time-domain (FDTD) software with the different thickness of AR-coating layer and try to find the optimum result. For the later, we change the ratio of SiO₂ and TiO₂ materials on different location and the reflect index will be changed with SiO₂ and TiO₂ different component concentration. We design the AR-coating layer form ITO layer to air with linear variation and find the suitable thickness for the LED device. Finally, the experiment result shows the output power behavior of LED device with AR-coating layer is improved above 10%.

9363-87, Session PWed

Extracting carrier Injection Efficiency of InGaN Light Emitting Diode depending on current injection level

Kyu-Sang Kim, Sangji Univ. (Korea, Republic of); Dong-Pyo Han, Hyun-Sung Kim, Jong-In Shim, Hanyang Univ. (Korea, Republic of)

To extract the carrier injection efficiency depending on the current injection level, we investigated the L-I characteristics plotted in log scales (denoted as log(L)-log(I)) of InGaN green LEDs.

The S values are obtained from the differential slope of log(L) versus log(I), i.e., $S = \frac{d \log(L)}{d \log(I)}$.

It is believed that the S value at the bias varies with the dominant carrier recombination process.

We can extract the normalized injection efficiency (NIE) from the S-I curves with considering the rate equation.

NIE curve of InGaN green LED in which the peak value of the external quantum efficiency (EQE) and the Auger coefficient of $10^{(-34)} \text{ cm}^6/\text{s}$ are adopted to the normalization process.

Interestingly, the NIE curves of LED continues to decrease with increasing current. This result suggests that some part of the carriers injected into QWs overflow without recombining there and their overflowing rate

**Conference 9363:
Gallium Nitride Materials and Devices X**

gradually becomes large with increasing current level. Although the Auger coefficient C is assumed as high as 10^{16} cm⁶/s, the reduction rate of NIE is not so much different from the previous value within less than 10% error. As a result, we thought that the EQE droops in InGaN LEDs are mainly determined by carrier overflow from QWs and their recombination outside QWs.

9363-88, Session PWed

Hybrid MOCVD-MBE growth of high In-content laser structures on semipolar (20-21) GaN plane

Lucja Marona, Marcin Sarzynski, Institute of High Pressure Physics (Poland); Robert Czernecki, TopGaN Ltd. (Poland); Grzegorz Muziol, Czeslaw Skierbiszewski, Piotr Perlin, Institute of High Pressure Physics (Poland)

High indium content InGaN optoelectronic structures are challenging because of much more pronounced influence of the internal electric field on the light emission properties. Strong quantum confined Stark effect causes difficulty in obtaining long-wavelength emission devices (blue-green) by substantially reducing the gain and optical transitions probability. To minimize the influence of the internal electric field we grew the laser structure on semipolar plane of GaN. However growth on semipolar plane entails numerous problems: more difficult In incorporation, faster relaxation of InGaN and AlGaIn layers, decomposition of quantum wells after the growth of p-type layers, and problems with growth of high quality p-type. While the strain relaxation can be controlled by using a specially patterned substrate, the problem of InGaN thermal decomposition and p-type layers quality can be addressed by combining two different epitaxial growth methods – MOCVD and MBE. The n-type layers and active region are grown in MOCVD reactor. After that the sample is placed in MBE reactor to grow the p-type layers. The main advantages of such a solution are: avoiding quantum wells decomposition due to low temperature growth and possibility to obtain good quality p-type due to the lack of hydrogen.

9363-89, Session PWed

Nonradiative recombination mechanisms in InGaN/GaN light-emitting diodes analyzed by various device characterization techniques

Dong-Soo Shin, Dong-Guang Zheng, Chan-Hyoung Oh, Hyun-Sung Kim, Hanyang Univ. (Korea, Republic of); Kyu-Sang Kim, Sangji Univ. (Korea, Republic of); Jong-In Shim, Hanyang Univ. (Korea, Republic of)

The nonradiative recombination affects light-emitting diodes (LEDs) in a detrimental way as it reduces the quantum efficiency. In InGaN/GaN blue LEDs widely used for general lighting currently, there exist various material issues that lead to the unwanted nonradiative recombination. Since different devices have different material issues related closely with the growth conditions, one needs to analyze the inherent nonradiative recombination mechanism in each device as a first step for further improving its quantum efficiency. In this work, we utilize various characterization techniques to investigate the nonradiative recombination mechanisms in LED devices. With the characterization techniques such as temperature-dependent external quantum efficiency, current-voltage, and electroluminescence spectra, we show that different nonradiative recombination processes such as the Shockley-Read-Hall (SRH) recombination and the defect-assisted tunneling play roles in LED devices. Useful information can be gathered on the carrier loss mechanisms especially from the temperature and electric-field dependences. For an LED device identified as having the SRH process as the dominant nonradiative recombination mechanism, it is shown that

the carrier overflow from the multiple-quantum-well active region to the p-GaN layer is the main carrier loss mechanism. On the other hand, it is demonstrated for another device that the defect-assisted tunneling from the active layer to the p-GaN constitute the dominant carrier loss mechanism. The type of defects that are considered to play roles in different loss mechanisms are to be discussed.

9363-91, Session PWed

Optical and structural properties of semipolar (11-22) GaN grown on m-plane sapphire using nanoporous SiNx interlayers

Morteza Monavarian, Virginia Commonwealth Univ. (United States); Sebastian Metzner, Otto-von-Guericke-Univ. Magdeburg (Germany); Natalia Izyumskaya, Serdal Okur, Fan Zhang, Saikat Das, Vitaliy Avrutin, Ümit Özgür, Virginia Commonwealth Univ. (United States); Frank Bertram, Jürgen Christen, Otto-von-Guericke-Univ. Magdeburg (Germany); Hadis Morkoç, Virginia Commonwealth Univ. (United States)

Enhancement of optical and structural quality for semipolar (11-22) GaN grown by metal-organic chemical vapor deposition on planar m-sapphire substrates was achieved by using an in-situ epitaxial lateral overgrowth (ELO) technique with nanoporous SiNx layers employed as masks. In order to optimize the procedure, the effects of SiNx deposition time and temperature were studied by steady-state and time-resolved photoluminescence (PL), and spatially resolved cathodoluminescence (CL), and X-ray diffraction. The intensity of room temperature PL for the (11-22) GaN layers grown under optimized conditions was about two orders of magnitude higher and the PL decay times were approximately one order of magnitude longer compared to those for the reference samples having the same thickness but no SiNx interlayers. These findings are attributed to the blockage of extended defect propagation toward the surface by the SiNx interlayers as evidenced from the suppression of emissions associated with basal plane stacking faults and prismatic stacking faults with regard to the intensity of donor bound excitons (D0X) in low-temperature CL and PL spectra. In agreement with the optical data, full width at half maximum values of (11-22) X-ray rocking curves measured for two different in-plane rotational orientations of [1-100] and [11-23] reduced from 0.33° and 0.26° for the reference samples to 0.2° and 0.16° for the nano-ELO structures grown under optimized conditions, respectively.

9363-92, Session PWed

Enhancement of coherent acoustic phonons in InGaN nanocavities

Shopan D. Hafiz, Fan Zhang, Morteza Monavarian, Vitaliy Avrutin, Hadis Morkoç, Ümit Özgür, Virginia Commonwealth Univ. (United States)

Enhancement of coherent zone folded longitudinal acoustic phonon (ZFLAP) oscillations at terahertz frequencies was demonstrated in nanocavities incorporating InGaN multiple quantum wells (MQWs) by using wavelength degenerate time resolved differential transmission spectroscopy. Screening of the piezoelectric field in InGaN MQWs by photo-generated carriers upon femtosecond pulse excitation gave rise to terahertz ZFLAPs, which were monitored at the Brillouin zone center in the transmission geometry. MQWs composed of 10 pairs of 2 nm In_{0.14}Ga_{0.86}N wells and 11.5 nm In_{0.01}Ga_{0.99}N barriers provided coherent phonon frequencies of 0.73 THz. Enhanced phonon oscillations were achieved by placing the InGaN MQW in a phonon cavity formed between two AlN/GaN phonon mirrors designed to exhibit large acoustic gaps at the zone center: 0.70 THz to 0.78

**Conference 9363:
Gallium Nitride Materials and Devices X**

THz at the zone center for phonon mirrors having 10 pairs of 10.5 nm/3 nm AlN/GaN layers. When the folded acoustic phonon mode frequency was adjusted, by changing the MQW composition and period, to fall into the phonon mirror acoustic gap, resulting full reflection of ZFLAPs at the zone center frequency led to subsequent enhancement of phonon oscillation amplitudes and increase of decay times. Dependences of nanocavity ZPLAP frequency and amplitude on excitation density and wavelength were also investigated.

9363-93, Session PWed

Fabrication and characterization of GaN-based p-i-n photodetectors on cone-shaped patterned sapphire substrates

Hsu-Hung Hsueh, Sin-Liang Ou, Chiun-Hao Lin, Dong-Sing Wuu, Ray-Hua Horng, National Chung Hsing Univ. (Taiwan)

The GaN p-i-n epitaxial structures were prepared on the cone-shaped patterned sapphire substrates (PSSs) by metalorganic chemical vapor deposition. The epitaxial structure includes a 3- μ m-thick undoped GaN nucleation layer, a 1.5- μ m-thick n-type GaN:Si layer, a 500-nm-thick undoped GaN layer, and a 50-nm-thick GaN:Mg p-contact layer. To reduce the dry-etched induced damage in the cone-shaped PSSs, these PSSs were further treated with wet etching process, and it resulted in a higher crystal quality of the subsequent GaN epilayer. Therefore, after the dry etching process, the fabricated cone-shaped PSSs were soaked in a H₂SO₄:H₃PO₄ (3:1) solution for 1, 3, 5, 7 and 10 min. Moreover, the epitaxial structure was grown on the conventional sapphire substrate (CSS) as a contrasted sample. For the photodetector device process, the thermal evaporation, standard photolithography, and wet etching processes were all employed. In comparison to the GaN growth on the CSS, the defect density was reduced when the GaN epilayer was grown on the cone-shaped PSS. The device performance was also enhanced by using the PSS, especially for the PSS with further wet etching for 3 min. Under a -5V applied bias, the reverse leakage currents for the photodetectors fabricated on the CSS and cone-shaped PSS with wet etching for 3 min were 1.2 \times 10⁻⁴ and 5.3 \times 10⁻⁸ A, respectively. The significant decrease in the magnitude of reverse leakage current for the photodetector on this cone-shaped PSS was owing to the improvement of epilayer quality.

9363-94, Session PWed

Time-resolved photoluminescence studies of GaN-nanowire based AlN/GaN heterostructures doped with Germanium

Nils Rosemann, Philipps-Univ. Marburg (Germany); Pascal Hille, Jan Müßener, Pascal Becker, Justus-Liebig-Univ. Giessen (Germany); Maria de la Mata, Institut de Ciència de Materials de Barcelona (Spain); César Magén Domínguez, Instituto de Nanociencia de Aragon (Spain); Jordi Arbiol, Institut de Ciència de Materials de Barcelona (Spain) and Institució Catalana de Recerca i Estudis Avançats (Spain); Jörg Teubert, Jörg Schörmann, Martin H. Eickhoff, Justus-Liebig-Univ. Giessen (Germany); Sangam Chatterjee, Philipps-Univ. Marburg (Germany)

GaN nanowires (NWs) exhibit a large surface-to -volume ratio that makes them an ideal systems to investigate surface-related effects such as the influence of, e.g., band bending. Due to band bending these structures show a quenching of the luminescence which opens the possibility to use such a structure for gas sensing. Additionally, these NWs exhibit a low defect density due to the self-assembly during growth which provides an ideal base for the growth of AlN/GaN hetero-structures. The low defect concentration also makes them an ideal system to investigate the influence

of doping on the crystal structure and the related optical properties. Previous studies investigated the influence of Si- and Mg-doping on such NWs[1]. As a next step the doping was changed to germanium, which has a much larger covalent radius than Si or Mg. We studied several ensembles of AlN/GaN structures based on GaN, with different barrier thicknesses and Ge-doping using a standard streak-camera setup. By this the spectral shift and changes in the dynamics of carriers, due to the doping are obtained. For comparably high Ge-concentrations, the photoluminescence emission energy of the hetero-structures is shifted to higher energies accompanied by a decrease of the photoluminescence decay time. Additionally, the thickness-dependent shift in emission energy is significantly reduced.

In spite of the high donor concentration a quench of the photoluminescence is not observed.

[1] F. Furtmayr et al., J. Appl. Phys. 104(7), 074309, (2008)

9363-95, Session PWed

Widely-spectral tuning from GaN nanowire lasers using hydrostatic pressure

Sheng Liu, Sandia National Labs. (United States); Changyi Li, The Univ. of New Mexico (United States); Igal Brener, George Wang, Sandia National Labs. (United States)

We report widely tunable lasing from 367 to 337 nm (-30 nm tuning) with sub-nanometer resolution from single GaN nanowire by applying hydrostatic pressure up to -7 GPa. The GaN nanowire lasers, with heights of 4-5 μ m and diameters -130 nm, are fabricated using a lithographically defined two-step top-down technique. At lower optical pump powers below the lasing threshold, we observe that the single nanowire photoluminescence spectrally shifts -35 nm to shorter wavelengths as pressure increases up to -9 GPa. This is caused by an increasing γ direct bandgap at higher pressure.

9363-96, Session PWed

Strong carrier localization in basal plane and prismatic stacking faults in semipolar (11-22)GaN

Serdal Okur, Morteza Monavarian, Natalia Izyumskaya, Fan Zhang, Vitaliy Avrutin, Hadis Morkoç, Umit Özgür, Saikat Das, Virginia Commonwealth Univ. (United States)

The effects of basal plane and prismatic stacking faults (BSF and PSF) on optical processes in epitaxially grown semipolar (11-22)GaN on m-sapphire have been investigated in detail using steady-state photoluminescence (PL) and time- and polarization-resolved PL. We demonstrate that the carrier recombination dynamics are substantially influenced by strong carrier localization in the stacking faults. In addition to nonradiative recombination, carrier trapping/detrapping and carrier transfer between the stacking faults and donors are found to be among the mechanisms affecting the recombination dynamics at different temperatures. PL decay times of both BSFs and PSFs do not show any temperature dependence up to 80 K while PSFs exhibit significantly longer PL decay times (-3 ns) as compared to BSFs (-1 ns). Above 80 K, PL decay times decrease with temperature (T) following -T⁻¹ and -T⁻² dependence for PSFs and BSFs, respectively, which suggests that the carrier localization is stronger in PSFs. However, intensity of PL from BSFs is higher, which may be attributed to larger BSF density, and therefore, larger contribution to recombination dynamics as compared to PSFs. In addition, polarization-resolved PL measurements reveal that the degree of polarization for the BSFs (0.30) is twice that for the PSFs due to different orientations of the stacking faults, which makes it easier to distinguish the contributions from the two.

9363-97, Session PWed

Strong exciton-photon coupling in hybrid InGaN-based microcavities on GaN substrates

Serdal Okur, Virginia Commonwealth Univ. (United States); Alexander Franke, Otto-von-Guericke-Univ. Magdeburg (Germany); Fan Zhang, Vitaliy Avrutin, Hadis Morkoç, Virginia Commonwealth Univ. (United States); Frank Bertram, Jürgen Christen, Otto-von-Guericke-Univ. Magdeburg (Germany); Umit Özgür, Virginia Commonwealth Univ. (United States)

A 5?-thick hybrid semiconductor/dielectric GaN-based microcavity grown by metal-organic chemical vapor deposition on a c-plane bulk GaN substrate was investigated using angle-resolved photoluminescence and angle-resolved cathodoluminescence techniques at room and low temperature (5.8 K), respectively. The cavity structure consisted of an InGaN multiple quantum well (MQW) active region emitting at 400 nm and sandwiched between 29.5 pair bottom semiconductor AlN/GaN and 13.5 pair top dielectric SiO₂/SiN_x distributed Bragg reflectors. The cavity supported strong exciton-photon coupling with a record 75 meV vacuum Rabi splitting energy at 5.8 K. The measured room temperature Rabi splitting energy of 45 meV is still close to the highest Rabi splitting energies reported in literature confirming that the strong coupling regime still persists at room temperature.

9363-98, Session PWed

Indium-incorporation efficiency for semipolar (11-22) GaN as compared to polar c-plane in GaN-based light-emitting diodes

Morteza Monavarian, Virginia Commonwealth Univ. (United States); Sebastian Metzner, Otto-von-Guericke-Univ. Magdeburg (Germany); Natalia Izyumskaya, Serdal Okur, Fan Zhang, Saikat Das, Vitaliy Avrutin, Umit Özgür, Virginia Commonwealth Univ. (United States); Frank Bertram, Jürgen Christen, Otto-von-Guericke-Univ. Magdeburg (Germany); Hadis Morkoç, Virginia Commonwealth Univ. (United States)

Reduced electric field in semipolar (11-22) GaN/InGaN structures makes this orientation a promising candidate for high efficiency light emitting diodes. We investigated indium incorporation in semipolar (11-22) GaN grown by metal-organic chemical vapor deposition on planar m-plane sapphire substrates. Indium content in the semipolar material was compared with that in polar c-plane samples grown under the same conditions simultaneously side by side on the same holder. The studied structures contained single and multiple GaN/InGaN/GaN double heterostructures of different widths. In order to improve optical quality, both polar and semipolar templates were grown using an in-situ epitaxial lateral overgrowth (ELO) technique in order to achieve the highest optical quality. By comparing samples with and without nano-ELO for the semipolar orientation, we investigated the effects of extended defects, such as grain boundaries, stacking faults, and threading dislocations, on indium incorporation using spatially resolved cathodoluminescence and time-resolved photoluminescence (PL). Indium incorporation efficiency was derived from the comparison of PL spectra measured at the highest excitation density on the semipolar and polar structures to minimize the effect of quantum confined Stark effect on the emission wavelength. Preliminary data suggests increased indium content in the semipolar variety by up to 4% in the layers containing 23.5% In.

9363-99, Session PWed

Formation of reflective Ag ohmic contacts to semipolar GaN for high-power GaN-based light-emitting diodes

Jae-Seong Park, Sung-Ki Kim, Hwa-Seub Lee, Tae-Yeon Seong, Korea Univ. (Korea, Republic of)

Group III-nitride-based LEDs are of significant importance because of the ability to replace general illuminations. LEDs grown on the polar (0001) sapphire substrates experience the spontaneous and piezoelectric polarization fields, spatially separating electron and hole wave functions within quantum wells and inducing the quantum-confined Stark effect. Thus, semipolar growth has been performed to alleviate the Stark effect. To increase the light extraction, highly reflective and low resistance p-type ohmic contacts should be formed. However, the electrical characterization of Ag-based contacts to semipolar GaN has not been extensively carried out so far. In this study, we investigated the electrical characteristics of Ag contacts to (0001) c-plane and (11-22) semi-polar plane GaN. The effect of polarity on the electrical properties of Ag contacts was characterized by X-ray photoemission spectroscopy (XPS). The (0001) c-plane samples become ohmic after annealing in air, whereas the (11-22) semi-polar samples are non-ohmic after annealing. The XPS results show that unlike the c-plane samples, the semipolar samples contain some amounts of oxygen at the Ag/GaN interface regions. On the basis of the electrical and XPS results, the polarity dependence of the electrical properties is described. In addition, we also investigated the effect of an interfacial Zn layer on the electrical characteristics of Ag contacts to the (11-22) semi-polar p-type GaN. Based on the XPS and electrical results, the possible mechanisms underlying the improved electrical properties of the Zn/Ag samples are discussed.

9363-100, Session PWed

Monolithically-integrated RGB photonic crystal surface-emitting lasers

Chu-Hsiang Teng, Univ. of Michigan (United States); Kuo-Bin Hong, Yu-Hsun Chou, Chun-Chieh Yang, Tien-Chang Lu, National Chiao Tung Univ. (Taiwan); Pei-Cheng Ku, Univ. of Michigan (United States)

The photonic crystal surface-emitting laser (PCSEL) has attracted a lot of attention recently because it possesses the advantages of vertical-cavity surface-emitting lasers (VCSELs) and yet can produce high output power and exhibits a very small beam divergence angle. The latter can enable a lens-free configuration. Visible-wavelength PCSEL is particularly attractive for display, biological fluorescence assay, and solid-state lighting applications. The capability of integrating multi-color PCSELs in one single chip can significantly reduce the system size and complexity. In this work, we utilize the InGaN/GaN nanopillar structures and the diameter-dependent emission wavelength to achieve wavelength tunability. Photonic crystal designs were investigated to confirm the feasibility and potential of monolithically integrated multi-color InGaN/GaN PCSELs. Here we report a scheme to monolithically integrate multi-color (e.g. red, green, and blue) photonic crystal surface emitting lasers in one single chip. Potential applications include display, sensing, and lighting. Via the control of strain in InGaN nanopillar structures, we realized active regions of different colors on the same epitaxial wafer. Due to a large lattice mismatch, InGaN quantum wells pseudomorphically grown on GaN suffer from a large piezoelectric field and quantum-confined Stark effect (QCSE). Nanostructures are known to be able to relax the strain via free surfaces. Previously, we have demonstrated effective strain relaxation of nanopillar structures and significant wavelength modulation as a result of reduced strain and piezoelectric field. It enables the possibility of having both green and blue emission monolithically integrated in one single chip simply by designing proper nanopillar diameters. We have investigated potential designs of photonic crystal structures that will incorporate these nanopillars with various dimensions and can be fabricated in one lithographic step to form

multi-color PCSEL pixels. Periodic and closely packed nanopillars lead to diffraction in normal direction and sufficient gain media for lasing behavior. The design rule of nanopillar PCSELS is studied by FDTD and finite element simulation, and the lasing characteristics are verified by photoluminescence measurements.

9363-101, Session PWed

Optimization of mode pattern and transmission analysis of GaN LED with ITO grating

Juliet Chico, Gabriela Aleman, Xiaomin Jin, California Polytechnic State Univ., San Luis Obispo (United States)

Optimization of mode pattern and transmission analysis of an LED is a recent topic gaining significant interest. Modal and transmission analyses are performed on a gallium nitride (GaN) based light emitting diode to achieve maximum light extraction. Optimization is achieved when the cavity and waveguide modes are in their best condition, emitting waves that interfere constructively with the nano-grated LED, produced by the best grating case. The various structural effects of the nano-gratings on light transmission are investigated, thus concluding that the transmission efficiency has a strong dependence upon these structural effects brought forth by the parameters of the nano-grated structure. By varying the period, height, and width of the ITO grating, we generated a 69.42% efficiency increase in the light extracted compared to a non-grated LED with 54.74%, producing a 27% difference. The grating location is investigated through modal analysis, which shows that the optical confinement factor (OFC) is greatly dependent on this parameter, reaching a maximum of 13.21%. With the improved grating location, a transmission analysis is performed, producing the light transmission of 81.88%, compared to a non-grated LED with 55.89%, achieving 47% improvement.

9363-102, Session PWed

Breakdown voltage improvement of AlGaIn/GaN HEMTs grown on silicon substrate with an LT-AlN interlayer

Geng-Yen Lee, Chien-Yu Pao, Nien-Tze Yeh, National Central Univ. (Taiwan); Jen-Inn Chyi, National Central Univ. (Taiwan) and Research Ctr. for Applied Sciences (Taiwan)

AlGaIn/GaN high-electron mobility transistors (HEMTs) grown on Si (111) substrate is emerging due to its low cost and large substrate size availability compared to SiC and sapphire. However, GaN grown on Si encounters high dislocation density and surface cracking, which adversely affect the breakdown property of GaN HEMTs. In this work, a low-temperature grown AlN ((LT-AlN) interlayer is implemented in the GaN buffer layer of AlGaIn/GaN HEMTs to block leakage current and improve breakdown voltage.

This study is performed on three samples with different buffer layers designated as A, B and C. Sample A is a reference structure, which consists of an AlGaIn graded buffer layer, followed by a 2.5 μm GaN buffer, a 1 nm AlN, and a 30 nm AlGaIn barrier layer. Sample B has the same heterostructure as sample A except an additional LT-AlN layer being inserted in the middle of the 2.5 μm -thick GaN buffer layer. Sample C then has the LT-AlN layer inserted between the AlGaIn graded layer and the GaN buffer layer. The 3-terminal breakdown voltage of sample A, B and C is 790 V, 926 V, and 750 V, respectively. Having an LT-AlN layer inserted in the middle of the GaN buffer layer increases the breakdown voltage significantly, while putting the LT-AlN below the GaN buffer layer does not. This is correlated well with the resistivity of their buffer layers.

9363-103, Session PWed

Active region dimensionality and quantum efficiencies of InGaIn LEDs from temperature-dependent photoluminescence transients

Nuri Can, Virginia Commonwealth Univ. (United States) and Balikesir Univ. (Turkey); Serdal Okur, Morteza Monavarian, Fan Zhang, Vitaliy Avrutin, Hadis Morkoç, Virginia Commonwealth Univ. (United States); Ali Teke, Balikesir Univ. (Turkey); Umit Özgür, Virginia Commonwealth Univ. (United States)

Temperature dependent carrier dynamics in c-plane InGaIn light emitting diodes (LEDs) with different well thicknesses, 1.5, 2, and 3 nm, were investigated to reveal the radiative and nonradiative recombination rates and determine the internal quantum efficiency at different temperatures. It was confirmed that the photoluminescence (PL) transients are governed by radiative recombination at low temperatures while nonradiative recombination dominates at room temperature for the samples investigated. At photoexcited carrier densities of $3 - 4.5 \times 10^{16} \text{ cm}^{-3}$ at room temperature, the Shockley-Read-Hall (A) and the bimolecular (B) recombination coefficients (A, B) were estimated as ($9.2 \times 10^7 \text{ s}^{-1}$, $8.8 \times 10^{-10} \text{ cm}^3 \text{ s}^{-1}$), ($8.5 \times 10^7 \text{ s}^{-1}$, $6.6 \times 10^{-10} \text{ cm}^3 \text{ s}^{-1}$), and ($6.5 \times 10^7 \text{ s}^{-1}$, $1.4 \times 10^{-10} \text{ cm}^3 \text{ s}^{-1}$) for the six period 1.5, 2, and 3 nm well-width LEDs, respectively. From the temperature dependence of the radiative lifetimes, $[\tau]_{\text{rad}} [\alpha] T^n$, the dimensionality n of the active region wells was observed to decrease consistently with decreasing well width. 3 nm wells exhibited ~ 1.5 dependence, suggesting a three-dimensional nature, whereas the 1.5 nm wells were confirmed to be two-dimensional (~ 1) and the 2 nm wells close to being two-dimensional. It is shown that a combination of temperature dependent PL and time-resolved PL techniques can be used to evaluate the dimensionality as well as the quantum efficiencies of the LED active regions for a better understanding of the active region design on the efficiency limiting processes in InGaIn LEDs. The relative external quantum efficiencies obtained from electrical measurements on fabricated LEDs were also correlated with the results from optical measurements.

9363-55, Session 12

High-power UV-B LEDs with long lifetime (Invited Paper)

Jens Rass, Tim Kolbe, Neysha Lobo-Ploch, Ferdinand-Braun-Institut (Germany) and Leibniz-Institut für Höchstfrequenztechnik (Germany); Tim Wernicke, Frank Mehnke, Christian Kuhn, Johannes Enslin, Martin Guttman, Christoph Reich, Technische Univ. Berlin (Germany); Johannes Glaab, Christoph Stölmacker, Mickael Lapeyrade, Sven Einfeldt, Markus Weyers, Ferdinand-Braun-Institut (Germany) and Leibniz-Institut für Höchstfrequenztechnik (Germany); Michael Kneissl, Ferdinand-Braun-Institut (Germany) and Technische Univ. Berlin (Germany)

UV light emitters in the spectral range between 280nm and 320nm, commonly described as UV-B range, are of great interest for applications such as phototherapy, gas sensing, plant growth lighting, and UV curing. In contrast to the conventional mercury discharge lamps, UV LEDs offer significant advantages such as low operation voltages, efficient heat dissipation, long lifetimes and small footprint. These features allow not only the one-to-one replacement of conventional UV lamps, but also enable completely new applications. In order to make UV-B-LEDs efficient with regard to power conversion and competitive with regard to the costs per power, key parameters such as the external quantum efficiency, light extraction efficiency, and device lifetimes need to be improved.

**Conference 9363:
Gallium Nitride Materials and Devices X**

In this paper we present high power UV-B LEDs grown by metal-organic vapor phase epitaxy on sapphire substrates. By optimizing the LED heterostructure design, growth parameters and the processing technologies, significant progress was achieved with respect to the internal efficiency, injection efficiency and light extraction. Highly conductive UV-transparent n-AlGaIn layers were grown and low resistance vanadium-based ohmic contacts have been developed. An electron blocking heterostructure guarantees efficient current injection for single peak UV-B emission. By using reflective metal layers and improved chip designs, the light extraction was enhanced. The LEDs were flip-chip mounted on AlN submounts. Using this approach, UV-B LEDs with output powers of up to 18 mW per chip at 310nm with approximately 20% decrease in emission power after 1000 operational hours at 100 mA / 5mW output power have been realized.

9363-56, Session 12

Progress of high-power deep-ultraviolet LEDs (Invited Paper)

Akira Fujioka, Kohji Asada, Hiromi Yamada, Takumi Ohtsuka, Toshiaki Ogawa, Takao Kosugi, Daisuke Kishikawa, Takashi Mukai, Nichia Corp. (Japan)

High output power 255/280/310-nm deep ultraviolet light-emitting diodes (DUV LEDs) suitable for high-current operation are reported. Two types of 1-mm-sized chips are installed in a commercial package either in a two series configuration or a single mounting. Initial and lifetime characteristics were measured at different temperatures and driving currents. First, the two series devices with a footprint of 6.8 x 6.8 mm² were operated at a forward current of 350 mA. We measured powers of 45.2, 93.3, and 65.8 mW for the 255, 280, and 310-nm LEDs, respectively. The corresponding external quantum efficiencies per serial circuit were 1.3, 3.0, and 2.4%, respectively. Next, single-chip device with a smaller footprint of 3.5 x 3.5 mm² was developed. We succeeded in lowering the forward voltage considerably by optimization of the epitaxial structure and device processing. Peak wavelengths, output powers, forward voltages, and external quantum efficiencies at a forward current of 350 mA were 258.0 nm, 34.8 mW, 8.25 V, 2.07% for the 255-nm LED, 282.8 nm, 40.5 mW, 5.69 V, 2.64% for the 280-nm LED, and 312.3 nm, 40.1 mW, 6.36 V, 2.89% for the 310-nm LED, respectively. Lifetime tests were performed by varying the junction temperatures. The 70% lifetime of the 280/310-nm LED die was estimated to be over 3000 h at a junction temperature of 45degC and a driving current of 350 mA. 255-nm LED die, however, showed much shorter lifetime below 1000 h. The output power decay was found to depend on the driving conditions.

9363-57, Session 12

High-efficiency UV LEDs on sapphire (Invited Paper)

Max Shatalov, Sensor Electronic Technology, Inc. (United States)

A detailed analysis of the quantum efficiency of deep ultraviolet LEDs confirms that the dislocation density of 10^8 cm^{-2} in AlGaIn MQW layers grown on sapphire substrates is sufficiently low to achieve the EQE above 10 % for LEDs emitting at 278 nm. Further IQE improvements could be achieved by optimization of growth parameters that affect concentration of point defects, sharpness of QW interfaces, and uniformity of the alloy composition. A layer structure transparent in DUV region is critical for obtaining high light extraction of LED chip. Residual absorption in the MQW and p-side of the structure, as well as optical losses due to the ohmic contacts, play a significant role in limiting the LEE to below 50 % in the deep UV range. The high efficiency LEDs with the output power of 100 mW CW at 300 mA provide a clear demonstration of DUV LED technology capabilities for disinfection, decontamination, curing and medical applications.

9363-58, Session 12

UVC LEDs on bulk aluminum nitride (Invited Paper)

Leo J. Schowalter, Crystal IS, Inc. (United States)

Ultraviolet light-emitting diodes, designed to emit at wavelengths shorter than 280nm, are attractive light sources for chemical analysis and disinfection applications. Their small size, robustness, ability to turn on and off instantly, stability, and ability to fabricate tuned to a specific wavelength are inherent advantages over alternate sources such as mercury, deuterium and xenon lamps. Recent improvements in efficiencies and lifetimes from the light-emitting diodes opened up new applications. Much of the improvement has been driven by improved quality of the epitaxial nitride semiconductor layers that are used to fabricate the LEDs.

Crystal IS has pursued an approach where the device structure is formed by using OMVPE to grow pseudomorphic (fully strained to the substrate) epitaxial layers on a suitably prepared, bulk AlN single crystal wafer. This approach achieves dislocation densities lower than $1E5$ per sq. cm in the active device region. This results in a significant improved internal efficiency over devices with higher dislocation densities. The low dislocation density also leads to long operating lifetimes for the devices even at high current operation. This approach has been used in the recently released Optan LED product which represents the first commercial product based on AlN substrates. Additional products can be anticipated based on the superior performance of high quality epitaxial nitride layers grown on single-crystal AlN substrates.

9363-59, Session 12

Strong TE polarized emission from deep UV AlGaIn quantum well LEDs

Christoph Reich, Martin Guttman, Tim Wernicke, Frank Mehnke, Technische Univ. Berlin (Germany); Jens Rass, Technische Univ. Berlin (Germany) and Ferdinand-Braun-Institut (Germany); Christian Kuhn, Technische Univ. Berlin (Germany); Mickael Lapeyrade, Sven Einfeldt, Arne Knauer, Viola Kueller, Markus Weyers, Ferdinand-Braun-Institut (Germany); Michael Kneissl, Technische Univ. Berlin (Germany) and Ferdinand-Braun-Institut (Germany)

Ultraviolet (UV) light emitters in the UV-C spectral region are of great interest for many applications, e.g., water purification, disinfection of medical systems, gas sensing, biomolecule detection, and non-line-of-sight communication. However, the external quantum efficiencies of AlGaIn-based light emitting diodes (LEDs) drops rapidly for emission wavelength below 265 nm. Besides the drop in the current-injection efficiency and the internal quantum efficiency, the decrease in the extraction efficiency is just as important. This effect is due to a change in the order of the valence bands with decreasing wavelength resulting in a change in the polarization of light emission from TE to TM. In this paper we present a detailed study of polarization and temperature dependent electroluminescence and photoluminescence measurements on AlGaIn multiple quantum well (MQW) LEDs emitting between 239 nm and 265 nm. All samples were grown by metal organic vapor phase epitaxy on low dislocation density (0001) AlN/sapphire templates fabricated by epitaxial lateral overgrowth. Dominant TE emission was observed for compressively strained AlGaIn MQW LEDs with an emission wavelength as short as 239 nm. The degree of polarization, i.e. $(I[TE]-I[TM])/(I[TE]+I[TM])$, decreases from 0.85 at 265 nm to 0.5 at 239 nm. This effect can be explained by a strain induced shift of the AlGaIn QW valence band. From temperature dependent measurements the energy difference between the two topmost valence bands was determined, i.e. 30 meV for 243 nm emission, which is significantly smaller than the expected negative splitting energy of -150 meV for unstrained Al_{0.7}Ga_{0.3}N QWs.

**Conference 9363:
 Gallium Nitride Materials and Devices X**

9363-60, Session 12

Current spreading optimized UV-C LEDs emitting at 235 nm

Mickael Lapeyrade, Florian Eberspach, Neysha Lobo-Ploch, Ferdinand-Braun-Institut (Germany); Christoph Reich, Martin Guttmann, Tim Wernicke, Frank Mehnke, Technische Univ. Berlin (Germany); Sven Einfeldt, Arne Knauer, Markus Weyers, Ferdinand-Braun-Institut (Germany); Michael Kneissl, Technische Univ. Berlin (Germany)

Deep UV emitters in the wavelength range between 220 nm and 280 nm are of great interest for many applications like water purification, disinfection of medical systems, and gas sensing. In order to reach these wavelengths, low resistance AlGaIn layers with high Al mole fraction exceeding 80% have to be realized posing serious challenges for materials growth and device fabrication technologies. Due to the high Al content, obtaining highly conductive p-doped and the n-doped AlGaIn layers is very difficult as well realizing low resistance and ohmic p- and n-metal contacts. Due to the limited conductivity of the n-doped AlGaIn layers and restrictions on the layer thickness, current crowding poses a serious problem for UV-C LEDs. Hence the chip design of the LEDs as well as the layout of the metal contacts is important to obtain a uniform current-injection into the active region.

In this paper we will present simulation and experimental data on UV-C LED emitting around 235 nm, grown by metal organic vapor phase epitaxy on ELO AlN/sapphire substrates. After a first stage of development in which heterostructures design and growth parameters were optimized, test structures were processed and the emission wavelength and power were measured. Using this data as input parameters for 3-D current spreading simulations, the influence of the segmentation of the emitting area and of the contact resistance on the homogeneity of the current injection was investigated. We show that the p-contact resistance and the number of segments are the two most critical parameters influencing the homogeneity of the emission. Furthermore the emission distribution of 235nm LEDs with the simulated chip geometries will be experimentally determined and compared to the simulation results.

9363-61, Session 13

study of efficiency droop in InGaIn/GaN light emitting diodes with V-shape pits
(Invited Paper)

Heng Li, Chiao-Yun Chang, Tien-Chang Lu, National Chiao Tung Univ. (Taiwan)

InGaIn/GaN light emitting diodes (LEDs) are now widespread used in solid-state lighting, because of their high luminescence efficiency and potential to replace traditional lighting sources. However, there are plenty threading dislocations occurred during the epitaxial process due to lattice mismatch between the GaN and sapphire substrate. The high threading dislocations density will lead to the enhancement of non-radiative recombination centers and current leakage. In this study, the relationship between the light emission efficiency of InGaIn/GaN MQWs and the formation of V-shaped pits were characterized by using scanning electron microscopy, photoluminescence, and cathodoluminescence. In order to clarify the effects of V-shaped pits, we insert different periods of InGaIn/GaN superlattice (SL) layers ranging from 0, 10, 15, 30 and 60 to control the properties of V-shaped pits. It could be observed that the V-pit size on InGaIn MQWs increases with increasing pairs of SLs layers, which would result in the formation of thinner sidewall quantum wells and create higher local energy barriers around V-shaped pits. The emission of 430 nm from the V-shaped pit sidewall was observed by the plane-view monochromatic CL measurement. It could be confirmed local energy barriers will go along with the formation of V-shaped pits and can assist the InGaIn MQWs to resist the carriers into the nonradiative recombination centers. By properly controlling

the V-shape defect formation, the excellent IQE of the InGaIn MQWs was found in 15 periods SLs layers about 70%.

9363-62, Session 13

Efficiency droop in nitride LEDs revisited: Impact of excitonic recombination processes

Andreas Hangleiter, Torsten Langer, Technische Univ. Braunschweig (Germany); Marina Gerhard, Dimitry Kalincev, Philipps-Univ. Marburg (Germany); Heiko Bremers, Uwe Rossow, Technische Univ. Braunschweig (Germany); Martin Koch, Philipps-Univ. Marburg (Germany)

One of the key limitations of visible light emitters based on III-nitrides is the so-called efficiency droop. Among the physical mechanisms being discussed are Auger recombination, density-activated defect recombination, and carrier leakage. The analysis is often based on the dependence of the internal efficiency on current density, using the so-called ABC model.

However, this is based on a single-particle picture, neglecting many-particle effects. With III-nitrides being wide-gap semiconductors with large effective masses and large exciton binding energies, excitonic effects can not be neglected even at room temperature.

Our time-resolved photoluminescence studies show that the radiative lifetime in thin GaInN/GaN quantum wells is independent of carrier density up to about 10^{13}cm^{-2} , which can only be explained by free excitons being the dominant species. On the other hand, the nonradiative lifetime is reduced towards high densities approximately proportional to the inverse of the carrier density. Converting these data to an efficiency vs. current density representation, a strong efficiency droop is revealed, resembling the typical LED behavior.

In a more general view, both radiative and Auger recombination are subject to an excitonic enhancement of the recombination probability. The enhancement, depending on carrier density, is calculated using a simplified many-body theory approach, in good agreement with our experimental findings. At the highest densities, a transition to single-particle radiative and Auger recombination is found, consistent with earlier results on Auger recombination.

Our results clearly show that a consistent explanation of the efficiency droop can be obtained taking into account the excitonic enhancement of recombination processes.

9363-63, Session 13

Hot carrier transport and efficiency droop in III-N LEDs

Pyry Kivisaari, Toufik Sadi, Jani Oksanen, Jukka J. Tulkki, Aalto Univ. School of Science and Technology (Finland)

Recent measurements have revealed significant hot carrier populations in III-N LEDs in the high injection regime roughly at the onset of the efficiency droop. These hot carriers have been suggested to result from Auger recombinations in the quantum wells (QWs), thereby backing up Auger recombination as the main cause of the droop. However, detailed information about the generation, relaxation, and transport of hot carriers in multi-quantum well (MQW) LED structures is still missing. This has resulted in a dynamic debate about the origin and contribution of hot carriers as well as renewed interest in theoretical studies of the topic. Theoretical studies from hot carrier currents caused by Auger recombination have also been somewhat controversial, and more detailed device-level simulations of Auger-excited hot carriers are needed.

We recently introduced the Monte Carlo--drift-diffusion (MCDD) method to study the physics of hot electrons in MQW LEDs. In the current work we introduce and discuss full bipolar Monte Carlo simulations to also account

**Conference 9363:
 Gallium Nitride Materials and Devices X**

for generation and relaxation of hot holes in III-N LED structures. Our simulations account for the self-consistent electrostatic potential profiles of the structures and all important scattering and recombination mechanisms. The results provide detailed information about the magnitude and relaxation of hot carrier currents and contributions of Auger recombination, Auger-generated leakage current and other hot carrier mechanisms on the efficiency droop of III-N LEDs.

9363-64, Session 14

Semi/non-polar nitride quantum wells for high-efficient light emitters (*Invited Paper*)

Mitsuru Funato, Yoichi Kawakami, Kyoto Univ. (Japan)

InGaN and AlGaIn quantum wells (QWs) on semi/nonpolar planes offer alluring features for light emitting devices. For example, compared with (0001) QWs, high optical transition probability is expected from lower internal electric fields, and threshold carrier density for lasing operation may be lower due to the optical anisotropy. One promising way to realize high quality semi/nonpolar QWs is homoepitaxial growth. Recent remarkable progress of bulk crystal growth has enabled us to demonstrate high-quality InGaIn and AlGaIn semipolar QWs using homoepitaxy technique. In this presentation, we mainly discuss deep ultraviolet (DUV) light emitting properties of AlGaIn QWs. Semipolar AlGaIn QWs on AlN (10-12) r-plane substrates were fabricated by metalorganic vapor phase epitaxy. Increasing growth pressure from 76 Torr, which is a good condition for the c-plane growth, to 500 Torr realized atomically flat AlN homoepitaxial layers. On top of AlN, AlGaIn QWs were fabricated. The surface remained flat in the atomic level, and abrupt QW interfaces were suggested from x-ray diffraction and transmission electron microscopy. Their photoluminescence was assessed under the selective excitation of AlGaIn QWs, using the 4th harmonic of a Ti:Sapphire laser. Their radiative lifetime was shortened by about two orders of magnitude, compared with similar QWs on the (0001) plane. This is due to suppressed internal electric fields. As a consequence, the emission intensity at room temperature is much stronger for semipolar (1-102) AlGaIn QWs, indicating that the semipolar AlGaIn QWs are promising for optical devices such as light emitting diodes and laser diodes in the DUV spectral range.

9363-65, Session 14

Spatial variations of optical properties of semipolar InGaIn quantum wells

Saulius Marcinkevicius, Kristina Gelzinyte, Ruslan Ivanov, KTH Royal Institute of Technology (Sweden); Yuji Zhao, Shuji Nakamura, Steven P. DenBaars, James S. Speck, Univ. of California, Santa Barbara (United States)

Semipolar InGaIn/GaN quantum wells (QWs) have a great potential for light emission applications, especially in the green spectral region, because, compared to polar structures, they have smaller intrinsic electric fields and a good In uptake. In spite of a recent progress in semipolar device fabrication, their efficiency is can still be improved. To assess the intrinsic limitations semipolar QWs, a number of issues, such the role of localized states, features of carrier recombination, and relation between them remain to be understood.

In this work, scanning near-field optical microscopy (SNOM) and time-resolved photoluminescence (TRPL) techniques were applied to examine recombination and spatial band gap variations in single (20-21) and (20-2-1) plane QWs. The studied samples contained single 3 nm QWs with In percentage between 11% and 36% grown by MOCVD on low defect density GaN substrates.

SNOM scans showed that spatial variations of band potentials are small (tens of meV), and islands of uniform potentials are large (a few μm). Recombination properties were found to be spatially uniform, and carrier redistribution between different potential sites weak, which suggests that

semipolar InGaIn QWs are prone to hot spot formation.

TRPL was used to estimate radiative and nonradiative recombination. With increased In content, the low temperature radiative lifetimes increase from a few to tens of ns, which is attributed to increased intrinsic electric field. At temperatures over ~ 200 K, nonradiative recombination, probably via N vacancy and C acceptor related traps, prevails. Still, room temperature carrier lifetimes are in the ns range, which is important for light emitting applications.

9363-66, Session 14

Investigation of facet-dependent InGaIn growth for core-shell LEDs

Ionut Girgel, Univ. of Bath (United Kingdom); Paul R. Edwards, Univ. of Strathclyde (United Kingdom); Emmanuel Le Boulbar, Duncan W. E. Allsopp, Univ. of Bath (United Kingdom); Robert W. Martin, Univ. of Strathclyde (United Kingdom); Philip A. Shields, Univ. of Bath (United Kingdom)

Core-shell GaIn/InGaIn nanostructures are sought after due to their large-area and high-quality non-polar facets, which are not subject to the detrimental quantum confined Stark effect. However, uniform InGaIn growth is difficult because the three-dimensional (3D) growth mode leads to facet-dependent growth rates and indium inclusion, resulting in emission at multiple peak wavelengths. Therefore this work examines facet-dependent InGaIn growth on 3D GaIn substrates.

An initial faceted GaIn structure was obtained by a short Metal Organic Vapour Phase Epitaxy (MOVPE) regrowth on plasma-etched 4-10 micron GaIn disks to reveal a-, m-, c- and semipolar planes. InGaIn layers were then grown under different reactor conditions to understand the influence of reactor parameters on growth rates and alloy fraction. The growth rates were determined by the analysis of scanning electron microscope images. Cathodoluminescence was used to examine the emission characteristics and estimate the indium fraction on individual facets.

For the largest structures the different reactor parameters regulate non-polar growth rates from 35 to 70 nm/min. Lower temperature growth inhibits c-plane emission but favours semipolar emission. Lower pressure enhances the indium fraction on the non-polar planes while reducing it on the semipolar plane. Reducing the size of the 3D GaIn structures to $1\ \mu\text{m}$ with the same growth conditions blue-shifts the non-polar InGaIn peaks by 200 meV corresponding to a decrease of indium nitride fraction from $\sim 20\%$ to $\sim 15\%$. This understanding and the subsequent control of the InGaIn growth rates on the various crystal facets will guide the design of core-shell LEDs.

9363-67, Session 14

Tapering process of a multiple-section GaIn nanorod

Charng-Gan Tu, Che-Hao Liao, Ta-Wei Chang, Yean-Woei Kiang, Chih-Chung Yang, National Taiwan Univ. (Taiwan)

With the nano-imprint lithography and the pulsed growth mode of metalorganic chemical vapor deposition, a regularly-patterned, c-axis nitride nanorod (NR) light-emitting diode array of uniform geometry with m-plane core-shell InGaIn/GaN quantum wells (QWs) is formed. To grow an NR with uniform cross-sectional size, in the pulsed growth mode, the sources of groups III and V are switched on and off alternatively with fixed supply durations. By varying the supply duration of group III source (TMGa) in the pulsed growth process, the NR cross section can be tapered for growing another uniform section of NR of a smaller cross-sectional size. Based on this growth technique, a multiple-section GaIn NR of changing cross-sectional size can be obtained. In this paper, we present the detailed study on the tapering process between two uniform sections of a multiple-

**Conference 9363:
Gallium Nitride Materials and Devices X**

section NR. By using the HAADF technique in TEM observation, we can trace the grown morphology after each pulsed growth cycle. It is found that in a uniform NR section, there is a small slant facet at the edge in the {1-102}-plane (-43 degrees). During the tapering process, the slant facet gradually changes into the {1-101}-plane (-62 degrees). When the growth returns to the next uniform section, the slant facet returns to the {1-102}-plane. Because of the changing slant-facet angle in the tapering process, QWs can be deposited onto the slant facet of the tapering section, even though no clear QW is grown on the slant facet of the {1-101}-plane.

9363-68, Session 14

Tunnel-junction-enhanced ultraviolet nanowire light-emitting diodes integrated on silicon

A. T. M. G. Sarwar, Roberto C. Myers, The Ohio State Univ. (United States)

Polarization-induced nanowire light emitting diodes (PINLEDs) are fabricated in a p-down orientation on silicon wafers from catalyst-free nanowires grown by plasma assisted molecular beam epitaxy [1]. The polarization charge is engineered into the nanowires using a double composition grading of digital AlGaIn alloy leading to a polarization-induced pn-junction. Due to the N-face [0001 ?] orientation [2] of the nanowires, previously designed p-down heterostructures suffer from a -2 eV hole injection barrier at the p-GaN/p-Si interface which results in a large turn-on voltage [3] for PINLEDs. Here, we demonstrate n⁺⁺/p⁺⁺ GaN tunnel junctions within an ultraviolet nanowire LED integrated on Si wafers. Electrical characterization of tunnel junction enhanced PINLEDs shows at least 1.65 V reduction in the turn on voltage. The electroluminescence (EL) from these devices shows characteristics quantum confined Stark effect (QCSE) and peaks at ~310 nm at an injection current of 100 mA which indicates band to band radiative recombination at AlGaIn multiple quantum wells. This work opens the pathway towards the development of high efficiency cascaded nanowire UV and Deep UV solid state emitters. Study of InGaIn and GdN insertion on the tunnel junction resistance and overall LED performance is in progress and will be presented.

This work is supported by the National Science Foundation CAREER award (DMR-1055164) and the Army Research Office (W911NF-13-1-0329).

[1] Carnevale, S. D.; Kent, T. F.; Phillips, P. J.; Mills, M. J.; Rajan, S.; Myers, R. C. Nano Letters 2012, 2, 915-920.

[2] Carnevale, S. D.; Kent, T. F.; Phillips, P. J.; Sarwar, ATM Golam; Selcu, C.; Kile R. F.; Myers, R. C. Nano Letters 2013, 13, 3029-3035.

[3] Sarwar, ATM Golam; Carnevale, S. D.; Kent, T. F.; Yang, F.; McComb, D. W.; Myers, R. C. Submitted.

9363-70, Session 14

Performance of nitride-based blue LED fabricated on sapphire substrate with nanostructured SiO₂

Shun Hanai, Motoaki Iwaya, Tetsuya Takeuchi, Satoshi Kamiyama, Meijo Univ. (Japan); Isamu Akasaki, Meijo Univ. (Japan) and Akasaki Research Ctr. (Japan); Tsukasa Kitano, Meijo Univ. (Japan)

Patterned sapphire substrates (PSSs) with a micron-scale periodicity are widely used in nitride-based light-emitting diodes (LEDs) for an enhancement of the light extraction efficiency. In addition, a submicron-scale-pattern on sapphire has also been proposed for further enhancement of the light extraction and control of a light emission dispersion. In latter case, due to a limited domain size of an initial GaN crystals by a small pitch pattern, a threading dislocation density (TDD) in an overgrown GaN layer tends to increase, compared with the case of PSS.

In this study, growth of GaN and characterization of LED on the sapphire substrate with a submicron-scale periodic SiO₂ pattern are investigated. The SiO₂ periodic corns with a height of 200 nm and a pitch of 460 nm were prepared. A conventional GaN growth with a low-temperature-deposited GaN buffer layer by metal-organic vapor phase epitaxy was carried out. The overgrown GaN layer has the TDD of 7?10⁷ cm⁻², which is twice lower than that in GaN on PSS and four-times lower than that in GaN on flat sapphire. A conventional nitride-based blue LED stack was also grown on the substrate with the patterned SiO₂.

Flip-chip type LEDs with a emitting area of 320 nm?320 nm were fabricated. An output power of this LED was 1.4 times higher than that of the LED with a flat sapphire substrate. This improvement may be mainly due to the enhancement of the light extraction efficiency, and slightly due to the improved internal quantum efficiency by reduced TDD.

9363-71, Session 15

InGaIn LEDs prepared on Ga₂O₃ substrates (Invited Paper)

Kazuyuki Iizuka, Yoshikatsu Morishima, Akito Kuramata, Tamura Thermal Device Corp. (Japan); Yu-Jiun Shen, Chang-Yu Tsai, Ying-Yong Su, Gavin Liu, Ta-Cheng Hsu, J. H. Yeh, Epistar Corp. (Taiwan)

?-Ga₂O₃ is optically transparent from the visible to the UV region and has n-type conductivity through impurity doping. These characteristics make ?-Ga₂O₃ very attractive as a substrate for vertical light emitting diodes (LEDs) that have a large driving current.

A previous study demonstrated InGaIn LEDs prepared on (100) ?-Ga₂O₃ [1]. However, as the reported LED characteristics were limited, the potential of this substrate has yet to be clarified. There were also problems in the form of epi-peeling and an electrical potential barrier at the GaN/Ga₂O₃ interface. Recently, we solved these problems by changing a surface orientation of the substrate from (100) to (-201) and by using a substrate partially masked with SiN_x [2].

In this paper, we report on the characteristics of LEDs prepared on (-201) ?-Ga₂O₃ substrates. The structure of LED is a vertical structure with a p-side down configuration. The LED layers were grown on the substrate by using the MOCVD method. Ag-alloy was used for the 300?300?m² p-type contact and reflective electrode. Ti/Au was used for the n-type contact.

The output power did not saturate at 1000 A/cm². The forward voltage was 4.7 V at 1000 A/cm². These characteristics are superior to conventional lateral LEDs and strongly indicate that LEDs prepared on ?-Ga₂O₃ substrate have excellent potential for power applications.

[1] K. Shimamura et al., Jpn. J. Appl. Phys. Vol.44 (2005) L7

[2] Y. Morishima et al., submitted to ISGN2014.

9363-72, Session 15

The novel design of white LED (Invited Paper)

Chia Liang Hsu, Epistar Corp. (Taiwan)

In recent years, white LED is rapidly developed for applications of flash, lighting, and BLU due to potential of package-less, low cost, high flux density, and possibility of optical design.

However, conventional white LED with narrow view angle results in problems about non-uniform light emitting, hot spot and color shift in application of planar light source. And therefore more LEDs need to be used in light source to maintain light uniformity but to increase electrical power consumption. And furthermore thermal management of H/C ratio, R_{th}, and heat spreading also should be improved in white LED for over drive. Moreover, huge capacity requirement for wire bonding, testing, and sorting by labor will impact on cost reduction of white LED.

**Conference 9363:
 Gallium Nitride Materials and Devices X**

In this lecture, development and application (ex. filament) of improved white LED will be introduced. It includes white LED with BD (Batwing Design) could achieve wide angle to improve light uniformity and to decrease quantities of LEDs used for electrical energy conservation. The technologies about high H/C ratio, low Rth, and good thermal conduction in application of white LED by modification of die bond process and LED structure will be also presented. Stable and simplified process about handling white LED with flip chip structure for cost reduction will be mentioned and explained. Finally we will report the approach to high lm and high lm/\$ by improved white LED in application.

9363-73, Session 15

Light output power enhancements of green light-emitting diodes by digital InN/GaN growth thick InGaN wells (*Invited Paper*)

Shoou-Jinn Chang, Wei-Chi Lai, National Cheng Kung Univ. (Taiwan)

We demonstrate the properties of LEDs containing thick InGaN wells with high crystal quality by digitally growing InN/GaN for InGaN wells. Compared with conventionally grown thin InGaN wells, thick InGaN wells with digitally grown InN/GaN exhibit superior optical properties. Green InGaN/GaN MQWs with InN/GaN growth-switched InGaN wells have a lower pit density and a smaller surface roughness than those with conventional InGaN wells. InN/GaN growth switching enhances the migration of the adatoms of In, Ga, and N during InGaN well growth, and the green InGaN/GaN MQW LEDs with InN/GaN growth-switched InGaN wells have a lower η_{ext} reverse leakage current than those with conventional InGaN wells. Obtained from the Arrhenius plot of the integrated PL intensity with respect to the measurement temperature, the activation energy for defect-related thermal quenching of thick InGaN wells with digitally grown InN/GaN (48 meV) is larger than the activation energy of conventionally grown thin InGaN wells (25 meV). Moreover, thick InGaN wells with digitally grown InN/GaN exhibit a lower η_{ext} value of 19 meV than conventionally grown thin InGaN wells (23 meV). Finally, compared with green LEDs with conventionally grown thin InGaN wells, the 20-A/cm² output power of green InGaN/GaN MQW LEDs containing thick InGaN wells with digitally grown InN/GaN has been improved by approximately 23%.

9363-74, Session 15

Enhancement of internal quantum efficiency in InGaN-based light-emitting diodes by additional growth of the p-ZnO layer

Jong-In Shim, Dong-Soo Shin, Hanyang Univ. (Korea, Republic of); Junghyun Kim, Sungki Hong, Yungryel Ryu, MOX, Inc. (Korea, Republic of); Ja-kyung Lee, Sang Ho Oh, Pohang Univ. of Science and Technology (Korea, Republic of)

We have recently proposed and demonstrated a novel method for generating high-quality white light with both the warm correlated color temperature (2500 - 3000 K) and the high color rendering index (> 90). The proposed white-light source consists of a blue light-emitting-diode (LED) encapsulated with a yellow phosphor and a green LED coated with a red phosphor, which greatly intensifies the yellowish spectral region and improves the stability and conversion efficiency of the red spectral region. A shortcoming of this white-light source arises from the fact that the internal quantum efficiency (IQE) of a commercially available green LED is still inferior to that of a blue LED. In this work, by utilizing additional growth of the p-ZnO layer on the p-GaN layer of an LED, we experimentally

demonstrate that this shortcoming can be overcome. We fabricated blue and green LEDs with and without the p-ZnO layers and compared their optoelectronic properties by employing various characterization tools such as the IQE, current-voltage, electroreflectance and photocurrent spectroscopies, strain distribution analysis by electron holography, and electroluminescence spectra. A record-high IQE of 80% was experimentally obtained in a green LED with the p-ZnO layer, which was an increase of more than 20% compared to the one without the p-ZnO layer. Overall characterization results such as the reduced sheet charge caused by the strain field and the blue shift of emission wavelength indicated that the p-ZnO layer was very effective in reducing the local strain in the multiple-quantum-well active region, which in turn improves the radiative recombination rate as well as the hole injection.

9363-75, Session 15

Chemically-doped graphene films as a transparent conductive layer in GaN LEDs

Jihyun Kim, Byung-Jae Kim, Sooyeoun Oh, Korea Univ. (Korea, Republic of)

Transparent conductive electrodes play an important role in displays, photovoltaic devices, and light-emitting diodes. Until now, indium-tin oxide (ITO) has been a common material due to its excellent electrical conductivity and optical transparency. However, the drawbacks include the restricted resources, poor chemical stability, low transmittance in the ultra-violet and infra-red spectral regions, poor adhesion, and low failure strain. Therefore, high performance transparent conductive electrodes to replace current ITO materials are needed. Since graphene grown by the chemical vapor deposition method can be chemically doped, different configurations of the doped graphene layers were prepared and analyzed by using sheet resistance measurements, optical transmittance measurements, SEM, and micro-Raman spectroscopy to compare the optical and electrical properties of the different graphene samples. In our experiments, terminal-layer doping was very effective, compared with middle-layer or bottom-layer doping. The details of the experimental procedure and results will be presented. Also, the integration of graphene-based transparent conductive electrodes with GaN LEDs will be demonstrated.

Conference 9364: Oxide-based Materials and Devices VI

Sunday - Wednesday 8-11 February 2015

Part of Proceedings of SPIE Vol. 9364 Oxide-based Materials and Devices VI

9364-1, Session 1

Physical model of mobility thickness dependence in thin-film ZnO

David C. Look, Wright State Univ. (United States); Kevin D. Leedy, Arnold M. Kiefer, Bruce B. Claflin, Air Force Research Lab. (United States)

The dependence of mobility μ on thickness d in thin films of highly conductive ZnO and other TCOs is a well-known phenomenon. To quantify this dependence, we have earlier introduced formulas for sheet concentration n_s and mobility μ that seem to be applicable over a wide range of samples: $n_s = n(d - \delta)/d$ and $\mu = \mu_{inf}/(1 + d^*/(d - \delta))$, where n , μ_{inf} , δ , and d^* are fitting parameters. The first formula implies a constant volume concentration n while the second has a parameter d^* which is useful as an interface figure of merit but otherwise has no strong theoretical basis. In the present work, we offer a quantitative physical model for all fitting parameters, based on two hypotheses: (1) n is constant throughout the entire film, even in the dead layer δ ; and (2) μ increases with d because scattering by extended defects, such as dislocations, typically decreases with d , following a form such as $\exp[-(d - \delta)/z_0]$. The measured Hall mobility and concentration can then be calculated from classical multi-layer theory, either in closed form or as integrals, conveniently set up in symbolic programs such as MathCad. It is often possible to cast the "exact" formulas for n_s and μ in terms of the simple formulas above, with the phenomenological parameter d^* becoming a weak function of d . Applications of the new formalism will be presented.

9364-2, Session 1

Influence of impurities and annealing procedures on optical and electrical properties of ZnO:Al

Florian Ruske, Steffi Schönau, Sven Ring, Sebastian Neubert, Bernd Rech, Helmholtz-Zentrum Berlin (Germany)

Post-deposition annealing can lead to significant changes in optical and electrical properties of ZnO:Al films. While annealing under a protective capping layer or vacuum annealing has shown to lead to improved transmission and electron mobility, annealing without capping layer in flowing nitrogen or air usually results in strong increases of resistivity caused by both a decline in carrier concentration and mobility. The strong influence of the annealing ambient could be caused by incorporation or emission of volatile species like oxygen and nitrogen. In order to clarify the effect either element has been deliberately added to the ZnO:Al growth process. Film properties have been studied after deposition and after various annealing treatments.

For oxygen-rich samples a strong influence of oxygen content has been found for as-deposited samples. Interestingly, the influence on electrical properties diminishes strongly after thermal treatments, both for annealing with and without a protective capping layer.

For nitrogen containing samples on the contrary the influence of nitrogen content remains strong even after annealing. Additionally nitrogen causes a considerable sub-bandgap absorption that cannot be removed by any thermal treatment. This is in contrast to sub-bandgap absorption as observed for nitrogen-free samples grown at moderate temperatures that can be eliminated by annealing.

As annealing effects on nitrogen-free samples are mostly reversible, nitrogen uptake during annealing in air or flowing nitrogen seems unlikely.

Along with an analysis of electrical transport data it can be concluded, that annealing procedures, depending on ambient, create or annihilate acceptor type point defects originating from deviations from the ideal oxygen-to-metal ratio within the lattice.

9364-3, Session 1

Electron transport in ITO and In₂O₃ : limits, scattering mechanisms, and carrier systems (*Invited Paper*)

Oliver Bierwagen, Paul-Drude-Institut für Festkörperelektronik (Germany)

Knowing the fundamental limits of material properties is important for deciding on their application. This contribution discusses, the measured and modeled transport properties of In₂O₃ for electron concentrations from 10^{17} (unintentionally doped In₂O₃) to 10^{21} cm⁻³ (ITO). High-quality, single crystalline, thin film samples grown by plasma-assisted molecular beam epitaxy were used to determine the relevant scattering mechanisms that fundamentally limit the electron mobility. Polar optical phonon (POP) scattering and ionized impurity scattering were found to dominate whereas acoustic phonon scattering is negligible. The model parameters for POP scattering were determined by fitting the model to the measured temperature dependent mobility of a sample with maximized relative phonon contribution (low dopant concentration, high temperature). Our modeling predicts a low-carrier concentration drift mobility limit at room temperature of 190 cm²/Vs (Hall mobility 270 cm²/Vs) and can do so for other application-relevant temperatures. Comparison of the measured mobility of single crystalline and textured films shows a strong influence of grain boundaries at low carrier concentrations which decreases at higher concentrations.

The measured and modeled (thermoelectric) Seebeck coefficient proved invaluable --- in combination with sheet electron concentrations from Hall measurements --- for clarifying the type of carrier system (bulk or surface/interface) and estimate the effective electron mass.

Further issues in transport analysis such as the correct assignment of the conductivity type (p- or n-type) and the influence of potential surface and interface carrier systems will be highlighted.

Natalie Preissler (PDI), and Ashok T. Ramu and James S. Speck (UCSB) contributed to this work.

9364-4, Session 1

Characterization of multilayered Molybdenum doped Indium Oxide/Zinc Oxide thin film stacks for optoelectronic applications (*Invited Paper*)

Jaime Viegas, Elangovan Elamurugu, Raquel Flores, Ricardo Janeiro, Marcus S. Dahlem, Masdar Institute of Science & Technology (United Arab Emirates)

Multilayered thin film stacks of molybdenum doped indium oxide (IMO) and zinc oxide (ZnO) deposited by RF sputtering with and without post-deposition annealing steps are optical, electrical and structural characterized for assessing their suitability for optoelectronic applications. IMO is a known transparent conductive oxide, which interlayered with ZnO can render similar optical properties to the Al:ZnO/ZnO multilayer, with applications to near infrared plasmonics. We present a discussion of optimal

**Conference 9364:
 Oxide-based Materials and Devices VI**

process conditions for maximizing optical and electrical properties, linking these to TEM and AFM nanostructure mapping. Additionally, waveguides based on an IMO/ZnO multilayered stack were fabricated by electron beam lithography and their optical losses and electro-optic parameters measured in a realistic photonic circuit environment.

9364-5, Session 1

**Progress in solution-based oxide devices
 (Invited Paper)**

Rebecca L. Peterson, Univ. of Michigan (United States)

Solution-processing is an attractive deposition approach for oxide thin films due to the high quality of material produced, the ease of manipulating oxide composition, and the future potential for low-cost, high-throughput commercial manufacturing. Liquid-ink approaches are particularly useful for amorphous oxide alloys because alloys do not require a high energy or high temperature process to induce crystallization. Using amorphous layers also avoids traps and defect states that characterize crystalline boundaries, yielding high-quality semiconductor films that are smooth and homogeneous. This talk will describe recent work on devices made of amorphous oxide alloys deposited via liquid inks. Solution-processed zinc tin oxide, indium gallium zinc oxide, or zinc oxide nanoparticles are used to make thin film transistors with electron mobility of up to $14 \text{ cm}^2\text{cm}/(\text{V}\cdot\text{s})$, and introduction of a quaternary alkaline earth metal into the zinc oxide alloy improves bias stability. Cryogenic measurements show that these planar devices exhibit band-like electron transport. I also will report recent results on Schottky diodes that exhibit excellent vertical conduction through multiple spin-coated layers of amorphous oxide semiconductors, and on solution-processed high-k insulators with homogeneous nano-crystalline morphology. Such thin film oxide materials have the potential to transform and enhance civilian and military capabilities through UV optoelectronics, heterogeneously integrated RF/power/sensor circuitry, and new adaptive devices, while the study of these materials can yield transformative insight into physics of disordered and semi-ordered oxides.

9364-6, Session 2

Direct Visualization of Atomic and Electronic Structure on Perovskite Oxide Film Surface (Invited Paper)

Yoshinori Okada, Ryota Shimizu, Susumu Shiraki, Taro Hitosugi, Tohoku Univ. (Japan)

Recent progress in epitaxial film techniques opened great opportunities for designing materials in atomic scale. Especially, exploring novel functionalities at oxide surface/interface has been one of the challenging topics, thus understanding the physics and chemistry at atomic scale has become crucial. However, direct experimental information at the atomic scale has been still limited.

Recently, we have developed pulsed laser deposition (PLD) system combined with highly stable low temperature UHV scanning tunneling microscope (STM)[1]. This particular set up introduced a way to probe ionic arrangement together with site selective high resolution tunneling spectra on fresh surface. So far, we have succeeded in probing SrTiO₃ surface[2] and initial growth process in LaAlO₃/SrTiO₃ system[3]. Our approach has been continuously giving new insight for understanding phenomena at atomic scale in oxide electronics field.

[1]K. Iwaya et al., Rev. Sci. Instrum. 82, 083702 (2011).

[2]R. Shimizu et al., ACS Nano 5, 7967 (2011)

[3]T. Ohsawa et al., ACS Nano, 8, 2223 (2014)

9364-7, Session 2

Antimony doping and defects in ZnO nanowires (Invited Paper)

Axel Hoffmann, Thomas Kure, Alexander Franke, Sarah Schlichting, Emanuele Poliani, Felix Nippert, Markus R. Wagner, Technische Univ. Berlin (Germany); Marcus Müller, Peter Veit, Sebastian Metzner, Frank Bertram, Jürgen Christen, Otto-von-Guericke-Univ. Magdeburg (Germany); Eswaran Senthil Kumar, Faezeh Mohammadbeigi, Simon Fraser Univ. (Canada); Janina Maultzsch, Technische Univ. Berlin (Germany); Simon Watkins, Simon Fraser Univ. (Canada)

Doping with group-V elements such as Sb on the O site could in general lead to p-type conductivity. We investigated the morphology of metalorganic vapor phase epitaxy (MOVPE) grown c-axis aligned Sb doped ZnO NWs as well as the doping distribution and structural defects of single NWs. First-principles calculations indicate that a SbZn+2VZn complex acts as an acceptor and SbZn+VZn as a shallow donor in ZnO [1]. Low-temperature photoluminescence spectroscopy (PL) under an external magnetic field up to 5 T clearly reveals that the Sb attributed emission at 3.3637 eV stems from an exciton bound to a neutral donor. The formation of a complex is favored in agreement with the observed strain behavior in Raman measurements.

Spatially-resolved PL and Cathodoluminescence spectroscopy (CL) along several single NWs reveal that the luminescence stems predominately from the tip and decreases towards the bottom of the NW. Raman measurements on ensemble NWs show additional vibrational modes, where the observed modes at 536 cm⁻¹ and 686 cm⁻¹ appear exclusively in Sb doped ZnO [2]. Tip-enhanced Raman spectroscopy (TERS) was performed to investigate the local doping concentration. The significant increase of Sb-related Raman modes towards the apex confirms the increase of Sb along the NW.

[1] S. Limpijumnong et al., Phys. Rev. Lett. 92, 155504 (2004);

[2] C. Bundesmann et al., Appl. Phys. Lett. 83, 1974 (2003).

9364-8, Session 2

Growth of GaZnO nanoneedles for low-threshold field emission

Yu-Feng Yao, Charng-Gan Tu, Ta-Wei Chang, Hao-Tsung Chen, Yean-Woei Kiang, Chih-Chung Yang, National Taiwan Univ. (Taiwan)

We report the growth and characterization results of GaZnO nanoneedles (NNs) based on the vapor-liquid-solid growth mode of MBE with Ag nanoparticles (NPs) as the catalyst. The Ag NPs on a GaN template are formed through thermal annealing of an Ag thin film of 2 nm in thickness at 300 degrees C for 30 min with ambient nitrogen. In the MBE reactor at 350 degrees C in substrate temperature, with melting Ag NPs, the VLS growth mode leads to the formation of GaZnO NNs on a GaZnO thin film. With the growth duration of 60 min, the NNs of 80-100 nm and 400-500 nm in maximum cross-sectional size and height, respectively, are formed along with a GaZnO thin film of ~200 nm in thickness. From the measurement of energy dispersive X-ray spectroscopy, it is found that the Ga content in the NNs is about the same as that in the thin film, within the range of 4-8%. Based on the diffraction pattern analysis of high-resolution TEM images, it is found that the grown GaZnO film and NNs consist of a multi-grain crystal structure of mild tilts and twists. During the NN growth, Ag atoms are mixed into GaZnO such that the catalytic Ag NP size diminishes. Based on a field emission test, it is found that the turn-on and threshold electrical fields of field emission are about 0.33 and 0.6 V per micron, respectively.

**Conference 9364:
Oxide-based Materials and Devices VI**

9364-9, Session 2

Atmospheric pressure chemical-vapor deposition of ZnO crystal structure: effects of substrate temperatures and porous silicon surface

Yousif M. Hassan, Shayda A. Kakil, Salahaddin Univ.-Hawler (Iraq)

Zinc oxide [ZnO] crystals were deposited on Silicon [Si] and porous silicon [Psi] substrate surfaces using atmosphere pressure chemical vapor deposition (APCVD), ZnCl₂ powder and O₂ gas were used as Zn and O sources respectively and N₂ as a carrier gas, electrochemical etching was used to porous Si surface. The substrate temperature was varied in the range of 450°C to 750°C. The structural, morphological, and atomic composition of ZnO products on Si and Psi substrate have been studied using X-ray diffraction (XRD) and field emission scanning electron microscopy (FESEM) and energy dispersive X-ray (EDX). The XRD analyses indicate that ZnO crystals have hexagonal wurtzite structures with (002) preferential orientation, whereas the diffraction patterns sharpen with the increase in substrate temperatures. EDX indicated that the atomic ratio (Zn/O) increases with increasing substrate temperature. The FESEM image reveals that the product has micro-size rods with diameters ranging from 100 to 600 nm. The XRD of crystals implies a superior c-axis preferred orientation and high quality crystals of ZnO at substrate temperature 650 °C with forming of Zn₂SiO₄ compound at the temperatures higher than this temperature.

9364-10, Session 2

Optical and thermal properties of doped ZnO thin films and nanostructures (Invited Paper)

Markus R. Wagner, Juan S. Reparaz, Institut Català de Nanociència i Nanotecnologia (Spain); Clivia M. Sotomayor Torres, Institut Català de Nanociència i Nanotecnologia (Spain) and ICREA (Spain); S. Dilger, D. Lehr, M. Gerigk, C. Lizandara-Pueyo, S. Polarz, Univ. Konstanz (Germany); S. Schlichting, Thomas Kure, Axel Hoffmann, Technische Univ. Berlin (Germany); Matthew R. Phillips, Univ. of Technology, Sydney (Australia); Jean-Michel Chauveau, Univ. de Nice Sophia Antipolis (France) and Ctr. de Recherche sur l'Hétéro-Epitaxie et ses Applications (France); Bruno K. Meyer, Justus-Liebig-Universität Giessen (Germany)

The optical, electronic and thermal properties of ZnO based materials strongly depend on the choice of dopants, polarity, size effects and the structural design of heterostructures. Here, we review recent advances in the modification of these properties both in thin films and nanostructures. The temperature dependent polariton dispersion of homoepitaxially grown ZnO by MBE is directly derived by the observation of Fabry-Perot interference fringes in the luminescence spectra of ZnO thin films. These results are discussed in comparison with reflectivity measurements and theoretical modeling [1]. Nitrogen doping of such ZnO epilayers in the high doping regime is found to give rise to a second DAP type luminescence band around 3.06 eV in addition to the typical N related DAP around 3.24 eV. The origin of this transition is discussed based on low energy electron beam irradiation (LEEBI) and photoluminescence excitation (PLE) measurements [2]. Furthermore, the effects of doping with less common elements such as Sb, S, Li, Cl, and Eu are studied in ZnO nanostructures [3-6]. The effects of these dopants on the optical and vibrational properties of ZnO nanostructures are investigated by micro-Raman, time resolved PL, magneto-PL and hydrostatic pressure measurements. Finally, we apply the recently developed 2-laser Raman thermometry technique [7] in order to analyze the thermal properties of these doped thin film and nanostructured

ZnO materials [5] and discuss potential applications in the field of thermoelectrics.

References:

- [1] B. K. Meyer, M. R. Wagner et al., to be published (2014)
- [2] M. R. Wagner, M. R. Phillips, B. K. Meyer et al., to be published (2014)
- [3] S. Schlichting, M. R. Wagner et al., to be published (2014)
- [4] C. Lizandara-Pueyo, M. R. Wagner et al., CrystEngComm 2014, 16, 1525 (2014)
- [5] S. Dilger, M. R. Wagner et al., Cryst. Growth Des., 2014, 14, 4593 (2014)
- [6] D. Lehr, M. R. Wagner et al., Chem. Mater. 2012, 24, 1771-1778 (2012)
- [7] J. S. Reparaz, M. R. Wagner et al., Rev. Sci. Instr. 85, 034901 (2014)

9364-11, Session 2

Fabrication of ZnO crystals by UV-Laser Annealing on ZnO Nanoparticles prepared by Laser Ablation Method

Tetsuya Shimogaki, Hirotaka Kawahara, Mitsuhiro Higashihata, Hiroshi Ikenoue, Daisuke Nakamura, Tatsuo Okada, Kyushu Univ. (Japan)

Various zinc oxide (ZnO) crystals such as nanoparticles (NPs), thin films and nano/microcrystals are expected as new building blocks for optoelectronic devices. We have studied about fabricating ZnO nano and microcrystals using nanoparticle-assisted pulsed laser deposition (NAPLD). In this report, we approach the study of ZnO crystals from a new angle. ZnO NPs with diameters of a few dozen nanometers were generated by ablating a ZnO sintered target with focused beam of the third harmonic of a Q-switched Nd:YAG laser ($\lambda = 355$ nm, $\tau = 10$ ns) at a fluence of 1.5 J/cm². The ZnO target was placed in a vacuum chamber at relatively high pressures (500-30000 Pa). In this study, bare ZnO NPs were collected at room temperature, then they were laser-annealed with a KrF excimer laser ($\lambda = 248$ nm, $\tau = 20$ ns). It was found that the optical properties of ZnO NPs improved by laser annealing. Additionally, their x-ray diffraction peaks originated from wurtzite ZnO crystals had narrower full width half maximum than those before laser annealing. We believe that these effects were resulted by ultrafast melting and recrystallizing of ZnO NPs. These techniques can be applied to fabricating ZnO nano/microcrystals and low-temperature film formation using ZnO NPs as a seed layer.

9364-12, Session 2

ZnO growth at low temperature and application as a buffer layer for LT-GaN growth

Nazmul Arefin, Preston Larson, Vince R. Whiteside, The Univ. of Oklahoma (United States); Khalid Hossain, Amethyst Research Inc. (United States); Jijun Qiu, The Univ. of Oklahoma (United States); Matthew H. Kane, Texas A&M Univ. at Galveston (United States); Brittany N. Pritchett, Matthew B. Johnson, Patrick J. McCann, The Univ. of Oklahoma (United States)

ZnO was deposited on sapphire and Si(100) at 300°, 500°, and 700°C in an Ar (7mTorr) atmosphere. High power electron gun pulses were used to ablate the 99.99% pure ZnO target, stationed at 5 cm vertical distance from the substrate. The electron pulses were generated at 12KV, 0.3 J/pulse at 1Hz for initial few nm of growth, and then increased to a 3Hz pulse rate. Scanning electron microscopy (SEM), x-ray diffraction (XRD), Rutherford backscattering (RBS), photoluminescence (PL) and Hall Effect measurement were performed to evaluate structural, morphological, optical and electrical properties. SEM imaging confirmed a rough surface morphology with

**Conference 9364:
Oxide-based Materials and Devices VI**

the presence of 30-100nm scaled ZnO crystallites (for the ZnO/Sapphire samples), while smaller but more coalesced crystallites of 30-70 nm size were observed for ZnO/Si(100) samples. XRD θ - 2θ scans from $2\theta=0^\circ$ to $2\theta=70^\circ$ on the ZnO on sapphire showed only two other peaks near $2\theta=34.3^\circ$, besides the peaks from the sapphire. The peaks consist of a stronger peak at 34.320° and a much weaker peak at 35.951° corresponding to the (0002) and (10-11) orientations for ZnO, respectively. XRD for the ZnO on Si(100) samples showed of a strong peak at $2\theta=34.402^\circ$ corresponding to polar ZnO(0002) plane and a very weak peak at $2\theta=61.67^\circ$ corresponding to ZnO(103) plane, besides the silicon substrate peaks. Room temperature PL measurements showed near band edge (NBE) emission in the region of 3.3eV. Hall measurements confirmed growth of n-type ZnO films with mobility in the range of 10-44 cm²/V-sec. ZnO/sapphire templates grown in 300oC were used to grow GaN at same temperature. Characterization results confirm epitaxial GaN on ZnO/Sapphire with c-plane orientation and NBE emission. These results demonstrate that PED-grown ZnO and LT-GaN on ZnO/Sapphire are highly c-axis oriented and have the potential for the initial growth of ZnO on various substrate materials for initial buffer layer growth for future optoelectronic and device applications based on III-nitride technology.

9364-13, Session 3

Orbital control of metal-insulator transition in VO₂

Naga Phani B. Aetukuri, IBM Research - Almaden (United States) and Stanford Univ. (United States); Alexander X. Gray, SLAC National Accelerator Lab. (United States); Marc Drouard, Matteo Cossale, Li Gao, IBM Research - Almaden (United States); Alexander H. Reid, SLAC National Accelerator Lab. (United States); Roopali Kukreja, Stanford Univ. (United States) and SLAC National Accelerator Lab. (United States); Hendrik Ohldag, SLAC National Accelerator Lab. (United States); Catherine A. Jenkins, Elke Arenholz, Lawrence Berkeley National Lab. (United States); Kevin P. Roche, IBM Research - Almaden (United States); Hermann A. Durr, SLAC National Accelerator Lab. (United States); Mahesh G. Samant, Stuart S. P. Parkin, IBM Research - Almaden (United States)

Controlling the conductivity of correlated electron insulators is considered to be one of the most promising approaches towards realizing energy-efficient electronic devices. Vanadium dioxide (VO₂), a prototypical correlated electron material, undergoes a metal-insulator transition (MIT) at -340 K, with an accompanying crystalline phase transition. In this work, we used pulsed laser deposition to deposit high quality single-crystalline thin films of VO₂ (001) on TiO₂ (001) substrates with varying RuO₂ (001) buffer layer thickness. We exploit the epitaxial strain provided by the variable thickness RuO₂ (001) buffer layer to vary the MIT transition temperature of thin VO₂ (001) films from -285 to -345 K. The high quality films enabled us to do a very fundamental physics experiment where in we measured the changes in electronic occupation of the transition metal d-orbitals by distorting an oxygen octahedron. The changes in orbital occupation were measured using strain-, polarization- and temperature-dependent x-ray absorption spectroscopy (XAS). Using XAS in conjunction with x-ray diffraction and electrical transport measurements, we show that the transition temperature of VO₂ is controlled by the orbital occupancy in its metallic state. We also observe that the structural distortion across the MIT is strongly correlated with the orbital occupation in the metallic state. Our results suggest that the MIT in VO₂ can be orbitally controlled, for example by hetero-structural engineering.

9364-14, Session 3

Dynamic tuning of refractive index profile over phase change regions in vanadium dioxide thin films

Shuyan Zhang, Mikhail A. Kats, Yanjie Cui, Yu Yao, You Zhou, Shriram Ramanathan, Federico Capasso, Harvard Univ. (United States)

Phase change materials have received great attention in the research of realizing active metamaterials and metasurfaces, as well as reconfigurable optical and optoelectronic devices. Vanadium dioxide (VO₂) is an archetypal phase change material featuring an insulator-to-metal transition (IMT) that can be triggered thermally, electrically, optically, or via strain. We utilize a simple two-terminal structure consisting of source and drain electrodes patterned on a 200-nm VO₂ thin film with a sapphire substrate which allows for dynamic control of the size and shape of localized regions of the metal-phase VO₂ within an insulator-phase background. By applying current through the device, a localized conducting path with a tunable width is formed within the gap, which we study by optical microscopy, electrical characterization, Raman spectroscopy, and Fourier transform infrared (FTIR) spectroscopy. The Raman intensity distribution at the edge of the conducting path shows that there is a phase co-existence region indicating the percolative nature of the IMT; we utilize this region as a disordered, natural metamaterial. Our FTIR spectrometer is equipped with a focal plane array which is capable of obtaining an infrared image of the conducting path region and the spectrum at each pixel simultaneously. We can use this spectral information to infer the refractive index profile of the conducting path region which shows a gradient distribution. Dynamic control of the size and shape of metal- and insulator-phase regions within a phase change material can enable a wide range of reconfigurable optical and optoelectronic devices exploiting sharp changes in carrier density.

9364-15, Session 3

Electronic control of germanium telluride (GeTe) phase transition for electronic memory applications

Alex H. Gwin, Ronald A. Coutu Jr., Air Force Institute of Technology (United States)

Germanium telluride (GeTe) is a phase change material that undergoes an exponential decrease in resistance from room temperature to its glass temperature near 200°C. Its resistivity decreases by as much as seven orders of magnitude between amorphous and crystalline phases as it is heated. Chalcogenide glasses such as GeTe typically have been utilized in non-volatile optical memories such as CDs, DVDs, and Blu-ray discs, where the change in reflectivity between phases gives enough contrast for “on” and “off” bits. Research over the past several years has begun to characterize the electronic control of GeTe thin films for advanced electronic memory applications. By applying a voltage to control its resistance and crystallinity, GeTe has become a candidate for ultra-fast switching electronic memory, perhaps as an alternative to flash memory. In this research, micro-scale resistors were fabricated in a cleanroom using RF sputtering of GeTe targets and electron-beam evaporation on c-Si, SiO₂/Si, Si₃N₄/Si, and Al₂O₃. Characterizations of the change in resistance were completed with varied voltage and temperature in order to draw a comparison of the switching mechanism between thermally and electronically induced transition. The resistors show approximately six orders of magnitude change in resistance when heated via conduction and five orders of magnitude via Joule heating. Hysteretic behavior is also evident in the current-voltage curves. The behavior of the resistors is compared for all four substrates. The results prove the feasibility of implementing GeTe thin films in electronic memory applications.

9364-16, Session 3

Real-space and nanoscopic observation of phase transition behaviors of VO₂ thin films using Kelvin probe force microscopy

Ahrum Sohn, Ewha Womans Univ. (Korea, Republic of); Teruo Kanki, Koutaro Sakai, Hidekazu Tanaka, The Institute of Scientific and Industrial Research (Japan); Dong-Wook Kim, Ewha Womans Univ. (Korea, Republic of)

VO₂, a representative correlated electron system, undergoes metal-insulator transition (MIT) and a monoclinic-tetragonal structural phase transition (SPT) near room temperature. For several decades, numerous researchers have continued investigations to unveil the underlying mechanism of the MIT of VO₂. In particular, in-situ and real-space observation of the MIT behaviors are highly desirable to reveal the distinct electronic and/or structural phases in the sample while spanning the transition.

In this study, we carry out transport and KPFM (Kelvin probe force microscopy) measurements on epitaxial VO₂/TiO₂ thin films simultaneously in the temperature range of 285 - 330 K. The samples have large grains due to very small lattice mismatch, which allows us to study inherent nature of the phase transition in quasi-2D VO₂ system. The sample's work function decreases from 5.08 eV to 4.96 eV, while the sample undergoes the transition, indicating a notable change in its electronic band structure. The work function maps can clearly reveal coexistence of the two distinct phases at the intermediate temperature range. Thus, the KPFM images allow us to extract metallic domain fraction at each temperature from the real-space domain configurations. The 2D percolation theory well explains the relation between the metallic fraction and conductivity of the VO₂/TiO₂ thin films. This work demonstrates that KPFM enables in-situ and nanoscopic observation of the intriguing MIT behavior of VO₂.

9364-17, Session 3

Thermal conductivity of VO₂ thin film deposited by RF-sputtering

Motohisa Kado, Toyota Research Institute North America (Japan); Jyothi S. Sanhu, Univ. of Illinois at Urbana-Champaign (United States); Gaohua Zhu, Debasish Banerjee, Toyota Research Institute North America (United States); David G. Cahill, Univ. of Illinois at Urbana-Champaign (United States)

Ultrafast nature of the phase transition near room temperature in VO₂ makes it attractive material for applications in electronics and optical devices, however utilization of corresponding drastic change in thermophysical properties are rarely reported. In this study, we investigate thermal and electronic properties of VO₂ thin films on various substrates across the transition temperature to seek possibility of utilizing VO₂ based thermal switches for applications in thermal devices. All films are deposited by radio frequency (RF) sputtering on various substrates with varying lattice mismatch. The sputtering is performed in argon environment from a V₂O₅ target at 550-600°C. Thermal properties are measured by time domain thermo-reflectance (TDTR) method. Electrical conductivity and carrier concentration of the films are measured by a temperature varying four-probe and Hall-Effect measurements. We will discuss interplay of phononic and electronic component to thermal conductivity in the light of Wiedemann-Franz law across MIT of VO₂ films deposited under various conditions.

9364-18, Session 3

Electric field-assisted metal insulator transition in vanadium dioxide (VO₂) thin films: optical switching behavior and anomalous far-infrared emissivity variation *(Invited Paper)*

Aurelian Crunteanu-Stanescu, XLIM Institut de Recherche (France); Julie Cornette, Maggy Colas, Jean-Christophe Orlianges, Univ. de Limoges (France); Annie Bessaudou, Françoise Cosset, XLIM Institut de Recherche (France)

VO₂ is an electron-correlated material undergoing a reversible insulator-to-metal transition (MIT) when heated above ~341 K. The transition is accompanied by a crystalline structure change of the material from a monoclinic (below 341 K, insulating state) to a tetragonal rutile structure in its metallic state. In VO₂ thin films, the MIT is usually described as percolative coexistence of the insulating- metallic domains in the film structure and can be triggered by thermal, electrical or photonic excitations. Activation times as short as 100 fs has been reported for the optically driven MIT transition, while the electronic transition occurs within nanoseconds.

Here we present the VO₂ thin films deposition using electron-beam evaporation of a vanadium target under oxygen atmosphere on different substrates (sapphire, SiO₂/Si..) and we focus on their electrical and optical properties variations as the material undergoes the MIT under electrical stimuli. The phase transition induces extremely abrupt changes in the electronic and optical properties of the material: the electrical resistivity increases up to 5 orders of magnitude while the optical properties (refractive index) are drastically modified. The thin films were further integrated in simple planar devices and we demonstrated electrical-activated optical modulators for visible-infrared signals with high discrimination between the two states.

We will highlight a peculiar behavior of the VO₂ material in the infrared and far infrared regions (2- 20 microns), namely its anomalous emissivity change under thermal- end electrical activation (negative differential emittance phenomenon) with potential applications in active coatings for thermal regulation, optical limiting or camouflage coatings.

9364-19, Session 3

Flexo printed sol-gel derived vanadium oxide films as an interfacial hole-transporting layer for organic solar cells

Terho Kololuoma, National Research Council Canada (Canada) and VTT Technical Research Ctr. of Finland (Finland); Salima Alem, Jiangping Lu, Neil Graddage, Ye Tao, National Research Council Canada (Canada)

In this paper we report on the synthesis and development of flexo-printable vanadium oxide precursor ink to be used as a hole-transporting layer in organic solar cell applications. For the synthesis of vanadium oxide inks, a sol-gel methodology was utilized. By selecting the right type of coordinating ligands flexo printable and stable ink was successfully developed and flexo printed on different substrates demonstrating its potential to be used as a hole-transporting layer in both conventional and inverted solar cell architectures. The conversion process of the synthesized vanadium oxy-alkoxide precursor into a corresponding oxide hole-transporting layer under different conditions was followed by DSC/TGA and XPS analyses. Flexo-printable vanadium oxide precursor inks and developed processing methodologies were utilized for the fabrication of inverted organic solar cells. Results reveal that depending on the formulation and the applied thermal conversion process, power conversion efficiencies between 1.3 % and 4.2 % can be achieved when PCDTBT:PC70BM is used as active solar harvesting materials.

9364-20, Session 4

High-rate growth of high-crystallinity LiCoO₂ epitaxial thin films by pulsed laser deposition (*Invited Paper*)

Tsuyoshi Ohnishi, National Institute for Materials Science (Japan)

Pulsed laser deposition is widely used to form complex oxide thin films due to the relatively small deviation in composition between the target and the film. The deviation, although small, is not completely prevented: it highly depends on the ablation conditions. Furthermore, gas pressure affects it in the case of lithium compounds, because lithium is even lighter than oxygen. In other words, the difference in composition between the target and the film is controllable by adjusting these parameters. In this study, we succeeded in the high-rate epitaxial growth of stoichiometric LiCoO₂ films from a lithium-enriched target through composition control.

9364-21, Session 4

Metal oxides single-walled carbon nanotube macrofilms-based lithium-ion batteries (*Invited Paper*)

Zeyuan Cao, Univ. of Delaware (United States); Bingqing Wei, Univ. of Delaware (United States) and Northwestern Polytechnical Univ. (China)

Lithium ion batteries are one of the most significant energy storage components in the current information age of human history. They are playing an essential role in various applications from portable electronic devices to hybrid electric vehicles and smart stationary grids. To build better batteries with higher energy and power densities for the increasing demands of emerging technologies, nanostructured metal oxide materials have been extensively investigated and developed as both cathodes and anodes. They have exhibited many unique characteristics within nanoscale such as a large surface area, a shortened lithium diffusion length and effectively enhanced electrochemical activity. Based on the electrode reactions, the oxides can be divided into two groups. The classical layered oxides represent one group, the mechanism of lithium reactivity of which is attributed to lithium ion intercalation and deintercalation, such as vanadium pentoxide (V₂O₅) with a high valence that undergoes a series of complicated structural transformation behavior during the lithiation/delithiation processes. Another group is a big family of transition-metal oxides (MO, where M is Cu, Fe, Co, and Ni) which experience a different conversional reaction where metal atoms would be reduced and oxidized by lithium ions. However, they also suffer delicate challenges. The specific capacity is typically restricted by poor electronic and ionic conductivity and the lifespan is limited by the cyclic instability resulted from structural deformation such as phase transition by lithium alloying as well as formation and growth of passivation layers such as solid electrolyte interlayers. In order to overcome these shortcomings, we have combined a variety of oxides with single walled carbon nanotube (SWNT) macrofilms, which have been previously demonstrated to exhibit a superior conductivity, high chemical stability, binder-free mechanical robustness, and excellent flexibility. In this invited talk, we will present a brief review of V₂O₅/SWNT, Cu_xO_y/SWNT, iron oxides (Fe₂O₃, Fe₃O₄)/SWNT representatives of such composite systems regarding the synthesis, characterization, electrochemical performance, and kinetics analysis.

9364-22, Session 4

Hybrid TiO₂-graphene and TiO₂-multi wall carbon nanotubes below the percolation threshold as high-efficiency electrode in excitonic solar cells (*Invited Paper*)

Kadiatou Therese Dembele, Institut National de la Recherche Scientifique (Canada); Gurpreet S. Selopal, Riccardo Milan, Univ. degli Studi di Brescia (Italy); Charles Trudeau, ETS (Canada); Afsoon Soudi, Institut National de la Recherche Scientifique (Canada); Marta Maria Natile, Univ. degli Studi di Padova (Italy); Giorgio Sberveglieri, Univ. degli Studi di Brescia (Italy); Sylvain G. Cloutier, Ecole de Technologie Supérieure (Canada); Isabella Concina, Univ. degli Studi di Brescia (Italy); Federico Rosei, Univ. du Québec (Canada); Alberto Vomiero, Univ. degli Studi di Brescia (Italy)

We demonstrate a fast, scalable and effective strategy for the assembly of hybrid organic-inorganic graphene- and multi wall carbon nanotubes-TiO₂ nanoparticles composites to be applied as high efficiency electrodes in dye sensitized solar cells (DSSCs). Amounts of graphene or carbon nanotubes below the percolation threshold, conformally dispersed inside a TiO₂ nanoparticles network, result in dramatic enhancement of DSSC functional performances, guaranteeing solar to energy conversion efficiency systematically as high as 9%. Scanning electron microscopy analysis demonstrates a conformal coverage by TiO₂ nanoparticles on graphene sheets (carbon nanotubes), which preserves the compactness of the photoanode, critical for charge transport, while 2D Raman spectroscopy allows the monitoring of spatial distribution of carbonaceous materials inside the metal oxide scaffold.

A rational understanding of device behavior is provided by electrochemical impedance spectroscopy: according to the composition of the hybrid composite, chemical capacitance is increased and recombination resistance diminished (for high amounts of graphene/carbon nanotubes), thus indicating that a careful design of materials is critical for the fabrication of high efficiency devices, whose performances are boosted by an increase in electron lifetime and the preservation of the energy position of anode conduction band, which is downshifted when high amounts of graphene/carbon nanotubes are integrated in the metal oxide scaffold. Adopted approach allowed not only to greatly overcome previous achievements in term of device functional performances for similar anode configurations, but also to rationally understand the electrical mechanisms behind the behavior of hybrid organic-inorganic composited in excitonic solar cells.

9364-23, Session 5

Engineering metal oxide semiconductors for excitonic solar cells (*Invited Paper*)

Alberto Vomiero, Univ. degli Studi di Brescia (Italy)

The typical photoanode in dye- and quantum dot- sensitized solar cells is composed of a wide band gap semiconductor, which acts as electron transporter for the photoelectrochemical system. Anatase TiO₂ nanoparticles are one of the most used oxides and are able to deliver the highest photoconversion efficiency in this kind of solar cells, but intense research in the last years was also addressed to ZnO and other composite systems. Modulation of the composition and shape of nanostructured photoanodes is key element to tailor the physical chemical processes regulating charge dynamics and, ultimately, to boost the efficiency of the end user device, by favoring charge transport and collection, while reducing charge recombination. We investigated several systems: (i) TiO₂ nanoparticles / ZnO nanowires [1]; (ii) Multiwall carbon nanotubes (MWCNTs) / TiO₂ nanoparticles; (iii) TiO₂ nanotubes [2]; (iv) Hierarchically self-assembled ZnO sub-microstructures [3]. Both dye molecules and

**Conference 9364:
 Oxide-based Materials and Devices VI**

semiconducting quantum dots were applied as light harvesters. Possible tailoring of structure and morphology of the photoanodes, and their implication in improving the functional properties of these kinds of excitonic solar cells will be discussed in detail.

References

- [1] A. Vomiero, I. Concina, M.M. Natile, E. Comini, G. Faglia, M. Ferroni, I. Kholmanov, G. Sberveglieri, *Applied Physics Letters* 95 (2009) 193104.
 [2] A. Vomiero, V. Galstyan, A. Braga, I. Concina, M. Brisotto, E. Bontempi, G. Sberveglieri, *Energy and Environmental Science* 4 (2011) 3408–3413.
 [2] N. Memarian, I. Concina, A. Braga, S. M. Rozati, A. Vomiero, G. Sberveglieri, *Angewandte Chemie In Ed* 50 (2011) 12321-12325.

9364-24, Session 5
ZnO-based semiconductors with tunable band gap for 3rd-generation solar cells
(Invited Paper)

Naho Itagaki, Kyushu Univ. (Japan)

ZnO is a remarkable material with a distinctive property set and a huge range of applications. Recently, some research has been directed towards development of ZnO based materials with smaller band gap, which allow light emission/absorption over a broad spectrum from the UV to the visible. In this context, we have developed a new compound, ZnInON (ZION), which is a pseudo-binary alloy of ZnO with InN. Since both ZnO and InN have the same wurtzite crystal structure and different band gaps (ZnO: 3.4 eV; InN: 0.7 eV), the mixed crystal may possess wide-range tunability of the band gap. Here, we report the physical properties of ZION synthesized by RF magnetron sputtering. The advantages of ZION as light-absorbing layers of multi-quantum-well (MQW) solar cells, the theoretical efficiency of which is over 50 %, are discussed in this paper.

From XRD analysis, ZION is deduced to be a pseudo-binary system of wurtzite ZnO and wurtzite InN. Optical measurements revealed the tunability of the band gap that covers the entire visible spectrum as well as the high optical absorption coefficient of 10^5 cm^{-1} . Furthermore, we found advantages of ZION in terms of applications in multi-quantum-well (MQW) solar cells. The lifetime of photo-generated carriers in QWs has been significantly increased by using ZION instead of conventional GaAs-based materials, owing to the large piezoelectric field (several MV/cm^{-1}) that separate electrons and holes. These results indicate that ZION is a promising material that opens new pathways for realizing 3rd generation solar cells with very high efficiency.

9364-26, Session 5
Design of ZnO charge carrier layers for efficient solid-state perovskite-sensitized solar cells

Thierry Pauporté, Jie Zhang, Ecole Nationale Supérieure de Chimie de Paris (France)

Zinc oxide is a n-type semiconductor with a wide bandgap of 3.3 eV that can be prepared at low temperature from solution with controlled conductivity and (nano)structure. Its use as electron carrier layer in Perovskite-Sensitized Solar Cells (PSSC) has attracted recently much attention. The preparation of lead iodide perovskite/ZnO composite layers by impregnation and chemical conversion of a precursor soaking various ZnO structured films is presented. These layers have been used as photoelectrodes in excitonic solid-state solar cells with the structure: ZnO/perovskite $\text{CH}_3\text{NH}_3\text{PbI}_3/\text{Spiro-OMeTAD}/\text{Ag}$. Well-conducting ZnO layers are electrodeposited in chloride medium and grown with tailored (nano) structures ranging from arrays of nanowires to a compact film. Moreover, the effect of a thin intermediate overlayer of ZnO conformally electrodeposited in nitrate medium and with a low n-type doping (i-ZnO) is discussed. Planar

i-ZnO structures have also been investigated. Our results show higher power conversion efficiencies for the nanostructured perovskite/oxide composite layers compared to the dense one. Moreover, we show that the presence of the i-ZnO layer in contact with the perovskite improves markedly the cell short circuit current and the open-circuit voltage due to charge recombination reduction. For the best cells, the active layers efficiently absorb light over a large spectral range from near-UV to near infra-red region and exhibit excellent charge collection efficiencies. Solar cells based on an optimized design generate a very large photocurrent and a power conversion efficiency above 10%.

9364-27, Session 6
Characterization of shallow traps in ZnO by charge-based deep level transient spectroscopy
(Invited Paper)

Cuong Ton-That, Laurent L. C. Lem, Matthew R. Phillips, Univ. of Technology, Sydney (Australia); Frédéric Reisdorffer, Thien-Phap Nguyen, Institut des Matériaux Jean Rouxel (France); Christian Nenstiel, Axel Hoffmann, Technische Univ. Berlin (Germany)

Charge-based deep level transient spectroscopy (Q-DLTS) has been used to investigate shallow traps in a- and c-plane ZnO crystals (grown hydrothermally by MTI Corp.). Gold Schottky contact pads with a thickness of 150 nm were deposited by thermal evaporation on one face of the crystal through a shadow mask, while In ohmic contact was established on the opposite face. Q-DLTS spectra were obtained from the ZnO/Au diodes at various temperatures up to 300 K. Both diodes of a- and c-plane ZnO show a broad Q-DLTS peak at relatively low temperatures, suggesting a complex distribution of shallow interface traps. Arrhenius plots of the Q-DLTS data reveal an average activation energy of 23 meV and 19 meV for a- and c-plane ZnO crystals, respectively. Their capture cross-sections are similar, in the range of $10^{-17} - 10^{-16} \text{ cm}^2$. Doping the ZnO crystals with hydrogen by plasma annealing did not affect this interface trap but introduced a new trap designated E11 with an activation energy of 11 meV. The formation of E11 trap coincides with an increase in the electron density from 4.4×10^{15} to $7.1 \times 10^{17} \text{ cm}^{-3}$. Temperature-resolved photoluminescence (PL) reveals a strong enhancement of the emission at 3.336 eV in H-doped ZnO, attributable to Y-line structural defects. This Y-line emission exhibits Arrhenius-like thermal quenching behaviour with a thermal activation energy of 11 meV, consistent with the E11 trap depth. Based on a multitude of Q-DLTS and luminescence results, it can be concluded that Y-like defects act like an electron trap.

9364-28, Session 6
Experimental observation of doping-induced defects in ZnO

Norbert H. Nickel, Nicole Karpensky, Marc A. Gluba, Helmholtz-Zentrum Berlin für Materialien und Energie GmbH (Germany)

Zinc oxide (ZnO) is attracting a lot of interest because of its electrical and optical properties for a variety of applications ranging from UV light emitting diodes and lasers to transparent conducting electrodes. For most applications reliable doping is essential to control properties of films and devices. Dopants introduced at low concentration substitute Zn or O host atoms thereby mainly changing the electrical properties of the host lattice. However, for applications such as transparent conductive electrodes and for attempts to achieve stable p-type ZnO doping concentrations exceeding 10^{20} cm^{-3} are commonly used.

In this paper, we show experimentally that the introduction of donors and acceptors into the ZnO lattice results in the formation of localized defects in the optical band-gap. For this purpose undoped, nitrogen -, and aluminum - doped ZnO layers were grown on sapphire substrates and

**Conference 9364:
 Oxide-based Materials and Devices VI**

single crystal ZnO using pulsed laser deposition. Al doping was achieved by fabricating ceramic ZnO:Al targets with an Al concentration of up to 4 at.%, while N-doping accomplished by microwave assisted plasma dissociation of N₂O. The samples were characterized with photothermal deflection spectroscopy (PDS), which is a sensitive method to measure the sub band-gap absorption coefficient. Al and N-doping resulted in an increase of the sub band-gap absorption coefficient by more than a factor of 2 in a broad energy range. Al-doping results in a significant broadening of the band tail. For N-doping an absorption peak occurs at E-ET = 0.88 eV and changes with the N concentration. The data indicate that this peak might be due to substitutional N.

9364-29, Session 6

High-temperature photoluminescence and absorption of undoped ZnO single crystals and thin films (Invited Paper)

Samuel Margueron, Univ. de Lorraine (France); David R. Clarke, Harvard Univ. (United States)

The photoluminescence of undoped ZnO single crystals up to 1350°C and the optical absorption of stress-relaxed, epitaxial ZnO thin films up to 1100°C are reported. The photoluminescence intensity and power dependence with illumination flux are related to the crystal growth methods and stabilize after high temperature annealing. Zero Phonon Line model reproduces the shift and the band gap narrowing as well as the free excitonic transition up to the cross-over with a defect level at 2.83 eV that occurs at 800°C. A phenomenological model of the photoluminescence band shape, taking account exciton-phonon losses and defect levels provides an excellent fit up to 2.2-2.4 eV (1100°C). At these cross-over temperatures, an energy transfer is observed between the free exciton transition and defect transitions. However, at temperature above 1100°C, the decrease of the band gap and the increase of thermal radiation, as well as the restrictions of our experimental set-up and particularly the illumination flux of the exciting laser, limit the analysis of the photoluminescence spectra measurements.

9364-30, Session 6

The impact of time-varying phosphorus doping on ZnMgO thin films and achievement of dominant acceptor-bound-exciton peak

Shantanu Saha, Saurabh Nagar, Subhananda Chakrabarti, Indian Institute of Technology Bombay (India)

We report on the achievement of p-type Zn_{1-x}Mg_xO (x=0.15) by doping phosphorus ions and varying the implantation time from 10 to 70 seconds. Plasma Immersion Ion Implantation was used to implant phosphorus ions on ZnMgO thin films deposited over Si substrate by RF sputtering. The samples were subsequently annealed at 700, 800, 900 and 1000°C. Temperature dependent photoluminescence (PL) measurements revealed the dominant acceptor-bound-exciton (A[°]X) peak at 3.36 eV. With increasing implantation time the intensity of the A[°]X peak was found increasing. The increased acceptor concentration in the films might be due to the formation of shallow acceptor levels due to phosphorus implantation. The best optimized parameter was found for sample implanted for 70 seconds, followed by annealing at 800°C. This sample exhibited dominant A[°]X peak for all the implanted samples. The peak position got red-shifted with increasing temperature which possibly occurs due to lattice dilation or carrier localization effect. Although the as-implanted samples revealed this acceptor peak at 3.33 eV but after annealing this peak was found at 3.36 eV which might be due to the fact of substitution of Zn into Mg at high annealing temperature because Mg has lower ionic radius (0.57Å) than Zn (0.60Å). Free exciton peak and inelastic exciton-exciton scattering peak were found at 3.37 and 3.66 eV respectively. The as-grown sample also

revealed the Branch point energy and 1H peak at 3.52 and 3.59 respectively. DST, India is acknowledged.

9364-31, Session 6

Nitrogen dopants in ZnO nanowires (Invited Paper)

Cuong Ton-That, Laurent L. C. Lem, Univ. of Technology, Sydney (Australia); Bruce Cowie, Australian Synchrotron (Australia); Matthew R. Phillips, Univ. of Technology, Sydney (Australia)

X-ray absorption near-edge spectroscopy and cathodoluminescence spectroscopy have been used to investigate the chemical states of nitrogen species incorporated in the ZnO nanowires. It was established that nitrogen plasma annealing produces three N-related defects in the nanowires: NO, free N₂ that is loosely bound to the ZnO lattice and (N₂)Zn. and that N₂ incorporation increased with plasma annealing time. The work establishes a direct link between a donor-acceptor pair (DAP) emission at 3.24 eV and the concentration of molecular N₂, suggesting that this N acts as a shallow acceptor.

9364-32, Session 6

Improvement of photoluminescence and lasing properties in ZnO submicron spheres by eliminating surface-trapped states

Hsu-Cheng Hsu, Tsen-Fang Dai, Wei-Chih Hsu, National Cheng Kung Univ. (Taiwan)

We report the enhancement of photoluminescence and laser action behaviors of ZnO submicron spheres fabricated by the sol-gel process. The influences of annealing treatment on the crystal structure of the ZnO micro-spheres were investigated. The intensity of UV emission becomes stronger as annealed temperature gradually increases. For the as-grown sample, the FX emission peak position is centered at 3.29 eV, which is slightly large compared with the FX emission in bulk ZnO due to the quantum confinement effect. After annealing, the FX emission is red-shifted due to enlargement of the nanocrystallites. Moreover, an enhancement of the intensity ratio of the UV emission to the visible emission and the decrease of the full width at half maximum of the UV emission intensity as a function of annealed temperature indicate that the ZnO microstructures have superior optical quality after performing annealing. When the pulsed excitation intensity exceeds certain threshold, sharp lasing peaks appear. The lowest lasing threshold value is two orders of magnitude lower than that of the similar ZnO micro-spheres grown by the sol-gel route and also is competitive with that of other ZnO structures grown by high-cost vacuum techniques or hybrid structures. The lasing threshold gradually decreases as annealed temperature increases, consistent with the result of the ratio of surface-trapped exciton to donor-bound exciton emissions at low temperature. X-ray photoelectron spectroscopy confirmed adsorbed OH bonds play critical roles of the trapping species of exciton at the ZnO surface. The superior optical properties of high-annealing ZnO mainly result from the elimination of the surface-trapped state.

9364-79, Session 6

Pronounced mobility change in MBE-grown ZnO thin-films after illumination (Invited Paper)

Adam R. Hyndman, Alana M. Hyland, Martin Allen, Roger J.

**Conference 9364:
 Oxide-based Materials and Devices VI**

Reeves, MacDiarmid Institute for Advanced Materials and Nanotechnology, Univ. of Canterbury (New Zealand) and Univ. of Canterbury (New Zealand)

In this paper we show that the electrical mobility of high quality ZnO films grown by plasma assisted molecular beam epitaxy varies significantly after both, UV and ambient room light exposure. Single field (0.51 T) Hall Effect measurements with the Van Der Pauw contact geometry showed typical mobilities for our films of 70 cm²/Vs. However, when left in a dark environment for a week the mobility of all our samples decreased dramatically to less than 10 cm²/Vs. We found that by exposing these samples to low intensity ambient room light we were able to restore the majority of the loss in mobility and that further illumination with UV light (365 nm) enhanced the mobilities up to 120 cm²/Vs. These results suggest more consideration of light exposure needs to be taken when measuring the mobility of ZnO thin films. In addition we will present results from our current investigations on the mechanisms responsible for the change in mobility and its effect on UV photodiode performance.

9364-33, Session 7

Optical Properties of One-dimensional Disordered Multilayer Photonic Structures
(Invited Paper)

Francesco Scotognella, Politecnico di Milano (Italy); Alessandro Chiasera, CNR-Istituto di Fotonica e Nanotecnologie (Italy) and Univ. degli Studi di Trento (Italy); Luigino Criante, Istituto Italiano di Tecnologia (Italy) and Politecnico di Milano (Italy); Stefano Varas, CNR-Istituto di Fotonica e Nanotecnologie (Italy) and Univ. degli Studi di Trento (Italy); Ilka Kriegel, Politecnico di Milano (Italy); Michele Bellingeri, Univ. degli Studi di Parma (Italy); Giancarlo C. Righini, Istituto di Fisica Applicata Nello Carrara (Italy); Roberta Ramponi, Politecnico di Milano (Italy); Maurizio Ferrari, CNR-Istituto di Fotonica e Nanotecnologie (Italy)

The investigation of the differences between ordered and disordered materials (in the hundreds of nanometer lengthscale) is a crucial topic for a better understanding of light transport in photonic media. Here we study the light transmission properties of 1D photonic structures in which disorder is introduced in two different ways.

First, we grouped the high refractive index layers in clusters, randomly distributed within layers of low refractive index. We control the maximum size of such clusters and the ratio of the high-low refractive index layers (here called dilution). We studied the total transmission of the disordered structure within the photonic band gap of the ordered structure as a function of the maximum cluster size, and we observe a dip of the total transmission for a specific maximum cluster size. This value increases with increasing dilution. Moreover, within one dilution we observe oscillations of the total transmission with increasing cluster size.

Second, we realized structures with a random variation of the layer thickness. The structures were fabricated by rf-sputtering technique. The transmission spectrum of the disordered structure was simulated by taking into account the refractive index dispersion of the materials, resulting in a good agreement between the experimental data and the simulations. We found that the transmission of the photonic structure in the range 300-1200 nm is lower with respect the corresponding periodic photonic crystal.

This study envisages the use of disordered 1D photonic structures for the modelization and realization of broad band filters and light harvesting devices.

9364-34, Session 7

Photonic glass-ceramics: consolidated outcomes and prospects
(Invited Paper)

Maurizio Ferrari, Istituto di Fotonica e Nanotecnologie (Italy); Brigitte Boulard, Univ. du Maine (France); Van T. T. Tr?n, Univ. of Natural Sciences (Viet Nam); Anna Lukowiak, Institute of Low Temperature and Structure Research (Poland); Adel Bouajaj, Ecole Nationale des Sciences Appliquées de Tanger (Morocco) and Univ. Abdelmalek Essaâdi (Morocco); Rogéria R. Goncalves, Univ. de São Paulo (Brazil); Andrea Chiappini, Istituto di Fotonica e Nanotecnologie (Italy); Alessandro Chiasera, Istituto di Fotonica e Nanotecnologie (Italy); Wilfried Blanc, Univ. de Nice Sophia Antipolis (France); Alicia Durán, Spanish National Research Council (Spain); Sylvia J. Turrell, Univ. des Sciences et Technologies de Lille (France); Francesco Prudeniano, Politecnico di Bari (Italy); Roberta Ramponi, Politecnico di Milano (Italy); Marian Marciniak, National Institute of Telecommunications (Poland); Giancarlo C. Righini, Centro di Studi e Ricerche “Enrico Fermi” (Italy) and MipLAB. IFAC - CNR (Italy)

Transparent glass-ceramics are nanocomposite materials which offer specific characteristics of capital importance in photonics. This kind of two-phase materials is constituted by nanocrystals embedded in a glass matrix and the respective composition and volume fractions of crystalline and amorphous phase determine the properties of the glass-ceramic. Among these properties transparency is crucial, in particular when confined structures, such as dielectric optical waveguides and optical fibers, are considered, and the number of papers devoted to this topic is continuously increasing. Another important point is the role of the nanocrystals when activated by luminescent species, as rare earth ions, and their effect on the spectroscopic properties of the glass-ceramic. The presence of the crystalline environment around the rare earth ion allows high absorption and emission cross sections, reduction of the non-radiative relaxation thanks to the lower phonon cut-off energy, and tailoring of the ion-ion interaction by the control of the rare earth ion partition. This last point is crucial and still object of intense experimental and theoretical studies. The composition of the glass matrix also impacts the properties of the rare earth ions located in nanoparticles. Moreover, some kinds of nanocrystals can play as effective rare earth sensitizers. Fabrication, assessment and application of glass-ceramic photonic systems, especially waveguides, deserve an appropriate discussion which is the aim of this paper, focused on luminescent glass-ceramics. In this work, a brief historical review, consolidated results and recent advances in this important scientific and technological area will be presented, and some perspectives will be outlined.

9364-35, Session 7

Guiding properties of zinc oxide-on-silica nanowire array

Igor V. Melnikov, Dmitry G. Gromov, Mikhail Y. Nazarkin, Andrey A. Machnev, Alexey S. Shuliatyev, National Research Univ. of Electronic Technology (Russian Federation); Andrey E. Mironov, J. Gary Eden, Univ. of Illinois at Urbana-Champaign (United States)

Versatile coupling silica fibers to ZnO nanowires offers a reliable research tool for optical, both linear and nonlinear, properties of nanowires, however, coupling ZnO nanowire and a standard fiber has not been addressed so far, to the best of our knowledge. In this Report, we successfully monitor the growth of ZnO nanowires on the tip of a standard single-mode fiber by means of fiber reflection spectroscopy and scanning electron microscopy

**Conference 9364:
Oxide-based Materials and Devices VI**

(SEM) and also study optical properties in details.

The procedure exploited to create an array of ZnO nanowires on the tip of a single-mode optical fiber is based on a standard technological procedure. In order to provide required level of the surface quality, the magneto-sputtering of 30-nm ZnO film is executed immediately after the fiber (SMF-28 Corning) cleaving. This film serves as a catalyst for ZnO nanowires to grow and also provides proper adhesion and ordering for the structure to be created. In the next step, a low-temperature chemical deposition is exploited to create an array of ZnO nanowires. The solution, has a concentration of 0.01 M of Zn (NO₃)₂·6H₂O a 0.4 M of NaOH, and pH of this solution is equal 13.2. It is kept for ten minutes in a water bath heated to 80°C, and the tip of the fiber is immersed into it and kept there for twenty minutes. The fiber with ZnO nanowires grown on its end is cleaned in a de-ionized water and then air-dried. The length of the nanowires is equal 800 nm, diameter varies from 50 to 90 nm, and surface density is 5x10 cm², correspondingly.

In the next step, the transmission and reflection spectra of the fiber that comprises a bundle of ZnO nanowires grown on its cleaved facets, are studied using experimental setup as follows. The output of the Er³⁺ broadband source MPB EBS-7210 is launched into one piece of SMF-28 followed by a circulator and another length of the SMF-28 that has ZnO nanowires on its facet and is connected by means of an adapter to the optical spectrum analyzer AQ6370 by Yokogawa. The circulator is introduced into the set-up in order the reflection spectrum to be analyzed simultaneously.

The reflection spectra are measured for the clean cleaved facet, facet with a seed layer of ZnO on its cleaved surface, and with ZnO nanowires that are being grown on this cleaved facet, correspondingly, and the reflection spectrum is analyzed in the report. What is even more, we also present here spectra for both the seed layer and nanowire array grown on the fiber tip immersed into a liquid. It is readily seen a profound asymmetry in the reflection spectrum that does not match the transmission one hence making a temptation to claim an observation of surface polaritons excited along the ZnO nanowires. Further basic measurements that are again the spectral measurement but with tilt and variable spacing introduced between the nanowires and collecting fiber confirm this assumption.

In conclusion, measurements of the transmission and reflection spectra of the single-mode optical fiber that end facet is modified by a disordered (but yet controllable) array of ZnO nanowires, exhibit spectral asymmetry of the reflection due to the excitation of surface polaritons that propagate along the surface of the nanowire. The behavior reported here is of interest for the implementation of new sub-wavelength optical waveguides.

9364-36, Session 7
Mechanisms of direct laser writing on a tailored silver-containing zinc phosphate glass: dual-color laser writing, UV post-illumination thermal influence, and sub-diffraction structures

Yannick G. Petit, Institut de Chimie de la Matière Condensée de Bordeaux (France); Konstantin Mishchik, Lab. Ondes et Matière d'Aquitaine (France); Nadezda Varkentina, Univ. Bordeaux 1 (France); Arnaud Royon, Lab. Ondes et Matière d'Aquitaine (France); Nicolas Marquestaut, Etienne Brasselet, Univ. Bordeaux 1 (France); Thierry Cardinal, Institut de Chimie de la Matière Condensée de Bordeaux (France); Lionel S. Canioni, Univ. Bordeaux 1 (France)

Phosphate glasses provide a very good solubility for silver ions, leading to an enhanced photosensitivity that allows very interesting behaviors under femtosecond direct laser writing (DLW). In particular, laser structuring such glasses leads to strong and 3D localized optical contrasts of both linear and nonlinear optical properties, such as the fluorescence emission from silver clusters or the enhanced third-harmonic generation [1]. More recently, we

have also demonstrated a strong and perennial second-harmonic generation in such glasses, originating from a laser-induced intense static electric field (up to 108-9 V/m) buried inside the glass bulk. The resulting electro-optic coupling process leads to a unique effective second-order nonlinearity (estimated to 0.6 pm/V), opening the way to nonlinear photonic devices [2].

In order to better understand the mechanisms at play during DLW, but also to enlarge our abilities for material structuring, we have applied additional external constraints either simultaneously or successively to the laser writing process. Namely, we have performed dual-color DLW, which leads to the promising feedback control of the laser writing efficiency for STED-like approaches for sub-diffraction 3D laser patterning. Finally, thermal influence on laser structuring is also presented [3], to discuss the tailoring of the mechanisms at play during DLW in our silver-containing phosphate glass, and to better control the laser/matter interaction [4] for future laser-manufactured photonic applications such as composite metal-dielectric materials with plasmonic properties or artificial materials.

[1] A. Royon et al., "Femtosecond Laser Induced Photochemistry in Tailored Materials," *Opt. Mat. Expr.* 1(5), 866-882 (2011).

[2] G. Papon et al., "Femtosecond single-beam direct laser poling of stable and efficient second-order nonlinear optical properties in glass," *Appl. Phys. Lett.* 96, 113103 (2014).

[3] N. Marquestaut, Y. Petit, A. Royon, T. Cardinal, and L. Canioni, "3D silver nanoparticles formation using femtosecond laser irradiation in phosphate glasses: analogy with photography," *Adv. Funct. Mat.* (2014) – Accepted: to appear in press.

[4] K. Mishchik, Y. Petit, E. Brasselet, I. Manek-Hönninger, N. Marquestaut, A. Royon, T. Cardinal, and L. Canioni, "Femtosecond laser processing of silver-containing glass with optical vortex beams," *Proc. SPIE 8974, Advanced Fabrication Technologies for Micro/Nano Optics and Photonics VII*, 897405 (2014).

9364-37, Session 7
Towards high-quality LiNbO₃ and LiTaO₃ thin films (*Invited Paper*)

Ausrine Bartasyte, FEMTO-ST Institute, Univ. of Franche-Comté, CNRS (France); Valentina Plausinaitiene, Arturas Abrutis, Vilnius Univ. (Lithuania); Samuel Margueron, Lab. Matériaux Optiques, Photonique et Systèmes, Univ. Lorraine and Supelec (France); S. Huband, Pamela A. Thomas, The Univ. of Warwick (United Kingdom)

LiNbO₃ (LN) and LiTaO₃ (LT) are two of the most important crystals in the field of optics, nonlinear optics, optoelectronics and acoustics. Thus, LN and LT thin films are attracting interest due to miniaturization and integration of devices into silicon technologies. The deposition of LN and LT thin film by different techniques has been studied for more than twenty years. However, the high quality LN films suitable for acoustic and optic applications are not available at present. First of all, alternative methods to standard $\theta/2\theta$ spectra of X-ray diffraction (XRD) have to be used to identify the presence of parasitical phases in the films [1], which were rarely considered in the literature. One more difficulty is the estimation and control of Li concentration, the key parameter determining the physical and structural properties of LN and LT, within the films. The methods for the identification of parasitical phases and the estimation of residual stress and Li stoichiometry by means of Raman scattering have been reported [1, 2]. It is known that the structural quality of the films highly affects the physical properties of the films. The most complicating structural factors are twinning and cracking of LN and LT films, which induce high acoustical and optical losses and contribute to the degradation of physical properties. The appearance of in-plane epitaxial variant was reported in numerous literature works. However, only a few groups studied the twinning system in LN films, which presence cannot be identified in standard $\theta/2\theta$ spectra of XRD. Thus, very little known effects of deposition and annealing conditions, non-stoichiometry and residual stresses on the mechanical twin structure in thin films, which might degrade the physical properties considerably, were investigated. It was shown that the twinning contributed significantly

**Conference 9364:
 Oxide-based Materials and Devices VI**

to the stress relaxation in the thick films. The stresses in thin films can alter the mechanical, optical, structural, and electrical properties, which play a direct part in the reliability of devices. Many literature works report high residual stresses in the epitaxial LN and LT films, but the effect of stresses on the physical and structural properties remains not well understood. The significant changes of the in-plane and out-of-plane thermal expansions of LN films due to the clamping by the substrate, which could be useful in the creation of thermally stable surface acoustic wave devices, was recently reported [2]. To be able to tune the thermal expansion of LN films in a controlled way, the relationships between the thermal expansion and the thickness of the film/residual stresses/clamping were studied. Moreover, the inelastic deformation and elastic hysteresis of lattice parameters during the heating-cooling cycles were observed. The residual stresses and thermal expansion of films were highly thickness dependent.

[1] A. Bartasyte, V. Plausinaitiene, A. Abrutis, et al., J. Phys.: Condens. Matter 25, 205901(2013).

[2] A. Bartasyte, V. Plausinaitiene, A. Abrutis, et al., Appl. Phys. Lett. 101, 122902 (2012).

9364-77, Session 7

Enhanced ZnO-stimulated emission-based UV photonics and related applications
(Invited Paper)

Komla Dunyo Nomenyo, Roy Aad, A.-S. Gadalah, Christophe Couteau, Univ. de Technologie Troyes (France); David J. Rogers, Nanovation (France); Vincent Sallet, Univ. de Versailles Saint-Quentin-en Yvelines (France); Gilles Lerondel, Univ. de Technologie Troyes (France)

No Abstract Available

9364-38, Session 8

Metal oxide nanostructures as catalysts and chemical sensors on flexible and solid substrates *(Invited Paper)*

Magnus Willander, Linköping Univ. (Sweden)

A review of our last findings on different metal oxide nano-structures in NiO, CuO, ZnO etc. on different solid substrates but also flexible substrates like paper and textiles will be discussed. The motivation for this is to show how cheap sensors with high selectivity and sensitivity can be done. Photocatalytic degradation will also be analyzed. Finally toxicity of the nano-particles is discussed.

9364-39, Session 8

Surface modification, heterojunctions, and other structures: composing metal oxide nanocrystals for chemical sensors *(Invited Paper)*

Mauro Epifani, Istituto per la Microelettronica e Microsistemi (Italy); Elisabetta Comini, SENSOR Lab, Department of Information Engineering, Brescia University and CNR-INO (Italy); Raül Díaz, IMDEA Energy Institute (Spain); Aziz Genç, Institut de Ciència de Materials de Barcelona, ICMAB-CSIC (Spain); Jordi Arbiol, Institut de Ciència de Materials de Barcelona, ICMAB-CSIC and ICREA (Spain); Teresa Andreu, Catalonia Institute for

Energy Research, IREC (Spain); Pietro Siciliano, Istituto per la Microelettronica e Microsistemi (Italy); Guido Faglia, SENSOR Lab, Department of Information Engineering, Brescia University and CNR-INO (Italy); Joan R. Morante, Catalonia Institute for Energy Research, and Departament d'Electrònica, Universitat de Barcelona (Spain)

The modification of the surface reception properties of nanocrystalline structures is of great interest in environmental, catalysis and energy related applications. For instance, an oxide surface covered with a layer of another oxide opens the possibility of creating the nanosized counterparts of bulk catalytic systems. Relevant examples include TiO₂-V₂O₅ and TiO₂-WO₃, which are active catalysts in a broad range of reactions. The chemical synthesis of the colloidal, nanocrystalline versions of such systems will first be reviewed, by coupling suitable sol-gel chemistry with solvothermal processing. Then, the range of obtained structures will be discussed, with particular focus onto the versatile TiO₂-WO₃ system, capable of providing both WO_x-surface modified TiO₂ and TiO₂-WO₃ heterojunctions. The complex structural evolution of the materials will be discussed, depending on the W concentration. A review of the gas-sensing properties of these systems will be shown. In particular, the surface activation of the otherwise almost inactive pure TiO₂ by surface deposition of V₂O₅ or WO₃-like layers will be highlighted. Addition of the smallest W concentration boosted the sensor response to values comparable to those of pure WO₃, ranging over 2-3 orders of magnitude of conductance variation in presence of ethanol or acetone gases. The same activating effect was found in the case of surface modification by a dense layer of V₂O₅ species. Simple analysis of the sensing data will evidence that the combination of such nanocrystalline oxides results in catalytic activation effects, with exactly opposite trend, with respect to pure TiO₂, of the activation energies and best responses.

9364-40, Session 8

Luminescence of sensitive materials: towards new optical sensing *(Invited Paper)*

Lucile Cornu, Manuel Gaudon, Evgeniy Ilin, Philippe Veber, Alain Garcia, Institut de Chimie de la Matière Condensée de Bordeaux (France); Myrtil Kahn, Yohan Champouret, Lab. de Chimie de Coordination (France); Van-Son Nguyen, Hélène Débéda, Univ. Bordeaux 1 (France); Veronique Jubera, Institut de Chimie de la Matière Condensée de Bordeaux (France)

In the last decades, considerable efforts have been carried out to develop new tools and research efforts in the domain of functionalized materials, for application ranging information, lighting, communication, energy, optical sources or detection [1]. As an illustration, to correlate the optical response of a material to another of its property is possible through the monitoring of the luminescence. The control of the structural symmetry, oxidation state or surface chemistry are tools enabling the chemists to precisely tune the emission. For instance:

- (i) A red to green luminescence switch occurred for manganese doped spinel treated between 1200 °C and 1350 °C. By modifying the stoichiometry, it is possible to change the temperature range of this blue shift [2,3].
- (ii) UV irradiation of cerium doped Indium elpasolite matrix leads to the decrease of the doping element emission in favor of a bright orange emission which results from the reduction of indium. The redox process is reversible under adequate irradiation or heat treatment temperature. The sensitized materials are stable over two decades [4,5].
- (iii) Emission of ZnO are strongly related to synthetic route. Low operating temperature can result in the appearing of surface and bulk defects. Their existence impact not only the emission wavelength but also its stability under specific atmosphere [6,7].

**Conference 9364:
Oxide-based Materials and Devices VI**

Tunable emission properties of these materials make them potential candidates for highly sensitive thermal, gas or photo-sensors.

References

- [1] C. Ronda, *Luminescence, from theory to applications*, (2008) Wiley VCH, Weinheim
- [2] L. Cornu, M. Gaudon, V. Jubera, "ZnAl₂O₄ as potential sensor : variation of luminescence with thermal history," *J. Mater. Chem. C*, 1(34), 5419-5428 (2013).
- [3] L. Cornu, M. Duttine, M. Gaudon, V. Jubera, "Luminescence switch of Mn-Doped ZnAl₂O₄ as thermal sensor", *J Mater Chem C*, submitted (July 2014)
- [4] L. Cornu, M. Gaudon, P. Veber, A. Villesuzanne, A. Garcia, V. Jubera, "Ce-Doped Elpasolite Phase Exhibiting Unusual Reversible Luminescence: A New Photosensor.", *Adv Funct Mater*, submitted (July 2014).
- [5] J. P. Chaminade, A. Garcia, T. Gaewdang, M. Pouchard, J. Grannec, B. Jacquier, "Reversible photoionization process in luminescent Ce³⁺ doped elpasolite-type fluorindates," *Radiat. Eff. Defects Solids*, 135, 137-141 (1995)
- [6] E. Ilin, S. Marre,, V Jubera, C Aymonier, "Continuous supercritical synthesis of high quality UV-emitting ZnO nanocrystals for optochemical applications," *J. Mater. Chem. C* 1(33), 5058-5063 (2013).
- [7] M.L. Kahn, T. Cardinal, B. Bousquet., M. Monge, V. Jubera, B. Chaudret, "Optical properties of zinc oxide nanoparticles and nanorods synthesized using an organometallic method," *ChemPhysChem*, 7(11), 2392-2397 (2006)

9364-41, Session 8

Photocatalytic degradation of Rhodamine B by metal oxide nanocomposites

Rajeswari Ponnusamy, Bharathidasan Univ. (India);
Prabhu S., Jothi Venkatachalam K., Anna Univ. (India);
Sivasubramanian Dhanuskodi, Bharathidasan Univ. (India)

ZnO nanomaterials have been recognized as excellent materials for photocatalytic processes due to their high photosensitivity, high catalytic activity, suitable bandgap, low cost, and environmental friendliness. Because of the photo-corrosion and poor quantum yield caused by the fast recombination rate of photogenerated electron-hole pairs, enhancing the photocatalytic efficiency of ZnO nanomaterials are still a challenge. One of the best ways to reduce the photo-corrosion and undesired recombination rate is by making composites with other metal oxides. In the present study, a facile microwave assisted synthesis route (2.45 GHz, 190° C) was followed for the preparation of ZnO, NiO, SnO₂ nanomaterials and ZnO-NiO, NiO-SnO₂, SnO₂-ZnO (1:1) nanocomposites. XRD reveals the hexagonal phase (ZnO), cubic phase (NiO) and tetragonal phase (SnO₂). The characteristic peaks observed in FTIR at 484, 424 and 622 cm⁻¹ are attributed to Zn-O, Ni-O and Sn-O vibrations respectively. UV-diffuse reflectance spectra show the absorption peaks at 365, 297, 290 nm for ZnO, NiO, and SnO₂ respectively whereas composite materials show overlapping absorption peaks. ZnO shows the highest (100 %) photocatalytic activity against the Rhodamine B dye whereas ZnO-NiO exhibits the appreciable (40 %) catalytic activity among other catalysts. By the formation of p- type and n-type band edge under UV light irradiation, NiO-ZnO composite reduces the electron-hole recombination and photo-corrosion processes. ZnO-NiO nanocomposite can be used as a good photocatalyst for the degradation of organic pollutants.

References:

1. F. Xu, Z. Y. Yuan, G. H. Du, T. Z. Ren, C. Bouvy, M. Halasa, B. L. Su, *Nanotechnology* 2006,17, 588.
2. Yuanhui Zheng, Chongqi Chen, Yingying Zhan, Xingyi Lin, Qi Zheng, Kemei Wei, Jiefang Zhu, *J. Phys. Chem. C* 2008, 112, 10773.
3. Abdul Hameed, Tiziano Montini, Valentina Gombac, Paolo Fornasiero, *Photochem. Photobiol. Sci.* 2009, 8, 677.

9364-42, Session 8

Red persistent luminescence and magnetic properties of nanomaterials for multimodal imaging

Celine Rosticher, Corinne Chaneac, Lab. Chimie de la Matière Condensée de Paris, Univ. Pierre et Marie Curie (France); Bruno Viana, Ecole Nationale Supérieure de Chimie de Paris (France)

We present a new generation of nanotracers with persistent luminescence properties in the red-near IR range for small animal imaging. Silicates, oxysulfides and calcium phosphates nanoparticles doped with transition metal and lanthanide ions were developed in this aim with focus on biocompatibility. CaMgSi₂O₆:Eu²⁺, Dy³⁺, Mn²⁺ compounds synthesized by sol gel method were the starting material for this study and has shown an emission in the red-near infrared range lasting for several hours. Gd₂O₂S:Eu²⁺, Mg²⁺, Ti⁴⁺ nanoparticles, hydrothermally synthesized, were developed as multimodal agents for in vivo optical imaging and MRI imaging. Fully biocompatible calcium phosphates nanoparticles were also obtained. A review and comparison of the different hosts for optical imaging and bimodal (optical and MRI) applications will be presented.

9364-43, Session 8

Strategy for introducing antibacterial activity under ambient illumination in titania nanoparticles

Alexander Hsu, Fangzhou Liu, Yu Hang Leung, Angel P. Y. Ma, Aleksandra B. Djurisic, Frederick C. C. Leung, The Univ. of Hong Kong (Hong Kong, China)

Titanium dioxide (TiO₂) is a wide bandgap (~3.4 eV) semiconductor material which is commonly used as a photocatalyst and antibacterial material. UV illumination with energy similar to the bandgap is often needed to make the material active. It would be favorable for practical applications, if its action can also be activated under ambient. Recently, robust antibacterial action was demonstrated on ZnO nanoparticles under ambient illumination. It was observed that material properties such as defects states and surface conditions play a major role on determining the antibacterial properties. The antibacterial activity of ZnO nanoparticles can be modified by modification with different surfactant molecules.

In this study, we demonstrated robust antibacterial activity under ambient illumination on TiO₂ nanoparticles induced by annealing. It was found that the antibacterial activity could be significantly changed by tuning the annealing temperatures and using different crucibles containing the nanoparticles. Bacterium *Escherichia coli* was used as the model organism in the test. It was observed that although no significant antibacterial activity was observed on the starting material (untreated commercial TiO₂ nanoparticles), the activity increases significantly if the nanoparticles were annealed above 650 °C with crucible lined with copper foil. The survival rate of *E. coli* bacteria approaches to zero if the nanoparticles annealing temperature reaches 850 °C. Under optimized conditions, three different titania nanoparticle samples exhibited antibacterial activity under ambient illumination. This work sheds light on the development of ambient-active antibacterial coating and in particular, on the modification of any TiO₂ material to become ambient-active with a suitable treatment.

9364-78, Session 8

Metal oxides nanowires chemical sensors (Invited Paper)

Elisabetta Comini, A. Bertuna, Univ. degli Studi di Brescia

**Conference 9364:
Oxide-based Materials and Devices VI**

(Italy) and Istituto Nazionale di Ottica (Italy); Dario Zappa, Guido Faglia, Giorgio Sberveglieri, Univ. degli Studi di Brescia (Italy) and Istituto Nazionale di Ottica (Italy)

Easy and cheap growth techniques for the production of nanostructures in a variety of morphologies are constantly proposed by the research community. Metal oxides in forms of nanowires are interesting materials for chemical sensors. Their peculiar morphology assures a high surface to volume ratio necessary to maximize surface related properties like the ones governing chemical sensing transduction principles. Their exceptional crystalline features guarantees stable crystalline and therefore electrical properties over long-term operation, a required quality for an industrial application of any kind of sensor or device in real environments. Metal oxide nanowires were integrated in functional devices for chemical sensing and then tested towards a wide range of chemicals.

Acknowledgements

The research leading to these results has received funding from the European Community's FP7-ICT-2013-10, MSP— Multi-Sensor-Platform for Smart Building Management under the project n° 611887.

9364-44, Session 9

Monolithic integration of complex oxides on semiconductors for new functionalities
(Invited Paper)

Catherine Dubourdieu, Institut des Nanotechnologies de Lyon, CNRS (France)

Oxides exhibit a wide range of electrical, magnetic, optical, mechanical properties, which may even be coupled. This extraordinary wealth of physical properties offers a huge potential for developing new functionalities in devices that can address societal needs related to health, efficient energy or information & communication technologies. Ferroelectrics are particularly attractive for their applications in nanoelectronics, communication devices, electro-mechanical systems or sensors; however, their properties can only be exploited if complex oxide integration can be performed in a seamless manner with semiconductor technologies. The first direct epitaxy of a perovskite (SrTiO₃) on silicon by molecular beam epitaxy in 1998 opened the door to such integration.

We will first review the scientific and technological challenges related to the monolithic integration of complex oxides on a semiconductor. We will then present the epitaxial growth by molecular beam epitaxy of complex oxides on silicon and illustrate how MBE provides unique advantages to precisely construct, almost atom by atom, the oxide/semiconductor interface. With the example of BaTiO₃ on silicon, we will discuss the crystalline structure and domain configuration of ferroelectric heterostructures. Nanoscale characterization of the polarization is realized using advanced transmission electron microscopy and piezoresponse force microscopy methods. Size effects on the ferroelectric properties will be addressed. Finally, we will conclude with current perspectives for applications of epitaxial ferroelectrics on semiconductors in nanoelectronic and electro-optic devices.

9364-45, Session 9

GaN-on-graphene technology: grow, release, transfer of thin-film GaN devices
(Invited Paper)

Can Bayram, Univ. of Illinois at Urbana-Champaign (United States); Jeehwan Kim, Hongsik Park, Cheng-Wei Cheng, IBM Thomas J. Watson Research Ctr. (United States); Christos D. Dimitrakopoulos, Univ. of Massachusetts Amherst (United States); John Ott, Kathleen Reuters, Stephen W. Bedell, Devendra K. Sadana, IBM Thomas J.

Watson Research Ctr. (United States)

Gallium Nitride semiconductor technology is unique as (1) GaN high electron mobility transistors outperform existing ones in high power and high frequency applications thanks to inherently high critical electric field (~3.5 MV/cm) and saturation velocity (~2.5·10⁷ cm/s), and (2) GaN visible light emitting diodes enable high efficiency deep ultraviolet to visible devices thanks to composition-independent direct-bandgap.

Conventional substrates for GaN epitaxy are sapphire, SiC, and Si that have around 14%, 3%, and 17% lattice-mismatch and 34%, 25%, and 53% thermal-mismatch with GaN, respectively. Among these mainstream substrates, SiC stands out for having the lowest lattice-mismatch, the lowest thermal-mismatch, and the highest thermal-conductivity. However, the \$/cm² for SiC is around an order and more than two orders of magnitude more than sapphire and silicon, respectively, limiting the broader adoption of SiC substrates.

In this work, we show that graphene grown on SiC can be a template for the growth and transfer of single-crystalline films. We, for the first time, demonstrated direct growth of high-quality single-crystalline GaN films&devices on this graphene. The GaN film was released and transferred onto Si substrates. The post-released graphene/SiC substrate was reused for multiple growth and transfer cycles of GaN films. To further this concept, we have grown visible LED structures on graphene/SiC substrates that have been previously used multiple-times. Fully-functional vertical blue LED on plastic was obtained by releasing this heterostructure demonstrating versatility of our technique. This technique could potentially be applied for growing other single-crystalline 3D and 2D materials on graphene and transfer.

9364-46, Session 9

Electrochromism: from oxide thin films to devices
(Invited Paper)

Aline D. Rougier, Institut de Chimie de la Matière Condensée de Bordeaux (France)

In respect of their adaptability and performance, electrochromic devices, ECDs, which are able to change their optical properties under an applied voltage, have received significant attention. Target applications are multifold, both in the visible (automotive sunroofs, smart windows, ophthalmic lenses, domestic appliances..) and in the infrared region (satellites thermal control, IR furtivity). In a standard configuration, ECDs, also described as optical batteries, are based on a 5 layers stack, schematized by TCO/EC/Electrolyte/CE/TCO, in which TCO stands for Transparent Conducting Oxides, EC for Electrochromic material and CE for Counter Electrode. At ICMCB, aiming at improving materials and devices in respect of specific applications modified NiO [1] thin films as counter electrode, ZnO based thin films as transparent conducting layer [2] WO₃ [3] and PEDOT electrochromic layers are particularly studied. In this presentation, we will discuss how we can (i) modulate the materials characteristics in terms of morphology, composition, structure, (ii) adapt the synthesis process to the substrate nature, considering paper, plastic, glass or metal substrate, (iii) evidence new electrochemical reactivity in ionic liquid based electrolytes and (iv) optimize the device architecture in order to improve the ECDs performances.

[1] Improved electrochromic performances of NiO-based thin films by lithium addition : From single layers to devices. H. Moulki, D.H. Park, B.K. Min, H. Kwon, S.J. Hwang, J.H. Choy, T. Toupance, G. Campet, and A. Rougier. *Electrochimica Acta*, 74, 46-52 (2012).

[2] Low Temperature Transparent Conducting Oxides based on Zinc Oxide Thin Films. J. Clatot, G. Campet, A. Zeinert, C. Labrugère, M. Nistor, and A. Rougier. *Solar Energy Materials and Solar Cells*, 95(8), 2357-2362 (2011).

[3] Room Temperature UV treated WO₃ thin films for electrochromic devices on paper substrate, A. Danine, L. Cojocar, C. Faure, C. Olivier, T. Toupance, G. Campet and A. Rougier, *Electrochimica Acta*, 129(20) 113-119 (2014).

9364-47, Session 9

Metal oxide based memristor: from homojunction diode to complementary 1D1R application and bias polarity-induced transformation of filamentary and homogeneous resistive switching with controllable multistate

Yu-Lun Chueh, National Tsing Hua Univ. (Taiwan)

In this talk, we will present the growth of ZnO_{1-X} nanorod arrays (NRs) on a ZnO thin film (TF) as homojunction diode and memory devices, containing uniquely double behaviors, namely rectifying and high performance resistive switching behaviors, depending on the applied voltages simultaneously. The ZnO_{1-X} NRs play as the reservoir for the supplement of oxygen vacancies to reduce the operation voltage, thereby significantly improving the ReRAM device performance. Next, a bias polarity-induced transformation from filamentary to homogeneous resistive switching was demonstrated on a Pt/ZnO thin films/Pt device. Two types of switching behaviors, which exhibit different resistive switching characteristics and memory performances, were investigated in detail. The detailed transformation mechanisms are systematically proposed. By controlling different compliance currents and reset-stop voltages, controllable multistate resistances at LRS and HRS in the ZnO thin films MIM structure under the homogeneous resistive switching were demonstrated. The findings would open up opportunities to explore not only for the resistive switching mechanisms in the metal oxide but also for next generation multistate high performance memristor.

9364-49, Session 10

Tuning the built-in electric field in ZnO-based quantum heterostructures with crystal orientation for optoelectronic applications (Invited Paper)

Jean-Michel Chauveau, Ctr. de Recherche sur l'Hétéro-Epitaxie et ses Applications (France)

The wurtzite wide band gap semiconductors exhibit built-in electric fields along their c-axis, affecting the electronic properties. Therefore the use of the non-polar surfaces is an alternative route to the fabrication of wide quantum wells (QWs) with no reduction of the exciton binding energies as compared to bulk in wide QWs. ZnMgO/ZnO QW heterostructures have attracted much attention due to their opportunity of combining band gap engineering, with large excitonic binding energies. So far studies on ZnO have mainly focused on films grown in c-(0001) orientation. In this presentation, we will demonstrate that the quantum confined Stark effect governs the electronic properties of wide Quantum Wells (QWs) We shall discuss the possible origins of the different values of the electric field found in the literature.

Growing non polar heterostructures represent a very exciting challenge. Unfortunately wide band gap nonpolar QWs grown on sapphire usually exhibit a large density of stacking faults, reducing the emission efficiency [1]. ZnO offers a particularly striking advantage in the field of wide band gap semiconductors: substrates are available in every crystal orientations. We show a drastic improvement of the structural and optical properties when the QWs are grown on ZnO substrates [2-3]. In addition the polarization dependent PL evidences the expected selection rules in these orientations [4]. Then we shall compare the different nonpolar orientations (m- or a-planes). The PL intensity of an m-plane QW is constant as a function of the temperature up to RT with a linear dependence of the decay time as a function of the temperature [5].

Then there is no report on ZnO based quantum heterostructures grown along semipolar orientations, along which the internal electric field can be reduced in nitrides based heterostructures. Therefore we have grown high quality semipolar QWs on (10-12) ZnO bulk substrates. Atomically

flat terraces are observed and no plastic relaxation is detected in such heterostructures. The emission of wider QWs is below the ZnO band gap owing to the presence of an electric field, which can be estimated around 400kV/cm (17% Mg) [6]. The emission is strongly polarized perpendicular to the projection of the c axis on the (10-12) plane, in agreement with the selection rules.

Finally we will present and discuss the possible applications as a function of the crystal orientation (Polarization sensitive photodetectors [7], non and semipolar LEDs,...)

References

- [1] P. Vennegues, et al., J. Appl. Phys. 103 083525 (2008).
- [2] J.-M. Chauveau, et al., App. Phys Lett. 97 081903 (2010)
- [3] J.-M. Chauveau, et al., J. Appl. Phys. 109 102420 (2011)
- [4] L. Beaur, et al., Appl. Phys. Lett. 98 101913 (2011)
- [5] L. Beaur, et al., Phys. Rev. B. 84 165312 (2011)
- [6] J.-M. Chauveau, et al. Appl. Phys. Lett. 103 262104 (2013)
- [7] G. Tabares et al., Appl. Phys. Lett. 99 071108 (2011)

9364-50, Session 10

Progress in NixMg1-xO thin films for optoelectronic applications (Invited Paper)

Jeremy W. Mares, Vanderbilt Univ. (United States); Ryan C. Boutwell, CREOL, The College of Optics and Photonics, Univ. of Central Florida (United States); Sharon M. Weiss, Vanderbilt Univ. (United States); Winston V. Schoenfeld, CREOL, The College of Optics and Photonics, Univ. of Central Florida (United States)

No Abstract Available

9364-51, Session 10

Optical and electrical properties of ZnMgBeO and ZnMgBeGaO thin films sputtered at various growth conditions

Ba Cuong Hoang, Sang-Hun Jeong, Byung-Teak Lee, Chonnam National Univ. (Korea, Republic of)

Recently, it was proposed that the ZnMgBeO and ZnMgBeGaO films would be a potential material for the UV optoelectronic devices, as their Eg values can be continuously modulated from 3.7 to 4.9 eV by changing the concentration of MgO and BeO. As it is well known that the optical and electrical properties of the ZnO-based films are strongly dependent on the growth conditions such as growth temperature (Tg) and growth ambient, in-depth study of the properties and the mechanisms affecting the phenomena would be very interesting and important.

Results indicate that the energy band gap (Eg) of the films drastically decreases and the resistivity of the films drastically increases with the addition of oxygen gas to the Ar plasma. With increasing Tg, the Eg decreases and the resistivity increases. It is observed that the film composition changed with the oxygen addition and/or the Tg increase, leading to the reduced Eg. This might be related to the suppression of the Zn evaporation during the sputtering by the presence of the oxygen. It is also suspected that density of the stoichiometry related point defects would decrease and passivation of the Ga donors would also occur with the oxygen addition, resulting in the reduced free electron concentration. It was suggested that combined effects of these phenomena resulted in the observed reduction in Eg and increase in resistivity by the oxygen addition and/or the Tg increase. Further studies are in progress to understand defect chemistry of the films and the mechanisms affecting the phenomena. Its results and the further details will be discussed during the presentation.

9364-52, Session 10

MOVPE growth of InGaN alloys with high In content on ZnO template substrates
(Invited Paper)

Suresh Sundaram, Renaud Puybaret, Georgia Tech-Lorraine (France); David J. Rogers, Ferechteh H. Teherani, Vinod Eric Sandana, Philippe Bove, Nanovation (France); Youssef El Gmili, Georgia Tech-Lorraine (France); David Troadec, Univ. des Sciences et Technologies de Lille (France); Gilles Patriache, Lab. de Photonique et de Nanostructures (France); Paul L. Voss, Georgia Tech-Lorraine (France); Jean Paul Salvestrini, Georgia Tech-Lorraine (France) and Lab. Matériau Optiques, Photonique et Systèmes (LMOPS) (France); Abdallah Ougazzaden, Georgia Tech-Lorraine (France); Ryan McClintock, Manijeh Razeghi, Northwestern Univ. (United States)

No Abstract Available

9364-80, Session 10

ZnO/ZnMgO multiple quantum well light polarization sensitive photodetectors
(Invited Paper)

Adrian Hierro, Gema Tabares, Elias Muñoz, Univ. Politécnica de Madrid (Spain); Borge Vinter, Ctr. de Recherche sur l'Hétéro-Epitaxie et ses Applications, CNRS (France) and Univ. de Nice Sophia Antipolis (France); Jean-Michel Chauveau, Ctr. de Recherche sur l'Hétéro-Epitaxie et ses Applications, CNRS (France) and Univ. de Nice Sophia Antipolis (France)

We review in this work the application of ZnO/ZnMgO quantum wells to the photodetection of the polarization state of UV light. This photodetection is achieved by using the natural anisotropy that exists in non-polar and semi-polar ZnO/ZnMgO quantum wells, which separates the excitonic absorption from the three valence bands to the conduction band depending on the incident light polarization. The device structures covered here consist of Schottky photodiodes on a-, m- and r-plane orientations, grown by MBE both on sapphire and ZnO substrates, and are analyzed and compared to nitride-based technology, showing the best reported figures of merit.

9364-53, Session 11

(-201) [beta]-Ga2O3 substrate for high optical and structural quality GaN materials
(Invited Paper)

Iman S. Roqan, Mufasila M. Muhammed, King Abdullah Univ. of Science and Technology (Saudi Arabia); Marco Peres, Univ. Técnica de Lisboa (Portugal); Y. Yamashita, Y. Morishima, S. Sato, Tamura Thermal Device Corp. (Japan); N. Franco, K. Lorenz, Instituto de Plasmas e Fusão Nuclear (Portugal) and Instituto Superior Técnico (Portugal); A. Kuramata, Tamura Thermal Device Corp. (Japan)

Producing highly efficient GaN-based optoelectronic devices has been a challenge for a long time due to the large lattice mismatch between

III-nitride materials and the most common substrates, which causes a high density of threading dislocations. Therefore, it is essential to obtain alternative substrates with small lattice mismatches, appropriate structural, thermal and electrical properties and a competitive price. We show that (-201) oriented β -Ga₂O₃ has the potential to be used as a transparent and conductive substrate for high quality GaN. Photoluminescence spectra of GaN epilayer found to be dominated by intense bandedge emission. Atomic force microscopy studies show a modest threading dislocation density of $\sim 10^8$ cm⁻². X-ray diffraction studies show the high quality of the single-phase wurtzite GaN thin film on (-201) β -Ga₂O₃ with in-plane epitaxial orientation relationships between the β -Ga₂O₃ and the GaN film defined by (010) β -Ga₂O₃ || (11-20) GaN and (-201) β -Ga₂O₃ || (0001) GaN leading to a lattice mismatch of $\sim 4.7\%$. The XRD and Raman measurements showed a slight biaxial strain in GaN epilayers. This work shows that β -Ga₂O₃ is a promising substrate for the growth of high-quality GaN films. Under systematically optimized growth conditions, the growth of highly efficient LEDs and LDs based on III-nitrides should be possible and will allow new device designs such as vertically structured LEDs thanks to the increased transparency and high conductivity of bulk β -Ga₂O₃ substrates.

9364-54, Session 11

Ternary and quaternary wurtzite-type oxide semiconductors: new materials and their properties
(Invited Paper)

Takahisa Omata, Osaka Univ. (Japan)

β -NaFeO₂ structure is an orthorhombic wurtzite-derived structure, in which divalent zinc ions in wurtzite ZnO are regularly replaced by monovalent sodium and trivalent iron ions similar to the structural relationship between the zincblende and chalcopyrite structures. β -LiGaO₂, β -AgGaO₂ and β -AgAlO₂ are known as materials possessing the β -NaFeO₂ structure; however, studies on the wurtzite-derived ternary oxide semiconductors are quite limited.

Recently, we demonstrated the band gap engineering of zinc oxide by alloying with wurtzite-type β -AgGaO₂, and we successfully reduced the band gap of ZnO to 2.55 eV [1]. We also found the wurtzite-type β -CuGaO₂ recently. Its energy band gap was 1.47 eV, and it exhibited p-type conduction [2]. The first principle calculation using LDA+U functional indicated that β -CuGaO₂ is a direct semiconductor; therefore it is suitable to use in optoelectronic devices. Taking the 1.47 eV of the band gap and p-type electronic conduction into account, β -CuGaO₂ is a promising material for the absorber in thin film solar cells. The band gap of the wurtzite β -CuGaO₂ can be widened up to 2.1 eV by alloying with CuAlO₂. These new ternary oxide semiconductors possessing wurtzite-derived structure expanded the covering energy region of oxide semiconductors into visible and infrared region.

[1] I. Suzuki, H. Nagatani, Y. Arima, M. Kita, T. Omata, Appl. Phys. Lett., 103, 222107(2013).

[2] T. Omata, H. Nagatani, I. Suzuki, M. Kita, H. Yanagi, N. Ohashi, J. Am. Chem. Soc. 136, 3378(2014).

9364-55, Session 11

Piezoelectric microelectromechanical systems (MEMS) across length scales
(Invited Paper)

Derek Wilke, Margeaux L. Wallace, Chris D. Rahn, Thomas N. Jackson, Susan E. Troler-McKinstry, The Pennsylvania State Univ. (United States); Vincenzo Cotroneo, Harvard-Smithsonian Ctr. for Astrophysics (United States); Dennis M. Newns, Glenn J. Martyna, Thomas N. Theis, IBM Thomas J. Watson Research Ctr. (United States)

**Conference 9364:
Oxide-based Materials and Devices VI**

Piezoelectric thin films are of increasing interest in low voltage microelectromechanical systems (MEMS) for sensing, actuation, and energy harvesting. They also serve as model systems to study fundamental behavior in piezoelectrics. Piezoelectric MEMS devices range over a wide range of length scales. On the extreme upper end are large area devices for applications such as adaptive optics. In this case, the piezoelectric film can be used to produce local deformation of a mirror surface, in order to correct figure errors associated with fabrication of the component or to correct for atmospheric distortion. For example, should a mission such as Gen-X be flown, it would require up to 10,000 m² of actuatable optics in order to correct the figures of the nested hyperboloid reflecting segments. In this case, the "micro" in "microelectromechanical systems" is clearly a misnomer, although the fabrication techniques would involve conventional micromachining for patterning of the electrodes. Many piezoelectric MEMS devices are fabricated at intermediate length scales (tens of microns to 1 cm). Here, examples will be given of piezoelectric energy harvesting devices with integrated electronics. We have recently demonstrated improvements in the energy harvesting figure of merit for the piezoelectric layer by factors of 4 - 10. Finally, piezoelectric MEMS are also attracting attention at a substantially smaller size scale (tens of nm) as a potential replacement for CMOS electronics. Examples of the materials choice as well as specific devices at all three of these length scales will also be discussed.

9364-56, Session 11

Theoretical investigations of Ni- and Cu-doped TiO₂

Esakkimuthuraju Murugan, Mahesh Rajendran, Venugopal Reddy Paduru, Vidya Jyothi Institute of Technology (India); Sreekanth Tirumala, Jawaharlal Nehru Technological Univ. (India)

Understanding the origin of the magnetism in oxide diluted magnetic semiconductors, ODMS, is actually a subject of intensive research and it is greatly enhancing our knowledge of wide band gap room temperature magnetism. Transition metal (TM) doped titanium dioxide, which belongs to these class of materials has been attracting significant research interest in the field of renewable energy and next generation spintronic devices. With a view to study the structural, electronic, magnetic, and optical properties of anatase and rutile forms of TM doped TiO₂ diluted magnetic semiconductor, systematic theoretical investigations have been undertaken. The density of states and band structure calculations are performed for doped TiO₂ and undoped TiO₂ using quantum espresso pw code. For the band gap calculations, we have used both local density approximation (LDA) and generalized gradient approximation (GGA). The magnetic and optical properties of the materials using the above package have been discussed in this paper. These results are useful in understanding the origin of magnetism, band structural variations with doping and other related properties in oxide based diluted magnetic semiconductors such as TiO₂.

9364-57, Session 11

Investigations of p-NiO/n-ZnO heterojunctions grown by pulsed laser deposition

Vinod Eric Sandana, David J. Rogers, Ferechteh H. Teherani, Philippe Bove, Nanovation (France)

No Abstract Available

9364-76, Session 11

Controlling photon emission from Si/SiO_x quantum structures for photonic applications (Invited Paper)

Seref Kalem, TUBITAK-BILGEM (Turkey)

An electron injected optical amplifier is yet to be realized due to the indirect nature of the silicon energy band structure. This emphasizes the importance of a photon source that would be compatible with silicon (Si) circuitry. Ideally, a light emission directly originating from the silicon and a monolithic integration of this source with other silicon components would be the best solution. Indeed, Si can emit in a broad range of spectral region in visible and in near infrared at telecommunication wavelengths. However, these photon sources are mainly related to defects and interface states between Si and SiO_x in related quantum structures. Quantum confinement in reduced dimensions can be another reason for the emission due to an increased electron and hole density of states. In such quantum structures, photon or electron pumping usually results in a fast decay time due to trapping at interface states, leading to a low efficiency of injection. In near infrared, even at telecommunication bands, a photon emission can be obtained from silicon, which are originated from band edge and dislocations. By engineering energy band structure, these emissions can be controlled favoring a certain emission in each structure. One of such control involves the treatment of Si surface by deuterium D, resulting in an emission at 1320 nm. The emission can also be favored in wafers wafers consisting of the following structures: black silicon formed as a result of plasma etching, silicon nanowires (NW) and Si/Ge superlattice and heterostructured NWs. It was shown that the spectral positions can be tuned and their photoluminescence (PL) efficiencies can be controlled by treatment conditions. Some of wafers exhibit a broad visible and near infrared emission bands while others treated under different conditions can reveal single luminescence bands at 1100 nm, 1300 nm or 1550 nm. Single emission bands can also be induced at around 600 nm and 750 nm. The results of time-resolved PL have been combined with those of CW measurements in order to clarify the nature of the observed bands. According to these results, an ultra fast blue component of about 15 picoseconds and a slow state of about 4 nanoseconds in the red region are of typical life times.

9364-58, Session PWed

Photocatalytic degradation of Rhodamine B by C-N-S tridoped TiO₂ nanoparticles

Amreetha Seetharaman, Sivasubramanian Dhanuskodi, Bharathidasan Univ. (India); Nithya A., Jothi Venkatachalam K, Anna Univ. (India)

One of the most intriguing applications of TiO₂ is the degradation of organic pollutants in aqueous solution. C-N-S doped TiO₂ was synthesized using titanium isopropoxide and thiourea as source materials. 15 wt% of thiourea was used for dopants at different calcining temperatures (300, 400, 500 and 600 °C). XRD results show that the C-N-S doping could effectively restrain the phase transformation of anatase to rutile at 600 °C calcination (undoped TiO₂: anatase 14%, rutile 86% and for doped TiO₂: anatase 100%). The crystallite size decreases with the addition of dopants (undoped TiO₂ is 36 and doped TiO₂ is 26 nm). FTIR analysis shows that the peaks at 1384, 1128 and 1051 cm⁻¹ are attributed to N-H bond, bidentate S-O coordination to Ti⁴⁺ and Ti-O-C bond respectively. UV-Vis absorption spectra reveal that the light absorption of doped TiO₂ is redshifted compared to undoped TiO₂. PL spectra were recorded under the excitation wavelengths of 280, 290, 300, 310 and 320 nm. The band edge emission at 390 nm is due to self trapped excitons (STE) which originates by the interaction of conduction band electrons localized on Ti 3d orbital with holes present in O 2p orbital in TiO₂ lattice. The luminescence at 483 nm is due to the oxygen vacancy. Photodegradation of Rhodamine B (RhB) in aqueous suspension under visible light irradiation of C-N-S doped TiO₂ shows higher photocatalytic activity (99%) than that of undoped TiO₂. The excellent

photocatalytic activity is attributed to the small crystallite size and strong light absorption in the visible region.

9364-59, Session PWed

Zinc oxide nanoparticles with controlled properties for application in dye-sensitized solar cells

Thierry Pauporté, Mongia Hosni, Yuly Kusumawati, Ecole Nationale Supérieure de Chimie de Paris (France); Samir Farhat, Noureddine Jouini, Univ. Paris-Nord (France)

The forced hydrolysis in polyol medium is a versatile synthesis method for the preparation of metal oxide particles with controlled properties. ZnO mesoporous film electrodes have been prepared with different types of nanoparticles prepared in polyol medium and having various sizes and morphologies. They have been sensitized by the D149-organic dye and the TG6 Ru-dye. The corresponding dye-sensitized solar cell (DSSC) performances have been investigated. The photoanode dye loadings have been determined. The cells have been studied by I-V curve measurements and by impedance spectroscopy (IS) at various applied voltages. The effects of dye and ZnO particle shape and size on the electron transport and recombination as well as on the electronic structure are analyzed. The best efficiency was as high as 5.3% for the TG6 dye.

[1] M. Hosni, Y. Kusumawati, S. Farhat, N. Jouini, Th. Pauporté, Effects of Oxide Nanoparticle Size and Shape on Electronic Structure, Charge Transport and Recombination in Dye-Sensitized Solar Cell Photoelectrodes, J. Phys. Chem. C, (2014) DOI: 10.1021/jp412772b.

9364-60, Session PWed

Silicon-based heterojunction thin film phototransistor with porous layer for short-wavelength detection at bio-sensing application

Yao-Chin Wang, Bor-Shyn Lin, Ming-Che Chan, National Chiao Tung Univ. (Taiwan)

The paper proposed a silicon-based device with porous-Si / c-Si structures were fabricated and short-wavelength characterized. We showed that the short-wavelength responses in the developed devices were enhanced as compared to the silicon based homojunction transistors; this comparably optical gain indicated that the developed porous-Si / c-Si heterojunction thin film phototransistor got potential for practical Si-based integrated circuit applications. The study proposed a short-wavelength responsivity of the Si-based thin film phototransistor can be enhanced by introducing thin porous layer as the base region of transistor. The porous process of device manufacture is suitable for applications in design of short-wavelength photo sensitive detector. Therefore, the more applications of short-wavelength are the trend for non-invasively bio- medical and sensing application.

9364-62, Session PWed

Graphene nanosheets supported Ag/ZnO hybrid for effective acetylene sensor

A. S. M. Iftekhar Uddin, Gwi-Sang Chung, Univ. of Ulsan (Korea, Republic of)

This paper investigates the acetylene gas sensing properties of graphene nanosheets supported Ag/ZnO hybrid synthesized via a chemical route. Field emission scanning electron microscopy (FESEM), transmission electron microscopy (TEM), energy dispersive spectroscopy (EDS) and X-ray

diffraction (XRD) were used to characterize the morphology and crystal structure of the Gr-Ag/ZnO hybrid. It was shown that the well-dispersed Ag/ZnO nanoparticles (NPs) mixer were deposited on few layer graphene nanosheets homogeneously. Graphene nanosheets supposedly acted as a support catalyst, that may promoted the preferential attachment of the Ag and ZnO NPs, and may prevented the agglomeration of the NPs in the synthesis process. Gas sensing properties of the synthesized hybrid were studied at various operating temperatures (25-250oC) for various concentrations of acetylene gas in air atmosphere and compared with Gr-ZnO composite and pristine ZnO NPs. The Gr-Ag/ZnO hybrid showed two times higher response magnitude than Gr-ZnO composite (18.2) while the pristine ZnO NPs had response value of only 1.3 at optimum temperature of 150oC. The response time of the Gr-Ag/ZnO hybrid was also reduced to 25s from 100s (Gr-ZnO composite). The fabricated sensor device showed excellent selectivity towards other reducing (H₂, CO, CO₂) and oxidizing (NO₂, O₂) gases. This study suggested that Ag NPs is an effective candidate for acetylene detection which may provide challenges and more opportunities in the near future and can be developed by further detailed investigations.

9364-63, Session PWed

Hydrogen sensor based on Pd nanocube-graphene hybrid

Duy-Thach Phan, Faisal Iqbal, Univ. of Ulsan (Korea, Republic of)

Graphene-supported palladium (Pd) nanocubes were synthesized via a simple chemical method for hydrogen sensing. Pd nanocubes were synthesized by chemical route in two-steps (seed-mediated growth). Pd nanocube with highly uniform of 70 nm size in colloidal state were simply reduced into graphene flakes by hydrazine in facile one-step. Resulting in graphene wrapped Pd nanocube were applied as new hydrogen sensing materials with high sensitivity and good selectivity. The resistivity-type sensor used Pd cube-graphene had detectable range from 1000 ppm to 6 ppm with good linearity at room temperature. In comparison with H₂ sensor based pure Pd cube, the Pd cube-graphene had more reliability properties in term of sensitivity, linearity and stability. Moreover, new H₂ sensor based Pd cube-graphene had the sensitivity 2-fold higher than our previous work on Pd nanoparticles-graphene composite. The new Pd nanocube-graphene hybrids are also promising for optically H₂ sensor based on surface plasmon resonance sensing technology.

9364-64, Session PWed

PbOx/Au-Pd core-shell structures for Schottky junction solar cells

Dipal B. Patel, Indrajit Mukhopadhyay, Pandit Deendayal Petroleum Univ. (India)

Since the beginning of the era of third generation solar cells, researchers are motivated to explore various semiconductor-metal configurations for the efficient solar energy conversion. We first time report the use of non-stoichiometric PbOx electrodes in the Schottky junction solar cell. This metal oxide makes an efficient Schottky junction with the high work function alloy of Au-Pd. It was found that the anodized lead metal via potential pulse technique results in the nanowall assemblies. When a few nanometer layer of Au-Pd was sputtered on these assemblies, we obtained a core-shell structure of PbOx/Au-Pd. With these newly developed structures, we obtained highest Jsc of 2.1 mA/cm² with Voc of 600 mV achieving an overall efficiency of 0.38%. The diode was assessed by the two diode model representing a solar cell which takes care of the recombination mechanisms present in the diode. It was found that the trap assisted recombination process dominates the charge transfer mechanism in the diode.

9364-65, Session PWed

Zinc oxide tetrapods as efficient photocatalysts for organic pollutant degradation

Fangzhou Liu, Yu Hang Leung, Aleksandra B. Djuricic, Changzhong Liao, Kaimin Shih, The Univ. of Hong Kong (Hong Kong, China)

Organic pollutants from industrial wastewater have long been a worldwide concern. Organic dyes form a common class of pollutants. In addition, endocrine disruptors, typically Bisphenol-A (BPA), have resulted in increasing risks for both marine environment and public health. Hence developing strategies of effective degradation of BPA and other organic pollutants is imperative. Metal oxide nanostructures, in particular titanium oxide (TiO₂) and zinc oxide (ZnO), have been demonstrated to exhibit efficient photodegradation of various common organic dyes. ZnO tetrapods are of special interest due to their low density of native defects which consequently lead to lower recombination loss and higher photocatalytic efficiency. Tetrapods can be obtained by relatively simple and low-cost vapor phase deposition in large quantity; the micron-scale size would also be advantageous for catalyst recovery.

In this study, the photodegradation of BPA with ZnO tetrapods and TiO₂ nanostructures under UV illumination were compared. The concentration of BPA dissolved in DI water was analyzed by high-performance liquid chromatograph (HPLC) at specified time intervals. It was observed that the photocatalytic efficiency of ZnO tetrapods eventually surpassed Degussa P25 in free-standing form, and more than 80% of BPA was degraded after 60 min. Photodegradation of other organic dye pollutants including acid red 27 and cresyl violet by tetrapods and TiO₂ nanostructures were also examined. The superior photocatalytic efficiency of ZnO tetrapods for degradation of BPA and other organic dye pollutants and its correlation with the material properties were discussed.

9364-66, Session PWed

White-light luminescence of Dy³⁺:bismuth borate glasses

Udaya Kumar K., Sri Venkateswara Univ. (India); C. R. Kesavulu, Univ. de São Paulo (Brazil); Patarawagee Yasaka, Keerati Kirdsiri, Ctr. of Excellence in Glass Technology and Materials Sciences (Thailand); Parnuwat Chimalawong, Chandrakasem Rajabhat Univ. (Thailand); Jakrapong Kaewkhao, Ctr. of Excellence in Glass Technology and Materials Sciences (Thailand); Chalicheemalapalli K. Jayasankar, Sri Venkateswara Univ. (India)

Dy³⁺-doped bismuth borate glasses with composition (mol %) of 30 Bi₂O₃ + (60-x) B₂O₃ + 10 ZnO + x Dy₂O₃ (x= 0.6, 0.8, 1.0, 2.0, 3.0, 4.0 and 5.0) have been prepared by melt-quenching technique. The spectral properties of these glasses are investigated through absorption, emission and decay measurements. Using Judd-Ofelt (JO) analysis the intensity parameters (10²⁰ cm²) are found to be $\Omega_2 = 6.38$, $\Omega_4 = 4.24$ and $\Omega_6 = 2.92$. From JO parameters the radiative properties of the 4F_{9/2} luminescent level of 1.0 mol % of Dy₂O₃ doped glass have been evaluated. The radiative lifetime for 4F_{9/2} level is found to be 1002 μ s. The effective bandwidth and the stimulated emission cross-section for the 4F_{9/2} \rightarrow 6H_{13/2} (J = 15/2, 13/2 and 11/2) transitions of Dy³⁺ ion have been calculated from the emission spectra. Decay profiles for the 4F_{9/2} level of Dy³⁺ ions have been measured by monitoring the 4F_{9/2} \rightarrow 6H_{15/2} transition. The decay curves exhibit non-exponential nature for all the concentrations which are analyzed under the framework of Inokuti-Hirayama model. The white light emission generated from 4F_{9/2} \rightarrow 6H_{15/2} (blue) and 4F_{9/2} \rightarrow 6H_{13/2} (yellow) transitions have been characterized with the help of CIE 1931 chromaticity diagram. The analyzed results suggest that these glasses are useful for making the mercury free display device applications.

9364-67, Session PWed

Effects of Low Energy H- ion implantation on the optical properties of ZnMgO Thin Films

Shantanu Saha, Saurabh Nagar, Indian Institute of Technology Bombay (India); Shree K. Gupta, Bhabha Atomic Research Ctr. (India); Subhananda Chakrabarti, Indian Institute of Technology Bombay (India)

Owing to the large exciton binding energy and direct bandgap at room temperature ZnO and its alloys are the most promising semiconductor in the area of optoelectronics. The effects of H⁻ ions on the optical properties of ZnMgO thin films were investigated by temperature dependent photoluminescence (PL) measurements. H⁻ ion implantation has been performed by applying 10¹³, 5x10¹³, 10¹⁴ and 5x10¹⁴ ions/cm² doses which are assigned as sample A, B, C and D respectively keeping the energies at 40 and 50keV respectively. The PL spectra revealed that the optical properties were severely degraded when the dosage of implanted ions were 10¹⁴ ions/cm² and beyond of that. Sample C and D only exhibited defect related peaks. Several weak deep level emission peaks were revealed by these samples at 3.03 and 3.10eV respectively. A comparative study between the as-grown and as-implanted samples signifies that after H⁻ ion implantation, the luminescence efficiency decreases. We attribute this to the increase of concentration of effective non-radiative centers which effectively suppresses the luminescence efficiency. A dominant peak was observed around 3.66eV for as-grown sample and samples A and B. The PL spectra also revealed the presence of 11H and branch point energy at 3.59 and 3.52eV respectively. The de-localized exciton peak along with acceptor-bound exciton peak, free-electron acceptor, donor-bound-acceptor peak were found at 3.44, 3.33, 3.28 and 3.24eV respectively. With increasing dosage, the intensity of all the acceptors peak got reduced which also justifies that hydrogen atoms act as a shallow donor. DST, India is acknowledged.

9364-68, Session PWed

Structural, optical, and electrical properties of ZnMgBeGaO/Ag/ZnMgBeGaO transparent conductive multilayer films with UV range bandgap

Ba Cuong Hoang, Byung-Teak Lee, Chonnam National Univ. (Korea, Republic of)

The TCO/metal/TCO (transparent conductive oxide) structures have been studied intensively, to achieve the optical properties comparable to the TCO layers as well as the electrical performances comparable to the metallic films at the same time. In this work, we report on thin multilayer structures with UV-range energy bandgap (E_g), composed of the ZnMgBeGaO TCO films and the Ag films, deposited by the magnetron and the DC sputtering, respectively. Effects of silver layer and top ZnMgBeGaO layer were investigated in detail, and the optimized ZnMgBeGaO/Ag/ZnMgBeGaO structure with the thickness of 50/10/50 nm is obtained, with the wide bandgap energy of 3.8 eV.

Results indicated that, while the electrical resistivity is dominated by the Ag middle layer irrespective of the ZnMgBeGaO nature, the optical transmissions critically depend on the nature of the top and bottom layers, mainly due to the change in reflectivity of the multilayers. It is observed that the resistivity substantially decreases from 10⁻³ Ω cm to 10⁻⁵ Ω cm by increasing Ag thickness from 0 to 20 nm. The resistivity also decreased by decreasing thickness of the top ZnMgBeGaO layer. To improve the crystal quality and the optical properties of the sandwich structures, samples were annealed in various ambient such as air (mixed oxygen gas) and nitrogen using the rapid thermal annealing system. Further details of the structural, electrical and optical properties of the structures as well as results of the annealing experiments will be discussed during the presentation.

9364-69, Session PWed

Anomalous transmission of Ag/ZnO nanocomposites prepared by a magneto-sputtering

Igor V. Melnikov, National Research Univ. of Electronic Technology (Russian Federation) and Univ. of Illinois at Urbana-Champaign (United States); Dmitry G. Gromov, National Research Univ. of Electronic Technology (Russian Federation); Joseph W. Haus, Univ. of Dayton (United States); Andrey A. Machnev, National Research Univ. of Electronic Technology (Russian Federation); Andrey E. Mironov, Univ. of Illinois at Urbana-Champaign (United States); Mikhail Y. Nazarkin, Alexey S. Shuliatjev, National Research Univ. of Electronic Technology (Russian Federation)

Noble-metal nanoparticles embedded in a wide-gap semiconductor such as zinc oxide have been widely studied to exploit their electronic and optical properties; the nanoparticles are recognized primarily as an effective tool to overcome carrier trapping by structural defects. A simple and inexpensive approach to the preparation of Ag/ZnO nanostructures is by using a magneto-sputtering tool. However, the effect of the preparation on optical properties of this nano-composite still requires more detailed studies. In this presentation, we successfully determine the correlation between optical properties of the Ag/ZnO nanostructure and annealing of the continuous silver film.

9364-70, Session PWed

Highly-flexible, robust, and conductive ZnO nanowire arrays with superhydrophobic property

Yuanzhi Cao, Jun Zhou, Huazhong Univ. of Science and Technology (China)

Flexible electronics have attracted a wide range of interest in science and technology due to modern society's demand of portable and stretchable electronic devices, such as wearable electronics, roll-up displays, foldable sensors and other basic components used in multifunctional devices. In our study, ZnO nanowire arrays have been grown on conductive polydimethylsiloxane (c-PDMS) via a dry transfer and hydrothermal method. The conductive PDMS (c-PDMS) substrate retains highly flexible and highly stable after the growth of ZnO nanowire (NW) arrays. After the growth of ZnO NW arrays, the c-PDMS demonstrated great superhydrophobic property with a water contact angle (CA) of 155.21° and a roll-off angle of -3°. These results indicate that ZnO NW arrays grown on c-PDMS have potential applications in flexible electronic devices with self-cleaning function.

9364-71, Session PWed

Extremely low temperature growth of high-optoelectronic quality one- and two-dimensional ZnO nanostructures

Matthew Erdman, Tito L. Busani, The Univ. of New Mexico Ctr. for High Technology Materials (United States); Julio Martinez, The Univ. of New Mexico (United States); Olga Lavrova, The Univ. of New Mexico Ctr. for High Technology Materials (United States)

ZnO nanostructures are typically grown via Chemical Vapor Deposition at temperatures higher than 400 °C or in aqueous solution between 70 and 100 °C. Proposed is a reliable aqueous solution growth and vapor growth process to synthesize one and two dimensional ZnO and ZnO:Al doped nanostructures at 50 °C. In both growth processes, two dimensional ZnO nanoplatelets with the same aspect ratio were grown. By varying the temperature of the aqueous solution, either nanowires, interwoven nanoplatelets, or single nanoplatelets can be grown. The substrate used for the seeding layer was an Al doped ZnO thin film deposited on glass or crystalline Silicon via physical vapor deposition. The grown nanoplatelets appear to be the first stage growth of large diameter nanowires, but are limited in the growth of the C-crystal plane due to the available concentration of reactants, and the limited thermal energy of the solution. Transmission electron microscopy (TEM) diffraction patterns and X-Ray diffraction (XRD) patterns of the two structures confirms they share a Wurtzite crystal structure. Lattice parameters Analysis via TEM and XRD, transmissivity via spectrophotometer, and conductivity using contact conductive atomic force microscopy for doped and undoped nanostructures has been studied. Both the nanoplatelets and the nanowires present a very low resistivity between 2×10^{-4} and 10^{-5} ohm/cm and a very high transitivity in the ultraviolet/visible range to be approximately 85-91%. Integration of the ZnO nanostructures as Transparent Conductive Oxide with hybrid solar cell and thermoelectric devices shows a very low defect density between the inorganic material and the ZnO nanostructures interface, resulting in a promising low cost solution for energy harvesting systems.

9364-72, Session PWed

Deep red radioluminescence from a divalent bismuth-doped strontium pyrophosphate Sr₂P₂O₇:Bi²⁺

Liyi Li, China-Germany Research Ctr. for Photonic Materials and Devices, State Key Lab. of Luminescent Mat. (China); Bruno Viana, Ecole Nationale Supérieure de Chimie de Paris (France); Mingying Peng, China-Germany Research Ctr. for Photonic Materials and Devices (China)

Scintillation materials have been used widely in either military or civil areas, but most of them emit lights in the spectral range of ultraviolet or visible. There are few candidates with an emission in the spectral range of 650 to 1200nm, which exactly lies in the transparent region of human tissue [1]. Here, we report a Bi²⁺ doped phosphor of Sr₂P₂O₇:Bi²⁺, which once exposed to X-ray can emit deep red lights peaking at ~700nm due to the typical transition of Bi²⁺ from 2P_{3/2} to 2P_{1/2} [2]. As the bismuth content is lower, blue and green emissions were observed possibly due to residual Bi³⁺ centers occupying the two different strontium sites in the compound. They will be greatly weakened immediately once bismuth content increases and the 700nm peak becomes dominant (see Fig.1). This might be due to the enhanced energy transfer efficiency from Bi³⁺ to Bi²⁺ with content of bismuth in view of the perfect spectral overlap of the Bi³⁺ emissions to the Bi²⁺ excitations. The 700nm peak is stronger when bismuth content rises to 0.5%. The deep red radioluminescence manifests the potential application of the phosphor as implantable scintillator which can obtain real time dose information and reduce serious radiation accidents in the case of radiation therapy.

Fig.1 The radioluminescence of Sr₂P₂O₇:Bi²⁺ with different nominal bismuth contents as the label says upon X-ray (40 KV, 20 mA Cu tube) excitation. Tiny amount of bismuth in the 0% sample perhaps comes from the contamination by bismuth vapor as the samples were sintered together at high temperature.

1. T. Maldiney, A. Bessiere, J. Seguin, E. Teston, S. Sharma, B. Bruno, A. Bos, P. Dorenbos, M. Bessodes, D. Gourier, D. Scherman and C. Richard, Nature Mater., 2014, 13, 418-426.

2. M. Peng and L. Wondraczek, Opt. Lett., 2010, 35, 2544-2546.

9364-73, Session PWed

Wafer-scale chemical lift-off of GaN thin films from sapphire substrates using ZnO sacrificial layers

David J. Rogers, Nanovation (France); A. Rajan, Heriot-Watt Univ. (United Kingdom); Ferechteh H. Teherani, Vinod Eric Sandana, Philippe Bove, Nanovation (France); Suresh Sundaram, Youssef El Gmili, Paul L. Voss, Abdallah Ougazzaden, Georgia Tech-Lorraine (France); K. A. Prior, Heriot-Watt Univ. (United Kingdom); Ryan McClintock, Manijeh Razeghi, Northwestern Univ. (United States)

We demonstrate the development of the chemical lift-off (CLO) technology for lifting off full 2 inch diameter layers of MOVPE grown GaN thin films from c-plane sapphire substrates using ZnO sacrificial layers. Here, GaN was grown on c- ZnO /Al₂O₃ heterostructures using MOVPE with N₂ as a carrier and dimethylhydrazine as a N source. Full 2 inch, epitaxial GaN layers were lifted-off the c-Al₂O₃ substrates by chemically etching away the ZnO sacrificial layers. Structures were characterized before and after the CLO using HRXRD, AFM, SEM, PL and optical transmission techniques. This method offers the freedom to remove GaN-based devices from expensive single crystal substrates and subsequent bonding onto foreign substrates with a superior cost/performance profile. Furthermore, this technique opens ways to reclaiming / recycling the expensive single crystal substrate for further regrowths.

9364-74, Session PWed

Electrochemical deposition and characterizations of adherent NiO porous films for photovoltaic applications

Sana Koussi, Thierry Pauporté, Ecole Nationale Supérieure de Chimie de Paris (France)

NiO is a wide bandgap semiconductor with a p-type conductivity. In the literature, NiO is the most studied hole transport material in inverted "p-type" dye-sensitized solar cells (p-DSSC). In p-DSSCs, excitons are photogenerated in a dye molecule and the charge separation occurs due to the driving forces induced by the contact to two adjacent phases. NiO receives the holes whereas the redox couple in the electrolyte receives the electrons from the photoexcited dye. For good performances, the oxide layer must present a large internal surface area, must be well-adherent and electrically contacted to the FTO conducting substrate.

We have tested the electrochemical preparation of NiO layers using various conditions. Adherent homogeneous films have been prepared by pulsed anodic techniques using an aqueous bath. We have also developed the cathodic potentiostatic deposition of NiO in a DMSO bath. The films have been characterized by XRD, by Raman spectroscopy and by cyclic voltammetry. The layer bandgap has been measured by spectrophotometry. The layers have also been characterized by impedance spectroscopy and Mott-Schottky measurements.

We have evaluated the PV performances of the electrodeposited NiO layers after sensitization by an ad-hoc dye.

9364-75, Session PWed

Optical studies of nickel oxide growth on Si (111), c-Al₂O₃, and FTO/glass by pulsed laser deposition

Vinod Eric Sandana, David J. Rogers, Ferechteh H. Teherani, Philippe Bove, Nanovation (France); Teresa Monteiro, N. Ben Sedrine, Maria R. Correia, Univ. de Aveiro (Portugal); Ryan McClintock, Manijeh Razeghi, Northwestern Univ. (United States)

Face centred cubic (fcc) nickel oxide (NiO) is a direct [1] wide bandgap semiconductor material [2-4] with excellent electrochemical stability. It also has a relatively high ionization potential and an elevated conduction band energy level. While stoichiometric NiO is electrically insulating, oxygen-poor NiO shows p-type conduction with a hole concentration that increases with oxygen content. This is generally attributed to positive charge compensation at Ni²⁺ vacancies. As a result of these properties, and their tunability, NiO has been investigated for a number of emerging uses including photocatalysis [5, 6], water treatment [7], electrochromics [8], UV photodetectors [9], thermoelectrics [10], chemical/gas sensing, [11], hole-transport/electronblocking in organic electronic devices [12], supercapacitor electrodes, lithium ion battery anodes [13], fuel cells [14], hybrid LEDs [15] and p-type field effect transistors [16]. The samples of NiO under study were grown on Si (111), c-Al₂O₃ and FTO/Glass substrates by PLD [17]. In this work, we report the room temperature NiO optical bandgap for as-grown and annealed NiO samples obtained from transmission measurements. We have found that the bandgap blueshifts from 3.60 to 3.68 eV after post-growth annealing for NiO layers grown on sapphire substrate. Furthermore, the room temperature micro-Raman analysis, in the 300-1500 cm⁻¹ range, reveals clear one and two-phonon (TO, LO, 2TO, LO+TO and the most intense 2LO) contributions, in good agreement with reported values in single crystal [18] and nanosized NiO powders prepared by plasma synthesis method [19]. The positions of the phonon modes are found to be independent of the nature of the substrate.

REFERENCES

- [1] S. Chakrabarty and K. Chatterjee, Journal of Physical Sciences, 13, 245 (2009).
- [2] P. S. Patil & L. D. Kadam, Appl Surf Sci 199:211–221 (2002).
- [3] S. Huffner S, Adv Phys 43:183 (1994).
- [4] L. Ai et al. Applied Surface Science 254 (8), 2401 (2008).
- [5] C.G. Granqvist, Handbook of Inorganic Electrochemicals Materials, Elsevier, Amsterdam, 1995.
- [6] Z. Zhai et al. Nanoscale 4, 547 (2012).
- [7] Xiaowei et al. J. Mater. Chem. 22, 14276 (2012).
- [8] A. Azens et al. Solid State Ionics 113–115, 449 (1998).
- [9] H. Ohta et al. Thin Solid Films 445, 2, 317 (2003).
- [10] W. Shin & N. Murayama Materials Letters 45, 6, 302 (2000).
- [11] A. Dirksen, et al. Sensors and Actuators B: Chemical 80, 2, 20 106 (2001).
- [12] S. Bai et al. Adv. Energy Mater. 4, 1301460 (2014).
- [13] A. Vu et al. Adv. Energy Mater. 2, 1056 (2012).
- [14] P. I. Cowin, et al. Adv. Energy Mater. 1, 314 (2011).
- [15] Y. Y. Xi et al. Appl. Phys. Lett. 92, 113505- 1 (2008).
- [16] H. Shimotani et al. Appl. Phys. Lett. 92 24, 242107 (2008).
- [17] V. E. Sandana et al. Proc. SPIE Vol. 8987, 89872P-1 (2014).
- [18] Dietz R E, Parisot G I and Meixner A E, Phys. Rev.B 42302 (1971).
- [19] N. Mironova-Ulmane, A. Kuzmin, I. Steins, J. Grabis, I. Sildos, and M. Pārs, Journal of Physics: Conference Series 93, 012039 (2007).

Conference 9365: Integrated Optics: Devices, Materials, and Technologies XIX

Monday - Wednesday 9-11 February 2015

Part of Proceedings of SPIE Vol. 9365 Integrated Optics: Devices, Materials, and Technologies XIX

9365-1, Session 1

Active and Passive Silicon Photonic Structures for Optical Communications (Invited Paper)

David V. Plant, McGill Univ. (Canada)

We review silicon photonic based 400G/IT short reach optical interconnects for application in data center communications.

9365-2, Session 1

Hybrid and heterogeneous photonic integrated circuits for high-performance applications (Invited Paper)

Martijn J. R. Heck, Aarhus Univ. (Denmark)

Photonic integration, based on silicon, silica, or indium phosphide technologies, has reached a level of maturity, where it has now become an integral part of telecom and datacom networks. However, although impressive levels of integration and bandwidth have been achieved, the performance of these technologies is relatively low, compared to fiber-optics and discrete bulk optics counterparts. This limits their application in more demanding fields like microwave photonics, e.g., for 4G/5G wireless communications, more advanced complex modulation formats for telecommunications, and highly energy-efficient interconnects.

The invention of the ultra-low loss waveguide (ULLW) platform, by me and my co-workers at UC Santa Barbara, heralds a new range of applications for photonic integrated circuits. Fiber-like loss performance, with waveguide propagation losses < 0.1 dB/m, has been realized in waveguides with silicon nitride cores. This performance level represents an order of magnitude lower loss than silica-based waveguides, and 2 - 3 orders of magnitude lower than the silicon-on-insulator and indium phosphide PIC platforms.

Using hybrid or heterogeneous integration, silicon, ULLW, and indium phosphide platforms can be combined. Using "the best of both worlds" approach, improved performance can be achieved. I will discuss the opportunities that these technologies offer to various high-performance applications, such as low-noise lasers and oscillators, high-resolution radars and gyroscopes, and high-bandwidth photonic analog-to-digital converters.

9365-3, Session 1

Extremely small electro-optic polymer/silicon hybrid modulator with low operational power

Shin-ichiro Inoue, Akira Otomo, National Institute of Information and Communications Technology (Japan)

Silicon-based optical modulators fabricated using CMOS compatible nanofabrication technology are critical components to enable high-speed optical transceivers and optical interconnects for intra- and inter-chip networks. However, the bandwidths of these Si modulators are usually limited by the free carrier dynamics. Moreover, it is known that these modulation characteristics strongly depend on temperature owing to the high thermo-optic (TO) coefficient of Si. In this study, we report on the design and experimental demonstration of a Mach-Zehnder modulator based on electro-optic (EO) polymer/silicon hybrid one-dimensional (1D) photonic crystal (PhC) waveguides. Organic EO polymers can provide

extremely high modulation speeds in excess of 100 GHz, and very high EO coefficients that are much higher than that of lithium niobate ($r_{33} = 30$ pm/V). The optical field in the 1D PhC waveguide is designed to be concentrated in the low index EO polymer clad and to compensate the positive TO coefficient of Si by using the negative TO coefficient of EO polymer. We have successfully demonstrated enhancement of the EO modulation efficiencies as a result of the slower group velocity in an MZI modulator that incorporates 80- μ m-long PhC phase-shifters. The observed in-device effective EO coefficient ($r_{33} = 504$ pm/V) is about 15 times larger than that of lithium niobate. Good agreement was obtained between the enhanced modulation efficiency and the photonic band structure, indicating that our EO polymer/silicon hybrid PhC platform effectively enables temperature-independent EO modulation using a simple geometry and an extremely small device footprint at potentially ultrafast modulation speeds.

9365-4, Session 1

Reflection type optical voltage sensors incorporating polymeric photonic ICs.

Woo-Sung Chu, Min-Cheol Oh, Sung-Moon Kim, Pusan National Univ. (Korea, Republic of)

Optical voltage sensors are indispensable devices for the accurate monitoring of high electric voltages in the environment suffering from severe electromagnetic interference. This paper reports on the study of an optical voltage sensors based on the EO crystal (z-cut LiTaO₃). A voltage sensing probe consists of polarization maintaining collimator, Faraday rotator, LiTaO₃ and dielectric mirror. In order to reduce the risk of electrical breakdown through the sensor probe, Teflon dielectric spacers used to sandwich the crystal. LiTaO₃ has different size by dicing in the experiment, dielectric mirror used for the reflective type that placed at the end of crystal. LiTaO₃ voltage applied to the way used electrodes that the deposited Au, Cr on glass using a photo-mask lithography, and it's located crystal above and below to applied voltage. And the incident light was 45 degree linearly polarization for the optical axis of EO crystal using the Faraday rotator. The reason of the 45 degree linearly polarization incident to EO crystal is electro-optic effect to take the maximum due to the most sensitive at the 45 degree. Electric field sensing signals are analyzed by polarization rotated reflection interferometry (PRRI). The PRRI is integrated on a single chip, which consists of 3-dB couplers, polarizers, TE/TM polarization converters, and thermo-optic phase modulators. In the experiment of voltage measurement, the optical signal exactly followed the 4 kVpp, 60 Hz sinusoidal waveform source voltage. Photonic integrated circuits (ICs) reduce the complexity of the interferometry, and enables mass-production of low-cost high performance electric field sensors.

9365-5, Session 1

Heterointegrated III-V/Si distributed feedback lasers

Hélène Duprez, Antoine Descos, CEA-LETI (France); Thomas Ferrotti, STMicroelectronics (France); Christophe Jany, Julie Harduin, André Myko, Corrado Sciancalepore, CEA-LETI (France); Christian Seassal, INL - Institut des Nanotechnologies de Lyon (France) and INSA (France); Badhise Ben Bakir, CEA-LETI (France)

With an ever-growing transmission data rate, electronic components reach a limit silicon photonics may overcome. This technology provides integrated circuits in which light is generated within hybrid III-V/Si lasers

**Conference 9365: Integrated Optics:
 Devices, Materials, and Technologies XIX**

and modulated to transmit the desired information through silicon waveguides to input/output active/passive components such as wavelength (de-)multiplexers, fiber couplers and photodetectors. Nevertheless, high aggregate bandwidth through wavelength division multiplexing demands for spectrally narrowband lasers with high side-mode suppression ratio (SMSR). Distributed feedback (DFB) lasers offer such a great selectivity. We report hybrid III-V on Silicon DFB lasers emitting at 1550nm and 1310nm. The III-V material is wafer-bonded to patterned silicon-on-insulator (SOI) wafers. The laser cavity is obtained by etching a grating in the silicon, while silicon adiabatic tapers are used to couple light from/to III-V waveguides to/from the passive silicon circuitry, in order to maximize the laser available gain and output power. Gratings are either etched on the top of the silicon waveguide or on its sides, thus relaxing the taper dimension constraint. At 1550nm, the investigated device operates under continuous wave regime with a room temperature threshold current of 70mA, an SMSR as high as 45dB and an optical power in the waveguide higher than 40mW. At 1310nm, a threshold current of 35mA, an SMSR of 45dB and an optical power coupled into a single-mode fiber higher than 1.5mW are demonstrated.

9365-6, Session 2

Ultra-wide bandwidth and low insertion loss bi-level grating couplers on silicon
(Invited Paper)

Joyce K. Poon, Wesley D. Sacher, Univ. of Toronto (Canada); Ying Huang, Guo-Qiang Lo, A*STAR Institute of Microelectronics (Singapore)

Grating couplers are attractive for fiber-to-chip coupling for silicon photonics because they can be used with standard single mode fibers, can be placed anywhere on the chip, and are compatible with wafer-scale measurements. However, traditional silicon grating couplers have limited optical bandwidths less than about 50 nm, and achieving insertion losses of 1 dB typically reduces the 1-dB bandwidth to less than 40 nm. Reducing the index contrast increases the bandwidth but reduces the directionality and increases the insertion loss. In this talk, we will describe a novel bi-level grating coupler design that has silicon nitride grating teeth aligned atop silicon grating teeth. Even without any bottom reflectors, the grating coupler achieves an insertion loss of -1.3 dB when coupled to a standard single-mode fiber and a record wide 1-dB bandwidth of 80 nm.

9365-7, Session 2

Low-crosstalk fabrication-insensitive echelle grating multiplexers and passives for the silicon photonics toolbox

Corrado Sciancalepore, CEA-Leti (France); Lycett J. Richard, Photon Design (United Kingdom); Jacques-Alexandre Dallery, Vistec Electron Beam GmbH (Germany); Sébastien Pauliac, Karim Hassan, Julie Harduin, Hélène Duprez, CEA-LETI (France); Ulf Weidenmueller, Vistec Electron Beam GmbH (Germany); Dominic F. G. Gallagher, Photon Design (United Kingdom); Sylvie Menezo, Badhise Ben-Bakir, CEA-LETI (France)

In this communication, we report about the design, fabrication, and testing of Echelle grating (de-)multiplexers for the 100GBASE-LR4 norm and other passive architectures such as vertical fiber-couplers and slow-wave waveguides in the O-band (1.31-um) for Silicon-based photonic integrated circuits (Si-PICs). In detail, two-point stigmatic 20th-order echelle gratings (TPSGs) on the 300-nm-thick SOI platform designed for 4x800-GHz-spaced wavelength division multiplexing featuring extremely low crosstalk (< -35 dB), precise channel spacing and optimized average insertion losses (< -3 dB) are presented. Distributed Bragg reflectors (DBRs) are used to

improve the grating facets reflectivity, while multi-mode interferometers (MMIs) are used in optimized perfectly-chirped echelle gratings (PCGs) for pass-band flattening. Moreover, 200-mm CMOS pilot lines processing tools including e-beam lithography are employed for the fabrication. In addition, wafer-level statistics of the multiplexers clearly shows the echelle grating to be inherently fabrication-insensitive to processing drifts, resulting in a minimized dispersion of the multiplexer performances over the wafer. In particular, the echelle grating spectral response remains stable over the wafer in terms of crosstalk, channel spacing and bandwidth, with the wavelength dispersion of the filter comb being limited to just 0.8 nm, thus highlighting the intrinsic robustness of design, fab pathways as well as the reliability of modeling tools.

As well as that, apodized one-dimensional vertical fiber couplers and extremely low-losses slow-light waveguides are demonstrated and discussed. The adiabatic apodization of such 1-D gratings is capable to provide band-edge group indices as high as 30 with propagation losses equivalent to the index-like propagation regime.

9365-8, Session 2

Experimental design and homogenization properties of a double zero refractive index metamaterial

Daryl I. Vulis, Yang Li, Shota Kita, Philip Munoz, Orad Reshef, Marko Loncar, Eric Mazur, Harvard School of Engineering and Applied Sciences (United States)

We experimentally demonstrate a double zero refractive index metamaterial structure consisting of a silicon pillar array embedded within an SU-8 matrix that takes advantage of the Dirac cone dispersion relation at the center of the Brillouin zone to achieve a double zero refractive index within the telecom regime. The recent advent of materials with simultaneously zero effective permittivity and permeability avoids the impedance mismatch associated with current epsilon near zero materials. Properties of such "double zero" refractive index materials include impedance matching and low loss.

To experimentally verify the zero refractive index, we fabricate a prism consisting of the metamaterial structure coupled with either a silicon or an SU-8 slab waveguide, and an input coupled silicon waveguide. Through optimization of the prism device and its associated slab waveguide, we are able to fully observe an unambiguous demonstration of the effective index of the metamaterial. We observe a linear dispersion in the positive and negative index regions, separated by a finite bandgap corresponding to a zero refractive index; the latter can be attributed to minor imperfections in fabrication. This design offers the advantage of in-plane isotropy and the potential for on-chip integration of zero refractive index materials with current optical platforms.

Finally, we consider the dependence of transmission on incident angle for both the photonic crystal based metamaterial and its equivalent homogenous medium. Comparable transmission results validates that this metamaterial can be homogenized as a bulk medium.

9365-9, Session 2

A new surface plasmon resonance spectral sensor using plasmon photonic crystal grating

Hong Guo, Xueli Tian, Junpeng Guo, The Univ. of Alabama in Huntsville (United States)

Surface plasmon resonance in metal nanostructures is very sensitive to surrounding surface conditions. Bonding of biomolecules on nanostructured metal surface can cause shift of surface plasmon resonance. The shift of surface plasmon resonance can be measured by using an optical spectrometer. Recently, we demonstrated a new method for measuring

**Conference 9365: Integrated Optics:
Devices, Materials, and Technologies XIX**

localized surface plasmon resonance by creating diffraction grating patterns of metal nanostructures, such as nanoholes, nanoslits, and metal nanoparticles. Surface plasmon resonance of nanostructures still provide sensing mechanism. But the diffraction grating pattern diffracts different surface plasmon resonance radiation frequency components into different directions. Therefore, a linear detector array can be used to capture the surface plasmon resonance spectrum. In this talk, we will present our recent progress on using metal-dielectric plasmon photonics crystal gratings for measuring surface bonding of bio-molecules such as bovine serum albumin (BSA) proteins. It will also be shown that surface plasmon resonance that cannot be measured by conventional optical spectrometers, can be measured by using this new technique.

9365-10, Session 3

Short-range plasmons and nanofocusing below 100 nm in atomically flat metal films
(Invited Paper)

Harald Giessen, Univ. Stuttgart (Germany)

We are going to present atomically flat and single crystalline gold films, which support a variety of nanostructures. Upon illumination with 800 nm light, nanofoci well below 100 nm are formed on these flat surfaces. PEEM measurements confirm this observation. Furthermore, interference of short-range surface plasmons is experimentally observed using PEEM. Time-resolved PEEM measurements demonstrate slowdown of the plasmon propagation by more than a factor of 5.

We acknowledge experimental and theoretical support by Bettina Frank, Liwei Fu, Thomas Weiss, Philipp Kahl and Frank Meyer zu Heringdorf.

9365-11, Session 3

Hyperbolic plasmonic metamaterials for nanophotonic applications: active functionalities (Invited Paper)

Wayne Dickson, Greg A. Wurtz, Anatoly V. Zayats, King's College London (United Kingdom)

We will discuss optical properties and photonic applications of active hyperbolic metamaterials based on assemblies of aligned plasmonic nanorods. These metamaterials can be designed to exhibit hyperbolic dispersion and epsilon-near-zero behaviour with tuneable optical properties across the visible and telecom spectral range. They can be used instead of conventional plasmonic metals for designing integrated active nanophotonic functionalities. In this talk, we will overview fundamentals and applications of plasmonic nanorod metamaterials as subwavelength waveguides, plasmonic crystals, label-free bio- and chemical sensors. The enhanced nonlinear response and its temporal behaviour can also be engineered by controlling metamaterial geometry. Hyperbolic plasmonic metamaterials provide flexible and universal platform for designing active nanophotonic components.

9365-13, Session 3

Plasmonic waveguide modulator based on bismuth ferrite as low-loss switchable material

Viktoriia E. Babicheva, DTU Fotonik (Denmark); Sergei V. Zhukovsky, DTU Fotonik (Denmark) and ITMO Univ. (Russian Federation); Andrei V. Lavrinenko, DTU Fotonik (Denmark)

We study the modal properties of the metal-insulator-metal (MIM) plasmonic waveguide with the bismuth ferrite (BFO) core, aiming to utilize it as a device for dynamic signal switching in photonic integrated circuits. The bismuth ferrite core is sandwiched between metal plates, which also serve as electrodes so that the core changes its refractive index by means of partial in-plane to out-of-plane reorientation of ferroelectric domains in bismuth ferrite under applied voltage. This domain switch results in changing of propagation constant and absorption coefficient, and thus both phase and amplitude control schemes can be implemented. From the material point of view, low losses of BFO (nearly zero for $\lambda > 1400$ nm) do not cause additional attenuation from waveguide core, and thus do not increase insertion loss of the whole device, in contrast to transparent conductive oxides or vanadium dioxide. From the design point of view, MIM configuration allows cut-off of the propagating mode and thus makes it possible to modulate propagation signal by switching it on and off through metal layers serving as electrodes. For the phase control scheme, π phase shift is provided by 0.8- μ m length device having propagation losses 0.29 dB/ μ m. For the amplitude control scheme, we predict up to 38 dB/ μ m extinction ratio with 1.2 dB/ μ m propagation loss.

9365-14, Session 3

Direct on-chip optical plasmon detection with an atomically thin semiconductor

Chitrleema Chakraborty, Kenneth M. Goodfellow, Ryan Beams, Univ. of Rochester (United States); Lukas Novotny, ETH Zürich (Switzerland); Nick Vamivakas, Univ. of Rochester (United States)

We demonstrate the potential for integrating nanoplasmonic based light guides with atomically thin materials for on-chip near-field plasmon detection. This allows us to build a fully integrated photonic circuit that is not only faster than its electronic counterpart but also miniaturized way below the diffraction limit of light because of the use of surface plasmons. We use silver (Ag) nanowires (NW) to enable sub-wavelength light guiding and transfer a single layer molybdenum disulfide flake to cover one end of the nanowire. Gold source drain contacts are then fabricated on either side of the flake for detecting photocurrent. When laser is focused on the uncovered end of the Ag NW, surface plasmon polaritons propagate along the length of the NW and reach the MoS₂ covered end where it gets converted to free space photons. These photons are absorbed by the MoS₂ flake to create electron hole pair which can generate a plasmon-current in the detector. Our fully integrated plasmon detector exhibits plasmon responsivities of 225 mA/W which corresponds to highly efficient plasmon detection (0.5 electrons-per-incident plasmon). Further evidence of electrical plasmon detection is provided by the polarization anisotropy of current. Photocurrent in maximum when incident laser is polarized along the length of the wire and smallest when perpendicular. This matches the throughput of the nanowire which shows similar dependence. Further we study the spectral responsivity of our plasmon detector and present its sensitivity over a broad wavelength range only limited by detector-band-gap absorption and wire coupling in the upper and lower regime respectively.

9365-15, Session 3

Analytical model of the modal characteristics of plasmonic slot waveguide

Rehab K. Abd-Allah, The American Univ. in Cairo (Egypt); Yehea Ismail, The American Univ. in Cairo (Egypt) and Zewail City of Science and Technology (Egypt); Mohamed A. Swillam, The American Univ. in Cairo (Egypt)

An analytical model to the modal characteristics of Metal-Insulator-Metal

**Conference 9365: Integrated Optics:
Devices, Materials, and Technologies XIX**

(MIM) plasmonic waveguide is proposed for the first time. An expression to the propagation constant and losses as function in the refractive index, the waveguide width, and the wavelength is obtained and verified using finite difference based mode-solver. These expressions are used to develop a theoretical model to the behavior of a plasmonic nano-filter based MIM configuration. The proposed filter works as optical Fabry-Perot resonator. Therefore, its transmission function based on the modal parameters and the reflection coefficients of its two mirrors. The reflection coefficients are calculated by investigating the physical parameters and the circuit model of plasmonic waveguide. By impeding the analytical expressions of modal parameters into the circuit model, a pure analytical model to the filter behavior is demonstrated without need to any FDTD simulations. As a result, the simulation time and the computational costs are reduced significantly. The proposed model shows a good agreement with FDTD simulations. Using this model, the sensitivity of the filter to different design parameters is investigated and analyzed analytically using closed form expression. Therefore, the optimum values of different design parameters can be obtained analytically. By using this theoretical model, a sharp resonance filter with narrow bandwidth, compact size, low loss, and good sensing characteristics can be demonstrated. The proposed filter can be used in different applications such as, biological sensing and communication systems.

9365-18, Session 3

Hybrid metallic-ion exchanged waveguides for SPR biological sensing

Sandie de Bonnault, Davide Bucci, IMEP-LAHC (France) and Univ. Grenoble Alpes (France); Pierre-Jean Zermatten, Paul G. Charette, Univ. de Sherbrooke (Canada); Jean-Emmanuel Broquin, IMEP-LAHC (France) and Univ. Grenoble Alpes (France)

Glass substrates have been used for decades to realize biosensors thanks to their biocompatibility, low thermal conductivity and limited fluorescence. Among the different types of sensors, the ones based on surface plasmon resonance (SPR) allow concentrating the sensing lightwave at the very vicinity of the sensor surface, where small entities like DNA or proteins are located.

Ion exchange on glass is a technology that already permitted realizing several high-quality integrated optical sensors for chemistry, physics and biology.

In this paper, we show how selectively buried ion-exchanged waveguides and SPR can be combined to realize a multianalyte optical sensor integrated on glass and aimed at parallel DNA studies.

After presenting the principle of operation, we use an in-house developed software based on Aperiodic Fourier Modal Method (AFMM) to design the detection zone. We show how the interaction between the ion-exchanged waveguide and the gold-layer deposited on its top can be tailored via various parameters like the gold layer thickness or the waveguide refractive index profile.

The sensor fabrication and characterization techniques are then provided and the preliminary experimental results are finally displayed and discussed.

9365-16, Session 4

Silicon photonics non-resonant wavelength filters: comparison between AWGs, echelle gratings, and cascaded Mach-Zehnder filters (Invited Paper)

Wim Bogaerts, Univ. Gent (Belgium) and IMEC (Belgium) and Luceda Photonics (Belgium); Shibnath Pathak, Alfonso Ruocco, Sarvagya Dwivedi, Univ. Gent (Belgium) and

IMEC (Belgium); Peter De Heyn, IMEC (Belgium) and Univ. Gent (Belgium); Pieter Dumon, Univ. Gent (Belgium) and IMEC (Belgium) and Luceda Photonics (Belgium); Dries Van Thourhout, Univ. Gent (Belgium) and IMEC (Belgium); Joris Van Campenhout, Philippe P. Absil, IMEC (Belgium)

Silicon photonics offers a platform for very compact wavelength filters. These can be either resonance-based (Infinite impulse response filters) or non-resonant (finite impulse response). The advantage of non-resonant devices is that they are less susceptible to non-linear effects, and in this paper we will present a qualitative and quantitative comparison between different FIR wavelength filter concepts: Arrayed Waveguide Gratings (AWG), echelle gratings, and cascades of Mach-Zehnder interferometers. We will discuss the operational principles, and the key differences between the components, and from that explain their strengths and weaknesses, and indicate for which operational specifications the different filters will perform better or worse, and how this performance scales. We confirm these with a large set of experimental data on demultiplexers in the 1550nm wavelength with a range of channel spacings and number of channels. We show that Echelle gratings are best performing for large channel spacings (> 10nm) CWDM and spectrometer applications, while AWGs perform significantly better in terms of crosstalk and insertion loss for channel spacings between 0.5 and 5nm. Echelle gratings and AWGs can be designed for flat-top behavior with a limited impact on performance (1-2 dB higher insertion loss). Mach-Zehnder cascades (e.g. lattice filters) can be tailored in much more detail, but many stages (8-12) are required to obtain a good flat-top behavior, but many stages can also give rise to higher phase errors and crosstalk. Based on these comparisons, we can make first-order recommendations for a choice of device for application in different types of WDM communication, but also for sensor read-outs and spectrometers.

9365-17, Session 4

Polarization independent electro-optical waveguides with liquid crystals in isotropic phase

Florenta A. Costache, Martin Blasl, Kirstin Bornhorst, Fraunhofer-Institut für Photonische Mikrosysteme (Germany)

Electro-optical waveguides are used in fiber optic networks for switching and modulating of optical signals transmitted over optical fibers. Highly reliable operation is ensured with this type of waveguides owing to their non-mechanical principle of operation. Their polarization dependent behavior could limit however their practical applications.

We report on a method to reduce the polarization dependent loss in electro-optically induced waveguides with a core made of special liquid crystals in isotropic phase. The design proposed is based on a particular electrode arrangement, which permits a controlled adjustment of the electrical field distribution responsible for inducing the waveguide. A spatial coexistence of both TE and TM modes allows guiding for both TE-polarization and TM-polarization in an equivalent way. A chip based on this concept was designed, fabricated and characterized. The electrode configuration, the waveguide geometry as well as the fiber to waveguide coupling were optimized using FEM simulations. A single mode, fiber pigtailed waveguide chip was fabricated by means of bulk silicon micromachining technology. In particular, the chip consists of a bottom silicon part with structured electrodes, integrated tapers and V-grooves for fiber to chip coupling, a top silicon part with a counter electrode layer and a liquid crystal layer. The device tested with increasing driving voltage revealed equally transmitted power for both TE and TM modes. Low insertion loss and very low polarization dependent loss of < 0.1 dB over a 20 dB wide dynamic attenuation range were obtained.

9365-19, Session 4

Integrated impedance-matched photonic Dirac-cone metamaterials

Yang Li, Shota Kita, Philip A. Muñoz, Orad Reshef, Daryl I. Vulis, Marko Loncar, Eric Mazur, Harvard School of Engineering and Applied Sciences (United States)

Optical metamaterials have received significant attention and progressed rapidly over the last decade. Materials with a zero index have been demonstrated in applications of supercoupling and cloaking. To date, a refractive index of zero has been achieved in the optical regime through plasmonics, metallic resonators, and dielectric resonators.

Alternatively, zero index metamaterials can be achieved using a Dirac-cone at the center of the Brillouin zone of a purely dielectric photonic crystal. This approach offers three important advantages: low loss, free-space impedance matching, and isotropy.

Recently Dirac-cone metamaterials were demonstrated in an out-of-plane geometry in the infrared regime. However, on-chip Dirac-cone metamaterials for integrated photonics in the optical regime have not yet been accomplished. Here, we demonstrate an in-plane Dirac-cone metamaterial platform with zero index in the optical regime. The design consists of a square array of low-aspect-ratio silicon pillars on a silicon-on-insulator substrate embedded in an SU-8 slab waveguide, and clad above and below by gold thin-films. We demonstrate its zero index by measuring the angle of refraction from a prism made of such a metamaterial.

This metamaterial platform represents a major step toward on-chip Dirac-cone metamaterials in the optical regime. The metamaterial is effectively two-dimensional as energy propagates in the plane of the array. Using standard planar processes, the metamaterial can be easily fabricated with consistent unit cells making it a versatile platform for the implementation of various on-chip Dirac-cone devices and geometries. Finally, the in-plane structure can be readily accessed using silicon waveguides to interface with standard integrated photonic circuits.

9365-20, Session 4

Nanoparticles generation inside Ag-doped LBG glass by annealing or femtosecond direct laser writing

Marie Vangheluwe, Univ. Laval (Canada); Yannick G. Petit, Institut de Chimie de la Matière Condensée de Bordeaux (France); Nicolas Marquestaut, Evelyne Fargin, Alexia Corcoran, Univ. Bordeaux 1 (France); Feng Liang, Réal Vallée, Ctr. d'Optique, Photonique et Laser (Canada) and Univ. Laval (Canada); Thierry Cardinal, Institut de Chimie de la Matière Condensée de Bordeaux (France) and Univ. de Bordeaux (Canada); Lionel S. Canioni, Univ. Bordeaux 1 (France)

Glassy matrix doped with noble metal ions can lead to metallic nanoparticle (NP) formation, either with a random spatial distribution from thermal annealing or with 3D localization from femtosecond direct laser writing (DLW). The associated NP surface plasmon resonances bring interesting local properties for plasmonic applications, since laser-induced composite metal-dielectric can lead to dichroic structures related to aspherical silver NPs in silicate after ion exchange process. However, silicate glass matrices are mostly considered, despite the related low solubility of silver ions and weak plasmon resonance magnitude. Besides, Lanthanum borogermanate (LBG) matrix is of interest because it combines good solubility of the silver ions, high refractive index and good optical quality, as well as the localized dielectric phase transition by means of either thermal annealing or laser structuring.

Here, we report on the silver ion insertion in the LBG glassy matrix. Such

silver-doped glass can undergo metallic silver NP precipitation, under thermal annealing or DLW. Thermal annealing has led to the homogeneous spatial creation of small NPs (6.6 ± 3.5 nm), while DLW at room temperature has produced much highly concentrated localized micro-structure of NPs.

We present macroscopic transmission measurements and localized micro-fluorescence emission spectra that correlatively reveal the plasmon resonance behavior of silver NPs. Additionally, for very high laser fluencies, polarization-dependent linear absorption coefficients showed anisotropic plasmon bands, which may open to 3D dichroic polarization-dependent optical responses.

9365-37, Session 4

Microtube optical ring resonators for integrated photonic and optofluidic applications (*Invited Paper*)

Oliver G. Schmidt, Leibniz-Institut für Festkörper- und Werkstoffforschung Dresden (Germany)

We employ rolled-up SiO_x based microtubes as a new type of vertical optical ring resonator by at the same time exploiting the microfluidic capability of these components. We report microtube optical ring resonators with quality factors larger than 5000 and demonstrate first add-drop filters at 1.55 μm by coupling two tapered fibers to the microtube. When exploited as microfluidic or gas channel, single cells, thin condensates and minute amounts of fluids can be detected optofluidically. The potential for ever new device concepts such as cylindrical 3D photonic crystals will be discussed.

9365-21, Session 5

Spiral amplifiers in a-Al₂O₃:Er on a silicon chip with 20 dB internal net gain

Sergio A. Vázquez-Córdova, Edward H. Bernhardt, Kerstin Wörhoff, Jennifer L. Herek, Sonia M. García-Blanco, Markus Pollnau, Univ. Twente (Netherlands)

Spiral-waveguide amplifiers in erbium-doped amorphous aluminum oxide are fabricated by RF reactive co-sputtering of 1-μm-thick layers onto a thermally-oxidized silicon wafer and chlorine-based reactive ion etching. The samples are overgrown by a SiO₂ cladding. Spirals with several lengths ranging from 13 cm to 42 cm and four different erbium concentrations between $0.5\text{--}3.0 \times 10^{20} \text{ cm}^{-3}$ are experimentally characterized. A maximum internal net gain of 20 dB in the small-signal-gain regime is measured at the peak emission wavelength of 1532 nm for two sample configurations with waveguide lengths of 13 cm and 24 cm and erbium concentrations of $2 \times 10^{20} \text{ cm}^{-3}$ and $1 \times 10^{20} \text{ cm}^{-3}$, respectively. The obtained gain improves previous results by van den Hoven et al. in this host material by a factor of 9. Gain saturation as a result of increasing signal power is investigated. Positive net gain is measured in the saturated-gain regime up to $\sim 100 \mu\text{W}$ of signal power, but extension to the mW regime seems feasible.

The experimental results are compared to a rate-equation model that takes into account migration-accelerated energy-transfer upconversion (ETU) and a fast quenching process affecting a fraction of the erbium ions. Without these two detrimental processes, several tens of dB/cm of internal net gain per unit length would be achievable. Whereas ETU limits the gain per unit length to 8 dB/cm, the fast quenching process further reduces it to 2 dB/cm. The fast quenching process strongly deteriorates the amplifier performance of the Al₂O₃:Er³⁺ waveguide amplifiers. This effect is accentuated for concentrations higher than $2 \times 10^{20} \text{ cm}^{-3}$.

**Conference 9365: Integrated Optics:
 Devices, Materials, and Technologies XIX**

9365-22, Session 5

Liquid crystal clad waveguide laser scanner and waveguide amplifier for LADAR and sensing applications

Scott R. Davis, Scott D. Rommel, Seth T. Johnson, Michael H. Anderson, Vescent Photonics Inc. (United States); Anthony W. Yu, NASA Goddard Space Flight Ctr. (United States)

We will present a high speed, non-mechanically scanned, laser system that is coupled to a custom planar waveguide optical amplifier. The system provides high speed (10 kHz) scanning of >200 far-field resolvable spots, with a path toward >500 spots at 10 kHz demonstrated. EO scanners with Gaussian output beams, throughputs greater than 50%, and a 500 ? 150 FOV will be discussed. We will also present slab waveguide amplifiers to which our EO scanner can be coupled. This will enable long-range, eye-safe LADAR and trace gas sensing.

9365-23, Session 5

Advances in planar photonic integration with a novel ultrafast laser plasma fabrication process

Jayakrishnan Chandrappan, Matthew Murray, Tarun Kakkar, Univ. of Leeds (United Kingdom); Kenneth L. Kennedy, EPSRC - National Ctr. of III-V Technologies (United Kingdom) and Univ. of Sheffield (United Kingdom); Richard A. Hogg, The Univ. of Sheffield (United Kingdom); David P. Steenson, Gin Jose, Animesh Jha, Univ. of Leeds (United Kingdom)

We report a novel method for the simultaneous implantation of multiple, atomically dissimilar ions into silica matrix using ultrafast laser processing for developing a variety of functional optoelectronic materials. High index contrast (>10%) waveguides ($n=1.6$) in silica with rare earth co-doping and sequential doping are realized with femtosecond plasma implantation, assisted by physicochemical reactions at the plasma-silica interface. Homogenous rare earth doped and undoped waveguides with no dopant segregation are fabricated, having the potential for devices like loss-less splitters, waveguide amplifiers and laser platforms. For an Er³⁺-ion doped waveguide, the absorption and emission cross sections at 1534 nm are estimated as 3×10^{-22} cm² with a measured fluorescence lifetime of 12.9 ms. The 1 mm thick substrates with the planar waveguides on it were measured to have a high optical transparency of 95 % and the waveguide propagation losses of < 0.5 dB/cm at 1550 nm. Selective doping and un-doped regions are achieved with a masked implantation approach in the same substrate with a good control over the step index waveguide formation. Multi-rare earth ion doped channel waveguides are accomplished on this platform in a single step process, reported for the first time in ultrafast laser processing. This can support the mass manufacturing of photonic integrated circuits in a CMOS foundry line. Further, this method can be extended for engineering the optical devices and sensors with hybrid integration of silica, silicon, metal and polymer materials.

9365-24, Session 5

High-index contrast potassium double tungstate waveguides towards efficient rare-earth ion amplification on-chip

Mustafa A. Sefunc, Frans B. Segerink, Sonia M. García-Blanco, Univ. Twente (Netherlands)

Rare-earth ion doped KY(WO₄)₂ amplifiers are proposed to be a good candidate for many future applications by benefiting from the excellent gain characteristics of rare-earth ions, namely high bit rate amplification (>Tbps) with low noise figure (<5-6 dB). However, KY(WO₄)₂ optical waveguide amplifiers based on rare-earth ions were conventionally fabricated on layers overgrown onto undoped KY(WO₄)₂ substrates. Such amplifiers exhibit a refractive index contrast between the doped and undoped layer of typically <0.02, leading to large devices not suited for the high degree of integration required in photonic applications. Furthermore, the large mode diameter in the waveguide core requires high pump input powers to fully invert the material.

In this study, we experimentally demonstrate high index contrast waveguides in crystalline KY(WO₄)₂, compatible with the integration onto passive photonic platforms. Firstly, a layer of KY(WO₄)₂ is transferred onto a silicon dioxide substrate using bonding with UV curable optical adhesive. A subsequent polishing step permits precise control of the transferred layer thickness, which defines the height of the waveguides. Small-footprint (in the order of few microns) high index contrast waveguides were patterned using focused ion beam milling. When doped with rare-earth ions, for instance, Er³⁺ or Yb³⁺, such high contrast waveguides will lead to very efficient amplifiers, in which the active material can be efficiently pumped by a confined mode with very good overlap with the signal mode. Consequently, lower pump power will be required to obtain same amount of gain from the amplifier leading to power efficient devices.

9365-25, Session 5

Polymer optical waveguide composed of europium-aluminum-acrylate composite core for compact optical amplifier and laser

Marina Mitani, Keio Univ. (Japan); Kenichi Yamashita, Kyoto Institute of Technology (Japan); Toshimi Fukui, KRI, Inc. (Japan); Takaaki Ishigure, Keio Univ. (Japan)

We successfully fabricate polymer waveguides with Europium-Aluminum (Eu-Al) polymer composite core (50-um circular core) using the Mosquito method that utilizes a microdispenser for realizing a compact waveguide optical amplifiers and lasers.

Rare-earth (RE) ions such as Erbium are well known as a fluorescent material, and widely used as the gain medium for fiber lasers and optical fiber amplifiers. However, high concentration doping of rare-earth-ion leads to the concentration quenching resulting in observing less gain in optical amplification. For addressing the concentration quenching problem, a rare-earth metal (RE-M) polymer composite has been proposed by KRI, Inc. to be a waveguide core material. Actually, 10-wt% RE doping into organic polymer materials was already achieved. Hence, realization of compact and high-efficiency waveguide amplifiers and lasers have been anticipated using the RE-M polymer composite. In this paper, for the core material, Eu-Al-benzyl methacrylate (Eu-Al-BzMA) composite is adopted, while for the cladding a photo-curable acrylate resin is used. The fabricated Eu-Al-BzMA-core waveguide is characterized: near-field and far-field patterns, optical insertion loss and the optical gain are measured. Because of tight light confinement effect in to the circular core, the insertion loss is sufficiently low, and it is experimentally confirmed that the low-loss waveguides are fabricated with a high reproducibility. Amplification rate is estimated by measuring the amplified spontaneous emission using the valuable stimulated length method. The fabricated waveguide laser exhibits gain of the amplification as high as 4.4 dB/cm at 616-nm wavelength.

9365-26, Session 6

Recent progress in InP/polymer-based devices for telecom and data center applications (*Invited Paper*)

Moritz Kleinert, Ziyang Zhang, David de Felipe, Crispin Zawadzki, Fraunhofer-Institut für Nachrichtentechnik Heinrich-Hertz-Institut (Germany); Alejandro Maese, Fraunhofer-HHI (Germany); Walter Brinker, Martin Möhrle, Norbert Keil, Fraunhofer-Institut für Nachrichtentechnik Heinrich-Hertz-Institut (Germany)

Highly functional and low-cost photonic devices are paving ways for the fast development of optical communication networks. To bring multiple optical functionalities together and to provide interfaces with the electronic domain, a polymer-based motherboard integration platform has been established and is fast evolving, tailoring to various demands from photonic applications. Optical filters based on polymer grating assisted directional couplers have been demonstrated with bi-directional wavelength tuning range exceeding 300 nm. Variable optical attenuators can reach >50 dB dynamic range on a heater power of a few mW. Thermo-optic switches have been tested achieving extinction ratios >70 dB with optical loss values < 1 dB. A TM-emitting tunable laser has been assembled in which a vertically inserted half-wave plate converts the otherwise TE-emitting laser into TM polarization. The same integration concept has been applied to more advanced devices such as optical network units for WDM-PON. Multi-core polymer waveguides have been fabricated to bridge the gap between the spatial division multiplexing technology using multi-core fibers and the well-established photonic components based on planar light wave circuits (PLCs), as well as to open up the third dimension for dense photonic integration. The matching multi-depth 45° mirrors deflect light from each individual layer to be received by the surface PDs mounted passively on top of the polymer boards. With its full flexibility, the polymer motherboard technology is providing solutions for compact, multifunctional optical modules for polarization-multiplexed, three-dimensional photonic integration. The technology is setting off to address various challenges in telecom and data center discipline.

9365-27, Session 6

Determination of thermo-optic characteristics in electro-optic polymer materials based on polymeric Bragg grating waveguides

Kyung-Jo Kim, Oscar D. Herrera, Soha Namnabat, Roland Himmelhuber, Robert A. Norwood, The Univ. of Arizona (United States); Jingdong Luo, Alex K. Y. Jen, Univ. of Washington (United States)

The thermo-optic characteristics of poled and the unpoled electro-optic (EO) polymer SEO250 have been determined based on characterizing polymer Bragg grating waveguides incorporating EO polymers. For Bragg reflection grating design, the perturbation to the effective index of the guided mode caused by the presence of the grating structure was calculated, and the transmission matrix method was used to find the grating reflectivity. Due to the large index contrast between the core and the cladding materials, an oversized rib structure was adopted for satisfying the single mode propagation condition. The grating was formed by using two-beam laser interference on a photoresist and was inscribed into the cladding layer by the oxygen plasma etching. The fabricated waveguide device was poled using top and bottom electrodes which can apply an electric field to the polymer waveguide structure. After poling, the device was pigtailed with optical fibers on both endfaces. To compare their respective temperature dependence, the unpoled device was also pigtailed. Both waveguides were placed in an environmental chamber and the Bragg reflection peak

shift was measured by using an erbium ASE light source and an optical spectrum analyzer. The poled and the unpoled devices both show a highly linear Bragg reflection peak shift as the temperature changes between -60 °C and 60 °C. The calculated thermo-optic coefficients of the poled and unpoled devices are $-1.104 \times 10^{-4} / ^\circ\text{C}$ and $-1.416 \times 10^{-4} / ^\circ\text{C}$, respectively. This indicates the feasibility of developing hybrid devices that use both EO and TO characteristics of EO polymers.

9365-28, Session 6

Air suspended polymer rib waveguides

Christoph Prokop, Univ. of Applied Sciences Karlsruhe (Germany) and RMIT Univ. (Australia); Arnan Mitchell, RMIT Univ. (Australia); Christian Karnutsch, Fachhochschule Karlsruhe Technik und Wirtschaft (Germany)

Polymers are a very popular material platform for low-cost, mass-producible photonic application such as telecommunication or sensing. Their simple and easy processing allows polymers to take on almost any desired shape. However, due to the low refractive index contrast between various polymer materials, the efficiency of such devices is often limited. The most elegant way to achieve maximum index contrast, not only in polymer photonic devices, is to use air as cladding layers.

We exploit a method for laminating thin polymer films over open polymer structures in order to provide a high refractive index contrast for air suspended photonic devices. Polymer films with thicknesses down to single-mode conditions can be transferred over areas of several hundred square microns by using a simple PDMS stamp. To define photonic devices on this platform two methods have been investigated. Firstly, ridge waveguide photonic structures can be directly transferred from the PDMS stamp requiring a sophisticated alignment due to the similar refractive indices of the materials. Alternatively, the ridge waveguides could be formed using a second layer of photo resist, spun on top of the existing laminated film. By using standard photolithography structures can then be defined on top of the air suspended polymer slab. We present optical modeling and experimental results of several different air suspended quasi single-mode rib waveguides formed using these techniques.

9365-29, Session 6

Waveguide collimators for integrating free-space components with waveguide devices

Jin Soo Shin, KAIST (Korea, Republic of); Min-Cheol Oh, Pusan National Univ. (Korea, Republic of); Chang-Hee Lee, Korea Advanced Institute of Science and Technology (Korea, Republic of); Sang-Yung Shin, KAIST (Korea, Republic of); Guang-Hao Huang, Woo-Sung Chu, Pusan National Univ. (Korea, Republic of); Young-Ouk Noh, Hyung-Jong Lee, ChemOptics Inc. (Korea, Republic of)

Array type of optical device are highly demanded in wavelength-division multiplexing optical communication systems to achieve the compactness, mass-production, and reliability. However, many essential optical components such as collimating lens, wavelength filter, isolator, wave plate are realized as free-space optical component and still difficult to be implemented as a waveguide component. To realize array type of LDs, an isolator device with few hundred micron thickness should be inserted, which require a collimating lens to reduce the coupling loss. In this work, we proposed and demonstrated an array type waveguide collimator device by using a low contrast large core polymer waveguide. The diffraction of guided mode propagating through a free-space region was highly suppressed by increasing the size of guided mode to 25 μm . However, it caused significant the fiber coupling loss by mode size mismatch between

**Conference 9365: Integrated Optics:
 Devices, Materials, and Technologies XIX**

the fiber and large core waveguide. To resolve the fiber coupling loss, an adiabatic taper structure was incorporated. The extra loss of array type waveguide collimator by the propagation through free-space of 400 μm was 0.8 dB. The extra loss by two taper was as small as 0.5 dB. The waveguide collimator would play an important role for the integrating of free-space component and enables low-cost solution of array type transceiver device.

9365-30, Session 6

Low-loss sharp bends in low contrast polymer hybrid metallic waveguides

Mustafa A. Sefunc, Willemijn van de Meent, Ashley R. Coenen, Meindert Dijkstra, Antonio Pace, Sonia M. García-Blanco, Univ. Twente (Netherlands)

Surface plasmon polaritons have drawn significant attention in recent years not only thanks to their capability of confining the field in the dielectric/metal interface, but also thanks to their potential to produce highly efficient thermo-optical and electro-optical devices such as modulators and switches due to the presence of the metal layer amidst the electromagnetic field. However, the high confinement comes at the cost of high propagation losses due to the metal's highly absorptive nature at visible and near-IR wavelengths. In order for plasmonic devices to find a widespread use in integrated optics, an advantage over dielectric waveguides needs to be found that justifies their utilization.

In this work, we present an application in which plasmonic waveguides perform better than their dielectric counterparts. By adding a thin metallic layer underneath the waveguide core, the total bend losses (dB/90°) are reduced with respect to the bend losses of the equivalent dielectric structure without the metallic layer for radii below 35 micrometers. The results show a dramatic reduction of total bend losses in TE-polarization with values as low as 0.02 dB/90° bend for radii between 6 and 13 micrometers. The mechanism for the reduction of bend losses is the shielding action of the metal layer, which prevents the field from leaking into the substrate. In this paper, both detailed theoretical calculations as well as experimental results for SU8 channel waveguides will be presented.

9365-31, Session 7

Toward building-block-based approach for generic integration photonic technologies
(Invited Paper)

Andrea I. Melloni, Daniele Melati, Politecnico di Milano (Italy); Emanuele Parrinello, Filarete s.r.l. (Italy); Francesco Morichetti, Politecnico di Milano (Italy)

In the last years the concept of building-block approach and circuit-model simulation in photonics has been thoroughly developed and is now becoming a pervasive methodology for Silicon, Indium Phosphide and dielectric based generic integration technologies. The current status and prospects of the BB approach, the concept, the potential and the limits are discussed focusing on materials, technologies, software tools and characterization techniques. Statistical analysis, yield and tolerance aspect are addressed too. The effort of introducing Photonics Design Kits is described and a comparison between the various technologies is presented. Successful examples based on our experience are presented and discussed and a tentative roadmap proposed.

9365-32, Session 7

A fully static OCT sensor using a glass integrated optic chip bonded to a CCD linear camera

Alain Morand, Adriana Warzecha, IMEP-LAHC (France); Fabrice Thomas, IPAG (France); Pierre Benech, IMEP-LAHC (France); Etienne P. Le Coarer, Institut de Planétologie et d'Astrophysique de Grenoble (France); Renaud Puget, Christophe Bonneville, Bruno Martin, Resolution Spectra Systems (France); Cédric Cassagnettes, Denis Barbier, Teem Photonics S.A. (France)

Optical Coherence Tomography (OCT) sensors traditionally use optical delay line with moving parts. In other way, OCT systems with linear detector array are more simples and do not need moving elements. They can be based on the measurement of a Fourier interferogram made along the linear pixel array. Nevertheless, optical bulk parts are often used. In order not to reach these limitations, an entire integrated system is proposed from the two input signals to compare (reference and probe) to the linear optical detector. Leaky Loop Integrated Fourier Transform Spectrometer technology (LLIFTS) is used to have a large fourier interferogram along an edge of the glass chip which is glued on a 4 megapixels CCD linear detector array without protective glass window. After describing the system principles, first measurements will be presented. For that an optical signal coming from a SLED is divided in two equal parts injected respectively in the reference input and the probe input. The optical phase difference between the two signals is controlled previously by an optical bulk Mach Zehnder interferometer. It will be demonstrated that an optical phase difference measurement higher than 1 mm in the air can be achieved with an optical contrast of 30dB without a specific signal treatment.

9365-34, Session 7

Using photo-sensitive glass ceramics for advanced optoelectronic IC packages

Jeb H. Flemming, Kevin Dunn, James Gouker, Carrie F. Schmidt, 3D Glass Solutions (United States)

Novel assembly and packaging technologies have the ability to become primary differentiators for many manufactures of optoelectronics devices and the main enabler of cost-effective on-chip systems integration. Unfortunately, today's packaging solutions have become a limiting component in system design, integration, and performance for compact optoelectronic devices. Therefore, a single material that is capable of integrating (1) copper plated through glass vias (TGVs) for I/O interconnects, (2) trenches for fiber optic alignment, and (3) in-plane 45° turning mirrors for optical turning would provide optoelectronic designers with increased toolsets for systems integration, compactness, and manufacturing simplicity.

In this paper, 3D Glass Solutions will present on our research efforts to create advanced optoelectronic packaging solutions using APEX® Glass Ceramic. The historical benefits of glass have typically been related to its optical transparency; however, APEX® Glass Ceramic is a photo-definable material that is processed in three simple steps to create a variety of 3D structures in glass including through holes, cavities, and trenches among other features. Through exposure, baking, and etching steps, complex 3D architectures, with micron-scaled precision may be microfabricated using wafer-level batch processing techniques, enabling the cost effective production of complex optoelectronic packages that contain copper filled TGVs, trenches for fiber optic alignment, and 45° turning mirrors. In this paper we will present on our efforts of creating (1) electronic packages with TGVs ranging in size from 30-100 μm in diameter, (2) fiber optic alignment trenches with micron-scaled precision in width and depth, and (3) optically smooth 45° horizontal and vertical turning mirrors.

9365-35, Session 7

Inductively coupled plasmas (ICP) etching of PZT thin films for fabricating optical waveguide with photoresist/aluminum bilayer masking

Zhipeng Qi, Guohua Hu, Qin Zhu, Lixing Zhang, Manqing Li, Yiping Cui, Southeast Univ. (China)

Waveguide morphology and etched surface are two of the most important factors deciding the performance of PZT waveguide devices. Smooth, clean and accurate waveguide patterns on PZT thin film could be fabricated through optimizing etching conditions (pressure, gas components, and RF power) and etching methods (single-/dual-electrode etching) of inductively coupled plasmas (ICP) in this work. Etch rate of PZT thin film and etch selectivity of mask to PZT in a CHF₃/Ar plasma have also been investigated in this paper.

Before etching, photoresist/aluminum bilayer mask was fabricated on PZT thin film. ICP etching was conducted by varying the ratio of Ar flow rate to study the effects of argon on the etched surface of PZT thin film during etching. It was found that Ar could play a role of buffer gas to protect the etched surface from defects in the etching process. Furthermore, as the pressure was decreased, etch rate of PZT thin film was increased obviously. However, the surface roughness of etched surface increased with the pressure decreasing below 3Pa. For the reason that increasing etch rate often results in thermal distortion of the photoresist mask [1], it was important to keep etch rate slow while make etch selectivity of mask to PZT as high as possible. In order to meet these two requirements, 250W/60W (antenna RF power/bias RF power) and 150W (bias RF power) was chosen as the etching power of dual-electrode ICP and single-electrode ICP respectively in 30/10sccm CHF₃/Ar mixture plasma, 3Pa of pressure. The results show that PZT ridge waveguide morphology etched by single-electrode ICP was much better than that of etched by dual-electrode ICP.

9365-12, Session 8

Nanoscale devices based on plasmonic coaxial waveguide resonators

Amirreza Mahigir, Pouya Dastmalchi, Louisiana State Univ. (United States); Wonseok Shin, Shanhui Fan, Stanford Univ. (United States); Georgios Veronis, Louisiana State Univ. (United States)

Waveguide-resonator systems are particularly useful for the development of several integrated photonic devices, such as tunable filters, optical switches, channel drop filters, reflectors, and impedance matching elements. In this paper, we introduce nanoscale devices based on plasmonic coaxial waveguide resonators. In particular, we investigate three-dimensional nanostructures consisting of plasmonic coaxial stub resonators side-coupled to a plasmonic coaxial waveguide. We use coaxial waveguides with square cross sections which can be fabricated using lithography-based techniques. The waveguides are placed on top of a silicon substrate, and the space between inner and outer coaxial metals is filled with silica. We use silver as the metal. We first investigate structures consisting of a single plasmonic coaxial resonator, which is terminated either in a short or an open circuit, side-coupled to a coaxial waveguide. We show that the incident waveguide mode is almost completely reflected on resonance, while far from the resonance the waveguide mode is almost completely transmitted. We also investigate structures consisting of two plasmonic coaxial stub resonators side-coupled to a coaxial waveguide. We show that this system is a plasmonic analogue of electromagnetically induced transparency and exhibits a transmission spectrum with a narrow transparency peak in the center of a broader transmission dip. We also show that the properties of the waveguide systems can be accurately described using a single-mode scattering matrix theory. The transmission and reflection coefficients at waveguide junctions are either calculated using the concept of the

characteristic impedance or are directly numerically extracted using full-wave three-dimensional finite-difference frequency-domain simulations.

9365-36, Session 8

Mid-IR frequency comb generation based on crystalline microresonators (*Invited Paper*)

Caroline Lecaplain, Erwan Lucas, Clément Javerzac-Galy, Victor Brasch, Martin H. P. Pfeiffer, Tobias Herr, John J. Jost, Arne Kordts, Michael Geiselmann, Tobias J. Kippenberg, Ecole Polytechnique Fédérale de Lausanne (Switzerland)

Optical frequency combs have become enabling tools for a growing number of applications, from calibration of astrophysical spectrographs to molecular science. They now enable dramatically improved acquisition rates, resolution and sensitivity for molecular spectroscopy mostly in the visible and the near-infrared ranges. Extension to the mid-infrared "molecular fingerprint region" (2-20 μ m) is crucial as many molecules undergo strong characteristic vibrational transitions in this domain. So far only a limited number of frequency comb sources produced by frequency conversion of near-infrared radiation through nonlinear processes have been demonstrated. These comb systems require complicated optical setups and the spectral bandwidth and power per comb line are restricted by the phase-matching condition of the nonlinear processes.

A novel and promising route to mid-infrared frequency comb generation is based on ultra-high Q crystalline optical microresonators. Recently, our group has demonstrated for the first time a Kerr comb in the mid-infrared by pumping a crystalline magnesium fluoride resonator with a continuous-wave laser at 2.5 μ m.

An appropriate choice of the resonator material and proper engineering are crucial to realize broad spectral span and low-phase noise in the mid-infrared region. The reason to choose magnesium fluoride is threefold: broad transparency window in the mid-infrared, anomalous group velocity dispersion, and the ability of self thermal-locking. Furthermore, the choice of the material is not limited to dielectric crystals. Many semiconductors such as silicon, germanium and indium phosphide also exhibit wide transparency windows in the mid-infrared and enable the development of a whole class of on-chip microresonators frequency combs for molecular spectroscopy. Progress on both the fabrication of ultra-high Q microdisk crystalline resonators and integrated silicon nitride microcavities for mid-infrared frequency comb generation will be presented.

Furthermore, the broad transparency window of magnesium fluoride includes the region of 3-5 μ m - a range where quantum cascade laser - are prevalent. Crystalline resonators can in this context allow overcoming the challenge of mode-locking quantum cascade laser. The unique combination of crystalline microresonators with high power narrow linewidth quantum cascade laser could open the path to novel, simple and compact mid-infrared comb generators. Preliminary results will be presented.

9365-38, Session 8

Design and performance analysis of a hybrid optofluidic ring resonator

Romeo Bernini, Genni Testa, Gianluca Persichetti, Istituto per il Rilevamento Elettromagnetico dell'Ambiente (Italy)

This paper reports the performance simulations and design optimization of an integrated liquid core optofluidic ring resonator (ORR) based on liquid core hybrid antiresonant reflecting optical waveguides (h-ARROWs). H-ARROWs have the potential to provide simple integration between the fluidic and optical elements, toward a fully integrated optofluidic platform. Single mode operation and low loss propagation of these waveguides is achieved through an accurate optimization analysis. Performance

**Conference 9365: Integrated Optics:
Devices, Materials, and Technologies XIX**

optimization of the ORR includes the analysis of any optical elements forming the ring: the liquid core hybrid MMI coupler and the bend h-ARROW waveguides. Furthermore, a new design strategy for improving the surface sensitivity of h-ARROWs is proposed and studied. H-ARROW, in fact, presents very high bulk sensitivity due to confinement of the entire optical mode in the liquid core. Meanwhile, it suffers of low surface sensitivity due to a poor coupling efficiency of the mode with the core sidewalls. A solution to this problem that is based on the addition of a suitable nanolayer during fabrication process is proposed and discussed.

9365-39, Session 8

Slot waveguide ring resonators for visible wavelengths in ALD titanium dioxide

Markus Häyrinen, Matthieu Roussey, Markku Kuittinen, Seppo K. Honkanen, Univ. of Eastern Finland (Finland)

The high refractive index and its transparency make titanium dioxide (TiO₂) a suitable material for nano-photonics devices in the visible spectral range. In the case of bio-sensing applications where the analyte is often in an aqueous environment, operating in the visible offers the advantage to avoid the absorption peak of water (in the near-infrared). We propose here a TiO₂ ring resonator working around $\lambda=650$ nm and based on a slot waveguide. The strong confinement of the field combined with the resonant structure offers a potential for high sensitivity to refractive index variations. The ring resonator has a radius of 6 μm and the slot has a width of 20 nm, in order to guide the fundamental quasi-TE slot mode. The structure is fabricated by e-beam lithography and an additional layer of TiO₂ is re-deposited by atomic layer deposition (ALD) on the sample afterwards in order to decrease the slot width and reach the ideal parameters. The design, fabrication and characterization of such a device will be presented for the visible wavelength range, where the bus is a strip waveguide and, for comparison, for the near-infrared region where the bus is a slot waveguide. As expected, in the visible, the propagation losses in the slot waveguide are higher. The transmission spectra, quality factors, propagation losses and effective index of the slot waveguides have been measured. Moreover, this is the first time, to our knowledge, that such a structure is fabricated and characterized.

9365-40, Session 8

Resonant enhanced low-power nonlinear tuning capability using an As₂S₃ waveguide on LiNbO₃

Yifeng Zhou, Christi K. Madsen, Texas A&M Univ. (United States)

A hybrid optics platform consisting of LiNbO₃ waveguides vertically coupled to high-index-contrast As₂S₃ waveguides can provide tight bend radii for ring resonators and strong tuning capability via third-order Kerr nonlinear effects in As₂S₃ waveguide. A vertically integrated As₂S₃ ring resonator side-coupled to a low-index Ti:diffused LiNbO₃ straight waveguide was designed and fabricated. At 1.55- μm wavelength, a low 1.2 dB/cm propagation loss and an over 30-dB extinction ratio were demonstrated on the fabricated As₂S₃-on-LiNbO₃ ring resonator waveguide with 400- μm bend radius, which corresponded to an intrinsic Q value as high as 3.5×10^5 . Operated close to the resonant wavelength, the incident optical power could be accumulated and stored inside the resonant cavity, to harness resonant enhancement effects. The waveguide nonlinear efficiency of the As₂S₃-on-LiNbO₃ ring waveguide was calculated at 3.85 radian/m \cdot W and a pump-signal measurement platform was setup to observe the nonlinear tuning phenomenon of the ring resonator waveguide. To avoid the thermal induced nonlinear effects inside the As₂S₃ materials, the As₂S₃ ring waveguide chip was placed on a thermally-conductive aluminum sample stage connected to a thermo-electric controller box. With the continuous wavelength signal power at 5 mW and the single tone pump power at 100 mW coupled into

the waveguide via a 5%:95% ratio fiber multiplexer, the resonant spectrum was measured blue-shifted and a 0.40- π phase shift was demonstrated at the resonant wavelength of 1554.935 nm.

9365-41, Session 9

Femtosecond laser micromachining for the realization of fully-integrated photonic and microfluidic devices (Invited Paper)

Roberta Ramponi, Istituto di Fotonica e Nanotecnologie (Italy)

Femtosecond-laser micromachining is an enabling technology that allows maskless realization of fully integrated photonic and microfluidic devices. Indeed, direct femtosecond laser writing can be used both for the fabrication of high-quality waveguides, and, combined with chemical etching, for the realization of microfluidic channels. By properly choosing the irradiation conditions and geometry, it is possible to fully control the device layout in 3D, the waveguide characteristics (e.g. possible anisotropy) and the microchannel internal shape. Indeed, the main advantage of this technique is its intrinsic capability of realizing 3D structures with high precision in a single fabrication step, thus making it the ideal choice both for fast prototyping and for the realization of complex or custom devices. Moreover, it allows easy integration of optical functionalities in microfluidic chips.

In this work, the basics of femtosecond laser writing will be discussed, together with the main aspects influencing induced material modifications. Some typical applications will be presented to better illustrate the versatility and peculiarities of the technique. In particular, reported examples will include microoptofluidic devices where by filling the microchannels with suitable organic materials, it is possible to realise devices with different optical functionalities (gain switch, polarisation control, etc.). The results obtained show the strong potential of this microfabrication technology, paving the way to increasingly compact and multifunctional photonic and microfluidic devices.

9365-42, Session 9

Optofluidics: manipulation and sorting of nanoparticles and cells (Invited Paper)

Ai Qun Liu, Nanyang Technological Univ. (Singapore)

Microfluidics represents the science and technology that process or manipulate small amount of fluids (10⁻⁹ to 10⁻¹⁸ liters) in microfluidic chip with dimensions of tens to hundreds of micrometers. Working with microfluidics, optofluidics becomes a significant research interest in the field of manipulation and sorting of small particles and molecules. Optofluidics aims at manipulating light and fluid at microscale and exploiting their interaction to create highly versatile devices that are significant scientific and interests in many areas. The novelties of the optofluidics are twofold. First, fluids can be used to carry substances to be analyzed in highly sensitive optical micro-devices. Second, fluids can also be exploited to control optical micro-devices, making them tunable, reconfigurable and adaptive. It is a new breakthrough research area that can provide new solutions and opportunities for a wide range of traditional photonic devices, allowing tuning and reconfiguration at the micrometer scale using microfluidic manipulation. This new innovation allows scientists and researchers to tackle many classical problems with new tools and new research ideas. Many novel innovations have been demonstrated such as liquid-liquid waveguide, liquid lens, liquid bubbles grating and microfluidic waveguide laser, etc. In this talk, the state-of-arts of optofluidic force research will be reviewed, with further discussion on its high potential applications in micro- and nano-particle manipulation, sorting and detection study, and some showcases such as a single molecule manipulation and sorting.

9365-43, Session 9

Integrated opto-microfluidics platforms in lithium niobate crystals for sensing applications

Cinzia Sada, Annamaria Zaltron, Giacomo Bettella, Gianluca Pozza, Univ. degli Studi di Padova (Italy)

Droplet microfluidic technology holds great promise for the development of efficient lab-on-chip systems of sure interest in micro-analytical chemistry, diagnostic testing, bio-sensing and the synthesis of biomolecules: the high versatility of droplets generation and manipulation inside micro-devices, in fact, can be successfully coupled to other external stages such as fluid pumping as well as optical analysis devices. In this scenario the integration of a large number of different stages on a single substrate chip would promote new insights in many applications that need portable devices to speed the analysis and allow investigation of new phenomena. This goal is still under debate since in polymers and glasses, i.e. on the most common used substrates for microfluidics, this full level of integration has not been achieved yet.

Towards this direction, we present recent results on the full integration of opto-microfluidic functionalities in the same substrate of lithium niobate (LiNbO₃) crystals. Thanks to its wide optical transparency, in fact, high performant optical waveguides can be realised to illuminate droplets generated by T-junctions that have engraved on the same LiNbO₃ substrate. The transmitted light can be therefore analysed by a holographic grating stage recorded on the material by exploiting its photorefractive properties. The perspectives of integrating a tailored light source by Second harmonic generation in Periodically Poled structures (PPLN) as well as the possibility of adding micro-pump stage based on Surface Acoustic Wave generation (SAW), both on the same substrate, will be also discussed.

9365-44, Session 9

Optofluidic waveguides written in hydrophobic silica aerogels with a femtosecond laser

Berna Yalızay, Yagiz Morova, Istanbul Technical Univ. (Turkey); Yagmur Ozbakir, Koç Univ. (Turkey); Alexandr Jonas, Istanbul Technical Univ. (Turkey); Can Erkey, Alper Kiraz, Koç Univ. (Turkey); Selcuk Akturk, Istanbul Technical Univ. (Turkey)

In this work, we present a new method to form 3D optofluidic waveguides inside hydrophobic silica aerogels. Although, aerogels are very attractive materials for a wide variety of applications due to their unique properties, it is very challenging to process them with traditional methods such as milling, drilling, or cutting because of their fragile structure. Therefore, there is a need to develop alternative processes for formation of complex structures within the aerogels without damaging the material. In our study, we used femtosecond laser pulses which provide precise machining and good quality feature definition to ablate hydrophobic silica aerogels. During the ablation, we directed the laser beam with a Galvo mirror system and focused through a scanning lens to the surface of bulk aerogel which was placed on a translation stage. We succeeded to obtain high quality 3D linear microchannels inside aerogel monoliths with simultaneous motion of Galvo mirror and translation stage.

In order to demonstrate waveguiding and measure optical attenuation of these microchannels, we filled the channels with ethylene glycol and coupled light inside the microchannel with a fiber. We measured the propagation loss as 8.83 dB/cm which demonstrates that these microchannels can be used as well optofluidic waveguides. These results show that, forming channels inside hydrophobic silica aerogels with femtosecond laser ablation is easier and more precise than mechanical methods. Furthermore, the results of optical attenuation show that the light

guiding properties of aerogels are much better than the ones produced by mechanical methods of ablation.

9365-45, Session PWed

Multi-functional optical signal processing using optical spectrum control circuit

Shuhei Hayashi, Tatsuhiko Ikeda, Keio Univ. (Japan); Takayuki Mizuno, NTT Photonics Labs. (Japan); Hiroshi Takahashi, Sophia Univ. (Japan); Hiroyuki Tsuda, Keio Univ. (Japan)

Processing ultra-fast optical signal without optical/electronic conversion is in demand and time-to-space conversion has been proposed as an effective method. We designed and fabricated arrayed-waveguide grating (AWG) configuration optical spectrum control circuit (OSCC) using silica planar lightwave circuit (PLC) technology. This device is composed of an AWG, tunable phase shifters and a mirror. The principle of signal processing is to decompose the signal's frequency components spatially by the AWG. Then, the phase of each frequency component is controlled by tunable phase shifters. Finally, the light is reflected back to the AWG by the mirror and synthesized. Amplitude of each frequency component can also be controlled by increasing coupling loss. The spectral controlling range of the OSCC is 100 GHz and the resolution is 1.67 GHz, respectively.

In this paper, we propose optical coded division multiplex (OCDM) encoder/decoder function. The encoding principle is to apply certain phase patterns to signal's frequency components and intentionally disperse the signal. The decoding principle is to also apply certain phase patterns to frequency components at the receiving side. If the phase pattern is applied that compensate intentional dispersion, the waveform is regenerated, but if the pattern is not appropriate, the waveform remain dispersed. We also propose an arbitrary filter function by exploiting amplitude and phase controlling feature. For example, the filtered optical signal transmitted through multiple optical nodes with wavelength multiplexer/demultiplexer can be equalized.

9365-46, Session PWed

Homogenization of two-dimensional Dirac-cone metamaterial

Yang Li, Shota Kita, Philip A. Muñoz, Orad Reshef, Daryl I. Vulis, Marko Loncar, Eric Mazur, Harvard School of Engineering and Applied Sciences (United States)

Impedance-matched metamaterials with zero refractive index can be achieved by exploiting a Dirac cone at the center of the Brillouin zone. We theoretically and experimentally demonstrated an in-plane Dirac-cone metamaterial consisting of low-aspect-ratio silicon pillar arrays in an SU-8 matrix with top and bottom gold layers in the optical regime.

To verify the fact that it is proper to treat the presented Dirac-cone metamaterial macroscopically as a homogeneous bulk medium in the in-plane direction near the Gamma-point, we conduct a systematic homogenization analysis on two aspects: the homogenization criterion and conditions of locality.

For the homogenization criteria, we analyze the homogenization of our metamaterial within the array and at the boundary, separately. Within the array, the metamaterial can be treated as an infinite array, which can be analyzed using bandstructure. We compare bandstructures obtained using two different methods: a macroscopic method treating the metamaterial as a homogeneous bulk medium and a microscopic method regarding the metamaterial as an infinite array. Results show that those two bandstructures agree with each other well even in the range far away from the Dirac point. At the boundary of the metamaterial, to quantitatively investigate the transition layer in which the local effective constitutive parameters vary from their value of the infinite array to their value of the background medium, we compare the phase of the electric field at the

**Conference 9365: Integrated Optics:
 Devices, Materials, and Technologies XIX**

interface of our Dirac-cone metamaterial with that of a bulk zero-index medium with retrieved constitutive parameters. Results show that, similar to its homogenized model, the metamaterial also has a deterministic boundary.

Results also show that the effective constitutive parameters of the presented metamaterial satisfy the conditions of locality: passivity, causality, and isotropy.

9365-47, Session PWed

Tunable wavelength filters based on thermo-optic polymer waveguide device

Tae-Hyun Park, Min-Cheol Oh, Won-Jun Lee, Pusan National Univ. (Korea, Republic of); Jin Soo Shin, KAIST (Korea, Republic of); Woo-Sung Chu, Pusan National Univ. (Korea, Republic of)

Optical transceiver is one of the key components in wavelength division multiplexing and it is important to realize the device with low-cost and small-foot print. In this work, Tunable wavelength filters with Bragg gratings are demonstrated based on thermo-optic polymer waveguide for the optical transceiver. To achieve high reflectivity, small core waveguide realized by using a high refractive index polymer is implemented. The reflectivity of the Bragg gratings is over 90 % with 5 mm length. However, the fiber coupling loss is significantly increased due to the mode size mismatch between small core waveguide and optical fiber. To resolve this problem, large core waveguide with a low refractive index polymer and an adiabatic taper structure for mode size conversion are implemented. A 3-dB directional coupler is included in the device for the separation of the reflected signal into the other path. However, the total loss and cross-talk are increased by the phase difference due to the slight error of the position of two Bragg gratings. To reduce the total loss and cross-talk, the electrode on the directional coupler region is implemented to compensate the phase difference.

9365-48, Session PWed

Low-loss segmented joint structure between a slab waveguide and arrayed waveguides designed by simple optimization method

Kosuke Shibuya, Bin Idris Nazirul Afham, Hideaki Asakura, Hiroyuki Tsuda, Keio Univ. (Japan)

An arrayed-waveguide grating (AWG) is a key device of the optical communication systems with wavelength division multiplexing (WDM). Low-loss AWGs are strongly required. We propose the low-loss segmented joint structure between a slab waveguide and arrayed waveguides for AWGs. A taper waveguide of each arrayed waveguide is separated into M sections, and the widths of both ends of each section and the length are optimized using the downhill simplex method. The coupling efficiencies are calculated by beam propagation method. Usually, the simulated coupling efficiency is converged on the local maximum value in only 100 iterations due to small number of variables. The higher coupling efficiency can be obtained with larger M, but it is almost saturated at around $M = 3$. The optimized coupling efficiency between a slab waveguide and arrayed waveguides is 91%, and it is 16% better than that of the joint structure with a conventional taper waveguide; when the input taper waveguide width is 15.0 μm , the slab waveguide length is 4171.6 μm , the number of the arrayed waveguides is 37, the pitch of the arrayed waveguides is 10.9 μm , and $M = 1$, respectively. The coupling efficiency is further improved to 92% when $M = 5$. The prototype silica planer lightwave circuits are under fabrication.

9365-49, Session PWed

Total internal reflection mirror-based ultra-sensitive triangular ring resonator sensor on the surface plasmon resonance condition

Hong-Seung Kim, Tae-Ryong Kim, Chung-Ang Univ. (Korea, Republic of); Doo-Gun Kim, Korea Photonics Technology Institute (Korea, Republic of); Young Wan Choi, Chung-Ang Univ. (Korea, Republic of)

In this paper, we have theoretically analyzed using a finite-difference time domain (FDTD) methods and realized a high sensitive triangular ring resonator sensor based on the total internal reflection (TIR) mirror with a thin metal film for surface plasmon resonance (SPR) phenomenon. One of advantages is a high sensitivity with large phase variation at TIR mirror facet with SPR. Previously, the sensing region of the general ring resonator sensor is located on the cladding region or upper core region. However, the triangular ring resonator has a very high sensitivity using the sensing region of the TIR mirror facet, because the length of the evanescent field at TIR mirror is longer than the evanescent field length at the cladding region. Another is a high Q-factor by the round-trip loss compensation through an active medium in the waveguide. Proposed sensor also has an integrated light source using an InP-based semiconductor optical amplifier. The sensitivity of triangular ring resonator with SPR is extremely enhanced by large phase shift at TIR mirror facet on SPR. Optimized metal thickness is a 33.4 nm at the SPR angle of 24.125 degree. The simulation result of the sensitivity for the triangular ring resonator sensor with SPR is 940 nm/RIU using by FDTD method. To measure the biosensor, we used an antigen/antibody reaction.

More detailed results on an integrated 1D PhC microcavity sensor with TIR mirror will be presented.

9365-50, Session PWed

Silica-on-silicon based 650/1550nm wavelength mux/demux for swept source OCT

Zhongwei Wu, Hui Zhou, Suiwen Wan, Xiaohan Sun, Southeast Univ. (China)

Swept source optical coherence tomography (SS-OCT) has been considered as an active imaging technology and will have many applications in biomedical diagnoses, by measuring the backscattering light from in vivo organization to acquire its cross-sectional imaging. Photonic integrated circuit (PIC) based SS-OCT system is required to achieve low power consumption, miniaturization and handheld, in which the red/infrared lightwave mux/DeMux is a very important component because red light should be used for guiding light to achieve accurate positioning of the probe location, and infrared light is used as detecting light with the structure information of the organization. However, the bandwidth of swept laser in SS-OCT system can be up to 100nm, so the red/infrared lightwave mux/DeMux should be optimized with such wide bandwidth.

We propose a 650/1550nm wavelength Mux/DeMux for SS-OCT system based on silica-on-silicon (SoS), in which mixing red/infrared lightbeams can be fully separated at low insert loss through special cascade multimode interference (MMI) structure. Each independent lightbeam is entered into its respective channel by selecting proper width and length of the MMI. By using of Finite Difference Beam Propagation Method (FD-BPM), the Mux/DeMux is optimally designed in size of 1?0.1mm², working at 650nm and 1550nm simultaneously. The results show the degrees of separation between two lightwaves are super high, loss of infrared light is less than 0.5dB and 1dB, and its output power stability is less than 0.25dB and 0.8dB, in 1510nm-1570nm and in 1500nm-1600nm, respectively. The Mux/DeMux can be used in SS-OCT PIC based on SoS.

9365-51, Session PWed

Design and characterization of integrated optical interferometers fabricated in polymer foils

Yanfen Xiao, Univ. of Freiburg (Germany); Yixiao Wang, Leibniz Univ. Hannover (Germany); Meike Hofmann, Hans Zappe, Univ. of Freiburg (Germany)

Integrated optical interferometric sensors are amongst the most attractive means to measure the refractive index of liquids or gases for applications in the chemical and biochemical fields. These sensors are based on single mode waveguides whose upper cladding is removed in the sensing region, enabling the evanescent field to interact with the analytes absorbed on the surface. The interaction between the optical field and analytes changes the properties of the guided wave and induces a phase shift which is used as an indicator for the analyte-dependent refractive index of the surrounding media.

We present here a new means of producing cost-efficient Mach-Zehnder interferometers for sensing by applying the fabrication techniques of roll-to-roll processing. This fabrication approach allows realization of distributed all-polymer sensors and arrays in a printable large-area foil. However, when compared to glass or silicon based systems, the very small refractive index contrast in polymer integrated optics requires new approaches for optimization of printable interferometric sensors.

In this context, we present the design and characterization of polymer-based Mach-Zehnder interferometers combined with hybridly-integrated light sources for sensing of refractive index changes in solutions. Simulations of the modal and loss behavior of different waveguide structures, in particular curves and couplers, as well as waveguide-to-waveguide coupling efficiency are investigated, yielding design rules for the interferometers. The coupling efficiency and stability between light sources bonded to the substrate and waveguides are also addressed. Finally, measurement results from printed Mach-Zehnders made from tailored polymers support these design considerations.

9365-52, Session PWed

Characterization of mid-infrared sidewall gratings in As₂S₃-on-Ti:LiNbO₃ waveguides with optical low-coherence interferometry

Xin Wang, Chen Zhang, Christi K. Madsen, Texas A&M Univ. (United States)

Arsenic tri-sulfide (As₂S₃) on titanium-diffused lithium niobate (Ti:LiNbO₃) is a proven powerful hybrid design platform for integrated optical device. Recently, sidewall Bragg gratings on this platform were fabricated by electron-beam lithography (EBL) and their spectral response were characterized at near-infrared (near-IR). Such hybrid sidewall Bragg gratings can be extended to mid-infrared (mid-IR) regime. Complex grating profiles (such as sinusoidal, square, trapezoidal, chirping, apodizing and sampling) can be easily implemented and fabricated by a single lithography step. A difficulty resides in measuring the narrowband response in the mid-IR range because of limitations in the availability and cost of wavelength-swept laser sources. We explore the use of optical low-coherence interferometry (OLCI) with a supercontinuum source to make the critical measurements in the mid-IR. With an optical pass-band filter over a desired wavelength range, the OLCI and Fourier spectroscopy can be carried out at mid-IR. The OLCI setup with supercontinuum source has been tested at near-IR, and the results are in good agreement with the measurements by a commercial optical vector analyzer. Both the amplitude and group delay characteristics can be measured for a device under test, enabling measurements on advanced grating structures ranging from multi-channel filters to tunable delay filters.

9365-53, Session PWed

A quantitative method to measure the carbon particles density in an electroactive layer of a polymer-based supercapacitor

Mohamad Rezaei, Jasbir N. Patel, Bozena Kaminska, Simon Fraser Univ. (Canada)

Supercapacitors (SCs) are a promising technology for the storage of electrical energy due to their very high power and energy storage capacity and fast charging with slow discharging cycles. The supercapacitor electrodes consist of a conductive current collector, an active material with a high specific surface area, and a separator. Ionomers such as Nafion and Aquivion are good candidate polymers to use as a polymeric solid electrolyte in SCs.

Activated carbon is the most commonly used high surface electrode material. It is less expensive than other electrode materials like carbon nanotubes and graphene. Its complex porous structure can provide a very high specific surface area. The size, volume percentage and distribution of carbon particles in electrolyte have a significant effect on the electrical properties of a SC. Our supercapacitors are fabricated using simple low-cost spray coating system designed in our lab. The activated carbon particle based ink is directly sprayed on to the ionomer sheets to realize a working supercapacitor.

In this research, a quantitative analysis of optical microscope images using image-processing algorithms is proposed. Image processing of the microscope images of novel supercapacitor electrodes is performed to examine the effect of carbon particle distribution and to calculate the density of carbon particles. The inks with different volume ratio of carbon particles and ionomer are sprayed, imaged and analyzed. The resultant capacitance is directly related to the quantified particle density. We obtained the average 5F/g without any enhancements.

9365-54, Session PWed

External cavity laser using a InGaAs quantum dot gain chip and an arrayed-waveguide grating for T-band optical communication

Hideki Shibutani, Keio Univ. (Japan); Yasunori Tomomatsu, Koshin Kogaku Co., Ltd. (Japan); Yoshinori Sawado, Katsumi Yoshizawa, Pioneer Micro Technology Corp. (Japan); Hideaki Asakura, Bin Idris Nazirul Afham, Hiroyuki Tsuda, Keio Univ. (Japan)

The use of the T-band (1030 nm to 1260 nm) is promising for short reach, large capacity optical communication in a data center or an access network for short reach, large capacity optical communication in a data center or an access network. It is feasible with low-cost coarse wavelength division multiplexing (WDM). The tunable wavelength light source is necessary for such an application.

In this paper, we propose new configuration of the external cavity laser, which uses a silica-based arrayed waveguide grating (AWG) for a wavelength selection element.

The external cavity laser consisted of the gain chip, which facets were high reflection (HR) and anti-reflection (AR) coated, coupling lenses, the AWG with AR/HR coatings, and the output fiber. The AWG had 17 connecting ports, which corresponded to 17 wavelengths with a channel spacing of 1.67 nm. The width of the connecting port waveguide was optimized to have high coupling efficiency. The AWG chip size was 15 mm x 30 mm. The active layer in the gain chip had InGaAs quantum dots. The spontaneous emission 3-dB bandwidth was 48 nm (1108 nm to 1156 nm) when the injection current to the gain chip was 150 mA.

The lasing wavelength of the external cavity laser was successfully tuned

**Conference 9365: Integrated Optics:
 Devices, Materials, and Technologies XIX**

from 1129.9 nm to 1154.4 nm by selecting the connecting ports of the AWG. The typical threshold current was about 130 mA.

9365-55, Session PWed

LED absorption sensor system for the detection of organics in water

Chi Hoon Kim, Chonnam National Univ. (Korea, Republic of) and Korea Photonics Technology Institute (Korea, Republic of); Taeksoo Ji, Chonnam National Univ. (Korea, Republic of)

Determination of organic compound concentration in water is an imperative key to the control of water quality since it provides important information on pollution control of water supply. This work proposes an optical sensor where the organic compound concentration in water determined by LED light(280nm). The absorbance was quantified according to the concentration of organic compound by means of linear regression modeling. Thus, suitability of the regression model was 0.996 and also explained 99.6% of the total variation.

9365-56, Session PWed

Experimental demonstration of directive Si3N4 optical leaky wave antennas with semiconductor perturbations

Qiancheng Zhao, Caner Guclu, Yuwang Huang, Salvatore Campione, Filippo Capolino, Ozdal Boyraz, Univ. of California, Irvine (United States)

Optical leaky-wave antennas (OLWAs) with tunable radiation pattern are promising integrated optical-modulation and -scanning devices. OLWAs fabricated using CMOS-compatible semiconductor planar waveguide technology have the potential of providing high directivity with electrical tunability. We experimentally demonstrate directive radiation from a silicon nitride (Si3N4) waveguide-based OLWA. Such waveguides have a width of 1.2 μm and a height of 735 nm, and the leaky-wave radiation is enabled by periodic silicon (Si) perturbations buried inside the waveguide. This OLWA design comprises 50 crystalline Si perturbations with a period of 1 μm, each with a length of 260 nm and a height of 150 nm leading to a directive radiation pattern at telecom wavelengths. The measured far-field radiation pattern at the wavelength of 1540 nm is highly directive, with the maximum intensity at the angle of 85.7° relative to the waveguide axis and a half-power beam width around 2.4° which are consistent with our theoretical prediction. The wavelength effect on the far-field radiation pattern is also studied. The use of semiconductor perturbations facilitates electrical radiation control by changing the refractive index with governing carrier density in the perturbations or by manipulating the optical losses through the Franz-Keldysh effect. We show that the Franz-Keldysh effect has the potential to generate fast modulation in radiation control at telecom wavelengths.

Conference 9366: Smart Photonic and Optoelectronic Integrated Circuits XVII

Wednesday - Thursday 11-12 February 2015

Part of Proceedings of SPIE Vol. 9366 Smart Photonic and Optoelectronic Integrated Circuits XVII

9366-1, Session 1

Devices and system measurements of mode- and wavelength-division-multiplexing in the Si wire platform (Invited Paper)

Richard M. Osgood Jr., Jeffrey B. Driscoll, Christine P. Chen, Richard R. Grote, Brian B. Souhan, Jerry I. Dadap, Columbia Univ. (United States); Aaron Stein, Ming Lu, Brookhaven National Lab. (United States); Keren Bergman, Columbia Univ. (United States)

On-Chip photonic networks for information exchange between multiple cores based on Si-wire waveguide interconnects can support a substantial aggregate bandwidth since the supported optical states have many degrees of orthogonality and, thus, potential data channels. The most widely used orthogonality is wavelength and WDM has already demonstrated ultrahigh data rates of 1.28 Tb/s transmission through a Si-wire waveguide. However, other orthogonalities can be used to extend bandwidth scaling or to diminish system-level cost and complexity. Here, we will discuss our silicon devices developed for two of these orthogonal degrees, viz spatial modes (MDM) and polarization, and fabrication and design to reduce crosstalk and wavelength uniformity. In the first example, these devices are used for on-chip MDM and MDM-WDM transmission through a multimode Si waveguide. This capability uses completely passive and compact asymmetric-Y-junction modes to mux and demux. With these asymmetric Y-junction, we measure an aggregate bandwidth of 60 Gb/s using 23?10 Gb/s MDM-WDM over a 1.2 mm link with power penalties of < 1 dB/channel. In the second example, polarization division multiplexing (PDM) is simultaneously employed, and the power penalty resulting from both polarizations is measured. Our experiments show power penalties of < 5 dB with a BER of 10⁻⁹, for combined MDM-PDM operation of error-free transmission. These measurements are the first to show the potential for implementing full-spatial MDM with both polarizations on an integrated Si-wire platform. Finally we will conclude with a discussion of the potential for scaling MDM devices to larger branching numbers.

9366-2, Session 1

Two probe writing and electrical measurements of oriented carbon nanotubes

Aaron Lewis, Talia Yeshua, The Hebrew Univ. of Jerusalem (Israel); Christian Lehmann, Stephanie Reich, Freie Univ. Berlin (Germany); Kristin Strain, Eleanor Campbell, The Univ. of Edinburgh (United Kingdom)

A multiprobe scanning probe microscope (SPM) system has been used to perform multiprobe electrical measurement of carbon nanotubes. In this system two probes can be used across an isolated carbon nanotube. A variety of probes have been developed that are compatible with multiprobe operation. These include probes for writing oriented single single walled carbon nanotubes which have a high degree of alignment and this is demonstrated with on-line Raman. The interconnection of the multiprobe system with the Raman System will be described in detail. The combination has the potential to cross the fabrication/measurement gap that will allow for both production and nanocharacterization of such single molecule carbon nanotube molecular devices both with chemically sensitive Raman measurements (with and without plasmonic enhancement) and with on-line electrical transport on isolated carbon nanotubes.

9366-3, Session 1

Optical routers for photonic networks-on-chip

Lin Yang, Qiaoshan Chen, Fanfan Zhang, Ruiqiang Ji, Rui Min, Institute of Semiconductors (China)

With CMP continuously requiring more communication bandwidths, metallic-based electrical NoC gradually becomes the bottleneck for improving the performance of CMP due to its high power consumption, limited bandwidth and long latency. Photonic NoC is considered as a potential solution to overcome the limitations of its electrical counterpart. Optical router is a key device in photonic NoC, which is responsible for routing data from one optical link to another optical link.

In this paper, we will review the status of the optical routers for photonic networks-on-chip and introduce our efforts on this topic. Firstly, we will introduce several demonstrated optical routers based on microring or Mach-Zehnder optical switches. Then, we will introduce a universal method for constructing an N-port non-blocking optical router for photonic NoC. The optical router constructed by this method has minimum optical switches, in which the number of the optical switches is reduced about 50% compared to the reported optical routers based on microring optical switches and about 30% compared to the reported optical routers based on Mach-Zehnder optical switches, and therefore is more compact in footprint and more power-efficient. Finally, we will introduce the fabricated 4- and 5-port optical routers constructed by this method.

9366-4, Session 2

Monolithic electro-optic CMOS Mach-Zehnder transmitters (Invited Paper)

Douglas M. Gill, Jonathan E. Proesel, Chi Xiong, Jessie C. Rosenberg, Yurii Vlasov, Marwan Khater, Jason S. Orcutt, IBM Thomas J. Watson Research Ctr. (United States); Steven M. Shank, Carol Reinholm, John J. Ellis-Monaghan, Edward Kiewra, IBM Microelectronics Div. (United States); Wilfried Haensch, William M. J. Green, IBM Thomas J. Watson Research Ctr. (United States)

Complementary metal-oxide semiconductor (CMOS) integrated nano photonics (CINPs) could bring traditional semiconductor industry efficiency and low cost manufacturing to the application space of optical interconnects, which has the potential to enable large scale deployment of broadband communication links. To address this potential IBM has recently announced its sub-100nm CIMP technology (CMOS9WG) that has silicon modulators, germanium photodetectors, WDM filters, optical couplers, etc., monolithically integrated with analog and mixed-signal circuits.

In this talk I will give a brief technical review of the IBM CMOS9WG technology with a specific focus on the design and performance of monolithically integrated electro-optic transmitters. I will present technical results from monolithic 25 Gb/s transmitters fabricated in the CMOS9WG technology. The design and performance of transmitters that have CMOS drive circuitry monolithically integrated with traveling-wave and lumped-element Mach-Zehnder modulators (MZMs) will be discussed. On-chip drive amplitude and thermal optic heater control is also enabled via monolithically integrated CMOS circuitry. In addition, the incorporation of monolithically integrated inductors as well as periodic PN-junction loading of the MZMs will be addressed. Furthermore, link considerations regarding the relationship between the modulator efficiency-loss figure of merit (with units of V-dB) and the attainable CMOS drive voltage and resulting optical loss will be reviewed.

9366-5, Session 2

Multi-parameter extraction from SOI photonic-integrated circuits using circuit simulation and evolutionary algorithms

Alfonso Ruocco, Univ. Gent (Belgium); Wim Bogaerts, Univ. Gent (Belgium) and Luceda Photonics (Belgium)

We propose a procedure to extract multiple parameters from the spectral characteristic of a photonic integrated circuit. We applied the method on high-order silicon Mach-Zehnder lattice filters: these filters are realized by cascading delay stages and directional couplers. Because of their cascaded nature and roll-off properties, these devices can be used to accurately extract properties of the waveguides and the directional couplers. The spectral transmission is measured between the inputs and the outputs. This result is compared to a full CAPHE optical circuit simulation with parametric behavioral model for the waveguide and the directional couplers. An evolutionary fitting algorithm based on the covariance matrix adaptation method is used to match the circuit simulation with the measurement. This "black box" approach gives fast and accurate parameter extraction of reduced iteration steps. The quadratic error between measurement and simulation of each iteration is used as feedback for the evolutionary algorithm that adapts the test values for the following step. Target of the analysis are an accurate, wavelength-dependent model for the group index and the directional couplers. The proposed method has been used for wafer scale parameter extraction. Our fast method makes it possible to extract the parameters in real time, and correlate the functional parameters of the waveguides with process statistics collected during fabrication. The obtained parameters are in substantial agreement with the results of the simulations used in the design, and can be used further to improve behavioral models that correlate the manufacturing process specifics with the optical performance.

9366-6, Session 3

Quantum and ultrafast precision measurements in mesoscopic mode-locked architectures *(Invited Paper)*

Chee Wei Wong, Columbia Univ. (United States)

Recent advances in sub-wavelength nanoscale platforms have afforded the control of light from first principles, with impact to ultrafast sciences, optoelectronics and precision measurements. In this talk I will highlight two coherent examples where emerging micro-scale architectures can make a difference. First, I will describe recent advances in chip-scale Kerr frequency comb oscillators, where we have achieved sub-100-fs pulse mode-locking, one of the shortest pulse Kerr comb to date. Coherent mode-locking is observed in the normal dispersion regime, verified by phase-resolved ultrafast spectroscopy at sub-100-attojoule sensitivities. The normal dispersion architecture uncovers the mode-locking mechanisms in Kerr frequency combs, matched with first-principles coupled-mode theory, complementing our efforts on precision optical clocks.

Second, I will describe our recent quantum entanglement advances on high-dimensional frequency mode-locked two photon states for dense quantum communications. We first demonstrate revival of the Hong-Ou-Mandel interferences, long postulated by theorists more than a decade ago, up to 19-dimensions and with visibilities up to 96.5%. The phase-locked high-dimensional qubit state is further witnessed through a stabilized Franson interferometer, as a generalized Bell's inequality test and hyperentangled through multiple degrees-of-freedom. Entanglement revivals of the non-local interference at discrete time-bins are uncovered for the first time, up to 97.8% visibility, as a fundamental resource for dense secure information processing.

9366-7, Session 3

Controlling light at the exceptional points with whispering gallery microresonators *(Invited Paper)*

Sahin K. Ozdemir, Lan Yang, Washington Univ. in St. Louis (United States)

Whispering-Gallery-Mode (WGM) optical microcavities with their high-quality factors and microscale mode volumes have emerged as versatile platforms for exploring basic science and for fabricating functional devices. In this talk, we will focus on systems of coupled WGM resonators (WGMRs) for on-chip control of optical processes and light transmission. WGMRs represent open physical systems that are characterized by non-Hermitian Hamiltonians, and thus by appropriately steering the system parameters, their complex eigenvalues and the corresponding eigenstates can be made to coalesce giving rise to a degeneracy referred to as Exceptional point (EP). In this talk, we will present two applications enabled by driving coupled WGM microcavities through exceptional points. First we will show parity-time (PT) symmetry and its breaking in a system composed of two coupled WGM microcavities, one of which has passive loss (passive resonator) and the other has optical gain (active resonator) balancing the loss of the other. By controlling the inter-cavity coupling strength, one can drive the system from PT-symmetric phase to the broken PT-symmetry phase through an EP. The broken phase enables localization of light in the active resonator, leading to nonlinearity-based nonreciprocal light transmission. Then we will show that modulating the loss contrast between two coupled passive resonators can bring the system to an EP where the total intracavity field intensity increases despite increasing loss. This enables us to control and reverse the effects of loss in optical systems. We will end the talk discussing some of the opportunities and challenges in the WGM research.

9366-8, Session 3

Optodic bonding of optoelectronic components in transparent polymer substrates-based flexible circuit systems

Yixiao Wang, Meriem Akin, Lisa Jogschies, Ludger Overmeyer, Lutz Rissing, Leibniz Univ. Hannover (Germany)

In the field of modern information technology, optoelectronics are being widely used and playing an increasingly important role. Meanwhile, the demand for more flexibility of circuit carriers is rapidly growing, since it facilitates the realization of diverse functions and applications. As a potential candidate, transparent polymer substrates with a thickness of about hundred micrometers by virtue of their low cost and sufficient flexibility are getting more attention. Thus, accomplishing an integration of optoelectronic components in polymer based flexible circuit systems increasingly becomes an attractive research topic, which is of great significance for future information transmission and processing. We are committed to developing a new bonding process to realize it. Taking into account the fact that most economical transparent polymer substrates can only be processed with restricted thermal loading, we design a so-called optode instead of a widely adopted thermode. We employ UV-curing adhesives as bonding materials; accordingly the optode is equipped with a UV irradiation source. An investigation facing commercial optoelectronic components is conducted, in which their dimensions and structures are studied. In selecting appropriate transparent polymer substrates, we take the characteristics such as UV transmission degree, glass transition temperature, etc. as key criterions and choose PET and PMMA as carrier materials. Besides bonding using adhesives cured by optode, underfill is accordingly employed to enhance the reliability of the integration. We deposit electrical interconnects onto the polymeric substrate to be able to place the optoelectronic components into electrical operation. In order to enlarge the optical coupling zone from component to substrate within the proximity of the adhesive or underfill, we employ transparent interconnects made of indium-tin-oxide. We present

**Conference 9366: Smart Photonic and
Optoelectronic Integrated Circuits XVII**

the results of the performance tests, including the contact resistances, mechanical tests and environmental tests.

9366-25, Session PWed

Photoluminescence properties of [beta]-FeSi2 on treated Si surface by metals

Kensuke Akiyama, Kanagawa Industrial Technology Ctr. (Japan); Hiroshi Funakubo, Tokyo Institute of Technology (Japan)

Semiconducting iron disilicide (β -FeSi₂) has attracted much attention over the past ten years as one of the promising materials for fabricating infrared optoelectronic devices. This is because β -FeSi₂ has a band gap of approximately 0.80 eV, and a very large optical absorption coefficient of over $1E+5$ /cm at 1 eV, in addition to ability of epitaxially growth on Si substrates. It emits light of about 1.55 μ m suitable for silica optical fiber communications. Recently, photoresponsivity of β -FeSi₂ single crystals is reported to reach to 58 mA/W at 0.91 eV. These optical properties of this semiconducting material have been expected for a development of monolithic optical device on Si substrates. Moreover, this material is considered to be an environmentally friendly semiconductor since both Si and Fe are nontoxic and occurs abundantly in the Earth's crust.

For the application of this material to those optoelectronic devices, β -FeSi₂ thin film with low defect density is essential. In this study, we report the enhancement of photoluminescence(PL) intensities from β -FeSi₂ films by coating copper (Cu), silver (Ag) and gold (Au) layer on (100)Si wafers by using metal-organic chemical vapor deposition (MOCVD).

A clear PL spectrum for β -FeSi₂ was observed by Au, Cu and Ag coating on (100)Si. High-crystal-quality β -FeSi₂ with a low-level non-radiative center was formed on treated Si by these metals. This method of deposition can be applied to other materials requiring high crystal quality. This high quality β -FeSi₂ with low defect density opens the door for the real applications.

9366-26, Session PWed

Microphotonic filter applications of silicon microspheres

Ulas S. Gökay, Muhammad Zakwan, Ali Serpengüzel, Koç Univ. (Turkey)

Elastic light scattering has been performed in silicon microspheres with refractive index of 3.5 and radius of 500 micrometers at near-infrared telecommunication wavelength of 1427 nm. Lorentzian and Fano lineshape whispering gallery modes with quality factors on the order of 100000 have been observed. Possible microphotonic filter applications of the Lorentzian lineshape include sensing, whereas possible microphotonic applications of the Fano lineshape include channel dropping.

9366-9, Session 4

Novel distributed feedback lightwave circuit elements

Ceren B. Dag, Istanbul Teknik Üniv. (Turkey); Mehmet A. Anil, Istanbul Technical Univ. (Turkey) and Univ. of Colorado (United States); Ali Serpengüzel, Koç Univ. (Turkey)

The devices that are variations of inter- and intracoupled meandering optical waveguides are proposed as the lightwave circuit elements that exhibit distributed feedback. A preliminary transfer matrix method analysis is applied in frequency domain, taking the coupling purely directional and with constant coefficient on geometrically symmetric and anti-symmetric

devices. The meandering loop mirror is the building block of all meandering waveguide based lightwave circuit elements. The simplest uncoupled meandering distributed feedback structure exhibits Rabi splitting in the transmittance spectrum. The symmetric and antisymmetric coupled meandering distributed feedback geometries can be utilized as band-pass, Fano, or Lorentzian filters or Rabi splitters. Meandering waveguide distributed feedback structures with a variety of spectral responses can be designed for a variety of lightwave circuit element functions and can be implemented with generality due to the analytic approach taken. The conclusions are further intricated with the finite time domain simulations on the breathless scalar signals to utilize the delay line properties of the meandering waveguide distributed feedback structures.

9366-10, Session 4

Heterogeneous 2D and 3D integrated circuits for temporal, spectral, and spatial information processing (Invited Paper)

S. J. Ben Yoo, Univ. of California, Davis (United States)

We discuss heterogeneous integration technologies in 2D and 3D leading to new capabilities in signal processing in temporal, spectral, and spatial domains. Recent advances in photonic and electronic integration demands an addition of a new dimension in integration. 3D integration emerges as a new necessity in providing functional integrated microsystems for modern computing, networking, and imaging applications. Exponential increases in the amount of data that need to be sensed, communicated, and processed are continuing to drive the complexity of our computing, networking, and sensing systems. High degrees of integration is essential in scalable, practical, and cost-effective microsystems. In electronics, high-density 2D integration has naturally evolved towards 3D integration by stacking of memory and processor chips with through-silicon-vias. In photonics, too, we anticipate high-degrees of 3D integration of photonic components to become a prevailing method in realizing future microsystems for information and communication technologies. However, compared to electronics, photonic 3D integration face a number of challenges. This paper will review two methods of 3D photonic integration --- fs laser inscription and layer stacking, and discuss applications and future prospects.

9366-11, Session 4

Simple and compact tunable semiconductor lasers based on novel half-wave coupler (Invited Paper)

Jian-Jun He, Zhejiang Univ. (China)

Widely wavelength tunable semiconductor lasers are important components for next-generation optical networks, and for applications in spectroscopic measurements. Over the last two decades, high performance tunable lasers have been developed based on complex structures such as sampled grating distributed Bragg reflector, superstructure grating DBR, digital supermode DBR, modulated grating Y-branch, and so on. In addition to fabrication complexity involving non-uniform gratings and multiple epitaxial growths, multiple electrodes with complex control algorithms are usually required for wavelength tuning. With the dense wavelength division multiplexing technology extending towards access and datacenter networks, and the emerging demands of portable devices for biomedical analyses etc., the cost reduction and operational simplicity become more and more important.

Simpler designs known as coupled-cavity lasers with an etched trench or cleaved-coupled-cavity (C3) structure were investigated in the 1980's. However, they have not been widely used in practice because of their poor single-mode characteristics. Recently, compact tunable lasers based on a novel half-wave coupler have been proposed and experimentally demonstrated. Single-electrode controlled wide-band wavelength tuning was realized with an excellent side-mode suppression ratio of about 40dB. By combining temperature-induced gain spectrum shift with current

**Conference 9366: Smart Photonic and
Optoelectronic Integrated Circuits XVII**

controlled Vernier tuning mechanism, the tuning range was extended to over 50 channels. They are all-active devices with no epitaxial regrowth. The fabrication process is similar to simple Fabry-Perot lasers and the device size is only about 0.5?0.3 mm². High speed direct modulation has also been demonstrated. In this paper, the principle, design, packaging and measurement results of the tunable lasers are reviewed.

9366-12, Session 5

Undisturbed interferometric sensing through a fluid interface by electrically-tunable lenses and micro mirrors (*Invited Paper*)

Jürgen W. Czarske, Hannes Radner, Christoph Leithold, Lars Büttner, Technische Univ. Dresden (Germany); Moritz Stürmer, Ulricke Wallrabe, Univ. of Freiburg (Germany)

We have harnessed the power of various programmable photonics devices for an interferometric measurement technique. Distortion-free laser-based velocity measurements through a dynamic gas-liquid interface are enabled by a closed-loop optoelectronic system. We are employing electrically tunable lenses and micro mirrors to correct low-order wavefront distortions effectively. Our work represents a paradigm shift in interferometric velocity measurement techniques from using static to dynamic optical elements.

The novel sensing technique was designed to overcome a shortcoming of existing laser interferometers in fluid dynamics applications. Transmitted laser beams can be distorted due to the fluctuating interfaces between media with different refractive indices. Temporal fluctuations of these distortions cause deterioration of laser interferometers and result in increased measurement uncertainties, or inability to make successful measurements. With our adaptive interferometry technique it is possible to make fluid flow velocity measurements behind a rapidly fluctuating interface [1].

We present the experimental as well as the computational investigation of a velocity measurement system based on a laser interferometer. By the numerical investigation of the uncertainty budget with a Monte-Carlo-like simulation the strategy for an improved adaptive optics system has been identified. The employed electrically tunable lenses [2] are capable of a defocus range of 40 dpt. at modulation frequencies of over 60 Hz. The adaptive correction of the tip and tilt is accomplished by a 2-axis voice-coil driven micro mirror. With the vastly superior defocus range of electrically tunable lenses it will be possible to measure non-invasively behind two-dimensional fluid interfaces.

[1] L. Büttner, C. Leithold and J. Czarske, "Interferometric Velocity Measurements through a fluctuating Gas-Liquid Interface Employing Adaptive Optics" in *Optics Express*, 21(25), pp. 30653-30663, (2013).

[2] N. Koukourakis, M. Finkeldey, M. Stürmer, C. Leithold, N.C. Gerhardt, M.R. Hofmann, U. Wallrabe, J.W. Czarske, A. Fischer, "Axial scanning in confocal microscopy employing adaptive lenses (CAL)" in *Optics Express* 22(5), pp. 6025-6039, (2014).

9366-13, Session 5

Integrated optofluidics chips for efficient on-chip infectious disease detection (*Invited Paper*)

Hong Cai, Joshua W. Park, Univ. of California, Santa Cruz (United States); Tomas Wall, Brigham Young Univ. (United States); Ricardo Carrion Jr., Jean L. Patterson, Texas Biomedical Research Institute (United States); Richard A. Mathies, Univ. of California, Berkeley (United States); Aaron R. Hawkins, Brigham Young Univ. (United States);

Holger Schmidt, Univ. of California, Santa Cruz (United States)

Optofluidic devices based on liquid-core ARROW waveguides have been shown to provide single molecule and single bioparticle fluorescence detection sensitivity using a fully planar, waveguide-based silicon chip and fiber-optic readout. Here, we report recent progress on optofluidic integration and detection of infectious disease biomarkers.

9366-14, Session 5

Nanophotonic sensor for optofluidic detection of gas/water/oil fluids

Huub W. Salemink, Radboud Univ. Nijmegen (Netherlands); Yazhao Liu, Technische Univ. Delft (Netherlands)

Photonic crystal sensors have many advantages compared to other kinds of sensors and have become one of the hot research topics. Firstly, photonic crystal has very small footprint and high quality factor/volume. It has been proven that with fine structural optimization a photonic crystal cavity can have a quality factor (Q) as high as 10⁶ in very small dimensions on the order of wavelength cubed, which enhances the light-matter interaction effect but decreases the volume of interaction. Therefore, tiny variations in refractive index are measurable and reflected in the optical properties of the photonic crystal cavities. Secondly, photonic crystal can be easily integrated with other on-chip elements. A potential utilization of this feature is being used as a part of a lab on chip [optofluidics]. However, the widths of the transmission band gaps and the light confinement in the photonic crystal cavity strongly depend on the refractive index contrast between the solid material and periodically embedded materials. In previous reports, high Q factors were obtained under high refractive index contrast (silicon vs. air). In many practical applications, sensors are expected to work under liquid environment. A high refractive index of the liquid will unavoidably cause adverse results such as narrow band gaps, low Q factors, weak light confinement in both vertical and horizontal directions, and broad resonant peaks in transmission. These problems can seriously affect the functionalities of the sensors, lower the sensitivities or resolution in detection. Here we present our investigation towards the development of sensor based on a modified L3 cavity that can overcome the above difficulties. As will be demonstrated, our sensor is designed to work under high refractive index material infilling of $n = 1.5$, which is much higher than many typical liquids. Theoretical analysis shows that after modifying the structure of the sensor, the Q factor and intensity are highly increased. In experiment, an oil sample with a refractive index of 1.45 is used to demonstrate the sensing ability of our sensor. We observe a wavelength shift of 12.4 nm with a refractive index variation of 0.12.

9366-15, Session 6

Design, fabrication and demonstration of heterogeneously III-V/Si laser with a compact optical vertical interconnect access (*Invited Paper*)

Jing Pu, Kim Peng Lim, Doris Keh Ting Ng, Vivek Krishnamurthy, Chee Wei Lee, Kun Tang, Anthony, Yew Seng Kay, Ter Hoe Loh, Qian Wang, A*STAR - Data Storage Institute (Singapore)

The heterogeneous III-V/Si platform enables fully-integrated photonic system-on-chip technology and heterogeneous III-V/Si laser is the key component in this integration technology as it acts as an on-chip light source required for various functional photonic systems. Our recent development of the heterogeneous III-V/Si laser from the design, fabrication to experimental demonstration is presented.

The III-V/Si laser structure consists of III-V/Si rib waveguide section and

**Conference 9366: Smart Photonic and
 Optoelectronic Integrated Circuits XVII**

tapering section for light coupling to the silicon nanophotonic waveguide. The III-V epitaxial layers bonded on a 300 nm thick silicon layer is etched to form a rib III-V waveguide. A short optical vertical interconnect access is formed through tapering the III-V and silicon simultaneously in the same direction. The III-V/Si laser design ensures a sufficient light confinement in the bonded active gain medium and effective light coupling between the III-V semiconductor layer and silicon photonic layer. Another key advantage is it can provide a great flexibility in general functional photonic circuit development as the III-V is sitting on top of silicon without any trenches or predefined silicon waveguides beneath.

Fabrication details are given including silicon circuits module, III-V to silicon bonding module, III-V process module, and planarization and metallization module. With these established modules and process integration, we have demonstrated this heterogeneous III-V/Si Fabry-Pérot (FP) laser with characterized specifications as a proof-of-concept. A 2mm long FP laser with a 3um wide and 450um long III-V/Si waveguide gain section shows a lasing threshold of 65 mA under room temperature and continues wave operation. It is able to give a maximum output power of ~ 9mW at 100mA pumping current. The serial resistance of the whole structure is ~19 Ohm, which gives a space for further performance improvement through design and fabrication process optimization.

9366-16, Session 6

Heterogenous integration: the more than Moore path to silicon photonic microsystems *(Invited Paper)*

Gregory A. Fish, Alexander W. Fang, Aurion, Inc. (United States)

Aurion has developed a heterogeneous integration platform for integrating InP based semiconductor materials onto existing silicon photonic substrates. This enables all photonic functions including the laser, to be combined on a single silicon chip. The underlying photonic circuit is made up of low loss silicon and dielectric waveguides and is formed on a silicon on insulator substrate using established foundry infrastructure. There are several cost advantages to this platform including leveraging shared resources, use of 8 inch substrates instead of 2 inch substrates, and superior yield, which results from higher capacity foundries with greater capabilities and quality systems compared to traditional III-V photonics facilities.

The process features a bonding step to add InP materials to the silicon photonic circuit after the typical silicon photonic elements are formed.

This process is done at the wafer scale and involves placing "chiplets" of custom unprocessed InP material on the silicon photonic circuit.

Using standard lithography and etch steps, the chiplets are processed in parallel to form lasers, optical amplifiers, modulators, and photodetectors. These elements are all registered to the underlying silicon waveguides and are optically connected through evanescent mode converters which connect the silicon and InP layers. Once this has been completed, further processing steps encapsulate the InP with dielectrics and form metal interconnects and contacts for RF and control circuitry.

Leveraging system-in-package developments from the electronics industry, we are able to use 2.5D or 3D interposer technologies to tightly integrate the photonic chip with advanced node electronic driver chips.

9366-17, Session 6

III-V/Si hybrid integrated devices for optical interconnect *(Invited Paper)*

Liu Liu, Jin Liu, South China Normal Univ. (China)

As the increasing demand for information interconnect, the traditional electrical interconnect will encounter a bottleneck on speed and power consumption. As a comparison, optical interconnect can offer better performance considering the above aspects. Multifunctional, high-speed,

highly-integrated photonic circuits are necessary for the next generation optical interconnect. Due to the compatible fabrication processes with CMOS electronics, silicon photonics has drawn much attention towards large scale integration of photonic devices. In this presentation, we discuss our view of the on-chip interconnect structure for future multi-core processors based on wavelength-multiplexing and our recent results on some key devices of such structure. Cascading performances of various wavelength multiplexers and de-multiplexers including arrayed waveguide gratings and echelle gratings based on silicon-on-insulator platform are discussed and compared. Besides passive functions, active devices, including modulators, light sources, etc., are also important for interconnect applications. Due to the limitations of silicon, hybrid integration through combining active III-V components and passive silicon waveguide circuits by BCB adhesive bonding are employed to realize some active photonic functions. InP based electro-absorption (EA) modulators on silicon are analyzed. Ultra short adiabatic tapers for mode converters between passive silicon waveguides and InP active structures are designed. The integration of multi-channel EA modulators and wavelength (de)multiplexer are realized. In addition, we also demonstrate a novel doubled-side processed III-V nanowire waveguide. This waveguide contains asymmetric thin upper and lower InP layers for lateral current injection, which make the metal contacts away from optical field while keeping a high index contrast in all directions.

9366-18, Session 7

Fan-in/out polymer optical waveguide for a multicore fiber fabricated using the Mosquito method

Daisuke Suganuma, Takaaki Ishigure, Keio Univ. (Japan)

We fabricate fan-in/out polymer optical waveguides for a multicore (7 cores) fiber with a 25-um core diameter and 40-um inter-core pitch for improving the productivity, integration and miniaturization of current fan-in/out devices.

First, we design the fan-in/out waveguide to be inserted between the multimode multicore fiber and a fiber ribbon or parallel laser/detector array devices (horizontally aligned) with a 250-um pitch. In its fabrication, we need not only to expand the inter-core pitch in the horizontal direction but also to bend the cores horizontally in order to align the seven cores in one line.

Next, we fabricate the waveguides using the Mosquito method which is capable of drawing a circular-graded-index core three dimensionally. Here, the Mosquito method is a fabrication method of polymer waveguides we have developed: A viscous core monomer is dispensed into another viscous cladding monomer from a thin needle attached to a syringe, followed by curing the monomers to obtain a polymer waveguides. Hence, three dimensional needle scan in the cladding monomer allows us to fabricate the designed structure for fan-in/out waveguides. We succeeded in fabricating a 10-cm long fan-in/out waveguide with 25-um core diameter for the multicore fiber. The lowest insertion loss of the fabricated waveguide is measured as 3.21 dB at 850-nm wavelength. Although similar fan-in/out structure (a hexagonal core alignment is converted to one-dimensional alignment) was already reported in a glass waveguide with laser writing utilizing two-photon absorption, we experimentally demonstrate that even polymer waveguides can realize three-dimensional fan-in/out structure very easily.

9366-19, Session 7

Graded refractive index optics based on dual-layer ultrathin films: theory, design and applications in integrated photonics *(Invited Paper)*

Qian Wang, Kim Peng Lim, Doris K. Ng, A*STAR - Data Storage Institute (Singapore)

**Conference 9366: Smart Photonic and
 Optoelectronic Integrated Circuits XVII**

This paper presents an overview of graded refractive index optics based on dual-layer ultrathin films and the applications in integrated photonics as an on-chip lens for light coupling between nano-waveguide and optical fiber or off-chip laser. We firstly show our theoretical and experimental study of dual-layer ultrathin film optics. Using transfer matrix method, we present the detailed derivation to show the equivalence between the dual-layer ultrathin films and a negative birefringent thin film for the s-polarized and p-polarized light under arbitrary incidence angle. Analysis of the approximations shows the influence of thickness of dual-layer thin films and the incidence angle. Using ion-beam assisted deposition, a set of ultrathin films of titanium dioxide (TiO₂) and aluminium oxide (Al₂O₃) are deposited on silicon with different volume fractions and characterized. Measured results show a good agreement between the experiments and simulation of the equivalent thin film.

A graded refractive index lens based on the above dual-layer thin film stack is integrated on chip and optimized for light coupling between waveguide and optical fiber or off-chip laser. Conventional parabolic refractive index based GRIN lens suffers from the aberration and it affects the coupling efficiency severely for nanowaveguide. An aberration-free GRIN lens with a super-high numerical aperture and an optimal refractive index profile (generated by a computational algorithm) is developed for this sub-wavelength focusing and collimating. Two application examples are given for this dual-layer thin film stack based GRIN lens, which are optical coupling between silicon photonic chip and standard singlemode fiber for data interconnect, and optical coupling between the integrated light delivery system and off-chip laser for high-density data storage based on heat-assisted magnetic recording. With optimal design, both application examples give a design coupling efficiency ~90%.

9366-20, Session 7

**Bend insensitive graded index multimode
 polymer optical waveguides fabricated
 using the Mosquito method**

Asami Takahashi, Takaaki Ishigure, Keio Univ. (Japan)

In this paper, we fabricate low-loss graded index (GI) circular core multimode polymer optical waveguides with 90° bending using the Mosquito method, and demonstrate low bending loss even if the bend radius is as small as 1 mm. Utilizing the Mosquito method, we could fabricate waveguides with not only horizontally curved cores but also vertically curved ones.

Currently, optical interconnection technologies have been drawing much attention as a solution to maintain the advancement of computing performance. We have experimentally and theoretically demonstrated the capability of GI-core multimode polymer optical waveguides for chip-to-chip interconnection on printed circuit boards (PCBs). On PCBs, waveguides with curved structures as well as straight ones are required. In the several fabrication methods of GI-core polymer waveguides already proposed, we adopt the "Mosquito method" using a microdispenser because the Mosquito method makes it possible to fabricate waveguides directly on board at desirable position on PCBs and to draw various patterns of cores including curves. However, in the waveguides including such curved cores, the transmission loss could increase due to the bending (bending loss). In this paper, we characterize the fabricated GI-core polymer waveguides: we found when the NA of waveguides was as high as 0.3, no extra bending loss was observed compared to the straight waveguides with the same length even for a 1-mm bend radius. The core diameter of the fabricated waveguide is 50 μm, and it is possible to further decrease the bending loss in the waveguides with smaller core diameter.

9366-21, Session 8

**SPADAS: a high-speed 3D single-photon
 camera for advanced driver assistance
 systems**

Danilo Bronzi, Yu Zou, Federica A. Villa, Politecnico di Milano (Italy); Simone Tisa, Micro Photon Devices S.r.l. (Italy); Alberto Tosi, Franco Zappa, Politecnico di Milano (Italy)

Advanced Driver Assistance Systems (ADAS) are the most advanced technologies to fight road accidents. Within ADAS, an important role is played by radar- and lidar-based sensors, which are mostly employed for collision avoidance and adaptive cruise control. Nonetheless they have a narrow field-of-view and a limited ability to detect and differentiate objects. Standard camera-based technologies (e.g. stereovision) could balance these weaknesses, but they are currently not able to fulfill all automotive requirements (distance range, accuracy, acquisition speed, frame-rate). To this purpose, we developed an automotive-oriented CMOS single-photon camera for optical 3D ranging based on indirect time-of-flight (iTOF) measurements.

Single-photon avalanche diodes (SPAD)-based imagers offer higher sensitivity with respect to CCD/CMOS rangefinders, have inherent better time resolution, higher accuracy and better linearity. Moreover, iTOF requires neither high bandwidth electronics nor short pulsed lasers, hence allowing the development of cost-effective systems. The CMOS SPAD sensor is based on 64 × 32 pixels, each able to process both 2D intensity-data and 3D depth-ranging information, with background suppression. Pixel-level memories allow fully-parallel imaging and prevents motion artefacts (skew, wobble, motion blur) and partial exposure effects, which otherwise would hinder the detection of fast moving objects. The camera is housed in an aluminum case supporting a 12 mm F/1.4 C-mount imaging lens, with a 40° × 20° field-of-view. The whole system is very rugged and compact and a perfect solution for vehicle's cockpit, with dimensions of 80 mm × 45 mm × 70 mm, and less than 1 W consumption. To provide the required optical power (1.5 W, eye safe) and allow fast (up to 25 MHz) modulation of the active illumination, we developed a modular laser source, based on five laser driver cards, with three 808 nm lasers each.

We present the full characterization of the 3D automotive system, operated both at night and during daytime, in both indoor and outdoor, in real traffic, scenario. The achieved long-range (up to 45m), high dynamic-range (118 dB), high-speed (over 200 fps) 3D depth measurement, and high precision (better than 90 cm at 45 m), highlight the excellent performance of this CMOS SPAD camera for automotive applications.

9366-22, Session 8

**Smart optoelectronic 3D sensing systems
 (Invited Paper)**

Junichiro Fujita, Tomoyuki Izuhara, Louay A. Eldada, Quanergy Systems, Inc. (United States)

No Abstract Available

9366-27, Session 8

Image sensor innovations for low light levels with active imaging features

Gareth H. Powell, e2v semiconductors SAS (France)

Advances in CMOS imaging enable image capture at lower light levels. Colour detection is also possible where human vision becomes less sensitive in night conditions. In daytime conditions, there are a number of climatic conditions such as rain, fog, snow or smoke etc. that render traditional 'intelligent' outdoor cameras that perform various forms of detection and identification tasks relatively ineffective. It has been proven that an adapted five transistor pixel CMOS sensor can perform range-gated active imaging that extends considerably the usability of intelligent cameras in the most difficult conditions. This presentation discusses the most advanced state of the art image sensors and embedded features, with emphasis on the ever-important size, weight, power and cost benefits and discusses the new applications that are enabled.

9366-23, Session 9

Photonic-crystal-based all-optical NOT gate

Brahm R. Singh, Swati Rawal, Jaypee Institute of Information Technology (India)

Photonic crystal (PhC) is a promising candidate for fabrication of optical devices with dimensions of a few wavelengths of light for future photonic integrated circuits. Photonic crystals can be used for the implementation of logic gates like NOT gate which can be used as an inverter. The optical logic gate have a simple design. For realizing the inverting function, we report the design of a hexagonal lattice PhC channel waveguide with Silicon(Si) rods in air. The range of photonic band gap can be varied by changing radius of silicon rods. The lattice constant used is $a = 0.68\mu\text{m}$. The radius of silicon rods is kept at $r = 0.2318\mu\text{m}$, so that the photonic bandgap varies in the range of $0.3863 \leq a/\lambda \leq 0.4899$. The photonic crystal structure has a certain performance with optimum dimension of almost $12.92\mu\text{m} \times 9.42\mu\text{m}$. Normalised transmission has been calculated for the C-band and the simulation results show that the extinction ratio is above 10 dB for NOT gate. Moreover, the operational wavelength of the input ports is $1.554\mu\text{m}$. Since the structure has a simple geometric shape using hexagon geometry with clear operating principle, it is potentially applicable for photonic integrated circuits. The advantage of using this PhC based NOT gate is that they consume low power and their interfacing is very easy compared to other logic gates.

9366-24, Session 9

Topological spin-polarized states in photonic metacrystals waveguide

Jian-Wen Dong, Yabin Chen, Jiarong Wang, Sun Yat-Sen Univ. (China)

Singal process by flow of light rather than by electrical currents has been extensively investigated. Many photonic devices, e.g., optical filter, optical modulator and slowlight optical buffer, have been achieved. However, disorder and imperfection in realistic nanofabricated structures severely reduce device performance. Topologically spin-polarized states with its fantastic robust transport behavior have been proposed to cope with the problem of disorder. Here, we report our recent experimental and theoretical results on photonic topological insulator and the nontrivial characteristics. We experimentally propose a prototype of photonic metacrystal waveguide which is constructed by non-resonant meta-atoms sandwiched between two metallic plates. Broadband impedance-matching and strong bianisotropic metamaterials due to the coupling between transverse electric and transverse magnetic guided modes are both achieved. Topological transition between photonic topological insulator and photonic ordinary insulator has been found. Topologically nontrivial gaps are achieved by experimentally measured transmission spectra. Gapless spin-filtered edge states are demonstrated experimentally by the stable phase differences between E_z and H_z fields no matter where is the source position. High transmission of the EM fields is maintained even when the disorder is present. In addition, we demonstrate that topological index can be accurately calculated and predicted by group theory to predict topological characteristics in photonic metacrystals invariant under crystallographic point group symmetries. Light transport is then issued at the boundary between the air and the impedance-mismatching photonic crystal. Our results may enable the design of photonic spin-polarized states in a rational manner.

Conference 9367: Silicon Photonics X

Monday - Thursday 9 -12 February 2015

Part of Proceedings of SPIE Vol. 9367 Silicon Photonics X

9367-200,

Silicon integrated nanophotonics: from fundamental science to manufacturable technology

Yurii A. Vlasov, IBM Thomas J. Watson Research Ctr. (United States)

The IBM Silicon Nanophotonics technology enables cost-efficient optical links that connect racks, modules, and chips together with ultra-low power single-die optical transceivers. I will give an overview of its historical development, technology differentiators, current status and a roadmap.

9367-1, Session 1

High-speed detection at and above the telecommunication windows with monolithic silicon avalanche photodiodes (Invited Paper)

Andrew P. Knights, Jason J. Ackert, McMaster Univ. (Canada); David J. Thomson, Li Shen, Anna C. Peacock, Univ. of Southampton (United Kingdom); Paul E. Jessop, Wilfrid Laurier Univ. (Canada); Graham T. Reed, Goran Z. Mashanovich, Univ. of Southampton (United Kingdom); Abdullah S. Karar, Queen's Univ. (Canada); Dixon J. Paez, McMaster Univ. (Canada); John C. Cartledge, Queen's Univ. (Canada)

There is a fundamental challenge in using the same material for a waveguide and an absorptive photo-detector. In the case of silicon-based waveguides there exists essential transparency at wavelengths greater than the optical cut-off of 1100nm, making SOI a suitable waveguide structure. Photodetection has to date been provided at high-speed via the integration of germanium with the silicon waveguide. Work under-pinning this type of detector has been remarkable in its successful mitigation of issues of lattice mismatch. An alternative to the use of germanium has been the development of photodiodes in the all-silicon geometry. Sub-bandgap absorption can be created by the introduction of deep electronic levels via masked ion implantation. Such devices typically consist of a p-i-n junction integrated with a waveguide, with deep-levels (associated with lattice defects) selectively introduced into the intrinsic region of the junction. Our recent work has focussed on these structures operating in the avalanche regime. We demonstrate in this presentation both high responsivity at 1550nm of almost 5A/W and a high speed operation at a data-rate of 10Gbps. We extend these results to demonstrate operation at wavelengths up to 2500nm with responsivity of 0.3A/W at 1960nm and data-rate detection of 28Gbps. This latter result is significant because it opens the possibility of a high-speed silicon photonics optical link in the new communication window around 2000nm, serviced by thulium-doped fiber amplifiers. Finally, routes to increase in responsivity and speed of operation are discussed.

9367-2, Session 1

Improvements in the angled MMI multiplexer

Graham T. Reed, Youfang Hu, David J. Thomson, Frederic Y. Gardes, Goran Z. Mashanovich, Univ. of Southampton (United Kingdom)

We have previously reported experimental and theoretical studies of the angled MMI (AMMI) as a multiplexer and demultiplexer. The device is limited to small channel counts, but is simple to fabricate, robust, and tolerant to fabrication errors. The device also exhibits very low insertion loss (<1dB). We have increased channel count by interleaving two AMMIs via an imbalanced Mach-Zehnder interferometer, to experimentally demonstrate an 8 channel device with a channel spacing of 4.5nm. Furthermore, we have proposed additional interleaving via ring resonators to increase the channel count further, to perhaps 16 or 20 channels, depending on the performance required.

Whilst the device is more robust than other multiplexers to fabrication tolerances, like other multiplexers in silicon, it is still temperature sensitive. In this paper we discuss ways in which the temperature sensitivity can be reduced, and how to implement such a device within a communications link. Both theoretical and experimental results will be presented.

Therefore, the paper will overview the previous developments of the AMMI as well as discussing new experimental results, and providing an update on the current device performance.

9367-3, Session 1

Improved performance of a silicon arrayed waveguide grating by suppression of multimode generation near the boundary of a star coupler

Jaegyung Park, Jiho Joo, Hyundai Park, Myung-Joon Kwack, Gyungock Kim, Electronics and Telecommunications Research Institute (Korea, Republic of)

Arrayed waveguide grating (AWG) is one of the important building blocks in a wavelength division multiplexing system to expand a capacity of optical data communication and interconnection systems. A silicon (Si) AWG on a silicon-on-insulator (SOI) platform has been received much attentions due to the compact device size, an order of magnitude smaller than that of silica AWGs that result from the high refractive-index contrast between the Si core and the SiO₂ cladding. However, tightly-confining Si waveguides (WGs) induce a larger phase error and scattering/transition losses, which degrade the crosstalk and insertion loss of a Si AWG. The abrupt transition at the boundary between the slab region and the arrayed waveguides causes major transition loss, and affects the crosstalk characteristics. In this work, we focus on the reduction of the transition-loss across the star coupler boundary, by analyzing the multimode generation due to the field-mismatching effect. We fabricated Si AWGs on a 6" SOI wafer with various optimal conditions of deep/shallow etch-depths and aperture size of arrayed WGs for suppressing the multimode generation. Our experimental results demonstrate improved insertion loss and crosstalk characteristics. The fabricated 8-channel AWG shows an insertion loss less than 1 dB with a crosstalk of -23.2 ~ -25.8 dB, exhibiting -2 dB improvement of insertion loss and -5 dB improvement of crosstalk, compared to our reported Si AWG [1].
 [1] D. J. Kim et al, IEEE Photon. Technol. Lett. 20, 1615 (2008).

9367-4, Session 1

Architectures for evanescent frequency tuning of microring resonators in micro-opto-electro-mechanical SOI platforms

Hossam Shoman, Marcus S. Dahlem, Masdar Institute of Science & Technology (United Arab Emirates)

Microring resonators are important elements in a wide variety of optical

systems, ranging from optical switches and tunable filterbanks to optical sensors. In these structures, the resonant frequencies are normally controlled by tuning the effective index of refraction. In optical switches and filters, this has traditionally been achieved through electro-optic or thermo-optic effects, while in sensors the effective refractive index is changed by the presence of the measurand. Adding a mechanical degree of freedom to these optical systems allows additional evanescent frequency tuning. In particular, the presence of a cantilever in the near field of the optical mode can tune the effective refractive index. A known cantilever displacement can therefore induce a desired resonant frequency shift. Alternatively, a measured shift in the resonant frequency can be associated with a cantilever displacement, and be used for pressure or acceleration detection. In this paper, we explore different geometries that can be used for controlling the resonant frequency of a microring resonator through evanescent field perturbation, using a cantilever defined in the same silicon layer as the optical waveguides, in a silicon-on-insulator (SOI) platform. The effects of the cantilever geometry, lateral gap size and vertical displacement, on both the resonant frequency and quality factor of the resonator, are evaluated through FDTD computations for wavelengths centered at 1550 nm. The presence of the cantilever in the near field of the optical mode changes the effective refractive index, resulting in frequency tuning, but also lowers the quality factor due to additional coupling into the membrane.

9367-5, Session 2

Feedback and control in integrated optics enabled by contactless integrated photonic probe *(Invited Paper)*

Andrea I. Melloni, Francesco Morichetti, Stefano Grillanda, Andrea Annoni, Marco Sampietro, Marco Carminati, Politecnico di Milano (Italy)

The silicon photonics platform is now mature enough to enable large-scale integration circuits, however because of the lack of tools to reliably control their operation when many components are aggregated, the realization of complex systems-on-chip is still a challenge. A major unsolved issue is the concept of transparent probes to inspect and monitor the status of a device without affecting its behavior.

Here, we demonstrate non-invasive light observation in silicon photonics devices and circuits with a Contactless Integrated Photonics Probe (CLIPP), that neither introduces appreciable perturbations of the optical field nor requires photon tapping from the waveguide. The CLIPP exploits light induced variations of the waveguide electric conductance associated with intrinsic surface states absorption at the core-cladding interface. Light monitoring with sensitivity down to -30 dBm, across 40 dB dynamic range, in few tens of picoseconds, on both TE and TM polarizations, and on both monomode and multimode waveguides is achieved.

Moreover, we show advanced control functionalities, such as wavelength tuning, locking and swapping of high-quality-factor thermally actuated resonators assisted by the CLIPP that is integrated inside the microring. All the CLIPP read-out and feedback control operations are entirely managed by a CMOS integrated electronic circuit that is bridged to the silicon photonic chip. The non-perturbative behavior of the CLIPP and the inherent scalability of the CMOS electronic circuit offer a viable path for the realization and control of arbitrarily reconfigurable systems-on-chip aggregating several components.

9367-6, Session 2

Suspended silicon slotted microring resonators with ultra-high optical quality

Wei C. Jiang, Qiang Lin, Univ. of Rochester (United States)

We propose and demonstrate a unique suspended slot-waveguide structure supported by a thin slab to realize high-quality air-clad silicon slotted microring resonators (SMRs) on the silicon-on-insulator platform, based on

a fabrication process consisting of two-step electron beam lithography and inductively-coupled-plasma reactive-ion-etching. Our SMRs can achieve an intrinsic optical quality factor (Q) above 10^5 operating at the telecom band, which is the highest value for silicon SMRs reported to date. The demonstrated high-quality air-clad silicon SMRs enable great potential for broad applications in biosensing, nonlinear photonics, and cavity optomechanics.

9367-7, Session 2

Ge quantum well photonic platform on bulk silicon *(Invited Paper)*

Papichaya Chaisakul, Delphine Marris-Morini, Institut d'Électronique Fondamentale (France); Jacopo Frigerio, Daniel Chrastina, Politecnico di Milano (Italy); Mohamed-Said Rouified, Institut d'Électronique Fondamentale (France); Stefano C. Cecchi, Politecnico di Milano (Italy); Paul Crozat, Institut d'Électronique Fondamentale (France); Giovanni Isella, Politecnico di Milano (Italy); Laurent Vivien, Institut d'Électronique Fondamentale (France)

We propose and experimentally validate a new approach to monolithically integrate Ge quantum well photonic interconnections on silicon substrates. We experimentally show that Ge-rich Si_{1-x}Ge_x virtual substrates (VS) can act as a passive optical waveguide on which a low temperature (< 450°C) high quality epitaxial growth of Ge quantum wells can be performed, realizing active optical planar circuitry on a bulk silicon wafer. As a proof of concept, the photonic integration of a passive Si_{0.16}Ge_{0.84} waveguide and two Ge/SiGe multiple quantum well (MQW) active devices, an optical modulator and a photodetector, was realized by using a single epitaxial growth step. A Si_{0.16}Ge_{0.84} VS was engineered to meet the two conflicting requirements of (i) being a waveguide with minimized optical loss at the operating wavelength of the quantum-confined Stark effect (QCSE) modulator based on Ge/Si_{0.16}Ge_{0.84} MQWs (Ge mean fraction of ~ 92%), and (ii) forming a VS with minimized lattice mismatch to the MQW stack to ensure a high quality epitaxial growth. Low-voltage and broadband Ge quantum well interconnects integrated on bulk silicon chips were demonstrated. Our approach can be extended to any kind of Ge-based optoelectronic devices working within telecom wavelengths as long as a suitable Ge concentration x is selected for the Ge-rich Si_{1-x}Ge_x VS.

9367-8, Session 2

Low-loss delay lines with small footprint on a micron-scale SOI platform

Matteo Cherchi, Mikko Harjanne, VTT Technical Research Ctr. of Finland (Finland); Konstantinos Vyrsoinos, Aristotle Univ. of Thessaloniki (Greece); Sami Ylinen, Markku Kapulainen, Tapani Vehmas, Timo Aalto, VTT Technical Research Ctr. of Finland (Finland)

Long and yet compact spiral waveguides based on micron-scale silicon strip waveguides has been enabled very recently by the introduction of the Euler bends. By ensuring effective broadband single mode operation of otherwise highly multimodal waveguides, these bends can have very low losses (<0.01 dB/90°) even with effective radii of a few microns. Together with the low propagation losses (< 0.15 dB/cm) of micron-scale strip waveguides, these bends enable centimetre-long delay lines with negligible losses and very small foot-print (< 1 mm²). In particular, interferometers delayed by ≈ 1 cm long spirals on one of the two arms have been fabricated on SOI wafers with both 3 μm- and 4 μm-thick silicon layer, based on the well assessed process developed by VTT. The full devices have footprint smaller than 1.5 mm², and they have been measured to have extinction ratios > 15 dB (reaching up

to 21 dB) and about 3 dB excess losses. Functional characterization of the delayed interferometers at about 10 Gbps through demodulation of pseudo-random Differential Phase Shift Keying signals led to clearly opened eye diagrams with Q factor of 8.6 and bit error rates lower than 10⁻¹⁵.

9367-9, Session 2

Total internal reflection mirrors with ultra-low losses in 3 μm thick SOI waveguides

Timo Aalto, Mikko Harjanne, Sami Ylinen, Markku Kapulainen, Tapani Vehmas, Matteo Cherchi, VTT Technical Research Ctr. of Finland (Finland)

We present results from 90° strip waveguide turning mirrors that have a novel geometry and were fabricated on our 3 μm SOI waveguide platform. The new total internal reflection (TIR) mirrors have record-low insertion loss of 0.08 dB/mirror and they are compared with our previous (unpublished) mirror designs that have demonstrated insertion losses down to 0.15 dB/mirror. State-of-the-art TIR mirrors in the literature have insertion losses around 0.3 dB/cm, so the mirror loss has been reduced significantly. The mirror layout was optimized with the help of COMSOL Multiphysics software. In addition to loss minimization also the sensitivity of the loss to design parameter variation was analysed and compared to normal process variation. The new mirror design was tested on strip waveguides with widths of 1.0 μm and 1.875 μm, which correspond to the standard widths used in the 3 μm SOI platform. The test structures consisted of up to 96 consecutive mirrors and were fabricated in VTT's multi-project wafer run. Despite the multi-mode behaviour of the strip waveguides the test devices and circuits only propagate light in the fundamental mode, so that the mirrors can be used in single-mode photonic circuits. The new mirrors support the implementation of densely integrated waveguide circuits that combine low losses, small polarisation dependency, wide bandwidth, high performance and small footprint.

9367-10, Session 3

Design and characterisation of high-speed monolithic silicon modulators for digital coherent communication (*Invited Paper*)

Kensuke Ogawa, Kazuhiro Goi, Akira Oka, Yasuhiro Mashiko, Fujikura Ltd. (Japan); Tsung-Yang Liow, Xiaoguang Tu, Guo-Qiang Lo, Dim-Lee Kwong, A*STAR Institute of Microelectronics (Singapore); Soon Thor Lim, A*STAR Institute of High Performance Computing (Singapore) and Optic2Connect Pte Ltd. (Singapore); Min Jie Sun, Optic2Connect Pte Ltd. (Singapore); Ching Eng Png, A*STAR Institute of High Performance Computing (Singapore) and Optic2Connect Pte Ltd. (Singapore)

With the advent of high-speed photonics and signal processing, transmission at 128 Gb/s per wavelength channel has been realized in digital coherent communication in optical-fiber networks. Dual-polarization quadrature phase-shift keying (DP-QPSK) has been exploited as the major modulation format in the digital coherent communication. High-quality optical signal generation in DP-QPSK format requires complex optical modulators consisting of nested Mach-Zehnder (MZ) waveguides for in-phase (I) and quadrature-phase (Q) modulation and passive optical circuits for polarization-division multiplexing (PDM). Silicon photonics provides a device platform for design and fabrication of photonic integrated circuits with the advantage of significant footprint reduction. The advantage meets the demand of small-footprint optical transceivers for wide-spread application such as digital coherent communication in metro-area networks. This paper encompasses recent experimental and computational studies on high-speed silicon-based MZ modulators in the light of monolithic optical modulator for digital coherent communication. Lateral PN-junction rib-

waveguide phase shifters are elaborated with experimental characteristics of high-frequency electro-optic response and computational characteristics of refractive-index dynamics including electron and hole transport in the PN junction. Silicon-based passive optical circuit for PDM is another essential device block to construct the monolithic IQ PDM modulator. Silicon PDM waveguides are designed in common design rules with the rib-waveguide phase shifters. Loss reduction in the PDM waveguide is described as an effort for further reduction in insertion optical loss of the monolithic modulator. The performance in DP-QPSK signal generation is characterized in experimental and computational constellation diagrams. Long-haul transmission in 1000-km single-mode fiber link is confirmed.

9367-11, Session 3

Power-efficient carrier-depletion SOI Mach-Zehnder modulators for 4x25Gbit/s operation in the O-band

Thomas Ferrotti, STMicroelectronics (France) and CEA-LETI (France); Alain Chantre, STMicroelectronics (France); H  l  ne Duprez, Benjamin Blampey, Fr  d  ric Milesi, Andr   Myko, Corrado Sciancalepore, Karim Hassan, Julie Harduin, CEA-LETI (France); Charles Baudot, STMicroelectronics (France); Sylvie Menezes, CEA-LETI (France); Fr  d  ric Boeuf, STMicroelectronics (France); Badhise Ben Bakir, CEA-LETI (France)

In this paper, we communicate on the design, fabrication and testing of optical modulators for Silicon-based photonic integrated circuits (Si-PICs) in the O-band (1.31 μm), targeting the 100GBASE-LR4 norm. The modulators have been conceived to be later coupled with hybrid-III-V/Si lasers and an echelle grating multiplexer, forming a hetero-integrated optical transmitter on a silicon-on-insulator platform. Measurements show modulation efficiencies up to 19 deg/mm (2.4 V.cm) for a 2.5 V input voltage, with doping-related losses below 1 dB/mm. Finally, an electrical-electrical (EE) bandwidth of 16 GHz at 1.25 V bias is measured, while the electro-optical (EO) bandwidth is above 28 GHz.

9367-12, Session 3

Strain tuning of Ge bandgap by selective epigrowth for electro-absorption modulators

Yasutaka Mizuno, Motoki Yako, Luan M. Nguyen, Kazumi Wada, The Univ. of Tokyo (Japan)

Electro-absorption (EA) modulator has been intensively studied recently, because of its small footprint and low energy consumption. Ge is promising material for EA modulator among group IV. The challenging issue is, however, Ge cannot work at 1.55 μm because of built-in tensile strain; the bandgap is shrunk beyond 1.6 μm. Thus, GeSi with dilute Si alloy has been used to make it work at 1.55 μm. Recently, we have proposed a new approach of realizing tunable bandgap of Ge via stress (stress engineering), and demonstrated bandgap expansion of Ge toward 1.55 μm using SiNx stressor layers. The approach is advantageous over the GeSi alloy method in tunability of the operation wavelength window in C+L bands simply by changing thickness and/or width of the SiNx stressor. In this work, we further explore selective Ge growth with using SiO₂ mask to stress Ge: We first simulate strain in Ge waveguide shaped epilayer by FEM method, and it indicates that strain in Ge waveguides depend on width and thickness of stressor, and width of waveguide. We then demonstrate that SiO₂ selective epigrowth mask indeed stresses Ge waveguides as the simulations predicted. We obtain -0.25% strain in 0.6 μm wide Ge waveguide grown in 20 μm wide and 1 μm thick SiO₂ on Si as a stressor layers. -0.25% strain can expand Ge bandgap to 1.55 μm.

9367-13, Session 3

Accurate modelling and simulation of silicon optical modulators in QPSK

Ching Eng Jason Png, A*STAR Institute of High Performance Computing (Singapore) and Optic2Connect Pte Ltd. (Singapore); Min Jie Sun, Optic2Connect Pte Ltd. (Singapore); Soon Thor LIM, A*STAR Institute of High Performance Computing (Singapore) and Optic2Connect Pte Ltd. (Singapore); Kensuke Ogawa, Fujikura Ltd. (Japan)

Performance of silicon based optical phase shifters of high-speed optical modulators in quadrature phase shift keying (QPSK) for the most advanced optical-fiber telecommunications is explored with simulation approach. Emphasis of this simulation work is given to device simulation where device physics principles are employed to calculate individual phase shifter's performance. The phase shifter is based around a rib waveguide. Our device simulation method features a unique mapping step from electrical carrier concentrations to optical indices. It captures the exact carrier distribution in depletion region and accurately model the plasma dispersion effect of the device, which ensures an accurate phase shift and material attenuation calculation in optical simulation. With the device simulation as the basis, optical QPSK is implemented with four identical silicon phase shifters, arranged in Mach-Zehnder configuration. The system level performance is illustrated with computed constellation diagram. With the same simulation scheme, we vary the phase shifter device structure and demonstrate effects of these variances to the system by comparing their constellation diagrams. Initial device variance plan includes the adjustments of rib width, p-n junction location and doping concentration, and may include others like rib-to-contact distance, rib height to slab thickness ratio, etc. Structural variance will affect certain device properties including phase shift efficiency, optical loss, electrical conductance and capacitance, etc. We calculate how these properties are associated with device variances and present qualitatively their effects over the QPSK system with plotted constellation diagrams. Our aim is to explore the optimized device structure design for 50Gbps QPSK.

9367-15, Session 3

Silicon photonics cloud (SiCloud)

Peter T. S. DeVore, Yunshan Jiang, Michael Lynch, Univ. of California, Los Angeles (United States); Taira Miyatake, Univ. of Tokyo (Japan); Christopher Carmona, Andrew C. Chan, Kuhan Muniam, Bahram Jalali, Univ. of California, Los Angeles (United States)

We present SiCloud (Silicon Photonics Cloud), the first free, instructional web-based research and education tool for silicon photonics. SiCloud's vision is to provide a host of instructional and research web-based tools. Such interactive learning tools enhance traditional teaching methods by extending access to a very large audience, resulting in very high impact. Interactive tools engage the brain in a way different from merely reading, and so enhance and reinforce the learning experience. Understanding silicon photonics is challenging as the topic involves a wide range of disciplines, including material science, semiconductor physics, electronics and waveguide optics. This web-based calculator is an interactive analysis tool for optical properties of silicon and related material (SiO₂, Si₃N₄, Al₂O₃, etc.). It is designed to be a one stop resource for students, researchers and design engineers. The first and most basic aspect of Silicon Photonics is the Material Parameters, which provides the foundation for the Device, Sub-System and System levels. SiCloud includes the common dielectrics and semiconductors for waveguide core, cladding, and photodetection, as well as metals for electrical contacts. SiCloud is a work in progress and its capability is being expanded. SiCloud was developed at UCLA with funding from the National Science Foundation's Center for Integrated Access Networks (CIAN) Engineering Research Center.

9367-16, Session 4

Slow-light modulators (Invited Paper)

Toshihiko Baba, Yosuke Terada, Hong C. Nguyen, Yokohama National Univ. (Japan)

Mach-Zehnder optical modulators using carrier plasma dispersion have been developed actively in silicon photonics toward high-speed E/O conversion suitable optical interconnects. Conventional devices using rib waveguides have been designed carefully so as to balance high speed, low loss, high extinction ratio, low drive voltage, small footprint, temperature insensitivity, and so on, while they are approaching to the best balance and very small room for further optimization remains. Using slow light has potential of breaking this constraint. Slow light enhances the phase sensitivity for the material index change in proportion to its group index. For this purpose, we usually use p/n-diode-loaded lattice-shifted photonic crystal waveguides (LSPCWs), which can be fabricated easily by standard CMOS-compatible process. It exhibits wideband dispersion-free slow light with a typical group index of 20 and a wavelength bandwidth of 15 nm at wavelengths around 1550 nm. The group index is five-fold larger than that of rib waveguides. Here, we have to also consider the overlap of the modal field with the depletion region of the p/n diode; it is twice smaller than that of rib waveguides due to the lateral spreading of the slow light. Consequently, 2.5-fold enhancement is expected for slow light, which reduces the device size or drive voltage by the same factor. By further optimizing the doping concentration and profile, we obtain 25 Gbps operation with a 3 dB clear open eye with a < 6 dB on-chip loss even under modulation with < 2 V_{pp} push-pull drive in a 200-micron-long device.

9367-17, Session 4

Modulation efficiency enhancement of an optical phase modulator using one-dimensional photonic crystal structures

Seyedreza Hosseini, Kambiz Jamshidi, Technische Univ. Dresden (Germany)

By emerging CMOS compatible silicon photonics platform, optical modulators with higher efficiencies are required to map the electrical signal to the optical signal in a more energy efficient way. One approach to improve the efficiency of optical modulators is to use photonic crystals to enhance the optical field and increase the efficiency of the modulators. Using two dimensional photonic crystals higher slow down factors can be achieved but they are very sensitive in terms of fabrication and cannot be realized using ordinary photolithography techniques.

In this paper we will consider the effect of slow down factor on modulation efficiency of several optical phase modulator architectures. Based on the modal analysis, their dispersion diagram for TE like mode have been calculated and based on that, group velocity and group index of these designs have been determined. The voltage level requires to achieve π phase shift has been obtained through the semi analytical model. This model is based on modeling carriers in a pn diode and using both Drude and Soref models for carrier plasma dispersion effect. Sensitivity of the structures in terms of structure dimension variations has been investigated and limitations of these structures in terms of bandwidth and induced group velocity dispersion have been shown.

9367-18, Session 4

Silicon-based optical matrix processor for parallel computing (Invited Paper)

Lin Yang, Jianfeng Ding, Qiaoshan Chen, Lei Zhang, Ruiqiang Ji, Institute of Semiconductors (China)

Matrix-vector multiplication is a fundamental operation in modern digital

signal processing fields. Inspired by the intrinsic spatial parallelism of optics, much effort has been made to develop optical apparatuses that can perform such a parallelizable operation. The Stanford multiplier is one of the most notable demonstrations, which is composed of light source array, optical lens, spatial light modulator (SLM) matrix and photodetector array. Almost all implementations are large in volume and high in power consumption. Moreover, many removable elements adopted make them extremely sensitive to the environmental vibration. To overcome these limitations, we propose an on-chip optical matrix-vector multiplier (MVM), which is composed of laser-modulator array, multiplexer, splitter, microring modulator matrix and photodetector array. The fan-out and fan-in with optical lenses in the traditional optical MVMs are replaced by the power splitting and wavelength multiplexing with waveguide devices in the proposed optical MVM, which greatly reduces the complexity and size of the system. The discrete components in the traditional optical MVMs are replaced by the integrated ones in the proposed optical MVM, which improves the stability and power efficiency of the system. 1.6×10^9 multiplications and accumulations per second is implemented by a demo system with a 4×4 microring modulator matrix.

9367-19, Session 4

25 Gb/s photoreceiver based on vertical-illumination type Ge-on-Si photodetector and CMOS amplifier circuit for optical interconnects

Jiho Joo, Ki-Seok Jang, Sang Hoon Kim, In Gyoo Kim, Jin Hyuk Oh, Sun Ae Kim, Gyungock Kim, Electronics and Telecommunications Research Institute (Korea, Republic of); Gyu-Seob Jeong, Hankyu Chi, Deog-Kyoon Jeong, Seoul National Univ. (Korea, Republic of)

Silicon photonics technology can provide cost-effective low-power solutions beyond 10 Gb/s applications of system-to-system, board-to-board, and chip-to-chip optical interconnects. In this paper, we report a silicon photonic receiver based on the hybrid-integrated vertical-illumination type germanium-on-silicon photodetector and CMOS amplifier circuit, characterized up to data rate of 36Gb/s optical interconnects. The 30 μ m-diameter vertical-illumination type Ge photodetector, grown on a bulk-silicon wafer by RPCVD and fabricated with CMOS-compatible process, has a bandwidth of ~22 GHz. The CMOS amplifier chip was designed with 65nm ground rule, where the trans-impedance amplifier (TIA) is based on an inverter with resistive and inductive feedback, and the limiting amplifier (LA) employs negative capacitance generation. For high-speed module packaging, the low-cost Duriod/PCB hybrid substrate is used. The butterfly-packaged Ge photoreceiver exhibits a responsivity of 0.79 A/W, and a sensitivity of -11 dBm (-9.1 dBm) for the data rate of 25 (28) Gb/s at a BER of 10^{-12} . Also, the measured sensitivity at 36 Gb/s is -1.6 dBm at a BER of 10^{-12} . The Ge photoreceiver exhibits low-power characteristics of 2.67 pJ/bit energy-efficiency at 25 Gb/s and 2.17 pJ/bit at 36 Gb/s.

9367-20, Session 4

A hybrid photonic-electronic switching architecture for next-generation data centers (Invited Paper)

Hamid Mehrvar, Alan F. Graves, Dominic J. Goodwill, Nortel Networks (Canada); Eric Bernier, Huawei Technologies Co., Ltd. (Canada)

We provide an alternative architecture for the next generation datacenters by employing electronic and photonic switching cores. The capacity of electronic packet switching (EPS) cores is not enough for the bandwidth requirements of next generation datacenters. On the other hand, it is prohibitively costly to build pure photonic packet switching core (OPS)

which is capable of switching native Ethernet frames in nanoseconds. We propose a low cost hybrid OPS/EPS platform which significantly increases the switching capacity of datacenters for all traffic patterns while using the existing EPS cores. Our proposed architecture is a fat-tree hierarchy consisting of servers, top-of-racks, aggregation switches, and core switches. The aggregation switches are interconnected to the core hybrid OPS/EPS switch. Since the traffic inside datacenters is typically bimodal, the hybrid switch core becomes feasible by switching short and long packets using EPS and OPS cores, respectively. In order to prepare long packets for photonic switching, they undergo packet contention resolution, compression, and bitwise scrambling. Afterwards, a photonic destination label is added to the long packets, and they are sent out through an optical transmitter. For compressing the long packets, the clock rate is raised on the output of the physical layer. Packet compression increases inter-packet gap to insert the photonic label. Also, it provides more time for photonic switch connection set-up and receiver synchronization at the destination aggregation switch. We developed a test bed for our architecture and used it to transmit real-time traffic. Our experiments show successful transmission of all packets through OPS.

9367-21, Session 5

Monolithic silicon photonics in a sub-100nm SOI CMOS microprocessor foundry: progress from devices to systems (Invited Paper)

Milos A. Popovic, Mark T. Wade, Univ. of Colorado at Boulder (United States); Jason S. Orcutt, Massachusetts Institute of Technology (United States); Jeffrey M. Shainline, National Institute of Standards and Technology (United States); Sun Chen, Univ. of California, Berkeley (United States); Michael S. Georgas, Benjamin Moss, Massachusetts Institute of Technology (United States); Rajesh Kumar, Univ. of Colorado at Boulder (United States); Luca Alloatti, Massachusetts Institute of Technology (United States); Fabio Pavanello, Univ. of Colorado at Boulder (United States); Yu-Hsin Chen, Massachusetts Institute of Technology (United States); Kareem Nammari, Jelena Notaros, Univ. of Colorado at Boulder (United States); Amir Atabaki, Jonathan Leu, Massachusetts Institute of Technology (United States); Vladimir Stojanovic, Univ. of California, Berkeley (United States); Rajeev J. Ram, Massachusetts Institute of Technology (United States)

We review recent progress of an effort led by the Stojanovic (UC Berkeley), Ram (MIT) and Popovic (CU Boulder) research groups to enable the design of photonic devices, and complete on-chip electro-optic systems and interfaces, directly in standard microelectronics CMOS processes in a microprocessor foundry, with no in-foundry process modifications. This approach allows tight and large-scale monolithic integration of silicon photonics with state-of-the-art (sub-100nm-node) microelectronics, here a 45nm SOI CMOS process. It enables natural scale-up to manufacturing, and rapid advances in device design due to process repeatability. The initial driver application was addressing the processor-to-memory communication energy bottleneck. Device results include 5Gbps modulators based on an interleaved junction that take advantage of the high resolution of the sub-100nm CMOS process. We demonstrate operation at 5fJ/bit with 1.5dB insertion loss and 8dB extinction ratio. We also demonstrate the first infrared detectors in a zero-change CMOS process, using absorption in transistor source/drain SiGe stressors. Subsystems described include the first monolithically integrated electronic-photonic transmitter on chip (modulator+driver) with 20-70fJ/bit wall plug energy/bit (2-3.5Gbps), to our knowledge the lowest transmitter energy demonstrated to date. We also demonstrate native-process infrared receivers at 220fJ/bit (5Gbps).

These are encouraging signs for the prospects of monolithic electronics-photonics integration. Beyond processor-to-memory interconnects, our approach to photonics as a “More-than-Moore” technology inside advanced CMOS promises to enable VLSI electronic-photonics chip platforms tailored to a vast array of emerging applications, from optical and acoustic sensing, high-speed signal processing, RF and optical metrology and clocks, through to analog computation and quantum technology.

9367-22, Session 5

Photonic-electronic integration with polysilicon photonics in bulk CMOS (Invited Paper)

Rajeev Jagga Ram, Massachusetts Institute of Technology (United States)

For high-volume, high-density VLSI applications (e.g. microprocessors, systems-on-chip (SOCs), field-programmable gate arrays (FPGAs), and memory (DRAM), bulk-silicon wafers remain the dominant production platform. However, thick-buried-oxide (BOX), silicon-on-insulator (SOI) wafers have been the dominant monolithic silicon photonic platform due to the easy formation of low-loss waveguides. Here, we present a photonic platform that is optimized for integration with electronics fabricated on bulk silicon wafers.

We review recent progress of an effort led by the Stojanovic (UC Berkeley), Ram (MIT) and Popovic (CU Boulder) research groups to enable the integration of photonic components within the front-end processes of a bulk CMOS VLSI process. This approach allows tight and large-scale monolithic integration of silicon photonics with microelectronics. A complete photonic link has been demonstrated at 5 Gbps that transfers digital information from one Bulk CMOS Photonics chip to another. A single-polysilicon deposition and lithography mask were used to simultaneously define the transistor gate, the low-loss waveguides, the depletion modulators, and the photodetectors. The process was finely tuned to adjust the density of localized electronic states associated with the grain-boundaries in polysilicon. A low-defect state density was utilized for the waveguide and modulator layers. This defect state density could be tuned to be higher for the all-silicon photodetectors. The resulting microring resonant detectors exhibit a 20% quantum efficiency with 9.7 GHz bandwidth over a wide range of wavelengths. For link tests, 1280nm laser was coupled into the transmitter chip, modulated, and then coupled into a receiver chip several meters away.

9367-23, Session 5

Interferometric microscopy of silicon photonic devices

William S. Rabinovich, Rita Mahon, Peter Goetz, Doewon Park, Marcel W. Pruessner, Fredrik K. Fatemi, Michael J. DePrenger, U.S. Naval Research Lab. (United States)

Silicon photonics provides the ability to construct complex photonic circuits that act on the amplitude and phase of multiple optical channels. Many applications of silicon photonics depend on maintenance of optical coherence among the various waveguides and structures on the chip. For example, optical phased arrays depend on the relative phase of a set of waveguides. Other applications can depend on the modal structures of the waveguides. For example microwave photonic delay lines can be affected by multimode dispersion. All these applications require the ability to characterize the amplitude and phase of individual optical channels. Fourier imaging with high numerical aperture microscope objectives has been used to image the intensity of individual channels of photonic structures in both real and Fourier space. In other work, holographic imaging of multimode fibers has allowed modal decomposition. In this work we use interferometric microscopy to image the amplitude and phase of a variety of silicon photonic structures. These include a multimode interference splitter,

an optical phased array with an adjustable phase gradient and a multimode waveguide under various excitation conditions. Limitations of the technique and other applications are also discussed.

9367-24, Session 5

hybrid silicon mode-locked laser with improved RF power by impedance matching

Bassem M. Tossoun, Dennis J. Derickson, California Polytechnic State Univ., San Luis Obispo (United States); Sudharsanan Srinivasan, John E. Bowers, Univ. of California, Santa Barbara (United States)

We design and discuss an impedance matching solution for a hybrid silicon mode-locked laser diode (MLLD) to improve peak optical power coming from the device. In order to develop an impedance matching solution, a thorough measurement and analysis of the MLLD as a function of mode-locking bias on each of the laser segments was carried out. A passive component impedance matching network was designed at the operating frequency of 20 GHz to optimize RF power delivery to the laser. The hybrid silicon laser was packaged together in a module including the impedance matching circuit. The impedance matching design resulted in a 6dB (electrical) improvement in the detected modulation spectrum power from the MLLD. Also, looking ahead to possible future work, we discuss a Step Recovery Diode (SRD) driven impulse generator, which wave-shapes the RF drive to achieve efficient injection. This novel technique takes into account the time varying impedance of the absorber as the optical pulse passes through it, to provide optimum optical pulse shaping.

9367-25, Session 6

Group IV mid-infrared photonics (Invited Paper)

Goran Z. Mashanovich, Milos Nedeljkovic, Jordi Soler Penades, Colin J. Mitchell, A. Z. Khokhar, Callum Littlejohns, Stevan Stankovic, Univ. of Southampton (United Kingdom); Benedetto Troia, Politecnico di Bari (Italy); Scott Reynolds, Univ. of Southampton (United Kingdom); Vittorio M. N. Passaro, Politecnico di Bari (Italy); Li Shen, Noel Healy, Anna C. Peacock, Univ. of Southampton (United Kingdom); Carlos A. Alonso Ramos, Alejandro Ortega-Moñux, Juan Gonzalo Wangüemert-Pérez, Iñigo Molina-Fernández, Univ. de Málaga (Spain); David J. Rowe, James S. Wilkinson, Univ. of Southampton (United Kingdom); Pavel Cheben, National Research Council Canada (Canada); Jason J. Ackert, Andrew P. Knights, McMaster Univ. (Canada); David J. Thomson, Frederic Y. Gardes, Univ. of Southampton (United Kingdom)

In this paper we present SOI, suspended Si and Ge on Si photonic devices. We demonstrate low loss slot waveguides in SOI and show efficient strip-slot couplers. In order to extend transparency of Si waveguides, bottom oxide cladding needs to be removed. We report a novel design based on subwavelength structures that is more robust than previously reported suspended designs. We also report a record low loss Ge on Si waveguides, as well as several other passive devices in this platform. A Vernier configuration based on racetrack resonators in SOI has been used to show its potential for sensing. All optical modulation and two photon absorption measurements in Ge are also analysed. Mid-infrared detection using defect engineered silicon detectors is reported and high responsivity and data rates demonstrated at the wavelength of $\sim 2\mu\text{m}$.

9367-26, Session 6

GeSn photodetector and light emitter: mid-infrared devices in silicon photonics (Invited Paper)

Shui-Qing Yu, Wei Du, Benjamin R. Conley, Seyed A. Ghetmiri, Aboozar Mosleh, Thach Pham, Yiyin Zhou, Univ. of Arkansas (United States); Amjad Nazzal, Wilkes Univ. (United States); Greg Sun, Richard A. Soref, Univ. of Massachusetts Boston (United States); Joe Margetis, John Tolle, ASM America Inc. (United States); Baohua Li, Arktronics, LLC (United States); Hameed A. Naseem, Univ. of Arkansas (United States)

(Invited paper) Silicon-based optoelectronic devices have long been desired owing to the possibility of monolithic integration of photonics with high-speed Si electronics and the aspiration of broadening the reach of Si technology by expanding its functionalities well beyond electronics. To overcome the intrinsic problem of bandgap indirectness in the group-IV semiconductors such as Si and Ge, a new group-IV based material, GeSn alloy, has been proposed. Recently, GeSn related research has attracted increasing interest due to its tunable bandgap, which makes the direct bandgap material grown on Si attainable. Therefore GeSn-based optoelectronic devices can be widely used in Si photonics. Moreover, the narrowed bandgap of GeSn extends the device operating range into the mid-infrared, which is desired for wide-ranging applications in the fields of optical interconnects, et al.

In this work, firstly, the material growth of GeSn by chemical vapor deposition (CVD) system has been reviewed. Secondly, GeSn-based photodetectors and light emitting diodes (LEDs) have been systematically investigated. For photoconductive detector, a temperature dependence study was conducted using both electrical and optical characterizations from 300 to 77 K. For LED, room-temperature electroluminescence (EL) spectra under various electrical injection current densities have been investigated. These devices operate in the wavelength range beyond 2 μ m.

9367-27, Session 6

Enhanced gain of GeSn photoconductors by interdigitated electrodes for mid-infrared detection

Benjamin R. Conley, Wei Du, Univ. of Arkansas (United States); Richard A. Soref, Greg Sun, Univ. of Massachusetts Boston (United States); Joe Margetis, John Tolle, ASM America Inc. (United States); Baohua Li, Arktronics, LLC (United States); Shui-Qing Yu, Univ. of Arkansas (United States)

The GeSn alloy is a promising material for active and passive photonics on Si due to its possible direct band gap, industry scalable growth, and mid-infrared response. Integration of photoconductor devices on Si with increased gain would allow for low cost integration of short to mid-infrared active devices. Previous studies of GeSn photodetectors focused on optical manipulations, i.e., the enhancement of light absorption, but the electrical properties such as carrier collection efficiency of those photodetectors have not been considered. Therefore the enhancement factor introduced by the material and optical design could be cancelled due to inefficient collection of photo generated carriers. In this work, enhancement of photoconductive gain by incorporating interdigitated electrodes has been investigated. Photoconductors were fabricated with a GeSn (7 % Sn) active layer on Si substrates using CMOS compatible chemical vapor deposition growth. The interdigitated electrode spacing of the Ohmic contacts were varied at 6, 12, and 24 μ m with 3, 6, and 12 μ m wide metal fingers, respectively. The factor of two for each metal width and spacing pair keeps the active illumination

area constant whilst allowing an unambiguous study of the carrier collection time and photoconductive gain behavior of this material. The responsivity of each sample, measured at variable temperature from 77 K to 300 K, increases for decreased temperatures. The increased responsivity, due to the reduced interdigitated spacing and lower temperatures, is result of an increase in the photoconductive gain by reducing the carrier transit time and increasing the carrier effective lifetime.

9367-28, Session 6

Integrated photonic crystal waveguides on silicon-on-sapphire for volatile organic compounds detection in mid infrared

Yi Zou, The Univ. of Texas at Austin (United States); Swapnajit Chakravarty, Xiaochuan Xu, Omega Optics, Inc. (United States); Ray T. Chen, The Univ. of Texas at Austin (United States)

A chip-integrated infrared spectrometer for remote, in situ sensing and spectroscopic identification of volatile organic compounds (VOCs) in water taking advantage of large absorption cross-sections in the mid-infrared (mid-IR) is highly desired. Interband cascade lasers (ICL) in mid-IR wavelengths and quantum cascade lasers (QCLs) at longer wavelengths can probe the fundamental molecular vibrations of most molecules. We previously demonstrated on chip sensing by near infrared absorption signatures in a 300 micron long photonic crystal (PC) slot waveguide that enabled detection of 100ppb xylene in water. Based on Beer-Lambert absorption law, the PC waveguide device provides large slow light effect at the operation wavelength near the bandedge to enhance interaction between the optical field and the analyte which when combined with the large absorption cross-sections in the mid-IR increases the sensitivity to analyte detection. PC waveguide devices have been fabricated in silicon-on-sapphire with bandedge around 3.4micron wavelength were experimentally demonstrated. Light from an ICL guided by optical fibers is coupled into and out of the devices using integrated sub-wavelength grating couplers. Transmission spectrum of PC waveguide has been experimentally measured by scanning the lattice constants of PCs using a fixed wavelength. Devices are covered with nearly transparent poly dimethyl siloxane (PDMS). PDMS serves as the solid phase micro-extraction layer which extracts the VOC from water and enables absorbance measurements independent from the strong absorbance of water. Transmitted intensity is measured in presence and absence of xylene as a representative VOC and its absorbance determined on chip from the difference in transmitted intensity.

9367-29, Session 6

Strain engineering to create direct-bandgap GeSn films for monolithic Si integration

Birendra R. Dutt, APIC Corp. (United States); Elizabeth H. Edwards, PhotonIC Corp. (United States); Gerald M. Miller, APIC Corp. (United States); Colleen K. Shang, Stanford Univ. (United States); Milam Pender, John Borland, Advanced Integrated Photonics (United States); Yi-Chiau Huang, Yihwan Kim, Applied Materials, Inc. (United States)

First principles electronic band structure calculations predict that unstrained Ge_{1-x}Sn_{x} with x > 6.55% Sn will show direct-bandgap behavior. In practice, during epitaxial growth on Si, the larger atomic size of Sn induces compressive strain in GeSn which increases the energy separation between the direct (?) and indirect (L) conduction valleys, preventing direct bandgap behavior.

In this study, we first measured and compare the residual strain in both blanket Ge_{0.905}Sn_{0.095} and heterostructured Ge/Ge_{0.905}Sn_{0.095}

grown on Ge-buffered Si. We then developed and deposited heavily compressively strained nitride films on the GeSn samples. The strain in the GeSn layers was remeasured to determine the amount of tensile strain successfully transferred from nitride. We compare predictions of the resulting bandgap behavior with experimental PL taken from the samples before and after nitride deposition to determine whether a direct bandgap condition has been achieved in the GeSn to allow efficient lasing.

9367-35, Session 7

Imec ISIPP25G silicon photonics: a robust CMOS-based photonics technology platform

Philippe P. Absil, IMEC (Belgium)

Silicon photonics has become in the past years an important technology adopted by a growing number of industrial players to develop their next generation optical transceivers. However most of the technology platforms established in CMOS fabrication lines are kept captive or open to only a restricted number of customers. In order to make silicon photonics accessible to a large number of players several initiatives exist around the world to develop open platforms. In this paper we will present imec's silicon photonics active platform accessible through multi-project wafer (MPW) runs.

In particular we will review the performance achieved for the various components that are integrated in the platform: fiber couplers, WDM filters, p-n based modulators, integrated heaters and germanium-on-silicon based photo-detectors. We will particularly focus on performance statistics of the various devices in terms of within-wafer, wafer-to-wafer and lot-to-lot repeatability that is of importance to deliver the expected performance to the MPW runs customers. We will also present the CMOS-based "in-line" statistical process control methods used during the wafer fabrication that guarantees "end-of-line" performance control.

9367-36, Session 7

Mode-converting coupler for silicon-on-sapphire devices

Sanja Zlatanovic, Space and Naval Warfare Systems Command (United States); Bruce W. Offord, Space and Naval Warfare Systems Ctr Pacific (United States); Randy L. Shimabukuro, Space and Naval Warfare Systems Command (United States); Everett W. Jacobs, Space and Naval Warfare Systems Ctr. Pacific (United States); Michael W. Owen, Defense Microelectronics Activity (United States)

Silicon-on-sapphire devices are attractive for mid-infrared optical applications up to 5 microns due to the low loss of both silicon and sapphire in this wavelength band. Designing efficient couplers for silicon-on-sapphire devices presents a challenge due to the highly confined mode in silicon and the large values of refractive index of both silicon and sapphire. Here, we present the design, fabrication and measurements of a mode-converting coupler for silicon-on-sapphire waveguides. We utilize a mode converter that consists of a large waveguide that overlaps a silicon inverse tapered waveguide. While this geometry was previously utilized for silicon-on-oxide devices, the novelty in this approach is using materials that are compatible with a silicon-on-sapphire platform and a CMOS fabrication line. In the coupler that we will present, the overlapping waveguide is made of silicon nitride. Silicon nitride is a material of choice because of its large index of refraction and low absorption from near-infrared to mid-infrared. The silicon nitride waveguide is 5 microns wide and 2 microns tall, while the silicon waveguide height is 500nm. The inverse taper is 150 microns long and the tip size is approximately 100nm. The couplers were fabricated using a 0.25 micron silicon-on-sapphire process. The measured coupling loss

from tapered lensed silica fibers to the silicon was 4.8dB/coupler. We will describe some challenges in the fabrication process and discuss ways to overcome them.

9367-37, Session 7

Topology-optimized silicon photonic wire mode-multiplexer

Louise F. Frellsen, Technical Univ. of Denmark (Denmark); Lars H. Frandsen, Yunhong Ding, Technical Univ. of Denmark (Denmark) and DTU Fotonik (Denmark); Yuriy Elesin, Topsoe Fuel Cell (Denmark); Ole Sigmund, Technical Univ. of Denmark (Denmark); Kresten Yvind, Technical Univ. of Denmark (Denmark) and DTU Fotonik (Denmark)

In order to support the constantly increasing internet traffic demand, interest is being shown in the possibility of exploiting mode division multiplexing in the optical communication networks [1]. The key to realizing on-chip mode division multiplexing is an efficient mode (de)multiplexer. Using the powerful inverse design tool topology optimization (TO) [2], we have designed a silicon nanowire mode (de-)multiplexer which multiplexes two fundamental even (TE₀) modes onto a photonic wire supporting the TE₀ and the first order odd mode (TE₁), i.e. one TE₀ channel is converted to the TE₁ mode. A minimal device footprint allowing for mode-multiplexing with low-loss and low crosstalk has been investigated through 2D TO, while 3D TO has been applied to the optimal 2D configuration to obtain a design which is performing in practice. Designs exhibiting high extinction ratios and low losses with ultra-compact footprints of $\approx 3 \mu\text{m} \times 2.5 \mu\text{m}$ were obtained in this way. The designs have been fabricated in silicon-on-insulator material through e-beam lithography for experimental verification. Robustness has been investigated through alterations of the fabricated designs and the insertion losses have been experimentally recorded. Mode profiles of the (de-)multiplexed signals were recorded using vertical grating couplers and an infrared camera.

In this way, TO has proved to be an efficient method for designing compact devices for multiplexing between the fundamental and the first order mode of a silicon photonic wire and we believe that the method can readily be extended to work with a higher order of modes.

[1] R. Kirchain and L. Kimerling, "A roadmap for nanophotonics," Nat. Photonics, vol. 1, no. 6, pp. 303-305, 2007.

[2] M. P. Bendsøe and N. Kikuchi, "Generating optimal topologies in structural design using a homogenization method," Comput. Meth. Appl. Mech. Engng., vol. 71, pp. 197-224, 1988.

9367-38, Session 7

25 Gbps silicon photonics multi-mode fiber link with highly alignment tolerant vertically-illuminated germanium photodiode

Tadashi Okumura, Yuki Wakayama, Yasunobu Matsuoka, Katsuya Oda, Misuzu Sagawa, Takashi Takemoto, Etsuko Nomoto, Hideo Arimoto, Shigehisa Tanaka, Hitachi, Ltd. (Japan)

Optical interconnection has attracted much attention with increasing demand for high-performance IT devices with large bandwidth such as servers and routers. For this interconnect application, an active optical cable (AOC) with single-mode-fiber (SMF) and silicon (Si) photonics technologies is widely used, and Low cost is an important factor in regard to use of large amounts of AOCs in datacenters. One of technical challenges concerning Si photonics is highly efficient optical coupling between a transceiver

chip and the optical fiber. The precise fiber alignment assembly becomes a barrier fabricating a low cost module. To reduce fiber connection cost, Si-photonics-technology-based optical interconnection combined with a multi-mode-fiber (MMF) system has been proposed.

In this research, optical coupling problem between a Si photonics transceiver and a MMF for low cost assembly was studied. A germanium (Ge) photodiode with large alignment tolerance for high speed and low cost optical interconnection was developed. To achieve a large alignment tolerance, a surface-illuminated structure was employed and a Ge photodiode with 20 GHz bandwidth and 0.5 A/W responsivity with 1 dB-down alignment tolerance of $\pm 10 \mu\text{m}$, was realized. A sensitivity of -4.2 dBm optical-modulation-amplitude (OMA) was confirmed at 25 Gbps with a receiver, which consists of the Ge photodiode and a CMOS transimpedance-amplifier (TIA). In addition, a 25 Gbps transmission test of a MMF link was demonstrated with a Si photonics transmitter, which has alignment tolerance of $\pm 15 \mu\text{m}$, and the receiver with the Ge photodiode.

9367-39, Session 7

Silicon-based tunable optical delay lines and switches for next-generation optical telecommunications (*Invited Paper*)

Linjie Zhou, Shanghai Jiao Tong Univ. (China)

We report our recent progress on the implementation of reconfigurable optical true time delay lines and generalized Mach-Zehnder interferometer (GMZI) based optical switches on the silicon-on-insulator platform. The delay line consists of 7 stages of silicon waveguide pairs connected by 2x2 Mach-Zehnder interferometer (MZI) switches. Variable optical attenuators are embed to suppress the inter-symbol crosstalk caused by the finite extinction ratio of switches. The device can provide a maximum of 1.27 ns delay with a 10 ps resolution over a wide wavelength range. Eye diagram measurement of a 25 Gbps pseudo-random bit sequence signal reveals that the power penalty is only increased by 0.17 and 0.77 dB after transmission through the shortest and the longest paths, respectively. The GMZI optical switch is composed of a 4x4 multimode interferometer connected with four regular 2x2 MZIs, which can provide the full 24 states of non-blocking switching with integrated silicon resistive micro-heaters. Our preliminary measurement shows that the average insertion loss is around 9 dB and the crosstalk of all switching states is better than -12 dB at the 1550 nm optical communication band. The average switching power is 109 mW. The switching functionality is verified by the transmission of a 40 Gb/s quadrature phase shift keying (QPSK) optical signal.

9367-40, Session 8

Si-wire grating couplers for integrated optical transceivers based on single-mode fiber connection

Yohei Sobu, Fujitsu Labs., Ltd. (Japan) and Photonics Electronics Technology Research Association (Japan); Seok-Hwan Jeong, Photonics Electronics Technology Research Association (Japan); Shigeaki Sekiguchi, Fujitsu Labs., Ltd. (Japan) and Photonics Electronics Technology Research Association (Japan); Yu Tanaka, Photonics Electronics Technology Research Association (Japan); Ken Morito, Fujitsu Labs., Ltd. (Japan) and Photonics Electronics Technology Research Association (Japan)

Recently, grating couplers (GCs) have been extensively reported as a promising device to solve a main concern related to optical coupling between Si-wire waveguides and standard single-mode optical fibers. In this paper, we report Si-wire-type GCs fabricated by 248-nm KrF lithography foundry process on a 200-nm silicon-on-insulator wafer with a 220-nm-

thick Si layer. We studied two kinds of GCs, one for transmitters (Tx-GCs) and the other for receivers (Rx-GCs). The Tx-GCs consist of Si-wire grating and the Rx-GCs consist of square-type air holes and two output waveguides for polarization splitting. Since the shapes of Tx-GC and Rx-GC are quite different, the optimum condition of the optical lithography is not same for the two kinds of GCs. In order to fabricate them on the same fabrication process, square lattice air hole sizes in Rx-GCs were adjusted from the viewpoint of optical proximity correction. As a result, Tx-GC and Rx-GC were operated within the same wavelength regime at around 1.55- μm . As for Tx-GCs, we obtained insertion loss ($\sim 3\text{dB}$), operating bandwidth (1-dB bandwidth of $\sim 35\text{nm}$), and also confirmed manufacturing tolerance of spectral characteristics (deviation of operating range $< 5\text{nm}$) in intra-dies and inter-dies and 1-dB fiber misalignment tolerance ($\sim \pm 3\text{-}\mu\text{m}$ in-plane of the grating in the Tx-GC). In the case of Rx-GCs, we achieved nearly the same fiber coupling efficiency for the two output channels whose difference is less than 0.5dB within the wavelength range of 30 nm.

9367-41, Session 8

Low back-reflection CMOS-compatible grating coupler for perfectly vertical coupling

George Dabos, Aristotle Univ. of Thessaloniki (Greece); Nikos Pleros, Aristotle Univ. of Thessaloniki (Greece) and Informatics and Telematics Institute, Centre for Research and Technology Hellas (Greece); Dimitris M. Tsiokos, Aristotle Univ. of Thessaloniki (Greece) and Informatics and Telematics Institute (Greece)

In view of high volume manufacturing of silicon based photonic-integrated-circuits (Si-PICs), CMOS compatible low-cost fabrication processes as well as simplified packaging methods are imperatively needed. Silicon-on-Insulator (SOI) based grating couplers (GCs) have attracted attention as the key components for providing optical interfaces to Si-PICs due their fabrication simplicity compared to the edge coupling alternatives. GCs based on perfectly vertical coupling scheme become essential by introducing substantial savings in the packaging cost as no angular configurations are required but at the expense of high coupling efficiency values due to the second order diffraction. In this context, research efforts concentrated on designing GCs with minimized back reflection into the waveguide yet employing more than one etching steps or rather complex fabrication processes. Herein, we propose a fully etched CMOS compatible non-uniform one-dimensional (1D) GC for perfectly vertical coupling with low back reflected optical power by means of numerical simulations. A particle-swarm-optimization (PSO) algorithm was deployed in conjunction with a commercially available 2D finite-difference-time-domain (FDTD) method to maximize the coupling efficiency to a SMF fiber for TM polarization. The design parameters were restricted to the period length and the filling factor while the minimum feature size was 80 nm. A peak coupling loss of 4.4 dB at 1553 nm was achieved with a 1-dB bandwidth of 47 nm and a back reflection of -20 dB. The coupling tolerance to fabrication errors was also investigated. The proposed GC is currently being fabricated.

9367-42, Session 8

Mode conversion based on the acousto-optical interaction in hybrid photonic-phononic waveguide

Guodong Chen, Ruiwen Zhang, Xiong Huang, Heng Xie, Ya Gao, Danqi Feng, Junqiang Sun, Huazhong Univ. of Science and Technology (China)

We present a scheme for on-chip optical mode conversion in a hybrid photonic-phononic waveguide. The design exploits the idea that a silicon (Si) rectangle waveguide is buried in a silicon nitride (Si₃N₄) honeycomb

phononic crystal slab. Total internal reflection between Si and Si₃N₄ tightly confines the optical waves in the Si waveguide core, which can be designed to be multi-moded for optical waves. Simultaneously, the Si waveguide also serves as line defect to be inserted the phononic crystal slab to form a phononic crystal waveguide for guiding the acoustic wave. This compound-material waveguide not only restricts both the optical and acoustic waves, but also provides independent control of the photonic and phononic waveguide dispersion for realizing phase-matching-condition. Both propagating optical and acoustic wave can be tightly confined in the hybrid waveguide, and the acousto-optical interaction can be enhanced to realize optical mode conversion within a chip-scale size. The theoretical model of the acousto-optic interaction is established to explain the mode conversion. The numerical simulation results indicate that the high efficient mode conversion can be achieved by adjusting the intensity of the acoustic wave. We also show that the mode conversion bandwidth can be dramatically broadened to 13 THz by adjusting the frequency of the acoustic wave to match phase condition of the acousto-optic interaction. This mode converter on-chip is promising in order to increase the capacity of silicon data buses for on-chip optical interconnections.

9367-43, Session 9

Comparison of different types of MMI-resonators fabricated on a micron-scale SOI platform

Matteo Cherchi, Sami Ylinen, Mikko Harjanne, Markku Kapulainen, Tapani Vehmas, Timo Aalto, VTT Technical Research Ctr. of Finland (Finland)

1x1 optical resonators have been designed based on multi-mode interference (MMI) splitters of different splitting ratios (85/25 and 73/27) and different types of back-reflectors as feedback mechanism. They are basically 2x2 MMIs of uneven splitting ratios with one of the ports from both sides ending in a reflector. The reflectors include metal-dielectric mirrors, waveguide loops and MMI reflectors. The remaining two ports play the role of input and thru port respectively. The resonant wavelengths are reflected back in the input port, hence acting also as output port in reflection. The devices have been fabricated on SOI wafers with a 3 μm-thick silicon layer. In all cases, the quality factors of the resonances of a given resonator have been found to significantly change from peak to peak. This can be attributed to wavelength dependent losses in the feedback mechanisms, that is wavelength dependent reflectivity of the back-reflectors. Through a suitable transfer matrix model, we have found that best performing devices correspond to reflectivity as high as 96% for the metal/dielectric mirrors and 91% for the MMI reflectors, corresponding to a resonator finesse of 12 and 9 respectively. The free spectral ranges of the resonators vary from about 3 nm to about 1 nm, depending on the cavity length, which is constrained by the lengths of both the MMIs and the reflectors. When suitably combined with gain elements, the proposed resonators are promising candidates as fabrication tolerant wavelength selective reflectors for external cavity lasers.

9367-44, Session 9

Structural and optical properties of 200-mm optical germanium-on-insulator (GeOI) substrates for silicon photonics applications

Vincent Reboud, Julie Widiez, Jean Michel Hartmann, CEA-LETI (France); Alexei Chelnokov, MINATEC (France); Alban Gassenq, CEA-LETI (France); Kevin Guillo, Nicolas Pauc, Vincent Calvo, CEA-INAC (France); Richard Geiger, Hadi Rabbani, Paul Scherrer Institut (Switzerland); Jérôme Faist, ETH Zürich (Switzerland); Hans C. Sigg, Paul Scherrer Institut (Switzerland)

Integrated laser sources compatible with microelectronic technologies is currently one of the main challenges for silicon photonics. Germanium (Ge) has typically an indirect band gap leading to a very inefficient photo-generation process which, however, is drastically improved when high mechanical stress is induced [1]. Our objective was to obtain highest Ge crystalline quality to avoid mechanical breaking of the Ge when a strong tensile strain is applied. To combine the advantages of high quality Ge layers on a silicon host substrate with a SiO₂ layer that isolate optical modes, the Ge layer has been transferred to obtain a Germanium-On-Insulator (GeOI) substrates. Here, we report on the first 200 mm optical GeOI substrates for Silicon Photonics made from epitaxial wafers using the Smart Cut™ technology composed by a thick germanium layer (>500 nm and up to 1 μm) on 1 μm buried oxide (BOX). Compared with conventional GeOI fabricated for microelectronic applications, a deeper splitting step had to be optimized, requiring H⁺ implantation at higher energy and higher dose than for standard applications.

We demonstrate the feasibility of the process to provide optical GeOI for Silicon Photonics applications. Emission properties and carrier lifetimes modification [2] will be compared to the Ge grown on SOI. These results open the way to a wafer based fabrication process of new devices based on strained and doped germanium.

[1] Süess, M. J. et al. Nature Photonics 7, 466 (2013).

[2] Geiger, R. et al. Appl. Phys. Lett. 104, 062106 (2014).

9367-45, Session 9

Silicon photonics athermal Mach-Zehnder interferometer with wide thermal and spectral operating range

Jaime Viegas, Peng Xing, Masdar Institute of Science & Technology (United Arab Emirates)

In the context of 3D-integrated circuit (3DIC) integration of photonic and electronic components on vertical stacks covering different domains (digital, analog, RF, optical and MEMS), the control and minimization of adverse thermal effects on the behavior of the different parts of the microsystem is a major concern. Solutions based on passive athermal design are good candidates for enabling operation of optical components over electronic ICs with variable temporal and spatial thermal load while at the same time, minimizing energy loss on thermal biasing resistive loads. We propose a design method and the corresponding fabricated prototype to extend the spectral athermal operating range of a Mach-Zehnder interferometer (MZI) over wide thermal range with minimal temperature sensitivity. We have selected the MZI as a case-study since this is a typical optical component commonly used as the backbone of an optical modulator. The proposed approach is demonstrated with an in-house CMOS compatible silicon-on-insulator process flow fabrication run. The fabricated MZIs have a temperature sensitivity of 2.5 pm/K over a spectral range larger than 90 nm, covering both C and L bands and for operating temperatures in the range of 20°C to 45°C.

9367-46, Session 9

Bending behavior of a flexible single crystal nanomembrane photonic crystal cavity

Xiaochuan Xu, Harish Subbaraman, Omega Optics, Inc. (United States); Ray T. Chen, The Univ. of Texas at Austin (United States)

In this paper, we present experimental and theoretical studies on the bending induced resonance shift of a photonic crystal cavity. The photonic crystal devices are fabricated on a 2cm x 2cm large-area single crystal Si₃N₄ which is transferred defect-freely onto a Kapton substrate with an SU-8 bottom cladding. Photonic crystal tapers are implemented at the strip-

photonic crystal waveguide interfaces, which lowers the coupling loss and enables operation closer to the band edge. Subwavelength grating (SWG) couplers are employed at the input and output of the device in order to enable device characterization. The device is mounted on the two jaws of a caliper and it can be buckled up and down through sliding one of the jaws. The bending radius at the top of the curvature can be estimated with the length of the specimen and the distance between the two jaws. A minimum bending radius of 5 mm is achieved. Finite element method (FEM) is used to simulate the deformation and the strain of the nanomembrane. The results are used as the input of finite-difference time-domain (FDTD) simulation. The analysis shows that the strain sensitivities are 0.673, 0.656, 0.588, and 0.591 picometer per micro-strain for longitudinal face-out, longitudinal face-in, transverse face-out, and transverse face-in bending, respectively.

9367-47, Session 9

Compact 4X4 1250GHz silicon arrayed waveguide grating router for optical interconnects

Guanting Chen, Jun Zou, Zhejiang Univ. (China); Tingting Lang, China Jiliang Univ. (China); Jian-Jun He, Zhejiang Univ. (China)

A compact arrayed waveguide grating router (AWGR) based on silicon nanowires for optical interconnects is experimentally demonstrated. The design, fabrication and characterization of this 4x4 AWGR with a 1250GHz channel spacing and a 5THz free spectral range are discussed. The insertion loss for four output channels is 2.5-5.5dB and the crosstalk is better than -18dB. The functionality of the AWG as a router and its good rotation property are also presented. This device has a compact footprint of 0.46x0.26mm².

A SOI wafer with 220nm top Silicon and 2µm buried oxide layer is used. The waveguide width is designed to be 500nm. Silica is chosen as the upper-cladding material. A four-channel AWGR with central wavelength of 1550nm and a channel spacing of 10nm is considered. In order to obtain a 40nm free spectral range, the diffraction order should be 19.

For the fabrication, an 180nm-thick SiO₂ is first deposited as hard mask by plasma-enhanced chemical vapor deposition (PECVD). Then, the photomask ma-N-2405 is spin-coated on the wafer and the AWGR pattern is written by electron-beam lithography. The pattern is subsequently transferred to the SiO₂ mask by inductively coupled plasma reactive ion etching (ICP-RIE). Finally, a 2µm-thick SiO₂ upper-cladding is deposited by PECVD.

A tunable laser (Agilent 8600A) and a power sensor (Agilent 8600B) are employed to characterize the AWGR. The measured results show that the AWGR exhibits low insertion loss (2.5-5.5dB) and low crosstalk of -18dB, as well as an excellent cyclic rotation property for TM polarization.

9367-30, Session 10

Silicon-PDMS optofluidic integration *(Invited Paper)*

Romeo Bernini, Testa Genni, Gianluca Persichetti, Istituto per il Rilevamento Elettromagnetico dell'Ambiente (Italy); Pasqualina M. Sarro, Technische Univ. Delft (Netherlands)

Hybrid approaches that involve the combination of Silicon-based optical and polymer-based microfluidic devices have been successfully demonstrated and are becoming more and more widespread. In this work we show that integrated Hybrid Silicon-PDMS Antiresonant Reflecting Optical Waveguide (H-ARROW) can be used as a basic tool for the realization of complex optofluidic devices. The combination of different materials and fabrication processes allows a modular approach, enabling to benefit from the high optical quality achievable with silicon technology and low cost of soft lithography processing. H-ARROW is constituted by the optofluidic channel of a conventional ARROW, sealed with a thin polydimethylsiloxane (PDMS)

polymer layer. This configuration presents the great advantage to have the core channel with double functionality, as it works as waveguide and fluidic channel simultaneously. Furthermore, the device layout simplifies the integration of microfluidic parts to manipulate liquid samples, comprising fluidic inlet and outlet and channels for delivering the sample, which can be cost-effectively and easily fabricated in PDMS layer. Hybrid ARROWS have been fabricated and characterized. The experimental results show that optical performances could rival with that obtained with full-silicon ARROW. These waveguides have been used in order to design complex devices like an integrated hybrid liquid core optofluidic ring resonator (h-LCORR). An optofluidic platform prototype for fluorescence measurements has been also developed. In this device liquid core H-ARROW has been integrated with self-aligned solid core waveguide and microfluidic device are integrated with a multilayer approach, resulting in a three-dimensional device assembly.

9367-31, Session 10

Optofluidic metasurfaces: from physical fundamentals to lab-on-chip systems *(Invited Paper)*

Ahmet A. Yanik, Univ. of California, Santa Cruz (United States)

In the first part of my talk, I will introduce an ultrasensitive infrared (IR) nanospectroscopy technique for conformational dynamics of proteins at few molecule levels. Conformational dynamics of proteins is one of the most critical components of life-sustaining biomolecular processes. However, the small intrinsic absorption cross-section of IR active modes of proteins has been a fundamental limitation in absorption spectroscopy. I will demonstrate 100,000 fold signal enhancements in vibrational signatures of proteins by using collective excitation of plasmonic nanoantenna arrays leading to unprecedented near field enhancements and record low zeptomole detection limits. To eliminate the need for current surgical approaches, I will also show integration of our spectroscopic technique onto optical fiber surfaces to achieve real-time cancer biopsy in the human body.

In the second part of the talk, I will introduce an optofluidic-nanoplasmonic biosensor merging nanofluidics and biosensing to overcome fundamental mass transport limitations. I will introduce extra-ordinary light transmission effect through subradiant plasmonic resonances and demonstrate ultrasensitive biosensors with detection limits surpassing the gold standard surface plasmon sensors. Furthermore, I will introduce a novel sensing scheme enabling label-free detection of biomarker proteins "with the naked eye" using plasmonic analogs of Fano resonances, which has been discovered in atomic physics experiments in 1950s. I will show real world applications of our optofluidic biosensors for detection of live and intact viruses in biological media at medically relevant concentrations. In the final part of my talk, I will introduce optofluidic metasurfaces enabling isolation and analysis of Circulating Tumor Cells (CTCs) from human blood.

9367-32, Session 10

Index of refraction sensors and biosensors using 2D photonic crystal slab devices *(Invited Paper)*

Ofer Levi, Univ. of Toronto (Canada)

Optical techniques are widely used in clinical settings and in biomedical research to interrogate bio-molecular interactions and to diagnose and monitor a disease. We present the development of miniature optical index of refraction sensors for biomedical diagnosis and molecular studies. We have designed and fabricated photonic crystal slab (PCS) nanostructures in Silicon/Silicon Nitride/Silicon Dioxide devices that can be embedded inside micro-fluidic channels. The presence of analyte nearby the nano-sensor surface changes the local index of refraction and the resonance condition for TE-like and TM-like guided resonance modes (GMRs), leading to the analyte

detection. We show that parameters such as spectral sensitivity (nm/RIU) and quality factor, Q for an index of refraction sensors can be optimized simultaneously, leading to limit of detection better than 10^{-7} RIU and to sensing sensitivity >0.8 of the theoretical limit at near IR wavelengths. Breaking the symmetry in the photonic crystal unit cell by creating elliptical holes, removes the degeneracy in the guided modes, and allows an independent evaluation of the GMRs in each incoming polarization and a potential for mode mixing between orthogonal modes. This architecture can also be explored for "self referencing" sensor designs, further reducing the sensor sensitivity to changing environmental conditions.

9367-33, Session 10

4H-SiC detectors for ultraviolet light monitoring

Massimo C. Mazzillo, STMicroelectronics (Italy); Antonella Sciuto, Consiglio Nazionale delle Ricerche (Italy); Paolo Badala, Beatrice Carbone, Alfio Russo, Salvo Coffa, STMicroelectronics (Italy)

Silicon Carbide (SiC) provides the unique property of near-perfect visible blindness and very high signal-to-noise ratio due to the high quantum efficiency and low dark current. These features make SiC the best available material for visible blind semiconductor ultraviolet (UV) light detectors. Thanks to their properties, these devices have been extensively used for flame detection monitoring, UV sterilization and astronomy. Here we report on the electrical and optical performance of patterned continuous metal film NiSi/4H-SiC vertical Schottky photodiodes with different semiconductor exposed area suitably designed for UV light monitoring.

9367-34, Session 10

Enhanced light-matter interaction in cascaded cavities within a slotted photonic crystal slab on silicon-inorganic hybrid platform

Arijit Bera, Petri Stenberg, Matthieu Roussey, Markku Kuittinen, Seppo K. Honkanen, Univ. of Eastern Finland (Finland)

Silicon photonics offers a multi-functional platform for ultrahigh bandwidth optical interconnects as well as low-power all-optical signal processing via nonlinear optics. However, its high two-photon absorption (TPA) imposes limitation on its use for ultrafast signal processing. The slot waveguide geometry caters a potential solution enabling strong light-matter interaction between the slot mode and the low index cover material. Here, we investigate a silicon-inorganic hybrid platform using TiO₂ as the cover material with high third-order nonlinearity and negligible TPA. We have previously demonstrated experimentally, a resonant structure involving a photonic crystal cavity within two Bragg mirror segments, created by periodically patterning the two rails of a slot waveguide, enabling enhanced light-matter interaction and precise wavelength selectivity. Here, we extend this idea by introducing multiple cavities cascaded in series. By coupling three identical cavities, we excite three resonant peaks, equally spaced in wavelength within the photonic band-gap, due to the natural splitting of resonance. Since the spacing of the three resonance peaks follows the conservation of energy, the structure shows the promise to achieve spontaneous four-wave mixing by launching a single pump at the input. Moreover, by including a silicon nanowire within the cavity region, we have found that the field confined within the cavity is evanescently guided by the nanowire, leading to a strong overlap of the field with the cover material. This structure is fabricated on an SOI wafer by e-beam lithography and reactive ion etching, followed by the conformal coating of 180 nm TiO₂ film using atomic layer deposition.

9367-54, Session PWed

High-quality slot waveguide ring resonator based on atomic layer deposition

Anton Autere, Aalto Univ. School of Electrical Engineering (Finland); Lasse Karvonen, Antti Säynätjoki, Aalto Univ. (Finland); Matthieu Roussey, Univ. of Eastern Finland (Finland); Elina Färm, Marianna Kemell, Univ. of Helsinki (Finland); Xiaoguang Tu, Tsung-Yang Liow, Guo-Qiang Lo, A*STAR Institute of Microelectronics (Singapore); Mikko Ritala, Markku Leskela, Univ. of Helsinki (Finland); Seppo K. Honkanen, Univ. of Eastern Finland (Finland); Zhipei Sun, Aalto Univ. School of Science and Technology (Finland)

Ring resonators have found many different applications. High index contrast between the silicon core and the low index cladding material in silicon waveguides makes them suitable to create very compact ring resonators. However, strong two-photon absorption (TPA) in silicon limits the use of silicon in various applications where high intensity is needed to facilitate nonlinear effects [1]. This shortcoming of silicon can be avoided by using slot waveguides where light is confined in a low refractive index material outside the silicon core [2].

Atomic layer deposition (ALD) has been proven to be an excellent method to improve the slot waveguide quality, due to the high thickness precision and conformality of ALD grown films, and wide variety of available ALD materials. For example, it has been shown that ALD can be used to reduce losses in slot waveguides [3,4]. Here, we combine slot silicon waveguides with ALD technique for ring resonator performance improvement.

The slot waveguide samples were fabricated with 248 nm deep ultra violet (DUV) lithography onto SOI wafers. Similar chips were coated with two different ALD materials: Al₂O₃ and a nanolaminate which consist of altering layers of tantalum pentoxide (Ta₂O₅) and polyimide (PI).

We obtained Q-factors of over 10 000 for ring resonators coated with ALD grown Al₂O₃ and nanolaminate. Our results demonstrate that ALD can be used to create slot waveguide ring resonators with relatively high Q-factors. To our best knowledge this is the first demonstration of silicon photonic device coated with ALD grown nanolaminates, also ALD-based slot waveguide ring resonator have not been demonstrated before.

References

- [1] C. Koos et al, Nat. Photonics, 3, 216,(2009).
- [2] V.R. Almeida et al, Opt. Lett., 29, 1209,(2004).
- [3] T. Alasaarela et al, Opt. Express, 19, 11529,(2011).
- [4] A. Säynätjoki, Opt. Express, 19, 26275, (2011).

9367-55, Session PWed

Toward new design rule check of silicon photonics for automated layout physical verifications

Mohamed Ismail, Raghi S. El Shamy, The American Univ. in Cairo (Egypt); Kareem Madkour, Sherif Hammouda, Mentor Graphics Egypt (Egypt); Mohamed A. Swillam, The American Univ. in Cairo (Egypt)

A simple analytical model is developed to estimate the power loss and time delay in photonic integrated circuits fabricated using SOI standard wafers. This model is simple and can be utilized in physical verification of the circuit layout to verify its feasibility for fabrication using certain foundry specifications. This model allows for providing new design rules for the layout physical verification process in any electronic design automation (EDA) tool. The model is accurate and compared with finite element based full wave electromagnetic (EM) solver. The model is a closed form and circumvent the need to utilize any EM solver for the verification process. As

such it dramatically reduces the time of the verification process and allow fast design rule check.

9367-56, Session PWed

Strain analysis in silicon-based waveguides and couplers

Giovanni Battista Montanari, Lab. MIST E-R (Italy); Fulvio Mancarella, Roberto Balboni, Diego Marini, Franco Corticelli, Michele Sanmartin, Matteo Ferri, Gabriele Bolognini, Consiglio Nazionale delle Ricerche (Italy)

Strained silicon technology opens interesting perspectives for photonic applications, since, as recently demonstrated, the deposition of a straining layer on top of a silicon waveguide can break the silicon lattice inversion thus enabling significant linear electro-optic effect or second-harmonic generation.

In this work, we report a study of the lattice deformation induced by a Si₃N₄ film (350nm thickness) deposited on several silicon ribs and coupling structures with cross sections down to 450x220nm).

The stress and strain distribution inside the silicon waveguides core for both single and coupled waveguides were estimated through finite-element modeling as well as measured on manufactured chips employing the Convergent Beam Electron Diffraction (CBED) technique enabling nanometer-scale accuracy to evaluate the lattice silicon deformation induced by the nitride film. Planar silicon rib structures with different dimensions were manufactured on 4 inch <100> silicon wafers employing a spacer technology that allowed fabrication of submicrometric silicon waveguides starting from conventional near-UV micrometric photolithography. A stoichiometric LPCVD Si₃N₄ film was then deposited onto them, leading to an expected significant intrinsic stress at the silicon-to-nitride interface and inducing a substantial strain inside the waveguide.

The simulated and measured strain values showed strain values up to ~ 2 μ? for the ?_{zz} component near the straining layer interface; such values are in line with similar measurements carried out on micrometric strained silicon waveguides, and Si₃N₄-induced strain results high enough to obtain significant nonlinear optical effects, without exhibiting cracks or delamination issues, in perspective integrated photonic devices.

9367-57, Session PWed

Enhanced multiband photodetection in blocked impurity band detectors with antenna-coupled microcavities

Kaisheng Liao, Shanghai Institute of Technical Physics (China)

Multicolor photodetectors are of interest for a variety of application. In this work, we report on a method for multicolor photodetection by using Fabry-Perot (FP) cavity and subwavelength-period grating mirror on a high sensitivity arsenic-doped silicon Blocked-Impurity-Band (BIB) detector. Advantage is taken of flexibility of the FP cavity to generate a series of resonances in multispectral bands. Theoretical calculations of the efficiency of this approach for multiband photodetection is presented. Fabrication of this integrated antenna-coupled microcavities on the broadband-response BIB detectors is described. Finally, preliminary results and further development plans are discussed.

9367-58, Session PWed

Large scale silicon photonic MEMS switch using moving couplers

Sangyoon Han, Tae Joon Seok, Ming C. Wu, Univ. of California, Berkeley (United States)

Fast and large port count optical circuit switches are on demand for delivering reconfigurable bandwidth in datacenter networks. 3D MEMS optical switch has been used but the application was limited due to its slow switching speed. Silicon photonics platform is ideal for implementing large port count optical switch due to its high integration density. However the port count of silicon photonic switch has limited due to their optically lossy architecture.

In this work, we report largely scalable silicon photonic MEMS switch with microsecond response time. The switching in our switch is done by MEMS fashion with moving waveguide couplers. Two waveguides placed in parallel with proximity gap forms coupled waveguides and light from one waveguide is transferred to the other waveguide. By changing the gap between the two waveguides, the coupling strength between waveguides were changed and thus light transfer character between two waveguides were changed. The gap was controlled by moving one of the waveguide with electrostatic actuator. Thanks to the large working range (1 μm) of the actuator, we could completely couple and de-couple the waveguides by actuating the actuator and thus the high extinction on-off ratio (30dB) was possible.

We used standard silicon photonic SOI wafer (220 nm thick silicon layer and 3 μm thick buried oxide layer) to fabricate our switch. Waveguides and actuators were defined by standard CMOS process. HF vapor release was introduced to release MEMS actuators which were anchored on buried oxide layer. Light was coupled to the switch using grating couplers.

9367-59, Session PWed

Solar cell enhancement using metallic nanoparticle arrays embedded in titanium dioxide

Max A. Burnett, Michael A. Fiddy, The Univ. of North Carolina at Charlotte (United States)

Advances in nanotechnology and metamaterials, has stimulated research to increase solar panel efficiency. Engineered surfaces can reduce scattering and increase absorption, e.g. using arrays of optical nanoantennas, but they can be difficult to fabricate and may not be easily applied to existing solar panel manufacturing lines. Subwavelength gold and silver nanoparticles, with both spherical and cylindrical shapes of varying dimensions and spacings, were studied via FDTD computer simulations. For these simulations we used a plane-wave broadband source (400nm-1100nm) with multiple polarizations to simulate sunlight and a 500nm layer of silicon. We chose to embed the array within a dielectric as plasmonic effects at the dielectric-metal boundary enhance the light through near-surface effects. We chose titanium dioxide as the dielectric both for its large index of refraction and low absorption within the visible regime. As gold and silver have low indices of refraction in the visible regime, pairing titanium dioxide with silver or gold results in enhanced surface waves with large wavevector values. Also, as silver and gold both have low absorption coefficients in the visible regimes so losses are minimal. Our results show little difference in performance between gold and silver and so the lowest cost can be chosen and its stability is ensured as it is embedded in a dielectric. Thin films of this composite can be made and applied to existing solar panel surfaces to boost performance.

9367-60, Session PWed

Strained germanium-tin multiple quantum well microdisk resonators towards a light source on silicon

Colleen K. Shang, Robert Chen, Suyog Gupta, Stanford Univ. (United States); Yi-Chiau Huang, Applied Materials, Inc. (United States); Yijie Huo, Stanford Univ. (United States); Errol Sanchez, Yihwan Kim, Applied Materials, Inc. (United States); Theodore I. Kamins, Krishna C. Saraswat, James S. Harris, Stanford Univ. (United States)

Germanium-tin (GeSn) is an exclusively Group IV materials system that has the potential to enable new families of optoelectronic and photonic devices integrated on silicon. Although the development of a silicon-compatible light source has been traditionally limited by the indirect band gaps of Group IV materials, it is predicted that GeSn can exhibit direct band behavior by alloying 6-8% Sn. By controlling alloy composition and strain, GeSn demonstrates a high degree of tunability that is promising for the development of reduced threshold lasers.

Strain is one of the key parameters of tunability in the GeSn system. The application of tensile strain can be used to achieve a more direct band gap material to dramatically increase radiative recombination efficiency for improved light emission. We demonstrate an external straining mechanism on suspended Ge_{0.926}Sn_{0.074} multiple quantum well microdisk resonator cavities using recently developed highly compressively-stressed silicon nitride layers. Raman spectroscopy is used to probe the resulting strain distributions between stressed and unstressed microdisk cavities. Photoluminescence results show that the strain-induced by the external stressor layer dramatically enhances GeSn light emission and demonstrates its great potential towards achieving an efficient, compact germanium-based laser on silicon.

9367-48, Session 11

Title to be determined (*Invited Paper*)

Juergen Michel, Technische Univ. Muenchen (Germany)

No Abstract Available

9367-49, Session 11

Photoluminescence quenching effect by Si cap in n+ Ge on Si

Han Pan, Ryohei Takahashi, Koki Takinai, Kazumi Wada, The Univ. of Tokyo (Japan)

Monolithically integrated lasers on Si have long been one of the biggest challenges for electronic-photonic integration on Si CMOS platform. An electrically pumped Ge-on-Si laser has been demonstrated with relatively high threshold current, 280 kA/cm² [1]. The "last one mile" is to reduce threshold current. The present paper reports a possible reason for this high threshold current based on photoluminescence (PL) study of the n+ Si cap effect on n+ Ge. We have compared PL intensity of n+ Ge with and without 5 nm-thick n+ Si cap. With n+ Si cap the PL intensity was only 25% of that of n+ Ge without n+ Si cap. By etching off the cap, PL intensity increased to ~50% of n+ Ge without the cap, but no perfect (100%) recovery of PL intensity was observed. It turned out that it was due to in-depth reduction of PL intensity of the n+ Ge epilayer. This indicates that removing the cap actually showed 100% recovery of PL intensity. The PL reduction with the cap would be most likely due to defects formed at the Si/Ge interface because of 4% lattice mismatch. These defects should pin the Fermi level at the interface to deplete the interlayer (12 nm thick because of our doping level 1E19 /cm³), or act as non-radiative recombination centers.

The depletion layer corresponds to a half of the penetration depth of 457 nm PL laser. We present a Fermi level pinning (FLP) model, suggesting the significance of n+ Si/n+ Ge interface in Ge lasers, which could cause such a high threshold current reported.

[1] R. Camacho-Aguilera et al., Opt. Exp., 20, 11319, (2012).

9367-50, Session 11

Comparison of large photovoltaic power plants with conventional ones and prospects for photovoltaic plants use in Israel

Michael A. Slonim, Ben-Gurion Univ. of the Negev (Israel); Lev Pregerman, Boris Medres, Israeli Independent Academy for Development of Sciences (Israel)

The photo-voltaic (PV) and conventional power (CP) stations of large power are compared in article. The 500 MW units are chosen for comparison. A comparative evaluation between CP and PV stations is carried out in relation to: physical properties (location, physical size, etc.), economic indicators (cost of station, cost of kWh, estimation of payback time, etc.); electrical characteristics (steady state, transient and faulty conditions). It is shown, that for many parameters PV plants exceed those of conventional ones. The cost of kilowatt - hour produced on PV station is lower at least 30% and possibly more than one produced on conventional station. An impact of introducing of large PV stations is discussed. Thus, widespread use in large PV plants will increase power generation options in the country. It creates conditions for healthy competition between conventional and PV stations and price reduction of electricity for private and industrial consumers. Ecological influence of large PV plants is analyzed also.

9367-51, Session 11

GeSn waveguide structures for efficient light detection and emission

You-Long Lin, Yu-Hui Huang, Shao-Wei Chen, Guo-En Chang, National Chung Cheng Univ. (Taiwan)

Si and Ge are the building materials for Si electronics for decades. Recently, they are considered as photonic materials for the development of electron-photonic integrated circuits on a Si platform for next-generation telecommunication and chip-scale optical interconnection. However, the indirectness of energy band leads to inefficient direct optical transitions and limits the performance of SiGe photonic devices. Recently, Sn-another group-IV element, has been employed in the growth of IV-IV compounds. By incorporating Sn into Ge, GeSn alloys can become a true direct bandgap material for developing high-performance Si-based photonic devices. Here we report the fabrication and characterization of GeSn waveguide structures integrated on Si substrates. The Sn incorporation into Ge is realized by low-temperature molecular beam epitaxy to suppressed Sn segregation. The optical properties are characterized by different experiment techniques. For photodetectors, a significant increase in optical response of GeSn waveguide structures in comparison to the pure Ge devices as revealed by the photocurrent experiments. Photoluminescence experiments were carried at room temperature, showing a redshifted emission wavelength for the GeSn waveguides compared to the Ge reference due to the bandgap shrinkage by Sn-alloying. Besides, we observe rippling structures in the photoluminescence spectrum, which are attributed to the waveguide modes. Those results suggest that GeSn waveguide structures are promising for high-performance Si-based photonics integrable with Si electronics.

9367-52, Session 11

Comparison of EL emitted by LEDs on Si substrates containing Ge and Ge/GeSn MQW as active layers

Bernhard Schwartz, Tzanimir Arguirov, Brandenburgische Technische Univ. Cottbus (Germany); Martin Kittler, Brandenburgische Technische Univ. Cottbus (Germany) and IHP GmbH (Germany); Michael Oehme, Erich Kasper, Jörg Schulze, Univ. Stuttgart (Germany)

We analyzed Ge- and Ge/GeSn MQW-LEDs. The structures were grown by MBE on Si. In the Ge LEDs the active layer was 300nm thick. Sb doping was ranging from $1E18$ to $1E20$ cm⁻³. An unintentionally doped Ge-layer served as reference. The LEDs with the MQWs consist of ten alternating Ge/GeSn-layers. The Ge-layers were 10nm thick and the GeSn-layers were grown with 6% Sn and thicknesses between 6 and 12nm. The top structure of all LEDs was identical. Accordingly, the light extraction is comparable.

The EL analysis was performed under forward bias at different currents. Sample temperatures between >300 K and 80 K were studied. For the reference LED the direct transition at 0.8eV dominates. With increasing current the peak is slightly redshifted due to Joule heating. Sb doping of the active Ge-layer affects the intensity and at $3E19$ cm⁻³ the strongest emission appears. It is ~5 times higher as compared to the reference. Moreover a redshift of the peak position is caused by bandgap narrowing.

The LEDs with undoped Ge/GeSn-MQWs as active layer show a very broad luminescence band with a peak around 0.65eV, pointing to dominance of GeSn-layers. The light emission intensity is at least 20 times stronger as compared to the reference Ge-LED. Due to incorporation of Sn in the MQWs the active layer approaches to a direct semiconductor. This view is supported by the temperature behaviour of light emission. In indirect Si and Ge we observed an increase of intensity with increasing T, whereas the intensity of Ge/GeSn-MQWs was much less affected.

9367-53, Session 11

Ultra-low-cost near-infrared photodetectors on silicon

Mohammad Amin Nazirzadeh, Fatih Bilge Atar, Berk Berkan Turgut, Ali K. Okyay, Bilkent Univ. (Turkey)

We demonstrate Silicon-only near-infrared photodetectors (sensitive up to 2000 nm) that meet large-scale ultra-low-cost fabrication requirements. For the detection of infrared photons, we use metal nanoislands that form Schottky contact with Silicon. NIR photons excite plasmon resonances at metal nanoislands and plasmons decay into highly energetic charge carriers (hot electrons). These hot electrons get injected into Silicon (internal photoemission), resulting in photocurrent. Several groups has studied plasmonic nanoantennas using high resolution lithography techniques. In this work, we make use of randomly formed nanoislands for broad-band photoresponse at NIR wavelengths. We observe photoresponse up to 2000 nm wavelength with low dark current density about 50 pA/ μ m². The devices exhibit photoresponsivity values as high as 2 mA/W and 600 μ A/W at 1.3 μ m and 1.55 μ m wavelengths, respectively.

Thin metal layer was deposited on low-doped n-type Silicon wafer. Rapid thermal annealing results in surface reconstruction of the metal layer into nanoislands. Annealing conditions control the average size of the nanoislands and photoresponse of the devices. An Al-doped Zinc Oxide (AZO) layer was deposited on the nanoislands using thermal atomic layer deposition (ALD) technique to acts as a transparent conductive oxide (TCO) and patterned using photolithography. AZO film creates electrical connection between the nanoislands and also makes a heterojunction to Silicon.

Simple and scalable fabrication on Si substrates without the need for any sub-micron lithography or high temperature epitaxy process make these devices good candidates for ultra-low-cost broad-band NIR imaging and spectroscopy applications.

Conference 9368: Optical Interconnects XV

Monday - Wednesday 9-11 February 2015

Part of Proceedings of SPIE Vol. 9368 Optical Interconnects XV

9368-1, Session 1

Multimode/single-mode polymer optical waveguide circuit for high-bandwidth-density on-board interconnects (*Invited Paper*)

Takaaki Ishigure, Keio Univ. (Japan)

For further advancement of high-performance computers (HPCs) and servers, optical interconnects are highly anticipated because of the capability of high bandwidth density wiring with low power consumption. In current HPC systems, multimode fiber (MMF) links are already deployed for inter-rack connections, so that optical wirings for chip-to-chip interconnects are the next technology issue. In particular, optical printed circuit boards (O-PCBs) incorporated with multimode polymer optical waveguides are currently drawing much attention, because multimode polymer optical waveguides are easily processed for mounting on boards and suitable for high-density wiring. In order to realize higher-density wiring, we proposed to introduce graded-index (GI) cores into the polymer optical waveguides on board, and we have experimentally and theoretically demonstrated excellent optical characteristics of the GI-core waveguides, compared to the step-index (SI) core counterparts. For fabricating GI-core waveguides, in this paper, we spotlight a method utilizing a microdispenser: the Mosquito method, which were developed by us. The Mosquito method makes it possible to fabricate waveguides directly on-board. Furthermore, almost perfect circular-shaped cores are successfully formed in this method.

Meanwhile, for higher density channel alignment, small-core waveguides are desirable. Hence, single-mode waveguides are regarded as an ideal component. In this paper, we show the Mosquito method is capable of fabricating single-mode polymer waveguides. We use an organic-inorganic hybrid material for single-mode waveguides. A fabricated 5-cm long waveguide exhibited remarkably low insertion loss (8.39 dB) at 1.55- μ m wavelength, which is 10-dB lower than the loss of a silicone based polymer waveguide at the same wavelength.

9368-2, Session 1

Bandwidth studies on multimode polymer waveguides for high-speed board-level optical interconnects (*Invited Paper*)

Richard V. Penty, Nikos Bamiedakis, Jian Chen, Ian H. White, Univ. of Cambridge (United Kingdom)

Multimode polymer waveguides are being increasingly considered for use in short-reach board-level optical interconnects as they exhibit favourable optical properties and allow direct integration onto standard PCBs using conventional methods from the electronics industry. Various optical demonstrators have been developed in recent years featuring large number of polymer waveguides, interfaced with high-speed VCSELs and PDs through customised connectors. The use of relatively large waveguides (width ~30-70 μ m) offers relaxed alignment tolerances and therefore enables cost-effective system assembly. However, the continuous improvements in high-speed performance of VCSELs raises questions about the suitability of this optical technology due to the highly multimoded nature of the waveguides. In this paper, we present theoretical and experimental bandwidth studies on multimode polymer waveguides and demonstrate that the waveguides can exhibit bandwidth-length products in excess of 40 GHz \cdot m, even under overfilled launch conditions. The bandwidth performance of metre-long multimode polymer waveguides is studied under different launch conditions and in the presence of spatial input offsets. Record error-free (BER<10⁻¹²) 40 Gb/s data transmission over a 1 m long spiral waveguide is reported demonstrating the potential of this technology for use in high-speed board-level optical links.

9368-3, Session 1

Semi-analytic ray tracing method for time-efficient computing of transmission behavior of PCB level optical multipoint interconnects

Oliver Stübbe, Ostwestfalen-Lippe Univ. of Applied Sciences (Germany)

Optical interconnects on printed circuit board level are a promising choice to support high bandwidth for short distance interconnects. These interconnects consists of highly multimode step index waveguides with rectangular core cross-sections. Therefore ray tracing is an excellent method to determine the optical path parameters, e. g. optical power, ray path lengths and directions. Based on these parameters the step response, the transient transfer function and the coupling behavior can be calculated.

Classical ray tracing methods calculates the optical path parameters of each ray by successively computing internal reflections until a termination criterion is reached. Therefore the computing time depends on the number of internal reflections.

If the optical waveguide consists of cascaded straight and curved segments, e. g. point-to-point interconnects, one can use the analytic ray tracing method to determine the optical path parameters. The whole path parameters of each ray are determined by one analytical computation. The computing time depends on the number of segments. The analytic ray tracing method is unusable to determine ray path parameters of segments with varying core cross sections, e.g. tapers, crossings and multipoint interconnects.

In this paper a semi-analytic ray tracing method will be presented. This method combines the analytic ray tracing method with classical ray tracing. With this method it is possible to compute time-efficiently the optical path parameters of each ray within waveguide segments with varying core cross sections. Based on this method the simulation results of different kind of tapers and a complex multipoint waveguide topology will be presented.

9368-5, Session 1

Silicone polymer waveguide bridge for Si to glass optical fibers

Kevin L. Kruse, Nick Riegel, Christopher T. Middlebrook, Michigan Technological Univ. (United States)

Multimode waveguides, increasingly employed as the means to achieving high-speed communication, attain a low bit-error-rate at data rates greater than 10 Gb/s. Using several waveguides in parallel allows the overall capacity to reach transmission speeds upwards of 100 Gb/s. The size of multimode waveguides (50 to 60 μ m) allows for connections and misalignments to be somewhat forgiving in terms of the overall link power budget; however, intrinsic bandwidth limitations exist due to the modal dispersion within the waveguide. Single mode waveguides, which are not as limited by modal dispersion, will be required to further improve transmission speeds. The size of a single mode waveguide is significantly less than their multimode counterparts, allowing for a greater bandwidth capacity per layer. The challenge in using embedded single mode waveguides within printed circuit boards involves the mass production fabrication techniques to create precision dimensional waveguides, the required precision alignment tolerances necessary to launch a mode, and effective coupling between adjoining waveguides and devices. In order to fully implement single mode waveguides coupling and fan out techniques are required for effectively coupling on-chip transceiver devices that utilize common Si waveguide (SiWG) structures to traditional single mode optical fiber (SMF). This can be implemented using Dow Corning's single mode polymer materials at 1310

nm by utilizing a silicone PWG to link a SiWG and traditional SMF. Fabricated and measured prototype devices with modeling and simulation analysis is reported for a 12 member 1-D tapered PWG. Recommendations and designs are generated with performance factors such as numerical aperture alignment tolerances.

9368-6, Session 2

Nanophotonics and VCSEL arrays for optical interconnects (*Invited Paper*)

Werner H. Hofmann, Technische Univ. Berlin (Germany)

Future high-performance computers require optical interconnects to meet their bandwidth demands and keeping their energy consumption at reasonable levels. Densely packed arrays of vertical-cavity surface-emitting lasers (VCSELs) are expected to be the workhorse for this application. Even though, long-wavelength devices are better suited to match the silicon technology with matched Voltage and wavelengths, the GaAs technology has advantages in cost and thermal stability.

Besides of challenges in photonic integration, VCSEL performance and multiplexing schemes are still to be optimized.

Novel nanophotonic structures, so called high-contrast-gratings (HCG) can replace the thick top-mirror of VCSELs saving epitaxial thickness and cost. Additionally, this kind of reflector can ensure single-mode emission of larger aperture devices or define the cavity mode by structuring different patterns, making VCSEL arrays for wavelength-division-multiplexing feasible.

Nanostructures are used for the electro-optic transition in the active medium making lasers depend on the precision of crystal growth down to the sub-nanometer range. Utilizing the HCG technology, also the optical confinement can be realized by nanostructures. The properties of the laser-cavity can be tailored varying the geometric design of a single layer.

The design parameters are accessible by numerical properties only. Additionally, the finite properties of these HCGs have to be accounted for, with easier infinite models giving misleading results.

Being able to handle a precision in fabrication down to 10 nanometers and handling numerical error, HCG technology opens the additional degree of freedom in device design needed to handle the challenge of photonic integration of VCSEL arrays into optical interconnects.

9368-7, Session 2

Low-loss mode converter for coupling light into slotted photonic crystal waveguide

Xingyu Zhang, The Univ. of Texas at Austin (United States); Harish Subbaraman, Amir Hosseini, Omega Optics, Inc. (United States); Ray T. Chen, The Univ. of Texas at Austin (United States)

Silicon slot photonic crystal waveguides (PCWs) infiltrated with electro-optic (EO) active polymers have shown to enable high-performance optical interconnects, EO modulators, and photonic sensors. In these structures, efficient coupling between a strip waveguide and a slot waveguide is challenging due to the large mode mismatch. In this work, we demonstrate a mode converter that achieves highly efficient coupling from a strip waveguide to a slot waveguide with a slot width (S_w) as large as 320nm. The rail width (R_w) of the slot waveguide section is optimized to 225nm, yielding an optimized mode converter length of 30 μ m. The measured insertion loss of the optimized mode converter is below 0.08dB. The optimized R_w of 225nm provides a loss improvement of about 0.8dB, compared to conventional designs that require R_w to be 300nm. In addition, a comparison between our adiabatic mode converter and a conventional V-shape mode converter is presented, and an improvement of 0.1dB in loss is demonstrated for the adiabatic mode converter. Finally, in addition to coupling light between a strip waveguide and a 320nm-wide slot waveguide, our adiabatic mode converter is also utilized to couple light into

and out of a 320nm-wide EO-polymer refilled slot PCW. We experimentally demonstrate that our mode converter provides up to 3.5dB improvement in coupling efficiency compared to the V-shape mode converter in the slow-light wavelength region of the slot PCW. This adiabatic mode converter has some advantages, such as low loss, easy manufacturability and large fabrication tolerance.

9368-8, Session 2

High-optical coupling efficient quasi-vertical tapers for polymer waveguide devices

Zeyu Pan, The Univ. of Texas at Austin (United States); Harish Subbaraman, Omega Optics, Inc. (United States); Xingyu Zhang, The Univ. of Texas at Austin (United States); Qiaochu Li, Cheng Zhang, L. Jay Guo, Univ. Of Michigan (United States); Ray T. Chen, The Univ. of Texas at Austin (United States)

On-chip polymeric waveguide devices usually rely on butt coupling method to couple light between input/output (I/O) fibers, which usually has large mode profile mismatch in vertical direction and limits coupling efficiency. To address this problem, we design a Quasi-Vertical Taper to enable highly efficient coupling from a conventional single mode fiber into a single mode polymer rib waveguide. The waveguide (a 0.5 μ m height and 8.5 μ m width) comprises of a UV15LV bottom cladding, SU8 core layer and UFC-170A top cladding. The taper is adopted below the waveguide to adiabatically transform the fiber mode into the polymer rib waveguide mode, and comprises of a triangular region with a 7.5 μ m height, whose width is linearly tapered from 8.5 μ m at the fiber end to a narrow tip at the waveguide end. This structure works as an optical mode transformer. Because the taper trenches are deeper at the facets than the active regions of waveguide, the waveguide mode size in vertical direction becomes larger at the facets and can better match the I/O fiber mode. The effect of the tip width and taper length on the coupling efficiency is numerically calculated using beam propagation method. For a tip width = 1.0 μ m and taper length = 1200 μ m, 82.67% coupling efficiency is obtained. A coupling efficiency >99% is achieved when the tip width is <0.5 μ m. Our design is compatible with roll-to-roll (R2R) imprinting technique, which enables high throughput and low cost fabrication of polymeric phonic devices on both rigid and flexible platforms.

9368-9, Session 2

High efficiency silicon strip waveguide to plasmonic slot waveguide mode converter

Chin-Ta Chen, National Central Univ. (Taiwan); Xiaochuan Xu, Amir Hosseini, Omega Optics, Inc. (United States); Zeyu Pan, Ray T. Chen, The Univ. of Texas at Austin (United States)

Plasmonic devices enable linear and non-linear processing of light beyond the diffraction limit. However due to the high loss (-dB/10 μ m), plasmonic structures must be made as short as possible. Efficient dielectric-plasmonic waveguide converters that can couple light into subwavelength plasmonic structures make it possible for the plasmonic device to benefit from low-loss conventional dielectric waveguides for photon delivery purposes.

In this paper, we design a high-efficiency silicon strip waveguide to plasmonic slot waveguide mode converter based on a hybrid silicon-gold taper. The converter is based on silicon-on-insulator with 250 nm thick single crystal silicon. The silicon strip waveguide is 450 nm wide. The plasmonic slot waveguide has a slot width of 250 nm. The thickness of gold is 225 nm. The waveguides and mode converter is covered by 500 nm thick SU 8 to reduce the loss.

The mode converter is designed and optimized with the three-dimensional (3-D) finite-difference time-domain (FDTD) simulation. In order to achieve extremely low insertion loss, the mode matching between these two waveguides is investigated. Through a hybrid silicon-gold taper, a coupling efficiency of 92.1% is achieved at 1550 nm. The 1 dB bandwidth of the mode converter is more than 200 nm.

9368-10, Session 3

1060-nm VCSEL-based parallel-optical modules for optical interconnects (*Invited Paper*)

Naoya Nishimura, Kazuya Nagashima, Agyl F. Rizky, Yoshinobu Nekado, Toshinori Uemura, Yozo Ishikawa, Hideyuki Nasu, Furukawa Electric Co., Ltd. (Japan)

The capability of solder mounting of parallel-optical module onto PCB contributes reducing the number of piece parts, simplifying its assembly process, and minimizing a foot print for both AOC and on-board applications. We introduce solder-reflow capable parallel-optical modules employing 1060-nm InGaAs/GaAs VCSEL which leads to the advantages of realizing wider modulation bandwidth, longer transmission distance, and higher reliability. In particular, we designed very thin 4-channel parallel-optical modules which are able to withstand high temperature during Sn-Ag-Cu solder-reflow process. By adopting a miniature glass prism lens and a high temperature-resistant plastic fixture using high-precision molding, the module measures 1.5 mm in height and realizes the required temperature resistance as high as 250 deg.C for Sn-Ag-Cu solder-reflow process. We demonstrate four-channel parallel PRBS 2³¹-1 transmission at 28 Gb/s through a 50-micron-core MMF beyond 500 m. A 1060-nm optical signal has the advantages of lower chromatic dispersion and lower loss in silica fiber. A 1060-nm specialized MMF using the design technology for OM4 fiber realizes a wider modal bandwidth at 1060 nm. We also introduce a proposed technology to realize maintaining good optical coupling and robust electrical connection during solder-reflow process between optical module and polymer-waveguide embedded PCB. Twelve-channel optical modules are mounted to the PCBs where precisely positioned guide holes for the module and stud-pins for the PCB are interdigitated. We performed optical link test of twelve-channel parallel PRBS 2³¹-1 transmission at 14 Gb/s using transmitter and receiver PCBs mounted with the module, and then observed bit error-free for all channels.

9368-11, Session 3

Multi-wavelength transceiver integration on SOI for high-performance computing system applications

Timo Aalto, Mikko Harjanne, Sami Ylinen, Maarkku Kapulainen, Tapani Vehmas, Matteo Cherchi, VTT Technical Research Ctr. of Finland (Finland)

We present a vision for integrating multi-wavelength transceivers on a 3 μm silicon-on-insulator (SOI) waveguide platform for high-performance computing systems where the optical interconnect network is scalable to Pb/s systems by combining spatial and wavelength multiplexing. We also present experimental results from the first building blocks that have been developed in the EU-funded RAPIDO project. The optical interconnects that are being developed in this project operate at around 1.3 μm wavelength with up to 80 Gb/s data rate per wavelength. The overall concept is based on the hybrid integration of III-V optoelectronics on SOI. Revolutionary approaches aim to achieve athermal operation, and good high-temperature operation, as well as optical I/O coupling from SOI waveguides to standard optical fibers and to polymer waveguides with both low loss and ultra-wide bandwidth. Advanced modulation formats, wavelength multiplexing and optical packet switching will be used to increase the data rate and to enable

flexible communication within the system. The initial results include, for example, 4x4 cyclic AWGs with 5 nm channel spacing and 0.4 dB/facet I/O coupling loss to standard SM fibers. Center-to-center loss of the cyclic AWG is 3.5 dB, while adjacent channel crosstalk is less than -23 dB. The AWGs operate at both polarisations and their footprint is approximately 3.5x1.5 mm².

9368-12, Session 3

A CWDM photoreceiver module for 10 Gb/s x 4ch interconnection based on a vertical-illumination-type Ge-on-Si photodetectors and a silica-based AWG

Ki-Seok Jang, Jiho Joo, Taeyong Kim, Sanghoon Kim, Jin Hyuk Oh, In Gyoo Kim, Sun Ae Kim, Gyungock Kim, Electronics and Telecommunications Research Institute (Korea, Republic of)

For the next-generation high-speed data communication and interconnect systems, silicon photonics is regarded as a promising technology, providing cost-effective optical devices based on mature silicon CMOS fabrication technology. In this paper, we report a 40 Gb/s (10 Gb/s x 4 ch) photoreceiver based on vertical-illumination type Ge-on-Si photodetector arrays and a silica-based arrayed waveguide grating (AWG) demultiplexer by employing 4-channel coarse wavelength division multiplexing (CWDM). The 60μm-diameter Ge-on-Si photodetectors, grown on a bulk silicon wafer by RPCVD and fabricated with CMOS-compatible process, have -0.9 A/W responsivity with 3-dB bandwidth of 13 GHz at the wavelength of 1330nm. The 4-channel silica-based AWG demultiplexer has output wavelengths of 1271nm, 1291nm, 1311nm, and 1331nm. Ge-on-Si photodetectors are hybrid-integrated with TIA/LAs and directly-coupled to the AWG. 10.3 Gb/s x 4-channel interconnection of a low-cost FPCB-package based Ge photoreceiver module shows the sensitivity of -11 ~ -12.2 dBm at a BER = 10⁻¹².

9368-13, Session 3

Hybrid-Integrated WDM silicon photonics for inter-chip communications (*Invited Paper*)

Hiren D. Thacker, Oracle (United States)

In this talk, we describe progress on silicon photonic components (modulators, detectors, mux/demux, circuits) being developed at Oracle for building high bandwidth (>10Gbps/channel) and ultralow power (<1pJ/bit) WDM photonic links that will penetrate deep into the system hierarchy. These interchip communication links are based on our hybrid integration platform by which we mate best-in-breed photonic devices with state-of-the-art CMOS VLSI circuits. We detail a 10Gbps, 2.1pJ/bit complete digital CMOS silicon photonic link achieved by these methods and discuss scaling of this technology to achieve Tbps/mm² density and sub-pJ/bit energy-efficiency.

9368-14, Session 4

Towards high-precision manufacturing of 3D optical components using UV-curable hybrid polymers (*Invited Paper*)

Arne Schleunitz, Jan J. Klein, micro resist technology GmbH (Germany); Ruth Houbertz, Multiphoton Optics GmbH (Germany); Marko Vogler, Gabi Gruetzner, micro

resist technology GmbH (Germany)

With exceeding processing speeds in computing systems, fundamental challenges for the way that computing systems are built are created. Reduction of power for data transfer is one of the major topics to be addressed. Optical interconnects are seen on most interconnect levels to be a feasible solution, but limitations to the existing technical solutions still have to be overcome.

Aside of manufacturing equipment for creating optical packages, suitable polymer materials are an essential key for cost-efficient production. They have to satisfy numerous requirements concerning their optical (e.g. optical loss) and processing properties (e.g. temperature stability). Hybrid polymers [1] having already been applied in photonic applications [2], as microlenses or 2D and 3D waveguides [3, 4] are promising candidates to manufacture optical systems down to the chip level. The materials can be specifically tailored to the fabrication method to be used (e.g. UV lithography and UV molding [5]). In recent years, hybrid polymers were particularly adapted towards two-photon absorption (TPA) lithography, which is used as an innovative production method for directly manufacture individual 3D photonic structures impossible with 2D techniques. The evaluation of hybrid polymer materials developed by micro resist technology GmbH with support from Fraunhofer ISC for high-precision 3D lithography will be presented. Complex 3D photonic structures can be manufactured by means of this technique. Teaming up as material and equipment supplier, we will highlight the current launch of a collaboration targeting a closed technological ecosystem.

The work was partly supported by the German Priority Program (SPP 1327, grant HO 2475/3).

[1] ORMOCER®s for micro-optics licensed by the Fraunhofergesellschaft zur Förderung der Angewandten Forschung in Deutschland e.V.

[2] C. Sanchez, B. Julian, P. Belleville, and M. Popall, J. Mater. Chem. 15 (2005), 3559-3592.

[3] U. Streppel, P. Dannberg, Ch. Wächter, A. Bräuer, P. Nicole, L. Fröhlich, R. Houbertz, M. Popall, Proc. SPIE 4453, 61 (2001).

[4] R. Houbertz, V. Satzinger, V. Schmid, W. Leeb, G. Langer, Proc. SPIE 7053, 70530B (2008).

[5] G. Gruetzner, J. J. Klein, M. Vogler, A. Schleunitz, Proc. SPIE 8974, 897406 (2014).

9368-15, Session 4

Building blocks for actively-aligned micro-optical systems in rapid prototyping and small series production

Gunnar Böttger, Fraunhofer-Institut für Zuverlässigkeit und Mikrointegration (Germany); Marco Queisser, Norbert Arndt-Staufenbiel, Technische Univ. Berlin (Germany); Henning Schröder, Fraunhofer-Institut für Zuverlässigkeit und Mikrointegration (Germany); Klaus-Dieter Lang, Technische Univ. Berlin (Germany)

In recent years there has been considerable progress in utilizing fully automated machines for the assembly of micro-optical systems. Such systems integrate laser sources, optical elements and detectors into tight packages, and efficiently couple light to free space beams, waveguides in optical backplanes, or optical fibers for longer reach transmission. The required electrical-optical and optical components are placed and aligned actively in more than one respect. For one, all active components are actually operated in the alignment process, and, more importantly, the placing of all components is controlled actively by camera systems and power detectors for an optimal coupling efficiency.

The total number of optical components typically is in the range of 5 to 50, whereas the number of actors with gripping tools for the actual handling and aligning is limited, with little flexibility in the gripping width. The assembly process therefore is strictly sequential and, given that an

automated tool changing has not been established in this class of machines, yet, there are either limitations in the geometries of components that may be used, or time-consuming interaction by human operators is needed.

As a solution we propose and present lasered glass building blocks with standardized gripping geometries that enclose optical elements of various shapes and functionalities. These are cut as free form geometries with green short pulse and CO₂ lasers. What seems to add cost at first rather increases freedom of design and an economical flexibility to create very hybrid assemblies of various micro-optical assemblies also in small numbers.

9368-16, Session 4

Manufacturability and optical functionality of multimode optical interconnections developed with fast processable and reliable polymer waveguide silicones

Joe Liu, Allen Lee, Mike Hu, Lisa Chan, Sean Huang, Foxconn Electronics, Inc. (Taiwan); Brandon W. Swatowski, W. Ken Weidner, Joseph Han, Dow Corning Corp. (United States)

We report on the manufacturing, durability, and optical functionality of multimode optical waveguide devices developed with a fast processable optical grade silicone. The materials show proven optical losses of <0.05 dB/cm @ 850 nm, surviving >2000 hours 85°C/85% relative humidity testing as well as >4 cycles of wave solder reflow. Fabrication speeds of <10 minutes are shown for a full waveguide stack. Step index 50x50 mm waveguides were fabricated and passively MT connectorized on rigid FR4 and flexible polyimide substrates with precise alignment features (cut by dicing saw or drilled by UV laser). Two out-of-plane coupling techniques were demonstrated in this paper, a MT connectorized sample with a 45° turning lens as well as 45° dielectric mirrors on waveguides by dicing saw. Multiple connections between fiber and polymer waveguides with MPO and two out-of-plane coupling techniques in a complete optical link are demonstrated @ 10 Gbps data rates with commercial transceiver modules. Also, complex waveguide geometries such as bends, crossings and splitters are demonstrated by QSFP+ transceiver. The eye diagram analyses show comparable results in functionality between silicone waveguide and fiber formats.

9368-17, Session 4

Optical coupling structure made by imprinting between single-mode polymer waveguide and embedded VCSEL

Mikko Karppinen, Noora Salminen, Tia Korhonen, Teemu Alajoki, VTT Technical Research Ctr. of Finland (Finland); Erwin Bosman, Geert Van Steenberge, IMEC (Belgium); John Justice, Umar Khan, Brian Corbett, Tyndall National Institute (Ireland); Arjen Boersma, TNO (Netherlands)

Low-loss single-mode polymer waveguides are attractive for inter-chip optical interconnection applications. For example, they can be applied in communicating between micro-photonic integrated circuit chips, such as silicon PICs, or in enhanced integration and coupling of photonic devices to fibers for longer reach data links, such as, coupling high density VCSEL arrays to fiber ribbons.

In such a hybrid integration scheme, a key challenge is to achieve efficient optical coupling between the chips and waveguides. With the single-mode polymer waveguides, the alignment tolerances become especially critical as compared to the typical accuracies of the patterning processes. We study novel techniques for such coupling requirements.

In this paper, we present an embedded mirror structure, which is aligned

with very high precision. It enables 90 degree bending of light to couple between a single-mode waveguide and an embedded vertical-emitting/detecting photonic chip, such as, VCSEL or photodiode, or a VCSEL/PD array. Both the mirror and the polymer waveguide structures are fabricated in a process based on direct pattern nanoimprinting of low-loss UV-curable polymeric materials. This makes it promising for cost-efficient volume production. The mirror is imprinted onto a groove formed e.g. by laser ablation. The demonstrated waveguides were optimised for operation at around 1300..1600 nm wavelengths and had cross-sectional core dimensions of ca 5 μm and mode field diameter of ca 7 μm . This implies the alignment and patterning accuracy requirements are on the order of 1 μm or less.

Fabrication results of the coupling structure with waveguides are presented, and the critical alignment tolerances and manufacturability issues are discussed.

9368-18, Session 4

Optical printed circuit board with vertical waveguide structure for high-speed data link and high-efficient optical coupling

Sung Hwan Hwang, Woo-Jin Lee, Jong-Bae An, Nam-Won Moon, Gye Won Kim, Myoung Jin Kim, Eun Joo Jung, Korea Photonics Technology Institute (Korea, Republic of); Ki Young Jung, NewFlex Technology Co., Ltd. (Korea, Republic of); Ik-Bu Sohn, Gwangju Institute of Science and Technology (Korea, Republic of); Byung Sup Rho, Korea Photonics Technology Institute (Korea, Republic of)

This paper suggests an optical printed circuit board with a vertical waveguide structure (OPCB-VWS) for high speed data link and high efficient optical coupling. The OPCB-VWS consists of a polyimide sheet as a dielectric layer, an optical waveguide sheet with 45 degree mirrors, and a vertical waveguide. In this structure, the polyimide (PI) should have two main features of a low dielectric loss material for high speed transmission line and a high transparency material for the vertical waveguide. We searched a special PI with 2.8 dielectric constant, 0.003 dissipation factor, and 90% transparency. And the OPCB was fabricated using the PI. And then, we have used a femto-second laser system to fabricate the vertical waveguide with a thermal-damage-free and precise ring structure. Optical coupling efficiencies under various OPCB structure including the OPCB-VWS were simulated and the coupling losses were measured. As the results, the coupling loss of the OPCB-VWS was measured as an improved result of 7.8dB than that of the general OPCB. The electrical 3-dB bandwidth of the OPCB-VWS was also measured as above 40GHz in 2cm transmission line. In conclusion, the suggested OPCB-VWS is very applicable for both high speed data link and high efficient optical coupling.

9368-19, Session 5

VCSEL scaling for very low bit energy (Invited Paper)

Dennis Deppe, CREOL, The College of Optics and Photonics, Univ. of Central Florida (United States); Guowei Zhao, sdPhotonics, LLC (United States); Xu Yang, Mingxin Li, Yu Zhang, Sabine Freisem, CREOL, The College of Optics and Photonics, Univ. of Central Florida (United States)

VCSELs are the leading laser device to dominate optical interconnects for data centers and high performance computers, as well as future consumer photonics. Scaling the VCSEL to small size can be shown to increase its intrinsic speed and reduce electrical parasitics. Embedding the VCSELs in silicon electronics and silicon photonics could produce highly

parallel interconnects with 100's of channels. In this talk we will describe lithographic VCSELs that can reach power conversion efficiency of 50% even for small diameters, and reach the single mode regime. Device data will be presented on drive levels, threshold, and efficiency as the VCSEL is scaled. Schemes to integrate the VCSELs will be described along with important requirements in the optical, electrical, and thermal interfaces.

9368-20, Session 5

Broadband energy-efficient optical modulation by hybrid integration of silicon nanophotonics and organic electro-optic polymer

Xingyu Zhang, The Univ. of Texas at Austin (United States); Amir Hosseini, Harish Subbaraman, Omega Optics, Inc. (United States); Jingdong Luo, Alex K. Y. Jen, Univ. of Washington (United States); Robert L. Nelson, Air Force Research Lab. (United States); Ray T. Chen, The Univ. of Texas at Austin (United States)

Silicon slot photonic crystal waveguides (PCWs) infiltrated with electro-optic (EO) polymers combine the slow-light effect in the PCWs with the high polarizability of the EO polymers. The large EO coefficient (r_{33}), ultrafast response time, very low dispersion, and spin-coating feature of organic polymers promise "GREEN" photonic devices with low-power consumption, broadband operation, and clean manufacturing. Silicon photonics offers the potential of CMOS-compatible ultra-scale photonic integrated circuits. Silicon slotted PCWs infiltrated with EO polymers further reduce the device size and enhance the performance by combining the best of these two worlds. In this work, we report a broadband, low-energy, low-dispersion and compact optical modulator based on silicon slot PCW infiltrated with EO polymer. The voltage-length product of the modulator is measured to be $V\pi^2L=0.282\text{V}^2\text{mm}$, corresponding to a record-high effective in-device r_{33} of 1230pm/V. Silicon slot PCW is selectively doped to reduce RC time delay and then to achieve high-speed modulation. Assisted by a backside gate voltage, the 3-dB bandwidth of the modulator is demonstrated to be 15GHz, and a modulation response up to 50GHz is observed. An energy consumption of as low as 94.4fJ/bit at 10Gbit/s is demonstrated. Benefiting from the band-engineered PCW, the modulator is demonstrated to have a low-dispersion optical bandwidth as wide as 8nm, which is much better than other modulators based on non-band-engineered PCWs or ring resonators. This wide operational spectrum range can be potentially used for wavelength-division-multiplexing (WDM). Our silicon-organic hybrid integrated nanophotonic modulator has potential applications in next-generation optical communication components and high-performance optical interconnects.

9368-21, Session 5

Hybrid titanium dioxide strip-line/ electro-optic polymer waveguide optical modulators

Shiyoshi Yokoyama, Feng Qiu, Andrew M. Spring, Kyushu Univ. (Japan)

Recently, EO polymer has been explored to the silicon-organic-hybrid (SOH) waveguide for the low driving voltage and large bandwidth applications. In such modulators, all passive components are fabricated on silicon on insulator wafer to form a strip-line waveguide, micro-ring resonator, slot waveguide, and photonics crystal structure. Though the SOH waveguide modulator is expected in the range of silicon photonics applications, the poling efficiency is required to improve much higher EO activity and the total optical loss much smaller. In this study, we show the hybrid EO polymer modulators by using the titanium dioxide strip-line. After tuning

the refractive index contrast and the dimension of electrodes, the modulator is fabricated to show the low driving voltage and the small propagation loss. We used the EO polymer with a r_{33} value of 150 pm/V at 1330 nm, which is synthesized in our previous work. After showing some optical properties of the EO polymer waveguide, a few volts of the half-wavelength voltage and 50 GHz bandwidth, the detail fabrication for the hybrid EO polymer modulator will be discussed. We prepare 0.3 μm -thick and 0.3 μm -width strip-lines, and subsequently spin-coat the EO polymer as the cladding layer. The electrodes are designed around the waveguide to obtain the highest poling efficiency and minimum the propagation loss. The waveguide predicts a possible driving voltage of -1V in a push-pull Mach-Zhender modulator. The ring resonator is also shown and its properties will be present. All the optical measurements are examined at 1550 nm.

9368-22, Session 5

Comb laser and ring modulator resonator based optical interconnects (*Invited Paper*)

Jeremy Witzens, Juliana Müller, Johannes Hauck, Saeed Sharif Azadeh, Alvaro Mártir, Bin Shen, Sebastian Romero-García, Florian Merget, RWTH Aachen (Germany)

Single section passively mode-locked comb lasers have the potential to be compact and effective light sources for Silicon Photonics based WDM transceivers. High relative intensity noise typically seen in isolated, single lines of Fabry-Perot lasers is suppressed via the mode-locking mechanism, resulting in the joint generation of multiple optical carriers suitable for high-speed optical data transmission. We will discuss recent results obtained with several architectures and optical encoding schemes based on resonant optical modulators and add-drop multiplexers.

9368-23, Session 6

Equilibrium modal power distribution measurement of step-index hard plastic cladding and graded-index silica multimode fibers

Ruichen Tao, Univ. College London (United Kingdom); Takehiro Hayashi, HAT Lab Inc. (Japan); Manabu Kagami, Toyota Central R&D Labs., Inc. (Japan); Shigeru Kobayashi, TE Connectivity Ltd. (Japan); Manabu Yasukawa, Synergy Optosystems Co., Ltd. (Japan); Hui Yang, David Robinson, Arden Photonics Ltd. (United Kingdom); Hadi Baghsiahi, F. Aníbal Fernández, David R. Selviah, Univ. College London (United Kingdom)

A stable reproducible optical standard source for measuring multimode optical fiber attenuation is required as recent round robin measurements of such fibers at several international companies and national standards organizations showed significant variation when using a source having only the encircled flux in the near field emerging from it defined. The paper presents and compares the far field and near field modal power distributions for (i) 2 km and 3 km step-index multimode Hard Plastic Cladding Fibers, HPCF, (SI-MMF) with 200 μm silica core diameter, 0.37 numerical aperture (NA) and polymer cladding, (ii) a 10 m silica graded-index multimode fiber (GI-MMF) with 50 μm core diameter and 0.2 NA, and (ii) a near field Encircled Flux Mode Converter or "Modcon". A free space method for measuring the far field using a Light-emitting diode (LED) centered at 850 nm wavelength with 40 nm bandwidth and a charge-coupled device (CCD) camera is compared with an r-theta multi-element lens based far field pattern (FFP) system. Mandrels of different diameter and different numbers of turns of the fiber around them were used to achieve an equilibrium mode distribution (EMD) for the GI-MMF. The paper defines encircled angular flux (EAF) as the fraction of the total optical power radiating from a multimode

optical fiber core within a certain solid angle in the far field. The paper calculates the EAF both when the solid angle decreases from the far field edge and when it increases from the far field centroid. The mathematical expression of the EAF of the far field is found and the paper investigates the relationship between the far field and the near field in wide wavelength bandwidth systems.

9368-24, Session 6

Analytical (mathematical) predictive modeling in fiber optics structural analysis (FOSA): review and extension

Ephraim Suhir, ERS Co. (United States)

The review part of the paper addresses analytical (mathematical) modeling in structural analysis in fiber optics engineering, mostly fiber optics interconnects, and deals with optical fibers subjected to thermal and/or mechanical loading (stresses) in bending, tension, compression, or to the combinations of such loadings. Attributes and significance of predictive modeling are indicated and discussed. The addressed structures include, but are not limited to, optical fibers of finite length: bare fibers; jacketed and dual-coated fibers; fibers experiencing thermal loading; fibers soldered into ferrules or adhesively bonded into capillaries; as well as the roles of geometric and material non-linearity; dynamic response to shocks and vibrations; and possible applications of nano-materials in new generations of coating and cladding systems.

The extension part is concerned with a novel, fruitful and challenging direction in optical engineering- probabilistic design for reliability (PDFR) of opto-electronic and photonic systems, including optical fibers and interconnects. The rationale behind the PDFR concept is that there is no such thing as zero probability of failure, that the difference between a highly reliably optical system and an insufficiently reliable one is "merely" in the level of the never zero probability of failure and that when the operational reliability of the product is imperative, the ability to predict, quantify, assure and, if possible and appropriate, even specify its reliability is highly desirable. Accordingly, the objective of the PDFR effort is to quantify, on the probabilistic basis, the likelihood of operational failures of opto-electronic materials, devices and systems, including the field of fiber optics.

9368-25, Session 6

Theoretical and empirical qualification of a mechanical-optical interface for parallel optics links

Dirk Schoellner, Steven Chuang, Alan Ugolini, Jillcha Wakjira, Griffin Wolf, US Conec Ltd. (United States); Prashant Gandhi, Amphenol TCS (United States); Alex Persaud, Amphenol High Speed Products (United States)

As the implementation of parallel optics continues to evolve, development of a universal coupling interface between VCSEL/PD arrays and the corresponding photonic turn connectors is necessary.

A newly developed monolithic mechanical-optical interface efficiently couples optical transmit/receive arrays to the accompanying fiber optic connector. This paper describes the optical model behind the coupling interface and validates the model using empirical measurements. Optical modeling will address how the interface is adaptable to the broad range of VCSEL/PD launch parameters from commercially available VCSEL hardware manufacturers; the optical model will illustrate coupling efficiencies versus launch specifications. Theoretical modeling will examine system sensitivity through Monte Carlo simulations and provide alignment tolerance requirements.

Empirical results will be presented to validate the optical model predictions and subsequent system performance. Functionality will be demonstrated through optical loss and coupling efficiency measurements. System metrics

will include characterizations such as bit-error-rate testing, eye diagram results, and link loss measurements.

9368-26, Session 6

Polymeric demultiplexer component for wavelength division multiplex communication systems using polymer fibers

Ulrich H. Fischer-Hirchert, Matthias Haupt, Sebastian Höll, Mladen Joncic, Hochschule Harz (Germany)

Data communication over Polymer Optical Fibers (POF) is limited to only one channel for data transmission. Therefore the bandwidth is strongly restricted. By using more than one channel, it is possible to break through the limit. This technique is called Wavelength Division Multiplexing. It uses different wavelengths in the visible spectrum to transmit data parallel over one fiber. A demultiplexer (DEMUX) as a key component separates the light at the end of the fiber into the different fiber output ports. To separate the channels at the output ports, one interesting option for high multimode transmission systems is to use an optical grating placed on an aspheric mirror, which focuses the monochromatic parts of light into the outgoing fibers. In order to keep the advantage of cost-effective POFs it is necessary to mass-produce the component at reasonable prices by injection molding. A demonstrator is fabricated by directly machining it in the PMMA material by means of diamond turning technique. Thus, the same diamond-turning technology is used for the manufacture of the mold insert. This step is done due to validate the simulation results with the produced component. Several measurements are required to validate the demonstrator for example to locate the exact position of the focus points of the separated wavelength. The paper discusses the results of the different simulation and development steps, the measurements done with the first demonstrator and the challenges related to the injection molding process accompanied by the first BER measurements using a 4 channel WDM transmission.

9368-27, Session 6

Planar concave grating with flattened spectral response for wavelength demultiplexing optical interconnection

Guomin Jiang, Sarfaraz Baig, Hui Lu, Kai Shen, Michael R. Wang, Univ. of Miami (United States)

The demand of high aggregate bandwidth for optical communication and interconnection promotes the rapid development of the waveguide wavelength division multiplexing (WDM) system. Many different waveguide WDM techniques have been proposed, including planar concave grating (PCG), arrayed waveguide grating (AWG), ring resonator, Mach-Zehnder interferometers, and superprism-based photonic crystal. PCG and AWG have been widely researched and made great progress due to their compactness, low cost, large fabrication tolerance and high performance. We consider PCG because of its significant size advantage over AWG. A conventional design of PCG offers a Gaussian-like spectral response with small shift tolerance on spectral channels, which seriously restricts its practical application in dense or coarse WDM system. Various techniques have proposed to flatten the spectral response of the PCG. The most common method is to use a mode shaper such as multimode interference section to form a double-peak filed distribution in the input plane. In this paper, we present a compact 12-channel PCG with a flattened spectral response by using new mode-shaped Y-taper couplers as input apertures of the PCG for spectrally separated channels. The filed distribution in the input plane can be controlled by adjusting the width and length of the Y-taper mode shaper. The effects of Y-taper parameters on the performance of PCG are demonstrated in detail through simulation results. The coupling loss between mode shaper of input and slab mode of PCG is also taken

into account in our device simulation. The ratio of the 1dB bandwidth to the 10dB bandwidth is highly improved compared to a conventional PCG. The performance of the PCG is verified in experiment using UV cured polymer waveguide structures.

9368-28, Session 7

Electrical interconnect scaling and the transition to optical

Bryan K. Casper, Intel Corp. (United States)

The perception of short-distance electrical communication not keeping up with the virtually unlimited bandwidth of optical fiber has prompted predictions of the demise for electrical in computer systems. However, over the last two decades, aggregate electrical bandwidths for high-volume microprocessor-based systems have scaled by more than 3 orders of magnitude. However in spite of past scaling to 30Gb/s and beyond, even optimized electrical channels based on micro-coax, refined high-density connectors and modern packaging are starting to show signs of bandwidth limits. I will discuss the primary circuit and off-chip interconnect related limitations of electrical as well as power, performance and cost tradeoffs of forward looking systems now on the research roadmap. I will cover in detail recent work in electrical interconnect for both channels and circuit and show how the bar is continually being raised to limit optical adoption for short distances. Based on the tradeoffs presented, I will outline possible transition scenarios to optical interconnect and also provide an overview of current crossover points between optical and electrical in terms of distance.

9368-29, Session 7

Towards energy-efficient photonic interconnects

Yigit Demir, Nikos Hardavellas, Northwestern Univ. (United States)

Silicon photonics have emerged as a promising solution to meet the growing demand for high-bandwidth, low-latency, and energy-efficient on-chip and off-chip communication in many-core processors. However, current silicon-photonic interconnect designs for many-core processors waste a significant amount of power because (a) lasers are always on, even during periods of interconnect inactivity, and (b) microring resonators employ heaters which consume a significant amount of power just to overcome thermal variations and maintain communication on the photonic links, especially in a 3D-stacked design. The problem of high laser power consumption is particularly important as lasers typically have very low energy efficiency, and photonic interconnects often remain underutilized both in scientific computing (compute-intensive execution phases underutilize the interconnect), and in server computing (servers in Google-scale datacenters have a typical utilization of less than 30%). We address the high laser power consumption by proposing a laser control scheme that saves energy by predicting the interconnect activity and opportunistically turning the on-chip laser off when possible, and also by scaling the width of the communication link based on a runtime prediction of the expected message length. Our laser control scheme can save up to 62 - 92% of the laser energy, and improve the energy efficiency of a many-core processor with negligible performance penalty. We address the high trimming (heating) power consumption of the microrings by proposing insulation methods that reduce the impact of localized heating induced by highly-active components on the 3D-stacked logic die.

9368-30, Session 7

Electro-optical backplane demonstrator with integrated multimode gradient-index thin glass waveguide panel

Henning Schröder, Lars Brusberg, Fraunhofer-Institut für Zuverlässigkeit und Mikrointegration (Germany); Richard Pitwon, Seagate Technology LLC (United Kingdom); Simon Whalley, ILFA Feinstleiteteknik GmbH (Germany); Kai Wang, Allen Miller, Seagate Technology LLC (United Kingdom); Christian Herbst, Technische Univ. Berlin (Germany); Daniel Weber, Fraunhofer-Institut für Zuverlässigkeit und Mikrointegration (Germany); Klaus-Dieter Lang, Technische Univ. Berlin (Germany)

Optical interconnects for data transmission at board level offer increased energy efficiency, system density, and bandwidth scalability compared to purely copper driven systems. So far embedded optical architectures do not exist in such data center and network systems but the clear goal is to replace the electrical signal lines by optical interconnects for high-speed data transmission to overcome the bandwidth by length limitation of copper signal lines. We present recent results on manufacturing of electro-optical printed circuit board (PCB) with integrated planar glass waveguides. The graded index multi-mode waveguides are patterned inside commercially available thin-glass panels by performing an ion-exchange process. The glass waveguide panel is embedded within the layer stack-up of a PCB using proven industrial processes. As a result of the successful technology development the paper will describe the design, manufacture, assembly and characterization of the first electro-optical backplane demonstrator based on integrated planar glass waveguides. The electro-optical backplane in question is created by laminating the glass waveguide panel into a conventional multi-layer electronic printed circuit board stack-up. High precision ferrule mounts are automatically assembled, which will enable MT compliant connectors to be plugged accurately to the embedded waveguide interfaces on the glass panel edges. The demonstration platform comprises a standardized sub-rack chassis and five pluggable test cards each housing optical engines and pluggable optical connectors. The test cards support a variety of different data interfaces and can support data rates of up to 10 Gb/s per channel.

9368-31, Session 7

8 Gb/s single-wavelength bi-directional PAM-16 SI-POF link using blue uLEDs and avalanche photodiodes

Xin Li, Nikos Bamiedakis, Jinlong Wei, Univ. of Cambridge (United Kingdom); Jonathan D. McKendry, Enyuan Xie, Ricardo Ferreira, Erdan Gu, Martin D. Dawson, Univ. of Strathclyde (United Kingdom); Richard V. Penty, Ian H. White, Univ. of Cambridge (United Kingdom)

The use of step-index plastic optical fibre (SI-POF) in short-reach communication links such as in-home and automotive networks has drawn considerable interest owing to their advantage of low cost, ease of installation and compatibility with low-cost light-emitting-diodes (LEDs). However, the high-speed performance of such links is limited by the low bandwidth of POF and conventional LED devices. As a result, research work in recent years has been focused on improving the achievable data rates in such links using advanced modulation formats or multiplexing techniques. In this work, we demonstrate record error-free (BER<1E-10) 8 Gb/s bi-directional data transmission over a single SI-POF employing blue micro-pixelated light-emitting-diodes (uLEDs) and avalanche photodiodes (APDs). uLEDs exhibit larger modulation bandwidths than conventional broad-area LEDs and 20 µm diameter 450 nm GaN uLEDs with a -175 MHz bandwidth are used in this work. Meanwhile, APDs offer improved sensitivity

over conventional PIN photodiodes and thus, enhanced overall link power budget. The use of advanced modulation formats, and in particular 16-level pulse amplitude modulation (PAM-16), enables data transmission at high rates beyond the typical limit of conventional on-off-keying (OOK) systems. Such a configuration enables simultaneous 4 Gb/s signal transmissions in each direction and a record aggregate data rate of 8 Gb/s over a single SI-POF channel. The bit error rate (BER) performance of each directional link is evaluated and 8 Gb/s data transmission is achieved over 10 m of SI-POF with a BER<1E-10. The crosstalk for each directional link is measured to be less than 0.5 dB.

9368-32, Session 7

International standardisation of optical circuit board measurement and fabrication procedures

Richard C. Pitwon, Seagate Technology LLC (United Kingdom); Marika Immonen, TTM Technologies, Inc. (Finland); Jinhua Wu, TTM Technologies, Inc. (China); Kai Wang, Seagate Technology LLC (United Kingdom); Long Xiu Zhu, Hui Juan Yan, TTM Technologies, Inc. (China); Alex Worrall, Seagate Technology PLC (United Kingdom)

Widespread adoption of optical circuit boards will herald substantial performance, environmental and cost benefits for the data communications industry.

Though optical circuit board technology has advanced considerably over the past decade, commercial maturity will be gated by the availability of conformity standards to forge future quality assurance procedures.

One important prerequisite to this is a reliable test and measurement definition system, which is agnostic to the type of waveguide system under test and therefore can be applied to different optical circuit board technologies as well as being adaptable to future variants. A serious and common problem with the measurement of optical waveguide systems has been lack of proper definition of the measurement conditions for a given test regime, and consequently strong inconsistencies ensue in the results of measurements by different parties on the same test sample.

We report on the development of a new measurement identification standard to force testers to capture sufficient information about the measurement conditions for a given optical circuit board such as to ensure consistency of measurement results within an acceptable margin.

Furthermore we demonstrate how the application of the proposed measurement identification system can bring about a dramatic improvement in results consistency, by comparative evaluation of the results on multimode polymer waveguide based optical circuit test boards from a large selection of testing organisations.

9368-33, Session 8

Optimization of beam expansion characteristics in a silicon planar guided-wave structure

Siamak Abaslou, Robert Gatdula, Wei Jiang, Rutgers, The State Univ. of New Jersey (United States)

Efficient coupling of light with high bandwidth between high contrast planar waveguides with different width in compact integrated optical circuits is a challenging issue. A long enough taper is needed to achieve adiabatic transmission of light and the parabolic shape of taper leads to the highest coupling efficiency. This length requirement leads to fairly large structures which is not suitable for high-density photonic integration. In contrast, in short tapers due to fast changing the effective index back reflection and diffraction loss can happen; also light may couple to higher order modes in the wider waveguide, which cause low transmission and distortion of

beam front. In this work we employ 3D finite difference time domain (FDTD) method to simulate a multi-stage taper with less than 7 μm length. The beam expander connects two planar Silicon-on-insulator (SOI) waveguides with 1:18 ratio. We use genetic optimization algorithm on the segmented beam expander to find the optimal values of the width of each segment and the shape of the device to achieve high coupling efficiency and high beam waist.

The structures are patterned by electron beam lithography on a standard SOI wafer with a 2 μm buried oxide layer and a 260 nm top silicon layer. To characterize the efficiency of the beam expander we use subwavelength grating coupler and tunable laser source in communication wavelength.

9368-34, Session 8

Design, fabrication, and characterisation of nano-imprinted single-mode waveguide structures for intra-chip optical communications

John Justice, Umar Khan, Tyndall National Institute (Ireland); Tia Korhonen, VTT Technical Research Ctr. of Finland (Finland); Arjen Boersma, Sjoukje Wieggersma, TNO (Netherlands); Mikko Karppinen, VTT Technical Research Ctr. of Finland (Finland); Brian Corbett, Tyndall National Institute (Ireland)

In the Information and Communications Technology sector, the demands on bandwidth continually grow due to increased microprocessor performance and the need to access ever increasing amounts of stored data. The introduction of optical data transmission (e.g. glass fibre) to replace electronic transmission (e.g. copper wire) has alleviated the bandwidth issues for communications over distances greater than 100 metres, however, the need has arisen for optical data transfer over shorter distances as found inside computers. A low-cost solution for the optical transport is single mode polymer based optical waveguides fabricated using Nanoimprint Lithography (NIL). NIL has emerged as a scalable manufacturing technology capable of producing features down to the hundred nanometer scale with the potential for large scale (roll-to-roll) manufacturing.

In this paper, we present results on the modelling, fabrication and characterisation of single mode waveguides and optical components in low-loss ORMOCER materials. Single mode waveguides with a mode field diameter of 7 μm and passive structures such as bends, directional couplers and multi-mode interferometers (MMIs) suitable for use in 1550nm optical interconnects were fabricated using wafer scale processes. Process issues arising from the nano-imprint technique such as the residual layer and angled sidewalls are modelled and investigated for excess loss and higher order mode excitation. Conclusions are drawn on the applicability of nano-imprinting to the fabrication of circuits for intra-chip/board-level optical interconnect.

9368-35, Session 9

Silicon photonic devices based on SOI/ bulk-silicon platforms for chip-level optical interconnects (Invited Paper)

Gyungock Kim, In Gyoo Kim, Sanghoon Kim, Jiho Joo, Ki-Seok Jang, Sun Ae Kim, Jin Hyuk Oh, Jeong-Woo Park, Myung-Joon Kwack, Jaegyung Park, Hyundai Park, Gun Sik Park, Sanggi Kim, Electronics and Telecommunications Research Institute (Korea, Republic of)

Silicon photonics technology, providing CMOS-compatible platform for optical interconnects, is regarded as a future technology for computing and communication systems. When photonic devices are successfully

monolithic-integrated into major silicon chips in computing systems as chip-level optical I/O, it can bring innovative changes including computer architecture. Intensive work has been done in this area in recent years, and has made remarkable progress. However, further improvement is desired for the realization of practical chip-level optical I/O applications. In this paper, based on either a silicon-on-insulator (SOI) wafer or a bulk-silicon wafer, we discuss silicon photonic devices and integrations for chip-level optical interconnects. First, we overview over our work of the low-voltage silicon photonic integrated circuits (Si-PICs) on a SOI wafer, where Si modulators and Ge-on-Si photodetectors were monolithically integrated for intra-chip or inter-chip optical interconnects up to 40 Gb/s. As a potential candidate for future chip-level integration, the small-sized depletion-type Mach-Zehnder modulator based on the vertically-dipped PN-depletion-junction (VDJ) scheme is also presented, where the device with 100 μm -long depletion phase-shifter shows operations up to 50 Gb/s with a high-modulation efficiency. We report vertical-illumination-type Ge photodetectors on bulk-silicon wafers which demonstrate high performances comparable to the conventional III-V counterparts, and ready for practical applications up to 50 Gb/s. We present the bulk-silicon platform with the photonic TRx structure for the practical implementation of chip-level optical interconnects, and the performance of the photonic transceiver silicon chip.

9368-36, Session 9

Symmetric cavity modes in parallel-coupled waveguides with tapered distributed Bragg reflectors

Robert Gtdula, Siamak Abaslou, Wei Jiang, Rutgers, The State Univ. of New Jersey (United States)

As the development of silicon photonics progresses, there is a stronger need for devices in practical applications. Wavelength filtering, wavelength division multiplexing, and nonlinear signal processing can be achieved via Fabry-Perot nano-cavities integrated on a silicon-on-insulator platform. We implement these types of optical cavities by utilizing a tapered distributed Bragg reflector design made up of a 1-dimensional array of holes in a silicon waveguide. Placing two of these waveguides in close proximity induces a bimodal response of the device with even or odd transverse symmetry. In this work, we specifically observe the even-mode response and its shift due to the spacing of the two waveguides.

The structures are patterned by electron beam lithography on a standard silicon-on-insulator wafer with a 2 μm buried oxide layer and a 260 nm top silicon layer. Physical dimensions of the structures are characterized with scanning electron microscopy. We couple light into the devices through the use of grating couplers. Optical testing results will show the resonant wavelength and quality factor dependence on the waveguide spacing. In addition, we will characterize the fabrication tolerances of these characteristics.

9368-37, Session PWed

Development and qualification of a mechanical-optical interface for parallel optics links

Dirk Schoellner, Steven Chuang, Alan Ugolini, Jillcha Wakjira, Griffin Wolf, US Conec Ltd. (United States)

The application of parallel optics in data communications continues to expand. As the implementation of optical arrays grows, there remains a need for an effective coupling interface between the board-level active components and the passive components of the network. Miniature, multi-fiber photonic turn connectors are available, but efficient, repeatable, and cost-effective coupling is not available outside of proprietary solutions. Development of a universal mechanical-optical coupling interface opens the door for broader parallel optics implementation.

In this paper, a universal interface for use between the optical transmitter and the photonic turn connector is introduced. The interface is a monolithic injection molded component with an array of collimating lenses and customizable stand-offs to couple efficiently with various VCSEL/PD designs. Design considerations include clearances for numerous chip drivers and wire-bond footprints, as well as for heat-sinking of the active optical components. The component has precise adhesive features for controlled epoxy bond-line thickness and strength. Several methods for pick-and-place alignment and bonding to circuit board substrates will be addressed, including suitable thermal and UV-curable epoxies.

Performance evaluation will address the environmental and mechanical functionality of the component after alignment and adhesion to the circuit substrate. Testing procedures are in-line with industry-standard environmental and mechanical requirements. Tensile force testing and durability results will validate the mechanical characteristics of the interface. Thermal performance and stability results will be reviewed.

9368-38, Session PWed

Multiple-input multiple-output based high-density on-chip optical interconnect

Po-Kuan Shen, National Central Univ. (Taiwan); Xiaochuan Xu, Amir Hosseini, Omega Optics, Inc. (United States); Zeyu Pan, Ray T. T. Chen, The Univ. of Texas at Austin (United States)

In on-chip optical interconnect, dielectric waveguide arrays are usually designed with pitches of a few wavelengths to avoid crosstalk, which greatly limits the integration density. In this paper, we for the first time propose to use multiple-input multiple-output (MIMO), a well-known technique in wireless communication, to recover the data from entangled signals and reduce the waveguide pitch to subwavelength range.

In the proposed on-chip MIMO system, there is significant coupling among the adjacent waveguides in the high density waveguide region. In order to recover signals, the $N \times N$ transmission matrix of N high-density waveguides is calculated to describe the relation between each input ports and output ports. In the receiving part, homodyne coherent receivers are used to receive the transmitted signals, and obtain the signal in phase and $\pi/2$ out of phase with local oscillator. In the electrical signal processing, the inverse transmission matrix is utilized to recover the signals in the electronic domain.

To verify the proposed on-chip MIMO, we used the INTERCONNECT package in Lumerical software to simulate a 10×10 MIMO system. The cross section of each waveguide is $500 \text{ nm} \times 220 \text{ nm}$. The spacing is 250 nm . The simulation verifies the possibility of recovering 10 Gbps data from the heavily coupled 10 waveguides with a BER better than 10^{-12} . The receiver sensitivity at a fixed BER of 10^{-12} is smaller than -15 dBm .

Conference 9369: Photonic Instrumentation Engineering II

Wednesday - Thursday 11-12 February 2015

Part of Proceedings of SPIE Vol. 9369 Photonic Instrumentation Engineering II

9369-1, Session 1

Terahertz octave-spanning semiconductor laser for comb applications *(Invited Paper)*

Giacomo Scalari, Markus Roesch, Mattias Beck, Jérôme Faist, ETH Zürich (Switzerland)

We present a THz semiconductor injection laser operating in continuous wave with an emission covering more than one octave in frequency, and displaying homogeneous power distribution among the lasing modes. The gain medium is based on a heterogeneous quantum cascade structure. Laser emission in continuous wave takes place from 1.64 THz to 3.35 THz with optical powers in the mW range and more than 80 modes above threshold. Free-running beatnote investigations on narrow waveguides yield linewidths of 980 Hz limited by jitter indicating frequency comb operation on a spectral bandwidth as wide as 624 GHz. Such devices are ideal candidates for octave-spanning semiconductor-laser-based THz frequency combs.

9369-2, Session 1

The spatially-heterodyned spectrometer: an ideal tool for Raman work?

Christopher N. Pannell, Bill G. Zhang, Gooch & Housego, Orlando (United States); Murray K. Reed, Gooch & Housego (Torquay) Ltd. (United Kingdom)

Dispersive spectrometers are ubiquitous in portable Raman equipment. However, when viewing diffuse /extended sources such as those produced by the Raman pump laser it is well known that the spectrometer slit presents an unavoidable trade-off between throughput and spectral resolution. Several image-slicing schemes have been devised to mitigate this problem, essentially trading divergences in the dispersive and non-dispersive directions, but our approach has been to investigate high-throughput spectrometers based on interferometry. The advantage of high throughput in this class of instruments when viewing extended sources has been known from the early days of scanning FTIR spectroscopy, and these advantages carry over into the more recently investigated class of static Fourier transform spectrometers in which a linear CCD array is used in place of a time-varying path length. Several of these "static Fourier transform spectrometers" have been described in the literature, but the Spatially Heterodyned Spectrometer (SHS), first used for analyzing spectra of extended astronomical sources, is unique among them as it possesses extra degrees of design freedom that we believe are particularly useful for Raman work. We have performed careful characterization of the sensitivity and the spectral resolution of an SHS in head-to-head studies with several dispersive instruments, and we describe the results obtained. Sensitivities at the pW level and spectral resolution of 3.4 wavenumbers in the range 790-930nm were obtained viewing a sub-resolution spectral feature using an un-cooled 1k x 1k CCD array. We also present results obtained with a Raman probe coupled using a 3mm diameter light guide.

9369-3, Session 1

A compact LIBS system for industrial applications

Bertrand Noharet, Acreo Swedish ICT AB (Sweden); Tania Irebo, Jonas Gurell, Rein Vainik, Swerea KIMAB (Sweden); Håkan Karlsson, Elizabeth K. Ily, Cobolt AB (Sweden)

In recent years, laser-induced breakdown spectroscopy (LIBS) has been established as a promising analytical tool for on-line chemical analysis. Two major strengths of the technique are the possibilities to perform both fast and remote chemical analysis to determine the elemental composition of the samples under test. Traditional LIBS set-ups are based on the use of flash-pumped Q-switched lasers that deliver pulses with hundreds of mJ energies at relatively low pulse rates, typically 20 to 30Hz. In order to reduce the size of LIBS systems, the use of a compact Q-switched diode-pumped solid-state laser (DPSSL) in a LIBS system is evaluated for the industrial sorting of aluminium alloys. The DPSSL, which delivers 150µJ pulses of high beam quality at more than 7KHz repetition rate, provides irradiance on the target that is appropriate for LIBS measurements. Results from the aluminium alloy classification will be presented, and improvements in the design of LIBS systems will be discussed.

9369-5, Session 1

Hartmannometer vs Fizeau interferometer: advantages and drawbacks

Alexander N. Nikitin, Alexis V. Kudryashov, Julia Sheldakova, Active Optics Night N Ltd. (Russian Federation); Dmitrii Denisov, Valerii Karasik, Alexey Sakharov, Bauman Moscow State Technical Univ. (Russian Federation)

A device based on Shack-Hartmann wavefront sensor is considered in this paper for assessing quality of the optical elements. We compare the main features of this device (Hartmannometer) with characteristics of the traditional Fizeau interferometer. The main advantages of Hartmannometer like insensitivity to vibrations, large dynamic range of measuring optical aberrations, no need of radiation source with a large coherence length and drawbacks of this device such as limited spatial resolution are considered in this paper for the tasks of testing of optical elements.

9369-6, Session 2

A high-performance passband-agile hyperspectral imager using a large aperture acousto-optic tuneable filter

Christopher N. Pannell, Gooch & Housego, Orlando (United Kingdom); Jon D. Ward, Gooch & Housego plc (United Kingdom); Elliot S. Wachman, ChromoDynamics Inc. (United States); Bill G. Zhang, Gooch & Housego, Orlando (United States); Murray K. Reed, Gooch & Housego (Torquay) Ltd. (United Kingdom)

We have constructed a hyperspectral imager for use in bright field microscopy, this device employs a large aperture acousto-optic tuneable filter having several novel features that have greatly improved image quality, tuning range and rejection of out-of-band light. The acousto-optic tuneable filter (AOTF) is an optical component that generates a moving volume diffraction grating in (e.g.) a TeO₂ crystal. The grating is generated by a periodic electronic signal applied to a piezoelectric transducer bonded to the crystal via a specially designed broadband electrical matching network. By varying the acoustic drive frequency a specific wavelength of light can be diffracted. Up to 16 "random access" optical passbands of arbitrary amplitudes can be simultaneously created with our custom-made driver module, or these can be spaced closely together create a single composite passband with greater FWHM and optical throughput. The theoretical

**Conference 9369:
Photonic Instrumentation Engineering II**

minimum time for switching wavelengths is ~200 microseconds in our AOTF, although (avoidable) computer overheads add to this. Our instrument uses a Zemax-optimized telecentric-confocal optical system to eliminate various aberrations specific to AOTFs and we present MTF, point-spread and registration data showing good image quality. Our optical arrangement has several novel features and we use wire-grid polarizers, these features allow shortening of the optical train and reduced stray light. This instrument allows the spectral unmixing of a combination of cellular morphology staining and multiple biomarker staining on a single microscope slide. A hyper-spectral imaging bright field microscope using these advances has been characterized for pathology and some results will be presented.

9369-7, Session 2

Planarized fiber-FHD optical composite

Christopher Holmes, Lewis G. Carpenter, James C. Gates, Corin B. E. Gawith, Peter G. R. Smith, Univ. of Southampton (United Kingdom)

Traditionally the precision placement and adhesion of optical fiber to an optical planar substrate has been made through use of solder, glass frit, glues or epoxies. These generally have disadvantages that include mechanical weakness in harsh environments (e.g. high temperature, high pressure and exposure to common solvents) and poor optical characteristics (e.g. high optical loss, high scattering and modal/refractive index mismatch with optical fiber). In this work we shall present an approach that overcomes these disadvantages, through embedding and consolidating a fiber directly upon a planar substrate layer using Flame Hydrolysis Deposition (FHD). The result is a planarized composite that is mechanically robust in harsh environments and is of planar optical quality. The deposited silica layers can be tailored in thickness, refractive index and anisotropic stress, with the ability for multiple layers to be deposited sequentially to achieve planar guiding. The technique is compatible with a lithography toolset allowing full planar integration techniques; physical micromachining capability allowing fiber evanescent field access and Bragg grating writing. The components that can be developed using this technique include precision layer-up fiber (e.g. high density fiber packing, precision fiber lengths and delay lines), hybrid fiber-planar devices (e.g. MOEMS, evanescent field sensors and environmentally stabilized narrow line lasers) and optical pump schemes (e.g. fiber pumping, pump strippers and mode strippers). We shall report the latest developments in fabrication, capability and components.

9369-8, Session 2

Surface plasmon polariton generation using acousto-optic effect in fiber

Hao Li, Ying Zhang, Singapore Institute of Manufacturing Technology (Singapore); Wei Tao Yang, Nanyang Technological Univ. (Singapore)

Surface Plasmon Polariton (SPP) effect on all-fiber acousto-optic tunable filter is studied. A novel acousto-optic SPP generation and control scheme on standard single mode fiber with silver coating was proposed and demonstrated. Assisted by the SPP effect, acoustic wave induced core mode to cladding TE mode coupling was suppressed while core mode to cladding TM mode was enhanced with a resonant wavelength red shift. Proposed motion-free, SPP generation and control scheme has potential to be used as active surface sensor, high speed opto-plasmonic controller or polarization selective component for integrated optical-circuit & processor.

9369-9, Session 2

Interferometric characterization of few-mode fibers for mode-division multiplexing

Olena Muliar, Mario A. Usuga Castaneda, Jesper Lægsgaard, Karsten Rottwitt, DTU Fotonik (Denmark)

The rapid growth of global data traffic demands the continuous search for new technologies and systems that could increase transmission capacity in optical links and recent experiments show that to do so, it is advantageous to explore new degrees of freedom such as polarization, wavelength or optical modes.

Mode division multiplexing (MDM) appears in this context as a promising and viable solution for such capacity increase, since it utilizes multiple spatial modes of an optical fiber as individual communication channels for data transmission. In order to evaluate its performance, a MDM system requires advanced characterization methods with regard to the modal content of its photonics components and in particular of the fibers involved for data transmission.

In this contribution we present a time-domain interferometric technique for a full modal characterization of few mode fibers (FMF), commonly used in a MDM scenario. This experimental technique requires the use of a Mach-Zehnder interferometer, where the reference's path length is controlled by an optical delay line. The interference between the output beams of reference and fiber under test (FUT) is recorded on a CCD camera and a careful evaluation of the resulting interferograms allows us to have full access to key parameters such as number of modes, modal weight, differential time delay between propagating modes and intensity profiles.

In this work, we apply this simple and complete characterization method to the case of a short link with two optical modes propagating in a FMF, which illustrates its potential as a diagnostic tool for MDM systems.

9369-10, Session 2

Quantum tunneling photoacoustic spectroscopy for the characterization of thin films

Benjamin S. Goldschmidt, Univ. of Missouri-Columbia (United States); Anna M. Rudy, Swarnasri Mandal, Charissa A. Nowak, Univ. of Missouri, Columbia (United States); John A. Viator, Duquesne Univ. (United States); Heather K. Hunt, Univ. of Missouri-Columbia (United States)

Thin films continue to show great promise for improving a wide variety of devices in applications such as medical instrumentation, material processing, and astronomical instrumentation. While ellipsometry and reflectometry are standard characterization techniques for determining thickness and refractive index, these techniques tend to require highly reflective or polished films and rely on empirical equations like the Cauchy, Briot, Hartmann, Conrady, and Sellmeier empirical dispersion equations. While these empirical equations may be accurate in some wavelength ranges and for non-conductive materials, the researcher must identify which equation is appropriate for the film being tested and wavelength range desired. We have created Quantum Tunneling Photoacoustic Spectroscopy (QTPAS) that uses light induced ultrasound to measure the amount of optical tunneling that has occurred with frustrated total internal reflection through a thin film. The QTPAS system allows a researcher to obtain thickness and refractive index estimates of transparent films without polishing or knowledge of empirical equations prior to the experiment. Scans of three thicknesses of MgF2 films were used to compare ellipsometry with the QTPAS technique. An example of our results shows mean refractive index and thickness estimates of 1.38262 and 194.209 nm versus 1.3975 and 187.775 nm at 532 nm for ellipsometry that suggests a general agreement between the two techniques. We present QTPAS to be used for the determination of

**Conference 9369:
 Photonic Instrumentation Engineering II**

properties of single layer films in cases where empirical equations cannot be used or in cases of low optical reflection.

9369-11, Session 3

Plasmonic-enhanced sensors: figures of merit and practical limitations (*Keynote Presentation*)

Jacob B. Khurgin, Johns Hopkins Univ. (United States)

Fluorescence, resonance and off-resonance Raman spectroscopy are all precise and versatile techniques for identifying small quantities of chemical and biological substances. One way to improve the sensitivity of these techniques is to use enhancement of optical fields in the vicinity of metal nanoparticles. The degree of enhancement, however, is drastically different as Raman enhancement of 10 orders of magnitude or more has been consistently measured in experiment, while the enhancement of the fluorescence is typically far more modest. We shall present an analytical model that reveals the physics behind the strikingly different orders of magnitude in enhancement, provide a fundamental explanation for the quenching effect observed in fluorescence and resonance Raman but not in normal Raman, establish limits for attainable enhancement, and outline the path to optimization of all three processes.

9369-12, Session 3

Realization of high-sensitivity surface plasmon resonance (SPR) sensor applying 2[omega] harmonic lock-in detection

Chang-In Park, Kwang-Jin Kim, Chang-Gun Kim, Nam-Pyo Hong, Young-Wan Choi, Chung-Ang Univ. (Korea, Republic of)

Surface plasmon resonance (SPR) sensor has been studied for high sensitivity optical biosensor as a single molecule detection, virus detection, DNA sequencing, etc. SPR sensor requires an ultra-small signal detection system that measures very small intensity variation of reflected light along with the change of a refractive index near the sensor surface. In this reason, lock-in detection method which is able to detect small signal buried in noise has been applied to SPR sensor. In general lock-in detection method using multiplier and low pass filter measures DC value of output, and its sensitivity is determined by 1/f noise at DC. Unlike the DC measurement we have proposed 2nd harmonic lock-in detection method using multiplier and band pass filter. Sensitivity of the proposed lock-in detection method is much lower than 1/f noise at DC. In this paper we will show SPR sensor system using 2nd harmonic lock-in detection method providing the sensitivity enhanced of about 10 dB.

9369-15, Session 3

A fuel level sensor for aeronautical applications

Romeo Bernini, Luigi Petrazzuoli, Gianluca Persichetti, Immacolata A. Grimaldi, Genni Testa, Giovanni Onorato, Istituto per il Rilevamento Elettromagnetico dell'Ambiente (Italy)

A novel fuel level sensor for aeronautical applications is developed. The sensor is based on an array of total internal reflection (TIR) point sensors. Respect to conventional TIR sensors the new design permits to be sensitive to common jet fuels (JetA, JP4, JP7) but also to operate with new alternative fuels. The sensor doesn't require aircraft calibration, temperature compensation and furthermore is able to operate correctly when partially

or totally exposed to presence of condensed water on its surface. The point sensors are multiplexed on a single fiber by optical couplers and interrogated simultaneously by Optical Time Domain Reflectometry (OTDR) at a wavelength of 1550nm. Experimental results show a resolution of ±1.5mm could be achieved. The sensors is also able to measure the free water level in the fuel.

9369-13, Session 4

High spatial resolution distributed optical fiber magnetic field sensor based on magnetostriction by optical frequency-domain reflectometry

Yang Du, Tiegeng Liu, Zhenyang Ding, Bowen Feng, Kun Liu, Junfeng Jiang, Tianjin Univ. (China)

The distributed optical fiber magnetic field sensors have a capability of spatially resolving the magnetic field along the entire sensing fiber that is distinguishes from other sensing methods. We present a distributed optical fiber magnetic field sensor based on magnetostriction using Rayleigh backscattering spectra shift in OFDR (optical frequency-domain reflectometry). As the spectral shift of Rayleigh backscattering can be used to achieve a distributed strain measurements with high sensitivity and high spatial resolution using OFDR. In the proposed sensor, the magnetostrictive Fe-Co-V alloy thin films as sensing materials are attached to a 51 m standard single mode fiber (SMF). We detect the strain coupled to SMF caused by variation of magnetic field by measuring Rayleigh Backscattering spectra shift in OFDR. In our experimental, we measure the range of the magnet field is from 12.9 mT-143.3 mT using proposed method and obtain the linear relationship between Rayleigh backscattering spectra shift and magnet field with R-squared 0.9991. The minimal measurable magnet field variation is 12.9 mT when the spatial resolution is 4 cm. The minimal measurable magnet field variation can be improved to 5.3 mT by increasing the spatial resolution to 14 cm. If we use the magnetostrictive materials with more sensitive to magnet field, the higher sensitivity in this sensor can be obtained. The proposed method has the potential to be a distributed optical fiber magnetic field sensor with high sensitivity and high spatial resolution.

9369-14, Session 4

Detection of carbon monoxide based on an asymmetric microfiber with a Rhodium complex overlay

Min-Seok Yoon, Young-Geun Han, Hanyang Univ. (Korea, Republic of)

Carbon monoxide is an airborne contaminant that is produced from incomplete combustion of fossil fuels. The affinity of carbon monoxide for hemoglobin is about 240 times that of oxygen and carbon monoxide becomes toxic when it is inhaled by humans. Since, furthermore, carbon monoxide is colorless, tasteless, odorless and non-irritating, undetected exposure can be fatal. Most existing optical sensing techniques for carbon monoxide are based on absorption spectroscopy. However, the sensing accuracy of the Carbon monoxide sensor based on absorption spectroscopy is degraded caused by the overlap of the absorption spectra between Carbon monoxide and other airborne contaminant, such as, CO₂, N₂ and H₂O. To overcome this drawback, it is required to investigate a sensing technique for Carbon monoxide with a high selectivity.

In this paper, we investigate a selective carbon monoxide sensor based on an asymmetrical microfiber with the Rhodium complex overlay. The carbon monoxide is readily bound with the Rhodium complex resulting in the enhancement of refractive index of the Rhodium complex overlay of the asymmetrical microfiber. Consequently, the increase of the refractive index of the Rhodium complex overlay leads to the reduction of birefringence of the asymmetrical microfiber. The sensitivity of the proposed sensing probe

to variations in the concentration of carbon monoxide was measured to be ~ 8 pm/ppm.

9369-16, Session 4

Surface plasmon resonance based fiber optic ammonia gas sensor using Ag/ZnO thin films

Banshi D. Gupta, Sruthi P. Usha, Satyendra K. Mishra, Indian Institute of Technology Delhi (India)

Ammonia is a colorless gas with a stifling smell. Even though it has got different applications ranging from fertilizers, fermentation, pharmaceuticals, and preservatives to explosives, it is hazardous as well as corrosive. It is considered as toxic and dangerous to the environment. Ammonia is highly stable, but very reactive. It interacts with the moisture in eyes, skin, respiratory tract etc to form very noxious ammonium hydroxide which causes necrosis. Poisoning may occur if we breathe ammonia. Hence sensing of ammonia is important.

The collective oscillation of electrons at the metal-dielectric interface is known as surface plasmon resonance (SPR). Since the wave is at the boundary of the metal and dielectric, these oscillations are sensitive to any changes in the dielectric medium and hence has been used for the sensing of changes in the dielectric medium using Kretschmann configuration. Here, we report the fabrication and characterization of a SPR based fiber optic ammonia gas sensor. To prepare the sensing probe, we unclad around 1cm of the multimode optical fiber and coated with a 40 nm thick film of silver using thermal evaporation technique, followed by a 12 nm thick film of zinc oxide (ZnO). The probe is fixed in a gas chamber and light from a polychromatic source is launched in the fiber. The transmitted SPR spectrum for a given concentration of the ammonia gas around the probe is recorded. The ammonia gas changes the refractive index of the ZnO film. Increase in the concentration of gas increases the resonance wavelength.

9369-17, Session 4

Localized surface-plasmon-resonance-based fiber-optic chlorine gas sensor using zinc-oxide nanoparticles

Sruthi P. Usha, Satyendra K. Mishra, Banshi D. Gupta, Indian Institute of Technology Delhi (India)

Chlorine is a highly reactive poisonous gas with a choking smell. It is a potent irritant that damages eyes, lungs and throat and can even cause asphyxiation when exposed to high concentration. Its application ranges from daily use such as sterilizing water to consumer product manufacturing and organic chemistry, which makes its sensing important.

The phenomenon of surface plasmon resonance has gained much attraction in the recent decades due its demanding applications in sensing of different chemicals, gases and biological components that affects human life as well as the ecosystem. The use of localized surface plasmon resonance for sensing has gained momentum in the last few years. Confinement of surface plasmons in nanoparticles such that free electron of the particle participates in collective oscillation is known as localized surface plasmon resonance, hence makes it useful for nano-sensing applications.

We report the synthesis of zinc oxide (ZnO) nanoparticles and characterization of a fiber optic chlorine gas sensor utilizing the former. The ZnO nanoparticle seeds were prepared by Pancholski method. The sensor probe was prepared by coating the unclad core of the multimode optical fiber with the ZnO nanoparticles. The probe was checked for chlorine gas sensing using a polychromatic source and a spectrometer. Absorption spectra were recorded for different concentrations of the chlorine gas around the probe. A red shift in the peak absorption wavelength with the increase in the concentration of the chlorine gas has been observed. A shift of 19 nm has been observed for 0-100 ppm gas concentration.

9369-18, Session 4

Detection of melamine using a molecular-imprinted surface-plasmon-resonance-based optical fiber sensor

Anand M. Shrivastav, Satyendra K. Mishra, Banshi D. Gupta, Indian Institute of Technology Delhi (India)

Melamine is a non-protein nitrogen added in food stuffs to improve its protein content although it is harmful to living organism. Its excess exposure can cause cancer and damage reproductive system, eye, skin and respiratory system. However, it is widely used in plastics, dishes and adhesives as well. Due to its harmful nature its detection is very important. In this study we report the fabrication and characterization of a surface plasmon resonance (SPR) based molecular imprinted optical fiber sensor for detection of melamine. The probe is prepared by coating an unclad core of a multimode optical fiber with a thin film of silver followed by the coating of the molecular imprinted thin film. Molecular imprinting is a method used for the selective identification of templates. It creates binding sites or nano-cavities in polymer having shapes of templates and recognizes the template molecules by key and lock model. The target molecules, melamine, interact with these active sites and due to this interaction the change in the refractive index of the film occurs. The change in refractive index of the molecular imprinting film is detected using SPR technique. In SPR technique light from a polychromatic source is launched into the fiber and the transmitted SPR spectrum and hence the resonance wavelength is recorded for a fluid sample around the probe. The change in the melamine concentration in fluid shifts the resonance wavelength. For melamine concentration range 10⁻⁷ to 10⁻¹ M, we observed a shift of 20 nm in the resonance wavelength.

9369-28, Session PWed

Optical accelerometer design based on laser self-mixing interference

Ying Yang, Tianjin Univ. of Science and Technology (China); Xingfei Li, Ke Kou, Tianjin Univ. (China)

A novel optical accelerometer based on laser self-mixing effect is presented and experimentally demonstrated. The design consists of a mass-loaded elastic-beam assembly and laser self-mixing interferometer reading out the displacement of the proof mass while the sensor experience acceleration. Proof mass is a quartz pendulous reed suspended by two flexible beams. The laser self-mixing interferometer is composed of a vertical cavity surface emitting laser, a gold mirror attached to the quartz pendulous reed that scatters the laser beam with some of the emission re-entering the laser cavity. Under external acceleration, an inertial force is applied to the proof mass, flexible beams deflect from their equilibrium position. According to the calculation, the displacement of proof mass is proportional to the acceleration applied to the sensor. Acceleration is then detected by measuring the displacement. According to laser self-mixing effect, the displacement can be read out by the laser self-mixing interferometer. In order to reduce the impact of higher harmonic produced by the slope mutation of modulation current and diminish the disturbing of high-frequency noise effectively, wavelet analysis is introduced to remove singular points, which reduce the displacement error of self-mixing interferometer to 2.45nm. The performance of a prototype of the accelerometer is examined. Preliminary results indicate that the resolution is 0.19²g/Hz^{1/2} within a bandwidth of 100Hz. The optical accelerometer has the potential to achieve high-precision, compact accelerometers. Combined with micro-manufacturing, the proposed scheme can be used to design MOEMS accelerometer with high resolution.

9369-29, Session PWed

Miniaturized fiber inline Fabry-Perot interferometer based on fiber optic ferrule for refractive index measurement

Eun Joo Jung, Woo-Jin Lee, Myoung Jin Kim, Sung Hwan Hwang, Byung Sup Rho, Korea Photonics Technology Institute (Korea, Republic of)

A miniaturized fiber inline Fabry-Perot interferometer based on fiber optic ferrule for refractive index measurement fabricated using a one-step U-sawing technique was proposed and demonstrated. The sensor head consists of a short FP cavity near the fiber patch cord tip which was assembled by joining a ceramic ferrule and a single mode fiber together. The experimental result shows that the attenuation peak wavelength of sensor is shifted toward a shorter wavelength with refractive index increasing, and the refractive index sensitivity is about 92.5 nm/RIU and 73.75 dB/RIU. The proposed device would be used in realizing a robust and compact sensor for many potential applications. Moreover, the easy fabrication method provides the possibility of mass production of the in-fiber refractometer.

9369-30, Session PWed

Thickness measurement of thin film using wavelength-tuning interferometer

Yangjin Kim, The Univ. of Tokyo (Japan); Kenichi Hibino, National Institute of Advanced Industrial Science and Technology (Japan); Naohiko Sugita, Mamoru Mitsuishi, The Univ. of Tokyo (Japan)

Thin films are widely used in the optics, semiconductor and materials industries to provide the specific functions to the coated devices. Effective measurement of the surface shape of the film and the thickness are important to achieve a special function of, and better performance for, a coated device. Conventional measurement methods of thin film thickness, such as spectroscopy and ellipsometry, generally adopt a single point measuring method resulting in large measurement time for thickness measurement. To overcome this problem, we adopted wavelength tuning Fizeau interferometer which has an expansion capability to large diameter. In this research, the surface shape and absolute optical thickness distribution of thin film was measured by wavelength tuning Fizeau interferometry. The interference signal intensity at the thin film interference system was calculated and the phase difference appearing when measuring the thin film was also formulated. Using simulation and experimental results, we proposed new method determining the absolute optical thickness of the thin film.

9369-31, Session PWed

A new real-time polarimetric method for determining the distribution of stressed state in different constructions

George Kakauridze, Barbara N. Kilosanidze, Institute of Cybernetics (Georgia); Teimuraz Kvernadze, Georgi Kurkhuli, E. Kharadze Abastumani Astrophysical Observatory (Georgia)

A new real-time nondestructive polarimetric method is suggested for the determination of the stressed state distribution in different objects. Light reflected from the object is polarized in a varying degree, and the distribution of the polarization state in the object image is related to the distribution of stresses in it. Method is based on the obtaining the distribution pattern of the polarization state of light in the object image, which is formed by an objective. The integral polarization-holographic

diffraction element developed by us is used for real time complete analysis of the polarization state of light at each point of the image, formed by the element in the diffraction orders. The simultaneous measurement of the intensities in four diffracted beams by means of a matrix of photodetectors and the appropriate software enable the polarization state of an analyzable light and its change to be obtained in real time. The laboratory model is presented. The correlation relations between the polarization state of light reflected from the sample with the distribution of the dosated mechanical stresses is considered. The theoretical model is presented. The experimental results are shown for different samples with one- and two-axis stress distribution. The method is nondestructive, i.e. there is no need to drill holes or openings or sticking transparent photoelastic plates on the object to determine the stresses. This method will enable the distance monitoring and diagnosis of already existing constructions to be carried out. This method will differ by universality, simplicity, high speed and comparative cheapness.

9369-32, Session PWed

Optimizing experimental conditions for stimulated emission depletion microscopy in biophotonics

Karl Beeson, Mary J. Potasek, Evgueni Parilov, Simphotek Inc. (United States)

A type of optical microscopy called stimulated emission depletion (STED) microscopy has been developed. In STED microscopy, fluorescence emission from single organic molecules or nanoparticle is generated by the diffraction-limited focused spot of a pump laser pulse. A second STED laser pulse that is donut-shaped and red-shifted is directed at the focus of the first pulse after a short delay. The second STED beam de-excites and depletes the fluorescence emission from the outer regions of the first pulse and allows emission only in the center of the donut where the STED pulse has zero or low intensity. The resulting fluorescence emission that occurs only at the center of the focal spot of the exciting light pulse results in an effective resolution for fluorescence emission that can be much smaller than the diffraction-limited spot size of the exciting pulse. The highest resolution is done using pulsed laser sources. Using a novel numerical method we show how to optimize the resolution enhancement of STED by simulating the entire process including the absorption, overlapping multiple beams and stimulated emission. We find that for a fixed Donut pulse energy, a longer Donut pulse length can result in greater resolution enhancement than a shorter Donut pulse length.

These results show how it is possible to use our simulations to design the best experimental conditions for STED resolution enhancement and illustrate the importance of having a software program that includes both multiple beams and stimulated emission.

9369-33, Session PWed

Triple-illumination phase imaging

Behnam Tayebi, Yonsei Univ. (Korea, Republic of); Farnaz Sharif, Yonsei Univ. (Korea, Republic of)

We present a multiple-illumination phase interferometer as a technique to reduce phase uncertainty. The proposed technique has a simple setup that ?unwraps large stepped phases and use an intermediate angle to apply hierarchal optical phase ?unwrapping technique. A grating is used to illuminate a sample with ?different illumination directions. The selecting beams and a reference beam are combined to form an interference pattern. Different ?angles make different spatial frequencies and selecting appropriate signals in the Fourier ?spectrum makes single shot imaging possible. Multiple-illumination phase interferometer simultaneously records three phases ?with different incident angles. By employing hierarchal optical phase unwrapping method it ?can increase accuracy more than ten times of the reconstructed image accuracy by the dual-?illumination phase unwrapping technique.?

9369-34, Session PWed

Apparatus for analyzing the spectral characteristics of reflection, albedo, and color parameters of flat objects

Elena V. Gorbunova, Aleksandr N. Chertov, Vladimir S. Peretyagin, Elena Lastovskaia, Valery V. Korotaev, National Research Univ. of Information Technologies, Mechanics and Optics (Russian Federation)

Quality control of different coatings (colorful, paint, marker, safety, etc.) that are applied to the surface of various objects (both metallic and non-metallic) is an important problem. Also, there is a problem of dealing with counterfeit products. So it's necessary to distinguish the fake replicas of marking from the authentic marking of producer. To solve these problems, we propose an automated device (hardware and software complex) for analysis and control of spectral reflection characteristics, albedo and color parameters of extended (up to 150 mm ? 150 mm) flat objects. It allows constructing the color image of the object surface as well as its multispectral images in selected regions of the spectrum. Herewith the color of the object surface can be calculated for various standard light sources (A, B, C, D65, E, F2, F7, F11, GE), or to any light source with a predetermined emission spectrum. The paper presents the description of construction and working principles of the proposed hardware and software complex. All color settings calculations correspond to the requirements and recommendations of CIE.

9369-35, Session PWed

The possibilities analysis of the optical non-invasive diagnostics method for the blood sugar control

Elena A. Lastovskaia, Elena V. Gorbunova, Aleksandr N. Chertov, Valery V. Korotaev, National Research Univ. of Information Technologies, Mechanics and Optics (Russian Federation)

The relevance of noninvasive method for determining the blood sugar is caused by necessity of regular monitoring of glucose levels in diabetic patients blood. Traditional invasive method is painful, because it requires a finger stick. Despite the active studies in the field of non-invasive medical diagnostics, to date the painless and inexpensive instrument for blood sugar control for personal use doesn't exist.

It's possible to measure the concentration of glucose in the blood with help of spectrophotometry method. It consists in registering and analyzing the spectral characteristics of the radiation which missed, reflected or absorbed by the object.

The authors proposed a measuring scheme for studying the spectral characteristics of the radiation, missed by ear lobe. Visible and near infrared spectral ranges are considered. Special retaining clip and an optical system for efficient use of the radiation source are also were developed.

The measurement main purpose was to find spectral regions which are informative for determining the level of glucose in the blood. Also pure glucose solutions of various concentrations were studied.

Next, the prototype for studying the spectral characteristics of the radiation transmitted through the phalanx was designed. In this case emitting diodes are used as radiation sources. They're selected on the basis of the results obtained on the first stage.

The prototype intended for reveal the dependence between the concentration of glucose in the blood and the intensity of the transmitted radiation. Its detailed description and principle of operation are presented. Proposed method can also be used to monitor other blood components such as cholesterol, hemoglobin, bilirubin, insulin, toxins.

9369-36, Session PWed

Research of principles for estimating the freshness of meat products by color analysis method

Aleksandr N. Chertov, Elena V. Gorbunova, Daria B. Petukhova, Artem A. Alekhin, Valery V. Korotaev, National Research Univ. of Information Technologies, Mechanics and Optics (Russian Federation)

Color is one of the most important metrics of foodstuffs quality. It allows to judge the its freshness, ingredient composition as well as about the presence or absence of falsification. Most often, the color is estimated visually, and thus, the evaluation is subjective. By automating the color analysis a wide application for this method can be found.

The aim of this research is to study the principles of color analysis as applied to the task of evaluating the freshness of meat products using modern machine vision systems.

From a scientific point of view, the color of meat depends on the content of myoglobin. It's the main pigment that characterizes the freshness of meat. Further color of meat can change due to oxidation of myoglobin during storage. Myoglobin exists in three forms. There are oxygenated form, oxidized form and form without oxygen. The meat color changes are just due to the conversion of one form into another. The content of amino acids and ammonia are another characteristics and constant signs of meat products spoilage.

The paper presents the results of meat color computer simulation based on data on the content of various forms of myoglobin in different proportions. The spectral characteristic of the light source used to illuminate the meat sample is taken into account.

Also the experimental studies were conducted using samples of beef, pork and chickens. As a result the correlations between said biochemical indicators of the quality and color of the meat were found.

9369-19, Session 5

Structured light from lasers by dynamic and geometric phase control (*Invited Paper*)

Andrew Forbes, CSIR National Laser Ctr. (South Africa)

In this talk I will review the role of phase in creating customized modes from lasers. I will begin with the traditional approach of intra-cavity diffractive optical elements as a means to create high brightness lasers through dynamic phase control, illustrating the power of the technique through improved industrial laser performance. I will then show how inhomogeneous polarization optics may also be inserted into a laser cavity to modify the geometric phase of the light, leading to control of the handedness of the laser modes. Finally I will show how traditional approaches may be replaced with complex amplitude modulation on an intra-cavity spatial light modulator to form a digital laser for on-demand laser modes.

9369-20, Session 5

Synthesis and characterization of complex partially-coherent beams (*Invited Paper*)

Tatiana Alieva, Alejandro Cámara, José A. Rodrigo, Univ. Complutense de Madrid (Spain)

Partially coherent light provides attractive benefits for different applications in microscopy, astronomy, telecommunications, optical lithography, etc. However, generation of partially coherent beams with desirable properties is challenging. Moreover, the experimental characterization of the

Conference 9369:
Photonic Instrumentation Engineering II

spatial coherence is a difficult problem involving second-order statistics represented by four-dimensional functions that cannot be directly measured and analyzed. We discuss the techniques for design and generation of partially coherent structurally stable beams and the recently developed phase-space tomography methods supported by simple experimental setups for practical quantitative characterization of partially coherent light spatial structure, including its local coherence properties. The considered techniques are experimentally demonstrated.

9369-21, Session 5

Formation of propagation-invariant laser beams with anamorphic optical systems
(Invited Paper)

Yakov G. Soskind, DHPC Technologies (United States)

Propagation invariant laser beams play an important role in several photonics applications. Propagation invariant beams are usually produced as laser modes emanating from stable laser cavities. This paper shows that anamorphic optical systems can be effectively employed to produce a variety of propagation invariant structured laser beams by altering the shapes of laser resonator modes. I review several types of anamorphic lens systems suitable for transforming a variety of input laser modes into structured propagation invariant beams. I show that the transformation of laser modes with an anamorphic optical system results in a family of propagation invariant structured fields with opposite symmetry. The influence of the input laser mode characteristics on the resulting transformed output laser field are discussed as well.

9369-22, Session 6

Thermal signature identification system (TheSIS): a spread spectrum temperature cycling method *(Invited Paper)*

Scott Merritt, NASA Goddard Space Flight Ctr. (United States)

We characterize both nonlinear and high order linear responses of fiber-optic and optoelectronic components using spread spectrum temperature cycling methods. This thermal signature identification system (TheSIS) provides much more detail than quasi-static profiling or conventional narrowband temperature cycling methods. This detail allows us to 1) match components more thoroughly, 2) detect subtle reversible shifts in performance, and 3) investigate the cause of instabilities or irreversible changes in component or subsystem performance, e.g. aging. In particular, we create parameterized models of athermal fiber Bragg gratings (FBGs), delay line interferometers (DLIs), and distributed feedback (DFB) lasers then select winning models using the Akaike Information Criterion (AIC). Detailed pairing of components, e.g. FBGs, is accomplished by means of weighted distance metrics or norms, rather than on the basis of a single parameter, such as center wavelength.

TheSIS uses maximum length pseudo-random binary sequences (PRBS) with interval or "chip" durations shorter than the highest frequency in the response determined from an impulse-like thermal challenge. TheSIS uses PRBS sequence*chip duration products that are longer than the period of the lowest frequency components in the reversible portions of the responses.

We show the application of TheSIS-derived parameters to pairing of FBGs for low combined insertion loss and center wavelength control over temperature. Similarly, we show how detailed dynamical matching of DFB lasers and FBGs improves the robustness of subsystems containing these and other components which are subjected to random, system-relevant thermal challenges.

9369-23, Session 6

Measurement of polarization assemblies for the Daniel K. Inouye Solar Telescope

William H. Schubert, Erika Petrak, Thomas G. Baur, Meadowlark Optics, Inc. (United States)

We present here methodology and instrumentation for the precise measurement of retardance and optic axis orientation of retarder assemblies for the Daniel K. Inouye Solar Telescope. This solar telescope, soon to be the world's largest, will perform broadband polarimetry of the sun. Each Meadowlark assembly is made up of three retarders that must have a retardance variation of less than 6.33 nanometers across the greater than 110 millimeter clear aperture. The retardation of each component was measured using a combination of spectral transmission scans and ellipsometry, with test wavelengths of less than a 0.45 nanometer bandwidths and yielding a standard deviation in measurements of less than 0.0001 waves.

A technique for the measurement of the near zero window (Infrasil® and CaF2) retardance is shown, in addition to retardance measurements of the component waveplates. An average retardance of 0.63 nm for CaF2 and 0.28 nm for Infrasil® was found. Finally, a technique for determining the optic axis tilt of each crystal waveplate using laser ellipsometry is discussed.

9369-24, Session 6

Ellipsometry-like analysis of polarization state for latent flaws using stress-induced light scattering method

Yoshitaro Sakata, Kazufumi Sakai, Kazuhiro Nonaka, National Institute of Advanced Industrial Science and Technology (Japan)

Fine polishing techniques, e.g. the chemical mechanical polishing (CMP), are very important part of the manufacturing process for liquid crystal panel glass substrate. These techniques have mechanical interactions and these interactions, e.g. friction, occur between the abrasive and the substrate surface during polishing, which may cause formation of latent flaws (micro/hano scale cracks) on these products. In the glass substrate manufacturing, fine polishing-induced latent flaws may become obvious during a subsequent cleaning process if glass surfaces are eroded away by chemical interaction with the cleaning liquid. In general, non-destructive inspection techniques, e.g. the light-scattering technique, used to detect foreign matters on the glass substrate surface. However, it is difficult to detect latent flaws by these methods because the flaws remain closed under the surface. The presented authors propose a novel inspection technique for fine polishing-induced latent flaws by combining the light scattering method with stress effects (the stress-induced light scattering method; SILSM). SILSM can distinguish between latent flaws and tiny particles on the surface. The authors' previous research reported SILSM can detect latent flaws under the surface of a fine polished glass substrate selectively. However, detail evaluation that change in the stress concentration provides effect to the crack tip of the latent flaw is not carried out. In this study, SILSM applying to the fine polished glass substrate, change in the reflection coefficients and the polarization states at the crack tips of the latent flaw between before and after applied stress are calculated and evaluated ellipsometry like using Jones matrix.

9369-25, Session 6

In-line temperature-insensitive refractometer based on a thin core fiber in-line Mach-Zehnder interferometer

Jung-Koo Kim, Min-Seok Yoon, Young-Guen Han, Hanyang

**Conference 9369:
 Photonic Instrumentation Engineering II**

Univ. (Korea, Republic of)

Optical fiber refractometers based on in-line Mach-Zehnder interferometer (MZI) have attracted much attention in various application areas, such as chemical, physical, and even biological measurements, because of their high resolution, small size, good stability, fast responses, and resistance to electromagnetic interference. However, one of shortcomings of the conventional in-line MZI is the concurrent sensitivity to multiple perturbations, such temperature and ambient index changes. In order to improve measurement accuracy, it is necessary to suppress the temperature sensitivity. To solve these problems, the temperature-insensitive MZI based on the photonic crystal fibers (PCFs) have been proposed. However, the PCF-based MZI have drawbacks of low sensitivity and high insertion loss.

We propose a novel in-line temperature-insensitive refractometer based on a thin core fiber Mach-Zehnder interferometer (MZI). The thermal properties of the in-line MZI is effectively controlled by adjusting the diameter of the microtapered thin-core fiber. When the diameter of the microtapered thin core fiber is 75 μm , the temperature sensitivity of the in-line MZI is successfully mitigated to be 0.09 pm/?. The refractive index sensitivity of the proposed in-line MZI is measured to be 128.15nm/RIU which was 3 times larger than that of a conventional in-line MZI.

9369-26, Session 6

Time-to-digital converter card for multichannel time-resolved single-photon counting applications

Davide Tamborini, Davide Portaluppi, Politecnico di Milano (Italy); Simone Tisa, Micro Photon Devices S.r.l. (Italy); Alberto Tosi, Politecnico di Milano (Italy)

We present a high performance Time-to-Digital Converter (TDC) card that provides 10 ps timing resolution and 20 ps (rms) timing precision with a programmable full scale range from 160 ns to 10 μs . Differential Non-Linearity (DNL) is better than 1.3% LSB (rms) and Integral Non-Linearity (INL) is 5 ps rms. Thanks to the low power consumption (400 mW) and the compact size (78 mm x 28 mm x 10 mm), this card is the building block for developing compact multichannel time-resolved instrumentation for Time-Correlated Single-Photon Counting (TCSPC), Time-of-Flight (TOF) and Positron Emission Tomography (PET) instrumentation.

The TDC-card has two coaxial cable connectors for the START and STOP input pulses and edge-card connectors for I/O connectivity and power supplies. The core of the TDC-card is the integrated circuit TDC fabricated in 0.35 μm CMOS technology. The chip has the two independent START/STOP channels and the global circuitry for synchronization and data read-out. The TDC-card hosts: i) the TDC chip; ii) a signal conditioning electronics accepting any input signal pulse shape; iii) a processing electronics for the TDC data handling and calibration. The TDC-card outputs the time measurement results together with the rates of START and STOP signals and the number of valid TDC conversions. These additional information are needed by many TCSPC-based applications, such as: Fluorescence Lifetime Imaging (FLIM), Time-of-Flight (TOF) ranging measurements, time-resolved Positron Emission Tomography (PET), single-molecule spectroscopy, Fluorescence Correlation Spectroscopy (FCS), Diffuse Optical Tomography (DOT), Optical Time-Domain Reflectometry (OTDR), quantum optics, etc.

Conference 9370: Quantum Sensing and Nanophotonic Devices XII

Sunday - Thursday 8 -12 February 2015

Part of Proceedings of SPIE Vol. 9370 Quantum Sensing and Nanophotonic Devices XII

9370-1, Session 1

Plasmonic terahertz optoelectronics (Keynote Presentation)

Mona Jarrahi, Univ. of California, Los Angeles (United States)

Although unique potentials of terahertz waves for chemical identification, material characterization, biological sensing, and medical imaging have been recognized for quite a while, the relatively poor performance, higher costs, and bulky nature of current terahertz systems continue to impede their deployment in field settings. In this talk, I will describe some of the significant advancements in terahertz technology enabled by nanoplasmonics. In this regard, I will introduce new generation of terahertz optoelectronic components and imaging/spectrometry/spectroscopy systems that offer significantly higher performance compared to the state of the art. In specific, I will introduce new designs of high-performance terahertz sources and detectors that utilize plasmonic nanostructures to enhance terahertz radiation power by three orders of magnitude – at record-high power levels of several milliwatts – and terahertz detection sensitivity by two orders of magnitude. To achieve this significant performance improvement, plasmonic nanostructures and device architectures are optimized for operation at telecommunication wavelengths, where very high power, narrow linewidth, wavelength tunable, compact and cost-effective optical sources are commercially available. Therefore, the plasmonic terahertz optoelectronic devices pave the way to compact and low-cost terahertz sources, detectors, and spectrometers that could offer numerous opportunities for e.g., medical imaging and diagnostics, atmospheric sensing, pharmaceutical quality control, and security screening systems.

9370-2, Session 2

Superradiant optoelectronic devices (Invited Paper)

Yanko Todorov, Thibault Laurent, Angela Vasanelli, Univ. Paris 7-Denis Diderot (France); Isabelle Sagnes, Lab. de Photonique et de Nanostructures (France); Carlo Sirtori, Univ. Paris 7-Denis Diderot (France)

In a quantum structure collective effects enhance the interaction between light and matter proportionally to the number of particles involved in the interaction. In a dense 2-dimensional electron gas such effects can therefore be huge due to Coulomb dipole-dipole coupling that ties all free oscillating charges and form a collective density waves: the plasmons. Due to its giant coupling with light, plasmons are bound to have an extremely short spontaneous emission life-time. Indeed, we have measured spontaneous emission shorter than 100fs for quantum wells doped in the order of 10^{13} cm⁻². For these measurements we have realised electrically injected devices that show a strong electroluminescent signal at the plasmon energy, evidence of super-radiant emission in a solid at room temperature. The data collected are in excellent agreement with our theoretical model that shows that the optical properties of the plasmon are no longer related to the energy spectrum imposed by the confining potentials, but depends primarily on the many-body particle arising from the coherent sum of each individual electronic dipole. From an optical point of view, the system behaves as a macro-atom (composed of several thousands of billions of electrons), with an exceptionally strong interaction with light.

9370-3, Session 2

Metallic metasurface as a directional and monochromatic thermal emitter (Invited Paper)

François Marquier, Daniele Costantini, Institut d'Optique Graduate School (France); Anthony Lefebvre, CEA-LETI (France); Anne-Lise Coutrot, Ioana Moldovan-Doyen, Jean-Paul Hugonin, Institut d'Optique Graduate School (France); Salim Boutami, CEA-LETI (France); Henri Benisty, Jean-Jacques Greffet, Institut d'Optique Graduate School (France)

Mid to far infrared is an important wavelength band for material detection. Incandescent sources are often used in infrared spectroscopy because they are simple and cost effective. They are however broadband and quasi isotropic. As a result, the total efficiency in a detection system is very poor. Yet it has been shown recently that thermal emission can be designed to be directional and/or monochromatic [see for instance Nature 416, 61 (2002); Phys. Rev. Lett. 107, 045901 (2011); Nat. Photonics 6, 535 (2012)]. To do so, the concept of emissivity is necessary. At a given temperature, the blackbody radiation gives the maximum specific intensity that can be got. A real thermal source is also characterized by its emissivity, which gives the specific intensity of the source compared to the blackbody at the same temperature. The emissivity depends on the wavelength and the direction of emission and is related to the whole structure (materials, geometry...) of the source. Emissivity appears as a directional and frequency filter for the blackbody radiation. Playing with materials and structure resonances, the emissivity can be designed to optimize the properties of an incandescent source. We will see how it is possible to optimize a plasmonic metasurface acting as an incandescent source, which is directional and quasi monochromatic at a chosen wavelength. We will take the example of a CO₂ detection application to illustrate this topic.

9370-4, Session 2

Magnetic dipole and electric dipole resonances in TiO₂ microspheres at terahertz frequencies

Oleg Mitrofanov, Univ. College London (United Kingdom); Filip Domenic, Petr Kuzel, Institute of Physics of the ASCR, v.v.i. (Czech Republic); John Reno, Igal Brener, Sandia National Labs. (United States); Seu Chung, Cathy Elissald, Mario Maglione, Institut de Chimie de la Matière Condensée de Bordeaux (France); Patrick Mounaix, Univ. Bordeaux 1 (France)

The key element for metamaterials is a sub-wavelength size resonator with an effective magnetic response. Dielectric resonators have attracted much interest recently as an alternative to split ring resonators, which exhibit undesirable anisotropy, polarization dependent response and non-negligible metallic Ohmic losses. In a high-permittivity dielectric sphere, an effective magnetic response occurs as a result of the 1st Mie mode, known as the magnetic dipole (MD) resonance. Due to the permittivity of ~100, TiO₂ is a promising material for dielectric resonators. The MD resonance at 1 THz is expected for a 30 micrometer diameter microsphere made of TiO₂. However, detection and characterization of the Mie resonances in a sub-wavelength size object is difficult with the standard THz spectroscopy methods. We demonstrate that the MD as well as the electric dipole

**Conference 9370: Quantum Sensing and
Nanophotonic Devices XII**

resonances can be probed in single TiO₂ microspheres using a THz near-field microscopy approach. A near-field probe with a sub-wavelength ($\sim \lambda/50$) size aperture and the THz time-domain spectroscopy technique allow us to detect the Mie resonance signatures in the amplitude and phase spectra. The narrow line-width of the MD resonance and the sub-wavelength size of the TiO₂ microspheres make them excellent candidates for realizing low-loss THz metamaterials, which can be used in THz devices as well as in THz sensors. In comparison with SRR, the TiO₂ resonators can provide a narrower line-width at THz frequencies and eliminate the anisotropy and polarization dependence of the effective magnetic permeability. The near-field microscopy method opens a possibility for investigation of single high-permittivity dielectric resonators.

9370-5, Session 2
**Sub-wavelength infrared investigations
of complex metallic surfaces and doped
semiconductors (*Invited Paper*)**

Yannick De Wilde, Institut Langevin (France)

In an apertureless near-field scanning optical microscope, using a laser to illuminate the area of the sample where the tip is located causes some asymmetry in the illumination. This should not be the case when using an apertureless probe based on the scattering of the sole thermal near-field emission such as the thermal radiation scanning tunneling microscope (TRSTM) [1-4], which is symmetric in essence, and also much less coherent than a laser. We will present an experimental study of the influence of the type of source employed on the formation of super-resolved infrared near-field images. The test samples are made of homogeneous surfaces of gold with a disordered bumpy structure of Gaussian statistics prepared by means of three dimensional laser lithography and the investigation is based on the autocorrelation of the near-field images [5]. Besides the investigation of test samples, we will also present the use of infrared near-field imaging and spectroscopy combined with broadband sources like near-field thermal emission or infrared synchrotron radiation, in the practical case of the characterization of doped semiconductor heterostructures made of InAs. We demonstrate that our approach has the ability of characterizing the field in any regime between the near-field with 100 nm resolution and the far-field where the subwavelength structures are homogenized.

ACKNOWLEDGMENTS

Work performed in collaboration with Institut Langevin (F. Peragut, V. Krachmalnicoff, R. Carminati), Laboratoire Charles Fabry-IOGS (J.-J. Greffet), Synchrotron SOLEIL (P. Roy, J.-B. Brubach), Institut d'Electronique du Sud (T. Taliercio, V. Ntsame Guilengu), Institut Electronique Fondamentale (S. Collin, N. Bardou).

REFERENCES:

- [1] Thermal Radiation Scanning Tunnelling Microscopy, Y. De Wilde, F. Formanek, R. Carminati, B. Gralak, P.-A. Lemoine, J.-P. Mulet, K. Joulain, Y. Chen, J.-J. Greffet, NATURE, 444, 740 (2006).
- [2] Thermal Infrared Near-Field Spectroscopy, A. C. Jones and M. B. Raschke, NANO LETTERS, 12, 1475 (2012).
- [3] Blackbody Spectrum Revisited in the Near Field, A. Babuty, K. Joulain, P.-O. Chapuis, J.-J. Greffet, Y. De Wilde, PHYSICAL REVIEW LETTERS, 110, 146103 (2013).
- [4] Infrared near-field imaging and spectroscopy based on thermal or synchrotron radiation, F. Peragut, J.-B. Brubach, P. Roy, Y. De Wilde, APPLIED PHYSICS LETTERS, 104, 251118 (2014).
- [5] Direct reconstruction of surfaces from near-field intensity under spatially incoherent illumination, R. Carminati, J.-J. Greffet, N. Garcia, M. Nieto-Vesperinas, OPTICS LETTERS, 21, 501 (1996).

9370-6, Session 2
**Characterization techniques for
semiconductors and nanostructures: a
review of recent advances (*Invited Paper*)**

Olivier Acher, HORIBA Jobin Yvon S.A.S. (France)

Optical spectroscopy techniques are widely used for the characterization of semiconductors and nanostructures. Confocal Raman microscopy is useful to retrieve chemical and molecular information at the ultimate submicrometer resolution of optical microscopy. Fast imaging capabilities, 3D confocal ability, and multiple excitation wavelengths, have increased the power of the technique while making it simpler to use for material scientists. Recently, the development of the Tip Enhanced Raman Spectroscopy (TERS) has opened the way to the use of Raman information at nanoscale, by combining the resolution of scanning probe microscopy and chemical selectivity of Raman spectroscopy.

Significant advances have been reported in the field of profiling the atomic composition of multilayers, using the Glow Discharge Optical Emission Spectroscopy technique, including real-time determination of etched depth by interferometry. This allows the construction of precise atomic profiles of sophisticated multilayers with a few nm resolution. Ellipsometry is another widely used technique to determine the profile of multilayers, and recent development have provided enhanced spatial resolution useful for the investigation of patterned materials.

In addition to the advances of the different characterization techniques, the capability to observe the same regions at micrometer scale at different stages of material elaboration, or with different instrument, is becoming a critical issue. Several advances have been made to allow precise re-localization and co-localization of observation with different complementary characterization techniques.

9370-7, Session 3
**Optically-pumped continuous-wave
terahertz sources (*Invited Paper*)**

Philipp Latzel, Univ. des Sciences et Technologies de Lille (France) and Institut d'Electronique de Microélectronique et de Nanotechnologie (France); Fabio Pavanello, Emilien Peytavit, Mohammed Zaknoute, Institut d'Electronique de Microélectronique et de Nanotechnologie (France) and Univ. des Sciences et Technologies de Lille (France); Guillaume Ducournau, Xavier Wallart, Jean-François Lampin, Univ. des Sciences et Technologies de Lille (France) and Institut d'Electronique de Microélectronique et de Nanotechnologie (France)

Recently we have improved the efficiency and the output power of our optically pumped continuous-wave THz sources. These sources are based on the beating of two laser lines in a wide bandwidth photodetector. Its intrinsic nonlinear behaviour is used to produce a beatnote at the frequency difference between the two laser lines (photomixing). These photomixers are continuously tunable THz sources working at room temperature. We have developed two kinds of photomixers: GaAs-based for 0.8 μm pumping and InP-based for 1.5 μm pumping. On GaAs the best results has been obtained thanks to low-temperature-grown GaAs (LTG-GaAs) photoconductors (PC). Efficiency and power were optimized by designing a new type of thin PC placed in a Fabry-Pérot resonator. The high impedance of the PC is a well-known limitation of this device but with our approach it was possible to reduce its impedance by a factor 100. Moreover by designing an impedance matching network it was possible to obtain 1.8 mW at 252 GHz with a total efficiency of 0.5 %. On InP the best results are obtained with uni-travelling carrier photodiodes (UTC-PD). The device was improved by designing a new heterostructure and new semi-transparent contacts with sub-wavelength apertures. The active layer was also bonded

**Conference 9370: Quantum Sensing and
Nanophotonic Devices XII**

to a silicon substrate thanks to metal thermocompression. It is demonstrated that with this approach it is possible to obtain a power of 0.7 mW at 300 GHz with a total efficiency of 0.7 %. More generally the efficiency of optically pumped terahertz sources will be discussed.

9370-8, Session 3
**Opening new territory in THz using
coherent synchrotron radiation (*Invited
Paper*)**

Pascale Roy, Synchrotron SOLEIL (France)

Recently, an unprecedented high power source of THz radiation was made scientifically available: coherent synchrotron radiation (CSR). This radiation produced from relativistic electron bunches of picosecond duration opens up new territory in the THz range with intensities up to 4 orders of magnitude higher than conventional synchrotron sources. Its huge potential can however be hampered by its stability which is critically affected by accelerator and electron bunches properties. Investigating these intrinsic instabilities remained up to now an open problem because of the extreme speed of the phenomena, implying to record picosecond signals at MHz acquisition rates. We will show how this was recently made possible by adapting a photonic technique, called time-stretch, which allows to "slow-down" the signal prior to recording. As a result we will demonstrate the possibility to look continuously at electron bunch emission with sub-psec resolution. We will also describe new scientific opportunities made possible by CSR in particular, high rate terahertz spectroscopy, as well as ultra-high resolution spectroscopy based on heterodyne mixing technique.

9370-9, Session 3
**THz quantum cascade lasers based on a
hyperuniform design (*Invited Paper*)**

Riccardo Degl'Innocenti, Yash D. Shah, Univ. of Cambridge (United Kingdom); Luca Masini, Istituto Nanoscienze, CNR (Italy) and Scuola Normale Superiore (Italy); Alberto Ronzani, Istituto Nanoscienze, CNR (Italy) and Scuola Normale Superiore (Italy); Alessandro Pitanti, Istituto Nanoscienze, CNR and Scuola Normale Superiore (Italy); Yuan Ren, David S. Jessop, Univ. of Cambridge (United Kingdom); Alessandro Tredicucci, Univ. di Pisa (Italy); Harvey E. Beere, David A. Ritchie, Univ. of Cambridge (United Kingdom)

We realized a terahertz quantum cascade laser based on a hyperuniform disordered design. Particularly, we designed a stealthy hyperuniform pattern distribution, which is characterized by being transparent for certain wavenumbers. Such a system is characterized by an efficient depletion of long range interactions: the properties of the distribution are globally isotropic, while the system is locally anisotropic. By varying the degree of disorder of such a distribution, it is possible to realize a wider range of band-gaps with respect to standard photonic crystal materials. Bi-dimensional hyperuniform patterns were simulated for hexagonal tiles composed of pillars merged in a polymeric matrix. From our simulations, three frequency degenerated modes emerged out of the Fourier spectrum at the lower band gap edge for TM polarization. The hyperuniform distribution of scatterers have been realized by standard photolithography, Ti/Au metallic evaporation and lift-off on a half stack bound to continuum active region emitting around 2.8 Terahertz. This pattern was then etched through the whole active region by using a reactive ion etching process in order to realize a distribution of 3D pillars. An efficient surface planarization was realized by spinning and processing many layers of Cyclotene polymer. The final step consisted in the evaporation of a metallic top layer covering both pillars and thermally cured Cyclotene, acting as top contact of our structures. The voltage-current-light characteristics of the laser are compatible with those

of a double-metal quantum cascade lasers for this active region processed with standard techniques.

9370-10, Session 3
**Uni-travelling carrier photodetectors as
THz detectors and emitters**

Cyril C. Renaud, Martyn J. Fice, Lalitha Ponnampalam, Michele Natrella, Chris Graham, Alwyn J. Seeds, Univ. College London (United Kingdom)

The THz part of the spectrum (0.1 to 10 THz) has been gathering increasing interest over the past 10 years as it could enable interesting new applications. Key to its exploitation has been the development of photonic based sources and detectors. However there is a lack of room temperature operating devices for both sources and detectors.

One device that could potentially be used both as a receiver or an emitter is the uni-travelling carrier photodetectors (UTC-PDs). As a photomixing source we have demonstrated record breaking figure of merit (PTHZ/P2opt) for the range up to 2 THz with power of several mW for frequencies up to 300 GHz and several μ W up to 1.2 THz. This device have also the potential to be monolithically integrated within an optical heterodyne chip and demonstrated 100 μ W at 100 GHz. As a receiver it could be used as an optically pumped mixer, within a similar heterodyning system. In that case an intermediate frequency (the difference between the THz received signal and the optical heterodyne) is measured. With such a device at room temperature a flat conversion loss was observed up to 600 GHz, while for all the frequency range the receiver sensitivity of -95 dBm/Hz was limited by the optical noise from the system. In this paper we also discuss the different processes in optimizing the receiver sensitivity to -120 dBm/Hz.

9370-11, Session 3
**THz generation by optical rectification in
graphene at room temperature: beyond
the linear carrier dispersion (*Invited Paper*)**

Juliette Mangeney, Jean Maysonnave, Simon Huppert, Feihu Wang, Simon Maëro, Ecole Normale Supérieure (France); Claire Berger, Walter A. de Heer, Georgia Institute of Technology (United States); Theodore B. Norris, Univ. of Michigan (United States); Louis-Anne de Vaultier, Sukhdeep S. Dhillon, Jérôme Tignon, Robson Ferreira, Ecole Normale Supérieure (France)

Graphene is a particularly attractive material for the achievement of strong optical nonlinearities, in particular generation of terahertz radiation. However, owing to the peculiar symmetries of the C-lattice, second-order nonlinear effects are predicted to vanish in a graphene layer for optical excitations involving the two relativistic dispersion bands. Here, we show broadband coherent terahertz emission at room temperature in epitaxial graphene under femtosecond optical excitation via optical rectification effect. We fully interpret the emitted THz radiation characteristics with a model describing the electron and hole states beyond the usual massless relativistic scheme. This second-order nonlinear effect relies on the dynamical transfer of light momentum (dynamical photon drag effect) to the carriers by the ponderomotive electric and magnetic forces. We demonstrate that, in contrast to most optical processes in graphene, the next-nearest-neighbor couplings as well as the distinct electron-hole dynamics are of paramount importance in the observed second-order response. Finally, our results indicate that optical rectification in graphene can provide emission up to 60 THz, opening new routes for the generation of ultra-broadband terahertz pulses at room temperature.

9370-12, Session 4

Hydride vapour phase epitaxy assisted buried heterostructure quantum cascade lasers for sensing applications (*Invited Paper*)

Sebastian Lourduoss, Wondwosen Metaferia, KTH Royal Institute of Technology (Sweden); Carl Junesand, KTH Royal Institute of Technology (Sweden) and Epiclarus AB (Sweden); Balaji Manavaimaran, KTH Royal Institute of Technology (Sweden); Simon Ferré, Bouzid Simozrag, Matheiu Carras, Alcatel-Thales III-V Lab. (France); Romain Peretti, Valeria Liverini, Mattias Beck, Jérôme Faist, ETH Zürich (Switzerland)

Buried heterostructure (BH) lasers are routinely fabricated for telecom applications. Development of quantum cascade lasers (QCL) for sensing applications has largely benefited from the technological achievements established for telecom lasers. However, new demands are to be met with when fabricating BH-QCLs. For example, hetero-cascade and multi-stack QCLs, with several different active regions stacked on top of each other, are used to obtain a broad composite gain or increased peak output power. Such structures have thick etch ridges which puts severe demand in carrying out regrowth of semi-insulating layer around very deeply etched ($> 10 \mu\text{m}$) ridges in short time to realize BH-QCL. For comparison, telecom laser ridges are normally only $< 5 \mu\text{m}$ deep. We demonstrate here that hydride vapour phase epitaxy (HVPE) is capable of meeting this new demand adequately through the fabrication of BH-QCLs in less than 45 minutes for burying ridges etched down to 10-15 μm deep. This has to be compared with the normally used regrowth time of several hours, e.g., in a metal organic vapour phase epitaxy (MOVPE) reactor. In addition, HVPE is largely insensitive to etched ridge profile, mask overhang and does not lead to rabbit-ear growth near the ridge. The fabricated devices emitting at 4.7 μm exhibit an output power up to -2.4 W at room temperature and under CW operation with a wall plug efficiency up to 9% while at the same time maintaining spatially monomode, TM00. We also demonstrate HVPE capability to fabricate buried heterostructure photonic crystal QCLs.

9370-13, Session 4

Quantum-cascade-laser active regions on metamorphic buffer layers (*Invited Paper*)

Luke J. Mawst, Ayushi Rajeev, Jeremy D. Kirch, Tae Wan Kim, Dan Botez, Brian Zutter, Phillip Buelow, Kevin Schulte, Thomas F. Kuech, Adam Wood, Susan E. Babcock, Univ. of Wisconsin-Madison (United States); Thomas Earles, Intraband, LLC (United States)

Metamorphic buffer layers (MBLs) can be utilized as virtual substrates with a specified lattice constant, opening up the palette of III/V alloys available for new device architectures. We have investigated the use of MBLs for the realization mid-infrared semiconductor lasers employing either Interband or Intersubband transitions.

Semiconductor lasers in the 2-4 μm wavelength region on a conventional InP substrate would have a significant advantage over GaSb-based interband devices in terms of lower cost, mature processing technology, and better thermal conductivity. InAs_xP_{1-x}(Sb) MBL structures have been developed on (100) InP substrates by MOCVD. Laser emission at LT (77K) near 2.5 micron is achieved from structures employing an InAs QW active region grown on top of the MBL, and RT PL emission is demonstrated near 3micron.

Short emission wavelength (i.e., $< 4.0\mu\text{m}$) quantum cascade (QC) lasers on InP substrates require deep quantum wells and tall barriers (i.e. higher strain) to prevent excessive active-region carrier leakage, due to the large transition energy. However, the barrier and well compositions that can be

accessed are limited by strain-thickness considerations in order to avoid strain relaxation. Simulation studies suggest that significant enhancement of performance is possible over conventional InP-substrate devices by employing an MBL design on a GaAs substrate. 20-period In_xGa_{1-x}As (wells)/Al_yIn_{1-y}As (barriers) SLs are grown by MOCVD on an InGaAs step-graded, (HVPE)-grown MBL. Employing chemical mechanical polishing (CMP) on the top of the MBL results in significantly improved surface morphology. Electroluminescent devices grown on the MBL demonstrate intersubband emission near 3.6 μm .

This work was supported by NSF Materials Research and Engineering center (DMR-1121288), NSF 1317297, NSF 1232618, and Navy STTR N68335-11-C-0432

9370-14, Session 4

Low power-consumption quantum cascade lasers

Tsukuru Katsuyama, Jun-ichi Hashimoto, Hiroyuki Yoshinaga, Hiroki Mori, Yukihiko Tsuji, Makoto Murata, Mitsuru Ekawa, Toshiyuki Tanahashi, Sumitomo Electric Industries, Ltd. (Japan)

Quantum cascade lasers (QCLs) are promising light sources for real time high-sensitivity gas sensing in the mid-infrared region. For the practical use of QCLs as a compact and portable gas sensor, their power-consumption needs to be reduced. So far there have been few reports on the reduction of power consumption of QCLs. In this paper, we report a successful operation of a low power-consumption distributed feedback QCL.

For the reduction of power consumption, we optimized the number of stage in core region by considering the trade-off between optical gain and operating voltage. We also reduce the device size such as a mesa-width and a cavity-length.

QCL epitaxial growth was carried out by low-pressure OMVPE. The core region consists of AlInAs/GaInAs superlattices lattice-matched to InP. A first-order Bragg-grating was formed near the core region to obtain a large coupling coefficient. A mesa-strip was formed by reactive ion etching and a buried-heterostructure was fabricated by the regrowth of semi-insulating InP. High-reflective facet coatings were also performed to increase the optical feedback for the reduction of the threshold current.

A device (5x500 μm) showed a good single mode operation at 7.27 μm . The threshold current and threshold voltage under CW operation at 20 °C were 52mA and 8.37V respectively. A very low threshold power-consumption as low as 0.44 W was achieved, which is among the lowest values at room temperature to our best knowledge. Further reduction of the power consumption can be expected by optimizing wavelength detuning and core structure.

9370-15, Session 4

Novel techniques for electrical tuning in quantum cascade lasers (*Invited Paper*)

Alfredo Bismuto, Yves Bidaux, Camille Tardy, Stéphane Blaser, Romain Terazzi, Tobias Gresch, Antoine Müller, Alpes Lasers SA (Switzerland)

Coherent sources in the mid-infrared spectral range are of great interest due to the large number of scientific and industrial applications in this spectral range, e.g. high resolution spectroscopy, industrial control, clinical diagnostic. Quantum cascade lasers provide nowadays a compact and efficient source across the whole Mid-IR range. In particular, distributed feedback (DFB) QCLs provide stable monomode emission as required by most of the spectroscopic applications. Unfortunately the electrical tunability of these sources is limited reducing the capability to detect multiple molecular resonances at the same time or to properly detect broad resonances. In the present work we will analyse the tuning mechanism in standard QCLs and will present novel solutions for electrical tuning of the

**Conference 9370: Quantum Sensing and
 Nanophotonic Devices XII**

laser emission. In particular, we will show a novel generation of devices that allow for local control of the laser active region temperature using an integrated heating element. The application of this novel tuning method on different classes of sources will be presented. As will be presented both high modulation speed and wide tuning can be obtained using this technique. For the present work various wavelength ranges have been selected due to their commercial interest.

9370-16, Session 5
Impact of MBE deposition conditions on InAs/GaInSb superlattices for very long wavelength infrared detection

Gail J. Brown, Heather J. Haugan, Krishnamurthy Mahalingam, Lawrence Grazulis, Air Force Research Lab. (United States); Said Elhamri, Univ. of Dayton (United States)

In order to develop ternary antimonide-based superlattice (SL) materials for very long wavelength infrared (VLWIR) detection, systematic growth optimization studies were performed to produce high quality ternary materials. For the studies, a SL structure of 47.0 Å InAs/21.5 Å Ga_{0.75}In_{0.25}Sb was selected to create a very narrow band gap. Results indicate that an epitaxial process developed can produce a precisely controlled band gap around 50 meV, but the material quality of grown SL layers is particularly sensitive to growth defects formed during the growth process. Since Group III antisites and strain-induced dislocations are the dominant structural defects responsible for the low radiative efficiencies, our optimization strategies to eliminate these defects have focused on stabilizing III/V incorporation during surface reconstruction by manipulating the growth surface temperature and balancing the residual strain of the SLs by adjusting the As/Sb flux ratio. The optimized ternary SL materials exhibited an overall strong photoresponse over a wide wavelength range up to ~15 μm that is important for developing VLWIR detectors. A quantitative analysis of the lattice strain, performed at the atomic scale by aberration corrected transmission electron microscopy, provided valuable information about the strain distribution at the interfaces that was important for optimizing the strain balancing process during SL layer growth.

9370-17, Session 5
Progress in development of direct bandgap III-V LWIR detectors

Stefan P. Svensson, Wendy L. Sarney, Harry S. Hier, U.S. Army Research Lab. (United States); Ding Wang, Dimitri Donetsky, Gela Kipshidze, Leon Shterengas, Youxi Lin, Gregory Belenky, Stony Brook Univ. (United States)

Until recently it was assumed that no direct-bandgap III-V compound existed that could absorb light in the entire long wavelength infrared (LWIR) band (8-12 micron). We have demonstrated that the bandgap bowing parameter of InAsSb is 0.87 eV, which is considerably larger than previously thought. We have reached photoluminescence wavelengths up to 12.4 micron in bulk InAsSb grown without detectable alloy ordering or strain effects. Larger bandgaps can be achieved in AlGaInAsSb, which can be lattice matched to LW InAsSb. The tuning of the bandgap, independent of a binary substrate, allows engineering of novel detector structures.

The InAsSb carrier concentrations in the bulk, at the surface, and at the interface with AlInSb have been studied. The surface exhibits an electron accumulation layer which necessitates the use of barrier structures or development of a surface isolation (passivation) process. Another accumulation layer with similar density but even higher conductivity is formed at interfaces. This charge transfer is partially responsible for the need for counter doping in diode barrier layers. We have measured the 77 K absorption in InAs_{0.5}Sb_{0.5} with a bandgap around 0.1 eV to be about 4000

cm⁻¹ at 8.5 micron, comparable to that of HgCdTe at similar wavelengths. The minority carrier life time in n-type material has been determined to be ~165 ns using a new method based on the transient response from diodes with variable size front and back illumination. Examples of barrier diode designs will be demonstrated and the prospects for multi-color devices discussed.

9370-18, Session 5
Temperature dependent carrier lifetime measurements of InAs/InAsSb T2SLs

Yigit Aytac, The Univ. of Iowa (United States); Benjamin V. Olson, Jin K. Kim, Eric A. Shaner, Sam D. Hawkins, John F. Klem, Sandia National Labs. (United States); Michael E. Flatté, Thomas F. Boggess, The Univ. of Iowa (United States)

Temperature dependent measurements of carrier recombination rates using a time-resolved pump-probe technique are reported for mid-wave infrared InAs/In_{1-x}Sb_x type-2 superlattices (T2SLs). By engineering the layer widths and alloy compositions a 16 K bandgap of ~235±10 meV was achieved for four doped and five undoped T2SLs. Carrier lifetimes were determined by fitting lifetime models of Shockley-Read-Hall (SRH), radiative, and Auger recombination processes simultaneously to the temperature and excess carrier density (ECD) dependent data. The contribution of each recombination processes at a given temperature is identified and the total lifetime is determined over a range of ECDs. The minority carrier and Auger lifetimes were observed to increase with antimony content and decreasing layer thickness for the undoped T2SLs. It is hypothesized that a reduction in SRH recombination centers or a shift in the SRH defect energy relative to the SL band edges is the cause of this increase in the minority carrier lifetime. The lower Auger coefficients are attributed to a reduced number of final Auger states in the SL samples with greater Sb. An Auger limited minority carrier lifetime is observed for doped T2SLs and is found to be a factor of ten shorter than for undoped T2SLs. The Auger rates for all the InAs/InAsSb T2SLs were significantly larger than previously measured for InAs/GaSb T2SLs. Sandia National Laboratories is a multi-program laboratory managed and operated by Sandia Corporation, a wholly owned subsidiary of Lockheed Martin Corporation, for the U.S. Department of Energy's National Nuclear Security Administration under Contract No. DE-AC04-94AL85000. This research was funded by the U.S. Government.

9370-19, Session 5
Ideal performance of and defect-assisted carrier recombination in MWIR and LWIR InAs/InAsSb superlattice detectors

Michael E. Flatté, The Univ. of Iowa (United States); Christoph H. Grein, Univ. of Illinois at Chicago (United States)

Detector performance is calculated for mid-wavelength infrared and long-wavelength infrared InAs/InAsSb type-2 superlattices (T2SLs). The electronic structure, transport, optical and carrier recombination properties are calculated for a series of T2SLs with varying Sb content in the InAsSb layer, and strain balanced for growth on GaSb substrates. The electronic-structure calculations rely on a well-tested envelope-function formalism based on fourteen bulk bands that has been extensively tested for InAs/GaInSb superlattice detectors. Targeted cutoff wavelengths are 5.2 microns and 10 microns. Resonances in the electronic structure are identified that are predicted to reduce the non-radiative carrier recombination rate. As the Sb composition and the strain in the InAsSb layer is varied the conduction and valence band edges also shift, and the resulting effect of these shifts on the Shockley-Read recombination rates from defect states in the gap

Conference 9370: Quantum Sensing and Nanophotonic Devices XII

is calculated. If these defect states do not shift much with the band edges then the Shockley-Read recombination rates should change by over an order of magnitude. Anisotropy in the carrier masses can also reduce detector performance; we find that hole mass anisotropy can be moderate for high-performance InAs/InAsSb superlattices. This research was funded by the U.S. Government.

9370-20, Session 5

Magnetotransport potentials for anisotropic thin films with stripline and ground plane contacts (*Invited Paper*)

Yang Tang, Matthew Grayson, Northwestern Univ. (United States)

Superlattice layers in infrared emitters and detectors can be highly anisotropic in their thermal and electrical properties. For optimal device performance, it is therefore important to perfect methods whereby the respective anisotropic thermal and electrical conductivity tensors can be characterized for these thin layers. This work first reviews improvements in the two-wire three-omega method for characterizing the anisotropic thermal conductivity tensor in superlattice active- and cladding-layers of infrared devices such as interband cascade lasers and type II infrared detectors. Subsequently, we introduce a novel method for deducing the complete anisotropic electrical conductivity tensor of a resistive layer atop a highly conducting bottom contact. Three strip-line contacts are applied atop the resistive superlattice layer of interest, which, in turn, contacts with a highly conducting back-plane such as a doped back-contact. Laplace's equation is solved numerically to deduce the current distribution in a magnetic field, with Dirichlet boundary conditions at the grounded back-plane and Neumann boundary conditions at the floating front-plane. By conducting two 4-point measurements, a method is described whereby the full conductivity tensor can be deduced as a function of magnetic field B. Preliminary experimental data will be shown which demonstrates the validity of this new analysis method for measuring the anisotropic electrical conductivity tensor of a superlattice layer.

9370-21, Session 6

Room temperature performance of mid-wavelength infrared InAsSb nBn detectors

Alexander Soibel, Cory J. Hill, Sam A. Keo, Linda Hoglund, David Z. Ting, Sarath D. Gunapala, Jet Propulsion Lab. (United States)

During the last several decades great efforts were dedicated to the development of high operating temperature infrared detectors for applications in imaging and chemical sensing. Significant progress achieved in development of thermal detectors enabled infrared imagers operating at ambient temperature. Quantum detectors, which are typically based on semiconductor devices, can provide better sensitivity and higher operational speed but require cryogenic cooling to achieve desirable operational parameters. A number of novel semiconductor devices, which rely on the suppression of thermal currents and an enhancement in responsivity to improve high temperature performance, have been proposed and realized. Innovative detector architectures such as barrier structures, in particular nBn, devices and significant improvement in the performance GaSb-based alloys and superlattices offer pathways to further improve high temperature operation.

We investigate the high temperature performance of mid-wavelength infrared InAsSb-AlAsSb nBn detectors with cut-off wavelength around 4.5 μ m. The quantum efficiency of these devices is 35% without antireflection and does not change with temperature in the 77-325K temperature range, indicating their potential for ambient temperature operation. The current generation of nBn detectors shows an increase of operational bias with temperature. Analysis of the devices performance

shows that operational bias and Quantum Efficiency of these detectors can be further improved. The device dark current stays diffusion limited in the 150K-325K temperature range and become dominant by generation-recombination processes at lower temperature. Detector detectivity $D^*(?)=1 \times 10^9$ (cm Hz^{0.5}/W) at T=300K and $D^*(?)=5 \times 10^9$ (cm Hz^{0.5}/W) at T = 250K easily achievable with one stage TE cooler.

9370-22, Session 6

MWIR InSb detector with nBn architecture for high operating temperature

Jean-Philippe Perez, IES Institut d'Electronique et des Systèmes (France); Axel Evirgen, Johan Abautret, Philippe Christol, IES Institut d'Electronique et des Systèmes (France); Arnaud Cordat, Alexandru Nedelcu, SOFRADIR (France)

InAsSb bariode is currently the dominant III-V infrared detector technology to reach high operating temperature (HOT) in midwave infrared (MWIR) spectral region. Indeed, InAsSb nBn Focal Plane Array (FPA) operating at 150 K with cut-off wavelength $\lambda_c = 4.1 \mu\text{m}$ has recently been reported. For the MWIR domain, InSb remains the main established technology. However, InSb conventional planar detector arrays fabricated either by ion implantation or Molecular Beam Epitaxy (MBE), with $\lambda_c \sim 5.5 \mu\text{m}$ at 77 K, suffer from strong performance degradation inducing operating temperatures lower than 95 K. Consequently, to get rid of this low temperature constraint and to benefit of the radiometric properties of InSb material covering the entire MWIR domain ($\lambda_c \sim 5.6 \mu\text{m}$ at 110 K), the idea is to apply nBn concept to InSb detector.

In this communication, we report results obtained on a new InSb/InAlSb/InSb bariode, grown by MBE on (100)-oriented InSb substrate. Because of a very weak valence band offset with InSb (~ 25 meV), InAlSb is a good candidate as a barrier layer (BL) for electrons. However, due to lattice mismatch with the InSb substrate, careful growth study of InAlSb BL was made to insure high crystal quality.

As a result, nBn detector device exhibits dark current density equals to 7×10^{-7} A.cm⁻² at 110 K : one decade lower than InSb standard pin photodiode with similar cut-off wavelength. Such result demonstrates the potentiality of InSb detectors with nBn architecture to reach the HOT.

9370-23, Session 6

MTF performance: measurements, modelisation, and optimization for Sofradir II-VI IR photodetectors

Jocelyn Berthoz, Laurent Rubaldo, Magalie Maillard, Rachid Taalat, Romain Grille, Nicolas Péré-Laperne, Alexandre Kerlain, SOFRADIR (France); Alexandre Ferron, CEA - LETI (France); Olivier Gravrand, CEA-LETI (France)

SOFRADIR is widely present on the IR detector market for high-performance space, military and security applications thanks to a well mastered Mercury Cadmium Telluride (MCT) technology, and recently thanks to the acquisition of III-V technology: InSb, InGaAs, and QWIP quantum detectors. As a result, strong and continuous development efforts are deployed to deliver cutting edge products with improved performances in terms of sensitivity, spatial and thermal resolution. The actual trend in quantum IR detector development is the design of very small pixel, with high operating temperature. The self-confinement of neighboring diodes may not be efficient enough to maintain optimal modulation transfer function (MTF).

This paper presents the recent developments achieved in Sofradir in terms of MTF measurements protocol challenged by the pitch reduction. An overview of state of the art MTF results with optimized measurement

**Conference 9370: Quantum Sensing and
Nanophotonic Devices XII**

technic will be shown, from SWIR to VLWIR MCT focal plane and also for III-V arrays. In order to optimize device performances and reduce development cycles, this experimental approach has been coupled with finite elements modelisation (FEM), and optimized MTF results for 10 μ m pitch MCT technology will be exposed.

9370-24, Session 6

**New development of the Sb-based III-V
infrared detector material (*Invited Paper*)**

Meimei Tidrow, U.S. Army Night Vision & Electronic
Sensors Directorate (United States)

No Abstract Available

9370-25, Session 7

**High-frequency gallium arsenide nano-
optomechanical systems (*Invited Paper*)**

Ivan Favero, William Hease, Biswarup Guha, Dac Trung
Nguyen, Eduardo Gil Santos, Univ. Paris 7-Denis Diderot
(France); Pascale Senellart, Aristide Lemaitre, Lab. de
Photonique et de Nanostructures (France); Sara Ducci,
Giuseppe Leo, Univ. Paris 7-Denis Diderot (France)

I will present our recent research on Gallium Arsenide disk optomechanical resonators confining photons and phonons in a sub-micron interaction volume [1], and reaching an extreme optomechanical coupling of several MHz [2,3]. The understanding of mechanical and optical dissipation in these resonators [4], together with its control to the ultra-low dissipation limit [5], will be exposed. With their strong optomechanical cooperativity, these miniature disks are also compatible with on-chip integration [6] and optoelectronics technologies based on III-V semiconductors. We have taken advantage of these assets to explore the fluidic operation of Gallium Arsenide devices, their close-to-quantum operation, and their interface with Quantum Dots or Quantum Wells for novel polariton-optomechanical scenarios [7].

[1] L. Ding et al. Physical Review Letters 105, 263903 (2010).

[2] L. Ding et al. Applied Physics Letters 98, 113108 (2011).

[3] C. Baker et al. arXiv:1403.4269 (2014), to appear in Optics Express.

[4] C. Baker et al. Applied Physics Letters 99, 151117 (2011).

[5] D. Parraïn et al. Applied Physics Letters 100, 242105 (2012).

[6] D. T. Nguyen et al. Applied Physics Letters 103, 241112 (2013).

[7] J. Restrepo et al. Physical Review Letters 112, 013601 (2014).

9370-26, Session 7

**Chaotic behaviour of photonic crystals
resonators (*Invited Paper*)**

Andrea Di Falco, Univ. of St. Andrews (United Kingdom);
Changxu Liu, King Abdullah Univ. of Science and
Technology (Saudi Arabia); Thomas F. Krauss, The Univ. of
York (United Kingdom); Andrea Fratallocchi, King Abdullah
Univ. of Science and Technology (Saudi Arabia)

The efficiency of an optical resonator, also known as quality factor (Q), is determined by the ratio of the stored electromagnetic energy and the power dissipated through all the possible loss channels, at a given frequency. Most applications benefit of the highest possibly Qs, e.g. to fabricate sensors, delay lines, lasers, tunable filters and in general to promote a strong

interaction between light and matter. Usually this requirement is achieved at the expense of the bandwidth of the resonator. Here we present a class of photonic cavities that exploit chaos to trap efficiently light in a very broad range of wavelengths. To this extent we adopt Photonic Crystals (PhCs) resonators based on silicon-on-insulator platform in the near infrared range. The choice is motivated by the fact that PhCs resonators can be defined with an arbitrary topology and that they enable an extremely accurate control of the loss channels. In particular, we show here theoretically and experimentally how chaotic PhCs resonators can be used for energy harvesting applications, the generation of linear rare and extreme events and the demonstration of fundamental theories, like the onset of superradiance in quantum systems.

9370-27, Session 7

**Solitons and coherent dispersive wave
emission in SiN microresonators (*Invited
Paper*)**

Victor Brasch, Tobias Herr, Michael Geiselmann, Ecole
Polytechnique Fédérale de Lausanne (Switzerland);
Michael L. Gorodetsky, Lomonosov Moscow State Univ.
(Russian Federation); Tobias J. Kippenberg, Ecole
Polytechnique Fédérale de Lausanne (Switzerland)

Temporal solitons, and more generally optical pulses, can in the presence of higher order dispersion give rise to the emission of dispersive waves. The process enables efficient transfer of energy from the pulse to different spectral regions, that can be spectrally widely separated from the pump pulse. Dispersive wave emission is recognized as one of the most central nonlinear frequency conversion processes and has played a key role for optical frequency metrology, attaining broadband supercontinuum spectra for spectroscopy and has experimentally been studied extensively in optical and photonic crystal fibers. Recently temporal solitons in a crystalline microresonator have been reported and it has been theoretically predicted that temporal solitons and dispersive wave emission leading to ultrabroadband spectra, should be able to occur in chip-scale SiN microresonators. SiN micro-resonators are a unique platform, as they are CMOS compatible, can be further integrated with optical and electrical functionality and have in recent years emerged as a highly promising platform for nonlinear, parametric frequency conversion and frequency comb generation.

Here we report for the first time the observation of temporal solitons and soliton induced coherent dispersive wave emission in a fully planar, on chip micro-resonator based on SiN. By suitable dispersion and mode engineering, we observe formation and stable generation of multiple cavity solitons. Higher order dispersion leads the soliton to emit a dispersive wave into the normal dispersion regime, whose spectral coherence we demonstrate. These results demonstrate the remarkable ability to access the rich Physics of soliton induced spectral broadening phenomena with a continuous wave (CW) laser in on-chip dispersion engineered SiN microresonators. From a technological perspective it enables synthesis of coherent ultra-broadband frequency comb spectra that can find application in spectroscopy, frequency metrology and astrophysical spectrometer calibration. Moreover the temporal solitons may serve as on chip optical buffers or on chip low phase noise microwave generation. In conjunction with the ability to integrate additional electrical and optical functionality this could provide a route to compact, electrically driven low phase noise RF generators for timing, positioning and navigation applications or modules for coherent communication.

9370-28, Session 7

Converting mid-infrared signals to near-infrared through optomechanical transduction

Alexandros Kapsalis, Charis Mesaritakis, National and Kapodistrian Univ. of Athens (Greece); Adonis Bogris, Technological Educational Institute of Athens (Greece); Dimitris Syvridis, National and Kapodistrian Univ. of Athens (Greece)

Mid-infrared silicon photonics surface as the dominant technology to bridge photonics and electronics in multi-functional high-speed integrated chips. The transmission and processing of optical signals lying at the mid-infrared wavelength region is ideal for sensing, absorption-spectroscopy and free-space communications and the use of group IV materials becomes principally promising as the vehicle towards their realization. In parallel, optical forces originating from modes and cavities can reach to outstandingly large values when sizes drop into the nanoscale.

Here, we propose the exploitation of large gradient optical forces generated between suspended silicon beams and optomechanical transduction as a means of converting signals from the mid-infrared to the near-infrared region. A mid-infrared signal is injected into the waveguide system so as to excite the fundamental symmetric mode. In the 2-5 μ m wavelength range, separation gaps in the 100nm order and waveguide widths ranging from 300-600nm, the mode is mostly guided in the air slot between the waveguides which maximizes the optomechanical coupling coefficient and optical force. The resulting attractive force deflects the waveguides and the deflection is linearly dependent on the mid-infrared optical power.

A simple read-out technique using 1.55 μ m signals with conventional waveguiding in the directional coupler formed by the two beams is analysed. A positive conversion efficiency (>0dB) is foreseen for waveguides with suspending lengths up to 150 μ m. The converter could be ideal for use in sensing and spectroscopy rendering the inefficient mid-infrared detectors obsolete. The low-index unconventional guiding in mid-infrared could be a key component towards multifunctional lab-on-a-chip devices.

9370-29, Session 7

Electric and magnetic dipoles in the Lorentz and Einstein-Laub formulations of classical electrodynamics (*Invited Paper*)

Masud Mansuripur, College of Optical Sciences, The Univ. of Arizona (United States)

The classical theory of electrodynamics is built upon Maxwell's equations and the concepts of electromagnetic field, force, energy, and momentum, which are intimately tied together by Poynting's theorem and the Lorentz force law. Whereas Maxwell's macroscopic equations relate the electric and magnetic fields to their material sources (i.e., charge, current, polarization and magnetization), Poynting's theorem governs the flow of electromagnetic energy and its exchange between fields and material media, while the Lorentz law regulates the back-and-forth transfer of momentum between the media and the fields. As it turns out, an alternative force law, first proposed in 1908 by Einstein and Laub, exists that is consistent with Maxwell's macroscopic equations and complies with the conservation laws as well as with the requirements of special relativity. While the Lorentz law requires the introduction of hidden energy and hidden momentum in situations where an electric field acts on a magnetic material, the Einstein-Laub formulation of electromagnetic force and torque does not invoke hidden entities under such circumstances. Moreover, the total force and the total torque exerted by electromagnetic fields on any given object turn out to be independent of whether force and torque densities are evaluated using the Lorentz law or in accordance with the Einstein-Laub formulas. Hidden entities aside, the two formulations differ

only in their predicted force and torque distributions throughout material media. Such differences in distribution are occasionally measurable, and could serve as a guide in deciding which formulation, if either, corresponds to physical reality.

9370-30, Session 8

Quantum cascade laser-based sensor system for nitric oxide detection (*Invited Paper*)

Frank K. Tittel, J. J. Allred, Yingchun Cao, Nancy Sanchez, Rice Univ. (United States); Wei Ren, Chinese Univ. of Hong Kong (Hong Kong, China); Wenzhe Jiang, D. Jiang, Robert Griffin, Rice Univ. (United States)

Sensitive detection of nitric oxide (NO) at ppbv concentration levels has an important impact in diverse fields of applications including environmental monitoring, industrial process control and medical diagnostics. For example, NO can be used as a biomarker of asthma and inflammatory lung diseases such as chronic obstructive pulmonary disease. Trace gas sensor systems capable of high sensitivity require the targeting of strong rotational-vibrational bands in the mid-IR range. These bands are accessible using high heat load (HHL) packaged continuous wave (CW), distributed feedback (DFB) quantum cascade lasers (QCLs). Quartz-enhanced photoacoustic spectroscopy (QEPAS) permits the design of fast, sensitive, selective, and compact sensor systems [1]. A QEPAS sensor was developed employing a room-temperature (RT), CW, DFB-QCL emitting at 1900.08 cm⁻¹ (5.26 μ m) with an optical excitation power of 60 mW. The measured minimum detection limit (MDL) of the sensor is 7.5 ppbv with a 1 second averaging time and 1 ppbv with a 100 second averaging time. High sensitivity is achieved by targeting the absorption line at 1900.08 cm⁻¹ free of H₂O and CO₂ interference. This detection sensitivity is sufficient for detecting NO in exhaled human breath, with typical concentration levels ranging from 24.0 ppbv to 54.0 ppbv [2].

References:

[1] P. Patimisco, G. Scamaracio, F. K. Tittel, V. Spagnolo. "Quartz-enhanced Photoacoustic Spectroscopy: a review". *Sensors* 14, 6165-6206 (2014)

[2] F. K. Tittel, L. Dong, R. Lewicki, V. Spagnolo et al. "Sensitive detection of nitric oxide using a 5.26 μ m external cavity quantum cascade laser based QEPAS sensor". *Proc. SPIE* 8268, 82680F (2012)

9370-32, Session 8

Quantum cascade laser-based multipass absorption system for hydrogen peroxide detection

Yingchun Cao, Nancy Sanchez, Wenzhe Jiang, Rice Univ. (United States); Wei Ren, Chinese Univ. of Hong Kong (Hong Kong, China); Rafal Lewicki, D. Jiang, Robert Griffin, Frank K. Tittel, Rice Univ. (United States)

Hydrogen peroxide (H₂O₂) is a relevant species related to the oxidative capacity of the atmosphere, the production of radical species such as OH, the generation of sulfate aerosol via oxidation of S(IV) to S(VI), and the formation of acid rain, etc. The detection of atmospheric H₂O₂ involves specific challenges due to its high reactivity and low concentration (ppbv to sub-ppbv level). Traditional methods for measuring atmospheric H₂O₂ concentration are often based on wet-chemistry techniques that require transfer from the gas- to liquid-phase for subsequent determination by fluorescence spectroscopy, which can lead to problems such as sampling artifacts and interference by other atmospheric constituents.

We previously reported a quartz-enhanced photoacoustic spectroscopy-based system for H₂O₂ measurement with a detection limit of 75 ppb for 1-s integration time. In this paper, an updated H₂O₂ detection system based

**Conference 9370: Quantum Sensing and
 Nanophotonic Devices XII**

on long-optical-path-length absorption spectroscopy by using a distributed feedback quantum cascade laser (DFB-QCL) will be reported. A 7.73- μm CW-DFB-QCL and a thermoelectrically cooled infrared detector, optimized for wavelength of 8 μm , are employed for the sensing system. A commercial astigmatic Herriot multi-pass cell with an effective optical path length of 76 m is utilized for gas absorption. Wavelength modulation spectroscopy (WMS) with second harmonic detection is used for enhancing the signal to noise ratio. A minimum detection limit of 20 ppbv is achieved with a 2 s sampling time. Based on an Allan-Werle deviation analysis the minimum detection limit can be improved to 2 ppbv when using an averaging time of 300 s.

9370-33, Session 8
New approaches in quartz-enhanced photoacoustic sensing

Angelo Sampaolo, Univ. degli Studi di Bari Aldo Moro (Italy) and Rice Univ. (United States); Pietro Patimisco, Riccardo Pennetta, Gaetano Scamarcio, Univ. degli Studi di Bari Aldo Moro (Italy); Frank K. Tittel, Rice Univ. (United States); Vincenzo Spagnolo, Univ. degli Studi di Bari Aldo Moro (Italy)

Two novel approaches aimed to achieve enhanced detection sensitivities with quartz enhanced photoacoustic (QEPAS) sensing will be reported. The first approach has been investigated by employing an optical power buildup, cavity system in a QEPAS sensor in order to enhance the light-matter interaction path between the two prongs of a quartz tuning fork (QTF). The new spectroscopic technique is named Intracavity QEPAS (I-QEPAS) and the detection sensitivity with respect to the standard QEPAS approach increases proportionally to the resonator enhancement factor. Recently a custom electronic controller to force the resonant frequency of the cavity to follow fast laser frequency changes induced by the current dither at ~ 16 kHz applied to laser current driver was designed and implemented. A piezo actuator was mounted on one the four high-reflectivity mirrors create a bow-tie cavity. In this manner the I-QEPAS sensor can operate in the wavelength modulation regime with the advantage of background-free detection.

The second approach consists of employing QTFs of different geometries in a QEPAS system. A detailed analysis of the piezoelectric properties in terms of resonance frequencies, quality factors, gas damping effects and thermal noise level, with the aim of selecting the best design for sensing applications will be presented. Furthermore, an innovative design of a gold pattern for electrical contacts, which allows an enhancement of the piezoelectric response of a QTF in terms of output piezoelectric current versus mechanical deformation, will be described.

9370-34, Session 8
Quartz-enhanced photoacoustic sensors for H₂S trace gas detection

Vincenzo Spagnolo, Politecnico di Bari (Italy) and CNR-Istituto di Fotonica e Nanotecnologie (Italy); Pietro Patimisco, Angelo Sampaolo, Univ. degli Studi di Bari Aldo Moro (Italy) and CNR-Istituto di Fotonica e Nanotecnologie (Italy); Riccardo Pennetta, Univ. degli Studi di Bari (Italy); Mario Siciliani de Cumis, Istituto Nazionale di Ottica (Italy) and European Lab. for Nonlinear Spectroscopy (Italy); Silvia Viciani, Simone Borri, Paolo De Natale, Istituto Nazionale di Ottica (Italy) and European Lab. for Nonlinear Spectroscopy (Italy); Francesco D'Amato, Istituto Nazionale di Ottica (Italy); Miriam S. Vitiello, Consiglio Nazionale delle Ricerche (Italy); Gaetano

Scamarcio, Univ. degli Studi di Bari Aldo Moro (Italy) and CNR-Istituto di Fotonica e Nanotecnologie (Italy)

Environmental monitoring is among the topics of larger interest for both scientific and civil purposes and hydrogen sulfide (H₂S) is one of the most relevant gas molecules due to its high toxicity. In order to perform real-time monitoring of this molecule, we developed three different sensors based on quartz-enhanced photoacoustic spectroscopy (QEPAS) and compare their performances in terms of sensitivity and selectivity.

The first sensor makes use of a semiconductor diode laser emitting at 2.7 μm . Its strength lies in the compactness and very low cost of all the components. The QEPAS sensor operating in the mid-IR range employed an external-cavity quantum cascade laser (EC-QCL) tunable between 7.6 and 8.3 μm . We employ a single mode hollow waveguide (HWG) to deliver the laser beam to the QEPAS cell. The HWG allows cleaning the astigmatic beam exiting the QCL into a TEM₀₀ mode optimal for beam focusing through the quartz tuning fork (QTF). The QEPAS sensor operating in the THz range employs a QCL working at 2.95 THz and a custom QTF specifically designed to provide higher opto-transduction performances and shaped in order to allow the focusing of ~100 μm wavelength laser beam between the two QTF prongs without hitting them.

For the three QEPAS sensors we select H₂S absorption features with line-strengths in the range 10-21-10-20 cm/mol and QEPAS normalized noise-equivalent absorptions in the 10-9-10-10 W $\cdot\text{cm}^{-1}\cdot\text{Hz}^{-1/2}$ range were achieved. A detailed comparison between the performances, potentialities and cost-effectiveness of the three QEPAS sensors systems will be provided.

9370-35, Session 8
Use of external cavity quantum cascade laser compliance voltage in real-time trace gas sensing of multiple chemicals

Mark C. Phillips, Matthew S. Taubman, Pacific Northwest National Lab. (United States); Jason M. Kriesel, Opto-Knowledge Systems, Inc. (United States)

We describe a prototype trace gas sensor designed for autonomous real-time detection of multiple chemicals. The sensor uses an external cavity quantum cascade laser (ECQCL) swept over its tuning range of 940-1070 cm^{-1} (9.3-10.7 μm) at a 10 Hz repetition rate, with 10 scans averaged to provide an overall spectrum update rate of 1/second. The sensor was operated in two modes, with both modes using detection of the ECQCL compliance voltage. In the first operation mode, the ECQCL output was propagated through a 60 m path length astigmatic Herriott cell and detected using a TE-cooled infrared photo-detector. In this operating mode, the compliance voltage provided a reference power monitor to detect variations in optical power. In the second operation mode, the ECQCL was used for intracavity absorption via detection of the compliance voltage. The sensor was characterized for detection of gas-phase chemicals including ammonia, methanol, ethanol, isopropanol, and Freon-134a. The sensor opto-mechanics and electronics were housed in a portable, compact enclosure of dimensions 0.3x0.3x0.3 m and consumed 100 W of electrical power.

In addition to laboratory characterization results, we present an example of using the sensor for mobile detection of ammonia downwind of cattle facilities. The sensor was operated from battery power and placed inside an automobile. Ammonia concentrations were recorded from this mobile platform at 1 s intervals and correlated with GPS location data.

9370-36, Session 8
Field test results of compound specific isotope analyzer based on quantum cascade lasers and hollow waveguide

Sheng Wu, Andrei Deev, California Institute of Technology (United States)

Conference 9370: Quantum Sensing and Nanophotonic Devices XII

The shale boom helped the energy independence, and one requirement is to logging while drilling (LWD). One of the data logged is compound specific isotope analysis (CSIA) data for C_{1,2,3}, which used to be only available as an offline service at dedicated laboratories using Isotope Ratio Mass Spectrometer (IRMS). Our field deployable infrared isotope ratio spectrometer for CSIA has reached the stability as good as mass spectrometer based CSIA.

Both CSIA-IRMS and our newly developed Infrared Isotope Ratio (IR2) spectrometer for CSIA demonstrated the existence of the fine variations, i.e. <0.05‰, in isotopic ratio as the pulse width, backing pressure and flow rate are varied for reference gases. However, IR2 has better stability over longer period of time, i.e. >1,000 seconds, and therefore better divulge such variations. The demonstrated stability translates directly into accuracy of the IR2 instrument, and bodes well for a calibration free or minimal calibration CSIA instrument which fits best for field deployment.

We also present the test results, and show that the CSIA data provided at the well-site enable LWD that could help the well drilling stay inside the “sweet spot” during horizontal drilling process.

9370-37, Session 9
Quantum cascade laser stabilization at sub-Hz-level by use of a frequency comb and an optical link (*Invited Paper*)

Bérengrère Argence, Bruno Chanteau, Univ. Paris 13 (France); Olivier Lopez, Univ. Paris 13 (France) and Ctr. National de la Recherche Scientifique (France); Daniele Nicolodi, Michel Abgrall, Lab. National de Metrologie et d'Essais (France); Christian Chardonnet, Univ. Paris 13 (France) and Ctr. National de la Recherche Scientifique (France); Christophe Daussy, Univ. Paris 13 (France); Benoit Darquie, Univ. Paris 13 (France) and Ctr. National de la Recherche Scientifique (France); Yann Le Coq, Lab. National de Metrologie et d'Essais (France); Anne Amy-Klein, Univ. Paris 13 (France)

With their large mid-infrared spectral coverage, Quantum Cascade Lasers (QCL) are very promising for probing the molecular fingerprint region. Current applications to high-resolution spectroscopy are mainly limited by their large free-running frequency instability. A lot of efforts have thus been made recently to characterize and improve their spectral properties, especially the emission linewidth and the traceability to frequency standards. Here we demonstrate the frequency stabilization of a QCL emitting at 10 μm onto an optical frequency comb (OFC), itself controlled with a remote near-infrared ultra-stable laser. The latter is transferred from a metro-logical institute with an optical link of 43 km and its frequency is monitored by frequency standards. From the OFC stability, one can infer a QCL linewidth below 1 Hz and a relative frequency stability of 2×10^{-15} for an averaging time of 1 s. Moreover the QCL frequency is known with an uncertainty of at most 10⁻¹⁴ after 100 s averaging time, thanks to the traceability to primary standards. This performance overcome by at least two orders of magnitude what has been demonstrated up to now with a QCL. We further demonstrate the continuous tuning of this stabilized QCL and recorded a few OsO₄ molecular absorption lines which cannot be easily probed with gas lasers such as CO₂ lasers. The saturated absorption linewidth is 25 kHz, well below what has ever been recorded with a QCL. These results open the way to ultra-high precision measurements with molecules with the same performance than currently achieved with atoms.

9370-38, Session 9
Widely tunable quantum cascade lasers for spectroscopic sensing (*Invited Paper*)

Joachim Wagner, Ralf Ostendorf, Fraunhofer-Institut für

Angewandte Festkörperphysik (Germany); Jan Grahmann, André Merten, Fraunhofer Institute for Photonic Microsystems (Germany); Stefan Hugger, Jan Philip Jarvis, Frank Fuchs, Fraunhofer-Institut für Angewandte Festkörperphysik (Germany); Dusan Boskovic, Fraunhofer Institute for Chemical Technology (Germany); Harald Schenk, Fraunhofer Institute for Photonic Microsystems (Germany)

Continuous tuning of quantum cascade lasers (QCL) over a wide wavelength range can be achieved by placing a QCL chip with a broad gain spectrum into an external cavity (EC-QCL), employing e.g. a diffractive grating as wavelength-selective feedback-element. This way wavelength tunability over >25% of the central wavelength can be achieved routinely in the mid-infrared (MIR) spectral range, which is of particular interest for molecular fingerprint spectroscopy. Moreover, EC-QCL technology combines the benefit of a high spectral brightness with a collimated low-divergence output beam. This enables numerous new applications of MIR spectroscopy in non-contact analysis and sensing.

In this paper recent advances in broadband-tunable EC-QCL technology will be discussed with special emphasis on kHz scan rate EC-QCL employing optical MEMS components for wavelength tuning. Furthermore, exemplary case studies of EC-QCL based MIR spectroscopy will be presented. These include temporally resolved analysis of catalytic reactions in chemical process control as well as imaging backscattering spectroscopy for the detection of residues of explosives on arbitrary surfaces.

9370-39, Session 9
Quantum cascade lasers with optical feedback: regular multimode dynamics (*Invited Paper*)

Lorenzo L. Columbo, CNR-Istituto di Fotonica e Nanotecnologie (Italy) and Politecnico di Bari (Italy); Massimo Brambilla, CNR-IFN UOS Bari (Italy) and Politecnico di Bari (Italy); Francesco P. Mezzapesa, Maurizio Dabbicco, CNR-Istituto di Fotonica e Nanotecnologie (Italy) and Politecnico di Bari (Italy); Gaetano Scamarcio, CNR-IFN UOS Bari (Italy) and Politecnico di Bari (Italy)

Unipolar lasers such as THz and Mid-IR Quantum Cascade Lasers (QCLs) are unique in that their fast carrier recombination time (~1ps) endows them with a typical class-A laser dynamics. The search for ultrashort pulse generation is thus a challenging task and so far pulsed emission was achieved only in an actively mode-locked configurations [ref. e.g. S. Barbieri et al., Nat. Photonics 5, 306 (2011)]. When a QCL is provided with optical feedback by an external mirror, the interference of the intracavity and the retroinjected fields causes the dynamics to be dictated by the competition among a set of continuous wave (CW) modes, close to the resonances of the external cavity modes. We here show that, at difference from bipolar semiconductor lasers (e.g. diode lasers), the destabilization of the single CW emission does not occur via undamped amplification of the relaxation oscillations, but instead it involves the competition among a number of adjacent CW modes. In the framework of the Lang Kobayashi model, we provide the linear stability analysis of the single mode CW emission and numerically show that a) a regime of absolute stability thereof exists versus injection strength for THz emitters and b) in the case of Mid-IR emitters, who exhibit higher Henry factor, the laser shows dynamical regimes where a limited number of modes coherently compete to induce regular oscillations in the field intensity. This phase-locking among modes is a relevant feature that may be a track towards the still sought-after spontaneous pulse generation in QCLs.

9370-40, Session 9

Nonlinear dynamics of quantum cascade lasers with optical feedback

Louise Jumpertz, Télécom ParisTech (France) and III-V Lab. (France); Simon Ferré, III-V Lab. (France); Kevin Schires, Télécom ParisTech (France); Mathieu Carras, III-V Lab. (France); Frédéric Grillot, Télécom ParisTech (France)

Quantum (Q) Cascade lasers can be widely used in optical communications, high-resolution spectroscopy, imaging, and remote sensing due to the wide spectral range from mid-infrared to terahertz regime. The dynamics of Q-Cascade lasers is dominated by the ultrafast carrier lifetime, which is on the order of picoseconds [1]. The combination of optical nonlinearities and ultrafast dynamics is one of the major characteristics of Q-Cascade, and the nonlinear dynamics are extremely useful for understanding the underlying physics as well as for the next generation of Q-Cascade devices. A particular feature of Q-Cascade lasers is the clear absence of relaxation oscillations, which is the consequence of the relatively small carrier lifetime compared to the photon lifetime. Although optical feedback (ie. self-injection) is known to be a robust technique for stabilizing or synchronizing a free-running laser [2], its application to Q-Cascade lasers remains almost unexplored [3,4]. This work aims to discuss the nonlinear photonic properties of Q-Cascade lasers operating under optical feedback employing a set of developed rate equations, which takes into account the upper and lower lasing levels, the bottom state as well as the gain stage cascading. This work analyzes the laser properties subject to optical feedback and complex bifurcation scenarios. Experimental results reveal that Q-Cascade laser undergoes distinct feedback regimes depending on the phase and amplitude of the reinjected field and that the coherence-collapse regime only appears in a very narrow range of operation, making such lasers much more stable than their interband counterparts.

9370-41, Session 9

Nonlinear frequency mixing in QCL-based interferometry: beyond the intrinsic resolution

Francesco P. Mezzapesa, Lorenzo L. Columbo, Massimo Brambilla, Maurizio Dabbicco, Gaetano Scamarcio, Politecnico di Bari (Italy) and CNR-Istituto di Fotonica e Nanotecnologie (Italy)

We develop an all-optical sensing method, based on feedback interferometry in quantum cascade lasers (QCLs), to demonstrate position tracking with nanometer scale resolution. QCLs in the self-mixing scheme act as source and shot-noise limited detector of infrared radiation, allowing for extremely compact differential interferometer. Moreover, we recently reported that QCLs feature ultra-stable dynamics against strong optical re-injection (F.P. Mezzapesa et al., Opt. Express. 21 (11), 13748-13757 (2013)). Hence, QCLs do tolerate feedback strengths which enable to enhance the nonlinearity of the laser active medium, without inducing chaotic dynamics typically shown by bipolar semiconductor laser. Here, nonlinear frequency mixing in a QCL-based common-path interferometer is exploited to increase the sub-wavelength sensitivity to the differential motion far beyond the intrinsic limit of half-wavelength. Specifically, we introduce a simple configuration composed of a mid-IR QCL coupled to a reference oscillator inserted in its optical path to achieve spatial resolution down to the nanometer-scale. The experimental results are in excellent agreement with the numerical simulations based on the Lang-Kobayashi semiconductor rate equations for multiple external cavities. The extension to QCLs with frequency bandwidths that stretch across the THz-gap of the electromagnetic spectrum, may even bring to high specific applications including depth-resolved THz imaging with sub-wavelength accuracy and nano-step height profiling in materials non-transparent to visible light, paving the way towards high resolution 3D reconstruction of sub-surface and/or inbuilt microstructures.

9370-42, Session 9

Mid-IR quantum cascade laser mode coupling in hollow-core, fiber-optic waveguides with single-mode beam delivery

Pietro Patimisco, Angelo Sampaolo, Univ. degli Studi di Bari Aldo Moro (Italy) and CNR-Istituto di Fotonica e Nanotecnologie (Italy); Jason M. Kriesel, Opto-Knowledge Systems, Inc. (United States); Gaetano Scamarcio, Univ. degli Studi di Bari Aldo Moro (Italy) and CNR-Istituto di Fotonica e Nanotecnologie (Italy); Vincenzo Spagnolo, Politecnico di Bari (Italy) and CNR-Istituto di Fotonica e Nanotecnologie (Italy)

Hollow-core, fiber-optic waveguides (HCWs) consisting of a metal and dielectric coating deposited inside a silica tube provide a low-loss means of delivering mid-IR beams. Previously, waveguides with a bore size of 300 μm have been demonstrated to deliver laser beams in the range 8-11 μm with a single spatial mode. In general, single-mode beam profile output has been obtained when $d < 40 \lambda$, where d is the internal diameter of the hollow fiber. Thus in order to obtain single-mode propagation down to $\lambda = 5 \mu\text{m}$, a Ag/AgI HCW with $d \sim 200 \mu\text{m}$ should be employed.

In this work, we investigated the transmission properties of HCWs with bore size of 200 μm in both straight and bent configurations employing three commercial quantum cascade laser sources with wavelength emission of 5.3 μm , 6.9 μm , and 10.5 μm , respectively. Using lenses with different focal lengths, we have experimentally investigated and modeled the influence of the input launch conditions on the loss behavior. Input conditions varied from under filling the fiber bore to overfilling it. We have also examined the effect of input-beam mode quality on the fiber output-mode. The optical properties were found to depend strongly on the launch conditions and the mode quality of the input laser beam. With appropriate launch conditions, the 200 μm -bore HCW are shown to provide efficient single-mode transmission in the investigated mid-IR range with propagation losses down to 1.5 dB/m, bending losses < 0.3 dB and output divergence angle of ~ 15 mrad.

9370-43, Session 10

Selective area growth of III-nitride nanorods on polar, semi-polar, and non-polar orientations: device applications

Steven Albert, Ana Maria Bengoechea-Encabo, David Lopez-Romero, Univ. Politécnica de Madrid (Spain); Philippe De Mierry, Jesús Zúñiga-Pérez, CRHEA-CNRS (France); Xiang Kong, Achim Trampert, Paul-Drude Institut (Germany); Miguel Ángel Sánchez-García, Enrique Calleja, Univ. Politécnica de Madrid (Spain)

New advances on Selective Area Growth (SAG) of InGaN/GaN nanostructures by plasma-assisted MBE on GaN/sapphire templates and Si (111) substrates are presented. Both, axial and core-shell structures are considered. Very intense green electroluminescence is achieved on axial nanoLEDs grown on Si(111) with very small emission drift with current injection.

First results on core-shell InGaN/GaN structures grown by MBE on GaN templates are also presented. Two approaches are followed: i) top down, where cylindrical micro-rods are etched down by ICP from a 3 micron thick GaN/sapphire template, and bottom up, in which very high aspect ratio GaN cores are used. In both cases, GaN and InGaN shell layers are then grown both in axial and radial directions. Potential advantages of this core-shell structure as compared to the axial one are twofold: the increase of emission

**Conference 9370: Quantum Sensing and
 Nanophotonic Devices XII**

surface (lateral area) and the absence of internal electric fields (m-plane). The crystal perfection is much better than that of 2D InGaN films of similar In% composition.

Ordered arrays of GaN and InGaN axial nanostructures are also grown on non-polar and semi-polar directions and subsequently merged into a continuous film to produce high quality pseudo substrates. The resulting films exhibit a very strong luminescence, orders of magnitude higher than from the substrate used. Semi-polar GaN templates have a huge density of stacking faults (SFs) most of them are filtered upon coalescence of the nanostructures grown on top. In all cases there is a preferential growth direction along the c-plane (0001).

PL and spatially resolved CL measurements on individual nanostructures, either polar, non-polar, or semi-polar show that the In% incorporation depends strongly on the crystal plane considered.

9370-44, Session 11
**Enhanced two-photon-absorption using
 sub-wavelength antennas (*Invited Paper*)**

Benjamin Vest, ONERA (France); Benjamin Portier, Lab. de Photonique et de Nanostructures, CNRS (France); Fabrice Pardo, Lab. de Photonique et de Nanostructures (France); Nicolas Péré-Laperne, Emilie Steveler, Lab. de Photonique et de Nanostructures, CNRS (France); Julien Jaeck, ONERA (France); Christophe Dupuis, Nathalie Bardou, Aristide Lemaitre, Lab. de Photonique et de Nanostructures (France); Emmanuel Rosencher, ONERA (France); Riad Haïdar, ONERA (France) and Ecole Polytechnique (France); Jean-Luc Pelouard, Lab. de Photonique et de Nanostructures (France)

Degenerate two-photon absorption (TPA) in semi-conductors has recently drawn much interest, as it allows photocurrent generation by absorption of subbandgap photon pairs. However, as a third-order non-linear optical process, TPA processes in conventional photodiodes remain intrinsically inefficient under low power regimes.

In order to enhance the TPA in a photodiode, one of the conceivable approaches is to improve the light-matter interaction in the active region. Several solutions involving waveguide structures, Bragg microcavities or photonic crystals have already been proposed and have demonstrated a significant increase in TPA levels. Here, we investigate TPA enhancement in a thin photodiode embedded in a metallic nanoantenna, which makes use of multiple resonant effects to induce light confinement and thus field enhancement in the active region of the photodiode.

The full device consists in a 186 nm thick GaAs p-i-n diode embedded in a back reflecting gold mirror and a gold subwavelength lamellar grating on the illuminated side [1]. The electric field is confined in the intrinsic region, far from the metallic interfaces, which reduces the chances of having defect-assisted transitions at the interfaces causing current generation through single-photon absorption [2].

We have experimentally observed a resonance close to 1.47 μm for TM-polarized light, leading to a two-orders-of-magnitude increase of the TPA-photocurrent, while numerical simulations suggest that both gain in TPA-photocurrent and angular dependence can be further improved.

References :

[1] B. Portier, B.Vest et al. , Appl. Phys. Lett. 105, 011108 (2014)

[2] B.Vest et al. , Appl. Phys. Lett. 102, 031105 (2013)

9370-45, Session 11
**Investigation of plasmonic enhancement in
 a quantum dot-in-a-well structure**

Alireza Kazemi, Mohsen Nami, Jun Oh Kim, The Univ. of New Mexico (United States); Monica S. Allen, Jeffery W. Allen, Brett R. Wenner, Air Force Research Lab. (United States); Dean P. Brown, Air Force Research Lab. (United States) and UES, Inc. (United States); Augustine M. Urbas, Air Force Research Lab. (United States); Daniel Feezell, The Univ. of New Mexico (United States); Bill Mitchell, Univ. of California, Santa Barbara (United States); Sanjay Krishna, The Univ. of New Mexico (United States)

Large near-field-assisted coupling at the gap of metallic nanostructures and infrared (IR) photodetectors allows for field enhancement when the detector absorption peak overlaps spectrally with the localized surface plasmon resonance of the structure. To demonstrate this field enhancement effect, we have theoretically and experimentally studied the resonant coupling between plasmonic modes of a split-ring-resonator (SRR) array and a quantum dot-in-a-well (DWELL) heterostructure.

The DWELL sample with a ground state emission peak at 1.2 μm , was grown by molecular beam epitaxy (MBE) on a semi-insulating GaAs substrate. The active region is composed of one stack that consists of 2.3 monolayers (ML) of InAs quantum dots (QDs) embedded in an In_{0.15}Ga_{0.85}As quantum well (QW).

The near-field distribution from the SRRs on the GaAs substrate was first modeled by Comsol simulations and optimized SRR dimensions for maximum near-field coupling into the DWELL sample were extracted.

The DWELL sample was uniformly covered with an array of SRRs, with dimensions from the model, patterned by standard electron-beam-lithography. The resulting SRR arrays have unit cell dimensions of roughly 100nm x 100nm, are nominally 20 nm thick, have an element to element spacing of 1 μm and have a total footprint of 500 μm by 500 μm .

In order to assess the near field coupling of the plasmonic structure (SRR arrays) into the DWELL sample, optical characterization is performed on the SRR-DWELL heterostructure including: near-field scanning optical microscopy (NSOM), room temperature photoluminescence (PL), and IR transmission and absorption measurements are. The results are reported in this presentation.

9370-46, Session 11
**3D hollow nanostructures as high quality
 plasmonic nanocavities for multipurpose
 applications (*Invited Paper*)**

Andrea Jacassi, Michele Dipalo, Mario Malerba, Gabriele C. Messina, Francesco De Angelis, Istituto Italiano di Tecnologia (Italy)

We present a novel manufacturing process capable of defining three-dimensional hollow nanostructures made of noble metals of various shapes and spatial arrangements [1]. The process is robust and enables to structure nanomaterials into unconventional geometries whose characteristic length varies from hundreds of nm up to few tens of μm . We characterized the devices both theoretically and experimentally and we found distinctive optical properties on a wide electromagnetic spectrum spanning from the visible up to the mid infrared region where sharp resonances and extremely high quality factors can be achieved ($Q > 200$). When the devices are fabricated on suspended membranes, the inner hollow nanochannel that passes through the nanostructure can work as an optical nanocavity far below the Abbe diffraction limit. In addition we showed that the antennas are connected by an uninterrupted metallic layer that does not prevent their plasmonic functioning hence they can work as plasmonic

**Conference 9370: Quantum Sensing and
 Nanophotonic Devices XII**

antennas and nanoelectrodes at the same time. These devices are very promising for a wide range of applications spanning from optoelectronics, neuro-electronics, nanoelectrodes for photo-electrochemical catalysis, and photovoltaic. Among them, we show that the fabrication process is compatible with CMOS technology, thus enabling the fabrication of CMOS micro-electrode array with three-dimensional nanoelectrodes coming out of the CMOS surface. The latter enabled their exploitation for the investigation of intracellular action potential of cultured neuronal network together with the spectroscopic investigation of the neuronal biochemical activity.

[1] F. De Angelis et al., 3D Hollow Nanostructures as Building Blocks for Multifunctional Plasmonics. *Nano Letters* 2013, 13, 3353-3358.

9370-47, Session 11
Plasmonic characteristics of metallic nano-ring structures

Doo-Gun Kim, Byung Gue Jung, Seon Hoon Kim, Hyun Chul Ki, Tae Un Kim, Hwe Jong Kim, Korea Photonics Technology Institute (Korea, Republic of); Hong-Seung Kim, Young Wan Choi, Chung-Ang Univ. (Korea, Republic of)

The surface plasmon resonance (SPR) has been an essential technology in chemical and bio-chemical sensing, pharmaceutical research, and environmental monitoring area. It has many major features, such as high sensitivity, real time detection, and non-labeling. More development of different types of SPR sensors have been done recently, which are comparable to or better than the conventional SPR sensors in terms of sensitivity and compactness. Localized surface plasmon resonance phenomenon as a collective oscillation of free electrons in metallic nanostructures has attracted the considerable attention of the scientific society in recent. For an enhanced sensitivity of SPR sensor, we applied metallic nano-ring structure using Polystyrene lift-off process on the conventional SPR sensor. The metallic nano-ring structure can be utilized to perturb the propagation of the surface plasmon. We also have optimized the metallic nano-ring structure using finite-difference time-domain method for the width, thickness, and period of the Polystyrene beads. Then, we have fabricated the metallic nano-ring structures with Polystyrene beads of 400 nm wide. The 330 nm wide metallic nano-ring structures have been obtained. Here, the metallic nano-ring structures were also fabricated on various base metal layers such as thin silver or gold of 30 nm. We have used indirect coupling methods to measure the optical characteristics of the metallic nano-ring structure. Therefore, high sensitivity is obtained due to the surface plasmon on the edge of the bandgap when the metallic nano-ring structures are used to excite the surface plasmon. More detailed results will be presented.

9370-48, Session 11
Photonic and plasmonic modulators based on optical switching in VO₂ (Invited Paper)

Richard F. Haglund Jr., Sharon M. Weiss, Vanderbilt Univ. (United States); Kannatassen Appavoo, Brookhaven National Lab. (United States)

Researchers all around the world are engaged in a technology-driven quest for a new generation of ultrasmall, low power photonic and plasmonic devices. One route to this objective involves hybrid structures that incorporate a phase-changing material into the structure, creating a nanocomposite material in which the optical response of a plasmonic or photonic structure is modulated by a change in phase, crystallinity or dielectric function induced by thermal, optical or electrical stimulus. A number of phase-changing materials have been proposed for this purpose; germanium-antimony telluride (GST), for example, switches its optical properties dramatically during a laser-induced amorphous-to-crystalline

transition exhibiting a change in reflectivity.

Vanadium dioxide (VO₂) has been considered as a model switching material ever since its semiconductor-to-metal transition (SMT) was first described half a century ago. As is now widely known, the SMT is also accompanied by a structural phase transition (SPT) from the M1 (monoclinic) to a rutile (tetragonal, R) crystalline form. However, recent research has shown that this picture is oversimplified. For one thing, intermediate semiconducting phases – the so-called M2 with its antiferromagnetically ordered vanadium chains, and the triclinic (T) phase – lead to more complicated transition dynamics, especially on the ultrafast time scale. In this talk, I describe recent progress in understanding the physical mechanisms underlying the ultrafast optically induced phase transition in VO₂. That understanding, in turn, is leading to new concepts in developing hybrid nanocomposites that incorporate VO₂ in plasmonic and waveguides, enabling the construction of optical switches, modulators and memory elements.

9370-49, Session 12
Quantum cascade laser THz metrology (Invited Paper)

Paolo De Natale, Luigi Consolino, Davide Mazzotti, Annamaria Campa, Marco Ravaro, Istituto Nazionale di Ottica (Italy); Miriam Serena Vitiello, NEST-CNR (Italy); Saverio Bartalini, Istituto Nazionale di Ottica (Italy)

The realization and control of radiation sources is the key for proper development of THz-based metrology. Quantum Cascade Lasers (QCLs) are crucial, towards this purpose, due to their compactness and flexibility and, even more important, to their narrow quantum-limited linewidth. We recently generated an air-propagating THz comb, referenced to an optical frequency comb by nonlinear optical rectification of a mode-locked femtosecond Ti:Sa laser and used it for phase-locking a 2.5 THz QCL [1]. We have now demonstrated that this source can achieve a record low 10 parts per trillion absolute frequency stability (in tens of seconds), enabling high precision molecular spectroscopy [2]. As a proof-of-principle, we measured the frequency of a rotational transition in a gas molecule (methanol) with an unprecedented precision (4 parts in one billion). A simple, though sensitive, direct absorption spectroscopy set-up could be used thanks to the mW-level power available from the QCL. The 10 kHz uncertainty level ranks this technique among the most precise ever developed in the THz range, challenging present theoretical molecular models. Hence, we expect that this new class of THz spectrometers opens new scenarios for metrological-grade molecular physics, including novel THz-based astronomy, high-precision trace-gas sensing, cold molecules physics, also helping to improve present theoretical models.

1. L. Consolino et al., "Phase-locking to a free-space terahertz comb for metrological-grade terahertz lasers," *Nature Communications* 3, 1040 (2012).

2. S. Bartalini et al., "Frequency-Comb-Assisted Terahertz Quantum Cascade Laser Spectroscopy", *Phys. Rev. X* 4, 021006 (2014)

9370-50, Session 12
Octave-spanning THz quantum cascade laser

Markus Roesch, ETH Zürich (Switzerland) and Institute of Quantum Electronics, ETH Zurich (Switzerland); Giacomo Scalari, Mattias Beck, Jérôme Faist, ETH Zürich (Switzerland)

A broadband gain medium is desirable for a wide range of applications in laser science like widely tunable sources employing on-chip tuning, external cavity, or ultrashort pulse lasers. Broad gain is especially interesting when combined with locking techniques which enable the access to comb operation. We present a semiconductor injection laser

**Conference 9370: Quantum Sensing and
Nanophotonic Devices XII**

operating in continuous wave with an emission covering more than one octave in frequency, and displaying homogeneous power distribution among the lasing modes. The gain medium is based on a heterogeneous quantum cascade structure operating in the THz range. The ultra-broad gain bandwidth is achieved by fully exploiting quantum engineering of intersubband transitions, integrating in the same laser ridge different designs of a quantum cascade structure, tailored at different frequencies. Laser emission in continuous wave takes place from 1.64 THz to 3.35 THz (from 89.5 μm to 183 μm in wavelength) with optical powers in the mW range and more than 80 modes above threshold. We characterized the laser in the broadband regime by measuring its beatnote at the roundtrip frequency of about 13 GHz in free-running mode. We could measure linewidths as narrow as 980 Hz limited by jitter, that provide strong indication of frequency comb operation on a spectral bandwidth as wide as 624 GHz. A simple model which includes the dispersion of the waveguide together with the one produced by the gain shows zero or low GVD in the spectral region where narrow beatnote is observed. These results make such devices ideal candidates for octave-spanning semiconductor-laser-based THz frequency combs.

9370-51, Session 12
Mid-IR and terahertz digital holography based on quantum cascade lasers

Marco Ravaro, Massimiliano Locatelli, Eugenio Pugliese, Mario Siciliani de Cumis, Francesco D'Amato, Luigi Consolino, Saverio Bartalini, Istituto Nazionale di Ottica (Italy); Miriam S. Vitiello, Consiglio Nazionale delle Ricerche (Italy); Paolo De Natale, Istituto Nazionale di Ottica (Italy)

Infrared (IR) digital holography based on CO₂ lasers has proven to be a powerful coherent imaging technique due to the reduced sensitivity to mechanical vibrations, to the increased field of view, to the high optical power and to possible vision through scattering media, such as smoke. In this contribution we report IR digital holography based on the combination of quantum cascade laser (QCL) sources and a high resolution microbolometric camera. Our holographic system is suitable for the acquisition of both transmission holograms of transparent objects and speckle holograms of scattering objects, which can be processed in real time to retrieve both amplitude and phase.

QCLs combine highly desirable features for coherent imaging, such as compactness, high optical power, and spectral purity. The present availability of external cavity mounted QCLs having a broad tuning range, makes them suitable sources for multiple wavelength holographic interferometry. In addition, QCL emission covers several windows throughout a large portion of the IR spectrum, from the mid-IR to the terahertz region. This allows taking advantage of the different optical response of the imaged object at different frequencies, which is crucial for applications such as non-destructive testing and biomedical imaging. Such features will be discussed and their practical exploitation demonstrated by showing mid-IR and terahertz holograms.

9370-52, Session 12
Homogeneous anisotropic terahertz response by photo-designed sub-wavelength grating

Lorenzo L. Columbo, CNR-Istituto di Fotonica e Nanotecnologie (Italy) and CNR-IFN UOS Bari (Italy); Francesco P. Mezzapesa, Univ. degli Studi di Bari Aldo Moro (Italy) and CNR-Istituto di Fotonica e Nanotecnologie (Italy); Massimo Brambilla, Univ. degli Studi di Bari Aldo Moro (Italy) and CNR-IFN UOS

Bari (Italy); Maurizio Dabbicco, Univ. degli Studi di Bari Aldo Moro (Italy) and CNR-Istituto di Fotonica e Nanotecnologie (Italy); Miriam S. Vitiello, Consiglio Nazionale delle Ricerche (Italy); Carlo Rizza, Univ. degli Studi dell'Insubria (Italy); Gaetano Scamarcio, Univ. degli Studi di Bari Aldo Moro (Italy) and CNR-IFN UOS Bari (Italy)

We experimentally demonstrate a new scheme for active, all-optical control of the THz wave polarization by photo-imprinting sub-wavelength patterns on a semiconductor (SC) slab. In a pump-probe configuration, we photo-generate a 1D grating of free carriers on a silicon sample with a NIR pump beam passing through a spatial light modulator. The corresponding changes in the SC optical properties are detected using a high-sensitive THz-QCL based interferometer where the laser field nonlinearly interferes with the radiation reflected by the SC target and coupled back into the laser cavity (self-mixing scheme). For a spatial scale of the photo-excited grating much smaller than the THz wavelength the SC shows the typical birefringence of a homogeneous uniaxial crystal (different ordinary and extraordinary principal permittivity) as predicted in a recent work of C. Rizza et al. (C. Rizza et al., *Opt. Lett.* **38**, 1307 (2013)). This metamaterial response can be further tailored by a suitable tuning of the pump intensity. As suggested by the theory based on the Drude model for quasi-free carriers, new unusual THz e.m. behaviours can be induced by 2D photo-generated patterns. We believe that these results will open the door to development of a new class of "soft" (i.e. obtained without any time consuming and device dependent microfabrication), dynamically reconfigurable optical devices (switches, spatial and spectral filters, lenses, polarizers) in the THz frequency range with undoubted impact on both applications (imaging, sensing and material characterization) and fundamental physics.

9370-53, Session 12
Investigating the coherence properties of terahertz quantum cascade lasers with fs-laser combs (*Invited Paper*)

Stefano Barbieri, Univ. Paris 7-Denis Diderot (France)

A near-infrared fs-laser comb in combination with electro-optic mixing can be used to generate a multi-line THz heterodyne receiver spanning a bandwidth of several THz. The use of a fast balanced detection allows the achievement of broad IF bandwidths (>1GHz) with a shot noise limited detection sensitivity. This presentation will overview the application of this coherent detection technique to THz quantum cascade lasers, from early results up to the most recent progress [1]. A special emphasis will be given to the investigation of the coherence properties of this class of lasers, from the characterization of their frequency noise spectral density [2], their mode-locking operation [3], to the coherence properties of multimode broad band THz lasers

[1] Sirtori et al. *Nature Photon.* **7**, 691 (2014)

[2] Ravaro et al. *Opt. Expr.* **5**, 25654 (2012)

[3] Barbieri. et al. *Nature Photon.* **5**, 306-313 (2011)

9370-54, Session 12
All solid state mid-infrared dual-comb spectroscopy platform based on QCL technology (*Invited Paper*)

Andreas Hugi, Markus Geiser, IRsweep GmbH (Switzerland) and ETH Zürich (Switzerland); Gustavo F. Villares, ETH Zürich (Switzerland); Francesco Cappelli, ETH Zürich (Switzerland) and Istituto Nazionale di Ottica (Italy); Stéphane Blaser, Alpes Lasers SA (Switzerland);

Jérôme Faist, ETH Zürich (Switzerland)

We develop a spectroscopy platform for industrial applications based on semiconductor quantum cascade laser frequency combs. The platform's key features will be an unmatched combination of bandwidth (100 cm⁻¹), resolution (100 kHz), speed (100 μ s), size (semiconductor laser based, 7 mm) and robustness (no moving parts), opening doors to beforehand unreachable markets. The parallel acquisition of dual-comb spectrometers comes at the price of enormous data-rates. Due to the frequency-modulated nature of our sources, usual data-reduction techniques employed in conventional dual-comb setups, like coherent averaging, do not work. Therefore, our running laboratory dual-comb spectrometer generates 5 GB/sec. The data is acquired with a 12-bit, 1 GHz, 2.5 GS/sec digital oscilloscope. Afterwards, it is treated on the ETH cluster computer platform Brutus. A single data set occupies easily 150 GB or more of data. One main challenge an industrial dual-comb setup has to overcome is the development of suitable data-acquisition methods and fast data-treatment algorithms. In order to enhance the signal to noise ratio by averaging or to allow process observations, this data-rate must be acquired and reduced by at least one order of magnitude in real-time. We present the development of an integrated acquisition and data-treatment solution for dual-comb spectroscopy setups. Data-treatment has been optimized and allows a data-throughput of 12% using a standard Laptop-computer. This is combined with a commercial 12-bit 1 GHz PCI data-acquisition board to a stand-alone data processing unit. This allows real-time industrial process observation and continuous averaging to improve the signal to noise-ratio.

9370-55, Session 13

Mid-IR integrated photonics for sensing applications *(Invited Paper)*

Luca Carletti, Christelle Monat, Univ. de Lyon (France) and Ecole Centrale de Lyon (France); Regis Orobitchouk, Univ. de Lyon (France) and Institut National des Sciences Appliquées de Lyon (France); Pedro Rojo-Romeo, Zhen Lin, Univ. de Lyon (France) and Ecole Centrale de Lyon (France); Cecile Jamois, Univ. de Lyon (France) and Institut National des Sciences Appliquées de Lyon (France); Jean Louis Leclerc, Pierre Viktorovitch, Xavier Letartre, Christian Grillet, Univ. de Lyon (France) and Ecole Centrale de Lyon (France)

The mid infrared (mid-IR, wavelength range between 2 and 10 μ m) is of great interest for a huge range of applications such as medical and environment sensors, security, defense and astronomy.

Silicon, in the form of SOI waveguides, has attracted significant interest recently as a potential platform for integrated optical devices for the mid-IR. However, for applications at wavelengths $> 3.5 \mu$ m, the silica cladding layer of the SOI platform may become an issue due to its increasing absorption above 3.5μ m and it is therefore crucial to explore other platforms. In this context, SiGe alloys on Si has been suggested (and theoretically predicted) as an advantageous alternative platform to SOI for mid-IR applications. Not only SiGe has potentially a low loss transmission window in the 2 to 12 μ m range, i.e. much wider than Si but nonlinear effects are also meant to be stronger than in Si.

In this talk, I will first present our first experimental reports validating the potential offered by SiGe/Si waveguides (manufactured in CEA-LETI) both in the linear regime (with propagation losses as low as 0.5dB/cm at a wavelength of 4.75 μ m) and nonlinear regime including nonlinear transmission and self-phase modulation using picosecond optical pulses centered at wavelengths between 3 and 5 μ m.

I will then give a broad overview of the different activities recently launched in INL Lyon, in close collaboration with several French, Australian and Korean institutions, under the umbrella of "Mid-IR integrated photonics" with a particular focus on novel integrated sources for the Mid-IR.

9370-56, Session 13

Fabrication of silica integrated waveguide circuits for quantum enhanced sensing, quantum information processing and number resolving detection *(Invited Paper)*

Peter G. R. Smith, James C. Gates, Christopher Holmes, Corin B. E. Gawith, Lewis G. Carpenter, Paolo L. Mennea, Matthew T. Posner, Peter A. Cooper, Stephen G. Lynch, Univ. of Southampton (United Kingdom)

Scaling quantum optical effects from the optical bench to integrated optics yield tremendous benefits in terms of integration density, stability and fidelity. However, in developing this technology it is also vitally important to maintain compatibility with optical fiber for transmission and to achieve low-enough losses to allow for convincing demonstration.

This talk will review integrated optical approaches to quantum information processing, and in particular focus on the use of the industry standard - silica-on-silicon platform widely used within Optical Communications. We will discuss how materials, processing techniques and incorporation of novel elements can be used to create circuits for quantum information processing and sensing. Examples of unique fabrication will include design and fabrication of waveguide devices for operation at mK temperature as photon number resolving detectors. The use of direct UV writing allows the addition of Bragg gratings for loss measurement, path tomography and birefringence characterisation. New glass composition on silicon will be presented with potential for lower losses and operation at lower wavelengths. Further work will show how the use of physical machining and dicing technology can be applied for fabrication of new elements for quantum enabled sensing, detection and information processing.

9370-57, Session 13

Advances in three-dimensional integration technologies in support of infrared focal plane arrays *(Invited Paper)*

Dorota S. Temple, E. P. Vick, D. Malta, M. R. Lueck, RTI International (United States); M. R. Skokan, C. M. Masterjohn, M. S. Muzilla, DRS Technologies, Inc. (United States)

Staring infrared focal plane arrays (FPAs) require pixel-level integration with silicon circuits that provide detector bias, integrate detector current and further process the signals. These 3D integration technologies, for a long time in the shadow of impressive progress in the detector development, are increasingly coming into focus due to the decreasing FPA pixel size and the desire to enhance signal processing capability at the FPA level. The former trend leads to the increased information content within the same FPA die size. The latter trend opens the door to the detector behaving like a smart-system peripheral rather than a passive component—with complex functions like calibration, compensation and self-testing being executed on, rather than off, the FPA chip. This added flexibility could greatly enhance the device performance, increase its stability and reliability, and reduce the size, weight, power and cost of the overall system.

In this paper we will review recent advances in 3D integration technologies that support these key trends in the development of infrared FPAs. We will describe progress in the development of bonding technologies for the face-to-face integration of FPAs with Si readout integrated circuits (ROICs). We will also discuss approaches in which the infrared sensor is integrated with three-dimensional ROIC stacks composed of multiple layers of Si circuitry interconnected using through-silicon vias. We will describe a roadmap for the continued development of the integration technology for increasingly smaller and smarter pixels, and identify development needs that have to be met to transition research results to system-level applications.

9370-95, Session 14

Helmholtz resonator for electric field enhancement from visible to far-infrared

Paul Chevalier, Patrick Bouchon, ONERA (France); Jean-Jacques Greffet, Lab. Charles Fabry, Institut d'Optique (France); Jean-Luc Pelouard, Lab. de Photonique et de Nanostructures (France); Riad Haidar, ONERA (France); Fabrice Pardo, Lab. de Photonique et de Nanostructures (France)

Designing nanoantenna that could strongly and efficiently concentrate incident light into deep subwavelength volumes is a key issue to locally enhance the electric field and thus produce strong light-matter interactions.

Whereas many existing designs are inspired by structures widely used in the radiofrequency domain such as bowtie or Yagi-Uda antennas, here we present a 2D slit-box electromagnetic nanoantenna inspired by the acoustic Helmholtz resonator. It is able to concentrate the energy into tiny volumes, and a giant field intensity enhancement is observed throughout the slit.

We are able to propose a model based on a quasistatic approximation for the field enhancement, which gives reliable rules to design such resonator at various wavelengths. We have been able to demonstrate field intensity enhancement two orders of magnitude above values presented in the literature: from 10^5 in the near infrared to 10^8 in the THz domain (P. Chevalier et al., *Axiv Pre-print*). Eventually we demonstrate that this strong field enhancement is preserved when the incident field is focused on the structure thanks to the large angular acceptance of the Helmholtz structure. (P. Chevalier et al., *JOSAA* 31 (8)).

Noteworthy, we have shown that this field intensity enhancement can also be obtained in three-dimensional structures that are polarization independent.

In the Helmholtz nanoantenna, the field is enhanced in a hot volume and not a hot point, which is of great interest for applications requiring extreme light concentration, such as SEIRA, non-linear optics and biophotonics.

9370-106, Session 14

Polarimetric determination of the orientation of a single nano-emitter (*Invited Paper*)

Clotilde Lethiec, Institut des NanoSciences de Paris, Univ. Pierre et Marie Curie (France); Julien Laverdant, Institut Lumière Matière (France); H. Vallon, Institut des NanoSciences de Paris, Univ. Pierre et Marie Curie (France); Clémentine Javaux, Benoit Dubertret, Ecole Supérieure de Physique et de Chimie Industrielles de la Ville de Paris (France); Ferruccio Pisanello, Istituto Italiano di Tecnologia (Italy); Luigi Carbone, Istituto Nanoscienze-CNR (Italy); Alberto Bramati, Lab. Kastler Brossel, CNRS, Univ. Pierre et Marie Curie (France); Laurent Coolen, Agnès Maître, Institut des NanoSciences de Paris, Univ. Pierre et Marie Curie (France)

The emission of a single nanoemitter coupled to a photonic or plasmonic depends on its emitting dipole orientation and position with respect to the structure, as efficient coupling requires their fitting with the modes of the structures. Nevertheless controlling the dipole orientation remains an experimental challenge. Many experiments rely on statistical trials by the production of numerous samples whereas a more efficient deterministical approach only requires the knowledge of the nature of the emitter and its orientation. We propose here to determine these two parameters by a polarimetric analysis of the emission.

A nanoemitter can be considered either by a single radiating dipole (molecule for example), or by the sum of two orthogonal incoherent dipoles, called 2D dipole. This dimensionality of a given type of nanoemitter can be determined by polarimetric analysis of a statistical collection of several hundreds of individual emitters randomly oriented. Experimentally, for CdSe/CdS nanocrystals, the polarization anisotropy measurements reveal a clear signature of a 2D dipole. Once the emitter dimensionality is determined, the orientation of a single emitter can be inferred by further polarimetric analysis [1].

This polarimetric determination of dipole orientation is complementary to defocused microscopy, and remains suitable even when emission pattern fairly not depend on dipole orientation (2D dipole at a metallic interface...). We illustrate our analytical model by several measurements on high quality semiconductor nanocrystals and nanorods [2].

[1] C. Lethiec et al, *Phys. Rev. X* 4, 021037 (2014),

[2] C. Lethiec et al, *New Journal of Physics* 16, 093014 (2014)

9370-107, Session 14

THz and mid-IR integrated multiwavelength devices (*Invited Paper*)

Jérôme Faist, ETH Zürich (Switzerland)

Quantum cascade laser active regions can be designed to operate with very broad gain curves. Recently, in a recent extreme case, a THz device was demonstrated with a gain curve covering a full octave of frequency. Taking advantage of such broad gain is a challenging task. Recent results in devices based on sampled grating achieved tuning range in the hundred cm⁻¹. Another approach are devices based on arrays of distributed feedback lasers. We demonstrated recently an array of surface-emitting laser with single mode operation and excellent potential for c.w. operation as well as operation of a multi-color DFB laser.

9370-108, Session 14

Top-down and bottom-up fabrication of GaN core/shell micropillar arrays on Si (*Invited Paper*)

Albert V. Davydov, National Institute of Standards and Technology (United States); Sergiy Krylyuk, Jong-Yoon Ha, National Institute of Standards and Technology (United States) and Univ. of Maryland, College Park (United States); Ratan Debnath, Baomei Wen, National Institute of Standards and Technology (United States) and N5 Sensors Inc. (United States); Matthew King, Northrop Grumman Electronic Systems (United States); Marcus Müller, Frank Bertram, Jürgen Christen, Otto-von-Guericke-Universität Magdeburg (Germany); Abhishek Motayed, National Institute of Standards and Technology (United States) and Univ. of Maryland, College Park (United States) and N5 Sensors Inc. (United States)

GaN-based core-shell nanowires have gained significant attention in recent years due to their potential use in electronics, optoelectronics, sensing and energy. These structures show significant benefits including large active surface area, reduced density of structural defects, greater carrier confinement, enhanced light extraction etc. This talk discusses design and fabrication of periodic arrays of vertically aligned GaN core-shell micro- and nano- pillar arrays, realized with a combination of top-down etch and Halide Vapor Phase Epitaxy (HVPE).

ICP and wet etch of lithographically patterned GaN-on-Si epilayers produced a regular array of n-GaN micro- and nano-scale pillars on the (111) Si substrate, followed by selective HVPE growth of n- and p-type

Conference 9370: Quantum Sensing and Nanophotonic Devices XII

shells to complete the core/shell design. Optimization of both etching and epitaxial overgrowth resulted in reduction of dislocation density in the GaN shells aimed at improving transport and optical properties of these device platforms. Control of faceting in the HVPE-grown shells produced core/shell pillars shaped as a) truncated hexagonal pyramids with the {1-101} semi-polar sidewalls, or b) hexagonal prisms with the {1-100} non-polar sidewalls. XRD, electron-backscatter-diffraction (EBSD), TEM, PL, CL and Raman scattering measurements revealed improved crystal quality of GaN and significant strain relaxation in the shells.

Strategies toward fabricating 3D GaN-on-Si p-n and p-i-n heterostructures for large-area photodetectors and LEDs will also be discussed.

9370-31, Session 15

Nitrogen vacancies (NV) centers in diamond for magnetic sensors and quantum sensing *(Invited Paper)*

Mayeul Chipaux, Stéphane Xavier, Thales Research & Technology (France); Alexandre Tallaire, Jocelyn Achard, Lab. des Sciences des Procédés et des Matériaux, CNRS, Univ. Paris 13 (France); Sébastien Pezzagna, Jan Meijer, Univ. Leipzig (Germany); Vincent Jacques, Jean-François Roch, Lab. Aimé Cotton, CNRS, Univ. Paris-Sud and ENS de Cachan (France); Thierry Debuisschert, Thales Research & Technology (France)

Nitrogen Vacancy (NV) centers are point defects in diamond that allow magnetic field sensing based on Optically Detected Magnetic Resonance (ODMR). They are processed in ultrapure single-domain CVD grown diamond crystals and can be operated at room temperature. This results in solid-state sensors with a wide variety of applications. Ensemble of NV centers can be used to perform wide-field magnetic imaging with sensitivity in the nT range. Single NV centers can also be processed, which allows sensing at the atomic scale. This possibility, combined with its unique coherence properties, make NV center an ideal candidate for quantum sensing. The presentation will give an overview of recent progresses in the field.

9370-87, Session 15

Nanophotonic phenomena in atomically-thin van der Waals crystals *(Keynote Presentation)*

Dmitri N. Basov, Univ. of California, San Diego (United States)

Layered van der Waals (vdW) crystals consist of individual atomic planes weakly coupled by vdW interaction, similar to graphene monolayers in bulk graphite. These materials can harbor superconductivity and ferromagnetism with high transition temperatures, emit light and exhibit topologically protected surface states. An ambitious practical goal is to exploit atomic planes of vdW crystals as building blocks of more complex artificially stacked structures where each such block will deliver layer-specific attributes for the purpose of their combined functionality. Infrared (IR) nano-spectroscopy and nano-imaging experiments on hexagonal boron nitride (hBN) have uncovered rich optical effects associated with phonon polaritons in this prototypical van der Waals crystal. We launched, detected and imaged the polaritonic waves in real space and altered their wavelength by varying the number of crystal layers in our specimens [Dai et al. *Science*, 343, 1125, (2014)]. Unlike surface plasmons in graphene that we have imaged using a similar nano-IR toolset [Fei et al. *Nature* 487, 82 (2012)], highly confined phonon polaritons are immune to electronic losses and therefore can travel over distances exceeding 10-s of microns. Peculiar properties of phonon polaritons in hBN enabled sub-diffractive focusing and image

formation in infrared frequencies using a slab of this layered single crystal. I will also discuss an ability to control plasmonic response of graphene at femto second time scales that we have demonstrated using a unique pump-probe nano-IR apparatus [Wagner et al. *Nano Letters* 14, 894 (2014)].

9370-88, Session 15

Ultra fine pitch quantum infrared sensors *(Invited Paper)*

Olivier Gravrand, CEA-LETI (France)

No Abstract Available

9370-89, Session 15

Low noise InGaAs/InP single-photon detector for singlet oxygen detection

Gianluca Boso, Boris Korzh, Tommaso Lunghi, Univ. de Genève (Switzerland); Bruno Sanguinetti, id Quantique SA (Switzerland) and Univ. de Genève (Switzerland); Hugo Zbinden, Univ. de Genève (Switzerland)

Single-photon detectors are the best option for applications where low noise measurements and/or high timing resolution are required.

At wavelength of between 900nm and 1700nm, however, low noise detectors have typically been based on cryogenic superconducting technology, precluding their extended use in industrial or clinical applications.

Here we present a practical (i.e. compact, reliable and affordable) detector [1], based on a negative feedback InGaAs/InP avalanche photodiode [2,3,4,5] (900nm to 1700nm) and exhibiting dark counts < 1 count-per-second at 10% efficiency, and with efficiencies of up to 27%.

In our device, a negative-feedback avalanche photodiode [2,3,4,5] limits the number of charges flowing within the diode, and therefore reduces afterpulsing probability. We are then able to cool the device to 170K using a simple "Free-piston Stirling cooler" whilst maintaining low afterpulsing. Combining this with an appropriate low-noise passive-quench-active-hold-off electronic circuit we obtain the observed high performance.

We show how this novel detector enables long distance quantum key distribution over more than 300km of optical fiber, and how it can be used in a selection of scientific, industrial and medical applications.

[1] B. Korzh et al., *Appl. Phys. Lett.* 104, 081108 (2014)

[2] M. Itzler et al., *J. Mod. Opt.* 58, 174 (2011)

[3] T. Lunghi et al., *J. Mod. Opt.* 59 17 (2012)

[4] S. Cova et al., *Appl. Opt.* 35, 1956 (1996).

[5] F. Zappa et al, *Proc. 8th Int. Conf. IPRM* (1996)

9370-90, Session 15

InGaAs/InP single-photon detector with low noise, low timing jitter and high count rate

Mirko Sanzaro, Niccolò Calandri, Alessandro Ruggeri, Carmelo Scarcella, Gianluca Boso, Mauro Buttava, Alberto Tosi, Politecnico di Milano (Italy)

A growing number of applications in the wavelength range from 1 μm to 1.7 μm need single-photon detectors that both guarantee good performances and are practical to use. An excellent choice is the InGaAs/InP Single-Photon Avalanche Diode (SPAD), which requires moderate cooling and shows good

Conference 9370: Quantum Sensing and Nanophotonic Devices XII

features, but still needs some improvements for noise reduction.

We present a new InGaAs/InP SPAD with high detection efficiency and low noise, which has been employed in a sinusoidal-gated setup for achieving very low afterpulsing probability and high count rate.

The new InGaAs/InP SPAD has lower noise thanks to the improvement of Zinc diffusion conditions and the optimization of the vertical structure. A detector with 25 μm active-area diameter, operated in gated-mode with ON time of tens of nanoseconds, has a dark count rate of few kilo-counts per second at 225 K and 5 V of excess bias, 30% photon detection efficiency at 1550 nm and a timing jitter of less than 90 ps (FWHM).

In order to extremely reduce the afterpulsing probability, these detectors can be operated with a sinusoidal gate at 1.3 GHz. The extremely short gate ON time (less than 200 ps) reduces the charge flowing through the junction, thus reducing the number of trapped carriers and, eventually, lowering the afterpulsing probability. The resulting detection system achieves a maximum count rate higher than 650 Mcount/s with an afterpulsing probability of about 1.5%, a photon detection efficiency greater than 30% at 1550 nm and a temporal resolution of less than 90 ps (FWHM).

9370-91, Session 15

High linearity SPAD and TDC array for TCSPC and 3D ranging applications

Federica A. Villa, Rudi Lussana, Danilo Bronzi, Alberto Dalla Mora, Davide Contini, Politecnico di Milano (Italy); Simone Tisa, Micro Photon Devices S.r.l. (Italy); Alberto Tosi, Franco Zappa, Politecnico di Milano (Italy)

We present a single-photon imager based on an array of 32x32 Single-Photon Avalanche-Diodes (SPADs) and Time-to-Digital Converters (TDCs) fabricated in a 0.35 μm CMOS technology. Each pixel is able to detect photons in the 300 nm – 900 nm wavelength range and provides either the count of detected photon within a frame time or the time stamp of the photon arrival time. In “photon counting” mode an in-pixel 6-bit counter provides photon-number resolved intensity 2D videos at 100 kfps, whereas in “photon timing” mode the 10-bit in-pixel TDC provides time-resolved maps (e.g., fluorescence and Time-Correlated Single-Photon Counting TCSPC measurements) or 3D depth-resolved (through direct Time-of-Flight measurement) images and videos at 100 fps, with 350 ps (i.e. 5.2 cm) single-shot resolution.

The 1024 photon detectors are 30 μm diameter SPADs (3.14% Fill-Factor) with very low Dark Counting Rate (120 counts/s at room temperature, with less than 3% hot-pixels) and 55% peak Photon Detection Efficiency (PDE) at 450 nm wavelength. The 1024 TDCs are constituted by a 6-bit counter and a 4 bit fine interpolator, based on a Delay Locked Loop (DLL) line, which makes the Time-to-Digital conversion insensitive to process, voltage and temperature drifts. We implemented the sliding-scale technique to improve linearity to the excellent results of 2% LSB DNL and 10% LSB INL. The single-shot precision is 260 ps, comprising SPAD, TDC and board time-jitter. Experimental measurements show that optical and electrical crosstalks among SPADs and TDCs are both negligible. We present high-frame rate 2D and 3D videos at the single-photon level and also high resolution (160 x 160 and 160 x 320 pixels) 3D images.

9370-109, Session 15

Terahertz harmonic generation in graphene (*Invited Paper*)

Samwel K. Sekwao, Jean-Pierre Leburton, Univ. of Illinois at Urbana-Champaign (United States)

In this talk we review key features of hot carrier transport interacting with optic phonons in graphene. Specifically, we show that charge carriers under the influence of a DC and a-c fields exhibit sharp resonances in the presence of spatially and temporarily modulated scattering. Resonances occur when

the period of the a-c field corresponds to the time taken by quasi-ballistic carriers to drift over a spatial scattering period, provided the latter is shorter than the distance taken by carriers to emit an optic phonon. We show that such system can be achieved with inter-digitated gates energized with an a-c bias on graphene layers. Gate separation and fields to achieve ballistic transport would result in resonances in the terahertz range, with the generation of higher harmonics characterized by large Q-factors, which are tunable with gate spacing, and well suited for THz detection.

9370-112, Session 15

Photoluminescence quenching of InP/ZnS quantum dots by charge injection

Martin Möbius, Technische Univ. Chemnitz (Germany); Xiangyu Ma, Univ. of Delaware (United States); Jörg Martin, Fraunhofer-Institut für Elektronische Nanosysteme (Germany); Matthew F. Doty, Univ. of Delaware (United States); Thomas Otto, Thomas Gessner, Fraunhofer-Institut für Elektronische Nanosysteme (Germany)

Rising efforts concerning the reduction of CO₂ emission promote the use of fiber reinforced plastics, e.g. in automotive or aircraft engineering due to their production process. Although fiber reinforced plastics have critical properties such as low mass and high stiffness compared to classical materials, they also have unpredictable failures due to structural damage. Thus structural health monitoring is vital for the development of modern lightweight structures.

Our concept of material integrated sensor technology is based on a combination of a piezoelectric foil with a quantum dot polymer composite. By application of a mechanical (over-) load, electrical charges are generated and injected into the nanocrystals causing PL quenching, which is detectable as local optical contrast. A very efficient charge injection is crucial for sensitive load detection, because of limited amount of generated charges and transport losses.

Consequently we have investigated the charge injection and charge storage properties of various types of quantum dots, in particular core shell types CdSe/ZnS and InP/ZnS, embedded in semi-conducting poly(9-vinylcarbazole) (PVK). PL quenching was realized by application of external voltages smaller than 20 V. Initial results indicated a longer charge storage time in InP/ZnS quantum dots, which we achieved by engineering the offset in band level alignment between valence band levels of respective quantum dots and PVK.

9370-58, Session 16

Turning assistive machines into assistive robots

Brenna D. Argall, Northwestern Univ. (United States)

For decades, the potential for automation---in particular, in the form of smart wheelchairs---to aid those with motor, or cognitive, impairments has been recognized. It is a paradox that often the more severe a person's motor impairment, the more challenging it is for them to operate the very assistive machines which might enhance their quality of life. A primary aim of my lab is to address this conundrum by incorporating robotics autonomy and intelligence into assistive machines---turning the machine into a kind of robot, and offloading some of the control burden from the user. Robots already synthetically sense, act in and reason about the world, and these technologies can be leveraged to help bridge the gap left by sensory, motor or cognitive impairments in the users of assistive machines. This talk will overview some of the ongoing projects in my lab, which strives to advance human ability through robotics autonomy.

9370-59, Session 17

Flexibility properties of type-II InAs/ GaSb SL to design MWIR pin photodiodes (Invited Paper)

Philippe Christol, Marie Delmas, Jean-Baptiste Rodriguez, Institut d'Electronique du Sud (France); Edouard Giard, Isabelle Ribet-Mohamed, ONERA (France); Julien Imbert, ONERA (France) and III-V Lab. (France); Sophie Derelle, ONERA (France); Virginie Trinite, III-V Lab. (France)

The last past years, Type-II InAs/GaSb superlattice (T2SL) has emerged as a new material technology suitable for high performance infrared detectors. This was possible because T2SL is a particular quantum structure with several advantages such as the possibility to address, thanks SL bandgap engineering, the midwave and the longwave infrared domains or to design, thanks band offset engineering, barrier structures.

Among T2SL properties, one of the main interesting is that several structures, with different InAs to GaSb thickness ratios in each SL period, can target the same cut-off wavelength. Recent previous work reports the study of photodiodes with different SL periods having the same cut-off wavelength at 5 μ m at 77K. This study shows the strong influence of the SL composition on dark current measurements, shape of spectral responses, quantum efficiency and type of background doping concentration of n-d InAs/GaSb SL active zone.

The objective of this communication is to use the flexibility of T2SL to fabricate by MBE a pin photodiode where the active zone is made of different SL periods. Electrical and electro-optical characterizations are reported and discussed. The results show that optimized SL structure for the MWIR domain can be designed by combining the best of each SL periods.

9370-60, Session 17

Physics and technology of antimonide heterostructure devices at SCD (Invited Paper)

Philip C. Klipstein, SCD Semiconductor Devices (Israel)

SCD has developed a range of advanced infrared detectors based on III-V semiconductor heterostructures, grown on GaSb. The X_{Bn}/X_{Bp} family of detectors enables diffusion limited behavior with dark currents comparable with MCT Rule-07 and with high quantum efficiencies. InAsSb/AlSbAs based X_{Bn} Focal Plane Array detectors with a cut-off wavelength of ~ 4.2 μ m and formats presently up to 1024x1280/15 μ m, operate at 150K with sensitivity and image quality comparable with those of standard InSb detectors working at 77K. In an X_{Bp} configuration, the same concept has been applied recently to develop an InAs/GaSb type II superlattice (T2SL) detector which operates with background limited performance up to 90K at a cut-off wavelength of ~ 9.5 μ m. In order to design our detectors effectively, a suite of simulation algorithms has been developed based on the k · p and Optical Transfer Matrix methods. In a given T2SL detector, the complete spectral response curve can be predicted from a knowledge of the InAs and GaSb layer widths in a single period of the superlattice. Gallium free T2SL detectors in which the GaSb layer is replaced with InAs_{1-x}Sb_x (x ~ 0.15-0.5) have also been simulated and their performance agrees with reports in the literature. Some of the key concepts behind X_{Bn} and X_{Bp} detectors will be discussed and illustrated with results from test devices and detectors grown and fabricated at SCD.

9370-61, Session 17

High-responsivity photovoltaic intersubband detectors

Peter Reininger, Benedikt Schwarz, Hermann Detz, Aaron M. Andrews, Werner Schrenk, Gottfried Strasser, Technische Univ. Wien (Austria)

Spectroscopy drives the research in the mid-infrared spectral region. Detecting light plays an important role in such sensing applications.

Quantum cascade detectors have already proven to be a versatile concept for fast and compact photodetection. Still, the highest reported room-temperature responsivity for the spectral region around 8 μ m is only 2mA/W, which is far below the theoretical maximum.

By introducing a new design, the diagonal transition QCD, we were able to increase both the resistance and the internal quantum efficiency. At room-temperature, our device shows a responsivity of 17mA/W, which is an improvement of almost one order of magnitude.

9370-62, Session 17

10 μ m pitch design of HgCdTe diode array in Sofradir

Nicolas Péré-Laperne, Laurent Rubaldo, Alexandre Kerlain, Emmanuel Carrère, Loïc Dargent, Rachid Taalat, Jocelyn Berthoz, SOFRADIR (France)

Sofradir recently presented Daphnis HD, its latest 10 μ m pitch HD720 product. Daphnis XGA is a 10 μ m pitch 1024x768 mid-wave infrared focal plane array. Development of small pixel pitch is opening the way to very compact products with a high spatial resolution. This new product is taking part in the HOT technology competition allowing reductions in size, weight and power of the overall package.

This paper presents the recent developments achieved in Sofradir to make this 10 μ m pitch HgCdTe focal plane array. Electrical and electro-optical characterizations are presented to define the appropriate design of 10 μ m pitch diode array. The technological tradeoffs are explained to lower the dark current, to keep high quantum efficiency with a high operability above 110K, F/4.

9370-63, Session 17

Extended-shortwave infrared unipolar barrier detectors (Invited Paper)

Gary W. Wicks, Amethyst Research Inc. (United States) and Univ. of Rochester (United States); Terry Golding, Amethyst Research Inc. (United States); Manish Jain, Amethyst Research Inc. (United Kingdom); Gregory R. Savich, Daniel E. Sidor, Xiaoyu Du, Univ. of Rochester (United States); Mukul C. Debnath, The Univ. of Oklahoma Bioengineering Ctr. (United States); Tetsuya D. Mishima, M. B. Santos, The Univ. of Oklahoma (United States)

The e-SWIR wavelength band is a performance gap for detectors. At both shorter and longer wavelengths, high performance detector technologies exist: SWIR InGaAs detectors (1.7 micron cutoff), and MWIR (3-5 micron) detectors such as GaSb-based Unipolar Barriers, MCT, and InSb. This work discusses Amethyst Research's development of high performance e-SWIR detectors with cutoff wavelengths in the 2.5 - 3 micron range.

Two approaches were evaluated, lengthening the wavelength response of the SWIR InGaAs technology and shortening the wavelength response of MWIR GaSb-based technology. Both approaches use unipolar barrier device

Conference 9370: Quantum Sensing and Nanophotonic Devices XII

architectures. The InGaAs e-SWIR approach employs mismatched InGaAs absorber layers on InP substrates, using graded AlInAs buffer layers. The GaSb-based approach uses lattice-matched quaternary absorber layers on GaSb substrates.

The unipolar barrier device architecture enables both types of device to be free of effects of surface leakage currents and generation-recombination dark currents. GaSb-based devices show excellent performance, with diffusion-limited dark current within a factor of 2-4 of the MCT standard, Rule 07. They achieve background-limited (BLIP) performance at T=200K, accessible by thermo-electric coolers. As expected, defects associated with lattice-mismatch increase dark currents of the InP-based approach. Initial results exhibit dark currents that are an order of magnitude larger than those of the lattice-matched GaSb approach, however despite the defects, the devices still exhibit diffusion-limited operation, and achieve BLIP performance at T=175K. Further improvements in the InP-based approach are expected with refinements in the epitaxial structures. Both types of detector approaches are excellent alternatives to conventional e-SWIR detectors.

9370-64, Session 17

Military applications for high-performance thermal imaging (*Invited Paper*)

Kenneth J. McEwan, Defence Science and Technology Lab. (United Kingdom)

Recent developments in high performance thermal imaging in the UK will be reviewed against current sensing requirements.

- Traditional thermal imaging cameras operate around 80 K to reduce the dark current however recent material and ROIC (read out integrated circuit) developments have enabled operation of mid-wave cameras at much higher operating temperatures; approaching 200 K. This has important implications for size, weight and power (SWAP), bringing high performance thermal imaging into the domains dominated by uncooled thermal sensors.
- Developments towards high operating temperature (HOT) also have implications for very large format cameras for persistent wide area surveillance (PWAS). Operating a large format (≥ 16 Mpixel) thermal imaging camera at 80 K would traditionally require an unacceptably large cooling engine however the HOT developments offer significant reductions in cooling making large format cameras feasible.
- CMT based thermal imaging cameras can be operated with high avalanche gain and the pixel read-out circuitry can be designed to measure range when operating in an active imaging mode. Long range, burst illumination 3D imaging has been an aspiration for many years to provide reliable assisted target recognition (ATR). A number of challenges still exist in achieving high avalanche gain, accurate range finding and uniformity across the whole detector array. Recent work towards the high performance, long range 3D imaging will be discussed.

Finally we will describe some recent work on III-V materials exploiting the nBn detector format. This approach has the potential to provide low noise operation required for certain applications such as the stand-off detection of Raman scattered light from chemical contaminants. Recent results that exploit the low background noise will be described.

9370-65, Session 18

High-power non linear frequency converted laser diodes (*Invited Paper*)

Ole B. Jensen, Peter E. Andersen, Anders K. Hansen, Technical Univ. of Denmark (Denmark) and DTU Fotonik (Denmark); Dominik Marti, Risø DTU (Denmark) and DTU Fotonik (Denmark); Peter M. W. Skovgaard, Norlase ApS (Denmark); Paul M. Petersen, Technical Univ. of Denmark (Denmark)

Many applications, e.g., within biophotonics require laser sources in the blue-green spectral range. A preferred method for such lasers has been frequency doubled solid state lasers. Such technology tends to be bulky and expensive and therefore alternatives are desired. Tapered diode lasers are an established method to generate high power near-diffraction limited light at wavelengths ranging from red to infrared. Nonlinear frequency conversion of tapered diode lasers is an efficient method for generation of coherent light in the required blue-green spectral range.

We present different methods of generating light in the blue-green spectral range by nonlinear frequency conversion of tapered diode lasers. In the blue spectral range, we will present results using single-pass second harmonic generation (SHG) as well as cavity enhanced sum frequency generation (SFG) with watt-level output powers. SHG and SFG are also demonstrated in the green spectral range as a viable method to generate up to 4 W output power with high efficiency using different configurations. The presented power levels are state-of-the-art for nonlinear frequency converted diode laser systems.

Examples of applications using such frequency converted lasers as pump sources for Ti:sapphire lasers and use within biophotonics imaging will be presented. The low noise of the diode laser sources gives enhanced contrast in the biophotonics imaging, important for diagnostics.

9370-66, Session 18

High-power tunable two-color VECSEL for on-demand wavelength generation (*Invited Paper*)

Mahmoud Fallahi, Chris Hassenius, Michal Lukowski, College of Optical Sciences, The Univ. of Arizona (United States)

There are growing needs for new sources emitting at unconventional wavelengths for numerous new applications. While direct bandgap engineering of semiconductor heterostructures allows efficient fundamental wavelengths generation in the visible, near-infrared and mid-infrared regions, significant wavelength gaps still remain to be filled. Nonlinear frequency conversion in high power semiconductor lasers is an attractive approach to fill these gaps. Optically pumped Vertical-External-Cavity Surface-Emitting Lasers (VECSEL) are very attractive for their high power, high beam quality and wide tuning operation. Open cavity of VECSELs provide easy access to the high intracavity circulating power of hundreds of watts, allowing new functionalities such as linewidth control, wavelength tuning and efficient nonlinear frequency conversion. Tunable two-color VECSELs are particularly suitable for new color generation via intracavity nonlinear conversion. Recently we demonstrated a novel widely tunable T-cavity two-chip VECSEL in which the two cavities with orthogonally polarized beams share a collinear section. In this talk I present details and discuss our recent advances in two-color T-cavity VECSELs used for efficient intracavity nonlinear wavelength generation. Two-color wavelength separation in the range of 0-200 nm will be shown. I will also report our latest results on intracavity tunable type-II sum frequency generation (SFG) for visible and difference frequency generation (DFG) for long wavelengths.

9370-67, Session 18

Frequency conversion in AlGaAs microdisks in the telecom range (*Invited Paper*)

Giuseppe Leo, Silvia Mariani, Alessio Andronico, Univ. Paris 7-Denis Diderot (France); Aristide Lemaitre, Lab. de Photonique et de Nanostructures (France); Sara Ducci, Ivan Favero, Univ. Paris 7-Denis Diderot (France)

Frequency conversion can be very efficient in whispering gallery mode

Conference 9370: Quantum Sensing and Nanophotonic Devices XII

semiconductor microresonators, thanks to high optical confinement and modal overlap. The crystallographic symmetry of AlGaAs, along with the circular geometry, provides effective quasi-phase matching without the burden of domain inversion. In this framework, some experimental studies have been recently reported on Second Harmonic Generation (SHG) in GaAs WGM microdisks. However, GaAs does not allow working with a Fundamental Frequency (FF) mode in the third fiber window of the telecom range, since the SH photon energy exceeds the energy gap and two-photon absorption losses are high up to 1800 nm.

Here we report on the demonstration of CW SHG in Al_{0.4}Ga_{0.6}As suspended microdisks on GaAs pedestal, with FF wavelength around 1.55 μm and an efficiency $\eta = 0.7 \times 10^{-3} \text{ W}^{-1}$ comparable to state-of-the-art monolithic telecom devices. This result was obtained via the evanescent coupling between the disk and a tapered fiber, with 3.5 mW input power injected in the fiber.

Then we discuss the down-conversion that can occur in the same microdisk, with inverted roles for the SH (which becomes the input pump) and FF (which corresponds to the output signal and idler). In this case, with 3 ps pulses and a repetition rate of 300 kHz, a peak power of about 10 kW at 775 nm can provide signal and idler peak power of about 5 μW at degeneracy.

Finally, we illustrate the fabrication of the monolithic counterpart of such submicron-system, with a suspended AlGaAs nanowire in lieu of the fiber.

9370-68, Session 18
Integrated optical sensing technologies on Si (Invited Paper)

Amr S. Helmy, Payam Abolghasem, Janahan Ramanan, Dongpeng Kang, Dylan F. Logan, Univ. of Toronto (Canada)

An effective approach to achieve efficient phase matching for second order nonlinearities, in multilayer structures will be discussed. It uses dispersion engineering in Bragg reflection waveguides to harness parametric processes in conjunction with concomitant dispersion and birefringence engineering in active devices. This technology enables novel coherent light sources using frequency conversion in a self pumped chip form factor. These sources can also provide continuous coverage of spectral regions, which are not accessible by other technologies including quantum cascade lasers. Examples of niche applications served by this platform include sources for environmental and biomedical sensing elements in the 2-3 μm window and the 7-9 μm window. This approach has been recently demonstrated in multi-layer Silicon-Oxy-Nitride (SiON) waveguides. Harnessing $\chi^{(2)}$ in SiON offers a route for integration of broadband infrared sources using frequency mixing with optofluidics. Different approaches for implementing optofluidic structures on SOI will be discussed, where the root cause of enhancing the retrieved Raman and infrared signals in these structures will be explained. Recent progress in using this approach to study different nanostructures and biological molecules will be presented.

9370-69, Session 19
Interband cascade lasers with high CW power and brightness (Invited Paper)

Mijin Kim, Sotera Defense Solutions, Inc. (United States); Chul Soo Kim, William W. Bewley, Charles D. Merritt, Chadwick L. Canedy, Joshua Abell, Igor Vurgaftman, Jerry R. Meyer, U.S. Naval Research Lab. (United States)

We enhanced the external differential quantum efficiency of broad-area interband cascade lasers (ICLs) operating in pulsed mode by increasing the thickness of the n-doped GaSb separate-confinement layers and also increasing the number of stages from 5 to 7 or 10. When HR/AR-coated narrow ridges with corrugated sidewalls and emitting at $\approx 3.5 \mu\text{m}$ wavelength were mounted epitaxial-side-down using a proprietary process,

a 22-micron-wide 7-stage device with HR/AR-coated facets produced 384 mW cw at $T = 25^\circ\text{C}$, while a 32-micron-wide ridge generated 592 mW. At 25°C , the maximum WPE was 13.2% while it was 10.1% at the highest current. Measurements of the far-field intensity profiles along the slow axis yielded beam quality factors of $M^2 = 2.4$ and 3.7 for the 22- and 32-micron-wide devices, respectively.

Subsequent ridges with more pronounced sidewall corrugations produced slightly lower maximum cw powers, but substantially better beam quality. For example, a 7-stage 18-micron-wide ridge emitting at $\approx 3.1 \mu\text{m}$ wavelength produced 326 mW in a beam with $M^2 = 1.34$, which corresponds to the highest brightness observed to date for an ICL. A 4-mm-long tapered-ridge laser processed from the same wafer with 1° taper and 4 mm cavity length produced 180 mW with $M^2 = 1.05$. A 12-micron-wide ridge with 1 mm cavity length, HR/AR coatings, and emitting at $\approx 3.5 \mu\text{m}$ wavelength generated 74 mW cw with a record wallplug efficiency of 18.4%.

9370-70, Session 19
Widely-tunable interband cascade lasers for the mid-infrared (Invited Paper)

Michael von Edlinger, Julian Scheuermann, nanoplus GmbH (Germany); Robert Weih, Julius-Maximilians-Univ. Würzburg (Germany); Lars Naehele, Marc Fischer, nanoplus GmbH (Germany); Sven Höfling, Julius-Maximilians-Univ. Würzburg (Germany); Johannes Koeth, nanoplus GmbH (Germany); Martin Kamp, Julius-Maximilians-Univ. Würzburg (Germany)

A multitude of absorption lines of important gases is located in the infrared region between 3 μm and 6 μm , making it very interesting for tunable diode laser spectroscopy (TDLs). In recent years, interband cascade laser (ICL) have shown good laser performance in this spectral region, including very low threshold current densities below 100 A/cm² and emission at room temperature at wavelengths above 7 μm . The first part of the talk will discuss these results and the potential for further developments of ICLs. In addition to cw operation at room temperature, TDLs applications also require single mode or tunable laser emission. A widely-tunable laser allows sensing of multiple gas absorption lines in a gas mixture or can be used to determine the base line of a measurement by sampling a far-away spectral region. The most commonly used single mode lasers employ distributed feedback (DFB) for mode selection. They offer a limited degree of tunability (a few nanometers), mainly due to the temperature induced change of the refractive index when the drive current is varied. The second part of the talk will discuss devices with multiple segments and special grating structures that allow an increased tuning range. Tuning is achieved by changing the drive currents of the segments, resulting in a change of the refractive index and a corresponding shift of the modes. The design of such lasers, their tuning performance and applications to gas sensing will be presented.

9370-71, Session 19
Interband cascade laser based absorption sensor for ppb-level formaldehyde detection

Wei Ren, Rice Univ. (United States) and Chinese Univ. of Hong Kong (Hong Kong, China); Longqiang Luo, Yingchun Cao, Wenzhe Jiang, Frank K. Tittel, Rice Univ. (United States)

Formaldehyde (H₂CO) is an important intermediate in the photochemical production of ozone and carbon monoxide by hydrocarbon oxidation impacting the oxidative capacity of the atmosphere. Accurate and sensitive measurements of small changes in H₂CO mixing ratios (normally a few ppbv) are thus particularly useful for atmospheric chemistry research.

Conference 9370: Quantum Sensing and Nanophotonic Devices XII

The recent availability of interband cascade lasers (ICLs) with wavelength ranged between 3-4 μm enables the sensitive detection of trace gases such as formaldehyde that possesses a strong absorption band in this particular wavelength region. The recent development of a H₂CO sensor will be reported with ppb-level detectivity using a continuous wave, room temperature, low-power (threshold current 20 mA) consumed ICL at 3.6 μm . This absorption sensor detected a strong formaldehyde line at 2778.5 cm^{-1} in its v₁ fundamental band. A novel type of compact multipass cell (7.6 cm long physical length and 32 ml sampling volume) was utilized to obtain an effective optical path length of 3.7 m. By carefully choosing and alignment of the modematching lens for the multipass cell, the optical interference fringes inside the cell were diminished to enhance the signal-to-noise-ratio. A pressure of 150 torr was selected to eliminate the spectral cross-talk noise from ambient water vapor and methane. Wavelength modulation spectroscopy (5 kHz) with second harmonic detection was implemented to achieve a detection sensitivity of ~6 ppbv for H₂CO measurement at 1 Hz sampling rate. The Allan-Werle deviation plot reveals that a minimum detection limit of ~1 ppbv can be achieved for an averaging time of 150 seconds.

9370-72, Session 20
Review of Al-free active region laser diodes on GaAs for pumping applications
(Invited Paper)

Michel Krakowski, Thales Research & Technology (France) and III-V Lab. (France); Michel Lecomte, III-V Lab. (France) and Thales Research and Technology (France); Nicolas Michel, M. Calligaro, M. Carbonnelle, M. Tran, M. Lamponi, C. Cayron, V. Ligeret, III-V Lab. (France); Joseph P. Bebe Manga Lobe, Roberto Mostallino, Nicolas von Bandel, Alexandre Larrue, Yannick Robert, Eric Vinet, III-V Lab. (France) and Thales Research and Technology (France); Olivier Drisse, III-V Lab. (France); Michel Garcia, Olivier Parillaud, III-V Lab. (France) and Thales Research and Technology (France)

We have developed the building blocks to realize the different kinds of laser diodes needed for various pumping applications. We have developed Al free active region materials for wavelength emission at 780nm (for Rb pumping), 793nm (for Tm pumping), 852nm and 894nm (for Cs pumping), 915nm and 975nm (for Yb pumping). The Al free active region is less sensitive to facet degradation and dark line propagation than Al containing material. It allows the realization of a buried Bragg grating needed for single frequency operation or wavelength stabilization. We have developed such buried gratings allowing a side mode suppression ratio of 50dB in single frequency lasers. We have developed low internal losses structures, in order to get a high wall plug efficiency. We have achieved 70% wall plug efficiency on 975nm broad area (BA) laser diodes. At 852nm we have achieved 200kHz linewidth for an optical power of 110mW. DFB approach can also be used in broad area lasers in order to stabilize the wavelength. By this way, we have demonstrated lasers at 975nm with a low spectral width (<1nm) and a low wavelength evolution with temperature. In order to get high power together with a good beam quality, we have developed tapered structures for both lasers and amplifiers. By this way we have obtained amplifiers with 1W output power at 780nm. With a multi-section tapered laser, we have demonstrated the high modulation efficiency concept which allows the modulation of a few watts by the modulation of tens of mA only.

9370-73, Session 20
High-power ultrafast and broadly-tunable quantum-dot lasers (Invited Paper)

Maria Ana Cataluna, Ying Ding, Stephanie E. Haggett,

David Bajek, Univ. of Dundee (United Kingdom); Michel Krakowski, III-V Lab. (France)

In this talk, we will present our recent progress in the development of novel lasers with tapered InAs/GaAs quantum-dot devices at their core, unlocking the access to record-high output power from tunable and ultrafast laser diodes, in the spectral region between 1.2 - 1.3 μm .

9370-74, Session 20
High-performance GaSb laser diodes and diode arrays in the 2.1-3.3 micron wavelength range for sensing and defense applications

Edgaras Dvinelis, Augustinas Trinkunas, Mindaugas Greibus, Mindaugas Kauzilas, Tomas Ukauskas, Ieva Rimonyte, Ramunas Songaila, Augustinas Vizbaras, Kristijonas Vizbaras, Brolis Semiconductors UAB (Lithuania)

Mid-infrared spectral region (2-4 μm) is gaining significant attention recently due to the presence of numerous enabling applications in the field of gas sensing, medical, environmental and defense applications. Major requirement for these applications is the availability of laser sources in this spectral window. Type-I GaSb-based laser diodes are ideal candidates for these applications being compact, electrically pumped, power efficient and able to operate at room temperature in continuous-wave. Moreover, due to the nature of type-I transition, these devices have a characteristic low operation voltage, typically below 1 V, resulting in low power consumption, and high-temperature of operation.

In this work we focus on a family of type-I devices for different applications - ranging from multi-Watt high-power diode arrays for defense applications to single-TE00 angled facet ASE sources for ultra-broad tuning spectroscopy applications.

High-power multimode device family features single-emitter with CW output power > 1 W CW and WPE > 30 % and 19 emitter laser diode bar with 10 W CW output power and WPE > 29 % at room-temperature with preliminary lifetime evaluation indicating MTF > 10 000 hours.

Single-TE00 mode laser diodes and angled facet ASE sources at 2100 nm, 2330 nm, 2410 nm and 2700 nm are presented with CW output power in excess 100 mW together with ultra-low input threshold power of < 13 mW for laser diodes and tuning range > 100 nm for the ASE sources is presented.

9370-75, Session 21
Polarization-free GaN emitters in the ultraviolet and visible spectra via heterointegration on CMOS-compatible
Si (100) (Invited Paper)

Can Bayram, Univ. of Illinois at Urbana-Champaign (United States); John Ott, Kuen-Ting Shiu, Cheng-Wei Cheng, Yu Zhu, Jeehwan Kim, Devendra K. Sadana, IBM Thomas J. Watson Research Ctr. (United States); Manijeh Razeghi, Northwestern Univ. (United States)

Conventional approach to enable polarization-free GaN devices is switching the growth plane from inherently polar ones to inherently polarization-free (a.k.a. nonpolar) ones. Practically, common nonpolar substrate is the m-plane freestanding GaN one (i.e. making 90° with the respect to <0001> direction) that are sliced along {1100} planes out of GaN boules grown along <0001> direction. Hence, m-plane substrates are small (< cm^2) and expensive.

**Conference 9370: Quantum Sensing and
Nanophotonic Devices XII**

An alternative way of enabling polarization-free GaN devices is through controlling the material phase. Conventionally-grown GaN material is hexagonal (wurtzite) phase which is polar along $\langle 0001 \rangle$ growth direction. However, GaN material can also be cubic (zinc blende) phase which is polarization-free along $\langle 001 \rangle$ growth direction. Nonetheless, cubic phase of GaN is observed to form when grown on cubic substrates such as GaAs. Thermodynamical instability of cubic phase GaN, epilayer-substrate chemical incompatibility (i.e. III-N vs. III-As), and large lattice-mismatch (i.e. ~ 20%) are some of the key issues bottlenecking such bulk epitaxial deposition schemes.

In this work, CMOS-compatible integration of wurtzite and cubic phase GaN on on-axis Si (100) substrates are realized through nano-groove pattern and selective MOCVD process. XTEM data shows no discernable threading dislocations on the h- and c-GaN surfaces. InGaN/GaN MQWs regrown on c-GaN templates demonstrated strong room temperature emission in visible spectrum. GaN wurtzite to cubic phase transition can be particularly beneficial for light emitting devices as GaN cubic phase is nonpolar and polarization-free. Our MOCVD growth technique and unique groove structure are particularly beneficial for integrating GaN devices with Si CMOS technology.

9370-113, Session 22
High-performance dual-band mid-/long-wavelength infrared InAs/InAs_{1-x}Sb_x type-II superlattice-based photodetectors for medical thermography applications

Abbas Haddadi, R. Chevallier, Guanxi Andy Chen, Anh Minh Hoang, Manijeh Razeghi, Northwestern Univ. (United States)

We present the demonstration of a bias-selectable dual-band mid-/long-wavelength (MWIR-LWIR) photodetector based on InAs/InAs_{1-x}Sb_x T2SLs. We use a modified nBn photodetector structure that consists of two n-doped T2SL-based absorption regions, MWIR and LWIR, and a thin conduction-band-barrier which has zero valence band discontinuity with respect to both n-type absorption regions. The two absorption regions, or channels, can be addressed alternatively by changing the polarity of the applied bias voltage. A schematic diagram of the device structure and the superlattice band alignment of the absorption regions are shown in Figure 2. The MWIR channel is grown on top of the LWIR channel in order to allow response from both channels in the front-side illumination configuration. The MWIR channel plays a role as a low-pass filter for the underneath LWIR channel in this configuration. This structure takes advantage of the simplicity of the nBn photodetector design which does not need an additional middle contact and keeps each channel quite independent of each other.

9370-114, Session 22
High-power mid-IR frequency comb quantum cascade laser source

Quan-Yong Lu, Manijeh Razeghi, Steven Slivken, Neelanjan Bandyopadhyay, Yanbo Bai, Wei Zhou, M. Chen, David Heydari, Abbas Haddadi, Ryan McClintock, Northwestern Univ. (United States); Maria Amanti, Carlo Sirtori, Univ. Paris 7-Denis Diderot (France)

Optical frequency combs are valuable tool for spectroscopy in the mid-infrared (mid-IR) spectral region, where a large number of molecules have strong absorption features. The evenly spaced modes in the frequency domain enable the frequency comb to act as a ruler and provide unprecedented precision and speed compared with other spectrometric techniques. One can directly generate the mid-IR frequency comb by using mode-locked femtosecond lasers, however, the wavelengths are mainly

limited to 3 μm . However, deep in the mid-IR wavelength range (3-12 μm), there still are no available compact solid-state frequency comb sources.

Quantum cascade lasers (QCLs), on the other hand, are intrinsically compact and becoming the leading semiconductor laser source in the mid-IR realm thanks to developments in power, efficiency, and tuning range in the past few years. Recently, it has been demonstrated that when QCL are engineered with a sufficiently low group velocity dispersion using a broadband heterogeneous active region design, the device can emit a frequency comb via four wave mixing process. Frequency comb operation was identified from a free-running continuous wave (CW) broadband QCL at $[\lambda]-6.9 \mu\text{m}$ with a spectral range of 60-100 cm^{-1} and an output power of 20-40 mW. While this power level is sufficient for some applications, such as gas sensing in an enclosed environment with dual-comb spectroscopy, a high power output is always desired, especially for standoff detection of hazardous chemicals.

Here we extend the frequency comb further into the long-wave mid-IR frequency range. A frequency comb source based on a room temperature CW broadband QCL at $[\lambda]-9.0 \mu\text{m}$ is demonstrated. The frequency comb operation is observed with a narrow intermode beating linewidth of 3 kHz in a current range corresponding to a broad spectral coverage of 65 cm^{-1} and high power output of 180 mW for ~176 comb modes, nearly 1mW power for most of the modes. The spectrum generated by intermode beat spectroscopy reveals that nearly the entire spectral range contributed to the frequency comb operation. At higher currents, the device emits an output power up to 223 mW for ~350 modes, covering a spectral coverage of 130 cm^{-1} , while the intermode beating linewidth remains on the order of tens of kHz. A broader gain design with certain GVD dispersion engineering should be able to increase the spectral bandwidth of the frequency comb operation.

T. Udem, R. Holzwarth, and T.W. Hänsch, Optical frequency metrology. Nature 416, 233-237 (2012).

A. Schliesser, N. Picqué, and T.W. Hänsch, Mid-infrared frequency combs. Nature Photon. 6, 449 (2002).

M. Razeghi, High-performance InP-based mid-IR quantum cascade lasers. IEEE J. Select. Top. Quantum Electron. 15, 941-951 (2009).

A. Hugi, G. Villares, S. Blaser, H. C. Liu, and J. Faist, Mid-infrared frequency comb based on a quantum cascade laser. Nature 492, 229 (2012).

G. Villares, A. Hugi, S. Blaser, and J. Faist, Dual-comb spectroscopy based on quantum-cascade-laser frequency combs. Nature commun. 5, 5192 (2014).

D. Burghoff, T.-Y. Kao, N. Han, C. W. I. Chan, X. Cai, Y. Yang, D. J. Hayton, J.-R. Gao, J. L. Reno and Q. Hu, Terahertz laser frequency combs. Nature Photon. 8, 462-467 (2014).

9370-115, Session 22
World's first pMp superlattice photodetectors enables high operating temperature infrared imaging

Guanxi Andy Chen, Abbas Haddadi, Anh Minh Hoang, Romain Chevallier, Manijeh Razeghi, Northwestern Univ. (United States)

Infrared (IR) imaging has wide applications from military to civilian, such as aerial surveillance and reconnaissance, object identification in harsh environment, vascular and cancer detection, and industrial process monitoring, and type-II InAs/GaSb superlattice (T2SL) has proved to be an attractive material system to meet all these requirements. Raising the operating temperature of mid-wavelength infrared (MWIR) radiation focal plane array (FPA) to remove the cryogenic cooling system is one of the challenging to overcome to further wider its applications.

Recently, scientists in Center for Quantum Devices (CQD) led by Manijeh Razeghi, Walter P. Murphy Professor of Electrical Engineering and Computer Science in Northwestern University's McCormick School of Engineering and Applied Science, have made a breakthrough in demonstrating the world's first InAs/GaSb type-II superlattice MWIR infrared 320x256 unipolar FPA based on pMp architecture. The infrared imager exhibited excellent infrared

**Conference 9370: Quantum Sensing and
Nanophotonic Devices XII**

image from 81K up to 150K and ~98% operability, which illustrated the possibility for high operation temperature application. At 150K and -50mV operation bias, the 27 μm pixels exhibited dark current density to be 1.2×10^{-5} A/cm², with 50% cutoff wavelength of 4.9 μm , quantum efficiency of 67% at peak responsivity (4.6 μm), and specific detectivity of 1.2×10^{12} Jones. At 90K and below, the 27 μm pixels exhibited system limited dark current density, which is below 1×10^{-9} A/cm², and specific detectivity of 1.5×10^{14} Jones. From 81K to 100K, the FPA showed ~11mK NEDT by using F/2.3 optics and a 9.69ms integration time.

The noise equivalent temperature difference (NEDT), a measure of the FPA sensitivity, was measured by varying the blackbody temperature between 20 oC and 30 oC and mounting a MWIR Janos ASIO lens with F-number of 2.3. The signal and noise of each pixel were calculated as the mean and standard deviation over 100 frames. From the NEDT distribution shown in Figure 1, the median value of NEDT using 9.69 ms integration time was 11 mK at 81K and 15mK at 110K. The NEDT distributions from 81K to 110K do not show any tail in logarithmic scale, which is an indication of uniform processing over whole array. This results in high operability of the FPA, where 98% of pixels are operable. As shown in the inset of Figure 1, the minimum achievable NEDT does not vary significantly below 120K, changing from 11mK at 81K to 23mK at 120K. At 120K and above, the NEDT starts to increase and reaches 93mK at 140K due to the fast increment of the dark current density, which generates higher noise.

As shown in Figure 2, under 9.69ms integration at 81K, excellent infrared human body image was obtained, and from 81K to 120K, the image quality is excellent. Although the quality of image becomes poor at higher temperature, however, human blood veins can still be clearly observed as the temperature raise to 150K, which indicates its high potential for HOT application.

9370-116, Session 22
High-power continuous-wave surface-emitting quantum cascade ring laser in fundamental mode operation

Yanbo Bai, M. Chen, David Heydari, Neelanjan Bandyopadhyay, Steven Slivken, Manijeh Razeghi, Northwestern Univ. (United States)

Semiconductor laser sources have the advantage of being efficient, lightweight, compact, and cost effective compared to other types of laser sources. This is especially true in the mid-infrared (mid-IR) portion of the electromagnetic spectrum. The rapid development of quantum cascade lasers (QCLs) in recent years [1, 2] has greatly expedited the penetration of this laser technology into important applications, such as breathe analysis for the detection stomach cancer precursors, remote detection of improvised explosive devices, infrared countermeasure, and free space communication, in which conventional systems are based on solid state or gas lasers. This older technology is being replaced by semiconductor laser sources with comparable or even better performances at a lower cost, in order to enhance portability, reliability, and efficiency. Though traditional edge emitting semiconductor lasers can be used for this task, there are additional important properties of surface emitting semiconductor lasers that are even better suited to many applications. One of the biggest advantages is that surface emission eliminates the necessity of facet cleaving and allows for optical coating and pre-bond screening on the wafer scale, which is expected to significantly increase the manufacturing yield and reduce the cost.

9370-117, Session 22
Broadband quantum cascade laser tunable from 6.1 to 10.2 μm

Neelanjan Bandyopadhyay, Yanbo Bai, S. Sengupta, M. Chen, Steven Slivken, Manijeh Razeghi, Northwestern Univ. (United States)

Mid-Infrared spectral region between 6 to 10 μm , is important for spectroscopic detection of large number of molecules of industrial chemicals, pollutants, and explosives, which have their absorption signatures[1] in this region. Quantum cascade lasers has emerged as the leading compact, high power, room temperature (RT) mid-infrared semiconductor laser source[2]. The molecules can be identified by measuring the spectral features near the absorption resonances. Concentration of hazardous pollutants like NO, CH₄, N₂O, CO₂ etc., which are produced as byproducts in many industrial processes, needs to be continually monitored to reduce its impact on the human health and environment. In addition rapid stand-off detection of trace explosives like TNT, DNT, RDX by photo thermal imaging are important for homeland security and national defense, and can save lives of citizens and armed forces.

However, gain width of a single core QCL is relatively small, so laser emission cannot be tuned over a large spectral range. So a single QCL source cannot be used to detect multiple molecules having their peak absorptions far apart. In addition, for unique identification of chemical it is desirable to scan multiple absorptions features over a spectral range.

A broadband QCL consisting of multiple quantum cascade stages emitting at some energies spaced apart, can be put together inside a single active region to have a broad gain. Individual emission energy of the broadband device can be determined by distributed feedback mechanism[3]. The number of periods of each stage is calculated such that the summation of product of modal confinement factors and gain of each stage, is flat over the entire spectral range. It can be seen that the short wavelength stages absorb long wavelength photons, thus reducing the net gain at the long wavelength. So the absorption loss at long wavelength should be adjusted by increasing the confinement factor at these wavelength.

9370-118, Session 22
High-power quantum cascade lasers with angled cavities

David Heydari, Neelanjan Bandyopadhyay, Steven Slivken, Manijeh Razeghi, Northwestern Univ. (United States)

The quantum cascade laser (QCL) has experienced rapid development in recent years [1], reaching power levels that allow for local chemical sensing in parts per billion [2]. Such a detection level is of particular interest for application in medical diagnostics and exhaled breath analysis [3]. In addition, remote chemical sensing with a range of several meters is also demonstrated [4]. Because the sensitivity and range are directly proportional to the output power of the laser, further increasing the output power of a QCL would lead to more sensitive medical diagnosis systems and remote sensing in greater distances.

Broad area (BA) device is the most straightforward approach for power scaling of the QCL. Due to the increase in the size of the cavity, the output power can be hundreds of times higher than a narrow ridge device. Up to 120 W peak power has been demonstrated in a BA-QCL [5]. However, simply making the width larger without changing the shape of the cavity would induce a degradation of the beam quality. In fact, a "rabbit ear" shaped far field is the typical beam pattern for a BA-QCL [5]. In this work, angled Fabry-Pérot (AFP) lasers are investigated. It is shown that by changing the shape of the cavity, it is possible to avoid the degradation of the beam quality as the width is increased, since the shape of the cavity influences which lateral modes are excited in the waveguide.

The light propagation inside angled cavities is very different from that in straight cavities. Because laser operation automatically selects a path that is perpendicular to short edges (ends), which are usually the laser facets, in the simplest ray optics picture (Figure 1), this means that reflection off the long edges (sides) is inevitable for angled cavities. Geometrically, there is a simple relation among the width, length, and angle that allows for the best performance of the laser. This relation is $L=2m(W \cos\theta/\tan\theta)$, where $2m$ denotes the number of reflections off the sides, with m being an integer.

Based on previous results for lasers with 0 degree tilt (straight cavity standard FP), a 300 μm -width laser with 3 mm length produced a total peak output power of ~90 W [5]. The aforementioned formula was used in order

**Conference 9370: Quantum Sensing and
Nanophotonic Devices XII**

to determine the tilt angle necessary for the best performing AFP lasers: -12.0 degrees.

This work is carried out on a 30-stage QCL wafer with an emission wavelength of approximately 4.8 μm . The wafer was grown via gas-source molecular beam epitaxy on an InP substrate. After processing, the lasers were cleaved and bonded to copper heatsinks in epilayer-up configuration for testing.

At a ridge width of 300 μm , length of 5.8 mm, and tilt angle of 12°, a high-reflection/anti-reflection (HRAR) coated laser produced over 200 W of power with a low order, single mode far field. The slope efficiency of the device is $\eta_s \approx 2.35 \text{ W/A}$, and the threshold current density is $J_{th} \approx 2.75 \text{ kA/cm}^2$. The peak wall plug efficiency of the device is 10%. These results compare favorably with the straight cavity broad area QCL [5]. These high power single mode QCLs, which can operate in a very broad range of wavelengths, can be used for many applications, including chemical sensing and spectroscopy, communications, and materials processing.

This work is supported by the National Science Foundation (grants ECCS-1231289, ECCS-1306397, and ECCS-1359779), the Naval Air Warfare Center (grant N68335-13-C-0342), the Department of Homeland Security Science and Technology Directorate (grant HSHQDC-13-C-00034), and an Early Stage Innovations grant from NASA's Space Technology Research Grants Program. The authors would like to acknowledge the encouragement and support of all the involved program managers.

REFERENCES

- [1] M. Razeghi, "High-Performance InP-Based Mid-IR Quantum Cascade Lasers," *IEEE J. Sel. Top. Quantum Electron.*, vol. 15, no. 3, pp. 941-951, 2009.
- [2] C. B. Hirschmann, J. Lehtinen, J. Uotila, S. Ojala, and R. L. Keiski, "Sub-ppb detection of formaldehyde with cantilever enhanced photoacoustic spectroscopy using quantum cascade laser source," *Appl. Phys. B*, vol. 111, no. 4, pp. 603-610, Jun. 2013.
- [3] K. Wörle, F. Seichter, A. Wilk, C. Armacost, T. Day, M. Godejohann, U. Wachter, J. Vogt, P. Radermacher, and B. Mizaikoff, "Breath Analysis with Broadly Tunable Quantum Cascade Lasers," *Anal. Chem.*, vol. 85, no. 5, pp. 2697-2702, 2013.
- [4] X. Chen, D. Guo, F.-S. Choa, C.-C. Wang, S. Trivedi, A. P. Snyder, G. Ru, and J. Fan, "Standoff photoacoustic detection of explosives using quantum cascade laser and an ultrasensitive microphone," *Appl. Opt.*, vol. 52, no. 12, pp. 2626-2632, Apr. 2013.
- [5] Y. Bai, S. Slivken, S. R. Darvish, A. Haddadi, B. Gokden, and M. Razeghi, "High power broad area quantum cascade lasers," *Appl. Phys. Lett.*, vol. 95, no. 22, pp. 221104-221104-3, Dec. 2009.

9370-119, Session 22

Nano III-V plasmonic light-sources for monolithic integration on silicon

Ning Li, IBM Thomas J. Watson Research Ctr. (United States); Ke Liu, The George Washington Univ. (United States) and Beijing Univ. of Technology (China); Volker J. Sorger, The George Washington Univ. (United States); Devendra K. Sadana, IBM Thomas J. Watson Research Ctr. (United States)

We investigate the design of a III-V plasmonic nano-cavity-based laser and LED for monolithic integration on a Silicon substrate. Due to the compact laser footprint (250 nm \times 250 nm), this III-V plasmonic laser can be directly grown on patterned Silicon substrate and is anticipated to exhibit reduced crystallographic defects. Such lasers are expected to provide reliable monolithic light sources. The numerically obtained output power and modulation bandwidth of the light source are about 30 (5) μW and >40 (10) GHz for the laser (LED), respectively.

9370-120, Session 22

THz digital holography for real-time biomedical imaging

Marco Ravaro, Massimiliano Locatelli, Saverio Bartalini, Luigi Consolino, Istituto Nazionale di Ottica (Italy) and European Lab. for Non-linear Spectroscopy (Italy); Miriam Serena Vitiello, Istituto Nazionale di Ottica (Italy) and Istituto Nanoscienze and Scuola Normale Superiore (Italy); Riccardo Cicchi, Istituto Nazionale di Ottica (Italy) and European Lab. for Non-linear Spectroscopy (Italy); Francesco S. Pavone, Istituto Nazionale di Ottica (Italy) and European Lab. for Non-linear Spectroscopy (Italy) and Univ. di Firenze (Italy); Paolo De Natale, Istituto Nazionale di Ottica (Italy) and European Lab. for Non-linear Spectroscopy (Italy)

A key feature of THz waves as bio-medical probe is their non-ionizing nature, which prevents the exposure of biological tissues to harmful radiations. Indeed, thanks to their low energy, THz photons are well suited for both ex vivo and in vivo investigations of biological samples¹. The potential of THz radiation for cancer detection and diagnosis (skin cancer, breast cancer, ...) depends on the high absorption of THz waves in water, which enables the measurement of the abnormal hydration of damaged tissues²⁻⁶. In particular, image contrast based on water/fat content ratio in different tissues can be revealed as local transmission and refractive index variation in amplitude and phase images, respectively⁷. Coherent detection schemes are particularly well suited for such applications since they can provide depth-resolved, high contrast imaging of transparent samples and complex permittivity characterization. Until now, however, their deployment has been severely limited due to the use of single point detection schemes, which require time consuming raster scanning of the object to be imaged.

Here we report on a coherent imaging technique still unexplored in the THz range, Digital Holography⁸, providing unprecedented values for field of view and tolerance to vibrations, due to the long wavelength adopted. In particular, we have developed a real-time hologram processing system which allows to record and reconstruct high resolution holographic images both in scattering and transmission configuration. Such a real-time system is the key for fast coherent imaging in biomedical applications, enabling real-time, in-situ efficient characterization of histological samples.

With an experimental setup (fig.1) based on a compact QCL emitting 4 mW at 2.8 THz, as source, and a microbolometer focal plane array, as detector, we got high resolution amplitude (fig. 2b) and phase (fig. 2c) transmission images of a 30 μm thick histological blank slice of healthy human skin (fig. 2a). In the THz amplitude image, epidermis and dermis skin layers can be distinguished, similarly to the visible microscope image, while complementary information about optical path lengths through the sample can be extracted from the phase image. This first demonstration paves the way to 2D THz single shot amplitude and phase imaging of biological samples, with a wide application in histopathology.

1. MacPherson, E., Practical Considerations for in Vivo THz Imaging. *Terahertz Science and Technology*. 3, 163-171 (2010).
2. Yu, C., Fan, S., Sun, Y., MacPherson, E. The potential of terahertz imaging for cancer diagnosis: A review of investigations to date. *Quant. Imaging Med. Surg.* 2, 33-45 (2012).
3. Ashworth P.C. et al. Terahertz pulsed spectroscopy of freshly excised human breast cancer. *Opt. Express*. 17, 12444-54 (2009).
4. Woodward R. M. et al. Terahertz pulse imaging of ex vivo basal cell carcinoma. *J. Invest. Dermatol.* 120, 72-78 (2003).
5. Woodward, R. M., Wallace, V. P., Arnone, D. D., Linfield, E. H. & Pepper, M. Terahertz Pulsed Imaging of Skin Cancer in the Time and Frequency Domain. *J. Biol. Phys.* 29, 257-261 (2003).
6. Woodward, R.M. et al. Terahertz pulse imaging in reflection geometry of human skin cancer and skin tissue. *Phys. Med. Biol.* 47, 3853-3863 (2002).
7. Kim, S. M. et al. Biomedical terahertz imaging with a quantum cascade

**Conference 9370: Quantum Sensing and
Nanophotonic Devices XII**

laser. Appl. Phys. Lett. 88, 153903 (2006).

8. Schnars, U. & Jüptner, W. Digital Holography, Springer (2005).

9370-121, Session 22
**Unveiling the spatio-temporal organization
of TRPV1 nociceptor in live cell membranes**

Barbara Storti, Scuola Normale Superiore (Italy) and Istituto Nanoscienze, CNR (Italy); Carmine Di Rienzo, Scuola Normale Superiore (Italy) and Istituto Italiano di Tecnologia (Italy); Francesco Cardarelli, Istituto Italiano di Tecnologia (Italy); Ranieri Bizzarri, Scuola Normale Superiore (Italy) and Istituto Nanoscienze, CNR (Italy); Fabio Beltram, Scuola Normale Superiore (Italy) and Istituto Italiano di Tecnologia (Italy)

The Transient Potential Vanilloid 1 (TRPV1) belongs to that fascinating class of polymodal cell membrane receptors that integrate several physical and molecular stimuli and convey them into efficient intracellular signaling. TRPV1 is a nonselective voltage-dependent, temperature-dependent, ligand-dependent cation channel with a preference for Ca²⁺. TRPV1 is expressed both in sensory neurons, where it is involved in pain signaling, and in many other cell types. The research on TRPV1 is surely prompted by its intriguing nociception role and its activation mechanism relevant to the discovery and design of drugs capable of controlling pain stress in humans.

Among the unclear aspects of TRPV1 activity, a hot topic is represented by its interactions with cell cytoskeleton. Activation of TRPV1 was demonstrated to yield fast disassembly of microtubules possibly to regulate some specific neuronal functions through cytoskeleton reshaping. Yet, the alleged direct binding of TRPV1 to microtubules raises the question: do microtubules also modulate TRPV1 activity? A further lack of knowledge on TRPV1, with obvious therapeutic implications, resides in the observed long-term receptor desensitization when subjected to prolonged stimuli. A suggested hypothesis calls for the TRPV1 withdrawal from the cell surface by endocytosis followed either by receptor recycling to the plasma membrane or by its degradation through the proteosomal or lysosomal pathways. Indeed, a clathrin-free endocytotic pathway was reported for TRPV1. Notably, several members of the TRP family reside proximal to caveolin-1, the main structural protein in caveolae, raising the question: is caveolin-1 implied in the clathrin-free endocytosis of TRPV1? To answer both questions is not an easy task and requires the capability of monitoring the real-time physicochemical status of the receptor in live cells.

In my thesis I set out to address these issues by combining several fluorescence micro/nanoimaging techniques such as Förster Resonance Energy Transfer (FRET), Fluorescence Anisotropy Imaging (FAIM), and Spatio-Temporal Image Correlation Spectroscopy (TICS and STICS). I targeted the real-time visualization of receptor properties such as membrane mobility, microtubule and caveolin-1 binding, and TRPV1 oligomerization status. My experimental strategies benefited from the use of genetically-encodable fluorescent reporters belonging to the green fluorescent protein family. At first, I demonstrated the specific stabilization of functional TRPV1 by direct entanglement with microtubules, revealing for the first time a feedback cycle between nociception and cytoskeletal assembly/remodeling [1]. Then, I targeted the spatial and temporal organization of membrane TRPV1 complexes with caveolin-1 and microtubules by combining for the first time FRET with a STICS method based on the extraction of the molecular mean square displacement directly from imaging data (FRET-IMSD) [2] (Figs. 1 and 2). My findings show that membrane TRPV1 is split, at least, in three pools with distinct functional roles: 1) TRPV1-C, which is trapped in caveolae (binding to caveolin-1) (Fig 1) and likely governs receptor long-term desensitization, 2) TRPV1-T, which is organized in large sub-micron membrane domains (Fig 2) and oversees the subtle feedback interaction between receptor and microtubules, and 3) TRPV1-I that diffuses on the membrane in a fast and isotropic fashion and might represent a reservoir of the receptor [2].

I believe that these results do unveil new and relevant properties of TRPV1, possibly with biomedical implications, beside representing a

paradigmatic model of how protein receptors, cytoskeleton and lipoprotein domains on the plasma membrane interplay to regulate cell functions and communication of cells with the external environment.

1. Storti B, Bizzarri R, Cardarelli F, Beltram F (2012) Intact Microtubules Preserve Transient Receptor Potential Vanilloid 1 (TRPV1) Functionality through Receptor Binding. J Biol Chem 287: 7803-7811.

2. Storti B, Di Rienzo C, Bizzarri R, Cardarelli F, Beltram F Unveiling TRPV1 Spatio-Temporal Organization in Live Cell Membranes, in press, 2015

9370-122, Session 22
**Quantum-cascade-laser-based
optoacoustic detection for breath sensor
applications**

Pietro Patimisco, Univ. degli Studi di Bari Aldo Moro (Italy); Angelo Sampaolo, Univ. degli Studi di Bari Aldo Moro (Italy) and Rice Univ. (United States); Gaetano Scamarcio, Univ. degli Studi di Bari Aldo Moro (Italy); Frank K. Tittel, Rice Univ. (United States); Vincenzo Spagnolo, Univ. degli Studi di Bari Aldo Moro (Italy)

Breath analysis, a promising new field of medicine and medical instrumentation, potentially offers noninvasive, real-time, and point-of-care disease diagnostics and metabolic status monitoring for the diagnosis and monitoring of airway inflammation. The use of biomarkers to differentiate between inflammatory phenotypes in clinical practice would allow improved targeting of therapy, and might permit titration of therapy to the inflammatory response in individual patients. To date, researchers have identified over 500 different compounds contained in human breath, some of which are present at ppb or even parts per trillion (ppt) concentration levels. For example, Hydrogen Sulphide (H₂S) is one of biomarkers in breath used for airway inflammation monitoring. Therefore, the development of H₂S trace gas sensor technologies is a key factor in the advancement of breath analysis.

Laser spectroscopic detection techniques not only have high-sensitivity and high-selectivity, as equivalently offered by the gas chromatography-mass spectrometry (MS), but also have the advantageous features of near real-time response, low instrument costs, and point-of-care function. Among the most robust and sensitive optical trace-gas detection techniques, quartz-enhanced photo-acoustic spectroscopy (QEPAS) is capable of record sensitivities with a compact and relatively low-cost detection module. It is based on the opto-acoustic effect and exploit the enhancement of acoustic energy density provided by a quartz tuning fork, which acts as high quality factor piezoelectric acoustic transducer. QEPAS is particularly suited for applications where continuous monitoring of targeted exhaled gases with sensitivity, selectivity and fast response are required, such as in critical care and operating room settings. To date, our QEPAS sensor for SF₆ detection has reached the record sensitivity of part-per-trillion concentration. The successful results achieved by our group have paved the way to the realization of QEPAS sensors for the detection of H₂S, using either conventional near-IR diode lasers or mid-IR quantum cascade lasers (QCLs) with part-per-billion detection sensitivities. On the other hand, the strongest absorption lines of H₂S fall in the terahertz (THz) spectral range. This fact, together with the simpler gas species THz spectral features, may lead enhance the sensor sensitivity and selectivity. In fact, the demonstration of the first QEPAS system operating in the THz range for methanol detection by our group was awarded the cover of the July 2013 issue of the "Applied Physics Letters" journal. Very recently, we reported a THz QEPAS sensor for H₂S trace gas detection, with a normalized noise equivalent factor comparable with the best results obtained for H₂S in the mid and near-IR spectral range. These advancements are paving the way for laser-based H₂S breath analysis and eventually taking it from laboratory research to clinical testing. Although current advanced laser sources are still too expensive for a home-owned breath sensor, laser-based breath QEPAS sensors (for NO and NH₃ detection) have already proven to be significantly less expensive than an MS-based system and play its unique role in real-time, non-invasive disease diagnosis and metabolic status monitoring.

9370-92, Session PWed

Towards graphene photonics and plasmonics

Shin Mou, Don Abeysinghe, Air Force Research Lab. (United States); Joshua Myers, Wright State Univ. (United States) and Air Force Research Lab. (United States); Justin W. Cleary, Nima Nader, Joshua R. Hendrickson, Air Force Research Lab. (United States)

Graphene has remarkable optical properties that it is highly transparent while owning large optical absorption coefficient. However, from an optical sensing point of view, it is less attractive due to the low interband optical absorbance resulting from its thinness. An alternative method to achieve optical absorption/ sensing is to utilize the tunable resonant absorption by plasmons in the two-dimensional electron gas (2DEG) of grating-gated field effect transistors (FETs), which is known for a variety of semiconductor systems, giving promise of frequency-agile Infrared/THz image sensors and spectrometers. Graphene-based plasmonics shows highly tunable and sharp plasmon THz resonance at room temperature while all other semiconductor 2DEG systems generally have plasmon resonance at much lower temperatures (< 77 K). In addition, graphene has the capability to operate at higher frequencies (shorter wavelength in mid-infrared) due to higher sheet carrier density. As a result, graphene grating-gated detectors have the potential to be the next-generation frequency-agile infrared detectors. We investigate the dc transport of both CVD graphene (grown on Cu) and epitaxial graphene (grown on SiC) with Hall measurement, by which we obtain important parameters such as Hall mobility and sheet carrier density helping us estimate the plasmon resonance frequency and the absorption spectrum. Furthermore, to complement the dc transport characterization, optical transmission/reflection measurements are carried out in Fourier transform infrared spectrometers (FTIRs) to obtain the infrared ac conductance. From that, the carrier density, carrier mobility, sheet resistivity, intraband scattering rate, and graphene layer number can be inferred. Last, we observe graphene plasmon resonances in far-infrared (~ 100 cm⁻¹) by optical transmission measurements through graphene ribbon grating structures.

9370-93, Session PWed

Long-wavelength interband cascade infrared photodetectors operating above room temperature

Hossein Lotfi, Lin Lei, Lu Li, Rui Q. Yang, Joel C. Keay, Matthew B. Johnson, The Univ. of Oklahoma (United States); Yueming Qiu, Dmitri Loubychyev, Joel M. Fastenau, Amy W. K. Liu, IQE Inc. (United States)

Theoretical studies projected that the device performance limit of Type-II superlattice (T2SL) infrared photodetectors can be improved by utilizing the interband cascade (IC) architecture. Recent experimental results obtained from mid-wavelength T2SL based on IC architecture have confirmed the advantage for high temperature operation. Because the absorption coefficient and diffusion length become smaller in T2SL detectors at longer wavelengths, interband cascade approach is expected to be more advantageous in long-wavelength infrared (LWIR, 8-12 μ m) and very long wavelength infrared (VLWIR, 12-30 μ m) windows.

In this study, we report our recent experiments on a set of interband cascade infrared photodetectors (ICIPs) that are able to operate at temperatures up to 340 K with cutoff wavelength longer than 8 μ m. Our preliminary characterization studies show that these two- and three-stage detectors have a 100% cutoff wavelength of 6.2 μ m at 78 K increasing to about 8.6 μ m at 340 K. The three-stage detectors had ROA of as high as 1.5×10^{-4} Ω cm² at 78 K. The corresponding Johnson-noise-limited detectivity for a three-stage ICIP was 3×10^{11} Jones ($\approx 5.5 \mu$ m) at 78 K and 1.1×10^8 Jones ($\approx 6.5 \mu$ m) at 300 K. Detailed results and analysis on this set of ICIPs will be presented at the conference.

9370-94, Session PWed

All-optical reservoir computing system based on InGaAsP ring resonators for high-speed identification and optical routing in optical networks

Charis Mesaritakis, Alexandros Kapsalis, Dimitris Syvridis, National and Kapodistrian Univ. of Athens (Greece)

Reservoir computing (RC) is a decade old mathematical paradigm that has been utilized efficiently in order to allow classification of time-dependent signals with minimum training overhead. The principle of operation relies on the expansion of the dimensionality of the classification task by the high-nonlinearity and interconnection complexity of the RC's nodes. The expansion of the RC concept to photonic applications like network routing can allow all-optical data processing with multi-gigabit rates, low power consumption and inherent parallelism.

Towards this direction, we propose an all optical RC scheme based on nodes realized as integrated InGaAsP micro ring resonators. In this case the node's nonlinearity stems from ultra-fast optical effects like Kerr effect and two photon absorption. Through a numerical model the structural parameters of each ring-node were optimized aiming at high nonlinearity. Furthermore, a matrix of 36 ring resonators with random interconnection has been modeled and the system's performance was evaluated.

In particular, 32bit long digital headers, encoded as optical NRZ pulses with stable extinction ratio of 10dB, 240Gbps rate, and varying level of optical noise (SNR of 20dB to 5dB) have been used as targeted patterns. These patterns were fed to the RC and triggered a nonlinear response at each node. The output of the system exhibited strong perturbations compared to the initial signal, due to the complex interaction inside the system. The outputs were fed to a simple one stage neural network that was trained offline with typical back propagation algorithms, exhibiting classification error of 0.5%.

9370-97, Session PWed

Multifunctional diffractive optical elements for the generation of higher order Bessel-like-beams

Anand Vijayakumar, Shanti Bhattacharya, Indian Institute of Technology Madras (India)

Higher Order Bessel Beams (HOBBs) have many useful applications in optical trapping experiments. The generation of HOBBs is achieved by illuminating an axicon by a Laguerre-Gaussian beam generated by a spiral phase plate. In this paper, the design of a spiral axicon is proposed by combining the phase profiles of a spiral phase plate with that of an axicon for the generation of HOBBs. Two techniques namely modulo- π phase addition method and an analog method were employed for the generation of the composite element. The elements were fabricated using electron beam direct writing. The fabricated elements were evaluated using a diode laser and the generation of ring shaped intensity profiles is confirmed. The angular momentum in the beam is evaluated by the interference of the generated HOBB with a direct beam both derived from the same source. The forked fringe pattern confirmed the presence of angular momentum present in the beam.

9370-100, Session PWed

Nanomaterials coated multiplexed fiber Bragg grating for multiparameter sensing

Shivananju B. N., Vishnu Prasad, Aravind C. G., Indian Institute of Science (India); Abha Misra, Indian Institute

**Conference 9370: Quantum Sensing and
 Nanophotonic Devices XII**

of Science (India) and Applied Photonics Initiative, Indian Institute of Science (India); Manoj M. Varma, Sundarrajan Asokan, Indian Institute of Science (India)

Fiber Bragg Grating (FBG) sensors have been extensively used for strain and temperature sensing. However, there is a need for intelligent sensing of multiple environmental parameters with a single sensor system. In this work we demonstrate a novel multiplexed FBG sensor whose core/cladding surface is coated with functional nano materials for sensing multiple parameters such as gas concentration (Polyallylamine-amino-carbon-nanotube coated on the surface of the core FBG for detecting the concentrations of CO₂ gas at room temperature in ppm levels over a wide range of 1000–4000 ppm with a limit of detection of about 75 ppm), humidity (Carbon nanotubes coated on the surface of the core FBG for detecting Relative Humidity (RH) over a wide range of 20%–90% RH at room temperature with a sensitivity of 31 pm/%RH), light (Carbon nanotubes coated on cladding FBG to sense light over a wide, 248-1500 nm, range of optical wavelengths such as Infrared (33 pm/mW), Visible (12 pm/mW) and Ultraviolet (1 pm/mW) radiation), pH (Polyelectrolyte multilayer structure (100 nm thick) coated on the core FBG for detecting pH over a wide, 1–12, range at room temperature with a sensitivity of 64 pm/pH), protein concentration (Polyelectrolyte coated on the core FBG for detecting Bovine Serum Albumin (BSA) protein with a sensitivity of 5 pm/?g/ml), temperature (Aluminum and Lead with an average thickness of about 80 nm coated on the cladding FBG for measuring thermal response with a sensitivity of 15 pm/oC).

9370-101, Session PWed

Ultra-wide tuning of a nanofiber Bragg grating cavity

Hideaki Takashima, Hokkaido Univ. (Japan) and Osaka Univ. (Japan); Andreas W. Schell, Humboldt-Univ. zu Berlin (Germany); Shunya Kamioka, Yasuko Oe, Osaka Univ. (Japan); Masazumi Fujiwara, Hokkaido Univ. (Japan) and The Institute of Scientific and Industrial Research (Japan); Oliver Benson, Humboldt-Univ. zu Berlin (Germany); Shigeki Takeuchi, Kyoto Univ. (Japan) and Hokkaido Univ. (Japan) and Osaka Univ. (Japan)

The development of optical microcavities with small mode volume, low-loss coupling to the single mode fibers (SMFs), and wide tuning of the resonant wavelength is necessary to realize devices for photonic quantum network such as single photon sources and quantum memories.

Tapered optical fibers with the diameter of about half-wavelength (nanofibers) are capable of efficient coupling photons from light emitters to the SMFs, and we have demonstrated efficient single photon sources using the nanofiber coupled with single light emitters. Recently, nanofiber Bragg grating cavities (NFBCs) has been proposed and realized as novel microcavities with small mode volume and the low-loss coupling to the SMFs.

Here, we report ultra-wide tuning of the NFBCs by controlling the tension to the fiber. Our NFBC was fabricated in a tapered optical fiber with a diameter of 300 nm using a focused ion beam milling. The tuning range is up to 20 nm at room temperature at around 640 nm, and the behavior of the tuning was reversible and hysteresis free. We also performed the tuning at cryogenic temperature (85 K) and observed the ultra-wide tunability similar with the room temperature. Furthermore, we coupled CdSe/ZnS/quantum dots to the NFBCs and observed the enhancement of the photon emission.

9370-102, Session PWed

Electrical isolation of type-II InAs/InGaSb superlattices from GaSb substrates

William C. Mitchel, Air Force Research Lab. (United States); Said Elhamri, Univ. of Dayton (United States); Heather J. Haugan, Air Force Research Lab. (United States); R. Berney, Univ. of Dayton (United States); Shin Mou, Gail J. Brown, Air Force Research Lab. (United States)

There is continued interest in type-II InAs/InGaSb superlattices (SL) because of their important applications as infrared detectors and lasers. The SL material with the best structural quality is grown on GaSb substrates where lattice mismatch induced dislocations are at a minimum. Infrared transparent substrates are preferred for detector applications because the sensor is usually mounted upside down to facilitate contacting of the sensor to read-out electronics by bump bonding so the signal must come through the substrate before being absorbed in the sensor. However, free carrier absorption in standard n-type tellurium doped substrates significantly reduces the transmittance, and infrared absorption in undoped p-type substrates is even higher. Recently lightly doped n-type GaSb substrates, n-GaSb, have become available with significantly reduced infrared absorption enabling backside illumination. However, while superior for SL crystal quality, all GaSb substrates are conductive which hinders measurement of in-plane electrical transport properties. So, it is desirable to isolate the substrate from the SL to enable these measurements. We here show that n-type InAs/InGaSb superlattices can be electrically isolated from n-type GaSb substrates at much higher temperatures than from the more common undoped p-type GaSb substrates without the use of a large band gap buffer layer. Temperature dependent Hall effect measurements show superlattice conduction up to near room temperature, which is significantly higher than the 20 K observed for p-type substrates. We argue that the isolation is due to the depletion layer at the p-n junction between the p-type buffer layer and the n-type substrate.

9370-103, Session PWed

High-speed multichannel time-correlated single-photon counting electronics based on SiGe-integrated time-to-digital converters

Uwe Ortmann, Michael Wahl, Tino Roehlicke, Hans-Jürgen Rahn, PicoQuant GmbH (Germany); Nick Bertone, PicoQuant Photonics North America, Inc. (Canada); Gerald Kell, Fachhochschule Brandenburg (Germany)

Time Correlated Single Photon counting with picosecond timing has become a key method in many areas of applied physics. One of the most important areas is that of fluorescence lifetime measurement in biophysics and the life sciences. Precisely timed photon counting for the purpose of coincidence correlation is now also emerging as the most common approach to quantum state interpretation in experimental quantum optics. Therefore, time-correlated single photon counting (TCSPC) electronics, traditionally mostly used in time-resolved fluorescence research are facing new challenges in different emerging areas. Consequently such instruments are undergoing a fresh cycle of innovation, some of which we try to highlight here. The new picosecond TCSPC system we specifically present provides several interesting new features resulting from a high speed monolithic integration in one of the fastest semiconductor technologies available today.

The result is a high timing resolution by direct digital conversion and a very short deadtime. Apart from conventional histogramming over a very long time span, we can implement continuous single photon recording modes that allow picosecond timing of all photon events with respect both to a sync signal as well as on a virtually infinite time scale. Multiple timing channels can also be operated independently and in parallel, e.g. for picosecond

**Conference 9370: Quantum Sensing and
 Nanophotonic Devices XII**

correlation analysis between signals from multiple photon detectors. In this paper we describe some implementation details and the results of an evaluation of the new electronics in synthetic benchmarks and real quantum optical applications.

9370-104, Session PWed

**MWIR interband transitions in type-II
 In(GaAl)Sb quantum dots**

Qin Wang, Acreo Swedish ICT AB (Sweden); Mehrdad Jafari, Halmstad Univ. (Sweden); Laiq Hussain, Lund Univ. (Sweden); Jindong Song, Won Jun Choi, Il Ki Han, Eun hye Lee, Suk In Park, Korea Institute of Science and Technology (Korea, Republic of); Ju Young Lim, Korea Photonics Technology Institute (Korea, Republic of); Amir Karim, Jan Y. Andersson, Acreo Swedish ICT AB (Sweden); Håkan Pettersson, Halmstad Univ. (Sweden)

Nowadays infrared (IR) detection and sensing technologies are used in many IR systems (0.7 to 14 μm) for security, defence and industrial applications. In particular, advanced light emitting lasers/LEDs and photodetectors in the mid-wave infrared (MWIR, 3-5 μm) regime are becoming important devices for the growing sensor, health and environment markets. To meet the demands imposed by market, various III-V semiconductor quantum structures are intensively explored as optical active absorption or emission materials, including quantum wells/wires/dots and strained-layer superlattices.

We focus on a promising approach utilizing In(GaAl)Sb quantum dots (QDs) embedded in an InAs matrix grown by MBE to achieve the desired IR device's operating wavelengths in the MWIR region. These QDs display spatially indirect interband transitions in a type-II broken bandgap alignment. The transition energy can be tuned by bandgap and strain engineering either by varying the QD size or by incorporation of Ga (or GaAl) into InSb-based QDs. An advantage of these quantum materials is that the growth doesn't require sophisticated epitaxial designs as for growth of superlattices or quantum cascade structures with their multitude of alternating layers and very exact interfaces. The QD structures are expected to provide advantages such as higher operating temperatures, lower power consumption and a general reduction of device size, weight and cost. The structural and optical properties of the In(GaAl)Sb QDs were characterized with AFM, TEM, XRD, photoluminescence and absorption spectroscopy at different temperatures. Moreover, the effect of annealing at 650 oC on the optical properties was analyzed in detail.

9370-77, Session 23

**Probing the real-world via terahertz nano-
 devices (Keynote Presentation)**

Miriam S. Vitiello, Consiglio Nazionale delle Ricerche (Italy)

Terahertz (THz) radiation lies in the region of the electromagnetic spectrum, loosely defined as the 30-300 μm wavelength region, that is often called "THz gap". Recent technological innovation in photonics and nanotechnology is now enabling THz frequency research to be applied in an increasingly widespread range of applications, such as information and communications technology, sensing, medical diagnostics, global environmental monitoring, homeland security, and quality and process controls. Most of these applications require systems with targeted sensitivity and specificity exploiting advanced quantum devices, novel materials and technologies. To address the above application requirements, high power, widely tunable sources with controlled and directional beam profiles, together with high-speed and high-sensitivity resonant detectors need to be developed. This requires parallel developments in semiconductor materials and heterostructures, including micro/nanostructuring and plasmonics, as well as related multifunctional THz optical components. The talk will

provide an overview of our recent technological developments of Terahertz photonics nano and micro devices

9370-78, Session 24

**Quantum optics with semiconductor
 quantum dots (Invited Paper)**

Pascale Senellart, Valérian Giesz, Simone Luca Portalupi, Olivier Gazzano, Aristide Lemaitre, Isabelle Sagnes, Loïc Lanco, Lab. de Photonique et de Nanostructures (France)

By deterministically coupling a semiconductor quantum dot to a pillar microcavity [1], we fabricate very bright single photon sources: a photon is generated for each excitation pulse and collected with a 79% probability. When controlling the electrostatic environment of the dot, the photons are shown to be highly indistinguishable [2]. We also study the quantum interference between photons emitted by two bright single photon sources. The Purcell effect is shown to enhance the indistinguishability of the photons emitted by two distinct dots.

Finally, we present a novel cavity design and technology that allows an electrical tuning of a bright single photon source [3].

[1] A. Dousse, et al. Controlled Light-Matter Coupling for a Single Quantum Dot Embedded in a Pillar Microcavity Using Far-Field Optical Lithography, Phys. Rev. Lett. 101, 267404 (2008)

[2] O. Gazzano, et al. Bright solid-state sources of indistinguishable single photons, Nature Communications 4, 1425 (2013)

[3] A. Nowak, et al., Deterministic and electrically tunable bright single-photon source. Nature Communications 5, 3240 (2014)

9370-79, Session 24

**Control of spontaneous emission by
 shaping the vacuum field in nanophotonic
 structures (Invited Paper)**

Andrea Fiore, Chaoyuan Jin, Technische Univ. Eindhoven (Netherlands); Robert Johnne, Technische Univ. Eindhoven (Netherlands) and Max-Planck-Institut für Physik komplexer Systeme (Germany); Ron Schütjens, Milo Swinkels, Thang Hoang, Leonardo Midolo, Rene van Veldhoven, Technische Univ. Eindhoven (Netherlands)

Spontaneous emission (SE) lies at the heart of cavity quantum electrodynamics (CQED) and its control in real time is required for quantum information processing applications. However, this control has not been possible so far in nanophotonic structures due to the ultrafast timescales (ps) involved. Here we report an approach to the control of spontaneous emission via the ultrafast molding of the cavity vacuum field. As the emitter-photon interaction rate g is directly related to the intensity of the vacuum field at the emitter's position, a modification of the electromagnetic environment results in a SE change. In a nanophotonic structure, this can be obtained by a change of the refractive index, which can be realized on a ps timescale by the injection of free carriers or by third-order nonlinearities. We provide a first demonstration of this concept in a photonic crystal coupled-cavity structure where the injection of free carriers in a "control" cavity changes its detuning with a "target" cavity, thereby changing the mode volume and quality factor seen by quantum dots in the target cavity, and report a change in SE intensity by over a factor of two over a 200 ps timescale. A more advanced scheme to tailor the g -factor with arbitrary contrast using arrays of coupled cavities is then discussed. These schemes open the way to the ultrafast control of CQED processes in nanophotonic structures, and particularly to the shaping of single-photon waveforms and the dynamic control of Rabi oscillations at optical frequencies.

9370-80, Session 24

Orbital angular momentum injection in a polariton superfluid. *(Invited Paper)*

Thomas Boulier, Quentin C. Glorieux, Emiliano Cancellieri, Elisabeth Giacobino, Alberto Bramati, Univ. Pierre et Marie Curie (France)

We will present two experiments :

1-The generation of squeezed and entangled light fields is a crucial ingredient for the implementation of quantum information protocols. In this context, semiconductor materials offer a strong potential for the implementation of on-chip devices operating at the quantum level. Here we demonstrate a novel source of continuous variable squeezed light in pillar-shaped semiconductor microcavities in the strong coupling regime. Degenerate polariton four-wave mixing is obtained by exciting the pillar at normal incidence. We observe a bistable behaviour and we demonstrate the generation of squeezing near the turning point of the bistability curve. The confined pillar geometry allows for a larger amount of squeezing than planar microcavities due to the discrete energy levels protected from excess noise. By analysing the noise of the emitted light, we obtain a measured intensity squeezing of 20.3%, inferred to be 35.8% after corrections.

2 - We report the formation of a ring-shaped array of vortices after injection of angular momentum in a polariton superfluid. The angular momentum is injected by a Laguerre-Gauss beam, whereas the global rotation of the fluid is hindered by a narrow Gaussian beam placed at its center. In the linear regime a spiral interference pattern containing phase defects is visible. In the nonlinear (superfluid) regime, the interference disappears and the vortices nucleate as a consequence of the angular momentum quantization. The radial position of the vortices evolves freely in the region between the two pumps as a function of the density. Hydrodynamic instabilities resulting in the spontaneous nucleation of vortex-antivortex pairs when the system size is sufficiently large confirm that the vortices are not constrained by interference when nonlinearities dominate the system.

9370-81, Session 24

Photon pair sources in AlGaAs: from electrical injection to quantum state engineering *(Invited Paper)*

Sara Ducci, Guillaume Boucher, Claire Autebert, Fabien Boitier, Ivan Favero, Giuseppe Leo, Univ. Paris 7-Denis Diderot (France)

Integrated quantum photonics is a very active field of quantum information communication and processing. One of the main challenges to achieve massively parallel systems for complex operations is the generation, manipulation and detection of many qu-bits within the same chip. Here we present our last achievements on AlGaAs quantum photonic devices emitting non-classical states of light at room temperature by spontaneous parametric down conversion (SPDC). The choice of this platform combines the advantages of a mature fabrication technology, a high nonlinear coefficient, a SPDC wavelength in the C-telecom band and the possibility of electrical injection.

The first device presented in this talk is an electrically injected photon pair source working at room temperature, directly compatible with the existing telecom network. Based on type-II intracavity SPDC in an AlGaAs laser diode the source generates pairs around 1.57 μ m. We will describe its optoelectronic and nonlinear optical behavior, as well as its performances as photon pair source.

The second device is a microcavity in a transverse pump configuration leading to a great versatility in the frequency correlation engineering through the spatial and spectral characteristics of the pump beam, opening the way to dense coding of information.

We will conclude the talk by presenting some novel techniques to tailor/reconstruct the generated bi-photon state.

9370-82, Session 24

Exciton-polariton Bose-Einstein condensation with a polymer at room temperature *(Invited Paper)*

Thilo Stoefler, IBM Research - Zürich (Switzerland); Johannes D. Plumhof, IBM Research - Zurich (Switzerland); Lijian Mai, IBM Research - Zürich (Switzerland); Ullrich Scherf, Bergische Univ. Wuppertal (Germany); Rainer F. Mahrt, IBM Research - Zürich (Switzerland)

We create exciton-polariton quasiparticles by exciting optically a microcavity filled with a ladder-type conjugated polymer in the strong coupling regime. At room temperature thermalization of these quasiparticles occurs while it is suppressed at low temperature because of a relaxation bottleneck. Above a certain excitation threshold with incoherent off-resonant picosecond laser pulses, we observe the emergence of non-equilibrium Bose-Einstein condensation in the lower polariton branch. This is evidenced by several distinct features such as a blue-shifted emission peak at zero in-plane momentum, accompanied by a nonlinear increase in the emission intensity and a sudden drop of the linewidth. Furthermore, the emission becomes polarized and the emission dynamics is drastically shortened. Spatially-resolved measurements with a Michelson interferometer show a macroscopic phase relation over almost the whole spot, and the fringe pattern exhibits non-flat phase fronts and fork-like dislocations, indicating a large number of vortices and excitations. In contrast to conventional lasing, we find a strong increase in threshold when decreasing the temperature, which can be explained by the peculiar thermalization properties. As we are able to obtain single-shot measurements of the spectrum and the interference patterns, we can study single realizations of the condensate. This gives access to non-averaged properties from each individual condensation process. Our approach demonstrates a radically simplified route to investigate Bose-Einstein condensation physics at ambient conditions with easy-to-process non-crystalline materials.

9370-111, Session 24

Manipulation of electrical flicker-noise and line narrowing in free-running quantum cascade-lasers *(Invited Paper)*

Masamichi Yamanishi, Toru Hirohata, Hamamatsu Photonics K.K. (Japan)

Intrinsic linewidths of quantum-cascade lasers are found to be astonishingly narrow, ~ 100 Hz. However, the free running linewidths (usually ~ 1 MHz) of existing quantum-cascade lasers are governed by flicker ($1/f$) frequency-noise that is identified to originate from electrical flicker-noise in the devices. Obviously, substantial suppression of the electrical flicker noise is required for substantial narrowing of free-running LWs. In this presentation, we show systematic experimental results of flicker voltage-noise power-spectral density obtained with mid-infrared QCLs of designed positioning of impurities in injectors. The measured noise-levels depending strongly on impurity position as well as device-temperature are evaluated with an ad hoc model based on fluctuating charge-dipole induced by trapping and de-trapping at impurity states. It is shown that quasi-delta doping of impurities in their injectors leads to strong suppression of electrical flicker noise by minimization of the dipole-length at a certain temperature, for instance ~ 300 K and, in turn, is expected to substantially narrow the free-running line-width down below 10 kHz without assistances of any types of feedback schemes.

9370-83, Session 25

Graphene vs more conventional narrow band semiconductors (*Keynote Presentation*)

Jacob B. Khurgin, Johns Hopkins Univ. (United States)

Graphene, a gapless two-dimensional material with Dirac-like dispersion has been in the focus of attention for the last decade due to its unusual electronic and optical properties, but those properties have not been compared directly with those of conventional III-V and II-VI narrow gap materials and 2D structures. In this talk we show that most of the electronic and optical properties of graphene are comparable, but not dramatically superior to those of more conventional semiconductors and which material is more practical should be determined on the basis of cost and fabrication issues rather than on performance alone.

9370-84, Session 25

Monolithic coupling of QCLs in evanescent waveguides on InP (*Invited Paper*)

 Clément Gilles, Gregory Maisons, Bouzid Simozrag,
 Mathieu Carras, III-V Lab. (France)

We present the realizations of an array of Distributed Feedback (DFB) Quantum Cascade Lasers (QCL) and passive Multiplexers (MUX) based on Indium Phosphide wafers. The aim of these preliminary results is to realize a monolithic, widely tuneable, source in the mid-Infrared (mIR) for laser spectroscopy.

In the Mid-Infrared the DFB Quantum Cascade Lasers (QCL) are among the most promising sources for the Laser Spectroscopy [1]. In order to detect complex molecules or a set of simple molecules, one needs a narrow-linewidth tunable source suitable to scan few tens of wavenumbers. Single DFB QCL have a limited tuning range ($<10\text{cm}^{-1}$) and can only be used for one or two simple molecules. External cavities are widely tunable [2]. However they could suffer from mechanical vibrations and are not relevant for miniaturized spectroscopic system. To achieve a broadband source, a DFB array needs tens of emitters. This configuration is not suitable for integration in a spectroscopic system and optical sources have to be multiplexed to get only one beam. External solution could be use [3] however, for the same reasons external cavities have been dismissed, a monolithic approach is preferable to combine all optical beams. These optical multiplexing needs low losses passive waveguide which cover all the spectral range. Monolithic tuneable sources are very appealing for spectroscopy applications because of the compactness, the robustness and the usability.

In order to be able to combine all the beams from the array, the light generated in the active region of the QCL has to be transferred to a low losses passive waveguide. Evanescent coupling has been studied in order to be able to transfer all light adiabatically.

References

- [1] P. Gorrotxategi-Carbajo, E. Fasci, I. Ventrillard, M. Carras, G. Maisons, D. Romanini, "Optical-feedback cavity-enhanced absorption spectroscopy with a quantum-cascade laser yields the lowest formaldehyde detection limit" *Appl. Phys. B*, 110, 309 (2013).
- [2] A. Hugi, R. Terazzi, Y. Bonetti, A.O Wittmann, M. Fischer, M. Beck, J. Faist and E. Gini, "External cavity quantum cascade laser tunable from 7.6 to 11.4 μm " *Appl. Phys. Lett.*, 95, 061103 (2009).
- [3] B. G. Lee, J. Kansky, A. K. Goyal, C. Pflugl, L. Diehl, M. A. Belkin, A. Sanchez and F. Capasso, "Beam combining of quantum cascade laser arrays" *Opt. Exp.*, 17, 16216 (2009).

9370-85, Session 25

Monolithic optical frequency comb based on quantum dashed mode locked lasers for Tb/s data transmission (*Invited Paper*)

Anthony Martinez, Cosimo Calò, V. Panapakkam, Kamel Merghem, Lab. de Photonique et de Nanostructures (France); Regan T. Watts, Vidak Vujicic, Colm Browning, Dublin City Univ. (Ireland); Alain Accard, François Lelarge, III-V Lab. (France); Liam P. Barry, Dublin City Univ. (Ireland); Abderrahim Ramdane, Lab. de Photonique et de Nanostructures (France)

Optical frequency combs have a great potential for ultra-high bit rate telecommunications based on e.g. optical orthogonal frequency-division multiplexing superchannels. For frequency comb generation, monolithic Quantum Dash semiconductor mode-locked lasers are very attractive candidates owing to their broadband optical spectrum, inherent intrinsic low noise and compactness.

The active region is based on InAs nanostructures grown on InP for operation in the 1.55 μm window. Owing to enhanced non linear effects, single gain section generates short pulses in the mode-locking regime without resorting to an absorber section. An optical bandwidth over 1.3 THz yielding over 100 channels, 10 GHz spaced, is reported. Mode-locking properties are analyzed using the frequency domain based on the concept of super-modes. An Allan deviation down to $\sim 10^{-9}$ is reported for these passively mode-locked lasers. The low timing jitter, long-term stability and high channel count of these QD based combs are of great potential for Tb/s data transmission with only one single FP type laser source.

9370-86, Session 25

Tuning of superconducting nanowire single-photon detector parameters for VLSI circuit testing using time-resolved emission

 Andrea Bahgat Shehata, Franco Stellari, IBM Thomas J.
 Watson Research Ctr. (United States)

Time-Resolved Emission (TRE) is a truly non-invasive technique based on the detection of intrinsic light emitted by integrated circuits that is used for the detection of timing related faults from the backside of flip-chip VLSI circuits. Single-photon detectors with extended sensitivity in the Near InfraRed (NIR) are used to perform time-correlated single-photon counting measurements and retrieve the temporal distribution of the emitted photons, thus identifying gates' switching events. The noise, efficiency and jitter performance of the detector are crucial to enable ultra-low voltage waveform sensitivity. For this reason, cryogenically cooled Superconducting Nanowire Single-Photon Detectors (SNSPDs) offer superior performance compared to state-of-the-art Single-Photon Avalanche Diodes (SPADs). In this paper we will discuss how electronics parameters, such as bias current, RF attenuation and threshold comparator, can be tailored to optimize the measurement signal-to-noise ratio, defined as the ratio between the switching emission peak amplitude and the standard deviation of the noise in the time interval in which there are no photons emitted from the circuit. For example, lowering the attenuation and the comparator threshold leads to an improvement of the jitter, due to the better discrimination of the detector's firing. On the other hand, increasing the bias current both the detection efficiency and the jitter improve, but the noise increases as well, leading to an optimal SNR. For this work, TRE waveforms were acquired from a 32 nm Silicon On Insulator (SOI) chip operating down to 0.4V using different SNSPDs.

9370-98, Session 25

Low-dimensional II-VI oxide-based semiconductor nanostructure photodetectors for light sensing (*Invited Paper*)

Jae Su Yu, Yeong Hwan Ko, Goli Nagaraju, Kyung Hee Univ. (Korea, Republic of)

Photodetectors which convert light into electrical signals are essential elements in a variety of fields of optical and optoelectronic systems. Conventionally, Si- or Ge-based and III-V-based semiconductors have been employed for these photodetection applications. Recently, one-dimensional metal oxide inorganic semiconductor nanostructures, such as ZnO and b-Ga₂O₃, a-Fe₂O₃, TiO₂, Cu₂O, CdO, SnO₂, etc., are very promising for photodetectors and sensors in the ultraviolet and visible wavelength regions due to their excellent physical and chemical properties. These nanostructured materials which are fabricated with a simple and low-cost process by various methods provide many advantages such as larger surface areas and superior properties over bulk or thin-film structures. Thus, the development of multifunctional nanostructures is required for their applications into photodetectors to enhance the device performance. In this presentation, low-dimensional II-VI oxide-based semiconductor nanostructure photodetectors for light sensing are described. Depending on the absorption edge and energy bandgap of the nanostructured materials, the detection wavelength range can be controlled. The physical properties of the fabricated nanostructures are investigated. Metal-semiconductor-metal type photodetectors are fabricated by integrating the oxide-based semiconductor nanostructures. Their photoresponse characteristics are evaluated in a specific spectral range.

9370-110, Session 25

Introducing Fourier-domain mobility spectrum analysis (FMSA) to deduce multi-component carrier mobility and density

Boya Cui, Yang Tang, Matthew Grayson, Northwestern Univ. (United States)

Heterostructures in optical devices often host multiple carrier species that contribute simultaneously to the total electrical conduction, making it difficult to distinguish the characteristics of each type. Although previous analysis methods such as improved QMSA (i-QMSA) [1] and Maximum Entropy MSA (ME-MSA) [2] tackle this problem of parallel conduction, they all have limitations: i-QMSA requires the conductivity derivatives as additional fitting parameters to minimize unphysical features [2], and both i-QMSA and ME-MSA do not accurately consider the lowest mobility species at the limits of their mobility range [2][3]. Here a simpler Fourier-domain mobility spectrum analysis (FMSA) [3] is introduced to sort the conductivity contributions of different carrier species from magnetotransport measurements. A MOCVD-grown high-mobility heterostructure InP/InGaAs is characterized to obtain the temperature-dependent conductivity and mobility of two different electron species from the doping layer and from the high-mobility two dimensional electron gas (2DEG), respectively. Unlike previous techniques, FMSA employs a background subtraction to isolate extremely low mobility contributions, and then iteratively adjusts the spectral densities in either the mobility domain or its Fourier reciprocal space to fit the mobility range spanning almost five orders of magnitude ($m = 10 - 1000,000 \text{ cm}^2/\text{Vs}$). Background subtraction gives more reliable information in the low-mobility regime below $1/B_{\text{max}}$. With its alternating local and global adjustments, FMSA is able to recover the mobility distribution of test data, as verified in convergence plots of the total error as a function of iteration times. This technique resolves more accurate linewidths than competing MSA techniques with a simple and elegant algorithm while precisely resolving the smoothness of wide mobility peaks and without artificially broadening peaks.

[1] I. Vurgaftman, et al, J.Appl. Phys. 84, 4966 (1998).

[2] S. Kiatgamolchai, et al, PR E 66 (2002). Copyright © 2014 by Northwestern University, All Rights Reserved

Conference 9371: Photonic and Phononic Properties of Engineered Nanostructures V

Monday - Thursday 9-12 February 2015

Part of Proceedings of SPIE Vol. 9371 Photonic and Phononic Properties of Engineered Nanostructures V

9371-202,

Tunable and quantum metaphotonics

Harry A. Atwater Jr., DOE Light-Material Interactions Energy Frontier Research Ctr. (United States) and Resnick Institute (United States) and California Institute of Technology (United States)

Progress in understanding resonant subwavelength structures has fueled an explosion of interest in fundamental processes and nanophotonic devices. The carrier density and optical properties of photonic nanostructures are typically fixed at the time of fabrication, but field effect tuning of the potential and carrier density enables the photonic dispersion to be altered, yielding new approaches to energy conversion and tunable radiative emission. Electrochemical in metals yields tunable resonances and reveals the plasmoelectric effect, a newly-discovered photoelectrochemical potential. Finally, while plasmons are usually described in a classical electromagnetic theory context, under single photon excitation quantum coherent states emerge. We demonstrate entanglement or coherent superposition states of single plasmons using two plasmon-quantum interference in chip-based plasmon waveguide directional couplers.

9371-1, Session 1

Nanoscale engineering optical nonlinearities and nanolasers (*Invited Paper*)

Yeshiahu Fainman, Univ. of California, San Diego (United States)

Dense photonic integration requires miniaturization of materials, devices and subsystems, including passive components (e.g., engineered composite metamaterials, filters, etc.) and active components (e.g., lasers, modulators, detectors). This paper discusses passive and active devices that recently have been demonstrated in our laboratory and design, fabrication and testing of nanolasers constructed using metal-dielectric-semiconductor resonators confined in all three dimensions and operating at room temperature.

9371-2, Session 1

Electrical control and detection of nanoscale optical fields with 2d materials (*Invited Paper*)

Frank H. Koppens, ICFO - Institut de Ciències Fotòniques (Spain)

In this talk, we use 2d materials to tailor novel nano-optoelectronic capabilities, exploiting strong-light matter interactions at the nanometer scale.

First, we will discuss the strong near-field interactions between graphene and nanoscale light-emitters. Because graphene is gapless with tunable carrier density, it can effectively behave as a semiconductor, a dielectric, or a metal. We exploit this to electrically control optical emitter relaxation pathways. Specifically, we control whether emitter excitations are converted into either photons, electron-hole pairs, or plasmons with confinement to the graphene sheet below 15 nm. Additionally, we electrically detect the transferred energy from the emitter into the graphene, enabling all-electrical

detection of the diamond NV center spin.

Second, we address the highly confined optical fields (plasmons) in heterostructures of graphene and hexagonal boron nitride. We find unprecedented low plasmon damping, while the device structures enable even stronger field confinement than for earlier graphene plasmon devices. Based on these results, we address new configurations to electrically control and detect plasmons, and develop a detailed understanding of their decay mechanisms and coupling to electronic excitations. Finally, we discuss the carrier dynamics in graphene from a broader perspective.

9371-3, Session 1

Detecting and controlling coherent acoustic phonons in complex nanostructures with plasmons (*Invited Paper*)

Kevin O'Brien, Norberto D. Lanzillotti-Kimura, Junsuk Rho, Haim Suchowski, Xiaobo Yin, Xiang Zhang, Univ. of California, Berkeley (United States)

The interplay between phonons and photons is increasingly important in modern photonics. Nanoplasmonic resonators are promising systems for generating and detecting coherent acoustic phonons due to their large optical absorption cross sections and high sensitivity to refractive index perturbations. To investigate this interplay between phonons and plasmons, we design and fabricate arrays of plasmonic nanostructures in the shape of Swiss Crosses which have visible frequency optical resonances and phonon eigenfrequencies near 10 GHz. We perform polarization resolved transient absorption spectroscopy on the plasmonic nanostructures and observe interference features in the frequency domain response due to the symmetric and anti-symmetric phonon modes. From this phonon interference, we can resolve the spatial properties of the phonon modes. In addition, manipulating the polarization of the probe laser allows dynamic control over the region in which mechanical motion is detected. The multiple vibrational states in nanostructures can be tailored by manipulating the geometry and dynamically enhanced or eliminated by coherent control. These nanostructures allow detection and generation of coherent strains using localized plasmons.

9371-4, Session 1

Noise in microphotonic oscillators (*Invited Paper*)

Lute Maleki, Andrey Matsko, OEwaves, Inc. (United States)

Photonics oscillators have demonstrated extremely high spectral purity, outperforming their electronic counterparts. In particular, Microwave and mm-wave oscillators based on optical frequency combs currently feature the highest spectral purity achieved with room temperature devices. These advances have promoted research into the sources of noise in photonics oscillators. In the case of microphotonic oscillators, such as those based on miniature Kerr frequency comb generator, sources of fundamental and technical noise are often intertwined with the noise of the laser that excites the oscillation. An example for this is the limitation of the oscillator's spectral purity set by the RIN of the laser. We will discuss these and other sources that influence the performance of the oscillator, with the aim of deducing the ultimate achievable spectral purity with a microphotonic oscillator.

9371-5, Session 2

Processable organic materials with large figures-of-merit for all-optical signal processing (*Invited Paper*)

Joseph W. Perry, Ali Adibi, Stephen Barlow, Jean-Luc Brédas, Ali A. Eftekhar, Yulia A. Getmanenko, Rebecca L. Giesecking, Joel M. Hales, Amir H. Hosseinnia, Georgia Institute of Technology (United States); Khanh Kieu, The Univ. of Arizona (United States); Hyeongeun Kim, Seth R. Marder, Hesam Moradinejad, Georgia Institute of Technology (United States); Robert A. Norwood, The Univ. of Arizona (United States); Chad M. Risko, Georgia Institute of Technology (United States); Shiva Shahin, The Univ. of Arizona (United States); Yadong Zhang, Georgia Institute of Technology (United States)

Polymethine dyes have been shown to have promising molecular third-order nonlinear optical (NLO) properties but have not shown adequate figures-of-merit (FOM) for all-optical signal processing (AOSP). This is largely due to the strong attractive interactions between molecules, which leads to aggregation and alterations of the electronic energy level structure that deleteriously affect the optical nonlinearity and optical loss. We have employed a molecular design strategy to achieve AOSP that is based on substitution of polymethines with bulky groups that prevent aggregation leading to high-number-density films with macroscopic NLO close to those needed for AOSP with exceptionally high two-photon FOM ($\text{Re}[\chi^{(3)}]/\text{Im}[\chi^{(3)}]$). The use of bulky groups on polymethine compounds results in dilute-solution like properties in 50wt.% blend films with amorphous polycarbonate and, remarkably, for neat molecular films. These thio- or seleno-pyrylium based polymethines exhibit a negative $\text{Re}[\chi^{(3)}]$ that can be useful in the compensation of self phase modulation (spectral broadening) that is associated with the propagation of strong optical signals in optical fibers. We demonstrate the use of a 50 cm liquid core optical fiber filled with a 20 mM solution of a thiopyrylium based polymethine was able to reverse the spectral broadening due to self-phase modulation from propagation of the pulses through a solution of CCl₄ and CS₂. In a similar vein, we will report on solutions and films with near-zero nonlinearity. Finally, we report on the successful integration of such polymethine based solid-state materials into nanoslot waveguide structures, which opens new possibilities in silicon-organic hybrid devices for AOSP.

9371-6, Session 2

Sub-diffractive volume-confined polaritons in a natural hyperbolic material: hexagonal boron nitride

Joshua D. Caldwell, U.S. Naval Research Lab. (United States); Andrey V. Kretinin, The Univ. of Manchester (United Kingdom); Yiguo Chen, Vincenzo Giannini, Imperial College London (United Kingdom); Michael M. Fogler, Univ. of California, San Diego (United States); Yan Francescato, Imperial College London (United Kingdom); Chase T. Ellis, Joseph G. Tischler, U.S. Naval Research Lab. (United States); Colin R. Woods, The Univ. of Manchester (United Kingdom); Alexander J. Giles, U.S. Naval Research Lab. (United States); Minghui Hong, National Univ. of Singapore (Singapore); Kenji Watanabe, Takashi Taniguchi, National Institute for Materials Science (Japan); Stefan A. Maier, Imperial College London (United Kingdom); Kostya S. Novoselov, The Univ. of Manchester (United Kingdom)

Strongly anisotropic media where principal components of the dielectric tensor have opposite signs are called hyperbolic. These materials permit highly directional, volume-confined propagation of slow-light modes at deeply sub-diffractive size scales, leading to unique nanophotonic phenomena. The realization of hyperbolic materials within the optical spectral range has been achieved primarily through the use of artificial structures typically composed of plasmonic metals and dielectric constituents. This has enabled the realization of a number of exciting physical phenomena, but the high optical losses of plasmonic metals and the inhomogeneous nature of these materials have lowered the efficiency of these systems and have limited the spectral range of operation to the visible and near-infrared. Recently, hexagonal boron nitride (hBN) was identified as a natural hyperbolic material (NHM), offering a low-loss, homogeneous medium that can operate in the mid-infrared. We have exploited the NHM response of hBN within periodic arrays of conical nanoresonators to demonstrate 'hyperbolic polaritons,' deeply sub-diffractive guided waves that propagate through the volume rather than on the surface of a hyperbolic material. We have identified that the polaritons are manifested as a four series of resonances in two distinct spectral bands that have mutually exclusive dependencies upon incident light polarization, modal order, and aspect ratio. The resonances exhibit exceptional optical confinement (up to $\lambda/86$) and record-high quality factors (Q up to 283) for sub-diffractive modes. These observations represent the first foray into creating NHM building blocks for mid-infrared to terahertz nanophotonic and metamaterial devices.

9371-7, Session 2

Zinc oxide nanophotonics

Sumin Choi, Cuong Ton-That, Univ. of Technology, Sydney (Australia); Stefania Castelletto, RMIT Univ. (Australia); Brett C. Johnson, The Univ. of Melbourne (Australia); Matthew R. Phillips, Igor Aharonovich, Univ. of Technology, Sydney (Australia)

ZnO is a wide band gap semiconductor with remarkable optical properties. ZnO nanostructures can be easily grown using simple CVD methods and it hosts a variety of optically active defects. In this work, we study ZnO suitability for applications in nanophotonics. We first show that ZnO hexagonal microdisks can be easily grown using the carbothermal reduction method of ZnO powder. The microdisks have smooth edge facets that support propagation of whispering gallery modes. We employ monochromatic cathodoluminescence (CL) imaging to show that the green luminescence is enhanced at the hexagonal boundary of the microdisk and present modelling to support the mode propagation.

Second, we study single photon emission from 20 nm ZnO nanoparticles. The nanoparticles exhibit ultra bright single photon emission and broad luminescence at the red spectral range, at room temperature. We study the blinking behaviour of the nanoparticles using various surface termination techniques, and show that the blinking can be suppressed by coating the nanoparticles with PMMA.

ZnO can be considered as an emerging platform to study nanophotonics and spectroscopy of single defects as it requires easy fabrication techniques. It is therefore an interesting candidate for future efficient LEDs and quantum communication networks.

9371-8, Session 2

Silicon carbide tetrapods: novel room temperature quantum systems

Igor Aharonovich, Univ. of Technology, Sydney (Australia); Zoltan Bodrog, Wigner Research Ctr. for Physics of the H.A.S. (Hungary); Andrew P. Magyar, Harvard Univ. (United States); Angus R. Gentle, Univ. of Technology, Sydney (Australia); Adam Gali, Budapest Univ. of Technology and

**Conference 9371: Photonic and Phononic Properties
 of Engineered Nanostructures V**

Economics (Hungary); Stefania Castelletto, RMIT Univ. (Australia)

Semiconductor nanocrystals have enabled research in technologically important areas including bio-labeling, solid state lighting, and quantum information. However, most of the quantum dots are only emitting single photons at cryogenic temperatures due to low exciton binding energy. Recently, a new class of materials has attracted a considerable attention – namely crystal phase quantum dots. These nanomaterials have identical chemical composition with alternating polytypes – for instance wurtzite (WZ) and zincblend (ZB).

In this work we report on a novel quantum system – SiC tetrapods. The tetrapod are approximately 100 nm in size, and consists of a cubic (3C) core and hexagonal (4H) arm. The nanometer size core forms a quantum confined exciton that results in room temperature, narrowband, fully polarized, single photon emission at the near infrared. The origin of the quantum confinement effect is the spontaneous polarization between the 4H and the 3C polytypes.

Low temperature measurements are done to provide insights into the photo-luminescence dynamics and modelling is performed to understand the emission pattern from the nanostructured tetrapods. Finally, we compare the emission from SiC tetrapods with SiC nanoparticles, to unambiguously prove that the tetrapods exhibit a quantum confinement effect at room temperature. Control over the nanometer size and emission wavelength of a single tetrapod can be exploited in using the SiC tetrapods for nanophotonics, sensing and quantum information processing.

9371-9, Session 3

Flat free-space optical components and systems based on sub-wavelength high-index dielectric structures (Invited Paper)

Amir Arbabi, Yu Horie, Alexander J. Ball, California Institute of Technology (United States); Mahmood Bagheri, Jet Propulsion Lab. (United States); Andrei Faraon, California Institute of Technology (United States)

Flat optical devices based on sub-wavelength high index dielectric structures promise to revolutionize the field of free-space optics. I discuss our work on high contrast transmitarrays and reflectarrays that enable precise phase control with high spatial resolution. We demonstrate high numerical aperture lenses with applications in microscopy, and custom phase plates to collimate and circularize the mode of semiconductor lasers operating in mid-infrared and telecom. Multiple flat optical elements are integrated in optical systems such as planar retro-reflectors that combine flat lenses and mirrors. New functionalities enabled by flat optical components and the prospects for tunable devices are discussed.

9371-10, Session 3

Enhancing and inhibiting stimulated Brillouin scattering in photonic integrated circuits (Invited Paper)

Benjamin J. Eggleton, The Univ. of Sydney (Australia)

On-chip nonlinear optics is a thriving research field which creates transformative opportunities for manipulating classical or quantum signals in small-footprint integrated devices. Since optical nonlinearities are weak, nonlinear interactions are commonly enhanced by exploiting materials with large nonlinearity in combination with high-Q resonators or slow-light structures. This, however, often results in simultaneous enhancement of competing nonlinear processes, which limit the efficiency and can cause signal distortion. Here, we exploit for the first time the frequency dependence of the optical density of states near the edge of a photonic-bandgap to selectively enhance or inhibit nonlinear interactions on a chip.

We demonstrate this concept for one of the strongest nonlinear effects, stimulated Brillouin scattering (SBS) using a narrow-band one-dimensional photonic-bandgap structure: a Bragg grating. The SBS enhancement enabled the generation of a 15-line Brillouin frequency comb. In the inhibition case, SBS-free operation was achieved at a power level twice the SBS threshold.

9371-11, Session 3

Strategies for optical integration of single-photon sources (Invited Paper)

Oliver Benson, Andreas W. Schell, Tanja Neumer, Humboldt-Univ. zu Berlin (Germany); Qiang Shi, Karlsruhe Institute of Technology (Germany); Johannes Kaschke, Joachim Fischer, Martin Wegener, Karlsruher Institut für Technologie (Germany)

Stable and efficient single photons are key elements for various tasks in optical quantum information processing. Sources based on solid-state single-photon emitters, like quantum dots, molecules or defect centers in diamond are of particular interest. Their integration in complex integrated structures is a very demanding task. A lot of progress was achieved in architectures based on a single material platform, e.g. III-V semiconductors. However, other solid-state sources require a hybrid platform.

Here, we introduce an approach using photon emission from defect centers in diamond and laser-written photonic structures. Direct laser-writing offers a tremendous variety of possible structures. Waveguides, microresonators, and optical antennas can be fabricated and oriented with respect to the single emitters. In this contribution we describe our general approach before we specifically address the problem of efficient single photon collection through optical antennas. We discuss the limitations of the method, its potential for scalability as well as its extension towards optical sensing applications.

9371-12, Session 3

Ultra-compact waveguide devices in thin film lithium niobate

Abdoulaye Ndao, Wentao Qiu, Xin Xu, Clement Guyot, Roland Salut, Gwen Ulliac, Nadege Courjal, Hervé Maillotte, Fadi Issam Baida, Maria Pilar Bernal, FEMTO-ST (France)

Micrometric size optical devices in a multiphysical (it is acousto-optic, electro-optic, pyroelectric, piezoelectric, nonlinear, etc.) dielectric like lithium niobate (LN, LiNbO₃) bring exciting perspectives for multifunctional integrated optics as well as highly sensitive non-metallic electric field sensors. In this talk we will present novel optical nanodevices based on thin film lithium niobate and innovative waveguide geometries. In particular, we will show strip loaded and nonlinear slot waveguides fabricated on 700 nm thick lithium niobate (NanoLN) in which photonic crystals have been milled. Due to the well-known electro-optic effect of lithium niobate, and combined with suitable slow light geometries these devices can present an enhancement in the electro-optic coefficient and therefore can potentially be used for electric field sensing of very small electric field amplitudes (pV/m) which can find for instance applications in biosensing.

9371-13, Session 3

Local resonance control of high-Q coupled nanocavities

Sergei Sokolov, Jin Lian, Univ. Twente (Netherlands); Alfredo De Rossi, Sylvain Combrie, Thales Research

**Conference 9371: Photonic and Phononic Properties
 of Engineered Nanostructures V**

& Technology (France); Allard P. Mosk, Univ. Twente (Netherlands)

Arrays of coupled high-Q nanocavities are fascinating for their slow-light applications and light-matter interaction enhancement [1, 2]. Due to inevitable disorder in the fabrication process some cavities are detuned from the intended frequency leading to degradation of the transmission. Achieving local resonance control of high Q cavities will not only restore the arrays to perfect, but also provide a route to have programmable photonic integrated circuits. Thermal switching equipped with wavefront shaping allows us to change resonance properties of cavities in the array [3]. This gives an opportunity to counteract the disorder and push the application of coupled cavity arrays forward.

In order to use thermal switching to control nanocavities, there are two key pieces of information which are required. The first is the resonance shift in wavelength versus the power of the pump light. This decides how much power is needed to shift the resonance to the desired wavelength. The second is the thermal profile of the pump light. This determines the thermal coupling between the neighbor cavities. Knowing the amount of disorder of each cavity, the problem of counteracting disorder is transformed to solve linear algebra equations.

In our experiments we retrieved the linear relation between the pump power of a 405 nm heating laser and the red shift of the resonance of an InGaP nanocavity. Most importantly, the thermal switching profile has been measured for the first time for such cavities. The thermal profile can be described accurately by our 2D analytic heat diffusion model. Our research sets up the foundation for the local resonance control of the coupled nanocavity arrays .

[1] A. Yariv, Y. Xu R. K. Lee and A. Scherer Opt. Lett. 24 711 (1999).

[2] M. Notomi, E. Kuramochi and T. Tanabe Nature Photon. 2 741 (2008).

[3] A.P. Mosk, A. Lagendijk, G. Lerosey, and M. Fink, Nature Photon. 6, 283-292 (2012).

9371-14, Session 4
Nano-spectroscopy using fabricated photonic crystals and plasmonic geometries (*Invited Paper*)

Axel Scherer, Sameer Walavalkar, William S. Fegadolli, California Institute of Technology (United States)

We describe the integration of optical systems within microfluidic environments to perform spectroscopy on small volumes of analytes. Effects such as Raman emission and the observation of binding reactions are observed when high optical fields are generated within nanofabricated geometries. We review different choices of such measurements at the molecular scale, and show how they can be used in biomedical applications.

9371-15, Session 4
Experimental observation of Anderson localization modes in a compositionally-disordered photonic crystal system

Myungjae Lee, Jeongkug Lee, Minsu Kang, Heonsu Jeon, Seoul National Univ. (Korea, Republic of)

Anderson localization is a spatial localization of physical waves as a result of multiple-scatterings in disordered systems. In this study, we have directly observed strong localization of photons in two-dimensional (2D) photonic crystal (PC) structure by introducing compositional disorder for which the relative compositional ratio of constituent atoms varies while the translational symmetry of crystalline structure is conserved. A quaternary disordered system was designed and fabricated by arranging air-holes of four different kinds of radii across the hexagonal lattice 2D PCs at various

configurations and ratios. Disorder patterns were generated using electron-beam lithography and then transferred to InAsP/InP multiple-quantum-well slab via reactive ion etching with the aid of silicon nitride hard mask layer. As a way of identifying Anderson-localized modes in this system, we measured the emission spectra using a micro-photoluminescence setup. Weak but well-defined emission peaks newly popped out from the spectral region that corresponds to the forbidden photonic bandgap of the non-disordered reference PC structure. Subsequently, we confirmed this photon mode to be a spatially localized one by comparing the spatial modal pattern of the mode with the topographical image of the PC structure, both measured using a wavelength-tuned near-field scanning optical microscope. Finite-difference time-domain simulations also reproduced the experimental outcome reasonably well. Some of the localized modes exhibited sharp emission linewidths and clear thresholds, indicating that the localized modes led to lasing action.

9371-16, Session 4
Polarization sensitive beam bending using a spatially-variant photonic crystal

Jennefir Digaum, CREOL, The College of Optics and Photonics, Univ. of Central Florida (United States); Javier J. Pazos, Raymond C. Rumpf, The Univ. of Texas at El Paso (United States); Jeffrey Chiles, Sasan Fathpour, Stephen M. Kuebler, CREOL, The College of Optics and Photonics, Univ. of Central Florida (United States)

A spatially-variant photonic crystal (SVPC) that can control the spatial propagation of electromagnetic waves in three dimensions with high polarization sensitivity was fabricated and characterized. The geometric attributes of the SVPC lattice were spatially varied to make use of the directional phenomena of self-collimation to tightly bend an unguided beam coherently through a 90° turn. Despite the bend, both the lattice spacing and the fill factor of the SVPC were maintained to be nearly constant throughout the structure. A finite-difference frequency-domain computational method confirms that the SVPC can self-collimate and bend light without significant diffuse scatter caused by the bend. The SVPC was fabricated using multi-photon direct laser writing in photo-polymer SU-8. Mid-infrared light of 2.94 μm was used to experimentally characterize the SVPC by scanning the different sides with optical fibers. Results have shown that the SVPC is capable of directing power flow of one polarization through a 90° turn, confirming the self-collimating and polarization selective light-guiding properties of the lattice.

9371-17, Session 4
The circular Bragg phenomenon for oblique incidence

Sema Erten, Akhlesh Lakhtakia, The Pennsylvania State Univ. (United States); Greg D. Barber, Pennsylvania State Univ (United States)

Structurally chiral materials such as cholesteric liquid crystals (LCs) and chiral sculptured thin films (STFs) exhibit the circular Bragg phenomenon (CBP). These materials preferentially reflect circularly polarized light of the same handedness while transmitting circularly polarized light of the opposite handedness within a range of wavelengths called circular Bragg regime. The CBP has been extensively investigated experimentally for normal incidence, but not for oblique incidence. The aim of the study was to investigate the CBP for oblique angles of incidence to experimentally prove the theoretical predictions. The results can be used for applications depending on angular tuning of CB regime. The CBP exhibited in chiral STFs is examined using a custom-made experimental set-up to measure specular and non-specular reflectance and transmittance. Chiral STFs of zinc selenide were deposited on BK7 glass substrates via a resistive heating physical vapor deposition technique. The films used in this study have 20

**Conference 9371: Photonic and Phononic Properties
of Engineered Nanostructures V**

periods, each period being 325 nm in thickness. The results clearly indicate the circular Bragg regime for all angles of incidence. A blue-shift in the wavelength regime of the CBP with increasing angle of incidence was observed and agrees with previous theoretical predictions, qualitatively.

9371-18, Session 4
Linear and nonlinear optical responses in chiral metamaterials

Wenshan Cai, Sean P. Rodrigues, Shoufeng Lan, Yonghao Cui, Lei Kang, Georgia Institute of Technology (United States)

The past few years have witnessed an explosive development of chiral optical metamaterials that exhibit circular dichroism and optical rotation orders of magnitude larger than conventional materials. Though chirality is most commonly applied in linear optical regime, opposing circularly polarized waves can also display parity as a property of higher order optics. Here we present a chiral metamaterial that produces both distinguishable linear and nonlinear resonant features when probed with left and right circularly polarized incident beams in the visible to near-infrared regime. Using an array of dual-layer twisted-arcs with a total thickness of approximately one-fifth of the applied wavelength of light, our experimental results show a circular dichroism of over 0.4 in the absolute value, and a maximum polarization rotation of over 300 degrees per wavelength of light. A transmission of greater than 50% is achieved at the frequency where the polarization rotation peaks. Retrieved parameters from measured quantities further indicate an actual optical activity of 76 degrees per wavelength, and a difference of 0.42 in the indices of refraction for the two circularly polarized waves of opposite handedness. Moreover, the metamaterial demonstrates a 20x contrast between second harmonic responses from the two circular polarizations. Linear and nonlinear response images probed with circularly polarized lights show strongly defined contrast, and the second-harmonic circular-dichroism images are produced to reveal the chiral characteristics of a metamaterial pattern consisting of opposite meta-enantiomers. The coupled twisted-arcs nanostructure is further exploited for chiral-selective two-photon luminescence of quantum emitters embedded in the metamaterial matrix.

9371-19, Session 4
Introducing high-quality planar defects into colloidal crystals via self-assembly at the air/water interface

Kuo Zhong, Katholieke Univ. Leuven (Belgium); Pieter-Jan H Demeyer, Olga Kruglova, University of Leuven (Belgium); Niels Verellen, University of Leuven (Belgium) and IMEC (Belgium); Victor V Moshchalkov, University of Leuven (Belgium); Kai Song, Technical Institute of Physics and Chemistry, Chinese Academy of Sciences (China); Koen Clays, University of Leuven (Belgium); xingping zhou, National Laboratory of Solid State Microstructures and Department of Physics, Nanjing University, Na (China)

We demonstrate an extremely facile method to insert a planar defect into colloidal photonic crystals. The defect layer itself is introduced by direct assembly at air/water/substrate contact line. Firstly, a two-dimensional monolayer of solid SiO₂ microspheres (guest spheres) was formed at the air/water interface by compressing the individual microspheres with surfactant into long-range ordered arrays. The floating monolayer, which served as our defect layer, was then transferred onto a pre-deposited colloidal crystal slab consisting of PS@SiO₂ microspheres (host spheres). Due to the presence of surfactant molecules, acting as a soft barrier, a high-quality 2D monolayer of solid SiO₂ spheres was obtained and layer

transfer was facilitated. After deposition of the second colloidal crystal slab on the surface of the defect layer, a sandwich-like structure was obtained. The high-quality of defect layer resulted in pronounced and fairly narrow (FWHM-16 nm) pass bands within the Bragg peaks in reflectance spectra, which is narrower than previous reported results. By varying the diameter of guest spheres, the different defect modes were studied. Furthermore, it is easy to convert our system to inverse opal-like structure (CPC of hollow spheres), and defect modes with different dielectric nature were also discussed. The experimental results are in good agreement with simulations performed using the FDTD method.

9371-20, Session 5
From light modulation to far-field excitation of graphene plasmons: science and applications of graphene-integrated plasmonic metasurfaces (*Invited Paper*)

Gennady B. Shvets, The Univ. of Texas at Austin (United States)

Graphene has emerged as a promising optoelectronic material because its optical properties can be rapidly and dramatically changed using electric gating. Graphene's weak optical response, especially in the infrared part of the spectrum, remains the key challenge to developing practical graphene-based optical devices such as modulators, infrared detectors, and tunable reflect-arrays. Here it is experimentally and theoretically demonstrated that a plasmonic metasurface with two Fano resonances can dramatically enhance the interaction of infrared light with single layer graphene. Graphene's plasmonic response in the Pauli blocking regime is shown to cause strong spectral shifts of the Fano resonances without inducing additional non-radiative losses. It is shown that such electrically controllable spectral shift, combined with the narrow spectral width of the metasurface's Fano resonances, enables reflectivity modulation by nearly an order of magnitude. We also demonstrate that metasurface-based enhancement of the interaction between graphene and infrared light can be utilized to extract one of the key optical parameters of graphene: the free carrier scattering rate. Numerical simulations demonstrate the possibility of strong active modulation of the phase of the reflected light while keeping the reflectivity nearly constant, thereby paving the way to tunable infrared lenses and beam steering devices based on electrically controlled graphene integrated with resonant metasurfaces.

9371-21, Session 5
Holographic metasurface for wavelength and polarization demultiplexing via focused surface plasmon polariton beams

Daniel Wintz, Harvard Univ. (United States); Patrice Genevet, Harvard School of Engineering and Applied Sciences (United States); Antonio Ambrosio, Alex Woolf, Harvard Univ. (United States); Federico Capasso, Harvard School of Engineering and Applied Sciences (United States)

Recently developed nanostructured optical interfaces, known as metasurfaces, can be designed to exploit the potential and exceptional optical properties of surface plasmon polariton (SPP) waves. Here, we report a simple holographic metasurface design strategy that can be used for focusing, polarization beam splitting, waveguide coupling, and even phase control at the focus of an SPP beam. We experimentally verify our holographic metasurface by creating a four wavelength plasmonic demultiplexer, which also has polarization selectivity (on/off). The wavelength demultiplexer is designed such that each of the four wavelengths is focused to a completely different spot outside of the

**Conference 9371: Photonic and Phononic Properties
 of Engineered Nanostructures V**

structure. Focusing and demultiplexing is achieved by reverse engineering a thin gold film metasurface by way of a combination of holography and Huygen's principle. Coupling of free space light to the surface plasmon modes is achieved by milling subwavelength apertures into a thin gold film. This methodology can be easily extended to any wavelength where surface plasmons exist, for an arbitrary number of wavelengths, and with polarization selectivity and phase control at the focus as well. This affords the possibility to further control light-matter interaction on the nanoscale and in the surface optics regime, opening up new possibilities in the realm of integrated photonics and optoelectronics.

9371-22, Session 5

Spectral and spatial manipulation of the polarization by metasurface made of v-shaped plasmonic MIM nanoantennas

Patrick Bouchon, Quentin Lévesque, ONERA (France); Mathilde Makhsian, ONERA (France) and Lab. de Photonique et de Nanostructures (France); Julien Jaeck, ONERA (France); Fabrice Pardo, Jean-Luc Pelouard, Lab. de Photonique et de Nanostructures (France); Riad Haidar, ONERA (France)

The ability to control the polarization of an electromagnetic wave has a wide range of applications, like quarter wave plates, circular polarizers or polarization scramblers.

This is classically done thanks to dichroic crystals or birefringent materials, but can also be achieved with plasmonic diffraction gratings or chiral structures.

More recently, polarization conversion using plasmonic metasurfaces or metamaterials has attracted a wide attention.

Here, we demonstrate, both theoretically and experimentally, how V-shaped plasmonic metal-insulator-metal (MIM) nanoantennas are able to manipulate efficiently the polarization. In this nanoantenna, only the top metallic layer is patterned by coupling two dipolar nanorods. This leads to a splitting of the degenerate energy levels of the nanoantenna. At these non degenerated energy levels, the V-shaped nanoantenna is able to rotate the linear polarization of the reflected wave with a very high efficiency (all the reflected energy has a rotated polarization).

We have developed an analytical model based on the Jones formalism which fairly describe the behavior of the V-shaped MIM nanoantenna.

Eventually, we also demonstrate that it is possible to design a wideband polarizer converter with a high efficiency of 80% between 3.25 μm and 4.25 μm (Lévesque et al., Appl. Phys. Lett. 104, 111105 (2014)). This is obtained in the particular case of L-shaped MIM nanoantennas, and due to the localized nature of the resonance, the conversion is independent of the angle of incidence.

9371-23, Session 5

Metallic metasurface anti-reflective coating in mid-wave infrared regime

Joshua R. Hendrickson, Air Force Research Lab. (United States); Nima Nader, Air Force Research Lab. (United States) and Solid State Scientific Corp. (United States); Boyang Zhang, The Univ. of Alabama in Huntsville (United States); Hou-tong Chen, The Ctr. for Integrated Nanotechnologies (United States); Junpeng Guo, The Univ. of Alabama in Huntsville (United States)

Historically, anti-reflective coatings have been composed of layers of dielectric materials specifically chosen for both their index of refraction and their ability to be deposited, in a high quality fashion, onto a substrate

of interest. Using the Fresnel equations, one can determine the necessary refractive index and film thicknesses needed. Such traditional structures can be, at their thinnest, a quarter wave thick. However, since the materials available are limited, one cannot always find a sufficient material for a given substrate index and operational wavelength. This often necessitates multiple layers which can be expensive, environmentally unstable, and, at longer wavelengths, impractical due to the required thickness of each layer. By designing an anti-reflection coating based on a metallic metasurface, many of these shortcomings can be overcome. Through the excitation of a surface plasmon resonance in a subwavelength thin structured metal - dielectric coating, one can gain control of the magnitude and phase of the reflection coefficient, allowing for passively tunable anti-reflection with dimensions less than that of a quarter wave. The metasurface device consists of a periodic gold cross array fabricated onto a germanium substrate with a nanoscale dielectric spacer layer of magnesium fluoride (MgF₂) on the top. Using a microscope coupled Fourier transform infrared spectrometer, optical transmission and reflection were measured. At a wavelength of 5 microns, greater than 95% transmission was observed over a large angular range for an anti-reflective coating on a single germanium surface.

9371-24, Session 6

Electrical manipulation of nonlinear optical processes in metamaterials (Invited Paper)

Wenshan Cai, Lei Kang, Shoufeng Lan, Yonghao Cui, Sean P. Rodrigues, Georgia Institute of Technology (United States)

Metamaterials have offered not only the unprecedented opportunity to generate unconventional electromagnetic properties that are not found in nature, but also the exciting potential to create customized nonlinear media with high-order properties correlated to linear behavior. Two particularly compelling directions of current interests are active metamaterials, where the optical properties can be purposely tailored by external stimuli in a reversible manner, and nonlinear metamaterials, which enable intensity-dependent frequency conversion of light waves. By exploring the interaction of these two directions, in this work we leverage the electrical and optical functions simultaneously supported in nanostructured metals and demonstrate electrically-controlled nonlinear optical processes from a photonic metamaterial. We show that a variety of nonlinear optical phenomena, including the second harmonic generation and the optical rectification, can be enhanced by the resonance behavior in the metamaterial absorber and purposely modulated by applied voltage signals. In addition, electrically-induced and voltage-controlled nonlinear effects facilitate us to demonstrate the backward phase matching in a negative index material, a long standing prediction in nonlinear metamaterials. By utilizing two distinct modes in an electrically-biased plasmonic waveguide, we confirm that the phase-matched harmonic wave propagates along a direction opposite to that of the incoming fundamental light. Our results reveal a grand opportunity to exploit optical metamaterials as self-contained, dynamic electrooptic systems with intrinsically embedded electrical functions and optical nonlinearities.

9371-25, Session 6

High temperature applications enabled by refractory plasmonic materials

Urcan Guler, Nano-Meta Technologies, Inc. (United States); Alexander V. Kildishev, Purdue Univ. (United States); Alexandra Boltasseva, Vladimir M. Shalaev, Purdue Univ. (United States) and Nano-Meta Technologies, Inc. (United States)

Plasmonic applications where high operational temperatures are desired, or

**Conference 9371: Photonic and Phononic Properties
 of Engineered Nanostructures V**

unavoidable due to ohmic losses, are hindered by the material limitations such as chemical instability, softness, low melting point etc. Refractory materials are chemically stable at temperatures above 2000 C and they can address most of the problems associated with material limitations at high temperatures. Transition metal nitrides are plasmonic in the visible region and durable at high temperatures, enabling the use of plasmonic components for high temperature applications such as heat assisted magnetic recording (HAMR) and solar/thermophotovoltaics (S/TPV) [1, 2]. Furthermore, properties of transition metal nitrides can be tailored for device-specific requirements via deposition parameters [3]. In this contribution, optical properties and high temperature stability of refractory plasmonic materials are investigated. Application specific components such as near field transducers (NFTs) for HAMR, and selective metamaterial absorbers and emitters for S/TPV are designed and tested. Opportunities and challenges in the field of high temperature plasmonics are discussed. It is shown that titanium nitride (TiN) nanoparticles are promising for use in HAMR NFTs. Broadband absorbers and selective emitters for S/TPV devices employing TiN as the plasmonic component exhibit high optical performance as well as durability at high temperatures.

[1] U. Guler, A. Boltasseva, and V. M. Shalaev, "Refractory Plasmonics," *Science* 344, 263-264 (2014).

[2] U. Guler, J. C. Ndukaife, G. V. Naik, A. G. A. Nnanna, A. V. Kildishev, V. M. Shalaev, and A. Boltasseva, "Local Heating with Lithographically Fabricated Plasmonic Titanium Nitride Nanoparticles," *Nano Letters* 13, 6078-6083 (2013).

[3] G. V. Naik, V. M. Shalaev, and A. Boltasseva, "Alternative plasmonic materials: beyond gold and silver," *Adv Mater* 25, 3264-3294 (2013).

9371-26, Session 6
Genetic algorithm for true negative index in plasmonic metamaterials

Ian A. Goforth, Max A. Burnett, Daniel B. Fullager, Christopher Rosenbury, Hossein Alisafae, Michael A. Fiddy, The Univ. of North Carolina at Charlotte (United States)

Negative refractive index is one of the most interesting properties of metamaterials with various applications. There are, however, cases in which negative refraction occurs without the fundamental property in which magnetic and electric dipoles simultaneously exhibit a negative response to the excitation. Negative refraction is seen in photonic crystals or sometimes in a naturally occurring material. Distinguishing between the two cases is complicated by the periodic structure of most metamaterials, albeit subwavelength in scale) and the relatively narrow bandwidths involved. In some cases, both phenomena might occur simultaneously. We studied the fundamental response of metamaterials with non traditional designs for a better understanding of the relation between true negative index and spatial dispersion.

We investigated negative refractive index in plasmonic metamaterials with an emphasis on distinguishing and isolating possible Bragg-like effects arising from periodic properties. We also considered the significance of homogenization at different feature scales in the metamaterial (e.g. $\lambda/5$ to $\lambda/15$). In our approach, we utilized a genetic algorithm to modulate the spatial structure of metamaterial on a subwavelength scale thereby creating aperiodicities within the medium. The results are compared with those from more conventional designs having the same negative index properties. We performed fullwave finite element simulations on some specific designs to investigate the internal fields and the differences a genetic approach can introduce. This provides insight into some fundamental properties of metamaterials and how to improve their designs, especially broadening the bandwidth of negative index properties.

9371-27, Session 6
Quality-factor enhancement of fano resonance in asymmetric-double-bar metamaterials by alternately arranging inversed unit cells in the optical region

Yuto Moritake, Yoshiaki Kanamori, Kazuhiro Hane, Tohoku Univ. (Japan)

Metamaterials are artificial structures with exotic electromagnetic response: negative refraction, sub-wavelength focusing, and so on. Although characteristics of metamaterials are almost determined by unit cell structure, coupling effects among unit cells also have an important role in engineering electromagnetic response of metamaterials. For example, coupling among unit cells leads a shift of resonant wavelength and a change in a quality factor (Q-factor) of resonance. In this study, we investigated Q-factors of Fano resonance in optical metamaterials having alternate arrangement of inversed asymmetric double bars (ADBs) to study effects of neighboring unit cell. ADB is a pair of metal bars with slightly different bar lengths. Fano resonance with the high Q-factor can be excited because of small asymmetry of ADB. Alternate arrangement of inversed unit cells, in which the positions of the long bar and the short bar in neighboring unit cells were interchanged each other, was introduced into ADB metamaterials and its effect on the Q-factor was investigated. ADB metamaterials were fabricated by a lift-off method and optical spectra were measured. The Q-factors of Fano resonance around a wavelength of 1500 nm were estimated from absorption peaks, and dependence of a degree of asymmetry was studied. There was the best asymmetry condition, and the highest Q-factor of 30.2 was obtained by alternate arrangement. Moreover, the Q-factors for alternate arrangement of inversed unit cells were higher than for normally periodic arrangement. The relations between the Q-factors and concentrated electromagnetic fields in the unit cells were discussed by electromagnetic field calculations.

9371-28, Session 7
Macroscopic broadband 3D invisibility cloaking for diffusive visible light (Invited Paper)

Robert Schittny, Andreas Niemeyer, Muamer Kadic, Tiemo K. Bückmann, Andreas Naber, Martin Wegener, Karlsruhe Institut für Technologie (Germany)

In many situations, propagation of light can adequately be described by the Maxwell equations for macroscopic continua. However, in disordered media composed of many spatially randomly distributed scattering micro- or nanoparticles (e.g., fog or clouds), this is not possible and one can often rather describe the random walk of photons by Fick's diffusion equation. Recently (*Science* 345, 427-429 (2014)), we have presented experiments on macroscopic three-dimensional omnidirectional invisibility cloaking working throughout the entire visible spectrum in the diffusive regime under quasi-static conditions. We review these results and additionally present more recent (unpublished) experiments in the time-dependent diffusive regime.

9371-29, Session 7
3D optical metamaterials by self-assembly and templated directed solidification of eutectics (Invited Paper)

Paul V. Braun, Univ. of Illinois at Urbana-Champaign (United States)

Nanoscale integration of phases with metallic and non-metallic character

**Conference 9371: Photonic and Phononic Properties
 of Engineered Nanostructures V**

is critical for the realization of optical metamaterials. However, in the near-infrared and visible wavelength regime, the creation of useful metamaterials requires the ability to fabricate three-dimensional (3D) complex structures with high precision using techniques that ultimately enable large-scale manufacturing. A new paradigm for the design and fabrication of metamaterials is therefore needed. Our team is applying unique template-based and post-synthetic materials transformations in conjunction with powerful computational design tools to develop the scientific underpinnings of and to produce 3D metamaterials derived from directionally solidified eutectics. Our approach involves close interactions among computational design, photonic theory, eutectic materials development, template fabrication, materials chemistry, and optical characterization.

9371-30, Session 7

Photonic orbital Hall effect in double negative metamaterials

Zhicheng Xiao, Han Li, Partha P. Banerjee, Univ. of Dayton (United States)

We study the photonic orbital Hall effect in double negative metamaterials both theoretically and experimentally. In the theory part, we derive the transverse spin displacements of elliptical vortex beam at air-double negative metamaterial interface. The vortex beam bears an asymmetric spin split since the polarized vortex beam has angular momentum \hbar per photon along the propagation axis. The Lorentz-Drude model is adopted to take into account the effects of dispersion. The formulae of magnified spin split are demonstrated in the quantum weak measurement setup. By applying this method, we observe and measure the orbital Hall effect of reflected vortex beam at air-double negative metamaterial for the first time. Our experiment indicates that the beam shifts are the same as air-normal material interface when normal material and metamaterial have identical absolute value of refractive index. The unreversed orbital Hall effect in metamaterials provides direct evidence that the orbital angular momentum is unreversed in metamaterials. These experimental results substantiate some findings of our previous paper [Z. Xiao et al Phys. Rev. A 85, 053822 (2012)].

9371-31, Session 7

Epsilon near-zero metamaterials for ultra-low-power nonlinear applications

Monika Pietrzyk, Univ. of St. Andrews (United Kingdom); Rishad Kaipurath, Daniele Faccio, Heriot-Watt Univ. (United Kingdom); Andrea Di Falco, Univ. of St. Andrews (United Kingdom)

We report on the theoretical and experimental demonstration of enhanced nonlinear effects in epsilon-near-zero (ENZ) metamaterials, at optical frequencies. The samples were fabricated stacking several layers of silver (5 nm) and SiO₂ (70 nm). Their nonlinear properties were measured via z-scan measurements, using a pulsed Ti:sapphire laser. The results show that the ENZ samples have a nonlinear coefficient one order of magnitude higher than what expected by averaging the values of the metal and the dielectric layers.

This result could lead to the demonstration of ultralow power nonlinear optical devices.

9371-32, Session 7

Advanced applications of flexible metamaterials at visible frequencies

Blair Kirkpatrick, Peter J. Reader-Harris, Jingzhi Wu,

Yufang Shen, Andrea Di Falco, Univ. of St. Andrews (United Kingdom)

Flexible metamaterials (FMMs) implement the physics of MMs in a flexible substrate. This enables a wide range of exciting applications that take advantage of the conformability to complex shapes and post-fabrication tuning of the optical response. Here we demonstrate how FMMs can be used for robust and versatile lab-on-fibre applications, optomechanics and nonlinear applications.

9371-81, Session 7

Paraxial ray optics cloaking

Joseph S. Choi, Institute of Optics, Univ. of Rochester (United States)

Despite much interest and progress in optical spatial cloaking, a three-dimensional (3D), transmitting, continuously multidirectional cloak in the visible regime has not yet been demonstrated. Here we experimentally demonstrate such a cloak using ray optics, albeit with some edge effects. Our device requires no new materials, uses isotropic off-the-shelf optics, scales easily to cloak arbitrarily large objects, and is as broadband as the choice of optical material, all of which have been challenges for current cloaking schemes. In addition, we provide a concise formalism that quantifies and produces perfect optical cloaks in the small-angle ('paraxial') limit.

9371-33, Session 8

Hybrid nanoplasmonics for nonlinear optics, sensing, and biomiaging (*Invited Paper*)

Stefan A. Maier, Imperial College London (United Kingdom)

The first part of this talk will discuss designs of planar plasmonic nanoantennas for applications in enhanced higher harmonic generation and broadband optical biosensing. In particular, hybrid nanoantennas consisting of nonlinear material placed into the gap of dimer antennas will be shown to be efficient generators of higher harmonic light, due to enhanced light matter interactions mediated via the hot spot. Antennas designs inspired by RF log periodic antennas will be discussed in the context of broadband light concentrators for surface enhanced spectroscopies from the visible to the mid infrared.

The second part of the talk will focus on hybrid metal nanoparticles incorporating fluorescent dyes, and evaluate their potential for biological tagging for stimulated emission depletion microscopy (STED). Preliminary evidence on a reduction of the power requirement for STED will be shown in optimized particles.

9371-34, Session 8

Plasmonic interferometry for non-invasive glucose sensing (*Invited Paper*)

Domenico Pacifici, Brown Univ. (United States)

A non-invasive method for the detection of glucose is sought by millions of diabetic patients to improve personal management of blood glucose over a lifetime. In this work, the synergistic advantage of combining plasmonic interferometry with an enzyme-driven dye assay yields an optical sensor capable of detecting glucose in saliva with high sensitivity and selectivity. The sensor, coined a "plasmonic cuvette," is built around a nano-scale groove-slit-groove (GSG) plasmonic interferometer coupled to an Amplex-red/Glucose-oxidase/Glucose (AR/GOx/Glucose) assay. The

**Conference 9371: Photonic and Phononic Properties
of Engineered Nanostructures V**

proposed device is highly sensitive, with a measured intensity change of $1.7E5\% / M$ (i.e. one order of magnitude more sensitive than without assay) and highly specific for glucose sensing in picoliter volumes, across the physiological range of glucose concentrations found in human saliva ($20 - 240 \mu M$). Real-time glucose monitoring in saliva is achieved by performing a detailed study of the underlying enzyme-driven reactions to determine and tune the effective rate constants in order to reduce the overall assay reaction time to ~ 2 min. The results reported suggest that by opportunely choosing the appropriate dye chemistry, a plasmonic cuvette can be turned into a general, real-time sensing scheme for detection of any molecular target, with high sensitivity and selectivity, within extremely low volumes of biological fluid (down to femtoliters). Hereby, we present the results on glucose detection in artificial saliva as a notable and clinically relevant case study.

9371-35, Session 8

Imaging with multimode fibers (Invited Paper)

Demetri Psaltis, Ecole Polytechnique Fédérale de Lausanne (Switzerland)

Holography and phase conjugation were proposed in the middle 1960's for correcting the distortions in imaging systems due to aberrating or scattering media. These early methods have been revisited in recent years and successful experimental demonstrations have been reported with digital holographic methods in which the recording and reconstruction of the hologram is done with the help of a digital computer. The digital holographic methods offer a lot more flexibility and control compared to the all-optical methods of the past making holographic imaging practical. In addition, adaptive wavefront shaping techniques have been recently developed providing a set of related and synergistic methods for imaging in complex media. In this presentation we will focus primarily on the application of the modern tools of holography to the control of light transmission through multi-mode fibers. The modal dispersion that severely scrambles images propagating through multi-mode fibers can be compensated allowing us to exploit the many degrees of freedom available in the multi-mode fiber for imaging and sensing.

9371-36, Session 8

Mid-infrared opto-nanofluidics for on-chip chemical sensing

Pao T. Lin, Sen Kwok, Massachusetts Institute of Technology (United States); Hao-Yu G. Lin, Harvard Univ. (United States); Dawn T. H. Tan, Singapore Univ. of Technology & Design (Singapore); Lionel Kimerling, Massachusetts Institute of Technology (United States); Anu Agarwal, Massachusetts Institute of Technology (United States); George Whitesides, Harvard Univ. (United States) and Harvard Univ. (United States)

A mid-infrared (mid-IR) label-free chemical sensor was developed using opto-nanofluidics consisting of a Si-liquid-Si slot-structure. A broadband mid-IR lightwave can be strongly confined within a nanofluidic capillary by utilizing the large refractive index contrast ($n \sim 2$) between the liquid core waveguide and the Si cladding. Through an optical-field enhancement together with a direct interaction between the probe light and the analyte, the sensitivity for chemical detection is increased by 50 times when compared to evanescent-wave sensing. This spectral characterization distinguished several common organic liquids (e.g., n-bromohexane, toluene, isopropanol) accurately, and could determine the ratio of chemical species (e.g., acetonitrile and ethanol) at low concentration ($< 5 \mu L/mL$) in a mixture through spectral scanning over their characteristic mid-IR absorption peaks. The combination of CMOS-compatible planar mid-IR microphotronics, and a

high-throughput nanofluidic sensor system, provides a unique platform for chemical detection.

9371-37, Session 9

Photonics and plasmonics with 2D atomic membranes: physics and device applications (Invited Paper)

Farhan Rana, Cornell Univ. (United States)

The optical and plasmonic properties of 2D materials like graphene and transition metal dichalcogenides have made them promising candidates for different device applications. Plasmons in graphene are robust collective excitations. The large carrier mobility in graphene coupled with the large oscillator strength and wide tunability of its plasmon modes have made graphene extremely promising for plasmonics in the far-IR to near-IR wavelength range. We present experimental results on plasmon modes in several different graphene micro and nanostructures. Confined plasmon modes in graphene structures are well described by an eigenvalue equation. Plasmon modes in neighboring structures interact strongly and these interactions can be described by a coupled mode theory. Plasmons in graphene are strongly coupled to interband electronic transitions as well as to graphene and substrate phonons. These interactions offer opportunities for interesting and novel devices, such as plasmon lasers, as well as pathways for plasmon damping. Confined plasmons in graphene micro and nanostructures can be probed optically thereby providing a laboratory to study electron-electron and electron-phonon interactions in graphene. Accurate electromagnetic FDTD models have been developed that can help design graphene plasmonic devices for various applications. Results on devices, such as plasmonic detectors, filters, and micro-mechanical devices will be presented. Besides graphene, other 2D materials also offer unique optical properties. For example, transition metal dichalcogenides have extremely robust excitons that have binding energies and oscillator strengths that are almost two orders of magnitude larger than the excitons in III-V semiconductors. We will discuss the optical physics associated with these excitons and opportunities for novel devices.

9371-38, Session 9

Realizing a point cavity with near-field engineering of sub-wavelength plasmonic cavity

Myung-Ki Kim, Hongchul Sim, Yong-Hee Lee, KAIST (Korea, Republic of)

Over the past decade, various types of plasmonic cavities have been studied. One of the most promising features of plasmonic cavity is to enable us to funnel electromagnetic energy into a very small space of deep-subwavelength scale. The strongly amplified electric-field in the cavity has opened up the possibility to realize super-resolution optical-imaging, subwavelength-scale optical communications, and efficient single-photon sources. Some of their key advantages are their subwavelength sizes, superior optical performances, and very low energy consumption. However, as minimizing their sizes, several significant issues emerge-1) huge energy absorption into the metal and 2) very inefficient light coupling with conventional photonics and optics. To fundamentally solve those issues, the reliable and effective near-/far-field engineering method for plasmonic cavity should be studied. However, due to very small sizes, it's still a major challenge.

In this talk, we present our recent experimental study for the highly efficient gap-plasmon point-cavity that confines the light three-dimensionally within a volume of $\sim 10^{-6} \mu m^3$ at the sub-5-nm gap. The device was designed by three-dimensionally tapering the cavity structure which strongly confines the cavity mode to the minimum-gap region. The simulation study shows our sub-5-nm-gap point-cavity can boost the intensity enhancement up to more than 10^6 for the incident $1.56 \mu m$ light. We fabricated the three-

**Conference 9371: Photonic and Phononic Properties
 of Engineered Nanostructures V**

dimensional point-cavity with a 4.8-nm gap by employing the FIB proximal milling technique and observed the extreme intensity enhancement ($>10^4$) from the cavity by measuring the second-harmonic generation. The scanning cathodoluminescence image straightly demonstrates the extreme field-intensity stems from the sub-5-nm gap in the point-cavity.

9371-39, Session 9

Sub-wavelength confinement of the orbital angular momentum of light probed by plasmonic nanoantennae resonances

Marta Carli, Gianluca Ruffato, Pierfrancesco Zilio, Denis Garoli, Univ. degli Studi di Padova (Italy); Valentina Giorgis, IOM-CNR (Italy); Filippo Romanato, Univ. degli Studi di Padova (Italy) and IOM-CNR (Italy)

In this work, we theoretically and experimentally study how the OAM of a Plasmonic Vortex (a SPP with in general non-zero topological charge j) produced by a Plasmonic Vortex Lens (PVL) can be probed by the Localized Surface Plasmon Resonances of nanoantennae suitably placed inside the PVL. First of all, we recall the mechanism by which PVLs can couple a plane wave, convert it into a Plasmonic Vortex and focus it to their center. A hole milled at the center of the PVL then allows to convert the focused PV into an in-plane field. The antennae are either excited by this field or not, depending on their orientation and on j , thus acting as a fingerprint of the OAM of the PV at the nanoscale. We elucidate different aspects of this coupling and we study in particular the two cases ($j=0$ and $j=2$) which can be obtained by illuminating a single-arm PVL with circularly polarized light. If four nanoantennae are tangentially arranged inside the hole, they are excited for $j=2$, while for $j=0$ they are off. The integrated structure is fabricated and experimentally characterized in the two configurations mentioned above, by monitoring its near field using SNOM. Our results are in good agreement with the simulations and seem to prove the capability of PVLs to transfer OAM properties control to the nanoscale as well as engineering spin-orbit interactions in the sub-wavelength regime. Moreover, they suggest an efficient coupling with nanostructures, thus paving the way for many possible applications and developments.

9371-40, Session 9

Strong atom-field interactions in metallic coaxial nanocavities

Hossein Hodaie, Ahmed El Halawani, Parinaz Aleahmad, Mercedeh Khajavikhan, CREOL, The College of Optics and Photonics, Univ. of Central Florida (United States)

In this work, we investigate the prospect of using nanoscale metallic coaxial cavities as a viable platform for cavity-quantum electrodynamics (c-QED). Along these lines we show that it is possible to observe for the first time vacuum Rabi oscillations in such ultra-small volume configurations via strong atom-field interactions. Our atomic system comprises of a single InAs quantum embedded in GaAs. The entire structure is in turn surrounded by a silver coaxial resonator that has no cut-off (always supports a mode). The modes and their respective quality factors of these cavities are electromagnetically investigated at low temperatures (4-10 K) so as to minimize dephasing effects on the quantum dot. At these temperatures, we find that this class of cavities exhibit modes with quality factors as high as ~ 2300 while their volume is exceptionally low $\sim 0.01(\lambda/n)^3$. Unlike other arrangements previously considered (photonic crystal cavities, Bragg structures etc) that rely mostly on high Q-factors, our cavity instead promotes strong atom-field interactions through its very small volume that directly enhances the local vacuum field. Our results indicate that a Rabi splitting in excess of 150 GHz can be expected in these systems. Different cavity designs and their role on Rabi oscillations will also be discussed. Our study suggests that this platform can be used not only to

observe fundamental aspects of c-QED but also paves the way towards the realization of on-chip high-speed quantum processing units.

9371-41, Session 10

Complex and hybrid functional plasmonics: from basics to applications (Invited Paper)

Harald Giessen, Univ. Stuttgart (Germany)

We present a number of new materials and hybrid structures for active and reconfigurable nanoplasmonics. In particular, we use the metal-to-insulator transition of yttrium hydrides to completely switch the particle plasmon on and off in nanoantennas with their spectral response tuned to the near infrared. A key challenge for the development of active plasmonic nanodevices is the lack of materials with fully controllable plasmonic properties.

In this work we demonstrate that a plasmonic resonance in top-down nanofabricated yttrium antennas can be completely and reversibly turned on and off using hydrogen exposure. We fabricate arrays of yttrium nanorods and optically observe in extinction spectra the hydrogen-induced phase transition between the metallic yttrium dihydride and the insulating trihydride. Whereas the yttrium dihydride nanostructures exhibit a pronounced particle plasmon resonance, the transition to yttrium trihydride leads to a complete vanishing of the resonant behavior. The plasmonic resonance in the dihydride state can be tuned over a wide wavelength range by simply varying the size of the nanostructures. Thus, our nanorod system serves as a versatile basic building block for active plasmonic devices ranging from switchable perfect absorbers to active local heating control elements.

Additionally, we are going to demonstrate switching functionalities in phase change hybrid plasmonic materials. For example, perfect absorbers as well as chiral plasmonic structures can be tuned over a large wavelength range or even switched on and off and have their handedness reversed.

9371-42, Session 10

Controlling surface plasmon propagation by tilted optical beams Incident on a 1D Grating

Doron Bar-Lev, Itai Epstein, Ady Arie, Jacob Scheuer, Tel Aviv Univ. (Israel)

Controlling surface plasmon (SP) waves is a key feature in enabling various applications as surface sensing, particle trapping, plasmonic circuitry and more. Consequently, several methods were suggested that enable the generation of any desired SP beam by applying static, specifically tailored gratings and apertures. When considering dynamic control, the use of fixed 2D structures incident by a varying optical beam was experimentally demonstrated. Nonetheless, a full theoretical model was not given hitherto. Moreover, a common belief asserts that this control is not possible using lower order structures. In this study we show that a 1D grating incident by a superposition of tilted optical beams can be applied to control and reshape SP waves. Based on the momentum condition, an analytical model is developed and numerically demonstrated and an optimal grating is derived. By setting the angles of incidence of an optical plane wave incident on this grating the propagation angle of the resulting SP can be varied between ± 82.46 degrees. In addition, we explore the effect of the optical polarization and derive an optimum for which there is practically no polarization loss. Finally, we show that a superposition of tilted optical beams can shape the SP beam. An analytical formalism is described and applied to design a varying SP lens which focus is tuned by varying the incident optical beam. Following, a position varying SP hotspot is numerically demonstrated. This work opens the way for applying optical beam shaping techniques to dynamically control SP waves thus yielding exciting future applications.

9371-43, Session 10

Hybrid optoplasmonic structures for efficient long-range energy transfer

Wonmi Ahn, Xin Zhao, Yan Hong, Björn M. Reinhard, Boston Univ. (United States)

Plasmonic nanostructures demonstrate excellent light focusing capabilities at the nanometer scale, which allow for their uses as promising optical nanocircuits. Metals, however, exhibit substantial dissipative heat losses when interacting with light, and this ultimately challenges practical applications of plasmonic nanocircuits. To address this challenge, we introduced on-chip integrated optoplasmonic structures, which combine high-Q optical microcavity (OM) resonators with plasmonic nanoantennas into well-defined hybrid structures through a guided self-assembly strategy [1]. The optoplasmonic structures achieved an efficient directed photon transfer from fluorescent dye-tethered nanoantennas into the OMs [2]. To further implement active optoplasmonic structures, we will show in this talk resonance energy transfer based spectral coupling between quantum dot (QD)-coated OMs and fluorescent dye-tethered metal nanoantennas. By spectrally modulating excitation and emission of respective elements in the optoplasmonic structures, photons guided by the OMs were efficiently coupled out and precisely measured via fluorescence microscopy. Finally, we will provide experimental evidences that validate a theoretically proposed concept of optoplasmonic superlenses [3], by measuring photons transferred to the metal nanoantennas that are separated from the emitter by the micrometer-sized OMs. The optoplasmonic structures will open up new possibilities for fast, near-lossless optical circuits for future energy and optical information processing and sensing.

References

- [1] Ahn, W.; Boriskina, S. V.; Hong, Y.; Reinhard, B. M. "Photonic-Plasmonic Mode Coupling in On-Chip Integrated Optoplasmonic Molecules" *ACS Nano*, 2012, 6, 951-960.
- [2] Ahn, W.; Hong, Y.; Boriskina, S. V.; Reinhard, B. M. "Demonstration of Efficient On-Chip Photon Transfer in Self-Assembled Optoplasmonic Networks" *ACS Nano*, 2013, 7, 4470-4478.
- [3] Boriskina, S. V.; Reinhard, B. M. "Spectrally and Spatially Configurable Superlenses for Optoplasmonic Nanocircuits" *Proc. Natl. Acad. Sci. USA*, 2011, 108, 3147-3151.

9371-44, Session 10

Dispersion analysis and manipulation of TiN 2D plasmonic waveguides

Hosam I. Mekawey, Yehea Ismail, Mohamed A. Swillam, The American Univ. in Cairo (Egypt)

An investigation has been performed of the low order guided modes in 2D hollow metallic waveguide. The dispersion characteristics of the 2D hollow metallic waveguides key guided modes are identified and analyzed. Dispersion manipulating is proposed by either changing the geometrical shapes of rectangular to trapezoidal waveguide or changing the material of the cladding region. The dispersion analysis of 2D plasmonic waveguide using TiN has been investigated for the first time. A study has been conducted on the effect of varying the shape parameters on the cutoff in the modes dispersion. The trapezoidal shape waveguide that causes the most significant shift in the cutoff has been selected and detailed dispersion analysis of its guided modes is performed. The effect of changing the plasmonic material on the dispersion curve key characteristics is also identified. Finally the effect of shifting the cutoff on the enhanced transmission phenomena is investigated.

9371-45, Session 11

Non-linear optical effects in plasmonic gold nanoantennas

Michael Kaniber, Konrad Schraml, Johannes Bartl, Glenn Gashagen, Armin Regler, Walter Schottky Institut (Germany); Tom Campbell, Virginia Polytechnic Institute and State Univ. (United States); Jonathan J. Finley, Walter Schottky Institut (Germany)

Plasmonic nano-particle dimers are well known to create strongly enhanced electromagnetic fields, localized within nanometer-sized optical volumes in the feed-gap separating the component particles. As such they enhance the local non-linear optical response, a key ingredient for nanoscale optical switching technologies or frequency conversion in future integrated photonic circuits.

Here, we present detailed numerical, structural and optical studies of the non-linear response of lithographically defined gold nano-triangles arranged in a tip-to-tip geometry, so-called bowtie antennas. Such plasmonic structures provide very large electromagnetic intensity enhancements of up to 10^3 in the feed-gap. We fabricated gold bowties on glass and GaAs substrates with triangle sizes and feed-gaps down to 100nm and 5nm, respectively. Those structures enable the generation of coherent and incoherent optical fields in the visible region of the spectrum arising from non-linear optical processes. We demonstrate second harmonic generation and two-photon photoluminescence and explore the dependence of the non-linear optical signals on antenna geometry, substrate, fundamental excitation frequency and polarization. This facilitates optimization of the non-linear signal and, moreover, provides a tool to directly quantify the maximum field enhancement in experiments. Simulations suggest local field enhancements up to 500 and a s^{-3} dependence on the feed gap. Moreover, after first excitation of the bowties we observe a strong increase of the non-linear signal, attributed to structural modifications of the antenna feed-gap due to short (~ 100 fs), high power (0.15 GW/cm² per pulse) excitation pulses. This attribution is supported by high resolution SEM images of the feed-gap before and after illumination.

9371-46, Session 11

Nano-patterning of KTiOPO4 nonlinear crystal for plasmonic applications

Itai Epstein, Gat Maman, Daniel Krol, Ady Arie, Tel Aviv Univ. (Israel)

Surface plasmons have attracted great interest in the last decade due to their two main characteristics: strong spatial confinement and large enhancement of the optical field. The latter is very appealing for applications in nonlinear plasmonics due to the dependence of the nonlinear process' efficiency on the intensity of the optical field. To excite surface plasmons by a free-space beam one commonly uses a grating. However, to realize plasmonic nonlinear light-matter interactions at the interface between a metal and a nonlinear crystal, it is required to couple the surface plasmon into that interface. Until now, structures which enabled the above included a three-layered configuration: a top grating layer above the metal layer, which coupled the plasmon from air, through the metal, and into the interface between the metal and the nonlinear crystal layer residing under it. This highly reduces the coupling efficiency and sometimes introduces difficulties to calculate the propagation modes of the structure. Here we demonstrate grating structures, which have been etched using micro-electronics processes, directly into a KTiOPO4 nonlinear crystal. When covered with a metal layer and illuminated from the KTiOPO4 side, they create unique structures that can couple surface plasmons directly into the metal/ KTiOPO4 interface. These structures not only simplify the aforementioned three-layered structure but also, according to our calculations, can increase the nonlinear process' efficiency by more than an order of magnitude. Other application for nonlinear optics, such as beam shaping, functional facets, and ridge waveguide arrays, can also be realized using this fabrication process.

9371-47, Session 11

Shaping plasmonic light beams with near-field plasmonic holograms

Itai Epstein, Ady Arie, Tel Aviv Univ. (Israel)

Surface-plasmon waves have been utilized in many applications such as biological and chemical sensing and trapping, sub-wavelength optics, nonlinear optics, optical communication and more. Controlling the shape and trajectory of these waves is a key feature in enabling all of the above applications, and a challenging task. The fundamental challenges resides in the different wave properties of surface plasmon waves, with comparison to free-space waves: First, coupling a surface plasmon wave from a free-space wave requires a compensation for the missing momentum between the two wave-vectors. Second, owing to the limited propagation length of surface plasmons and the limited measurement range of their characterization tools, the resulting beams should be formed directly in the near-field. Third, unlike planar phase plates, surface plasmons are excited over a finite propagation distance and therefore their phase cannot be simply defined at a specific one-dimensional plane. Fourth, dynamic tools for controlling the wavefront of free-space beams, like spatial-light-modulators, do not exist for surface plasmons. Here we demonstrate, both numerically and experimentally, a robust holographic scheme that provides complete control over the amplitude and phase of surface-plasmons, thereby enabling the engineering of any desired plasmonic light beam. We show how all of the above challenges can be overcome by introducing a new class of binary plasmonic holograms, which are designed specifically for the near-field. We demonstrate a large variety of plasmonic beams, such as "self-similar", "non-diffracting", "self-accelerating", "self-healing", paraxial and non-paraxial plasmonic beams, and also the dynamic generation of plasmonic bottle-beams for micromanipulation of particles.

9371-48, Session 11

Extremely-high near-field enhancement in a novel plasmonic nanomaterial used for photovoltage generation

Debadrita Paria, Kallol Roy, Shishir Kumar, Haobijam J. Singh, Srinivasan Raghavan, Arindam Ghosh, Ambarish Ghosh, Indian Institute of Science (India)

Electric field localization enhancement near metal (plasmonic) nanostructures can have various interesting applications, such as in sensing, imaging, photovoltage generation etc., for which significant efforts are aimed towards developing plasmonic systems with well designed electromagnetic response. In this paper, we discuss the wafer scale fabrication and optical characterization of a unique three dimensional, plasmonic material. The near field enhancement in the visible range of the electromagnetic spectrum obtained in these structures (order of 10^6), is close to the fundamental limit that can be obtained in this and similar EM field enhancement schemes. The large near field enhancement has been reflected in a huge Raman signal of graphene layer in close proximity to the plasmonic system, which has been validated with FEM simulations.

Graphene is the thinnest material known till date having many exotic properties like very high electrical mobility, broad band optical response etc. Smart integration of graphene with such a plasmonic material has enabled record photovoltage generation with responsivity in the order of A/W. As far as we know, this is the highest photovoltage obtained in any plasmonic-graphene hybrid photodetection system till date.

9371-49, Session 11

Control of radiative processes of molecules and quantum dots using plasmonic structures

Thang B. Hoang, Gleb M. Akselrod, Christos Argyropoulos, Cristian Ciraci, David R. Smith, Maiken H. Mikkelsen, Duke Univ. (United States)

We experimentally demonstrate large enhancements of fluorescence and spontaneous emission rate of molecules and quantum dots coupled to single plasmonic nanoantennas. The nanoantennas consist of colloiddally synthesized silver nanocubes coupled to a metallic film separated by a -5 nm self-assembled polyelectrolyte spacer layer with embedded emitters. Each nanocube resembles a nanoscale patch antenna with highly directional emission whose plasmon resonance can be changed independent of its local field enhancement. By varying the size of the nanopatch, we tune the plasmonic resonance by ~200 nm throughout the excitation, absorption, and emission spectra of the embedded molecules. Using this colloiddally synthesized and tunable plasmonic platform, design rules for observing large fluorescence or Purcell enhancements are revealed. Utilizing these, we observed fluorescence enhancements of Cy5 fluorophores coupled to individual plasmonic nanopatch antennas exceeding a factor of 30,000 accompanied by a significantly increased spontaneous emission rate. Next, we directly probe and control the nanoscale photonic environment of the embedded emitters including the local field enhancement, dipole orientation and spatial distribution of emitters. This enables the design and experimental demonstration of Purcell factors ~1,000 while maintaining high quantum efficiency and directional emission. Full-wave simulations incorporating the nanoscale environment accurately predict the experimentally observed emission dynamics and reveal design rules for future devices. Progress on coupling single colloiddal CdSe/ZnS core-shell quantum dots to the plasmonic nanopatch antennas will also be discussed. Additionally, the plasmonic platform developed here enables straightforward and large-area fabrication using colloiddal synthesis without the need for electron-beam lithography techniques.

9371-50, Session 11

Optical magnetism in asymmetric plasmonic structures

Faezeh Tork Ladani, Vartkess A. Apkarian, Eric O. Potma, Univ. of California, Irvine (United States)

Single molecule studies are of great interest to researchers in different disciplines such as biomedical and chemical sciences as well as quantum communication technologies. Thanks to plasmonic structures and engineered nano-junctions, enormous advances have been made in the study of light-molecule interactions in hot spots. However, virtually all plasmon-molecule interactions considered so far have been with the electric field, whereas the interaction through the magnetic field has received relatively little attention. Since the electric polarizability of plasmonic structures is dominant, no significant magnetization is observed at optical frequencies near hot spots. However, strong circulation of the electric field, leading to magnetic field enhancement, may be achieved if the structures are engineered properly. We study certain configurations of plasmonic objects with structural asymmetry and different material properties to induce magnetic field enhancement at optical frequencies. We investigate the enhanced magnetic field for exciting the molecular magnetic transitions in spectroscopy and imaging applications.

9371-69, Session PWed

Tunable infrared extraordinary transmission through 2D hole arrays in conductive ZnO

Nima Nader, Shiva R. Vangala, Solid State Scientific Corp. (United States); Junpeng Guo, The Univ. of Alabama in Huntsville (United States); Joshua R. Hendrickson, Kevin D. Leedy, Air Force Research Lab. (United States); David C. Look, Wyle Labs. (United States); Justin W. Cleary, Air Force Research Lab. (United States)

Extraordinary optical transmission (EOT), or transmission greater than that predicted by conventional optics theory, through highly conductive ZnO films with sub-wavelength hole arrays is investigated in the mid- to long-wavelength infrared regime. EOT is facilitated by the excitation of surface plasmons on Ga-Doped ZnO films and can be tuned utilizing the physical structure sizes; i. e. film thickness, period, hole diameter, and hole shape. Ga-doped ZnO films are grown via pulsed laser deposition (PLD) as have plasma frequencies in the near-infrared. The sub-wavelength 2D hole arrays are fabricated in the Ga-doped ZnO films via standard lithography and etching processes, with the optical transmission then being measured with a microscope coupled FTIR system and quantum cascade lasers. EOT through the structures is observed and compared with finite difference time-domain simulations. This highly conductive ZnO EOT structure may prove useful in novel integrated components such as tunable biosensors or surface plasmon coupling mechanisms.

9371-70, Session PWed

The analog of superradiant emission in thermal emitters

Ming Zhou, Soongyu Yi, Univ. of Wisconsin-Madison (United States); Ting S. Luk, Sandia National Labs. (United States); Qiaoqiang Gan, Univ. at Buffalo (United States); Zongfu Yu, Univ. of Wisconsin-Madison (United States)

Superradiance is first used to describe the phenomenon that when N quantum emitters are put together within subwavelength dimension, the total emission power scales quadratically with the number of emitters N . It originates from the coherent interaction between emitters. On the contract, due to the lack of coherence, superradiant emission has never been considered for thermal emitters which is typically considered as incoherent source. Here we show that the analog of superradiant emission can be realized resonant thermal emitters. Usually the thermal photons is stored in thermal emitters through reabsorption, which can be described by an absorption or emission rate γ_a . The resonator provides a reservoir of thermal photons and introduce another way of photon storage, which can be described by a coupling rate γ_c . The rebalance of these two different process will lead to a power scaling law that significantly deviates from the conventional well-known linear relationship. To illustrate this new idea, we first develop a general theory for the thermal emission of N resonant emitters. We show that when the coupling process is predominate, the emission power scales inverse linearly with the number of emitters! In addition, when the reabsorption process is predominate, our theory successfully predict the conventional linear scaling of emission power. Second, we validate our theory by performing numerical simulation through solving full-wave Maxwell's equations in the frequency domain. The simulation results agree with theory very well.

9371-71, Session PWed

Determination of enhanced excitation rate of quantum dots mediated by Bloch-like surface plasmon polaritons

Min Lin, Zhaolong Cao, Hock Chun Ong, The Chinese Univ. of Hong Kong (Hong Kong, China)

Excitation of plasmonic resonance generates strong localized electromagnetic fields which enhance the excitation of nanostructures. Understanding and controlling the excitation are of great importance in fluorescence, sensing, photovoltaics, photocatalysis, and photothermal effect. However, to date, the exact determination of the excitation rate is not yet available and most of the studies reveal only the excitation efficiency which is very system dependent and sometimes is difficult to quantify. Here, we devise a new method to determine the excitation rate quantitatively, by employing temporal coupled mode theory and rate equation model to formulate the excitation rate in terms of measurable quantities such as reflectivity, emission power ratio, and decay rates of surface plasmon polaritons. More importantly, from the formalism, we learn how to maximize and tailor the excitation rate by adjusting these quantities, which are geometry dependent. Experimentally, we use angle- and polarization-resolved reflectivity and Fourier space microscopy to measure them and determine the excitation rate of different plasmonic systems that support propagating and localized surface plasmon. For example, for quantum dots deposited on 2D Au nanohole array, we find the excitation rate to be 8.55 meV, and the excitation efficiency increases by 6 times. On the other hand, for nanoparticles, the rate is 152 meV and the efficiency increases by 110 times. Our results are found to be consistent with finite-difference time-domain simulations.

9371-72, Session PWed

Optical Helmholtz resonators

Paul Chevalier, Patrick Bouchon, ONERA (France); Fabrice Pardo, Lab. de Photonique et de Nanostructures (France); Riad Haidar, ONERA (France)

Metallic nanostructures could be tailored to manipulate the light on a sub-wavelength scale, for instance perfect absorbers at a single frequency can be designed using metal-insulator-metal resonators.

Here, based on an analogy between acoustics and electromagnetism wave equations, we present an electromagnetic resonator analogous to the Helmholtz resonator in acoustics. This structure is made of a tiny slit above a cavity, and in opposition to Fabry-Perot slit resonators, it neither relies on the propagation of electromagnetic waves, nor does it exhibit any harmonic resonances.

At the resonance, the incident light is totally funnelled through the nanometre-wide slit aperture and is further absorbed within the cavity. A quasi static model is proposed to describe the resonance mechanism and predict the resonance wavelength of a given structure geometry; it has been successfully validated with rigorous numeric computations for 100 000 different configurations. Interestingly the slit acts as a capacitor and the slit as an inductance which explains why the dielectric index of the material filling the cavity has no influence on the resonance.

The properties of the resonance (absence of harmonic resonance, quasi static behaviour) are appealing for components based on this resonator such as spectral filters, thermal emitters or photodetectors. Eventually the strong field intensity enhancement that appears within the whole slit volume may be of great interest for applications requiring strong confinement such as SERS or biophotonics.

**Conference 9371: Photonic and Phononic Properties
 of Engineered Nanostructures V**

9371-73, Session PWed

Highly-tolerant and reflective titanium dioxide stacks with tunability for visible wavelength applications

Jung Woo Leem, Jae Su Yu, Kyung Hee Univ. (Korea, Republic of)

Distributed Bragg reflectors (DBRs) have been increasingly applied in a wide variety of optical and optoelectronic devices such as light-emitting diodes, semiconductor laser diodes, optical sensors, solar cells, and photodetectors. Conventional DBRs composed of two different materials have fundamental limitations such as low refractive index contrast, material selection, and thermal mismatch. Thus, the DBRs consisted of the same material are desirable in practical applications. In this view, using an oblique angle deposition (OAD) technique, the same material-based DBRs can be realized. The OAD which allows for the formation of inclined nanocolumnar structures enables to form easily porous films with a low refractive index compared to dense films in the same materials due to the self-shadowing effect and limited atom mobility. Furthermore, the high reflective band of DBRs can be adjusted by varying the by adjusting the $\lambda/4$ thicknesses of alternating two films. In this work, we fabricated the tunable DBRs, which have different center wavelengths, with different pairs consisting of nanoporous/dense titanium dioxide (TiO₂) film stacks by the OAD method using an electron-beam evaporation system, suggesting high tolerance and reflectivity at visible wavelengths. Their optical reflection characteristics were investigated at normal incidence including different light incident angles. For the TiO₂ DBR with 5 pairs, the wafer-scale uniformity on a 3 inch-sized silicon wafer was studied. For optical reflectance properties, a theoretical analysis was also performed using the rigorous coupled-wave analysis method.

9371-74, Session PWed

Nonlinear light interaction in an array of dielectric subwavelength waveguides

Gregorio Mendoza González, Jesús Manuel Muñoz Pacheco, Erwin A. Martí Panameño, Benemérita Univ. Autónoma de Puebla (Mexico)

We study the dynamics of nonlinear propagation and interaction of two optical fields in arrays of dielectric subwavelength waveguides of circular cross section. Applying the finite difference time-domain (FDTD) method, we numerically solve the Maxwell's equations considering real values for the constitutive relations. The arrays under study are formed by a finite number of parallel waveguides with identical parameters: subwavelength dimensions, Kerr nonlinearity, length of tens of micrometers and the separation between the waveguides is constant. In our study, we focus on the determination of specific values for the physical parameters before mentioned, to obtain light self-trapping. For this, we also determine the properties of the incident optical fields: complex amplitude, wavelength, angle of incidence and phase difference. As a result we observe the strong dependence of the total energy output to the parameters of phase difference and angle of incidence. This allows us to conclude about the possibility to control the nonlinear interaction properties of two optical fields, generating a single output beam, whose position can be controlled by the selection of the system parameters. These results may contribute to the development of logic gates based on subwavelength waveguides

9371-75, Session PWed

Towards practical realization of plasmonic waveguides cladded by hyperbolic metamaterials

Viktoriia E. Babicheva, DTU Fotonik (Denmark) and Purdue

Univ. (United States) and ITMO Univ. (Russian Federation); Mikhail Shalaginov, Purdue Univ. (United States); Satoshi Ishii, Purdue Univ. (United States) and National Institute for Materials Science (Japan); Alexandra Boltasseva, Purdue Univ. (United States) and DTU Fotonik (Denmark); Alexander V. Kildishev, Purdue Univ. (United States)

Engineering plasmonic metamaterials with anisotropic optical properties enables us to tune the properties of waveguides. In particular, utilizing a nanostructure with hyperbolic dispersion as a cladding can provide more advantages in comparison to standard metal-insulator-metal and insulator-metal-insulator plasmonic waveguides, especially in terms of propagation length and mode confinement. We investigated properties of plasmonic waveguides with a dielectric core and a multilayer metal-dielectric cladding with hyperbolic dispersion (HIH waveguides). First, we studied the validity of effective medium theory (EMT) for homogenizing the multilayers and showed that EMT can be applied only when the number of periods is more than ten. Rigorous calculations need to be applied for the thinner cladding. Further, we studied eigenmodes inside the cladding of the HIH waveguides of finite width. Finally, by finding the eigenmodes of the cladding layers, we have discovered that their corresponding propagation constants match the dispersion anomalies of the studied HIH waveguides. Henceforth, to avoid excitation of these anomalous modes leading to unfavorable regimes, the waveguide cladding should be properly designed.

9371-76, Session PWed

Lattice resonances of plasmonic nanoparticle array in TM-polarization

Viktoriia E. Babicheva, National Research Univ. of Information Technologies, Mechanics and Optics (Russian Federation); Andrey B. Evlyukhin, Laser Zentrum Hannover e.V. (Germany); Sergei V. Zhukovsky, DTU Fotonik (Denmark) and ITMO Univ. (Russian Federation)

It is well known that dipole coupling in one- and two-dimensional plasmonic nanoparticle arrays can produce narrow collective plasmon resonances in light transmission spectra. These resonances appear at the wavelength of scattered light close to the wavelength corresponding to the Rayleigh anomaly. The strength and width of the resonances are characterized by the spectral distance between the closest Rayleigh anomaly and the single-particle plasmon resonance. The wavelengths corresponding to the Rayleigh anomaly are determined by the array periods, and the wavelength of the single-particle plasmon resonance is determined by particle size and shape. The spectral sensitivity to the environmental properties of collective resonances makes them very attractive for sensing applications. In the electric dipole approximation the collective resonances (excitation of lattice waves) involves only dipole moments of the nanoparticles oriented perpendicular to the lattice wave propagation (TE-polarization). Recently it was shown that for plasmonic nanoparticle arrays located on substrates the collective (lattice) plasmon resonances can be excited in the TM-polarization configuration. In this work, we theoretically study collective plasmon resonances in plasmonic nanoparticle arrays for the TM-polarization configurations taking into account the magnetic-dipole and electric quadrupole nanoparticle modes. The analysis is based on rigorous numerical calculations and on the coupled multipole approach. Results show that inclusion of these multipoles into the theoretical model provides conditions for excitation of the collective (lattice) resonances in the TM-polarization configurations. Moreover, if substrate is present, reflectance and dipole coupling between nanoparticles causes a band of transparency in transmission spectrum.

9371-77, Session PWed

Numerical and experimental investigation of plasmonic properties of silver nanocrescent structures for sensing applications

Ahmed A. Abumazwed, Andrew G. Kirk, McGill Univ. (Canada); Wakana Kubo, Takuo Tanaka, RIKEN (Japan)

Metallic U shaped structures have proven to be good candidates for biosensing applications due to their multiresonance extinction properties. However, fabrication of such structures typically requires expensive and time consuming electron beam lithography. Here, we present a simple fabrication method based on the sidewall lithography technique, where an oblique metal evaporation is suggested to produce engineered nanocrescent structures. Nanocrescents support multiresonance extinction spectra, making them good candidates for sensing applications. In this work, silver nanocrescents are arrayed on a glass substrate. A silicon mold was used to imprint an array of polymer nanopillars that were coated using an obliquely evaporated silver producing a difference in the wall thickness around the pillars. The thin part of the silver wall and the inner pillars were then removed under a vertical hydrogen plasma shower and nanocrescents were formed. Scanning electron microscopy was used to characterize the surface morphology, and the optical properties have been investigated by using spectroscopy. We then performed a FDTD analysis of the nanocrescent structures to investigate their plasmonic properties emphasizing the multiresonance behaviour. A comparison between the measured and simulated extinction spectra for two different polarizations of the incident plane wave showed a slight redshift in the case of the simulated spectra in both polarization states. This slight discrepancy is attributed to the roughness of the fabricated nanostructures. The existence of multiple resonances was clearly seen in the case of measured spectra. Microfluidic channels were fabricated and integrated with the nanostructured chip to investigate the sensitivity of the structures.

9371-78, Session PWed

3D microfabrication and bioimaging by using two-photon absorbing chromophores

Ha Neul Chae, Jin Sun Park, Jin-Kyung Park, Ju Hyoung Jung, Hannam Univ. (Korea, Republic of); Cheolwoo Ha, Dong-Yol Yang, KAIST (Korea, Republic of); Chang Su Lim, Bong Rae Cho, Korea Univ. (Korea, Republic of); Kwang-Sup Lee, Hannam Univ. (Korea, Republic of)

Two-photon absorption (TPA) is a third non-linear optical process with many promising applications. In this study, four TPA compounds were synthesized (EMPA, EMPA-4Br, EMPA-4Branch, PASN) and their optical properties were analyzed in the organic solvents and water. Their TPA cross-sections (TPACS) were measured by using fluorescence two-photon excitation method in the each solvent. The TPACS of EMPA-4Branch showed highest value in both solutions. Four compounds were applied for the 3D microfabrication and bioimaging, and each results were compared on the basis of the compounds TPACS. The imagings of HeLa cell were obtained by using the PASN nanoparticles and EMPA-4Br solution. And the 3D microstructures were made by SU8 resin containing EMPA and EMPA-4Br.

9371-79, Session PWed

Saturation-limited second harmonic generation in a quantum well-nanoresonator coupled system

Omri Wolf, Salvatore Campione, Sandia National Labs. (United States); Arvind Pawan Ravikumar, Princeton Univ. (United States); Alexander Benz, Sheng Liu, Emil A. Kadlec, Benjamin V. Olson, Eric A. Shaner, John F. Klem, Michael B. Sinclair, Igal Brener, Sandia National Labs. (United States)

We experimentally demonstrate very efficient (up to 0.1%) second harmonic (SH) generation using subwavelength, phase-matching free, engineered nanoresonators, strongly coupled to a III-V quantum-well (QW) heterostructure supporting intersubband transitions at mid-infrared wavelengths. Near-perfect polarization separation between the pump and the SH signal, in transmission, is achieved through proper design of the nanoresonators. Due to the efficient resonator-QW coupling, shown previously to be in the strong-coupling regime, saturation is observed for moderate pump intensities ($\sim 6\text{ kW/cm}^2$); this technique may allow probing dynamic, non-equilibrium states in quantum-well systems without the need for extremely high pump powers ($\sim \text{MW/cm}^2$) and the negative side effects, e.g. heating, associated with such excitations. In addition, this design scheme could enable fabrication of high intensity sources across the entire infrared spectrum through proper choice of QW and nanoantenna design.

9371-80, Session PWed

Design of water molecule and its surrounding

Rostyslav I. Danylo, Boris A. Okhrimenko, National Taras Shevchenko Univ. of Kyiv (Ukraine)

This research is devoted to the vibrational spectroscopy inverse problem solution that gives a possibility to design a molecule and make conclusions about its geometry. The valent angle finding based on the usage of inverse spectral vibrational spectroscopy problem is a well-known task [1,2]. 3N-matrix method [3,4] was chosen to solve the proposed task. The usage of this method permits to make no assumptions about the molecule force field, besides it can be applied to molecules of matter in liquid state. First results about this investigation were presented in [5]. Found valence angle value [Equation Missing] provoked our researches to be continued.

The calculation algorithm [5] was developed and improved. The main idea to minimize the function y called a divergence parameter stayed the basis of the algorithm: [Equation Missing] where [Equation Missing] is a calculated theoretically vibration frequency, [Equation Missing] is a measured experimentally. The valent angle assessment was reduced to the divergence parameter minimization. The B value concerning divergence parameter minimum was interpreted as the desired valent angle.

The method mistake can be approximately assessed presently as $1, 2[\text{deg}]$. Proposed algorithm was applied for different molecules in gaseous state. Calculated values were compared with measured ones and algorithm capacity was verified in such a way. The proposed method was applied then for water molecule in liquid state and the calculated value correlates with [5]: [Equation Missing].

References

- [1] G. Herzberg. Infrared and Raman spectra of polyatomic molecules (New York, 1945; Inosrannaya literatura, Moscow, 1949).
- [2] Bilyi M. U. and Okhrimenko B.A., "Assessment of force matrix of water molecule in liquid state," Ukrainian Journal of Physics 44 (3), 326 (1999).
- [3] M. U. Belyi, B. A. Okhrimenko, and S. M. Yablochkov, Izv. Vyssh. Uchebn. Zaved., Fiz., 4. 52, (1987).
- [4] B. A. Okhrimenko and O. A. Yushko. Optics and Spectroscopy, 110 (2).

**Conference 9371: Photonic and Phononic Properties
 of Engineered Nanostructures V**

184, (2011).

[5] R. I. Danylo and B. A. Okhrimenko, "Spectroscopic modeling of water molecule," *Micro/Nano Materials, Devices, and Systems*, edited by James Friend, H. Hoe Tan, Vol. 8923, (Proc. Of SPIE, Melbourne, VIC; Australia, 2013), pp. 89235K-1-89235K-8.

9371-52, Session 12

Nano-optomechanics: Feedback control with zero point motion resolution at the thermal decoherence rate *(Invited Paper)*

Dalziel J. Wilson, Vivishek Sudhir, Nicolas Piro Mastracchio, Tobias J. Kippenberg, Ecole Polytechnique Fédérale de Lausanne (Switzerland)

In real-time (Markovian) quantum feedback protocols the outcome of a continuous measurement is used to stabilize a desired quantum state. Extending such protocols to macroscopic systems is a significant challenge, as the measurement must in this case compete with rapid environmental decoherence. We report on the realization of a sensor that approaches the requirements of quantum feedback for a solid state, 4.3 MHz nanomechanical oscillator — namely, the ability to resolve its zero-point motion at a rate comparable to that of its thermal decoherence. The sensor is based on near-field optomechanical coupling and achieves an imprecision - 39 dB below that at the standard quantum limit (SQL) for a weak continuous position measurement while maintaining an imprecision-backaction product only - 5 times in excess of the Heisenberg uncertainty limit. As a demonstration of its utility, we employ the measurement to feedback cool the oscillator to an occupation of - 5 quanta. Our results establish qualitatively new benchmarks for the readout and control of a macroscopic mechanical device, and underscore the potential and the challenge of extending such systems to the quantum regime.

9371-53, Session 12

Gallium arsenide and silicon nitride optomechanical crystals *(Invited Paper)*

Kartik Srinivasan, Krishna C. Balram, Karen Grutter, Marcelo I. Davanco, National Institute of Standards and Technology (United States)

We present optomechanical crystals, in which localized GHz frequency phonons interact with localized optical photons via radiation pressure, in both the gallium arsenide (GaAs) and silicon nitride (Si₃N₄) material systems. In GaAs, we develop devices in which the optomechanical coupling is due to the photoelastic effect, and show that its magnitude strongly depends on the device's in-plane orientation, with a maximum coupling strength $g_0/2\pi \sim 1.1$ MHz demonstrated. In Si₃N₄, we demonstrate sideband-resolved devices suitable for observing coherent coupling between photons and phonons. We present experimental results on slot mode cavity geometries tailored for multimode applications such as wavelength conversion, where widely separated electromagnetic resonances are mutually coupled to the same mechanical mode.

9371-54, Session 12

Diamond waveguide optomechanics *(Invited Paper)*

Paul E. Barclay, Univ. of Calgary (Canada)

Diamond nanophotonic and nanomechanical devices are promising for applications including sensing, quantum information processing and nonlinear optics. We have demonstrated that optomechanical coupling

to single crystal diamond nanobeam waveguides allows readout of their mechanical resonances with ultrahigh sensitivity over a broad optical bandwidth. Using this waveguide optomechanical coupling interface, we have probed mechanical resonances of diamond nanobeams with $Q > 100000$, and have show that actuation of their mechanical motion is possible. The single crystal diamond nanobeams under study were fabricated from bulk diamond samples using a highly scalable isotropic etching technique which is compatible with a wide range of nanophotonic structures.

9371-55, Session 12

Optomechanical and strain coupling in diamond phoxonic crystal cavities *(Invited Paper)*

Laura Kipfstuhl, Christian Hepp, Christoph Becher, Univ. des Saarlandes (Germany)

A photonic and phononic crystal (phoxonic crystal, PxC) is a periodically patterned material that at the same time localizes optical and mechanical modes. The simultaneous confinement of photons and phonons gives rise to optomechanical nano-resonators offering strong phonon-photon coupling and integration of acoustic and optical functionalities on the same chip. At the same time, the strongly localized mechanical modes result in very high dynamical strain fields. Adding an active solid-state spin system or optical emitter to the system introduces yet another functionality allowing for mutual coupling of optical, mechanical and internal (spin, electronic) degrees of freedom.

We here consider diamond as very promising material for realization of such systems: fabrication of photonic crystal cavities has been demonstrated [1], the unique material properties allow for high mechanical resonance frequencies, and diamond hosts a large number of color centers acting as single quantum emitters or spin qubit systems.

As specific system we theoretically model one-dimensional PxC in diamond and find mechanical resonances with high frequencies > 12 GHz, large optical and acoustical quality factors up to 10^7 and optomechanical coupling strengths in the MHz range [2]. The strong strain field in the PxC cavity can also exert a large strain splitting of electronic states of color centers, e.g. nitrogen vacancy (NV) centers placed in the center of the structure. We calculate a splitting of the NV ground state spin levels and excited electronic states by up to 400 Hz and 19 MHz per single confined phonon, respectively.

[1] I. Aharonovich and E. Neu, *Adv. Optical Mater.* (2014), DOI: 10.1002/adom.201400189

[2] L. Kipfstuhl, F. Guldner, J. Riedrich-Möller, and C. Becher, *Opt. Express* 22, 12410 (2014).

9371-56, Session 13

Chip-scale phonon-based scalable quantum computing *(Invited Paper)*

Ihab El-Kady, Sandia National Labs. (United States)

Quantum computing fundamentally depends on the ability to concurrently entangle and individually address/control a large number of qubits. In general, the primary inhibitors of large scale entanglement are qubit dependent; for example inhomogeneity in quantum dots, spectral crowding brought about by proximity-based entanglement in ions, weak interactions of neutral atoms, and the fabrication tolerances in the case of Si-vacancies or SQUIDs. We propose an inherently scalable solid-state qubit system with individually addressable qubits based on the coupling of a phonon with an acceptor impurity in a high-Q Phononic Crystal resonant cavity.

Due to their unique nonlinear properties, phonons enable new opportunities for quantum devices and physics. We present a phononic crystal-based platform for observing the phonon analogy of cavity quantum

**Conference 9371: Photonic and Phononic Properties
 of Engineered Nanostructures V**

electrodynamics, called phonodynamics, in a solid-state system. Practical schemes involve selective placement of a single acceptor atom in the peak of the strain field in a high-Q phononic crystal cavity that enables strong coupling of the phonon modes to the energy levels of the atom. A qubit is then created by entangling a phonon at the resonance frequency of the cavity with the atomic acceptor states. We show theoretical optimization of the cavity design and excitation waveguides, along with estimated performance figures of the phonon system. Qubits based on this half-sound, half-matter quasi-particle, may outcompete other quantum architectures in terms of combined emission rate, coherence lifetime, and fabrication demands.

9371-57, Session 13

**Generation of spin waves in nanomagnets
 in a phononic crystal (*Invited Paper*)**

Yu Yahagi, Univ. of California, Santa Cruz (United States);
 Bruce D. Harteneck, Lawrence Berkeley National Lab.
 (United States); Stefano Cabrini, The Molecular Foundry
 (United States); Holger Schmidt, Univ. of California, Santa
 Cruz (United States)

Densely packed arrays of nanomagnets are the prototype approach to next generation spintronic devices with applications in next generation data storage and magnetic memories. The dynamic behavior of individual nanomagnetic elements is of great interest in terms of attainable device speed, statistical variations across the array, and the effect of neighboring magnets and, more generally, the array geometry itself. We have previously shown that magneto-static interactions between neighboring magnets can affect the spin wave spectrum.

Here, we describe a different mechanism to affect and control the dynamic magnetic properties based on magneto-elastic coupling with propagating surface acoustic waves (SAWs).

When metallic nanomagnets are optically excited by an intense laser pulse, propagating SAWs are generated at distinct frequencies determined by the substrate and the array geometry. The mechanical vibrations created by the SAWs can trigger magnetization precessions in the nanomagnets due to magneto-elastic coupling. As a result, the field-dependent spin wave spectrum is strongly disturbed by the presence of phononic resonances. This phenomenon is illustrated using time-resolved magneto-optical Kerr spectroscopy on arrays of nickel nanomagnets. Both local and nonlocal control of the magnetic properties (spin waves) using phononic resonances (SAWs) are demonstrated.

9371-58, Session 13

**GHz complete elastic bandgap in pillar-
 based membrane structures**

Reza Pourabolghasem, Saeed Mohammadi, Ali Asghar
 Eftekhar, Ali Adibi, Georgia Institute of Technology (United
 States)

We report the experimental evidence for the existence of a complete elastic bandgap around 800MHz in a pillar-based phononic crystal slab of Au pillars in a AlN/Mo/Si structure with good agreement with theoretical design. The observed attenuation in the experiments for the bandgap region is at least 20dB; however, the extent of the observed attenuation is wider than the theoretical prediction. We investigate the physical justification behind this observation and discuss the effects of different Bloch modes, their symmetry, and changing group velocity in affecting the attenuation levels inside and outside the theoretical bandgap region.

9371-59, Session 14

**Inverse design and implementation of
 nanophotonic structures (*Invited Paper*)**

Jelena Vuckovic, Stanford Univ. (United States)

Nanophotonics has emerged as a powerful tool for manipulating light on chips. Almost all of today's devices, however, have been designed using slow and ineffective brute-force search methods, leading in many cases to limited device performance. We present an inverse design technique, wherein the user specifies design constraints in the form of target fields rather than a dielectric constant profile. We then employ this method to demonstrate highly compact and functional nanophotonic devices, including frequency splitters, mode converters, and spatial mode multiplexers.

9371-60, Session 14

**Cylindrical and spherical space equivalents
 to the plane wave expansion technique of
 Maxwell's wave equations**

Robert C. Gauthier, Mohammed A. Alzahrani, Seyed
 Hamed Jafari, Carleton Univ. (Canada)

The plane wave expansion (PWM) technique applied to Maxwell's wave equations provides researchers with a supply of information regarding the optical properties of dielectric structures. The technique is well suited for structures that display a linear periodicity. When the focus is directed towards optical resonators and structures that lack linear periodicity the eigen-process can easily exceed computational resources and time constraints. In the case of dielectric structures which display cylindrical or spherical symmetry, a coordinate system specific set of basis functions have been employed to cast Maxwell's wave equations into an eigen-matrix formulation from which the resonator states associated with the dielectric profile can be obtained. As for PWM, the inverse of the dielectric and field components are expanded in the basis functions (Fourier-Fourier-Bessel, FFB, in cylindrical and Fourier-Bessel-Legendre, FBL, in spherical) and orthogonality is employed to form the matrix expressions. The theoretical development details will be presented indicating how certain mathematical complications in the process have been overcome and how the eigen-matrix can be tuned to a specific mode type. The similarities and differences in PWM, FFB and FBL are presented. In the case of structures possessing axial cylindrical symmetry, the inclusion of the z axis component of propagation constant makes the technique applicable to photonic crystal and other waveguide structures. Computational results will be presented for a number of different dielectric geometries including Bragg ring resonators, cylindrical space slot channel waveguides, bottle resonators and others as computation results become available. Steps to further enhance the computation process will be reported.

9371-61, Session 14

**Spherical space Bessel-Legendre-Fourier
 mode solver for Maxwell's wave equations**

Mohammed A. Alzahrani, Robert C. Gauthier, Carleton
 Univ. (Canada)

For spherically symmetric dielectric structures, a basis set composed of Bessel, Legendre and Fourier functions, BLF, are used to cast Maxwell's wave equations into an eigenvalue problem from which the localized modes can be determined. The steps leading to the eigenmatrix are reviewed and techniques used to reduce the order of matrix and tune the computations for particular mode types are detailed. The BLF basis functions are used to expand the electric and magnetic fields as well as the inverse relative dielectric profile. Similar to the common plane wave expansion technique, the BLF matrix returns the eigen-frequencies and eigenvectors, but in BLF

**Conference 9371: Photonic and Phononic Properties
 of Engineered Nanostructures V**

only steady states (non-propagated) are obtained. The technique is first applied to a spherical structure void of internal dielectric detail and results are compared to, and match, those commonly available in textbooks and journal publications. The technique is then applied to a number of non-traditional spherically symmetric structures, (Bragg shell, meridian wedges, ...) and the steady state modes supported are reported. An interesting alternate configuration is that of a slot channel running the equator of the sphere. The results predict the existence of orbital whispering gallery modes in spherical space where the electric field maximum is located within the channel comprising the external ambient medium. Such a structure seems suited for sensor applications. To close is discussed the application of the FBL technique to Schrodinger and Navier-Stokes equations.

9371-62, Session 14

Cross-slot waveguide Bragg grating

Matthieu Roussey, Petri Stenberg, Arijit Bera, Somnath Paul, Jani Tervo, Markku Kuitinen, Seppo Honkanen, Univ. of Eastern Finland (Finland)

A silicon cross-slot waveguide is a two dimensional slot waveguide composed of four 180 nm-wide silicon rails separated by a narrow gap of 50 nm, in our case. The structure is fully symmetric and is embedded in silicon dioxide. After presenting the optimization of this guiding structure at the wavelength of 1550 nm, we will show the potential of this device to be sensitive or insensitive to polarization. A Bragg grating cavity is merged to the cross-slot waveguide in order to create a band-pass filter. A photonic band gap with a resonant peak in its center appears in the transmission spectrum of the device. By changing the cavity, i.e., by adding a silicon sub-structure in the cavity, one can modify the dependence on the polarization of the structure. Six cavity types are studied in order to understand how the field distribution can be shaped in the cavity. Moreover one can also play on the confinement of the field and achieve light guiding in a two-dimensional slot waveguide of 50 nm width where both polarizations are present at the same time. We also show that including a nanowire in the cavity allows a better guidance of the field inside the cavity. It appears then that the structure has potential in sensing applications. A preliminary study of the fabrication of this structure will be presented. It consists of a combination of Atomic Layer Deposition for the silicon dioxide layers and the use of amorphous silicon instead of crystalline silicon.

9371-63, Session 14

Optical biosensor based on silicon nanowire ridge waveguide

Rania Wahdan, Yehia Ismail, The American Univ. in Cairo (Egypt) and Zewail City of Science and Technology (Egypt); Mohamed A. Swillam, The American Univ. in Cairo (Egypt)

We propose a silicon nanowire ridge waveguide (SNRW) to work as an optical biosensor. This structure is comprised of an array of vertically aligned silicon nanowires on an insulator that have the envelope of a ridge waveguide. The SNRW inherently maximizes the overlap between the material under test and the incident light wave by introducing voids to the otherwise bulk structure. When a sample is injected, the voids within the Silicon nanowires adopt the refractive index of the material under test; hence, the strong contribution of the material under test to the overall modal effective index will greatly augment the sensitivity. FDTD simulations are conducted to show that the percentage change in the effective index due to a 1% change in the surrounding environment is more than 170 times the amount of change perceived in an evanescent detection based bulk silicon ridge waveguide. In addition, the detection limit for this structure was revealed to be as small as 10^{-8} .

9371-64, Session 15

Total absorption by degenerate critical coupling

Jessica R. Piper, Victor Liu, Shanhui Fan, Stanford Univ. (United States)

We consider a planar, mirror-symmetric optical resonator with two ports. We show that, when excited from a single port, complete absorption can be achieved through critical coupling to degenerate resonances with opposite symmetry. Moreover, any time two resonances with opposite symmetry are degenerate in frequency, absorption is always significantly enhanced. In contrast, when two resonances with the same symmetry are nearly degenerate, there is no absorption enhancement. We numerically demonstrate these effects using a graphene monolayer on top of a photonic crystal slab, illuminated from a single side in the near-infrared.

9371-65, Session 15

Application of Fourier-Bessel technique for computing Eigen-states in a Bragg cylindrical space slot channel waveguide

Seyed Hamed Jafari, Robert C. Gauthier, Carleton Univ. (Canada)

Maxwell's wave equations can be solved using different techniques in order to extract optical properties of a variety of dielectric structures. For structures that contain an extended axis which serve for the reference for cylindrical symmetry, we have shown that an expansion of the fields and inverse of relative dielectric profile using a simplified and complete set of basis functions of Fourier-Bessel terms provide access to an eigenvalue formulation from which the eigen-states can be computed. We review the steps used to convert Maxwell's equation into an eigenvalue formulation, and then proceed to discuss several applications of the technique. For cylindrically symmetric structures, the computational technique provides a significantly reduced matrix order to be populated and diagonalized. New target structure for the presentation consists of cylindrical space slot channel waveguide in which the channel extends in azimuthal (?) direction. The channel is provided by considering the etching of external side walls of "Bragg fiber". The configuration is similar to a structure that can support whispering-gallery modes, except that the modes highest field locations are within the ambient medium of the channel. Optical properties of this structure can be best examined through Ez field component which is discontinuous by ratio of relative dielectric constants when passing air-Bragg interfaces. The ability to select Bragg dielectric properties and to introduce non-uniformities in Bragg plane spacing provides access to tuning slot channel waveguide properties and design several novel configurations. Latest simulation results will be presented with focus on potential applications.

9371-66, Session 15

Dispersion of mode-gap cavities

Jin Lian, Sergei Sokolov, Univ. Twente (Netherlands); Alfredo De Rossi, Sylvain Combrie, Thales Research & Technology (France); Allard P. Mosk, Univ. Twente (Netherlands)

Arrays of coupled nanocavities are fascinating for their slow-light applications and light-matter interaction enhancement [1]. High Q and wavelength sized cavities, especially the photonic crystal mode gap cavities are more attractive for people to making large scale arrays [2]. For a long time, the tight binding (TB) model is the most widely used model for modeling and optimizing the light transport in such systems [3, 4]. However, the distinction between symmetric spectrum which predicted by

**Conference 9371: Photonic and Phononic Properties
 of Engineered Nanostructures V**

the TB model and asymmetric spectrum which has been calculated and measured on arrays of coupled mode gap cavities [5] proves that the TB model should be modified in order to make the modelling and optimization more accurately. Thus, to investigate the origin of the deviation from the TB model becomes crucial.

Here we represent systematic numerical calculation of the dispersion of coupled mode-gap cavities. We show the dispersion deviates strongly from the TB model especially depending on the resonant frequency of the single cavity. We prepare an improved TB model to account for this dispersion.

- [1] A. Yariv, Y. Xu, R. K. Lee and A. Scherer *Opt. Lett.* 24 711 (1999).
- [2] M. Notomi, E. Kuramochi and T. Tanabe *Nature Photon.* 2 741 (2008).
- [3] P. Chak and J. E. Sipe *Opt. Lett.* 31 2568 (2006)
- [4] M. Sumetsky and B. J. Eggleton, *Opt. Express* 11, 381 (2003).
- [5] N. Matsuda, E. Kuramochi, H. Takesue, and M. Notomi *Opt. Lett.* 39 2290 (2014).

9371-67, Session 15
Coherent control of coherent anti-Stokes Raman scattering by chiral sculptured thin films

Joseph B. Geddes III, Rolith, Inc. (United States)

Chiral sculptured thin films (STFs) comprise assemblages of helical nanowires grown on a substrate via physical vapor deposition. The nanowires are tightly packed, and hence the STFs can be modeled as anisotropic, inhomogeneous continua. The periodicity of the helical nanowires endows sufficiently thick chiral STFs with a circular polarization dependent photonic bandgap, known as the circular Bragg phenomenon. Chiral STFs can be deposited from materials possessing Raman-active vibrational modes, or Raman-active fluids can infiltrate their interstices. Hence they make a good model system for the study of coherent control of stimulated Raman scattering in complex media. Using a numerical finite-difference method, we studied the temporal response of Raman-active chiral STFs to ultrashort optical pulses. We show how the amplitudes and spectral phases of such pulses can be shaped to increase the coherent anti-Stokes Raman scattering signal produced by the chiral STF, and how this signal depends on the circular polarization state of the incident pulse and the structural handedness of the film.

9371-68, Session 15
All-optical control of form birefringence

Subhajit Bej, Jani Tervo, Yuri Svirko, Jari Turunen, Univ. of Eastern Finland (Finland)

In this work, we report a way for all-optical control of form birefringence of a sub-wavelength 1-D grating structure (SWG) with isotropic dielectric materials. Form birefringence is a well known physical phenomenon where the source of the birefringence is structural anisotropy in the sub-wavelength scale. With the variation of grating periods, depths and duty cycles, it is also possible to tailor the amount of anisotropy and hence the amount of form birefringence. Form birefringent structures can be used to construct commercial optical devices like wave plates, phase plates, beam splitters etc. However, no one to our knowledge has considered yet the effect of Kerr nonlinearity on form birefringence. Here, starting from the Maxwell's equations and using the first order effective medium theory approach we derive an analytical formula for an estimation of the nonlinear form birefringence from a linear grating composed of isotropic, dielectric, Kerr-nonlinear material. We also present comparisons between the results produced with the analytical formula and those obtained with the full rigorous FMM (Fourier Modal Method). We find out that even under the influence of strongly intense light, the assembly still behaves like an uniaxial crystal under normal incidence of light as in the linear case but as one varies the input light intensity, the amount of birefringence is also varied. Hence, the assembly behaves as a tunable birefringent material under the influence of strongly intense field. Finally, we investigate the effect of Kerr nonlinearity on the dispersion (wavelength dependence) of form birefringence.

Conference 9372: High Contrast Metastructures IV

Wednesday - Thursday 11-12 February 2015

Part of Proceedings of SPIE Vol. 9372 High Contrast Metastructures IV

9372-1, Session 1

Advances of high-contrast gratings (*Invited Paper*)

Connie J. Chang-Hasnain, Univ. of California, Berkeley (United States)

No Abstract Available

9372-2, Session 1

High-index contrast-integrated optics in the cylindrical coordinate (*Invited Paper*)

Siyuan Yu, Univ. of Bristol (United Kingdom) and Sun Yat-Sen Univ. (China); Xinlun Cai, Sun Yat-Sen Univ. (China); Ning Zhang, Univ. of Bristol (United Kingdom)

Recently the developments of high contrast optics, such as high contrast grating (HCG), have attracted much attention. Much of the existing work have been focused on structures that can be characterized as 'Cartesian', i.e., their are easily described by functions that are separable in the Cartesian coordinate. Yet optical fields with cylindrical rather than Cartesian symmetries, such as Laguerre-Gaussian (LG) modes and their relatives including both the scalar LG modes and cylindrical vectorial (CV) modes, can be more efficiently manipulated by high contrast structures that have the same kind of cylindrical symmetries, hence best described in a polar or cylindrical coordinate. An example of such a structure is the angular grating based silicon photonics micro-ring optical vortex emitter device we reported.

An efficient treatment of cylindrical high contrast structures requires the decomposition of Fourier components of both the field and the structure in the cylindrical coordinate, so that the coupling process between the field Fourier component via the structure can be calculated. We have implemented a semi-analytical model that fully describes the 3D vectorial coupling process using a transverse spatial Fourier analysis in the cylindrical space. This model can deal with HGC structures in cylindrical coordinates with high precision and fast speed, enabling rapid yet accurate simulation of the coupling of planar waveguide modes with optical vortex modes carrying photonic orbital angular momenta and allowing optimization of the emission coefficient and emitted beam quality. The details of the method and optimized silicon photonics integrated OAM emitter devices will be presented.

9372-3, Session 1

Electrical tuning and control of photonic crystal cavities for photonic quantum information processing (*Invited Paper*)

Andrea Fiore, Tian Xia, Maurangelo Petruzzella, Leonardo Midolo, Francesco M. Pagliano, YongJin Cho, Frank W. M. van Otten, Technische Univ. Eindhoven (Netherlands); Lianhe Li, Edmund H. Linfield, Univ. of Leeds (United Kingdom)

Large-scale quantum photonic integrated circuits, as needed for scalable quantum information processing with photons, require optical nanocavities and other components (e.g. phase modulators) with a large degree of reconfigurability and operating at low temperatures. This reconfigurability must be realised at ultralow power levels, in order to avoid excessive thermal load. The most promising solution to this formidable technical challenge is

the use of nano-opto-electro-mechanical systems (NOEMS), which exploit mechanical motion at the nanoscale to change the distribution of optical fields in a waveguide or a cavity. We have recently demonstrated the electromechanical tuning of the resonant modes of III-V double-membrane photonic crystals over 20 nm with very small static power consumption, and used it to control the spontaneous emission of quantum dots. This concept can be extended to phase modulation and other types of reconfigurability in quantum and classical photonic integrated circuits. In this talk, after an introduction on the concept, recent results on cavity tuning, coupling of NOEMS structures to waveguides, and integration of cavity tuning with the electrical control of the exciton energy in quantum dots via the Stark effect will be presented.

9372-4, Session 2

High-speed high-contrast grating VCSELs (*Invited Paper*)

Werner H. Hofmann, Technische Univ. Berlin (Germany)

The Vertical-Cavity Surface-Emitting Laser (VCSEL) has evolved to a mature device technology enabling novel products like the laser-mouse.

VCSELs feature a very short optical cavity and only a very small amount active media has to be pumped compared to typical edge-emitters.

Modal properties can be defined at levels of dedicated distributed feed-back laser diodes. Featuring a designed cavity with Bragg-reflectors, mode-filters or high-contrast gratings can be used. This yields a low-cost laser-diode with superior modal behavior which can be operated up to the thermal roll-over. Together with a well-designed mode-gain offset or detuning, very temperature-stable devices with intrinsic power limiter can be realized.

Utilizing High-contrast metastructures, so-called high-contrast gratings (HCG) open up another degree of freedom in VCSEL device design and performance. Being novel not only a replacement technology of the thick distributed Bragg reflectors, but adding various novel properties like polarization mode stability, the HCG-VCSEL will be the future workhorse of energy-efficient, low-cost and high-performance light source. Additionally, this kind of reflector can ensure single-mode emission of larger aperture devices or define the cavity mode by structuring different patterns, making VCSEL arrays for wavelength-division-multiplexing feasible.

The HCG design has to found by a large effort of numerics. Utilizing the Finite-difference time-domain method, close attention on the grid-size and other parameters has to be given. Additionally, the finite properties of these HCGs have to be accounted for, with easier infinite models giving misleading results.

Finally, we present our standing in realizing high-performance HCG-VCSEL devices for highest modulation speeds.

9372-5, Session 2

High-contrast grating reflectors for 980-nm vertical-cavity surface-emitting lasers (*Invited Paper*)

Marcin Gebiski, Olga Kuzior, Maciej Dems, Lodz Univ. of Technology (Poland); Anna Szerling, Anna Wojcik, Institute of Electron Technology (Poland); Norbert Palka, Military Univ. of Technology (Poland); Michal Wasiak, Lodz Univ. of Technology (Poland); Qi Jie Wang, Dao Hua Zhang, Nanyang Technological Univ. (Singapore); Tomasz G. Czystanowski, Lodz Univ. of Technology (Poland)

High reflectivity mirrors are crucial element of low threshold VCSELs. Typically used Distributed Bragg Reflectors (DBR) provide reflectivity over 99.8% in the spectral range of 75 nm. It has been shown that High Contrast Gratings (HCG), if properly designed, provide extremely large polarization discrimination as well as 150 nm spectrum of high reflectivity which makes them superior to DBRs and potentially opens a way to the next generation HCG based VCSELs. We present extensive numerical analysis of a high-contrast grating VCSEL emitting at 980 nm. Using a three-dimensional, fully vectorial optical model, we investigate the influence of a non-uniform grating with a broad range of geometrical parameters on the modal behavior of the VCSEL. Properly designed and optimized, the high-contrast grating confines the fundamental mode selectively in all three dimensions and discriminates all higher order modes by expelling them from its central region. This mechanism makes single mode operation possible under a broad range of currents and could potentially enhance the single-mode output power of such devices. The high-contrast grating design proposed here is the only design for a VCSEL with three-dimensional, selective, optical confinement that requires relatively simple fabrication.

9372-6, Session 2

Fabrication of SiC membrane HCG blue reflector using nanoimprint lithography

Ying-Yu Lai, National Chiao Tung Univ. (Taiwan); Akihiro Matsutani, Tokyo Institute of Technology (Japan); Tien-Chang Lu, Shing-Chung Wang, National Chiao Tung Univ. (Taiwan); Fumio Koyama, Tokyo Institute of Technology (Japan)

In recent years, blue vertical microcavity (MC) emitters fabricated by III-N based materials such as resonant cavity light emitting diodes (RCLEDs) and vertical cavity surface emitting lasers (VCSELs) have attracted much attention for various applications. To further intensify the functionality of III-N MC, high contrast grating (HCG) is a good platform due to its high reflectivity, compactness, polarization selectivity, and so on. So far, the development on short wavelength HCG has been still limited due to difficulties in nitride based membrane structures. Furthermore, making HCG structures on the III-N material may have a possibility to damage the active layer, which is a tough issue for realizing an efficient MC emitter. In view of these issues, SiC, a wide-bandgap material which has a low absorption at short optical wavelength and a high etching selectivity against SiO₂ as a sacrificial layer is a good candidate for fabricating a high reflectivity blue HCG reflector. In this paper, we fabricated a high quality membrane SiC blue HCG reflector using nanoimprint lithography followed by two-step etching process. Such membrane SiC HCG provides a functional single layer cavity mirror without damage to the III-N-based active layer, which offers a platform for nitride-based microcavity devices.

9372-7, Session 2

Heterogeneously-integrated VCSEL using high-contrast grating on silicon

James E. Ferrara Jr., Weijian Yang, Li Zhu, Connie J. Chang-Hasnain, Univ. of California, Berkeley (United States)

A light source integrated with silicon will play a key role in applications such as optical interconnects for multi-core computing, lab-on-a-chip systems, and range detection. Part of the allure is that photonics circuits on silicon can be very small and leverage over 50 years of existing microelectronics infrastructure. VCSELs have inherent advantages over their edge-emitting counterparts because they can be easily tested in vast 2D arrays and are energy efficient at high data rates. By employing MEMS actuators, they can also offer the flexibility necessary for circuit or network designers to reduce wavelength inventory and reduce integrated system costs.

Our scalable approach targets the thermal resistance of VCSELs by: (i) employing a unique eutectic metal bonding process that acts as an efficient heat sink; and by (ii) substituting traditional III-V distributed Bragg reflector (DBR) mirrors used in VCSELs – which are thermally inefficient – with ultra-thin high contrast gratings (HCGs).

We report an electrically pumped AlGaInAs-silicon VCSEL structure using a high contrast grating (HCG) mirror on silicon. The VCSEL operates in the L band

with >1.5 mW CW output power, and single-mode operation up to 65 °C. The thermal resistance of our device is measured to be 1.46 K/mW. We demonstrate >2.5 GHz 3-dB direct modulation bandwidth, and we show 5 Gb/s direct modulation through a fiber link of 2.5 km single mode fiber (SMF). We also explore the possibility of an all-HCG VCSEL structure that would benefit from stronger thermal performance, higher tuning efficiency, and faster direct modulation speeds.

9372-8, Session 3

Optomechanics with high-contrast gratings (*Invited Paper*)

John R. Lawall, National Institute of Standards and Technology (United States) and Joint Quantum Institute (United States); Haitan Xu, National Institute of Standards and Technology (United States) and Joint Quantum Institute (United States); Yi-Chen Shuai, National Institute of Standards and Technology (United States) and Joint Quantum Institute (United States); Utku Kemiktarak, Corey Stambaugh, National Institute of Standards and Technology (United States) and Joint Quantum Institute (United States); Jacob M. Taylor, National Institute of Standards and Technology (United States) and Joint Quantum Institute (United States)

High-contrast gratings (HCGs) fabricated from silicon nitride can realize an extremely lightweight mirror with a very high mechanical quality factor, offering a fruitful platform for optomechanics. By using a highly reflective HCG as the end mirror of a Fabry-Perot cavity, we have optically cooled mechanical modes of the HCG to cryogenic temperatures. In related experiments, we have studied the multimode dynamics of a “phonon laser.” More recently, we have used a HCG to couple two optical cavities, both optically and mechanically. From careful analysis of the mode structure we are able to independently characterize the losses from absorption and scattering, as well as infer a reflectivity of over 99.8%. Our current effort involves HCGs with a two-dimensional pattern, which should be insensitive to polarization, provide better dissipation of heat, and have better mechanical properties. Metrological motivations for this work include the creation of squeezed light and force detection beyond the standard quantum limit.

9372-9, Session 3

High-contrast gratings for active-cavity optomechanics

Stephen A. Gerke, Weijian Yang, Connie J. Chang-Hasnain, Univ. of California, Berkeley (United States)

Recently, optomechanical cavities with integrated optical gain have been demonstrated to produce very large amplitude mechanical regenerative oscillation, with applications as self-driving wavelength swept sources. Instead of the detuning-based mechanism of passive-cavity optomechanical oscillators, active-cavity optomechanical oscillators create negative damping using the delayed response time of the photon pressure to mechanical perturbations of the cavity, giving a more complex dynamical system incorporating the dynamics of the semiconductor quantum well

active medium. By removing the requirement of an external low-noise laser, optomechanical lasers show significant promise in developing microscale integrated optomechanical systems for use in clock generation and on-chip sources for swept-source imaging. Here, we show the crucial role of high-contrast metastructure reflectors in enabling active-cavity optomechanical systems. These mirrors offer not only high reflectivity in a low-mass structure, but also offer the ability to design optomechanical behaviors based on the reflectivity spectrum of the grating mirror and mechanical modes of the mirror and support structure. We further demonstrate design principles for active-cavity optomechanical self-oscillation and cooling, and show the latter as a way to address serious issues of thermal phase noise affecting micromechanically-tunable lasers.

9372-10, Session 3

Optical resonator for gas/liquid sensing based on high-contrast gratings

Tianbo Sun, Univ. of California, Berkeley (United States); Krishanan Parameswaran, Physical Sciences Inc. (United States); Connie J. Chang-Hasnain, Univ. of California, Berkeley (United States)

HCGs are formed by a thin layer of semiconductor subwavelength grating surrounded by low index material. Unlike traditional gratings, which are etched on high index substrates, HCG has high index contrast at both entrance and exit planes. One feature of this configuration is that HCGs can be designed to have high-quality factor optical resonance. By carefully designing the grating period, duty cycle and thickness, HCG resonator can be designed to: (i) operate within a large wavelength range (from visible, near infrared to mid infrared). (ii) work at surface normal or oblique incident angles. All these features make HCG a suitable platform for compact while efficient sensing system.

We report design, fabrication and measurement of HCG resonators. Devices are fabricated on Si SOI wafer with one step of lithography and one step of etching. Two designs are shown here: Optical resonators (i) working at 1550nm with surface normal input light, (ii) working at 2004nm (CO₂ absorption peak) with 36 degree input light. In both cases, optical Q is measured to be ~ 7000. Flexible combination of input angle and resonance wavelength can be achieved by different design parameters (i.e. grating period, duty cycle and thickness).

Index sensing has been demonstrated using our HCG resonator. A sensitivity of 700nm/RIU (refractive index unit) has been shown in the measurement. Index change as small as 10^{-4} can be resolved basing on this sensitivity. We also explore the possibility graphene-HCG structure that would benefit from tunable optical quality factor and additional sensitivity gain from low density of states in graphene.

9372-11, Session 3

Lasing characteristics of nonpolar a-plane GaN-based photonic crystal defect cavities *(Invited Paper)*

Tsung-Sheng Kao, Tien-Chang Lu, Hao-Chung Kuo, Shing-Chung Wang, National Chiao Tung Univ. (Taiwan)

Nonpolar GaN-based materials in the a-plane or m-plane direction have drawn much attention due to their great potentials in high-performance lasers and high-brightness light-emitting diodes. In this paper, we exploited the features of the free polarization fields in the quantum wells and the anisotropic gain in different nonpolar directions, developing low threshold and high power photonic crystal (PC) cavity lasers. The PC pattern with a L7 line-type defect cavity was defined by the e-beam lithography (EBL) on the nonpolar a-plane GaN films, while the thin membrane structures were milled by focused-ion beam (FIB), forming a free-standing thin slab of 235nm. The hole radius and lattice constant are 29nm and 122nm, respectively. By

conducting the micro-photoluminescence at 77K, the lasing properties of the nonpolar a-plane GaN-based photonic crystal with the L7 nanocavities were characterized. One dominated resonant mode was observed at 419.3nm with a quality factor around 2×10^3 . Moreover, the degree of polarization of the emitted light was measured to be 51.3%. The numerical calculations showed a good agreement with the experimental results. In the comparison with the PC line cavities fabricated on the c-plane, the nonpolar a-plane GaN-based PC cavity laser not only showed higher polarization ratio for the output emission, but also exhibited an invariant resonant mode with an increase of the injection carriers, resulting from absent of the quantum confined Stark effect (QCSE) in the nonpolar GaN quantum wells.

9372-12, Session 3

TiO₂/air high-contrast grating reflectors for GaN-based vertical-cavity light emitters

Seyed Ehsan Hashemi, Jorgen Bengtsson, Johan S. Gustavsson, Chalmers Univ. of Technology (Sweden); Georg Rossbach, Ecole Polytechnique Fédérale de Lausanne (Switzerland); Åsa Haglund, Chalmers Univ. of Technology (Sweden)

High-reflectivity broad-stopband feedback mirrors necessary for GaN-based vertical-microcavity light emitters, e.g. VCSELs, in the UV-blue-green wavelength regime are truly challenging to produce. Rather than conventional distributed Bragg reflectors (DBRs) high contrast gratings (HCGs) may be used, which may offer stronger higher-order-mode suppression, post-epitaxial setting of resonance wavelength, and better polarization selectivity. Since III-nitride-based materials are difficult to selectively wet etch, we have investigated an alternative approach using an air-suspended TiO₂ grating with a SiO₂ sacrificial layer. The deposition processes for the dielectric layers were carefully fine-tuned to minimize the residual stress. To achieve an accurate control of the grating duty cycle, a newly developed lift-off process using HSQ and sacrificial PMMA was applied to deposit the hard mask, providing sub-10nm resolution. TiO₂/air HCGs with a range of duty cycles and periods were fabricated and characterized in a micro-reflectance measurement setup. A pinhole was used to limit the acceptance angle of incident and collected light ($\sim 13^\circ$ full-angle). The measured HCG reflectance spectra were compared to corresponding calculated spectra obtained from rigorous coupled-wave analysis. Good agreement was found and the change in the reflectivity spectrum with a change in grating parameters was also well reproduced. A peak power reflectivity in excess of 90-95% was achieved for TM polarization at the design wavelength of 435 nm, with a reflectivity stopband width of about 75 nm (FWHM). Within the explored range of grating duty cycles (45-50%) and periods (325-370 nm), the center wavelength of the stopband could be varied as much as 50 nm.

9372-13, Session 4

Virtually-imaged phased array based on Bragg reflector waveguide for large-port optical switching *(Invited Paper)*

Fumio Koyama, Tokyo Institute of Technology (Japan)

We review a new type of dispersion elements based on a Bragg reflector waveguide, which provides a large angular dispersion of $1-2^\circ/\text{nm}$. The device functions as sub-wavelength virtually imaged phased array grating. We obtain a number of resolution-points (possible channel-count in demultiplexing) over 1,000. We demonstrate a large-scale wavelength switch based on a Bragg reflector waveguides array. The waveguides array has a small footprint of 2.4 mm^2 , but provides both ultra-large numbers (>100) of output-ports and wavelength-channels at the same time. Prospects for further increase in the wavelength channel count and output ports will be discussed.

9372-14, Session 4

Bringing mirrors to rest: grating concepts for ultra-precise interferometry (*Invited Paper*)

Stefanie Kroker, Friedrich-Schiller-Univ. Jena (Germany); Ernst-Bernhard Kley, Friedrich-Schiller-Univ. Jena (Germany) and Fraunhofer IOF (Germany); Andreas Tünnermann, Friedrich-Schiller-Univ. Jena (Germany) and Fraunhofer-Institut für Angewandte Optik und Feinmechanik (Germany)

Multilayer mirrors based on amorphous coating materials are known for their excellent optical properties which enable a reflectance of virtually 100%. However, they reach a limitation when it comes to applications where an extreme precision of length measurement is required. Fields of interest are for example the realization of frequency stabilized lasers for high-resolution spectroscopy, of optical clocks or the detection of gravitational waves. The latter demands a relative precision in the range of 10-21. Here, tiny fluctuations of the mirror surface (e.g. caused by Brownian motion) can severely disturb the length measurement. By reducing the thermal noise of the optical components the experiments' sensitivity can thus be substantially improved. A promising possibility in order to decrease these fluctuations is to replace conventional amorphous coating stacks by highly reflective silicon based grating components. Instead of multiple beam interference these gratings employ the effect of resonant light coupling to provide a high reflectivity. They are known as resonant waveguide gratings, guided mode resonance filters, or particularly in the case of high-index materials, high contrast gratings (HCGs).

In this contribution we present the current state of knowledge of high contrast gratings as components for gravitational wave interferometers. We discuss how the properties of HCGs can be tailored such that beside highly reflective mirrors also diffractive beam splitters can be realized. Further, we show the impact of such gratings on the sensitivity of future detectors which can pave the way for the new field of gravitational wave astronomy.

9372-15, Session 4

Low-loss adiabatically-tapered high-contrast gratings for slow-wave modulators on SOI

Corrado Sciancalepore, Karim Hassan, CEA-LETI (France); Thomas Ferrotti, STMicroelectronics (France) and CEA-LETI (France); Julie Harduin, H el ene Duprez, Sylvie Menez, Badhise Ben Bakir, CEA-LETI (France)

In this communication, we report about the design, fabrication, and testing of Silicon-based photonic integrated circuits (Si-PICs) including low-loss flat-band slow-light high-contrast-gratings (HCGs) waveguides at 1.31 μm . The light slow-down is achieved in 300-nm-thick silicon-on-insulator (SOI) rib waveguides by patterning adiabatically-tapered high-contrast gratings, capable of providing flat-band slow-light propagation with extremely low optical losses, back-scattering, and Fabry-P erot noise. In detail, the one-dimensional (1-D) grating architecture is capable to provide band-edge group indices as high as 30, characterized by a flattened transmission over several nanometers bandwidth with overall propagation losses equivalent to those of the index-like propagation regime ($\sim 1\text{-}2$ dB/cm). Such photonic band-edge slow-light regime at low propagation losses is made possible by the adiabatic apodization of such 1-D HCGs, thus resulting in a win-win approach where light slow-down regime is reached without additional optical losses penalty. As well as that, a tailored apodization optimized via genetic algorithms allows the flattening of slow-light regime over the wavelength window of interest, therefore suiting well needs for group index stability for modulation purposes and non-linear effects generation. In particular, by tailoring the grating corrugation strength

experienced by the optical mode envelope while propagating in the slow-wave waveguide, it is possible to address a continuously-varying photonic bandgap, resulting in flat-band slow-light transmission. In conclusion, such architectures provide key features suitable for power-efficient high-speed silicon modulators as well as an extremely low-loss building block for non-linear optics (NLO) which is now available in the Si photonics toolbox.

9372-16, Session 4

Highly-efficient polarization control using high-contrast transmit arrays

Amir Arbabi, California Institute of Technology (United States); Mahmood Bagheri, Jet Propulsion Lab. (United States); Yu Horie, Andrei Faraon, California Institute of Technology (United States)

Light polarization is conventionally modified using wave plates made of birefringent materials such as crystalline quartz and polymer liquid crystals. Due to the small birefringence of these materials, the thickness of the wave plates is tens to hundreds of microns. Large birefringence may also be achieved using thin 1D or 2D dielectric and metallic gratings with subwavelength periods, and wave retarders have been implanted using these gratings. Here, we present efficient wave retarders with different retardations and orientations of fast and slow axes implemented using periodic arrays of silicon elliptical cylinders resting on a fused silica substrate. The high refractive index contrast between the silicon cylinders and their surrounding media (i.e. air and fused silica) leads to a weak coupling among cylinders that allows for local modification of light polarization by gradually changing the in-plane geometrical dimensions of the scatterers composing the array. We show that novel polarization devices which locally rotate the polarization of the light by different angles while preserving its phase front can be realized using such a high contrast transmitarray. We present design, fabrication and experimental characterization results for near infrared transmissive wave retarders with efficiencies in excess of 90%. We also discuss the applications of the arbitrary local polarization control provided by these novel polarization devices in the generation of cylindrical vector beams, and the possibility of their integration with other flat elements.

9372-17, Session 5

Self-similar optical properties of fractal high-contrast gratings (*Invited Paper*)

Bala Pesala, Ameen E., CSIR Madras Complex (India); Connie J. Chang-Hasnain, Univ. of California, Berkeley (United States)

Fractal structures are common in nature as evident from the structure of snowflakes, blood vessels and tree branches. Fractals have an interesting self-similar property i.e. the physical structure appears similar at various length scales. This interesting property has been explored in various scientific fields ranging from optics, chemistry to biology. For example, significant size reduction in antennas is achieved by using fractal based designs, change in the fractal structure of heart beats is shown to be a good indicator in predicting the onset of various cardiovascular diseases. The self-similarity of physical structure can manifest into self-similarity of optical properties. Earlier studies on fiber Bragg gratings comprising of Cantor set based fractal structures have shown interesting reflection properties with self-similarity.

High-contrast grating is a novel platform with applications ranging from ultra-broad bandwidth reflectors, high-Q resonators, low loss hollow-core waveguides to compact lenses. Here, we explore the optical properties of fractal high-contrast gratings. Simulations are performed using Rigorous Coupled Wave Analysis (RCWA) for various orders of Cantor gratings. The results show interesting reflection, transmission and diffraction properties that demonstrate self-similarity. Fractal HCGs can have various applications

in Surface Enhanced Fluorescence (SEF), Surface Enhanced Raman Scattering (SERS) and towards building compact high-Q resonators.

9372-18, Session 5

Design and fabrication of 3D high-contrast metastructure THz cage waveguides

Gerard T. Dang, Monica Taysing-Lara, Weimin Zhou, U.S. Army Research Lab. (United States); Tianbo Sun, Weijian Yang, Connie J. Chang-Hasnain, Univ. of California, Berkeley (United States)

Previously we developed a new type of 3D high-contrast metastructure hollow-core cage waveguide that displayed slow-light effects at 1550 nm wavelength operation. One of the potential applications for this waveguide is in chemical gas sensing, because the cage design provides an open form of a high-Q cavity that can be integrated with a light source and detector. However, it is desirable to perform the chemical sensing in the THz regime where there is a less busy spectrum for easier chemical identification. We therefore designed and developed a new technique to fabricate a 3D THz metastructure cage waveguide in Si wafers. The waveguide is fabricated using the entire Si wafer thickness (~550 μm) and a modified "SCREAM" method which involves deep Si etch to form the top high-contrast grating (HCG) as cladding, SiO₂ oxidation of the HCG, etching the hollow core with both a Bosch etch and an isotropic undercut etch. The bottom HCG cladding and vertical HCG on each side of hollow-core can be processed from the bottom side of the Si wafer. Using these methods, we have produced waveguides with a 100 μm HCG period. We will discuss the details of these methods and our experimental results. We are also developing a THz waveguide experimental test setup. The next step is to experimentally test and characterize these waveguide in THz spectrum range.

9372-19, Session 5

Active coloration with flexible high-contrast metastructures

Li Zhu, Univ. of California, Berkeley (United States); Jonas Kapraun, Julius-Maximilians-Univ. Würzburg (Germany); James E. Ferrara Jr., Connie J. Chang-Hasnain, Univ. of California, Berkeley (United States)

The ability to actively control the perceived color of objects is highly desirable for a variety of applications, such as camouflage, sensing, and displays. Such a phenomenon can be readily found in nature - the chameleon is an excellent example. However, the capability to change color at-will has yet to be reproduced by humans. The conventional optical coating relies on accumulative interference across multiple layers to provide high reflection or transmission of specific wavelengths and, thereby, display a corresponding coloration. Such structures can never provide substantial color change since layer thicknesses cannot be significantly modified.

In this work, We report a completely new flexible high contrast metastructure (HCM) whose color can be varied by stretching the membrane. This is accomplished with a novel HCM design that annihilates the 0th order diffraction in a grating while enhancing the -1st order. The color perception of the HCM, determined by the -1st diffraction order, is thus easily changed with the variation of its period. The ultra-thin HCM is patterned on a silicon-on-insulator wafer and transferred onto a flexible membrane. We measure more than 15 times stronger intensity in the -1st order diffraction than the 0th order, in excellent agreement with theoretical results. We experimentally demonstrate brilliant colors and change the color of a 1 cm² cm sample from green to orange (39 nm wavelength change) with a stretch of 4.9% (25 nm period change). The same effect can be used for steering a laser beam. We demonstrate more than 36 resolvable beam spots.

9372-20, Session 5

Gap-plasmon metasurfaces for circular dichroic spectroscopy and broadband optical activity

Amr Shaltout, Jingjing Liu, Vladimir M. Shalaev, Alexander Kildishev, Purdue Univ. (United States)

We design, fabricate, and experimentally demonstrate ultrathin metasurfaces that enable circular dichroic (CD) spectroscopy and optical rotation of linearly polarized light over a broadband wavelength range in the near IR region. Each metasurface utilizes a planar array of 30-nm thick gold nano-antennae above a 50-nm gold film reflector and spaced by a 50-nm layer of alumina. The metaldielectricmetal sandwich excites gap-plasmonic waves that cause a significant phase and polarization change to the back-reflected beam. As a result of their dichroism, the metasurfaces respond differently to right circularly polarized (RCP) and left circularly polarized (LCP) light. One metasurface reflects RCP and LCP in two opposite directions at a wavelength dependent angle allowing for detection of RCP and LCP spectra, and hence, acting as a CD spectrometer. The other metasurface rotates linearly polarized light by 45-degree by generating a fixed phase-shift between the reflected LCP and RCP components of light. Previously, both metasurfaces would require complicated chiral antennae to achieve the desired functionality. However, we achieve an effective chiral metasurface through a collective operation of non-chiral antennae. Our approach is built on a supercell metasurface design methodology, where performance is obtained through careful design of location and orientation of individual antennae in the structural supercells. This removes the requirement of chirality for individual antennae and enables a metasurface functionality which quantitatively depends on the supercell geometry. This also simplifies the structure and allows for greater tolerance against fabrication and/or temperature effects. Applications include bio-sensing, DNA structural analysis, crystallography, and secure quantum communications.

9372-21, Session 5

PT symmetric metamaterials and polarisation phase transitions

Mark Lawrence, The Univ. of Birmingham (United Kingdom); Ningning Xu, Oklahoma State Univ. (United States); Xueqian Zhang, The Univ. of Birmingham (United Kingdom) and Tianjin Univ. (China); Longqing Cong, Jianguang Han, Tianjin Univ. (China); Weili Zhang, Oklahoma State Univ. (United States) and Tianjin Univ. (China); Shuang Zhang, The Univ. of Birmingham (United Kingdom)

In recent years PT symmetric photonics has received a great deal of attention, inspired by theoretical investigations of non-hermitian or open quantum systems. By engineering artificial structures such as coupled waveguides, Bragg gratings, ring resonators and microwave cavities with balanced loss and gain, PT symmetric photonic systems have been shown to reveal exciting properties including anomalous transparency, power oscillations, unidirectional transparency and coherent perfect absorption. Here we theoretically and experimentally explore novel polarisation phase transitions induced by PT symmetry breaking in anisotropic terahertz metasurfaces. By using terahertz time domain spectroscopy, giving both amplitude and phase information for all four transmission coefficients, we gain complete knowledge of the polarisation response of our samples. After constructing a metasurface unit cell out of coupled orthogonally orientated split ring resonators with the same resonant frequency but different absorption coefficients, a phase transition is observed for the polarisation eigen states of transmission upon varying the coupling strength. In this case PT symmetry breaking is found to cause a sudden 45° rotation of the eigen polarisation ellipses. Moreover, precisely at the point separating these two regimes, known as the exceptional point, the eigen modes coalesce

into a single circular polarized state which is highly unusual given the metasurface's lack of rotational symmetry. Our study therefore points to increased freedom for controlling the polarisation states of light beyond apparent spatial symmetries and may lead to the exploration of more exotic polarisation phase transitions for 3D metamaterials.

9372-22, Session 6

Parameter-tolerant design of HCGs (*Invited Paper*)

Christyves Chevallier, Supélec (France) and Georgia Tech-CNRS Joint Research Lab. (France); Nicolas Fressengeas, Univ. de Lorraine (France); Joël Jacquet, Captoor (France); Guilhem Almuneau, Youness Laaroussi, Olivier Gauthier-Lafaye, Lab. d'Analyse et d'Architecture des Systèmes (France); Laurent Cerutti, Univ. Montpellier 2 (France); Frédéric Genty, Supélec (France)

Grating structures made of materials which provide a high optical index contrast between the grating slabs and the surrounding medium have shown many extraordinary properties. In fact, with a sub-wavelength grating period, the propagation is possible only for the 0th order of diffraction and the grating layer can be seen as a 1D photonic crystal supporting only a few propagative Bloch modes. The resonance of these modes between the two grating interfaces and their coupling can be adjusted to obtain different and promising properties in a large range of applications such as broadband mirrors, high-Q filters, planar lenses, circular polarizer... In particular, structures made of a high contrast grating (HCG) layer combined with a low index sublayer has already demonstrated that can advantageously replace Bragg reflectors in VCSEL structures for example.

The work presented here is devoted to the design of high contrast grating mirrors and takes precisely into account the technological constraints and tolerance of fabrication. In a first part, a global optimization algorithm has been combined to a numerical analysis of grating structures (RCWA) to automatically design HCG mirrors. In a second part, the tolerances of the grating dimensions have been precisely studied to develop a robust optimization algorithm. This algorithm allows to design high contrast gratings which exhibit not only a high efficiency but also large tolerance values required by the manufacturing process. Finally, in a last part, several structures integrating previously designed HCGs has been simulated to validate and illustrate the interest of such gratings.

9372-23, Session 6

On-chip broadband spectral filtering using planar double high-contrast grating reflectors

Yu Horie, Amir Arbabi, Andrei Faraon, California Institute of Technology (United States)

Miniaturized spectrometers built using monolithic integration on silicon chips will enable low-cost spectroscopy and sensing. For free-space spectroscopy, one attractive design consists of an array of narrowband optical filters placed on top of a photodetector array. Collimated light is incident on the device and then analyzed. We present an on-chip narrowband filter array realized by Fabry-Perot (FP) resonators formed by double high-contrast grating (HCG) reflectors. It is advantageous to use HCG reflectors instead of traditional distributed-Bragg reflectors because the resonance wavelength of each filter can be controlled by varying the lateral geometrical parameters of the grating such as the period and the duty cycle, while the vertical dimensions including the HCG's height and cavity thickness are kept constant. Thus, a filter set covering a broadband wavelength range can be designed and fabricated using only one substrate. To investigate the resonance wavelength tunability and verify the performance of double HCG FP resonators, we performed

numerical simulations using the rigorous coupled-wave analysis and the finite-difference time-domain methods. We found that broadband operation of $\lambda \approx 120$ nm around the central wavelength of 1550 nm can be achieved only by altering the lateral grating dimensions. The HCG reflectors were fabricated in silicon on insulator substrates and high reflectivity was measured. Double HCG devices were developed using a wafer bonding process and their filtering function was measured.

9372-24, Session 6

Efficient high NA flat microlenses realized using high-contrast transmit arrays

Amir Arbabi, California Institute of Technology (United States); Mahmood Bagheri, Jet Propulsion Lab. (United States); Alexander J. Ball, Yu Horie, Andrei Faraon, California Institute of Technology (United States)

Flat microlenses with high NAs that can focus the light to small spot sizes are attractive in many applications including data recording and retrieval, high speed detectors, and integrated micro-optical systems. Multi-level low NA Fresnel microlenses are commonly realized by approximating the height profiles of Fresnel microlenses by a set of quantized height levels. However, high NA microlenses have rapidly varying height profiles which lead to large quantization error and low efficiency of these microlenses. Here, we present design procedure, fabrication details, and measurement results of high NA microlenses based on high contrast transmit arrays. A high contrast transmit array is made by periodic arrangement of potentially dissimilar scatterers with large refractive index compared to their surrounding materials. The high index contrast results in weak coupling among the scatterers and enables realization of rapidly varying phase profiles required for implementation of high NA microlenses. As scatterers, we use 940nm tall amorphous silicon posts with different diameters located on a fused silica substrate and arranged in a periodic hexagonal lattice. We report near infrared high NA microlenses with unparalleled measured performance metrics such as spot sizes as small as 0.57λ and focusing efficiencies in excess of 80%. We demonstrate a trade-off relation between the NAs and efficiencies of high contrast array flat microlenses, and attribute it to the spatial discretization of the microlens phase profile.

9372-25, Session 6

Tailoring the angular transmission behavior of high-contrast gratings (*Invited Paper*)

Stefanie Kroker, Thomas Käsebier, Friedrich-Schiller-Univ. Jena (Germany); Ernst-Bernhard Kley, Friedrich-Schiller-Univ. Jena (Germany) and Fraunhofer IOF (Germany); Andreas Tünnermann, Friedrich-Schiller-Univ. Jena (Germany) and Fraunhofer-IOF (Germany)

Reflective grating structures been demonstrated to enable the realization of filters selective to wavelength, angle and polarization state of the incident light. They are known as resonant waveguide gratings, guided mode resonance filters or in the presence of high index-materials as high contrast gratings (HCGs). During the past decade they have become a promising alternative to conventional multilayer interference filters. However, there is still a lack of grating elements selective in transmission which are of interest for sensor applications. Hereby the main challenge is to realize narrowband filtering properties which cannot be as easily implemented as for their reflective counterparts.

In this contribution we present an approach to realize grating based filter elements with angular bandpass behavior. In order to minimize the bandwidth of the transmission window we exploit the nearly angular independent high reflectivity of high contrast gratings with two-dimensional periodicity. The coupling of two such HCGs enables the realization of a well-defined transmission window. As material combination which is

particularly promising for applications in the near infrared spectral region we focus our investigations on silicon as high index and silicon dioxide as low index material. This choice provides a high index contrast of about 3.5 to 1.5, a fairly low absorption and an excellent compatibility to fabrication processes in semiconductor industry. We show that the approach allows for transmissive filters with a full width at half maximum of less than 3° for light of a wavelength of 1550 nm and transversal-electric polarization.

9372-26, Session 6

Polariton system control through surface pattern design in a subwavelength-grating-based microcavity

Bo Zhang, Zhaorong Wang, Univ. of Michigan (United States); Sebastian Brodbeck, Christian Schneider, Martin Kamp, Julius-Maximilians-Univ. Würzburg (Germany); Sven Höfling, Univ. of St. Andrews (United Kingdom); Hui Deng, Univ. of Michigan (United States)

Exciton-polaritons are quasi-particles in semiconductors formed through the strong coupling of microcavity photons and quantum well excitons. With the demonstration of polariton condensation, polaritons promise to be a model system for novel manybody phenomena if confined-, coupled-, and lattice-polariton systems can be created. To date, lattice-polariton condensation have been created via surface patterning and pillar etching for Distributed Bragg Reflector (DBR) devices, and 1D or OD polariton condensation have been created in etched pillars. Recently, we have demonstrated a OD polariton system by using a cavity with a designable sub-wavelength grating (SWG) mirror. It uniquely enabled strong confinement of polaritons while non-destructive to the coupled exciton media. Here we demonstrate coupled- and lattice-polariton systems in this SWG-based cavity, where the coupling and dimensionality are controlled by controlling both the SWG's optical and mechanical properties. In particular, we show that potentials for polaritons can be created by design of surface tension control patterns surrounding the SWG. The designed patterns control the deformation of the SWG, which is mostly in the normal direction and thus changes the thickness of the air-gap beneath the SWG. The variation in the air-gap thickness leads to variation of the cavity photon resonance, resulting in an effective potential for the photon as well as the polariton modes. We present three devices with different surface tension control patterns corresponding to decoupled OD polaritons, coupled polaritons in a double-well potential, and a coupled quasi-1D polariton lattice. Finally, we show a device that demonstrates the construction of an arbitrary photon potential by design.

9372-27, Session 7

GaAs/AIOx high-contrast grating mirrors for mid-infrared VCSELs *(Invited Paper)*

Guilhem Almuneau, Youness Laaroussi, Lab. d'Analyse et d'Architecture des Systèmes (France) and Ctr. National de la Recherche Scientifique (France); Christyves Chevallier, Frédéric Genty, Nicolas Fressengeas, Lab. Matériaux Optiques, Photonique et Systèmes (France) and Supélec (France); Laurent Cerutti, Univ. Montpellier 2 (France); Olivier Gauthier-Lafaye, Lab. d'Analyse et d'Architecture des Systèmes (France) and Ctr. National de la Recherche Scientifique (France)

Mid-infrared Vertical cavity surface emitting lasers (MIR-VCSEL) are very attractive compact sources for spectroscopic measurements above $2\ \mu\text{m}$, relevant for molecules sensing in various application domains. A long-standing issue for long wavelength VCSEL is the large structure thickness affecting the laser properties, added for the MIR to the tricky technological

implementation of the antimonide alloys system. In this paper, we propose a new geometry for MIR-VCSEL including both a lateral confinement by an oxide aperture, and a high-contrast sub-wavelength grating mirror (HCG mirror) formed by the high contrast combination AlOx/GaAs in place of GaSb/AlAsSb top Bragg reflector. In addition to drastically simplifying the vertical stack, HCG mirror allows to control through its design the beam properties. The robust design of the HCG has been ensured by an original method of optimization based on particle swarm optimization algorithm combined with an anti-optimization one, thus allowing large error tolerance for the nano-fabrication. Oxide-based electro-optical confinement has been adapted to mid-infrared lasers, by using a metamorphic approach with (Al) GaAs layer directly epitaxially grown on the GaSb-based VCSEL bottom structure. This approach combines the advantages of the well controlled oxidation of AlAs layer and the efficient gain media of Sb-based for mid-infrared emission. We finally present the results obtained on electrically pumped mid-IR-VCSELs structures, for which we included oxide aperturing for lateral confinement and HCG as high reflectivity output mirrors, both based on AlxOy/GaAs heterostructures.

9372-28, Session 7

Antireflection subwavelength gratings on optical fiber tips fabricated by a dedicated UV nano imprint lithography system

(Invited Paper)

Yoshiaki Kanamori, Masaaki Okochi, Kazuhiro Hane, Tohoku Univ. (Japan)

Antireflection (AR) layers at the tips of optical fibers are indispensable in order to reduce propagation loss and optical noise. Conventional thin-film AR layers have problems about high cost due to vacuum apparatus usage in the fabrication and requirement of many thin-film layers to obtain broadband AR characteristics. So, easy AR coating methods are needed to reduce Fresnel reflection. AR structures consisting of subwavelength gratings (SWGs), which have periodic structures with the periods smaller than operating wavelengths, have been extensively investigated. The desired refractive index to realize the ideal AR condition can be obtained by SWGs. Nano imprint lithography (NIL) is known as the low cost fabrication technology of SWGs. However, it is difficult to do an NIL process on the tips of the flexible and long optical fibers. In this study, we developed a dedicated UV-NIL system for optical fiber end-faces. Using this system, ideal AR-SWG structures with desired refractive indices can be realized at low cost in principle. An SWG with a period of 700 nm, a width of 560 nm, and a height of 250 nm was successfully fabricated at the tip of a single-mode optical fiber for optical communications system. We evaluated that reflectance decreased by using the SWG over measured spectral range. For example, reflectance decreased to 0.2% at a wavelength of 1550 nm.

9372-29, Session 7

Integration of GaAs-based VCSEL array on SiN platform with HCG reflectors for WDM applications

Sulakshna Kumari, Univ. Gent (Belgium) and IMEC (Belgium); Johan S. Gustavsson, Chalmers Univ. of Technology (Sweden); Ruijun Wang, Univ. Gent (Belgium) and IMEC (Belgium); Emanuel P. Haglund, Petter Westbergh, Chalmers Univ. of Technology (Sweden); Dorian Sanchez, Univ. Gent (Belgium); Erik Haglund, Asa Haglund, Jorgen Bengtsson, Chalmers Univ. of Technology (Sweden); Gunther Roelkens, Univ. Gent (Belgium) and IMEC (Belgium); Anders Larsson, Chalmers Univ. of Technology (Sweden); Roel G. Baets, Univ. Gent (Belgium)

and IMEC (Belgium)

To meet the demands for optical interconnects in future datacom applications, there is a need for dense integration of low-cost, high-bandwidth, and power-efficient WDM transmitters. A similar need exists in spectroscopic approaches for chemical and biological sensing. An attractive route is to use III/V-based VCSEL arrays bonded to a Si-based platform. We present a novel design of a GaAs-based VCSEL, bonded to a Si₃N₄ waveguide platform using benzocyclobutene (BCB), where one of the distributed Bragg reflectors is completely substituted by a free-standing Si₃N₄ high-contrast-grating (HCG) reflector made in the Si₃N₄ waveguide layer. This solution offers a WDM transmitter operating at the standard 850-nm-wavelength for datacom and spectroscopic sensing, where the individual channel wavelengths can be set using standard CMOS fabrication technology. The wavelength separation is simply achieved by varying the HCG parameters (duty cycle and period) of the VCSELS.

Assuming a typical 300-nm-thick Si₃N₄ waveguide layer, we find from RCWA calculations that a corresponding 300-nm-thick, non-absorbing free-standing Si₃N₄ HCG with an 800-nm period and a 40% duty cycle reflects strongly (>99%), for TE-polarization around 850-nm-wavelength, although with a limited 9% stopband-to-center-wavelength ratio. To theoretically investigate the wavelength setting range, a 1D-TMM model is applied to simulate the detailed VCSEL layer structure, where the HCG is replaced by an "artificial" interface having spectral reflectance/transmittance properties obtained from the RCWA calculations. We find that a design with a standing-optical-field minima at the III/V-material/airgap interface will maximize the HCG's influence on determining the VCSEL resonance wavelength, and thereby allowing for a 15-nm-wide wavelength setting range with low threshold gain (<1000 cm⁻¹).

9372-30, Session 7

Photonic crystal membranes for the coherent control of thermal radiation: application to narrow-band and directive sources

Cedric Blanchard, Ecole Centrale de Lyon (France); Cecile Jamois, Institut National des Sciences Appliquées de Lyon (France); Pierre Viktorovitch, Christian Grillet, Ecole Centrale de Lyon (France); Xavier Letartre, Institut des Nanotechnologies de Lyon (France)

Incandescent sources, brought at temperatures of some hundreds of Kelvin, are heavily employed as active element in gas sensors. In order to reduce the energy consumption, a filament exhibiting low thermal inertia must be chosen. The filament can be that way repeatedly heated within a few microseconds at each measure of the gas concentration. There exist mid infrared sources that exploit the high conductivity of platinum to reduce the power consumption well below 50 mW [1].

However, conventional incandescent sources are inherently inefficient owed to their broadband radiation, though the signature of molecules takes the form of narrow absorption rays. What is more, the thermal radiation of a bare object is omnidirectional. To improve the consumption, the power radiated in directions and wavelength ranges that are useless must be inhibited.

In this communication, we employ high index contrast gratings to achieve the coherent control of the emission of incandescent sources. We will present several resonant structures capable of engineering their spectral properties such that the emission of the device is that of the blackbody in the directional and spectral window of interest while the emissivity is remarkably low elsewhere. Our designs and experimental realizations are a response to energy efficiency concerns inasmuch as they are suitable candidates for the development, at the industrial level, of autonomous gas sensors, i.e., able to operate for several years with a simple AA commercial battery.

[1] P. Barritault, M. Brun, S. Gidon, S. Nicoletti. Mid-IR source based on a free-

standing microhotplate for autonomous CO₂ sensing in indoor applications. Sensors and Actuators A: Physical. 379-385. 172(2). 2011.

9372-31, Session 7

Guided resonance reflective phase shifters

Yu Horie, Amir Arbabi, Andrei Faraon, California Institute of Technology (United States)

Optical phased arrays (OPAs) are versatile platforms for various applications such as beam steering, adaptive optics, Fourier optics, and holography. In a reflective-type OPA, each pixel element reflects the incoming light, and controls the phase shift. Commercial OPAs are based on liquid crystals or movable MEMS mirrors. We propose and fabricate phase shifters consisting of sub-wavelength high contrast grating, resting on a low-index spacer backed by a metallic mirror. The guided resonance of the grating combined with the reflection from the metallic mirror leads to an all-pass filter with 2π phase shift variation and unity reflectivity across the resonance. Rigorous coupled-wave analysis was used to verify the phase shifting scheme. We present fabrication and measurement of passive devices operating at telecom wavelengths, fabricated in silicon over gold using a polymer spacer layer. Active control at high modulation speeds can be achieved by shifting the guided resonance frequency using carrier injection or thermo-optic effect that changes the refractive index. Integration of an array of such phase shifters will lead to reflective OPAs operating at faster speed than state-of-the-art devices.

Conference 9373: Quantum Dots and Nanostructures: Synthesis, Characterization, and Modeling XII

Monday - Wednesday 9 -11 February 2015

Part of Proceedings of SPIE Vol. 9373 Quantum Dots and Nanostructures: Synthesis, Characterization, and Modeling XII

9373-1, Session 1

Combining fast electrical control and resonant excitation to create a wavelength-tuneable and coherent quantum-dot light source *(Invited Paper)*

Anthony J. Bennett, Toshiba Research Europe Ltd. (United Kingdom); Yameng Cao, Toshiba Research Europe Ltd. (United Kingdom) and Imperial College London (United Kingdom); David J. P. Ellis, Toshiba Research Europe Ltd. (United Kingdom); Ian Farrer, David A. Ritchie, Univ. of Cambridge (United Kingdom); Andrew J. Shields, Toshiba Research Europe Ltd. (United Kingdom)

One of the building blocks of quantum photonics is a single photon source with high spectral coherence. Semiconductor quantum dots are a promising technology in this regard, as they can integrate monolithic microcavities and electric control to create a versatile and compact device. We report here a device that utilises these advantages, in combination with resonant excitation, to create a wavelength tuneable coherent photon source.

Our dot is embedded in a low RC-constant diode-heterostructure that allows transitions to be tuned by tens of meV around 1324 meV. This device is irradiated by a linearly-polarised coherent laser, whilst emission is collected along the orthogonal linear polarisation. Laser scatter by a factor of up to 1 billion so that it is 1/200th the intensity of the fluorescence.

We show that jitter in the exciton energy broadens the transition to 20 microeV, but that the use of a narrowband laser effectively "filters" this out, leading to fluorescent photons with a linewidth of 1.3 microeV. Thus, it is still possible to observe the signature of coherent light-exciton coupling, the Mollow Triplet, as the laser intensity is increased. Taking advantage of the fast response of the device we are able to switch the transition into and out of the laser energy faster than the transition lifetime, and observe single photon emission with $g(2)(0) = 0.028$. We shall also discuss using multiple dots to create an array of identical single photon sources, frequency locked to a single laser.

9373-2, Session 1

High-performance nanopillar optical antenna avalanche diodes

Pradeep N. Senanayake, Alan Farrell, Diana L. Huffaker, Univ. of California, Los Angeles (United States)

Avalanche photodetectors (APDs) are essential components in active imaging systems requiring both ultrafast response times to measure photon time of flight and high gains to detect low photon fluxes. APDs improve system Signal to Noise Ratio by combining photon detection and amplification eliminating the need for front end amplifiers. An emerging trend in active imaging focal plane array technologies is reducing the pixel pitch (detector volume) for higher resolution images. However, there is an inherent trade-off between reduced detector volume and APD figures of merit.

This talk will focus on the nanowire growth, fabrication and electro-optic characterization of a novel detector architecture "3D Nanopillar Optical Antenna Avalanche Detectors" (3D-NOAADs) for shrinking both the absorption and multiplication volumes using III-V nanopillars, while enhancing the optical absorption via a self-aligned 3D plasmonic antenna. The nanowire growth is achieved via selective area epitaxy of catalyst free

InGaAs nanowires on (111)B GaAs substrates in an Emcore vertical-flow reactor. A passivation shell was subsequently grown in situ.

Wavelength tuning and hybridization of the optical absorption is achieved via Surface Plasmon Polariton Bloch Waves (SPP-BWs) and Localized Surface Plasmon Resonances (LSPRs). Single pixel 3D-NOAADs exhibit substantially lower excess noise factors ($k_{eff} \sim 0.13$) compared to bulk, low breakdown voltages ~ 8 V and gain-bandwidth products > 100 GHz.

9373-3, Session 1

Low-noise four-wavelength simultaneous oscillation of a 1.3-um external-cavity quantum-dot laser

Nami Yausoka, The Univ. of Tokyo (Japan); Mitsuru Ishida, Kan Takada, Masaomi Yamaguchi, Tsuyoshi Yamamoto, Fujitsu Labs., Ltd. (Japan); Yasuhiro Arakawa, The Univ. of Tokyo (Japan)

An external-cavity laser with quantum-dot (QD) gain medium is attractive because it's possible to combine advantages of both the QD medium and the external-cavity configuration. Recent investigations on the external-cavity QD lasers demonstrated high-performances such as the wide wavelength tuning range, stable lasing oscillation, and 10-Gbps transmission.

In this study, we demonstrate an external-cavity QD comb laser of four wavelength channels with 800-GHz spacing. We employed an 800-GHz etalon-filter inserted into the external-cavity, and obtained the four-channel spectrum coincided with LAN-WDM grid. Each mode of four channels oscillated stably at the single longitudinal mode of the external-cavity even when increasing the driving current. We sliced the four-channels into single-channel by an inline band-pass filter. The filtered single-channel has the high optical signal-to-noise ratio (OSNR) of 43.9 dB, and the relative intensity noise (RIN) was as low as -137.9 dB/Hz in the frequency range from 500 MHz to 20 GHz. For comparison with a multi-quantum well (MQW) gain medium, we managed to obtain the four-channel spectrum coincided with LAN-WDM grid using the same setup. However, the four-channel simultaneous oscillation could not be maintained for only several minutes. Furthermore, when we sliced the four-channels into single-channel, the spectrum became hopping, therefore we could not measure the RIN of the filtered single-channel. It was found that the low RIN in the QD comb laser is inheritance in the QD medium. This indicates that the external-cavity comb laser with the QD gain medium is promising for the light source in WDM transmission.

9373-4, Session 1

On-chip generation, routing, and detection of non-classical light

Michael Kaniber, Technische Univ. München (Germany); Günther Reithmaier, Fabian Flassig, Walter Schottky Institut (Germany); Kai Müller, Stanford Univ. (United States); Rudolf O. Gross, Walther-Meissner-Institute (Germany); Jonathan J. Finley, Walter Schottky Institut (Germany)

Photonic information technologies using semiconductors are ubiquitous and are rapidly being pushed to the quantum limit [1] where single photons can be generated on-chip and routed into waveguides [2]. The ability

**Conference 9373: Quantum Dots and Nanostructures:
 Synthesis, Characterization, and Modeling XII**

to integrate sources and detectors with nanophotonic hardware would represent a major step towards the realization of semiconductor based quantum optical circuits. Superconducting single photon detectors (SSPDs) provide high detection efficiencies, low dark count rates, sensitivity up to the infrared and ps timing resolution [3,4,5].

Here, we report the generation, routing and detection of quantum light emitted by resonantly pumped self-assembled InGaAs quantum dots (QDs) in an all-optical circuit using an on-chip integrated SSPD. Applying a temporal filtering technique, we observe common QD excited state resonances both in on-chip and off-chip detection geometries and demonstrate resonant fluorescence from a single quantum dot with a line-width of $10.2 \pm 1.3 \mu\text{eV}$, guided in the optical modes of a GaAs ridge waveguide and efficiently detected via evanescent coupling to an NbN-SSPD integrated on the same chip. Finally, by measuring the autocorrelation function with off-chip detection, we prove the non-classical character of the on-chip detected light.

[1] J. C. F. Matthews et al., Nature Phot. 3, 346 (2009)

[2] A. Laucht et al., Phys. Rev. X 2, 011014 (2012)

[3] C. Natarajan et al., Sup. Sci. and Tech. 25, 063001 (2012)

[4] G. Reithmaier et al., J. Appl. Phys. 113, 143507 (2013)

[5] G. Reithmaier et al., Sci. Rep. 3, 1901 (2013)

9373-5, Session 2
High efficiency AlGaIn deep ultraviolet light emitting diodes on silicon (Invited Paper)

Zetian Mi, Songrui Zhao, Ashfiqua Connie, Mohammad Hadi Tavakoli Dastjerdi, McGill Univ. (Canada)

No Abstract Available

9373-6, Session 2
Tailoring of GaAs/GaAsSb core-shell structured nanowires for IR photodetector applications

Pavan K. Kasanaboina, Sai K. Ojha, Shifat U. Sami, Lew Reynolds, Shanthi Iyer, North Carolina A&T State Univ. (United States)

Ga assisted GaAs/GaAsSb core-shell structured nanowires (NWs) were successfully grown on chemically etched p-type Si(111) substrate by molecular beam epitaxy (MBE). Growth temperature was found to have a strong influence on the Sb incorporation in the NWs and hence the NW morphology. Optical characteristics of the NWs as measured by 4K photoluminescence (PL) exhibit red shift to 1.2 eV with increasing Sb incorporation to 12%. The Raman spectra of reference GaAs NWs shows TO and LO modes of zinc blende structure at 291 cm^{-1} and 267.8 cm^{-1} , respectively. The red shifts of both TO and LO modes in conjunction with corresponding asymmetrical peak broadening with increasing Sb incorporation are attributed to the enhanced strain and disorder in the structure. Raman peak in the reference sample near GaAs LO mode (287 cm^{-1}) attributed to surface optical mode (SO), commonly observed in thin NWs, is absent in core-shell NWs due to their larger diameters (~180 nm). When compared with segmented axial structured NWs of similar Sb composition, core-shell structure was found to yield NWs of uniform composition and diameter. GaAs passivation layer on both core-shell and axial structured NWs significantly enhanced the PL signal and PL was observed even at room temperature. Structural characterization of the NWs by transmission electron microscopy (TEM) will also be presented.

Funding of this work from ARO Grant No. W911NF-11-1-0223 (technical monitor-William Clark) is acknowledged.

9373-7, Session 2
Optical characterisation of catalyst free GaAsP and GaAsP core-shell nanowires grown directly on Si substrates by MBE

Jonathan R. Orchard, The Univ. of Sheffield (United Kingdom); Yunyan Zhang, Jiang Wu, Huiyun Liu, Univ. College London (United Kingdom); David J. Mowbray, The Univ. of Sheffield (United Kingdom)

There is significant interest in the development of vertical nanowires, either singularly or in ensembles, for optoelectronic devices such as single photon sources, nanowire lasers or solar cells. Of the different methods developed to produce these nanowires, deposition directly on to Si substrates using Ga-assisted vapour-liquid-solid growth has a number of benefits. These include reduced costs of Si substrates, no Au contamination and the ability to make a dual junction solar cell using Si and nanowire layers. Peak solar cell efficiency is achieved in combination with a 1.7eV band gap top cell, given by GaAs_{0.8}P_{0.2} nanowires.

However, the optimum growth conditions and nanowire physics is still not fully understood. In this paper we study the optical properties of a number nanowire samples grown under different growth conditions. The samples are characterised by both photoluminescence and micro-photoluminescence at a range of temperatures and excitation wavelengths as well as photoluminescence excitation (PLE). PLE reveals that strong emission only results for excitation within 40 meV of the band edge. For higher energy excitation energetic carriers are lost to non-radiative recombination at the nanowire sidewalls. Temperature dependent PL allows the activation energy associated with carrier loss to be determined.

9373-8, Session 2
GaAsP nanowires on silicon substrates for high-efficiency and low-cost multi-junction solar cells

Ramesh Babu Laghumavarapu, Univ. of California, Los Angeles (United States)

No Abstract Available

9373-9, Session 2
Complex emission dynamics from InGaAs/GaAs core-shell nanopillars

Katarzyna Komolibus, Tomasz J. Ochalski, Bryan Kelleher, Cork Institute of Technology (Ireland); Adam C. Scofield, Univ. of California, Los Angeles (United States); Guillaume Huyet, Cork Institute of Technology (Ireland); Diana L. Huffaker, Univ. of California, Los Angeles (United States)

In this work, the optical properties and emission dynamics of InGaAs/GaAs nanopillars have been investigated using low-temperature photoluminescence and time-resolved photoluminescence. These novel structures have recently attracted much interest within the silicon photonics scientific community because of their potential employment as a gain medium for monolithically integrated lasers on silicon substrates. The optimization of the emission properties of these heterostructures is essential to obtain full compatibility with silicon photonics and requires an accurate tailoring of the pillar geometry (size and pitch) and composition. Therefore it is critical to gain deeper insights into the optical and dynamical properties of different nanopillar designs to achieve optimal device performance. GaAs axial nanostructures with InGaAs inserts and GaP surface passivation layers were grown on native GaAs (111)B substrates by selective-area metal-organic

**Conference 9373: Quantum Dots and Nanostructures:
Synthesis, Characterization, and Modeling XII**

chemical vapor deposition. The NPs were arranged in patterns differing in pillar composition, diameter and pitch. The indium content was estimated from photoluminescence measurements and showed a change in the In to Ga ratio from 0.1 to 0.25. The time evolution of the emission peak showed a strong excitation-dependent blue-shift attributed to the band-filling effect and a slow initial intensity rise followed by exponential decay. For small diameter nanopillars there are two independently saturating emission peaks, suggesting a lack of electronic coupling between them. Measured emission decay times were strongly pattern-dependent varying from nanoseconds to a hundred picoseconds. A dramatic reduction of the decay time was observed for the highest indium concentration due to the dominant contribution of the strain-induced non-radiative recombination processes.

9373-11, Session 3
**Carrier lifetime measurements for 1.3-
um InAs/GaAs quantum dot lasers using
impedance matching**

Xiao Sun, Alcatel-Lucent Shanghai Bell Co. Ltd. (China)

InAs/GaAs QD material system allows emission at 1.3 μm wavelength, which is suitable for optical fibre data communication. The importance of carrier loss mechanisms in these lasers has not been studied in much detail. In particular the role of Auger loss and mono-molecular losses with p-doping need analysis.

This work presents experimental results of carrier lifetime studies in QD lasers using an impedance matching measurement technique. The carrier lifetime analysis can be related to the usual loss coefficients associated with monomolecular (A), radiative recombination (B) and Auger (C) loss processes. The lifetime is measured in the frequency range 0.045-2GHz and for various temperatures. We have used an InAs/GaAs QD laser with a threshold current $I_{th}=48$ mA at 298K and an emitting wavelength temperature dependence of 0.395 nm/K. The laser emission spectrum is 3 nm wide at FWHM with gain of 2 cm^{-1} at 298K at the threshold current.

By comparing the recombination coefficients of the QD lasers, shown in table 1, with those of the QW lasers, we found that A coefficients of both structures are similar. However, B coefficients of the QD lasers are one order of magnitude bigger than those of the QW lasers. The most significant difference of the results between the QD and QW lasers is the Auger recombination coefficient which has much smaller values in QDs than in QWs, at about ten orders of magnitude. Analysis of these results will be presented.

9373-12, Session 3
**Enhanced single-photon emission of InGaN
quantum dots coupled to a silver cavity**

Brandon J. Demory, Tyler Hill, Chu-Hsiang Teng, Lei Zhang, Hui Deng, Pei-Cheng Ku, Univ. of Michigan (United States)

We demonstrate enhanced single photon emission from individual InGaN Quantum Dots (QDs) coupled to a silver (Ag) cavity. InGaN QDs are of interest because of their potential for operation beyond the cryogenic temperature range. To address the inverse relationship between collectable intensity and temperature, we present a metallic cavity capable of broadband (~100nm width) enhancement with a fabrication process that can tolerate QD size and position variations. The cavity comprises of the QD coated with an aluminum oxide layer (Al_2O_3) deposited by atomic layer deposition and a silver film layer deposited by electron beam evaporation. Tuning the thicknesses of the coating layers changes the Localized Surface Plasmon Resonance peak of the cavity, allowing us to better align with the emission wavelength of the QDs. Using angled deposition for the Ag evaporation, we are able to achieve a pseudo conformal Ag coating, to reduce non-radiative losses. Initially, the TRPL lifetime, PL intensity, and g_2 autocorrelation of the uncoated single QDs was measured. Then, the sample was divided into three sections: section 1 being coated in a silver

cavity, section 2 being coating in an aluminum cavity, and section 3 left uncoated as a control. Repeating the same measurements revealed a reduction of the TRPL lifetime and an increase in the PL intensity measured from the Ag section, which was not observed in the other sections. The g_2 autocorrelation measurement of the QDs in the Ag cavity shows photon antibunching. The combination of photon antibunching and enhanced emission signifies single photon-plasmon coupling.

9373-13, Session 3
**Plasmon-coupled CuInS₂/ZnS core-shells
for developing hybrid white LEDs**

Quinton Rice, Hampton Univ. (United States); Sangram Raut, Texas Christian Univ. (United States); Rahul Chib, Univ. of North Texas Health Science Ctr. at Fort Worth (United States); Zygmunt K. Gryczynski, Texas Christian Univ. (United States); Ignacy Gryczynski, Univ. of North Texas Health Science Ctr. at Fort Worth (United States); Wenjin Zhang, Xinhua Zhong, East China Univ. of Science and Technology (China); Mahmoud Abdel-Fattah, Bagher Tabibi, Jaetae Seo, Hampton Univ. (United States)

Plasmon-coupled CuInS₂/ZnS (CIS/ZnS) core-shells are of great interest in developing hybrid white light-emitting-diodes. Cadmium- or lead-free semiconductor nanocrystals are essential components for environmentally green nanophotonic and optoelectronic devices. The plasmon-exciton coupling provides a large amplification of excitation and emission rates. The time-resolved spectroscopy reveals the plasmon effect on the correlation between the fast, intermediate, and slow decay components and the interface-trapped, shallow, and deep-trapped defect states. The plasmon has strong interaction with the pairs at all defect states, and the plasmon-exciton interaction leads to the large photoluminescence enhancement at all defect states. The time-resolved spectroscopy indicates that the fractional amplitudes of PL decay components are widely distributed over the entire spectra. The temperature-resolved PL study suggests that the PL thermal quenching rate of plasmon-coupled CIS/ZnS is dominant at the shallow-trapped donor-acceptor (DA) state, while that of bare CIS/ZnS is dominant at the deep-trapped states. It implies that the Coulomb interaction of plasmon-exciton is dominant between the collective electron cloud oscillation and the pairs at the shallow-trapped DA states, while the Coulomb interaction between the pairs is dominant at the deep-trapped states. The large amplification of excitation and emission by the LSPR, and the good spectral coupling between the blue diode excitation and the PL from CIS/ZnS lead to the realization of hybrid white LEDs. Acknowledgement: This work at HU is supported by NSF HRD-1137747 and ARO W911NF-11-1-0177.

9373-14, Session 3
**Nonlinear versus linear optics transition
selection rules in CdTe quantum dots**

Diogo B. Almeida, Instituto de Física "Gleb Wataghin" (Brazil); André A. de Thomaz, Univ. Estadual de Campinas (Brazil) and Instituto de Física (Brazil); Vitor B. Pelegati, Instituto de Física "Gleb Wataghin" (Brazil); Hernandes F. Carvalho, Univ. Estadual de Campinas (Brazil); Carlos L. Cesar, Univ. Estadual de Campinas (Brazil) and Instituto de Física (Brazil)

By measuring the one photon and two photon absorption in the same quantum dot sample at the same temperature we can discriminate interband and intersubband transitions. We have performed these measurement using one and two-photon Photoluminescence Excitation spectra of CdTe quantum dots at cryogenic temperatures. The measurement

**Conference 9373: Quantum Dots and Nanostructures:
Synthesis, Characterization, and Modeling XII**

required the adaptation of a small cryostat in a nonlinear optics confocal microscope. The 1-photon PLE was performed using a commercial lamp system and a monochromator as the excitation source. The two-photons excitation source was a Ti:Sapphire fs laser, automatically scanned from 780 to 1000 nm in 5 nm steps. The signal collecting optics, including dichroic mirrors, monochromator grating and CCD, was calibrated with a black body radiation source. The fact that two photons absorption depends on the square of the power, the spot size and the pulse duration of the incident beam, all parameters that change with the wavelength, makes it harder to perform a normalization of the spectra. We solved this calibration problem by using the Second Harmonic Generation of urea microcrystals embedded in the sample. Both 1 and 2 photon PLE were performed in the same temperature and the same wavelength collecting window. Our results show clearly the difference in the selection rules between 1 and 2 photon PLE. We used the simplest parabolic effective mass confinement model to analyze the one versus two photons transition oscillator strengths and show that our results agree well with the calculations.

9373-15, Session 3

Modification of photon antibunching behavior of single quantum dots near gold nanoparticles

Swayandipta Dey, Univ. of Connecticut (United States); Yadong Zhou, Univ. of Central Florida (United States); Xiangdong Tian, Julie Jenkins, Univ. of Connecticut (United States); Ou Chen, Massachusetts Institute of Technology (United States); Shengli Zou, Univ. of Central Florida (United States); Jing Zhao, Univ. of Connecticut (United States)

Manipulating plasmon-exciton coupling in a judiciously engineered nanostructure provides a fundamental basis for the development of many emerging fields, such as nano-photonics and photovoltaics. The emission of the QDs get quenched or enhanced, depending upon the distance between the QDs and the metal NPs. The degree of emission enhancement depends also on the spectral overlap between the excitation and emission of the QDs and the plasmon resonance of the MNPs. Thus in order to systematically investigate the effect of plasmon resonance on exciton and multiexciton dynamics, we will perform time-dependent fluorescence measurements of the QDs on MNPs at both the single QD and ensemble level. At the same time, we will monitor the plasmon resonance of the MNPs by absorption or scattering spectroscopy. Our preliminary studies were performed on QDs deposited on Au NPs coated with a silica layer of 5 nm and 10nm thickness. Briefly, Au NPs coated with a silica shell were immobilized on a glass substrate. Then dilute solution of QDs was spin-coated on the Au@SiO₂ surfaces. The QDs formed a very dilute layer on the Au@SiO₂ nanoparticles so that individual QDs could be studied with confocal fluorescence spectroscopy. Then, the second-order photon intensity correlation measurements were carried out to determine the biexciton quantum yield of individual QDs. The preliminary study has proved that when QDs are close to metal nanostructures, the presence of the strong plasmonic field dramatically alters the multiexciton recombination rates therefore affecting the photon antibunching behavior of the single QDs.

9373-16, Session 4

Growth of InGaAs quantum dots on Si and tensile GaAs quantum dots on InP (Invited Paper)

Minjoo Larry Lee, Yale Univ. (United States)

No Abstract Available

9373-17, Session 4

Optimising the defect filter layer design for III/V QDs on Si for integrated laser applications

Jonathan R. Orchard, The Univ. of Sheffield (United Kingdom); Jiang Wu, Siming Chen, Qi Jiang, Univ. College London (United Kingdom); Thomas Ward, Richard Beanland, The Univ. of Warwick (United Kingdom); Huiyun Liu, Univ. College London (United Kingdom); David J. Mowbray, The Univ. of Sheffield (United Kingdom)

Integration of optical and electronic components on the same chip is highly desirable; offering increased data transmission rates, reduced cost and improved power efficiency. However full integration is prevented by the lack of a Si laser. There have been recent promising advances using direct epitaxial growth of III-V materials onto Si with quantum dots (QDs), which are less sensitive to the defects resulting from the large GaAs-Si (4%) lattice mismatch, as the active region. The introduction of strained defect filter layers (DFLs) above the GaAs-Si interface significantly reduces the defect density in the optical layers, the strain causing lateral movement and annihilation of the defects. An open question is the best choice for the DFL.

DFLs based on InAs QDs, InGaAs and InAlAs QWs are studied. Despite QDs having the highest strain, both theoretical, structural and optical measurements show QWs to act as the best DFLs due to their higher strain-thickness product. Selectively excited PL reveals that defects act on carriers thermally excited from the QDs and do not affect the initial carrier capture. The different DFLs result in different QD densities. Limited area PL via apertures in gold masks is used to probe both residual defect densities in the active region and provides a probe of QD densities which can be compared with AFM measurements of surface grown QDs. Both defect and QD densities are critical for devices, laser results for the different DFLs will be presented.

9373-18, Session 4

Heuristic method to calculate quantum dots energy levels

André A. de Thomaz, Diogo B. Almeida, Vitor B. Pelegati, Univ. Estadual de Campinas (Brazil); Luiz G. Ferreira, Univ. de São Paulo (Brazil); Carlos L. Cesar, Univ. Estadual de Campinas (Brazil)

In this work we propose a new method to calculate the energy levels of Quantum Dots (QDs). The most used method, known as kp, presents a set of equations for the calculation of the energy levels of electrons and holes of the QDs. This method provides satisfactory results for the energies at the bottom of the bands, (k=0, large QDs). However, for smaller QDs it fails when compared to experimental results of the measurement of the QD size. The main problem of the kp method is the choice of a set of parameters that can only be measured indirectly. Another problem is that the energy dispersion for electrons and holes provided by the method differs significantly from the energy dispersion of the semiconductor bulk. In order to avoid these problems we decided to employ a heuristic method to calculate the energy bands of QDs, using the energy dispersion relation of the bulk directly and applying the same boundary conditions of the kp theory, that were defined by the symmetry of the system. Each boundary condition provides a k for the electron or hole and we used this k to obtain its respective energy from the energy dispersion relation of the bulk. This way we guarantee that in the limit of the QD radius going to infinity we recuperate the bulk dispersion and also guarantee that we are using the correct bulk parameters. Our predicted QDs sizes obtained by the heuristic method were very close to the sizes measured experimentally.

**Conference 9373: Quantum Dots and Nanostructures:
 Synthesis, Characterization, and Modeling XII**

9373-19, Session 4

**Stability in peak emission wavelength
 in strain coupled multilayer InAs/GaAs
 quantum dot heterostructures upon
 subjected to high-temperature rapid
 thermal annealing**

 Saikalash Shetty, Sourav Adhikary, Hemant Ghadi,
 Subhananda Chakrabarti, Indian Institute of Technology
 Bombay (India)

InAs/GaAs quantum dots (QDs) are of substantial interest in optoelectronic device applications now days. In laser and solar cell structures, high temperature is required for the growth of good quality cladding or window layer. Therefore it is much needed to check for the thermal stability of the peak emission wavelength of the QDs at high temperature. We are reporting the effect of high temperature post growth annealing on photoluminescence (PL) properties of strain coupled InAs/GaAs QDs capped with two different type of thin spacer layer-one with InGaAs (sample A) and another quaternary InAlGaAs (sample B). The samples are grown by MBE and subsequently annealed at 650, 700, 750 and 800 degree Celsius respectively for 30 second. Low temperature and power dependent PL shows a multimodal distribution of the QDs in all the samples. Most significantly, till 700oC annealing temperature, no significant shift in peak emission wavelength is observed for InGaAs capped sample (Sample A). The vertical strain propagating from underlying QDs arising due to lattice mismatch prevents the inter-diffusion by maintaining a strain relaxed state due to coupling. This stability i.e. inhibition in blue shift is more prominent for quaternary InAlGaAs capped coupled QDs where we observed stability in emission peak till 800oC (Sample B). Presence of Al in the capping layer helps in reduction of the thermal energy at high temperature. This stability is essential for optoelectronic devices like vertical cavity surface emitting laser, distributed feedback lasers or photovoltaic device like solar cell. Riber, France and DST, India is acknowledged.

9373-20, Session 5

**Room temperature continuous-wave
 pumped lasing with colloidal CdSe
 nanosheets**

 Joel Q. Grim, Sotirios Christodoulou, Francesco Di Stasio,
 Roman Krahne, Istituto Italiano di Tecnologia (Italy);
 Roberto Cingolani, Istituto Nazionale per la Fisica della
 Materia (Italy); Liberato Manna, Iwan Moreels, Istituto
 Italiano di Tecnologia (Italy)

Emerging photonic applications are creating a growing demand for low-threshold, spectrum-spanning laser gain media. For more than a decade, colloidal nanocrystals (NCs), particularly 0D quantum dots (Qdots), have been investigated with this objective, driven by their tunable optoelectronic properties and ease of solution synthesis. However, efficient Auger recombination has presented a significant roadblock, and until this work, the state-of-the-art colloidal lasers only operated under pulsed laser pumping conditions. To reach the continuous-wave excitation regime, we synthesized 2D colloidal CdSe nanosheets. From an optoelectronic perspective, these form the solution-based counterpart to epitaxial quantum wells. Hence, in contrast to 0D Qdots, stricter momentum conservation rules apply, which is evidenced by the observation of significantly reduced Auger recombination rates. Secondly, (nearly) unrestricted exciton motion in the CdSe plane results in a giant oscillator strength transition, further suppressing Auger recombination through sub-nanosecond radiative recombination rates. We also demonstrate that the colloidal quantum wells, with their 1.5 nm thickness and large dielectric contrast with the surrounding medium, have large exciton and biexciton binding energies of 132 meV and 30 meV, respectively. This enables a stable biexciton population at room

temperature. A stimulated emission gain of 161 cm⁻¹ and threshold of 6.5 W/cm² under CW-pumping conditions were determined (with variable-stripe length and power-dependent measurements, respectively, using CW excitation on close-packed thin films). Finally, CW-pumped lasing at room temperature was achieved by imbedding a 40 μm thin film of CdSe nanosheets in a surface-emitting microcavity, thus providing the first demonstration of CW-pumped solution-processed lasers.

9373-21, Session 5

**Low-loss mid infrared surface phonon
 polariton modes in polar dielectric crystals**

 Jeffrey C. Owrutsky, U.S. Naval Research Lab. (United
 States)

There is interest in identifying nanostructured materials capable of supporting sub-diffraction confinement without the high optical losses inherent in metals that are typically employed for surface plasmon resonances. Polar dielectrics, such as SiC, support narrow band, high quality factor (Q) surface phonon polariton (SPhP) modes because they rely on optical phonons with inherently longer lifetimes and dephasing times than similar plasmonic resonances based on electronic properties. SPhP resonances are demonstrated for nanopillar antenna arrays fabricated in 6H-silicon carbide which are characterized by reflection infrared spectroscopy. The spectra reveal bands due to a dipolar resonance transverse to the nanopillar axis and a monopolar resonance associated with the longitudinal axis that depends on the SiC substrate. The bands are located within the Reststrahlen band of the bulk material and tune with nanopillar dimensions. Both bands are observed with narrow linewidths (??24 cm⁻¹) and high Q factors (40?135). Some of the modes are Raman-active so they can also be observed and characterized in the visible spectral range. Because the SPhP bands are based on optical phonons with longer lifetimes, narrower bandwidths and higher Q than for the plasmonic bands that rely on electronic properties, they are promising for nanophotonic applications.

9373-22, Session 5

**Water-soluble CdTe nanocrystals under
 high pressure**

Yan-Cheng Lin, National Chiao Tung Univ. (Taiwan)

The application of static high pressure provides a method for precisely controlling and investigating many fundamental and unique properties of semiconductor nanocrystals (NCs). Here we systematically investigate the high-pressure photoluminescence and time-resolved carrier dynamics of thiol-capped CdTe NCs of different sizes, at different concentrations, and in various stress environments. The zincblende-to-rocksalt phase transition in thiol-capped CdTe NCs is observed at a pressure far in excess of the bulk phase transition pressure. Additionally, the process of transformation depends strongly on NC size, and the phase transition pressure increases with NC size. These peculiar phenomena are attributed to the distinctive bonding of thiols to the NC surface.

9373-23, Session 5

**Shape and size controlled lead sulfide
 (PbS) quantum dots for optical
 refrigeration applications**

 Gurinder K. Ahluwalia, Mandeep S. Bakshi, College of
 The North Atlantic (Canada); Raman Kashyap, Ecole
 Polytechnique de Montréal (Canada)

Lead sulfide (PbS) quantum dots are attractive candidates for optical

**Conference 9373: Quantum Dots and Nanostructures:
 Synthesis, Characterization, and Modeling XII**

refrigeration due to the tunability of their band gap as a function of size and the resulting quantum confinement*. This study focuses on the simple and straightforward method of synthesis of PbS NPs coated with zein protein and conventional surfactants with well-defined morphologies which show remarkable pH responsive behavior and excellent photo physical properties. The synthesis of PbS NPs in the presence of zein depicts a fine shape control effect as indicated in TEM images. At 0.4 % zein produces nanocubes of ~42 nm which convert into spheres of almost equal dimensions with 0.2 % and 0.1 % zein. Since all reactions contain equal amount of precursor with identical conditions except the amount of zein, the shape transformation from nanocubes to spheres is mainly due to the decrease in the amount of zein from 0.4 to 0.2 %. Close up images indicate a thin coating of zein on the surface of NPs. XRD patterns demonstrate the rock salt crystal structure of NPs with prominent growth at {100} crystal planes. The presence of protein coating makes the NPs bioactive and pH responsive. An increase in the pH systematically increases the absorbance of PbS NPs with a significant red shift which is simultaneously shown by remarkable color change in the solution from light grey with orange tinge to dark brown. The light grey color with weak absorbance at 320 nm is the original color of the solution with pH = 2.55 after the completion of the reaction. Fluorescence behavior of these NPs was investigated under steady state and transient conditions. The implications of the resulting material properties on laser cooling will be discussed.

9373-24, Session 5

Towards the fabrication of high-quality superstructures from ionic liquid electrolytic bath

Khushbu Chauhan, Indrajit Mukhopadhyay, Pandit Deendayal Petroleum Univ. (India)

Abstract: One dimensional superstructures are of great interest in the field of optics, opto-electronics and photonics. Over a period of time, researchers have developed various new and low cost techniques to prepare nanostructures of metals as well as semiconductors. We found that the room temperature ionic liquid can be used to synthesis nanostructured film directly on the substrate by means of electrodeposition. It was found that spindle like CdTe superstructure assemblies over the commercial F:SnO₂ substrate gives a Schottky junction, resulting in the highest rectification ratio of 6000. It was also possible to manipulate the structure dimensions by changing the precursor molar ratio in the ionic liquid bath. It was observed that by varying the structure size, electrical properties of the diodes improve significantly. The admittance measurements reveal that by increasing the diameter of the structures, the conductance of the diode increases linearly. We believe that proper arrangement of the fabricated CdTe thin films will find many applications in near future.

9373-25, Session PWed

Capping layer growth rate and the optical and structural properties of GaAsSbN-capped InAs/GaAs quantum dots

Jose María M. Ulloa, Univ. Politécnica de Madrid (Spain); Daniel Reyes, Univ. de Cádiz (Spain); Antonio D. Utrilla, Alvaro Guzmán, Adrian Hierro, Univ. Politécnica de Madrid (Spain); Teresa Ben, David Gonzalez, Univ. de Cádiz (Spain)

Changing the growth rate during the heteroepitaxial capping of InAs/GaAs quantum dots (QD) with a 5 nm-thick GaAsSbN capping layer (CL) strongly modifies the QD structural and optical properties. A size and shape transition from taller pyramids to flatter lens-shaped QDs is observed when the CL growth rate is decreased from 1.5 to 0.5 ML/s. This indicates that the QD dissolution processes taking place during capping can be modulated by

the GaAsSbN CL growth rate, with high growth rates allowing a complete preservation of the QDs. However, the erosion processes are shown to have a leveling effect on the QD height, giving rise to a narrower size distribution for lower growth rates. Contrary to what could be expected, these effects are opposite to the strong blue-shift and improvement of the photoluminescence (PL) observed for higher growth rates. Nevertheless, the PL results can be understood in terms of the strong impact of the growth rate on the Sb and N incorporation into the CL, which results in lower Sb and N contents at higher growth rates. Besides the QD-CL band offsets and QD strain, the different CL composition alters the band alignment of the system, which can be transformed to type-II at low growth rates. These results show the key role of the alloyed CL growth parameters on the resulting QD properties and demonstrate an intricate correlation between the PL spectra and the sample morphology in complex QD-CL structures.

9373-26, Session PWed

Strong visible electroluminescence in silicon nanocrystals embedded in a silicon carbide matrix

Chul Huh, Tae-Youb Kim, Chang-Geun Ahn, Bong Kyu Kim, Electronics and Telecommunications Research Institute (Korea, Republic of)

Recently, Si nanocrystals (NCs) has attracted the most attention as a promising light sources for the next generation of Si nanophotonics. Generally, Si NCs are created into insulating matrices such as Si oxide and Si nitride films. Because Si oxide and Si nitride films, however, have a relatively high band gap (approximately 9 eV for Si oxide and 5.3 eV for Si nitride, respectively), the tunneling probability between Si NCs decreases due to a high barrier height, resulting in a reduction in light emission efficiency. An alternative surrounding matrix to synthesize Si NCs should be, therefore, developed to realize an efficient Si NC LED. In this work, we investigate the strong visible light emission from the LEDs by employing the Si NCs in a SiC matrix. The structure of Si NC LED investigated here is ITO (100 nm)/n-SiC (10 nm)/Si NCs in SiC (50 nm)/p+-Si. I-V curves of Si NC LEDs with SiC and SiNx matrices were measured at room temperature, respectively. The turn-on voltage of Si NC LED with a SiC matrix was decreased by around 5 V. This was attributed to a lower barrier height caused by a lower band gap of SiC matrix (approximately 2.5 eV) compared to that of SiNx matrix. Electroluminescence intensity was increased with increasing the forward voltage. The light from the Si NC LED was uniformly emitted. We will discuss on the electrical and light emission properties of Si NC LED in detail.

9373-27, Session PWed

Optimization of Er³⁺/Yb³⁺ co-doped LaF₃ nanoparticles for enhanced upconversion emission

Kagola Upendra Kumar, Tasso de Oliveira Sales, Carlos Jacinto da Silva, Univ. Federal de Alagoas (Brazil)

The lanthanide ions doped nanocrystals can generate higher energy emission from lower energy excitation through sequential absorption of photons or energy transfer, which is upconversion (UC) process. Upconverting phosphors have several compelling advantages such as low photobleaching, multicolor labeling, and improved signal-to-noise ratio, which are suitable for using in biomedical applications. LaF₃ works as a host efficiently (maximum phonon vibration frequency <400 cm⁻¹) and is non-hygroscopic, whereas its oxides and sulfides are either hygroscopic or unstable. Er³⁺/Yb³⁺ combination gives number of UC emission bands with two most intense bands at 520–550 and 657 nm under 976-nm diode laser excitation. It is highly desirable in some applications to have UC emission only in green 520–550 nm region because human eyes are most sensitive to this wavelength region. However, the nanoparticles (NPs) have lower luminescence quantum yields and shorter fluorescence lifetime than

**Conference 9373: Quantum Dots and Nanostructures:
 Synthesis, Characterization, and Modeling XII**

their bulk counterparts due to their large number of defects present on the surface, such as unsaturated bonds, surface-adsorbed ions/molecules (H₂O, CO₂), impurities, ligands, and an inhomogeneous distribution of lanthanide (Ln) ions. Improved crystallinity and reduction in the surface defect are possible with annealing of samples at particular temperature, which helps enhancement in the emission of Ln ions. In the present work LaF₃:Er³⁺/Yb³⁺ NPs were synthesized and were heat treated at different temperatures. Their structural characterization and fluorescent properties were demonstrated in details. For further improvement in the efficiency, core/shell nanoparticles were investigated, in which the core is doped with the lanthanide ion and the shell is undoped and similar crystalline structure between the shell and core to decrease lattice mismatch, could confine the excited state well away from the surface and in this way reduce surface quenching. Finally, the surface of the nanoparticles were modified with different ligands (Oleic acid, PEG and SiO₂). Their solubility in the liquid without aggregation and the effect of the ligands on the luminescence properties of the NPs were analyzed in details.

9373-28, Session PWed

Cross sectional TEM (XTEM) analysis for vertically-coupled quaternary InAlGaAs capped InAs/GaAs quantum dot infrared photodetectors

Binita Tongbram, Sourav Adhikary, Hemant Ghadi, Arjun Mandal, Subhananda Chakrabarti, Indian Institute of Technology Bombay (India)

Self-assembled InAs/GaAs quantum dots (QDs) play crucial roles in producing high performance optoelectronics devices such as solar cell, lasers, infrared photodetectors etc. The QDs are grown in MBE by strain driven process which arises due to lattice mismatch. Therefore it is essential to investigate structural morphology of these QD heterostructures to analyze the defects and dislocations, dimensions, stacking and uniformity etc. A detailed XTEM analysis of size, shape, morphology of vertically strain coupled 30 layer InAs QDs with 30 Å quaternary (InAlGaAs) capping and different GaAs capping (90, 120, 150 and 180 Å namely A,B,C,D respectively) is reported along with thick 500 Å uncoupled sample. XTEM micrograph depicted multimodal dot size distribution which was confirmed by power dependent photoluminescence spectra. TEM images report maximum defects and non uniformity in sample A with thin 90 Å capping thickness. With increasing capping thickness, coupling reduces and dot size increases. The average QD height for sample A, B, C and D are 6-9 nm, 8-10 nm, 10-12 nm and 7-13 nm and similarly width as 36-45 nm, 37-49 nm, 39-51 nm and 32-61 nm respectively. For the thick uncoupled sample, the height and width of the QDs are 4 nm and 24 nm which is relatively small compared to coupled QDs. Red shift in spectral response peak is observed from the fabricated coupled quantum dot infrared photodetector compared to uncoupled. Most significantly, peak detectivity is increased by one order for optimized coupled photodetector compared to uncoupled sample.

Acknowledgement: DST, India and Riber, France.

Conference 9374: Advanced Fabrication Technologies for Micro/Nano Optics and Photonics VIII

Sunday - Wednesday 8-11 February 2015

Part of Proceedings of SPIE Vol. 9374 Advanced Fabrication Technologies for Micro/Nano Optics and Photonics VIII

9374-1, Session 1

Fabricating microscopic tools: Towards optically actuated micro-robotics (*Invited Paper*)

David B. Phillips, Miles J. Padgett, Univ. of Glasgow (United Kingdom); Simon Hanna, Daniel Ho, Univ. of Bristol (United Kingdom); David Carberry, The Univ. of Queensland (Australia); Mervyn J. Miles, Univ. of Bristol (United Kingdom); Stephen H. Simpson, Univ. of Brno (Czech Republic)

Direct laser writing is a powerful and flexible tool with which to create 3D micro-scale structures with nanoscale features. If these structures are dispersed in aqueous media, they can be picked up and dynamically actuated in three dimensions using optical tweezers - focussed beams of light that can trap and manipulate dielectric particles. The ability to trap and actuate complex microscopic structures heralds a variety of new applications - optically actuated micro-robotics.

In this presentation, I will describe the design, fabrication and actuation of such a system to develop a scanning probe microscope for imaging surface topography inside a sealed microfluidic chamber. When submerged and held with optical tweezers, the structures are constantly bombarded by water molecules and consequently undergo Brownian motion. Integration of a stereo-scopic imaging system enables three dimensional tracking of the position and orientation of our optically controlled structures to nanometer accuracy, and in real-time (at up to ~2kHz). This allows control of their motion to be handed over to a computer, and they become fully autonomous robotic agents. I will also discuss a variety of other applications of this technology, which have yet to be fully realised but promise exciting developments for the future.

9374-2, Session 1

Fabrication and characterization of micro-structures created by direct laser writing in multi-layered chalcogenide glasses

Casey M. Schwarz, Univ. of Central Florida (United States); Chris N. Grabill, The College of Optics and Photonics, Univ. of Central Florida (United States); Benn Gleason, Spencer Novak, Univ. of Central Florida (United States) and Clemson Univ. (United States); Anna M. Lewis, Gerald D. Richardson, Univ. of Central Florida (United States); Clara Rivero-Baleine, Lockheed Martin Missiles and Fire Control (United States); Kathleen A. Richardson, The College of Optics and Photonics, Univ. of Central Florida (United States); Alexej Pogrebnjakov, Theresa S. Mayer, The Pennsylvania State Univ. (United States); Stephen M. Kuebler, The College of Optics and Photonics, Univ. of Central Florida (United States)

Arsenic trisulfide (As₂S₃) is a chalcogenide (ChG) material with excellent infrared (IR) transparency (620 nm to 11 μm), low phonon energies, and large nonlinear refractive indices. These properties directly relate to commercial and industrial applications including sensors, photonic waveguides, and acousto-optics. Multi-photon exposure can be used to

photo-pattern thermally deposited As₂S₃ ChG glassy films of molecular clusters. Immersing the photo-patterned cross-linked material into a polar-solvent removes the unexposed material leaving behind a structure that is a negative-tone replica of the photo-pattern. Nano-structure arrays that were photo-patterned in single layered As₂S₃ films through multi-photon direct laser writing (DLW) resulted in the production of nano-beads as a consequence of a standing wave effect. To overcome this effect, an anti-reflective (AR) layer of arsenic triselenide (As₂Se₃) was thermally deposited between the silicon substrate and the As₂S₃ layer, creating a multi-layered film. The chemical composition and refractive index of the unexposed and photo-exposed multi-layered film was examined through Raman spectroscopy and near infrared ellipsometry. Nano-structure arrays were photo-patterned in the multi-layered film and the resulting structure, morphology, and chemical composition were characterized, compared to results from the single layered film, and correlated with the conditions of the thermal deposition, patterned irradiation, and etch processing.

9374-3, Session 1

Hybrid type-I/II waveguide embedded Bragg gratings in lithium niobate by direct femtosecond laser writing

Sebastian Kroesen, Jörg Imbrock, Cornelia Denz, Westfälische Wilhelms-Univ. Münster (Germany)

Optical waveguides and integrated optical devices are fundamental components of optical communications and signal processing. In addition to common lithographic techniques, direct femtosecond laser writing is nowadays recognized as a versatile tool to inscribe arbitrary three-dimensional refractive index landscapes into various materials including glasses, crystals and ceramics [1]. Particularly with respect to direct integration of functional optical devices it is indispensable to inscribe waveguide structures, couplers, and gratings into nonlinear optical materials to exploit their inherent reconfigurability [2, 3]. However, the intrinsic anisotropy of crystalline materials e. g. lithium niobate complicate direct write approaches and new complex designs and writing schemes are required.

In this contribution we present a hybrid design that consists of a circular type-II waveguide and an embedded type-I Bragg grating. The structure supports both, ordinary and extraordinary polarized modes, which is mandatory to access features based on the largest electro-optic coefficient r_{33} for extraordinary polarization. Second order Bragg gratings with a period of $\Lambda = 705$ nm are inscribed into the waveguide core using a multiscan technique with high transverse resolution. Finally, narrow spaced integrated electrodes are realized using femtosecond laser material ablation.

We demonstrate that the waveguide embedded Bragg gratings exhibit low loss symmetric guiding and narrowband reflections in the c-band of optical communications. Moreover, we show high bandwidth spectral tuning of more than a peak width and nearly preserved electro-optic coefficients.

[1] Nature Photon 2, 219 (2008).

[2] Laser Photonics Rev. 8, 251 (2014).

[3] Opt. Express 20, 26922 (2012).

9374-4, Session 1

Nano-scale optical actuation based on two-dimensional heterostructure photonic crystal cavities

Tong Lin, Guangya Zhou, Fook Siong Chau, Feng Tian, National Univ. of Singapore (Singapore); Jie Deng, A*STAR Institute of Materials Research and Engineering (Singapore)

Nowadays, the nanoelectromechanical systems (NEMS) actuators using the electrostatic force are facing the bottleneck of the electromagnetic interference which greatly degrades their performance. On the contrary, the hybrid circuits driven by optical gradient force actuation which is immune to the electromagnetic interference show prominent advantages in communication, quantum computation systems. In this paper we propose an optical actuator utilizing the optical gradient force generated by the heterostructure photonic crystal cavities. This type of cavity has a longitudinal slot and is characteristic of ultrahigh quality factor (Q) and ultrasmall mode volume (V) which is capable of producing much larger force compared with waveguide-based structures. Due to the symmetry property, attractive optical gradient force is generated. Additionally, the optomechanical coefficient (gom) of this cavity is up to 200 GHz/nm which is hundreds times larger than that of coupled nanobeam photonic crystal cavities. The 2D hetero-structure cavity, comb drives, folded beam suspensions and the displacement sensor compose the whole device. The cavity serves as the optical actuator whilst the butt-coupled waveguide acts as the displacement sensor which is theoretically proved to be insensitive to the ambient temperature within large range. As known, the thermo-optic effect prevails especially in the cavity-based structures. The comb drive can actuate the movable structure with controllable nanometer precision when no light is pumped into the cavity. Therefore no heat is generated throughout the calibration. When light is continuously launched into the cavity, the overall motion is measured by the displacement sensor. Thus the butt-coupled waveguide can be efficiently used to decouple the thermal effect and the optomechanical effect (OM). The experiment results demonstrate that the proposed optical gradient force actuator show great potential in the future of all-optical reconfigurable circuits.

9374-5, Session 2

Recent progress on triple-helix gold-based metamaterials (Invited Paper)

Johannes Kaschke, Karlsruher Institut für Technologie (Germany); Mark Blome, Sven Burger, Konrad-Zuse-Zentrum für Informationstechnik Berlin (Germany); Martin Wegener, Karlsruher Institut für Technologie (Germany)

Metamaterials based on metal helices have been introduced as broadband and compact circular polarizers. Recently, we have shown that square arrays of intertwined helices, so called N-helices, can eliminate circular polarization conversions by recovering four-fold rotational symmetry. Here, we discuss the possibility of reducing N from 4 to 3, which eases our micro-fabrication considerably. We show analytically that N = 3 helices arranged on a hexagonal lattice exhibit strictly vanishing circular polarization conversions as three-fold rotational symmetry is recovered for the overall structure.

We furthermore investigate numerically N = 3 helices with a tapered diameter along the helix axis. Tapering the helix diameter leads to an increased circular polarizer bandwidth and a higher extinction ratio while maintaining zero circular polarization conversion and high transmission for the wanted polarization. We find operation bandwidths as large as 2.4 octaves.

Furthermore, we present our current progress in the fabrication and characterization of metamaterials based on N = 3 helices. We create polymer templates for subsequent electrochemical deposition of gold using STED inspired direct laser writing (STED-DLW). STED-DLW is a fully

three-dimensional lithography tool with an enhanced resolution not limited by diffraction. The major drawback however, is the lack of a positive-tone photo-resist. We employ a negative-tone photo-resist instead by writing part of the complementary structure. These highly complex structures become feasible by the enhanced aspect ratio and increased axial resolution achieved by STED-DLW. The obtained hollow polymer templates are subsequently filled with gold by electro-chemical deposition.

9374-6, Session 2

Three-dimensional plasmonic nanostructures for enhanced circular dichroism

Negar Otrooshi, Abraham Vazquez-Guardado, Daniel Franklin, Debashis Chanda, Univ. of Central Florida (United States)

The chirality of any molecule can be detected by using the differential absorption of left and right circularly polarized light. Due to small size of such molecules compared to the wavelength the circular dichroism is not strong enough for accurate detection with high degree of certainty. Chiral metal nanostructures are shown to enhance the circular dichroism by many folds due to plasmonic field localization and molecules located near the surface of nanostructures interact with electromagnetic field strangely. A three dimensional (3D) chiral nanostructure outperforms two-dimensional spiral designs due to longer interaction length along the propagation direction. However, fabrication of such 3D metal chiral nanostructure remained as an extreme technological challenge. We propose to use a direct laser writing approach to form inverse replica of the 3D chiral inside a photosensitive polymer. A post electroplating step completes the fabrication process by growing metal through the hollow chiral tubes. A novel cavity based design approach will be investigated to form superchiral light to further enhance the interaction between the chiral nanostructures and chiral molecules. Emphasis will be given to detect various organic molecules like proteins, viruses and DNAs. One of the most important applications of detection of chiral molecules is in medicine where the drug molecules with chiral centers can be accurately identified. Both left and right handed enantiomers have different effect on our body and hence recognition of the enantiomers will enable design of more effective and potent drugs. The proposed technique can detect such molecules at nanogram level or lower.

9374-7, Session 2

Reversible deformation in hybrid organic-inorganic photoresists processed by ultrafast direct laser write technique

Vygantas Mizeikis, Shizuoka Univ. (Japan); Sima Rekstyte, Vytautas Purlys, Vilnius Univ. (Lithuania); Saulius Juodkasis, Swinburne Univ. of Technology (Australia)

This study focuses on volume modification and deformations of sub-micrometer sized features fabricated in hybrid organic-inorganic negative tone photoresist using ultrafast direct laser write (DLW) technique. Typically, photoresist shrinkage is widely recognised as the principal origin of deformations in extended structures (e.g., photonic crystals) fabricated by DLW technique. Here we demonstrate that, at least in some photoresists, significant swelling may also take place during sample development and rinse stages, and is especially pronounced for thin photoresist features characterised by large surface-to-volume ratio. Feature swelling and linear expansion in excess of 10% may dislodge the fabricated samples from substrates already during development, leading to their complete loss or deformations. In order to assess photoresist swelling and expansion, we have fabricated test structures composed of thin lines suspended between massive supporting walls, and observed them shapes during post-DLW wet development and rinse using optical microscope. In developer or alcohol-

**Conference 9374: Advanced Fabrication
 Technologies for Micro/Nano Optics and Photonics VIII**

based rinse solutions, photoresist swelling becomes apparent from buckling of the thin lines, and increases with decreasing line width. However, swelling can be reversed to shrinkage within ~10% linear range by replacing alcohol with water-based rinse. This process is reversible, and thin photoresist features can exhibit actuator-like response during alcohol-water cycling. For larger extended structures, such as diffractive optical elements and photonic crystals, this behaviour may also enable one to tune the lattice period. Qualitative explanation of physical mechanism underlying photoresist swelling and its reversibility will be presented.

9374-8, Session 2

Enhanced nanograting formation assisted by silver ions in a sodium gallophosphate glass: Correlation between surface nanostructuring, fluorescence, and effective second-order nonlinear optical properties

Marie Vangheluwe, Univ. Laval (Canada); Feng Liang, Ctr. d'Optique, Photonique et Laser (Canada); Yannick Petit, Patricia H  e, Institut de Chimie de la Mati  re Condens  e de Bordeaux (France); Yannick Ledemi, Ctr. d'Optique, Photonique et Laser (Canada); S  bastien Thomas, Institut de Chimie de la Mati  re Condens  e de Bordeaux (France); Nicolas Marquestaut, Univ. Bordeaux 1 (France); Evelyne Fargin, Thierry Cardinal, Institut de Chimie de la Mati  re Condens  e de Bordeaux (France); Youn  s Messaddeq, Ctr. d'Optique, Photonique et Laser (Canada); Lionel S. Canioni, Univ. Bordeaux 1 (France); R  al Vall  e, Ctr. d'Optique, Photonique et Laser (Canada)

Sub-wavelength nanoscale gratings are important building blocks for optics and photonics devices, to allow advanced light manipulation. However, the fabrication of large areas and high-quality structures is challenging. Here, we report the first demonstration of the significant role of silver ions included in tailored sodium gallophosphate matrix during nanograting (NG) surface formation by femtosecond direct laser writing (DLW). By comparing the glass behavior with and without silver ions, we observed significant improvements due to the presence of ions in the glass: the NG formation threshold is lower, with smoother NG shape.

Moreover, we recently demonstrated intense and permanent electric-field induced second-harmonic generation and fluorescence emission from silver clustering associated to DLW on silver doped zinc-phosphate glass. Fluorescence and SHG microscopies are perfect tools to monitor silver cluster generation. Here, we extend such laser-induced linear and nonlinear optical properties to the gallophosphate glass.

Noble metal ions act as electron donors which also allow overcoming the stochastic nature of the defects positions in glassy matrices. The silver cluster production is locally stabilized by the electric potential modification resulting from space charges distribution. During ablation, the large reservoir of available free electrons from silver elements drives the NG formation and its incubation process.

Tailored glasses and correlative microscopy were developed to investigate the mechanisms of NG formation. Such approaches, in advanced fabrication technologies, should further provide enhanced abilities for manufacturing high-quality and multi-functional NGs.

9374-9, Session 2

Femtosecond laser writing of phase-tuned multi-level volume gratings for holographic fabrication of symmetry-controlled 3D photonic crystal structure

Liang Yuan, Peter R. Herman, Univ. of Toronto (Canada)

Diffractive optical elements (DOEs) provide powerful opportunities over spatial and spectral beam shaping by means of controlling the beam transmission or reflection from high-resolution surface relief structures. Alternatively, volume gratings offer further utility in manipulating the phase and amplitude of the beam as it propagates and subsequently diffracts over multiple phase layers. Volume gratings also avoid the highly sensitive surface relief structures of traditional DOEs to serve in more robust and high power applications.

Femtosecond laser direct writing is emerging as a highly promising and flexible fabrication technique for structuring internally in transparent optical materials, opening a practical direction for 3D-patterning of permanent refractive index change. In this way, femtosecond lasers are enabling 3D writing of volume DOEs, in which weak phase contrast of $\Delta n = 0.01$ can be accumulated over long propagation distance to modulate and shape the spatial and spectral beam properties. However, a major limitation of volume gratings arises as diffraction dephases over long grating distance, particularly from a weakly contrasting and high resolution grating structure.

Femtosecond lasers provide a novel solution for generating multi-layered phase levels that can coherently stitch and build strong diffraction by aligning the multiple phase levels on Talbot self-imaging planes. These principles are applied in the present work to optimally pattern and order the stacking of laser formed phase layers that enhance and balance the diffraction efficiencies amongst several first order beams in a 2D volume phase mask. Laser writing is further applied to tune phase offsets between orthogonal grating patterns and thereby control the symmetry of 3D diffraction interference such that body centered tetragonal (BCT) and woodpile-like tetragonal (TTR) structural symmetry could be recorded in photoresist. The results demonstrate the utility of low index contrast phase masks in managing both the beam phase and amplitude in new directions of high-resolution 3D holographic lithography.

9374-10, Session 2

Volumetric integration of photorefractive micromodifications in lithium niobate using femtosecond direct laser write technique

Domas Paipulas, Vilnius Univ. (Lithuania); Vygantas Mizeikis, Shizuoka Univ. (Japan); Vytautas Purlys, Ausra Cerkauskaitė, Vilnius Univ. (Lithuania); Saulius Juodkazis, Swinburne Univ. of Technology (Australia)

Capability to modify material's local refractive index using tightly focused ultrashort laser pulses promises fabrication of integrated photonic devices, networks, and data storage structures in the bulk of optically transparent materials. In most optical materials, such as silica glass or sapphire, laser-induced refractive index change typically occurs due to irreversible damage (optical breakdown or near-breakdown), and hence can not be erased or otherwise modified afterwards. On the other hand, lithium niobate, a material widely used in photonics, exhibits bulk photovoltaic effect, which allows metastable and reversible refractive index photomodification without permanent damage, thus enabling optical erasure or modification of previously recorded features. Photorefractive photomodification is widely exploited in recording of holographic memory elements using continuous-wave laser irradiation. Here demonstrate that photorefractive structures in lithium niobate can be tailored with even greater flexibility using femtosecond direct laser write (DLW) technique. Using a traditional

**Conference 9374: Advanced Fabrication
 Technologies for Micro/Nano Optics and Photonics VIII**

DLW setup with a femtosecond Ti:Sapphire oscillator as the light source, combined with specially tailored DLW trajectory, fabrication of small discrete regions with spatial variation of local refractive index on a micrometer length scale, as well as larger regions with quasi-homogeneous modification of refractive index are realized. With this approach we demonstrate multiple writing and local erasure of photorefractive features in the previously recorded volume of lithium niobate, and realization of extended periodic and non-periodic refractive index modification structures can be created. Moreover, refractive index change achievable using femtosecond pulses is by one order of magnitude higher than that achievable with continuous-wave laser irradiation. This approach is suitable for processing of both pure and iron-doped lithium niobate, and can be realized using relatively cheap femtosecond laser oscillator instead of more expensive amplified laser system. Strategies to control the spatial profile of refractive index modification, and prototypes of laser-fabricated diffractive optical elements will be presented.

9374-11, Session 3

Direct laser writing of complex photonic structures *(Invited Paper)*

Harald Giessen, Timo Gissibl, Univ. Stuttgart (Germany)

We combine direct laser writing and fiber technology to fabricate functional devices. We demonstrate a number of different functionalities and present their design, their experimental realization, and their validation. We discuss the sources of error such as writing and shrinking. We are going to demonstrate a number of exciting novel perspectives for the combination of direct laser writing and fiber technology.

9374-12, Session 3

Fiber endface Fabry-Perot vapour microsensors fabricated by multiphoton polymerization technique

Vasileia Melissinaki, Foundation for Research and Technology-Hellas (Greece) and Univ. of Crete (Greece); Ioannis Konidakis, Maria Farsari, Savros Pissadakis, Foundation for Research and Technology-Hellas (Greece)

We report on a Fabry-Perot optical resonator fabricated on the endface of a SMF28 fiber, by employing the direct laser writing technique. We explore this fiber sensing probe for measuring the vapour concentration of common organic solvents. The material used for the fabrication of the microstructure is a zirconium-silicon, photosensitive organic-inorganic hybrid material. The sensing head consists of a "prism" like structure suspended on pillars, attached onto the silica fiber endface. This architecture allows the formation of a small air cavity, between the fiber endface and the microstructure, which acts as a Fabry-Perot resonator, providing interrogation capabilities of the intermediate optical medium. To avoid multiple Fabry-Perot resonance between the two surfaces of the fabricated microstructure, which can complicate the interrogation spectrum, an inclination of about 20° was given across the outer surface of the microstructure. A 20 μm air cavity results a periodic modulation of the reflected optical spectrum by notches of -20dB in amplitude strength and a free spectral range of ~88nm.

We have tested the operation of this sensing probe for different alcohol vapours, succeeding detectivities of the order of 4ppm, resulting sensitivity of 1503 nm/RIU. Also, chlorinated organic solvents of different chlorine valence have been probed (dichloromethane, chloroform and carbon tetrachloride), for investigating selectivity capabilities of this sensing device. Preliminary experiments lead to promising results related to selectivity of different chlorinated vapours. The behavior of the sensing probe presented herein is explained in terms of standard physisorption and molecule packing mechanisms, of organic vapours onto porous surfaces.

9374-13, Session 3

Focused ion beam 3D nano-patterned optical fiber tips for advanced beam profile engineering

Jaime Viegas, Masdar Institute of Science & Technology (United Arab Emirates); Ana R. Ribeiro, Masdar Institute of Science & Technology (United Arab Emirates) and Univ. do Porto (Portugal); Pedro A. S. Jorge, INESC Porto (Portugal); Ricardo Janeiro, Raquel Flores, Masdar Institute of Science & Technology (United Arab Emirates)

Focused ion beam (FIB) patterning of 3D topography on optical fiber tips for application in stand-alone, rugged and simplified setups for optical tweezers manipulators, optical near-field lithography and beam profile engineering are reported. We demonstrate various configurations based on single/multi-step FIB patterning and hybrid approaches based on optical fiber pre- and post-FIB treatment for optical fiber texture, topography and composition engineering. Optimal beam parameters and sample preparation for accurate pattern replication and positioning are presented. Measured experimental field profiles are compared with numerical simulations of fabricated optical fiber tips for fabrication accuracy evaluation. Applications employing these fiber tips are presented.

9374-14, Session 3

Large-scale fabrication of 3D photonic nanostructures

Norbert Schneider, Alexander Kolew, Marc Schneider, Senta Schauer, Radwanul H. Siddique, Karlsruher Institut für Technologie (Germany); Juerg Leuthold, ETH Zürich (Switzerland); Hendrik Hoelscher, Matthias Worgull, Karlsruher Institut für Technologie (Germany)

Sophisticated nanostructures are an integral part of today's state of the art optical components. Here, we present a replication method combining the ability to create hierarchical 3D structures on large scales beyond the current state of the art.

To this day, the fabrication of photonic structures is still limited to basically two-dimensional setups, unlike nature's complex templates as the renowned blue Morpho's "Christmas trees". These structures are the basis for the brilliant blue iridescence and can be replicated in plane [1].

To overcome limitations restricting high throughput fabrication to two dimensions we combined nanoimprint with thermoforming to create 3D structures. Utilizing the unique features of shape memory polymers (SMPs), we are able to downscale the process to sizes feasible for optical elements.

First, we use hot embossing/nanoimprint for the fabrication and preparation of an active SMP-based mould-insert. A second polymer foil is deposited on it and embossed as well. This embossing step is followed by nanothermoforming, where the foil is shaped on the micro- or nano-scale [2].

As a result, we present a process combination to fabricate complex hierarchical surfaces encompassing even arbitrary shapes with structure sizes several orders of magnitude smaller than conventional thermoforming.

[1] Siddique et al., Opt. Exp. 21, 14351 (2013)

[2] Schneider et al., Optical Materials Express, acc. (2014)

**Conference 9374: Advanced Fabrication
 Technologies for Micro/Nano Optics and Photonics VIII**

9374-15, Session 3

**Optochemically organized light filaments:
 From wide-eyed polymer lattices to
 encoded beams**

Kalaichelvi Saravanamuttu, Ian D. Hosein, Hao Lin, Matthew Ponte, Dinesh K. Basker, McMaster Univ. (Canada)

Optochemical organization is a powerful single-step route that employs low-intensity incandescent light to generate complex, optically functional 3-D polymer architectures. In this technique, we exploit the instability of broad light beams in photopolymerizing media and their spontaneous division into large populations ($> 10,000 \text{ cm}^{-3}$) of self-trapped filaments. Each filament is a microscopic thread of light, which inscribes a polymer channel – a multimode waveguide – along its path. By employing multiple, spatially modulated beams, we can corral filaments into a richly diverse collection of lattices with square, near-cubic, simple cubic, BCC and woodpile geometries.

This talk highlights two recently developed applications of our approach to optochemical organization. The first is a multidirectional waveguide lattice – which like an insect's compound eye – possesses a significantly enhanced field of view. Because they are fabricated in flexible, robust photopolymer media, waveguide lattices could serve as intelligent encapsulants of light-harvesting devices or light-shaping conformal coatings on LEDs. More generally, this approach opens pathways to a fundamentally new generation of planar, flexible, thin film optics that can capture, steer, guide, transmit and focus light. The second application exploits the interactions of optochemically organizing filaments to elicit the spontaneous transfer of information between light beams and develop a new technology to encode optical data.

9374-16, Session 4

**Large area fabrication of light trapping
 nanostructures for high efficiency silicon
 solar cells (Invited Paper)**

Debashis Chanda, Univ. of Central Florida (United States)

Mono-crystalline silicon (c-Si) remained number one material of choice for harnessing solar energy due to natural abundance, superior electronic properties and chemical/radiation hardness. Thinner, lighter and high efficiency solar cells are extremely important for all practical applications. In this context trapping sunlight inside thin-film c-Si cells holds the key to generate high energy density from a low cost, light weight solar module. We have shown that the direct laser writing and soft nanoimprint lithography can form a unique combination for large area mask-less nanomanufacturing of light trapping patterns where the master pattern is written once using direct laser writing and then replicated repeatedly following stamping based nanoimprinting process. Other known nanopatterning techniques based on electron/ion beam, deep-UV lithography lacks the throughput and large area scalability needed for commercial c-Si cells which are typically 156 mm x 156 mm area and are produced at over 2000 wafers/hr. In that context a stamping based rapid imprinting offers a true low cost, large area and high throughput approach. The key advantage of the proposed scheme is that any arbitrary periodic as well as aperiodic pattern can be made over large area in order to maximize light absorption which gives enormous design options to optimize and/or customize light trapping scheme for a specific cell geometry without involving any complicated lithographic steps. This will translate to enormous cost and material savings as well as will provide other mechanical attributes like lightweight, flexibility and bendability of the resultant solar modules.

9374-17, Session 4

**Integrating III-V compound
 semiconductors with silicon for advanced
 multijunction solar cells (Invited Paper)**

Gregory N. Nielson, Sandia National Labs. (United States)

Traditional multijunction solar cells are epitaxially grown with series connected junctions directly on top of each other. This architecture imposes important constraints on the multijunction cell such as requiring current-matching between the junctions and lattice-matched materials. We have developed methods that allow the integration of III-V materials with silicon to eliminate both the lattice matching requirement and the current matching requirement. These methods allow wafer-level processing of the cells, wafer reuse, and are targeted toward micro-scale solar cells that have been shown to provide significant advantages over macro-scale cells.

We have fabricated and experimentally demonstrated four terminal InGaP/GaAs/Si cells and a low bandgap InGaAs cell that is bonded to Si using these fabrication techniques. The InGaP/GaAs/Si cell has demonstrated efficiencies up to approximately 23%. The InGaAs cell transferred to Si provided 3% efficiency behind the silicon handle. The fabrication methods for these cells have been designed for cells at the scale of hundreds of microns which allow the exploitation of numerous beneficial scaling effects at the cell, module, and system levels. These cells, and the fabrication techniques used to produce them, provide the building blocks that should allow an optimized cell to achieve over 50% conversion efficiencies by eliminating the current matching and lattice matching constraints traditional multijunction cells face.

9374-18, Session 4

**Thermal to electrical energy converter
 based on black Si**

Ryosuke Komatsu, Takuya Yamamura, Yokohama National Univ. (Japan); Gediminas Seniutinas, Swinburne Univ. of Technology (Australia) and Melbourne Ctr. for Nanofabrication (Australia); Pierrette Michaux, Swinburne Univ. of Technology (Australia); Yoshiaki Nishijima, Yokohama National Univ. (Japan); Basil T. Wong, Swinburne Univ. of Technology (Malaysia); Saulius Juodkazis, Swinburne Univ. of Technology (Australia) and Melbourne Ctr. for Nanofabrication (Australia)

Harvesting of thermal energy and its conversion into electrical will increase efficiency of energy use, reduce greenhouse gas emissions, and power miniaturized sensors and monitoring devices. We made black-Si (b-Si) by plasma etching achieving about 1-2% reflection across the entire 300-1000 nm spectral window due to sub-micrometer height nano-needles formed randomly on the surface. The aspect ratio of needles and the air-Si volume fraction is controlled by plasma etching. We use a commercial Peltier element for thermal-to-electrical power conversion by placing b-Si in a thermal contact (vacuum grease) with p- and n-type contacts of the Peltier element. Under a metal halide lamp illumination which has spectrum close to that of Sun within a 400-1000 nm range, a 62.5% increase in generated voltage (25 to 40 mV) was detected. The output voltage was proportional to the absorbed power and temperature increase. Under 532 nm laser illumination an additional 50% increase was observed when b-Si was infiltrated with 50-nm-diameter Au nanoparticles at optimal density of $1.4 \times 10^{16} \text{ cm}^{-2}$. For reference, output voltage from the Peltier element with Ag film and at different density of Au nanoparticles on b-Si was systematically measured. Largest gains in terms of thermal to electrical conversion were observed for the Au decorated b-Si in the spectral window 600-750 nm where up to 6 times larger voltages were generated.

**Conference 9374: Advanced Fabrication
Technologies for Micro/Nano Optics and Photonics VIII**

9374-19, Session 4

Nanotextured CuO: Sensing and light harvesting platform

Armandas Balcytis, Swinburne Univ. of Technology (Australia) and Ctr. for Physical Sciences and Technology (Lithuania); Gediminas Seniutinas, Swinburne Univ. of Technology (Australia) and Melbourne Ctr. for Nanofabrication (Australia); Jurga Juodkazyte, Biochemijos Institutas (Lithuania); Saulius Juodkazis, Swinburne Univ. of Technology (Australia) and Melbourne Ctr. for Nanofabrication (Australia)

The ever present challenge for the large scale adoption of solar power harvesting is fabricating efficient, low cost solar cells from abundant and environmentally friendly materials. Despite the broad range of materials investigated, presently none of them seems to be able to satisfy all of the aforementioned requirements. The search might have come full circle with one of the first discovered transition metal oxide semiconductors – CuO. It is abundant, simple to fabricate, has a tunable band gap in the optimal range 1.6 -2.3 eV and is nontoxic. The major challenges for the material, however, are the low efficiency of carrier extraction, and photocorrosion of the semiconductor.

Most noteworthy features of chemically nanotextured CuO are its band gap and nano-rough surface structure. In this work we use thin film deposition techniques to modify the surface of CuO, thereby harnessing specific features of the complex surface for distinct applications. We show how noble metal coating of CuO nano-flakes makes the surface plasmonic, and its roughness strongly facilitates the formation of hotspots for highly efficient SERS sensing. On the other hand, we show how the semiconducting nature of p-type CuO can be utilized by creating a p-n junction by physical vapor deposition (PVD) of n-type Si, thereby overcoming the low charge extraction efficiency, which until now has been the major stumbling block CuO application as a solar energy harvesting platform. Additionally, the chemical oxidation method of CuO creation and PVD techniques used for its surface modification make the processes cost-effective and highly scalable.

9374-20, Session 4

Electron beam-induced etching and restructuring of diamond

Cameron J. Zachreson, Aiden A. Martin, Igor Aharonovich, Milos Toth, Matthew R. Phillips, Univ. of Technology, Sydney (Australia)

Electron beams used in scanning electron microscopy can dramatically alter the structural, optical, and electronic properties of diamond. Here, we demonstrate the versatility of electron beam-induced chemical etching in direct-write fabrication of optical devices, show an example of electron beam restructuring of luminescent defects, and discuss the rate-limiting mechanism of etching in ultra nanocrystalline diamond.

To investigate the restructuring of optical defects we used time-resolved cathodoluminescence (CL) spectroscopy to measure the intensities of NVO, A-band, and H3 centers in a sample of polycrystalline diamond as a function of irradiation time. Our results suggest that electron catalyzed, thermally-driven restructuring of extended defects activates luminescent NVs and A-band centers at room temperature, without thermal annealing. We attribute the activation kinetics to electron-induced dehydrogenation of nitrogen-vacancy-hydrogen clusters and dislocations. During CL analysis, etching was observed due to residual H₂O in the sample chamber.

The etching kinetics in nanocrystalline samples indicate that etching proceeds via chemical volatilization at active sites created by beam-induced material restructuring. Etching of single crystal diamond, however, proceeds through a damage-free mechanism, allowing the fabrication of

optical devices. To demonstrate this, we have etched direct-write patterns into inclined surfaces of single crystal microdiamonds. Additionally, we fabricated pillars in bulk single-crystal diamond that enhance the nitrogen vacancy emission.

Taken together, our results demonstrate the potential of electron beam processing for the fabrication of diamond-based devices.

9374-21, Session 5

Nanoimprinted metallic arrays for highly directional light-emitting devices (*Invited Paper*)

Gabriel Lozano, Spanish National Research Council (Spain)

The development of efficient and versatile light sources based on light-emitting diodes (LEDs) is a central goal for solid-state lighting (SSL). The most widely employed route to achieve white light using LEDs consists in combining an electrically driven blue LED and a material, usually known as a phosphor, that absorbs part of the blue light and emits in the green-to-red region of the electromagnetic spectrum. Metallic nanoparticles behaving as optical antennas provide unique ways of controlling light at length scales smaller than the wavelength through the excitation of surface plasmons. Herein, it is demonstrated that large-area nanoimprinted periodic arrays of aluminum antennas strongly shape the directionality of the emission of light-emitting devices. The coupling of a thin layer of a dye-doped polymer acting as a phosphor to lattice modes sustained by the array enhances the spatial coherence of the emitters, allowing the efficient beaming of its emission along specific angular and spectral ranges. In contrast to localized surface plasmon resonances, lattice resonances have a large spatial extension and can couple very efficiently to free space radiation due to their hybrid photonic-plasmonic character. Such features yield highly directional light-emitting devices in which the angular distribution of the emission can be controlled through the shape and dimensions of the metallic nanoparticles and by the lattice geometry. This demonstration opens a new path for fundamental and applied research in SSL in which plasmonic nanostructures are able to mold the emission of illumination devices with unprecedented precision.[1,2]

[1] G. Lozano, D. J. Louwers, S. R. K. Rodríguez et al., *Light: Sci. Appl.* 2, e66 (2013)

[2] G. Lozano, G. Grzela, M. A. Verschuuren et al., *Nanoscale*. 6, 9223 (2014)

9374-22, Session 5

Design and fabrication of 3D meta-optics for beam customization and propagation (*Invited Paper*)

Eric G. Johnson, Aaron J. Pung, Matthew Byrd, Kaitlyn Morgan, Indumathi Raghu Srimathi, Clemson Univ. (United States)

3D meta-optics has become a topic of great interest for engineering electromagnetic field profiles in optical systems. Fabrication of these devices utilizes conventional lithography processes, commonly used in integrated circuit technology. By properly designing the exposure pattern, a variety of devices can be made. The ability to spatially modify a periodic structure enables an incident beam to be customized in terms of its spatial profile and spectral content with a resonant structure. Such devices take the form of resonant mirrors, with applications in locking laser diodes, beam combining, and spectral filtering. Alternatively, diffractive optics may be created by overlaying concentric designs of increasing detail through multiple exposures. Experimentally, the concentric designs are used to impart a specific phase profile on the incident beam. These find use in communication, imaging, and beam propagation. This paper discusses the design and fabrication of resonant and phase optics for applications where spectral and spatial modifications are desired. Both simulation and

**Conference 9374: Advanced Fabrication
 Technologies for Micro/Nano Optics and Photonics VIII**

experimental data are given to demonstrate the versatility of 3D meta-optic technology.

9374-23, Session 5

Rapid Origination of Structural Colorful Images and Data Storage for Security Purposes

Mohamad Rezaei, Simon Fraser University (Canada); Hao Jiang, Reza Qarehbaghi, Mohammad Naghshineh, Bozena Kaminska, Simon Fraser Univ. (Canada)

Metallic nano-structures are often referred to as plasmonic nano-structures, owing to the surface plasmon. Plasmonic nano-structures allow for manipulation of light at the nanoscale and can display intense colors and unique visual effects tunable over the entire visible spectrum. In this paper, we present a technology called 'Nano-Media' that allows rapid production of a multi-channel image display and information storage using nano-structures as pixels. Owing to the ultra-small scale of nanostructures, they can be used as pixels to print color images at ultra-high resolutions, potentially 100,000 DPI. The Nano-Media consists of a pre-fabricated pixelated nanostructures and an intensity control layer (ICL). By engineering the optical properties of the metal nano-structures, they can display visible primary colors and infrared radiation, for light being transmitted, reflected or diffracted due to the extraordinary optical transmission and the nano-grating effects. The ICL is used to tune the brightness of individual RGB sub-pixels and to obtain the desired color in each pixel in the RGB color system. Experimental work demonstrated that Nano-Media can be used for image storage and display, and the multispectral layers of stored information. Full-color, high resolution images were produced using an ICL fabricated with a mask writing technique. We embedded covert information into the visible images and successfully retrieved the information by a reader device. We have also deposited a photo-sensitive layer on top of the nano-structures and successfully embedded information into the Nano-Media by visible light exposure.

9374-24, Session 5

Nanoscale precision in ion milling for THz and optical antennas

Gediminas Seniutinas, Gediminas Gervinskas, Saulius Juodkazis, Swinburne Univ. of Technology (Australia) and Melbourne Ctr. for Nanofabrication (Australia)

Direct nanoscale fabrication and modification of complex 3D structures opens possibilities for implementing new device concepts and sophisticated designs. Conductive materials are preferably used for precise focused ion beam milling as they do not suffer surface charge accumulation effects. However, terahertz and optical antennas are usually made on high resistivity or insulating substrates to prevent electron leakage. This makes modification challenging as surface charging distorts the patterns to be milled. We demonstrate high precision and fidelity ion beam milling of insulating materials using UV light illumination to mitigate surface charging during the process. This approach was used to modify terahertz antennas for enhanced emission and detection. Down to 40 nm tip-to-tip spaced and interdigitated electrodes were milled in the detection area of photoconductive THz antenna. The milled nanostructures help to collect more photogenerated electrons thus enhance the output signal. Furthermore, using ion beam milling the antenna arrays can be fabricated with operational range extending into optical wavelength region and allows light manipulation at the nanoscale. Identical 15 nm width chiral inscriptions were written on 8 μm x 8 μm arrays of 560 nm gold discs fabricated on strongly charging glass substrate. The arrays are used for polarization sensitive "hot-spot" control.

9374-25, Session 6

Template-guided self-assembly strategies for discrete and extended optoplasmonic materials (Invited Paper)

Yan Hong, Wonmi Ahn, Xin Zhao, Björn M. Reinhard, Boston Univ. (United States)

Optoplasmonic materials that contain both metallic (plasmonic) and dielectric building blocks can sustain synergistic interactions between photonic and plasmonic resonances and, thus, pave the way to overcoming the limitations of the respective building blocks. A significant challenge in realizing the full potential of these unique electromagnetic materials is the integration of building blocks with different chemical composition and size into defined morphologies. Template guided self-assembly strategies have shown some promise in realizing intricate discrete and extended optoplasmonic materials. The underlying fabrication methods and selected optoplasmonic materials obtained through them will be discussed in this paper. The first class of materials discussed combines dielectric microspheres as whispering gallery mode resonators with plasmonic antennas at defined locations in close vicinity of (but not attached to) the dielectric microsphere. The interaction of WGMs with plasmonic resonators located in their evanescent field is analyzed. The second example describes two-dimensional interdigitated arrays of 250 nm diameter TiO₂ NPs and clusters of electromagnetically strongly coupled 60 nm gold nanoparticles. It is demonstrated that delocalized photonic-plasmonic modes in the arrays achieve a cascaded E-field enhancement in the gap junctions of the Au NP clusters and that this boost is accompanied by a general increase of the E-field intensity throughout the entire array.

9374-26, Session 6

Parallel fabrication of wafer-scale plasmonic metamaterials for nano-optics

Sahand Eslami, John G. Gibbs, Alberto Castillo, Hyeon-Ho Jeong, Andrew G. Mark, Tung Chun Lee, Max-Planck-Gesellschaft (Germany); Peer Fischer, Max-Planck Institut für Intelligente Systeme (Germany) and Univ. Stuttgart (Germany)

Recently we have shown how glancing angle deposition on nano-seeded (and cooled) substrates enables the growth of 3D hybrid nanostructures with 10nm resolution. More than a hundred billion complex nanoparticles are grown in an hour on entire wafers. This has allowed us to fabricate plasmonic nanohelices with large chiroptical responses, where the precise control over the helix composition and dimension permits the spectral response to be tuned.

We present the details of this advanced fabrication scheme and demonstrate hybrid nanostructures that combine plasmonic as well magnetic properties. Direct evidence is provided by a higher-order chiral-magnetic coupling effect, magneto-chiral dichroism, that is observed in transmission. We discuss how the complex dielectric tensor of a structured sub-wavelength film can be tuned using different materials or by controlling the shape of the nanostructures.

Our technique permits the realization of nanophotonic metamaterials as thin films or as colloidal solutions. The latter is of interest for isotropic metamaterial applications. We show how the circular and linear birefringence of the thin-film structures can be measured and how this can be exploited to engineer the refractive index in the visible.

**Conference 9374: Advanced Fabrication
 Technologies for Micro/Nano Optics and Photonics VIII**

9374-27, Session 6

Scalable and 3D nanofabrication toward optical metamaterials and plasmonic nanostructures

Junsuk Rho, Pohang Univ. of Science and Technology (Korea, Republic of) and Univ. of California, Berkeley (United States) and Lawrence Berkeley National Lab. (United States)

Metamaterials, artificially structured nanomaterials, have enabled unprecedented phenomena such as invisibility cloaking and negative refraction. In this talk, I will discuss our efforts in achieving the unique optical property overcoming diffraction limit, so to demonstrate the extraordinary metamaterials and metadevices. First, I will present super-resolution imaging device called "hyperlens", which is the first experimental demonstration of near- to far-field imaging at visible light with resolution beyond the diffraction limit in two lateral dimensions. Second, I will show another unique application of metamaterials for miniaturizing optical cavity, a key component to make lasers, into the nanoscale for the first time. It shows the cavity array which successfully captured light in 20nm dimension and show very high figure of merit experimentally. Then, I will show the recent achievements of photo-induced switching of reconfigurable negative index metamaterial device and large scale negative index metasurface with anomalous spin-Hall effect. Finally, if time allows, I will show our effort to realize those proof-of-concepts in scientific level into the real engineering applications as developing the scalable fabrication techniques. It will include high-resolution/high-throughput flying head nanolithography and scalable fabrication methods. Scalable fabrication techniques are, but not limited to, large scale 2D metasurfaces, multilayered 3D bulk metamaterials and top-down/bottom-up combined hybrid plasmonic structures. I believe our efforts in sub-wavelength metamaterials and scalable manufacturing methods will lead extreme light control and manipulation with the metamaterials and metadevices, and further advanced nanooptics, nanophotonics and nanomanufacturing.

9374-28, Session 6

Fabrication of two-dimensional aperiodic Vogel spiral photonic lattices by optical induction

Falko Diebel, Patrick Rose, Martin Boguslawski, Cornelia Denz, Westfälische Wilhelms-Univ. Münster (Germany)

Designing the optical properties of materials by tailoring their band structures is an active field of research and has led to groundbreaking developments in various fields of optics [1]. These so-called photonic crystals exhibit characteristic response properties, including complete photonic band gaps, a key requirement for exciting effects and applications, e.g., band gap optical waveguides or lasing structures [2,3].

Recently, the focus of realizing spatial band gap structures turned towards deterministic aperiodic structures showing distinctive band gap properties. Due to the lack of rotational and translation symmetry, these aperiodic structures offer more isotropic band diagrams which makes complete band gaps more easy to achieve. In particular, the golden angle Vogel spiral has attracted much attention since its topology remarkably differs from many other lattices, implying effects like optical angular momentum-bearing discrete diffraction [4]. However, fabrication of these kind of structures is challenging and mostly relies on point-by-point methods which up to now excluded generation with the most prominent method: optical induction of photorefractive index landscapes.

In the past, the complexity of the achievable structures has continuously increased [5], nevertheless these approaches rely on extended nondiffracting beams and thus are not capable to fabricate 2d deterministic aperiodic structures.

In this contribution, we present a new holographic optical induction method based on spatially multiplexed nondiffracting Bessel beams, thereby allowing for the first time longitudinal extended point-by-point techniques implemented in the optical induction of photorefractive index landscapes. This technique allows us to realize a huge class of two-dimensional photonic structures, including deterministic aperiodic golden-angle Vogel spirals as well as Fibonacci lattices.

[1] J. D. Joannopoulos, S. G. Johnson, J. N. Winn, and R. D. Meade, *Photonic Crystals: Molding the Flow of Light*, 2nd ed. (Princeton University Press, 2008).

[2] P. Russell, *Science* 299, 358 (2003).

[3] H.-G. Park, S.-H. Kim, S.-H. Kwon, Y.-G. Ju, J.-K. Yang, J.-H. Baek, S.-B. Kim, and Y.-H. Lee, *Science* 305, 1444 (2004).

[4] L. Dal Negro and S. V. Boriskina, *Laser Photon. Rev.* 6, 178 (2012).

[5] M. Boguslawski, P. Rose, and C. Denz, *Phys. Rev. A* 84, 013832 (2011).

9374-29, Session 7

3D optical printing of piezoelectric nanoparticle-polymer composites (Invited Paper)

Donald J. Sirbuly, Kanguk Kim, Wei Zhu, Shaochen Chen, Univ. of California, San Diego (United States)

The ability to convert compressive/tensile stresses to an electrical charge, or vice versa has long been an intriguing and valuable property of piezoelectrics. As such these materials have found use in a stellar number of applications including imaging technologies, energy harvesting devices, electronics, and nanopositioning systems. Most piezoelectric materials in today's systems are based on brittle ceramic materials which are extremely difficult to scale down in size and shape into higher order 3D structures. To address this researchers have been actively pursuing nanostructured piezoelectrics in the form of nanowires, thin films, and nanoparticle composites. Unfortunately manufacturing high-efficiency piezoelectric materials into well controlled, 3D architectures has been nearly impossible and will require the development of novel fabrication techniques. In this talk I will discuss a solution to this problem by leveraging piezoelectric nanoparticles in a photoliable polymer solution. Upon light exposure the polymer solution is cross-linked and the piezoelectric nanoparticles are grafted to the polymer matrix which is shown to significantly enhance the stress transfer efficiency from the polymer to the piezoelectric nanoparticles. 3D printing is achieved by projecting dynamic optical masks onto the polymer solutions or point scanning a light source. The photopolymerized materials show excellent piezoelectric properties with piezoelectric coefficients that exceed that of pure polymer piezoelectrics. These results demonstrate that flexible, biocompatible piezoelectric materials can be fabricated into any user defined 3D shape which could have a huge impact on technologies such as acoustic imaging, nano/microelectromechanical systems and biodiagnostics.

9374-30, Session 7

Spatial light modulator based holographic fabrication of 3D spatially varying photonic crystal templates

Jeffrey R. Lutkenhaus, David George, Usha Philipose, Hualiang Zhang, Yuankun Lin, Univ. of North Texas (United States)

In this work, we present holographic fabrication of spatially varying photonic crystal templates of gradient index structures in photosensitized polymer using the interference of multiple beams with specified phases generated by an engineered grayscale phase patterns displayed on a phase only spatial light modulator (SLM) in conjunction with a 4f imaging system.

**Conference 9374: Advanced Fabrication
Technologies for Micro/Nano Optics and Photonics VIII**

Simple spatially varying 3D structures are fabricated by the interference of four 1st order beams with desired phases plus a central 0th order beam generated by pixel-by-pixel assignment of the gray levels of cells and supercells within the phase pattern displayed on the SLM. Additionally, a low order simple gradient or vortex phase can be added to a multi-beam-generating phase pattern to also create an angularly varying 3D structure. We also demonstrate 2D and 3D spatially variant photonic crystal templates in photoresist with variation in lattice orientation and spacing using interference of modified beams with specified phases produced by an engineered phase pattern displayed on a SLM. By using the SLM to holographically fabricate spatially varying photonic crystal templates, greater control over the manipulation of light is possible.

9374-31, Session 9

Design and fabrication of sub-wavelength athermal resonant waveguide replicated gratings on different polymer substrates

Muhammad Rizwan Saleem, Univ. of Eastern Finland (Finland) and National Univ. of Sciences and Technology (Pakistan); Seppo Honkanen, Jari Turunen, Univ. of Eastern Finland (Finland)

We demonstrated the design, fabrication and characterization of three Resonant Waveguide Gratings (RWGs) with different polymer substrate materials [polycarbonate (PC), cyclic-olefin-copolymer (COC) and Ormocoms). The RWGs are designed by Fourier Modal Method and fabricated by Electron Beam Lithography, Nanoimprinting and Atomic Layer Deposition. RWGs are investigated for athermal filtering device operation over a wide range of temperatures. Spectral shifts of RWGs are described in terms of thermal expansion and thermo-optic coefficients of the selected substrate and waveguide materials. Furthermore, the spectral shifts are explained on the basis of shrinkage strains, frozen-in stresses and the molecular chain orientation in polymeric materials.

The thermal spectral stability of these filters was compared by theoretical calculations and experimental measurements. For PC gratings, there is a good agreement between calculated and measured results with a net spectral shift of 0.8 nm over 75 °C wide temperature range. Optical spectral characterization of COC and Ormocomp gratings showed larger red spectral shifts than predicted by theoretical calculations. The deviation (0–1.5 nm) for the COC grating may result in by high modulus and inherent stresses which were relaxed during heating and accompanied with the predominance of the thermal expansion coefficient. The Ormocoms gratings were subjected to UV-irradiation, causing the generation of compressive (shrinkage) strains, which were relieved on heating with a net result of expansion of material, demonstrated by thermal spectral shifts towards longer wavelengths (0–2.5 nm). The spectral shifts might also be caused partially by the reorientation and reconfiguration of the polymer chains.

9374-32, Session 9

Mask aligner lithography for TSV-structures using a double-sided (structured) photomask

Tina Weichelt, Lorenz Stuerzebecher, Friedrich-Schiller- Univ. Jena (Germany); Uwe D. Zeitner, Fraunhofer-Institut für Angewandte Optik und Feinmechanik (Germany) and Friedrich-Schiller- Univ. Jena (Germany)

Through-silicon vias (TSV) became an important part for wafer level packaging (WLP) as they provide patterning holes through thick silicon dies to integrate and interconnect devices which are stacked in z-direction. First of all, TSV fabrication needs to be cost-effectively combined with a high throughput to allow an economic processing. Furthermore, a lithography process for TSV has to be stable enough to allow patterning

on pre-structured substrates with inhomogeneous topography. This can be addressed by an exposure process which offers a large depth of focus. We have developed a mask-aligner lithography process based on the use of a double-sided photomask to realize aerial images which meet these constraints.

The mask enables structuring various thin and thick photoresist in proximity distances between 30 µm to 100 µm. With this kind of technology a reliable transfer of non-periodic via-hole arrangements like e.g. 3x3-arrays with 20 µm diameter has been demonstrated.

Compared to a standard binary amplitude photomask with a chromium layer the exposure time has been halved and the photoresist prints are of significant better quality; in particular having steeper sidewalls and being less conic.

The diffractive elements on the backside of the photomask have to be precisely aligned to circular chrome apertures on the frontside. Therefore, a special technology has been developed. It allows an accurate relative alignment of structures on both sides of the mask. Special diffractive elements on the backside are used to transfer alignment marks to the front side by means of UV exposure. As this step is a significant part of the photomask fabrication process it will be discussed in detail in the paper and the presentation. The results for via-hole exposures additionally prove the successful alignment of front- and backside of the photomask.

9374-33, Session 9

Design and fabrication of diffractive optics for orbital angular momentum space division multiplexing

Kaitlyn Morgan, Indumathi Srimathi Raghu, Eric G. Johnson, Clemson Univ. (United States)

This work presents the design and fabrication of diffractive optical elements for use in optical communication systems. The device geometry uses a vortex pattern to impart orbital angular momentum (OAM) onto an incident beam, providing a robust method for transmitting information through free space. Furthermore, multiple beams of the same wavelength can be transmitted the same spatial path. Two refractive elements were designed and fabricated to use log-polar coordinate transformation of an incident OAM beam at 1550 nm for communications systems. Furthermore, diffractive elements were designed based on the phase profile of this refractive element. These transform elements were designed and simulated using MATLAB. Fabrication of the devices uses conventional photolithography on a fused silica substrate. Experimental power measurements are then contrasted against similar measurements for the beam splitting method. Applications of the OAM diffractive elements improve and enable more compact multiplexing and de-multiplexing systems for optical communication.

9374-34, Session 9

Design and fabrication of a resonant mirrors for locking blue laser diodes

Matthew Byrd, Joshua Baghdady, Aaron J. Pung, Eric G. Johnson, Clemson Univ. (United States)

Recently, a great amount of attention has been placed on high power sources for use in underwater communication systems. Blue light is ideal for underwater transmission due to the low absorption coefficient of water at this frequency. The development of Gallium nitride (GaN) blue laser diodes provides an ideal solution to both problems, offering an efficient, high power source capable of strong underwater transmission. However, many issues remain with respect to underwater propagation. The most significant of these involves ambient light saturating the highly sensitive photodetectors used to detect the signal from the GaN diode. Further issues arise from scattering due to impurities in the water, as well as reflections

**Conference 9374: Advanced Fabrication
 Technologies for Micro/Nano Optics and Photonics VIII**

from the air/water boundary. Both issues cause temporal spreading of the input signal.

We demonstrate the simulation and subsequent fabrication of a guided-mode resonance filter (GMRF) that can be used to lock the wavelength of a GaN laser diode. Successful locking of the emission wavelength with respect to fluctuations in the surrounding environment addresses challenges associated with underwater communications. Our experiment uses an optical cavity with a GaN blue laser diode source and an off-axis narrowband GMRF fabricated for 445 nm. Based on spectral drift of the diode emission caused by an increase in input current, experimental measurements were taken with the GMRF installed to verify wavelength locking capability.

9374-35, Session 9

Multilevel micro-structuring of glassy carbon for precision glass molding of diffractive optical elements

Karin Prater, Ecole Polytechnique Fédérale de Lausanne (Switzerland); Julia Dukwen, Fraunhofer-Institut für Produktionstechnologie (Germany); Toralf Scharf, Hans Peter Herzig, Ecole Polytechnique Fédérale de Lausanne (Switzerland); Andreas Hermerschmidt, HOLOEYE Photonics AG (Germany)

Precision compression molding has been used for low and high glass-transition temperature materials. The mold needs to withstand friction, corrosion and chemical reactions with the glass. Glassy Carbon is a good choice as a mold material since its high temperature resistance allows to mold a wide variety of glasses including fused silica.

We discuss process flows to micro-structure GC with 3D shapes. The efficiency of diffractive optical elements is the lowest for binary structures with ca. 40%. For 8 level features with a 3 step photolithography process the efficiency increases theoretical to 95%. It is thus important to widen the possibilities for 3D structuring of the mold material glassy carbon.

We introduce a process based on O₂/SF₆ reactive ion etching and a multistep photolithography. The possibility to use maskless photolithography will also be discussed. The use of titanium as a hard mask allows a reasonable selectivity of 4:1, which has so far been one of the main problems in micro-structuring glassy carbon. We studied the suitability of different hard mask materials like Si and SiO₂ for the O₂/SF₆ reactive ion etching of GC.

The fabricated GC molds were applied to thermal imprinting onto glass and fused silica.

GC molds with thicknesses up to 3 mm were tested for multilevel structuring. We discuss the suitability of the fabricated GC samples as molds for cost efficient mass production with a high quality.

9374-36, Session 10

Finely control groove-depth variations of large-area diffraction gratings

Lixiang Wu, Yanchang Zheng, Keqiang Qiu, Shaojun Fu, Univ. of Science and Technology of China (China)

Ion beam etching (IBE) has been widely applied to fabricate large-area diffraction gratings such as beam sampling gratings (BSG), pulse compression gratings (PCG) and vacuum ultraviolet (VUV) gratings. However, it is still challenging to finely control groove-depth variations of large-area diffraction gratings, and there seem to be a trade-off between the depth control accuracy and the processing efficiency. We introduced a technique for conducting on-the-fly fine adjustment of etch depths with sub-nanometer accuracy during the IBE process. The working efficiency would be slightly lowered due to a newly mounted fine

adjustment component (FAC), but not evidently. The FAC has a dynamic leaf and it is vertically positioned between the substrate platform and the radio frequency (RF) linear source. As the dynamic leaf with two degrees of freedom (i.e., traveling along the vertical axis and swinging about the horizontal axis) sweeps over the grating substrate, dwell times of the leaf shadow projected onto the grating substrate vary. Etch depths decrease with the increase of dwell times. The motion trajectory of the leaf is pre-programmed and calculated on the basis of the raster-scan dwell time algorithm. Simulations were performed to evaluate the depth control accuracy. The simulation predictions show that the accuracy of fine adjustment of etch depths is less than 0.1 nm when the adjustable ratio is around 10%. The preliminary experimental were conducted, and the results and the predictions are in good agreement with each other. With the high accuracy of depth control, this efficient approach is feasible for finely controlling groove-depth variations of large-area diffraction gratings, and will be promisingly applied to more fields as an economical and low-energy solution.

9374-37, Session 10

Electron beam written subwavelength gratings for polarization separation in the infrared

Vayalamkuzhi Pramitha, Lakshmi R., Gayathri M. Sridharan, Shanti Bhattacharya, Indian Institute of Technology Madras (India)

A subwavelength grating is a diffraction grating with physical dimensions less than the wavelength of incident light. The ability of subwavelength structures to create an artificial effective index opens up new perspectives in designing highly efficient diffractive optical elements. These gratings have potential applications as anti reflection filters, wave plates, polarizing beam splitters and so on. The present work reports the design and fabrication of subwavelength grating structures for polarization separation in the infrared. The grating was designed for 1550 nm (period - 936 nm, width - 374 nm, index of ridge, n=1.485, depth- 1815 nm) using simplified modal method. When a subwavelength grating is excited by a linearly polarized plane wave at oblique incidence, discrete modes in the grating get excited as predicted by the modal theory. The simplified modal method ensures a time saving and cost-effective realization of the element with good efficiency. Studies were done to fabricate subwavelength grating structure on poly methyl methacrylate ((PMMA) 950k, A11) spin coated on indium-tin-oxide coated quartz substrates. Raith 150TWO e-beam lithography system was used for fabrication. The e-beam writing parameters and the development time in MIBK: IPA (1:3) solution were optimized to fabricate good quality gratings. The grating fabricated using an optimized exposure parameters with acceleration voltage of 20 kV and 30 μm aperture matches well with the design. Scanning electron microscopy and surface profiler were used for the surface morphology analysis and depth measurement of the fabricated gratings. The fabricated grating exhibited good diffraction efficiency on illumination using a 1550 nm laser beam.

9374-38, Session 11

Fluorescent signal enhancement using vapor-condensed micro-reflectors

Zoltán S. Göröcs, Euan McLeod, Shiv Acharya, Aydogan Ozcan, Univ. of California, Los Angeles (United States)

We introduce a novel method of fluorescent signal enhancement, which uses self-assembled vapor-condensed droplets as micro-reflectors in order to redirect the light emitted by fluorescent microparticles towards the detector plane. This procedure creates a liquid meniscus around the fluorescent particle of interest, which confines the uniformly emitted fluorescent light into a specific solid angle using total internal reflection at the surface of the meniscus. We present the method of fabricating

Conference 9374: Advanced Fabrication Technologies for Micro/Nano Optics and Photonics VIII

these self-assembled micro-reflectors around fluorescent particles, which is based on the condensation of polyethylene glycol around the target particles, also giving us the ability to tune their shape as a function of time, contact angle, and temperature. We also demonstrate experimental proof of ~3-fold enhancement of the emitted signal from 2-10 micron sized fluorescent microspheres and present a theoretical analysis of the formation and the optical properties of these self-assembled micro-reflectors using non-sequential ray-tracing simulations, which agree very well with our experimental results. This practical method can provide an advantageous sample preparation technique for relatively low numerical aperture (NA) fluorescent imaging systems, such as field-portable cellphone based devices, as it can be used to reflect the emitted fluorescent light towards the angular aperture of the low NA optical system and thus increase the signal-to-noise ratio of the acquired fluorescent image.

9374-39, Session 11

A tiny, VIS-NIR snapshot multispectral camera

Bert Geelen, Murali Jayapala, Pilar Gonzalez, Klaas Tack, Andy Lambrechts, IMEC (Belgium)

Spectral imaging can reveal a lot of hidden details about the world around us, but is currently confined to laboratory environments due to the need for complicated, costly and bulky cameras. Imec has developed a unique spectral sensor concept in which the spectral unit is monolithically integrated on top of a standard CMOS image sensor at wafer level, hence enabling the design of compact, low cost and high acquisition speed spectral cameras with a high design flexibility. This flexibility has previously been demonstrated by imec in the form of both high spatial and spectral resolution scanning cameras and video-rate snapshot multispectral cameras in multichannel and single optical channel per-pixel mosaic implementations. These snapshot spectral cameras sense an entire multispectral data cube at one discrete point in time, extending the domain of spectral imaging towards dynamic, video-rate applications. This paper describes the integration of our per-pixel mosaic snapshot spectral sensors inside a tiny, portable and extremely user-friendly camera. Our prototype demonstrator cameras can acquire multispectral image cubes of 272x512 pixels over 16 bands, either in the VIS (470-620nm) or in the VNIR (600-1000nm) at 90 cubes per second for normal machine vision illumination levels. The cameras themselves are extremely compact based on Ximea xiQ cameras, measuring only 26x26x30mm and can be operated from a laptop-based USB3 connection, making them easily deployable in very diverse environments.

9374-40, Session 11

Process optimization for a 3D optical coupler and waveguide fabrication on a single substrate using buffercoat material

Chris Summitt, Sunghin Wang, Tao Ge, Jilin Yang, Lee Johnson, Melissa Zaveron, Tom Milster, Yuzuru Takashima, College of Optical Sciences, The Univ. of Arizona (United States)

Silicon photonics devices can be used to achieve increased data transfer rates within microchip systems. By using optical interconnects, optical data transmission technology currently used for long haul applications can be implemented in local computer peripherals. Integration of this technology has not yet been perfected due to a number of key difficulties, among them, the coupling of the light across multiple planes. An optical via would allow light coupling across multiple physical layers. By using an in-plane light coupler, the direction of incoming light can be bent by 90 degrees into a parallel plane. In order to introduce optical components such as these into a microchip system, the fabrication process must be CMOS compatible. Recently, we have proposed a solution which uses a buffercoat material to

create a 45 degree mirror based optical coupler. Also, we reported a hybrid lithography approach by which two kinds of micro optical structures, a well-defined waveguide structure and free-form structure including 45 degree mirror, can be simultaneously fabricated by combining mask-less gray scale lithography with conventional mask-based lithography. In this paper, major improvements on the hybrid lithography process are reported. Especially, sample preparations for mirror and waveguides, alignment process by using conventional metallic structure as well as newly developed phase-based alignment mark, fine tuning of the mirror surface angle by double exposure methods are described in detail.

9374-41, Session 11

Low-stress silicon nitride for mid-infrared microphotonics

Pao T. Lin, Massachusetts Institute of Technology (United States); Hao-Yu G. Lin, Harvard Univ. (United States); Tom Tiwald, J.A. Woollam Co., Inc. (United States); Dawn T. H. Tan, Singapore Univ. of Technology & Design (Sierra Leone); Lionel Kimerling, Anu Agarwal, Massachusetts Institute of Technology (United States)

We experimentally demonstrate a sophisticated mid-IR microphotonics platform adopting engineered Si-rich and low-stress silicon nitride (SiN_x) thin films where an extensive infrared transparency up to $\lambda = 8.5 \mu\text{m}$ is achieved. Furthermore, because of the designed low-stress property, the SiN_x deposition is able to reach a thickness $> 2 \mu\text{m}$ that significantly reduces mid-IR waveguide loss to less than 0.2 dB/cm. We show directional couplers functioning over a broad infrared spectrum, thus enabling monolithic mid-IR multiplexing schemes for integrated linear and nonlinear photonics leading to sophisticated label-free sensing technologies.

9374-42, Session PWed

Investigation of all-optical laser-based direct-write techniques

Ugis Gertners, Univ. of Latvia (Latvia); Janis Teteris, Institute of Solid State Physics (Latvia)

The demand of lower cost surface-relief based optical instruments such as grating-based resonators or filters for waveguides, diffractometers, spectrometers, etc. is one of the main driving forces for the investigation of direct light-induced relief formation. The most common techniques for fabricating and investigating these surface-relief gratings involve an interferometric or holographic recording setup.

We have investigated that the light-induced mass transfer process strongly depends on the material itself and polarization of the light. The behavior of mass transfer and thus the resulting recording could be related to interaction between the polar photo-induced defects and the polarized electric field of recording beam. It has been shown that the mass transfer can be directed both ways – towards or away from the electric field intensity gradient. The evolution of surface relief in dependence from the recording time and polarization has been investigated in detail. The mechanism of the direct recording of surface relief on amorphous organic and inorganic films based on the photo-induced plasticity has been discussed.

A direct recording technique is a comparatively new solution for lithography and, as shown in this report, provides new experimental techniques for better understanding of the interaction between the light and matter. The obtained gratings are very stable at room temperature, so this method can replace some of the chemical etching techniques and find a practical application in the applied physics.

**Conference 9374: Advanced Fabrication
 Technologies for Micro/Nano Optics and Photonics VIII**

9374-43, Session PWed

Fabrication of sine-top broadband gold-coated gratings

Bilali Muhutijiang, Keqiang Qiu, Xiangdong Xu, Shaojun Fu, Univ. of Science and Technology of China (China)

Large aperture broadband gold-coated grating (BGCG) is the key component in the large pulse compression systems. BGCG is simpler in structure and lower cost compared with other pulse compression gratings. Furthermore, high diffraction efficiency can be got within a broadband range (usually 200 nm or more) by using this kind of grating. Because of the advantages the BGCG has attracted wide attention in the fields of the short-pulse (shorter than 100fs) and high-power pulse compression systems. In this paper, a new method for fabrication of sine-top BGCG is proposed. The grating fabrication process: Firstly, spin-coating photoresist onto a fused silica substrate. Secondly, patterning sinusoidal photoresist grating by holographic lithography. Thirdly, form the desired fused silica grating structure by reactive-ion beam etching. Finally, the sine-top BGCG can be got after coating the surface of the grating with gold deposition. When gratings are intended for use with high-power lasers, their laser-damage threshold has an importance equal to that of the diffraction efficiency. In pulse compression, the damage threshold limits the amount of energy that can be tolerated in the pulse for a given grating area. These gratings fabricated by this method differ from conventional metal-on-photoresist pulse compression gratings in that the gratings patterns are generated by etching the fused silica substrate directly. This can improve the laser damage threshold. The groove depth and duty cycle of the photoresist mask were controlled by changing photoresist thickness and adjusting exposure and development time. The duty cycle of the fused silica grating was further corrected by oxygen plasma etching. Using this method, broadband, high efficiency sine-top BGCG with line densities of 1740 lines /mm, duty cycle of 0.5 and groove depth of 210 nm was fabricated successfully.

9374-44, Session PWed

A novel fabrication process of digital encoding grating ruler for optical displacement sensors

Yu Wang, Zhengkun Liu, Huoyao Chen, Yilin Hong, Shaojun Fu, Univ. of Science and Technology of China (China)

Due to its immunity to electromagnetic interference, optical displacement sensors have become an essential component in the aircraft control system. Among those optical sensors, digital wavelength encoding optical absolute displacement sensor is quite promising. And the core element of the sensor is a digital encoding grating ruler (DEGR), which is practically a substrate on which several blazed grating units with different line densities are parallel arranged in certain orders. And this paper introduces a novel fabrication process of the DEGR. In this process, the pattern of DEGR is firstly fabricated on a (111) silicon wafer by combining UV lithography and holography lithography with wet etch technique and then replicated to a hard substrate using polyurethane acrylate (PUA), which is UV curable. Using this process, one DEGR contains 11 kinds of blazed grating units with the linear densities ranging from 1000-1800l/mm has been successfully fabricated. Unit size is 200µm while the length of the whole DEGR is 100 mm. Experimental results show this process is highly repeatable. The replicated DEGR with PUA can works in the temperatures range from -55° to 70°, and its diffraction efficiency is higher than 90% of the master one. The fabrication precision meets the requirements of the optical sensor, and the signal response accuracy is nearly 100%. Moreover, this process could also be used to fabricate other micro-nano structures with high precision, complex graph and poor working environment.

9374-45, Session PWed

Monte Carlo simulations applying rigorous coupled-wave analysis for tolerance analysis of diffractive optical elements

Toru Inomata, Kayoko Fujimura, Masato Okano, Kazuya Yamamoto, Takeshi Yamamoto, Hitoshi Kimura, Tomohiro Kanakugi, Seiichiro Kitagawa, Nalux Co., Ltd. (Japan)

The rigorous coupled-wave analysis (RCWA) has been used for determining the periodic grating structures of diffractive optical elements (DOE) such as rectangular surface-relief gratings. While we observed the cross-sectional image of a manufactured rectangular grating by the scanning transmission electron spectroscopy (STEM), we found that the rectangular part was deformed to trapezoid shape with the corner radius. Therefore, we assumed that we could derive more accurate diffraction efficiencies by RCWA using parameterized values of the trapezoid with the height, inclination angles and the corner radius as well as the grating pitch. However, each parameter has a distribution with variation resulting the variations in diffraction efficiencies. In order to predict quantitatively that the diffraction efficiencies are in the allowable ranges, the tolerance analysis in the design stage is effective. Therefore, we have developed a Monte Carlo simulation program by applying RCWA which can deal with distributions of these trapezoid parameters. The program can also deal with the distributions of the thickness and refractive indices of thin films vaporized on the grating part. The distributions of the trapezoid parameters were obtained by multiple measurements of the base gratings without thin films by atomic force microscopy and by STEM. The distribution of the thickness and refractive indices of the thin films were obtained from analyzed data measured in the vacuum deposition equipment. According to our measurements of the diffraction efficiencies of the manufactured gratings, the diffraction efficiencies have been in the allowable range, and have also been consistent with the results of the tolerance analysis.

9374-46, Session PWed

Simple volume expanding fabrication method for focal length controlled micro-lens array

Junoh Kim, Muyung Lee, Cheoljoong Kim, Jinsu Lee, Yonghyub Won, KAIST (Korea, Republic of)

This study describes easy fabrication method for micro-lens array which has desired focal length in such a way that without the use of reflow technique. The process includes conventional lithographic process only which can be compatible with general semiconductor process. As constituent material, Negative photo-resist SU-8 with its developer PGMEA is used. Two main phenomena during lithography process are adjusted to expand the volume of the PR. During UV exposure, hardening proceeds from the top of the PR. Just after first exposure, using this property, very thin membrane on the top of the surface of the PR can be formed by short time exposure. In the development process, unexposed area of the PR is removed by chemical reaction with developer which causes the volume expansion if the unexposed area is covered with thin cured film. This method is to form the lens as the molecules in the volume are not easily escaped from the covered region. The thickness of the thin film depends on the exposure dose of 2mJ/cm² which determines the degree of expansion. The symmetrical volume expansion creates the membrane of lens shape and the focal length is directly related with second exposure dose. An extended research of affecting the change of the focal length of lens using volume expansion method by changing any other elements is discussed. This process can achieve a focal length selective for the applications of micro-optics.

**Conference 9374: Advanced Fabrication
Technologies for Micro/Nano Optics and Photonics VIII**

9374-47, Session PWed

Fabrication of bilayer metal wire-grid polarizer

Quan Liu, Qiufeng Jin, Jianhong Wu, Soochow Univ. (China)

In this paper, a bilayer metal nanowire-grid is designed by finite difference time domain method. Herein, considering the high reflection of metal aluminum in the manufacturing process, we propose using the copper as anti-reflection coating. Numerical results show that: the reflection on the substrate is suppressed with the optimal thickness of the Cu layer. Considering the resist-substrate reflectivity and the final performance of the nanowire-grid, the structure with an 120nm Al layer, and a 50nm anti-reflection Cu layer is chosen; and the TM transmission efficiency is more than 70%, and the extinction ratio is more than 25dB with the wavelength from 1500nm to 3000nm. A bilayer metal nanowire-grid with the period of 300nm has been fabricated by the holographic ion beam etching. Experimental measurements show that the TM transmission efficiency is more than 70% and the maximum extinction ratio can reach 30dB.

9374-48, Session PWed

Production of waveguides on borate glass doped with transition metals by femtosecond laser pulses

Juliana M. Almeida, Univ. de São Paulo (Brazil); Paulo Henrique D. Ferreira, Univ. Federal de Sao Carlos (Brazil); Ruben D. F. Rodriguez, Leonardo De Boni, Antonio C. Hernandez, Cleber R. Mendonca, Univ. de São Paulo (Brazil)

Femtosecond micromachining allows the fabrication of waveguides inside the volume of a material without damaging its surface. Due to its features, fs-laser micromachining has been used in a broad variety of materials to fabricate waveguide-based photonic devices. Among several interesting candidates for such application, glasses have received special attention due to their high third order optical nonlinearities and ultrafast response times, as well as the easiness to tailor their properties by compositional changes. In this work, we produced waveguides using extended-cavity femtosecond laser irradiation (50-fs, 800-nm and 5.1 MHz) in a new transparent glassy matrix (Eg = 3.92 eV) doped with transition metals, in order to introduce electronic transitions in visible spectrum, since nonlinear optical properties are enhancement when the excitation energy approaches an electronic transition. The glassy matrix, containing mainly boron, zinc and lead oxides, was doped with 0.1% mol of CdCl₂, Fe₂O₃, MnO and CoO, which produced samples with broad absorption bands in different spectral regions. The beam was focused under the sample surface through microscope objectives. We demonstrated the waveguides functionality by measuring the near-field intensity distribution at the waveguide output and their efficiency. Their influence on the nonlinear index of refraction (n₂) was also evaluated through z-scan from 550 up to 1500 nm. Similar results were found for both doped and undoped samples (average value of n₂ = 4.5x10⁻²⁰ m²/W), indicating that the dominant transitions contributing to the nonlinear process are located in the UV region of the spectrum and, therefore, associated to the glass matrix.

9374-49, Session PWed

High-efficiency encapsulated transmission gratings for chirped pulse amplification

Stephan Ratzsch, Ernst-Bernhard Kley, Friedrich-Schiller- Univ. Jena (Germany); Andreas Tünnermann, Fraunhofer-Institut für Angewandte Optik und Feinmechanik

(Germany); Adriana Szeghalmi, Friedrich-Schiller-Univ. Jena (Germany)

Diffraction optical elements are essential optics in high power laser systems due to their higher laser-induced damage threshold compared to metallic optics. In a chirped pulse amplification (CPA) system of a high power laser, diffraction gratings in transmittance or reflectance are used for pulse manipulation in the Littrow configuration. The final laser power scales with the fourth power of the efficiency of the diffraction grating. Additionally, highly dispersive gratings are preferred for compact compressor layouts. Thus gratings with a small period are required. However, due to the Littrow mount the maximum transmission efficiency of standard fused silica gratings reduces with decreasing period because of increasing incident angle and the correspondingly increasing reflections at the air-grating interface. Encapsulating such gratings will result in up to 100% diffraction efficiency in the -1st diffraction. The Fresnel reflections can be completely suppressed in such systems by additional anti-reflective coatings.

In this study, we present a novel fabrication process for encapsulated dielectric gratings based on atomic layer deposition without mechanical bonding. We demonstrate the feasibility of the process based on the design and characterization of encapsulated transmission gratings with an efficiency of 97.5 % in the -1st diffraction order for TM polarized light. The experimentally measured efficiency is in excellent agreement with the theoretical value obtained by rigorous wave coupled analysis. The efficiency can be further improved by optimizing the grating parameters such as height and fill factor. Furthermore, the encapsulation ensures mechanical stability and protection of the fragile gratings against environmental damage.

9374-50, Session PWed

High contrast and metal-less alignment process for all polymer optical interconnect devices

Tao Ge, Jilin Yang, Chris Summitt, The Univ. of Arizona (United States); Sunglin Wang, Lee Johnson, Melissa Zaveron, Tom Milster, Yuzuru Takashima, College of Optical Sciences, The Univ. of Arizona (United States)

A polymer-based flat, flexible and parallel optical interconnect has become an attractive approach for short-range data transfer. For such a device, a low cost fabrication technique is required for light couplers to redirect light from source to waveguides. Recently, we demonstrated a mask-less gray scale lithography process, which used a CMOS compatible polymer for a 45-degree mirror coupler. Polymer materials such as polyimide and SU-8 photoresist can be used to fabricate flexible substrates and waveguides, respectively. We propose an all-photopolymer lithography process to fabricate the flexible and parallel optical interconnect in conjunction with the mirror couplers. In the process, a buried polymer structure is used to precisely align the mirror coupler to waveguides, which make it possible to avoid an additional metallization process. However, the contrast of such buried fiducial mark is low since the structure is a phase structure. As a result, it is not feasible in general to use the buried polymer structure as an alignment mark with conventional amplitude based imaging modalities. To increase the contrast of the buried alignment marks, we propose a feature specific alignment system for which the shape and depth of the buried alignment marks are optimized for phase-based imaging, such as phase contrast and Schlieren imaging. Our results show that an optimized alignment mark provides a significant contrast enhancement while using a phase contrast imaging system compared to that of a conventional imaging system. In addition, we have fabricated an optimized alignment mark specifically for use with a Schlieren imaging system.

**Conference 9374: Advanced Fabrication
 Technologies for Micro/Nano Optics and Photonics VIII**

9374-51, Session PWed

Engineering of the extraordinary optical transmission of metallic gratings via Er³⁺-doped tellurite glass

Otávio de Brito Silva, Victor A. G. Rivera, Euclides Marega Jr., Univ. de São Paulo (Brazil)

We present a systematic analysis both theoretical and experimental of the optical properties of slit arrays in gold films that can be integrated on wide number of devices, especially in optical communications. Although the properties of extraordinary optical transmission (EOT) due surface plasmon polaritons (SPP), which are coupled in such nanostructures have been widely studied in the last two decades, their influence on the absorption and transmission spectra from their dielectric substrates has not been deserved the same attention. The choice of a good substrate for implementation not just for metallic gratings, but also for other devices, it is extremely important in order to achieve great applications of the EOT. A good candidate to replace the conventional semiconductor based substrates it is the rare-earth ions (REI) doped glass, which it is applicable in light wave technologies, like optical waveguides and fiber optics due the signal amplification in these devices. The specific case of Erbium ions and its implementation into glasses for the fabrication of fiber optics, as Erbium doped fiber amplifiers (EDFA) for instance, had shown an incredible success in order to replace optoelectronic devices. With this motivation, we performed exhaustive experimental and theoretical investigations of geometrical and dispersive properties of metallic slit arrays built on the Er³⁺-doped tellurite glass in the visible region, which reveals the resonance features of these plasmonic arrays, including the role of surface waves and their relationship with features in the transmission spectrum of the white light and this specific REI. The observed transmission (EOT from the Er³⁺ ion via slits arrays) is elucidated considering the following effects: (i) white light absorption by the Er³⁺ ions, (ii) coupling between the light and the nanostructure via the creation of surface plasmon polariton where the wavelengths with minimum transmission corresponds to the $4l/15/2 \approx [2H9/2, 4F3/2, 4F5/2, 4F7/2, 2H11/2, 4S3/2, 4F9/2]$ absorption levels the Er³⁺, which propagates through the nanoholes, and, finally, (iii) the Er³⁺ transmission intensity and the spectral shape -symmetry depend on the nature of metallic film and the number of nanoholes constituting the arrays, for which the resonant properties are strongly affected. Furthermore, in order to compare the influence of substrate in the transmission properties, we also performed the same measurements and computational simulations on slit arrays fabricated on the BK 7 glass.

times increase in cut depth and an eight times improvement in surface roughness over previously reported silica slot micromilling. We will present our latest machining results with studies into sequential slot milling and report on the subsequent slot form, surface roughness, and mill wear from prolonged sequential machining. We will also show results of integrating milled slots with optical waveguides and Bragg gratings to create refractometer devices.

9374-53, Session PWed

Quantification of microscopic surface features of single point diamond turned optics with subsequent chemical polishing

Nelson Cardenas, Matthew Kyrish, Daniel Taylor, Margaret Fraelich, Oscar Lechuga, Richard Claytor, Nelson Claytor, Fresnel Technologies Inc. (United States)

Phosphoric/nitric acid baths are routinely used for chemical polishing of aluminum optics, mirrors and molds. The acid bath functions by leveling the microscopic peaks and valleys of the substrate, thereby increasing specularly and reducing light scattering. The rate of attack of the acid is dependent of the physical characteristics (height, depth, and width) of the microscopic structures that constitute the surface finish. To prepare the sample, mechanical polishing such as buffing or grinding is typically required before acid etching. This type of mechanical polishing produces random microscopic structures at varying depths and widths, thus the chemical polishing parameters are determined in an ad hoc basis. Alternatively, single point diamond turning offers excellent repeatability and highly specific control of substrate polishing parameters. While polishing, the diamond tool leaves behind an associated tool mark, which is related to the diamond tool geometry and machining parameters. Machine parameters such as tool cutting depth, speed and step over can be changed in situ, thus providing control of the spatial frequency of the microscopic structures characteristic of the surface topography of the substrate. By combining single point diamond turning with subsequent chemical etching, ultra smooth polishing of both rotationally symmetric and free-form mirrors and molds is possible. Additionally, machining parameters can be set to optimize post polishing for increased surface quality and reduced processing times. In this work, we present a study of substrate surface finish based on diamond turning tool mark spatial frequency with subsequent chemical etching.

9374-52, Session PWed

Micromilling with nanoscale roughness for silica photonics

Lewis G. Carpenter, Peter A. Cooper, Christopher Holmes, Corin B. E. Gawith, James C. Gates, Peter G. R. Smith, Univ. of Southampton (United Kingdom)

We present Flame Hydrolysis Deposition (FHD) silica micromilled with nanoscale surface roughness, sub-micron form control and micron scale depths of cut for photonic applications. Using our in-house developed high-precision micromill and industrially standard micromill tools, we have machined slots 1.5 mm long and 17 μm deep, enabling access and interaction with the evanescent field of nearby UV-written waveguides. Potential applications vary from: biological sensing, plasmonic devices, refractometers and chemical sensing. The micromilling approach offers advantages over conventional cleanroom and laser-based machining of optical materials in both form control and achievable surface roughness. To assess optimum cutting conditions a wide parameter test was conducted, where the rotational and translational speeds were varied and feed speeds optimized to allow cutting in the high-quality low-chipping ductile regime. Whilst milling in the ductile regime our smoothest form slots had a surface roughness of 3.0 nm (Sa) at a 17.0 μm depth of cut. This represents a forty

Conference 9375: MOEMS and Miniaturized Systems XIV

Monday - Thursday 9 -12 February 2015

Part of Proceedings of SPIE Vol. 9375 MOEMS and Miniaturized Systems XIV

9375-1, Session 1

Maskless fabrication of micro-optical elements for functional endomicroscopic fiber tips

Jae-Beom Kim, Ki-Hun Jeong, KAIST (Korea, Republic of)

We present a simple and low-cost technique for the rapid fabrication of micro-optical elements at the end of an optical fiber using maskless lithography. The maskless lithography platform is developed using a Digital Micromirror Device (DMD) to create dynamic photomask patterns as a spatial light modulator, low cost illumination part with UV LED, and an optical microscopic imaging system with objective lens. The DMD based maskless lithography platform allows fabrication of arbitrary micro patterns on a photoresist layer coated at the end of an optical fiber. A commercial SU-8 negative photoresist (PR) is used as a photopolymer for microfabrication. The photopolymer is deposited on the tip of optical fiber by dip coating to fabricate micro-optical elements. However on the small diameter optical fiber tip, surface tension can dominate to create curved and non-planar coatings. This work presents novel concept for PR planarization on the cleaved facet of an optical fiber using a commercially available optical fiber splicing machine. The photoresist micro-optical element was exactly formed on the cleaved facet of an optical fiber by exposing a reflected UV light from DMD and conventional development, rinse processes. The optical characterizations of resulting micro structures were analyzed experimentally and theoretically.

The proposed microfabrication process can be extended to fabricate diffractive and refractive optical elements for medical endoscopy or fiber-based sensing applications with rapid and inexpensive manners.

9375-2, Session 1

Monolithic microfabrication of micropism arrays for 3D stereoscopic endoscope

Sung-Pyo Yang, Jae-Jun Kim, Kyung-Won Jang, Ki-Hun Jeong, KAIST (Korea, Republic of)

Three dimensional (3D) endoscopes can provide depth information of the real physical world to the surgeons during the surgeries and help them to perceive and understand the patient's anatomy more accurately compared to the traditional two dimensional endoscope. However, conventional 3D endoscope techniques to acquire stereo image pairs with two image sensors or other bulky optical components has limitations on miniaturization of endoscopic systems and high cost. We report a monolithically microfabricated micropism arrays for 3D stereo endoscopic imaging with simple method using two-step lithography and geometric guided resist reflow in a wafer scale, and demonstrate the formation of stereo image pair with single image sensor chip by the fabricated micropism arrays. Microfabrication of micropism arrays utilizes thermoset photoresist SU-8, thermoplastic photoresist AZ9260, and thermal reflow of thermoplastic photoresist to form 3D inclined microstructures. After making micropism array structures above the silicon substrate through microfabrication, microstructures were transferred onto the glass substrate with soft lithography using PDMS mold and UV curable resin. Transferred micropism arrays with UV curable resin were placed in front of optimized lens set to form stereo image pair for 3D stereoscopic imaging. The fabricated micropism arrays has advantages over other techniques, such as capability of shooting image pairs simultaneously, favorable size for compact packaging of endoscopic system, and also easy to control the binocular disparity through changing micropism apex angle.

9375-3, Session 2

An update on scanning micro mirror performance and its extended application range (*Invited Paper*)

Jan Grahmann, Fraunhofer-Institut für Photonische Mikrosysteme (Germany)

Scanning micro mirrors as MEMS respectively MOEMS devices are around for about two decades now. This paper gives a short historical summary on MEMS scanning mirrors their addressed applications and performance. It describes key features but also disadvantages of MEMS-Scanner technology compared to established Scanner technologies and shows in combination with recent results at IPMS how mature the technology has been evolved to extend the application area. A scanner with 38 kHz and low dynamic deformation suitable for laser projection is presented. Progress on integrated position detection technology will be shown, a strongly required feature for many applications where very exact trajectory precision is desired. Coating concepts allow to serve high laser power applications and very precise reproducible integrated diffraction gratings make mirrors suitable for high performance spectroscopy. Large mirror diameters allow a high etendue and quasistatic operation of electrostatic mirrors is enabled through functionalized wafer bonding techniques.

9375-4, Session 2

Hybrid assembly of micro scanner arrays with large aperture and their system integration

Thilo Sandner, Michael Wildenhain, Markus Schwarzenberg, Fraunhofer-Institut für Photonische Mikrosysteme (Germany)

Laser scanners are widely used for Time of Flight (ToF) 3D-distance measurements systems. In comparison to ToF-3D cameras laser scanners have an advantage of higher measurement accuracy due to scanning principle, because only single measuring points are illuminated sequentially within the scanned FOV. Hence, the LIDAR detector collects light of signal- & background (noise) in short time only from a small measured area of the target reducing significantly the influence of background (noise). Also a nearly unlimited number of voxels can be measured with high measuring rates of up to 1 Mio voxel/s and low measurement uncertainty of typically 2...10 mm. One the other hand, traditional laser scanners for 3D distance measurement involve expensive, heavy and large rotating or vibrating mirrors for light deflection of the scanning TOF (time of flight) distance measurement. Typically, the precision of ToF distance measurements is limited by the amount of signal light available at the detector. Hence, a scanning mirror with large aperture is required for LIDAR systems to collect small amounts of light reflected or scattered by the measured target. Its replacement by a micromechanical scanning mirror is not straightforward, since a large mirror aperture of the receiver optics must be guaranteed in addition to sufficiently large optical scan angles (> 40°) and high scan frequency of more than 100Hz. Contrary, the aperture of a single MEMS scanning mirror is limited to small values of typically 1...4mm diameter due to the dynamic mirror deformation. To overcome the mentioned problems, Fraunhofer has developed a new concept for a MEMS-based LIDAR which is based on an array of identical synchronized driven MEMS mirror elements.

9375-5, Session 2

MEMS scanner mirror based system for retina scanning and in eye projection

Franziska Woittennek, Jens Knobbe, Tino Pügner, Hans-Georg Dallmann, Uwe Schelinski, Heinrich Grüger, Fraunhofer-Institut für Photonische Mikrosysteme (Germany)

Many applications could benefit from miniaturized systems to scan the blood vessels behind the retina in the human eye, so called „retina scanning“. This reaches from access control to sophisticated security applications and medical devices. High volume systems for consumer applications need low cost and simple operation. For example this means no need for removal of glasses and self-adjustment, in turn guidance of focus and point of attraction by simultaneous projection for the user.

A new system has been designed based on the well-known resonantly driven 2D scanner mirror of Fraunhofer IPMS. A combined NIR and VIS laser system illuminated the eye through an optic designed for an operating distance allowing the use of glasses and granting sufficient field of view. This was considered to be more important than higher miniaturization. The VIS laser is modulated for image generation. The backscattered light from the NIR laser is detected by a high sensitivity photo diode. The absorption of the NIR radiation in the hemoglobin generates an image of the blood vessel in the eye.

A demonstration unit has been realized including readout and drive electronics. The laser power was adjusted to a proven eye-secure level. Additional security features were integrated. Test measurement revealed promising results. In a first demo application the detection of biometric pattern of the blood vessels were evaluated for authentication issues.

9375-6, Session 2

Rotational MEMS mirror with latching arm for silicon photonics

Jonathan Briere, Philippe-Olivier Beaulieu, Menouer Saidani, Frederic Nabki, Michael Menard, Univ. du Québec à Montréal (Canada)

This paper presents an innovative rotational MEMS mirror that can control or scan the direction of propagation of light beams inside of planar waveguides implemented in silicon photonics. Potential applications include but are not limited to optical telecommunications, medical imaging and spectrometry.

The mirror has a half-cylinder shape with a 300 μm radius that provides low and constant optical losses over the full angular displacement range. Its reflective surface can be shaped to focus the light signal. A circular comb drive structure is anchored such that it allows free or latched rotation experimentally demonstrated over 8.5° (X-Y planar rotational movement) using 290V electrostatic actuation. The entire MEMS structure was implemented using the MEMSCAP SOIMUMPs process. The anchor is a 3.0 μm x 70 μm flexible beam that directly connects the MEMS mirror to the substrate. The middle of the beam is designed to be the rotation point of the circular comb drive to counter the rotation offset of the mirror displacement. A complete mechanical characterization of the MEMS mirror will be presented in the full paper.

The latching mechanism provides up to 20 different angular locking positions allowing the mirror to counter any resonance or vibration effects and it is actuated with an electrostatic linear comb drive. An innovative gap closing structure was designed to reduce optical propagation losses due to beam divergence in the interstitial space between the mirror and the planar waveguide. The gap closing structure is also electrostatically actuated and includes two side stoppers to prevent stiction.

9375-37, Session 2

A MEMS based electrically pumped tunable VCSEL operating at 1060 nm for SS-OCT

Keiji Isamoto, Santec Corp. (Japan); Kiyotaka Yamashita, Santec Corp. (Japan) and Tokyo Institute of Technology (Japan) and The Univ. of Tokyo (Japan); Mohammed Saad Khan, Santec Corp. (Japan); Nicolas Lafitte, The Univ. of Tokyo (Japan); Kouki Totsuka, Changho Chong, Santec Corp. (Japan); Nobuhiko Nishiyama, Tokyo Institute of Technology (Japan); Hiroshi Toshiyoshi, The Univ. of Tokyo (Japan)

We report a MEMS (microelectromechanical systems) based tunable VCSEL operating at 1060-nm wavelength range for the SS-OCT (Swept Source Optical Coherence Tomography) application. An electrically pumped VCSEL is used for its superior reliability and simple optical configuration as a light source. The developed tunable VCSEL is composed of an SOI-MEMS based diaphragm mirror with a high reflective coating and is mounted by the thermo-compression bonding of gold onto a half-VCSEL chip with an InGaAs multi-quantum well gain medium and with a bottom DBR. The resonant frequency of MEMS mirror is designed around 100 kHz for operation voltage of 200 V maximum. Wavelength tuning range of the tunable VCSEL is 42 nm, and the maximum optical output power is 2 mW. Coherence length in the OCT application is more than 100 mm thanks to the single mode lasing of the VCSEL of short cavity. Both the forward (from shorter wavelength to longer) and backward (longer to shorter) scans are available at high stability, thereby doubling the wavelength scan frequency to 200 kHz maximum. Wavelength tuning is also performed at different frequencies such as 3 kHz, 50 kHz and 200 kHz to realize SS-OCT measurement of different depth ranges with a single light source. Image from deep inside the skin clearly is observed without typical artifact associated to the long external cavity. OCT images obtained by the newly developed instrument will be reported at the conference.

9375-7, Session 3

Centimeter-scale MEMS scanning mirrors for high power laser application (*Invited Paper*)

Ulrich Hofmann, Frank Senger, Fraunhofer-Institut für Siliziumtechnologie (Germany); Peter Gawlitza, Patrick Herwig, Fraunhofer IWS Dresden (Germany); Thomas von Wantoch, Fraunhofer-Institut für Siliziumtechnologie (Germany); Christoph Grune, Moises A. Ortega Delgado, Fraunhofer IWS Dresden (Germany); Joachim Janes, Christian Mallas, Wolfgang Benecke, Fraunhofer-Institut für Siliziumtechnologie (Germany)

There has been very limited effort but also very little potential so far to apply MEMS mirror technology in high power laser applications like laser cutting, laser welding, laser hardening, laser marking or high power laser projection displays. These are applications where the use of conventional classic scanning technology based on galvanometric scanners and polygon scanners still is required. This paper will report on a new concept to adapt MEMS mirror technology to the target of kilowatt laser power loads. This new approach includes the design and the fabrication of single axis and biaxial MEMS scanners with mirror aperture sizes in the range of 0.7 to 2 centimeters.

Multilayer dielectric coating of that large mirrors has been applied in order to achieve a reflectivity exceeding 99.9% which is a prerequisite to minimize heating up the mirror. However, multilayer dielectric coating is well-known for causing mirror deformation by its high residual stress. Therefore,

**Conference 9375:
 MOEMS and Miniaturized Systems XIV**

MEMS mirror thickness of 725 μ m was chosen which provides mirrors with excellent flatness. Wafer level vacuum packaging in combination with electrostatic actuation has been applied to enable high speed scanning at the required scan angle amplitudes. In addition to MEMS mirror design, fabrication and opto-electro-mechanical characterization this paper will also report about first results in applying these MEMS mirrors in high power laser applications.

9375-8, Session 3

High brightness MEMS mirror based head-up display (HUD) modules with wireless data streaming capability

Veljko Milanovic, Abhishek Kasturi, Volker Hachtel, Mirrorcle Technologies, Inc. (United States)

A high brightness Head-Up Display (HUD) module was demonstrated utilizing a fast, dual-axis MEMS mirror that displays vector images and text, utilizing its >6kHz bandwidth on both axes. Mirror steers a 405nm laser at wide angles of >40° on transparent emissive foils directly on the windshield, or on reflective emissive plates reflected off the windshield as a virtual image toward the driver/viewer, in two different HUD methodologies. The laser module optical cell is compact and combined with a MEMS controller enabling the precise movement of the mirror's X- and Y-axes to deflect the laser beam and communicating wirelessly to a host via Bluetooth. The wireless capability and a complete library of functions for vector displaying allows simple integration with smart phones or other mobile devices, or with car's computers. As an example, a phone number for an incoming calls or SMS to a smart phone is displayed on the windshield.

The compact display unit is resistant to vibrations and shock, and requires low power to operate, mainly supplied to the 405nm laser diode. The low power requirement is in part due to a vector graphics approach, allowing the efficient use of laser power. Vector display creates the brightest images since the laser power is concentrated on the content, with the laser being turned on nearly 80% of the time, compared to raster HUD designs where lasers are on <5% of the time.

9375-9, Session 3

A study of integrated piezoelectric position sensors for PZT resonant micromirrors

Shanshan Gu-Stoppel, Hans-Joachim Quenzer, Felix Heinrich, Joachim Janes, Wolfgang Benecke, Fraunhofer-Institut für Siliziumtechnologie (Germany)

PZT driven resonant micromirrors offer advantages of large scan angles and low power consumption due to benefits of resonant driving and high torque delivered by PZT actuators. Therefore they are entering different application fields recently, as for example laser projection or head-up displays. For many uses position sensing of the micromirrors is necessary to set up closed loop controls. Often position detections of micromirrors are based on optical principle and require accordingly external laser source and detector, which affects the device compactness and production cost. Thus, in this work the development of integrated position sensors is aimed and investigation and evaluation of different position sensing principles have been performed.

In previous works 1D and 2D PZT driven resonant micromirrors have been presented, which feature divergent spring suspensions and thin-film PZT actuators as drivers. Since these micromirrors have considerably different motion modes and resonant frequencies, which vary from 100 Hz up to 64 kHz, various position detection methods have been investigated. This work presents the study of the integrated piezoelectric position sensors for the previously introduced PZT micromirrors. Designs, fabrication and characterization of these position sensors have been performed and the results will be reported. Analyses of the sensitivity, linearity and dynamic

behavior of these integrated sensors have been executed, by comparing the sensor signals with the micromirror position signals measured by a Position-Sensitive-Device. Advantages, drawbacks of the sensors are itemized and methods for eliminating the drawbacks are proposed.

9375-10, Session 3

2D tilting MEMS micro mirror integrating piezoresistive sensors position feedback

Sebastien Lani, Dara Z. Bayat, Michel Despont, Ctr. Suisse d'Electronique et de Microtechnique SA (Switzerland)

An integrated position sensor for a dual-axis electromagnetic tilting mirror is presented. This tilting mirror is composed of a silicon based mirror directly deposited on a silicon membrane supported by flexible beams. The position sensors are constituted by 4 Wheatstone bridges of piezoresistors which are fabricated by doping locally the flexible beams. A permanent magnet is attached to the membrane and the scanner is mounted on planar coils deposited on ceramic substrate to achieve electromagnetic actuation. The performances of the piezoresistive sensors are evaluated by measuring the output signal of the piezoresistors in function of the tilt of the mirror and the temperature. White light interferometry was performed on all measurement to measure the exact tilt angle. The minimum detectable angle with such sensors was 30 μ rad in the range of the minimum resolution of the interferometer. The tilt reproducibility was 0.0186% obtained by measuring the tilt after repeated actuations with a coil current of 50mA during 30 min and the stability over time was 0.05% in 1h without actuation.

9375-33, Session PWed

Mechanical analysis and optimal design of a new kind of spherical mobile robot with two modes of locomotion

Hanxu Sun, Beijing Univ. of Posts and Telecommunications (China); Wei Zhao, Beijing university of post and telecommunication (China); Ping Sun, Beijing Normal Univ. (China)

The advantage of the spherical mobile robot includes high maneuverability, and that the robot can resume stability even if a collision happened with the other obstacles. So it is very suitable to be used in those environments, such as industrial building, civil application, defense construction and space exploration domain. But, till now, because of the feature of the point contact between the spherical shell and the ground, there are no effective methods that can solve the problems about the motion analysis and control technology of a spherical mobile robot, which prevents further research and application of the robot. So, in order to solve these problems, this thesis discusses deeply the motion analysis and control technology of the robot. The following aspects are contained in this thesis.

Firstly, based on the Euler-Lagrangian method, the dynamics model of the spherical mobile robot was developed, treated by reduced-order and transformed to normal nonlinear system using coordinate and input control transformation. Secondly, the spherical mobile robot was simplified as the "spheroid-pendulum" and the "spheroid-frame" model, and their dynamics differential equations were developed, respectively. The motion characteristic of the drive mechanism along the two drive shafts was discussed by solving the approximate solutions of the differential equations. For the sake of robust control, the uncertainty dynamics model of spherical mobile robot was developed while the coupling effect of the drive mechanism was regarded as the interference items of the spheroid motion. Then, the robust motion controllers were designed, using the slide-mode variable structure method, and the stability analysis, simulation and test verification were finished for the control strategies.

9375-34, Session PWed

Fiber-optical endoscopy with MEMS scanner technology

Wibool Piyawattanametha, King Mongkut's Institute of Technology Ladkrabang (Thailand) and Chulalongkorn Univ. (Thailand); Chanikarn Pipitsombat, King Mongkut's Institute of Technology Ladkrabang (Thailand)

Currently, performing clinical tissue diagnosis has to be performed through excised tissues by observing them under a microscope for histopathological interpretation. While this process has been the standard of care for over 50 years, there are significant limitations that include processing artifact, sampling error, time consumption, and interpretive variability. Light can achieve spatial resolution that is far superior to that of other imaging modalities, including computed tomography (CT), magnetic resonance imaging (MRI), and ultrasound. Recently, tremendous progress has been made in the development of MEMS based fiber-optical microendoscopes that can be used inside the human body to directly visualize tissue in vivo. These advances have been made possible by significant technological progress in flexible optical fibers, micro-optics, and compact scanning mechanisms such as MEMS scanners. A novel combination of MEMS scanners and advanced optical imaging modalities such as confocal microscopy or two-photon microscopy will provide new directions for advanced endoscopic diagnosis. Currently, these instruments are being used with medical endoscopes to collect high-resolution fluorescence images from the inner lining of hollow organs, such as the mucosa of the digestive and respiratory tract, to guide tissue biopsy. In this work, we will introduce recent development of MEMS based fiber-optical endoscopy.

9375-35, Session PWed

Inkjet printing of all-solid-state supercapacitors

Cristina Cordoba, Simon Fraser Univ. (Canada)

Supercapacitors have been studied and developed over the past few decades. Parameters such as surface area and pore size distribution have been underlined as major contributors to the capacitance of these devices. However, production of repeatable supercapacitors continues to be of great importance.

To address this concern, symmetric all-solid-state supercapacitors are manufactured using inkjet-printing technology (using DMP-2800 series from Dimatix Fujifilm) due to its flexibility of operation and lateral resolution. Aquivion® ionomer is used as a solid electrolyte which acts as both an ionic membrane as well as a binding substance. The electrodes are manufactured by preparing an activated carbon-based ink, Aquivion® suspension, ethylene glycol and a surfactant. The ink is printed on both sides of a cleaned Aquivion® membrane. The inkjet printing technology overcomes multiple challenges that the ionomer imposes like extreme sensitivity to humidity and relatively low working temperatures. Repeatable supercapacitors are successfully fabricated using the proposed inkjet printing technology. Once printed, supercapacitors are doped in 18% NaOH solution for 24 hours.

The electrochemical characterization of the printed devices is carried out by cyclic voltammetry and electrochemical impedance spectroscopy (EIS) in a two-electrode configuration. The values of capacitance are between 0.35 and 0.4 mF. Moreover, the fabricated devices are found to be highly flexible (bendable) and thin (~70 μm). Morphological characterization is obtained through scanning electron microscopy (SEM).

9375-36, Session PWed

Optical metrology of AlN piezomachined ultrasonic transducer arrays and piezopumps

Jaime Viegas, Inas Taha, Mateusz Madzik, Raquel Flores, Ricardo Janeiro, Masdar Institute of Science & Technology (United Arab Emirates)

Piezomachined ultrasonic transducer (PMUT) arrays are commonly found in applications in the field of ultrasonography and gesture recognition systems. Their application for bio and chemical sample preparation is another possibility, based on their beam steering and acoustic field manipulation capabilities. Post-fabrication non-destructive measurement of key device temporal and spatial parameters is required in order to adjust either simulation models or tune fabrication steps. In this work we report an optical testing setup for measuring the acoustic spectrum of PMUT devices and arrays, characterize maximum deflection of PMUTs and piezopumps and investigate the load effect of electrical contacts on the spatial and temporal oscillation behavior of these piezoelectric structures. We employ this testing setup to measure our designed PMUT structures which were fabricated by IME-Singapore, evaluating the relative merits of the PMUT design parameters.

9375-11, Session 4

Spatially resolved contrast measurement of diffractive micromirror arrays

Cornelius Sicker, Jörg Heber, Dirk Berndt, Fraunhofer-Institut für Photonische Mikrosysteme (Germany); Florian Ruckerl, Jean-Yves Tinevez, Spencer Shorte, Institut Pasteur (France); Michael Wagner, Harald Schenk, Fraunhofer-Institut für Photonische Mikrosysteme (Germany)

The manufacturing of optical MEMS modulators requires precise, nondestructive characterization techniques including, but not limited to thin film inspection, CD measurement, and hinge-stress measurement to guide the development process of high performance elements. Standard optical measurement techniques such as interference microscopy, light scattering, scanning white light interferometry, and spectrophotometric techniques have been adopted for general wafer-based MEMS processing tasks. Since their usability may strongly vary with the application range of specific MEMS modulators, essential performance parameters are often obtained only with specialized characterization techniques. We investigate a specifically designed Fourier imaging principle that resolves scattered light with regard to the analysis of the diffractive characteristics of micromirror arrays (MMA). As a central example, the optical quantity "display contrast" has been chosen to illustrate the distinct opportunities of spatially resolved scattering methods and MMA's diffractive operation principle. We present our concept for a spatially resolved contrast measurement and its experimental implementation. The setup comprises a laser beam combiner, an achromatic beam homogenization unit, a MMA imaging optics, and a CCD camera offering multispectral measurement capabilities. Key aspects of the development such as camera linearity, stray light reduction, and automation are discussed. The experimental results are compared with contrast calculations based on surface roughness parameters, which were obtained by scanning white light interferometry. Contrast values of up to 10,000 in selected samples demonstrate the high dynamic range of the setup, as well as the potential of the diffractive MMA technology.

**Conference 9375:
MOEMS and Miniaturized Systems XIV**

9375-12, Session 4

Image based wavefront compensation with deformable mirror for small satellite remote sensing

Norihide Miyamura, Meisei Univ. (Japan)

We are developing an adaptive optics system for earth observing remote sensing sensor. In this system, high spatial resolution has to be achieved by a lightweight sensor system due to the launcher's requirements. Moreover, simple hardware architecture have to be selected to achieve high reliability. Image based AOS realize these requirements without wavefront sensor. In remote sensing, it is difficult to use a reference point source unless the satellite controls its attitude toward a star. We propose the control algorithm of the deformable mirror on the basis of the extended scene instead of the point source.

9375-13, Session 4

Advanced MEMS spectral sensor for the NIR

Jarkko E. Antila, Uula Kantojärvi, Jussi Mäkyinen, Matti Tammi, Janne Suhonen, Spectral Engines Oy (Finland)

Near Infrared (NIR) spectrometers are widely used in many fields to measure material content, such as moisture, fat and protein in grains, foodstuffs and pharmaceutical powders. These fields include applications where only highly miniaturized and robust NIR sensors can be used due to small usable space, weight requirements and/or hostile working environment. Handheld devices for material inspection, online process automation and automotive industry introduce requirements for size, robustness and cost, which is currently difficult to meet. In this paper we present an advanced spectral sensor based on a tunable Microelectromechanical (MEMS) Fabry-Perot Interferometer. The sensor is fiber-coupled, weighs less than 100 grams and fits to an envelope of 25x55x55 mm³. Three types of sensors cover the wavelength ranges from 1.35-1.7 μm , 1.55-2.0 μm and 1.7-2.2 μm , utilizing only a single pixel InGaAs or extended InGaAs detector, avoiding the expensive linear array detectors. We describe the design, principle of operation and calibration methods together with the control schemes. Environmental tests are described and their results and finally application measurement results are presented along with discussion and conclusions.

9375-14, Session 4

Far infrared microbolometers for radiometric measurements of ice cloud

Linh Ngo Phong, Canadian Space Agency (Canada); Christian Proulx, El-Hassane Oulachgar, François Châteauneuf, INO (Canada)

We report on the development of focal plane arrays of 80x60 far infrared microbolometers for the TICFIRE (Thin Ice Cloud in Far Infrared Experiment) microsatellite payload. The latter is intended for the multispectral radiometric measurements of thin ice cloud in the range from 7.9 to 50 μm . A goldblack coating design was established for the arrays to achieve spectrally uniform absorption of far infrared radiation. Because of the large pitch required (104 μm), the microbolometer used a special central post structural design instead of conventional design. To avoid rises in thermal conductance of the microbolometer hinges through contact with goldblack material, the design includes an added platform as a cover for the hinges. The wafer yield for one wafer entirely manufactured was found to be about 60%. The examination of the first devices showed that they have a good structural integrity and a spectral absorbance uniformity better than 97% in all spectral channels. The effects of pixel addressing conditions on noise and responsivity were investigated to establish a baseline operational scenario

for the payload. For operating temperatures in the range from 10 to 20 deg C, a noise equivalent power below 80 pW was measured. This confirms that the mission required radiometric resolution of 100 mW/m²/sr could be met, considering the worst case in-band transmission of 0.3 and a working F# of 1.6 for the far infrared telescope.

9375-15, Session 4

Compact MEMS mirror based Q-switch module for pulse-on-demand laser range finders

Veljko Milanovic, Abhishek Kasturi, Bryan Atwood, Yu Su, Kevin Limkrailassiri, Mirrorcle Technologies, Inc. (United States); John E. Nettleton, Lew Goldberg, Brian J. Cole, U.S. Army RDECOM CERDEC NVESD (United States); Nathaniel Hough, Fibertek, Inc. (United States)

A highly compact and low power consuming Q-switch module was developed based on a fast single-axis MEMS mirror, for use in eye safe battery-powered laser range finders. The module's 1.6mm x 1.6mm mirror has >99% reflectance at 1535nm wavelength and achieves mechanical tilt angle slew rates of over 500 rad/s when switching the Er/Yb:glass lasing cavity from pumping to lasing state. The design targeted higher efficiency, smaller size, and lower cost than the traditional Electro-Optics Q-Switch. MEMS mirrors can offer a more cost-effective and compact solution with higher lasing efficiency, however the requirements are very challenging for MEMS design. Specifically, application requires pulse-on-demand capability and therefore cannot rely on resonant devices to achieve the needed performance. Instead, a highly efficient point-to-point capable device was designed with custom-coated dielectric mirror to withstand the high intra-cavity laser fluence levels. A compact MEMS controller was designed and implemented behind the MEMS mirror package with average ~90mW power consumption during the short switching cycle and 0mW in standby mode. The controller is designed to receive an external 3V power supply and a digital trigger and perform the Q-switch operation within 50ms. HR-coated mirror is bonded on top of the actuator in final assembly. Hence, mirror size can be adjusted to accommodate various beam shapes and sizes. Existing module prototypes are ~ (15mm)³ in size and have passed 500G shock tests. Successful operation in a laser cavity was demonstrated with high quality ~3mJ pulses generated. Future design focuses on increased shock tolerance to >1500G.

9375-16, Session 4

Tuning mechanical resonant frequencies of nanoelectromechanical systems with light

Feng Tian, Guangya Zhou, Fook Siong Chau, Jie Deng, National Univ. of Singapore (Singapore)

In this paper, mechanical resonant frequencies of nanoelectromechanical systems (NEMS) are tuned by light, in which optical spring effect plays a role. Optical spring effect has been investigated by the research in optomechanical field. This paper reports its application in a practical NEMS device. In our device, a multi-degree of freedom (DOF) NEMS spring system consisting of three nanoscale folded-beam-springs is adopted here. A NEMS comb drive is integrated into the spring system to excite its resonances. The resonance modes of the mechanism can be categorized into in-plane translational (I), out-of-plane translational (O), and torsional (T) modes according to their motion directions. The double-coupled nanobeam photonic crystal cavities (PCCs) are utilized to generate the optical spring effect. One of PCCs is fixed and connects with the input and output rib waveguides, while the other movable cavity is attached to the multi-DOF spring mechanism and the optical forces between the coupled cavities react on the mechanism. In the coupled cavities, resonance modes in each order split into even and odd modes. We investigate the shift of the mechanism's first-order in-plane translational (I1) resonance mode tuned

**Conference 9375:
 MOEMS and Miniaturized Systems XIV**

by the incident laser wavelengths across the fourth-order even (TE_{e,4}) and odd (TE_{o,4}) cavities' modes. Results show a nonlinear relationship between the 11 frequency and the wavelength, which can be explained by the model of optical spring effect. We also investigate the frequency of the third-order torsional (T3) mode versus the wavelengths across the fourth-order even (TE_{e,4}) mode and it shows a weaker torsional optical spring effect.

9375-17, Session 5

Large-aperture MOEMS Fabry-Perot interferometer for miniaturized spectral imagers

Anna Rissanen, Andreas Langner, Kai H. Viherkanto, Rami Mannila, VTT Technical Research Ctr. of Finland (Finland)

Microspectrometers enable novel applications based on optical MEMS – these small, robust and light-weight devices have found their way into medical-, automotive- and space instruments as well as environmental analysis. VTT's optical MEMS Fabry-Perot interferometers (FPIs) are tunable optical filters, which enable miniaturization of spectrometers into mass producible hand-held sensors with versatile measurement capabilities. FPI technology has also created a basis for various hyperspectral imaging instruments, ranging from nanosatellites, environmental sensing and precision agriculture with UAVs to instruments for skin cancer detection. Until now, these application demonstrations have been realized with piezo-actuated FPIs fabricated by non-monolithical assembly method, suitable for achieving very large optical apertures and with capacity to small-to-medium volumes; however large-volume production of MEMS manufacturing supports the potential for emerging spectral imaging applications in consumer wellness and wearable devices. So far optical apertures of MEMS FPIs in the visible range have been up to 2 mm in size; this paper presents the design, successful fabrication and characterization of MEMS FPIs for central wavelengths $\lambda = 500$ nm and $\lambda = 650$ nm with optical apertures up to 4 mm in diameter. The characterized optical properties are compared to the simulated values. The mirror membranes of the FPI structures consist of ALD (atomic layer deposited) TiO₂-Al₂O₃ 2/4-thin film Bragg reflectors, with the air gap formed by sacrificial polymer etching in O₂ plasma. The entire fabrication process is conducted below 150 °C, with possibility to monolithically integrate the filter structures on other IC-devices such as detectors.

9375-18, Session 5

Large size MOEMS Fabry-Perot interferometer filter for focal plane array hyperspectral imaging

Julian L. Chee, EPIR Technologies, Inc. (United States)

Commercial Micro Opto-Electro-Mechanical System (MOEMS) Fabry-Perot Interferometer (FPI) devices are currently available for single element (SE) infrared photo detectors (IR-PD) devices. Existing FPI designs are between 500 by 500 μ m to 2 by 2 mm in size to satisfy 30 by 30 μ m square IR-PD filtering requirements. With the growing trend of hyperspectral thermal imaging and chemical detection using IR focal plane arrays (FPAs), the planar mirror size of MOEMS FPI must scale upwards to 12 by 12 mm square, so to ensure full coverage for 9.6 x 7.7 mm sized (640 x 512 pixel, 15 μ m pitch) FPAs. In this paper, we will present our Multi-User MEMS Processes (MUMPs) fabrication approach which allows us to fabricate FPI devices to target SE to FPA size, and short-, mid-, and long wave bandwidth requirements, while using the same set of process and metrology tools. The critical features of the FPI are the deflection of the moving mirror membrane, deposition of the dielectric materials on a thin silicon membrane, to form the cavity mirror, and the assembly of the mirrors to form the cavity. The moving membrane will be a MEMS-actuated large size membrane with deposited dielectric mirrors for IR filtering. The dielectric stack consists of alternating layers of germanium and zinc sulfite, of high and low refractive

index properties respectively. The surface roughness of dielectric layers, the radius of curvature of the dielectric mirror, and reflectance of the assembled FPI between the bandwidth of 8 to 12 μ m, will be characterized.

9375-19, Session 5

Technological platform for vertical 3D multi-wafer integration of miniature imaging instruments

Sylwester Bargiel, Maciej Baranski, Nicolas Passilly, Christophe Gorecki, FEMTO-ST (France); Maik Wiemer, Joerg Froemel, Dirk Wuensch, Wei-Shan Wang, Fraunhofer-Institut für Elektronische Nanosysteme (Germany)

MOEMS-based microscopes and interferometers have recently gained significant attention in response to a strong need for handheld, low-cost imaging instruments for medicine and biotechnologies. In particular, on-chip confocal microscopes or Optical Coherence Tomography devices, capable of performing non-invasive optical biopsy of tissue with cellular resolution are expected to reduce or even eliminate the need of surgical biopsy. However, batch fabrication of such MOEMS is challenging. It requires an appropriate strategy of optical system miniaturization and a technological platform, providing wide port-folio of processes to 3D integrate, join, interconnect and package heterogeneous components.

In this work we describe a technological platform, which allows wafer-level batch fabrication of individual or arrayed instruments on-chip, based on free-space micro-optics. Its potential is exemplified by optical 3-D microlens microscanner, a key part of laser scanning confocal microscope on-chip.

The platform employs multi-wafer vertical integration approach, combined with integrated glass-based micro-optics and heterogeneous bonding / interconnecting technologies. The wafers of different functionality (lids, MEMS wafers, separators, etc.) are aligned and stacked using anodic bonding. We demonstrate bonding of five silicon/glass wafers at the temperature below 400°C with max. misalignment of 16 μ m. All the micro-optical components are made of glass to withstand multi-step bonding. We present the technology of monolithically integrated plano-convex lenses for beam collimation/focusing and hybrid laser-assisted integration of glass ball microlenses on the silicon MEMS actuators for transmissive beam scanning. Finally, the methods of distribution of electrical signals in a vertically stacked device using SiO₂-filled insulation trenches and gold-filled through wafer interconnects are described.

9375-20, Session 5

A biaxial PZT optical scanner for pico-projector applications

Keiichi Ikegami, Takaaki Koyama, Takao Saito, Yoshiaki Yasuda, Stanley Electric Co., Ltd. (Japan); Hiroshi Toshiyoshi, The Univ. of Tokyo (Japan)

We report a newly developed two-dimensional MEMS optical scanner based on the ADRIP (Arc Discharge Reactive Ion-Plating) deposited piezoelectric PZT film of typical 4 μ m. A circular mirror of 1.2 mm in diameter is suspended within a pair of resonant mechanism that oscillates at 25 kHz for $\pm 12^\circ$ mechanical angle with a typical voltage of 10 V. A gimbal plate including the mirror is supported with another pair of meandering suspensions to tilt the plate in the orthogonal direction at 60 Hz for the off-resonant vertical motion of $\pm 8^\circ$ mechanical. Overall power consumption of the piezoelectric actuation was 100 mW or less. As a mechanical reinforce, a rib-structure was designed on the backside of the mirror by using a structural optimization tool TOSCA to suppress the dynamic curvature to 100 nm or less. A piezoelectric sensor was also integrated in the identical PZT film after optimizing the electrode shape to pick up the mechanical angle of the scanner and to give a trigger signal to the control system. A

**Conference 9375:
 MOEMS and Miniaturized Systems XIV**

plug-in type pico-projector optics and electronics has been assembled in a 7.5 cm × 12 cm × 5 cm volume with RGB lasers to demonstrate a HD (high definition) class image projection of 720 horizontal lines. The fundamental resonance of the entire scanner mechanism was made to be 1 kHz or higher, thereby exhibiting a compatibility with vehicle applications.

9375-21, Session 6

CMOS compatible fabrication of 3D photonic crystals by nanoimprint lithography

Martin Eibelhuber, Gerald Kreindl, Thomas Glinsner, EV Group (Austria)

The major part of today's semiconductor technology is based on electrons rather than on photons. However, photonic applications are emerging rapidly and nanoscale manipulation of light is the core to develop the full potential of this technology. For that reason nanopatterning of optical structures will play an essential role in the photonics market.

To this end direct writing methods as e-beam lithography have been extensively used for research and development but these techniques cannot be easily scaled up for cost efficient production. Even though steppers can warrant cost efficient production when high volume production is established, they are nonetheless mainly designed for the needs of the electronic and not of the photonic industry.

Nanoimprinting techniques are an attractive solution for next generation lithography methods. Nanoimprint lithography can here not only be considered for bridging the gap from R&D to high volume manufacturing as it is in addition capable to adapt to the needs of the fragmented and less standardized photonic market more easily. In this work UV-NIL has been selected for the fabrication process of 3D-photonic crystals.

It was shown that UV-NIL using a multiple layer approach is well suited to fabricate a 3D woodpile photonic crystal. The necessary alignment accuracies below 100nm were achieved using a simple optical method. In order to obtain sufficient alignment of the stacks to each other a two stage alignment process is performed: at first proximity alignment is done followed by the Moiré alignment in soft contact with the substrate. Multiple steps of imprinting, etching, Si deposition and chemical mechanical polishing were implemented to create high quality 3D photonic crystals with up to 5 layers. This work has proven the applicability of nanoimprint lithography in a CMOS compatible process on 3D photonic crystals with alignment accuracy down to 100nm. Optimizing the processes will allow scaling up these structures on full wafers while still meeting the requirements of the designated devices.

9375-22, Session 6

Piezoelectrically driven translatory optical MEMS actuator with 7mm apertures and large displacements

Joachim Janes, Shanshan Gu-Stoppel, Hans-Joachim Quenzer, Fabian Stoppel, Christian Mallas, Ulrich Hofmann, Wolfgang Benecke, Fraunhofer-Institut für Siliziumtechnologie (Germany)

The FEM supported design studies and manufacturing of a piezoelectrically driven translatory MEMS actuator is presented, which features a 7 mm aperture and four thin-film PZT actuators achieving large displacements. The actuator performs torsion mode oscillation as well as piston oscillation, which can serve for Fourier Transform Infrared Spectroscopy (FTIR). Mode analysis using Laser Doppler Vibrometry is applied to study the dynamic and quasi-static performance of the actuator. Thereby displacement of up to ± 250 μm in piston mode has been achieved under ambient conditions driven by 30 V sinusoidal voltages. Besides, total optical scan angle of

16.6° has been obtained by 10 V driving voltage. The resonant frequencies of the two motion modes are 143 Hz and 339 Hz, respectively. Due to the low frequencies and the low driving voltages only low power consumption is required. The effect of residual gas friction, squeezed film damping and internal friction on the piezo-driven MEMS actuator is analyzed by measuring Q-values associated with the piston mode and torsion modes. Vibrometry has been also used to analyze other oscillatory motions of this actuator.

9375-23, Session 6

Multi-wafer bonding technology for the integration of a micromachined Mirau interferometer

Wei-Shan Wang, Fraunhofer-Institut für Elektronische Nanosysteme (Germany); Justine Lullin, FEMTO-ST (France); Maik Wiemer, Joerg Froemel, Fraunhofer-Institut für Elektronische Nanosysteme (Germany); Sylwester Bargiel, Nicolas Passilly, Christophe Gorecki, FEMTO-ST (France); Thomas Gessner, Fraunhofer-Institut für Elektronische Nanosysteme (Germany)

A multi-wafer bonding technology combined with electrical connection functionality for the integration of a micromachined array-type Mirau interferometer is presented. A Mirau interferometer, which is a key-component of OCT microsystem, consists of a microlens doublet, a MEMS Z scanner, a focus-adjustment spacer and a beam splitter plate. Therefore, heterogeneous bonding of Si, glass and SOI wafers is necessary for the integration of this MOEMS device. Previously, most of the existing methods for multilayer wafer bonding require annealing at high temperature, i.e., 1100°C. To be compatible with MEMS devices, bonding of 3 different wafer stacks lower than 400°C has also been investigated. However, if more components are involved, it becomes less effective due to the alignment accuracy or degradation of surface quality of the not-bonded side after each bonding operation.

The proposed technology focuses on 3D integration of heterogeneous building blocks, where the assembly process is compatible with the materials of each wafer stack and with position accuracy which fits optical requirement. A demonstrator up to 5 wafer stacks bonded lower than 400°C is presented and bond interfaces are evaluated. To avoid the complexity of through wafer vias, a design which creates electrical connections along vertical direction by mounting a wafer stack on a flip chip PCB is proposed.

The approach, which adopts vertically-stacked wafers along with electrical connection functionality, provides not only a space-effective integration of MOEMS device but also a design where the Mirau stack can be further integrated with other components of the OCT microsystem easily.

9375-24, Session 6

Tunable optical buffer based on III-V MEMS design

Wing H. Ng, Univ. College London (United Kingdom); Nina Podoliak, Peter Horak, Univ. of Southampton (United Kingdom); Huiyun Liu, Univ. College London (United Kingdom); William J. Stewart, Univ. of Southampton (United Kingdom); Anthony J. Kenyon, Univ. College London (United Kingdom)

We present a tunable optical buffer device based on the III-V semiconductor platform for telecommunication applications. The device comprises two InP suspended parallel waveguides with cross sectional dimensions of 200nm × 300nm, separated by an air gap. Due to the small dimensions of the waveguides, the propagating optical mode is confined in both the waveguides and the space between them. Our simulation shows we could

**Conference 9375:
 MOEMS and Miniaturized Systems XIV**

achieve up to 100% change in optical propagation delay time when the waveguide spacing is increased by ~500nm, which reduces the effective refractive index of the structure.

The variation of the spacing between the two waveguides is achieved using a MEMS technique. In our simulation, our waveguides has an initial spacing of 50nm. When a voltage of the same polarity is applied to both waveguides, their separation increases due to electrostatic repulsion. We estimate that only 3V is required to increase the separation distance from 50nm to 500nm; this translates to a change in the propagation delay by a factor of 2.

An optical buffer device designed to operate under the MEMS actuation scheme is being fabricated. The sample is grown on an InP substrate by molecular beam epitaxy. The waveguide pattern is written onto a 300nm thick InP device layer by electron beam lithography and plasma etching. Electrodes are incorporated into the structure to apply voltages for MEMS actuation. We estimate that with a 1mm long device, we could induce a change of the propagation delay in the order of ~10ps.

9375-25, Session 6

Integrated packaging of 2D MOEMS mirrors with optical position feedback

Andreas Tortschanoff, Martin Lenzhofner, Marcus Baumgart, Matthias P. Kremer, Carinthian Tech Research AG (Austria)

Many applications of MOEMS microscanners rely on accurate position feedback, scanning of arbitrary trajectories in particular. For MOEMS devices which do not have intrinsic on-chip feedback, position information can be provided with optical methods, most simply by using a reflection from the backside of a MOEMS scanner. By measuring the intensity distribution of the reflected beam across a quadrant diode, one can precisely detect the mirror's deflection angles. Previously, we have presented a position sensing device, applicable to arbitrary trajectories, which is based on the measurement of the position of the reflected laser beam with a quadrant diode.

In this work, we present a novel setup, which comprises the optical position feedback functionality integrated into the device package. The new device's design is based on a flip-folded 2.5D PCB layout and fully assembled as small as 9.2x7x4mm³ in total. The device contains of four layers, which supply the MOEMS mirror, a spacer to provide the required optical path length, the quadrant photo-diode and a laser diode to serve as the light source.

Additionally to describing the mechanical setup of the novel device in detail, we will present first experimental results and optical simulation studies. Accurate position feedback is the basis for closed-loop control of the MOEMS devices, which is crucial for some applications as image projection for example. In-package integration of position feedback and the possibility of closed-loop control will significantly improve the performance of these devices.

9375-26, Session 7

Improvement of Varioptic's liquid lens based on electrowetting: How to obtain a short response time and its application in the design of a high resolution iris biometric system

Benjamin Burger, Varioptic-A BU of Parrot SA (France); Serge C. Meimon, Cyril Petit, ONERA (France); Minh Chau Nguyen, Varioptic-A BU of Parrot SA (France)

A few years ago, Varioptic started the business of a new electro-optical device : the liquid lens. The actual products proposed by Varioptic provide real time focus, tilt and astigmatism correction with short response time. In

our research for improvement of the performance of the liquid lenses, we have investigated solutions to decrease the response time of these devices. For example, a response time of 6 ms was required for the conception of a new IRIS biometric system demonstrator. This program (IRISEM) is supported by the French agency for research and technology. In this paper, we present how we achieved this result and what are the key parameters to decrease the response time of the liquid lens. We will present the optimum designs and control law of the lens in order to obtain the lowest response time. Fluid reorganization hydrodynamic models which explain the choice of the optimization parameters are presented and discussed

9375-27, Session 7

Volume refractometry of liquids using stable optofluidic Fabry-Pérot resonator with curved surfaces

Noha A. Gaber, Univ. Paris-Est (France); Yuto Takemur, Kagawa Univ. (Japan); Maurine Malak, Ecole Polytechnique Fédérale de Lausanne (Switzerland); Frédéric Marty, Univ. Paris-Est (France); Daa Khalil, Ain Shams Univ. (Egypt); Dan Angelescu, Elodie Richalot, Tarik Bourouina, Univ. Paris-Est (France)

This work reports a simple, optical miniaturized sensing module for liquid refractometry. It adopts a stable Fabry-Perot resonator consisting in two silicon cylindrical mirrors with a cylindrical lens in the core. The lens is formed by a capillary tube with the analytes to be analyzed passing through it. This setup enables volume refractometry, where light propagates through the sample realizing high interaction depth. The cylindrical surfaces achieve light confinement, reducing the light escaping loss known in usual cavities having straight mirrors; and hence attain high quality factors Q over 1,000. Exploiting this high Q, we adopt uncommon refraction index (RI) measuring criterion: operate at a fixed wavelength and detect the power drop caused due to the spectral shift with RI change.

Performing experimental testing using a tunable laser and a power-meter, the normalized spectra for different mixture ratios between acetone and deionized water are obtained. The maxima wavelength of pure acetone curve is taken as a reference. A vertical line at this wavelength cuts the successive curves in the linear region enables measuring the power drop, and from it the refractive index change Δn above the reference solution by $0.0023 < \Delta n < 0.0045$ can be determined. Sensitivity up to 4,094 dBm/RIU is achieved. A wider range is still accessible by the conventional method of tracing the shift in peak wavelengths: a range of $\Delta n = 0.0163$ RIU can be scanned, with a sensitivity of 221 nm/RIU. Error analysis has been also accomplished, and the design parameters of the device are discussed to evaluate the performance.

9375-28, Session 7

Fiber-coupled Fabry-Pérot notch filter combining in-plane axis, high speed MEMS tunability and large etching depth

Yasser M. Sabry, Si-Ware Systems (Egypt) and Ain-Shams Univ. (Egypt); Yomna M. Eltagoury, Ain Shams Univ. (Egypt); Ahmed Shebl, Si-Ware Systems (Egypt) and Ain Shams Univ. (Egypt); Mostafa Solimanb, Mohamed Sadek, Si-Ware Systems (Egypt); Daa Khalil, Ain Shams Univ. (Egypt) and Si-Ware Systems (Egypt)

Notch filters based on fiber-coupled Fabry-Pérot cavity are formed by a reflector placed in close proximity to a dielectric-coated end of an optical fiber. This kind of optical filters is easy to tailor for a given application because the external mirror has less mechanical and optical constraints. Notch filter are used in spectroscopy, multi-photon microscopy, fluorescence

**Conference 9375:
MOEMS and Miniaturized Systems XIV**

instrumentation, optical sensors and other life science applications. In this paper we present a fiber-coupled Fabry-Pérot filter based on dielectric-coated optical fiber inserted into a fiber groove facing a metallized micromirror, where the latter is driven by a high-speed MEMS actuator. The microsystem is fabricated using Deep Reactive Ion Etching (DRIE) technology on SOI wafer. The optical axis is in-plane and the components are self-aligned. The DRIE etching depth is 150 μm ; chosen for improving the out-of-plane stiffness of the actuator and increasing the micromirror optical throughput. The etching verticality is better than 0.1 degree and the surface roughness is less than 60 nm peak-to-peak. The MEMS actuator type is closing-gap while its quality factor is improved by slotting the fixed plate. The actuator, therefore, achieves a travel distance of 800 nm and a resonance frequency of 90 kHz. The notch filter exhibits a free spectral range up to 100 nm and a notch rejection ratio of 20 dB around a wavelength of 1300 nm. The presented device provides low cost wafer level production of the tunable filter

9375-29, Session 7

MEMS-based frequency modulation of fiber ring laser

Kamal Khalil, Ain Shams Univ. (Egypt); Khaled Hassan, Ahmed Shebl, Mostafa Soliman, Si-Ware Systems (Egypt); Fares Al-Arifi, Mohammed Al-Otaibi, King Abdulaziz City for Science and Technology (Saudi Arabia); Yomna M. Eltagoury, Ain Shams Univ. (Egypt); Yasser M. Sabry, Ain Shams Univ. (Egypt) and Si-Ware Systems (Egypt); Diaa Khalil, Ain Shams Univ. (Egypt) and Si-Ware Systems (Egypt)

Fiber lasers are gaining wide attention nowadays due to their high stability, high reliability, low cost and compactness. They have applications in material processing, optical telecommunications, medical imaging and spectroscopy. Frequency or phase modulation of the laser system is important in wavelength tuning, active mode locking, generation of frequency combs and sensors in general. In this work, we report frequency modulation of fiber ring laser system using transmission-type corner cube in-plane MEMS phase modulator fabricated by DRIE technology on an SOI substrate. Optical phase modulation is achieved through variations in the optical path length based on a corner-cube microreflector driven by a comb-drive MEMS actuator. Input/output lights are supplied/collected using optical fibers inserted into micromachined grooves self-aligned with the microreflector and the MEMS actuator. The mechanical system has a resonance frequency of 11.2 kHz and a maximum stable travel range of 5.5 μm at resonance. The ring laser system is composed of a semiconductor optical amplifier used as the gain medium, a single-mode fiber coil of 570 m length, the fiber-coupled MEMS-based phase modulator and a 90/10 tapping coupler. The coupler output is connected to a high speed optical detector module and the output is measured on an RF spectrum analyzer. The results show beating modes at 345 kHz and its harmonics corresponding to the free spectral range of the cavity. The number of side bands due to frequency modulation is related to the modulation index. A wide range of the frequency modulation index could be achieved by varying the applied DC and AC voltages on the MEMS comb-drive actuator.

9375-30, Session 7

Large MOEMS diffraction grating results providing an EC-QCL wavelength scan of 20%

Jan Grahmann, Fraunhofer-Institut für Photonische Mikrosysteme (Germany)

External cavity quantum cascade lasers (EC-QCL) are very promising light sources in the mid infrared wavelength range for spectroscopy applications

and contribute drastically due to their output power of a few 10 mW up to 100 mW to a nice signal to noise ratio. Addressed in the presented project is a wavelength region between 3 μm to 12 μm . Due to their intersubband crossings a wide range of wavelengths can be emitted by a single semiconductor QCL. Combined with an external cavity and a scannable grating the wavelength is supposed to be tuned around 30% of the center wavelength. The first experimental results presented here are for a center wavelength of 4.7 μm . Emphasis is on the large MOEMS diffraction grating used as wavelength selective element in the external cavity. The diameter of the grating is 5mm with a resonance frequency of 1 kHz and mechanical deflections up to 10°. The optical diffraction grating is fabricated on the mirror single crystal silicon plate to scan the first diffraction order in the MIR-wavelength range over the laser facet. The development of the grating technology module to integrate it with high accuracy and reproducibility into the IPMS AME75 process flow is one major part of the paper. The principle EC-QCL setup with the scanning grating is described and first measurement results concerning laser output power and tuning range are presented.

9375-31, Session 7

Resonant micro optic gyro using tens of centimeters long optical fiber coil

Huilian Ma, Jianjie Zhang, Zhejiang Univ. (China); Linglan Wang, Zhejiang Univ (China); Zhonghe Jin, Zhejiang Univ. (China)

Micro-electromechanical system (MEMS) gyros have captured many rate-gyro applications for their small size and low cost. However, they can hardly provide the precision and dynamic performance required for stabilization and navigation applications. In addition, MEMS-based gyros are susceptible to instantaneous shock and vibration that further deteriorate their performance and limit their applications. A resonator micro optic gyro (RMOG) is a promising candidate for applications requiring small, light and robust gyros. A High-performance RMOG requires a micro ring resonator of high finesse, and thus a resonator having low loss. For planar waveguide ring resonators, the limit to propagation losses is an ongoing research area, however, and is yet to be determined. The achieved finesse of mostly explored low-loss planar waveguide ring resonator to be used for RMOGs are less than 100. In this paper, we experimentally demonstrate a new record for high-finesse micro ring resonators by using low-loss optical fiber coils. Both the simulation and experimental results show that a 30-cm long spliceless optical fiber ring resonator is sufficient to build a tactical-grade RMOG. Additionally, silicon is quickly proving to be an ideal substrate platform for RMOGs because it permits the fabrication of low loss planar waveguides and active componentry. By etching a silicon substrate to form a V-groove, the spliceless optical fiber ring resonator is then inserted in the etched groove and embedded within the coating. Thus, the silicon-based platform can allow integrating all optoelectronic components of the RMOGs.

9375-32, Session 7

Modeling and simulations of new electrostatically driven, bimorph actuator for high beam steering micro-mirror deflection angles

John P. Walton, Ronald A. Coutu Jr., Air Force Institute of Technology (United States)

There are numerous applications for micromirror arrays seen in our everyday lives. From flat screen televisions and computer monitors, found in nearly every home and office, to advanced military weapon systems and space vehicles, each application bringing with it a unique set of requirements. The microelectromechanical systems (MEMS) industry has researched many ways micromirror actuation can be accomplished and the different constraints on performance each design brings with it. This paper

**Conference 9375:
MOEMS and Miniaturized Systems XIV**

investigates a new 'zipper' approach to electrostatically driven micromirrors with the intent of improving dual plane beam steering by coupling large deflection angles, over 30°, and a fast switching speed. To accomplish this, an extreme initial deflection is needed which can be reached using high stress bimorph beams. Currently this requires long beams and high voltage for the electrostatic pull in or slower electrothermal switching. The idea for this 'zipper' approach is to stack multiple beams of a much shorter length and allow for the deflection of each beam to be added together in order to reach the required initial deflection height. This design requires much less pull-in voltage because the pull-in of one short beam will in turn reduce the height of the all subsequent beams, making it much easier to actuate. Using modeling and simulation software to characterize operations characteristics, different bimorph cantilever beam configurations are explored in order to optimize the design. These simulations show that this new 'zipper' approach increases initial deflection as additional beams are added to the assembly without increasing the actuation voltage.

Conference 9376: Emerging Digital Micromirror Device Based Systems and Applications VII

Tuesday - Wednesday 10-11 February 2015

Part of Proceedings of SPIE Vol. 9376 Emerging Digital Micromirror Device Based Systems and Applications VII

9376-2, Session 1

Software developments for DLP 3D printings

Badia Kouksi, Optecks, LLC (United States)

A common method for 3D printing utilizes ultraviolet light incident on an appropriately chosen liquid to solidify portions of the liquid that combine to form the three-dimensional object. These printers use digital light projection (DLP) technology and a z-scanner to address all of the volume pixels (voxels) on a slice-by-slice basis. Drawbacks of this approach are the time required to convert an object into a format suitable for use with the printer, especially for large objects, and the inability of current systems to provide editing and other control options to the operator. We have developed a software package for image segmentation and DLP control that provides significant improvements in printing time and image control. The Optecks software can rapidly convert 3D objects from any software tool to the printer's platform and allow editing and image controls. This reduces the time to printing and minimizes problems with interfacing the printer to the applications that utilize it. The Optecks software can render both solid and surface representations of an object. Combined with projector optics, objects of different sizes and resolution can be printed. Voxel depth can be altered by simply printing the same slice at multiple, successive depths. The software provides interactive graphic tools that provide the operator the ability to edit the properties of each slice, including deleting and adding voxels, rotation, mirroring, and duplication of voxel patterns to different parts of the slice. The capabilities of the software and its suitability to this form of 3D printing will be discussed.

9376-3, Session 1

Large area maskless photopolymerization (LAMP): Disruptive technology for additive manufacturing using scanning spatial light modulators

Suman Das, Marvin Kilgo, Michael Middlemas, Erica Davis, DDM Systems (United States)

This presentation will cover Large Area Maskless Photopolymerization (LAMP™), an additive manufacturing (AM) technology being commercialized by DDM Systems. LAMP utilizes scanning spatial light modulators to pattern large areas of photosensitive materials for the layer-by-layer production of macroscale objects with microscale feature. LAMP has a strong potential for disruption across diverse industries including the aerospace, energy, defense, healthcare and automotive sectors. The technology was developed with support from DARPA's Disruptive Manufacturing Technologies program to produce highly intricate ceramic components such as cores and integral-cored ceramic molds for the investment casting of turbine airfoils directly from digital design data, without any tooling. Equiaxed and single-crystal turbine airfoils with a high degree of conformance to the design geometry have been cast in nickel-base superalloys using LAMP-manufactured molds, demonstrating LAMP's ability to meet production requirements. LAMP technology is thus on the path to disrupting the state-of-the-art of investment casting by eliminating all the tooling, handling and sources of scrap, and multiple process steps, and by achieving the ability to manufacture advanced designs that are today considered non-manufacturable through conventional casting. This presentation will describe the research and development paths that are being pursued to commercialize LAMP. It will conclude with an outlook towards future directions for achieving further advances in this technology.

9376-4, Session 1

Digital micromirror devices for laser-based manufacturing on the micro-scale

Ben Mills, Univ. of Southampton (United Kingdom); Dan Heath, Matthias Feinäugle, Rob W. Eason, Optoelectronics Research Ctr. (United Kingdom)

Digital micromirror devices (DMD), such as the DLP range developed by Texas Instruments, have found many applications in scientific research. Here, we show how a DMD can be used as a spatial light modulator for an 800nm wavelength, femtosecond laser system, to enable image-projection-based laser machining, for both additive and subtractive manufacturing. Laser pulses incident on the DMD were spatially shaped by the DMD pattern and demagnified, via a microscope objective, to a size of $\sim 30\mu\text{m}$ by $30\mu\text{m}$ onto a target sample, hence providing a ~ 1000 increase in laser fluence compared to that on the DMD surface. Typically $1-10\text{J}/\text{cm}^2$ was achieved on the target sample, which enabled ablative patterning of a range of materials ranging from thin-film semiconductors to bulk diamond. As only a single laser pulse was required to machine an entire pattern, through the use of automated stages, stitched cm^2 -sized regions, with diffraction-limited resolution, were machined on a time scale of minutes. The ability to synchronise the DMD updating with the arrival time of the laser pulses enabled each laser pulse to be individually spatially shaped providing significant flexibility to machine arbitrary cm^2 structures. We will present examples of both subtractive (laser-ablation) and additive (photo-polymerisation and laser-induced-forward-transfer) manufacturing, show how this approach can fabricate structures smaller than $1/10$ th of the laser wavelength, and demonstrate a technique that modifies a surface to produce complex multi-coloured patterns (achieved via the ablation of micron-sized variable-period-gratings) that may have applications in the security and marking industries.

9376-5, Session 1

Concepts for 3D print productivity systems with advanced DLP photoheads

Alfred Jacobsen, Visitech AS (Germany); Oyvind Tafjord, Trond Jorgensen, Endre Kirkhorn, Visitech AS (Norway)

Direct Imaging with DLP® Photoheads is becoming an established technology in productivity systems for PCB Lithography and similar applications. Scrolling technology is used to expose large areas and is enabling highest levels of productivity and efficiency, while maintaining full flexibility of direct imaging concepts. Specific features such as SPX (subpixelation) and PPC (pixel power control) technologies have further enhanced resolution of printed structures, as well as precision and uniformity of the exposure across the entire field.

3D print systems with photosensitive resins can conceptually be seen as an extension of 2D Direct Imaging systems into the third dimension. The scrolling technique then allows to enlarge the build area by freely multiplying the photohead's static build area with native pixel pitch in both, X and Y dimensions. In addition, SPX technology in 3D print systems would enable 2 different advanced options. Either it offers improved (reduced) edge roughness of structures, by fine pitching the native pixel pitch. Or a larger native pixel pitch can be chosen, still providing the same fine pitched edge roughness as a native system with its proportionally smaller build area.

**Conference 9376: Emerging Digital Micromirror
 Device Based Systems and Applications VII**

9376-6, Session 2

Transport-aware imaging (*Invited Paper*)

 Kyros Kutulakos, Matthew O'Toole, Univ. of Toronto
 (Canada)

When we snap a photo with a conventional camera, we record all light incident on the sensor no matter what path it followed to get there. In this talk I will discuss a new family of cameras that gives us many more degrees of freedom: these cameras record just a fraction of the light coming from a controllable source, based on the actual 3D path followed. Photos and live video captured this way offer an unconventional view of everyday scenes in which the effects of scattering, refraction and other phenomena can be selectively blocked or enhanced, visual structures that are too subtle to notice with the naked eye can become apparent, and object appearance can depend on depth. I will discuss the basic theory behind these cameras, their DMD-based implementation, and three applications: (1) live imaging of complex everyday scenes, (2) reconstructing the 3D shape of scenes whose geometry or material properties make them hard or impossible to scan with conventional methods, and (3) acquiring time-of-flight images that are free of multi-path interference.

9376-7, Session 2

3D microscopy for microfabrication quality control

 Matthew S. Muller, Paul D. De Jean, Swept Image Inc.
 (Canada)

A novel stereo microscope adapter, the SweptVue, has been developed to rapidly perform quantitative 3D microscopy for cost-effective microfabrication quality control. The SweptVue system replaces the observation module on an Olympus SZX7 stereo microscope, and uses the right and left stereo channels for sample illumination and detection, respectively.

Samples are illuminated using a sequence of 42 rapidly projected lines from a Texas Instruments' DLP LightCrafter. The lines are temporally synchronized to the electronic rolling shutter of a Point Grey Flea3 USB3.0 CMOS camera. The stereo optical arrangement causes a shift in line position with respect to the rolling shutter according to sample depth and microscope magnification. To generate a depth map of features within the focal volume, a series of 1280x960 image frames is acquired at 24Hz with 1-3msec trigger delays.

Depth is assigned in real-time to each pixel based on its maximum detected intensity. A 40-step depth map of the entire field of view is obtained in approximately 5 seconds. With a 1X objective lens, 0.1msec sensor exposure time, and 5.6-0.8x adjustable magnification, depth resolutions of 2.5-17.8 μ m were achieved over a 0.8-5.0mm field of view. Calibration is performed by acquiring depth maps of a microscope slide mounted on a 3-axis translation stage at various positions.

A selection of 3D printed, micromilled, and soft lithography microfabricated samples have been examined for quality assurance and conformance to design specifications. The modular SweptVue microscope adapter provides a means to quickly and cost-effectively perform quality control measurements for microfabrication applications.

9376-8, Session 2

Characteristics of digital micromirror projection for 3D shape measurement at extreme speed

Roland Höfling, Petra Aswendt, Frank Leischnig, Matthias Förster, ViALUX GmbH (Germany)

Nowadays, 3D shape measurement is one of the growing industrial

applications of the digital micro-mirror device (DMD). This paper will present investigations on precision and repeatability of that spatial light modulator output when it is driven up to its high-speed limit. The study focuses on 3D shape measuring methodologies based upon phase-shifting projection of sinusoidal patterns. The DMD is a bi-stable device providing an on/off pattern at each certain moment in time, i.e. it has a native binary output. Sinusoidal patterns are the result of either a temporal average of multiple on/off patterns or a spatial average in one on/off pattern. Both approaches are studied experimentally with respect to precision and stability of the pattern output. The pattern switching rates cover the range of 250 Hz to 50,000 Hz.

9376-9, Session 3

High-speed phase modulation using the DLP: Application in imaging through complex media (*Invited Paper*)

 Eyal Niv, Antonio M. Caravaca-Aguirre, Donald B. Conkey,
 Rafael Piestun, Univ. of Colorado at Boulder (United States)

We present a configurable high-speed wavefront phase modulation and control system based on a DLP deformable mirror device (DMD) system. We demonstrate a hardware implementation that reduces latency and computation times for real-time experiments. A custom driver and the FPGA included in the DLP system reduce data transfer enabling adaptive wavefront shaping at kilohertz frame rates for use in multimode fiber endoscopes and focusing through scattering media.

In order to acquire feedback phase information we implement a phase shifting method directly on the FPGA. The FPGA controls the DMD indirectly via the digital controller and power and reset driver. It is also responsible for triggering of the analog signal conversion and storage of the digitized output.

We demonstrate the system measuring the amplitude and phase corresponding to 256 different input modes (with three different reference phases per input mode) in 34 ms, corresponding to a frequency of 22,727 Hz per phase mask. The information processing to create the optimal phase mask, the data transmission, and the projection on the DMD takes 3 ms.

9376-10, Session 3

DMD-based open-loop wavefront shaping technique: Turbidity suppression in biological tissues

 Mooseok Jang, Haowen Ruan, Haojiang Zhou, California
 Institute of Technology (United States); Daifa Wang,
 BeiHang Univ. (China); Changhui Yang, California Institute
 of Technology (United States)

Since most biological tissues are highly scattering, the utility of optical imaging and therapy in biomedicine has long been limited to the superficial layer of tissue. However, as the wavefront distortion from the multiple scattering is deterministic and has a time-reversal symmetry, the obstacle can be circumvented with a proper wavefront manipulation. Along with the recent emergence of spatial light modulators, the concept-turbidity suppression in biological tissues with the time-reversed beam- has been experimentally demonstrated, in turn, an optical focusing and imaging through the turbid medium has been achieved. However, the system latency is still one of the key technical hurdles for the practical in-vivo use of the turbidity suppression technique: though highly dynamic tissues decorrelate within 1 ms, the liquid crystal-based spatial light modulator, which is widely used due to its capability to directly modulate the phase of the light field, can refresh typically in every 10ms. In this study, we introduced several ways to generate the time-reversed beam and explained the benefits and

**Conference 9376: Emerging Digital Micromirror
Device Based Systems and Applications VII**

challenges of using digital micromirror device (DMD), whose refresh rate is around 20000 Hz. Then, we proposed the DMD-based open-loop time-reversed beam generation method and described its potential in biomedical applications. The proposed DMD-based system was experimentally implemented and confirmed to provide the turbidity suppression fidelity that is theoretically expected. This method paves the way toward the in-vivo deep-tissue optical interrogation.

9376-11, Session 3

**Head mounted DMD for visual stimulation
in freely moving rats: A novel tool for
visual neuroscience research**

Yossi Mandel, Tamar Arens-Arad, Nairouz Farah, Alex Zlotnik, Zeev Zalevsky, Bar-Ilan Univ. (Israel)

Novel technologies are constantly under evaluation for vision restoration in blind patients. Some of these techniques, such as photodiode implants or optogenetics based treatment, rely on a glasses mounted optical system which projects the visual scene onto the retina. The projection system is characterized by a relatively high power, a localized retinal stimulation area and wavelengths that are specific for the technology at hand. Current research techniques used for evaluation of visual function in animals utilize computer screens for retinal stimulation, and are therefore inefficient in the evaluation of retinal implant performance or optogenetics based treatment.

Here we present a head mounted customized DMD illuminated by a 915nm diode laser and 530nm LED and imaged on the rat retina to stimulate a prosthetic retinal chip or normal retinal areas, respectively. Optical designs constitutes of four spherical lenses and two folding mirrors. Simulation based results, using Zemax tool, revealed that our customized optical system achieves retinal projected patterns with contrast of 0.95 and 0.85 for 5 and 30 cycles/mm, respectively, and a field of view of 15 degrees. The system's low weight and its wireless capabilities, enable the training of freely moving rats to respond to visual stimuli and the studying of the visual function obtained by the treatment. An alternative system's design approach uses a customized divergent contact lens, which cancels the anterior corneal surface of the rat's eye.

This novel presented approach enables scientists to evaluate various artificial vision techniques in a behaving animal model.

9376-12, Session 4

**Generation 3 programmable array
microscope (PAM) for high speed, large
format optical sectioning (*Invited Paper*)**

Anthony H. de Vries, Stephan Kramer, Donna J. Arndt-Jovin, Thomas M. Jovin, Max-Planck-Institut für Biophysikalische Chemie (Germany)

This paper reports on the development of the latest generation Programmable Array Microscope (PAM) which utilizes the Texas Instruments 1080p micromirror device as a spatial light modulator and two sCMOS cameras for dual-path detection. Optically sectioned images of 2 megapixels can be acquired at up to 200 fps.

The PAM achieves optical sectioning by projecting a sequence of binary illumination patterns in the focal plane of the microscope objective using the DMD as a spatial light modulator (SLM). The resulting patterned fluorescence emission is captured by the objective, and sent back to the same SLM, where the conjugate (~ in-focus) and non-conjugate (~ out-of-focus) light is separated optically and captured simultaneously on camera. Use of the non-conjugate image and pseudo-random illumination/detection patterns allows pixel duty cycles of up to 50% without degradation in optical sectioning performance, and therefore high imaging speed and efficiency.

The DMD runs at 25 kHz binary frame rate, which with typical PAM sequences allows optical sectioning frame rates well above 1000 fps. We are currently limited in speed by the camera. The fastest sCMOS cameras presently available allow us to record the full 2MP PAM image at 200 fps. Cropping to a narrower image (128px), allows a speed of 1600 fps.

Because the PAM uses a freely programmable spatial light modulator, many "advanced" fluorescence imaging modes are readily available, such as photo conversion and FRAP in arbitrary regions of interest, Minimized Light Exposure (MLE) to reduce photo bleaching, and superresolution strategies.

9376-13, Session 4

**In vivo confocal imaging of the retina
using patterned illumination**

Mathivanan Damodaran, Kari V. Vienola, Rotterdam Ophthalmic Institute (Netherlands) and Vrije Univ. Amsterdam (Netherlands); Boy Braaf, Vrije Univ. Amsterdam (Netherlands); Koenraad A. Vermeer, Rotterdam Ophthalmic Institute (Netherlands); Mattijs de Groot, Johannes F. de Boer, Vrije Univ. Amsterdam (Netherlands)

The human chorioretinal system is associated with a number of diseases owing to its complicated structure. Structural information of the retina obtained from a confocal scanning laser ophthalmoscope (cSLO) helps to improve disease diagnosis and clinical care but eye motion demands high-speed imaging to prevent image artifacts. Digital micromirror devices (DMD's) have found applications in confocal imaging, especially in microscopy and helps to achieve high-speed imaging without compromising resolution or contrast. We present a cSLO using a DMD for high resolution retinal imaging.

Confocal imaging depends on directing the illumination beam via pinholes to a single focus spot that is scanned over a region of interest (ROI) in the sample. In a DMD, a single mirror or group of mirrors can be used to create illumination and/or detection pinholes. A system is presented in which a DMD is used to create a large number of parallel illuminations spots. In order to increase flexibility and have control over the system confocality, pinholes in the detection path are applied digitally (virtual pinholes). A confocal image over the full ROI is reconstructed from a sequence of subsampled images corresponding to a series of shifted DMD illumination patterns.

In contrast to conventional SLOs which typically use a single spot scanning method, this system has two advantages. Firstly, the DMD creates parallel spots and continuously scans the retina over the entire ROI. Secondly, virtual pinholes offer great flexibility in post-processing, as it is not necessary to choose a pre-defined pinhole size for detection.

9376-14, Session 4

**Non-mydratric confocal retinal imaging
using a digital light projector**

Matthew S. Muller, Aeon Imaging, LLC (United States); Jason J. Green, Karthikeyan Baskaran, Indiana Univ. (United States); Allen Ingling, Jeffrey Clendenon, Thomas J. Gast, Aeon Imaging, LLC (United States); Ann E. Elsner, Indiana Univ. (United States)

A 3rd generation confocal non-mydratric retinal camera, the Digital Light Ophthalmoscope (DLO), is presented, which uses digital light projector (DLP) technology to achieve advantages in size, cost, robustness, and flexibility over standard retinal cameras.

The DLO substitutes a DLP for the traditional illumination and scanning elements in a confocal imaging system. To simulate continuous line scanning, the DLP rapidly projects adjacent lines across the field of view. The backscattered light from each illumination line is not descanned, but

Conference 9376: Emerging Digital Micromirror Device Based Systems and Applications VII

rather synchronized to a CMOS sensor's rolling shutter to achieve spatial filtering.

The 3rd generation DLO uses Texas Instruments' DLP LightCrafter 4500 to perform real-time imaging at 42 Hz using a USB3.0 camera (IDS Imaging Development Systems GmbH). The retina is illuminated using the DLP's built-in red (640 nm) or green (530 nm) LED channels with 48 lines that cover a maximum field of view of 42 deg. A small, minimum 1 mm, entrance/exit pupil permits non-mydratic imaging. Image frames are registered, averaged, and overlaid to produce pseudo-color fundus photos with a resolution of 1024 x 768 pixels. Retinal images of undilated subjects demonstrate good vessel contrast across the field of view.

The DLO is a cost-effective platform that can be modified to use dynamic illumination patterns sent from a PC video card to perform vision research tests such as static and kinetic perimetry. With the addition of optical filters, the DLO can perform autofluorescence imaging, as well as high contrast confocal imaging using less pupil constricting orange (~570nm) illumination.

9376-15, Session 5

Micro-mirror arrays for Raman spectroscopy (*Invited Paper*)

Walter M. Duncan, The Univ. of Texas at Dallas (United States)

In the Computational Imaging and Photonic Systems group at the University of Texas at Dallas, we are studying Raman and fluorescence spectroscopies as non-destructive and non-invasive methods for probing biological material and "living systems." Particularly in living systems any probe technology need be non-destructive and non-invasive, as well as provide real time measurement information and be cost effective in order to be generally useful. Over the past few years the components needed to measure weak and complex processes such as the Raman scattering have evolved substantially with the ready availability of lasers, dichroic filters, low noise and sensitive detectors, digitizers and signal processors. A Raman spectrum consists of a wavelength or frequency spectrum of the inelastic Raman photon signal that result from a material that has been optically injected usually using a single frequency laser. The Raman fingerprint that results from a Raman spectrum can be determined from the light frequencies scattered and received by an appropriate detector then the spectra is usually "digitized" and numerically matched to a reference sample or reference material spectra. Fortunately today with the many "commercial off-the-shelf" components that are available, weak intensity effects such as Raman and fluorescence spectroscopy are available technologies in a number of applications.

One of the experimental limitations for the Raman effect and other inelastic measurement methods is the spectrometer itself. The spectrometer is the section of the system that either by interference and detection, or by dispersion and detection that signal amplitude versus energy/frequency signals are measured. Particularly in Raman spectroscopy but in fluorescence spectroscopy as well, optical signals carrying desired "information" about the analyte are extraordinarily weak and require special considerations when measuring. We will discuss here the use of micro-mirror arrays for analyzing dispersed light as needed in Raman and fluorescent applications as well as compare to results from a standard dispersive Raman spectrometer and to interference spectroscopy (e.g. FT Raman) as well.

9376-16, Session 5

DMD-based programmable wide field spectrograph for Earth observation

Frédéric Zamkotsian, Patrick Lanzoni, Lab. d'Astrophysique de Marseille, CNRS (France); Arnaud Liotard, Thierry Viard, Thales Alenia Space (France); Vincent Costes, Philippe-Jean Hébert, Ctr. National d'Études Spatiales (France)

In Earth Observation, Universe Observation and Planet Exploration, scientific return could be optimized in future missions using MOEMS devices. In Earth Observation, we propose an innovative reconfigurable instrument, a programmable wide-field spectrograph where both the FOV and the spectrum could be tailored thanks to a 2D micromirror array (MMA).

For a linear 1D field of view (FOV), the principle is to use a MMA to select the wavelengths by acting on intensity. This component is placed in the focal plane of a first grating. On the MMA surface, the spatial dimension is along one side of the device and for each spatial point, its spectrum is displayed along the perpendicular direction: each spatial and spectral feature of the 1D FOV is then fully adjustable dynamically and/or programmable. A second stage with an identical grating recomposes the beam after wavelengths selection, leading to an output tailored 1D image.

A mock-up has been designed, fabricated and tested. The micromirror array is the largest DMD in 2048 x 1080 mirrors format, with a pitch of 13.68µm. A synthetic linear FOV is generated and typical images have been recorded at the output focal plane of the instrument. By tailoring the DMD, we could modify successfully each pixel of the input image: for example, it is possible to remove bright objects or, for each spatial pixel, modify the spectral signature.

The very promising results obtained on the mock-up of the programmable wide-field spectrograph reveal the efficiency of this new instrument concept for Earth Observation.

9376-17, Session 5

Techniques and applications of programmable spectral pattern coding in DLP spectroscopy

Eric Pruett, Texas Instruments Inc. (United States)

The architecture of a DLP spectrometer allows techniques of spectrum measurement through programmable patterns previously not possible by conventional spectrometers. Certain industry applications of spectroscopy have constraints on sampling methods or sampling time. Other applications have a priori knowledge of expected substances or contaminants. By defining custom scan patterns and decoding techniques to take advantage of this information, we can optimize a system by maximizing detection accuracy and minimizing scan time. Various techniques are shown, along with the applications that may find these techniques useful.

9376-18, Session 5

Programmable spectroscopy enabled by DLP

Bjarke Rose, Ibsen Photonics A/S (Denmark)

Ibsen Photonics has since 2012 worked to deploy Texas Instruments DLP® technology to high efficiency, fused silica transmission grating based spectrometers and programmable light sources. The use of Digital Micromirror Devices (DMDs) in spectroscopy, allows for replacement of diode array detectors by single pixel detectors, and for the design of a new generation of programmable light sources, where you can control the relative power, exposure time and resolution independently for each wavelength in your spectrum.

We present the special challenges presented by DMD's in relation to stray light and optical throughput, and we comment on the possibility for instrument manufacturers to generate new, dynamic measurement schemes and algorithms for increased speed, higher accuracy, and greater sample protection. We compare DMD based spectrometer designs with competing, diode array based designs, and provide suggestions for target applications of the technology.

**Conference 9376: Emerging Digital Micromirror
Device Based Systems and Applications VII**

9376-19, Session 6

Replacing scanning based laser processing applications with variable mask image amplification systems using TI DMD, pulsed Nd:YAG lasers, and amplifiers
(Invited Paper)

Farzan N Ghauri, Vardex Laser Solutions LLC (United States); Raymond Jones, Montana Laser Technologies (United States); Ryan Feeler, Mark E. Kushina, Northrop Grumman Cutting Edge Optronics (United States)

Laser processing methods based on projection of amplified images provide significant benefits compared to scanning based methods in applications with variable high resolution information. Using the Texas instrument Digital Micromirror Device (DMD) as a Variable Mask, an image amplification architecture is presented that provides pulse energies (50mJ ~ 250mj) and peak powers necessary to process large areas (several cm²) with variable high resolution information. The seed lasers and the amplifiers used in the architecture are pulsed Nd:YAG systems. Results of the DMD based image amplification architecture as a laser marking system show that compared to scanning based marking, the system can mark larger areas of materials with superior resolution in shorter times.

9376-20, Session 6

Angularly sensitive detector for transmission Kikuchi diffraction in a scanning electron microscope

Bryce Jacobson, Kaley Woods, RadiaBeam Technologies, LLC (United States)

New methods in thin-film analysis have been developed which take advantage of elastic scattering of incoherent electrons (Kikuchi Diffraction) providing information of the exit surface of the sample material. Instead of the high-energy probe beams of TEM machines where Kikuchi lines are usually observed along with the coherent primary diffraction pattern, the new form of analysis employs low energy SEM beams. This method has been described as TEM-in-SEM (t-SEM), Transmission EBSD, and Transmission Kikuchi Diffraction (TKD) and requires the detection and indexing of dim and diffuse Kikuchi patterns in the presence of bright field backgrounds.

In order to best take full advantage of this new method of material analysis, an arbitrarily reconfigurable detector with ultra-fine angular selectivity is needed for the SEM. We have developed a unique and novel detector which allows for simultaneous Bright Field and Kikuchi Diffraction imaging of thin samples in SEM machines. Unlike EBSD cameras with limited field of view and orientation to the beam column, our prototype detector has achieved a 20 degree field of view in the scattering plane with better than 0.5 degree selectivity and ultra-high dynamic range capability. Integration into an SEM is underway with initial tests forthcoming.

This paper will discuss the experimental methods, results, and technological implications of this system.

9376-21, Session 6

The Si elegans connectome: A neuromimetic emulation of neural signal transfer with DMD-structured light

Alexey Petrushin, Lorenzo Ferrara, Axel W. Blau, Istituto Italiano di Tecnologia (Italy)

The parallel computational power of even the simplest biological neural

system cannot be taken advantage of without a deeper understanding of its function. The Si elegans project (www.si-elegans.eu) aims at developing a hardware-based computing framework that accurately replicates nervous system function and behavior of the tiny worm *Caenorhabditis elegans*. The nervous system of the *C. elegans* hermaphrodite is composed of exactly 302 neurons and about 8000 connections. In its Si elegans emulation, each neuron will be simulated by an individual field-programmable gate array (FPGA) board that carries a neuron-specific response model. To mimic the parallel nature of nervous system interconnectivity and information flow, these FPGA neurons will be linked and communicating through an electro-optical connectome. Individual FPGA I/O pins will act as synaptic or electrical junctions and be connected to separate photodetectors. Information will be transmitted between neurons by spatially structured light. An axonal beam from an active neuron will be simultaneously distributed onto the receptive field of post-synaptic neurons by one of 302 digital micromirror devices (DMDs). For this purpose, a dedicated custom circuit demultiplexes the control signal of a digital light processing (DLP) device (LightCrafter, Texas Instruments) to drive an array of DMDs on a time-shared basis. A LabVIEW (National Instruments) application downloads a sequence of 302 patterns onto the respective DMDs. A microcontroller supervises the timing. This paper gives an overview of the electro-optical *C. elegans* connectome emulation concept and the required components along with an early small-scale implementation of the optical communication between FPGA boards.

9376-22, Session 7

Applications of DMDs in quantum information science

Robert W. Boyd, Univ. of Rochester (United States) and Univ. of Ottawa (Canada); Mohammad Mirhosseini, Omar S. Magaña-Loaiza, Brandon Rodenburg, Robert Cross, Univ. of Rochester (United States)

We describe our use of digital micromirror devices (DMDs) in our research on quantum communication. The goal of our research is to develop a quantum key distribution (QKD) system that can carry many bits of information onto a single photon by encoding in the basis of Laguerre-Gauss (LG) modes. As these modes constitute an infinite-dimensional set, there is in principle no limit on how much information can be encoded onto a single photon. Previous workers have usually made use of liquid-crystal spatial light modulators (SLMs) to form beams in LG modes. However, we have found that we can obtain enhanced performance in terms of higher configuration rates and lower system costs by replacing the SLMs with DMDs. In this presentation we will also present results describing the performance of our current QKD system. We also describe how we use a DMD to create light field with controllable spatial coherence.

9376-23, Session 7

Controlling the phase and amplitude of light using a digital micromirror device

Sebastianus A. Goorden, Univ. Twente (Netherlands); Jacopo Bertolotti, Univ. of Exeter (United Kingdom) and Univ. Twente (Netherlands); Allard P. Mosk, Univ. Twente (Netherlands)

Shaping of light waves is of great importance in areas such as holography, microscopy, optical micromanipulation, optical communication, security and imaging inside scattering media. A very promising device for shaping light is the digital micromirror device (DMD), because of its very high speed and large number of pixels.

We present a superpixel method for full spatial phase and amplitude control of a light beam using a DMD combined with a low-pass spatial filter in the Fourier plane. The spatial filter averages the field responses of a group of

**Conference 9376: Emerging Digital Micromirror
 Device Based Systems and Applications VII**

DMD pixels to a superpixel response. The DMD is illuminated under an angle such that the pixels within a superpixel have phase responses uniformly distributed between 0 and 2π . The superpixel responses of all possible superpixel settings cover a disk in the complex plane, allowing full and independent control over phase and amplitude.

The superpixel method leads to a modulation fidelity $F=0.98$ for a high resolution test field with fully independent amplitude and phase and $F=0.99993$ for a LG10 orbital angular momentum mode. Our method is more accurate than state of the art Lee holography and equally efficient, easy to use and robust to misalignment. A DMD in combination with our superpixel method offers an excellent platform for measuring transmission matrices of e.g. fibers and scattering materials.

9376-24, Session 7

**Fast and stable polarization state
 generation using DLP technology**

Alan She, Federico Capasso, Harvard Univ. (United States)

We have developed an approach for polarization state generation using a Texas Instruments DLP digital micromirror device (DMD). The DMD as a spatial light modulator is used to modulate spatially-separated Stokes polarization components of a input laser beam to digitally generate a laser beam with arbitrary state of polarization (SOP), including control over the degree of polarization. Current methods of polarization state generation often rely on the addition of control systems to compensate for the lack of stability and repeatability of generated polarization states due to the use of moving parts, such as rotating wave plates or bending fibers. The approach here aims to improve on the speed and stability using DMD over existing methods, while also enabling a compact and robust form in future device applications. Measurements of the performance of this approach, such as SOP settling time, SOP accuracy, degree of polarization accuracy, etc., are compared to the advertised specifications of existing commercial technologies. Polarization state generation has found applications in optics and telecommunications, as well as other areas of science, including chemistry, biology, and astronomy.

9376-25, Session 7

**Non diffraction beam generation using
 digital micromirror device (DMD)**

Yongdong Wang, Yilei Zhang, Nanyang Technological Univ. (Singapore)

Bessel beams have very interesting and useful properties, such as non-diffraction over propagation distance and self-healing beyond an obstacle. A straightforward but powerful method to generate Bessel beams with continuous control of spot size, intensity and non-diffraction zone length has been successfully developed and verified based on annular reflections using a Digital Micromirror Device (DMD). Reflective circular ring patterns were loaded in a DMD placed in the focal point of a converging lens to generate Bessel beams with tremendous flexibility and control. The generated Bessel beam could propagate more than one meter without any diffraction. Furthermore, a systematic study shows that the spot size of the generated Bessel beam could be controlled within a large range by varying diameters of the ring patterns while varying the ring thickness will not have significant effects on it. On the other hand, the intensity of the generated Bessel beam could be varied significantly by controlling the ring thickness. The non-diffracting zone length of the generated Bessel beam could be precisely controlled in a large range by varying the ring diameter and/or thickness loaded on the DMD. A new explicit model was also developed and shows good agreement with experimental results. This method has great potential in many applications, such as high resolution imaging and particle manipulation.

Conference 9377: Advances in Photonics of Quantum Computing, Memory, and Communication VIII

Tuesday - Thursday 10-12 February 2015

Part of Proceedings of SPIE Vol. 9377 Advances in Photonics of Quantum Computing, Memory, and Communication VIII

9377-1, Session 1

Fluorescence imaging and quantum sensing using nitrogen-vacancy centers in nanodiamonds (*Invited Paper*)

Huan-Cheng Chang, Academia Sinica (Taiwan)

Much of the studies on negatively charged nitrogen-vacancy (NV⁻) centers in diamond have been focused on their unique photophysical properties and quantum optical applications at room temperature using bulk crystals. Our group, on the other hand, has been interested in the characterization and use of these color centers in nanoscale diamonds (known as fluorescent nanodiamonds, FNDs) for super-resolution microscopy, bioimaging, and nanoscale sensing applications. For FNDs with a size in the range of 100 nm, they typically have a fluorescence lifetime of ~20 ns, which is distinctly different from those (<10 ns) of cell and tissue autofluorescence, making it possible to achieve background-free detection *in vitro* and *in vivo* by time gating. Moreover, the centers in the particles exhibit a distinct magnetic resonance peak at 2.87 GHz for the $m_s = 0 \rightarrow m_s = \pm 1$ transitions, similar to that of NV⁻ in bulk diamond. In this presentation, we will discuss how FNDs can be applied as photostable contrast agents for *in vivo* imaging by fluorescence lifetime imaging microscopy (FLIM) and quantum sensors for nanoscale thermometry with optically detected magnetic resonance (ODMR) at the single particle level. Also, we demonstrate that gold-nanorod-conjugated FNDs can serve as both a nanoheater and a nanothermometer in solution and cells. The integration of heating and temperature sensing functions on the same particles offers an opportunity for active and high-precision control of temperature at the nanoscale by pure optical means.

9377-2, Session 1

Neurons on diamond: towards optical sensing of action potential (*Invited Paper*)

Milos Nesladek, Mathew McDonald, Univ. Hasselt (Belgium); Micha Spira, The Hebrew Univ. of Jerusalem (Israel)

Brain Machine Interface Technologies (BMITs) require novel highly parallel neural interfaces permitting readout from a large number of interacting neurons. At the same time, techniques allowing coupling single neurons to individual nano-sized electrodes are of high demand for further progress in neuroscience engineering. A critical part of the active interface is the biocompatible device, a microelectrode array that is physically and electrically interfaced with neurons. Based on the original work of Spira [1], tight extracellular interfaces of engulfing electrodes were fabricated, allowing access even to sub threshold synaptic potentials. Such nanoscale devices can also be used for effective intracellular stimulation. However a complex optimization of the cell-electrode interface and tuning the electrode properties, such as the seal and junction resistances is required. One of the further limitations of multiparallel microelectrode arrays is high number electrical leads.

Optical contactless readout is anticipated to bring progress to BMITs; however, the practical realization is still far away. Current devices rely mainly on extrinsic fluorescent indicators or genetically encoded molecular probes, suffering from reliability, cell toxicity and not allowing chronic operations (stimulations, recording). In this work we come with novel a paradigm that combines 3D engulfing electrodes with optical sensing. We discuss Nitrogen-Vacancy color centre sensors, to be used for reading the action potential. Fabrication of the sensor and experimental contactless detection

arrangement is discussed. 3D diamond electrodes are interfaced to cortical and hippocampus neural cells. The interface is studied by using Focused Ion beam, demonstrating a tight engulfment of electrodes by the neurons. We discuss the experimental setup employing NV color centers, engineered in each of the electrodes, to be used as a contactless sensor for optical magnetic resonance detection of the action potential. The biocompatibility of the fabricated interfaces is established. We demonstrate reliable and durable growth of primary neurons on diamond electrodes using chemical functionalization.

[1] M. Spira and A. Hai, *Nature Nanotechnology* 8, (2013).

[2] A.M. Ojovan, M. McDonald, N. Rabieh, N. Shmuel, H Erez M Nesladek, M.E. Spira, *Front Neuroeng.*, doi: 10.3389/fneng.2014.00017 (2014).

9377-3, Session 1

Nanoscale magnetic resonance detection and imaging using nitrogen-vacancy centers in diamond (*Invited Paper*)

Daniel Rugar, IBM Research - Almaden (United States)

Nuclear magnetic resonance (NMR) is the basis of powerful spectroscopic and imaging techniques, but extension to nanoscale samples has been a longstanding challenge due to the insensitivity of conventional detection methods. We are exploring the use of individual, near-surface nitrogen-vacancy (NV) centers in diamond as atomic-size magnetometers to detect proton NMR in organic material located external to the diamond. Using a combination of electron spin echoes and proton spin manipulation, the NV center senses the nanotesla field fluctuations from the protons, enabling both time-domain and spectroscopic NMR measurements on the nanometer scale. By scanning a small polymer test object past a near-surface NV center, we have recently demonstrated proton magnetic resonance imaging (MRI) with spatial resolution on the order of 12 nm.

Work performed in collaboration with H. J. Mamin, M. Kim, M. H. Sherwood, C. T. Rettner, K. Ohno, and D. D. Awschalom

9377-4, Session 2

Microplasma synthesis of sub-5 nm nanodiamonds (*Invited Paper*)

R. Mohan Sankaran, Case Western Reserve Univ. (United States)

Nanodiamonds are nanometer-sized clusters of diamond-phase carbon nanoparticles that have received interest for their unique structure, diamond-like mechanical and thermal properties, photoluminescence, and biocompatibility. Nanodiamonds have been detected in outer space and synthetically produced by high pressure/high temperature (HPHT), detonation of carbon-containing explosives, and chemical vapor deposition (CVD). Despite the availability of various forms of nanodiamonds, the controlled formation of nanodiamonds in terms of size, chemical composition, purity, and surface chemistry remains a challenge.

In this talk, I will present our development of a plasma-based process that dissociates carbon feedstock vapors and homogeneously nucleates carbon nanoparticles including nanodiamonds. The plasma is formed over confined electrode geometries and referred to as a microplasma. The limited residence time for particle nucleation and growth quenches the particle size, resulting in sub-5 nm particles. We have characterized the nanodiamonds by several techniques including UV micro Raman spectroscopy, X-ray

**Conference 9377: Advances in Photonics of
 Quantum Computing, Memory, and Communication VIII**

diffraction, transmission electron microscopy, and X-ray photoelectron spectroscopy. Details of the process as well as the materials analysis will be discussed.

9377-5, Session 2
Sub-diffraction optical manipulation of the charge state of nitrogen vacancy center in diamond

Fang-Wen Sun, Xiang-Dong Chen, Chang-Ling Zou, Guang-Can Guo, Univ. of Science and Technology of China (China)

Owing to the stable fluorescence and long coherence time of its spin state, the negatively charged nitrogen vacancy center (NV⁻) has the potential in quantum computation and nanoscale sensing. To further extend the study of multi-NV-center, it is necessary to detect and control the NV center spin state dynamics with high spatial resolution.

Here we demonstrated the optical image and manipulation of the state of NV center with sub-diffraction resolution based on the charge state conversion. There are two charge states in NV center, NVO and NV⁰, which are stable in the absence of optical excitation and can be distinguished by measuring the fluorescence. The highest population of about 75% (95%) for NV⁻ (NVO) can be obtained by excitation with a 532 nm green (637 nm red) laser. Also, the transition between them can be well controlled with lasers. In the experiment, a red (green) Gaussian beam was used to initialize the NV center to NVO (NV⁰). Then a doughnut-shaped green (red) laser pulse was applied to deplete NVO (NV⁻) charge state except for the NV at the beam center. Finally, the charge state was detected using a weak 589 nm laser pulse. By changing the duration and power of laser pulses, we optimized the charge state depletion (CSD) microscopy to improve the resolution to 4.1 nm without oil immersion lens. With the charge state manipulation, we were able to control and detect the electron spin state dynamics of NV centers with sub-diffraction resolution, which can be used for the nanoscale sensing of electromagnetic field and biological molecules, and the study of spin state quantum coherent dynamics for quantum information techniques.

9377-6, Session 3
Control of the cavity reflectivity using a single quantum dot spin (*Invited Paper*)

Shuo Sun, Hyochul Kim, Univ. of Maryland, College Park (United States); Glenn S. Solomon, National Institute of Standards and Technology (United States) and Joint Quantum Institute (United States); Edo Waks, Univ. of Maryland, College Park (United States)

The implementation of quantum network and distributive quantum information processing relies on interaction between stationary matter qubits and flying photons. The spin of a single electron or hole confined in a charged quantum dot is considered as a promising matter qubit as it possesses long coherence time and allows picosecond timescale control using optical pulses. The quantum dot spin can also interact with a photon by strongly coupling with an optical cavity, in which the spin can significantly alter the cavity spectrum. Yet all the experimental demonstrations of the cavity spectrum control have used neutral dots. Recently there has been demonstration of coherent control of a quantum dot spin trapped inside a photonic crystal cavity (Nature Photonics 7, 329–334 (2013)). However the system is in the very weakly coupling regime and the spin thus has negligible effects on the cavity spectrum. Here, we report an experimental realization of a spin-photon interface using a strongly coupled quantum dot and cavity system. We show large modulation of the cavity reflection spectrum by manipulating the spin states of the quantum dot. The spin-photon interface is crucial for realizing a quantum logic gate or generating hybrid entanglement between a quantum dot spin and a

photon. Our results represent an important step towards semiconductor based quantum logic devices and on-chip quantum networks.

9377-7, Session 3
Hybrid nanophotonic resonators for coupling to rare-earth ions

Evan Miyazono, Alex Hartz, Tian Zhong, Andrei Faraon, California Institute of Technology (United States)

With an assortment of narrow line-width transitions spanning the visible and IR spectrum and long spin coherence times, rare-earth doped crystals are the leading material system for solid-state quantum memories. Integrating these materials in an on-chip optical platform would create opportunities for highly integrated light-matter interfaces for quantum communication and quantum computing. Nano-photonics resonators with high quality factors and small mode volumes are required for efficient on-chip coupling to the small dipole moment of rare-earth ion transitions. However, direct fabrication of optical cavities in these crystals with current nanofabrication techniques is difficult and unparallelized, as either exotic etch chemistries or physical milling processes are required.

We fabricated hybrid devices by mechanically transferring a nanoscale membrane of gallium arsenide (GaAs) onto a neodymium-doped yttrium silicon oxide (Y₂SiO₅) crystal and then using electron beam lithography and standard III-V dry etching to pattern ring resonator cavities, a technique that is easily adapted to other frequency ranges for arbitrary dopants in any rare earth host system. Single crystalline GaAs was chosen for its low loss and high refractive index at the transition wavelength. We demonstrated evanescent coupling between the cavity field and the 883 nm 4I_{9/2}-4F_{3/2} transition of nearby neodymium impurities in the host crystal by examining transmission spectra through a waveguide coupled to the resonator with a custom-built confocal microscope. The prospects and requirements for using this system for scalable quantum networks are discussed.

9377-8, Session 3
Qubits, qutrits, and ququads stored in single photons (*Invited Paper*)

Axel Kuhn, Univ. of Oxford (United Kingdom)

Photons acting as flying information carriers are key to many modern applications of quantum technologies, and the arbitrary control of their quantum state in space and time is crucial. Here we show how to accomplish this task in the deterministic single-photon emission from coupled atom-cavity systems. We encode arbitrary qubits, qutrits and even ququads within their spatio-temporal mode profile, with a fidelity verified in quantum-homodyne measurements better than 96%. Such a close-to-perfect control of photonic wavefunctions might well change the way we think about quantum logic today. For instance, when using qutrits or ququads, powerful ternary or quaternary quantum logic concepts can be realised without the need for additional resources. We furthermore took first steps towards implementing this technique in atom-cavity arrays controlled by optical tweezers, which will open new avenues towards large-scale quantum processing.

9377-9, Session 3
Coherent control of energy transfer in a quantum dot strongly coupled to a photonic crystal molecule

Tao Cai, Univ. of Maryland, College Park (United States); Ranjoy Bose, Univ. of Maryland, College Park (United States); Kaushik R. Choudhury, Univ. of Maryland, College

**Conference 9377: Advances in Photonics of
Quantum Computing, Memory, and Communication VIII**

Park (United States); Glenn S. Solomon, National Institute of Standards and Technology (United States) and Univ. of Maryland, College Park (United States); Edo Waks, Univ. of Maryland, College Park (United States) and Joint Quantum Institute (United States)

Vacuum Rabi oscillation is a damped oscillation in which energy can transfer between an atomic excitation and a photon when an atom is strongly coupled to a photonic cavity. This process is challenging to be coherently controlled due to the fact that interaction between the atom and the electromagnetic resonator needs to be modulated in a quick manner compared to vacuum Rabi frequency. This control has been achieved at microwave frequencies, but has remained challenging to be implemented in the optical domain. Here we demonstrated coherent control of energy transfer in a semiconductor quantum dot strongly coupled to a photonic crystal molecule by manipulating the vacuum Rabi oscillation of the system. Instead of using a single photonic crystal cavity, we utilized a photonic crystal molecule consisting two coupled photonic crystal defect cavities to obtain both strong quantum dot-cavity coupling and cavity-enhanced AC stark shift. In our system the AC stark shift modulates the coupling interaction between the quantum dot and the cavity by shifting the quantum dot resonance, on timescales (picosecond) shorter than the vacuum Rabi period. We demonstrated the ability to transfer excitation between a quantum dot and cavity, and performed coherent control of light-matter states. Our results provides an ultra-fast approach for probing and controlling light-matter interactions in an integrated nanophotonic device, and could pave the way for gigahertz rate synthesis of arbitrary quantum states of light at optical frequencies.

9377-10, Session 3

Few-photon nonlinearities mediated by Rydberg interaction (*Invited Paper*)

Sebastian Hofferberth, Univ. Stuttgart (Germany)

Mapping the strong interaction between Rydberg excitations in ultracold atomic ensembles onto single photons via electromagnetically induced transparency enables manipulation of light on the single photon level. We report the realization of a free-space single-photon transistor, where a single gate photon controls the transmission of many source photons. We show that this transistor can also be operated as a quantum device, where the gate input state is retrieved from the medium after the transistor operation. This forms the basic building block of multi-photon quantum gates and may enable the non-destructive detection of single photons.

9377-11, Session 4

Continuous-variable quantum computing: toward an experimental assessment (*Invited Paper*)

Olivier Pfister, Univ. of Virginia (United States); Nicolas C. Menicucci, The Univ. of Sydney (Australia); Moran Chen, Pei Wang, Wenjiang Fan, Univ. of Virginia (United States)

Proposed in 1999 by Lloyd and Braunstein, continuous-variable quantum computing (CVQC) surfaced only recently as a viable paradigm for practical implementations. In 2008, Menicucci, Flammia, and Pfister showed that a single optical parametric oscillator (OPO) is sufficient to implement an optically based quantum computing register of size up to 10^4 "quomodes" (resonant modes of the OPO, equivalent to qubits). This QC implementation is based on the "entanglement engine" of the OPO, i.e., the multimode squeezing (quantum noise reduction, a signature of entanglement) that it creates between its quomodes, entangled in one fell swoop into a CV cluster state suitable for one-way QC.

The Pfister group has pursued the experimental implementation of

these ideas and demonstrated the simultaneous generation of fifteen quadripartite cluster states, as well as, more recently, two 30-partite, and one 60-partite, cluster states in the quantum optical frequency comb (QOFC) of a single OPO. The latter realization is the largest entangled state ever created in the laboratory on any physical system whose subsystems are all simultaneously available.

On the theory side, Menicucci recently proved the existence of a fault-tolerance threshold for one-way CVQC using a qubit implementation proposed in 2001 by Gottesman, Kitaev, and Preskill, an error rate of 10^{-6} corresponding to 20.5 dB of squeezing in the entangled resources. For topological encodings such as proposed by Raussendorf in 2006, the threshold error rate raises to about 1%, which mandates about 15 dB of squeezing.

These advances have opened up tantalizing prospects for the practical implementation of CVQC, which will be assessed in this talk.

9377-12, Session 4

Extensions to the Wigner inequality for high-loss experimental scenarios

William N. Plick, Institut für Quantenoptik und Quanteninformation (Austria); Johannes Kofler, Max-Planck-Institut für Quantenoptik (Germany)

The original Wigner inequality - which was first derived in 1969 - presented an easy and straightforward way to understand the contradiction between local realistic theories and quantum mechanics. However it has been mostly inequities based on Bell's original inequality that have become familiar in experiments - most notably CHSH, CH, and Eberhard. We will show how - by extending the counterfactual logic of Wigner's inequality - new formulas can be derived which may have advantages over other more traditional approaches.

9377-13, Session 4

New concepts and laboratory protocols for quantum technologies (*Invited Paper*)

Robert W. Boyd, Univ. of Ottawa (Canada) and Univ. of Rochester (United States)

We first discuss some fundamental issues in quantum technologies. One issue is an analysis of a recent experiment of Menzel et al. that appears to violate the tenet that fringes in two-path interference must disappear when "which path" information is known [1]. Another issue is the use of weak values to perform direct measurements of the photon wave function [2]. The second part of the talk describe improved laboratory procedures for encoding information onto a single photon by using modes that carry orbital angular momentum (OAM). These procedures include better computer-generated holograms, more efficient projective measurements [3], and construction of plasmonic q-plates [4].

1. Wave-particle dualism and complementarity unraveled by a different mode, Ralf Menzel, Dirk Puhlmann, Axel Heuer, and Wolfgang P. Schleich, *Publ. Nat. Acad. Science*, www.pnas.org/cgi/doi/10.1073/pnas.1201271109

2. Amplification of angular rotations using weak measurements, O.S. Magaña-Loaiza, Mohammad Mirhosseini, Brandon Rodenburg, and R.W. Boyd, *Phys. Rev. Lett.* 112, 200401 (2014).

3. Limitations to the determination of a Laguerre-Gauss spectrum via projective, phase-flattening measurement, H. Qassim, F.M. Miatto, J.P. Torres, M.J. Padgett, E. Karimi, and R.W. Boyd, *J. Opt. Soc. Am. B.* 31, A20-A23 (2014)

4. Generating optical orbital angular momentum at visible wavelengths using a plasmonic metasurface, E. Karimi, S. Schulz, I. De Leon, H. Qassim, J. Upham, and R.W. Boyd, *Light: Science & Applications* (2014).

**Conference 9377: Advances in Photonics of
 Quantum Computing, Memory, and Communication VIII**

9377-14, Session 4

An ultrahigh-resolution quantum optical coherence tomography with dispersion-tolerance (*Invited Paper*)

Shigeki Takeuchi, Osaka Univ. (Japan) and Kyoto Univ. (Japan); Masayuki Okano, Ryo Okamoto, Kyoto Univ. (Japan); Sunao Kurimura, National Institute for Materials Science (Japan); Norihiko Nishizawa, Nagoya Univ. (Japan)

In this talk, we will report our recent progresses on quantum metrology.

 Optical coherence tomography has been a key technology in medicine and biology as an invasively tomographic imaging technique. However, the axial resolution in a sample has been limited to the order of 10 μm due to the dispersion effect. As an alternative technique, quantum optical coherence tomography has been demonstrated in the low-resolution regime with 19 μm -resolution and it shows dispersion-tolerance by virtue of the quantum entanglement of entangled photon pairs.

 In this presentation, we report the demonstration of the dispersion-tolerance of the quantum optical coherence tomography in the high-resolution regime. We show that the high resolution of 3 μm can be completely remained even in the presence of 25-mm thick water (a diameter of a human eye) [1]. In contrast the resolution of 4.2 μm in the optical coherence tomography degrades to 38 μm with the 25-mm thick water. We also discuss the resolution-enhancement in comparison with optical coherence tomography. This experimental demonstration will open the door for the broad application of quantum metrology from medicine and biology to material science. In the talk, we will also report the most updated result using the ultra-broadband spontaneous parametric fluorescence (over 160 THz) generated from a chirped quasi-phase matching device [2]. Sub-micron resolution with dispersion-tolerance will be discussed.

[1] M. Okano, S. Takeuchi, et. al., PRA88, 043845 (2013).

[2] A. Tanaka, S. Takeuchi, et. al., Opt. Express20, 25228 (2012).

9377-15, Session 5

Time-bin entangled photon pairs from spontaneous parametric down-conversion pumped by
a cw multi-mode diode laser (*Invited Paper*)

Yoon-Ho Kim, Pohang Univ. of Science and Technology (Korea, Republic of)

Generation of time-bin entangled photon pairs requires the use of the Franson interferometer which consists of two spatially separated unbalanced Mach-Zehnder interferometers through which the signal and idler photons from spontaneous parametric down-conversion (SPDC) are made to transmit individually. There have been two SPDC pumping regimes where the scheme works: the narrowband regime and the double-pulse regime. In the narrowband regime, the SPDC process is pumped by a narrowband cw laser with the coherence length much longer than the path length difference of the Franson interferometer. In the double-pulse regime, the longitudinal separation between the pulse pair is made equal to the path length difference of the Franson interferometer. In this paper, we propose another regime by which the generation of time-bin entanglement is possible and demonstrate the scheme experimentally. In our scheme, differently from the previous approaches, the SPDC process is pumped by a cw multi-mode (i.e., short coherence length) laser and makes use of the coherence revival property of such a laser. The high-visibility two-photon Franson interference demonstrates clearly that high-quality time-bin entanglement source can be developed using inexpensive cw multi-mode diode lasers for various quantum communication applications.

9377-16, Session 5

Quantum sensing meets compressive sensing (*Invited Paper*)

John C. Howell, Gregory Howland, James Schneeloch, Daniel Lum, Univ. of Rochester (United States)

I will give a brief overview of compressive sensing. I will then discuss our recent efforts to use compressive sensing for measuring quantum signals. I will discuss three experiments where we used compressive sensing to efficiently measure high-dimensional quantum signals: compressive wave function measurement, simultaneous measurement of complementary observables and transverse momentum position entangled photons.

9377-17, Session 5

Quantum-secure authentication without secret information

Sebastianus A. Goorden, Marcel Horstmann, Allard P. Mosk, Univ. Twente (Netherlands); Boris Koric, Technische Univ. Eindhoven (Netherlands); Pepijn W. H. Pinkse, Univ. Twente (Netherlands)

Modern society strongly relies on secret information for authentication. Human as well as computer-based parties typically verify each other's identity before engaging in transaction. With the exception of direct human-to-human interaction, this is almost exclusively done through the possession and verification of secret information. This information must be simultaneously secret and accessible, preferably without human intervention. In modern society this is exceedingly difficult to achieve.

We experimentally demonstrate an authentication method that does not require keeping secret information: Quantum-Secure Authentication (QSA) [1] with an optical Physical Unclonable Function (PUF) as a key. We illuminate the key using light with a quantum character: containing fewer photons than spatial degrees of freedom. Upon entering the key the photons are multiple-scattered by millions of randomly organized nanoparticles. The spatial shape of the returned ("response") photons depends strongly on the positions of the scatterers and on the incident ("challenge") photons. Assuming its challenge-response behavior is known, the key can be authenticated by illuminating it with a challenge and verifying whether the response is as expected.

Quantum-physical principles forbid an attacker to fully characterize the challenge. Therefore, he cannot digitally construct the correct response even if the challenge-response behavior of the key is publicly known. QSA is secure if the physical key is impossible to copy. This is believed to be the case for e.g. the random arrangement of scattering nanoparticles in dried white paint. QSA forms a valuable alternative to authentication methods that rely on keeping secret information.

[1] Goorden et al., arXiv:1303.0142 (2013)

9377-18, Session 6

Device-independent verification of entanglement and entangled measurements (*Invited Paper*)

Geoff J. Pryde, Griffith Univ. (Australia)

Shared entanglement (between two remote parties, for example) can provide the basis for absolutely secure communication, the basis for guaranteed randomness, and allows the teleportation of quantum information, because it establishes strong 'nonlocal' correlations.

The existence of such correlations between distant parties can be tested without trusting the measurement devices used, or the parties themselves.

**Conference 9377: Advances in Photonics of
Quantum Computing, Memory, and Communication VIII**

This leads to device-independent unconditionally secure quantum information tasks, but requires loophole-free Bell inequality violations, with their challenging requirements on detection and transmission efficiency. An easier test, EPR-steering, can tolerate high losses, but requires complete trust in one party and their equipment. We have demonstrated how to overcome this limitation in using EPR-steering for device-independent entanglement verification [1]. In this technique, the use of quantum states (instead of classical information) to encode some measurement settings removes the need for either party to be trusted.

Entangled *measurements* also play a very important role in remote entanglement sharing, being a central part of quantum teleportation, entanglement swapping, repeater (etc.) protocols. We experimentally demonstrate a procedure for witnessing entangled measurements [2] that, similar to Bell inequalities for states, relies on only experimental statistics. Our procedure is termed semi-device-independent, as it uses uncharacterized quantum preparations of fixed Hilbert space dimension.

[1] S. Kocsis, M. J. W. Hall, A. J. Bennet and G. J. Pryde, arXiv:1408.0563

[2] A. J. Bennet, T. Vertesi, D. J. Saunders, N. Brunner and G. J. Pryde, accepted to Phys. Rev. Lett; arXiv:1404.1422

9377-19, Session 6

Preserving flying qubit in single-mode fiber with Knill Dynamical Decoupling (KDD) (Invited Paper)

Manish Kumar Gupta, Louisiana State Univ. (United States); Erik Navarro, California State Univ., Chico (United States); Todd Moulder, Jason Mueller, Ashkan Balouchi, Katherine L. Brown, Hwang Lee, Jonathan P. Dowling, Louisiana State Univ. (United States)

Quantum computer have been theoretically shown to have far reaching application from interferometric measurement, prime factoring to crypto systems. Quantum information and quantum cryptographic systems use photon as their information carrier and they encodes information into polarization degree of freedom of photon. Achieving secure long-distance communication over single mode fiber is plagued by the interaction of qubit with the environment that causes loss of coherence and subsequently loss of information. This effect is called decoherence and it limits the distances over which quantum information can be retained and transmitted.

The implementation of information theoretic crypto protocol is limited by decoherence caused by the birefringence in a single mode fiber. We propose a scheme to preserve the polarization qubit from from birefringent dephasing in a single mode fiber by implementing Knill dynamical decoupling pulse sequence, where we implement the π pulses sequence by introducing half-wave plate (HWP) at specified distances in the fiber.

We numerically show that diagonal state of polarization can be preserved in a single mode fiber with our scheme even in presence of 0.5% pulse error, a fidelity greater than 96% between input and output state can be achieved. We also show that KDD performs better than CPMG in presence of pulse error.

9377-20, Session 6

Entanglement assisted time-energy QKD employing Franson interferometers and cavity quantum electrodynamics (CQED) principles

Ivan B. Djordjevic, The Univ. of Arizona (United States)

The study of efficient quantum key distribution (QKD) over either free-space optical or fiber-optics channels is an active research topic. Even though that significant advance has been made in QKD research and commercialization,

the secure key rates are still low, and transmission distance even over optical fiber is still limited. Most research efforts have been focused on two-dimensional qubits, implemented based on a photon polarization. Several methods have recently been proposed to increase the secure key rates. These methods rely on encoding information either using time and frequency, linear momentum, orbital angular momentum (OAM), or using multiple degrees of freedom made available through hyper-entangled states.

In this paper, we propose an entanglement assisted QKD protocol based on time-energy encoding with the number of mutually unbiased bases (MUBs) larger than two. We describe how to implement this protocol based on Weyl gate, representing a generalization of both quantum Fourier transform (QFT) gudit gate and generalized CNOT gate. The proposed gate can be implemented with a help of Franson interferometers and cavity quantum electrodynamics (CQED) principles. We then analyze the security of the proposed protocol and provide the finite key secure key rates in the presence of various imperfections including background errors, time jitter, frequency offset; to mention few. Finally, we provide the improvements in secure key rates of proposed protocol over conventional two-base time-energy QKD protocol.

9377-34, Session PWed

Domain-engineered PPLN for generation of polarization-entangled photons

Paulina Kuo, National Institute of Standards and Technology (United States); Jason Pelc, Hewlett-Packard Labs. (United States); Oliver Slattery, Lijun Ma, Xiao Tang, National Institute of Standards and Technology (United States)

Type-II spontaneous parametric downconversion can be used to generate polarization-entangled photon pairs, useful for quantum communications and distributing entanglement in quantum information systems. Typically, the polarization-entangled twin photons are generated in two distinct crystals. Here, we demonstrate production of polarization-entangled photons in a single, domain-engineered, periodically poled lithium niobate (PPLN) crystal. The domain-engineering of the quasi-phases matching allows both $|HV\rangle$ and $|VH\rangle$ states to be generated simultaneously in a distributed fashion throughout the nonlinear optical crystal. The crystal is pumped at 775 nm and produces near-degenerate, telecommunications-wavelength photon pairs at 1532 nm and 1567 nm. Near-degenerate operation results in nearly matched bandwidths for the signal and idler photons even though the crystal is birefringent. We observed 1 nm bandwidths for both $|HV\rangle$ and $|VH\rangle$ states in our 25 mm long, domain-engineered PPLN crystal. We investigate optimization of this source for entanglement visibility and collection efficiency. We study loose pump focusing for more collimated output, which enhances collection efficiency at the expense of source brightness. Such a source of entangled photons may be used for demonstration of quantum teleportation and tests of local realism.

9377-35, Session PWed

Singular layer transmission for continuous-variable quantum key distribution

Laszlo Gyongyosi, Budapest Univ. of Technology and Economics (Hungary) and Hungarian Academy of Sciences (Hungary); Sandor Imre, Budapest Univ. of Technology and Economics (Hungary)

We propose a singular layer transmission model for continuous-variable quantum key distribution (CVQKD). The singular layer uses the singular value decomposition of the Gaussian quantum channel, which yields an additional degree of freedom for the phase space transmission. The singular layer defines the eigenchannels of the Gaussian physical link, which can

**Conference 9377: Advances in Photonics of
 Quantum Computing, Memory, and Communication VIII**

be used for the simultaneous reliable transmission of multiple user data streams. Our transmission model also includes the singular interference avoider (SIA) precoding scheme. The proposed SIA precoding scheme prevents the eigenchannel interference to reach an optimal transmission over a Gaussian link. We demonstrate the results through the adaptive multicarrier quadrature division–multiuser quadrature allocation (AMQD-MQA) CVQKD multiple-access scheme. We define the singular model of AMQD-MQA and characterize the properties of the eigenchannel interference. We propose the SIA precoding of Gaussian random quadratures and the optimal decoding at the receiver. We show a random phase space constellation scheme for the Gaussian sub-channels. The singular layer transmission provides improved simultaneous transmission rates for the users with unconditional security in a multiple-access scenario, particularly in crucial low signal-to-noise ratio regimes.

9377-36, Session PWed

Abstract probabilistic CNOT gate model based on double encoding: study of the errors and physical realizability

Amor Gueddana, Attia Moez, Rihab Chatta, SUP'COM (Tunisia)

In this work, we study the error sources standing behind the non-perfect linear optical quantum components composing a non-deterministic quantum CNOT gate model, which performs the CNOT function with a success probability of $4/27$ and uses a double encoding technique to represent photonic qubits at the control and the target. We generalize this model to an abstract probabilistic CNOT version and determine the realizability limits depending on a realistic range of the errors. Finally, we discuss physical constraints allowing the implementation of the Asymmetric Partially Polarizing Beam Splitter (APPBS), which is at the heart of correctly realizing the CNOT function.

9377-37, Session PWed

Quantum secure communication using multi-photon tolerant protocols

Mayssaa El Rifai, Pramode K. Verma, The Univ. of Oklahoma - Tulsa (United States)

This paper proposes a quantum secure communication protocol using multiple photons to represent each bit of a message to be shared. The protocol proposed is a multi-stage protocol; an explanation of its operation and implementation are provided. The multi-stage protocol is based on the use of unitary transformations known only to Alice and Bob. This paper studies the security aspect of the multi-stage protocol by assessing its vulnerability to different quantum attacks. It is well known that as the number of photons increases, the level of vulnerability of the multi-stage protocol increases. This paper sets a limit on the number of photons that can be used while keeping the multi-stage protocol a multi-photon tolerant quantum secure method for communication. The analysis of the number of photons is based on the probability of success of a Helstrom discrimination done by an eavesdropper on the channel. Limiting the number of photons up to certain threshold per stage makes it impossible for an eavesdropper to decipher the message sent over the channel. The multi-photon tolerant approach to quantum cryptography provides a quantum level security while using more than a single photon per transmission. This obviates the disadvantages associated with single photon implementations, such as limited data rates and distances along with the need to have no more than single photon per time slot. The multi-stage protocol is a step toward direct quantum communication rather than quantum key distribution associated with single photon approaches.

9377-21, Session 7

**Topological physics in photonic devices
 (Invited Paper)**

Mikael C. Rechtsman, Technion-Israel Institute of Technology (Israel); Julia Zeuner, Friedrich-Schiller- Univ. Jena (Germany); Yonatan Plotnik, Yaakov Lumer, Mordechai Segev, Technion-Israel Institute of Technology (Israel); Alexander Szameit, Friedrich-Schiller-Univ. Jena (Germany)

In this talk I will demonstrate the experimental realization and discuss the mathematical underpinnings of photonic topological protection. In a photonic topological insulator, light is able to flow without being obstructed by disorder, with a similar mechanism to the quantized transport of the quantum Hall effect. Specifically, I will show that in a honeycomb array of helical waveguides, light flows via topological edge states, unscattered around corners and past defects. Time permitting, I will discuss an experimental realization of a topological transition in a non-Hermitian system, wherein bulk propagation can yield topological numbers.

9377-22, Session 7

Photons in synthetic gauge fields (Invited Paper)

Mohammad Hafezi, Joint Quantum Institute (United States)

Electronic transport is localized in low-dimensional disordered media. The addition of gauge fields to disordered media leads to fundamental changes in the transport properties. We implement a synthetic gauge field for photons using silicon-on-insulator technology. By determining the distribution of transport properties, we confirm that waves are localized in the bulk and localization is suppressed in edge states. Furthermore, we discuss how similar physics can be observed in the microwave domain using circuit-QED architecture. The addition of nonlinearity to such photonic systems with synthetic gauge fields could lead to the generation of quantum many-body states similar to that of the fractional quantum Hall effect in electronic systems. We investigate various schemes to prepare and detect such states. Such systems provide a new platform for investigating the transport properties of photons in the presence of synthetic gauge fields with potential applications in quantum simulation and fault-tolerant quantum computation.

9377-23, Session 7

Engineering topological order for light in bianisotropic metacrystals with and without time-reversal symmetry (Invited Paper)

Alexander B. Khanikaev, Queens College (United States)

Topologically nontrivial photonic states have been recently shown to exist in photonic crystal with broken time-reversal symmetry, such as magnetic photonic crystals, as well as in periodic systems with time-reversal symmetry, such as photonic metacrystal with bianisotropic response. Here we demonstrate that topological order for light can also be found in periodic materials with special class of bianisotropic response violating time-reversal symmetry known as "Tellegen medium". Numerical simulations of Tellegen metacrystals reveal nonvanishing values of topological invariants and presence of topologically robust edge states. These states are also shown to be insensitive to structural imperfections and defects deliberately introduced into the crystal.

**Conference 9377: Advances in Photonics of
Quantum Computing, Memory, and Communication VIII**

9377-24, Session 7

Guiding electromagnetic waves around sharp corners: topologically-protected photonic transport in meta-waveguides *(Invited Paper)*

Gennady B. Shvets, The Univ. of Texas at Austin (United States)

The wave nature of electromagnetic radiation prevents it from propagating around sharp corners because of the inevitable scattering by any non-smooth obstruction. Similar restriction for fermion matter waves is overcome in topological insulators, where topological protected edge states can propagate without scattering. Guided by the analogy between electromagnetic and matter waves, we demonstrate that a simple photonic structure based on a periodic array of metallic cylinders attached to one of the two confining metal plates acts as a photonic topological insulator with emulated spin-orbital interaction and a complete photonic topological band gap. First-principles numerical simulations demonstrate that when two such meta-waveguides with opposite signs of the effective spin-orbital interaction are interfaced with each other, the resulting topological boundary supports photonic edge states which are robust against sharp bends and other obstructions. We demonstrate that the photonic transport of such edge states through arbitrarily shaped cavities and pathways exhibits unique non-resonant broadband character unattainable with edge states supported by conventional topologically trivial photonic structures.

9377-25, Session 7

Breaking reciprocity on-chip *(Invited Paper)*

Michal Lipson, Cornell Univ. (United States)

No Abstract Available

9377-26, Session 8

Prospects for photonic integration of rare-earth quantum memories *(Invited Paper)*

Matthew J. Sellars, The Australian National Univ. (Australia)

The implementation of a quantum repeater network will require the integration of a large number of components including quantum memories, quantum sources, detectors and modulators in to complex optical circuits. The prospect of developing a rare-earth doped crystal planar waveguide platform to achieve this goal will be discussed.

In particular the demonstration of planar waveguide components including memories and modulators based on passive glass waveguides on an active crystalline substrate controlled electronically via Stark shifting the optical transitions of the rare earth ions will be described.

9377-27, Session 8

Spin properties and optical interfacing of silicon vacancy color centers in diamond *(Invited Paper)*

Jonas N. Becker, Univ. des Saarlandes (Germany); Benjamin Pingault, Univ. of Cambridge (United Kingdom); Carsten Arend, Univ. des Saarlandes (Germany); Christian Hepp, Univ. des Saarlandes (Germany) and Univ. of

Cambridge (United Kingdom); Janine Riedrich-Möller, Univ. des Saarlandes (Germany); Mete Atatüre, Univ. of Cambridge (United Kingdom); Christoph Becher, Univ. des Saarlandes (Germany)

Spin impurities in diamond are versatile tools for a wide range of solid-state-based quantum technologies. The most prominent example is the nitrogen vacancy (NV) center providing very long spin coherence times. On the other hand, its optical properties are limited by a dominant emission into a very broad phonon sideband hindering efficient optical spin access. Thus, identifying a spin impurity which offers sufficient quality in both photonic and spin properties remains a challenge. Silicon vacancy (SiV) centers have attracted large interest due to their spin-accessible optical transitions [1,2] and the quality of their optical spectrum, i.e. narrow zero phonon lines and weak phonon sidebands [3]. What remains unknown so far is the spin coherence time being essential for applying SiV centers as spin-photon quantum interface.

We report on the nature of the SiV electronic structure and selection rules giving rise to spin-selective fluorescence, and all-optical access to spin coherence in the ground state using coherent population trapping. We further investigate the role of phonon-assisted coupling between orbital states as a source of irreversible spin decoherence. Our results indicate that all-optical coherent control of silicon-vacancy spins can be feasible. Efficient spin-readout of color centers can be further promoted by coupling their optical transitions to micro-cavities. We recently have demonstrated fabrication of photonic crystal cavities at the predetermined position of single SiV centers [4] where the cavities can be aligned to the emitter's dipole orientation. We observe a large Purcell enhancement (~ 19) and a reduction (~ 2.5) of the spontaneous emission lifetime.

[1] C. Hepp, T. Müller, V. Waselowski, J. N. Becker, B. Pingault, H. Sternschulte, D. Steinmüller-Nethl, A. Gali, J. R. Maze, M. Atatüre, C. Becher, Phys. Rev. Lett. 112, 036405 (2014).

[2] T. Müller, C. Hepp, B. Pingault, E. Neu, S. Gsell, M. Schreck, H. Sternschulte, D. Steinmüller-Nethl, C. Becher, M. Atatüre, Nature Commun. 5, 3328 (2014).

[3] E. Neu, D. Steinmetz, J. Riedrich-Möller, S. Gsell, M. Fischer, M. Schreck, C. Becher, New J. Phys. 13, 025012 (2011).

[4] J. Riedrich-Möller, C. Arend, C. Pauly, F. Mücklich, M. Fischer, S. Gsell, M. Schreck, and C. Becher, Deterministic coupling of a single color center to a photonic crystal cavity in diamond, Nano Lett. (2014); DOI: 10.1021/nl502327b.

9377-28, Session 8

Coupling of rare-earth ions to a YSO nanophotonic resonator for efficient quantum memory

Tian Zhong, Jonathan Kindem, Evan Miyazono, Alex Hartz, Andrei Faraon, California Institute of Technology (United States)

Rare-earth ions (REI) are promising candidates for implementing solid-state quantum memory and quantum repeater devices. The high spectral stability, long coherence times, and small inhomogeneous broadening makes REIs a good choice for nano-scale quantum photonic applications. We report the coupling of the 883 nm $4I_{9/2}-4F_{3/2}$ transition of Neodymium (Nd^{3+}) ions to a Yttrium orthosilicate Y_2SiO_5 (YSO) photonic crystal nano-beam resonator, achieving enhanced spontaneous emission rate of Nd^{3+} photoluminescence and increased optical absorption. This platform could enable efficient nano-scale optical quantum memory devices.

The triangular nano-beam resonator in 0.2% doped Nd:YSO was fabricated using focused ion beam milling. $\sim 50\%$ efficient coupling in/out of the cavity was realized by 45° angled reflectors milled in YSO, allowing vertical excitation and collection of the cavity emission using a confocal microscope setup. Measured resonance of $Q=2150$ and mode volume of $1.65 (\lambda_{bd}/n)^3$ at 881.4 nm were tuned to the Nd:YSO transition by N2

**Conference 9377: Advances in Photonics of
 Quantum Computing, Memory, and Communication VIII**

nitrogen gas condensation at <10 k temperature. When coupled, enhanced photoluminescence and reduced lifetime from 250 ps to 130 ps were observed. Factoring in the branching ratio of the transition, this corresponds to a spontaneous emission rate enhancement (Purcell Factor) F-21.

We measured an enhanced absorption of ~80%, which can be compared to < 5% absorption by the same ensemble of ions in a nano-beam waveguide without a cavity. Photon echo experiments were performed in the same waveguide and a 0.5% echo efficiency was measured at 1 ps delay. We expect a significantly enhanced echo intensity and thus high memory storage efficiency to be measured using our nano-resonator.

9377-29, Session 9

**Optical control and readout of single spins
 in diamond (Invited Paper)**

Fedor Jelezko, Univ. Ulm (Germany)

Colour centres in diamond are attracting growing interest owing to their applications in quantum information processing, sensing and as sources of single photons. In this talk I will highlight recent progress on optical control of spins associated with single SiV defects in diamond lattice including optical pumping, spin readout and electromagnetically induced transparency.

9377-30, Session 9

**Quantum memory based on nuclear spin in
 nitrogen vacancy in diamond for quantum
 repeater (Invited Paper)**

Sen Yang, Ya Wang, Thai Hien Tran, S. Ali Momenzadeh, Helmut Fedder, Rainer Stöhr, Univ. Stuttgart (Germany); Naofumi Abe, Tohoku Univ. (Japan); Philipp Neumann, Univ. Stuttgart (Germany); Hideo Kosaka, Tohoku Univ. (Japan); Jörg Wrachtrup, Univ. Stuttgart (Germany)

Quantum repeater is one of the key elements to realize long distance quantum communication. In the heart of a quantum repeater is quantum memory. There are a few requirements for this memory: it needs to couple to flying qubits: photon; it needs to have long coherence time, so quantum error correction algorithm can be performed in the quantum repeater nodes; it needs to be stable under optical illuminations.

Nitrogen nuclear spin is available for every nitrogen vacancy center (NV) in diamond. Besides it can be a robust quantum memory for spin qubit operations, nitrogen nuclear spin can couple to photon by taking advantage of optically resonant excitation of spin-selective transitions in low temperature. Here we demonstrate the coherent storage of quantum information from photon into nuclear spin. We show this quantum memory fulfills requirements as quantum memory for quantum repeater. Coherent time beyond 3 seconds is measured in ^{13}C natural abundant sample. Under resonant laser excitations, the excited state quadruple and hyperfine interaction could lead to decoherence of nuclear spin. We show those interactions are low and nuclear spin can keep its coherence over 1000 times resonant laser excitation of electron spin. We also demonstrate effective initialization of this memory.

9377-31, Session 9

**Quantum networks based on diamond
 spins: From long-distance teleportation to
 a loophole-free Bell test (Invited Paper)**

Hannes Bernien, Bas Hensen, Wolfgang Pfaff, Anais Dreau, Andreas Reiserer, Machiel Blok, Suzanne van Dam, Just

Ruitenbergh, Technische Univ. Delft (Netherlands); Matthew Markham, Daniel Twitchen, Element Six Ltd. (United Kingdom); Tim H. Taminiau, Ronald Hanson, Technische Univ. Delft (Netherlands)

The realization of a highly connected network of qubit registers is a central challenge for quantum information processing and long-distance quantum communication. Diamond spins associated with NV centers are promising building blocks for such a network as they combine a coherent optical interface (similar to that of trapped atomic qubits) with a local register of robust nuclear spin qubits [1].

Here we present our latest progress towards scalable quantum networks. We have realized unconditional teleportation between long-lived qubits residing in independent setups [2]. The teleportation exploits entanglement between distant NV electronic spins that is generated through spin-photon entanglement and subsequent photon detection [3]. By encoding the source state in a separate qubit (a single nuclear spin) we realize a Bell state measurement that distinguishes between all four outcomes in a single shot. Analysis shows that the obtained fidelities are in principle high enough for a loophole-free violation of Bell's inequalities. We will present our latest efforts towards reaching this ultimate goal.

References

- [1] T. H. Taminiau et al., Nature Nanotechnology 9, 171 (2014).
- [2] W. Pfaff et al., Science 345, 532 (2014).
- [3] H. Bernien et al., Nature 497, 86 (2013).

9377-32, Session 9

Diamond photonics (Invited Paper)

Marko Loncar, Harvard School of Engineering and Applied Sciences (United States)

Diamond possesses remarkable physical and chemical properties, and in many ways is the ultimate engineering material. For example, diamond is transparent from the ultra-violet to infra-red, has a high refractive index ($n = 2.4$), strong optical nonlinearity (Kerr and Raman) and a wide variety of light-emitting defects. These properties make diamond a highly desirable material for many applications, including quantum optics, nonlinear optics, magnetic and electric field sensing, and NEMS. One particularly exciting application of diamond is in the field of quantum information science and technology, which promises realization of powerful quantum computers capable of tackling problems that cannot be solved using classical approaches, as well as realization of secure communication channels. At the heart of these applications are diamond's luminescent defects—color centers—and the nitrogen-vacancy (NV) color center in particular. This atomic system in the solid-state possesses all the essential elements for quantum technology, including storage, logic, and communication of quantum information.

I will review advances in nanotechnology that have enabled fabrication of nanoscale optical devices in diamond that can generate, manipulate, and store optical signals at the single-photon level. Examples include a room temperature source of single photons based on diamond nanowires and plasmonic apertures, as well as single-photon generation and routing inside ring and photonic crystal resonators. Novel and scalable fabrication technique – angled-etching – suitable for realization of nanophotonic and nanomechanic devices in bulk diamond crystals will also be discussed. Our work on diamond based on-chip frequency combs will also be presented.

9377-33, Session 9

**Multidimensional quantum interferometry
 on a chip**

Zachary Chaboyer, Thomas D. Meany, Luke G. Helt, Michael J. Steel, Michael J. Withford, Macquarie Univ. (Australia)

Conference 9377: Advances in Photonics of Quantum Computing, Memory, and Communication VIII

We perform a non-classical characterization of a multiport interferometer waveguide circuit. This device is fabricated using an ultrafast laser inscription process which permits uniquely three-dimensional circuit fabrication not possible using standard lithographic means.

Multiport interferometric circuits are unique devices which permit the injection of photon states distributed across multiple individual modes, while arbitrary phase relationships between individual modes can be varied to enhance phase precision or to produce exotic output states. However, the extreme sensitivity to small phase variations phase of such devices means that fibre based components are unsuitable.

The femtosecond laser direct-write technique (FLDW) offers the ability to produce waveguides at multiple depths in a glass substrate using no lithographic mask or clean room facilities. This method has been used to fabricate a three arm Mach Zehnder interferometer composed of two individual three-way beamsplitters. One arm exiting the plane and interacting with the surface of the glass chip.

To characterize the devices phase response a heater has been used to apply a local refractive index variation to the surface of the chip imparting a phase in the selected arm of the interferometer. This allows us to observe the behaviour for the cases of single and two-photon inputs while the phase of one arm is varied. By comparing these we see an increased sensitivity to phase for the two-photon case matching theoretical predictions of Fisher information, maximum extracted phase information, of 2.8. This shows the potential of using multiple photon inputs in a multiport circuit for quantum metrology applications.

9377-38, Session 9

Toward remote ion-ion entanglement with barium

Thomas Noel, Carolyn Auchter, Chen-Kuan Chou, Boris Blinov, Univ. of Washington (United States)

We present work toward remote entanglement of barium ions in traps separated by a few meters. A new version of an ion trap specialized for remote entanglement is introduced. The new trap allows for highly efficient collection of ion fluorescence while simultaneously minimizing ion micromotion and aligning the trap position precisely to the focus of an in-vacuum parabolic mirror by using a set of bias electrodes and a piezoelectric micro-positioning system. The success rate of the remote entanglement procedure depends strongly on the efficiency with which ion fluorescence can be coupled into an optical fiber. Characterization of our system in terms of ion fluorescence collection and fiber coupling efficiency is presented. Results demonstrating entanglement between a single barium ion and single spontaneously emitted photons are shown. The entanglement fidelity of the ion-photon state is measured to be 0.84(1) and a CHSH Bell signal of 2.303(36) finds violation of the CHSH version of the Bell inequality by over eight standard deviations. Barium's relatively long wavelength transitions make it an ideal candidate for our longer term goal of remote entanglement of ions separated by a kilometer or more. Such long distance remote entanglement should allow for a loophole-free verification of the violation of the Bell inequality.

Conference 9378: Slow Light, Fast Light, and Opto-Atomic Precision Metrology VIII

Sunday - Thursday 8 -12 February 2015

Part of Proceedings of SPIE Vol. 9378 Slow Light, Fast Light, and Opto-Atomic Precision Metrology VIII

9378-1, Session 1

Group velocity and extraordinary subwavelength imaging in graphene waveguides *(Invited Paper)*

Zheng Wang, The Univ. of Texas at Austin (United States)

No Abstract Available

9378-2, Session 1

Recent progress in waveguide-based atom photonics *(Invited Paper)*

Holger Schmidt, Jennifer A. Black, Univ. of California, Santa Cruz (United States)

No Abstract Available

9378-3, Session 1

Induced transparency in optical whispering gallery microcavity systems *(Invited Paper)*

Yun-Feng Xiao, Peking Univ. (China)

Electromagnetically induced transparency (EIT) in atomic systems is an important phenomenon in quantum optics, and its analogy in photonic structures can be found in whispering gallery microcavity systems. In this talk, we present some experimental works on EIT-like resonances in three different whispering gallery microcavity systems. In these systems, there exists a common property that coupling between two different modes is necessary. Specifically, the origins of the mode coupling in these three systems are (i) a fiber taper mediated indirect coupling of two modes belonging to two different microcavities; (ii) a fiber taper induced indirect coupling of two different modes in a single microcavity; and (iii) tunneling induced coupling of a chaotic mode and a whispering gallery mode in a deformed microcavity.

9378-4, Session 1

Ultra-slow light in erbium-doped whispering gallery mode microresonators

Vincent Huet, Alphonse L. Rasoloniaina, Ecole Nationale Supérieure des Sciences Appliquées et de Technologie (France); Michel S. Mortier, Ecole Nationale Supérieure de Chimie de Paris (France); Kamel Bencheikh, A. Yacomotti, A. Levenson, Lab. de Photonique et de Nanostructures (France); Patrice Féron, Yannick Dumeige, Ecole Nationale Supérieure des Sciences Appliquées et de Technologie (France)

No Abstract Available

9378-5, Session 1

Optical microfiber knot resonator (OMKR) and its slow-light performance *(Invited Paper)*

Liyong Ren, Xi'an Institute of Optics and Precision Mechanics (China)

No Abstract Available

9378-6, Session 2

Compact cold-atom clocks and interferometers based on stimulated Raman transitions *(Invited Paper)*

Elizabeth Donley, National Institute of Standards and Technology (United States)

No Abstract Available

9378-7, Session 2

AC stark shift in Raman-Ramsey interference using a multi-level system calculation *(Invited Paper)*

Gour S. Pati, Zachary Warren, Delaware State Univ. (United States); Selim M. Shahriar, Northwestern Univ. (United States)

Determining AC Stark shift (or light shift) is important for the development of compact, high-performance atomic clocks. We have estimated frequency shifts in Raman-Ramsey interference using a multi-level system calculation. Frequency shifts associated with coherent density-matrix terms are calculated. These are relevant to the detection of Raman-Ramsey interference in transmission (or absorption) through the medium. We have also investigated the effect of Doppler-broadening in the medium on various sources of frequency errors. Dependencies of light shift on laser intensity and frequency detuning have been investigated in detail.

9378-8, Session 2

Broadband rotational optical cooling of AIH⁺ to the rotational ground state

Brian Odom, Chris Seck, Northwestern Univ. (United States)

No Abstract Available

**Conference 9378: Slow Light, Fast Light, and
 Opto-Atomic Precision Metrology VIII**

9378-9, Session 2

**Atomic clock based on a coherent
 population trapping resonance in 87Rb
 with improved high-frequency modulation
 parameters** *(Invited Paper)*

Sergey M. Kobtsev, "Tekhnoscan - Lab" LLC (Russian Federation); Daba A. Radnatarov, Sergey A. Khripunov, Novosibirsk State Univ. (Russian Federation)

Due to their high long-term stability, compactness, and low energy consumption, atomic frequency references based on coherent population trapping resonances (CPT) in vapours of alkali metals are often used in many applications related to precision positioning, rigorous security, and others. One of key technologies behind CPT frequency references relies on a laser spectrum having two frequencies with difference equal to that between levels of a hyper-fine splitting transition (for D1-line of 87Rb it is 6.835 GHz). Usually, in order to generate two frequencies with the difference required for creation of CPT in 87Rb, injection current modulation of a single-frequency diode laser is used at the frequency of 6.835 or 3.417 GHz is used. In this case, the parameters of CPT are highly dependent on the amplitude of high-frequency modulation and on the ratio of this amplitude to the constant component of the laser diode injection current. Experiments conducted on our set-up allowed to determine optimal values of both constant and high-frequency components of the injection current, which resulted in CPT peak contrast of 10% and peak width of 15 kHz. Optimisation of high-frequency modulation parameters was also key to achievement of long-term stability (over more than 300 s) of the compact laboratory atomic frequency reference prototype around 2010-10. Stability of the master oscillator without frequency stabilisation over the same period was not better than 5 \times 10⁻⁹. The present work further provides detailed description of the experimental installation and discusses prospects of improvements in long-term stability.

9378-10, Session 3

**Tunable optical delays for implementing
 high-speed optical signal processing
 functions** *(Invited Paper)*

Alan E. Willner, The Univ. of Southern California (United States)

No Abstract Available

9378-11, Session 3

Co-propagating slow-light pulse system *(Invited Paper)*

Toshihiko Baba, Keisuke Kondo, Yokohama National Univ. (Japan)

Lattice-shifted photonic crystal waveguide produces wideband low-dispersion slow light, which is suitable for short pulse transmission, nonlinear enhancement, tunable dispersion and tunable delay. In Si devices, intense slow light pulse at fiber communication wavelengths generates efficient two-photon absorption and carrier plasma dispersion (CPD). If two slow light pulses: signal pulse and more intense control pulse, are launched with a close timing and similar group velocity, the CPD induced by the control pulse dynamically interact with the signal pulse, and achieves the following three different functions, depending on each pulse width: 1) adiabatic wavelength conversion when the control pulse width is wider than signal pulse's, 2) pulse compression in the opposite case, and 3) ultrafast delay tuning when they are nearly equal. For 1), we show that the co-propagating two pulses break the limit of the conventional adiabatic

wavelength conversion using a resonator and nearly 5 nm spectral shift is observed. For 2), a compression factor of 6.0 \times 9.5 is demonstrated using the above interaction as well as heater-controlled integrated dispersion compensator. For 3), the delay of the signal pulse is shifted up to 10 ps with a switching time as short as 10 ps, which not limited by the carrier lifetime but by the pulse width. Therefore, it enables the delay tuning of one target pulse in a high-speed pulse train.

9378-12, Session 3

**Slow light in ruby: delaying energy beyond
 the input pulse**

Emma Wisniewski-Barker, Graham Gibson, Sonja Franke-Arnold, Univ. of Glasgow (United Kingdom); Zhimin Shi, Univ. of South Florida (United States); Robert W. Boyd, Univ. of Ottawa (Canada) and Univ. of Rochester (United States); Miles J. Padgett, Univ. of Glasgow (United Kingdom)

The mechanism by which light is slowed through ruby has been the subject of great debate. To distinguish between the two main proposed mechanisms, we investigate the problem in the time domain by modulating a laser beam with a chopper to create a clean square wave. By exploring the trailing edge of the pulsed laser beam propagating through ruby, we can determine whether energy is delayed beyond the input pulse. The effects of a time-varying absorber alone cannot delay energy into the trailing edge of the pulse, as a time-varying absorber can only attenuate a coherent pulse. Therefore, our observation of an increase in intensity at the trailing edge of the pulse provides evidence for a complicated model of slow light in ruby that requires more than just pulse reshaping. In addition, investigating the Fourier components of the modulated square wave shows that harmonic components with different frequencies are delayed by different amounts, regardless of the intensity of the component itself. Understanding the difference in delays of the individual Fourier components of the modulated beam reveals the cause of the distortion the pulse undergoes as it propagates through the ruby.

9378-13, Session 3

**Strong slow-light resonances in apodized
 deuterium-loaded femtosecond FBGs** *(Invited Paper)*

George Skolianos, Arushi Arora, Stanford Univ. (United States); Martin Bernier, Univ. Laval (Canada); Michel Dignonnet, Stanford Univ. (United States)

We report the generation of record low group velocities and high optical confinements in strong apodized fiber Bragg gratings (FBGs). The gratings were fabricated in deuterium-loaded fiber using a 400-nm femtosecond laser and a phase mask, followed by annealing to reduce residual losses. In an FBG of this type 12.4 mm in length, a group delay of 43 ns was observed, corresponding to a group velocity of only ~288 km/s and a group index of ~1040. In a shorter and therefore lower loss device (5.1 mm) we were able to observe the fundamental mode, and infer a Purcell factor as high as 25.5. These exceptional features are made possible in part by the gratings' strong index modulation (~2 \times 10⁻³) and ultra-low single-pass loss (~0.02 dB).

**Conference 9378: Slow Light, Fast Light, and
 Opto-Atomic Precision Metrology VIII**

9378-14, Session 3

**Optimizing delaying strength and
 distortion in linear slow light systems**
(Invited Paper)

 Luc Thévenaz, Ecole Polytechnique Fédérale de Lausanne
 (Switzerland)

No Abstract Available

9378-15, Session 4

**Wideband perfect coherent absorber
 based on white-light cavity**

Omer Kotlicki, Jacob Scheuer, Tel Aviv Univ. (Israel)

Coherent Perfect Absorbers (CPAs) are optical cavities which can be described as time-reversed lasers where light waves that enter the cavity, coherently interfere and react with the intra-cavity losses to yield perfect absorption. In contrast to lasers, which benefit from high coherency and narrow spectral linewidths, for absorbers these properties are often undesirable as absorption at a single frequency is highly susceptible to spectral noise and inappropriate for most practical applications.

Recently, a new class of cavities, characterized by a spectrally wide resonance has been proposed. Such resonators, often referred to as White Light Cavities (WLCs), include intra-cavity superluminal phase element, designed to provide a phase response with a slope that is opposite in sign and equal in magnitude to that of light propagation through the empty cavity. Consequently, the resonance phase condition in WLCs is satisfied over a band of frequencies providing a spectrally wide resonance. WLCs have drawn much attention due to their attractiveness for various applications such as ultra-sensitive sensors and optical buffering components. Nevertheless, WLCs exhibit inherent losses that are often undesirable.

Here we introduce a simple wideband CPA device that is based on the WLC concept along with a complete analytical analysis. We present analytic and FDTD simulations of a practical, highly compact (12 μ m), Silicon based WLC-CPA that exhibits a flat and wide absorption profile (40nm) and demonstrate its usefulness as an optical pulse terminator (>35db isolation) and an all optical modulator that span the entire C-Band exhibiting high immunity to spectral noise.

9378-16, Session 4

**Proof of principle experiment on
 minimizing propagation time in optical
 communications**

 Federico Tommasi, Emilio Ignesti, Univ. degli Studi di
 Firenze (Italy); Lorenzo Fini, Stefano Cavalieri, Univ. degli
 Studi di Firenze (Italy) and European Lab. for Non-Linear
 Spectroscopy (Italy)

Any optical transmission line of some extent presents two key steps: propagation in a slow media with reduction of the signal amplitude and a further propagation in an amplifying media.

Our idea is to combine, in a proof of principle experiment, the delay induced in a slow light propagation with a subsequent superluminal propagation in a tailored amplifying medium to achieve the whole minimum propagation time. In addition we show that this possibility can be optically controlled.

The experiment, based on an incoherent scheme that we proposed [1] and realized for fast and slow light optical control [2,3], is performed in two cells containing sodium vapor by means of two control pulses.

Results showed that the second fast-light stage can be optically controlled to not only completely recover the delay experimented in the first slow light stage, but also produce an advance. In this way the previous history of the pulse propagation can be canceled in a timescale of 1.0 ns.

Our experiment may lead to interesting scenarios in optical signal transmission, by the use of a tailored amplification stage.

References:

- [1] M. V. Tognetti et al. Phys. Rev. A 81 023812 (2006)
- [2] E. Ignesti et al. Phys. Rev. A 86 063818 (2012)
- [3] E. Ignesti et al. Phys. Rev. A 87 033828 (2013)

9378-17, Session 4

**Suppression of sensitivity due to length
 variation in a subluminal ring laser**

Zifan Zhou, Northwestern Univ. (United States)

No Abstract Available

9378-18, Session 4

**Towards long-distance superluminal
 propagation in optical fibers via cascaded
 Brillouin lasing resonators *(Invited Paper)***

 Li Zhan, Liang Zhang, Minglei Qin, Shanghai Jiao Tong
 Univ. (China); Jinmei Liu, Shanghai Jiao Tong Univ. (China)
 and East China Normal Univ. (China)

No Abstract Available

9378-19, Session 5

**Towards fast-light gyroscope, modification
 of dispersion, and pulling sensitivity
*(Invited Paper)***

 Eugeniy E. Mikhailov, Matt T. Simons, The College of
 William & Mary (United States); Simon Rochester, Dmitry
 Budker, Univ. of California, Berkeley (United States); Irina
 Novikova, The College of William & Mary (United States)

No Abstract Available

9378-20, Session 5

**Enhancement of bandwidth of a LIGO
 interferometer using white light cavity and
 signal recycling**

 Minchuan Zhou, Zifan Zhou, Selim M. Shahriar,
 Northwestern Univ. (United States)

No Abstract Available

**Conference 9378: Slow Light, Fast Light, and
Opto-Atomic Precision Metrology VIII**

9378-21, Session 5

**Passive fast-light optical gyroscope
(Invited Paper)**

David D. Smith, NASA Marshall Space Flight Ctr. (United States); Krishna Myneni, U.S. Army Research, Development and Engineering Command (United States); Hongrok Chang, Ducommun Inc. (United States); Heather A. Luckay, The Univ. of Alabama in Huntsville (United States)

No Abstract Available

9378-22, Session 5

**Superluminal enhancement of rotation
sensitivity in a laser gyroscope based
on stimulated Raman scattering (Invited
Paper)**

Sean M. Spillane, Los Gatos Research, Inc. (United States); Selim M. Shahriar, Northwestern Univ. (United States)

No Abstract Available

9378-23, Session 5

**Quantum noise limited linewidth of super-
and sub-luminal lasers (Invited Paper)**

Jacob Scheuer, Tel Aviv Univ. (Israel); Selim M. Shahriar, Northwestern Univ. (United States)

No Abstract Available

9378-24, Session 5

**Theoretical design of a superluminal
helium-neon ring laser via coupled cavities
(Invited Paper)**

Tianliang Qu, National Univ. of Defense Technology (China)

No Abstract Available

9378-77, Session 5

**Quantum noise of white-light cavity using
double-pumped gain medium (Invited
Paper)**

Yiqiu Ma, The Univ. of Western Australia (Australia); Haixing Miao, Univ. of Birmingham (United Kingdom); Chunnong Zhao, The Univ. of Western Australia (Australia); Yanbei Chen, California Institute of Technology (United States)

We developed an input-output formalism to study the quantum noise of white light cavity using double gain medium. Specifically, we studied the additional noise associated with the parametric amplification process. We found that the effect of this additional noise may limit the integrated shot-noise limited sensitivity of a gravitational wave detector with double gain

medium so that it is still bound by the Mizuno limit. Other gain media may allow one to overcome this limit.

9378-25, Session 6

**Enhanced wavelength conversion and
photon pair generation using slow light
effects and electronic carrier sweepout in
silicon photonics devices (Invited Paper)**

Marc Savanier, Shayan Mookherjea, Univ. of California, San Diego (United States)

No Abstract Available

9378-26, Session 6

**Controlling photonic transport using
synthetic gauge field (Invited Paper)**

Mohammad Hafezi, Joint Quantum Institute (United States)

No Abstract Available

9378-27, Session 6

**Measuring the propagation of
entanglement and information in
dispersive media (Invited Paper)**

Jeremy B. Clark, Joint Quantum Institute (United States); Paul D. Lett, National Institute of Standards and Technology (United States)

No Abstract Available

9378-28, Session 6

**Entangled photons from hot vapors
(Invited Paper)**

John C. Howell, Justin Winkler, Univ. of Rochester (United States)

No Abstract Available

9378-29, Session 6

**Towards noiseless integrated quantum
memories (Invited Paper)**

Joshua Nunn, Univ. of Oxford (United Kingdom)

No Abstract Available

**Conference 9378: Slow Light, Fast Light, and
Opto-Atomic Precision Metrology VIII**

9378-30, Session 7

Spin squeezing: a tutorial review (*Invited Paper*)

Eugene S. Polzik, Niels Bohr Institute (Denmark)

No Abstract Available

9378-31, Session 7

Photon-correlation amplifiers and interferometers for quantum metrology

Weiping Zhang, East China Normal Univ. (China)

Interferometers usually consist of linear elements such as beam splitters for wave splitting and recombination. Their sensitivity for phase measurement is limited by the shot noise, which can be suppressed with squeezed states of light. Here we demonstrate a different type of interferometer in which beam splitters are replaced by nonlinear elements such as parametric amplifiers which generate photon-correlated beams. Although such an interferometer still operates near shot noise level, its nonlinear property enhances the phase signal, leading to a phase measurement sensitivity beyond the shot noise limit set by a conventional interferometer with coherent state. We observe an improvement of 4.1 ± 0.3 dB in signal-to-noise ratio beyond the shot noise limit. Combined with squeezed state technique for shot noise suppression, this interferometer promises further improvement in sensitivity. Such an interferometer can find potentials in quantum metrology.

9378-32, Session 7

Generation of a squeezed state of an oscillator by stroboscopic quantum nondemolition measurement

Eugene S. Polzik, Niels Bohr Institute (Denmark)

No Abstract Available

9378-33, Session 7

Spatial profile of the squeezed quantum noise generated and modified by resonant atomic ensembles (*Invited Paper*)

Mi Zhang, Irina Novikova, Eugeniy E. Mikhailov, The College of William & Mary (United States); Jonathan P. Dowling, Louisiana State Univ. (United States)

No Abstract Available

9378-34, Session 7

Sensing of magnetic and gravitational fields beyond standard quantum limits

Eugene S. Polzik, Niels Bohr Institute (Denmark)

No Abstract Available

9378-35, Session 8

Title to be determined (*Invited Paper*)

Andrey A. Sukhorukov, The Australian National Univ. (Australia)

No Abstract Available

9378-36, Session 8

Enhancing the nonlinearity at ultra-low-light levels using spatial bunching of cold atoms (*Invited Paper*)

Bonnie L. Schmittberger, Daniel Joseph Gauthier, Duke Univ. (United States)

No Abstract Available

9378-37, Session 8

Photon drag effects in a rubidium slow-light medium (*Invited Paper*)

Robert W. Boyd, Israel De Leon, Univ. of Ottawa (Canada); Mohammad Mirhosseini, Univ. of Rochester (United States)

No Abstract Available

9378-38, Session 8

Speed-of-light management via RF-photon coupling in a nonlinear photonic crystal (*Invited Paper*)

Igor V. Melnikov, National Research Univ. of Electronic Technology (Russian Federation)

No Abstract Available

9378-39, Session 9

Precision magnetometry with diamond color centers (*Invited Paper*)

Philip R. Hemmer, Texas A&M Univ. (United States)

There has been much recent interest in magnetometers based on diamond color centers for applications ranging from material science to biological sensing. In this talk I will review some of the recent progress for two diamond color centers; the nitrogen vacancy (NV) and the silicon vacancy (SiV). Briefly the NV is preferred for magnetometer applications involving room temperature measurements and the SiV is preferred for low temperatures.

Conference 9378: Slow Light, Fast Light, and
Opto-Atomic Precision Metrology VIII

9378-40, Session 9

New developments in precision metrology with nitrogen-vacancy centers in diamond *(Invited Paper)*

Andrey Jarmola, Univ. of California, Berkeley (United States)

No Abstract Available

9378-41, Session 9

Microwave saturation spectroscopy and coherence of nitrogen-vacancy ensembles in diamond

Pauli Kehayias, Dmitry Budker, Univ. of California, Berkeley (United States)

No Abstract Available

9378-42, Session 9

Cavity-enhanced magnetometry with nitrogen-vacancy ensembles in diamond based on infrared absorption *(Invited Paper)*

K. Jensen, Nathan Leefer, Andrey Jarmola, Univ. of California, Berkeley (United States); Yannick Dumeige, Ecole Nationale Supérieure des Sciences Appliquées et de Technologie (France); Victor M. Acosta, Pauli Kehayias, Brian Patton, Univ. of California, Berkeley (United States); Mayeul Chipaux, Thierry Debuisschert, Thales Research & Technology (France); François Treussart, Vincent Jacques, Jean-Francois Roch, Ecole Normale Supérieure de Cachan (France); Dmitry Budker, Univ. of California, Berkeley (United States) and Mainz Johannes Gutenberg Univ. (Germany)

No Abstract Available

9378-43, Session 9

Optically-addressed spin sensors in nanostructured diamond *(Invited Paper)*

Victor M. Acosta, Google (United States)

No Abstract Available

9378-44, Session 10

Slow light and narrow resonances in electromagnetic-induced deflection *(Invited Paper)*

David Eger, Slava Smartsev, Nir Davidson, Weizmann Institute of Science (Israel)

No Abstract Available

9378-45, Session 10

Formation of dark states of atoms near metallic nanoparticles *(Invited Paper)*

Yuri V. Rostovtsev, Suman Dhayal, Univ. of North Texas (United States)

No Abstract Available

9378-46, Session 10

Slow exciton polaritons in 2D materials *(Invited Paper)*

Jacob B. Khurgin, Johns Hopkins Univ. (United States)

We show that a single monolayer of newly-recognized 2-dimensional materials such as MoS₂ and WSe₂ is capable of supporting a well confined guided TE mode propagating with reduced group velocity. Implications for integrated and nonlinear optics will be considered.

9378-47, Session 10

Slow light optofluidics *(Invited Paper)*

Misha Sumetsky, Aston Institute for Photonics Technologies (United Kingdom)

No Abstract Available

9378-48, Session 10

Slow light and its application to semiconductor lasers *(Invited Paper)*

Jesper Mørk, Technical Univ. of Denmark (Denmark)

No Abstract Available

9378-49, Session 11

Recent achievements in chip scale and miniaturization of hybrid photonic-atomic devices *(Invited Paper)*

Liron Stern, Meir Grajower, E. Talker, N. Mazurski, R. Zektzer, A. Neiman, Boris Desiatov, Uriel Levy, The Hebrew Univ. of Jerusalem (Israel)

No Abstract Available

9378-50, Session 11

Cold and thermal atoms in kagome fiber *(Invited Paper)*

Fetah A. Benabid, Univ. of Bath (France); Thomas D. Bradley, Ekaterina Ilinova, XLIM Institut de Recherche (France); Hidetoshi Katori, S. Okaba, Tetsushi Takano, The Univ. of Tokyo (Japan)

No Abstract Available

**Conference 9378: Slow Light, Fast Light, and
Opto-Atomic Precision Metrology VIII**

9378-51, Session 11

Title to be determined (*Invited Paper*)

Alexander L. Gaeta, Cornell Univ. (United States)

No Abstract Available

9378-52, Session 11

**Dual wavelength and dual resonance on
chip vapor spectroscopy in the telecom
band**

 Liron Stern, Meir Grajower, Uriel Levy, E. Talker, N. Mazurski,
R. Zektzer, A. Neiman, The Hebrew Univ. of Jerusalem
(Israel)

No Abstract Available

9378-53, Session 11

**Experimental observations of slow light
using the EIT-like resonance in a self-
coupled resonator**

 Yundong Zhang, Xuenan Zhang, Chi Xu, Xianxin Zhai,
Yongfeng Wu, Chunyu Zhang, Ping Yuan, Harbin Institute
of Technology (China)

We report the experimental observations of slow light using the EIT-like (electromagnetically induced transparency-like) resonance in a self-coupled ring resonator (SCRR). We fabricate the SCRR using fiber directional couplers with various coupling coefficients. When the coupling coefficients of the two couplers composing the SCRR are close to each other, we observe that the transmission spectrum of the SCRR exhibits the EIT-like resonance line shape as that in conventional coupled resonators. The frequency-dependent phase response of the SCRR is experimentally measured by coupling the SCRR to a fiber Mach-Zehnder interferometer (MZI). The measured experimental results of the phase response of the SCRR indicate that the steep phase shift depending on frequency detuning and the resulting significant group delay (dispersion) can be achieved in the vicinity of the EIT-like resonance. Also, we demonstrate the pulse propagation through the SCRR, and acquire the significant pulse delay and advance using the EIT-like resonance in the SCRR. The theoretically simulated results of the transmission intensity and phase responses of the SCRR are obtained from the transfer matrix theory, and they are in good agreement with the foregoing experimental results. The slow light using the EIT-like resonance in a SCRR holds wide and important implications for tunable optical delay line, optical storage, quantum information processing, nonlinear optical effect enhancement, slow light Fourier transform (FT) interferometric spectrometers, white light cavities (WLCs), and optical sensors.

9378-54, Session 12

**Light-matter interaction in plasmonic
groove waveguides** (*Invited Paper*)

N. Asger Mortensen, DTU Fotonik (Denmark)

No Abstract Available

9378-55, Session 12

Coherent atomic gas metamaterials
(*Invited Paper*)

Susanne F. Yelin, Univ. of Connecticut (United States)

No Abstract Available

9378-56, Session 12

**The crucial role of slow light in
metamaterials: from theory (zero index
media) to practice (efficient cascade
detectors)** (*Invited Paper*)

 Meir Orenstein, Technion-Israel Institute of Technology
(Israel)

No Abstract Available

9378-57, Session 12

**From slow light to single-photon lasing
and neutral-atom acceleration in a
plasmonic crystal**

 Igor V. Melnikov, National Research Univ. of Electronic
Technology (Russian Federation) and Univ. of Illinois at
Urbana-Champaign (United States); Joseph W. Haus, Univ.
of Dayton (United States)

In the recent years, quantum plasmonics has quickly become a major research field in nanoscale optics. In future integrated nanoscale plasmonic circuits quantum sources of light will provide the input signal which then will be used to channel along plasmonic waveguides and the propagating plasmons will be used as carriers of information. Integration of quantum and classical plasmonic units in a single device is projected to be a driving force in the development of next generation optoelectronic devices. Photoluminescence (PL) from silver nanoparticles is a poorly understood phenomenon and requires thorough investigation from both classical (such as local field enhancement and coupling to the LSPR) and quantum mechanical description, such as interband electronic transitions, size-dependent electronic band structure or grain effects in a single nanoparticle.

Quantum photonics integrated metamaterials will require multi-functionality in a single device. For example, quantum emitters embedded in a hyperbolic metamaterial with a gradient of the effective dielectric permittivity. Organic dyes can be used as quantum emitters integrated close to the metamaterial. However, organic dyes suffer from photobleaching degradation. Silver nanoparticles, with or without surface functionalization, are more photostable and are reported to exhibit photoluminescence with a quantum yield comparable to organic dyes. Integrating silver nanoparticles in a layered or graded metamaterial is a promising route to develop novel multi-functional quantum plasmonic metamaterials. These novel quantum plasmonic metamaterials might be used for photovoltaic, quantum computing, near-field sub-diffraction optics, super-lensing, and optical cloaking.

Metals exist as bulk, thin films, nanoparticles, nanoclusters, molecules or atoms. They exhibit fundamentally different electronic and optical behavior, such as collective electronic excitations (LSPR) as opposed to electronic transitions between individual electronic levels, exhibited as single or discrete lines in the absorption spectra of atoms or molecules. The intermediate state - nanoparticles often exhibits both discrete energy levels (discrete absorption lines) and band electronic structures which leads to collective electronic behavior such as LSPR excitations. The evolution

**Conference 9378: Slow Light, Fast Light, and
 Opto-Atomic Precision Metrology VIII**

of the electronic structure from molecular-like clusters to nanoparticles can lead to deeper understanding of the physical mechanism of the LSPR enhanced PL from silver nanoparticles. Similar interactions may be used/ explained in SERS, surface enhanced spectroscopy. It has been known that nanostructured semiconductors or quantum dots (QD) exhibit photoluminescence. Photoluminescence is an inelastic scattering process in which a light photon is absorbed by the QD and then re-irradiated as a photon with a different wavelength. The photoluminescence of QD's is well understood in terms of the radiative transition between conduction and valence bands across the band gap of semiconductors. Bulk metals and metal nanoparticles, on the other hand, do not have a band gap, leaving one with the conclusion that metal nanoparticles would never exhibit any signature of photoluminescence. Yet, recent experimental studies do show luminescence from metal nanoparticles. Astonishingly, the efficiency of the photoluminescence, a quantity known as the quantum yield, is enhanced a million times as compared to bulk metals.

In this Report, we explore the population, polarization, and optical field dynamics that is the excitation transport inside both a plasmonic crystal and continuous medium of quantum emitters where isotropic spontaneous decay organizes itself into a correlated high-gain process. The objective is to develop a model that includes (i) both the spatiotemporal dynamics of the radiation field and the dynamic properties of two-level atoms; (ii) is applicable to a plasmonic crystal where excitation (LSPR) is initially localized inside a narrow area; and (iii) can be extended onto a two-dimensional geometry in a physically transparent way.

We add up this Report with a theoretical model that drives plasmonic crystal into a totally novel area of exploitation – laser acceleration of neutral atoms. Indeed, recent technological advances in coupling atoms to photonic crystal fibers and nanophotonic waveguides have been accompanied by tremendous success in single-atom trapping, self-organization, and neutral-atom transport. However, to the best of our knowledge no one has addressed issues as to whether or not basic concepts like the principle of Macmillan phase stability could be exploited in accelerating neutral atoms by an optical field that, in turn, propagates inside (or in the vicinity) of a specially tailored plasmonic structure.

Our aim here is to make a qualitative analytic assessment of neutral-atom acceleration problem and to provide direct physical insight to an otherwise complicated problem. In particular, our goal in this presentation is to show that the mechanism of continuously varying recoil, which may be implemented by the engineered dispersion, provides an effective acceleration tool. Introduction a dipole-dipole interaction into the model will provide a better connection, and hence understanding, on how to balance between atom bunching and repulsion can be created and applied to atom beam acceleration inside a plasmonic crystal.

Our method is based on the two-level density-matrix equation modified to include dipole-dipole interaction which has the advantage of providing a semi-analytic result without resorting to cumbersome numerical simulations. Specifically, we find conditions at which distribution function collapses and examine bounds for dispersion tailoring that provides corresponding gradual increase of the speed of light. Additionally, we simulate density-matrix equations for the plasmonic crystal made of metal/semiconductor nanowires that provide an additional tool to keep the atom bunching.

9378-58, Session 13

**Rotation sensitivity analysis of a two-dimensional array of coupled resonators
 (Invited Paper)**

Kiarash Zamani-Aghaie, Stanford Univ. (United States);
 Pierre Vigneron, Ecole des Mines (France); Michel
 Digonnet, Stanford Univ. (United States)

No Abstract Available

9378-59, Session 13

Optimization of gyroscope properties with passive and active coupled resonator optical waveguide structures (Invited Paper)

Jiayang Chen, Hao Zhang, Long Zhao, Junjie Jin, Jian Lin,
 Zhuanfang Bi, Anping Huang, Zhisong Xiao, BeiHang Univ.
 (China)

No Abstract Available

9378-60, Session 13

High-resolution Brillouin metrology of strain and temperature (Invited Paper)

Yair Yair Antman, Bar-Ilan Univ. (Israel); David Eloo, Elbit
 Systems Electro-Optics El-Op Ltd. (Israel); Yosef London,
 Raphael Cohen, Avinoam Zadok, Bar-Ilan Univ. (Israel)

No Abstract Available

9378-61, Session 13

Phase modulation detection with liquid crystal devices (Invited Paper)

Umberto Bortolozzo, Stefania Residori, Institut Non
 Linéaire de Nice Sophia Antipolis (France)

No Abstract Available

9378-62, Session 13

Nonlinear holography for acoustic wave detection (Invited Paper)

Stefania Residori, Institut Non Linéaire de Nice Sophia
 Antipolis (France)

No Abstract Available

9378-78, Session 13

Nuclear magnetic resonance gyroscope (Invited Paper)

Michael S. Larsen, Northrop Grumman Corp. (United
 States)

No Abstract Available

9378-63, Session 14

Precise navigation and timing with atom-interferometric sensors (Invited Paper)

David Butts, Draper Lab. (United States)

No Abstract Available

9378-64, Session 14

Collective state atomic interferometer with ultra-high Compton frequency

Resham Sarkar, May Kim, Selim M. Shahriar, Northwestern Univ. (United States)

No Abstract Available

9378-65, Session 14

Towards an interferometer with thermal atoms trapped on a microwave chip
(Invited Paper)

Sylvain Schwartz, M. Dupont-Nivet, Thales Research & Technology (France); Peter Rosenbusch, Observatoire de Paris (France); Isabelle Bouchoule, Institut d'Optique Graduate School (France); Christoph I. Westbrook, Institut d'Optique Theorique et Appliquee (France); C. Guerlin, J. Reichel, Lab. Kastler Brossel (France)

No Abstract Available

9378-66, Session 14

Atom interferometry using Bose-Einstein condensates on Earth and in space *(Invited Paper)*

Charles Sackett, Univ. of Virginia (United States)

No Abstract Available

9378-67, Session 14

Photonic requirements for magnetically-guided cold atom gyroscopes *(Invited Paper)*

John H. Burke, Air Force Research Lab. (United States)

No Abstract Available

9378-68, Session 15

Optical lattice clocks for ultra-precise atomic timekeeping *(Invited Paper)*

Andrew D. Ludlow, National Institute of Standards and Technology (United States)

No Abstract Available

9378-69, Session 15

Materials for on-chip optical combs

Michal Lipson, Cornell Univ. (United States)

No Abstract Available

9378-70, Session 15

Fiber-laser frequency combs for the generation of mm- and THz-waves, sinc-shaped Nyquist pulses, and tunable single-frequency laser lines *(Invited Paper)*

Thomas Schneider, Karlsruher Institut für Technologie (Germany)

No Abstract Available

9378-71, Session 15

Cascaded optical link on a telecommunication fiber network for ultra-stable frequency dissemination *(Invited Paper)*

Olivier Lopez, Nicola Chiodo, Lab. de Physique des Lasers (France); Fabio Stefani, Observatoire de Paris (France); Fabrice Wiotte, Nicolas Quintin, Anthony Bercy, Lab. de Physique des Lasers (France); Christian Chardonnet, Observatoire de Paris (France); Giorgio Santarelli, Observatoire de Paris (France) and Lab. de Physique des Lasers (France); Paul-Eric Pottie, Anne Amy-Klein, Lab. de Physique des Lasers (France)

The transfer of ultra-stable frequencies between distant laboratories is required by many applications in time and frequency metrology, fundamental physics, particle accelerators and astrophysics. Optical fiber links have been intensively studied for a decade and brought the potential to transfer frequency with a very high accuracy and stability thanks to an active compensation of the propagation noise.

We are currently developing an optical link of 1500 km using the fibers of the French National Research and Education Network. Using the so-called dark-channel approach, the ultrastable signal is copropagating with data traffic using wavelength division multiplexing. Due to significant reflections and losses along the fibers, which cannot be compensated with amplifiers, we have developed some repeater stations for the metrological signal. These remotely-operated stations amplify and filter the ultrastable signal and compensate the propagation noise. The link is thus composed of a few cascaded spans. It gives the possibility to increase the noise correction bandwidth, which is proportional to the inverse of the fiber length for each span. These stations are a key element for the deployment of a reliable and large scale metrological network.

We will report on the first implementation of a four-span cascaded link of 1100 km reaching a relative stability of a few 10^{-19} after 10000 s averaging time. Extension to longer links and alternative transfer methods will be discussed.

9378-72, Session 16

A matter wave clock *(Invited Paper)*

Holger Muller, Consultant (United States)

No Abstract Available

**Conference 9378: Slow Light, Fast Light, and
Opto-Atomic Precision Metrology VIII**

9378-73, Session 16

**Collective state Raman-Ramsey atomic
clock with trapped atoms**

May Kim, Resham Sarkar, Selim M. Shahriar, Northwestern Univ. (United States)

No Abstract Available

9378-74, Session 16

**Measurements and characterization of
a Rb-based Raman-Ramsey vapor cell
atomic clock**

Gour S. Pati, Zachary Warren, Renu Tripathi, Delaware State Univ. (United States); Selim M. Shahriar, Northwestern Univ. (United States)

Raman-Ramsey technique has been demonstrated as an effective method for producing narrow optical resonance and reduced light shift for developing high-performance vapor cell atomic clocks. We have designed an experimental testbed for a Rb-based Raman-Ramsey vapor cell atomic clock. This apparatus allows us to measure the frequency-stability of a microwave oscillator by locking it to the clock transition. In order to achieve high frequency stability (Allan deviation below 10^{-11} at 1 sec), high magnetic-shield enclosure and low phase noise electronics have been assembled. Pulsed optical interrogation and clock servo control have been performed through a computer-controlled digital board. We will present basic measurements and characterizations of the experimental testbed. This will include measurements of light shift, and characterizations of short- and long-term frequency stability performance of the Rb-based atomic clock.

9378-75, Session 16

**Investigation of atomic shot noise
spectrum in a warm vapor cell** (*Invited
Paper*)

Yanhong Xiao, Fudan Univ. (China)

No Abstract Available

9378-76, Session 16

**Precision measurement with ultra-
broadband bi-photons** (*Invited Paper*)

Avi Pe'er, Bar-Ilan Univ. (Israel)

Broadband time-energy entangled photon pairs (bi-photons) and broadband squeezed light offer a rare resource for quantum information – extreme quantum correlation in the femtosecond time-scale combined with an ultra-high photon flux (up to $10^{14}/s$). Despite these advantages, the bandwidth resource of bi-photons is rarely used in current experiments, mainly because standard detection with photo-detectors and homodyne measurement is narrowband and cannot access the broad bandwidth. I will present our efforts to develop a complete set of detection methods for broadband squeezed light and bi-photons, which exploit the optical nonlinearity as an efficient broadband physical detector of quantum correlation in both the low power regime of single photons and high-power regime of broadband squeezed light. I will discuss applications for quantum information, such as high bit-rate quantum communication and precision measurement of optical phase.

1. Yaakov Shaked, Roey Pomerantz, Rafi Z. Vered and Avi Pe'er, "Observing the nonclassical nature of ultra-broadband bi-photons at ultrafast speed", *New J. Phys.* 16, 053012 (2014).
2. Rafi Vered, Yaakov Shaked, Michael Rosenbluh and Avi Pe'er, "The Classical-to-Quantum Transition with Broadband Four-Waves Mixing - Observing Bi-photon Generation with Real or Imaginary Gain", Submitted (2014)
3. Faina Shikerman and Avi Pe'er, "Sum-frequency generation as a detector of high-power two-mode squeezing", *Phys. Rev. A.* 88, 043808 (2013)

Conference 9379: Complex Light and Optical Forces IX

Wednesday - Thursday 11-12 February 2015

Part of Proceedings of SPIE Vol. 9379 Complex Light and Optical Forces IX

9379-1, Session 1

The physics of “self-healing” of structured wavefields (*Invited Paper*)

Sabino Chávez-Cerda, Instituto Nacional de Astrofísica, Óptica y Electrónica (Mexico)

During the last three decades, the property of self-healing or self-reconstruction of wavefields has amazed the scientific community. It has been reported for wavefields propagating in linear and nonlinear media, for optical pulses in the temporal domain and also for acoustic wavefields. Self-healing can be defined as the reappearance of a wavefield after being partially blocked by an obstruction, or temporal shutter in its case, with similar characteristics of amplitude and phase that it would have if no obstacle was encountered.

Self-healing was originally studied for nondiffracting beams and, interestingly enough, since these diffraction-free beams have been surrounded by many mysterious properties, self-healing inherited this uncanny perception. What made self-healing a mysterious property is that it is not observed in common optical wavefields, like a Gaussian beam. Even in recent literature we can read about the remarkable, intriguing and unique property of self-healing of wavefields that historically had been mainly attributed to diffraction-free or propagation invariant wavefields. Nevertheless, more recently they have also been demonstrated in vortex, lattice, nonparaxial, acoustic, optical caustic and other more complex wavefields.

The physics behind this mysterious property will be exposed. Gaussian beams and plane waves are characterized for not having a complex transverse phase structure. It will be shown that it is precisely only wavefields having a particular complex phase structure that can be subject to self-healing. The approach is based on the complementarity principle in optics using wave and ray optics to have a complete physical picture of self-healing of optical wavefields.

9379-2, Session 1

Adaptive self-reconstruction and autocorrelation of nondiffracting wavepackets

Alexander Treffer, Stefan Koenig, Max-Born-Institut für Nichtlineare Optik und Kurzzeitspektroskopie (Germany); Jens Brunne, Ulrike Wallrabe, Univ. of Freiburg (Germany); Ruediger Grunwald, Max-Born-Institut für Nichtlineare Optik und Kurzzeitspektroskopie (Germany)

The reliable autocorrelation of ultrashort laser pulses, in particular such emitted by Ti:sapphire laser oscillators with pulse durations in few-cycle range, is a challenging task. Related techniques are important for the exploration of physical and chemical processes on this extreme time scale and required for ultrafast information processing. The transfer of spatial and temporal information, however, is sensitive against amplitude and phase distortions. It is well known, e.g. from microscopy, that it can be improved by exploiting the propagation features of distortion-tolerant nondiffracting beams. The availability of new, fast switching, reflective, piezo-based MEMS components enables to realize even smarter and more robust autocorrelator systems which combine the low-dispersion, nondiffracting beam shaping and adaptive functionality. Two basic concepts of adaptive non-collinear nonlinear autocorrelation are presented here: (a) autocorrelation with adaptive self-reconstruction of nondiffracting sub-beams, and (b) discrete phase shifting methods. By tuning the angle

of superposition in non-collinear autocorrelation it is possible to bypass the corruption of temporal information by distortions. This is demonstrated by recent experimental results with a prismatic linear axicon (Fresnel mirror). By means of adaptively self-reconstructive autocorrelation with hysteresis compensation, a spatially located distortion can be sampled in temporal domain. The phase-shifting approaches promise to enable a significant improvement with respect to the possible time resolution. It is expected that measurements at pulse durations even down to the attosecond range are realistic. Analogies to the classical interferometric and holographic phase shifting techniques are addressed and system requirements are analyzed in detail for different geometries.

9379-3, Session 1

Deconvoluting principal modes for mode-division multiplexing

Daniel A. Nolan, Corning Incorporated (United States); Giovanni Milione, Robert R. Alfano, The City College of New York (United States)

In mode division multiplexing (MDM) optical fiber modes are used as separate channels carrying independent signals over a multimode optical fiber. Mode coupling and mode dispersion severely limit MDM, yet can be mitigated by a method of digital signal processing referred to as MIMO. In principle, it is possible to avoid MIMO using what are referred to as principal modes, i.e., superpositions of optical fiber modes that do not exhibit mode dispersion. In this presentation, we propose an alternative method of MDM where the optical fiber modes are (de)multiplexed but then deconvolved without MIMO by separately measuring the principal modes.

9379-4, Session 1

Spiral phase plates for the generation of high-order Laguerre-Gaussian beams with non-zero radial index

Gianluca Ruffato, Marta Carli, Filippo Romanato, Univ. degli Studi di Padova (Italy)

Azimuthally higher and radially lowest-order Laguerre-Gaussian (LG) beams have been extensively studied, while radially higher-order LG beams have not attracted much attention. In the specific, a few groups described the generation of high-order LG beams with the use of spatial light modulators or fork-holograms. Here we extend the use of spiral phase plates (SPP) for the generation of high-order LG beams with non-zero radial index and present the work of design, fabrication and characterization of such optical elements. These engineered SPPs were designed and fabricated by electron beam lithography (EBL) on poly(methyl methacrylate) (PMMA) over glass substrates. The optical response was theoretically considered and experimentally measured and the purity of the experimental beams was investigated in terms of LG modes contributions. The far-field intensity pattern was compared with theory and numerical simulations, whereas interferometric analyses confirmed the expected phase features of the generated beams. The high quality of output beams confirms the applicability of these SPPs for the generation of high-order LG beams with remarkable applications in many areas: optical tweezing and trapping, spiral-phase contrast microscopy, telecommunication systems based on OAM multiplexing. We present a novel and promising application concerning high-security holograms based on twisted light. Diffractive optical elements encoding information for impinging light generated by high-order SPPs are designed and fabricated with EBL.

**Conference 9379:
 Complex Light and Optical Forces IX**

G. Ruffato, M. Massari and F. Romanato, "Generation of high-order Laguerre-Gaussian modes by means of Spiral Phase Plates", accepted by Optics Letters.

G. Ruffato, M. Carli and F. Romanato, "High-security holograms for twisted light", in preparation.

9379-5, Session 1

Attenuation-compensated Airy beams

Miguel A. Preciado, Kishan Dholakia, Michael Mazilu, Univ. of St. Andrews (United Kingdom)

Propagation-invariant light fields have attracted significant attention due to their ability to retain their transverse profile during propagation over finite distances. The Airy wave-packets exhibit a parabolic path and self-healing properties. These beams have been used for spatio-temporal light-bullets under linear and non-linear conditions, plasmonics, micro-manipulation and have recently been used for super-resolved and light-sheet microscopy. Here, we present a novel form of the propagation-invariant Airy beam that is attenuation-compensated. This beam exhibits an evanescent attenuation that can be adjusted to compensate for the losses originating from the propagation through absorbing media. We generate and study finite-energy versions of these beams using a digital micro-mirror device.

9379-6, Session 2

Pancharatnam-Berry phase optical elements for generation and control of complex light and weak measurements without post-selection for probing the orbital angular momentum content of complex light (Invited Paper)

Bruno Piccirillo, Univ. degli Studi di Napoli Federico II (Italy); Lorenzo Marrucci, Univ. degli Studi di Napoli Federico II (Italy) and CNR-SPIN (Italy); Enrico Santamato, Univ. degli Studi di Napoli Federico II (Italy)

We present the state-of-the-art in the development of liquid-crystal-based Pancharatnam-Berry phase Optical Elements (PBOE) for highly efficient generation and control of complex light. The prototype of PBOE for light shaping is the q-plate[1]. It is an electrically tunable retardation waveplate having an axis distribution with topological charge q. A circularly polarized plane beam traversing a q-plate suffers a handedness reversal and the orbital angular momentum (OAM) is shifted by $\pm 2q$ opposite to the handedness change. q-plate technology has proved to be useful for applications both in quantum and classical optics.

Full azimuthal control of the optical axis is now available and a variety of q-plate-like devices can be fabricated[2]. These devices reshape wavefronts by birefringence, impressing to the extraordinary component of a polarized beam an inhomogeneous transverse phase-retardation reflecting the inhomogeneity of the axis distribution. Devices based on this principle can be fabricated to generate complex superpositions of multiple OAM eigenmodes or light beam with polarization singularities.

We also address the problem of fast and reliably measuring the orbital angular momentum of light in structured beams. Exploiting quantum weak measurements without post-selection, we worked out a method for measuring both the mean and the variance of the OAM content of beam without acquiring its entire spectrum.

[1] Marrucci et al. Phys. Rev. Lett. 96, 163905 (2006)

[2] Slussarenko et al. J. Opt. 15 025406 (2013)

9379-7, Session 2

Holographic modulation of polarization singularities in the transverse plane of Poincaré beams

Eileen Otte, Christian Schlickriede, Christina Alpmann, Cornelia Denz, Westfälische Wilhelms-Univ. Münster (Germany)

Within the last ten years a growing interest in the theoretical and experimental investigation of polarization singularities could be observed [1]. Vector singularities as L-Lines, V-Points and C-Points can appear in the transverse plane of Poincaré beams, which contain a spatially inhomogeneous distribution of states of polarization [2]. Typically, Poincaré beams and polarization singularities are generated exploiting birefringence, q-plates, or by interferometric methods. However, these methods do neither allow an arbitrary transverse location of polarization singularities nor a full combination of amplitude phase, and polarization modulation of the complete transverse plane.

In our contribution, we present a holographic method which is not only capable of tailoring complex light fields by amplitude and phase modulation but also allows arbitrarily modulating the states of polarization such that Poincaré beams with polarization singularities can be created. Our experimental system employs a single reflective phase-only spatial-light-modulator operating in a split-screen-mode. We will demonstrate the capabilities of our method ranging from the modulation of higher order Gaussian modes including desired polarization characteristics to the generation of polarization singularities at arbitrary points in the transverse plane of Poincaré beams. The properties of these beams can be applied in optical micromanipulation, where polarization properties are used to align anisotropic particles. Moreover, application in information technology for advanced information encoding is possible.

[1] M. R. Dennis et al., Progress in Optics 53, 293-363 (2009)

[2] T. G. Brown, Progress in Optics 56, 81-129 (2011)

9379-8, Session 2

Is Monstar topologically the same as Lemon?

Nirmal K. Viswanathan, Vijay Kumar, Univ. of Hyderabad (India)

Singularities in pi-symmetric fields are associated with lemon, star and monstar topological structures. Symmetric cases of these structures were first proposed by Berry and Hannay in 1977 [1] and Dennis in 2008 [2] generalized them to asymmetric cases. Monstar with index and three radial lines ending at the C-point is an intermediate structure having properties of both lemon and star. The monstar structure though are statistically rare in random Gaussian fields but can be experimentally realized in specially prepared optical fields by means of superposition of vortex beam(s) and / or uniform phase Gaussian – Hermite-Gaussian beams under appropriate phase and polarization conditions [3].

We experimentally realized the monstar pattern in polarization ellipse orientation via three different routes from lemon pattern using topologically-invariant squeezing and / or rotation transformations. This raised the question "is monstar topologically the same as lemon?" Our results suggest that lemon and monstar can smoothly transform into each other under any or combination of topologically-invariant transformations leading to one interpretation that monstar is an anisotropic lemon, the two structures being topologically the same. However, if lemon and monstar structures are to be topologically different we have to look for physical situations where these structures have their respective manifestations.

References:

[1] M.V. Berry and J.H. Hannay, J. Phys. A 10, 1809 (1977)

[2] M.R. Dennis, Opt. Lett., 33, 2572 (2008)

[3] E.J. Galvez et al., Phys. Rev. A 89 (R), 013801 (2014)

**Conference 9379:
 Complex Light and Optical Forces IX**

9379-10, Session 2

Mobius strips and twisted ribbons in 3-dimensional optical fields

Enrique J. Galvez, Jonathan J. Zeosky, Colgate Univ. (United States)

We investigate three-dimensional ellipse fields produced by two intersecting beams of light. One beam is prepared in either a pure or a superposition of Laguerre-Gauss modes with $l = 1, 2$ and in a circular polarization state. The other beam is in Gaussian $l = 0$ mode and with orthogonal polarization. We diagnosed the field patterns by projective polarization measurements. The results are consistent with either Mobius strips or twisted ribbons described by the polarization ellipses on a circle about the center of the intersection.

9379-11, Session 3

Real-time imaging of spin-to-orbital angular momentum quantum state teleportation (Invited Paper)

Ebrahim Karimi, Manuel Erhard, Hammam Qassim, Harjaspreet Mand, Robert W. Boyd, Univ. of Ottawa (Canada)

Quantum teleportation is a process in which an unknown quantum state is transferred between two spatially separated parties, namely Alice and Bob, that share an entangled state and communicate classically. In the case of photonic states, this process is probabilistic due to the impossibility of performing a two-particle complete Bell state analysis with linear optics. In order to achieve a deterministic teleportation scheme, it has been proposed to harness other degrees of freedom of Alice particle, rather than using the quantum state of a third particle. Indeed, this suggestion leads to a novel type of deterministic teleportation, so-called hybrid teleportation. Here we report the first realization of photonic hybrid quantum teleportation from spin to the orbital angular momentum degree of freedom. In our scheme, the polarization state of photon A is transferred to orbital angular momentum of photon B . The teleported states are visualized in real-time by means of an intensified CCD camera. The quality of the teleported states is verified by performing quantum state tomography, which confirms an average fidelity higher than 99.4%. We believe that this experiment paves the way towards a novel means of quantum communication in which encryption and decryption are carried out in naturally different Hilbert spaces, and therefore may provide a means for enhancing security.

9379-12, Session 3

Quantum nonlinear optics with strongly interacting atoms: from few-photon applications to quantum many-body physics with light (Invited Paper)

Thomas Pohl, Max-Planck-Institut für Physik komplexer Systeme (Germany)

The generation of optical nonlinearities, sufficiently strong to operate on the level of few photons, remains an outstanding challenge for many years. Recently, the combination of electromagnetically induced transparency with strong, long-ranged particle interactions has emerged as a promising approach to this goal.

In this talk, I will describe the basic mechanisms that give rise to unique nonlocal optical nonlinearities, which yield very strong photon-photon interactions acting over long distances of several micrometers. I will discuss the potential of such settings for few-photon applications to

deterministically create and manipulate quantum states of light. Propagating multi-photon pulses are shown to provide a well suited platform for exploring the transition from few-photon bound states to unusual optical solitons with a nonlinear group velocity. Finally, I will discuss the properties of stationary light fields in such optical media. Quantum Monte-Carlo simulations of this scenario reveal a rich spectrum of strongly correlated phases of photons, atoms or both, illustrating its potential for realizing exotic quantum many-body physics with light. Implications for experiments using ultracold Rydberg atoms or ion crystals will also be discussed.

9379-13, Session 3

Quantum zeno suppression of a quantum phase transition

Wolfgang A. Ertmer, Bernd Luecke, Jan Peise, Carsten Klempt, Frank Deuretzbacher, Luis Santos, Leibniz Univ. Hannover (Germany); Luca Pezzé, Istituto Nazionale di Ottica (Italy); Augusto Smerzi, European Lab. for Non-linear Spectroscopy (Italy)

The quantum Zeno effect predicts that a quantum mechanical transition can be suppressed by frequent measurements. Here, we demonstrate that a quantum phase transition can be suppressed by the continuous detection of the output phase. In our experiment we investigate spin changing collisions in a Rb-87 Bose-Einstein condensate. A BEC of 30,000 atoms is initially prepared in the $F=2, m_F=0$ state. The collisional energies and the quadratic Zeeman energy define a critical magnetic field for which the BEC becomes unstable towards a production of atom pairs in the states $m_F=\pm 1$. This process resembles parametric-down conversion in optics, where the output states in $m_F=\pm 1$ correspond to the signal and idler beams in optics. We experimentally demonstrate that a continuous measurement of the number of atoms in $m_F=-1$ (signal) during the spin changing collisions introduces the quantum Zeno effect for the phase transition. We observe the suppression of the transition by detecting the atoms in $m_F=+1$ (idler). For the first time, it is thus possible to detect the quantum Zeno effect indirectly. Our setup allows for interesting applications such as interaction-free measurements on the basis of neutral atoms

9379-14, Session 4

Classical entanglement: more than an oxymoron (Invited Paper)

Andrea Aiello, Max-Planck-Institut für die Physik des Lichts (Germany) and Friedrich-Alexander-Univ. Erlangen-Nürnberg (Germany); Falk Toeppel, Friedrich-Alexander-Univ. Erlangen-Nürnberg (Germany); Christoph Marquardt, Gerd Leuchs, Max-Planck-Institut für die Physik des Lichts (Germany); Elisabeth Giacobino, Lab. Kastler Brossel (France)

Quantum approaches relying on entangled photons have been recently proposed to increase the efficiency of optical measurements. We demonstrate that, surprisingly, the use of classical light with entangled degrees of freedom can also bring outstanding advantages over conventional measurements in polarization metrology. Specifically, we show that radially polarized beams of light allow to perform real-time single-shot Mueller matrix polarimetry. Our results also indicate that quantum optical procedures requiring entanglement without nonlocality can be actually achieved in the classical optics regime. Moreover, other useful applications of classical entanglements are presented.

**Conference 9379:
 Complex Light and Optical Forces IX**

9379-15, Session 4

Spatially-varying polarization singular pattern: degree of polarization and coherence

Nirmal K. Viswanathan, Samlan C. T., Rishabh Pandey, Anusuya Pal, Univ. of Hyderabad (India)

Superposition of optical vector waves can result in light fields with spatial modulation of not only its state of polarization (SOP) but also the degree of polarization (DOP) and coherence. Unraveling this interconnection between the polarization and coherence characteristics of light fields in the context of singular optics is of recent research interest with far-reaching consequences of both fundamental and applied nature [1].

Spatially-varying polarization modulation (with different singularity features) is realized in the observation plane using a birefringent wedge depolarizer (WD), which modifies the mutual coherence of orthogonally polarized components of the beam. Using Stokes polarimetric technique we understand the polarization singular patterns generated by the WD. The polarization changes leading to the changes in the visibility of interference patterns of the Stokes parameters is used to extract information on the degree of polarization and coherence of the superposed vector optical fields. Different experimental parameters including the SOP of the incident plane and helical wavefront beams, orientation of the WD with respect to the input beam polarization at a fixed plane and along the direction of propagation are explored to realize vector optical beam-fields with variable degree of polarization and coherence.

References:

[1] O.V. Angelsky et al., "Optical measurements: Polarization and coherence of light fields," "Modern Metrology Concerns", book edited by Luigi Cocco, DOI: 10.5772/36553

9379-16, Session 4

Imaging polarimetry of single-photon states

Enrique J. Galvez, Xinru Cheng, Colgate Univ. (United States); Behzad Khajavi, Colgate Univ. (United States) and Florida Atlantic Univ. (United States)

We prepare single photons in non-separable states of polarization and spatial mode. The spatial modes can be any of the low-order ($l = 0, 1, 2$) Laguerre-Gauss modes. When the photons prepared in qubit-qubit and qubit-qutrit states are projected onto a transverse position basis, polarimetry analysis reveals polarization singularity features shown previously in classical beams: lemons, stars and monstars. This polarimetry analysis also gives information about the purity of the quantum state, which is also diagnosed by quantum state tomography.

9379-17, Session 4

Quantum optics of non paraxial vortex beams

Jörg B. Götte, Max-Planck-Institut für Physik komplexer Systeme (Germany); Matt M. Coles, Imperial College London (United Kingdom)

Using a fully quantised description we investigate the effect of focussing of vortex beams on the energy, momentum and angular momentum of the light. We calculate the various quantities as functions of the numerical aperture of the lens used for the focussing the light beam. Our results can be expressed simply in terms of differences and sums of the number operators for left and right handed circular polarization and the azimuthal

winding number of the vortex. We relate the different measures to the spin and orbital parts of the optical momentum. In contrast to the collimated or paraxial case we show a direct coupling between the individual parts of the optical momentum are coupled which increases with the numerical aperture.

We predict that any experiment designed to detect orbital angular momentum of focussed light will be affected by a contribution depending on the helicity of the light beam. Conversely, we discuss the consequences of focussing for the interaction of light with chiral matter by means of general optical processes which have different absorption rates for the different handedness of circular polarization. Using our formalism we are able to show that within the dipole approximation the orbital angular momentum does not contribute to the differential absorption.

9379-32, Session PWed

Constrained Brownian motion of nanoparticles near an interface using optical tweezers

Hui Yang, Matteo Cornaglia, Thomas Lehnert, Martin A. M. Gijs, Ecole Polytechnique Fédérale de Lausanne (Switzerland)

It is well known that the diffusivity of a particle in unbound space is different from that of the particle positioned nearby a solid boundary. The former follows the Stokes-Einstein relation, which balances the fluid thermal energy with the particle's hydrodynamic mobility. However, when the particle is near the boundary, it experiences an increased hydrodynamic drag force, which reduces its mobility. This phenomenon can be studied by monitoring the constrained Brownian motion of particles near an interface. Most previous experimental results were obtained by measuring the diffusion coefficient of the particle in the evanescent optical field near the interface using video imaging microscopy techniques. Here, we demonstrate a method to directly determine the diffusion coefficient of the particle over an extended range in the direction normal to the interface by using optical tweezers. Fluorescent polystyrene nanoparticles are dispersed in de-ionized water, and then the sample solution is introduced in a micro-chamber. A single particle is trapped by the tweezers and moved to certain distances away from the substrate. By analyzing the time-dependent trajectory of the nanoparticle, the diffusion coefficient parallel to the substrate, for a Brownian particle constrained by the substrate, is determined as a function of the distance between the substrate and the nanoparticle. The experimental result directly indicates the drag effect on the nanoparticle arising from the substrate, and the measurement shows that the viscous drag for a particle nearby the substrate is about three times higher than for a particle in the bulk fluid.

9379-33, Session PWed

Force calibration of structured light in optical tweezers

Ann A. Bui, Alexander B. Stilgoe, Timo A. Nieminen, Halina Rubinsztein-Dunlop, The Univ. of Queensland (Australia)

Optical tweezers are strongly focussed beams which can trap transparent microscopic particles by exerting piconewton forces. Tracking of the trapped particles is usually done using a camera or quadrant photodiode (QPD). It is common to assume that the camera and QPD give the same information. However, the camera gives the position of the particle and the QPD gives the force acting on the particle. For rotationally symmetric beams, the distributions of positions and forces have similar shapes. For nonrotationally symmetric beams, it is clear that the position and force distributions are not the same, but have complementary shapes. This is intuitive as a greater force more restricts the thermal motion of the trapped particle. Here we use computational simulation of trapping a particle in a nonrotationally symmetric beam to compare the relation between position and force measurements.

**Conference 9379:
Complex Light and Optical Forces IX**

9379-34, Session PWed

Cylindrical polarization analyzers

Roger M. Herman, The Pennsylvania State Univ. (United States); Daniel A. Nolan, Corning Incorporated (United States) and New York State Ctr. for Complex Light (United States)

We describe a new method to fabricate analyzers for cylindrically polarized and vortex beams. The method requires only linear polarization elements and a transparent cylindrical tube. In this method an incoming beam incident onto and then propagating within the interior of a tube parallel to the z axis, is redirected onto the tube's surface, which includes the linear polarizers. Light is refracted and components of polarization are absorbed by the linear polarizers. Light then incident onto a plane above and perpendicular to the z axis of the tube is cylindrically polarized. The orientation of the linear polarizers on the tube's surface determines the orientation of the output radial or azimuthally polarized light. Vortex beams are obtained by orientating the linear polarizers at an angle to the x, y plane. We analyze the polarization components using a three dimensional Stokes analysis, SU(3) group theory and the Gell Mann matrices. Using this formalism, we define a 3 dimensional degree of polarization, which is dependent on the symmetry and the width of the incoming beam in relation to the geometry of the tube and the orientation of the linear polarizers.

9379-35, Session PWed

Classical entanglement in polarization metrology

Falk Töppel, Andrea Aiello, Christoph Marquardt, Elisabeth Giacobino, Gerd Leuchs, Max Planck Institute for the Science of Light (Germany)

Quantum information theory shows that coherent measurements have the essential capability to provide more information than incoherent ones, as emphasized by many authors [1, 2]. Several works based on the concept of coherent measurements have appeared recently [3-5]. However, for the purpose of such measurements, not all the features of quantum entanglement, as nonlocality, are necessary. For example most coherent measurements require entanglement as primary resource, but not nonlocality. Classical systems are known to obey the rules of locality. Nevertheless, some classical systems show the remarkable feature of nonseparability, that is "classical entanglement" between different degrees of freedom [6]. In particular, classical entanglement has been demonstrated in optical beams with nonuniform polarization patterns. Typical examples are the so-called cylindrically polarized beams of light [7, 8], which can be represented by linear superpositions of the transverse electro-magnetic modes TEM₁₀ and TEM₀₁ with different linear polarizations. So the question arises: Can one also use the unique properties of nonseparable classical light to benefit from the advantages of coherent measurements?

Our work demonstrates that classical entanglement in cylindrically polarized beams of light permits achieving coherent measurement of the Mueller matrix of an optical element affecting polarization [9, 10]. In principle, our method allows the Mueller matrix reconstruction in real time from a single shot, whereas conventionally four probe beams of different polarizations are required. This example furnishes a proof of principle that tasks requiring entanglement but not nonlocality may be accomplished by using classical systems.

[1] N. Gisin, J. Mod. Opt. 48, 1397 (2001)

[2] S. Massar. and S. Popescu, Phys. Rev. Lett. 74, 1259 (1995)

[3] A. Aiello, and J. P. Woerdman, arXiv:0412061v3 [math-ph]

[4] M. Legré M, M Wegmüller, and N. Gisin, Phys. Rev. Lett. 91, 167902 (2003)

[5] N. Brunner, A. Acín, D. Collins, N. Gisin, and V. Scarani, Phys. Rev. Lett. 91, 180402 (2003)

[6] R. J. C. Spreeuw, Foundations of Physics 28, 361 (1998).

[7] A. Holleczek, A. Aiello, Ch. Gabriel, Ch. Marquardt, and G. Leuchs, Opt. Exp. 19, 9714 (2011).

[8] X.-F. Qian and J. H. Eberly, Opt. Lett. 36, 4110 (2011).

[9] F. Töppel, A. Aiello, Ch. Marquardt, E. Giacobino, and G. Leuchs, New J. Phys. 16, 073019, (2014).

[10] A. Aiello, F. Töppel, Ch. Marquardt, E. Giacobino, and G. Leuchs, arXiv:1409.0213 [quant-ph].

9379-18, Session 5

Mode-division multiplexing using the basis of vector modes over free space and optical fibers

Giovanni Milione, The City College of New York (United States); Martin P. J. Lavery, Univ. of Glasgow (United Kingdom); Hao Huang, Yongxiong Ren, Yan Yan, The Univ. of Southern California (United States); Ebrahim Karimi, Univ. of Ottawa (Canada); Thien An Nguyen, The City College of New York (United States); Ming-Jun Li, Dan A. Nolan, Corning Incorporated (United States); Robert R. Alfano, The City College of New York (United States); Alan E. Willner, The Univ. of Southern California (United States)

Mode division multiplexing (MDM) is a method of optical communication where each spatial mode of an optical communication link, such as free space or an optical fiber, is used as a separate information channel carrying an independent signal. MDM can multiplicatively increase the information capacity and in turn the spectral efficiency optical communication in an amount proportional to the number of modes used. Spatial modes can be represented by many bases. In principal, any basis of modes can be used for MDM. In this talk, we will provide new context and insight into our recent work on MDM using the basis of vector modes over free space and optical fibers. A mode (de)multiplexer for vector modes based on a liquid crystal device referred to as q-plate is described. Using q-plates, four vector modes are (de)multiplexed over free space, comprising an aggregate 160 Gbit/s information capacity on a single wavelength channel, with a bit error rate above the forward error correction limit. Also, four vector modes are (de)multiplexed over 5 kilometers of a conventional multimode optical fiber, comprising an aggregate 160 Gbit/s information capacity on a single wavelength channel, in concert with 4X4 multiple input multiple output (MIMO) digital signal processing to mitigate mode coupling.

9379-19, Session 5

Optical vortex position detection with a Shack-Hartmann wavefront sensor using extended closed-contour method

Hongxin Huang, Hamamatsu Photonics K.K. (Japan); Jia Luo, Zhejiang Univ. (China); Yoshinori Matsui, Haruyoshi Toyota, Takashi Inoue, Hamamatsu Photonics K.K. (Japan)

Optical vortex (OV) beams having spiral phase structures around zero-amplitude-points have many applications. With increasing demands, adaptive control of the OV beam becomes necessary, which requires direct detection of OV fields, especially detection of their center positions. We have proposed a detection method using a Shack-Hartmann wavefront sensor for the detection of OV center position. The method has steps of calculating circulation values of phase slope vectors along a closed contour path connecting the centers of the 2x2 neighboring lenslets and of comparing the circulation values around the OV center with a set of pre-calculated reference values. The accuracy experimentally confirmed was approximately 0.056, in units of the lenslet size. However, we found that the measurement accuracy depends on the relationship between the

**Conference 9379:
 Complex Light and Optical Forces IX**

lenslet centers and the OV center, due to the nature of zero-amplitude of OV field. Here we propose an alternative method to avoid the problem, thus to improve measurement accuracy and robustness to noise. In the new method, we used a closed contour line connecting the centers of 3x3 neighboring lenslets. While it was expected that the larger close-line path would reduce the influence of the zero-amplitude of OV field, and the characteristics of circulation values would also differ from those with the 2x2 lenslet closed-line. We will present both theoretical analysis and experimental evaluation by using a phase-only spatial light modulator to generate OV beams.

9379-20, Session 5

Characterization of OAM carrying beams by means of holographic correlation filters

Robert Brüning, Christian Schulze, Daniel Flamm, Friedrich-Schiller-Univ. Jena (Germany); Andrew Forbes, CSIR National Laser Ctr. (South Africa); Michael Duparré, Friedrich-Schiller-Univ. Jena (Germany)

Laser beams carrying orbital angular momentum (OAM) attained a lot of interest in the last years owing to their unique properties and enable a variety of exciting applications, e.g. in optical mode- multiplexing communication strategies, nonlinear optics and particle manipulation. To control and improve such systems the complete characterization of the OAM carrying beams becomes essential to understand the underlying physical effects. We present an all optical analysis scheme based on holographic correlation filters, which enables the real time observation of OAM carrying beams and their properties, like underlying OAM state spectrum, total OAM, OAM density and position of occurring phase singularities. For this purpose, the beam under investigation is modally decomposed by a holographic correlation filter into a complete set of orthogonal modes. Using an adapted mode set of vortex modes, typical for cylinder symmetric systems, and where the azimuthal field dependency is given by a unique OAM value, such parameters like OAM state spectrum, total OAM and OAM density can be directly received from the achieved mode content of the beam. After reconstruction of the complete optical field based on the results of modal decomposition, including the transversal phase distribution, even the position of occurring phase singularities is determinable. By application of a spatial multiplexing technique all needed filter functions can be implemented into a single hologram, resulting in a real-time procedure to investigate arbitrary OAM carrying beams.

9379-21, Session 6

**Dynamical stabilisation in optical tweezers
 (Invited Paper)**

Philip H. Jones, Christopher J. Richards, Thomas J. Smart, Univ. College London (United Kingdom); David Cubero, Univ. de Sevilla (Spain)

The phenomenon of dynamical stabilisation is well-known from the famous Kapitza pendulum experiment, in which a rigid pendulum with negligible damping is stabilised in the inverted position by a high-frequency modulation of the point of suspension. Here we present a study of dynamical stabilisation of a pendulum in a regime with non-negligible friction. In the presence of high damping the inverted pendulum position is predicted to be no longer stable, however new positions of equilibrium are shown to emerge depending on the magnitude of the friction, and the frequency and amplitude of driving.

The damped pendulum is realised experimentally using a spherical microparticle in a ring-shaped optical trap that is subject to an additional controllable viscous drag force induced by fluid flow at constant velocity. Driving of the pendulum is achieved by modulation of the position of the trapping potential parallel to the direction of the fluid flow. The dynamics of the particle are recorded and analysed by video tracking microscopy.

We show that the location of the particle in the trap can be stabilised against the viscous drag for sufficiently high amplitude of driving. We track the motion of the trapped particle and use the resulting trajectory to characterise the effective potential in the region of the new equilibrium position. Experimental results are in good agreement with theory and Brownian motion simulations of the trapped particle.

9379-22, Session 6

Real-time dynamic coupling of GPC-enhanced diffraction-limited focal spots

Mark Jayson M. Villangca, Andrew Rafael Bañas, Oleksii Kopylov, DTU Fotonik (Denmark); Darwin Palima, Jesper Glückstad, Technical Univ. of Denmark (Denmark)

We have previously proposed and demonstrated on-demand dynamic coupling of an optically manipulated wave-guided optical waveguide (WOW) using diffractive techniques [1,2]. The use of diffractive techniques enables creation of diffraction-limited focal spots that can efficiently couple through the WOWs in 3D space. Aside from on-demand light targeting, continuous addressing is also useful in some applications. In this work, we add a particle tracking routine in our Biophotonics Workstation to determine the position of the WOW and calculate the necessary phase pattern to diffractively send coupling light in that position. We also improve the intensity and efficiency of the coupling focal spots by employing the Generalized Phase Contrast (GPC) method to create the matching input beam in the spatial light modulator using optimal parameters [3]. Because of the gain in intensity, we can couple multiple WOWs using the same laser power compared to using only hard-truncated Gaussian input beam. The ability to switch from on-demand to continuous addressing with efficient illumination leverages our WOWs for potential applications in stimulation and nonlinear optics.

References:

1. D. Palima, a R. Bañas, G. Vizsnyiczai, L. Kelemen, P. Ormos, and J. Glückstad, "Wave-guided optical waveguides," *Opt. Express* 20, 2004–2014 (2012).
2. M. Villangca, A. Bañas, D. Palima, and J. Glückstad, "Dynamic diffraction-limited light-coupling of 3D-manuevered wave-guided optical waveguides," *Opt. Express* 22, 17880 (2014).
3. A. Bañas, D. Palima, M. Villangca, T. Aabo, and J. Glückstad, "GPC light shaper for speckle-free one- and two- photon contiguous pattern excitation," 7102, 5299–5310 (2014).

9379-23, Session 6

The efficiency of fiber optical tweezers for cell manipulation using distinct fabrication methods

Ana Rita S. Rodrigues Ribeiro, INESC TEC (Portugal) and Masdar Institute of Science and Technology (United Arab Emirates) and Univ. do Porto (Portugal); Jaime Viegas, Masdar Institute of Science & Technology (United Arab Emirates); Ariel Guerreiro, Univ. do Porto (Portugal) and INESC TEC (Portugal); Pedro A. S. Jorge, INESC Porto (Portugal)

Looking at a single cell can provide insights into the cell dynamics and heterogeneity yielding information otherwise unattainable with traditional biological methods. Optical tweezers are nowadays exceptional tools in studies of single cells, molecular motors or even single molecules, with the unique ability to accurately trap and manipulate nano to micron sized particles without physical contact. Usually bulk optical trapping systems come upon serious difficulties, regarding their cost, dimension and portability. On the other hand, fiber optical tweezers (FOT) are a turning

**Conference 9379:
 Complex Light and Optical Forces IX**

point technology enabling its use in a compact miniaturized tool.

In this work, the trapping efficiency of FOT structures fabricated using chemical etching, photo polymerization and focused ion beam milling techniques is evaluated. The first two fabrication methods may present limited capabilities on the tailoring of the structures, and therefore limited operation features. On the other hand, with focused ion beam milling a vast myriad of structures may be accurately fabricated, and contrarily to conventional fabrication methods, more specialized manipulation tools can be developed. In this regard, the performance of FOT for the trapping of yeast cells using axicons (chemical etching), spherical lenses (photo polymerization), Fresnel zone plates (FIB) and optical vortices (FIB) will be presented. In addition, finite difference time domain (FDTD) simulations of the full vectorial optical propagation through the designed structures and the corresponding calculation of the optical forces are presented and different designs are evaluated.

9379-24, Session 6

Optimal illumination of phase-only diffractive element using GPC light shaper

Mark Jayson M. Villangca, Andrew Rafael Bañas, DTU Fotonik (Denmark); Oleksii Kopylov, Darwin Palima, Jesper Glückstad, Technical Univ. of Denmark (Denmark)

Many optical tweezers array and custom optical landscapes (e.g. vortex beams, non-diffracting beams, accelerating beam, etc) are generated using holography. Nowadays, holography uses programmable phase-only diffractive element to modify the incident wavefront such that a desired intensity distribution is obtain at some output plane. There is a strong interest in the application of holography in neurophotonics where simultaneous multi-site two-photon photolysis is used to uncage neurotransmitters [1]. Increasing the number of light spots will decrease peak intensities for each spots. Since a high laser power is not always available, efficient illumination of the diffractive element is therefore necessary to utilize most of the photons. Among other things, one consideration in using phase-only diffractive element is geometry. Most diffractive elements are pixelated and consequently have a square or rectangular overall shape. The typical holography setup involves hard-truncation of the incident beam to match the shape of the modulation element and thereby waste photons. In this work, we use the Generalized Phase Contrast (GPC) method to reshape the incident wavefront to match the shape of the diffractive element using optimal parameters [2,3]. In addition to the shaping, there is an inherent gain in intensity which means more light spots can be made using the same laser power compared to a setup without GPC and applications that rely on intensity profiles of custom optical landscapes can benefit greatly. In our experiment we generate array of focal spots and we verify that reshaping the beam with GPC prior to phase modulation increases the intensity of the generated spots.

References:

1. M. A. Go, C. Stricker, S. Redman, H.-A. Bachor, and V. R. Daria, "Simultaneous multi-site two-photon photostimulation in three dimensions.," *J. Biophotonics* 5, 745-53 (2012).
2. D. Palima, C. a Alonzo, P. J. Rodrigo, and J. Glückstad, "Generalized phase contrast matched to Gaussian illumination.," *Opt. Express* 15, 11971-7 (2007).
3. A. Bañas, D. Palima, M. Villangca, T. Aabo, and J. Glückstad, "GPC light shaper for speckle-free one- and two- photon contiguous pattern excitation," 7102, 5299-5310 (2014).

9379-25, Session 7

Light shaping along 3D curves and particle manipulation (Invited Paper)

José A. Rodrigo, Tatiana Alieva, Univ. Complutense de Madrid (Spain)

Light shaping along three-dimensional (3D) curves is an attractive problem with relevant applications in imaging, laser micro-machining and optical trapping. In the last case not only the beam intensity distribution but also its phase have to be controlled. While the intensity gradients allow for trapping of the particle, the phase gradients drive it along the curved beam. For example, the well-known Laguerre-Gaussian vortex beam can be used to move a micron-sized particle around a circle. However, this kind of vortex only traps the particle against the cover-slip glass or other interface surface due to its weak axial intensity gradient which is unable to compensate the scattering force (2D trap). Up to now, few methods based on solving inversion problem of light propagation have been developed for generation of true 3D traps.

We have proposed and experimentally demonstrated a new non-iterative holographic technique for beam shaping along 3D arbitrary smooth curves (open or closed). It is based on the generalization of the mathematical formalism describing spiral Gaussian beams. Trapping beams with their intensity shaped in several geometries such as tilted ring, Viviani's curve, Archimedean spiral, and trefoil-knotted curve with insignificant cross-talk have been generated. The independent phase gradient control and high intensity gradients prescribed along the curve make them a versatile micro-manipulation tool. In particular, we demonstrated that a micron-sized polystyrene sphere moves along the curve forward and backward (tractor beam trap) to the light source.

9379-27, Session 7

Trapping atoms with laser written wave guides

Jörg B. Götte, Dario Juki?, Thomas Pohl, Max-Planck-Institut für Physik komplexer Systeme (Germany)

We show how simple waveguide structures written into fused silica with femtosecond lasers, can be operated to trap Caesium atoms in the evanescent field in close proximity to the fused silica to air interface. The use of the fundamental mode of red detuned light and two spatial modes of blue detuned light allows us to balance the attractive surface forces and to create a stable potential minimum a few hundred nanometers from the surface of the waveguide. The process is very flexible, cost effective and allows for the realisation of a variety of complex trapping geometries. Using counter propagating waves we can realise optical conveyor belts with this design which is why our setup lends itself ideally for integration in optical atom chips.

9379-29, Session 7

The viability of achieving chiral separation through the optical manipulation of molecules (Invited Paper)

David L. Andrews, David S. Bradshaw, Univ. of East Anglia (United Kingdom)

Several different optical methods have recently been proposed for the potential separation of chiral molecules according to their intrinsic handedness. Applying fundamental symmetry and electrodynamic principles provides a perspective that casts doubt over the viability of some of the more extravagant claims. However there is a genuine basis for achieving chiral separation by using circularly polarized light to deliver chirally sensitive optical forces. The mechanism comes into play when molecules (or nanoscale particles) are optically trapped in a laser beam by forward Rayleigh scattering, as a result of trapping forces that depend on positioning within the beam profile. In such a setup, chiral molecules experience subtle additional forces associated with a combination of electric and magnetic transition dipoles, and when circularly polarized light is used for the trapping, a discriminatory response can be identified that has the capacity to separate left- and right-handed molecular isomers. Here, clear differences can be observed between the behavior of isotropic liquids and

**Conference 9379:
 Complex Light and Optical Forces IX**

poled solutions or liquid crystals. Detailed analysis provides an objective basis to assess new prospects for the recognition and differentiation of molecules with opposite chiral form, identifying and paving the way for future commercial applications.

9379-28, Session 8

Spin and orbital angular momentum interactions probed using microparticles trapped in vacuum (*Invited Paper*)

Michael Mazilu, Yoshihiko Arita, Tom Vettenburg, Univ. of St. Andrews (United Kingdom); Ewan Wright, College of Optical Sciences, The Univ. of Arizona (United States); Kishan Dholakia, Univ. of St. Andrews (United Kingdom)

Micro particles trapped in vacuum offer a sensitive opto-mechanical system to probe various interactions between mesoscopic objects and light. We have demonstrated previously the rotation of microscopic gyroscopes at rates exceeding MHz using spin angular momentum. Here, we use Laguerre-Gaussian beams in various polarisation states to study the intricate interplay between spin and orbital angular momentum when light interacts with micro particles trapped in vacuum. We observe the effect of the relative handedness of the spin and orbital angular momentum and study the rotation rates as a function vortex charge and residual gas pressure.

9379-30, Session 8

Optical sculpting of ultra-low-interfacial-tension oil droplets using holographic optical tweezers

Jonathan M. Taylor, Univ. of Glasgow (United Kingdom); Andrew Kirby, Durham Univ. (United Kingdom); Guido Bolognesi, Imperial College London (United Kingdom); Oliver W. J. Burnham, Alex Hargreaves, David Tapp, Durham Univ. (United Kingdom); Alex Lubansky, Edith Cowan Univ. (Australia); Lian R. Hutchings, Gordon D. Love, Durham Univ. (United Kingdom); Oscar Ces, Imperial College London (United Kingdom); Buddhapriya Chakrabarti, Durham Univ. (United Kingdom); Mark Neil, Imperial College London (United Kingdom); Andrew Ward, Rutherford Appleton Lab. (United Kingdom); Colin D. Bain, Durham Univ. (United Kingdom)

We will present experimental results obtained from a novel microdroplet sculpting platform, allowing us to produce and manipulate ultra-low interfacial tension (ULIFT) oil-in-water droplets in the 1-10 micron size range. This allows us to sculpt the droplets into shapes of our choosing, by exploiting the interplay between laser tweezer and surface tension forces. Our sculpting platform consists an integrated microfluidic droplet generation system in combination with holographic optical tweezers and UV polymerization capabilities. Our system includes structured illumination imaging to allow the volumetric interrogation of the resultant shapes, as well as an integrated Raman spectroscopy system to monitor the compositional dynamics and polymerization kinetics of the ULIFT droplets.

Our experimental results include generation and characterization of user-selected droplet shapes, through the use of multiple laser tweezers to manipulate the forces acting on the droplet surface. We will also demonstrate that networks of interconnected oil droplets can be created using an array of holographic optical tweezers, and that 'optical pumping' between droplets can be achieved, opening up the possibility of performing chemical reactions on an attolitre scale.

Our experimental results are complemented by numerical and analytical

models that we have developed to understand and simulate the optomechanical forces involved in droplet deformation. This has helped us understand the physical processes involved in the sculpting, and has revealed the existence of threshold values defining the transition between different regimes involved in the sculpting process.

9379-31, Session 8

Optical assembly of zeolite-L-nanocontainer-based waveguides and sensors

Alvaro Barroso Peña, Katrin Dieckmann, Annika Uphoff, Christina Alpmann, Cornelia Denz, Westfälische Wilhelms- Univ. Münster (Germany)

Zeolite L is a type of porous micro-sized crystal which features a high number of strictly one-dimensional aligned nano-channels across the whole crystal axis. They are highly interesting as building blocks for functional nanoscale structures due to their potential to accommodate different guest molecules within their nano-pores and to assemble them in specific configurations. Recently, we have demonstrated that holographic optical tweezers (HOT) enable the optomechanical assembly of sophisticated microstructures based on zeolite L with full control over each individual constituent. This micro-optomechanical construction of zeolite-L based functional systems can be applied to create permanent two- and three-dimensional microstructures on surfaces as well as dynamic structures, as e.g. microscopic polarization sensors or chains consisting of several microcrystals [1-2].

In this work, we extend this concept and demonstrate the ability of empty zeolite L crystals to guide light when dispersed in media with lower refractive index and show exciting applications, as e.g., a microscopic shutter sensor. For this purpose, HOT are used in combination with single-mode fibers which, attached to the microscopic sample, launch light directly into optically arranged chains of zeolite L crystals. Loaded zeolite L crystals with fluorescent dyes are optically placed at the output of the chain and are exploited to detect the emitted light with high spatial precision. Finally, we discuss the use of abruptly tapered single-mode fibers for both trapping and illumination of the zeolite-L-based waveguides.

[1] M. Woerdemann et al., Adv. Mater. 22, 4176 (2010)

[2] M. Veiga-Gutiérrez et al, Adv. Mater. 24, 5199 (2012)

Conference 9380: Laser Refrigeration of Solids VIII

Wednesday - Thursday 11-12 February 2015

Part of Proceedings of SPIE Vol. 9380 Laser Refrigeration of Solids VIII

9380-1, Session 1

Optical refrigeration demonstrates the first cooling below 100 K (*Invited Paper*)

Seth D. Melgaard, Air Force Research Lab. (United States) and The Univ. of New Mexico (United States); Denis V. Seletskiy, Univ. Konstanz (Germany); Alexander R. Albrecht, Mansoor Sheik-Bahae, The Univ. of New Mexico (United States)

We report a milestone in optical refrigeration, cooling a 10% Yb:YLF crystal to 93K (?T-180K) at 1020 nm; obtaining the coldest solid-state refrigeration temperature to date. A multi-pronged approach including increased doping, alignment enhanced absorption increased by 75%, and reduced heat load allow us to approach the minimum achievable temperature (MAT) for the highest purity Yb:YLF crystal currently available. Identification of transition metal impurities via mass spectrometry allows further cooling through purification.

9380-2, Session 1

Intracavity-enhanced optical refrigeration of Yb:YLF crystal to cryogenic temperatures (*Invited Paper*)

Mohammadreza Ghasemkhani, Alexander R. Albrecht, Seth D. Melgaard, The Univ. of New Mexico (United States); Denis V. Seletskiy, Univ. Konstanz (Germany); Jeffrey G. Cedeberg, Sandia National Labs. (United States); Mansoor Sheik-Bahae, The Univ. of New Mexico (United States)

Laser cooling of solids has a great potential to achieve an all-solid-state optical cryocooler. The advantages of compactness, no vibrations, no moving parts or fluids, and high reliability have motivated intensive research. Increasing the absorbed power in the cooling sample is essential to reach lower temperatures. Here, using a high power, broadly tunable InGaAs/GaAs vertical external-cavity surface-emitting laser (VECSEL) we demonstrate how we have increased the pump power absorption in an intracavity geometry in a Yb:YLF crystal. We also discuss the progress, advantages, and challenges of laser cooling inside a VECSEL cavity, including the VECSEL active region design, cavity design, and cooling sample choice for optimal cooling.

9380-3, Session 1

Purification of precursors of Yb³⁺ doped YLF crystals by solvent extraction and electrochemical processing (*Invited Paper*)

William L. Boncher, Markus P. Hehlen, Los Alamos National Lab. (United States)

Optical refrigeration by laser irradiation of YLiF₄:Yb³⁺ (YLF) crystals has been shown to be strongly deteriorated by impurities, especially transition metal ions such as iron, copper and cobalt. These ions absorb energy at the laser wavelength, and relax non-radiatively, negating some of the cooling produced from anti-Stokes fluorescence. We aim to increase the efficiency of optical refrigeration through materials purification.

We start with the purest sources of yttrium, lithium, and ytterbium which are commercially available and process them in a cleanroom environment. Our initial efforts proceeded through a solvent extraction method, selective

chelating and sequestering transition metal ions from solution. This process resulted in an increase in the amount of impurities present, introduced from the various chemical reagents used for purification.

Our latest method proceeds through electrochemical purification, separating out the transition metal impurities by their redox potentials. This process uses significantly fewer reagents and thus minimizes sources of contamination. Furthermore, it can be scaled up with substantially less difficulty, in order to produce the amounts of material needed for crystal growth of the YLF crystal.

9380-4, Session 1

A novel approach for solid-state cryocooler (*Invited Paper*)

Mauro Tonelli, Alberto Dilieto, Azzurra Volpi, Univ. di Pisa (Italy)

Optical cooling in solids is based on anti-Stokes luminescence. Coherent excitation at wavelengths longer than the mean emission wavelength results in the spontaneous emission of more energetic photons, leading to a decrease of thermal energy via annihilation of lattice phonons. We present cooling efficiency measurements in Yb-doped LiYF₄ single crystals, as a function of the Yb doping level. Current studies on efficiency enhancement via energy-transfer processes between Yb and other rare-earth ions are also presented, along with investigation of LiLuF₄ crystal host for optical cooling. Details of Czochralski growth of cooling materials and spectroscopic analysis are reported.

9380-5, Session 2

Recent advances in proposed techniques for laser cooling of solids (*Invited Paper*)

Raman Kashyap, Galina Nemova, Elton S. L. Filho, Sebastien Loranger, Ecole Polytechnique de Montréal (Canada); Venkata Krishnaiah, Ecole Polytechnique de Montréal (Canada) and Univ. of Laval (Canada); Ye Jin Yu, Ecole Polytechnique de Montréal (Canada) and Univ. Laval (Canada); Younes Merssaddeq, Yannick Ledemi, Univ. Laval (Canada); Fiorenzo Vetrone, Marta Quintanilla, Institut National de la Recherche Scientifique (Canada); Gurinder K. Ahluwalia, College of The North Atlantic (Canada)

The cooling of solids with lasers is a demanding application requiring not only the best purity in materials but has also been restricted to low phonon-energy glasses and crystals. The principle of anti-Stokes emission generally used for cooling, requires a pump photon of lower energy than the one emitted, the difference being supplied by a small amount of vibration energy taken away from the material leading to net cooling. While this technique has developed from the embryonic demonstration of cooling from room temperature of 0.3K by Epstein et al. in 1995 [1], to a record temperature of 93K in 2014 [2], the widespread use of materials for laser cooling is fraught with significant challenges. Firstly, pump wavelengths are determined by the mean fluorescence wavelengths the very few set of rare-earths suitable for laser cooling, restricting their choice considerably. Secondly, parasitic effects such as background absorption and non radiative emission, severely degrade cooling. We have proposed and developed materials that may overcome some of these restrictions to make laser cooling ultimately ubiquitous. These include the use of quantum dots (QDs) to engineer the band-gap, allowing more lasers to be used for cooling, improving efficiency and to some extent mitigating the effects of parasitics. Other materials include nano-crystalline rare-earth doped oxy-fluoride

glasses, rare-earth doped semiconductors as well as novel schemes using superradiance. This paper will review our recent progress in these areas and propose possible solutions for future development.

1. R. I. Epstein et al., Nature (London) 377, 500 (1995).
2. S. Melgaard et al., CLEO 2014, FTh4D.4

9380-6, Session 2

laser-refrigeration of rare-earth-doped nanocrystals in water (*Invited Paper*)

Peter J. Pauzauskie, Paden B. Roder, Bennett E. Smith, Xuezhe Zhou, Univ. of Washington (United States)

Single-beam laser-tweezers have been demonstrated over the past several decades to confine nanometer-scale particles in three dimensions with sufficient sensitivity to measure the spring constants of individual biological macromolecules including DNA. Large laser-irradiance values (MW/cm²) commonly are used to generate laser traps which can lead to significant laser-heating within the 3D optical potential well. To date, laser-refrigeration of particles within an aqueous medium has not been reported stemming primarily from the large near-infrared (NIR) optical absorption coefficient of liquid water (0.2 cm⁻¹ at 1020nm). In this presentation we will demonstrate how single-beam laser-traps can be used to induce and quantify the refrigeration of optically trapped of individual Yb³⁺-doped yttrium lithium fluoride (Yb:YLiF₄) and sodium yttrium fluoride (Yb:NaYF₄) nanocrystals in both deionized water and Dulbecco's modified eagle medium (DMEM). A tunable NIR continuous-wave laser is used to optically trap individual nanocrystals with an irradiance on the order of 1 MW/cm². Analysis of the Brownian dynamics of individual nanocrystals via forward light scattering provides an absolute measurement of particle's temperature in agreement with complimentary measurements based on ratiometric photoluminescence. Heat is transported out of the crystal lattice (across the solid / liquid interface) by anti-Stokes photons following upconversion of Yb³⁺ excited states mediated by optical-phonon absorption. The Brownian motion of individual YLF crystals indicates local cooling of water by 20°C below ambient conditions suggesting a range of potential future applications of laser refrigeration of nanoscale materials in biotechnology and information technology sectors.

9380-7, Session 2

Optical refrigeration of Yb³⁺:YAG nanocrystals

Galina Nemova, Raman Kashyap, Ecole Polytechnique de Montréal (Canada)

The idea of cooling solids with light was proposed in 1929 by Peter Pringsheim [1]. It was realised experimentally for the first time with the Yb³⁺:ZBLANP sample in 1995 [2] only after the invention of the laser. Today this area of science is known as laser cooling of solids or optical refrigeration. Optical refrigeration with anti-Stokes fluorescence has been experimentally realised with Yb³⁺, Tm³⁺, and Er³⁺ rare-earth (RE) ions doped in wide variety of low-phonon glasses and crystals. Today's record temperature of 93K±1K was achieved in 2014 with a 10% Yb³⁺:YLF sample [3]. Contrary to all other RE ions the Yb³⁺ ions have only two [ground (2F_{7/2}) and excited (2F_{5/2})] manifolds and are consequently, free from excited state absorption, which generates heat and degrades cooling of the sample. Yb³⁺ ions can be considered as the best ions for optical refrigeration; however, the host material and the shape of the sample are very important for the cooling process as well. In this work we compare the laser cooling process in Yb³⁺:YAG nanocrystals with optical refrigeration in Yb³⁺:YAG bulk samples aiming to find the best sample shape for laser cooling. The impact of the size of the nanocrystal and Yb³⁺ concentration on laser cooling process in the Yb³⁺-doped YAG nanocrystals is considered. The association between the radius of nanocrystals and the final equilibrium temperatures is obtained. The influence of cooperative effects such as

re-absorption, energy migration in the dipole-dipole approximation and cooperative luminescence on the cooling process as well as dependence of all parameters on temperature has been taken into account. The impact of the "fill factor" on cooling is also analyzed.

- [1]. P. Pringsheim, Z. Phys. 57, 739 (1929).
- [2]. R.I. Epstein et al., Nature (London) 377, 500 (1995).
- [3]. S. Melgaard et al., CLEO 2014, FTh4D.4

9380-8, Session 2

Spectroscopy characterization and laser cooling performance of Yb³⁺-doped LuLiF₄ crystals (*Invited Paper*)

Biao Zhong, Lin Chen, East China Normal Univ. (China); Youhua Jia, Shanghai Second Polytechnic Univ. (China); Jianping Yin, East China Normal Univ. (China)

The resonant cavity enhancement absorption is adopted for laser cooling 5wt.% Yb³⁺:LuLiF₄ crystal. More than 90% pump laser is absorbed. The polarized fluorescence spectroscopy of 5wt.% Yb³⁺:LuLiF₄ crystal was measured within the temperature range of 77K-100K. And the Spectroscopic characterization reveals that this crystal is a potentially promising candidate for solid-state refrigeration.

9380-9, Session 2

Spectroscopic and thermal study of Er-doped oxysulfide crystal powders (*Invited Paper*)

Joaquín Fernández, Rolindes Balda, Macarena Barredo, Univ. del País Vasco (Spain); Odile Merdrignac, Noha Hakmeh, Univ. de Rennes 1 (France)

The investigation of new hosts for rare earth ions with low phonon energies appears to be a promising way to find efficient cooling materials, especially for dopant ions with low-energy band-gaps between active levels. Among the RE-doped oxides, oxysulfides (RE₂O₂S) are one of the most efficient phosphors investigated for commercial television and lighting applications [1]. In particular, lanthanum oxysulfide crystal matrix, a uniaxial wide-gap (36000 cm⁻¹) [2] semiconductor material, is known as an excellent host lattice for trivalent RE ions [3]. Each lanthanum atom is coordinated by four oxygen atoms and three sulfur atoms in its nearest neighborhood [4]. The lanthanum site symmetry is C_{3v}.

Here we report a detailed study of the spectroscopic properties of Er³⁺ ion in lanthanum erbium-doped oxysulfide crystal powders under excitation in the 4I_{9/2} manifold as well as experimental evidences of anti-Stokes laser-induced cooling. The wavelength and pump power dependence of the spectroscopic properties and temperature field are also considered.

- [1] I. W. M. Yen, S. Shionoya, and H. Yamamoto, Phosphor Handbook, 2nd ed. (CRC Press, 2007).
- [2] C. W. Struck and W. H. Fonger, Phys. Rev. B 4(1), 22-34 (1971).
- [3] R. V. Alves, R. A. Buchanan, K. A. Wickersheim, and E. A. C. Yates, J. Appl. Phys. 42(8), 3043-3048 (1971).
- [4] G. I. Abutalibov, D. I. Guseynov, and A. A. Mamedov, Phys. Status Solidi., C Curr. Top. Solid State Phys. 6(5), 1127-1129 (2009)

9380-23, Session PWed

Comparative spectroscopic studies of Ho: KPb₂Cl₅, Ho: KPb₂Br₂, and Ho: YAG for 2 μm laser cooling applications

EiEi Brown, Uwe H. Hömmerich, Hampton Univ. (United States); Eric Kumi-Barimah, Hampton Univ (United States); Althea G Bluiett, Elizabeth City State University (United States); Sudhir B. Trivedi, Brimrose Corp. of America (United States)

There is a continued interest in the development of rare earth doped materials for applications in anti-stokes fluorescence cooling [1-3]. In this work, the IR absorption and emission properties of Ho: KPC, Ho: KPB, and Ho: YAG were compared for possible applications in 2 μm laser cooling. Ho: KPC and Ho: KPB crystals were grown by vertical Bridgman technique using purified starting materials. A commercial Ho: YAG crystal was included in this study for comparison. Under resonant pumping at -1.9 μm, the Ho doped KPC/KPB crystals exhibited broad IR emission centered at -2 μm based on the Ho³⁺ intra-4f transition 5I₇ → 5I₈. Under similar experimental conditions, Ho: YAG showed a narrow-structured emission band reflective of individual stark levels. The average emission wavelength for Ho: YAG was determined to be -2.03 μm. Initial heat loading/cooling experiments under air were performed using a fiber laser operating at -2.036 μm with an output power of 2 W. The Ho: KPC/KPB crystals exhibited small temperature increases of -1.0 °C. A significantly larger temperature increase of -5 °C was observed for Ho: YAG. IR transmission studies revealed the existence of OH impurities in the Ho doped halides, which possibly lead to non-radiative decay channels. Results of the material preparation, optical spectroscopy, and initial heat loading studies will be reported at the conference.

References

[1] M. Sheik-Bahae and R.I. Epstein, "Optical refrigeration", *Nature Photonics* 1, 693-699 (2007).

[1] S. R. Bowman, S. O'Connor, N. J. Condon, E. J. Friebele, W. Kim, B. Shaw, and R. S. Quimby, "Non-radiative decay of holmium-doped laser materials", *Proc. of SPIE Vol.*

8638, 863803 (2013).

[2] E. Brown, U. Hömmerich, S. Hyater-Adams, O. Oyebola, A.G. Bluiett, S. B. Trivedi, "Infrared Absorption and Fluorescence Properties of Ho-doped KPb₂Br₅", *Proc. of SPIE* 8982, 89821S (2014).

9380-24, Session PWed

Nanocrystallization in Yb³⁺-doped oxyfluoride glasses for laser cooling

Venkata Krishnaiah Kummara, Ecole Polytechnique de Montréal (Canada); Yannick Ledemi, Younes Messaddeq, Ctr. d'Optique, Photonique et Laser (Canada); Raman Kashyap, Ecole Polytechnique de Montréal (Canada)

Glass-ceramics are composite materials consisting of crystals which are controllably grown within a glass matrix usually by applying an appropriate heat treatment. They possess outstanding optical properties with applications in laser induced cooling, solid state lasers, optical amplifiers, etc. For laser cooling, the material should exhibit specific properties like low phonon energy environment around the lanthanide ions, low background losses, high transparency and high photoluminescence quantum yield. In the present study, oxyfluoride glasses and ultra-transparent nano glass-ceramics doped with different concentrations (2, 5, 8, 12, 16 and 20 mol %) of Yb³⁺ ions have been prepared by conventional melt-quenching and subsequent thermal treatments at different temperatures, respectively. Differential scanning calorimetry (DSC) and X-ray diffraction (XRD) measurements have been performed to characterize thermal properties of the glass and structural changes in the glass-ceramics, respectively. The XRD

patterns confirm the growth of Yb³⁺-PbF₂ nanocrystals as well as progressive incorporation of Yb³⁺ ions. This enhances the Yb³⁺ ion emission intensity which depends on the doping concentration and ceramization temperatures. The nanocrystallite size (20 nm) estimated from the Sherrer's formula and found to increase with increasing ceramization temperature, small enough to avoid scattering losses and ensure an excellent transparency of the glass-ceramics comparable with that of the parent glass. An enhancement of the luminescence properties of Yb³⁺ ions surrounded by crystalline low phonon environment is observed. Finally, the utilization of these heavily Yb³⁺-doped ultra-transparent materials for laser cooling and solid state laser applications is discussed.

9380-25, Session PWed

Characterization of fluoride nanocrystals for optical refrigeration

Elton Soares de Lima Filho, Ecole Polytechnique de Montréal (Canada); Marta Quintanilla, Fiorenzo Vetrone, Institut National de la Recherche Scientifique (Canada); Galina Nemova, Raman Kashyap, Ecole Polytechnique de Montréal (Canada)

This paper reports the characterization of nanocrystalline powders of ytterbium doped YLiF₄ for application in optical refrigeration. Here we used powders with nanocrystals of Yb³⁺ concentrations of (10, 15, 20) mol % and lengths (70, 66, 96) nm. Our preliminary spectroscopic measurements did not show an enhancement in the absorption at the long-wavelength tail of the spectra of the nanocrystalline powder when compared with bulk Yb:YLiF₄, indicating that the increase of the phonon-assisted excitation is not large enough to play a significant role in cooling in the present conditions. One advantage of nanocrystalline powders over bulk crystals is the possibility of enhancing the absorption by the realization of cavity-less pump recycling through photon localization [1]. While photon localization also increases the reabsorption of the fluorescence depending on the quantum efficiency of the material and can mitigate cooling, it allows the use of crystals of low enough concentrations to avoid deleterious effects such as ion-ion energy transfer followed by quenching. The pump intensity enhancement favors upconversion luminescence to visible wavelengths, which can be used for optical refrigeration and extends the scope of application for the material. We observed both green and blue emission from the samples and investigate the processes which lead to it. We present the experimental investigation of the nanocrystals' absorption and emission spectra and the first excited state lifetime measurements, which are used to estimate the nanocrystal's photoluminescence quantum efficiency.

[1] X. L. Ruan and M. Kaviany, "Enhanced laser cooling of rare-earth-ion-doped nanocrystalline powders," *Physical Review B* 73, 155422 (2006).

9380-26, Session PWed

Prospects of optical refrigeration on oxyfluoride glasses and glass-ceramics: experiments

Elton Soares de Lima Filho, Kummara Venkata Krishnaiah¹, Ye Jin Yu, Ecole Polytechnique de Montréal (Canada); Yannick Ledemi, Ctr. d'Optique, Photonique et Laser (Canada); Younes Messaddeq, Univ. Laval (Canada); Raman Kashyap, Ecole Polytechnique de Montréal (Canada)

We report the characterization of oxyfluoride glasses and glass ceramics for their application in optical refrigeration. Oxide glasses are chemically and mechanically stable and relatively easy to handle and fabricate, but their high maximum phonon energy leads to a nonradiative decay rate which is unacceptable for optical refrigeration. On the other hand, low-maximum

phonon energy hosts such as fluorides lack the desirable mechanical and chemical stabilities to make them widely used. The combination of the high chemical and mechanical stability of oxides and the low maximum phonon energy of fluorides make oxyfluorides strong candidates for wide-spread use in optical refrigeration. Glasses and ultra-transparent glass-ceramics of molar composition $30\text{SiO}_2\text{-}15\text{Al}_2\text{O}_3\text{-}(27\text{-}x)\text{CdF}_2\text{-}22\text{PbF}_2\text{-}4\text{YF}_3\text{-}x\text{YbF}_3$, with $x = (2, 5, 8, 12, 16 \text{ and } 20)$ mol % were investigated. The absorption and photoluminescence spectra, as well as the lifetime and the external quantum efficiency of the photoluminescence for these samples using an integrating sphere are reported. The effects of reabsorption on the measured mean fluorescence wavelength are also investigated. The cooling efficiencies of the samples were measured as a function of the pump wavelength using a calorimetric method with a Ti:Sapphire laser pump source and a fiber Bragg grating sensor for a direct temperature measurement. Impurities and background absorption are also investigated using different pump sources and the calorimetric method. From a comparison of the cooling/heating performance of the oxyfluoride glasses and glass-ceramics containing various Yb^{3+} amounts, we developed a strategy to realize and enhance optical refrigeration in this class of material.

9380-27, Session PWed

Laser cooling of doped crystals by methods of coherent pumping

Andrei V. Ivanov, Yuri V. Rozhdestvensky, National Research Univ. of Information Technologies, Mechanics and Optics (Russian Federation)

Methods of coherent pumping through dipole-allowed 5d levels of RE ion are proposed for laser cooling. The coherent and complete population transfer between the ground and the first excited levels of 4f multiplet is achieved by using the different Raman techniques, namely two-photon scattering, adiabatic passage method, and π -pulse pumping. It is shown that the multiplication of the number of electrons that participate in cooling cycle leads to increasing of the cooling power and to acceleration of the cooling process. The increasing of cooling efficiency of 0.5% compared to the direct pumping between 4f levels is attained through the use of dipole-allowed optical transitions. Performed estimates show that the sample temperature can achieve 94° K for current purity materials. The calculations are obtained for $\text{Yb}^{3+}:\text{CaF}_2$ system.

9380-10, Session 3

Sideband Raman cooling of optical phonons in semiconductors (Invited Paper)

Jun Zhang, Nanyang Technological Univ. (Singapore); Leong C. Kwek, National Univ. of Singapore (Singapore) and Nanyang Technological Univ. (Singapore); Qi Hua Xiong, Nanyang Technological Univ. (Singapore)

Although the radiation pressure of lights has been widely used to laser cool the movements of trapped atoms and the mechanical vibration modes of cavity optomechanical systems, laser cooling of one specific lattice vibration in solids, saying phonons, has remained little studied. In 1980s, Dykman theoretically discussed the possibility of cooling, heating and amplification of specific phonon in solids by similar physics of laser cooling in atoms. Recently, by using electrostrictive forces of light acting on dielectrics, Bahl et al., experimentally demonstrated spontaneous Brillouin cooling and stimulated Brillouin excitation of whispering-gallery type acoustic mode, analogue of acoustic phonon in solids, in silica microsphere resonator. These works raise the question of whether it is possible to cool optical phonon modes in solid by means of a Raman process. For achieving Raman anti-Stokes cooling, the heating Stokes line needs to be filtered out. However, as high optical phonon frequencies have higher dissipation than acoustic phonon, eliminating the Stokes line against the anti-Stokes line is not easily available in solid materials. Here we experimentally demonstrate

spontaneous Raman cooling and heating of longitudinal optical phonon with a 6.23 THz frequency in polar semiconductor zinc telluride nanobelts. We use the exciton to resonate and assist photo-elastic Raman scattering from LOPs due to the large exciton-LOP coupling. The cooling (heating) is mediated by detuning the laser pump to lower (higher) energy sideband, and spontaneous scattering photon resonates with exciton at anti-Stokes (Stokes) side, that beat and photo-elastically attenuate (enhance) the dipole oscillation of the optical phonon.

9380-11, Session 3

Multi-phonon-assisted absorption and emission in semiconductors and its potential for laser refrigeration (Invited Paper)

Jacob B. Khurgin, Johns Hopkins Univ. (United States)

Laser cooling of semiconductors has been an elusive goal for many years, and while attempts to cool the narrow gap semiconductors such as GaAs are yet to succeed, recently, net cooling has been attained in a wider gap CdS. This raises the question of whether wider gap semiconductors with higher phonon energies and stronger electron-phonon coupling are better suitable for laser cooling. In this work we develop a straightforward theory of phonon-assisted absorption and photoluminescence of semiconductors that involves more than one phonon and use to examine wide gap materials, such as GaN and CdS and compare them with GaAs. The results indicate that while strong electron-phonon coupling in both GaN and CdS definitely improves the prospects of laser cooling, large phonon energy in GaN may be a limitation, which makes CdS a better prospect for laser cooling.

9380-12, Session 3

Anti-Stokes Raman processes based on second-order nonlinearities at phonon-polariton resonances for phonon removal and laser cooling (Invited Paper)

Yujie J. Ding, Lehigh Univ. (United States)

During this presentation, we review our most recent result on Raman oscillation, frequency upconversion, and amplification in a second-order nonlinear medium at the phonon-polariton resonance. For the co-propagating configuration, the small-signal gain for Raman oscillation reaches 2.2 per cm and per W of the input power. For the counter-propagating optical fields, frequency upconversion is feasible without any input at the anti-Stokes frequency with its conversion efficiency approaching 10% without an input and significantly higher with an input. These Raman processes can be used to effectively remove transverse-optical phonons before decaying to lower-frequency phonons. The counter-propagating configuration offers advantages for amplifying extremely weak signals, efficient phonon removal, and perhaps laser cooling.

9380-13, Session 3

Photoluminescence study of suspended MQW structures for laser refrigeration purposes

Iman Hassani Nia, Hooman Mohseni, Northwestern Univ. (United States)

Anti-Stokes laser cooling of bulk semiconductors is quite challenging and requires advanced thermometry measurements. Suspended structures are suitable candidates that offer high sensitivity for the measurement

of ultra-low dissipated thermal powers. Furthermore, their geometry can be designed to have high extraction efficiency in order to assist optical refrigeration. In this talk, we first describe our MQW structures designed for the purpose of laser cooling, then the fabrication processes of these structures and our measurements regarding their properties for anti-Stokes laser cooling purposes are presented. The various recombination processes after photogeneration of electron-hole pairs are of central importance to determine the feasibility of anti-Stokes laser cooling. On the other hand, we expected the change of recombination rates after suspending the MQW structures. For these reasons, time resolved and intensity dependent micro-photoluminescence measurements were employed to estimate the change of recombination rates. Finite difference time domain (FDTD) simulations have been used to determine the fraction of the pump laser absorbed in the active region. Since the pump laser is focused on a small spot and the mobility of the active region is significant, the effect of lateral carrier diffusion should be considered. Therefore, we performed finite-element time-resolved analysis of carrier recombination and diffusion using COMSOL. The measurements and simulations for different temperatures from 77 K up to room temperature reveal the potential of suspended structures for anti-Stokes laser cooling purposes.

9380-14, Session 3

High sensitivity background absorption measurements in semiconductors

Nathan Giannini, The Univ. of New Mexico (United States); Junior R. Silva, Univ. Estadual de Mato Grosso do Sul (Brazil) and The Univ. of New Mexico (United States); Chengao Wang, The Univ. of New Mexico (United States); Seth D. Melgaard, The Univ. of New Mexico (United States) and Air Force Research Lab. (United States); Alexander R. Albrecht, Mansoor Sheik-Bahae, The Univ. of New Mexico (United States)

Until now, laser cooling in semiconductors has been a nontrivial task. It was only in 2013 that semiconductor cooling has appeared in CdS nanoribbons, despite two decades of research. However, cooling of bulk semiconductors has remained elusive. The semiconductor GaAs is an appealing material due to its integration in circuits, detectors and lasers. External quantum efficiencies (EQE) as high as 99.5% have been reported using a double heterostructure (DHS) approach, involving InGaP to reduce surface recombination and bonding to a ZnS hemisphere for efficient fluorescence extraction. According to Sheik-Bahae Epstein (SBE) theory of optical refrigeration, such an EQE would allow cooling for background absorptions below -4 cm^{-1} . Such background absorptions have not been achieved until now. In this paper we report on a new minimum for MOCVD grown GaAs with a value ranging from $3\text{-}4 \text{ cm}^{-1}$. This result was obtained from a DBR mirror, 35.5 pair GaAs/AlGaAs, bonded to a ZnS substrate. To obtain this result we used a two-color excite-probe z-scan, with $\approx 1550 \text{ nm}$ probe and a tunable Ti:Sapphire pump between 900-1070 nm. Corrections were made for Fabry-Perot effects and heat transfer to ZnS. In order to check for systematic errors, the background absorption of 15%Yb:YLF was measured and compared with a laser induced temperature modulation spectrum (LITMoS) test. The results show good agreement, with our measurement at $2.7 \cdot 10^{-3} \text{ cm}^{-1}$ and the LITMoS measurement giving $2.2 \cdot 10^{-3} \text{ cm}^{-1}$. Further checks involved measuring additional DHS samples and comparing them with the results from DLT experiments.

9380-15, Session 4

Next-generation ultrastable lasers based on crystalline materials (Invited Paper)

Wei Zhang, Lindsay Sonderhouse, Jun Ye, JILA (United States)

The development of ultrastable lasers helps pushing the frontier of precision measurement [1]. Brownian noise arising from mechanical losses of spacer, mirror substrates and coatings represents a fundamental limit to the stability of an optical reference cavity [2].

The crystalline silicon cavity [3] with AlGaAs crystalline coating [4] provides a feasible implementation to achieve stability at the 10^{-17} level, thanks to the enhanced mechanical quality factors of crystalline materials for reduced thermal noise. The quality factor of silicon is on the order of 10^7 , which is two orders of magnitude higher than that of ultralow expansion glass. The mechanical quality factor of AlGaAs coating has been demonstrated to be ten-fold increased comparing to the standard amorphous SiO₂/Ta₂O₅ coatings.

A well-designed cryogenic cooling system is necessary for a stable silicon cavity. The coefficient of thermal expansion of silicon has two zero-crossing points at 17 K and 124 K, respectively, where the silicon cavity is insensitive to temperature fluctuations. The quality factor of crystalline material increases with decreasing temperature, resulting in a further reduction of the thermal noise.

The vibration noise induced by the cooling system can be a critical limit to the silicon cavity stability. By combining the solid-state optical refrigeration for vibration-free cooling [5] and vibration-insensitive cavity design, we expect to achieve the 10^{-17} stability level limited by thermal noise. This will represent a factor of 10 improvement over the current state-of-the-art [3,6].

Our research is based on extensive collaborations with T. Legero, D. Matei, U. Sterr, and F. Riehl at PTB for silicon cavity, G. Cole and M. Aspelmeyer of Univ. of Vienna for crystalline coating, Montana Instruments for a cryogenic system, and R. Epstein and M. Sheik-Bahae for optical refrigeration. We thank M. Martin for his important contributions. Funding for this work is provided by NIST and DARPA.

References

- [1] B. J. Bloom et al., *Nature* 506, 71 – 75 (2014).
- [2] M. Notcutt et al., *Phys. Rev. A* 73, 031804 (R) (2006).
- [3] T. Kessler et al., *Nature Photonics*, 6 687 – 692 (2012).
- [4] G. D. Cole et al., *Nature Photonics*, 7 644-650 (2013).
- [5] R. Epstein et al., *Nature*, 377 500-503 (1995).
- [6] M. J. Martin et al., *Science* 341, 632 – 636 (2013).

9380-16, Session 4

Low-thermal-noise and high-reflectivity crystalline coatings for the near- and mid-infrared (Invited Paper)

Garrett D. Cole, Crystalline Mirror Solutions, LLC (United States) and Vienna Ctr. for Quantum Science and Technology (Austria)

Ultrastable optical interferometers require mirrors that simultaneously exhibit excellent optical and mechanical quality. The current bounds of stability and sensitivity in these systems are dictated by the mechanical damping, and thus the corresponding Brownian noise level, of the high-reflectivity coatings that comprise the cavity end mirrors. A spin-off of fundamental research from the University of Vienna, Crystalline Mirror Solutions has developed a proprietary microfabrication technique that enables the transfer of low-loss single-crystal semiconductor heterostructures onto essentially arbitrary optical surfaces. These "crystalline coatings" exhibit both high reflectivity (with a demonstrated finesse of 150,000 at 1064 nm), as well as minimal mechanical damping, with room temperature loss angles an order of magnitude lower than state-of-the-art ion-beam sputtered dielectric coatings. These excellent optomechanical properties pave the way for the next generation of cavity-stabilized laser systems and interferometric gravitational-wave detectors. Beyond our initial demonstration devices developed for 1064 nm, we have now extended the operating wavelength of our crystalline coatings into the near- and mid-infrared (IR). Here I describe efforts towards realizing parts-per-million levels of optical absorption in semiconductor Bragg mirrors

at wavelengths from 1100 to beyond 3700 nm, opening up additional application areas in chemical and trace gas sensing as well as power buildup cavities for the mid IR.

9380-17, Session 4

Design study of a laser-cooled infrared sensor (*Invited Paper*)

Markus P. Hehlen, William L. Boncher, Steven P. Love, Los Alamos National Lab. (United States)

Solid state laser refrigeration is the only vibration-free cooling technology capable of reaching cryogenic temperatures. This is particularly attractive for sensor applications that are sensitive to mechanical vibrations, such as space-based infrared imaging systems. The majority of solid-state laser cooling studies to date have focused on cooling the Yb-doped crystal to record-low temperatures, usually without an attached payload such as an infrared sensor. These experiments are valuable for assessing the quality of the cooling crystal and the optical cavity. In this study we explore by numerical modeling the impact of attaching a thermal link and an infrared sensor to the cooling crystal in order to create a practical device. The calculations include the optical properties of the pump cavity, cooling crystal, and thermal link as well as the thermal properties of the clamshell, payload interface, and infrared sensor. We show results on the tradeoffs between pump laser power, payload heat lift, and payload temperature. We also discuss the effects of increasing the Yb ion density in the crystal, reducing background absorption, and pre-cooling the clamshell.

9380-18, Session 4

Thermal modeling of an optical refrigerator cold finger

Kyle W. Martin, Applied Technology Associates (United States); Jason Schomacker, Rensselaer Polytechnic Institute (United States); Christopher Dodson, Tom Fraser, Air Force Research Lab. (United States)

We model thermal losses, radiative and conductive, associated with the cold finger link to a Yb:YLF crystal used for optical refrigeration. We minimize these losses from the worst case scenarios and develop a robust cold finger to be installed on an optical refrigeration device. We show designs with conductive losses as small as 2 mW and conservative combined thermal losses to be as low as 50 mW.

9380-19, Session 5

Optically-cooled solid-state lasers (*Invited Paper*)

Steven Bowman, U.S. Naval Research Lab. (United States)

Waste heat generation is a generic problem in high power solid-state laser systems. Thermo-optic distortions or instability usually limits the laser's maximum brightness. Managing the thermal loading and distortions reduce system efficiency and increases its cost. Lasers that incorporate optical cooling directly into the gain medium can greatly reduce this problem. When the internal laser heat generation is precisely offset by fluorescence cooling, the gain medium is said to be Radiation Balanced. These lasers have the potential to produce very high average power with excellent beam quality. This paper will review the concept and theory of optically cooled lasers. High power ytterbium laser experiments will be discussed which illuminate some practical issues in maintaining Radiation Balance. Numerical simulations of these systems allow extrapolation of the potential and requirements for further average power scaling. Progress on the extension of this approach to high power lasers in the mid-infrared will also be reviewed.

9380-20, Session 5

Optical refrigeration for ultra-efficient photovoltaics (*Invited Paper*)

Assaf Manor, Leopoldo L. Martin, Carmel Rotschild, Technion-Israel Institute of Technology (Israel)

The Shockley-Queisser (SQ) efficiency limit for single-junction photovoltaic cell (PV) is to a great extent due to inherent heat dissipation accompanying the quantum process of electro-chemical potential generation. Concepts such as solar thermo-photovoltaics (STPV) and thermo-photonics aim to harness this dissipated heat, claiming very high theoretical limit. In practice, none of these concepts have been experimentally proven to overcome the SQ limit, mainly due to the very high operating temperatures, which significantly challenge electro-optical devices.

Here we experimentally study endothermic photoluminescence (PL) at high temperatures. We demonstrate the conservation in emitted photon number while increasing temperature and the inherent abrupt transition of PL to thermal emission. We also show how endothermic PL generates orders of magnitude more energetic photons than thermal emission at similar temperatures. Relying on these observations, we study a highly efficient solar-energy converter, wherein solar radiation is absorbed by a low-bandgap PL material. The dissipated heat is emitted by endothermic PL, and harvested by a higher-bandgap photovoltaic cell. While such device operates at much lower temperatures than STPV, the theoretical efficiencies approach 70%, bringing its realization into reach.

9380-21, Session 5

A Kennard-Stepanov relation study on redistributional laser cooling in dense gaseous ensembles (*Invited Paper*)

Stavros Christopoulos, Anne Sass, Peter Moroshkin, Lars Weller, Roberto Cota, Benedikt Gerwers, Katharina Knicker, Martin Weitz, Rheinische Friedrich-Wilhelms-Univ. Bonn (Germany)

We report on experiments investigating laser cooling of atomic gases by collisional redistribution of radiation, a technique applicable to ultradense atomic alkali noble gas mixtures. Thermal deflection spectroscopy indicates a relative gas cooling of 500 K in the laser focus, starting from an initial gas cell temperature near 700 K. We are currently investigating different techniques for precise determination of the local temperature within the gas cell. In recent work, we investigate the Kennard-Stepanov relation, a thermodynamic, Boltzmann-type scaling between the absorption and emission spectral profiles of an absorber, which applies in many liquid state dye solutions as well as in semiconductor systems. To this end, absorption and emission spectra of rubidium atoms in dense argon buffer gas environment have been recorded. We demonstrate experimentally that the Kennard-Stepanov relation between absorption and emission spectra is well fulfilled in the collisionally broadened atomic gas system. Our experimental findings are supported by a simple theoretical model.

9380-22, Session 5

Excitation strategies and propagation effects in laser cooling of solids via superradiance (*Invited Paper*)

Guang-Zong Dong, Xin-Lu Zhang, Harbin Engineering Univ. (China)

Since the pioneer work of Petrushkin and Samartsev, laser cooling of solids in superradiance (SR) regime is receiving increased attention, because it

could facilitate ultra fast optical refrigeration. Originally, a red-detuned continue-wave laser and a resonant pulsed laser are needed to achieve SR emission in a rare-earth activated solid for cooling. Alternatively, Nemova and Kashyap suggested that cooling of a solid in SR regime can be achieved only by adopting a red-detuned pulsed laser. In this paper, we propose other possible excitation schemes that enable optical refrigeration in SR regime. Specifically, we consider the case that two laser pulses (one is red detuned and the other is resonant to the manifold transition) interact with a rare-earth active solid of a few millimeters in dimension. The temporal and spatial evolution of the ionic ensemble being prepared for SR emission under various excitation orders is analyzed. The characteristic time scales of SR are estimated, and the temporal evolution of SR emission is presented. Moreover, the propagation effects related to the attention of the input pulses, the cooperation length and the direction and shape of SR emission are also investigated. The analytical expressions of the cooling power density and total cooling power are deduced by considering the energy exchange of the ionic ensemble with the surrounding host material during the recovery of thermal equilibrium, based on which, the temperature dependent cooling performance of optical refrigeration via triggered SR is simulated.

Conference 9381: Vertical-Cavity Surface-Emitting Lasers XIX

Wednesday - Thursday 11-12 February 2015

Part of Proceedings of SPIE Vol. 9381 Vertical-Cavity Surface-Emitting Lasers XIX

9381-1, Session 1

New applications boost VCSEL quantities: recent developments at Philips (*Invited Paper*)

Martin Grabherr, Philips Technologie GmbH U-L-M Photonics (Germany)

Along with the mature and steadily growing traditional datacom business (Transceivers, AOC, MBOM) VCSELs have proven to be key components also for further volume applications.

Laser mice emerged 2004 and dominated the shipped quantities of VCSELs for some years, followed by various applications like atomic clock, TDLAS oxygen sensing, encoders, and many more.

Recently, two additional major applications came into focus: smart sensors for mobile devices and integrated optical interconnects in systems like high performance computers, servers or core routers.

On top of this, VCSELs are penetrating more and more power applications, primarily for illumination or IR heating.

We present recent developments in technology, products, and addressed market segments within Philips that will have an impact on the VCSEL industry.

9381-2, Session 1

Vertical-cavity surface-emitting lasers enable high-density ultra-high bandwidth optical interconnects (*Invited Paper*)

Nicolae Chitica, TE Connectivity Ltd. (Sweden)

Vertical-Cavity Surface-Emitting Lasers (VCSELs) are key components enabling power- and cost-efficient, high-density, ultra-high bandwidth parallel optical interconnects for data center and high-performance computing applications. This paper presents recent developments at TE Connectivity in the area of 25 Gb/s per channel-class VCSEL and optical transmitter technology for applications such as 100G Ethernet and Enhanced Data Rate InfiniBand pluggable and mid-board connectivity solutions.

9381-3, Session 1

Mode partition noise characterization of 25 Gb/s VCSELs (*Invited Paper*)

M. V. Ramana Murty, Laura Giovane, David G. Cunningham, Jingyi Wang, Avago Technologies Ltd. (United States); Zheng-Wen Feng, Avago Technologies Ltd. (Singapore); Thomas R. Fanning, Avago Technologies Ltd. (United States)

Directly-modulated multi-mode 850 nm VCSELs operating at 25 and 28 Gb/s are helping meet the bandwidth demands of short reach links in data centers and enterprise applications. As data transmission rate continues to increase, impairments such as modal and chromatic dispersion in the fiber, and device parameters such as relative-intensity noise and spectral width become more important. In particular, mode partition noise (MPN) in the VCSEL may place a key limitation on link length. Fluctuations in the partition of energy among the transverse modes of the VCSEL combined

with chromatic dispersion in the fiber leads to a fluctuation in the received power. The resulting power penalty from MPN is characterized by measuring the k-factor, a ratio of standard deviation in received power due to MPN to that in the extreme limit where all power in a pulse is contained in one mode. The k factor is determined by isolating and observing the fluctuations of individual super-modes of high-bandwidth multi-mode VCSELs. Intensity noise in the super-modes is measured under large-signal modulation at 25 Gb/s. The observed mode partition noise in multi-mode VCSELs and its implications for link length will be discussed.

9381-4, Session 2

Concepts for long wavelength VCSELs above 2 μ m (*Invited Paper*)

Stephan Sprengel, Markus-Christian Amann, Technische Univ. München (Germany)

VCSELs are highly interesting for innovative gas sensing techniques like tunable diode laser absorption spectroscopy, due to excellent beam quality, inherent longitudinal single mode behavior and extremely low threshold powers. The strong increase in absorption strength for many gases towards longer wavelengths makes VCSELs above 2 μ m highly beneficial. In this talk different concepts for long wavelength VCSELs based on InP and GaSb will be compared. The presented lasers use buried tunnel junctions for current confinement and exhibit emission wavelengths of up to 2.36 μ m and 2.6 μ m for InP and GaSb respectively. Furthermore, concepts for wavelength extension by type-II active regions are presented.

9381-5, Session 2

Long wavelength VCSEL by VCSEL optically injection locked optoelectronic oscillator

Juan F. Coronel, Institut Supérieur de l'Aéronautique et de l'Espace (France) and Univ. Nacional de Colombia (Colombia); Angélique Rissons, Institut Supérieur de l'Aéronautique et de l'Espace (France); Margarita Varon, Univ. Nacional de Colombia (Colombia)

BACKGROUND

The aerospace industry is keen on the development of optical technology. This is due to the reduced size, cost, weight and reduced power consumption of optical technologies compared to electronics. Since 1994 the development of optical microwave devices using several techniques has been reported.

The VCSEL Based Oscillator (VBO) was presented as a low cost and low power consumption device using a directed modulated VCSEL source. Good performance of this carrier generator is reported for frequencies below 4 GHz. The intrinsic free running cut off frequency of the VCSEL has limited the increase of the carrier frequency and the advantage of using such relatively simple configuration in comparison to other optoelectronic oscillator topologies.

The VCSEL by VCSEL Optically Injection Locked VCSEL Based Oscillator (OILVBO) is presented. The injection locking technique give stability of the VCSEL source due to the reduction of the Relative Intensity Noise (RIN). This leads to a purer carrier. The optically injection locked VCSEL frequency response is enhanced by enabling the VCSEL to be modulated beyond 4 GHz. The OILVBO can generate carriers at higher frequencies than the single VBO with lower noise. A previous result making OILVBO using a DFB laser

**Conference 9381:
Vertical-Cavity Surface-Emitting Lasers XIX**

as a master was reported by our team last year.

RESULTS

In this article is presented a VCSEL by VCSEL OILVBO at 2.49 GHz with carrier phase noise lower than -120 dBc/Hz at 10 kHz offset using a 2 km length optical fiber is reported. Its effects in the carrier phase noise will be presented showing the feasibility of using low power lasers in high frequency communications. The VCSEL biasing and locking conditions will be analyzed in the article. More measurements and results at higher frequencies will be presented for the final paper submission, they are still being carried out.

9381-6, Session 2

Heat-assisted magnetic recording (HAMR) demonstration using C-shaped nano-apertures

Sajid Hussain, Charanjit S. Bhatia, Yang Hyunsoo, Aaron J. Danner, National Univ. of Singapore (Singapore)

Heat assisted magnetic recording (HAMR) is a next generation technology proposed for achieving magnetic storage densities beyond 1 Tb/in². However, the commercialization of heat-assisted magnetic recording faces substantial technical challenges that must be resolved before widespread adoption of the technology can commence. Foremost of these challenges, is the development of a precise method of delivering light to a very small, sub wavelength bit area with sufficient power to heat a high coercivity magnetic medium above its Curie temperature. Complex fabrication processes, low power transfer efficiency and high heat dissipation are the biggest problems faced in current HAMR light delivery systems. Nano-aperture VCSELs are potential candidates as a light delivery system in HAMR, and we have fabricated 850 nm VCSELs with C-shaped nano-apertures on their facets to be used as near-field transducers in order to produce a small localized optical spot; we then characterized their performance and compared power requirements with successful HAMR demonstrations with control C-shaped nano-aperture near-field transducers fabricated on glass substrates. Laser light at 850 nm wavelength was focused onto a magnetic medium, through the nano-apertures, and an external magnetic field of magnitude much lower than the coercivity (at room temperature) of the magnetic medium was simultaneously applied. Magnetic force microscopy images of the medium showed that C-apertures are capable of producing a magnetic spot much smaller than the diffraction limit using localized plasmonic effects. The power density required at this wavelength for HAMR process was experimentally measured using a pump-probe optical setup.

9381-7, Session 2

Optical power of VCSELs stabilized to 35 ppm/°C without a TEC

John Downing, USL Technologies LLC (United States)

This paper reports a hybrid optoelectronic method and device for stabilizing the output optical power from vertical-cavity surface-emitting lasers (VCSELs) and laser diodes (LDs) without a thermoelectric cooler. It is a sequel to Downing et al. (2013), which reported that 50 ppm/oC stability can be obtained from VCSELs using a weakly polarizing beamsplitter coating. The new method eliminates the need for custom interference coatings, polarization-angle adjustments (optical calibration), and extreme alignment tolerances and has diverse applications in battery-powered sensors and systems. A typical system comprises: 1) a semiconductor light emitter (VCSEL or LD) with integral thermistor, 2) a glass-wedge beamsplitter, 3) a monitor photodiode, 4) a digital controller, and 5) calibration firmware. The system can precisely compensate for the combined effects of temperature and wavelength on photodiode responsivity, as well as changes in beam divergence, power profile, and polarization angle over a 50o-C temperature range. Numerical simulations show that power stability better than 15 ppm/oC can be obtained with the

system. Data are reported that demonstrate 35 ppm/oC stability can be achieved with prototype systems built with single-mode, polarization-locked VCSELs and LDs. VCSELs are the emitter of choice when low power (a couple of mW) and optical simplicity drive system design whereas LDs can be used when higher optical power (100s of mW) is needed. Calibration at time of manufacture in batches is feasible. It is also shown that the method can deliver unpolarized, incoherent light from resonate-cavity light-emitting diodes for environmental sensing applications.

J. Downing, D. Babic, and M. Hibbs-Brenner, "An Ultra-Stable VCSEL Light Source", SPIE Photonics West 2013, Vertical-Cavity Surface-Emitting Lasers XVII, Conference OE121, Vol. 8638, pgs. 86390B-1 to 86390B-12 (2013).

9381-8, Session 2

Vertical-cavity surface-emitting laser for space applications

Sébastien Chaudron, Angélique Rissons, Veronique Gernigon, Institut Supérieur de l'Aéronautique et de l'Espace (France)

The Vertical-Cavity Surface Emitting Laser (VCSEL) is another kind of semiconductor laser, which, instead of the Edge Emitting Laser (EEL) like DFB, have his electromagnetic field oscillating parallel to the growing plan. This property allows the VCSEL to have many advantages compared to the EEL like they are very compact, they have a low weight, a low electrical consumption, a low threshold current, a low cost, a large bandwidth, a low line-width, a low relative intensity noise (RIN) and a circular beam (M² = 1). However, the VCSEL have also drawbacks like a low optical power at 1550 nm (few mW vs several hundred mW for the EEL), they have usually a multimode transverse emission. Nevertheless the VCSEL assets make them an excellent candidate for several applications, and particularly for space applications such as free space optical communications, attitude control (gyro-laser), microwave-photonics links and active remote sensing. In order to let these applications being possible, several studies on reliability of this component are needed. Indeed, we need to know the behavior of this component in space environment; in particular, the dynamic behavior of the 1.55 μm VCSEL operating in harsh environment is still an investigating point.

So, we have to study (characterization and modelling) wavelength, optical power, RIN, phase noise as a function of the temperature. Same studies of these parameters as a function of space radiations, depending of the orbit of the satellite, have to be made. We need also to do studies on shock, acceleration and vibration resistance during the launch phase.

9381-9, Session 3

High-power VCSEL arrays for consumer electronics (Invited Paper)

Luke A. Graham, Hao Chen, Jonathan Cruel, James Guenter, David Q. Kelly, Alirio Melgar, Jim A. Tatum, Edward Shaw, Finisar Corp. (United States)

Finisar has developed a line of high power, high efficiency VCSEL arrays. They are fabricated at 860nm as traditional P side up top emitting devices with -100 micron substrate thickness, leveraging Finisar's existing VCSEL fab and test processes for low cost, high volume capability. A thermal camera is used to accurately measure temperature profiles across the arrays at a variety of operating conditions and further allowing development of a full reliability model. The arrays are shown to demonstrate wear out reliability suitable for a wide range of applications. Typical 1/e² beam divergence is near 16 degrees under CW operating conditions at peak wall plug efficiency, narrowing further under pulsed drive conditions.

**Conference 9381:
Vertical-Cavity Surface-Emitting Lasers XIX**

9381-10, Session 3

Progress on high-power high-brightness VCSELs and applications *(Invited Paper)*

Delai Zhou, Jean-Francois Seurin, Guoyang Xu, Pu Zhao, Bing Xu, Tong Chen, Robert Van Leeuwen, Alexander Miglo, Chuni Ghosh, Princeton Optronics, Inc. (United States)

High power, high brightness semiconductor lasers are widely used for illumination, pumping as well as nonlinear frequency conversion. Compared with LED and edge emitters, vertical cavity surface-emitting lasers (VCSEL) provide combined advantages such as high efficiency, low diverging circular beam, stable and narrow emission spectrum, and low-cost manufacturability that include wafer level test and array integration. With the external-cavity configuration, large size VCSELs and two dimensional (2D) arrays can be excellent candidates for low-cost, high-brightness light source. Due to its very high intra-cavity field intensity, VCSELs are especially advantageous in the application of second-harmonic generation, for high power, reliable green, red and blue lasers, via intra-cavity frequency-doubling with nonlinear crystals.

We report our progress on such high-power high-brightness VCSELs and 2D arrays in the infrared wavelength range. Those GaAs-based VCSEL wafers are grown by MOCVD and processed into either top-emitting or bottom-emitting devices using reactive ion etch (RIE) and selective wet oxidation process. For self-lasing multimode devices, CW output of >6W and peak efficiency of > 60% were recorded from large single devices with 300um aperture diameter. Output of >500W and peak efficiency of >55% were also achieved from large 2D arrays. For single mode devices (M2<1.1) with external cavity configuration, we obtained CW output of >2.1W for single devices and >100W for 2D arrays. For single devices with intra-cavity frequency-doubling approach, record CW green laser output of ~4.4W is achieved, with overall electrical to optical efficiency of ~20.3%.

9381-11, Session 3

High-speed and scalable high-power VCSEL arrays and their applications *(Invited Paper)*

Mial E. Warren, Richard F. Carson, John R. Joseph, Thomas Wilcox, David J. Abell, Kirk J. Otis, TriLumina, Inc. (United States)

A unique architecture for two-dimensional arrays of VCSELs that allow for simultaneous high-power output and high-bandwidth modulation has been developed for a variety of applications. The arrays use integrated micro-lenses for beam shaping and control, and to enable incoherent beam combining to make compact, high-brightness sources with low coherence. The fabrication and performance of the laser arrays will be reviewed and some of the applications being developed will be discussed.

9381-12, Session 4

High-speed VCSELs and VCSEL arrays for single- and multi-core fiber interconnects *(Invited Paper)*

Anders Larsson, Petter Westbergh, Johan S. Gustavsson, Erik Haglund, Emanuel P. Haglund, Chalmers Univ. of Technology (Sweden)

Oxide confined 850 nm VCSELs operating at high speed have been realized using optimized active region and cavity designs, as well as techniques for reducing capacitance and thermal impedance. Investigations of the

impact of damping on the small and large signal VCSEL dynamics show that damping has a major impact on the modulation response. While a reduction of damping allows for a small signal modulation bandwidth approaching 30 GHz, it is found that the optimum damping under large signal modulation (digital data transmission) is bit rate dependent. Transmission at data rates up to 57 Gbps is demonstrated. Our VCSELs have also enabled the assembly of equalized transmitters and links operating at 64 Gbps (at IBM) and transmission over onboard polymer waveguides at 40 Gbps (at University of Cambridge).

To enable transmission over long distances of multimode fiber we use an integrated mode filter for single mode emission, thereby mitigating the effects of chromatic dispersion in the fiber. Such VCSELs have enabled transmission at 25 Gbps over 1300 m of multimode fiber and at 20 Gbps over 2000 m. The latter represents a record bandwidth-distance product of 40 Gbps*km.

To enable high bandwidth density interconnects using multicore fibers, we have developed dense 6-channel VCSEL arrays with each VCSEL operating up to a bit rate of 40 Gbps. The arrays have an aggregate capacity of 240 Gbps and show excellent uniformity. An investigation of RF and thermal crosstalk between the channels revealed very low levels of crosstalk.

9381-13, Session 4

850-nm Zn-diffusion VCSELs with oxide-relief structure for optical interconnects from very-short to medium (2km) reaches *(Invited Paper)*

Jin-Wei Shi, National Central Univ. (Taiwan); Chia-Chien Wei, National Sun Yat-Sen Univ. (Taiwan); Jyehong Chen, National Chiao Tung Univ. (Taiwan); Ying-Jay Yang, National Taiwan Univ. (Taiwan)

High-speed and "green" ~850 nm vertical-cavity surface-emitting lasers (VCSELs) have lately attracted lots of attention due to their suitability for applications in optical interconnects (OIs). To further enhance the speed and its maximum allowable linking distance of VCSELs are two major trends to meet the requirement of OI in next generation data centers. Recently, by use of the advanced 850 nm VCSEL technique, data rate as high as 64 Gbit/sec over 57m and 20 Gbit/sec over 2km MMF transmission have been demonstrated, respectively. Here, we will review our recent work about 850 nm Zn-diffusion VCSELs with oxide-relief apertures to further enhance the above-mentioned performances. By using Zn-diffusion, we can not only reduce the device resistance but also manipulate the number of optical modes to benefit transmission. Combining such device, which has excellent single-mode (SMSR> 30 dB) and high-power (~7mW) performance, with advanced modulation format (OFDM), record-high bit-rate-distance-product through MMF (2.3 km*26.5 Gbit/sec) has been demonstrated. Furthermore, by selective etching away the oxide aperture inside Zn-diffusion VCSEL, significant enhancement of device speed, D-factor, and reliability can be observed. With such unique VCSEL structure, >40 Gbit/sec energy-efficient transmission over 100m MMF under extremely low-driving current density (< 10kA/cm²) has been successfully demonstrated.

9381-14, Session 4

High-speed modulation, wavelength, and mode control in vertical-cavity surface-emitting lasers *(Invited Paper)*

Nikolay N. Ledentsov, Vitaly A. Shchukin, Joerg-Reinhardt R. Kropp, Gunther Steinle, Nikolay Ledentsov Jr., VI Systems GmbH (Germany); Kent D. Choquette, Univ. of Illinois at Urbana-Champaign (United States); Sven Burger, Frank Schmidt, Konrad-Zuse-Zentrum für

**Conference 9381:
 Vertical-Cavity Surface-Emitting Lasers XIX**

Informationstechnik Berlin (Germany); Jarek P. Turkiewicz, Warsaw Univ. of Technology (Poland); Bo Wu, Qiu Shaofeng, Yanan Ma, Zhiyong Feng, Huawei Technologies Co., Ltd. (China)

We address demands and possibilities in modern Vertical-Cavity Surface-Emitting Lasers.

(i) High Speed Modulation. High-speed modulation >25Gb/s is important for application in data transmission and microwave photonics. High speed can be realized by applying novel VCSEL concepts: anti-waveguiding design with AIAs-rich core, further increase in the optical confinement factor, engineering of the density of states to increase the material gain, using barriers preventing the leakage of the injected nonequilibrium carriers. For microwave photonics electrooptically-modulated VCSELS allow modulation bandwidth >35GHz.

(ii) Wavelength control. To multiplex many (>4) VCSEL wavelengths into the 840–860 nm range of low modal dispersion of multimode fiber, a VCSEL low shift of the wavelength with temperature is needed (<0.03 nm/K). The device where the gain medium is placed within the region of the bottom semiconductor distributed Bragg reflector (DBR) while the other part of the bottom DBR, the cavity and the top DBR are made of dielectric materials, can provide a complete temperature stability of the wavelength but also allow a high optical confinement factor for high-speed operation.

(iii) Single mode operation and mode control. Single mode operation is needed to counteract a significant spectral dispersion of the multimode fiber (MMF) in the 840–860 nm range. A 300 m error-free transmission over OM3 MMF at 25Gb/s is realized for parallel MMF links using commercially available driver and transimpedance amplifier array electronics and x16 Transceiver and Receiver boards. OM4 fiber allows >600 m transmission. To achieve single mode operation at moderate VCSEL it is possible to design and realize apertures to match the standard resistance and a strong leakage of the high order transverse optical modes into the selectively oxidized surrounding regions.

(iv) The oxide apertures may, as opposite, suppress the lateral leakage of the VCSEL mode in a broad range of the photon energies corresponding to a wide range of the mode tilt angles. High tilt angles beyond the angle of the total interval reflection at the semiconductor-air interface are realized. In this case single mode large aperture (9 μm) devices can be manufactured. The device may be used for near field light outcoupling into waveguides and does not require multilayer DBRs at the top surface.

9381-15, Session 4

Phased VCSEL array modulation

Kent D. Choquette, Stewart T. M. Fryslie, Bradley Thompson, Zihao Gao, Univ. of Illinois at Urbana-Champaign (United States)

Controlling the phase relationship between the pixels of a coherently coupled VCSEL array can create unique properties that may have several novel applications. We have previously reported record phase shift sensitivity with current and ultrafast beam steering. Here we show that independent current injection into phased photonic crystal VCSEL arrays can drive the arrays to exhibit either coherent or incoherent operation. In the condition of coherent operation, we have achieved a record 37 GHz small signal bandwidth with 3 mW output power and single mode (≤ 0.1 nm) emission.

9381-16, Session 4

Extraction and analysis of high-frequency response and impedance of 980-nm VCSELS as a function of temperature and oxide aperture diameter

Philip Wolf, Hui Li, Philip Moser, Gunter Larisch, James A. Lott, Technische Univ. Berlin (Germany); Dieter H. Bimberg, Technische Univ. Berlin (Germany) and King Abdulaziz Univ. (Saudi Arabia)

Vertical-cavity surface-emitting lasers (VCSELS) are decisive cost-effective, energy-efficient, and reliable light sources for short-reach (up to ~300 m) optical interconnects in data centers and supercomputers. To viably replace copper interconnects and advance to on-chip integrated photonics reliable VCSELS ideally must be able to operate highly energy efficiently at large bit rates without cooling at up to 85 °C with immunity to temperature variations.

For the first time we demonstrate that with our 980 nm VCSELS can achieve temperature-stable, energy-efficient, and high-speed operation coincidentally. A record low 139 fJ/bit of dissipated heat for 35 Gbit/s error-free data transmission at 85 °C is achieved. Carefully design of both the VCSEL's epitaxial structure and device geometrics is of essence in order to realize this contemporaneousness. By introducing a suitable quantum well gain-to-etalon wavelength offset simultaneously improves the temperature-stability, the maximum bit rate at high temperatures, and the energy efficiency. Tuning the photon lifetime additionally increases the bandwidth by changing the relation between damping and resonance relaxation frequencies. Via detailed systematic experimental temperature-dependent and oxide aperture-diameter-dependent measurements including static L-I-V and emission spectra measurements, small signal analysis, and data transmission experiments we report our VCSELS' most important figures-of-merit of intrinsic and extrinsic performance limitations. This includes the modulation bandwidth, the parasitic cut-off frequency, the relaxation resonance frequency, lumped-circuit elements, and the K- and D-factors. We report VCSEL device parameters useful for the development of energy-efficient optical interconnect systems based on 980 nm VCSELS with respect to the impact on energy efficiency and temperature stability.

9381-17, Session 4

Ultrafast polarization dynamics with controlled polarization oscillations in vertical-cavity surface-emitting lasers

Markus Lindemann, Henning Höpfner, Nils C. Gerhardt, Martin R. Hofmann, Ruhr-Univ. Bochum (Germany); Tobias Pusch, Rainer Michalzik, Univ. Ulm (Germany)

Spintronic lasers offer promising perspectives for new concepts superior to the options of purely charge-based devices. Especially spin-polarized vertical-cavity surface-emitting lasers (spin-VCSELS) exhibit ultrafast spin and polarization dynamics. Using pulsed spin-injection, oscillations in the circular polarization degree can be generated, which have the potential to exceed frequencies of 100 GHz. The oscillations evolve due to the carrier-spin-photon system that is coupled via the birefringence for the linear modes in the micro-cavity of the VCSEL. They are independent of the conventional relaxation oscillations and thus their usage can be the cornerstone for ultra-fast directly modulated spin-VCSELS in the near future. After giving a short overview of the state of the scientific and technical knowledge we will outline a method to control the polarization oscillations by multiple spin-injection pulses. It is possible to switch these oscillations on and off, depending on phase and amplitude conditions of two consecutive excitation pulses. Even half-cycles can be generated, which is the basis for short polarization pulses, only limited by the polarization oscillation resonance frequency. We investigate influences of the birefringence, which

**Conference 9381:
 Vertical-Cavity Surface-Emitting Lasers XIX**

directly determines the oscillation frequency, by means of calculations with the spin-flip-model and experimental verification using 850 nm VCSELs. Furthermore we discuss experimental possibilities of increasing the birefringence and therefore the oscillation frequency, so ultra short pulses come into reach.

9381-18, Session 5

Cold-cavity optical loss measurements of oxide-confined VCSELs

Stewart T. M. Fryslie, Charlene Tai, Univ. of Illinois at Urbana-Champaign (United States); Janice Blane, Univ. of Illinois at Urbana-Champaign (United States) and U.S. Military Academy (United States); Kent D. Choquette, Univ. of Illinois at Urbana-Champaign (United States)

A generalized method using sub-threshold spectral measurements matched to model calculations is demonstrated to determine optical loss in microcavity lasers. Cold-cavity spectral characteristics are used to extract the size-dependent optical loss for small diameter oxide-confined vertical-cavity surface emitting lasers. VCSELs with varying impurity concentrations are compared.

9381-19, Session 5

VCSEL modeling with self-consistent models: From simple approximations to comprehensive numerical analysis

Maciej Dems, Piotr Beling, Marcin Gebski, Lukasz Piskorski, Jaroslaw Walczak, Maciej Kuc, Leszek Frasunkiewicz, Michal Wasiak, Robert Sarzala, Tomasz Czystanowski, Lodz Univ. of Technology (Poland)

In the talk we show the process of modeling complete physical properties of VCSELs. First, we identify the most important phenomena that take place in their operation and then we apply a self-consistent approach not only to model each of these phenomena, but also to consider their mutual interactions. We use a VCSEL with buried tunnel junction as an analyzed structure and show how a step-by-step development of a complete multi-physics model allows with every step to represent its properties more accurately. Then we introduce structural complication to the VCSEL design, which renders most commonly used numerical models invalid. In particular, we show that introduction of high contrast gratings, while opening new ways to improve laser properties, strongly complicates its optical modeling. In such case, the comprehensive multi-physics VCSEL simulation becomes a challenging task. We show however, that a proper choice of a self-consistent simulation algorithm can still make such a simulation a feasible one, which is necessary for an efficient optimization of the laser prior to its costly manufacturing.

9381-20, Session 5

Spectrally-resolved imaging of the transverse modes in multimode VCSELs

Stephen M. Misak, Kelly R. Farner, Daniel J. Thul, Daniel G. Dugmore, Evan R. Hale, Kirsten A. Middleton, Rose-Hulman Institute of Technology (United States); Kent D. Choquette, Univ. of Illinois at Urbana-Champaign (United States); Paul O. Leisher, Rose-Hulman Institute of Technology (United States)

Vertical-cavity surface-emitting lasers (VCSELs) enable a range of applications such as data transmission, trace sensing, atomic clocks, and

optical mice. For many of these applications, the output power and beam quality are both critical (i.e. high output power with good beam quality is desired). Multi-mode VCSELs offer much higher power than single-mode devices, but this comes at the expense of lower beam quality. Directly observing the resolved mode structure of multi-mode VCSELs would enable engineers to better understand the underlying physics and help them to develop multi-mode devices with improved beam quality. In this work, a low-cost, high-resolution (<3 pm) Echelle grating spectrometer system is used to map the two-dimensional VCSEL near-field emission profile. This system spectrally disperses the emission profile and images it with high magnification onto a CMOS camera. The resulting two dimensional images of each LP mode allow direct observation of modal content of the VCSEL.

9381-21, Session 5

Efficiency optimization and analysis of 808nm VCSELs with a full electro-thermal-optical numerical model

Andreas P. Engelhardt, Univ. Kassel (Germany); Johanna S. Kolb, Philips Technologie GmbH (Germany); Friedhard Römer, Univ. Kassel (Germany); Ulrich Weichmann, Holger Moench, Philips Technologie GmbH (Germany); Bernd Witzigmann, Univ. Kassel (Germany)

A high electro-optical conversion efficiency of a VCSEL (Vertical-Cavity Surface-Emitting Lasers) is one of the key requirements for their application in high power systems for heating, illumination and pumping applications. The substantial amount of degrees of freedom in the epitaxial and structural design of a VCSEL demands numerical guidance in form of TCAD modeling for a straight forward and successful optimization of the devices.

We set up a full electro-thermal-optical model for the simulation of VCSEL devices. The electro-thermal part of the simulation follows a drift-diffusion model complemented by a customized, energy resolved, semi-classical carrier capture theory in the QW regions. Optical modes, eigensolutions of the vectorial electromagnetic wave equation, stem from a finite element vectorial solver. The electro-thermal and optical model are linked via the photon-rate equation using QW gain spectra (screened Hartree-Fock approximation) and iterated to self-consistency in a Gummel-type iteration scheme. For comparison and calibration, experimental reference data was extracted from oxide-confined, top-emitting VCSEL devices with an emission wavelength of 808 nm.

Our simulations are in good agreement with the electro-optical characteristics of the experimental reference. With the calibrated, microscopic model, routes of design adjustment for efficiency optimization are explored. Exemplarily, the maximal VCSEL efficiency of the simulated reference design increases by -10% (absolute) when free hole absorption is switched off. Accordingly, with the combination of an electro-thermal and optical description, a balancing of the tradeoffs of pDBR doping towards reduced free carrier absorption results in a noteworthy efficiency improvement which is validated with experimental data.

9381-22, Session 5

Electrical, thermal, and optical modeling of high-performance 25-50 Gb/s 980 nm VCSELs

Michal Wasiak, Tomasz Czystanowski, Jaroslaw Walczak, Robert Sarzala, Lodz Univ. of Technology (Poland); Philip Moser, Dieter H. Bimberg, James A. Lott, Technische Univ. Berlin (Germany)

An accurate model of oxide-confined VCSELs that includes for example 2-3D capacitance, resistance, current density, temperature, and optical modes is extremely valuable for optimizing the design and performance

**Conference 9381:
Vertical-Cavity Surface-Emitting Lasers XIX**

of VCSELs targeted for use in on-chip photonics, silicon photonics, and very-short-reach optical interconnects. Ideally given a foundry VCSEL technology - for example a visionary circa 2020 6-inch wafer foundry process that produces highly energy efficient, 25-85°C-rated, 25-50 Gbit/s VCSELs - this technology would have associated with it a set of measured device parameters that are entered into the simulator. Toward this end in our presentation and paper we report the results of our numerical modeling of the capacitance, resistance, temperature, optical modes, and cavity Q-factor in state-of-the-art 25-50 Gb/s oxide-confined 980 nm VCSELs. Several theoretical modifications of the laser's epitaxial and geometrical structure are considered, such as: the number, placement, and diameter of the oxide layers, and adjustment of DBR and other epitaxial layer or dielectric layer thicknesses to modify the VCSEL cavity photon lifetime. The electrical and thermal models are solved in a self-consistent way, providing the distribution of temperature and electric potential in the laser. These distributions allow us to calculate resistances and capacitances that are used to estimate modulation time constants and other high frequency figures-of-merit. We also find the 2-3D optical modes, their modal gains, and the resultant VCSEL Q-factors, and adjust our model to better fit, analyze, and thus understand our measured results.

9381-23, Session 5

Universal reliability model for VCSELs and other diode lasers

Dennis Deppe, Xu Yang, Yu Zhang, CREOL, The College of Optics and Photonics, Univ. of Central Florida (United States); Guowei Zhao, sdPhotonics, LLC (United States); Mingxin Li, CREOL, The College of Optics and Photonics, Univ. of Central Florida (United States)

Reliability has been one of the most important topics for commercial laser diodes, and continues to grow in importance as VCSELs are driven to increasingly high current densities to achieve high speed. The empirical results based on acceleration factors described by activation energy and current density are effective at modeling reliability of a specific device structure, but less effective at producing a useful defect model to predict how new laser structures will operate. In this presentation a specific defect model is described based on increased Frenkel defect creation in the laser diode active volume due to increased temperature and pressure in the active region when the laser diode is biased. Interstitial defect propagation out of the active volume, leaving increased vacancy concentration that can relax the lattice pressure, is presented as a likely cause of wear-out due to biasing. The model could enable corrections to be made to the acceleration factors and predictive analysis for future laser diodes. VCSELs in particular are predicted to increase in reliability for a given size reduction, as well as increasing in speed. The model is compared to existing and new experimental results.

9381-24, Session 6

Hybrid VCSEL: liquid crystal systems (Invited Paper)

Krassimir Panajotov, Vrije Univ. Brussel (Belgium); Yi Xie, Jeroen Beeckman, Kristiaan Neyts, Univ. Gent (Belgium); Carlos Belmonte, Vrije Univ. Brussel (Belgium); Maciej Dems, Lodz Univ. of Technology (Poland); Hugo Thienpont, Vrije Univ. Brussel (Belgium)

We study theoretically and experimentally the spectral and polarization characteristics of hybrid systems of Vertical-Cavity Surface-Emitting Lasers integrated within liquid crystal cells. For the case of nematic liquid crystal (NLC) - VCSEL system our model predicts the possibility of selecting between two orthogonal directions of linear polarization (LP) of the fundamental mode (x or y LP) by choosing appropriate NLC length as well

as by an active electro-optically tuning of the LC director. These theoretical predictions are confirmed experimentally after integrating VCSEL wafers in specially designed LC cells that allow for applying an electrical field. We also investigate such systems for the purpose of efficient electrical wavelength tuning.

Completely different is the behaviour of the hybrid system of cholesteric liquid crystal (CLC)-VCSEL: it becomes a coupled system with different spectral, threshold and polarization characteristics than the ones of the stand-alone VCSEL. Due to the existence of a band gap for circularly polarized light in the liquid crystal, lasing occurs in almost circularly polarized modes at the LC side. Theoretically, we predict that the threshold current significantly decreases while the CLC-VCSEL birefringence increases: wavelengths are separated due to the CLC birefringence rather than to the inherent VCSEL birefringence that determines the solitary VCSEL linearly polarized mode wavelength splitting. We confirm these predictions experimentally by measuring the polarization state of the emission from CLC-VCSEL at different temperatures: with the transition of nematic to isotropic phase of the LC the polarization changes from left-handed circular to linear polarization.

9381-25, Session 6

Small-sized lithographic single-mode VCSELs with high-power conversion efficiency

Xu Yang, Mingxin Li, Guowei Zhao, Yu Zhang, Sabine Freisem, Dennis Deppe, CREOL, The College of Optics and Photonics, Univ. of Central Florida (United States)

We believe that we have record results in power conversion efficiency, slope efficiency, and power level from small sized VCSELs. By eliminating the oxide we are able to reduce the electrical and thermal resistance, and use improved mirror materials for high slope efficiency. Size scaling from 6 μm to 1.5 μm diameter show that power conversion efficiency remains ~ 50 % over the size range of 6 μm to 2 μm . Slope efficiency actually increases for the smaller VCSELs, which may be a result of improved modal overlap with the gain volume. We believe these are the first VCSELs to show high performance at small size, and further scaling appears possible. We will present data on efficiency and spectral properties, along with temperature performance and polarization data.

9381-26, Session 6

Double HCG 980-nm VCSEL with non-oxide lateral mode confinement scheme (Invited Paper)

Marcin Gebiski, Maciej Dems, Lodz Univ. of Technology (Poland); Y. Y. Xie, Z. J. Xu, Qi Jie Wang, D. H. Zhang, Nanyang Technological Univ. (Singapore); James A. Lott, Technische Univ. Berlin (Germany); Tomasz Czyszanowski, Lodz Univ. of Technology (Poland)

Distributed Bragg Reflectors are typically used as highly reflecting mirrors of VCSELs. In order to provide optical field confinement, oxide apertures are incorporated in the process of wet oxidation of high aluminum content layers. This technology has several drawbacks from which poor control of resulting aperture diameter and low reliability of the device are the most important ones. A prospective alternative to the DBR mirror is the heterostructure High refractive index Contrast Grating (HCG). As with a DBR mirror the power reflectance and reflectivity phase of the HCG offers optical confinement by its intrinsic mirror properties controlled by the HCG's design parameters. We present self consistent, thermal, electrical, gain, and optical simulations of a double HCG 980 nm GaAs-based VCSEL. We propose optimized parameters of the VCSEL in order to obtain the lowest threshold current and the highest single mode output power.

**Conference 9381:
 Vertical-Cavity Surface-Emitting Lasers XIX**

This work is jointly supported by Polish NCR&D and Singapore A*STAR (grant no. 122 070 3063) project: 'A Novel Photonic Crystal Surface Emitting Laser Incorporating a High-Index-Contrast Grating'.

9381-27, Session 6

Compliant heterogeneous assemblies of micro-VCSELs as a new materials platform for integrated optoelectronics

Jongseung Yoon, The Univ. of Southern California (United States)

Vertical cavity surface emitting lasers (VCSELs) represent a ubiquitous light source with unique performance characteristics that excel edge-emitting lasers or light-emitting diodes. Despite their unique advantages, established modes of exploiting VCSELs have been intrinsically limited as they rely mainly on devices that operate on their native growth substrates, which is attributed to difficulties in materials growth, processing, and assembly methods that are not readily compatible with programmable distribution on unusual substrates over large area, as well as heterogeneous integration with dissimilar materials and devices. Furthermore, VCSELs, typically built on rigid and brittle semiconductor wafers, restricted their capacity to integrate effectively onto systems with a soft, non-planar interface, which can be extremely useful for many unconventional applications. Here we developed approaches that address these limitations in conventional VCSELs by exploiting strategic combinations of specialized epitaxial design, device configuration, and printing-based deterministic assembly. The outcome enabled defect-free release of ultrathin, microscale VCSELs (micro-VCSELs) from the growth wafer, and their device-level implementation on nearly any types of non-native substrates in scalable, precisely controlled layouts, with performance comparable to devices on the growth substrate. Systematic studies of electrical and optical characteristics of devices on the source wafer and foreign substrates, together with 3D mechanics and thermal modeling based on finite element method (FEM), provide essential aspects of underlying materials science and physics in the reported systems.

9381-28, Session 7

Maximizing temperature insensitivity and energy-efficiency of 25-50 Gb/s 980-nm VCSELs via small oxide-aperture diameters and photon lifetime tuning (*Invited Paper*)

Philip Moser, Maya Volwahren, Gunter Larisch, James A. Lott, Dieter H. Bimberg, Technische Univ. Berlin (Germany)

Energy-efficient oxide-confined vertical-cavity surface-emitting lasers (VCSELs) emitting at 980 nm particularly well suited for very short reach (< 2m) and ultra short-reach (< 2 mm) optical interconnects operating at high temperatures up to 85°C are presented.

The maximum modulation bandwidth f_{3dB} of a 5 μm oxide-aperture diameter VCSEL is 24.7 GHz at 25°C and decreases only slightly to a record-high 23 GHz at 85°C. At bias currents below the thermal rollover the modulation bandwidth f_{3dB} increases up to 90% when the temperature is increased from 25 to 85°C. As a consequence our VCSELs operate more energy-efficiently at 85°C than at 25°C.

The impact of the oxide-aperture diameter on the energy-efficiency and temperature stability of the static and dynamic properties of our VCSELs is demonstrated and discussed. Via cavity photon lifetime tuning we demonstrate how the energy-efficiency and temperature stability can be improved and discuss and analyze the existing trade-offs between energy-efficiency, temperature stability, and low current density operation.

9381-29, Session 7

Theory and characterization of elliptically-polarized modes in vertical-cavity surface-emitting lasers

Nicolas Volet, Ecole Polytechnique Fédérale de Lausanne (Switzerland)

We report on a detailed study of the polarization of the beam emitted from telecom-wavelength vertical-cavity surface-emitting lasers (VCSELs). The investigated devices are electrically-pumped double-wafer-fused VCSELs emitting around 1.31 μm. The laser cavity, grown on an InP substrate, contains an AlGaInAs quantum well active region and a regrown circular tunnel junction. The AlGaAs/GaAs distributed Bragg reflectors are not-intentionally doped.

Stokes parameters are extracted separately for the two polarization submodes of the fundamental spatial mode LP₀₁. This characterization was performed at room temperature and for a significant number of devices. This led to the discovery of stable optical modes with a polarization that differs from the linear case. This crucial result was obtained without immersing the device in an external magnetic field or driving it under external optical injection. In addition, the polarization handedness can be selected directly with the drive current.

The analysis shows that the values of certain parameters involved in the spin-flip model should be reconsidered. In particular, a generalization of this theory is presented and fantastic agreement is found with the experimental results.

This work paves the way for a broad range of novel applications with the VCSEL technology, in particular for spintronics, bio-chemical sensing and telecommunication.

9381-30, Session 7

Engineering of optical modes in vertical-cavity microresonators by the aperture placement: applications to single-mode and near-field lasers

Vitaly A. Shchukin, Nikolay N. Ledentsov, Joerg-Reinhardt R. Kropp, Gunther Steinle, Nikolay Ledentsov Jr., VI Systems GmbH (Germany); Kent D. Choquette, Univ. of Illinois at Urbana-Champaign (United States); Sven Burger, Frank Schmidt, Konrad-Zuse-Zentrum für Informationstechnik Berlin (Germany)

By a proper positioning of the thick oxide apertures in oxide-confined vertical-cavity microcavities one can realize unique opportunities for optical field engineering and achieve novel functionalities.

(i) A device is engineered where a strong leakage of the high order transverse optical modes into the selectively oxidized surrounding regions is realized. Single mode lasing up to large aperture diameters is demonstrated. A 5 μm-aperture vertical-cavity surface-emitting laser (VCSEL) lases with >20dB side mode suppression ratio at >10kA/cm² having a resistance below 900Ω suitable for standard VCSEL drivers.

(ii) In a different approach the oxide layers may, as opposite, suppress the lateral leakage of the VCSEL mode in a broad range of photon energies corresponding to a wide range of the mode tilt angles also those beyond the angle of the total interval reflection at the semiconductor-air interface. In this case single mode large aperture (9 μm) devices is realized. The device is well suited for diffraction-induced or near field light outcoupling and does not require multilayer distributed Bragg reflectors with a high reflectivity at normal incidence.

We address air gaps as an alternative to oxide confinement in other than (Al,Ga)As materials systems and the application of the concept to edge-emitting lasers.

**Conference 9381:
 Vertical-Cavity Surface-Emitting Lasers XIX**

9381-31, Session 7

Impact of a negative gain-to-cavity wavelength detuning on the performance of InGaAlAs oxide-confined vertical-cavity surface-emitting lasers

Sergey A. Blokhin, Mikhail A. Bobrov, Nikolay A. Maleev, Ioffe Physical-Technical Institute (Russian Federation); Alexander G. Kuzmenkov, Ioffe Physical-Technical Institute (Russian Federation) and Connector Optics LLC (Russian Federation); Alexey V. Sakharov, Ioffe Physical-Technical Institute (Russian Federation); Alexei A. Blokhin, Saint-Petersburg State Polytechnical Univ. (Russian Federation); Philip Moser, James A. Lott, Technische Univ. Berlin (Germany); Dieter H. Bimberg, Technische Univ. Berlin (Germany) and King Abdulaziz Univ. (Saudi Arabia); Victor M. Ustinov, Ioffe Physical-Technical Institute (Russian Federation)

Vertical-cavity surface-emitting lasers (VCSELs) based on the InGaAlAs-materials system on GaAs substrates are the key component for short-reach data and computer communications systems. Several different modulation schemes have been developed to realize high data bit rates based on various oxide-confined near-infrared VCSEL designs operated under direct current modulation. However, one open question to resolve is the optimal quantum well (QW) gain-to-cavity etalon wavelength detuning to employ for temperature-stable high-speed performance. We investigate the static and dynamic characteristics of 850 nm high-speed oxide-confined VCSELs with different negative QW gain-to-cavity wavelength detunings. Our oxide-confined 850 nm VCSELs with a more common -10 nm negative gain-to-cavity detuning demonstrate the conventional optical mode behavior with a classical single-relaxation resonance frequency response. With a larger (≥ 20 nm) negative detuning, our devices with large oxide-aperture diameters ($> 6 \mu\text{m}$) show an anomalous start of lasing via higher order modes with a subsequent switching to lasing via the lowest order modes at higher currents. At intermediate currents, co-lasing via two types of transverse modes and a two-resonance modulation response is observed. The increase of operation temperature as well as the reduction in the oxide-aperture area resulted in classical lasing of index-guided VCSELs. The observed optical mode behavior can be attributed to the specific index guiding profile caused by the oxide-apertures, low internal optical losses, and the large gain-to-cavity detuning. Moreover, one can suggest that the complex shape of the modulation response results from the mode competition for the available gain during an interesting co-lasing operating regime.

9381-32, Session 7

Effect of temperature on polarization switching in long-wavelength VCSELs

Ana Quirce, Vrije Univ. Brussel (Belgium); Angel Valle, Luis Pesquera, Univ. de Cantabria (Spain); Krassimir Panajotov, Hugo Thienpont, Vrije Univ. Brussel (Belgium)

The polarization behavior of VCSELs has attracted a great deal of attention over these last decades. Polarization switching (PS) has been observed in a great variety of devices. Only recently a single PS in long-wavelength VCSELs has been reported [1].

In this work we have measured the effect of the temperature on the polarization-resolved characteristics of 1550-nm wavelength VCSELs. Double polarization switchings (PS) are observed. For low temperatures a PS from longer to shorter wavelengths (Type II PS) followed by the opposite PS (Type I) is observed. For large temperatures Type I followed by Type II PS are measured. A single Type I PS is observed at intermediate temperatures. The current at which this Type I PS appears does not depend on the

temperature.

A simple expression of the spin flip rate in the VCSEL is derived from [2]. Spin flip rate is related to the minimum value of the effective dichroism, differential gain, threshold current and PS current. The dependence of these quantities with the temperature is measured and hence the dependence of the spin-flip rate on the temperature is obtained.

[1] T. Deng, Z.M. Wu, Y.Y. Xie, J.G. Wu, X. Tang, L. Fan, K. Panajotov, G.Q. Xia, Appl. Opt., 52, 16, 3833-3837, 2013.

[2] M. P. Van Exter, M. B. Willemsen, J. P. Woerdman, Phys. Rev. A, 58, 5, 4191-4205, 1998.

Conference 9382: Novel In-Plane Semiconductor Lasers XIV

Monday - Thursday 9 -12 February 2015

Part of Proceedings of SPIE Vol. 9382 Novel In-Plane Semiconductor Lasers XIV

9382-1, Session 1

GaAsBi lasers: Progress towards telecoms wavelengths

Stephen J. Sweeney, Konstanze Hild, Igor P. Marko, Shirong Jin, Univ. of Surrey (United Kingdom); Eoin P. O'Reilly, Tyndall National Institute (Ireland); Kerstin Volz, Philipps- Univ. Marburg (Germany); Arunas Krotkus, Ctr. for Physical Sciences and Technology (Lithuania)

GaAsBi is an attractive new material for laser applications due to the strong band gap (Eg) shrinkage and a large increase of the spin-orbit split-off energy due to Bi incorporation. It has been shown that in III-V bismides it is possible to suppress the dominant hot-hole producing Auger recombination and Inter-valance band absorption (IVBA) processes which limit current 1.55µm lasers. We report on the development of GaAsBi/GaAs QWs from semiconductor design through to the fabrication of devices. Electrically pumped GaAsBi/(Al)GaAs lasers with different Bi compositions in the active region have been grown by MOVPE and a hybrid MOVPE/MBE approach. Since MBE has the potential to reach higher Bi fractions than MOVPE, lasers were also grown using a combined MOVPE/MBE approach with the lower n-type cladding and waveguide initially grown with MOVPE followed by MBE growth of the QW active region, finally completed with the upper waveguide and p-type cladding grown again by MOVPE. The physical properties of broad area laser diodes were characterised as a function of temperature. For the MOVPE devices, lasing was achieved with 4.4% Bi in the QW up to 180K (current source limited) with a projected RT emission wavelength of ~1070nm. Combined MOVPE/MBE devices achieved room temperature operation above 1100nm but with a high Jth. Analysis of the devices reveals that defect-related recombination dominates Jth suggesting that further growth optimisation is required to improve device performance and to reach the higher Bi fractions required for 1550nm operation, as will be discussed in detail.

9382-2, Session 1

GaInSb/AlInSb coupled QWs on GaSb for telecom laser

Laurent Cerutti, Univ. Montpellier 2 (France) and Ctr. National de la Recherche Scientifique (France); Andrea Castellano, Univ. Montpellier 2 (France) and Ctr. National de la Recherche Scientifique (France) and III-V Lab. (France); Karine Madiomanana, Jean-Baptiste Rodriguez, Univ. Montpellier 2 (France) and Ctr. National de la Recherche Scientifique (France); François Lelarge, III-V Lab. (France); Eric Tournié, Univ. Montpellier 2 (France) and Ctr. National de la Recherche Scientifique (France)

One of the hot topics in photonic for this century is the direct integration of III-V semiconductor laser with Si photonics at wavelength around 1.55 µm. Although the most developed materials system for emission in this wavelength range is InP, it is still difficult to grow high quality InP directly on Si without buffer layers thinner than 5µm. One solution could come from GaSb materials, which yielded very promising results. But, due to their natural bandgap, achieving laser emission at telecom wavelength with GaSb-based heterostructures is difficult. Nevertheless, we have recently demonstrated laser emission around 1.55 µm in continuous wave at room temperature. Despite this result, there is still much room for improving the performance of GaSb-based laser at telecom wavelengths.

Previous result was obtained using 3.6 nm GaInSb QWs in AlGaAsSb barriers. We show that by inserting thin (< 0.5 nm) AlInSb layers within the GaInSb QW, it is possible to form coupled QWs emitting at the same 1.55 µm wavelength but exhibiting larger QW width and strain, higher electron-hole wavefunction overlap in the QW and high optical mode/QW overlap. With 2 AlInSb barriers inside the QWs, we demonstrate laser emission at 1.55 µm at temperatures higher than 45 °C. Optical power as high as 30 mW per facet is achieved at 15°C. This very promising result paves the way to the development of GaSb-based lasers for telecom applications and to their possible integration on Si platforms.

9382-3, Session 1

Highly stacked InAs quantum-dot laser grown on vicinal (001)InP substrate by strain-compensation technique

Kouichi Akahane, Naokatsu Yamamoto, Tetsuya Kawanishi, National Institute of Information and Communications Technology (Japan)

Semiconductor quantum dots (QDs) grown using self-assembly techniques in the Stranski-Krastanow (S-K) mode have potential applications in high-performance optical devices, such as QD lasers and QD semiconductor optical amplifiers (SOAs). To realize high-performance QD lasers and QD SOAs, the surface QD density should be increased by fabricating a stacked structure. We have developed a growth method based on the strain-compensation technique that enables the fabrication of a high number of stacked InAs QD layers on an InP(311)B substrate. However, a (311)B surface is uncommon, and we need to control the growth parameter to obtain high crystal quality. In this study, we developed a growth technique for an InAs QD on a vicinal (001)InP substrate, which yielded a highly stacked structure of InAs QDs. Using this structure, we successfully fabricated a highly stacked InAs QD laser. A stack of 30 InAs QD layers and 15-nm-thick InGaAlAs spacer layers were grown for an active region using a strain-compensation technique. Both n-type and p-type InAlAs was used for the cladding layer. The laser structure was a simple broad-area type, the line width and length of which were 50 µm and 0.6 to 1.4 mm, respectively. This QD laser shows lasing at 1550 nm with a threshold current density of approximately 3 kA/cm². The peak wavelength of the lasing spectrum was 1576 nm, which is almost same as the peak wavelength of QD ground levels in photoluminescence. Therefore, this lasing occurs at QD ground levels, which result from the large optical gain of the highly stacked QDs.

9382-5, Session 1

10Gb/s Direct modulation of widely tunable V-cavity-laser with chirp managed laser technology

Jianjun Meng, Zhejiang Univ. (China); Lei Wang, Lightip Technologies Co., Ltd. (China); Jian-Jun He, Zhejiang Univ. (China)

Widely tunable lasers are key components for dense wavelength division multiplexing (DWDM) systems. As WDM technology extends towards access and data center interconnection networks, there is an urgent demand for low-cost wavelength tunable lasers and a growing interest in using directly modulated lasers in these cost-sensitive optical links. Chirp managed laser technology which comprises a direct modulated laser and an optical spectrum reshaping filter can provide large dispersion tolerance and

**Conference 9382:
 Novel In-Plane Semiconductor Lasers XIV**

enhanced extinction ratio. Recently, a widely tunable V-cavity laser has been proposed and demonstrated, which does not require complex gratings and multiple epitaxial growths. Single-electrode controlled wavelength tuning of about 30 channels at 100GHz spacing has been demonstrated, and the channel number can go up to 50 by varying the TEC temperature. Without optimization on the high speed performance, the measured small-signal frequency response is about 5.7GHz. Well open eye diagrams with extinction ratio above 4.5dB are observed when the laser is directly modulated at 2.5Gb/s. When the laser is modulated at 10Gb/s, the eye diagram becomes very poor. However, by using the chirp managed laser technology with an optical spectrum reshaping filter placed after the output of the laser to convert the frequency chirp accompanying the direct modulation to amplitude modulation, well-open eye diagrams with 8dB extinction ratio under 10Gb/s modulation rate is achieved. The advantages of compactness, fabrication simplicity, easy wavelength control algorithm, and simple direct modulation offer great potential for the chirped managed V-cavity laser to be used in low-cost WDM links.

9382-6, Session 1

Low-chirp QD-based directly-modulated lasers monolithically integrated with a ring resonator for long-range access network

Siddharth Joshi, Nicolas Chimot, III-V Lab. (France); François Lelarge, III-V Lab. (France) and CEA-LETI (France)

As the standardization of next generation passive optical network is ongoing, it is necessary to develop innovative 10Gbit/s transmitters at 1.55 μ m for long reach, low cost and high capacity access and metropolitan networks. Directly modulated lasers (DML) are attractive candidates due to their high output power, high tolerance to optical feedback, and ability to operate in semi-cooled or un-cooled conditions. However, it remains difficult with DML to both reach transmission distances above 40km, because of frequency chirp at 1.55 μ m inherent to direct high bit rate modulation, and to achieve high dynamic extinction ratio (DER), typically more than 6dB, compatible with next generation PON requirements. The combination of low chirp Quantum dash DML with an optical filter are demonstrating data transmission performances with 10Gb/s transmission distances in the range of 0-100kms. This paper describes in details the operation of such transmitters, including the enhancement in modulation bandwidth of the laser induced by the passive filter. The monolithic integration of a low chirp DML with a ring resonator would open the way for a low cost transceivers for long range access network. In this paper, we report on the fabrication of a low losses InP based ring resonator with a buried technology identical to the one used to fabricate the DML. Ring resonators with steepness of -4dB/GHz are demonstrated allowing 10Gb/s transmissions over 0.65km with DER of -8dB. The challenge related to the integration of the active quantum dash based DFB laser with the passive ring resonators will be discussed in details.

9382-7, Session 2

InGaN/GaN quantum dot and nanowire single-photon sources (Invited Paper)

Pallab K. Bhattacharya, Saniya V. Deshpande, Thomas Frost, Arnab Hazari, Univ. of Michigan (United States)

Sub-Poissonian light sources that emit single photons have many promising applications in quantum information processing, communication and metrology. In particular, visible single-photons are suitable for free-space communication because they allow miniaturization of telescopes. Additionally, they are important because single-photon detectors are most sensitive in the visible wavelength range and polymer/plastic fibers have transmission windows in this range. Many two-level emitters have been investigated as single-photon sources but semiconductor quantum dots are important due to their stability, fast recombination lifetimes and potential

for electrical injection.

Nitride quantum dots are particularly attractive for these applications because of their large bandgap, exciton oscillator strength and exciton binding energy that allow higher operating temperatures. Single photon emission has been observed from InGaN quantum dot-in-AlGaIn nanowires up to 200 K, under optical excitation. Electroluminescence from single GaN nanowire p-n junction diodes containing a single InGaIn quantum dot, also shows photon anti-bunching up to 150 K, in the blue (?-430 nm)-green (?-520 nm) spectral range.

We have investigated electroluminescence from a single self-organized In_{0.4}Ga_{0.6}N/GaN quantum dot embedded in a planar p-i-n diode grown by plasma assisted molecular beam epitaxy. Atomic force microscopy shows a low quantum dot density of $\sim 2 \times 10^9$ /cm² and dot size ~ 15 nm x 3 nm. Under forward bias, the diode shows excitonic emission from a single quantum dot (?-620 nm) with linewidths ~ 22 meV at room temperature. Photon correlation measurements show a g(2)(0) value of 0.28 and exciton lifetime is ~ 1.3 ns, which indicates potential GHz operation of this device is possible.

9382-8, Session 2

Longitudinal mode dynamics in (Al,In)GaIn laser diodes

Ulrich T. Schwarz, Univ. of Freiburg (Germany); Thomas Weig, Fraunhofer-Institut für Angewandte Festkörperphysik (Germany); Thomas Hager, Georg Bruederl, Uwe Strauss, OSRAM Opto Semiconductors GmbH (Germany)

The development of blue and green (Al,In)GaIn ridge waveguide laser diodes (LDs) experienced great progress in the last years, pushing this technology toward longer wavelengths and higher optical output power. For many applications mode stability is a necessary prerequisite.

We present spectro-dynamical measurements of blue and green LDs showing longitudinal mode competition with frequencies ranging from 10 MHz to 150 MHz. Hereby, up to two dozen lasing modes pulsate with 100 % modulation depth. We show that the formalism of self-, symmetric and asymmetric cross gain saturation allows to model this dynamics of mode competition in (Al,In)GaIn LDs with high accuracy. The frequency dependence on current and spectrochronograms are described numerically with a set of multi-mode rate equations. While these effects have been studied in detail for GaAs- and InP-based LDs, these mechanisms are affected by piezoelectric polarization and large inhomogeneous broadening in InGaIn quantum wells.

In certain parameter ranges, mode competition disappears and single mode operation as well as mode clustering is found. We thus introduce a new explanation of mode clustering in (Al,In)GaIn LDs, which is discussed since the demonstration of the first violet LDs in 1997.

The described mechanisms of gain saturation perturb LDs in cw operation, interfere with wavelength stabilization in an external cavity, and with the generation of ultrafast pulses. Furthermore, the resulting spectro-temporal dynamics can lead to an intensity modulation when a wavelength selective optical element (edge filter, wave plate,...) is placed downstream in the optical path.

9382-9, Session 2

Strategies and Progress towards Compact Deep UV Laser Sources (Invited Paper)

Thomas Wunderer, Palo Alto Research Center, Inc. (United States)

The increasing interest in compact deep UV lasers is driven by applications such as native fluorescence or Raman spectroscopy for detection and identification of chemical species and bio-particles. Several possible

**Conference 9382:
 Novel In-Plane Semiconductor Lasers XIV**

strategies will be discussed to realize such lasers using the AlGaInN material system.

The first is an AlGaIn-based laser diode (LD) with direct current injection. PARC has pioneered the development of nitride UV lasers containing AlGaIn quantum wells and LDs on bulk single-crystal AlN substrates. More recently, we have demonstrated optically pumped UV lasers with AlGaIn MQWs on bulk AlN at wavelengths down to 237 nm and with record-low pump power thresholds, for example, 41 kW/cm² at $\lambda = 266$ nm. Fundamental work has included experimental observation and computational understanding of polarization switching of the laser emission at wavelengths near 250 nm. To overcome the limitations of thermally activated p-type doping, nano-structured AlGaIn-based composition- and doping-modulated superlattice materials were designed, developed, tested and integrated into sub-300-nm LD heterostructures and fully processed UV laser test devices. Significant progress has been made in all aspects of LDs, with maximum current density exceeding 40 kA/cm² and improved carrier injection. Yet, challenges remain to the realization of deep UV LDs. These include optical absorption losses as well as further heterostructure optimization and device design.

Alternative strategies have been proposed that are also based on AlGaInN semiconductors. One is the use of a high-energy electron beam to pump the UV laser heterostructures. Conceptual designs will be presented and the advantages of the approach discussed.

9382-10, Session 2

MOEMS integration of (Al,In)GaIn laser diodes with optical waveguides for applications in optogenetics (*Invited Paper*)

Ulrich T. Schwarz, Michael Schwaerzle, Annik Jakob, Linda Rudmann, Marie Alt, Eva Fiedler, Thomas Stieglitz, Patrick Ruther, Univ. of Freiburg (Germany)

Optogenetics provides new tools for fundamental research in neuroscience as well as for the prosthesis development, e.g. for optical cochlear implants or retina implants. Optogenetics relies on the principle that neurons are made sensitive to light by the incorporation of light-sensitive transport proteins in the cell membrane, most prominently Channelrhodopsin2 (ChR2) which triggers neuronal activity when illuminated with blue light at a wavelength of about 460 nm. We work on the development of miniaturized optical probes which can be directly implanted for in-vivo studies. The technological challenges are the direct integration of the LD chip within the optical probe as well as long-term stability and bio-compatibility.

We investigate two systems approaches, one with flexible silicone (PDMS) waveguides, the other with polymer waveguides on Si substrate, for surface and penetrating probes, respectively. In the first approach the laser diodes chips are encapsulated together with humidity and temperature sensors in a hermetically sealed package allowing out-of-plane coupling to the waveguide. In the second approach the laser diode chip is flip-chip bonded to the microfabricated Si substrate with bond areas, waveguides and additional electrodes, and subsequently encapsulated to provide mid-term sealing. Coupling of the laser diodes to the waveguides, absorption and scattering was investigated for the polymer waveguide in the wavelength range from 430 nm to 650 nm. For the PDMS waveguide low scattering losses (0.38 to 0.41 dB/cm) and an increase of the losses by 10% after 8 weeks in saline solution at 37°C is reported.

9382-11, Session 3

The role of optical delays for the dynamic behavior of passively mode-locked lasers (*Invited Paper*)

Kathy Lüdge, Lina Jaurigue, Technische Univ. Berlin (Germany)

Passively mode-locked semiconductor lasers are of broad interest as inexpensive sources of ultra-short, high-repetition-rate light pulses. In this work we study the effects of multiple optical feedback lines on the dynamics and performance of the mode-locked laser device. It has been previously shown both theoretically and experimentally that time-delayed optical feedback can lead to a variety of complex dynamics, from the stabilization of the fundamental mode-locking operation over the appearance of higher-order harmonics to a destabilization and chaotic dynamics. Furthermore, optical feedback can improve the device performance, with emphasis on a reduction of the timing jitter and tuning of the repetition frequency. In this work, we present a theoretical model of the passively mode-locked laser using a system of delay differential equations and include time-delayed optical feedback from multiple external passive cavities. We find complex dynamics that depend strongly on the delay times of the feedback cavities and the repetition rate of the laser. Optical feedback resonant to multiples of the repetition frequency can lead to a substantial reduction in the timing jitter, especially for long delay lines. For slightly off-resonant feedback the timing jitter reduction is not as effective, however the repetition rate of the laser can be shifted from the free running case. This effect is especially strong for short feedback cavities. We thus predict the possibility of simultaneous wide repetition rate tuning and strong timing jitter reduction by employing a combination of a short and a long feedback cavity.

9382-12, Session 3

Ultrafast pulse shortening through adjustment of the mode-locking threshold condition in passively mode-locked InAs quantum dot lasers

Patrick Finch, Tyndall National Institute (Ireland); Matthew Hutchings, Syracuse Univ. (United States); Angela D. Sobiesierski, Cardiff Univ. (United Kingdom); Russell M. Gwilliam, Univ. of Surrey (United Kingdom); Peter M. Snowton, Peter Blood, Cardiff Univ. (United Kingdom); Ian O'Driscoll, Tyndall National Institute (Ireland)

We have compared, for the first time, the bandwidth of mode-locked pulses in a two-section mode-locked laser and its relationship between its modal gain spectrum and the mode-locking threshold condition. By lowering the threshold condition for mode-locking, we have decreased the pulse width from 940 fs to 610 fs, with a corresponding increase in optical bandwidth from 16 meV to 30 meV, as the amount of gain available above the threshold condition for mode-locking increases in the non-thermal regime.

Using rate equations, which include a temperature dependent homogeneous linewidth, we describe the electronic transitions as interactions with a Bose-Einstein distribution of phonons for an inhomogeneous Gaussian distribution of energies and include a single mode photon rate equation for the cavity. As the threshold condition for mode-locking is decreased, the occupation of non-lasing dots, away from the peak of the gain spectrum, increases as more dots are available to be occupied. The occupation of lasing dots is the inverse of the dot distribution and remains clamped once lasing is initiated. Any additional carriers are supplied from the external current and the optical bandwidth increases, in contrast to the thermal regime, where the linewidth remains narrow due to the depletion of other dots in thermal equilibrium across the inhomogeneous distribution.

This work demonstrates that the optical pulse width may be significantly decreased by simply lowering the threshold condition for mode-locking when the dots are operated in a non-thermal regime, without the need for complex engineering techniques.

9382-13, Session 3

Ultrashort pulse generation with semiconductor lasers using intracavity phase- and amplitude pulse shaping

Benjamin Döpke, Jan C. Balzer, Rouven Pilny, Carsten Brenner, Ruhr-Univ. Bochum (Germany); Andreas Klehr, Götz Erbert, Günther Tränkle, Ferdinand-Braun-Institut (Germany); Martin R. Hofmann, Ruhr-Univ. Bochum (Germany)

Ultra-short pulse generation with semiconductor lasers is a promising technique that could lead to mass-market applications for fields of research that are still limited by the price and complexity of conventional ultra-short pulse sources, such as titanium-sapphire or fiber lasers. Even though decades have been spent improving the properties of mode-locked semiconductor lasers, it has proven difficult to utilize the complete gain spectrum of mode-locked semiconductor lasers, limiting the obtainable pulse widths as a result. While tuning ranges of more than 15 nm at 850 nm central wavelength are easily possible, the bandwidth in passively mode-locked operation is typically less than 7 nm at such wavelengths, with the exception of record devices which were usually quite sensitive to alignment. This has limited the applications that practical ultra-short pulse lasers can be used for. While in earlier work we have studied the influence of phase masks on the mode-locking dynamics, we now introduce spectrally resolved dispersion and absorption masks into the cavity of the anti-reflection coated laser with a resonator-internal pulse shaper, producing a significantly enhanced spectral bandwidth in stable passively mode-locked operation. Pulse widths of 200 fs are obtained.

9382-14, Session 3

Evaluation of free carrier effects on the gain and spontaneous emission spectra of InAs/GaAs quantum dot lasers

Negin Peyvast, David T. D. Childs, Kejia J. Zhou, Richard A. Hogg, The Univ. of Sheffield (United Kingdom); Takeo Kageyama, Kenichi Nishi, QD Laser, Inc. (Japan); Keizo Takemasa, QD lasers Inc. (Japan); Mitsuru Sugawara, QD Laser, Inc. (Japan)

Quantum dot lasers have attracted significant interest over more than thirty years due to the prediction of temperature insensitivity and enhanced material gain. The Stranski-Krastanov growth method has been employed to realise high quality laser devices and have been used to extend the wavelength of GaAs based lasers to 1300nm. The importance of the carrier distribution within quantum dot laser materials has been highlighted and discussed widely, and can be expected to play a key role in many aspects of the operation of the laser diode.

GaAs based InAs QDs operating at near 1000nm have been shown to exhibit a carrier distribution in thermal equilibrium at 300K, but a breakdown in this thermal equilibrium was observed at low temperatures where a random carrier population of isolated quantum dots was observed.

In this paper we describe simulation results that explore the effect of free-carrier induced red-shift and increased homogeneous broadening on the carrier distribution function. The different extreme cases for carrier statistics (Fermi-Dirac and random carrier distribution), QD ensemble inhomogeneity and state-separation are explored. We show that not only are free carrier effects important at high QD occupancies, but also at lower carrier densities where QD lasers would normally operate. We conclude that the free carrier effects dominate the form of the gain and spontaneous emission spectrum for the QD ensemble, rather than the carrier statistics.

9382-15, Session 3

Mechanism controlling threshold current temperature dependence in InP QD lasers at elevated temperature

Peter M. Smowton, Makarimi Kasim, Stella N. Elliott, Cardiff Univ. (United Kingdom); Andrey B. Krysa, The Univ. of Sheffield (United Kingdom)

Quantum dot lasers were introduced over 20 years ago [1] following predictions that the electronic state distribution in such systems would provide significant performance advantages for lasers [2]. Self assembled quantum dots have different state distributions from those originally envisaged but still can show excellent characteristics [3]. However, at elevated temperatures the rate of increase of threshold current with temperature is surprising poor without the application of p-modulation doping, which has led to temperature insensitive threshold current density in InAs quantum dot lasers [4]. The application of p-modulation doping in InP quantum dot lasers, emitting in the 630-780 nm range and of use for bio-sensing applications amongst others, is ineffective and as such we return to the origin of the sensitive threshold current temperature dependence. We characterise the processes responsible using experimental measurements and show that by minimising thermal spreading effects we can produce uncoated 2mm long lasers with a threshold current density of < 130 Acm⁻² at 25°C rising to < 250 Acm⁻² at 80°C without the application of p-modulation doping.

[1] N. Kirstaedter, N.N. Ledentsov, M. Grundmann, D Bimberg, VM Ustinov, SS Ruvimov, MV Maximov, Ps S Kop'ev, Zh I Alferov, U Richter, P Werner, U Gösele, J Heydenreich, "Low threshold, large To injection laser emission from In(Ga)As quantum dots", Electronics Letters, 30, 1416-1417 1994

[2] Y. Arakawa and H. Sakaki, "Multidimensional quantum well laser and temperature dependence of its threshold current" Applied Physics Letters, 40 939-941, 1982

[3] D. G. Deppe, K. Shavritranuruk, G. Ozgur, H. Chen and S. Freisem, "Quantum dot laser diode with low threshold and low internal loss", Electronics Letters, vol. 45, pp. 54-55. 2009

[4] T. Kageyama; K. Takada; K. Nishi; M. Yamaguchi; R. Mochida; Y. Maeda; H. Kondo; K. Takemasa; Y. Tanaka; T. Yamamoto; M. Sugawara; Y. Arakawa, "Long-wavelength quantum dot FP and DFB lasers for high temperature applications", Proc. SPIE 8277, Novel In-Plane Semiconductor Lasers XI, 82770C 2012; doi:10.1117/12.905873

9382-16, Session 4

Dynamic characteristics of double tunneling-injection quantum dot lasers

Levon V. Asryan, Virginia Polytechnic Institute and State Univ. (United States)

As an alternative to conventional pumping, tunneling-injection of carriers into a low-dimensional active region of diode lasers was proposed. In [1]-[3], double tunneling-injection (DTI), i.e., tunneling-injection of both electrons and holes into quantum dots (QDs) from two separate quantum wells (QWs) was proposed. A study of static characteristics [1]-[6] showed that DTI QD lasers possess the potential for higher temperature stability, lower threshold, and higher output power as compared to conventional QD lasers. In this work, dynamic characteristics of DTI QD lasers are studied. To reveal the potential of such lasers for high-speed direct modulation of their optical output by the pump current, the case of fast injection into QDs and no carrier leakage from QDs is considered. The small-signal analysis of rate equations is applied. The modulation bandwidth is calculated as a function of the dc component of the injection current density and parameters of the structure. The optimum dc component of the injection current density and the optimum cavity length maximizing the modulation bandwidth are calculated. While the maximum bandwidth is shown to be the same in DTI and conventional QD lasers and unaffected by the differential gain, the

**Conference 9382:
Novel In-Plane Semiconductor Lasers XIV**

optimum dc current density, being inversely proportional to the differential gain, is lower in a DTI QD laser.

- [1] L.V. Asryan, S. Luryi, IEEE J. Quantum Electron. 37, 905 (2001).
- [2] L.V. Asryan, S. Luryi, Solid-State Electron. 47, 205 (2003).
- [3] L.V. Asryan, S. Luryi, U.S. Patent 6870178 B2 (2005).
- [4] D.-S. Han, L.V. Asryan, Appl. Phys. Lett. 92, 251113 (2008).
- [5] D.-S. Han, L.V. Asryan, Nanotechnology 21, 015201 (2010).
- [6] D.-S. Han, L.V. Asryan, J. Lightw. Technol. 27, 5775 (2009).

9382-17, Session 4

Advances in nanowire quantum-dot lasers and single photon emitters (*Invited Paper*)

Yasuhiko Arakawa, Jun Tatebayashi, Mark Holmes, Satoshi Iwamoto, The Univ. of Tokyo (Japan)

(the same as that of the above abstract) We discuss fabrication and optical characterization of multi-stacked InGaAs/GaAs quantum-dots with a single GaAs nanowire Fabry-Pérot cavity. Lasing oscillation due to the quantum-dot gain was clearly observed at 6K by optical pumping method. In addition, we demonstrate single photon emission at room-temperature from a single GaN quantum-dot embedded in an AlGaIn-based nanowire. This result paves the way toward room-temperature quantum information photonics.

I hope this presentation is categorized as an invited talk.

9382-18, Session 4

Effect of difference-wavelength and temperature on the performance of Dual-[λ] InP-QD lasers

Samuel Shutts, Peter M. Smowton, Cardiff Univ. (United Kingdom); Andrey B. Krysa, The Univ. of Sheffield (United Kingdom)

Dual-wavelength (dual-?) lasers are used in applications including distance and position interferometric measurements, producing THz radiation via difference-frequency-generation and biomedical imaging/diagnostics. We employ a device which exploits the properties of InP-QDs, (emitting from 650-730 nm), to produce simultaneous dual-? lasing from a single ridge-waveguide comprising two sections. In a simple edge-emitting laser, the wavelength coincides with the peak of the gain spectrum and due to the effects of state-filling in an inhomogeneously broadened QD ensemble, the wavelength is strongly dependent on gain magnitude (or cavity loss). Therefore, by altering the loss of each section of the device we are able to demonstrate a large range of difference-wavelengths, up to 63 nm. Here, we test the performance of the device and measure effects of temperature and difference-wavelength on the stability of the two lasing modes. For large wavelength separations, the short wavelength is relatively unaffected by variations in light output at the longer wavelength. Due to gain-saturation effects, carrier competition of the two modes is not significant to suppress dual-state lasing, but as the difference-wavelength is reduced there is a reduction in the output at the short wavelength, when increasing the output at the longer wavelength. The temperature-dependence of the emission wavelength in a QD material is dependent on the fixed temperature coefficient of the band-gap and the magnitude of the gain. Adjusting the operating temperature of the device can be used to tune the difference-wavelength, for example a device with a 63 nm separation the tuning is 0.12 nm/K.

9382-66, Session 4

A new methodology and experimental results for designing semiconductor lasers for high-coherence narrow linewidth (*Invited Paper*)

Amnon Yariv, California Institute of Technology (United States)

No Abstract Available

9382-19, Session 5

Resonant self-injection locked ultra-narrow-line semiconductor lasers (*Invited Paper*)

Andrey B. Matsko, Elijah B. Dale, Anatoliy A. Savchenkov, Wei Liang, Danny Eliyahu, Vladimir S. Ilchenko, David J. Seidel, Lute Maleki, OEwaves, Inc. (United States)

We show that resonant self-injection locking is highly efficient for reducing linewidth of semiconductor lasers including both conventional diode lasers (DL) and quantum cascade lasers (QCL). We have demonstrated pigtailed self-injection locked DFB DL operating in visible and near-infrared as well as self-injection locked DFB QCL operating at mid-infrared. All the lasers have sub-kHz linewidth. Using an example of self-injection locked DFB DL operating at 795 nm we have shown agile tunability as well as high speed frequency dithering of the laser. The features enabled locking of the laser to rubidium D1 line to produce light with Allan deviation of 4×10^{-13} at 1,000s. This approach offers miniature narrow line lasers at any desirable wavelength.

9382-20, Session 5

Al-free active region laser diodes at 894nm for compact Cesium atomic clocks

Nicolas von Bandel, Joseph P. Bebe Manga Lobe, Michel Garcia, Alexandre Larrue, Yannick Robert, Eric Vinet, Michel Lecomte, Olivier Drisse, Olivier Parillaud, Michel Krakowski, III-V Lab. (France)

Time-frequency applications are in need of high accuracy and high stability clocks. Industrial Cesium atomic clocks optically pumped is a promising area that could satisfy these demands. However, the stability of these clocks relies strongly on the performances of laser diodes that are used for pumping. This issue has led the III-V Lab to commit to the European Euripides "LAMA" project that aims to provide competitive compact optical Cesium clocks for earth and space applications. We are in charge of the design, fabrication and reliability of Distributed-Feedback diodes (DFB) at 894nm (D1 line of Cesium) and 852nm (D2 line). The use of D1 line for pumping will provide simplified clock architecture compared to D2 line pumping thanks to simpler atomic transitions and larger spectral separation between lines in the 894nm case. The modules should provide narrow linewidth (<1MHz), very good reliability in time and be insensitive to optical feedback. The new development of the 894nm wavelength is grounded on our previous results for 852nm DFB (C. Cayron et al., Photonics West 2010). Thus, we show our first results from Al-free active region with InGaAsP quantum well broad-area lasers (100 μ m width, with lengths ranging from 2mm to 4mm), for further DFB operation at 894nm. We show that the internal losses are near 2,6cm⁻¹, the external differential efficiency is 0,44W/A with cleaved facets and a low threshold current density of 200A/cm², for 2mm lasers at 20°C. We are confident to present further results on DFB at 894nm that are currently being processed.

**Conference 9382:
Novel In-Plane Semiconductor Lasers XIV**

9382-21, Session 5

DBR grating stabilized ridge waveguide lasers emitting at 647 nm for real 3D holographic displays

David Feise, Johannes Pohl, Gunnar Blume, Katrin Paschke, Ferdinand-Braun-Institut (Germany)

Real 3D display applications require RGB light sources which provide a spectral bandwidth of less than 5 MHz for recording (and playing-back) a holographic film. Furthermore, these emitters must be small in size, efficient, robust and reliable. Therefore, diode lasers with internal wavelength filters are the devices of choice.

In our paper we will present a further development of our red-emitting distributed Bragg reflector ridge waveguide laser (DBR-RWL). In Ref. [1] a DBR-RWL emitting at a wavelength of 633 nm was presented with sub-MHz linewidth. Although the human eye is 1.9 times less sensitive at the now chosen wavelength of 647 nm compared to 633 nm [2], the reduced temperature sensitivity of the semiconductor layer structure and the greater available color space [3] compensate for such a reduction.

DBR surface gratings are implemented into the 2 mm long RWL by BCl₃-Ar reactive ion etching. Therefore, the fabrication process is single-epitaxy and industry-compatible. The laser's facets were coated to obtain a reflectivity of 4% at the front facet and less than 0.1% at the rear facet to suppress unwanted Fabry-Pérot modes.

At a heat sink temperature of 15°C the DBR-RWL provides 120 mW of optical output power in longitudinal single mode emission. Heterodyne linewidth measurements of two identical DBR-RWL show a FWHM linewidth of less than 2 MHz.

The excellent beam quality (M₂ = 1.1) enables the use of these chips for play-back of holographic films or as master oscillators in a future micro-integrated master oscillator power amplifier configuration for recording.

[1] Feise et al., Proc. SPIE, SPIE, 2013, 8640, 86400A-1-9

[2] Blume et al., Proc. SPIE, 2010, 7720, 77201B-1-12

[3] Commission internationale de l'Eclairage proceedings, "CIE 1931" (1931).

9382-22, Session 5

Theory and observation on non-linear and temperature-related effects limiting the coherence properties of semiconductor lasers

Yaakov Vilenchik, Christos T. Santis, Scott T. Steger, Amnon Yariv, California Institute of Technology (United States)

Recent theoretical and experimental developments have demonstrated that conventional semiconductor laser design may not be consistent with high coherence operation. It was demonstrated that a new design paradigm, in which the optical energy is stored away from the active region, in the low-absorption portion of a composite resonator, is essential to minimizing spontaneous emission into the laser mode thus improving, possibly by orders of magnitude, the coherence of the laser field.

Hybrid Si/III-V is a very promising platform for this approach, where Si takes the role of the low-loss material and is fashioned into a high-Q resonator. However, the large intra-cavity field intensity resulting from the high-Q operation gives rise to non-linear effects, which may limit the improvement in coherence described above, and causes a new domain of linewidth-limiting factors to emerge.

Fundamentally, two-photon absorption and subsequent free-carrier absorption are limiting the achievable cavity's quality factor. Interestingly, a more dominant effect at low frequencies is caused by fluctuations in the density of free carriers in silicon that couple to the frequency noise through both plasma and thermo-optic effects.

Moreover, due to the large thermo-optic coefficient of silicon, the effect of the inherent fluctuations of temperature also becomes dominant at intermediate frequencies as the spontaneous emission noise is reduced.

This paper presents a theoretical model based on modified rate equations and Langevin force approach to describe these non-linear and temperature-related effects. The derived theoretical frequency spectrum and other performance metrics are compared to experimental results from fabricated high-Q Si/III-V lasers.

9382-23, Session 5

Thermally-tuneable integrated planar Bragg-grating stabilized diode laser

Stephen G. Lynch, James C. Gates, Peter G. R. Smith, Univ. of Southampton (United Kingdom)

Integrated planar laser structures allow for greater flexibility in resonator design and improved coherence performance that would otherwise be possible in monolithic diode laser. Our device is an External Cavity Diode Laser (ECDL) with an integrated planar external-cavity grating that is butt coupled to a ThorLabs 1650nm semiconductor gain-chip. In our external cavity design we use a Flame-Hydrolysis Deposition fabricated planar silica-on-silicon chip with a direct UV-written waveguide and Bragg grating. The chip has a silicon substrate where the high thermal conductivity of the silicon thermalises the cavity improving device stability. The ECDL is fully integrated further improving stability and allowing greater potential for miniaturisation. The UV-writing process is fully computer controlled, enabling custom period (wavelength) and apodisation to be inscribed in the same process as defining the waveguide. Continuous tuning is enabled through localised micro heating-elements, allowing continuous thermal tuning of the cavity at modulation frequencies > 1kHz. This novel method of cavity tuning isolates frequency modulation from amplitude modulation without using an external EOM. Tuneable single-mode operation has been demonstrated at 1650nm, with ultra-low RIN (< -150dB). A matched pair of cavities were fabricated to measure the phase noise properties of the laser via heterodyne detection. The resulting beat note that was measured using a fast oscilloscope, a lorentz linewidth of < 10kHz was obtained. We will present our latest results including wavelength locking the laser emissions to each other and locking the lasers to external references using heater control.

9382-24, Session 5

400 mW output power at 445 nm with narrowband emission from an external cavity diode laser system

Norman Ruhnke, André Müller, Bernd Eppich, Martin Maiwald, Bernd Sumpf, Götz Erbert, Günther Tränkle, Ferdinand-Braun-Institut (Germany)

Recently, high-power broad-area laser diodes based on GaN with output powers beyond 1 W have become available. However, their broad spectral emission limits their applicability. Due to a lack of internal grating technology for GaN devices, narrowband emission with several hundreds of milliwatts in the blue-green spectral range has not been achieved with laser diodes thus far.

In this work, a high-power external cavity diode laser (ECDL) system with an optical output power of 400 mW and narrowband emission at 445 nm is presented. The system is based on a commercially available broad-area GaN laser diode from OSRAM Opto Semiconductors GmbH with an optical output power of P = 1.6 W at an injection current of I = 1.2 A. The laser emission of the Fabry-Perot (FP) laser diode shows a spectral width of about 1 nm full width at half maximum (FWHM). Longitudinal mode selection is realized by using a surface diffraction grating in Littrow configuration for optical feedback. At 0.49 A, the ECDL has an output power

**Conference 9382:
 Novel In-Plane Semiconductor Lasers XIV**

of 400 mW and the emission shows a spectral width of 20 pm (FWHM) with a side-mode suppression ratio larger than 40 dB.

With the above presented optical output power and narrowband laser emission at 445 nm, the ECDL is well suited as a pump light source for nonlinear frequency conversion into the ultraviolet spectral range.

9382-25, Session 6

Heterogeneously-integrated InP on Si microdisk lasers (*Invited Paper*)

Geert Morthier, Thijs Spuesens, Pauline Mechet, Univ. Gent (Belgium) and IMEC (Belgium); Philippe Regreny, Institut des Nanotechnologies de Lyon (France); Rama Raj, Fabrice Raineri, Lab. de Photonique et de Nanostructures (France); Nicolas Olivier, Jean-Marc Fedeli, CEA-LETI (France); Dries Van Thourhout, Gunther Roelkens, Univ. Gent (Belgium) and IMEC (Belgium)

We review recent theoretical and experimental work on InP membrane microdisk lasers heterogeneously integrated on SOI and coupled to a Si bus waveguide. After a general introduction on the fabrication and the operation principles, we will describe various improvements in the fabrication technology. This includes improvements to the yield of the bonding of the InP die on the SOI die and controllability of the bonding layer thickness, as well as optimization of the alignment of the microdisk with respect to the silicon waveguide and some proposals for better heat sinking and loss reduction. Improvement in the alignment and the bonding has led to interesting results on the uniformity in device characteristics.

In a second part, unidirectional behaviour and reflection sensitivity will be briefly discussed. Theoretical, numerical and experimental results will be shown about the unidirectional behavior and it will be explained how unidirectional microdisk lasers can be a lot less sensitive to external reflections than other lasers. We will also show how such lasers can be used as optical signal regenerators that can work with low optical input powers and that have small power consumption.

We will end with a description of demonstrations of optical interconnects based on heterogeneously integrated microdisk lasers and heterogeneously integrated photodetectors. Optical interconnects on chip have been demonstrated at 10 Gb/s. An epitaxial layer stack that contains both the laser and the detector structure has been used for this purpose.

9382-26, Session 6

Microwatt-threshold Raman silicon laser using photonic crystal high-Q nanocavity (*Invited Paper*)

Yasushi Takahashi, Osaka Prefecture Univ. (Japan); Susumu Noda, Kyoto Univ. (Japan)

Raman scattering has been a useful phenomenon for examining the static stress of various silicon devices since the 1970's. From the early 2000's, the Raman effect has also attracted attention due to its potential to add active functionality to pure silicon devices. Raman silicon lasers using rib waveguide resonators with reverse-biased p-i-n diodes have been an important advance in silicon photonics. Very recently, we have reported a micrometer-scale continuous-wave Raman Si laser with an ultralow threshold of 1 microwatt, using a photonic crystal heterostructure nanocavity without any p-i-n diode. This device utilizes an unusual pair of high-Q resonant modes in the heterostructure nanocavity. The pair is superior in terms of all of the aspects that are important for enhancing the Raman gain. We believe that this breakthrough will stimulate silicon photonics research in a number of areas.

9382-27, Session 6

A monolithic electrically-injected nanowire array edge-emitting laser on (001) silicon

Ethan M. Stark, Thomas Frost, Shafat Jahangir, Saniya V. Deshpande, Pallab K. Bhattacharya, Univ. of Michigan (United States)

It remains a major challenge to achieve practical high quality light sources on silicon, since silicon itself is a poor light-emitter. Approaches to this problem have included arsenide-based quantum well and dot lasers grown on 4-degree tilted-plane silicon, III-V lasers grown separately and bonded to silicon, and strained germanium on silicon with novel buffer layers. III-Nitride nanowires and disk-in-nanowire (DNW) structures can be grown, strain-relaxed and relatively defect-free, on standard (001) silicon substrates. These DNWs have lower polarization fields as compared to planar quantum well structures emitting at similar wavelengths due to strain relaxation during growth, leading to less quantum-confined Stark effect emission shift at high bias. We have used these nanowire structures to make monolithic edge-emitting lasers operating in the long-wavelength visible range on (001) silicon. Nanowire heterostructures were grown by plasma-assisted molecular beam epitaxy (PA-MBE) and planarized with parylene for surface passivation and to aid in processing. The parylene-planarized nanowire array forms a composite slab heterostructure through which a guided mode can propagate transverse to the growth direction. Ridge geometry laser devices were fabricated by standard etching and metalization techniques and cavity facets were formed by cleaving, focused ion beam (FIB) polishing, and dielectric DBR deposition for increased reflectivity. A low lasing threshold of $J_{th} = 1.8 \text{ kA/cm}^2$ is achieved for a 1.5mm cavity length device emitting at a wavelength of 533nm.

9382-28, Session 6

Membrane lasers on SiO₂/Si substrate (*Invited Paper*)

Shinji Matsuo, Koji Takeda, Takuro Fujii, Tomonari Sato, NTT Photonics Labs. (Japan)

Reduction of laser operating energy is a key issue to use the lasers in datacom and computercom networks because internet traffic is still increasing. Thus, the integration of buried heterostructure (BH) laser on SiO₂/Si substrate is essential because the increase of carrier and photon confinements is quite important to improve the device efficiency. For datacom application, we have developed membrane DFB lasers on SiO₂/Si substrate. We have employed epitaxial growth of buried InP layer on a directly bonded active layer on SiO₂/Si substrate, which enables us to grow the materials under a lattice-matching condition. However, we have to solve the problem that is the stress caused by the difference of thermal expansion coefficients of InP, Si, and SiO₂. We have found that reducing the total thickness of compound semiconductor is essential. Fabricated DFB laser with 73-um long was directly modulated by 25-Gbit/s NRZ signal with a bias current of 3.2 mA, resulting in an energy cost of 171 fJ/bit. For computercom application, we have developed photonic crystal (PhC) wavelength-scale cavity laser to obtain both ultra-low threshold current and operating energy. To integrate PhC laser on Si substrate, we also used directly bonding technique while BH and air holes was fabricated before bonding. The device exhibited a threshold current of 33 uA, and a maximum output power exceeding a microwatt. These results indicate that the membrane lasers on SiO₂/Si substrate are highly suitable for use as a transmitter in datacom and computercom applications.

9382-29, Session 7

InP-based type-II heterostructure lasers for wavelengths up to 2.7 μm (*Invited Paper*)

Stephan Sprengel, Ganpath K. Veerabathran, Technische Univ. München (Germany); Alexander Andrejew, Technische Univ. München (Germany) and Walter Schottky Institut (Germany); Anna Königer, Technische Univ. München (Germany); Gerhard Boehm, Christian Grasse, Markus-Christian Amann, Technische Univ. München (Germany) and Walter Schottky Institut (Germany)

Type-II heterostructures on InP substrates are an innovative concept for light sources with wavelengths ranging from 2 μm to the mid-IR. The devices are based on the type-II band alignment between GaInAs and GaAsSb to overcome the limitations of type-I heterostructures. Since the first demonstration of InP type-II heterostructure lasers beyond 2.3 μm in 2012, an increase in emission wavelength up to 2.7 μm was achieved. Furthermore, a drastically reduced threshold current density of 104 A/cm² per QW at infinite length (at 2.5 μm) was achieved, representing an improvement by more than a factor of two. Additionally CW operation above RT and up to 80 °C pulsed mode is presented.

9382-30, Session 7

Distributed feedback interband cascade lasers for applications in research and industry

Johannes Koeth, Michael von Edlinger, Julian Scheuermann, Lars Nähle, Lars Hildebrandt, Marc Fischer, nanoplus GmbH (Germany); Robert Weih, Martin Kamp, Wilhelm-Conrad-Röntgen-Research-Ctr. for Complex Material Systems (Germany)

In recent years, the use of laser sources in gas sensing applications has been increasing continuously. Tunable Laser Absorption Spectroscopy (TLAS) has proven to be a versatile tool in a variety of sectors including industry, health & security and modern environmental analysis. Especially the mid-infrared wavelength range is of great interest for high accuracy gas sensing applications, since many technologically and industrially relevant gas species have their strongest absorption features in the spectral region between 3 and 6 μm . These include, e. g., important hydrocarbons like methane or propane, as well as nitric oxide and formaldehyde.

Interband cascade lasers (ICL) provide mono mode continuous wave (CW) operation above room temperature in this wavelength range. Application-grade complex coupled distributed feedback (DFB) laser devices based on the ICL concept are presented, using lateral metal gratings as wavelength selective elements. The fabricated devices operate at specific, technologically relevant, emission wavelengths in the spectral region from 3 to 6 μm . CW operation up to 80 °C and mono mode wavelength tuning ranges above 20 nm were achieved with low energy consumption.

Application examples in industry and research are presented that demonstrate the high potential of DFB ICLs for the use in TLAS. E. g., formaldehyde gas sensor systems based on DFB ICL devices operating around 3.6 μm can provide real-time in-situ measurements with resolution limits in the low ppb range, even in dense background atmospheres. The low power consumption of ICL based devices makes them especially favorable for battery-powered or portable sensor applications.

9382-31, Session 7

High performance low-dissipation QCL across the mid-IR range

Alfredo Bismuto, Alpes Lasers SA (Switzerland)

The mid-infrared (IR) spectral region is of crucial importance in the spectroscopy, due to the very prominent absorption lines of substances in this region. The intensity of these lines enables the development of very compact sensing systems with high sensitivity.

Twenty years after their invention, quantum cascade lasers can now be considered as the most mature source in the Mid-IR region. Nevertheless, in order to enable the development of mass products based on these lasers, both low electrical dissipation and spectral control are crucial. For this work, different spectral regions across the Mid-IR range have been chosen due to their commercial interest and distributed feedback quantum cascade lasers have been fabricated. We will show single-mode QCLs working in continuous-wave operation with electrical dissipations smaller than 0.5 W and thresholds currents smaller than 50 mA.

The impact of the different factors that contributed to this dissipation level, i.e. active region design, waveguide design and thermal management, has been analysed through various theoretical models. Indeed, we have developed a set of modelling tools to predict the properties of QC lasers through cloud-based simulations, avoiding costly trial and calibration runs.

Another key parameter for the development of QCL-based products is the fabrication yield of the sources. An analysis of the laser performance and single mode yield as function of the device length will be presented.

9382-32, Session 7

Type-I QW cascade diode lasers with 830 mW of CW power at 3 μm (*Invited Paper*)

Leon Shterengas, Rui Liang, Takashi Hosoda, Gela Kipshidaze, Gregory Belenky, Stony Brook Univ. (United States); Sherrie S. Bowman, Richard L. Tober, U.S. Army Research Lab. (United States)

Cascade pumping leads to multifold improvement of the device efficiency and, hence, output power level of type-I quantum well (QW) GaSb-based diode lasers. We recently demonstrated 2.4 - 3.2 μm two-stage cascade diode lasers with 100% efficient carrier recycling between two gain stages. The next generation of the cascade diode lasers discussed in this work use the cascade pumping scheme to minimize the device threshold current via enhancement of the confinement factor and differential gain. The key achievement was the development of the design solution allowing for dense stacking of the type-I QWs gain sections while preserving strong carrier confinement and narrow gain bandwidth. This design approach facilitated the development of efficient multi-stage cascade diode laser heterostructures. The newly designed 3 μm cascade diode lasers demonstrated CW RT threshold current densities as low as 100 A/cm², a twofold improvement over the previous world record. Peak CW RT power conversion efficiency nearly doubled reaching 16% for 2-mm-long coated lasers. Three stage multimode (100- μm -wide, 2 mm-long, coated) cascade lasers demonstrated maximum CW RT output power level above 830 mW at an operating current of 3.7 A. These devices emitted 600 mW of CW power at 17 °C at 2 A at power conversion efficiency exceeding 12%. Additionally, narrow ridge (~6- μm -wide, 2-mm-long, coated) devices generated more than 100 mW of CW power at RT near 3 μm with conversion efficiencies near 10%.

**Conference 9382:
Novel In-Plane Semiconductor Lasers XIV**

9382-33, Session 8

Quantum cascade lasers for broadband spectroscopy (*Invited Paper*)

Jérôme Faist, ETH Zürich (Switzerland)

The possibility to design broadband gain medium using quantum cascade material has spurred a flurry of new approaches to use these devices in applications. We will report on our newest results using mid-infrared and THz Quantum cascade frequency combs as well as arrays of surface-emitting distributed feedback lasers.

9382-34, Session 8

Electrically-tunable quantum-cascade lasers

Alfredo Bismuto, Yves Bidaux, Camille Tardy, Stéphane Blaser, Romain Terazzi, Tobias Gresch, Antoine Muller, Alpes Lasers SA (Switzerland)

Coherent sources in the mid-infrared spectral range are of great interest due to the large number of scientific and industrial applications in this spectral range, e.g. high resolution spectroscopy, industrial control, clinical diagnostic. Quantum cascade lasers provide nowadays a compact and efficient source across the whole Mid-IR range. Nevertheless, in the development of spectroscopic applications is crucial the ability to tune the laser light emission with high modulation speeds. Distributed feedback (DFB) QCLs provide stable monomode emission, unfortunately due to the limited impact of injected current on the optical mode refractive index in QC structures, the electrical tunability of these sources is limited. In our work we developed a novel method to electrically tune the laser emission wavelength by locally controlling the laser active region temperature using a microscopic heating element. Temperature raises as elevated as 150 K were observed leading to tuning levels as high as 10 cm⁻¹ at modulation speeds of several kHz on QCLs operating in continuous wave operation. As we will show this method has been successfully applied to several spectral region, becoming an attractive solution for molecular resonances scanning.

9382-35, Session 8

Experimental investigation of intensity noise in injection locked mid-infrared quantum cascade lasers

Carsten Juretzka, Technische Univ. Darmstadt (Germany); Hercules Simos, National and Kapodistrian Univ. of Athens (Greece); Adonis Bogris, Technological Educational Institute of Athens (Greece); Dimitris Syvridis, Eugenia Roditi, National and Kapodistrian Univ. of Athens (Greece); Wolfgang E. Elsässer, Technische Univ. Darmstadt (Germany); Mathieu Carras, III-V Lab. (France)

The intensity noise properties of injection locked mid-infrared emitting quantum cascade lasers are experimentally investigated. The injection locking is realized below and near the threshold of the free running slave laser, resulting in an efficient technique to achieve low noise operation. It is found that below threshold the locking characteristics (locking range shape and bandwidth) are different in comparison to those above threshold. Furthermore, an alternative injection locking realization is also investigated: injection locking into longitudinal side modes of the slave laser. Here, similar characteristics were observed, however, with the potential to achieve even higher relative intensity noise reduction suppression with respect to the quantum noise limit. The measurements are confirmed by numerical simulations with a travelling-wave model which takes into account the multi-mode spectrum of the slave laser and the spectral profile of the

material gain. The simulations give the perspective for the achievement of a reduction of the relative intensity noise of the slave laser of up to 10 dB (above threshold) and up to 20 dB (below threshold) in comparison to the free running slave laser noise level.

9382-36, Session 8

Unique properties of quantum cascade lasers with applications to high-resolution molecular spectroscopy (*Invited Paper*)

Gerard Wysocki, Andreas Hangauer, Michael G. Soskind, Yin Wang, Princeton Univ. (United States)

Quantum cascade lasers (QCL) become a laser source of choice for high resolution spectrometry in the mid-IR, which is considered a molecular fingerprint region. In this paper several unique properties of the QCL technology that enable new capabilities in mid-IR spectroscopic sensing will be presented. One of the examples will present a very specific FM modulation behavior of QCLs, which allows for optical quasi single sideband (SSB) modulation through current injection and has not been observed in directly modulated semiconductor lasers before. This predestines QCLs in applications where SSB is required, such as telecommunication or high speed spectroscopy. Example applications to chirped laser dispersion spectroscopy with theoretical modeling and experimental verification of spectroscopic signals will be presented. Another set of spectroscopic sensing applications will include broadband mid-infrared spectroscopy with conventional, free-running, continuous wave Fabry-Perot (FP) QCLs. This measurement method is based on down-conversion of optical signals to the RF domain through a multi-heterodyne process. The paper will discuss the configuration of the experimental set-up of a robust dual-FP-QCL multi-heterodyne spectrometer, that is all electrically driven, contains no moving parts and assures high opto-mechanical stability, uses intrinsically small semiconductor devices, and shows a great potential for development of simple and compact broadband spectrometers that are able to access the fundamental molecular absorption bands in the mid-IR with high resolution (?15MHz, free-running). The evaluation of the amplitude and phase noise of the multi-heterodyne signals predicts relative intensity noise at <10⁻⁵ level as well as ultimate linewidth limit in the <200kHz regime. Examples of spectroscopic molecular sensing will be presented and discussed in details.

9382-67, Session 8

Light emission from III-nitride quantum cascade structures designed with effective interface grading

Yu Song, Princeton Univ. (United States); Rajaram J. Bhat, Corning Incorporated (United States); Andrew A. Allerman, Sandia National Labs. (United States); Tzu-Yung Huang, Princeton Univ. (United States); Chung-en Zah, Corning Incorporated (United States); Claire F. Gmachl, Princeton Univ. (United States)

A quantum cascade (QC) emitter in the III-nitride material system is designed, fabricated and characterized. The QC structure consists of GaN wells and Al_{0.65}Ga_{0.35}N barriers, which is sandwiched between the top and bottom contact layers, both Al_{0.26}Ga_{0.74}N with a Si doping of 1?10¹⁹ cm⁻³. The samples are grown by metal organic chemical vapor deposition on c-sapphire. The effective interface grading (EIG) is implemented in designing the structure. EIG arises due to a significant interface roughness (IFR), and has recently been identified with the help of non-equilibrium Green's functions. Here the effects of EIG in the active QC structure are discussed, which include repositioning of the subband Eigen-energies, remixing of the subband wave functions, and loss of confinement in the subband states at higher energies. These effects are confirmed experimentally by the measured photo-response spectra of the QC structure.

**Conference 9382:
 Novel In-Plane Semiconductor Lasers XIV**

The designed QC structure features a diagonal optical transition centered at ~ 250 meV (5 ?m). Efficient carrier injection and extraction are designed, with corresponding lifetimes of ~ 0.1 ps considering both longitudinal optical (LO) phonon and IFR scattering. The non-radiative decay from the upper to the lower emitter state is ≥ 10 ps. The leakage into the continuum above the quantum wells is also minimized with a scattering lifetime of ≥ 30 ps. Intersubband (ISB) Light emission is successfully observed from the structure up to 200 K, with a peak transition energy of 250 meV and a full width at half maximum of 110 meV, in agreement with the calculation. The emission is purely transverse magnetic polarized, verifying its origin in the ISB transition. The measured current-voltage characteristics shows a bias in the active layers of ≥ 120 kV/cm at a current density of above 3 kA/cm^2 , reaching the desired operation condition beyond flat-band.

9382-37, Session 9

Planarized process for resonant leaky-wave coupled phase-locked arrays of mid-IR quantum cascade lasers

Chun-Chieh Chang, Jeremy D. Kirch, Colin Boyle, Christopher A. Sigler, Luke J. Mawst, Dan Botez, Brian Zutter, Phillip Buelow, Kevin Schulte, Thomas F. Kuech, Univ. of Wisconsin-Madison (United States); Thomas Earles, Intraband, LLC (United States)

Resonant leaky-wave coupling has been used in the near-IR for phase-locking lasers to watt-range peak pulsed and CW powers. At and near resonance the structures are analogous to 2nd-order lateral distributed-feedback structures; thus, representing high-index-contrast ($n = 0.06\text{-}0.10$) photonic-crystal lasers that allow long-range coupling in a stable, in-phase array mode of uniform intensity profile. We have recently presented [1] the realization of resonant leaky-wave coupling of QCLs, which, in turn, has provided in-phase-mode operation to 3.0 W front-facet emitted power in a near-diffraction-limited far-field beam pattern, with 2.5 W in the main lobe. In that work, the interelement layers were grown selectively by using a SiN mask; thus, the regrown layers were curved. We have now developed a refined fabrication process to produce phase-locked arrays of a planar geometry. The process involves non-selective regrowth of Fe:InP after defining interelement trenches, followed by a chemical polishing (CP) step to planarize the surface. After CP planarization, the interelement layers are regrown over the entire surface. Finally, we selectively etch interelement-layer material, followed by an InP regrowth over the entire surface and a second CP step, to form element regions. This results in planar InGaAs/InP interelement regions, allowing for significantly improved control of the array geometry and the element/interelement dimensions. By removing the active-core material from the array interelement regions, we eliminate current spreading. We project from Full-Wave optical simulations that such arrays will support a single in-phase mode up to watt-range output powers.

[1] J. D. Kirch et al., CLEO: Science and Innovations Conf., Paper STh3G, June 8-13, 2014, San Jose, CA.

This work was supported by Air Force Research Laboratory under agreement number FA8650-13-2-1616.

9382-38, Session 9

Multiple quasi-stable spectral outputs at constant current from a continuous-wave high-power quantum cascade laser (Invited Paper)

Tobias S. Mansuripur, Harvard Univ. (United States); Guy-Mael J. de Naurois, Harvard School of Engineering and Applied Sciences (United States); Yongrui Wang, Texas A&M Univ. (United States); Wondwosen Metaferia, KTH

Royal Institute of Technology (Sweden); Carl Junesand, Epiclarus (Sweden); Sebastian Lourduoss, KTH Royal Institute of Technology (Sweden); Bouzid Simozrag, Mathieu Carras, III-V Lab. (France); Alexey A. Belyanin, Texas A&M Univ. (United States); Federico Capasso, Harvard School of Engineering and Applied Sciences (United States)

We have observed a continuous-wave Fabry-Perot (FP) quantum cascade laser (QCL) at wavelength 4.8 ?m that can emit multiple different spectra at a fixed current and temperature. The spectra can be qualitatively sorted into two classes: either the optical power is (1) highly concentrated in one mode or (2) spread rather uniformly over a "comb" comprising on the order of 100 adjacent FP modes. With the current fixed, we have observed that the laser spectrum remains stable at one of these states from anywhere between a few seconds to a few hours, and then suddenly transitions to a different state. These transitions appear to be random, as no external stimulus to trigger the transition has yet been found. The transitions are not correlated with temperature fluctuations, nor are they the result of optical feedback from the laser back into itself caused by stray reflections. Far-field measurements indicate that both spectral states are associated with the lowest order lateral mode of the cavity. The voltage across the QCL is roughly 0.03% larger for the "comb" state than for the "single-mode" state. Understanding the competition between these quasi-stable states could yield insight into the various intra-cavity phenomena—such as spatial hole burning and four-wave mixing, for instance—that determine the spectral output of the laser.

9382-39, Session 9

A mid-infrared on-chip sensor based on bi-functional quantum cascade structures and plasmonics

Benedikt Schwarz, Daniela Ristanic, Peter Reininger, Hermann Detz, Aaron M. Andrews, Werner Schrenk, Gottfried Strasser, Technische Univ. Wien (Austria)

Mid-infrared spectroscopy is one of the main techniques to investigate the composition of chemicals substances via their unique pattern of absorption lines. To access remote areas one has to develop more compact and cost-effective sensing systems. Until now, all miniaturized concepts have been demonstrated with external optics, lasers or detectors. Here, we present a monolithic sensor by integrating a laser, a plasmonic waveguide and a detector on the same chip (Schwarz et al. Nat Commun. 5, 2014). The laser and the detector are fabricated from a bi-functional quantum cascade structure. Surface plasmon polaritons (SPPs) are used to efficiently guide light from the laser to the detector and in parallel, to act as an interaction region. Due to the evanescent nature of SPPs the mode is mainly located outside, which provides a high interaction with surrounding chemical substances. In the mid-infrared, SPPs are commonly very weakly confined, as in this wavelength region metals have a large negative permittivity. By applying a thin (200nm) dielectric layer on top of an unpatterned metal surface, the propagation properties of the SPP can be modified in such a way, that it the SPP is strongly bound to the interface. This increased confinement enables an efficient coupling from and to the laser and the detector via spatial mode matching. To prove the functionality of the sensor, we submerged the entire unpassivated device in a solution of isopropyl alcohol (low absorption) and water (high absorption). In our first experiments we achieved a limit of detector of 100ppm.

**Conference 9382:
 Novel In-Plane Semiconductor Lasers XIV**

9382-40, Session 9

Nonlinear optics with quantum-engineered intersubband metamaterials *(Invited Paper)*

Jongwon Lee, Nishant Nookala, Mykhailo Tymchenko, Seungyong Jung, The Univ. of Texas at Austin (United States); Frederic Demmerle, Gerhard Boehm, Markus-Christian Amann, Technische Univ. München (Germany); Andrea Alù, Mikhail A. Belkin, The Univ. of Texas at Austin (United States)

Intersubband transitions in n-doped semiconductor heterostructures provide the possibility to quantum engineer one of the largest known nonlinear optical responses in condensed matter systems, limited however to electric field polarized normal to the semiconductor layers. We have recently integrated these nonlinearities into laser waveguides to produce room-temperature terahertz quantum cascade laser sources based on efficient intra-cavity difference-frequency mixing. Here we show that by coupling of electromagnetic modes in plasmonic metasurfaces with quantum-engineered intersubband transitions in semiconductor heterostructures one can create ultra-thin highly-nonlinear polaritonic metasurfaces for normal light incidence. Examples include mid-infrared metasurfaces with giant electro-optic effect that display ultra-fast electrical tuning of reflectivity and giant nonlinearity for second harmonic generation. Structures discussed here represent a novel kind of hybrid metal-semiconductor metamaterials in which exotic optical properties are produced by coupling electromagnetically-engineered modes in dielectric and plasmonic nanostructures with quantum-engineered intersubband transitions in semiconductor heterostructures.

9382-41, Session 10

Recent progress and future prospects of THz quantum-cascade lasers *(Invited Paper)*

Hideki Hirayama, Wataru Terashima, Tsung-Tse Lin, Miho Sasaki, RIKEN (Japan)

We are studying on terahertz-quantum cascade lasers (THz-QCLs) using GaAs/AlGaAs and GaN/AlGaIn semiconductor superlattices. We demonstrated 1.9-3.8 THz GaAs/AlGaAs QCLs with double metal waveguide (DMW) cavity. We demonstrated the highest temperature operation of low-frequency QCL ($T > 160\text{K}$ for 1.9 THz-QCL) by using indirect injection scheme (4-level design). GaN is a material having potentials for realizing wide frequency range of QCL including the unexplored frequency range from 5 to 12 THz, as well as realizing room temperature operation of THz-QCL. We demonstrated the first lasing action of GaN/AlGaIn THz-QCLs with lasing frequencies from 5.4-7 THz.

9382-42, Session 10

THz quantum cascade lasers operating on the radiative modes of a 2D photonic crystal *(Invited Paper)*

Yacine Halioua, Univ. Paris-Sud 11 (France); Gangyi Xu, Univ. Paris-Sud 11 (France) and Institut d'Électronique Fondamentale (France); Souad Moumdji, Univ. Paris-Sud 11 (France); Lianhe H. Li, Giles Davies, Edmund H. Linfield, Univ. of Leeds (United Kingdom); Raffaele Colombelli, Institut d'Électronique Fondamentale (France)

THz metal-semiconductor-metal photonic-crystal lasers naturally operates on the so-called "non-radiative" modes. Indeed, these modes, due to their low output coupling, possess a high Q factor favoring lasing. In this work, we propose a design based on anisotropic lattice and resonator allowing to control mode competition and favor lasing on radiative modes which are well suited for emission. As a result, with devices based on this design, surface emitting quantum cascade THz lasers with with diffraction-limited beams with 17 mW peak output power has been demonstrated.

9382-43, Session 10

Recent advances in the research toward graphene-based terahertz lasers *(Invited Paper)*

Taiichi Otsuji, Akira Satou, Takayuki Watanabe, Stephane A. Boubanga Tombet, Tohoku Univ. (Japan); Alexander A. Dubinov, Institute for Physics of Microstructures (Russian Federation) and Lobachevsky State Univ. (Russian Federation); Vyacheslav V. Popov, Institute of Radio Engineering and Electronics (Russian Federation); Vladimir Mitin, Univ. at Buffalo (United States); Michael Shur, Rensselaer Polytechnic Institute (United States); Victor Ryzhii, Tohoku Univ. (Japan)

[Invited] This paper reviews recent advances in the research toward creation of graphene-based terahertz (THz) lasers. Mass-less Dirac Fermions of electrons and holes in gapless and linear symmetric band structures in graphene yield a gain in a wide THz frequency range under optical or electrical pumping. Interband photon absorption under sufficiently intense pumping leads to population inversion after ultrafast energy relaxation of photoelectrons and photoholes via optical phonon emissions. When interband stimulated photon emission prevails over the intraband Drude-type absorption, the system yields a gain. However the maximal obtainable gain is limited to or below 2.3% of the interband photon absorbance of monolayer graphene. Excitation of surface plasmon polaritons (SPPs) in population-inverted graphene extremely enhance the THz gain by orders of magnitude. An experimental observation of the giant THz gain via SPPs in femtosecond infrared laser-pumped graphene is demonstrated. Resonant-type active plasmonic graphene heterostructures are also addressed. Photon-emission-assisted resonant tunneling in a double-graphene-layered nano-capacitor structure is another promising mechanism that can enormously enhance the THz gain. Novel graphene-based heterostructures that can install such physical mechanisms for current-injection-type THz lasing are proposed. Their superior gain-spectral properties and practical laser cavity structures are also addressed.

9382-60, Session PWed

Improved efficiency in room temperature $>3\mu\text{m}$ diodes using highly-strained quantum wells

Chunte A. Lu, Ron Kaspi, Tim C. Newell, Chi Yang, Sanh Q. Luong, Donald M. Gianardi Jr., Air Force Research Lab. (United States)

Diode lasers emitting above $3\mu\text{m}$ capable of operating at room temperature are of interest for spectroscopic detection and infrared counter measurement applications. The challenge for producing such mid-infrared wavelength devices remains due to the diminishing hole confinement barrier. Recent advancement has shown promising results using GaSb-based type-I InGaAsSb quantum wells (QWs) with AlInGaAsSb quinary barriers to improve the hole confinement. Here we further improve the hole confinement using highly strained QWs in addition to the use of quinary barriers. The strain compensated structure contains Al_{0.9}Ga_{0.1}As_{0.07}Sb_{0.93}

**Conference 9382:
 Novel In-Plane Semiconductor Lasers XIV**

clad layers, a 600-nm thick tensile strained AlInGaAsSb waveguide barrier with three compressively strained InGaAsSb QWs. We use the molecular beam epitaxy technology to conduct the laser growths and achieve strain >2.2% in the QWs. To the best of our knowledge, this is the highest strain in the QWs reported for >3 μ m GaSb-based type-I laser diode. For efficiency comparison, we also performed the growths for lasers with strain of 1.5% and 1.9% in the QWs. At near room temperature, the preliminary pulsed L-I results for the 1mm x 100 μ m uncoated devices show the diode with 1.9% strain is 4 times more efficient than the diode with 1.7% strain and the highly strained diode with >2.2% strain is 6.2 times more efficient than the diode with 1.7% strain. The measured spectra for all diode lasers are >3 μ m. The study demonstrates significant improvement in laser efficiency using highly strained QWs in GaSb-based type-I mid-infrared laser diodes.

9382-61, Session PWed

Electrical diagnosis of quantum cascade lasers

Peter G. Eliseev, Chi Yang, Tim C. Newell, Ron Kaspi, Air Force Research Lab. (United States)

In a relatively complex optoelectronic device such as the quantum cascade laser (QCL), extracting information concerning the pumping mechanism and recombination balance in the operational device can be very helpful. In the QCL, the junction resistance is associated with the penetration of carriers through a potential barrier where the height of the barrier depends on the applied voltage, leading to the electrical nonlinearity. We present an analysis of the electrical characteristics of QCLs emitting at the mid-IR at room temperature and demonstrate the separation of ohmic and nonlinear components of diode resistance.

We analyze a variety of high power QCL devices and demonstrate that the differential resistance dU/dI varies linearly with the inverse diode current ($1/I$), as evidence that the diode current vs the junction voltage has a simple exponential dependence. Consequently, the relationship for the differential resistance is given as:

$$dU/dI = R_s + (\eta/e)(1/I)$$

where R_s is the ohmic resistance, and $\eta = nkT$ where n is an ideality factor. In our analyses, we consistently observe junction voltage saturation above the threshold, and quantify the quasi-Fermi level separation in each stage. We also extract temperature dependent values for η that are near 1 eV at room temperature, and approach 2 eV as the temperature is reduced. We demonstrate that a considerable amount of information pertaining to the quality of the QCL device can be accessed by electrical diagnostics alone.

9382-62, Session PWed

Dynamic and static concept of laser-thyristor for high-peak power lasing

Sergey O. Slipchenko, Aleksandr Podoskin, Nikita A. Pikhtin, Valentin S. Yuferev, Il'ya S. Tarasov, Ioffe Physical-Technical Institute (Russian Federation)

A concept of a new type of high power pulsed laser generators based on epitaxial and operating integration of high-speed high power current switch and laser heterostructure, the so-called laser-thyristor, has been developed. In the developed concept laser-thyristor has been considered as an optocoupler heterophototransistor-diode laser. Analytical expressions describing static I-U curve have been obtained. It is shown that voltage blocking effect and negative differential resistance are connected with change in dependence behavior of photogeneration rate of control signal vs. total current through the structure. It has been determined that lasing switch on basically influences on injection efficiency of laser-thyristor. Above lasing threshold photogeneration rate of control signal is saturated and laser-thyristor goes into saturation regime. This regime is manifested in residual potential growth on collector p-n junction. Possible means

of laser-thyristor injection efficiency increase at ultrahigh pump current densities (dozens of kA/cm²) have been analyzed. Dynamic characteristics of laser-thyristor have been investigated using obtained relations for optical feedback. Possibility of low-signal control using both electrical and optical is shown. Facts of high energy efficiency of control as well as possibility to control turn-on time delay of lasing from several of nsec to dozens of μ sec are established. Avalanche effects and their influence on switch on dynamics of laser-thyristor are investigated. Approaches for pulse generation of nsec-duration and peak optical power of dozens of watt are considered.

9382-63, Session PWed

A ZnSe/BeTe p-grading superlattice with a low voltage drop for efficient hole injection in green-yellow BeZnCdSe quantum well laser

Ryoichi Akimoto, National Institute of Advanced Industrial Science and Technology (Japan)

Semiconductor laser diodes (LDs) in emission wavelength range of green-to-yellow are of importance for interesting applications such as full-color laser displays as a pure green light source, especially so-called pico-projectors for mobile devices, and a sensing of bio-chemical materials and medical cures. For those applications, continuous wave operation of BeZnCdSe quantum well laser diodes at room temperature in the green to yellow spectrum range have been demonstrated recently [1-4]. ZnSe-based alloy containing beryllium has a much higher degree of covalency than other II-VI compounds[5]. Thus the beryllium-containing material system is expected to overcome a problem of limited lifetime due to weakness inherent to II-VI materials.

In this contribution, a ZnSe/BeTe p-grading superlattice (p-GSL) layer with a low voltage drop for BeZnCdSe quantum well LDs is reported. A p-GSL is inserted between a p⁺-BeTe layer for ohmic contact to metals and a ZnSe/BeMgZnSe p-cladding layer in a LD layer structure, for an efficient hole injection in spite of a large potential barrier of -0.8 eV between telluride and selenide materials. GSL is considered to greatly influence a threshold voltage of lasing and thus reliability in LDs. To investigate performance of GSL, test devices of pn junction are fabricated where a p-ZnSe (0.5 μ m), a-GSL, and p-BeTe (20nm) are grown on n-GaAs homo epitaxial layer on n-GaAs wafer grown by two-chamber (II-VI, and III-V) molecular beam epitaxy system. In a p-GSL, BeTe thickness increases with fixed monolayer (ML) step, while ZnSe thickness decreases with the same step when next period of ZnSe/BeTe is grown, so that one period thickness is kept constant. In the previous LDs, a p-GSL with one period thickness of 13 ML with 1ML grading step is used. But we found that a grading of 1 ML step is still too thick and does not give a smooth potential shape for hole transport. A-GSL of 0.5 ML grading step gives better hole transport. In a GSL with one period thickness of 9 ML with 0.5ML step, bias voltage at 200A/cm² is as low as 3.0 V, while the previous one is 5.0 V, thus 2 V lower voltage is obtained. As for other factor that influences a performance of GSL is chemical bond (ZnTe or BeSe) at ZnSe/BeTe interface. Effect of chemical bonds influence valence band offset in ZnSe/BeTe [6] and hence hole transport across a p-GSL. This effect will be also presented.

References

- [1] J. Kasai et al., Applied Phys. Express 3, 091201 (2010).
- [2] J. Kasai et al, Applied Phys. Express 4, 082102 (2011).
- [3] S. Fujisaki et al., Applied Phys. Express 5, 062101 (2012).
- [4] R. Akimoto et al., SPIE Proceedings of SPIE Photonics West OPTO 2013, Vol. 8640, 8640F (2013).
- [5] A. Waag et al, J. Appl. Phys. 80, 792 (1996).
- [6] Nagelstrasser et al., J. Appl. Phys. 83, 4253 (1998).

9382-64, Session PWed

Selective and tunable red- or blue-shift of GaAsP quantum well heterostructures

WeiFu Wang, Kai-Yuan Cheng, National Tsing Hua Univ. (Taiwan); Ching-Yi Huang, National Tsing Hua Univ. (Taiwan) and Institute of Electronics Engineering (Taiwan); Wei-Ting Liu, Bao-Hsien Wu, National Tsing Hua Univ. (Taiwan); Yu-Chen Cheng, Union Optronics Corp. (Taiwan); Kuang-Chien Hsieh, National Tsing Hua Univ. (Taiwan)

Post-growth quantum-well intermixing (QWI) is a useful technique to realize optical integrated devices on III-V compound semiconductor heterostructures. Together with lithography, localized compositional intermixing can be achieved allowing bandgap alteration to facilitate wave guiding and reduction in optical absorption near the mirror facets of semiconductor lasers.

In this work, our research emphases focus on two areas: (i) the effect of dielectrics and arsenic or gallium overpressure on point defect generation and (ii) compositional mixing and wavelength shifting upon furnace anneals in GaAsP-based QW heterostructures.

Dielectric encapsulation layers including SiO_x and SiN_x deposited by Plasma Enhanced Chemical Vapor Deposition and SrF₂ films deposited by E-gun evaporation are used. An epitaxial laser structure having a 10-nm quantum well of nominal GaAs_{0.9}P_{0.1} confined with p-type upper and n-type lower Al_xGa_{1-x}As layers, is used in this work. Materials and processed structures are characterized with a depth profiler, ellipso-meter, transmission electron microscopy, secondary ion mass spectroscopy, and photoluminescence (PL). In this structure, intermixing of column-V species between QW and the confining layers will reduce the QW band-gap energy while an intermixing of Column III species will increase the energy conversely. The as-grown QW structure shows PL peaks around 800 nm.

For cap-less bare samples sealed in ampoules with little arsenic overpressure, furnace anneals at 800 C result in red PL shifts asymptotically as much as 75 meV with anneal time up to 40 hours. We attribute this red-shift to the inter-diffusion of phosphorous and arsenic in QW and the neighboring confinement layer through a small amount of built-in defects, most likely the Column-V vacancies formed during the epitaxial growth. For samples doubly capped with an initial layer of SrF₂ and a following SiO_x film, similar temporal red shifts appear suggesting the combined dielectrics either prohibit or slow down the diffusion of Column III vacancies during anneals.

The temporal PL shifts take a more complicated path for samples capped with either SiO_x or SiN_x alone. They first shift toward longer wavelength than shorter wavelength. We attribute the beginning red shift to the inter-diffusion of phosphorous and arsenic in QW and the neighboring confinement layer as before and the large turn-around blue-shift (up to 165meV for 40hr annealing under 800oC) because Ga in QW exchanges with Al in the confinement layer through column-III vacancies. Apparently, a single layer of SiO_x or SiN_x film actually allows the generation and diffusion of column III vacancies, which facilitate the intermixing of QW with its neighboring confining layers.

Additional complexity arises when As overpressure is replaced with Ga overpressure. For samples similarly capped with either SiO_x or SiN_x films, although an initial red-shift persists as before, the following blue-shift proceeds much faster. It takes place in a very short time (up to 281meV for only 5hr annealing under 800C). Since Ga overpressure favors the creation of Column III interstitials instead of vacancies, we believe that the reason for the large amount of blue-shift in a very short time as compared to that in arsenic-overpressure is due to the kick-out mechanism of dopants in the heavily doped contact layer. The Zn dopants in the contact layer are kicked out by Ga atoms introduced by the encapsulation layer under Ga overpressure, then diffuse very quickly downward to the QW region through interstitial sites.

It is useful through employing different combinations of dielectrics, Ga or As overpressure and anneal time that we can selectively control the red- or blue-shift of GaAsP QW to realize optical integrated devices for different applications.

9382-65, Session PWed

Analysis of dual-mode lasing characteristics in a 1310-nm optically-injected quantum dot distributed feedback laser

Ravi Raghunathan, Justeen Olinger, Virginia Polytechnic Institute and State Univ. (United States); Antonio Hurtado, Univ. of Essex (United Kingdom) and Univ. of Strathclyde (United Kingdom); Frédéric Grillot, Télécom ParisTech (France); Vassilios I. Kovanis, Luke F. Lester, Virginia Polytechnic Institute and State Univ. (United States)

Recent work has shown the Quantum Dot (QD) material system to be well-suited to support dual-mode lasing [1-4]. In particular, optical injection from a master laser (ML) into the residual Fabry-Perot (FP) modes of a 1310 nm Quantum Dot Distributed Feedback (QD-DFB) laser has been recently demonstrated to offer a highly reliable platform for stable dual-mode lasing operation. External controls on the ML, such as operating temperature and bias current, can be used to precisely adjust the spacing between the two lasing modes. This tunability of mode-separation is very promising for a range of applications requiring the generation of microwave, millimeter wave and terahertz signals. Considering the versatility and utility of such a scheme, it is imperative to acquire a deeper understanding of the factors that influence the dual-mode lasing process, in order to optimize performance.

This paper seeks to further our understanding of the optically-injected dual-mode lasing mechanism. Controlling the optical power injected into each FP residual mode and the wavelength detuning, the dual-mode lasing characteristics are analyzed with regard to important system parameters such as the position and the intensity of the injected residual mode (relative to the Bragg and the other residual FP modes of the device). Preliminary results indicate that for dual mode lasing spaced less than 5 nm apart, the relative intensity of the injected FP mode is important toward determining dual mode lasing behavior. Insight into the dual-mode lasing characteristics could provide an important design guideline for the master and QD-DFB slave laser cavities.

References:

- [1]. Hurtado, A., Henning, I.D., Adams, M. J., and Lester, L. F., "Dual-mode lasing in a 1310-nm quantum dot distributed feedback laser induced by single-beam optical injection", *Appl. Phys. Lett.*, vol. 102, no. 20, pp. 201117-1-201117-4 (2013).
- [2]. Hurtado, A. Mee, J. K., Nami, M., Henning, I. D., Adams, M. J., and Lester, L. F., "Tunable microwave signal generator with an optically-injected 1310nm QD-DFB laser", *Opt. Exp.*, vol. 21, no. 9, pp. 10 772-10 778 (2013).
- [3]. Hurtado, A, Henning, I. D., Adams, M. J., and Lester, L.F., "Generation of Tunable Millimeter-Wave and THz Signals With an Optically Injected Quantum Dot Distributed Feedback Laser", *IEEE Photonics Journal* , vol.5, no.4, pp.5900107-5900107 (2013).
- [4]. Grillot, F., Naderi, N. A., Wright, J. B., Raghunathan, R., Crowley, M. T., and Lester, L. F., "A dual-mode quantum dot laser operating in the excited state," *Appl. Phys. Lett.* 99, 231110 (2011).

9382-44, Session 11

Waveguide and PC design of photonic crystal surface-emitting lasers

Richard Taylor, Pavlo Ivanov, Alex Crombie, David T. D. Childs, Salam Khamas, Richard A. Hogg, The Univ. of Sheffield (United Kingdom)

In this work we theoretically investigate semiconductor photonic crystal (PC) surface-emitting lasers (PCSELS). Compared to other types of compact semiconductor lasers, the optical power of PCSELS can be scaled with area

**Conference 9382:
 Novel In-Plane Semiconductor Lasers XIV**

whilst keeping their emission single-mode. The PC embedded within the cavity of the PCSEL allows the control of many aspects of the emitted beam such as the divergence, direction, polarization, and emission wavelength.

We have demonstrated 980 nm GaAs-based PCSELS with all-semiconductor GaAs/InGaP and semiconductor-void InGaP/air PCs situated above laser active region. The PC was fabricated by etching a suitable pattern in an InGaP layer followed by the deposition of GaAs inside these holes (or the formation of voids) via MOVPE.

To improve PCSEL design and expand the application area of PCs to other lasers, we use a combination of an effective index approach and optical scattering models. Results justify the placement of the PC as close to the active zone as possible in order to achieve the maximum coupling of the mode with the PC. All-semiconductor PCs provide a higher coupling with the optical mode in most cases. It can be improved by moving the PC layer close to the active zone, reducing the ballast layer between the PC and upper cladding layers and using two PC layers with the active zone "sandwiched" between them.

9382-45, Session 11

785-nm dual wavelength DBR diode lasers and MOPA systems with output powers up to 750 mW

Bernd Sumpf, Martin Maiwald, Andreas Klehr, André Müller, Frank Bugge, Jörg Fricke, Peter Ressel, Götz Erbert, Günther Tränkle, Ferdinand-Braun-Institut (Germany)

Raman lines are often superimposed by daylight, artificial light sources or fluorescence signals from the samples under study. Shifted excitation Raman difference spectroscopy (SERDS), i.e. exciting the sample alternately with two slightly shifted wavelengths, allows to distinguish between the Raman lines and sources of interference.

In this work, monolithic dual wavelength Y-branch DBR ridge waveguide diode lasers and their application in master oscillator power amplifier (MOPA) systems at 785 nm suitable for Raman spectroscopy and SERDS will be presented. The definition of the wavelengths is made by implementing deeply-etched 10th order 500 nm long surface gratings with different periods using i-line wafer stepper lithography. Y-branch DBR lasers with a total length of 3 mm and a stripe width of 2.2 μm were manufactured and characterized.

The monolithic devices reach output powers up to 215 mW with emission widths of about 20 μm . At 200 mW the conversion efficiency is 25%, i.e. the electrical power consumption is only 750 mW. The spectral distance between the two laser cavities are about 0.6 nm, i.e. 10 cm⁻¹ as targeted. The side mode suppression ratio is better than 50 dB. Long-term test at output powers up to 75 mW show a reliable operation over more than 3,000 h. Amplifying these devices using a ridge waveguide amplifier an output power of about 750 mW could be achieved maintaining the spectral properties of the master oscillator.

These devices were tested in a Raman set-up and successfully applied for SERDS.

9382-46, Session 11

Using shape-memory polymer resonators for building continuously-tunable organic distributed feedback lasers

Senta Schauer, Xin Liu, Norbert Schneider, Matthias Worgull, Uli Lemmer, Hendrik Hoelscher, Karlsruher Institut für Technologie (Germany)

We demonstrate a novel way to fabricate tunable diffractive phase gratings as resonators utilizing shape-memory polymers (SMP). Such gratings are important tools for various applications in optics and photonics, e.g. they

serve as distributed feedback (DFB) resonators in organic semiconductor lasers. SMPs are able to remember a predefined shape and recover it even after strong deformations as long as they are driven by a proper stimulus like heat. The SMP we utilized is the thermally triggered polyurethane Tecoflex[®]. We used hot embossing to replicate nanometer scale one-dimensional 2nd order Bragg gratings onto SMP substrates. After stretching, these gratings feature an increased period which shrinks back to original length after activation of the recovery process. In order to demonstrate the practical applicability of these gratings as useful components for photonics, we successfully fabricated continuously tunable DFB-lasers based on SMP resonators with the organic semiconductor Alq₃:DCM serving as laser active material. The device includes a pre-stretched SMP substrate covered with organic material which is optically pumped and then heated with a Peltier element to initialize the recovery process. By changing the resonator's period via the shape-memory effect we achieved a continuously tunable and adjustable shift in the maximum of the emitted spectra of about 30 nm. To evaluate our novel device we quantified the lasing threshold to about 140 $\mu\text{J}/\text{cm}^2$ and the lifetime to $>10^7$ pulses. Due to their flexibility, our tunable lasers can be integrated in Lab-on-a-Chip devices to enable various applications for biomedical and chemical testing for point-of-care analysis.

9382-47, Session 11

Demonstration of continuous-wave microsquare lasers and comparison to microdisk laser

Chee-Wei Lee, Qian Wang, Yicheng Lai, Doris K. Ng, Siu Kit Ng, A*STAR - Data Storage Institute (Singapore)

Microcavity lasers are of great interest to the research community due to its much compact footprint, and low threshold as compared to the conventional fabry-perot lasers, which leads to its potential applications as compact on-chip light sources. In most literatures, circular-shaped cavity is amongst the commonly seen microlasers. However, recently some researchers have paid attention to the microcavity based on other polygonal shapes, such as square, triangle, hexagon and etc. Although each of them has their own unique properties, no comparison was done with the prevalent microdisk laser. In this paper, we aimed to demonstrate compact optically-pumped continuous wave microsquare laser on InP-based multiple-quantum-wells (MQW) material, and draw a comparison to microdisk laser realized on the same substrate. The comparison potentially acts as justification for using a microsquare laser instead of a microdisk laser. Numerical mode analysis and experimental characterization of the microsquare laser are conducted, and continuous wave operation is achieved with footprint as small as $4\text{?}4\text{?}\mu\text{m}^2$. The microsquare laser shows a lower lasing threshold and infers a higher differential efficiency than the microdisk counterpart. The microsquare cavity laser has also sufficiently high quality factor, and higher pumping injection efficiency due to the more evenly distributed field profile as compared to that of the microdisk. Experimental result also shows that the microsquare laser has better temperature stability than the microdisk. These results promise a potential alternative laser structure for on-chip light source applications. The lasers could also be possibly integrated with silicon platform for electronic-photonics integration.

9382-48, Session 11

On-chip PT-symmetric microring lasers

Hossein Hodaei, Mohammad-Ali Miri, Absar Ul Hassan, Enrique Sanchez Cristobal, Matthias Heinrich, Demetrios N. Christodoulides, Mercedeh Khajavikhan, CREOL, The College of Optics and Photonics, Univ. of Central Florida (United States)

The concept of parity-time (PT) symmetry has recently attracted considerable attention in optics. In general, PT-symmetric structures utilize

**Conference 9382:
 Novel In-Plane Semiconductor Lasers XIV**

gain and loss in a balanced fashion in otherwise symmetric cavities or waveguide arrangements. As recently demonstrated, such systems can exhibit altogether new properties and functionalities which are otherwise unattainable in Hermitian platforms. One such phenomenon is the transition from all real to partially complex spectra at the so-called PT-symmetry breaking threshold.

Here, we present the first experimental demonstration of stable single-mode operation in on-chip PT-symmetric micro-ring lasers. Along these lines, an active ring is paired with a lossy but otherwise identical partner. By choosing an appropriate coupling strength between them, one may withhold amplification from all undesired modes by keeping them below the PT-symmetry breaking. Therefore, the one mode which exceeds the symmetry-breaking threshold dominates the emission spectrum with high fidelity and enhanced extraction efficiency.

For our experiments we utilized InGaAsP micro-rings, which are partially buried in SiO₂. The amplification is provided by a total of six of quantum wells. Each single ring, having a width of 2 μm and a radius of 6 μm, supports four radial modes for each longitudinal resonance that falls within the amplification bandwidth. By judiciously tuning the coupling between the rings, we were able to suppress all higher-order transverse modes, and even obtain entirely single-longitudinal-mode operation at pump powers, which would yield highly multi-moded emissions from a conventional single microring resonator. This is achieved without negative impact on the lasing efficiency of the desired mode.

9382-49, Session 11

Low-spatial coherence chaotic cavity laser for speckle-free full-field imaging

Brandon Redding, Alexander Cerjan, Xue Huang, A. Douglas Stone, Minjoo L. Lee, Michael A. Choma, Hui Cao, Yale Univ. (United States)

High spatial coherence is a defining characteristic of traditional lasers, allowing us to focus light to a small spot or collimate it over long distances. Nevertheless, spatial coherence in the setting of imaging has one notorious consequence: speckle. Coherent artifacts such as speckle have precluded the use of lasers in full-field imaging applications, despite advantages such as higher power per mode and increased spectral control. To address this issue, we recently showed that random lasers, a kind of complex-cavity laser, can generate low spatial coherence laser emission. Unfortunately, this demonstration was performed in a pulsed dye-based laser which has well known practical limitations. In this work, we present a compact, electrically pumped semiconductor laser using a chaotic cavity design to facilitate multimode lasing and achieve low spatial coherence. The cavity shape consists of a microdisk with a flat edge known as a "D-cavity" which has been used as the outer core in fiber lasers to achieve uniform optical pumping. The chaotic laser was fabricated on a GaAs wafer and the number of lasing modes was estimated by monitoring the speckle formed by the laser emission. We found that a 500 μm radius chaotic cavity supported ~1000 mutually incoherent lasing modes in parallel. We then demonstrated speckle-free imaging using the chaotic cavity laser emission. In addition to precluding speckle formation, the chaotic laser provides much higher power per mode than traditional low spatial coherence sources and could be used for a range of high-speed full-field imaging applications.

9382-50, Session 12

Numerical simulation and optimization of microstructured high brightness broad area laser diodes (Invited Paper)

Hans-Christoph Eckstein, Uwe D. Zeitner, Andreas Tünnermann, Fraunhofer-Institut für Angewandte Optik und Feinmechanik (Germany); Christian Lauer, Uwe Strauss, OSRAM Opto Semiconductors GmbH (Germany)

The development of broad area laser diodes towards higher output power, efficiency and brightness is essential to gain progress in almost all laser applications because those devices provide the basis for high power laser sources. To systematically improve the characteristics of high power broad area laser diodes through a design process, it is necessary to have an accurate and efficient computation model self-consistently taking into account optical, electrical, and thermal properties. In this publication we present numerical techniques to compute the optical properties of the multimode beam generated by high-power AlGaAs broad area laser diodes with an operating wavelength of 970 nm. This simulation considers fluctuations of the carrier and power density as well as the temperature distribution. The numerical results show an excellent accordance to measured data of conventional and micro-structured high power broad area lasers. The high computation speed of the model allows to optimize microstructures inside the laser resonator with the use of a genetic optimization algorithm. We show that this design approach potentially leads to a high performance gain of the device. In particular degradation of the beam quality due to thermal effects at high injection currents can be controlled.

9382-51, Session 12

Generation of spectrally-stable continuous-wave emission and ns pulses at 800nm and 975nm with a peak power of 4W using a distributed Bragg reflector laser and a ridge-waveguide power amplifier

Andreas Klehr, Hans Wenzel, Jörg Fricke, Frank Bugge, Götz Erbert, Günther Tränkle, Ferdinand-Braun-Institut (Germany)

Semiconductor based sources which emit high-power spectrally stable nearly diffraction-limited optical pulses in the nanosecond range are ideally suited for a lot of applications, such as free-space communications, metrology, material processing, seed lasers for fiber or solid state lasers, spectroscopy, LIDAR and frequency doubling.

The aim of this paper is to present detailed experimental investigations of 975nm and 800nm diode-laser based master oscillator power amplifier (MOPA) light sources where the output power under CW and pulse excitation is spectrally stabilized and nearly-diffraction limited. The MOPA systems consist of distributed Bragg reflector lasers (DBR) as master oscillators driven by a constant current and ridge waveguide power amplifiers which can be driven DC and by current pulses. In pulse regime the amplifiers modulated with rectangular current pulses of about 5ns width and a repetition frequency of 200kHz act as optical gates, converting the CW input beam emitted by the DBR lasers into a train of short optical pulses which are amplified. With these experimental MOPA arrangements no relaxation oscillations occur. With a seed power of about 5mW output powers behind the amplifier of about 1W under DC injection and 4W under pulsed operation for 975nm, and 5.5W for the 800nm, are reached. The optical spectra of the emission of the amplifiers exhibit a peak at a constant wavelength with a line width < 10pm in the whole investigated current ranges. The ratios between laser and ASE level were > 50dB. The output beam is nearly diffraction limited with beam propagation ratios M_{2lat} - 1.1 and M_{2ver} - 1.2 up to 4W pulse power.

9382-52, Session 12

New approach for high-peak power lasing based on epitaxially-integrated AlGaAs/GaAs laser-thyristor heterostructure

Sergey O. Slipchenko, Aleksandr Podoskin, Aleksandr Rozhkov, Nikita A. Pikhtin, Il'ya S. Tarasov, Ioffe Physical-

**Conference 9382:
Novel In-Plane Semiconductor Lasers XIV**

Technical Institute (Russian Federation); Timur Bagaev, Maxim Ladugin, Aleksandr Marmalyuk, Anatolii A. Padalitsa, Vladimir Simakov, POLYUS Research and Development Institute (Russian Federation)

A new approach for generation of high peak optical power based on epitaxial and operating integration of high-speed high power current switch and laser heterostructure (the so-called laser-thyristor) is developed. Epitaxially-integrated AlGaAs/GaAs heterostructure of low-voltage laser-thyristor has been investigated and optimized for lasing of high power pulses at 900nm wavelength. It is shown, that an incomplete switch on of laser-thyristor at initial stage and nonlinear dynamics of radiated laser power are connected with an insufficient efficiency of vertical optical feedback in epitaxially-integrated heterostructure. An optimization of composition and interband absorption spectra of transistor base layers allows essentially increasing efficiency of control signals due to photogeneration speed growth. Experimental laser-thyristor samples with 200 μ m aperture have been manufactured and investigated. Maximal value of static block voltage hasn't exceeded 20V. It is shown that generated laser pulses have perfect bell-like shape without any features of nonlinear dynamics. It allows confirming that changes introduced in heterostructure design provide sufficient efficiency of control signal photogeneration. As a result maximal value of optical peak power has reached 40W at 95ns FWHM pulse duration. The analysis of potential dynamics has shown that the developed heterostructure provides pumping of active layer with up to 90A amplitude pulses. The developed devices demonstrate a unique possibility to control a turn-on time delay. It is experimentally shown that amplitude variation of control signal from 100mA to 0.5mA changes turn-on time delay in 10ns-3 μ s range. Minimal energy of control signal providing switching of maximal optical power reached 1nJ

9382-53, Session 12

Short-wavelength infrared defect emission as probe for degradation effects in diode lasers

Martin Hempel, Jens W. Tomm, Max-Born-Institut für Nichtlineare Optik und Kurzzeitspektroskopie (Germany); Fangyu Yue, Max-Born-Institut für Nichtlineare Optik und Kurzzeitspektroskopie (Germany) and East China Normal Univ. (China); Mauro A. Bettinati, 3S PHOTONICS S.A.S. (France); Thomas Elsaesser, Max-Born-Institut für Nichtlineare Optik und Kurzzeitspektroskopie (Germany)

The infrared emission from 980-nm single-mode high power diode lasers is analyzed in the wavelength range from 0.8 to 8.0 μ m. The short-wavelength infrared (SWIR) emission band with a maximum at 1.3 μ m is used to study the evolution of defect states located in the waveguide of the devices. The SWIR intensity is verified to represent a measure of the non-equilibrium carrier concentration in the waveguide, allowing for non-destructive waveguide mapping in spatially resolved detection schemes. The potential of this approach is demonstrated by measuring spatially resolved profiles of SWIR emission and correlating them with mid-wavelength infrared thermal emission along the cavity of devices undergoing repeated catastrophic optical damage. The enhancement of SWIR emission in the damaged parts of the cavity is due to a locally enhanced carrier density in the waveguide and allows for in situ analysis of the damage patterns. Moreover, spatially resolved SWIR measurements are a promising tool for device inspecting even in low-power operation regimes.

9382-54, Session 12

975 nm high-peak power ns-diode laser based MOPA system suitable for water vapor DIAL applications

Bernd Sumpf, Andreas Klehr, Ferdinand-Braun-Institut (Germany); Thi Nghiem Vu, Ferdinand-Braun-Institut (Germany) and Vietnam Academy of Science and Technology (Viet Nam); Götz Erbert, Günther Tränkle, Ferdinand-Braun-Institut (Germany)

Micro-DIAL (differential absorption LIDAR) systems require light sources with peak powers in the range of several 10 W together with a spectral line width smaller than the width of absorption lines under study. For water vapor at atmospheric pressure this width should be smaller than 10 pm at 975 nm.

In this paper, all semiconductor master oscillator power amplifier system at an emission wavelength of 975 nm will be presented. This spectral range was selected with respect to a targeted absorption path length of 5000 m and H₂O line strengths. A distributed feedback (DFB) ridge waveguide diode laser operated in continuous wave is used as master oscillator whereas a tapered amplifier consisting of a RW section and a flared section is implemented as power amplifier. The RW section acts as optical gate. The current pulses injected into the RW part have a length of 8 ns and the tapered part with 15 ns long pulses. The delay between the pulses is adjusted for optimal pulse shape. The repetition rate is in both cases 25 kHz.

A maximal pulse output power of about 16 W limited to the available current supply is achieved. The spectral line width of the system determined by the properties of the DFB laser is smaller than 10 pm. The tuning range amounts 0.9 nm and a SMSR of 40 dB is observed. From the dependence of the peak power on the power injected into the tapered amplifier, the saturation power is determined to 5.3 mW.

9382-55, Session 13

Above-threshold numerical modeling of high-index-contrast photonic-crystal quantum cascade lasers

Anatoly P. Napartovich, Nikolay N. Elkin, Dmitry V. Vysotsky, Troitsk Institute for Innovation and Fusion Research (Russian Federation); Jeremy D. Kirch, Christopher A. Sigler, Dan Botez, Luke J. Mawst, Univ. of Wisconsin-Madison (United States); Alexey A. Belyanin, Texas A&M Univ. (United States)

Three-dimensional above-threshold analyses of high-index-contrast (HC) photonic-crystal (PC) quantum-cascade-laser (QCL) structures, for operation at watt-range CW powers in a single spatial mode, have been performed. Three-element HC-PC structures are formed by alternating active- antiguided and passive-guided regions along with respective metal-electrode spatial profiling. The 3-D numerical code takes into account absorption and edge-radiation losses. Rigrod's approximation is used for the gain. The specific feature QCL lasers is that only the transverse component of the magnetic field sees the gain. Results of above-threshold laser modeling in various approximate versions of laser-cavity description are compared with the results of linear, full-vectorial modeling by using the COMSOL package. Additionally, modal gains for several higher-order optical modes, on a 'frozen gain background' produced by the fundamental-mode, are computed by the Arnoldi algorithm. The gain spatial-hole burning effect results in increases of the competing modes' gain with drive current. Approaching the lasing threshold for a competing higher-order mode sets a limit on the single-mode operation range. The modal structure and stability are studied over a wide range in the variation of the inter-element widths. Numerical analyses predict that the proper choice of construction parameters ensures stable single-mode operation at high drive levels above

**Conference 9382:
 Novel In-Plane Semiconductor Lasers XIV**

threshold. The output power from a single-mode operated HC-PC QCL at a wavelength of 4.7 micron is predicted to be available at levels higher than 6 W, although this power may be restricted by thermal effects.

This work was supported by Air Force Research Laboratory under agreement number FA8650-13-2-1616.

9382-56, Session 13

Broadband external cavity-QCL with MOEMS diffraction grating for spectral scan rates in the kHz range

Ralf Ostendorf, Daniela Bleh, Fraunhofer-Institut für Angewandte Festkörperphysik (Germany); André Merten, Jan Grahmann, Fraunhofer-Institut für Photonische Mikrosysteme (Germany); Stefan Hugger, Hans-Joachim Wagner, Fraunhofer-Institut für Angewandte Festkörperphysik (Germany)

Broad band tunable external cavity quantum cascade lasers (EC-QCL) are versatile mid-infrared (MIR) light sources combining high brightness and wide spectral coverage of more than 300 cm⁻¹. Therefore, EC-QCLs are well-suited for the integration in optical spectroscopy systems identifying complex chemical compounds, e.g. in chemical or pharmaceutical in-line process control. However, many of these applications require short analysis times in the range of seconds or even below to perform quasi real-time measurements. To meet these requirements the wavelength scan rate of the EC-QCL has to be in the range of several Hz up to even kHz.

We present an EC-QCL combining a broad gain quantum cascade laser with a tuning range of more than 240 cm⁻¹ at 4.7 μm and a resonantly driven Micro-Opto-Electro-Mechanical (MOEMS) scanner with an integrated diffraction grating for wavelength selection in Littrow configuration. The grating geometry was optimized to provide high diffraction efficiency over the wide tuning range of the QCL, thus assuring high power density and high spectral resolution in the MIR range. The MOEMS scanner has a resonance frequency of 1 kHz, hence allowing for a complete wavelength scan of the EC-QCL within 1 ms.

9382-57, Session 13

Open-path atmospheric spectroscopy using widely-tunable quantum cascade lasers

Anish K. Goyal, Erik R. Deutsch, Ninghui Zhu, Petros Kotidis, Mark Norman, Jim Ye, Kostas Zafiriou, Alexander Mazurenko, Raymond F. Connors, Block Engineering, LLC (United States)

Widely tunable quantum cascade lasers (QCLs) spanning the long-wave infrared (LWIR) atmospheric transmission window and an HgCdTe detector were incorporated into a transceiver having a 50-mm-diameter transmit/receive aperture. The transceiver was used in combination with a 50-mm-diameter hollow retroreflector for the monitoring of atmospheric gases. Two rapidly tunable QCLs spanned the wavelength range of 7.7 to 13 microns within <0.2 second. Transmission measurements between the transceiver and retroreflector were made with a spectral resolution of 2 cm⁻¹ as a function of distance to the retroreflector with a maximum round-trip distance of >500 meters. Freon 132 and other gases were sprayed into the beam path and the concentration-length product (CLP) was measured as a function of time. The system exhibited a noise-equivalent concentration (NEC) of 3 ppb for Freon 132 for a round-trip path of 310 meters. Algorithms based on correlation methods were used to both identify the gas and to determine its CLP as a function of time. This presentation will detail the system design and detection algorithm. Also discussed will be the relative advantages of QCL-based open-path spectrometers with those based

on Fourier-transform infrared (FTIR) spectrometers for the monitoring of atmospheric gases.

9382-58, Session 13

Characterization of an InGaAs/InP-based echelle mirror multiplexer for widely-tunable mid-IR sources based on quantum cascade lasers

Luis Jorge Orbe Nava, Guillermo Carpintero del Barrio, Univ. Carlos III de Madrid (Spain); Gregory Maisons, Clément Gilles, Fahem Boulila, Mathieu Carras, III-V Lab. (France)

We present the experimental characterization results of a 30-to-5 wavelength multiplexer for a Distributed Feedback Quantum Cascade Laser (DFB QCL) array operating in the 7-8.5 μm (mid-long) infrared (IR) range. This design is customized for its use among a DFB QCL array with a 0.05 μm wavelength channel space for spectroscopy applications, and it is proposed in order to achieve a continuous tuning range overcoming the limited tunability of individual QCLs, which is necessary for multi-gas or complex molecule detection.

This multiplexer design is based on an Echelle diffraction mirror grating scheme with multiple output waveguides, which allows us to characterize the wavelength deviation of the device and optimize the placement of the input and output guides for monolithic integration along with DFB QCL arrays, providing a number of advantages such as a higher stability, less complexity and lower cost over other technologies such as external cavities.

We discuss the effects over the device performance of the design, such as the diffraction effects, input channel width overlapping/crosstalk and input channel profile, which are very important to address in order to avoid unaccounted transmission losses. Other parameters such as the profile of the input and output waveguides and fabrication limitations are also discussed as their effect on the device is observed.

A series of characterization tests are presented in order to compare both simulated and experimental results, placing them as suitable options when comparing to other IR multiplexer schemes in terms of size and power transmission.

9382-59, Session 13

Destructive physical analysis of degraded quantum cascade lasers

Yongkun Sin, Zachary Lingley, Miles Brodie, Nathan Presser, Steven C. Moss, The Aerospace Corp. (United States); Jeremy D. Kirch, Chun-Chieh Chang, Colin Boyle, Luke J. Mawst, Dan Botez, Univ. of Wisconsin-Madison (United States); D. Lindberg III, Thomas Earles, Intraband, LLC (United States)

Remarkable progress made in QCLs has led them to find an increasing number of applications in remote sensing, chemical sensing, and free space communications, in addition to potential space applications. However, little has been reported on reliability and failure modes of QCLs although it is crucial to understand failure modes and underlying degradation mechanisms in developing QCLs that meet lifetime requirements for space missions. Focused-ion-beam (FIB) techniques have been employed to investigate failure modes in various types of laser diodes, but few groups have used this technique to investigate failure modes in QCLs. In our study, we report on destructive physical analysis (DPA) of degraded InGaAs-InAlAs QCLs using FIB and high-resolution TEM techniques.

The active region of QCLs that we studied consisted of 30-stage layers of lattice-matched InGaAs-InAlAs heterostructure. The MOVPE-grown laser

**Conference 9382:
Novel In-Plane Semiconductor Lasers XIV**

structures were fabricated into deep-etched ridge waveguide QCLs. Failures were generated via accelerated lifetesting of QCLs. FIB systems were used to study the damage area on the front facet and also to prepare TEM cross sections at different locations along the waveguide for defect and chemical analyses using a HR-TEM. In contrast to the COMD damaged area showing as a blister on the front facet of QW lasers, the damaged area of QCLs was significantly extended into the InP substrate due to a much less absorption of lasing photons in QCLs. Our DPA results from degraded QCLs lifetested under different conditions will be presented. We will also provide possible degradation processes responsible for failures in QCLs.

Conference 9383: Light-Emitting Diodes: Materials, Devices, and Applications for Solid State Lighting XIX

Tuesday - Thursday 10-12 February 2015

Part of Proceedings of SPIE Vol. 9383 Light-Emitting Diodes: Materials, Devices, and Applications for Solid State Lighting XIX

9383-1, Session 1

Pathways to ultra-efficient solid-state lighting (*Invited Paper*)

Mary H. Crawford, Sandia National Labs. (United States)

Solid-state lighting is a rapidly advancing technology with potential to provide decisive energy savings and functionality well beyond traditional lighting systems. Already, the efficiency of commercial white LEDs has surpassed that of incandescents and exceeds that of compact fluorescents in particular applications. Research efforts are now focused on achieving a system efficiency of 50%; a technology roadmap target that, along with quality-of-light metrics, is expected to realize the vision of solid-state lighting as a truly disruptive technology. While achieving this goal will have major impact, there is no fundamental reason why even higher efficiencies could not be achieved. In this presentation, we will explore the science challenges of achieving "ultra-efficient" solid-state lighting, focusing on the LED-chip level. In particular, we will review recent insights into the mechanisms behind "efficiency droop" of InGaN LEDs under high current operation. We will present recent advances that show promise for bridging the "green-yellow" gap in LED efficiency including nanostructured InGaN LEDs. We will further describe the continuing search for a higher-efficiency, red (~614 nm), narrow-band emitter, presenting challenges and potential solutions for direct emitters as well as down-conversion materials. Finally, we will show how overcoming these challenges may enable "smart lighting" concepts, providing a new paradigm for how we generate and use light. Acknowledgements: Jeffrey Tsao, Michael Coltrin, George Wang, Daniel Koleske, Weng Chow, Jonathan Wierer, Andrew Armstrong, Jeremy Wright, Igal Brener, May Nyman, James Martin, Lauren Shea-Rohwer, E. Fred Schubert, and Xiaoyang Zhu.

9383-2, Session 1

Synthesis and characterization of red emitting $\text{Eu}^{3+}:\text{K}_3\text{Y}_3(\text{BO}_3)_4$ phosphor

Basavapoorima Ch, Sowjanya G., Chalicheemalappalli K. Jayasankar, Rama Moorthy L, Sri Venkateswara Univ. (India); Venkata Krishnaiah, Ecole Polytechnique de Montréal (Canada)

Now-a-days the fabrication of new full-color displays using a single-emitting component is one of the major challenges of the solid state lighting technology. Rare-earth (RE) doped phosphors are important in the production of artificial light owing to their stable physical and chemical properties. Borate based luminescent materials exhibit interesting optical and luminescence properties allowing them to be used in lighting applications. In the present work, the detailed results on synthesis, structural and luminescent properties of a new inorganic phosphor, $\text{K}_3\text{Y}_3(\text{BO}_3)_4$ doped with Eu^{3+} ions, have been presented. The $\text{K}_3\text{Y}_3(\text{BO}_3)_4$ phosphor exhibits monoclinic structure with a particle size of 60 nm. From the SEM image, the particles are of irregular in shape with flake type structures and distributed non-uniformly. The excitation spectra were recorded by monitoring a red emission at 610 nm and broad excitation band observed in the lower wavelength region, 250 - 280 nm (O_2^- - Eu^{3+}). The PL spectrum exhibits typically Eu^{3+} emission lines at 578 nm ($5\text{D}_0?7\text{F}_0$); 585, 590 and 600 nm ($5\text{D}_0?7\text{F}_1$); 615, 620 and 626 nm ($5\text{D}_0?7\text{F}_2$); 651 nm ($5\text{D}_0?7\text{F}_3$); 689 nm ($5\text{D}_0?7\text{F}_4$). The chromaticity coordinates are found to be (0.62, 0.34) which is well with in the red region. The decay curves are found to be

single exponential for lower concentrations and tend to be non-exponential at high concentrations with shortening of lifetime (2.72 ms to 0.86 ms). The systematic investigation and results obtained indicate that this material is an ideal candidate for light emitting diode applications.

9383-3, Session 1

Application of airy beams to bending functions of automotive headlights

Ceren Altingöz, Magneti Marelli Mako Elektrik Sanayi Ticaret A.S (Turkey)

Contrary to common belief, light does not all the time propagate linearly. Hence it tends to bend when it takes the form of airy wave packets. This paper describes a first possible application of such wave packets to automotive lighting technology.

After a first brief description of the historical background of the airy beams principle and their potential applications, an analysis of these beams under potential-free Schrödinger equation with detailed physical formulations is proposed.

Considering that one of the most peculiar characteristic of airy waves is that they stay diffraction free when propagating, 'diffraction' and 'diffraction-free propagation' aspects and the physics behind them are then analyzed and described at the second step.

In the third part of the paper, the characteristics of Bessel beams, and their diffraction free behavior is explored and a comparison between Bessel beams and airy beams is crosschecked.

As airy beams do accelerate during propagation, they describe a ballistic trajectory and so bend. Up to now, these beams were mainly used to generate curved plasma channels in air and for particle separation in optical trapping applications.

We investigate in our paper how the bending property of Airy beams could be used to achieve illumination in curved roads and corners in an automotive lighting application.

Considering that so far, Airy beams were never thought to be a possible alternative to the current mechanical systems used to provide a "bending light" function, we describe how this could be achieved and what are the next steps to be investigated.

9383-4, Session 1

Rapid prototyping of reflectors for vehicle lighting using laser activated remote phosphor

Roland Lachmayer, Gerolf Kloppenburg, Roman Danov, Alexander G. Wolf, Leibniz Univ. Hannover (Germany)

Bright white light sources are of significant importance for automotive front lighting systems. Today's upper class vehicles mainly use HID or LED as light source. As a further step in this development laser diode based systems offer high luminance, efficiency and allow the realization of new styling concepts and new dynamic lighting functions. These white laser diode systems can either be realized by mixing different spectral sources or by combining diodes with specific phosphors.

Based on the approach of generating light using a laser and remote

Conference 9383: Light-Emitting Diodes: Materials, Devices, and Applications for Solid State Lighting XIX

phosphor, lighting modules are manufactured. Four blue laser diodes (450 nm) are used to activate a phosphor coating and thus to achieve white light. A segmented paraboloid reflector generates the desired light distribution for an additional car headlamp. We use high speed milling, selective laser melting as well as 3D-plastic-printing with coated surface to build the reflector system for this lighting module. We compare the spectral reflection grade of these materials. Furthermore the generated modules are analyzed regarding their efficiency, light distribution and the quality of the emitted white light. The use of Rapid Prototyping technologies allows an early validation of the chosen concept and is supposed to reduce cost and time in the product development process significantly. Therefore we discuss costs and times of the applied manufacturing technologies.

9383-5, Session 2

Regularly-patterned non-polar InGaN/GaN quantum-well nanorod light-emitting diode array *(Invited Paper)*

Charng-Gan Tu, Che-Hao Liao, Chia-Ying Su, Yu-Feng Yao, Horng-Shyang Chen, Chieh Hsieh, Hao-Tsung Chen, Yean-Woei Kiang, Chih-Chung Yang, National Taiwan Univ. (Taiwan)

Among the reported MOCVD-grown, regularly-patterned nanorod (NR) light-emitting diode (LED) arrays, which are expected to have a more uniform behavior among NRs, when compared with a randomly distributed NR array, either the mixed emission of non-polar and semi-polar quantum wells (QWs) or that of non-polar and polar QWs was observed. Also, detailed LED characteristics, such as non-polar emission behavior and QW internal quantum efficiency, have not been investigated yet. A regularly patterned NR LED array with pure non-polar emission can have higher emission efficiency. Meanwhile, the understanding of more detailed characteristics of such an NR LED array can guide us to further explore the potential of NR LED development. In this paper, the growth and process of a regularly patterned NR-array LED device with its emission completely from sidewall non-polar QWs are demonstrated. A pyramidal un-doped GaN structure is intentionally formed at the NR top for minimizing the current flow through this portion of the NR such that the injection current can be effectively guided to the sidewall m-plane InGaN/GaN QWs for emission excitation by a conformal transparent conductor (GaZnO). The electrical property of the NR LED device is similar to that of a planar c-plane or m-plane LED. The blue-shift trend of NR LED output spectrum with increasing injection current is caused by the non-uniform distributions of QW width and indium content along the height on a sidewall. The photoluminescence spectral shift under reversed bias confirms that the emission of the fabricated NR LED comes from non-polar QWs.

9383-6, Session 2

High-power phosphor-free InGaN/AlGaIn dot-in-a-wire core-shell white light-emitting diodes

Hieu P. Nguyen, New Jersey Institute of Technology (United States); Mehrdad Djavid, Xianhe Liu, Qi Wang, Zetian Mi, McGill Univ. (Canada)

III-nitride nanowire structures have been intensively studied and shown tremendous promise for applications in solid state lighting. However, the performance of nanowire LED structures suffers from large nonradiative surface recombination, leading to extremely low quantum efficiency and very low output power. In this regard, we have developed unique self-organized InGaN/AlGaIn dot-in-a-wire core-shell LED structures that can address the afore-mentioned critical challenges for achieving high efficiency, full-color LEDs. Strong white-light emission is recorded for this core-shell LED with an output power of >5 mW, measured under an injection current -

60 A/cm².

Self-organized InGaN/AlGaIn dot-in-a-wire core-shell LEDs were grown on Si(111) substrates by plasma-assisted molecular beam epitaxy under nitrogen-rich conditions. GaN segment was grown at - 770 oC while InGaN/AlGaIn quantum dot active region was grown at 640oC to enhance In incorporation. An AlGaIn shell layer is spontaneously formed during the growth of the quantum dot active region. The repeated growth of multiple, vertically aligned InGaN/AlGaIn quantum dots enables the formation of a relatively thick, uniform AlGaIn shell surrounding the device active region. The barrier of each quantum dot is modulation doped p-type using Mg to enhance hole transport. Moreover, the p-doped AlGaIn barrier layers can serve as distributed electron blocking layers to effectively reduce electron overflow. The resulting phosphor-free core-shell white-light LEDs exhibit record-high output power of > 5mW which is more than two orders of magnitudes higher compared to those of InGaN/GaN nanowire LEDs without AlGaIn shells. Additionally, such white LEDs exhibit high color rendering index of ~95.

9383-7, Session 2

Group III-nitride semiconductor nanostructures for LEDs and novel photonic devices *(Invited Paper)*

Yong-Hoon Cho, KAIST (Korea, Republic of)

(invited) Although much attention has been paid to group III-nitride semiconductors and their heterostructures due to their wide range of bandgap energy and versatile optoelectronic applications, there still exist serious problems such as large density of dislocations, poor material quality of high-In-content InGaIn, strong built-in internal electric field along the c-axis growth direction. To overcome these obstacles, low-dimensional semiconductor nanostructures have attracted a lot of attention due to their rich and unique optical properties. In this talk, we present various types of nitride semiconductor nanostructures and their applications in LEDs and novel photonic devices. Group III-nitride-based pyramidal, annular, columnar, and tapered structures were successfully fabricated by means of metal-organic chemical vapor deposition and/or vapor-phase chemical etching techniques. First, InGaIn/GaN multiple quantum wells were grown on GaIn-based pyramidal and annular templates, exhibiting broad-band multi-color visible light emission. Electrically driven light emitting diodes were also demonstrated using these GaIn-based hexagonal structures. Next, InGaIn/GaN multiple quantum wells were deposited on the surface of slightly tapered GaIn rods on Si substrates, and intriguing unidirectional photonic diode behaviour was observed. Finally, InGaIn-based single quantum dot arrays were formed on tapered and pyramidal GaIn nanostructures and ultrafast and high efficiency single photon generation was demonstrated by virtue of spontaneous formation of single quantum dot on the apex of tapered GaIn nanostructures. An overview and comparison of the characteristics of the above nanostructures will be given.

9383-8, Session 2

Optical properties and efficiency of nonpolar/semipolar InGaIn QWs on GaIn core-shell microrods for solid-state-lighting

Christian Mounir, Ulrich T. Schwarz, Univ. of Freiburg (Germany); Tilman Schimpke, Martin Mandl, Martin Strassburg, OSRAM Opto Semiconductors GmbH (Germany)

With their unique properties, core-shell group III nitride microrods are very promising candidates for solid state lighting. In addition to their almost perfect crystalline quality and the reduced quantum confined Stark effect on their semipolar/nonpolar facets, which potentially leads to higher radiative

Conference 9383: Light-Emitting Diodes: Materials, Devices, and Applications for Solid State Lighting XIX

efficiency, they allow to achieve very large active area compared to standard planar technology. This should allow operating the light emitting diode (LED) with reduced droop and hence increased efficiency. The efficiency of state-of-the-art group III nitride microrods remains however still behind the performance of conventional GaN-based LEDs.

In our work we investigate the optical properties and internal quantum efficiency (IQE) of InGaN QWs grown on GaN core-shell microrods with micro-photoluminescence (μPL) and micro-electroluminescence (μEL). The Ga-polar microrods were grown by selective area growth using a SiO₂ mask. Their side facets are nonpolar m-planes and their tip is formed by (10-11) semipolar facets. We confront our experimental results with k·p envelope function simulations of QWs of different crystal orientations.

The diffraction-limited spatial resolution of our measurement is at most one order of magnitude smaller than the microrods scale. μPL and μEL allow to access the optical polarization properties of the emission by adding a polarizer in the collection optics and the IQE of the active region by resonant excitation or electrically contact the device.

We discuss our results obtained on the different facets to get insight on the microrods and core-shell QW design for optimal efficiency.

9383-9, Session 2

Selective-area growth of InGaN/GaN nanocolumnar structures for classical and quantum light sources (*Invited Paper*)

Enrique Calleja, Ana Bengoechea-Encabo, Steven Albert, Arkar Gaevii, Miguel Angel Sanchez-Garcia, David Lopez-Romero, Univ. Politécnic de Madrid (Spain)

Selective Area Growth (SAG) by Molecular Beam Epitaxy (MBE) is applied to develop a variety of nanostructures on different substrates.

Axial InGaN/GaN NanoLED structures are fabricated on GaN templates as well as on Si(111) substrates with a thin GaN buffer. On the last substrate, by precise control of growth temperature and III/V ratio, the whole In composition range in InGaN alloys is achieved, covering most of the visible range and the near IR.

Core-shell InGaN/GaN microstructures have been developed following two methods: i) use of top-down (etched) GaN cores and ii) use of bottom-up GaN cores grown by MOVPE. In both cases a subsequent conformal growth of InGaN layers was achieved. The quality of the resulting layers is exceptionally high. In case ii), full core-shell LEDs are developed and individually characterized by measuring the electroluminescence spectra locally (micro needles contact).

A common feature in both cases is that the In incorporation depends significantly on the crystal plane considered, either m- or r-plane, giving rise to two InGaN related emissions. Based on this effect, dot-in-a-wire InGaN structures were grown embedded in ordered GaN nanowires. The resulting structures showed sharp and distinct intense peaks by micro PL. Single PL peaks as narrow as 500 microeV were observed in single nanostructures. Correlation measurements showed the emission of single photons up to 80K. Detailed analysis and discussion will be presented.

9383-10, Session 3

Fabrication of nitride LEDs on amorphous substrates by pulsed sputtering (*Invited Paper*)

Hiroshi Fujioka, The Univ. of Tokyo (Japan) and JST, CREST (Japan)

It is well known that group III nitride devices exhibit high performance but their applications are limited in high-end devices because their fabrication process involves low throughput high temperature epitaxial growth by MOCVD. It is quite natural to expect that group III nitride devices prevail

widely among various new application fields once low cost fabrication process is established. Large area nitride devices such as solar cells and displays are among these applications. For this purpose, we have recently developed a new low cost growth technique named PSD (pulsed sputtering deposition). PSD has already attracted much attention of industry engineers because its productivity is much higher than that of MOCVD. In this technique, surface migration of the film precursors is enhanced and, therefore, the temperature for epitaxial growth is dramatically reduced. This reduction allows us to utilize large area low cost substrates such as glass that were not used for growth of semiconductors so far due to their low softening temperatures. In this presentation, we will discuss feasibility of large area nitride devices such as LED displays or solar cells fabricated with a low temperature PSD technique and graphene buffer layers on amorphous substrates. We will also show that low temperature PSD is quite promising for growth of high In concentration InGaN which is necessary for fabrication long wavelength optical devices.

9383-11, Session 3

Flip-chip multiple-active-region AlGaInP light-emitting-diodes with transferred sapphire substrate

Guang-di Shen, Li Ma, Peng Lian, Beijing Univ. of Technology (China)

To reduce carrier leakage under high current injection level and enhance light extraction of light emitting diodes, a novel transferred substrate flip-chip multiple-active-region (FCMAR) structure was applied in AlGaInP-based LEDs. The FCMAR LED epitaxial layer was grown by MOCVD on n-GaAs substrate. Two active regions were fabricated in the LED epitaxial layer, between the two active regions there is a GaAs reverse tunneling junction. On the other hand, a 300 nm thick spin-on-glass (SOG) was coated on the top of the sapphire substrate as a transparent adhesive layer. The two wafers were then bonded together by applying a uniform pressure. Thereafter, GaAs substrate was lifted off by polishing and wet etching process. The surfaces of the bonded samples were then partially etched until the p-GaP layers were exposed. Be/Au and AuGeNi/Au were deposited as p-type and n-type ohmic contact. We then bumped gold studs onto the Si submount and subsequently flipped the processed LED chip onto the submount. In this way, the light can emit from the back side without substrate absorption; meanwhile, the high heat can be dissipated by a thermal conductive submount. For comparison, conventional multiple-active-region AlGaInP LEDs with transferred sapphire substrate were also fabricated. Optical, electrical and thermal characterizations of these LEDs were measured and analyzed, respectively. The results showed that the FCMAR LEDs presented better properties.

9383-12, Session 3

Aluminum-doped zinc oxide current spreading layer on P-side up thin-film AlGaInP-based light-emitting diodes by ALD

Ming-Chun Tseng, Chi-Lu Chen, Nan-Kai Lai Lai, Dong-Sing Wu, National Chung Hsing Univ. (Taiwan); Hsin-Ying Lee, National Cheng Kung Univ. (Taiwan); Yu-Chang Lin, Ray-Hua Horng Horng, National Chung Hsing Univ. (Taiwan)

A twice wafer-transfer technique can be used to fabricate high-brightness p-side-up thin-film AlGaInP-based light-emitting diodes (LEDs) with an aluminum-doped zinc oxide (AZO) thin films transparent conductive layer deposited on a GaP window layer. The GaP window layer consist of the two different doping profile, the carbon doped GaP (GaP:C) window layer of 50 nm is on the top of Mg doped GaP window layer of 8 μm. The GaP:C window layer is used to improved the ohmic contact properties of GaP:C/AZO. The

Conference 9383: Light-Emitting Diodes: Materials, Devices, and Applications for Solid State Lighting XIX

AZO with different cycle ratio of Zn:Al (15:1, 20:1 and 25:1) is deposited on GaP:C window layer as current spreading layer by atomic layer deposition. The AZO layer can be used to improve light extraction, which enhances light output power. The output power of p-side-up thin-film AlGaInP LED with an AZO layer of 20:1 cycle ratio has improved up to 19.2 % at injection current of 350 mA, as compared with that of LED without AZO film. The p-side-up thin-film AlGaInP LED with AZO current spreading layer exhibited excellent performance stability, the emission wavelength shift of p-side-up thin-film AlGaInP LED without and with AZO film are 18.2 nm and 11.2 nm under the injection current increased from 20 mA to 1000mA, respectively. This stability can be attributed to the following factors: 1) Refractive index matching, performed by introducing AZO thin film between the epoxy and the GaP window layer enhances light extraction; and 2) the favorable thermal dissipation of the silicon substrate reduces thermal degradation.

9383-13, Session 3
Green (In,Ga,Al)P-GaP light-emitting diodes grown on high-index GaAs surfaces

Nikolay N. Ledentsov, Vitaly A. Shchukin, VI Systems GmbH (Germany); Jari Lyytikäinen, Oleg Okhotnikov, Tampere Univ. of Technology (Finland); Yuri Shernyakov, Alexey Payusov, Nikita Y. Gordeev, Mikhail Maximov, Ioffe Physical-Technical Institute (Russian Federation)

Green (550–560 nm) electroluminescence (EL) from $(\text{Al}_{0.5}\text{Ga}_{0.5})\text{InP}/(\text{Al}_{0.8}\text{Ga}_{0.2})\text{InP}$ double p-i-n heterostructures grown on (100) and high-index GaAs substrates by molecular beam epitaxy is studied. As was previously proposed [1], growth of tensile-strained GaP-rich insertions on substrate orientations different from (100) may allow significant bandgap engineering in the In-Ga-Al-P/GaAs systems with extension of the direct bandgap. GaP has the highest conduction band energy among III-V semiconductors, furthermore, in the related In-Ga-Al-P heterostructures lattice-matched to GaAs substrate, GaP-rich insertions are under biaxial tensile strain which may further increase the barrier height. Growth on (100) surface is resulting in the splitting of the triply degenerated conduction band at the X-point of the Brillouin zone thus lowering the barrier. The splitting is maximum for the structures grown on GaAs(100) substrate but vanishes for the structures grown on GaAs(111) where the tensile strain only increases the X minimum energy further. The structures were grown side-by-side on (100), (311)A, and (211)A GaAs substrates. High-index surfaces are unstable towards surface nanofaceting resulting in spontaneous formation of natural tilted short period superlattices with InP- and GaP-rich domains [2] allowing self-organized band-engineering of the alloy. Furthermore we introduced additional monolayer scale GaP barriers into the p-doped $(\text{Al}_{0.8}\text{Ga}_{0.2})\text{InP}$ cladding layers. As (211) surface is the closest to (111) orientation in our experiment, the effect of GaP barriers is modeled to be the maximum one. LEDs fabricated in the ridge-stripe geometry are characterized. At low and moderate current densities ($\sim 5000\text{A}/\text{cm}^2$) the EL intensity of the structures is comparable for all substrate orientations. For (100) grown-structures the EL strongly saturates at higher current densities and a long wavelength tail evolves. We attribute the effects to the filling of the indirect minimum and the nonequilibrium carrier escape into the staggered-lineup $(\text{Al}_{0.8}\text{Ga}_{0.2})\text{InP}$ cladding layer. The (211) and (311)-grown devices demonstrate the EL spectra shifted towards the shorter wavelengths ($\sim 550\text{ nm}$ at room temperature). A much higher EL intensity is achieved in LEDs at high current densities ($>10000\text{A}/\text{cm}^2$) in this case. The integrated intensity of (311) grown structures gradually saturates above $4\text{ kA}/\text{cm}^2$. No saturation of the integrated intensity is revealed for (211)-grown structures up to $14\text{ kA}/\text{cm}^2$.

[1] N. N. Ledentsov, et al., Proc. 2012 Advanced Research Workshop (FTM-7), June 25–29, 2012: Corsica, France, in "Future Trends in Microelectronics: Into the Cross Currents", S. Luryi, J. Xu, and A. Zaslavsky, Eds, 2013, Wiley, pp. 142–160.

[2] V. Shchukin, et. al., Microelectronics Journal, 37, pp. 1451–1463 (2006).

9383-14, Session 3
A novel design and process for improving the efficiency and reliability of an AC direct LED chip (Invited Paper)

Yongil Kim, Chan M. Lim, Wanho Lee, Jin-Young Choi, Seunghwan Lee, Gi Bum Kim, Young Sun Kim, Yoon Joon Choi, SAMSUNG Electronics Co., Ltd. (Korea, Republic of)

We have developed a low-cost AC direct LED chip in which bridge rectifiers are implemented within multi-cell array. Within this talk, we will discuss effects of cell array design on the luminous efficiency, and present a process to improve the efficiency. Furthermore, a degradation mechanism of optical and electrical properties due to the high reverse voltage implied to a bridge rectifier and an advancement in the structure of the chip to overcome the degradation will be discussed.

9383-15, Session 4
Defects in GaN-based LEDs and lasers: impact on internal quantum efficiency and on reliability (Invited Paper)

Matteo Meneghini, Gaudenzio Meneghesso, Enrico Zanoni, Univ. degli Studi di Padova (Italy)

Over the last decade the technology of InGaN-based LEDs and lasers has shown impressive improvements: white LEDs with efficacies in excess of $270\text{ lm}/\text{W}$ have already been demonstrated, while watt-class laser diodes are already available. The performance and the reliability of InGaN-based optoelectronic devices strongly depend on the quality of the material; more specifically: (i) point and extended defects may act as SRH (Shockley-Read-Hall) recombination centers, thus limiting the efficiency of the devices at low current levels, and increasing the threshold current of laser diodes; (ii) high SRH recombination components can favor the thermal droop, i.e. the decrease in internal quantum efficiency (IQE) at high temperature levels; (iii) during long-term operation, the generation of lattice defects may lead to a significant degradation of the devices (decrease in IQE, increase in the threshold current of laser diodes).

This presentation reviews the properties of the defects which limit the performance and the reliability of LEDs and lasers based on GaN. More specifically: (i) we discuss the physical origin and properties of the defects responsible for SRH recombination in InGaN-based LEDs and lasers; (ii) we describe and discuss the properties of dislocation-related defects, and their impact on device performance; (iii) we describe the role of defects in favoring the degradation of InGaN-based lasers and LEDs; (iv) we present a detailed investigation of the properties of the lattice defects generated as a consequence of long-term ageing. Original data are compared to previous literature reports to provide a clear understanding of the topic.

9383-16, Session 4
Structural investigation of the deep-green InGaN LEDs by transmission electron microscopy

Maxim Korytov, Nikolay Cherkashin, Ctr. d'Elaboration de Matériaux et d'Etudes Structurales (France); Andrei F. Tsatsulnikov, Alexey V. Sakharov, Andrey Nikolaev, Wsevolod V. Lundin, Martin Hytch, Ioffe Physical-Technical Institute (Russian Federation)

We report on a systematic study of the luminous efficacy of single quantum well (QW) deep-green light-emitting diodes grown by metal-organic vapor phase epitaxy as dependent on the QW thickness and composition. When

Conference 9383: Light-Emitting Diodes: Materials, Devices, and Applications for Solid State Lighting XIX

the QW thickness increases from 1.7 nm to 3.0 nm the electroluminescence (EL) peak position shifts from 507 nm to 585 nm, while the EL peak intensity exhibits rather unexpected behavior: it increases with increase of the wavelength, reaches its maxima around 540 nm and then it begins to decrease monotonically.

The QW morphology, the strain relaxation mechanisms and the In distribution in the active region were investigated by various methods of transmission electron microscope (TEM). The local chemical composition was determined by a recently invented dark-field electron holography (DFEH) technique with the Hitachi HF3300 in-situ interferometry microscope (I2TEM), which allows precise composition measurement with a high spatial resolution up to 0.4 nm.

The TEM study showed that the thick QWs have a regular shape with abrupt interfaces and constant composition, while decrease of the QW growth time produces unintentional composition gradient inside the QW. Moreover an enhancement of the surface segregation effect causing penetration of In into the GaN barrier was evidenced. The observed effects of the composition redistribution were investigated by TEM as a function of the In content of the QW. Experimentally measured composition profiles were used to simulate the QW band structures with a Schrödinger-Poisson solver. Besides the factors governing incorporation of In during the growth of In-rich InGaN QWs are discussed.

9383-17, Session 4

Blue luminescence and quantum-confined Stark effect in green InGaN/GaN quantum wells

Felix Nippert, Technische Univ. Berlin (Germany); Anna Nirschl, Ines Pietzonka, OSRAM Opto Semiconductors GmbH (Germany); Tobias Schulz, Martin Albrecht, Leibniz-Institut für Kristallzüchtung (Germany); Thomas Kure, Christian Nenstiel, Steffen Westerkamp, Gordon Callsen, Technische Univ. Berlin (Germany); Martin Strassburg, OSRAM Opto Semiconductors GmbH (Germany); Axel Hoffmann, Technische Univ. Berlin (Germany)

We have investigated several InGaN/GaN quantum wells of high structural quality by means of (time-resolved) photoluminescence and photoluminescence excitation spectroscopy. We find that their optical properties are governed not only by the well-known quantum-confined Stark effect (QCSE), but also by a strong and very fast decaying "Blue Luminescence" (BL) in high excitation power density conditions, that we tentatively attribute to excited states of the quantum wells. The influences of QCSE and BL on the internal quantum efficiency are discussed as well as implications for optimal device design.

9383-18, Session 4

Trap-assisted tunneling in InGaN/GaN single-quantum-well LEDs

Matthias Auf der Maur, Univ. degli Studi di Roma "Tor Vergata" (Italy); Bastian Galler, Ines Pietzonka, Martin Strassburg, Hans-Juergen Lugauer, OSRAM Opto Semiconductors GmbH (Germany); Aldo Di Carlo, Univ. degli Studi di Roma "Tor Vergata" (Italy)

III-nitride LEDs often exhibit abnormally high ideality factors. Based on numerical simulations and comparison with measured current-voltage characteristics of blue single-quantum-well devices, we demonstrate that a trap-assisted tunneling model introduced for pn-junctions by Hurkx et al. in 1992 can accurately describe III-nitride quantum well LED currents at low forward bias. By adjusting trap energy level, density and spatial location, we obtain a good fit for a series of devices with different quantum well

thicknesses between 3-5 nm and Indium content in the range of 16-22%.

We find that the low forward leakage current of devices with ideality factors < 4 can be ascribed to tunneling in the electron blocking layer assisted by trap states with parameters compatible with the Magnesium dopants. The studied devices with higher leakage currents and ideality factors > 10 , on the other hand, can be well described by mid-gap trap states inside the active region. We also find that the density of trap states needed to fit the IV characteristics in the latter case is correlated with the planar strain energy density in the active region. Since the shape of the non-exponential current-voltage characteristics of these devices strongly depends on the electric field, we used a certain amount of polarization field relaxation as additional fitting parameter. The amount of this relaxation is also found to be correlated with the planar energy density.

Our results suggest the appearance of deep trap levels in the active region for Indium contents $> 18\%$, and a dependency of the amount of such traps on the amount of strain energy in the quantum well.

9383-19, Session 4

Nanolasers as solution to efficiency droop in solid-state lighting

Weng W. Chow, Sandia National Labs. (United States)

Considerable resources are being devoted to advancing light-emitting diodes (LEDs) for solid-state lighting. Particularly challenging is the saturation in output intensity with increasing current (dashed curve, Fig. 1a). The problem is often cast in terms of efficiency degradation with increasing excitation, i.e., efficiency droop (dashed curve, Fig. 1b). This paper proposes and analyzes a solution via replacement of LEDs with lasers. Important mechanisms are population clamping at high pump rate to limit Auger carrier loss, and unity spontaneous emission factor at low pump rate to efficiently channel light out of the cavity and into the output beam when operating below lasing threshold. The results are obtained using a semiconductor quantum-optical theory for InGaN quantum wells in a nanocavity. Spontaneous and stimulated emissions are treated on equal footing by quantization of both carriers and radiation.

9383-20, Session 5

GaN native substrate full-visible-spectrum LEDs for illumination (*Invited Paper*)

Michael R. Krames, Soraa, Inc. (United States)

Breakthroughs in Japan in the late 1980s and early 1990s enabled the synthesis of single-phase GaN on a foreign substrate (sapphire) and paved the way for practical violet, blue, and green emitting light-emitting diodes (LEDs). This was especially important since, unlike other semiconductor materials, GaN cannot be grown from the melt and so GaN substrates were not readily available. In addition, due to the optical properties of InGaN, a fairly high dislocation density (caused by heteroepitaxy on foreign substrates) was surprisingly well tolerated, and very efficient white-emitting LEDs were developed on platforms such as GaN-on-sapphire and GaN-on-SiC for lighting and display applications.

During the last decade, GaN-based laser diodes were developed as well. However, these devices, operating at about 100x the current density of LEDs, could not tolerate the high dislocation densities of standard heteroepitaxy from a reliability standpoint. This drove the development of dislocation density reduction technologies, which culminated in the development of quasi-bulk GaN substrates by thick hydride-vapor-phase-epitaxy (HVPE). However, due to their relatively high cost and the (perceived) lack of benefit for LEDs, they were (mostly) relegated as substrates for laser diodes.

We show that the myriad benefits of the native substrate do in fact have dramatic consequences for LEDs. These benefits, including lower dislocation density, improved thermal conductivity, optical, refractive index match, and simpler fabrication combine to provide unique cost and performance

Conference 9383: Light-Emitting Diodes: Materials, Devices, and Applications for Solid State Lighting XIX

characteristics. Results of this approach, termed GaN-on-GaN™, include higher potential external quantum efficiencies in the violet wavelength regime, very low “droop” characteristics by mitigating Auger recombination, and very high overall power conversion efficiencies (> 80%). Using this platform has offered, for the first time, full-visible-spectrum solid-state lighting products with combined inherent brightness advantages and power handling capability, and improved light quality including high color rendering, and whiteness rendering (from excitation of optical brighteners in many white materials). Details of GaN-on-GaN LED and product performance will be given in the oral presentation.

9383-21, Session 5

Flexible optical system for large-area LED luminaires with excellent light uniformity and efficiency

Oscar Fernandez, Rolando Ferrini, Frédéric Zanella, Martin Stalder, Benjamin Gallinet, Ctr. Suisse d'Electronique et de Microtechnique SA (Switzerland)

Today, most large-area LED-based products use relatively simple solutions to achieve the required spatial luminance uniformity. Such solutions require either inefficient light scattering sheets or costly short-pitch LED arrays.

We present a flexible, roll-to-roll compatible and thin form-factor innovative optical system that demonstrates excellent luminance uniformity and high efficiency in combination with large-area, long-pitch LED arrays. This excellent performance is the result of a highly engineered combination of diffractive and refractive optical elements with parameters carefully optimized using interfaced rigorous and ray-tracing modelling tools.

The optical system presented here is a fundamental part of a cost-efficient, large-area, intelligent lighting module whose targeted specifications include 180lm/W efficacy and 95% luminance uniformity and that is currently been developed in the framework of the EU-funded project LASSIE-FP7.

9383-22, Session 5

Large area lighting applications with organic dye embedded flexible film

Huang Yu Lin, National Chiao Tung Univ. (Taiwan)

A flexible large area lighting devices have been demonstrated by PDMS films. The (polydimethylsiloxane)PDMS film is favorable for heat stability, good transparency, and flexibility. This study aimed to combine both organic and inorganic materials for flexible large area lighting applications. The architecture consists of blue LEDs coupled to a leaky waveguide that is covered with the PDMS film. The white light was generated with the poly (9, 9-dioctylfluorene-co-benzothiadiazole)F8BT blended into the PDMS slurry. Organic wavelength conversion materials were chosen owing to their ability to decompose in nature. The more conventional inorganic phosphors such as YAG are difficult to decompose and may present environmental issues for light-area lighting applications.

These flexible PDMS films had thicknesses of 100µm, 440µm, and 980µm. The resulting white light devices had color temperatures of 8944K, 4863K, and 4429K, respectively. In this study, we have also compared the performance of the organic versus conventional YAG phosphor embedded films.

9383-23, Session 5

Flexible tandem organic light-emitting diodes with graphene anode (Invited Paper)

Tae-Hee Han, Min-Ho Park, Pohang Univ. of Science and Technology (Korea, Republic of); Sang-Hoon Bae, Yonsei Univ. (Korea, Republic of); Hong-Kyu Seo, Pohang Univ. of Science and Technology (Korea, Republic of); Jong-Hyun Ahn, Yonsei Univ. (Korea, Republic of); Tae-Woo Lee, Pohang Univ. of Science and Technology (Korea, Republic of)

Organic Light-Emitting diodes (OLEDs) have attracted great attention due to their potential use of next-generation flexible displays and solid-state-lighting. However, conventional indium-tin-oxide (ITO) electrode has very poor tolerance to the mechanical stress. To realize flexible organic optoelectronic devices, brittle ITO electrode should be replaced with flexible transparent conducting electrodes. In this regard, the use of graphene electrode in flexible OLEDs has been increasingly studied because graphene exhibits exceptional electrical properties and mechanical flexibility. However, high sheet resistance and low work function (WF) of pristine graphene have been critical weak points to be used as an anode and thus resulted in poor hole injection and low power efficiency in OLEDs. Use of chemical p-type dopants (HNO₃) reduces sheet resistance of graphene anode and high WF hole injection layer (HIL) (- 5.95 eV) on graphene anode facilitates hole injection from graphene anode for high-efficiency flexible OLEDs. Here, we fabricated tandem OLEDs by stacking two electroluminescent (EL) units vertically on the modified graphene anode to enhance the luminous efficiency and operational stability of flexible OLEDs with the graphene anode. Fabricating tandem OLEDs is an effective way to reduce current density at the same luminance and thus improves luminous current efficiency and device stability. We demonstrated that charge generation layer (CGL) composed of metal oxide and stable low-temperature processable n-type material effectively provides charges spouted between two EL units. By employing well-optimized CGL and the modified high WF graphene anode with low sheet resistance, we achieved extremely efficient flexible tandem OLEDs with the graphene anode (~ 200 cd/A). Our results provide a significant step toward the next generation flexible displays and solid-state-lighting.

9383-24, Session 6

Deep UV LEDs for sensing applications (Invited Paper)

Michael Kneissl, Technische Univ. Berlin (Germany) and Ferdinand-Braun-Institut (Germany) and Leibniz Institut für Höchstfrequenztechnik (Germany)

The development of deep UV light emitting diodes (UV-LEDs) opens up new opportunities for the realization of compact, selective, and highly sensitive optical sensors. For example, many amino acids, polymeric macromolecules and organic compounds, like tryptophan, tyrosine, DNA, and RNA, which are common in human cells, bacteria and viruses, exhibit absorption bands in the UV-C spectral range. The same is true for a number of gas molecules, like ammonia and NO. Based on optical absorption measurements or fluorescence excitation spectroscopy, UV-C LEDs can be applied to the detection of dangerous multi-drug-resistant (MDR) germs or to the monitoring of medical conditions. This paper will provide a review of recent advances in development of AlGaIn-based LEDs emitting in the UV-C spectral range. We will discuss the growth of low defect density AlN layers using epitaxial lateral overgrowth (ELO) on sapphire substrates to improve the quantum efficiencies of deep UV light emitters as well as the growth of highly conductive Si-doped AlGaIn current spreading layers that cover almost the entire aluminium composition range. We will also explore novel electron barrier heterostructures (EBH) for enhanced carrier-injection into

Conference 9383: Light-Emitting Diodes: Materials, Devices, and Applications for Solid State Lighting XIX

the AlGaIn quantum well active region and investigate the effects of strain on the optical polarization and light extraction from deep UV LEDs. Finally we will review the performance characteristics of UV LEDs emitting in the wavelength range between 265 nm and 233 nm, including an outlook for future developments.

9383-25, Session 6

Numerical study of current spreading and light extraction in deep UV light-emitting diode

Xinhui Chen, Yuh-Renn Wu, National Taiwan Univ. (Taiwan)

AlGaIn deep ultra-violet light emitting diodes (UVLEDs) have attracted attention due to the applications in industry and medical applications in lithography, phototherapy, disinfection, etc. However, the efficiency of deep UVLEDs is extremely low because of high defect densities in AlGaIn materials. Due to the high activation energy of p-AlGaIn layer, which makes the contact and sheet resistance much higher, we need to use the p-GaN layer as the contact and current spreading layer. However, the significant absorption in p-GaN layer makes the light extraction much lower. The common transparent conduction layer (TCL) material such as ITO or IGZO also has very strong absorption in deep UV range, which cannot be used to improve the current spreading issues. To solve this problem, we try to find the optimized condition for lateral and vertical UVLED. For the step, we study the influence of light absorption due to different p-GaN layer thickness for lateral LED. As expected that thinner layer provides the better light extraction. However, the current spreading and IQE is not good. Then the spacing between p-fingers has been studied to find the optimized condition. Due to the lack of TCL, the smaller spacing of fingers improves the current spreading, lowering forward voltage significantly. If the finger spacing of different p-contact is minimized to 60?m, the EQE (including the LEE) can be improved to 4.76% without surface roughness. The WPE can be further improved to 3.77% due to the significant reduction of forward voltage. If the p-GaN layer can be fully replaced by p-AlGaIn and minimized the contact resistance, the WPE can be further improve to be over 7%. We also studied the vertical deep UV LED. We found that with 30nm p-GaN layer and 60?m n-metal finger spacing, the EQE can be further improved to 6.28% and WPE can be improved to 5.52%. In the future work, we will further study the influence of surface texture and optimized condition of thin TCL such as graphene or ITO to improve the current spreading in deep UVLEDs.

9383-26, Session 6

Improved UV LED performance using transparent conductive films embedded with plasmonic structures

Shih-Hao Chuang, Cheng-Yi Lin, Sin-Liang Ou, Cheng-Sheng Tsung, Ching-Ho Chen, National Chung Hsing Univ. (Taiwan); Dong-Sing Wu, National Chung Hsing Univ. (Taiwan) and Da-Yeh Univ. (Taiwan)

Recently, ultraviolet light-emitting diodes (UV-LEDs) have been used in many applications such as light sources for ultraviolet curing, environmental cleaning, biomedical instrumentation, counterfeit bill detection and phosphor-based white LEDs. However, it is difficult to fabricate UV-LEDs with high emission efficiency. As the wavelength of UV-LED decreases, the most dominant emission will be photons with transverse-magnetic (TM) polarization. For LED structures grown on a c-plane sapphire substrate, TM-light propagates mainly in the lateral direction. It suffers strong effects of total internal reflection (TIR) due to the large incident angle on the interface. Therefore, light extraction efficiency of UV-LEDs is still lower than that of visible LEDs. In this study, a spin coating process in which the grating structure comprises the metallic nanoparticle layer coated on a p-GaN top layer was developed. Various sizes of metallic nanoparticles forming a

suspended nanoparticle layer (SNL) embedded in a transparent conductive layer were clearly observed after the deposition of indium tin oxide. The SNL enhanced the light extraction efficiency of UV-LEDs. Light output power was 1.4 times in magnitude as compared with that of conventional device operating at 350 mA, but retained nearly the same current-voltage characteristic. Unlike in previous research on surface-plasmon-enhanced LEDs, the metallic nanoparticles were consistently distributed over the surface area. Device performance can be improved substantially by using the three-dimensional distribution of metallic nanoparticles in the SNL, which scatters the propagating light randomly and is coupled between the localized surface plasmon and incident light internally trapped in the LED structure through TIR.

9383-27, Session 6

Investigation of uniformity field generated from freeform lens with UV LED exposure system

Fong-Yi Ciou, Yi-Chian Chen, Cheng-Tang Pan, Po-Hung Lin, Po-Hsun Lin, Feng-tzu Hsu, National Sun Yat-Sen Univ. (Taiwan)

In the exposure process, the intensity and uniformity of light in the exposure area directly influenced the precision of products. UV LED (Ultraviolet Light-Emitting Diode) exposure system was established to reduce the radiation leakage and increase the energy efficiency for energy saving. It is a trend that conventional mercury lamp could be replaced with UV LED exposure system. This study was based on the law of conservation of energy and law of refraction of optical field distributing on the target plane. With these, a freeform lens with uniform light field of main exposure area could be designed. The light outside the exposure area could be concentrated into the area to improve the intensity of light. The refraction index and UV transmittance of Polydimethylsiloxane (PDMS) is 1.43 at 385 nm wavelength and 85-90%, respectively. The PDMS was used to fabricate the optics lens for UV LED. The average illumination and the uniformity could be obtained by increasing the number of UV LEDs and the spacing of different arrangement modes. After exposure process with PDMS lens, about 4% inaccuracy was obtained. Comparing to 10% inaccuracy of general exposure system, it shows that it is available to replace conventional exposure lamp with using UV LED.

9383-28, Session 6

Development of high-performance UV-C LEDs and potential applications (*Invited Paper*)

S. David Roh, LG Innotek (Korea, Republic of)

Deep ultraviolet light emitting diodes with emission wavelengths shorter than 280 nm (UV-C LEDs) can be used in applications such as sterilization, chemical/biological detection, and spectroscopy. Recently, many reports have been published regarding the development and applications of UV-C LEDs. However, UV-C LEDs still have a number of challenges, such as output power, manufacturability, and customers' preconception, to overcome on its road to true mass adoption by the market.

In this talk, advances in epitaxial quality, device design, reliability, and manufacturability of UV-C LEDs will be presented. Also, potential power scaling techniques of UV-C LEDs will be discussed.

Conference 9383: Light-Emitting Diodes: Materials, Devices, and Applications for Solid State Lighting XIX

9383-48, Session PWed

Development of environmentally friendly LED light source module for photoacoustic imaging system

Toshitaka Agano, Naoto Sato, Hitoshi Nakatsuka, XTrillion, Inc. (Japan); Kazuo Kitagawa, Takamitsu Hanaoka, Koji Morisono, Yusuke Shigeta, Funai Electric Co., Ltd. (Japan)

We have developed near infrared LED (NIR-LED) array light source module for photoacoustic imaging system, which is ultra-small package and consumes extremely low power. Conventional photoacoustic imaging system uses solid state laser light source, which requires large space, consumes large amount of electricity, and generates high-energy output which is sometimes difficult to handle. Instead of the solid state laser, we have developed high intensity NIR-LED chips in matrix on a 1cm x 6cm board. Our module produces approx. 1.0kW output power and obtained photoacoustic signal by driving NIR-LED light source module with about 100 ns pulse. Comparing to the laser light source (ex. Nd:YAG-OPO system), our NIR-LED light source module is much smaller than 1/15000 the volume and less than 1/1000 the power consumption approximately.

We have achieved penetration depth of 30mm that is equivalent to the solid state laser system.

9383-49, Session PWed

Enhanced brightness from all solution processable biopolymer LED

Pradeep Chandran, Cochin Univ. of Science & Technology (India); Manoj A. Namboothiry, Indian Institute of Science Education & Research (India); C. P. Girijavallabhan, Cochin Univ. of Science & Technology (India); P. Radhakrishnan, International School of Photonics (India); V. P. N. Nampoori, Cochin Univ. of Science & Technology (India)

Since the discovery of light emission from polymers over two decades ago, especially conjugated polymers paved way for simpler technology viz. solution casting method to make light emitting devices. However in the past few years, biopolymers such as Deoxyribonucleic acid (DNA) has gained tremendous interest among researchers trying to develop BioLED. Marine derived DNA from salmon sperm has been exploited as biodegradable polymeric material for photonic and electronic applications. Many devices such as optical waveguides, bio-organic light emitting devices, bio field effect transistors and bio sensors are at the research table with promising results. What the DNA could offer in LED application is multifold. Through the emerging field of 'DNA Photonics', it could be exploited as a biodegradable polymeric material for photonics and optoelectronics application. Apart from being biodegradable, abundant, inexpensive and renewable resource, they hold a unique optical and electrical properties. Being optically transparent in the visible region, electrically conductive, tunable resistivity from 10¹⁵ to 10⁹ Ω-cm by varying its molecular weight, suitable refractive index and dielectric constant, all yielding to be a promising material for optical and optoelectronic devices. Additionally, the HOMO (5.6 eV) and LUMO (0.9 eV) levels support hole transportation and also effectively block electrons enabling it to use as an electron blocking layer in LED which has resulted in increased brightness and luminous efficiency.

Motivated by the potential of DNA as an interesting material in the field of light emitting diodes, much research was directed to designing and developing BioLED. Here, we present the effect of thickness of electron blocking DNA layer in polymer LEDs. In this investigations, a blend of F8BT based green emitting polymer and PFO based blue emitting polymer was used as active layer. We also show an 8 fold increase in brightness of polymer LED by introducing PFN as electron injection and DNA:CTMA as electron blocking layer on either side of the polyfluorene active layer. It has

been observed that the variation in thickness of DNA layer even at small values is very crucial.

9383-50, Session PWed

Lateral thin-film grating structure for enhanced phosphorescence

Kyungtaek Min, Serok Choi, Heonsu Jeon, Seoul National Univ. (Korea, Republic of)

The importance of phosphor cannot be overemphasized nowadays as the phosphor-capped white light-emitting diodes (LEDs) have hit hard the global lighting market. Consequently, there has been a great deal of efforts to develop efficient phosphors with tailored optical properties. In our previous work [Opt. Express, 20 (3), 2452-2459 (2012)], we showed that a periodically stacked multiple layer, or vertical one-dimensional (1D) photonic crystal (PC), can be used as a phosphor structure that improves phosphorescence efficiency; when pump photon energy is tuned to a stop-band edge where the photon group velocity is zero, the interaction between the pump photons and phosphorescent agents becomes greatly strengthened, resulting in a much improved phosphorescence. In that case, however, we had to keep the concentration of phosphorescent agents low in order to excite the entire phosphor structure, limiting the impact of the implement. Here we propose a thin-film grating as a phosphor backbone structure that can result in even higher phosphorescence efficiency without suffering from the problem with the previous vertical PC phosphor structure. The grating phosphor structure considered here is a kind of lateral 1D PC, where a thin-film grating of a high refractive index is filled with a phosphorescent agent of low refractive index. Theoretical simulations were performed based on finite-difference time-domain method, which revealed that phosphorescence from a model grating phosphor structure can be 5 times higher than from a bulk phosphor when the pump photon energy is tuned to a band-edge where $k_{\parallel} = 0$.

9383-51, Session PWed

Design of a new cheaper high-performance optical imaging system using commercial LED sources

Mohamed Darwiesh, Military Technical College (Egypt)

Optical imaging systems are widely used in different applications including tracking for portable scanners; input pointing devices for laptop computers, cell phones, and cameras; and fingerprint-identification scanners. Also in optical navigation (military target tracking where tracking sensors follow airplanes, missiles, and other targets). The basic structural elements of the optical imaging system include optical source and optical sensor that contains a small camera and a digital signal processor (DSP).

Since the main parameter affects the performance of the optical imaging systems is the optical source. So; The theoretical and experimental studies of the colorimetry of the optical sources (color correction is done in the color images captured by the optical imaging system to produce realistic color images which contains most of the information in the image by selecting suitable gray scale which contains most of the informative data in the image, this is done by calculating the accurate Red-Green-Blue (RGB) color components making use of the measured spectrum for light sources, and color matching functions of International Telecommunication Organization (ITU-R709) for CRT phosphorus, Tirinton-SONY Model)

From these studies we found that the electronic sensor can deliver the same accuracy of laser diodes when replacing it by commercial LEDs. So, we can design a new cheaper, high performance optical imaging system using commercial LED sources.

Conference 9383: Light-Emitting Diodes: Materials, Devices, and Applications for Solid State Lighting XIX

9383-52, Session PWed

Temperature dependence of efficiency in GaInN/GaN light-emitting diodes with a strain-control layer

Hyun Seok Song, Jaehee Cho, Chonbuk National Univ. (Korea, Republic of); David S. Meyaard, Guan-Bo Lin, E. Fred Schubert, Rensselaer Polytechnic Institute (United States); Jong Kyu Kim, Pohang Univ. of Science and Technology (Korea, Republic of)

Nitride-based light-emitting diodes (LEDs) have become increasingly prevalent in illumination applications. However, a long standing technical issue called "efficiency droop" has been impeding the speedy development and future prospects of LEDs as the ultimate illumination source. The efficiency droop can be categorized by two classifications: current-density droop and temperature droop. The former describes the decrease in radiative efficiency with increasing operating current. The latter is represented by the decrease in radiative efficiency with increasing temperature.

In this study, the temperature dependence of efficiency in blue LEDs with a strain-control layer is investigated. Firstly, the effect of a GaInN underlayer having several different indium mole fractions is investigated in a GaInN/GaN LED structure. An LED with an indium mole fraction of 8% shows a reduced temperature-driven droop. Better carrier confinement in the active region of the LED with the GaInN underlayer is proposed to reduce carrier leakage from the active region at high temperature. Secondly, dielectric material-induced strain is studied to find a practical use in GaInN/GaN LEDs. We found that a SiO₂ layer deposited on the as-grown AlGaIn/GaN template induces compressive strain on an AlGaIn layer, which resulted in an increase of polarization sheet charge density between AlGaIn and GaN interface. Some other dielectric materials such as ITO and ZnO are also investigated to get more flexibility of the strain engineering in LEDs.

9383-53, Session PWed

Improved thermal and optical performance of chip-on-board light-emitting-diode panel lamps

Wing Shing Cheung, Antony H. W. Choi, The Univ. of Hong Kong (Hong Kong, China)

Applications involving light-emitting diodes (LEDs) are abundant, in the form of display backlighting and general lighting. However, many of the LED products are not designed to enable the LED chips to deliver their optical performances, so that the benefits of LEDs are undermined. For example, packaged LEDs are employed for the assembly of LED lamps in common practice. Obviously this will unnecessarily increase the dimensions of the lamp, as well as an increase of production costs. More importantly, these individual packages will hinder the optical performances of the LEDs due to inefficient heat-sinking, given the close relation between chip temperatures and internal quantum efficiencies. In this paper, the superior optical and thermal performances of chip-on-board LED panel lamps are demonstrated.

Experiments are carried out to compare thermal performance of LEDs bonded directly to a ceramic panel, or through a ceramic package. The optical powers of the LEDs are measured in an integrating sphere, while their thermal performance is determined in by long-wave infra-red thermometry. The results indicate that while both devices operate similarly at lower currents, the optical power of the chip-on-package begins to increase at a slower rate at 250mA compared to the chip-on-board. LWIR data also shows that the chip-on-board operates at 20°C lower than the chip-on-package at an operating current of 400mA, explaining its better quantum efficiency. The package, no matter how well-designed, serves as a thermal resistance ultimately limiting thermal flow. A ceramic panel lamp consisting of 20 chips-on-board is built based on this design.

9383-54, Session PWed

Failure mechanisms for InGaN light-emitting diode chips with patterned sapphire substrates

Chia-Hung Sun, Optoelectronic Technology Lab. (Taiwan)

To improve light extraction and reduce threading dislocation density (TDD) of InGaN lighting emitting diodes (LEDs), patterned sapphire substrates have been used to grow GaN-based LEDs. In this paper, we investigated the failure mechanisms of blue InGaN LEDs grown on patterned sapphire substrates (P-LEDs) and demonstrated the influence of patterned sapphire substrates on the reliability of GaN LED by comparing with conventional LEDs (C-LEDs) grown on planar sapphire substrates.

Both samples were aged using a high DC current density of 220 A/cm² for two hours. Failure modes were studied with various measurements including current-voltage (I-V), Log I-V, light power-current (L-I), capacitance-voltage (C-V), surface temperature and light emission near field pattern (NFP) taken before and after aging tests. We found that P-LED had a higher turn-on voltage but a smaller series resistance compared with C-LED owing to rough inner patterns and small TDD. Therefore, they had similar surface temperatures driven under the same current. From the power evolution performance, we found that both C-LED and P-LED showed an initial increase in output power which should be attributed to thermal annealing effect, confirmed from the comparison of power increase amounts at different driving currents. After aging 10 minutes, the power of C-LED started to decay while the power of P-LED remained stable which can be understood from reverse leakage currents and tunneling currents observed from Log I-V characteristics and carrier concentration obtained from C-V data. During aging, operation voltage increased slightly which was caused by contact degradation. More discussion will be presented in the conference.

9383-55, Session PWed

Characteristics of nonpolar GaN:Mn grown by plasma-assisted molecular beam epitaxy

Yu-Jung Cheng, Yuan-Ting Lin, Ching-Wen Chang, Song-Sain Guo, National Sun Yat-Sen Univ. (Taiwan); Mu-Xin Ma, Wei-Chih Lai, National Cheng Kung Univ. (Taiwan); Li-Wei Tu, National Sun Yat-Sen Univ. (Taiwan)

In the recent years, nonpolar III-V nitrides light-emitting diodes (LEDs) with low droop have been fabricated and studied intensively. They have not only the high performances in optical output power and wavelength ranges, but also the polarized light emission characteristic which opens new fields of applications. Furthermore, III-V nitride semiconductors doped with Mn are expected to become ferromagnetic semiconductor materials with Curie temperature higher than room temperature. They have the potential to be developed into spintronic LEDs operated at room temperature. In this study, m-plane GaN:Mn were grown on m-plane GaN template by plasma-assisted molecular beam epitaxy. The morphology of thin film is presented by field-emission scanning electron microscopy. High-resolution x-ray diffraction shows a good crystal quality grown along the m-axis of a wurtzite structure. The strains of the m-plane nitrides films and the local structure of Mn atoms in GaN lattice were measured by micro-Raman spectroscopy, which were related to the degree of the polarization. The magnetic properties of m-plane GaN:Mn were investigated using a superconducting quantum interference device magnetometer. In the future, spin-LEDs will be fabricated by m-plane GaN:Mn on an m-plane p-GaN/InGaIn/n-GaN (p-i-n) structure.

Conference 9383: Light-Emitting Diodes: Materials, Devices, and Applications for Solid State Lighting XIX

9383-29, Session 7

X-ray scattering methods for R&D and process control of nitride LED and LD structures (*Invited Paper*)

Lars Grieger, Joachim F. Woitok, PANalytical B.V. (Netherlands)

High-resolution X-ray diffraction (XRD) has been extensively used to characterize GaN based epitaxial structures on all commercial and experimental substrates during its research and development phase. For a long time XRD was considered too difficult and time consuming for use in a production environment. But improved performance of laboratory XRD equipment and advances in analytical software enabled fast and reliable determination of relevant layer parameters. Nowadays XRD is a well-proven and established tool for the quantification of structural information on current layered epitaxial structures in the semiconductor industry.

Next to the common X-ray techniques advanced scattering methods are evolving to meet the upcoming requirements of the industry. While in the past for each analysis method dedicated instruments were applied modern lab equipment with exchangeable optics offers all techniques on one single instrument.

In this presentation a brief overview will be given about the experimental aspects including recent hardware developments and evaluation methods of X-ray characterization techniques. Their applicability to extract structural information of advanced layered structures is illustrated on some examples of technologically relevant materials.

9383-30, Session 7

Improvement of GaN epitaxial quality and LED performance by incorporating alumina cavity pattern into substrate

Yongjo Park, Advanced Institute of Convergence Technology (Korea, Republic of); Daeyoung Moon, Jeonghwan Jang, Hyo-Jeong Lee, Seoul National Univ. (Korea, Republic of); Duk-Kyu Bae, Hexa Solution (Korea, Republic of); Euijoon Yoon, Seoul National Univ. (Korea, Republic of)

GaN-based white LED, a combination of blue LED and phosphors, has attracted much attention for the replacement of conventional lighting sources like fluorescent lamps and incandescent bulbs, leading to a lighting revolution. However, the high cost of LED lighting is still an obstacle to the fast penetration into the illumination market. Many technical efforts to improve chip efficacy and manufacturing productivity have been made for the reduction of the cost. A new growth scheme using cavity engineered sapphire substrate was investigated to realize high efficiency and low cost GaN LED. An array of patterned alumina cavities was incorporated into the surface of sapphire substrate by photo-resist patterning and subsequent heat treatment for the crystallization of the cavity film. The growth of GaN on the cavity structure by metalorganic chemical vapor deposition results in improved crystal quality due to lateral epitaxial overgrowth. Moreover, well-defined voids embedded at the GaN/sapphire interface help scatter light effectively, improving the light extraction, and reduce wafer bowing due to partial alleviation of compressive stress in GaN. In this presentation, phase transformation in the cavity film, the improved crystal quality of the GaN film and the enhanced LED performance by the new epitaxy scheme will be reported in detail.

9383-31, Session 7

Robust diffuser and roughness metrology tool for LED manufacturing

Peter Walecki, Wojciech Walecki, Sunrise Optical LLC (United States)

We have built novel oblique angle scatterometer designed and optimized for measurements of rough surfaces having root mean square roughness (RMS Roughness) of the order of 100 nm - 1000 nm or larger.

Majority of existing techniques for measurement of such surfaces are slow, sensitive to vibration, provide short or no working distance, may result in generation of particles and have very small throughput [1]. In this paper we discuss two metrologies addressing the above limitations.

In the first implementation optical beam is probing a single spot of the sample. The interference from the stray light is reduced by optical and electronic means. We demonstrated that tool can provide fast (in a fraction of one second) and accurate (repeatability of about 5%) measurements while being immune to vibration and stray light.

In the second novel implementation we analyze an image of a pattern using the entire wafer surface as a mirror. We show that the image produced by sample reflecting light at an oblique angle provides information about roughness for even very rough samples (having RMS roughness of the order of 100 nm - 1000 nm). We do also discuss a simplified model providing quantitative estimate of the surface roughness.

Finally we discuss possible extensions of the described metrology to novel applications.

Whitehouse, David (2012). Surfaces and their Measurement. Boston: Butterworth-Heinemann. ISBN 978-0080972015.

9383-32, Session 7

High-performance epitaxial-lifted-off micro-GaN-LEDs for optoelectronics integration

Hsien-Yu Liao, Ahmed Ben Slimane, Tien Khee Ng, Boon Siew Ooi, King Abdullah Univ. of Science and Technology (Saudi Arabia)

We report on the fabrication of high performance micro-pixelated blue (445nm) InGaN LED structure on flexible PDMS substrate using a novel epitaxial-lift-off process. The LED lift-off process is achieved by selective etching of the undoped-GaN buffer layer below the LED epi-structure using a novel backside UV-irradiation photoelectroless chemical etching process at room temperature. As only the bottom GaN buffer layer is activated by the UV-irradiation, high etch selectivity of 100:1 between the undoped GaN-buffer and other GaN/InGaN layers was achieved. The lifted-off LED layer is 3.5 μm thick with lateral size ranges from 10 μm to 100 μm . Photoluminescence characterization shows a reduced power dependent peak emission shift in the lifted-off micro-membrane LED compared to the as-grown LED, indicating a reduced piezoelectric biaxial strain after the lift-off process. These micro-InGaN LEDs have been successfully transferred to PDMS substrate. The lifted-off LEDs gave 35% lower series resistance, R_s , and 60% higher output emission power, Pout, compared to the bulk LEDs fabricated directly on the conventional sapphire substrate. A significant improvement in turn-on voltage has also been observed. The micro-membrane LED technology enables heterogeneous integration, and can potentially be used for forming pixelated red, green, blue (RGB) display on flexible and transparent substrate.

Conference 9383: Light-Emitting Diodes: Materials, Devices, and Applications for Solid State Lighting XIX

9383-33, Session 7

In-situ monitoring during epitaxial growth of light emitters (*Invited Paper*)

André Strittmatter, Otto-von-Guericke-Univ. Magdeburg (Germany)

Heteroepitaxial growth of nitride-based LED structures on foreign substrates faces a number of challenges such as high dislocation densities as well as of stress accumulation within the structure. Controlling these issues is at the core of any successful approach to high-performance LEDs. In-situ monitoring of the epitaxial growth is an inevitable tool to understand and to optimize crucial steps within the layer structure. For that purpose, optical setups to measure surface reflectivity, surface temperature, and wafer curvature have been developed during the past decade. The evolution of reflectivity curves during growth of buffer layer structures are very well understood as arising from three-dimensional island growth and subsequent coalescence of these islands. Curvature measurements are successfully applied by us to realize stress-free LED structures on Si substrates which is upcoming as a low-cost approach to industrial LED fabrication. Insertion of thin interlayers at appropriate positions within the vertical buffer structure was a key step towards realization of buffer layers with dislocation densities as low as $2 \times 10^8 \text{ cm}^{-2}$. Recently, we used in-situ monitoring of reflectivity transients during growth of vertical surface emitting laser structures to control the optical properties of distributed Bragg reflectors and cavity resonances. Furthermore, the wafer asphericity of anisotropically strained materials becomes accessible by applying 3-beam curvature measurements. Such unusually curved wafer surfaces can be found during growth of a-plane GaN material, for instance.

9383-34, Session 8

Recent progress in the understanding of the efficiency droop in GaN-based LEDs (*Invited Paper*)

Bastian Galler, Anna Nirschl, Michael Binder, Hans-Juergen Lugauer, Marina Schmid, Roland Zeisel, Berthold Hahn, OSRAM Opto Semiconductors GmbH (Germany); Joachim Wagner, Fraunhofer-Institut für Angewandte Festkörperphysik (Germany); Matthias Sabathil, OSRAM Opto Semiconductors GmbH (Germany)

Significant progress in the understanding of the efficiency droop in GaN-based light-emitting diodes has been obtained during the last decade. In particular, novel experimental approaches were recently published which attempted to complement evidence for the important role of Auger recombination by detecting hot carriers associated to the droop [1,2]. While the observed constant ratios of measured hot carriers and droop losses further support the conclusion that Auger processes dominate the investigated phenomenon, clear proof requires that the respective proportionality factors approach unity or that the deviations are quantitatively understood.

An important step for this purpose is clarifying whether the recombination energy in Auger processes in InGaN is more likely transferred to an electron or hole. The approach chosen in Ref. 1 is entirely limited to the detection of the first process whereas the proportionality factor found in the approach in Ref. 2 is strongly dependent on the ratio of the respective rates.

To determine the dominant mechanism experimentally, we investigate single quantum well test structures featuring different type and levels of background carriers. By breaking charge neutrality in the active layer on purpose, the different dependencies of the Auger recombination rates on electron and hole concentrations become apparent. The series reveal that the loss process dominating the efficiency droop is superlinear in the electron density and thus can be assigned to nnp-Auger recombination [3]. Finally, we discuss how this knowledge contributes towards a quantification

of the total droop losses caused by Auger recombination using the approach discussed in Ref. 2.

[1] J. Iveland, L. Martinelli, J. Peretti, J. S. Speck, and C. Weisbuch: Phys. Rev. Lett. 110 177406 (2013).

[2] M. Binder, A. Nirschl, R. Zeisel, T. Hager, H.-J. Lugauer, M. Sabathil, D. Bougeard, J. Wagner, and B. Galler: Appl. Phys. Lett. 103 071108 (2013).

[3] B. Galler, H. Lugauer, M. Binder, R. Hollweck, Y. Folwill, A. Nirschl, A. Gomez-Iglesias, B. Hahn, J. Wagner, and M. Sabathil: Appl. Phys. Express 6, 112101 (2013).

9383-35, Session 8

Nitride heterostructure influence on efficiency droop

Oleg I. Rabinovich, Sergei Didenko, Sergei Legotin, National Univ. of Science and Technology "MISIS" (Russian Federation)

The influence of nitride heterostructures on efficiency droop is presented. It was developed a special method based on simulation for investigating the changes in the semiconductor devices characteristics due to different influencing factors. The cause of efficiency droop was detected - large difference in carrier lifetimes. The simulation results are used to suggest several techniques for improving LED efficiency about 12 %.

Investigation results discussed in this paper showed that the "optimum" heterostructure contains 4 QWs in the active region. In the central quantum wells, maximum recombination occurs, while the edge wells act as quasibuffers to protect the central region and to promote carrier currents to obtain a maximum recombination rate.

In the paper the quantum efficiency droop based on computer simulation was discussed.

It was found that the effect is based on large difference between the characteristic lifetime of the charge carriers by at least two orders of magnitude.

It is shown that the use of silicon substrates for growing nanoheterostructures can decrease efficiency droop.

The results obtained could be useful in the design of LEDs with high luminous efficiency.

9383-36, Session 8

Probing inhomogeneous absorption linewidth of purely disordered InGaN alloy

Lise Lahourcade, Marlene Glauser, Georg Rossbach, Raphaël Butté, Nicolas Grandjean, Ecole Polytechnique Fédérale de Lausanne (Switzerland)

InGaN alloy material properties are still attracting a lot of attention, even though this alloy has already proven to be perfectly suitable for optoelectronics applications. More particularly indium composition inhomogeneity and well-width fluctuations (WWFs) can generate localization of carriers in InGaN quantum wells (QWs), which in turn tends to detrimentally affect the performance of laser diodes (LDs). In this context, we have chosen to study InGaN layers instead of QWs to get rid of both the quantum-confined Stark effect and WWF-induced localization, hence aiming to probe the intrinsic inhomogeneous absorption linewidth of purely disordered InGaN alloy.

Covering a wide range of indium contents we investigated a series of uncapped InGaN layers focusing on the correlation between their optical properties and crystalline quality. By systematic analysis of their temperature-dependent optical features we will show that a statistical model of random atom distribution can well reproduce the increase of both the absorption linewidth and the Stokes shift between absorption edge

Conference 9383: Light-Emitting Diodes: Materials, Devices, and Applications for Solid State Lighting XIX

and photoluminescence peak when increasing the indium content. Given that stochastic alloy properties are preserved (i.e. before the formation of extended defects or strain-induced large-scale indium fluctuations upon plastic relaxation), relatively narrow absorption linewidths are measured. The implication of this finding on QW optical properties will be discussed, in particular in the light of the recent progress in InGaN-based green LEDs.

9383-37, Session 8
GaN-based tunnel-junction LED with 250% peak quantum efficiency (*Invited Paper*)

Joachim Piprek, NUSOD Institute LLC (United States)

GaN-based light-emitting diodes (LEDs) exhibit a severe efficiency droop with increasing current. Various physical mechanisms have been proposed to explain the efficiency droop. Among them are density-activated defect recombination, enhanced Auger recombination, and electron leakage. While the debate on the dominating mechanisms is still ongoing, all these proposals hold the rising carrier density inside the multi-quantum well (MQW) active region responsible for increasing carrier losses as cause of the efficiency droop. Therefore, a possible solution lies in the reduction of the QW carrier density required for a given output power by increasing the number of wells. However, this concept is hindered by the non-uniform vertical carrier distribution commonly observed with thick InGaN MQW regions. We here investigate an alternative approach by inserting tunnel junctions into the MQW region without changing the total thickness of the active layers. Such bipolar cascade design allows for the repeated use of electrons and holes for photon generation (carrier recycling). Advanced numerical simulations show that an LED with three tunnel junctions inside the MQW can achieve up to 250% peak quantum efficiency, despite photon absorption at the tunnel junctions. Naturally, the wall plug efficiency (WPE) remains below 100%. However, the WPE is still as high as 48% at 100 mW input power, compared to 32% with the conventional MQW and 40% with a single active layer of the same total thickness.

9383-38, Session 9
3D NanoLEDs: status and prospectives (*Invited Paper*)

Andreas Waag, Jana Hartmann, Johannes Ledig, Martin S. Mohajerani, Xue Wang, Hao Zhou, Frederik Steib, Sönke Fündling, Hergo-Heinrich Wehmann, Technische Univ. Braunschweig (Germany); Daniel Bichler, Barbara Huckenbeck, OSRAM GmbH (Germany); Tilman Schimpke, Ion Stoll, Martin Mandl, Hans-Jürgen Lugauer, Martin Strassburg, OSRAM Opto Semiconductors GmbH (Germany)

GaN nanorods and 3D columns are expected to be an exciting new route towards light engines for solid state lighting. Core-shell design of LEDs based on 3D GaN offer a dramatically enhanced active area per chip area, since the active area is scaling with height of the 3D structures. Aspect ratios of above 20 can easily be achieved. This will allow for operating conditions under lower current densities, possibly avoiding the droop problem and enhancing the output of photons per chip area. Meanwhile, detailed insight into MOCVD growth mechanisms has been gained and such core-shell structures can reproducibly be fabricated with high aspect ratios and relatively good homogeneity. Further processing into white LEDs as well as performing analysis of these 3D structures is a challenge and calls for novel approaches. This talk will give an overview on the state of the art of our 3D GaN research, particularly focusing on selective MOCVD growth mechanisms, 3D characterization and processing of white LEDs.

9383-39, Session 9
Investigation of optimal silver nanowires film as conductive wires for LED

Cheng-Tang Pan, I-Chou Wu, Tsung-Lin Yang, Yi-Chian Chen, Kun-Hao Hung, National Sun Yat-Sen Univ. (Taiwan)

In the study, the Polyol reduction process was used to fabricate silver nanowires (AgNWs). In the experiment, the ratio of PVP/Ag, silver seed, AgNO₃ and the amount of ethylene glycol (EG) were adopted to design orthogonal array with a constant temperature and heating time and the synthesis parameters of AgNWs were obtained. Therefore, the optimal AgNWs solution was obtained, followed by centrifuging to obtain AgNWs which were used to fabricate AgNWs film. The scanning electron microscope (SEM), Fourier Transform Infrared Spectroscopy (FTIR), Energy Dispersive Spectrometer (EDS) and four-point probe were used to measure the sheet resistance and transmittance of AgNWs film. Moreover, the AgNWs film was adopted to be the conductive wires of LED. From the experiment results, the synthesis parameter of 15ml EG, 0.01g AgCl, ratio 2 of PVP/Ag and 0.22g AgNO₃ could be used to fabricate optimal AgNWs with 45nm average diameter, 5 μ m average length and aspect ratio of 110. The sheet resistance and transmittance of film fabricated by centrifuged AgNWs was 0.1252 Ω /sq and 70%, respectively. Furthermore, the luminance of LED with conductive wires made of AgNWs film was better than that made of commercial silver plastic. In the future, the AgNWs film can be broadly applied to the conductive films of touch electric products, LCD display and solar panels.

9383-40, Session 9
Efficiency droop improvement for tip-free InGaN/GaN core-shell nanorods green light-emitting diodes

Da-wei Lin, An-Jye Tzou, Wei-Chi Hsu, Tzu-Pei Chen, Jia-Min Shieh, Chun-Yen Chang, Hao-Chung Kuo, National Chiao Tung Univ. (Taiwan)

In recent years, c-axis oriented nitride-based nanorod light emitting diodes (LEDs) have attracted a lot of attentions due to the enhancement of active region area, elimination of defect density for nanorods, enhancement of light extraction and further the non-polar/semi-polar plane multiple quantum wells (MQWs) would be grown on the sidewall of nanorods along c-axis, which is promising to decrease the polarization induced effect that we could reach to high efficiency LEDs without the influences from quantum confined Stark effect (QCSE).

In general core-shell nanorod LEDs, tip shaped nanorods are always fabricated on the topmost of the nanorods with composition fluctuation of indium and even indium clustering. Moreover, the inhomogeneous thickness of MQWs would be observed, hence the emission wavelength would be spatially distributed over the nanorods and further the electroluminescence peak with strong blue shift would be observed. To improve the nonideal effect from conventional nanorod LEDs, we utilize a SiN_x passivation on the top of the nanorods, which purpose to prevent tip-shape nanorod formation. The less area of semi-polar plane for MQWs is obtained and the area of non-polar is raised simultaneously. In addition, the SiN_x passivation attains to prevent the indium clustering and also obtained a less blue shift of emission peak. The less blue shift is contributed by the SiN_x passivation, hence the electric field distribution would be more uniform.

In this work, we will introduce the growth, optical, and electrical characteristics of our innovative nanorod LEDs and the potential for high efficiency LEDs would be demonstrated.

Conference 9383: Light-Emitting Diodes: Materials, Devices, and Applications for Solid State Lighting XIX

9383-41, Session 9

Effective efficiency improvement and droop effect reduction of a blue-emitting light-emitting diode with localized surface plasmon coupling

Chun-Han Lin, Yu-Feng Yao, Chung-Hui Chen, Chia-Ying Su, Pei-Ying Shih, Horng-Shyang Chen, Chieh Hsieh, National Taiwan Univ. (Taiwan); Yang Kuo, Tung Nan Univ. (Taiwan); Yean-Woei Kiang, Chih-Chung Yang, National Taiwan Univ. (Taiwan)

The enhanced surface plasmon (SP) coupling effects in a blue light-emitting diode (LED) with surface Ag nanoparticles (NPs) by adding a dielectric interlayer (DI) of a lower refractive index, when compared with that of GaN, between the Ag NPs and p-GaN is demonstrated. When the p-GaN is reasonably thin, the surface Ag NPs induce SP coupling with the quantum wells (QWs) in the LED, leading to the increases of internal quantum efficiency (IQE) and LED output intensity, the decrease of photoluminescence (PL) decay time, the reduction of the external quantum efficiency droop effect, and the increase of modulation cutoff frequency. By adding a DI, the SP coupling effect is enhanced, resulting in the further improvements of all the aforementioned factors. We also compare the SP coupling effects between the LEDs with regularly patterned (REG) and randomly distributed (RAN) Ag NPs. Although the REG Ag NPs can produce stronger localized surface plasmon (LSP) resonances with narrower spectral widths, the SP coupling effect depends only on the LSP resonance strength at the QW emission wavelength. Meanwhile, we compare the SP coupling effects between the LED samples with single- and multiple-QW. In all cases, the LED performance improvements are more significant through SP coupling in the samples with single-QW. This result can be attributed to the non-uniform SP coupling effects among the QWs in a multiple-QW sample. Also, the higher intrinsic IQE in the samples with multiple QWs can result in a less favorable SP coupling effect.

9383-42, Session 9

InGaN/GaN core-shell LEDs (*Invited Paper*)

Nathan F. Gardner, GLO-USA, Inc. (United States)

No Abstract Available

9383-43, Session 10

In-situ metrology: key enabling technology for LED and LD production (*Invited Paper*)

Stephanie Fritze, Oliver Schulz, Marcello Binetti, LayTec AG (Germany)

Solid state light emitters are increasingly dominating nowadays lighting industry, saving a huge amount of energy and enhancing the product lifetime compared to light bulbs and halogen lamps. In this regard, GaN and its related alloys (In,Al,Ga)N have revolutionized the optoelectronic devices for visible light. However, the further III-Nitride LED commercialization demands further reduction of manufacturing costs on the one hand and further performance improvement on the other hand. Focusing on cost benefits, the LED manufacturing proceeds towards larger substrate sizes, such as 6" sapphire or even 8" silicon. But in terms of larger diameters, additional effects like wafer bow become a crucial issue that needs to be precisely controlled in terms of homogeneous temperature distribution and consequently accurate and uniform InGaN QW compositions and doping levels. The growth on silicon requires additional complex buffer structures for maximum efficient stress reduction and defect elimination. Moreover, targeting further device quality improvement, high thermal conductivity

substrates like SiC or even fully lattice matched substrates like freestanding GaN provide excellent crystal quality for III-Nitride based high brightness LEDs or laser diodes.

However, during epitaxy all these different substrate materials have different physical properties (thermal conductivity and thermal emissivity) directly affecting the III-Nitride growth physics. By using advanced UV pyrometry we will present a detailed in-situ analysis of the real GaN surface temperature effects due to different underlying substrate types. The comparison of UV pyrometry to the commonly used IR pyrometry, which is not sensitive to the GaN surface, reveals the additional impact of substrate and buffer layer doping on the surface thermal emission during epitaxy. In conclusion a tight control of the absolute GaN surface temperature is essential for precise and lateral homogeneous bandgap and strain engineering during growth of advanced III-Nitride optoelectronic device structures.

9383-44, Session 10

Robust noncontact surface roughness metrology based on range from focus method

Wojciech Walecki, Peter Walecki, Sunrise Optical LLC (United States)

We present an application of range from focus metrology [1] to investigations of surface roughness of transparent, and reflective surfaces. "Range from focus" method is a topography measurement when measured sample is placed at several different working distances from objective of microscope, and a set of images is collected. The degree of "defocus" provides information of the topography of sample. "Range from focus" provides cost effective alternative to confocal microscopy and interferometry.

In order to improve speed and resolution of the system we use a novel, fast multi-frame algorithm utilizing change of blur of measured surface pattern. We compare and contrast our numerical method with those presented in literature [2].

Our method of measuring of sample roughness is quite cost effective. The "range from focus" can be implemented as a relatively inexpensive modification of existing microscope system, and unlike low coherence interferometry or confocal microscopy it does not require very specialized and costly dedicated hardware.

In this paper we discuss the technical challenges encountered when developing this metrology, results on calibration samples, and practical application of technology on metrology of optical diffusers. Finally we discuss in details speed and accuracy limitations of this metrology.

[1] Eric Krotkov and Jean-Paul Martin, "Range from Focus", Robotics and Automation. Proceedings. 1986 IEEE International Conference on (Volume: 3) pp 1093 - 1098

[2] Paolo Favaro and Stefano Soatto "3-D Shape Estimation and Image Restoration" Springer Berlin 2007 pp 37 -118

9383-45, Session 10

Large area LED package

Lena Goullon, Jörg Bauer, Tanja Braun, Rafael Jordan, Matthias Hutter, Karl Friedrich Becker, Hermann Oppermann, Martin Schneider-Ramelow, Klaus-Dieter Lang, Fraunhofer-Institut für Zuverlässigkeit und Mikrointegration (Germany)

Solid state lighting with LED-dies is a rapidly growing market. LED-dies with the needed increasing luminous flux per chip area produce a lot of heat therefor an appropriate thermal management is required for general lighting with LED-dies. One way to avoid overheating and shorter lifetime is the use of many small LED-dies (down to 70 µm edge length), so light

Conference 9383: Light-Emitting Diodes: Materials, Devices, and Applications for Solid State Lighting XIX

and heat can spread into a large area. The handling with such small LED-dies is very difficult because they are too small to be picked with common equipment. Therefore a new concept called collective transfer bonding using a temporary carrier chip was developed. A further benefit of this new technology is the high precision assembly as well as the plane parallel assembly of the LED-dies which is necessary for wire bonding. It has been shown that hundred functional LED-dies were transferred and soldered at the same time.

After the assembly a cost effective established PCB-technology was applied to produce a large-area light source consisting of many small LED-dies and electrically connected on a PCB-substrate. The top contacts of the LED-dies were realized by laminating an adhesive copper sheet followed by LDI structuring as known from PCB-via-technology. This assembly can be completed by adding converting and light forming optical elements. In summary two technologies based on standard SMD and PCB technology have been developed for panel level LED packaging up to 610x 457 mm² area size.

In addition, the light output power of blue LEDs with magnetic dot or line patterns is increased up to 28 %. The time-resolved photoluminescence (TR-PL) decay time of LEDs with ferromagnetic structures was faster than those of LEDs before magnetization due to an increase in the spontaneous emission rate by inhomogeneous magnetic field within the MQWs, resulting in the increased optical output power of LEDs. We believe that carriers under inhomogeneous magnetic field are easily confined in the localized potential minima of MQWs, which act as luminescence centers of InGaN-based LEDs. The length of carrier trajectory is increased by the external inhomogeneous magnetic fields and this can offer more chances for carriers to be trapped in a potential minima. In this presentation, the electrical and optical properties of InGaN/GaN MQW LEDs with various ferromagnetic structures will be addressed and propose a possible radiative recombination process under inhomogeneous magnetic fields.

9383-46, Session 10

Customized homogenization and shaping of LED light by micro cells arrays

Daniel Asoubar, Friedrich-Schiller-Univ. Jena (Germany) and LightTrans VirtualLab UG (Germany); Christian Hellmann, Hagen Schweitzer, Michael Kuhn, LightTrans (Germany); Frank Wyrowski, Friedrich-Schiller-Univ. Jena (Germany)

The energy-efficient use of LED light requires the development of compact illumination systems for the customized homogenization and shaping of partially-coherent LED light. Therefore a design concept which is based on arrays of aperiodic micro structures, namely cells, for primary or secondary optics is introduced. Each cell of the array deflects locally the light into predefined directions and results in a light spot in the target plane. The light spots of all array cells together form the desired light pattern. The performance of three different cell geometries (linear gratings, micro prisms and micro mirrors) on the homogenization and shaping of monochromatic as well as white light LEDs is demonstrated. For the realistic evaluation of the illumination system an LED model including power spectrum, polarization, spatial and temporal coherence is chosen. Furthermore wave-optical effects like diffraction at the cell apertures are taken into account. For the grating cells arrays a rigorous analysis of the diffraction efficiencies is included.

9383-47, Session 10

Enhanced optical output power of InGaN/GaN LEDs with ferromagnetic films on LEDs (*Invited Paper*)

Seong-Ju Park, Jae-Joon Kim, Young-Chul Leem, Gwangju Institute of Science and Technology (Korea, Republic of)

The general-purpose LED (light-emitting diode) requires high-brightness and high-energy efficiency. Although internal quantum efficiency (IQE) of LEDs has evolved dramatically, it is still seeking a new way to achieve additional enhancement for next-generation lighting sources. Here we address the effect of inhomogeneous magnetic fields on the performance of LEDs by incorporating ferromagnetic layers on gallium nitride (GaN)-based LED. We have observed the enhanced IQE of near UV, blue, and green LEDs by depositing ferromagnetic layers with various configurations such as films, stripe, and dot patterns on ohmic/reflector layers of InGaN/GaN multiple quantum wells (MQWs) LEDs. The light output power of the near UV, blue, and green LEDs with the CoFe or Co/Pt ferromagnetic layer after magnetization is enhanced by 5.7, 15.0, and 27.0% at an injection current of 20 mA, respectively, compared to those before magnetization of films.

Conference 9384: Emerging Liquid Crystal Technologies X

Monday - Wednesday 9 -11 February 2015

Part of Proceedings of SPIE Vol. 9384 Emerging Liquid Crystal Technologies X

9384-1, Session 1

Nematic topological line defects as optical waveguides (*Keynote Presentation*)

Slobodan Žumer, Miha Žula, Miha Ravnik, Univ. of Ljubljana (Slovenia)

Liquid crystals are recently attracting a lot of attention with applications far beyond the display technology. Their high birefringence, softness, and possibility to form complex topological defect structures allow for easy light manipulation in systems ranging from cholesteric lasers [Coles & Morris, Nat. Photonics 2010] to droplet resonators [Humar et al., Nat. Photonics 2009] and smectic filament wave guides [Peddireddy et al., Optics Exp. 2013]. Recent interest in light-induced topological defects [Smalyukh et al., Nat. Materials 2010; Porenta et al. Soft Matt. 2012] and light propagation along the disclinations [Lousiest et al., Phys. Rev. Lett 2013] stimulated us to develop a customized version of the Finite-Difference Time-Domain (FDTD) method for solving Maxwell's equations on a discrete time & space lattice and modeling the time-evolution of electromagnetic fields. With the numerical procedure we simulate the propagation of light beams along nematic disclination lines characterized by different winding numbers. We show how topological invariants of the nematic and polarization fields combine. For certain birefringence and appropriate light propagation distance, the linearly polarized light beam attains a polarization profile with twice the winding number of the liquid crystal disclination. Further possible focusing and defocusing of the light propagating along the disclinations is analyzed for weak intensity beams. Finally we also model self-reshaping of the high intensity optical beams by adding dielectric coupling to the free energy and, in parallel to FDTD calculation of electromagnetic fields, numerically solving the minimization equations for nematic fields.

9384-2, Session 1

Laser manipulation of colloids dispersed in an azo dye-doped liquid crystal cell (*Invited Paper*)

Andy Y. G. Fuh, Te-Wei Chang, Ming-Shian Li, Shing-Trong Wu, National Cheng Kung Univ. (Taiwan)

Recently, azo derivatives have been intensively studied because of their interesting anisotropic properties, in particular, the effects of adding azo derivatives in some organic materials, e. g. polymers and/or liquid crystals (LCs). In this paper, laser manipulation of micron-sized colloids dispersed in an azo dye-doped nematic liquid crystal by both unfocused and focused laser beams are studied. In the case of unfocused pumping laser, the results show that the laser-induced isothermal phase transition causes nematic/isotropic phase separation through nucleation process, and the isotropic domain is gradually increased with the exposure time of the pumping beam. It is observed that nematic colloids are bounded and move with the nematic-isotropic phase boundary. As the sample is pumped by a focused laser beam, an air-cavity can be induced, which can control the movement of colloids in a LC cell, and finally trap colloids. The distance of a colloid that can be trapped by the air-cavity is estimated to be approximate 200 μm . The details of sample fabrication, experimentals, and results are discussed.

The authors would like to thank the National Science Council of Taiwan for financially supporting this research under Grant No. NSC 101-2112-M-006-011-MY3. Additionally, this work is partially supported by the Top University Program of the National Cheng Kung University as well.

9384-3, Session 1

Self-assembly and self-alignment of plasmonic particles with complex shape and non-trivial topology in liquid crystalline dispersions

Ye Yuan, Univ. of Colorado at Boulder (United States); Ivan I. Smalyukh, Univ. of Colorado at Boulder (United States) and National Renewable Energy Lab. (United States)

Recent studies on topological colloids, including the ones with the surface topologies of handlebodies of different genus and torus knots [1,2], suggest the possibility of using geometric and topological features of colloidal particles in guiding their self-assembly and self-alignment in liquid crystals, which can be realized through surface anchoring and elasticity-mediated interactions or entanglement of particle-induced defects. However, most of the studies of topological colloids so far were performed for micrometer-sized particles. In this work, we describe development of topological nanocolloids. Plasmonic metal nanoparticles with non-trivial topology were synthesized and dispersed in a liquid crystal host after surface passivation. We demonstrate that this guest-host system shows different properties from previously reported ones, such as dispersions of metal nanorods and nanoplatelets homeomorphic to spheres[3]. Nanoparticles with strongly-pronounced geometric features like pentagonal stems, dubbed as "mesoflowers", are also studied both experimentally and numerically. Our findings indicate that topology and geometry of nanocolloids can be used as means of controlling self-alignment and self-assembly of nanoparticles in thermotropic liquid crystalline colloidal dispersions.

[1]. B. Senyuk, Q. Liu, S. He, R. D. Kamien, R. B. Kusner, T. C. Lubensky and I. I. Smalyukh. Nature 493, 200-205 (2013).

[2]. A. Martinez, M. Ravnik, B. Lucero, R. Visvanathan, S. Žumer, and I. I. Smalyukh. Nature Mater.13, 258-264 (2014)

[3]. Q. Liu, Y. Yuan, and I. I. Smalyukh. Nano Lett. 14, 4071-4077 (2014)

9384-4, Session 1

Plasmonic nanocomposites of gold nanorods and cellulose nanocrystals

Qingkun Liu, Michael G. Campbell, Ivan I. Smalyukh, Univ. of Colorado at Boulder (United States)

Fabricating nano-structured materials with plasmonic properties from renewable, biocompatible sources remains a challenge. In this work, we developed cellulose-based orientationally ordered soft matter composites with polarization-dependent properties. Gold nanorods (GNRs) self-assembled into nematic-like and helicoidally orientational order by use of colloidal dispersions of cellulose nanocrystals (CNCs) in mesomorphic phases as host materials. We observed a transition from an initial orientationally disordered dispersion of GNRs to that with a uniaxial order mimicking that of CNCs and exhibiting polarization-dependent plasmonic extinction with increasing the CNCs concentration. Cholesteric-isotropic phase coexistence and continuous domains of single-phase regions were observed and qualitatively discussed on the basis of entropic and electrostatic interactions in co-dispersions of rigid rods of different aspect ratios. Furthermore, using the ensuing GNRs-CNCs nano-dispersion, we obtained thin solid films with orientationally ordered organization of both CNCs and GNRs. These structured films can be converted into mesoporous silica films decorated with aligned GNRs obtained by using cellulose-based nanostructures as a replica. The ensuing long-range alignment of GNRs in both cellulose-based and nanoporous silica films results in a polarization-

**Conference 9384:
Emerging Liquid Crystal Technologies X**

sensitive surface plasmon resonance. Transmission electron microscopy, polarization-sensitive extinction spectra and two-photon luminescence imaging were used to characterize orientations and spatial distributions of GNRs. The demonstrated device-scale bulk nanoparticle alignment may enable engineering of new material properties arising from combining the orientational ordering of host nanostructures and properties of the anisotropic plasmonic metal nanoparticles, including biologically compatible plasmonic composite nanomaterials for solar biofuel production and polarization-sensitive plasmonic papers and nanoporous silica structures with polarization-dependent plasmonic effect.

9384-5, Session 2

Surface dynamics and mechanics in liquid crystal polymer coatings (*Invited Paper*)

Danqing Liu, Dirk Broer, Technische Univ. Eindhoven (Netherlands)

Based on liquid crystal networks we developed 'smart' coatings with responsive surface topographies. Either by pre-patterning or by the formation of self-organized structures they can be switched on and off in a pre-designed manner. Here we provide an overview of our methods to generate coatings that form surface structures upon the actuation by light. The basic principle is based on the change of molecular organization in ordered liquid crystal polymer networks. The change in order leads to anisotropic expansion and an increase in volume by the formation of free volume. These two effects work in concert to provide local expansion and contraction in the coating steered by the local direction of molecular orientation. The depth of modulation that we achieve by the various methods is of the order of 20% of the coating thickness. Switching occurs on a time scale of seconds. We present here an example of the dynamic formation of fingerprints texture in chiral nematic polymer networks. The coating has a flat surface but when actuated by light in the presence of a copolymerized azobenzene compound, 3D fingerprints structures appear in the coating. One of the applications of switchable topographies is the control over the surface tribology in a dynamic way. By forming or removing the coating surface textures the tribological behavior can be altered accordingly. Here, in this fingerprints sample, the friction coefficient drops by a factor of four to five when the fingerprint switched on because of reduced surface contacts.

9384-6, Session 2

Plasmon-exciton resonant energy transfer in soft optical metamaterials (*Invited Paper*)

Giuseppe Strangi, Case Western Reserve Univ. (United States)

INVITED TALK

The performance of all metamaterial-based applications is significantly limited by the inherent and strong energy dissipation present in metals, especially in the visible range. We experimentally demonstrate that the incorporation of excitonic material in the high-local-field areas of plasmon nanostructures induce coherent resonant energy transfer processes from chromophores (donors) to plasmon nanoentities (acceptor). Ultra-fast fluorescent time-resolved spectroscopy paired with transient absorption spectroscopy and spectroscopic ellipsometry in pump-probe configuration emphasize a strong exciton-plasmon coupling behind the process of non-radiative excitation energy transfer (RET). Across scales studies show how these energy transfer processes occurring at the nanoscale translate to liquid crystal based bulk materials. Multipronged strategies - bio-inspired and bottom up - allowed obtaining important advances in materials science and paves the way toward further promising scientific research aimed to enable the wide range of electromagnetic properties of optical metamaterials.

9384-7, Session 2

Properties and applications of nano-pore dispersed liquid crystals (*Invited Paper*)

Hiroyuki Yoshida, Junji Kobashi, Hoekyung Kim, Osaka Univ. (Japan); Yo Inoue, Kyoto Univ. (Japan); Yasutaka Maeda, Masanori Ozaki, Osaka Univ. (Japan)

One of the main properties of liquid crystals is that their refractive index can be tuned by an applied electric field. While large tuning of the refractive index reaching 0.2 or even greater can be realized, liquid crystals possess an inherent drawback - a slow response time, which originates from the fact that their response is due to reorientation of the bulk liquid crystal director. We have recently shown that in-situ polymerization of a mixture of a low molecular weight liquid crystal and a mesogenic monomer can produce nano-composites in which the liquid crystals are confined in nano-sized pores dispersed throughout the matrix. The confinement of liquid crystals in nano-sized voids can accelerate their response by more than a factor of 100, and moreover, strongly fixes the molecular orientation of the liquid crystal, allowing a 'deformation-free' response. The deformation-free response is particularly useful for the tuning of cholesteric liquid crystals as the optical properties can be tuned without disturbing the helical structure. In this presentation, we will show recent results on how the morphology of the polymer matrix changes depending on the fabrication conditions, and its relationship to the electro-optic response. We also discuss possible applications of this nano-composite.

9384-8, Session 2

Probing helical nanostructures in B4 and TGB phases with resonant x-ray scattering at carbon k-edge

Chenhui Zhu, Cheng Wang, Anthony T. Young, Feng Liu, Ilja Gunkel, Lawrence Berkeley National Lab. (United States); Wim Bras, ESRF - The European Synchrotron (France); David M. Walba, Noel Clark, Univ. of Colorado at Boulder (United States); Alexander Hexemer, Lawrence Berkeley National Lab. (United States)

Liquid crystals (LCs) form many interesting nano-scale structures, many of which can be probed with X-ray scattering techniques, such as layering in smectics, hexagonal packing in discotics, and layer modulation in bent-core smectics (e.g. B7 phase [1], SmAPFmod phase[2]). Typically hard X-rays are used due to its high penetrating power, however, the scattering cross section depends on x-ray energy, and is low for organic materials in the hard-x-ray regime, which makes it extremely difficult to characterize nanostructures of weak electron density modulation, such as the helical structure in B4 nanofilaments. Here we show that the scattering contrast can be dramatically improved by tuning the x-ray energy to carbon K-edge (- 284 eV). In addition, at resonance, the scattering cross section becomes sensitive to chemical bond orientation, thus enabling us to monitor the evolution of helical pitch as a function of temperature. The technique may be extended to investigate blue phase and clock phase in smectics [3].

[1] D.A. Coleman, et al. Science, 301, 5637 (2003).

[2] C. Zhu, et al. J. Am. Chem. Soc. 134, 9681 (2012).

[3] P. Mach, et al, Phys. Rev. Lett. 81, 1015 (1998).

**Conference 9384:
Emerging Liquid Crystal Technologies X**

9384-46, Session 2

Single-photon experiments with liquid crystals for quantum science and quantum engineering applications (*Invited Paper*)

Svetlana G. Lukishova, Univ. of Rochester (United States); Andreas C. Liapis, Brookhaven National Lab. (United States); Luke J. Bissell, Air Force Research Lab. (United States); Justin M. Winkler, George M. Gehring, Univ. of Rochester (United States); Robert W. Boyd, Univ. of Rochester (United States) and Univ. of Ottawa (Canada)

We present our results on using liquid crystals (LCs) in experiments with nonclassical light sources: (1) single-photon sources exhibiting antibunching, which are key components for secure quantum communication systems [1,2], and (2) entangled photon sources with photons exhibiting quantum interference in a Hong-Ou-Mandel interferometer [2, 3]. In the first part, LC hosts were used to create definite linear or circular polarization of antibunched photons emitted by single dye molecules, nanocrystal quantum dots, etc. In the second part (a) we measured with femtosecond resolution difference in propagation times through planar-aligned cholesteric LCs of two opposite handedness circular polarizations at different points of selective transmission curves along a bandedge; (b) we simulated quantum-mechanical barrier tunnelling phenomena using an electrically controlled planar-aligned nematic LC layer between two prisms in the conditions close to a frustrated total internal reflection.

[1] S.G. Lukishova, et al., *Opt. Lett.* 37, 1259 (2012)

[2] S.G. Lukishova, et al., *Liquid Crystal Reviews* 2, N 2, 111 (2014)

[3] G. Gehring, et al., *Phys. Rev. Lett.* 111, 030404 (2013).

9384-9, Session 3

Light-directing chiral liquid crystalline nanostructures: from 1D to 3D (*Keynote Presentation*)

Quan Li, Kent State Univ. (United States)

Liquid crystals (LCs) represent a fascinating state of matter which combines order and mobility on a molecular and supermolecular level. The unique combination of order and mobility results in that LC is typically “soft” and responds easily to external stimuli. The responsive nature and diversity of LCs provide tremendous opportunities as well as challenges for insights in fundamental science, and open the door to various applications. Conventional nematic LCs have become the quintessential materials of LC displays. With the LC displays ubiquitous in our daily life and annual more than \$100 billion market, the research and development of LCs are moving rapidly beyond display applications and evolving into entirely new and fascinating scientific frontiers. In my talk, I will focus on our recent research and development on light-directing chiral liquid crystalline nanostructures: from 1D to 3D.

9384-10, Session 3

The helical nanofilament phase for organic photovoltaics (*Invited Paper*)

David M. Walba, Rebecca A. Callahan, Michael T. Springer, Eva D. Korblova, Ranfan Shao, Univ. of Colorado at Boulder (United States); David Coffey, Garry Rumbles, National Renewable Energy Lab. (United States); Noel A. Clark, Univ. of Colorado at Boulder (United States)

The helical nanofilament (HNF) liquid crystal phase represents a unique

hierarchical assembly of bent-core mesogens.[1] In the bulk HNF phase, smectic stacks possess spontaneous negative Gaussian curvature, limiting the width of the layers (~ 40nm, and the number of layers in a stack (~40 nm), providing long helical nanofilaments ~ 40 nm diameter, which then self-organize into a porous hexagonal array of HNFs. Furthermore, half the surface area of the HNFs is composed of layer edges, putting the edges of the aromatic sublayers in direct contact with the surroundings, which may contain any one of many nanophase segregated dopants up to concentrations ~ 50% by weight. These dopants can be soluble fullerenes such as PCBM, in which case the doped sample represents nanostructured bulk heterojunction (BHJ) system with possible application in organic photovoltaics (OPV). This gains added attractiveness due to the additional hypothesis, supported by solid state NMR data, that the aromatic core sublayers in the HNF phase are effectively crystalline in nature. Recent studies using flash photolysis time-resolved microwave conductivity suggesting efficient exciton splitting from excited PCBM in a prototypical HNF mesogen/PCBM BHJ will be described.

References:

[1] Hough, L. E.; Jung, H. T.; Krüerke, D.; Heberling, M. S.; Nakata, M.; Jones, C. D.; Chen, D.; Link, D. R.; Zasadzinski, J.; Heppke, G.; Rabe, J. P.; Stocker, W.; Korblova, E.; Walba, D. M.; Glaser, M. A.; Clark, N. A. “Helical nanofilament phases,” *Science* 2009, 325, (5939), 456-460.

9384-11, Session 3

Chiral nano-pore arrays with bent-core liquid crystals and their applications

Dong Ki Yoon, Hanim Kim, Kiback Choe, Seong Ho Ryu, Sunhee Lee, KAIST (Korea, Republic of); Tae Joo Shin, Pohang Univ. of Science and Technology (Korea, Republic of); Eva D. Korblova, David M. Walba, Noel A. Clark, Univ. of Colorado at Boulder (United States); Sang Bok Lee, Univ. of Maryland, College Park (United States); Pilhan Kim, KAIST (Korea, Republic of)

We introduced a novel chiral nano-pore-system using bent-shaped liquid crystals (LCs) and porous anodic aluminium oxide (AAO) films to achieve functional 3-dimensional nanostructures. Bent-core LCs self-assemble to a unique superstructure called as helical nanofilaments (HNFs), which is occurred by the highly restrictive molecular packing process under nanoconfinement based on porous AAO film. As a result, individually controlled HNFs readily grow in nanochannels of AAO film, generating hierarchically self-assembled chiral nano-porous structures. Both helical pitch and width of chiral pores are tuneable with sub-nanometer precision by varying the size of AAO.

In such self-generated chiral nano-pore arrays, the other guest materials such as 5CB which is -CN containing polar nematic liquid crystal were guided to achieve unusual optical property, for example second harmonic generation (SHG) signal. A high power laser was shined to 5CB molecules, resulting in changes of electric energy state and order parameter of 5CB molecules. This simple procedure produces SHG activity with the broken centro-symmetry in the molecular polarization. Our 3-dimensional nano-confining system can give an extreme restriction on ordering and alignment of 5CB molecules, prohibiting thermal fluctuations of the molecules, resulting in the maximized non-linear properties of 5CB. Here, SHG signal was observed by multi-photon confocal microscopy as a function of rotation angle of the sample. We believe our system can suggest novel applications of controlled nematic LCs to open a way to enhance nonlinear optical properties of other soft matters.

**Conference 9384:
 Emerging Liquid Crystal Technologies X**

9384-12, Session 3

Thin film polariser and color filter based on photo-polymerizable nematic liquid crystal

Mohammad Mohammadimasoudi, Jeroen Beeckman, Kristiaan Neyts, Univ. Gent (Belgium)

We present a method to fabricate a 6 μm thin film color filter based on a mixture of photo-polymerizable liquid crystal and chiral dopant. A chiral nematic liquid crystal layer reflects light for a certain wavelength interval $\Delta\lambda$ ($= \Delta n \cdot P$) with P the period and Δn the birefringence of the liquid crystal. The reflection band is determined by the chiral dopant concentration. The bandwidth is limited to 100 nanometer and the reflectance is at most 50% for unpolarized incident light. The thin color filter is interesting for innovative applications like polarizer-free reflective displays, polarization-independent devices, stealth technologies, or smart switchable reflective windows to control solar light and heat. The reflected light has strong color saturation without absorption because of the sharp band edges.

A thin film polarizer is developed by using a mixture of photo-polymerizable liquid crystal and color-neutral dye. The fabricated thin film absorbs light that is polarized parallel to the c axis of LC. The obtained polarization ratio is 80 % for a film of only 12 μm.

The thin film polarizer and color filter feature excellent film characteristics without domains and can be detached from the substrate which is useful in e.g. flexible substrates.

9384-13, Session 3

Zero-orientational birefringence polymer with no temperature dependence

Mio D. Shikanai, Akihiro Tagaya, Yasuhiro Koike, Keio Univ. (Japan)

Birefringence which can be generated in optical polymer films used in liquid crystal displays (LCDs), degrades the contrast ratio by changing the polarization state of the incident light. Therefore, a film that does not generate birefringence is needed. In previous works of our group, zero-zero-birefringence polymer (ZZBP) which exhibits neither orientational birefringence nor photoelastic birefringence at room temperature was successfully designed in a ternary copolymerization system. LCDs are used under condition where temperature changes, such as inside cars. To materialize higher image quality in-car LCDs, ZZBP that shows no temperature dependence of birefringence in a certain temperature range is required. However, temperature dependence of birefringence of polymers, especially of ZZBP, has not yet been explained in details.

In this research, we elucidated that intrinsic birefringence shows temperature dependence. Orientational birefringence is the product of intrinsic birefringence and degree of orientation. Thus when intrinsic birefringence is zero, orientational birefringence will not generate. We defined the proportionality constant of intrinsic birefringence against temperature as temperature coefficient of intrinsic birefringence. We then suggested a method to control the temperature dependence of birefringence to zero by copolymerizing monomers with opposite signs of temperature coefficient of intrinsic birefringence. Intrinsic birefringence itself can also be adjusted to zero in the same manner. By copolymerizing monomers in a composition which fulfills both requirements simultaneously, a film that exhibits almost no temperature dependence of orientational birefringence and almost no orientational birefringence was designed. This is an essential step to materialize ZZBP with no temperature dependence of birefringence.

9384-14, Session 4

Dynamics of liquid crystal blue phases (Keynote Presentation)

Hirotsugu Kikuchi, Kyushu Univ. (Japan)

Blue phases (BPs) are liquid crystal (LC) phases which occurs for high chiral nematic liquid crystals in a temperature range between a chiral nematic and an isotropic phases, and are optically isotropic without birefringence because of their cubic lattice structure consisting of double twisted cylinders. If an electric field is applied to BPs, a field-induced birefringence obeying the Kerr law is observed due to both of an electrostriction of the BP lattice and a reorientation of local director of liquid crystal within the BP lattice. In this study, temperature dependences of Kerr coefficient and the electro-optic response of polymer-stabilized blue phases (PSBPs) with various polymer concentrations were investigated at a wide temperature range including lower temperature than room one.

Through measurements of E-O Kerr effect of PSBPs with various polymer concentrations at a low temperature, their local director reorientation was found to be abruptly decreased below 280 K. As a temperature was lowered, the E-O response times increased monotonously and could be fitted by the Arrhenius equation. The molecular relaxation time of LC molecules in PSBPs became gradually slower with lowering temperature. In addition, the temperature dependence of molecular relaxation time was well fitted by the Vogel-Fulcher equation. Therefore, the kinetic modes of electro-optical response and dielectric relaxation are different. The rotation of LC molecule about the short axis in PSBPs was not abruptly lowered in a temperature where the local director reorientation was frozen, and unaffected by the polymer network in BP. The results agree well with the proposed PSBP model, in which polymers are phase-separated from the LC ordered region to be concentrated in the disclinations where LC order is reduced.

9384-15, Session 4

Stabilizing blue phase liquid crystals with linearly polarized UV light (Invited Paper)

Daming Xu, Jiamin Yuan, CREOL, The College of Optics and Photonics, Univ. of Central Florida (United States); Martin Schadt, MS High-Tech Consulting (Switzerland); Jing Yan, Southeast Univ. (China) and CREOL, The College of Optics and Photonics, Univ. of Central Florida (United States); Shin-Tson Wu, CREOL, The College of Optics and Photonics, Univ. of Central Florida (United States)

Polymer-stabilized blue-phase liquid crystal (BPLC) has become an increasingly important technology trend for information display and photonic applications. BPLC exhibits several attractive features, such as reasonably wide temperature range, submillisecond gray-to-gray response time, no need for alignment layer, optically isotropic voltage-off state, and large cell gap tolerance when an in-plane switching (IPS) cell is employed. Fast response time not only suppresses image blurs, improves the overall transmittance but also enables color sequential display without noticeable color breakup. With time sequential RGB LED colors, the spatial color filters can be eliminated so that both optical efficiency and resolution density are tripled. High optical efficiency helps to reduce power consumption while high resolution density is particularly desirable for the future Ultra High Definition Television. However, some bottlenecks such as high operation voltage, relatively low transmittance, and noticeable hysteresis and prolonged response time at high field region for in-plane switching (IPS) mode, remain to be overcome before widespread application of BPLC can be realized. To reduce operation voltage, both new BPLC materials and new device structures have been investigated. In this paper, we investigate the electric field effects of PS-BPLC and evaluate quantitatively the individual contribution of Kerr and electrostriction effects. Especially, we will demonstrate a hysteresis-free PS-BPLC with 2X faster response time by implementing linear photo-polymerization approach. The sunrise for BP LCD is near.

**Conference 9384:
 Emerging Liquid Crystal Technologies X**

9384-16, Session 4

Electro-optical behavior of polymer dispersed blue phase liquid crystals

Emine Kemiklioglu, Liang-Chy Chien, Kent State Univ. (United States)

We have recently demonstrated polymer dispersed blue phase (PDBP) liquid crystal droplets that have low switching voltage with in-plane electric field. The PDBP films are prepared via solvent evaporation-induced phase separation of a mixture of blue phase liquid crystal and polymer latex. The PEBP films laminated between two indium-tin-oxide coated conductive substrates enable switching between light scattering and transparent states in response to applied electric fields across the films. The observed textures of PDBP samples show a uniform, reflecting, bluish-green color of the BPI at room temperature. Electro-optical behavior of the PDBP films of different compositions and will be discussed. We will compare and contrast the use of these materials for two different light modulator operation modes; the normal and reverse modes.

9384-17, Session 4

Field-induced Bragg diffraction in polymer stabilized cholesteric liquid crystal bubbles

Andrii Varanytsia, Liang-Chy Chien, Kent State Univ. (United States)

Cholesteric liquid crystals (CLC) with a specific confinement conditions are known to form bubble domain (BD) texture. The BD texture consists of a single layer of bubbles embedded into a uniform homeotropic matrix. Each bubble is formed by a vortices-like distortion of a LC director field around two distance separated defects stabilized by an energy barrier against nucleation, bigger than a thermal energy. We have developed the CLC BD texture stabilized with a small amount of polymer.

CLC bubbles of a BD texture have a particle-like behavior and self-assemble into domains with a hexagonal ordering. Hexagonally ordered BD texture is a diffraction grating, providing a high contrast far-field laser diffraction pattern with diffraction maxima representing positions of bubbles in the sample with respect to each other. By stabilization with a small amount of polymer we have improved optical quality of the diffractive CLC layer and at the same time increased its mechanical stability and durability.

We will discuss the approach for obtaining a well-ordered BD texture with an applied electric field, optimum polymerization conditions and will compare properties of samples with different amount of polymer. Detailed electro-optical performance of the polymer stabilized BD CLC samples as well as results of a thorough scanning electron microscopy morphological study of the polymer network formed in the bulk of the liquid crystal cells will be presented.

9384-18, Session 5

Dynamic LC/polymer systems (Keynote Presentation)

Timothy J. Bunning, Air Force Research Lab. (United States); Luciano De Sio, Svetlana V. Serak, BEAM Engineering for Advanced Measurements Co. (United States); C. Umeton, Univ. della Calabria (Italy); E. Ouskova, BEAM Engineering for Advanced Measurements Co. (United States); V. Tondiglia, Timothy J. White, Air Force Research Lab. (United States); Nelson V. Tabiryan, BEAM Engineering for Advanced Measurements Co. (United States)

Novel combinations of polymer and liquid crystals can be utilized to obtain useful photo- and electro-optic dynamic properties and several such examples will be explored. We discuss novel periodic structures formed through holography wherein the local chemical structure of the periodic wall induces well aligned initial conditions of the as-formed two-phase structure. We explore a new generation of a LC composite material system made of an anisotropic polymer and continuously dispersed NLC phase - LCPDLC. These represent a solid-state electro-optical modulator that possess low-voltage drive and large phase modulation capabilities. Finally, we explore the fabrication and characterization of curved periodic microstructures formed through the controlled phase separation of a liquid crystal and a polymerizing matrix comprising self-aligned liquid crystal. Imaging through a "Fresnel like" structure imparts an intensity profile onto a photosensitive mixture which subsequently forms periodic alternating curved polymeric and liquid crystal slices. The system exhibits high-quality and self-alignment of an ordered (liquid crystal) fluid without the need of surface chemistry or functionalization.

9384-19, Session 5

Liquid crystal waveguide technologies for a new generation of low-power photonic-integrated circuits (Invited Paper)

Antonio d'Alessandro, Rita Asquini, Luca Martini, Univ. degli Studi di Roma La Sapienza (Italy)

Future further development of datacom applications can be faced, only if tight power dissipation requirements will be satisfied, for the ever increasing demand of more dense and higher speed web interconnections. Replacing electronics with optics is a viable solution, therefore reliable low driving and consumption power photonic components are requested at reasonable low costs per chip. A low cost photonic component technology would also increase functionality in the micro-optofluidic circuits in the novel and increasing application field of lab-on-chips. In this talk we will propose and compare several approaches to fabricate photonic channels on several substrate technology platforms ranging from glass, silicon and polydimethylsiloxane (PDMS) for flexible photonic integrated circuits.

In particular the electro-optic effect and nonlinear optical properties of liquid crystals (LC) and doped LC novel materials allow the realization of low cost and low energy consumption optoelectronic devices. High extinction ratio and large tuning range guided wave devices will be presented. In particular we will show our recent results on light propagation in channel waveguides whose core consists of LC infiltrated in PDMS channels (LC:PDMS waveguides). Both theoretical and experimental results show polarization independent light transmission despite of the typical LC optical anisotropy due to the cigar-like shape of the LC molecules, which generally induce polarization dependence of light propagation.

Because of their sub-milliwatt power consumption such integrated optical devices can trigger the development of a new generation of low power, compact and low cost all-optical components for next generation fiber optic datacom and sensor systems.

9384-20, Session 5

Emerging liquid crystal waveguide technology for low SWaP active short-wave infrared imagers

Sean D. Keller, Gerald P. Uyeno, Ted Lynch, Raytheon Missile Systems (United States); Scott R. Davis, Scott D. Rommel, Juan M. Pino, Vescent Photonics Inc. (United States)

Raytheon's innovative active short wave infrared (SWIR) imager uses Vescent Photonics's emerging liquid crystal waveguide (LCWG) technology to continuously steer the illumination laser beam over the imager field of

**Conference 9384:
Emerging Liquid Crystal Technologies X**

view (FOV). This approach instantly illuminates a very small fraction of the FOV, which significantly reduces the laser power compared to flash illumination. This reduced laser power directly leads to a reduction in the size, weight and power (SWaP) of the laser. The reduction in laser power reduces the input power and thermal rejection, which leads to additional reduction in the SWaP of the power supplies and thermal control.

The high-speed steering capability of the LCWG enables the imager's SWaP reduction. The SWaP reduction is possible using either global or rolling shutter detectors. In both cases, the LCWG steers the laser beam over the entire FOV while the detector is integrating. For a rolling shutter detector, the LCWG synchronizes the steering with the rolling shutter to illuminate only regions currently integrating. Raytheon's approach enables low SWaP active SWIR imagers without compromising image quality.

This paper presents the results of Raytheon's active SWIR imager demonstration including steering control and synchronization with the detector integration.

Non-technical as defined under ITAR 120.10

9384-21, Session 5

Fast-response IR spatial light modulators with a polymer network liquid crystal

Fenglin Peng, Haiwei Chen, Shin-Tson Wu, Univ. of Central Florida (United States); Suvagata Tripathi, Robert J. Twieg, Kent State Univ. (United States)

Liquid crystals have widespread applications for amplitude modulation (such as flat panel displays) and phase modulation (such as adaptive optics and beam steering). For phase modulation, a 2π phase modulo is required. To extend the electro-optic application into infrared region (MWIR and LWIR), several key technical challenges have to be overcome: 1. low absorption loss, 2. high birefringence, 3. low operation voltage, and 4. fast response time. After three decades of extensive development, an increasing number of IR devices adopting liquid crystal technology have been demonstrated, such as liquid crystal waveguide, laser beam steering at 1.55 μ m and 10.6 μ m, spatial light modulator in the MWIR (3-5 μ m) band, dynamic scene projectors for infrared seekers in the LWIR (8-12 μ m) band. However, several fundamental molecular vibration bands and their overtones exist in the MWIR and LWIR regions, which contribute to high absorption coefficient and hinder its widespread application. Therefore, the inherent absorption loss becomes a major concern for IR devices. To suppress IR absorption, several approaches have been investigated: 1) Employing thin cell gap by choosing a high birefringence liquid crystal mixture; 2) Shifting the absorption bands outside the spectral region of interest by deuteration, fluorination and chlorination; 3) Reducing the overlap vibration bands by using shorter alkyl chain compounds. In this paper, we report some chlorinated terphenyl liquid crystals and mixtures with a low absorption loss in the near infrared and MWIR regions. To achieve fast response time, we have prepared several polymer network liquid crystal (PNLC) composites and studied their phase modulation properties. A PNLC with 2π phase change at MWIR and response time less than 5 ms is demonstrated.

9384-22, Session 6

Voltage-tunable liquid-crystal-based filters, resonators, and lasers (Invited Paper)

Kristiaan Neyts, Mohammad Mohammadimasoudi, Yi Xie, Inge Nys, Jeroen Beeckman, Univ. Gent (Belgium)

Liquid crystals are birefringent and depending on the orientation of the director the effective refractive index may be varied. In this work we consider optical filters and resonators that are based on selective reflectivity. Wavelength-selective reflectivity may be obtained by using two solid mirrors (metallic or Bragg-dielectric) or by taking advantage of the

reflection band in the self-organized periodic structures formed by chiral nematic liquid crystal. When two solid mirrors are used, nematic liquid crystal between the mirrors makes it possible to tune the wavelength of the resonance peaks by applying a voltage. When chiral nematic liquid crystal is used, the reflection band is determined by the pitch and the refractive indices.

Three different implementations will be discussed. The first is a partially-polymerized fast-switching chiral nematic liquid crystal filter that can continuously switch its reflection band. Secondly a vertical-cavity surface-emitting laser has been integrated in a liquid crystal device, which allows to switch the polarization state and the wavelength of the laser emission. Finally the laser emission from a dye-doped liquid crystal layer between two reflective surfaces is studied. For each of these examples, the device technology and electro-optical properties will be discussed. The results will be compared with numerical simulations that describe the optical properties of these devices.

9384-23, Session 6

Liquid crystal THz photonics with indium tin oxide nanowhiskers and graphene as functional electrodes (Invited Paper)

Ci-Ling Pan, National Tsing Hua Univ. (Taiwan)

We have constructed and characterized THz phase shifters based on liquid crystals (LCs) with graphene and indium-tin-oxide nanowhiskers (ITO NWs). A graphene-based phase shifter can achieve a phase shift of $\pi/2$ at 1.0 THz with the operating voltage of -2.2 V (rms) versus -5.6 V (rms) for ITO-NWs-based phase shifter in previous work. On the other hand, 2π phase shift at 1.0 THz was achieved in an ITO-NWs-based phase shifter with a multi-sandwiched structure by applying -2.6 V (rms). The low operation voltage of both two kinds of phase shifters imply the compatibility with thin-film transistor (TFT) and complementary metal-oxide-semiconductor (CMOS) technologies. The experimental results of phase shifters are in good agreement with the theoretical predictions. Both types of phase shifters exhibit excellent transmission characteristics in the THz frequency range. Further, ITO NWs can be used to align the LC cell

9384-24, Session 6

Multi-twist retarders in homogeneous and inhomogeneous alignment (Invited Paper)

Michael J. Escuti, Kathryn J. Hornburg, North Carolina State Univ. (United States)

Multi-Twist Retarders (MTRs) are a family of complex birefringent elements that offer remarkably flexible control of broadband polarization transformation and retardation. They are comprised of two or more twisted liquid crystal (LC) layers on a single substrate and with a single alignment layer, and as such, they are preferably formed with polymerizable LC (reactive mesogen) materials. Importantly, subsequent LC layers are aligned directly by prior layers, allowing simple fabrication, achieving automatic layer registration, and resulting in a monolithic film with a continuously varying optic axis through the thickness. Our initial study focused on achromatic and super-achromatic half- and quarter-wave retarders, and found their behavior matches or exceeds that of the analogous stacked homogeneous waveplate (e.g., Pancharatnam style), in both theory and experiment. This enables achromatic louvered waveplates (i.e., film patterned retarders), which have multiple domains of uniform orientation (i.e., homogeneous alignment), to be conveniently produced with MTRs for display and telecommunications applications. More recently, we have studied MTRs elements with highly chromatic behavior, e.g., acting as color filters, or acting as polarization gratings with high diffraction efficiency in the infrared but high transparency in the visible. Perhaps most interestingly, in cases where the optical axis of an MTR is spatially patterned within the film plane (i.e., inhomogeneous alignment), the geometric phase can

**Conference 9384:
Emerging Liquid Crystal Technologies X**

be controlled across a wide bandwidth. This has led to some of the most efficient and compelling broadband thin-film optical elements, including achromatic polarization gratings, white-light geometric phase lenses, and distortion-free holograms.

9384-25, Session 6

Electrically-regulated bandwidth broadening in polymer stabilized negative dielectric anisotropy cholesteric liquid crystals as color-tunable mirrors

Kyung Min Lee, Vincent P. Tondiglia, Chad Keister, Timothy J. Bunning, Timothy J. White, Air Force Research Lab. (United States)

We report on the color-tunable mirrors based on electrically-regulated bandwidth broadening of the circularly polarized reflection of polymer stabilized cholesteric liquid crystals (PSCLCs). A number of improvements including color and bandwidth stability, baseline optical properties, and response times will be discussed based on the study of structural chirality, viscoelastic properties of the polymer network architecture, and electro-optic drive schemes. The examination of PSCLC samples prepared in different conditions and compositions further elucidate the dominant role of structural chirality and the impact of crosslinking of the polymer stabilizing network on the threshold voltage and relative change in bandwidth per voltage. Furthermore, nonideal optical properties (scatter and haze) associated with the polymer/LC compatibility and effectiveness of structural templating will be also discussed.

9384-27, Session 6

Filtration and modulation of infrared radiation by the small particles: dual-frequency liquid crystal system

Tahir D. Ibragimov, Gazanfar M. Bayramov, Abbas R. Imamaliyev, Institute of Physics (Azerbaijan)

Possibility of application of the small particles - dual frequency liquid crystal (DFLC) system is studied for selective filtration and modulation of infrared (IR) radiation.

Aluminum oxide particles and DFCL consisting of 4-n-pentyl-4'-cyanobiphenyl (5CB), 4-hexyloxyphenyl ester 4'-hexyloxy-3-nitrobenzoic acid (C2), and 4-n-pentanoyloxy-benzoic acid-4'-hexyloxyphenyl ester (H 22) were used as a filler and a matrix, correspondingly. The preliminary study of transmission spectra of the LC mixture has shown its sufficient transparency up to 1800 cm⁻¹ at small layer thickness except for a set of the bands at 2800-3200 cm⁻¹ and a narrow band at 2220-2250 cm⁻¹ corresponding to vibrations of the CH₂, CH₃ and NO₂ groups and the refractive index of aluminum oxide dramatic changes in this spectral region. The cells for optical measurements had a "sandwich" structure with conductive p-type germanium substrates transparent in the mid-IR range.

Transmission spectra of the aluminum oxide particles-DFLC system in both the ordinary electro-optic cell and the twist-structure were carried out. Experiments showed that for certain changes in the frequency of the applied electric field, the transmission region maximum of the aluminum oxide particles - DFCL ordinary cell switched from one wavenumber to another. While the twist-structure of the system at low frequencies passed the IR radiation at the same wavenumbers but it became practically opaque at high frequencies. The basic optic and electro-optic parameters of both only DFCL and the entire system were determined.

The experimental results are explained by the optical homogeneity of the system in a narrow wavenumber interval when the refractive indices of the particle material and the matrix are close, and also by reorientation of the liquid crystal molecules as the frequency of the applied voltage changes.

This work was done with the support of the Science and Technology Center in Ukraine (grant no. 5821).

9384-45, Session 6

Dynamic and complex optical patterns from colloids of cholesteric liquid crystal droplets (*Invited Paper*)

Junghyun Noh, Univ. du Luxembourg (Luxembourg); Irena Drevensek-Olenik, Univ. of Ljubljana (Slovenia); Jun Yamamoto, Kyoto Univ. (Japan); Jan P. Lagerwall, Univ. du Luxembourg (Luxembourg)

Planar-aligned short-pitch cholesteric liquid crystals confined into a spherical sample, e.g. as a droplet or shell suspended in an aqueous continuous phase, exhibit unique and very attractive optical properties [1]. This is due to the combination of Bragg reflection and spherical sample symmetry, with consequent radial orientation of the cholesteric helix axis. If such a droplet is illuminated from above the reflected light is separated into a continuous set of cones, each with a narrow and well-defined wavelength regime. For the wavelength that fulfills the Bragg condition at 45° incidence the cone opening angle is 90° and the reflected light is thus directed into the plane of the sample, with equal intensity along all directions that are perpendicular to the incoming beam. This immediately makes spherical cholesteric samples useful for coupling light with a specific wavelength uniformly into a plane. Even more interestingly, if multiple cholesteric droplets are in one and the same sample, the horizontally reflected light from one droplet is reflected back up by the surrounding ones, but this happens only for the wavelength fulfilling the Bragg condition. A second mechanism for such photonic cross communication between droplets is mediated via total internal reflection at the surface of the continuous phase. The result is an intricate pattern of colored and circularly polarized spots that depends on the size of the illuminated area, the pitch of the cholesteric as well as the spectrum of the incident light. This could be the basis for a number of interesting applications, e.g. in identification and authentication devices. The presentation will describe these prospects as well as the basic optics governing the pattern generation.

[1] J. Noh, H.-L. Liang, I. Drevensek-Olenik, and J.P.F. Lagerwall, J. Mater. Chem. C, vol. 2, 806 (2014)

9384-28, Session 7

Nanosecond electric modification of nematic order parameter (*Keynote Presentation*)

Oleg D. Lavrentovich, Volodymyr Borshch, Bing-Xiang Li, Dergij Shiyanovskij, Kent State Univ. (United States)

An electric field applied to a dielectric can change the structural symmetry and thus the optical properties of the material. In an isotropic material, the field induces a uniaxial state; the effect is well known as the Kerr effect. The Kerr effect becomes more pronounced near the transition into the nematic. When the material is already in the nematic state, a similar effect may occur when the electric field does not cause macroscopic director reorientation, for example, when the electric field is applied perpendicularly to the director of a nematic with negative dielectric anisotropy. In this case, the applied electric field results in field-modified uniaxial order (FMUO) and also changes the overall symmetry of the NLC, inducing a secondary axis of molecular perpendicular to the main director so that the material becomes biaxial. This effect can be called field-induced biaxial order (FIBO). The challenge in characterizing the possible FIBO is that the field can also make the fluctuations of the main (uniaxial) director anisotropic, providing a 'differential quenching of uniaxial fluctuations' (DQUF). We present a special optical testing scheme to separate FMUO, FIBO and DQUF and demonstrate an ultrafast (nanoseconds) optical response with a large field-induced

**Conference 9384:
Emerging Liquid Crystal Technologies X**

modification of birefringence. The effect is tested for more than 10 different nematic materials with the goal of establishing a relationship between the materials parameters and efficiency of the nanosecond response.

9384-30, Session 7

Wide-color gamut multi-twist retarders

Kathryn J. Hornburg, Leandra L. Brickson, Michael J. Escuti, North Carolina State Univ. (United States)

It is well known that the color (i.e., transmittance spectrum shape) of a uniaxial retarder between polarizers does not depend on the orientation of the retarder's optical axis. However, this is not true for retarders which have a complex birefringence. In this work, we show how Multi-Twist Retarders (MTRs) can be used to create a single-film color filter wherein the color may be selected only by the MTR orientation angle. MTRs comprise two or more twisted liquid crystal layers on a single substrate and with a single alignment layer. We employ a patterned photoalignment material to set a spatially varying initial orientation angle for the MTR. In this work, we will in theory and experiment demonstrate continuous and discrete patterns to show the imaging possibilities, wherein different regions and pixels have different retardation spectra - and therefore various colored light outputs for the same MTR coating. A highly chromatic MTR design (thicknesses and twist angles) can be chosen to maximize the available color gamut (i.e., the range of colors and retardation), and the pattern in the photoalignment layer determines the image.

9384-31, Session 7

Epidermal photonic devices for quantitative imaging of temperature and thermal transport characteristics of the skin

Li Gao, Univ. of Illinois at Urbana-Champaign (United States); Yihui Zhang, Northwestern Univ. (United States); Viktor Malyarchuk, Lin Jia, Kyung-In Kang, Chad Webb, Univ. of Illinois at Urbana-Champaign (United States); Haoran Fu, Yan Shi, Guoyan Zhou, Northwestern Univ. (United States); Luke Shi, Deesha Shah, Xian Huang, Baoxing Xu, Univ. of Illinois at Urbana-Champaign (United States); Cunjiang Yu, Univ. of Houston (United States); Yonggang Huang, Northwestern Univ. (United States); John A. Rogers, Univ. of Illinois at Urbana-Champaign (United States)

Precision characterization of temperature and thermal transport properties of the skin can yield important information of relevance to both clinical medicine and basic research in skin physiology. Here, we introduce an ultrathin, compliant skin-like, or 'epidermal', photonic device that combines colorimetric temperature indicators with wireless stretchable electronics for precision thermal measurements when softly laminated on the surface of the skin. The sensors exploit thermochromic liquid crystals (TLC) patterned into large-scale, pixelated arrays on thin elastomeric substrates; the electronics provide means for controlled, local heating by radio frequency (RF) signals. Algorithms for extracting patterns of color recorded from these devices with a digital camera, and computational tools for relating the results to underlying thermal processes near the surface of the skin lend quantitative value to the resulting data. Application examples include non-invasive spatial mapping of skin temperature with milli-Kelvin precision and sub-millimeter spatial resolution. Demonstrations in reactive hyperemia assessments of blood flow and hydration analysis establish relevance to cardiovascular health and skin care, respectively.

9384-32, Session 7

Ferroelectric liquid crystal for photonics and display

Abhishek K. Srivastava, Vladimir G. Chigrinov, H. S. Kwok, Hong Kong Univ. of Science and Technology (Hong Kong, China)

The latest demand of the community, which has changed dramatically in recent time, includes high resolution displays (i.e. close to the human eye limits), low power consumption and undoubtedly the cost effective display and photonic devices. This is a big challenge for both scientists and engineers. The ferroelectric liquid crystal (FLC), because of the fast switching speed and low power consumption, is considered to be one of the potential candidates to serve as the building block for the modern high resolution devices. However, due to several limitations i.e. geometrical, optical and mechanical defects, these structures are less popular among the research and industrial regime. Recently, we have established that the Nano-scale photo -alignment technology could be used to improve characteristics of FLC systems. The photo- alignment, by different irradiance doses, offers good control on the anchoring energy and therefore provides good balance for elastic energy of the helix and the normalized anchoring energy. This balanced energy with proper selection of material parameter, that offers helix unwinding only in the presence of electric field i.e. ESHFLCs, manifests high contrast ratio of >10K: 1 at the driving frequency of > 3kHz at the cost of extremely small applied voltage and therefore have an edge over the other alternatives

9384-39, Session 7

Fast bistable switching of a chiral nematic liquid crystal cell induced by applying an in-plane electric field

Seung-Won Oh, Tae-Hoon Yoon, Pusan National Univ. (Korea, Republic of)

We propose a method for fast bistable switching of chiral nematic liquid crystals. Fast switching from the focal conic state to the planar state can be achieved by applying an in-plane electric field for a short time. The in-plane field induces a transient state, which relaxes rapidly to the initial planar state. We demonstrated that the switching time from the focal conic state to the planar state could be reduced from 150 to 5 ms by applying an in-plane field instead of a vertical field. We achieved a total response time of less than 10 ms. The proposed device is applicable to a reflective display and to other optical switching devices requiring both fast response time and low power consumption.

9384-33, Session 8

Large-aperture adaptive liquid crystal lenses for vision care (*Invited Paper*)

Guoqiang Li, The Ohio State Univ. (United States); Thomas Mauger, The Ohio State Univ. Havener Eye Institute (United States)

Adaptive liquid crystal (LC) lenses with variable focusing powers have a promising application in vision care, especially for correction of presbyopia. Presbyopia is due to an age-related loss of progressively diminished ability to focus on near objects. In most cases, bifocal or trifocal lenses are possible treatment for this problem. However, these lenses have limited field of view and cause discomfort or dizziness to the subjects when they use different parts of the lens for different vision tasks. To overcome these shortcomings, adaptive LC lenses can be a potential candidate due to their tunability of focal length and high-speed switching. However, to achieve LC lenses with a

**Conference 9384:
 Emerging Liquid Crystal Technologies X**

large aperture and high optical quality is still challenging. For conventional refractive LC lenses, the large thickness from the center to the periphery region results in significantly increased switching time and poor alignment of the liquid crystal materials. In this talk, we will present two kinds of large-aperture LC lens. One is the harmonic diffractive LC lens based on patterned electrodes with a 20 mm aperture and switchable powers such as plano, 3.5 diopter, and 7 diopter. The other is based on hybrid LC lens structure, in which a plastic substrate is micromachined with grooved structures and nanoparticles are doped into the LC for enhanced alignment. Switchable lenses with a 20 mm aperture and focusing powers up to 4 diopters will be demonstrated. These lenses are promising for correction of presbyopia.

9384-34, Session 8

A liquid crystal and polymer composite film for liquid crystal lenses (*Invited Paper*)

Yi-Hsin Lin, Hung-Shan Chen, Yu-Jen Wang, Chia-Ming Chang, National Chiao Tung Univ. (Taiwan)

Liquid crystal (LC) lenses offer novel opportunities for applications of ophthalmic lenses, camera modules, pico projectors, endoscopes, and optical zoom systems owing to electrically tunable lens power. Nevertheless, the tunable lens power and the aperture size of LC lenses are limited by the optical phase resulting from limit birefringence of LC materials. Recently, we developed a liquid crystal and polymer composite film (LCPCF) as a separation layer and an alignment layer for a multi-layered structure of LC lenses in order to enlarge the polarization-independent optical phase modulation. However, the physical properties and mechanical properties of the LCPCF are not clearly investigated. In this paper, we show the mechanical and physical properties of the LCPCF. The anchoring energy of the LCPCF is comparable with the standard rubbing-induced alignment layer by using different measurement methods. The transmission efficiency is over 97% neglecting the Fresnel reflection. The surface roughness is under 1 nm by using AFM scanning. The bending strength test indicates that the LCPCF can hold the LC material with reasonable deformation. A simple electrode and low voltage LC lens using LCPCF with spatially distributed dielectric constant is also realized. We believe this study provides a deeper insight to the LC lens structure embedded with LCPCF.

9384-35, Session 8

An electrically-tunable liquid crystal lens coupler for the fiber communication systems

Chyong-Hua Chen, Michael Chen, Yi-Hsin Lin, National Chiao Tung Univ. (Taiwan)

In this study, we demonstrated an electrically tunable lens coupler for both variable optical attenuation (VOA) and polarization selection. This coupler consists of a liquid crystal (LC) lens sandwiched between two GRIN lens. A GRIN lens is used to couple the light into the single mode fiber, and a LC lens is used to electrically manipulate the beam size of light. It is known that the lens power of a LC lens is tunable with high polarization sensitivity. Then, as the applied voltage on the LC lens is zero, the incident light is focused due to GRIN lens and coupled into the fiber. On the other hand, the beam size of the transformed e-ray becomes larger because the lens power of a LC lens for the e-ray decreases with the increase of the applied voltage. This results in the decrease of the coupling efficiency, and the optical power coupled into the fiber is smaller. This lens coupler for the e-ray functions as a VOA due to a continuous optical attenuation. On the contrary, the lens power of this LC lens for the o-ray does not vary because of optical anisotropy of the LC layer, and then the coupling efficiency for the o-ray remains high. For an arbitrary polarized incidence, this tunable lens coupler acts as a broadband polarizer for the fiber systems. The polarization dependent loss is larger than 30 dB and the switching time is around 1 second.

9384-36, Session 8

Super-fast refresh holographic liquid crystals for holographic 3D video display

Hongyue Gao, Yingjie Yu, Jicheng Liu, Shanghai Univ. (China)

Holographic display is a true 3D display, which has been demonstrated by static hologram recorded in materials. However, holography has not been applied in 3D video display because dynamic holography using optical media did not reach video-rate refresh. Recently, we achieved real-time dynamic holographic 3D display in dye-doped nematic liquid crystal films, which are super-fast refresh holographic media. The hologram formation time and self-erasable time can both reach ~ 1 ms in this films. Holographic video display was realized using it without any cross talk. This paper will focus on the mechanism of real-time hologram recording and self-erasure in the liquid crystal films with their extraordinarily high optical nonlinearity arising from laser-induced liquid crystal director axis reorientation. Hologram formed in the dye-doped liquid crystal film is based on the following process: dye molecules induced by laser orientate and lie in a new orientation, which are usually perpendicular to their original molecular direction, meanwhile, reorienting dye molecules result in a stable reorientation of liquid crystal molecules due to the interaction of the dye molecules with the liquid crystal molecules, and finally refractive-index modulation, which is a copy of the optical hologram, is generated in the liquid crystal films. This recorded hologram is transient, and not permanent. Therefore, once the recording light is turned off, all the dye and liquid crystal molecules go back to their original orientation, and the refractive-index hologram disappear immediately. This is the self-erasure process of the hologram in the film. Theory and experiments on the mechanism of real-time dynamic holographic 3D display will be presented using the holographic liquid crystal films. The super-fast refresh holographic liquid crystal films, which can be developed into large size holographic 3D TV, are very useful for true 3D display.

9384-37, Session 8

A polarized liquid crystal lens with electrically-switching mode and optically-written mode

Hung-Shan Chen, Yi-Hsin Lin, Chia-Ming Chang, Yu-Jen Wang, National Chiao Tung Univ. (Taiwan); Abhishek K. Srivastava, Jia-Tong Sun, Vladimir G. Chigrinov, Hong Kong Univ. of Science and Technology (Hong Kong, China)

A polarized liquid crystal (LC) lens composed of a LC layers as a polarization switch and an polymeric lens is demonstrated with electrically switching (ES) mode and optically written(OW) mode. The lens power of polymeric lens is related to the polarization of light modulated by the LC layers whose orientations are manipulated electrically or optically. The LC lens is not only electrically switchable, but also optically rewritable. Only two discrete lens powers (-1.39 Diopter or +0.7 Diopter) can be obtained in both ES mode and OW mode. No matter in ES mode or OW mode, the difference of two discrete lens power is identical. The aperture size is 10 mm. The image performance is demonstrated and the dispersion of the LC lens is discussed. Such a polarized LC lens can also be a special switch in optical systems.

9384-38, Session 8

The progress of light field real 3D display

Xu Liu, Haifeng Li, Zhejiang Univ. (China)

It is well known that what we see the real object in the world is the light rays from the object, no matter it emits or reflected light to the observers. So that we can use this property to create the 3D display by regeneration

**Conference 9384:
Emerging Liquid Crystal Technologies X**

of the light rays field distribution of the display object. That is the main principle of the light field display. In this talk we are going to use wave theory to describe the light rays' model, which will allow us to look in more detail of the principle of the light field display. The scanning type light field 3D display and the parallel projection light field 3D display will be reviewed in the talk, by emphasizing the difference in the data processing rate, and display performances.

9384-26, Session PWed

Green display: In-plane switching cholesteric liquid crystal devices with long-lived metastable display mode

Guan-Jhong Lin, National Taiwan Univ. (Taiwan); Tien-Jung Chen, Yu-Ting Lin, Jin-Jei Wu, National Taipei Univ. of Technology (Taiwan); Ying-Jay Yang, Chen-Kuo Wu, National Taiwan Univ. (Taiwan)

The electro-optical properties of cholesteric liquid crystal (LC) display, composed of chiral nematic LC with negative dielectric anisotropy, is investigated. The cell is operated between the standing-helix and lying-helix LC molecular arrangements after going through the applied electrical field. Bragg reflection, threshold voltage, and maximum bright-state voltage of a cell are significantly related with the chiral dopant concentration. The long-lived bright state for this cell can be kept without continuously supplying voltage.

9384-29, Session PWed

Fast gray-to-gray switching of a hybrid-aligned liquid crystal cell

Tae-Hoon Choi, Jung-Wook Kim, Tae-Hoon Yoon, Pusan National Univ. (Korea, Republic of)

Currently, liquid crystal displays (LCDs) have been widely used because of their low power consumption, light weight, and thinness. However, their slow response times are considered a major drawback which needs to be improved in order to display high-quality moving pictures and crosstalk-less three-dimensional displays. Furthermore, field sequential color (FSC) technology requires a liquid-crystal cell with total response time of less than 1 ms to avoid the color breakup. The FSC technology is considered as very attractive for enhancing both the light efficiency and display resolution by three times by eliminating the color filters in an LCD panel. In these display applications, the response times between grey levels are important but these are slower than those between the complete dark and the maximum bright states.

In this paper we demonstrate sub-millisecond switching of a hybrid-aligned liquid crystal cell by applying both vertical and in-plane electric fields to LCs using a four-terminal electrode structure. We demonstrated experimentally a total response time of 0.75 ms. Furthermore, fast gray-to-gray response could be achieved so that the proposed fast liquid crystal device can be a good candidate for applications, such as optical switching devices, FSC displays, and 3D displays.

9384-40, Session PWed

Double-layered liquid crystal light shutter for control of absorption and scattering of the light incident to a transparent display device

Jae-Won Huh, Byeong-Hun Yu, Pusan National Univ. (Korea, Republic of); Dong-Myung Shin, Hongik Univ.

(Korea, Republic of); Tae-Hoon Yoon, Pusan National Univ. (Korea, Republic of)

Recently, a transparent display has got much attention as one of the next generation display devices. Especially, active studies on a transparent display using organic light-emitting diodes (OLEDs) are in progress. However, since it is not possible to obtain black color using a transparent OLED, it suffers from poor visibility. This inevitable problem can be solved by using a light shutter. Light shutter technology can be divided into two types, light absorption and scattering. However, a light shutter based on light absorption cannot block the background image perfectly and a light shutter based on light scattering cannot provide black color.

In this work we demonstrate a light shutter using two liquid crystal (LC) layers, a light absorption layer and a light scattering layer. To realize a light absorption layer and a light scattering layer, we use the planar state of a dye-doped LC cell and the focal-conic state of a long-pitch cholesteric LC cell, respectively. The proposed light shutter device can block the background image perfectly and show black color. We expect that the proposed light shutter can increase the visibility of a transparent OLED display.

9384-41, Session PWed

Color-tunable mono-domain in blue phase I transitioned from blue phase III under anisotropic boundary condition

Min-Jun Gim, Gohyun Han, KAIST (Korea, Republic of); Suk-Won Choi, Kyung Hee Univ. (Korea, Republic of); Dong Ki Yoon, KAIST (Korea, Republic of)

Liquid crystalline blue phases (LCBPs), which consist of double-twisted cylinders (DTCs) as a building block, emerge between isotropic and cholesteric phase under excessive chirality in nematic liquid crystal. And there are three kinds of BPs (BP I, BP II and BP III). BP III has randomly ordered DTCs, showing the amorphous optical property, while BP I and BP II have cubic structures with multi-color domains. And their intriguing structural and optical properties have provided a great potential for BP lasing systems in which complex fabrication process is unnecessary and the laying wavelength can be tuned by external stimuli. However, the usual BPs show multi-color domains with micro-size, which results in the high excitation threshold energy and the low efficiency.

To obtain the uniform mono-domains with a single reflection color, we applied anisotropic surface boundary condition and phase transition via BP III. The BP mixture, which consists of bent-core nematogen and chiral dopant, exhibited only one BP III between isotropic and cholesteric phases in a sandwiched cell of which two substrates give planar anchoring to LC molecules. However, the BP III transitioned to BP I for a droplet sample in which the molecules exhibit planar anchoring on the bottom substrate and homeotropic anchoring near LC/air boundary. The homeotropic anchoring from air gave ordering to LC molecules in DTCs, and induced phase transition to ordered cubic BP I. The transitioned BP I showed uniform mono-domains with a single reflection color and a red-color shift as decreasing temperature.

9384-42, Session PWed

Design of retardation films with controlled birefringence dispersion using N-substituted maleimides

Hikaru Hotta, Shotaro Beppu, Houran Shafiee, Akihiro Tagaya, Yasuhiro Koike, Keio Univ. (Japan)

Retardation films are a polymer-based optical device which is used for improving image quality of flat-panel displays. Polymers exhibit birefringence and the birefringence is commonly known to exhibit

**Conference 9384:
 Emerging Liquid Crystal Technologies X**

normal wavelength dispersion which birefringence becomes larger as wavelength becomes shorter in the visible region. The retardation films exhibiting different birefringence dispersion which is normal, flat or reverse wavelength dispersion are required for many purposes. Birefringence dispersion of N-substituted maleimides is not clarified though N-substituted maleimides are utilized for heat resistant improvement. The purpose of this article is to design of retardation films with different birefringence dispersion using N-substituted maleimides based on the results of clarifying those intrinsic birefringence and birefringence dispersion. We proposed N-methylmaleimide (MeMI), N-ethylmaleimide (EMI), N-phenylmaleimide (PhMI) and N-(o-chlorophenyl)maleimide (o-CPMI) and the monomers were copolymerized with methyl methacrylate (MMA) in various composition ratios. Then, we measured birefringence dispersion of the copolymer films and calculated birefringence dispersion of PMeMI, PEMI, PPhMI and Po-CPMI from those of the copolymer films. These four homopolymers had positive birefringence, PMeMI and PEMI exhibited normal birefringence dispersion and PPhMI and Po-CPMI exhibited reverse birefringence dispersion. Based on the results, we calculated composition ratios of P(MMA/EMI/PhMI) with normal, flat or reverse birefringence dispersion and similar intrinsic birefringence at the wavelength of 548.9 nm and synthesized the copolymers with calculated composition ratios. Birefringence dispersion of synthesized P(MMA/EMI/PhMI) exhibited nearly the same tendency as designed by calculation. From the above results, we can design the retardation films which were controlled birefringence dispersion using N-substituted maleimides.

adaptive lenses, modulators, displays, photonic and other E-O devices. The possible reason behind the fast response time could be the combined effect viscosity and restoring force imparted by the locally ordered LCs induced by the FNPs. This restoring force help to reduce the decay time of the device. It reveals that low concentration NPs doping is essential for achieving dislocation-free fast response of the electro-optic devices. For higher concentration of the NPs, this restoring force slowed down due to higher viscosity and aggregation. Polarized optical microscopic textural observation shows that dislocation-free excellent contrast at 10 Vp may have significant impact for improving the image quality of the display devices.

9384-43, Session PWed

Effect of surface polymer networks on electrical and optical characteristics of vertically aligned liquid crystal displays

Guan-Jhong Lin, National Taiwan Univ. (Taiwan); Tien-Jung Chen, Yi-Wei Tsai, Jin-Jei Wu, National Taipei Univ. of Technology (Taiwan); Ying-Jay Yang, Chen-Kuo Wu, National Taiwan Univ. (Taiwan)

High transmittance and fast response of vertical alignment liquid crystal cell with polymer networks are demonstrated. Three different polymer morphologies are selected for a detailed investigation. Compared with the pure cell, polymer cell can modify the threshold voltage and the image responses. The fast response of planar cross-linking polymer cell is achieved at low driving voltage, attributed to the anchoring effect. In addition, the fabricated polymer cells can be operated at high voltage and keep the good light transmittance, as compared to the pure cell. This study also demonstrates that the suitable polymer will benefit the display performance.

9384-44, Session PWed

Tailoring fast electro-optic response by multiferroic bismuth ferrite nanoparticle: nematic liquid crystal composites

Prasenjit Nayek, Guoqiang Li, The Ohio State Univ. (United States)

Fast electro-optic (E-O) response time has been achieved with multiferroic bismuth ferrite (BiFeO₃/BFO) nanoparticles (NPs) doped in a nematic liquid crystal (NLC) host, E7. The BFO-NLC mixtures were injected into, indium-tin-oxide (ITO) coated, sandwich type, planar aligned cell of cell gap 5 μm. Polyimide coated substrates have complementary anti-parallel alignment to diminish performance degradation from non-uniformity. When the concentration of BFO is 0.15wt%, the total response time (τ_{On}+τ_{Off}) of the BFO-NLC mixture is two times faster than the intrinsic host NLC. The boosted total response time is ~ 2.5 millisecond. Interestingly, this faster response time has been achieved without significant change in threshold voltage of the mixture. This might be exploited for the construction of

Conference 9385: Advances in Display Technologies V

Wednesday - Thursday 11-12 February 2015

Part of Proceedings of SPIE Vol. 9385 Advances in Display Technologies V

9385-1, Session 1

Investigation of response time of vertically-aligned in-plane-switching LCD mode (*Invited Paper*)

Tien-Lun Ting, Cheng-Wei Lai, Yen-Ying Kung, Cho-Yan Chen, Wen-Hao Hsu, Jenn-Jia Su, AU Optronics Corp. (Taiwan)

In this paper, the rising and falling time of VA-IPS are discussed. The falling time, T_{off} , is monotonically increasing with the applied voltage, and this could be quite intuitive. As for the rising time, however, the intuition fails. It is not similar to the traditional VA mode whose T_{on} decreases first and then increases when the target voltage, V_{on} , escalates. As a matter of fact, it has a completely opposite behavior. This may refer to something having influences upon the dynamics of the liquid crystal molecules other than dielectric torque. We demonstrate the response time with respect to the different target voltages of PSA, one of the most popular mass-production VA modes in the current market. Next the response time of VA-IPS is shown to have the opposite behavior to PSA, and it's highly related to the dielectric torque but with certain anomaly. Finally, the observation of transient response of VA-IPS by fast CCD indicates the existence of torque caused by flexoelectricity which explains the anomaly. When the dielectric torque is very small, the deformation of the LC molecules is not strong, and thus the flexoelectric effect is not important. With the increase of the dielectric torque, the flexoelectric torque caused by stronger deformation is observed and the rising speed is slowed because of the unbalanced torques within the spacing of electrodes. If the dielectric torque is large enough, one can no longer perceive the existence of flexoelectricity, and the rising time is dominated by the dielectric torque. This is why the rising time of VA-IPS doesn't decrease monotonically with the applied voltage. A critical square of electric field is found to be $0.3V^2/\mu m^2$. Around this value, T_{on} will be extremely slow. However, the overdrive technique can be easily applied to the VA-IPS mode as long as one carefully chooses the voltage. VA-IPS has many characteristics worth studying, and through these studies one can seize more insights to novel nematic LCD modes.

9385-2, Session 1

Elimination of off-axis light leakage in a homogeneously-aligned liquid crystal cell (*Invited Paper*)

Tae-Hoon Yoon, Byung Wok Park, Seung-Won Oh, Pusan National Univ. (Korea, Republic of)

Among various liquid crystal display modes, the in-plane switching mode exhibits the widest viewing angle because the liquid crystals are homogeneously-aligned initially and rotate within a plane parallel to the substrates when an in-plane field is applied. However, further improvement is needed for viewing high-quality dark images from the bisector direction of the crossed polarizers. Several compensation schemes have been proposed to eliminate the off-axis light leakage in a homogeneously-aligned liquid crystal cell. Although a 100:1 iso-contrast contour at an optimized wavelength of 550 nm can cover the entire viewing cone, light leakage at other wavelengths still remains very severe. In this talk, we introduce achromatic optical compensation methods using uniaxial films to eliminate the off-axis light leakage at the dark state in homogeneously-aligned liquid crystal cell. For each compensation scheme, uniaxial films with different dispersion characteristics are used so that they can compensate one another to achieve achromatic optical compensation. The retardation values are optimized with the aid of the Poincaré sphere and through numerical research.

9385-3, Session 1

High-contrast LCD mode (*Invited Paper*)

Lachezar Komitov, Univ. of Gothenburg (Sweden)

In the conventional LCDs, operating in the regime of electric field applied across the display gap, the main obstacles for generating high contrast images is the light leakage through the display due mainly to the polarizers' quality, misalignment of the nematic liquid crystal (NLC) and remaining birefringence of the liquid crystal (LC) after switching to the dark state. The highest possible quality dark state in LCDs is achieved when the LCD exhibits optically isotropic state, such as the field-off state of antiferroelectric LCs with molecular tilt of 45° (AFLC 45°) [1] and the one of Blue Phase LCs [2].

Here, will be presented a LCD mode for generating high contrast images in which the applied electric field induces optically isotropic state and thus high quality dark state. This mode has been recently discovered in NLCs constituting of or consisting bent-core (BC) molecules [3].

References:

- [1] N. Olsson, I. Dahl, B. Helgee, and L. Komitov, *Liq. Cryst.* 31, 1 (2004).
- [2] H. Kikuchi, M. Yakota, Y. Hisakado, H. Yang and T. Kajiyama, *Nature Materials*, 1, 64 (2002).
- [3] O. Elamain, G. Hegde, K. Fodor-Csorba, and L. Komitov, *J. Phys. D: Appl. Phys.*, 46, 455101, (2013).

9385-4, Session 1

Control of pre-tilt angle of liquid crystal alignment by polymerized surfaces

Libo Weng, Kent State Univ. (United States); Pei-Chun Liao, Chen-Chun Lin, Tien-Lun Ting, Wen-Hao Hsu, Jenn-Jia Su, AU Optronics Corp. (Taiwan); Liang-Chy Chien, Kent State Univ. (United States)

A new method to improve the vertical alignment properties of liquid crystal devices by surface polymer stabilization is introduced. The mixture is made of a nematic liquid crystal with negative dielectric anisotropy and a minute amount of reactive monomer. It is filled into liquid crystal test cells, which are made of two glass substrates with ITO and homeotropic alignment layer. The cell is exposed to UV illumination to form sub-micron sized polymer protrusions on the two substrates of the cell. In order to generate the pretilt angle, different voltages are applied on the cell during polymerization. We will compare and contrast the pretilt angle and electro-optical performance of LC test cells with and without curing voltage and polymerized surfaces.

9385-5, Session 1

Low-power and high-quality reflective LCD with achromatic polarizer and novel anisotropic diffusion layers (*Invited Paper*)

Takahiro Ishinabe, Hideo Fujikake, Tohoku Univ. (Japan)

The development of bright color-reflective displays with low power consumption, a wide viewing angle, and broad color gamut, together with motion image capability, is desirable for next-generation display systems.

In this paper, we have developed an achromatic polarizer which has no wavelength dependency in both parallel and crossed states, high

**Conference 9385:
 Advances in Display Technologies V**

transmittance and high dichroic ratio by using new dichromatic pigments and manufacturing process. We synthesized new pigments that suppress the light absorption occurring in wavelength range except the dominant wavelength, and have the uniform dichroic ratio in visible wavelength range. In addition, we established the new technique for impregnation of dichromatic pigment and cross-linker and optimized stretch condition to control the alignment direction of each pigments and improve the dichroic ratio.

Moreover, we have established a novel technique to control the anisotropy of optical diffusion based on the optimization of the internal refractive-index distribution of the polymer film by controlling the degree of parallelization and angle of incidence of the UV light used for photo-polymerization, resulting in a high reflectivity across a wide angle range.

We have successfully developed monochrome-type reflective LCD using achromatic polarizer and achieved high reflectance of $L^*=71$, high contrast ratio (over 100:1), paper white characteristics superior to the electrophoretic display. In addition, we have developed a low-power color reflective LCD with wide color gamut (50% of NTSC), a wide viewing angle, as well as motion image capability.

We believe that this technology will create new display applications, including e-book readers, electronic shelf-edge labels and digital signage.

9385-6, Session 2

Viewing angle dependence of speckle contrast ratio in laser projection system

Qianli Ma, Changqing Xu, McMaster Univ. (Canada); Hai Ming, Univ. of Science and Technology of China (China)

The speckle, which is due to the interference of coherent light scattered by a random surface, can severely degrade the image quality. The speckle properties are usually measured by a camera, which takes images of the center of a projection screen. As a result, the effects of different viewing angles are not considered. In this paper, the dependence of speckle contrast ratio on the viewing angles in a laser projection system is studied. Two major effects have been considered in the studies. First, different viewing angles result in different projection distances. Secondly, for a rough screen, there exists an angular intensity distribution for the reflected/scattered light, which is determined by the structure of the screen surface. By combining these two effects, the experiment results show that the speckle contrast can vary significantly for different viewing angles. It is found that speckle contrast decreases with increase of viewing angle. As a result, when evaluating the speckle contrast in a laser projection system, the dependence of viewing angle should be considered.

9385-7, Session 2

Suppression of speckle patterns based on temporal angular decorrelation induced by a reflective diffuser

Sunduck Kim, Oh-Jang Kwon, Min-Seok Yoon, Young-Geun Han, Hanyang Univ. (Korea, Republic of)

Laser sources for illumination of projection systems have been attracting much attention because of their many advantages, such as high image brightness, high optical efficiency, and wider color gamut. The main issue in the laser based projector, however, is the emergence of speckle patterns that severely degrade the quality of the image. In order to mitigate speckle, a number of the speckle reduction methods have been reported. Among these methods, as the most effective way, the angular decorrelation methods can simply suppress speckle pattern by using the mechanical vibration or rotation of a diffuser. However, a diffuser exploited in a laser based projector to suppress speckle patterns has transmission optical loss of ~20%, which is not desirable in aspect of optical efficiency.

In this paper, we investigate a novel method to dramatically alleviate

the speckle contrast ratio by inducing angular decorrelation of light controlled by the diverging angle of a reflective diffuser. The enormously high divergence angle of light illuminating in a glass with random surface roughness is effectively controlled by adjusting the thickness and the refractive index of a polymer overlay. Aluminum was coated on the polymer-coated random phase glass to fabricate a reflective diffuser. The speckle contrast ratio was successfully suppressed to be ~7%.

9385-8, Session 2

Combining, homogenizing, and shaping beams from multiple laser emitters using multimode optical fibers and waveguides used in display systems

Hadi Baghsiahi, David Selviah, Univ. College London (United Kingdom)

Hollow mirrored square or rectangular cross section tubes or cylindrical tubes are commonly used as beam combiners and homogenizers for use in display backlights. These are large, heavy, cumbersome and difficult to align. This paper investigates whether very thin, lightweight multimode optical fibers and multimode optical waveguides can be used instead. Silica core optical fibers use total internal reflection, TIR, at the boundary between the transparent core and the transparent cladding materials. TIR offers lower loss in a more compact form factor, 1/50 smaller diameter, for portable displays. In the reported research, multimode optical waveguides are investigated for low power laser, high power laser and LED beam combining and color homogenization for display systems. Several light sources are coupled into a single multimode fiber, which acts as if it were a narrow light pipe. The light is homogenized by multimode propagation inside the fiber and the fiber can be easily vibrated to reduce any speckle due to use of long coherence length sources. A recently developed laser array with two rows of 24 emitters is characterized and several possible designs and waveguide configurations for beam combining are explored to be used in an auto-stereoscopic 3D display system. The best method is then selected based on simulation and experiment results and the results are presented. A lens system is designed and used to couple 20 coherently related red, 48 independent green and 48 independent blue laser beams into a silica core and silica cladding fiber having 200 μm core diameter and 80% power input coupling efficiency. Moreover a flexible slab waveguide was designed and simulated for used in beam shaping and beam homogenizing.

9385-27, Session PWed

Challenges in realizing a wind-driven mechanoluminescent display

Soon Moon Jeong, Seongkyu Song, Jaewook Jeong, Hyunmin Kim, Daegu Gyeongbuk Institute of Science & Technology (Korea, Republic of)

Mechanically-driven light generation (mechanoluminescence; ML) is an exciting and under-exploited phenomenon with a variety of possible practical applications. Until now, many materials have been known to emit light by the application of stress even though scientists have not yet arrived at a clear understanding of the effect [1]. Most studies of ML or triboluminescence (TL) have been performed using quartz, sugar, rocks, alkali halides and molecular crystals. Because the phenomenon is often weak and unreproducible, ML was initially assumed to have no major applications. Intense, reliable ML could lead to practical applications for these materials, such as displays and light sources driven by naturally vibrating mechanical actions.

Previously, we proposed a possible approach for producing durable [2], colour-tunable [3], and bidirectional [4] ML using zinc sulphide (ZnS) microparticles embedded in polydimethylsiloxane (PDMS) structures. The realization of wind-driven ML is also challengeable and would thus open a

**Conference 9385:
 Advances in Display Technologies V**

door for exploiting ML in various applications [5]. Here, we propose a high resolution wind-driven ML system that will have potential use in harvesting wind power for display. Compared with previous results [5], smaller vibrating rods (1 pixel can be considered as 1 rod) can make the smooth and detailed ML image. This result can be obtained by adjusting patterned hole size of molds and the weight fraction (wt %) of ML phosphors. Because wind power is a sustainable and environmentally friendly energy source, the findings of this study could create a significant new field in energy harvesting.

[1] B. P. Chandra, in *Luminescence of Solids* (Plenum, New York, 1998), p.361.

[2] S. M. Jeong, S. Song, S. -K. Lee and B. Choi, *Appl. Phys. Lett.* 102, 051110 (2013).

[3] S. M. Jeong, S. Song, S. -K. Lee and N. Y. Ha, *Adv. Mater.* 25, 6194 (2013).

[4] S. M. Jeong, S. Song, K. -I. Joo, J. Jeong and S. -H. Chung, *Opt. Mater. Express* 3, 1600 (2013).

[5] S. M. Jeong, S. Song, K. -I. Joo, J. Kim, S. -H. Hwang, J. Jeong and H. Kim, Submitted (2014).

9385-28, Session PWed

Analysis of outcoupling efficiency of OLED device incorporating a wrinkled polymer layer

Jun-Hwan Park, Min-Cheol Oh, Pusan National Univ. (Korea, Republic of)

To extract the light trapped in OLED device, a variety of research has been studied. OLED incorporating wrinkled polymer layer was proposed to enhance the outcoupling efficiency of device which has random period and direction. These features can improve the serious problem of the previous periodic diffraction structure which has color dispersion on the viewing angle. Performing these characteristics, the light extraction efficiency of a wrinkled-OLED depending on the wrinkle period, amplitude and refractive index of polymer inserted under the ITO anode for producing wrinkle was investigated by finite difference time domain (FDTD) numerical method. For designing the wrinkled-OLED in FDTD simulation, a point light source with a temporal coherence similar to green light emitted in OLED was incorporated, and the boundary condition of structure was set to periodic boundary to reproduce wide area device. According to FDTD simulation, the light guided in ITO/Organic layer called waveguided mode was extracted at flexion because of radiation mode coupling which has different mechanism from diffracted light and scattering of light. Finding optimized extraction efficiency of the wrinkled-OLED, simulation was conducted in accordance with wrinkle period and amplitude. Therefore, when period and amplitude was 1.6 μm , 0.4 μm separately, the maximum outcoupling efficiency by 1.6 times compared to the reference OLED device was found.

9385-29, Session PWed

A novel computer-generated hologram (CGH) achieved scheme using point cloud data based on integral imaging

Wei-Na Li, Mei-Lan Piao, Chungbuk National Univ. (Korea, Republic of); Seok-Hee Jeon, Incheon National Univ. (Korea, Republic of); Jong-Rae Jeong, Suwon Science College (Korea, Republic of); Nam Kim, Chungbuk National Univ. (Korea, Republic of)

We proposed a novel computer-generated hologram (CGH) achieved scheme, wherein the CGH is generated from a point cloud which is transformed by a mapping relationship of a series of elemental images captured from a real three-dimensional (3D) object by using a lens array. This scheme is composed of three procedures: mapping from elemental

images to point cloud, hologram generation, and hologram display. A mapping method is figured out to achieve a virtual volume data (point cloud) from a series of elemental images captured by a lens array. This mapping method consists of two steps. Firstly, the coordinate (x, y) pairs and its appearing number are calculated from the series of sub-images, which are generated from the elemental images. Secondly, a series of corresponding coordinates (x, y, z) are calculated from the elemental images. Then a hologram is generated from the volume data that is calculated by the previous two steps. Eventually, a spatial light modulator (SLM) and a green laser beam are utilized to display this hologram and reconstruct the original 3D object. In this paper, in order to show a more autostereoscopic display of a real 3D object, we successfully obtained the actual depth data of every discrete point of the real 3D object, and overcame the inherent drawbacks of the depth camera by obtaining point cloud from the elemental images.

9385-9, Session 3

Front and rear projection autostereoscopic 3D displays based on lenticular sheets *(Invited Paper)*

Qiong-Hua Wang, Shang-fei Zang, Sichuan Univ. (China)

A front projection autostereoscopic display is proposed. The display is composed of eight projectors and a 3D-image-guided screen which having a lenticular sheet and a retro-reflective diffusion screen. Based on the optical multiplexing and de-multiplexing, the optical functions of the 3D-image-guided screen are parallax image interlacing and view-separating, which is capable of reconstructing 3D images without quality degradation from the front direction. The operating principle, optical design calculation equations and correction method of parallax images are given. A prototype of the front projection autostereoscopic display is developed, which enhances the brightness and 3D perceptions, and improves space efficiency. The performance of this prototype is evaluated by measuring the luminance and crosstalk distribution along the horizontal direction at the optimum viewing distance. We also propose a rear projection autostereoscopic display. The display consists of four projectors, a projection screen, and two lenticular sheets. The operation principle and calculation equations are described in detail and the parallax images are corrected by means of homography. A prototype of the rear projection autostereoscopic display is developed. The normalized luminance distributions of viewing zones from the simulation and the measurement are given. Results agree well with the designed values. The prototype presents high resolution and high brightness 3D images. The research has potential applications in some commercial entertainments and movies for the realistic 3D perceptions.

9385-10, Session 3

30-view projection 3D display

Junejei Huang, Yuchang Wang, Delta Electronics, Inc. (Taiwan)

A compact 30-view 3D display using angle-magnifying screen is proposed. Small angle of Lamp-scanning on the stop of the projection lens is magnified into large field of view on the observing plane. The lamp-scanning is realized by the vibration of Galvano-mirror that synchronizing with the frame rate of the DMD and reflecting the laser illuminator to the scanning angles. To achieve 30-view, a 3-chip DLP projector with frame rate of 720 Hz is used. For one cycle of vibration of Galvano-mirror, steps of 0, 2, 4, 6, 8, 10, 12, 14 are reflected on going-path and steps of 13, 11, 9, 7, 5, 3, 1 are reflected on returning path. A frame is divided into odd lines and even lines for two views. For each view, 48 half frames per second are provided. A projection lens with aperture-relay system is used to double system etendue and separate odd and even lines into two half frames. Laser illuminator is required because at one time only 1/15 system etendue of the optical engine is utilized. After going through the Philips prism, three panels, the scanning 15 spots are doubled to 30 spots and emerge from the exit pupil of the

**Conference 9385:
Advances in Display Technologies V**

projection lens. The exit 30 light spots from the projection lens are projected to 30 viewing zones by the angle-magnifying screen. 30-view is scalable by adding more scanning steps to Galvano-mirror. A cabinet of rear projection with up-mirror and back-mirror is used because a projection lens of long throw distance is required.

9385-11, Session 3

Diffractive optics in large sizes: computer-generated holograms (CGH) based on Bayfol(R) HX film

Günther Walze, Bayer MaterialScience AG (Germany)

Volume Holographic Optical Elements (vHOE) offer angular and spectral Bragg selectivity that can be tuned by film thickness and holographic recording conditions. With the option to integrate complex optical function in a very thin plastic layer formerly heavy refractive optics can be made thin and lightweight especially for large area applications like liquid crystal displays, projection screens or photovoltaic. Additionally their Bragg selectivity enables the integration of several completely separated optical functions in the same film. The new instant developing photopolymer film (Bayfol® HX) paves the way towards new cost effective diffractive large optics, due to its easy holographic recording and environmental stability.

A major bottleneck for large area applications has been the master hologram recording which traditionally needs expensive, large high precision optical equipment and high power laser with long coherence length. Further the recording setup needs to be rearranged for a change in optical design.

In this paper we describe an alternative method for large area holographic master recording, using standard optics and low power lasers in combination with an x-y-translation stage. In this setup small sub-holograms generated by a phase only spatial light modulator (SLM) are recorded next to each other to generate a large size vHOE. The setup is flexible to generate various types of HOE's without the need of a change in the mechanical and optical construction by convenient SLM programming. Application examples and parameter studies of large area vHOE's based on Bayfol® HX Photopolymer will be given.

9385-12, Session 3

Depth-enhanced integral imaging display system with time-multiplexed depth planes using a varifocal liquid lens array

Cheoljoong Kim, Muyoung Lee, Junoh Kim, Jin su Lee, Yonghyub Won, KAIST (Korea, Republic of)

In this paper, we present a depth enhancing technique for integral imaging (II) system using a varifocal lens array. Expressible depth range of II is restricted in a specific region. If the image gets out of the region, displayed image becomes distorted and broken. The center of the region is called central depth plane (CDP), and its position is defined by the focal length of lens array. In our experiment, liquid lens array is used for II system instead of ordinary solid lens array. The liquid lens array is connected to the computer through a driver board, and the focal length of lens array varies depending on the applied voltage across. As a result, the proposed II system enables control of the location of image planes electrically. With this depth plane controllable system, time multiplexed II system is implemented. For this purpose, two objects of different positions and appropriate voltage level for each object are chosen. In display panel, elemental images for each object are alternately displayed with high frame rate. With the same ratio, calculated voltage levels are applied to the liquid lens array alternately. These two fast repeating signals are well synchronized so that the two objects are expressed in rotation. Because the time period between two sequences is very short, both objects are seems to appear simultaneously. Hence the depth range of the constructed image is enhanced.

9385-13, Session 3

Wide-angle color holographic 3D display with multi-source-based holographic content

Malgorzata Kujawinska, Weronika Zaperty, Tomasz Kozacki, Bartosz Wisniowski, Warsaw Univ. of Technology (Poland)

In this paper we present a multi SLMs color holographic 3D display. In order to provide best utilization of spatiotemporal bandwidth of the display a single SLM unit, equipped with a color (RGB) filter mask, is illuminated simultaneously with three color beams. After propagation the modulated wavefronts overlap in space and create a real color 3D image. The unit works with native SLM frame rate. This feature allows to apply temporal multiplexing method for extending the angular field of view of the display. In the paper we discuss the main features of the display and compare it with the performance of other solutions. We present the display implementation resulting in color reconstruction of holograms of computer generated and real world 3D objects. Finally, the data obtained from several sources including multiview 2D image capture, structured light systems, computer generation and holographic recording is converted into holographic representation and displayed at a wide angle holographic display. The applicability of this approach to allow holographic display of big 3D scenes is discussed.

9385-14, Session 4

Quantum-dot-enabled high color gamut LCDs (Keynote Presentation)

Jian Chen, Shihai Kan, Ernie Lee, Steve Gensler, Jason Hartlove, Nanosys, Inc. (United States)

Quantum dots are a new generation of phosphor material that have high quantum efficiency, narrow spectral line-widths and can be continuously tuned in their emission wavelengths. Since 2013, quantum dots have been adopted by the consumer electronics industry into LCDs to significantly increase their color performance. Compared to the OLED solution, quantum dot enabled LCDs have higher energy efficiency, larger color gamut, longer lifetime, and are offered at a fraction of the OLED panel cost. In addition, quantum-dot based LCDs can achieve more than 90% coverage of a much wider color gamut, Rec. 2020, which is the new color standard for UHD TV. Rec. 2020 displays were previously thought to be only possible with laser illumination sources.

9385-15, Session 4

A glasses-free random dot stereoacuity test using a multi-view display system

Jonghyun Kim, Keehoon Hong, Seoul National Univ. (Korea, Republic of); Hee Kyung Yang, Jeong-Min Hwang, Seoul National Univ. College of Medicine (Korea, Republic of); ByoungHo Lee, Seoul National Univ. (Korea, Republic of)

Stereoacuity is defined as the smallest disparity that provokes perception of depth or stereopsis. The exact measurement of stereoacuity of a patient is important to evaluate the disease associated with the disruption of normal binocular fusion. The most widely used stereoacuity test is the randot stereotest with polarization glasses and random dot targets. However, this method has some limitations such as limited range of stereoacuity or learning effect. Therefore, our group proposed a new stereoacuity test method with active shutter glasses and 120 Hz 3D monitor. That method showed the significant correlation with conventional randot stereotest,

**Conference 9385:
 Advances in Display Technologies V**

however, it still has some limitations. Firstly, the exactness of stereotest relies on the specification of 3D monitor, shutter glasses, and their synchronization. Secondly, it provides only binocular disparity to the patient not the accommodation or motion parallax.

In this paper, we propose a glasses-free random dot stereoacuity test using a multi-view display system. We use a multi-view display system with a liquid crystal display panel and a cylindrical lens array. We generate randot base images with different disparities to the patient. The multi-view system and the generated base image provide several randot stereotest images to the patient. The proposed method can offer not only binocular disparity but also motion parallax. The patient can change the position slightly within the viewing angle, and recognize the depth differences. Furthermore, we discuss about the future stereoacuity test with super multi-view display, which can provide binocular disparity and accommodation together.

9385-16, Session 4

Colorful holographic display of 3D object based on scaled diffraction by using non-uniform fast Fourier transform

Chenliang Chang, Jun Xia, Wei Lei, Southeast Univ. (China)

We proposed a new method to calculate the color computer generated hologram of three-dimensional object in holographic display. The three-dimensional object is composed of several tilted planes which are tilted from the hologram. The diffraction from each tilted plane to the hologram plane is calculated based on the coordinate rotation in Fourier spectrum domains. We used the nonuniform fast Fourier transformation (NUFFT) to calculate the nonuniform sampled Fourier spectrum on the tilted plane after coordinate rotation. By using the NUFFT, the diffraction calculation from tilted plane to the hologram plane with variable sampling rates can be achieved, which overcomes the sampling restriction of FFT in the conventional angular spectrum based method.

The holograms of red, green and blue component of the polygon-based object are calculated separately by using our NUFFT based method. Then the color hologram is synthesized by placing the red, green and blue component hologram in sequence. The chromatic aberration caused by the wavelength difference can be solved effectively by restricting the sampling rate of the object in the calculation of each wavelength component. The computer simulation shows the feasibility of our method in calculating the color hologram of polygon-based object. The 3D object can be displayed in color with adjustable size and no chromatic aberration in holographic display system, which can be considered as an important application in the colorful holographic three-dimensional display.

9385-17, Session 4

Holographic 3D video display of super-fast response liquid crystal film

Hongyue Gao, Yingjie Yu, Shanghai Univ. (China)

Holographic display, as a true 3D display technology, which can provide realistic 3D images without any special eyewear for observers, will be ultimately developed into holographic 3D TV.

However, dynamic holography is not applied in 3D video display because of limitations of spatial light modulators and slow-response dynamic holographic materials with hologram refresh rate, less than 25 Hz. Recently, we achieved real-time dynamic holographic 3D display in a super-fast response liquid crystal films. The hologram formation time and self-erasable time can both reach ~ 1 ms in this films. Holographic 3D video display with refresh rate, at least 60 Hz, was realized using it without any cross talk. Moreover, there is no need to apply any external electric field such that any SLMs or other holographic display devices resulting from this material need not to be pixilated. It is easier to fabricate large-size color video-rate holographic 3D displays by using this material. This paper will focus on holographic 3D video display of this liquid crystal film, and present its

potential applications in a large-size, high-definition, and color holographic 3D video display.

9385-18, Session 5

Video-rate optical holographic display based on nonlinear doped liquid crystals (Invited Paper)

Yikai Su, Shanghai Jiao Tong Univ. (China)

Among 3D display techniques, holographic display is considered as an ultimate goal to provide realistic image of a real object or a scene, because it has the ability to reconstruct both the intensity and phase information of a true nature of an object or a scene. Optical holography based on the dynamic recording materials might be an effective method for its wide viewing angle and scalability in display size. However, one major difficulty in optical holographic display is to dynamically show real-time, dynamic 3D images. This imposes challenges in materials, devices and system structures.

We present a real-time holographic display featured by an azo-dye-doped liquid crystal (LC). This material enables a video-rate display as each hologram can be refreshed in the order of several milliseconds. We have successfully demonstrated a real-time holographic video at a refresh rate of 25 Hz, sourced from an SLM and reconstructed by an azo-dye (DRI) doped nematic LC cell without any applied electric field. The performance of the proposed device is studied by the response time.

To further improve the diffraction efficiency, semiconductor nanoparticles doped liquid crystal materials show photorefractive (PR) effect based on of space charge field and liquid crystal's birefringence. By doping quantum dots into the liquid crystal, the PR effect is found to be greatly enhanced. With an external voltage applied to the material, our device exhibits fast response, and a significantly improved diffraction efficiency of 20%, up from 0.6% compared to the case of DRI doped LC. We also have demonstrated the R/G/B real-time videos and verified the feasibility as a color holographic display.

9385-19, Session 5

Three-dimensional display based on refreshable volume holograms in photochromic diarylethene polymer (Invited Paper)

Zheng Wang, Liangcai Cao, Hao Zhang, Guofan Jin, Tsinghua Univ. (China)

Holographic display has the ability to reconstruct both the intensity and wavefront of a three-dimensional (3D) object and can truthfully present a virtual window of 3D real-world scene for viewers without any eyewears. Real-time holographic display has been demonstrated in photorefractive polymers [1]. It is expected to carry out dynamic 3D display by recording holograms into a volume holographic polymer due to its high-density storage capacity and good multiplexing property [2]. In this work a updatable 3D display based on volume holographic polymer of photochromic diarylethene polymer is proposed. The photochromic diarylethene polymer is a promising rewritable recording material for holograms with high resolution, fatigue resistance and long life time. A phase-only spatial light modulator is utilized to modulate the object beam with the hogel information for 3D display. The computer-generated holograms carrying with wavefronts of 3D objects are written to the diarylethene polymer by using angular multiplexing, thus improving the space-bandwidth product by times. The 3D scenes can be reconstructed from the multiplexed hogels in the diarylethene polymer. The hogels can be easily erased in subseconds when exposed in ultraviolet light. This work paves a new way for practical dynamic holographic 3D display based on rewritable volume holographic polymer.

**Conference 9385:
 Advances in Display Technologies V**

9385-20, Session 5

Novel volumetric 3D display based on point light source optical reconstruction using multi focal lens array

Jin su Lee, Muyoung Lee, Junoh Kim, Cheoljoong Kim, Yong Hyub Won, KAIST (Korea, Republic of)

Generally, volumetric 3D display panel produce volume-filling three dimensional images. This paper discusses a volumetric 3D display based on periodical point light sources(PLSs) construction using a multi focal lens array(MFLA). The voxel of discrete 3D images is formed in the air via construction of point light source emitted by multi focal lens array. This system consists of a parallel beam, a spatial light modulator(SLM), a lens array, and a polarizing filter. The multi focal lens array is made with UV adhesive polymer droplet control using a dispersing machine. The MFLA consists of 30x30 circular lens array. Each lens aperture of the MFLA shows from 2mm to 300um. The polarizing filter is placed after the SLM and the MFLA to set in phase mostly mode. By the point spread function, the PLSs of the system are located by the focal length of each lens of the MFLA. It can also provide the moving parallax and relatively high resolution. However it has a limit of viewing angle and crosstalk by a property of each lens. In our experiment, we present the letter 'C', 'O', 'DE' and ball's surface with the different depth location. It could be seen clearly that when CCD sensor is moved to its position following as transverse axis of the display system. From our result, we expect that varifocal lens like EWOD and LC-lens can be applied for real time volumetric 3D display system.

9385-21, Session 5

Video-based 3D scanning integrated with a hand-held configuration of light-field photography

Chia-Ming Jan, Metal Industries Research & Development Ctr. (Taiwan)

This paper presents a new hand-held configuration of video-based 3D scanning integrated with the light field photography. This is achieved by inserting a microlens array or a micro-structure pattern on the MIM interface. By adopting a co-axial configuration, we proposed a combination of confocal scanner and light field camera to satisfy the high-performance 3D scanning of focus variation. To keep with consumer preferences for ever products, a precise and fast auto-focusing system for many inspection instruments were built up by utilizing a configuration of dual-confocal system. The traditional confocal auto-focusing system usually is consist of the only one single confocal optical configuration. It is often applied in the fields of the measurement, rebuilding of 3D image, medical imaging instrument, laser repair, and auto-focusing optical microscope. The dual-confocal optical system is one of the optics-based auto-focusing systems, which circumvent the response of the auto-focusing system with not real-time enough and principally enhanced the accuracy positioning of the focal plane with fast and precise depth information. The results showed that our design of 3D metrology can be widely used to a fast and precise scanning or RP(rapid prototype) in the industry with variable focal length. We demonstrated more detail including simulation and experiment particularity. In the future, the proposed auto-focusing system integrated with video-based light field photography can be further designed and developed for the precise additive layer manufacturing or minimally invasive surgery and its applications.

9385-22, Session 6

Viewing angle and imaging multispectral analysis of OLED display light emission (Invited Paper)

Pierre M. Boher, Thierry Leroux, Thibault Bignon, Véronique Collomb-Patton, ELDIM (France)

Organic Light Emitting Diodes (OLEDs) are presently one of the most promising new display technology. OLEDs provide a number of major technology enhancements for display and TV such as high contrast ratio, wide viewing angle, and very fast response time. Moreover, OLEDs could be used to make paper-thin display, transparent display, and flexible display. Currently the light emission properties of the OLED displays have only been studied using standard color and luminance measurements.

Nevertheless, OLED displays are not perfect and require very good manufacturing control to achieve optimized properties and homogeneous emissive properties. Presently the spectral emission has not been studied in details. One major source of problem is the lack on homogeneity of the emission of the different sub-pixels. In addition, the relative complex multilayer structure of the different sub-pixels introduces small spectral and angular modulation. In the present paper we use two systems to make multispectral imaging and viewing angle measurements. The Fourier optics viewing angle system has been introduced in 2008 for the characterization of LCDs. Spectral information is obtained with 31 band pass filters regularly distributed in the visible range. The imaging system is based on the same principle and one imaging optics instead of the Fourier one. The emission of red, green and blue states is measured with the two systems on different OLED displays. The homogeneity is evaluated on the entire surface of the displays and at the sub pixel level. Color fluctuations above the human eye sensitivity are measured in both cases. The viewing angle emission presents complex changes versus wavelength and angle. These changes due to interference fringes inside the OLED layered structure have a small impact on the color and luminance properties, but can be very useful to understand in depth the working conditions inside the OLED structures.

9385-23, Session 6

Anti-ambient light reflective type projection screen with angle-selective absorber

Liao Tianju, Qiao Junfeng, Li Xian, Zhaoyu Zhang, Peking Univ. (China)

Ambient light is destructive to the reflective type projection system's contrast ratio which has great influence on the image quality. In contrast to the conventional front projection, short-throw projection has its advantage to reject the ambient light. Fresnel lens-shaped reflection layer is adapted to direct light from a large angle due to the low lens throw ratio to the viewing area. The structure separates the path of the ambient light and projection light, creating the chance to solve the problem that ambient light is mixed with projection light. However, with solely the lens-shaped reflection layer is not good enough to improve the contrast ratio due to the scattering layer, which contributes a necessarily wide viewing angle, could interfere with both light paths before hitting the layer. So we propose a new design that sets the draft angle surface with absorption layer and adds an angle-selective absorber to separate these two kinds of light. The absorber is designed to fit the direction of the projection light, leading to a small absorption cross section for the projection light and respectfully big absorption cross section for the ambient light. We have calculated the design with Tracepro, a ray tracing program and find a nearly 8 times contrast ratio improvement against the current design in theory. This design can hopefully provide efficient display in bright lit situation with better viewer satisfaction.

**Conference 9385:
 Advances in Display Technologies V**

9385-24, Session 6

Low cost of ownership large area annealing of amorphous silicon films

Nick Hay, Ian A. Baker, Young Kwon, Powerlase Photonics Ltd. (United Kingdom)

Laser annealing of amorphous silicon films for OLED display production has historically been performed using laser sources based on excimer laser technology (ELA). The drive to improve system up-time and reduce running costs has promoted the development of alternative laser sources. We report the introduction of a scalable, stabilised, all solid-state laser system architecture designed for 24/7 production in typical semiconductor processing environments. The core laser system with power >1.6 kW at wavelength 532 nm is compared with existing technology. A description of the system architecture is given along with detailed characterisation data. Scalability to higher powers and higher throughput is shown along with applications examples. Stability, reliability, availability and cost of ownership data are given and compared to industry requirements.

9385-25, Session 6

360-degree table-top display with rotating transmissive screen

Kwang-Soo Kim, Hosung Jeon, Kyungpook National Univ. (Korea, Republic of); Sang Kil Lee, A-Optics Co., Ltd. (Korea, Republic of); Hwi Kim, Korea Univ. Sejong Campus (Korea, Republic of); Joonku Hahn, Kyungpook National Univ. (Korea, Republic of)

Three-dimensional(3D) display usually provides binocular disparity to observer. To construct 360degree table-top display, lots of views are required. In order to display a large amount of views to observer, time-multiplexing or spatial multiplexing techniques are applied. There have been several studies on table-top 3D displays. For example, Light field display suggested by A. Jones consists of the rotating reflective screen and high speed DMD(digital micromirror device). As an another example, fVision suggested by S. Yoshida consists of almost hundred mini-projectors which are arranged around of the circle pointing its center.

We suggest a new structure for view-sequential 360-degree table-top display system. In my system, transmissive screen is used and it is illuminated by the DMD. This system defines the direction of bundle of rays to configure the sequential view. It has some advantages resulting from the transmissive flat screen. When the transmissive screen is used instead of the reflective one, the light power efficiency is improved. Moreover, the arrangement of the pixel is more uniform when the screen is flat instead of conic screen. We construct a table-top display with about 300views around 360degree and its feasibilities are confirmed.

9385-26, Session 6

High-efficient photonic crystal embedded polymer light-emitting diodes with inkjet-printed conductive polymer anodes

Jaeheung Ha, Donghyun Kim, Jongjang Park, Seunghwan Lee, Heonsu Jeon, Changhee Lee, Yongtaek Hong, Seoul National Univ. (Korea, Republic of)

We fabricated the high efficient photonic crystal embedded polymer light-emitting diodes (PC-PLEDs) on a hybrid substrate (SiNx/quartz), where photonic crystal structures were fabricated in the SiNx layer by a holographic lithography. Our devices were composed of a conductive polymer (PEDOT:PSS, E-157, Con-Tech) which was used as anodes and planarization layers, a hole injection layer (Al4O83), an emission layer (SPG-01T), and a bi-layer cathode (LiF/Al). The anode was deposited by an inkjet printer, and HIL and EML were spun-coated, and the cathode was deposited by thermal evaporation. From the ellipsometry measurement, we could obtain a refractive index of the E-157, which was 1.5 at 500 nm. The refractive index difference of SiNx and E-157 was about 0.52 at 500 nm. Although the thickness of E-157 on the normal quartz substrate was slightly higher than that of E-157 films on the photonic crystal structure, the sheet resistance was similar each other. The transmittance of E-157 films on the hybrid substrate was higher than that of hybrid substrate at 500nm, where the main peak of PLEDs' spectrum was observed. The PEDOT:PSS-based PC-PLEDs showed 7.27 cd/A and 5.61 lm/W at 964 cd/m², which was higher than the efficiencies of normal (no PC-embedded) PEDOT:PSS or ITO-based PLEDs. When compared to the normal PEDOT:PSS-based PLEDs, the efficiencies of the PC-PLEDs were increased about 116% (Cd/A) and 121% (lm/W) at 964 cd/m². These results showed that our E-157 electrode and photonic crystal structure are key enabling technology for the high efficient lighting applications.

Conference 9386: Practical Holography XXIX: Materials and Applications

Sunday - Wednesday 8 -11 February 2015

Part of Proceedings of SPIE Vol. 9386 Practical Holography XXIX: Materials and Applications

9386-1, Session 1

Edge-lit volume holograms recorded by free space exposure: diffraction by 2nd Harmonics in Bayfol(R) HX film

Friedrich-Karl Bruder, Thomas Faecke, Rainer Hagen, Dennis Hönel, Bayer MaterialScience AG (Germany); David Jurbergs, Bayer MaterialScience LLC (United States); Enrico Orselli, Christian Rewitz, Thomas Roelle, Guenther Walze, Brita Wewer, Bayer MaterialScience AG (Germany)

Miniaturization of optical components specifically the reduction in thickness created by using planar optical devices makes light manipulation by diffraction more and more attractive. Optical gratings based on volume Holographic Optical Elements (vHOEs) have the advantage over surface gratings as they reconstruct only a single diffraction order and hence provide high diffraction efficiencies, selectivity and remain fully transparent in the off-Bragg condition.

Guiding light inside an optically transparent medium by total internal reflection (TIR) is common and useful in thin planar optical devices. vHOEs offer unique ways to create selective in- and out-coupling of TIR light. Respective vHOEs typically have to be recorded in an edge-lit configuration as necessary high diffraction angles could not be generated by two free-space beams outside the medium. To record such an edge-lit vHOE, bulky recording blocks or liquid bathes are used in complex and hard to align recording setups.

We present in this paper our findings to use instant-developing photopolymer film (Bayfol® HX) to generate 2nd harmonics in the index profile of phase gratings while using free-space recording setups. Those 2nd harmonic components enable the vHOE to diffract at such large angles that they replay in an edge-lit configuration. We will discuss in this paper selected materials and beneficial recording parameters to tune the diffraction efficiency towards 2nd harmonic replay. By this - in reported specific cases - the cumbersome and complex edge-lit recording can be substituted by easy-to-use free-space setups. This process significantly simplifies master recordings for vHOEs with edge-lit functionalities which later can be used in contact copy schemes for mass replication.

9386-2, Session 1

Beam propagation ratios measurement based on transmissive liquid crystal spatial light modulator

Lei Zhang, Dong Li, Jindong Tian, Shenzhen Univ. (China)

In this paper, the function of zoom lens could be obtained by loading a calculated digital lens of variable focal length to the LC-SLM. Then the intensity is measured by a camera at a fixed distance behind the LC-SLM without moving any components. Specially, a method of calculating the real focal length of the digital lens is proposed by paying attention to the practical phase modulation of the LC-SLM. The accurate position of the focus will be gotten, since the ability of phase modulation of SLM is less than 2π . Furthermore, the radius of laser beam at the focus could be determined by an improved algorithm of the second order moment. Therefore, the beam propagation ratios could be calculated by curve fitting based on the accurate focal point position. The experimental setups are simple because of the employment of the transmissive LC-SLM, which will be of significance for the application of measuring the beam propagation ratios with high-efficiency, high-precision and low-cost

9386-3, Session 1

Everything you need to know about resin interactions with PDMS as a window material and some new window materials for SLA 3D printers

Michael C. Cole, Univ. of Colorado at Boulder (United States) and Colorado Photopolymer Solutions (United States); Robert McLeod, Univ. of Colorado at Boulder (United States)

New, low cost SLA 3D printers are now available for regular consumers offering new possibilities for the hobbyist, jewelry makers, and the curious. These new printers offer good resolution and are starting to offer a larger range of materials properties. However, all these new printers currently use PDMS (polydimethylsiloxane) as a window material. PDMS works so well in these applications because it provides an optically clear window, rapid oxygen diffusion which prevents adhesion to the window, and ease of manufacturing. We present how to design a resin for use with PDMS taking into account the major degradation mechanisms such as monomer solubility in PDMS, oxygen diffusion rates, and polymer grafting onto the PDMS surface. We also note how light intensity, modulus of the PDMS, and size of the cure area affect the lifetime of the PDMS window. Lastly we demonstrate several new materials that were tested as a substitute for PDMS as a window material.

9386-4, Session 1

Hyperspectral digital holography of microobjects

Georgy S. Kalenkov, Moscow State Technical Univ. MAMI (Russian Federation); Georgy S. Kalenkov, Moscow Institute of Physics and Technology (Russian Federation); Alexander E. Shtanko, Moscow State Univ. of Technology Stankin (Russian Federation) and Moscow Institute of Physics and Technology (Russian Federation)

Novel method is suggested for a hyperspectral wave field holographic recording, based on asymmetrical Fourier spectrometer with a flat microobject placed in one of its arms. The output signal, which is the interference of the reference field with the field diffracted by the object, is registered by CCD. The process of recording is reduced to consecutive registration of two-dimensional interferograms by changing the optical length of the reference arm of the interferometer. One-dimensional Fourier transform of the interferogram in each pixel gives a spatial distribution of the complex amplitude for all spectral components of a hyperspectral object field. Inverse Fresnel transform of this field gives a hyperspectral object field in the object plane. Hyperspectral amplitude and average-phase profile images of standard microscope samples obtained experimentally are presented. Spectrally-spatial resolution related to Fellgett's advantage, coloring, and speckle noise reduction are discussed.

9386-5, Session 2

Generalized experimental phase extraction algorithm for speckle interferometry

Antonio Barcelata-Pinzón, Rigoberto Juárez-Salazar,

**Conference 9386:
 Practical Holography XXIX: Materials and Applications**

Carlos Ignacio Robledo-Sánchez, Cruz Meneses-Fabián, Benemérita Univ. Autónoma de Puebla (Mexico); Manuel Durán-Sánchez, Univ. Tecnológica de Puebla (Mexico) and Instituto Nacional de Astrofísica Óptica y Electrónica (Mexico); Ricardo I. Álvarez-Tamayo, Univ. Tecnológica de Puebla (Mexico)

A novel effective and straightforward alternative methodology for phase-shifting interferometry by using a Speckle interferometer experimental setup is proposed. The proposed method is based on phase shifting interferometry (PSI) technique. By the proposed experimental method we demonstrate that the necessary phase shift is not required to be calibrated because the uses of an appropriate fringe-pattern processing allowing the use of arbitrary phase steps. The acquired fringe patterns are processed by well-established phase-shifting algorithms in order to compare phase results with consecutive and calibrated phase results. High accuracy in the evaluated phase is achieved. Simulated and experimental results are provided to probe the proposed method efficiency and reliability.

Acknowledgements.

Grant 209335 Fondomixto CONACYT project.

9386-6, Session 2

Differentiation methods for phase recovery.

Meriç Özcan, Sabanci Univ. (Turkey)

Accurate phase measurement is important in optical metrology for a wide range of applications such as surface profiling to holographic imaging to radar imaging.

In almost all of the optical measurements, fringe patterns, interferograms or the phase of the reconstructed hologram is related to the quantity measured such as displacement, depth profile or temperature gradient, etc., such that the recovery of the phase will lead to desired physical quantity.

However the measured phase is in sinusoidal form (sine and/or cosine of the phase is measured), hence the actual phase is usually recovered using arctangent method. If the range of the phase is greater than 2π , phase will be wrapped and it will be necessary to employ some phase unwrapping methods.

For this purpose there were many algorithms developed, such as 2π phase jump counting, Fourier and wavelet transforms methods, integration of the phase gradients to unwrap the wrapped phase.

Here we summarize phase gradient base methods used for the phase recovery and then concentrate on a numerical method that can be described as differentiate and cross multiply operation to obtain the phase gradient.

This method uses quadrature phase data that is in sine and cosine form which is a natural outcome of holographic reconstruction. Since the differentiation is performed on trigonometric functions which are discrete, it is shown that the method of differentiation and the sampling rate are important considerations especially for the noise corrupt signals. The method is initially developed for 1D and then later extended to 2D phase recovery.

Once the phase gradient is obtained a simple integration produce the phase map.

Noise performance of the method is also investigated and it is shown that for the extremely noisy signals, the method can be adapted to an iteration routine which recovers the phase successfully.

We present simulations and the experimental results which show the validity of the approach.

9386-7, Session 2

Diffraction pattern of gratings with erosion

Arturo Olivares-Pérez, Israel Fuentes-Tapia, Instituto Nacional de Astrofísica, Óptica y Electrónica (Mexico)

We present a theoretical study of amplitude diffraction gratings using computer simulating. Which consists of a random sampling of points on the image grating to determine the points to be plotted and the points to remove, to simulate an erosion in amplitude on the grating. We show their behavior in the diffraction patterns and the induced noise by limiting the number of points that representing the image of the eroded gratings.

9386-8, Session 2

Spatial domain Fraunhofer computer hologram

Jian-Wen Dong, Yigui Chen, Sun Yat-Sen Univ. (China)

Three-dimensional (3D) displays have been made great progress in recent years, due to the development of the fields on optical information and computer science technologies. Holography enables to provide accurate depth cues of 3D objects and has attracted much attention. Computer generated hologram (CGH) is one of the exceptional way to utilize vivid 3D scene of both virtual and real objects. However, time-consuming holographic computation, ultra-narrow viewing angle, and unavoidable speckle noise are main disadvantages to restrict the development. Here, I will review the CGH in spatial domain. I will show you that the Fraunhofer formulism can be used in Fresnel region. Spatial domain Fraunhofer computer hologram can be encoded the diffraction pattern of polygon-based 3D model, no matter either analytical or fast Fourier transform is used. Based on this method, we have solved the problems on occlusion, shading, and texture. In addition, we have proposed a 4f optical system by time division multiplexing and spatial tiling technique to enlarge the viewing angle so as to make the naked eye view smooth. The coherence of reconstructed LED light is also investigated. The correlation between the coherence of light, the blur effect and the speckle noise is established. Spatial domain Fraunhofer computer hologram can be used in the computation of complicated 3D scenes with large amounts of data, which is helpful to the development of holography display.

9386-10, Session 3

Distortion-free broadband holograms: A novel class of elements utilizing the wavelength-independent geometric phase

Xiao Xiang, Matthew N. Miskiewicz, Michael J. Escuti, North Carolina State Univ. (United States)

We demonstrate a novel class of elements called Far-Field Geometric Phase Holograms (FGPH) capable of producing far-field output images free of chromatic distortion for a broad range of input wavelengths. The FGPH utilizes the geometric phase which applies the same phase profile to any incident wave regardless of wavelength. Thus, the fidelity of an image produced by an FGPH is the same for all wavelengths. However, being a diffractive element, the FGPH is still dispersive in that the size of a generated image depends on the replay wavelength according to the diffraction equation. In this paper, we give theory for the ideal FGPH element, describing its replay characteristics and unique polarization properties. Then, we experimentally realize an FGPH element using photo-aligned liquid crystals patterned with a direct-write system. We utilize a multi-twisted retarder (MTR) coating to achieve high diffraction efficiency over a broad wavelength range. We characterize the fabricated element and show the theory to be valid. Generally, this new class of polarization sensitive elements can produce broadband undistorted images with high diffraction efficiency.

9386-11, Session 3

Computation of Fresnel holograms and diffraction-specific coherent panoramagrams for full-color holographic displays based on anisotropic leaky-mode modulators

Sundeep Jolly, Ermal Dreshaj, V. Michael Bove Jr., MIT Media Lab. (United States)

We have previously introduced a computational architecture suitable for driving full-color holographic display systems based around anisotropic leaky-mode modulators; this architecture appropriately handles single-sideband modulation and frequency-division multiplexing of spectral bands that correspond to the independent red, green, and blue color channels in the display output. In this paper, we describe an implementation for driving the MIT Mark IV holographic display system with such a computational approach, in cases of both pre-computed Fresnel CGHs and real-time, GPU-based diffraction-specific coherent panoramagrams. Real-time holographic images of nearly VGA-resolution (468 lines) are generated via three dual-head NVIDIA GPUs via a CUDA-based implementation that encompasses the requisite orthographic view generation from 3-D data sources, parallel vector-based fringe computation per hogel and per color, single-sideband modulation, and frequency-division multiplexing. We present the first results of this scheme in driving the Mark IV display system and review the resulting holographic video output and performance metrics.

9386-12, Session 3

Improved real-time holographic video display using a super-fast-refresh liquid crystal film

Hongyue Gao, Yingjie Yu, Jicheng Liu, Huadong Zheng, Shanghai Univ. (China)

Holographic three-dimensional (3D) display is a true 3D display technology, which can provide realistic 3D images without any special eyewear for observers. A static hologram recorded in a permanent holographic storage material using holographic stereography is able to provide excellent resolution and depth reproduction on a large scale. However, dynamic holography has not been applied in 3D video display because the limitations of dynamic holographic materials and current holographic display devices, spatial light modulators (SLMs). Therefore, a development of updatable holographic materials and improvement of SLMs have attracted wide attention. For a holographic video material, its holographic response must be fast enough for video-rate 3D display. In 2012, we reported real-time dynamic holographic display with holographic response time under an order of a microsecond using a liquid crystal film. A transient hologram can be formed and completely self-erased both in ~ 1 ms in the film. Holographic videos were realized using it without any cross talk between the holograms. However, they need to be improved in image quality. We found that this fast-response holographic liquid crystal film is more sensitive to green and blue lasers than red laser, and diffraction efficiency and resolution of the hologram in it can be enhanced by choosing suitable sample parameters and recording parameters. Therefore, this paper focuses on improvement of holographic display of this film, and presents improved holographic videos reconstructed by red, green, and blue lasers. This work may be helpful to develop a large-size, high-definition, and color holographic 3D video display, such as holographic 3D TV, based on this liquid crystal film.

9386-13, Session 4

Time within time: 3D printed sculptures within holographic art practice

Yin-Ren Chang, Martin J. Richardson, De Montfort Univ. (United Kingdom)

Holography is a time-based medium that brings its own aesthetics and techniques to interpret colour and light. This exclusive descriptive language represents the scenario of the moment it is recording, but also documents the whole light activity during the shooting process.

3D graphic software and Internet propose practitioners more mobility to develop and deliver their artworks; furthermore, the diverse web-based social media opens various space to facilitate artists to be able to exchange or collaborate their projects with external links (audience or specialist).

Within analogue holography art practice, there is a primarily lack of interface to attach digital creative tools. 3D printing makes it possibility to bridge the gap between cyber space and holographic world; meanwhile, this emerging technique also becomes a platform to connect computational data and light information.

Applying 3D printing to contemporary art will reshape the process of creation, but also the form of visual narrative. New technologies continually and increasingly involve the projection of another artistic dimension, and the term "visual" embarks on challenging the generally accepted notion of understanding art and interacting with it.

As new pathways of practice are established, interest needs to take years to understand and use this new medium. This paper's aim is looking for the potential of artistic expression in between analogue holography and 3D printing, and to make an articulate assessment of 3D printing within the dynamic holographic aesthetic.

9386-14, Session 4

Seeing yourself seeing

Maria Isabel Azevedo, Martin J. Richardson, Elizabeth Sandford-Richardson, De Montfort Univ. (United Kingdom); Luís Miguel Bernardo, Helder Crespo, Univ. do Porto (Portugal)

The rapid evolution of the computer, compared to that of previous technologies, and the lack of progress in the human form, took the theoretical and artist from the virtual art, Myron Krueger, to predict that the last computer-people interface will be directed toward the human body and the human senses. It is accordingly that, the importance that is given in this paper to metamorphosis, most often invisible to the human body and changes in sensitivity that have been explored by artists and inspiring the development of that series of digital art holograms and lenticulars. Starting from a belief in the human body as emotional tool, as courier of memories, and the idea that the virtual colour image behind a holographic plate, shows the most realistic 3D image of "what" we want.

Through two temporal modalities, the time of the holographic image (the performance recorded time) and the time of the performance by the public, we create "a new space for the image", whose structure is influenced by the holographic images and the public as performer. In the tension between the space of the action of the participants and the virtual space of holographic images, we have the time image, that goes beyond the issue of the movement and has a direct relationship with the participant's thought.

Gilles Deleuze reflects about memory and, from his point of view, the "matter" is an aggregate of "images", something placed halfway between the thing (object) and its representation. He calls the "crystal image" as the image that combines the memory of a past event to that of the present time, and it ("crystal image") is sometimes characterized by spatial and temporal links between images (the images from the memory and the present time).

In this series of digital holographic images and lenticulars, we are using

an old camera Canon IS3 and a new HD Canon, on the rail, to capture the scenes that have an old fashion look with a look of “nowadays”, and then mixing them on the surface of the holographic plate.

Some think, that the present time/moment, is a singularity of the infinitesimal time duration, what exists is past and future, thus we are mixing images from a remote past with the near past...

9386-15, Session 4

Archiving Saudi heritage using the holographic medium

Amani D. Althagafi, Martin J. Richardson, De Montfort Univ. (United Kingdom)

Althagafi. A. De Montfort University, Leicester, Faculty of Technology, The Imaging & Display Research Group, 2.27 Queens Building, The Gateway, LE1 9BH, UK & Professor Richardson, M. De Montfort University, Leicester, Faculty of Technology, The Imaging & Display Research Group, 2.27 Queens Building, The Gateway, LE1 9BH, UK.

This paper focuses on the use of the Yuri Nikolaevich DENISYUK holographic recording process to document, preserve and display Saudi heritage. The goal of this research is to develop a technique of preserving heritage by using a high-tech holographic process to capture a three-dimensional presentation of ancient jewelry artifacts of the Saudi Heritage in particular. This study concentrates on five particular items of handmade authentic ancient metal jewelry from different parts of Saudi Arabia. When conducting this research experiments were conducted using both red-green sensitive plates sensitive to 633 nm and 532 nm respectively. Material thickness ranged between 1.5 and 3 millimeters were used, consequently in the dark room, varied chemicals for developing the holograms were employed. Red and green laser devices were also used with exposure times between 8 to 18 seconds of laser light dispersion through diffused surfaces in reflection holography. The outcome in each case was varied. The holograms captured the jewelry pieces with all the engravings and minute details, thus preserving the Saudi Heritage of that time. What makes holograms a revolutionary method for presenting valuable and/or ancient artifacts is the fact that they offer a more practical and convenient solution to travel around the world than displaying the originals items. Thus, museum visitors can enjoy and appreciate the precious artifacts otherwise unseen and lost without holography.

9386-16, Session 5

Holography: past, present, and future (Invited Paper)

Ian M. Lancaster, Reconnaissance International Ltd. (United Kingdom)

Two months after this Practical Holography conference I will be relinquishing the editorship of Holography News® and leaving Reconnaissance International. This will be the formal end to my career of almost 40 years in holography, during which time I have made holograms commercially, written about the commercial aspects of holography most months since 1987, run the Museum of Holography in New York, run the industry conference and generally been a participating observer of the holography industry and the holography community.

So this is my personal review of how holography has developed in that time, where it is now and where it might be going in the next few years. Forgive the immodesty implied!

In the paper I will reminisce about the state of holography over the last 40 years, since I first saw a hologram at the 1976 Light Fantastic exhibition. I gave my first paper to Practical Holography in 1987, so I will consider how this conference and others have evolved since then.

I will describe, review and try to offer explanations for the successes and disappointments in display and technical holography in four decades. I

will consider how visible holograms have established a US\$4-5bn global industry while (not yet?) fulfilling the aspirations that holograms would become the leading visual medium, especially the leading 3D medium. I will trace the parallel path of HOEs, and consider the potential for both visual and technical holograms in the next 5 and 10 years.

9386-17, Session 5

Holographic data storage at 2+ Tbit/in²

Mark R. Ayres, Ken E. Anderson, Fred Askham, Brad Sissom, Akonia Holographics, LLC (United States); Adam C Urness, Akonia Holographics LLC (United States)

The onslaught of big data continues even as growth in data storage density tapers off. Meanwhile, the physics of holography continues to suggest the possibility of digital data storage at densities far exceeding those of today's technologies. We report on recent results achieved with a demonstrator platform incorporating several new second-generation techniques for increasing holographic data storage (HDS) recording density and speed.

Since the highest reported areal densities for hard disk drive products currently hover in the 1 Tbit/in² range, we have adopted 2 Tbit/in² as a milestone likely to generate interest in the technology. The demonstrator is based on an advanced pre-production prototype, and so inherits highly functional electronic, mechanical, and optical subsystems. It employs a high-NA monocular architecture with proven angle-polytopic multiplexing.

The demonstrator design includes several second-generation innovations. The first, dynamic aperture multiplexing, greatly increases the number of multiplexed holograms. The second, the DRED medium formulation, provides dramatically higher dynamic range to record these holograms. These two features alone allow the demonstrator to exceed 2 Tbit/in². Additionally, it is equipped with the capability of quadrature homodyne detection, permitting phase quadrature multiplexing (QPSK modulation), and the potential to further increase user capacity by a factor of four or more. The demonstrator has thus been designed to achieve densities supporting the multi-terabyte storage capacities required for competitive products, and to demonstrate the potential for Moore's-Law growth for years to come.

9386-18, Session 5

Compensation of laser wavelength drift in collinear holographic storage system

Xiaotong Li, Yabin Cheng, Xiao Lin, Guoguo Kang, Xiaodi Tan, Beijing Institute Of Technology (China)

Collinear holographic storage system is one of the advantages of the promising candidate as its unique system design. The wavelength margin is a very important characteristic which can make a laser diode to be used possible as a light source in a holography storage system, because of the bit-error-rate (BER) of a reconstructed page data pattern will be so high that we cannot decode it correctly, even though the wavelength drift of the diode was small enough. To solve the problem, we studied a method of decreasing BER by adjusting the focal length of the lens to compensate the wavelength drifted in the collinear holographic storage system. In the simulation, when the wavelength drift was 5nm, the BER was grown up to 12.5%. However, if the focal length of the lens was decreased of 0.003mm, the BER was also decreased to zero. By decreasing the focal length, the wavelength drift can be compensated to some extent. In a two plane wave holographic theory, when the wavelength of the reference beam for reconstruction is different from recording process, in order to satisfy the Bragg condition, the incident angle should be also changed. In the collinear holographic storage system, the angles can be changed by adjusting the focal length of the lens. So we find that decreasing the focal length of the lens can compensate the wavelength drift up effectively and vice versa.

**Conference 9386:
 Practical Holography XXIX: Materials and Applications**

9386-19, Session 5

Automated determination of volume phase hologram parameters

Robert D. Brown, Rockwell Collins Aerospace & Electronics Inc. (United States); James H. Stanley, Rockwell Collins, Inc. (United States)

Commercially available ray tracing programs by themselves are not adequate for modelling waveguide based structures utilizing holographic gratings. In this paper we describe a suite of tools that we have developed specifically for working with volume phase holograms. One tool measures the diffraction efficiency of a grating with respect to angle and position. The automated measurement process is described, including steps taken to optimize speed, repeatability, and accuracy. This tool further analyzes measured diffraction data to extract key grating parameters; such as film thickness and index modulation. The theoretical basis for this extraction is described. The grating parameters are then used to directly model the real hologram performance in raytracing with a DLL to enable direct comparisons of the theoretical performance to measured performance. In our environment, data is collected and grating parameters are extracted using LabView; and ray tracing is performed using Zemax. The concepts, however, are quite general. Measurements of real photopolymers are given and compared to published specifications.

9386-20, Session 5

Applied digital holography for evaluating hard metal chip

José Luis V. Valin Rivera, Univ. de São Paulo (Brazil); Jaime M. Monteiro, Mario A. P. Vaz, Univ. do Porto (Portugal); H. M. Lopes, Institute Politecnico de Braganca (Portugal); Reginaldo T. Coelho, Meylí V. Fernández, Edison Goncalves, Univ. de São Paulo (Brazil)

The main objective of this work is the application of an interferometry method for validating the result of wear in a cutting tool insert of hard metal. We describe in this paper the experimental setup for the application of Digital Holography technique, used with digital recording of holograms on a CCD camera. The cutting insert inspected with the optical technique was previously mounted on a support structure and slightly heated with a halogen lamp for evidence of defective regions. In the test of the chip, implementing Digital holography system was used for the image processing software, ProITec. With this technique, it was possible to detect, with high resolution and contactless defects that could compromise the structural integrity of the insert analyzed for this particular case, no defect was found. Analysis of the images obtained, it is verified that the object is deformed as a whole, not to present any visible alteration in their pattern of fringes.

9386-21, Session 5

Design of wide angle holographic waveguide monocular head-mounted display using photopolymer

Meilan Piao, Chungbuk National Univ. (Korea, Republic of); Sangkeun Gil, Univ. of Suwon (Korea, Republic of); Nam Kim, Chungbuk National Univ. (Korea, Republic of)

The head-mounted display (HMD) has a huge potential market when used as a mobile display, and in applications for mixed reality, games, and navigation. In comparison with other waveguide HMDs, the holographic waveguide technique has the advantage of having a small volume, low price, and good command of angular and spectral selectivity of optical elements.

This work presented the design and proof of the concept of a wide angle holographic waveguide for monocular HMD's. The intended use of this device is using holographic optical element (HOE) to in-couple collimated light entering the waveguide at a particular angle, then the light travels through the waveguide using the principle of the total internal reflection, and finally the light is extracted to the eye with another set of HOE. Both ends of the designed waveguide, which were wedge-shaped at a certain angle, were attached to the HOEs. Structurally, the thickness of the waveguide can be reduced by a large angle of total internal reflection. Even though the conventional reflective optics without holographic mirror can make the total internal reflection and give the perfect color uniformity, the main problem arises due to the limited size of the resulting eye box and the thickness of the waveguide optics. Also one of the characteristic of reflection HOE is wide angular selectivity that is the reflection in reconstruction depends on the incident angle of illuminating beam which is equivalent to reference beam used in recording. The advantages of designed holographic waveguide monocular HMD that uses HOEs can use to make a wide angle, thin and flexible device for future commercial system.

9386-22, Session PWed

Optimization of the switch-back technique used for fast occlusion-processing in computer holography

Sachio Masuda, Kyoji Matsushima, Sumio Nakahara, Kansai Univ. (Japan)

Through the past few years, the spatial 3D images reconstructed by high-definition computer-generated holograms (HD-CGH), created by the polygon based-method, are being comparable to that by the conventional optical holograms. These HD-CGHs can reconstruct very impressive deep 3D scene and give a strong sensation of depth to viewers. This is because continuous motion parallax is generated both in horizontal and vertical directions by occlusion-processing based on the silhouette method.

Recently, we have proposed a new technique called the switch-back technique that makes it possible to realize very fast occlusion-processing in strongly self-occluded objects. This technique uses silhouette apertures based on Babinet's low instead of conventional silhouette masks, and partial field propagation instead of whole field propagation.

In this technique, it is reported that computation becomes even faster by splitting an object into several sub-objects along with depth direction, because the computation time strongly depends on the average distance between the polygons and the object plane in that final object field is obtained. However, there is an optimum number of sub-objects, because the computational cost for numerical propagations increases with increasing the number of sub-objects, while splitting object reduces the computational cost of the switch-back technique itself. In this paper, we propose a method to predict the optimum number of sub-objects by estimating the total computational complexity of the switch-back technique with object splitting. Moreover, another acceleration technique of the switch-back technique is also proposed in this paper. We will demonstrate several actual HD-CGHs created by the proposed method.

9386-23, Session PWed

Holographic gratings with NOA65(R) adhesives with edible colorant

Arturo Olivares-Pérez, Israel Fuentes-Tapia, Instituto Nacional de Astrofísica, Óptica y Electrónica (Mexico); Santa Toxqui-López, Benemérita Univ. Autónoma de Puebla (Mexico)

We present preliminary results on diffraction gratings made with holographic techniques, using as matrix the NOA 65[®] adhesive, photosensitized with neon food colors purple Mc Cormick[®]. The diffraction

**Conference 9386:
 Practical Holography XXIX: Materials and Applications**

gratings were recorded with a laser diode, $\lambda = 457\text{nm}$, we show the curves of diffraction efficiency vs exposure time. The gratings have a mixed behavior, of amplitude and phase, and have the ability of itself developed.

9386-24, Session PWed

Optimization of design wavelength for unobtrusive chromatic aberration in high-definition color computer holography

Takashi Miyaoka, Kyoji Matsushima, Sumio Nakahara, Kansai Univ. (Japan)

In a past few years, optical reconstruction of the high-definition computer-generated hologram (HD-CGH) created by computer holography is being comparable with that by conventional optical holography. However, the 3D image optically reconstructed by these HD-CGHs was commonly a monochromatic. Full-color reconstruction of HD-CGHs is simply realized by combining reconstructed images of three HD-CGHs for primary color. However, a chromatic aberration commonly occurs for each HD-CGH, because incoherent and non-monochromatic light source, such as LED, is used for illumination in order to avoid strong speckle noises and an injury to the viewer's retina. The chromatic aberrations change depending on the wavelength used for calculation of the CGH, which is referred to as the design wavelength in this paper, as well as the spectral shape of the illumination light. Since the illumination light has broadband spectrum, we have some flexibility to choose the design wavelength of HD-CGHs in order to make the color aberration be unobtrusive. In this paper, we present a technique based on simulated reconstruction of CGHs to measure quantitative unobtrusiveness of the chromatic aberration. We also propose an optimization technique of the design wavelength so that the color aberration is most unobtrusive in appearance of full-color reconstruction of HD-CGHs. Optical reconstruction of a full-color HD-CGH actually created using the proposed technique is presented to verify the validity of the technique.

9386-25, Session PWed

Holographic gratings in dichromated gelatin with edible dyes

Arturo Olivares-Pérez, Israel Fuentes-Tapia, Yessenia Jauregui-Sanchez, Instituto Nacional de Astrofísica, Óptica y Electrónica (Mexico); Santa Toxqui-López, Benemérita Univ. Autónoma de Puebla (Mexico); Rosario Juárez-Néstor, CONALEP (Mexico)

We present preliminary results on diffraction gratings made with holographic techniques using dichromated gelatin (AD) matrix with edible dyes, the purple red, Layar[®]; and blue Sabofrut[®]. The gratings were recorded with a laser diode, $\lambda = 530\text{nm}$. Curves show diffraction efficiency vs exposure time. The recorded gratings show different diffraction efficiencies of gratings prepared with AD, purple red + AD, and blue+ AD. We observed high diffraction efficiency with purple red. All exposure conditions and reconstruction were thereof for all gratings with the same concentration of dichromate for each one of the photosensitive emulsions prepared.

9386-26, Session PWed

Optimum phase-shift for off-axis digital holographic microscopy in phase volume measurement

Mohammad Reza Jafarfard, Yonsei Univ. (Korea, Republic of)

In this report, we analyze the inherent error of QPM that mainly caused by coherent transfer function (CTF) of system or band-pass filter in frequency domain used in numerical phase calculation processes. We propose an optimum amount of phase, existed that can effectively decrease the influence of band-pass filter in Fourier domain. We show that phase signal in frequency domain nonlinearly depends on the phase-shift between sample and its medium and this nonlinearity can be applied for overcoming the unwanted effect of band-pass filter in frequency domain. Because we have freedom to adjust the phase-shift value by different methods such as changing illumination wavelength using tunable laser or in some instances by alteration of refractive index of medium, our proposed method can be applied for different applications in morphology measurement. Here, we firstly propose a simple method for finding a proper band-pass filter for each system, and then we introduce our method to overcome the undesirable and inherent effects of the band-pass filter in the phase measurement by choosing a proper value of phase-shift in QPM. We also provide an empirical formula that can be used to choose the best amount of phase for a given size of a sample for a fixed width of a band-pass filter. To our knowledge, this is the first investigation that shows the influence of illumination wavelength or refractive index of medium on the phase signal in frequency domain and consequently the accuracy of phase morphology measurement in QPM. A cube can represent many man-made parts used in industry such as MEMS or micro-channels and a bead is a simplified shape for a cell. Our proposed method is not restricted to a cube or a bead, but can be applied to any unknown sample shapes.

9386-27, Session PWed

Stability of holographic gratings recorded on photopolymer films using acrylamide as monomer and N,N'-methylenebisacrylamide

Keiichi Osabe, Nagaoka Univ. of Technology (Japan); Hiroshi Saito, TDK-Lambda Corp. (Japan)

The stability of holographic gratings recorded on photopolymer films, using acrylamide as a monomer and N,N'-methylenebisacrylamide as a crosslinker, was experimentally examined. The photopolymer films contained acrylamide, N,N'-methylenebisacrylamide, eosin Y, and triethanolamine in the polyvinyl alcohol matrices. Four sets of films were fabricated, varying the concentration of N,N'-methylenebisacrylamide. The concentration of N,N'-methylenebisacrylamide was determined from the molar ratio between the crosslinker and the acrylamide. The relative molar rate between N,N'-methylenebisacrylamide and acrylamide was 0.1, 0.02, 0.004, or 0.

The photopolymer films were exposed by two intersecting laser beams at 532 nm, produced by a YVO laser, to form a holographic grating with a spatial frequency of 653 lines/mm, 100 s. The intensity of the impinging beams was 10 mW, and the beam diameter was 2.25 mm.

During recording, the diffracted intensity was simultaneously measured using a He-Ne laser at 633 nm, and again after one, two, and three days, in a dark storage using a YVO laser beam.

The photopolymer film having a relative molar ratio of 0.1 showed the highest diffraction efficiency during the recording (90%) and the best stability after three days (80%).

9386-28, Session PWed

Increasing reconstruction quality of diffractive optical elements displayed with LC SLM

Vitaly V. Krasnov, Pavel A. Cheremkhin, Nikolay N. Evtikhiev, Vladislav G. Rodin, Sergey N. Starikov, National Research Nuclear Univ. MEPhI (Russian Federation)

Phase liquid crystal (LC) spatial light modulators (SLM) are actively used in various applications. However, majority of scientific applications require stable phase modulation which might be hard to achieve with commercially available SLM due to its consumer origin. The use of digital voltage addressing scheme leads to phase temporal fluctuations, which results in lower diffraction efficiency and reconstruction quality of displayed diffractive optical elements (DOE). Due to high periodicity of fluctuations it should be possible to use knowledge of these fluctuations during DOE synthesis to minimize negative effect. We synthesized DOE using accurately measured phase fluctuations of phase LC SLM "HoloEye PLUTO VIS" to minimize its negative impact on displayed DOE reconstruction. Synthesis was conducted with versatile direct search with random trajectory (DSRT) method in the following way. Before DOE synthesis begun, two-dimensional dependency of SLM phase shift on addressed signal level and time from frame start was obtained. Then synthesis begins. First, initial phase distribution is created. Second, random trajectory of consecutive processing of all DOE elements is generated. Then iterative process begins. Each DOE element sequentially has its value changed to one that provides better value of objective criterion, e.g. lower deviation of reconstructed image from desired one. If current element value provides best objective criterion value then it left unchanged. After all elements are processed, iteration repeats until stagnation is reached. It is demonstrated that application of SLM phase fluctuations knowledge in DOE synthesis with DSRT method leads to noticeable increase of DOE reconstruction quality.

9386-29, Session PWed

UV recording with ethyl acetate and muicle dye film

Santa Toxqui-López, Benemérita Univ. Autónoma de Puebla (Mexico); A. Olivares-Pérez, Instituto Nacional de Astrofísica, Óptica y Electrónica (Mexico); V. Santacruz-Vazquez, Benemérita Univ. Autónoma de Puebla (Mexico); Israel Fuentes-Tapia, J. Ordóñez-Padilla, Instituto Nacional de Astrofísica, Óptica y Electrónica (Mexico)

Now days there are many types of holographic recording medium some of them are photopolymer systems that generally consist of a polymeric host matrix, photopolymerizable monomer, photosensitizing dye and charge transfer agent but some of them have an undesirable feature, the toxicity of their components. Therefore, the present research study material recording, ethyl acetate is selected as binder and natural dye from "muicle plant" is used as the photoinitiation these components are not toxic. The films are fabricated using gravity settling method at room temperature by this method, uniform films is obtained with good optical quality. To characterize the medium, interferometric studies including the recording of transmission gratings have been done; good diffraction efficiency have been obtained when the coherent reed light (632.8 nm) was sent normally to the grating.

9386-30, Session PWed

Improved hidden surface removal method for computer-generated alcove hologram

Takeshi Yamaguchi, Hiroshi Yoshikawa, Nihon Univ. (Japan)

We have investigated the floating image display, which named computer-generated alcove hologram. The viewing angle was enlarged by changing the shape of the computer-generated hologram from flat to semi-half cylindrical. To employ the calculation method of the computer-generated rainbow hologram, the full color floating image which has the wide viewing angle is reconstructed. Since these computer-generated holograms have the wide viewing angle, the correct hidden surface removal method is required.

In our previous work, the computer-generated hologram was calculated by using the large number of object data from different viewpoints. When the fringe pattern was calculated, the calculation area is divided into small segments, and each small segment is calculated from one object data. The

reconstructed image of the computer-generated hologram should not show the hole or overlap on the different viewing position. The small segment needs the several viewpoints information, especially the reconstructed image is close to the hologram plane. Therefore, the reconstructed image of the previous computer-generated hologram is concerned about the possibility of the hole or overlap.

In this paper, we have proposed the improved hidden surface removal method which uses the virtual window. The calculation area, which is determined by the virtual window, is added to the object data. To apply the improved hidden surface removal method, we have achieved the more correct reconstructed image.

9386-31, Session PWed

Security enhanced optical one-time password authentication method by using digital holography

Sangkeun Gil, Univ. of Suwon (Korea, Republic of); Seok-Hee Jeon, Incheon National Univ. (Korea, Republic of); Jong-Rae Jung, Suwon Science College (Korea, Republic of)

We propose an optical one-time password(OTP) authentication method by using digital holography, which enhances security strength in the cryptosystem compared to the conventional electronic OTP method. OTP authentication is a scheme which is a kind of challenge and response. In this paper, challenge and response of OTP authentication are performed by 2-step phase-shifting digital holography, where 2-step phase-shifting digital interferograms are acquired by moving the PZT mirror with phase step of 0 or $\pi/2$ in the reference beam path and are recorded on CCD. An OTP generated from the server is expressed by random binary code for convenience. This OTP information is encrypted with the secret key by applying phase-shifting digital holographic method, and this encrypted information is delivered to the valid user. Firstly, the user decrypts this encrypted OTP and encrypts it again with the secret key by the same phase-shifting digital holography. Then the user responses it to the server for authentication. After decryption of the OTP, the server verifies the user and allows login. Encrypted digital hologram in our method is Fourier transform hologram and is recorded on CCD with 256 gray-level quantized intensities. These encrypted digital holograms are able to be stored by computer and be transmitted over a communication network. The proposed optical method has an advantage that it does not need time-synchronized OTP and can be applied to various security services.

9386-32, Session PWed

Hologram-like interactive three-dimensional display using LED array type persistence of vision

Youngmin Kim, Jisoo Hong, Sunghee Hong, Sangkyun Kim, Hoonjong Kang, Korea Electronics Technology Institute (Korea, Republic of)

A three-dimensional display using persistence of vision (POV) has its own benefits for natural image expression. Conventional POV display using light emitting diode (LED) array was connected with high speed motor, so it could be possible to express curved-type two-dimensional display or volumetric three-dimensional display. However, it is necessary to consider interactive three-dimensional display. For example, this kind of volumetric display is hardly applied on interactive display since light emitting parts are placed in the center of rotating screen.

To provide a complementary effort to this need, we propose here a hologram-like interactive volumetric display using LED array type persistence of vision and a pair of parabolic mirrors. We build volumetric

**Conference 9386:
 Practical Holography XXIX: Materials and Applications**

POV display by using small size LED arrays. This POV display is located below a pair of parabolic mirrors so the mirrors make hologram-like volumetric POV display to be reimaged such as 4f system of lenses. Unlike this 4f system, the geometric distortion can be generated by a pair of mirrors. We assume our display as point cloud type display, it can be deduced the geometric distortion relationship between a hologram-like volumetric POV display and reimaging region by a pair of parabolic mirrors. Several preliminary experiments will be provided for our proposed method and compensation method by inverse homography matrix will be discussed.

9386-33, Session PWed

Non-destructive testing of an original XVI century painting on wood by ESPI system

Giovanni Arena, Pasquale Memmolo, Istituto Nazionale di Ottica (Italy); Giancarlo Fatigati, Mariangela Grilli, Univ. degli Studi Suor Orsola Benincasa (Italy); Melania Paturzo, Luca Pezzati, Pietro Ferraro, Istituto Nazionale di Ottica (Italy)

This work shows an applications of ESPI (Electronic Speckle Pattern Interferometry) in the context of diagnostics of Cultural Heritage. ESPI is a non-contact and non-destructive technique originally developed for high sensitivity NDT utilization in industrial applications. It is increasingly utilized as diagnostic tools in the Cultural Heritage field, providing relevant information about the structure and the state of conservation on different types of artefacts and has been demonstrated as a high valuable tool for largely improving traditional techniques used in the artworks diagnostics. By ESPI it is possible to reveal hidden damages not detectable by traditional methods. Detachments in paintings and frescoes, presence and extension of micro-cracks in statues and a huge typology of archaeological finds, quantitative measurements of deformation due to variations of environmental parameters, are possible. We used ESPI for the structural characterization and for revealing hidden defects of an original painting on wood, supposed dating from XVI century. Wooden substrates are affected by deformations produced by continuous contractions or expansion due to the moisture exchange. Pictorial layers protect the front of the board. Moisture absorption occur prevalently on the back of the panel, causing dangerous compressions and tractions on the preparation and painted layers. We obtained valuable information for the painting conservation and its restoration, by performing a long term monitoring of the structural deformations, resulting from the air conditioning system daily cycles, and measurements in restricted critical regions for revealing local damages. Understanding specific artwork behaviour is crucial in designing adequate micro-climatic conditions for its conservation.

9386-34, Session PWed

Recovering data from noisy fringe patterns from a portable digital speckle pattern interferometer for in-situ inspection of painting hanging on the wall

Giovanni Arena, Pasquale Memmolo, Istituto Nazionale di Ottica (Italy); Giancarlo Fatigati, Mariangela Grilli, Univ. degli Studi Suor Orsola Benincasa (Italy); Melania Paturzo, Luca Pezzati, Pietro Ferraro, Istituto Nazionale di Ottica (Italy)

We report on recovering data from a simple portable Digital Speckle Pattern Interferometer operating outside of laboratory conditions, without anti-vibration devices. The system was intended for potential in-situ utilization. In such a situation fringes produced by the true object displacements are affected by randomly unpredictable distortions caused by environment vibrations. The effects of environmental perturbations can be reduced by

capturing the fringe patterns with a short integration-time of the camera. By observing the evolution of the fringe-patterns, during an adequate time interval, it is possible to unambiguously distinguish the fringes produced by the object displacements and clearly recognize the distortions produced by environmental perturbations. In many cases undistorted or barely distorted interferograms, usable for recovering data, were found. Obviously blindly capturing random frames results ineffective as the fringes are erratically affected by distortions and their visibility and shape are continuously varying. As the reference hologram needs to be updated at regular time intervals, we implemented a strategy consisting on continuously recordings a large number of consecutive interferograms just prior each updating. The recorded frames were evaluated off-line, to retrieve suitable fringe patterns for processing through Hilbert Transform and PUMA unwrapping algorithms approach. We tested the method in monitoring a painting on wood, gaining the measurement of distortions caused by thermo-hygrometric fluctuations, verifying the usefulness of the system in a noisy location. The proposed method is intended for a qualitative evaluation tool for the routinely activity in art restoration laboratories and requires the active role of a skilled operator.

9386-35, Session PWed

Experiment on three-dimensional display using spatial cross modulation method

Yuta Kan, Atsushi Okamoto, Akihisa Tomita, Atsushi Shibukawa, Hokkaido Univ. (Japan); Hisatoshi Funakoshi, Gifu Univ. (Japan)

A well-known method for generating complex amplitude fields is displaying an off-axis computer-generated hologram (CGH) on a spatial light modulator (SLM). However, in this method, optical diffraction efficiency is considerably reduced. In addition, several tens of SLM pixels must be sacrificed for displaying a single data pixel, in an effort to form an interference fringe pattern.

To overcome these problems, we developed a spatial cross modulation (SCM) method using a random diffuser and phase-only SLM. In the proposed method, a scattered wavefront is obtained by first passing the original wavefront through a random diffuser on the Fourier plane and then converting the resultant distribution on the image plane. This step can be performed using virtual optical processing with a computer. The phase conjugate component of the scattered wavefront is displayed on the SLM, and the phase conjugate light is then optically reconvered through the random diffuser. Thus, the original wavefront is reconstructed on the image plane.

In this study, we performed an experiment on a 3D display using SCM. In our experiment, a 3D object constructed using four 2D images acquired from different spatial positions along the optical axis is generated, and the encoded 3D object is then displayed on a SLM. The different object images are observed when the image sensor is moved to a new spatial position. The experimental results revealed that the SCM method allows the generation of arbitrarily complex amplitude fields with higher diffraction efficiency compared to the CGH method, and with much lower speckle noise compared to the kinoform method.

9386-36, Session PWed

Interferometric study on Gouy phase anomaly of microlens array

Myun-Sik Kim, SUSS MicroOptics SA (Switzerland) and Ecole Polytechnique Fédérale de Lausanne (Switzerland); Toralf Scharf, Ecole Polytechnique Fédérale de Lausanne (Switzerland); Wilfried Noell, SUSS MicroOptics SA (Switzerland); Hans Peter Herzig, Ecole Polytechnique Fédérale de Lausanne (Switzerland); Reinhard Völkel,

Conference 9386:
Practical Holography XXIX: Materials and Applications

SUSS MicroOptics SA (Switzerland)

We experimentally and theoretically investigate the Gouy phase anomaly of light in the focus of cylindrical and spherical microlens array. Experiments are conducted by using longitudinal-differential interferometry and the theoretical study relies on a finite-difference time-domain (FDTD) method. We primarily discuss the classical definition for the Gouy phase for a conventional lens system, and compare with that of very small-size microlenses, where the size of the lens affects the phase properties near the focus. We put emphasis on determining the amount of the Gouy phase shift for line and point foci within the limited axial space, which is the fundamental difference from the conventional concept that concerns the \pm -infinite distance from the focus. Contrary to macroscopic lenses, the optical properties of microlenses are strongly governed by the effect of diffraction when their size tends to be comparable to the operation wavelength. In this study, we clearly show how such diffraction features affect the axial phase shift. For example, phase singularities, which occur at discrete points on the optical axis where the total intensity vanishes for spherical microlenses, cause an additional axial phase shift when compared to the cylindrical microlens where those axial phase singularities are absent. The rotational symmetry of the Fresnel zones is the origin of such a difference between point and line foci. In this way, we successfully demonstrate the Gouy phase measurements near the focus of small-size microlenses, and verify the results by rigorous simulation.

Conference 9387: Broadband Access Communication Technologies IX

Tuesday - Thursday 10-12 February 2015

Part of Proceedings of SPIE Vol. 9387 Broadband Access Communication Technologies IX

9387-1, Session 1

Prospects for millimetre-wave-over-fibre and THz-over-fibre systems *(Invited Paper)*

Alwyn J. Seeds, Haymen Shams, Martyn J. Fice, Katarzyna Balakier, Lalitha Ponnampalam, Cyril Renaud, Univ. College London (United Kingdom)

Optical fibre transmission has enabled greatly increased transmission rates, with 10Gb/s common in local area networks. End users find wireless access highly convenient, however limited spectrum availability at microwave frequencies results in per-user transmission rates which are limited to much lower values, 500 Mb/s for 5 GHz band IEEE 802.11ac, for example. Extending the high data-rate capacity of optical fibre transmission to wireless devices, requires greatly increased carrier frequencies. This paper will describe how photonic techniques can enable ultra-high capacity wireless data distribution and transmission using signals at millimetre-wave and TeraHertz (THz) frequencies.

Following an introduction to wireless over fibre system architectures and their deployment at microwave frequencies, architectures for millimetre wave over fibre and THz over fibre systems will be described. Simple wireless propagation models will be used to illustrate system requirements and constraints. Photonic technologies for the generation and detection of wireless signals will be described. Millimetre wave over fibre and THz over fibre system experiments will be presented and related to the system model. Key technology challenges that will need to be overcome to enable widespread deployment of millimetre wave over fibre and THz over fibre system further will also be described.

9387-2, Session 4

Next-generation optical wireless communications for data centers *(Invited Paper)*

Shlomi Arnon, Ben-Gurion Univ. of the Negev (Israel)

Data centers have become the leading technology for accumulating and handling information. The data-rates required for transferring the information through the server's backplane and between the servers has been increasing from year to year at an almost exponential pace. Therefore a technology-shift from the electronic to the optic domain has already been initiated in order to meet the required

data-rate and low latency demands for next-generation servers and data center. The technology that is present in this talk is optical wireless communication (OWC) or free space optics (FSO) for server and the data center applications.

9387-3, Session 4

Space division multiplexing in access networks *(Invited Paper)*

Frank J. Effenberger, FutureWei Technologies, Inc. (United States)

Access networks have requirements that differ from transport networks. Transport systems are mostly concerned with maximum capacity and distance capability; however, the emphasis in access is on low cost, low-loss, and service flexibility. This paper considers mode division multiplexing

(MDM) in the access application. In addition to MDM's natural capability to increase capacity, we explore its potential to reduce the optical combining loss in time division multiple access (TDMA) passive optical network systems (PON), and to reduce the overall cost of the system.

The first concept to be explored is the use of a photonic lantern to provide lossless combining of several single mode fibers (SMF) into a single few-mode fiber (FMF). This can be used in a PON system to combine several conventional splitter-based PONs into a hybrid fiber PON. It is possible to losslessly couple each input SMF into one mode of the FMF. In the simplest realization, the signal from the FMF could be detected by a single detector, and the TDMA of the underlying PON system would prevent collisions. More advanced realizations are possible where simultaneous transmissions are possible, but with interference reduction schemes. The intent is to avoid employing full MIMO techniques, due to their high cost.

Initial experimental evaluations of these concepts have been completed, and the basic principles have been confirmed. The practicality of these systems hinges on the availability of the fiber components, which should be solved over time. This suggests that applications of MDM in access might be closer than expected.

9387-4, Session 4

New development in optical fibers for data center applications *(Invited Paper)*

Yi Sun, Roman shubochkin, Benyuan Zhu, OFS Fitel LLC (United States)

VCSEL-multimode optical fiber based links is the most successful optical technology in Data Centers. Laser-optimized multimode optical fibers, OM3 and OM4, have been the primary choice of physical media for 10 G serial, 4 x 10 G parallel, 10 x 10 G parallel, and 4 x 25 G parallel optical solutions in IEEE 802.3 standards. As the transition of high-end servers from 10 Gb/s to 40 Gb/s is driving the aggregation of speeds to 40 Gb/s now, and to 100 Gb/s and 400 Gb/s in coming years, industry experts are coming together in IEEE 802.3bm 400 Gb/s study group and preliminary discussion of Terabit transmission for datacom applications has also been commenced. To meet the requirement of speed, capacity, density, power consumption and cost for next generation datacom applications, optical fiber design concepts beyond the standard OM3 and OM4 MMFs have a revived research and developmental interest. For example, wide band multimode optical fiber using multiple dopants for coarse wavelength division multiplexing; multicore multimode optical fiber using plural multimode cores in a single fiber strand to improve spatial density; and perhaps 50 Gb/s per lane and few mode fiber in spatial division multiplexing for ultimate capacity increase in far future. This talk reviews the multitude of fiber optic media being developed in the industry to address the upcoming challenges of datacom growth. We conclude that multimode transmission using low cost VCSEL technology will continue to be a viable solution for datacom applications.

9387-5, Session 5

SDN based millimetre wave radio over fibre (RoF) network *(Invited Paper)*

Ahmed Mohammed Amate, Milos Milosavljevic, Pandelis Kourtessis, Matthew Robinson, John M. Senior, Univ. of Hertfordshire (United Kingdom)

A software defined millimetre wave (mm-Wave) Radio over fibre (RoF) network is introduced for fifth (5G) generation mobile with gigabit connectivity. It enables effective open access where providers can manage

**Conference 9387:
 Broadband Access Communication Technologies IX**

and lease the infrastructure to service providers through un-bundling. The proposed network therefore presents network operators with suitable technologies that can effectively complement the toolkit of access methods they can utilize to best address the backhaul needs of the various classes of cell sites existing in their network.

Exploiting the inherited benefits of RoF, complete base station functionalities are centralised at the edges of the metro and aggregation networks leaving remote radio heads (RRHs) with only tuneable filtering and amplification. The software defined network (SDN) central controller (SCC) is responsible for managing the resource across several mm-Wave radio access networks (RANs) providing a global view of several network segments. This ensures flexible resource allocation with reduced overall latency and increased throughput. The SDN based mm-Wave RAN also provides inter edge node communication where specified packets are routed between RANs, bypassing the mobile core. A new layer 2.5 therefore allows end-to-end latency for wireless packets to be significantly reduced. Alternatively, packets can also be routed between RANs supported by the same edge node. System level simulations have shown significant improvement of the overall network throughput and latency of wireless users by providing effective resource allocation and mapping mechanisms.

9387-6, Session 5

Investigation of the SIW technology for low cost 60 GHz radio over fiber based array antenna units (*Invited Paper*)

Dimitrios Makris, Panagiotis K. Tsiakas, Konstantinos Voudouris, Technological Educational Institute of Athens (Greece); Manoj P. Thakur, Spiros Mikroulis, Univ. College London (United Kingdom)

The growing demand for ultra broadband wireless services (HD video, multimedia) lead to the use of Radio over Fiber (RoF) for 60 GHz links at indoor access. In this case, RoF systems use as a carrier a mm wave frequency (30-300 GHz) imposed onto an optical carrier and the modulated signal is then transmitted over the fiber from a Central Office (CO) to Base Stations (BSs), onwards defined as Remote Antenna Units (RAUs) providing low losses, high data rates and low implementation costs. Millimeter-waves, especially from 57 to 64 GHz, is an unlicensed frequency band, capable of secure and high bandwidth point to point wireless connections.

In general, mm-wave RAU performance is limited by the adaptation between the optical and microwave components, while cost-effectiveness and potential for integration are driving factors. System on Chip (SoC) approach is difficult to be implemented on mm wave photonics (absence of common substrates), while System on Package (SoP) has potential performance limitations especially due to the high interface/bonding losses. A promising candidate for developing all microwave/photonic components in the same substrate (System on Substrate- SoS) is the Substrate Integrated Waveguide (SIW) technology, which ensures low loss due to radiation.

In this paper, a SIW based O/E interface is presented compatible to RoF applications. The microwave design is based on a diplexer, two Chebyshev bandpass filters, one for uplink (61,7 GHz to 62,7 GHz) and one for downlink (59,3 GHz to 60,3 GHz) and one common 8x8 Slot array antenna, integrated in the same substrate. E/M simulations of fully integrated planar RF Front End provide very good performance, either in diplexer and filters or in antenna characteristics, comparing common substrates, and considering transition requirements for integration with a coplanar waveguide (CPW) photodiode. Last but not least, a proposed beamforming scenario is analyzed.

9387-7, Session 5

Deep optical access on multi-core and multi-mode fiber for integrated wireless applications (*Invited Paper*)

Roberto Llorente, Maria Morant, Marta Beltrán, Andrés Macho, Univ. Politècnica de València (Spain)

Deep optical access networks has been subject of study in the last years. Deep optical access should provide a range one order of magnitude over typical implementations supporting optical connectivity and mm-wave services at customer premises. This permits great capillarity and multiple ONTs. A radio-over-fiber bundle is proposed in the framework of the EU-FIVER project for the provision of quintuple-play services using fully standard signals as 3GPP LTE and IEEE802.16 WiMAX. Experimental results demonstrate 125 km reach including bend-insensitive ClearCurve in-building distribution supporting legacy coaxial distribution of DVB-T signals.

This concept has been extended with the introduction of plastic multimode fiber (POF) for in-building distribution applications capable of LTE, WiMAX and UWB wireless provision after 25 km SSMF optical access transmission. Also POF in-building transmission from satellite master antenna television (SMATV, 950-2150 MHz) and MATV (470-790 MHz) broadcasting is demonstrated over 25 m of 1-mm diameter graded-index POF. Mm-wave radio in this scenario benefits from optical signal processing. An optical comb based on gain-switched laser is demonstrated generating a 12.5 Gb/s 16QAM signal after 25 km SSMF distribution at 60 GHz. A 4-band OFDM signal with 9.6 Gb/s/band in 14.4-GHz bandwidth can also be provided to the user with 1.3-m wireless reach in the 75-110 GHz band.

Finally, wireless fronthaul on multicore transmission is proposed and demonstrated with dual 20-MHz LTE and WiMAX channels along 150 m in 4-core fiber. Linear and nonlinear inter-core crosstalk impact is minimized using core interleaving meeting EVM requirements in the wireless fronthaul.

9387-8, Session 5

Class AB radio-over-fiber link based on highly-linear ring resonator modulators

Stavros Iezekiel, Univ. of Cyprus (Cyprus)

A key figure of merit for analog optical links for radio-over-fiber applications is the spurious-free dynamic range (SFDR). In most links, shot noise associated with the residual optical carrier dominates SFDR. Class AB techniques have been used previously in order to improve the shot-noise limited SFDR for intensity-modulated links, but this has been for Mach-Zehnder modulators. In order to approach the theoretical improvement of 12 dB in SFDR for the class B scheme, an ideal linear static characteristic for the modulator is required; hence we propose the use of ring-resonator modulators which have been proven to approach quasi-linear voltage-light characteristics.

A class-AB photonic link uses two complementary modulators, each biased at opposite sides of the extinction point. By using a balanced photodetector to subtract the photocurrent due to modulator 1 from that of modulator 2, an effective transfer function is created. Through biasing ring-resonator modulators at complementary low-bias points, a highly linear effective transfer function results which leads to a linear output from the balanced photodetector with a near-zero average photocurrent, thus leading to SFDR enhancement approaching the 12 dB improvement that is theoretically possible for ideal linear modulator transfer characteristics. Moreover, through correct alignment of the two modulator transfer characteristics, the slope efficiency of the effective transfer function of the resulting analog link is double that of a single modulator, thus leading to a 3 dB enhancement of link gain. A theoretical analysis of the above scheme is currently being validated through development of a prototype system.

**Conference 9387:
Broadband Access Communication Technologies IX**

9387-9, Session 6

Integrated coherent radio-over-fiber units for millimeter-wave wireless access
(Invited Paper)

Andreas Stöhr, Sebastian Babel, Rattana Chuenchom, Matthias Steeg, Univ. Duisburg-Essen (Germany); John E. Mitchell, Cyril Renaud, Manoj Thakur, Univ. College London (United Kingdom); Frederic van Dijk, Alcatel-Thales III/V-Lab. (France); Andreas Steffan, Finisar Corp. (Germany); Matthew O'Keefe, Finisar Corp. (United Kingdom); Yigal Leiba, SIKLU Communications (Israel); Pawel Polis, Pawel Parol, Orange Polska (Poland); Juan J. Vegas Olmos, Technical Univ. of Denmark (Denmark); Idelfonso T. Monroy, DTU Fotonik (Denmark)

This paper will concentrate on recent key technological developments that were achieved within the European IPHOBAC-NG project for constructing such CRoF units capable to provide wireless services within the E-band (60-90 GHz). In detail, GaAs-based single-sideband millimeter-wave Mach-Zehnder modulators, InP-based millimeter-wave photodiodes featuring rectangular waveguide outputs and monolithically integrated low-linewidth tunable laser diodes as well as SiGe-based millimeter-wave RF amplifier technology will be reported.

In addition, a new coherent optical heterodyne radio-over-fiber scheme is proposed for seamless integration of next generation millimeter-wave wireless access systems into a next generation passive optical network employing dense or even ultra-dense WDM. We propose and demonstrate novel radio access units (RAU) using coherent optical heterodyne detection for the generation of the millimeter-wave radio signals in the RAUs. The proposed CRoF concept supports the provision of multiple services over a single optical distribution network including next generation optical and wireless access services and high-capacity fixed wireless links for mobile backhaul. Proof-of-concept system experiments are reported including the wireless transmission of a 2.5 Gb/s data signal over 40 m (limited by lab space) at 76 GHz carrier frequency after 20 km fiber-optic transmission.

9387-10, Session 6

Fiber-wireless system techniques for millimeter-wave wireless access
(Invited Paper)

Anthony Ng'oma, Corning Incorporated (United States)

Wireless data continues to grow exponentially – driven by the high proliferation of smart mobile devices and the popularity of video-centric mobile applications. As a result, new technologies are needed to address the growing gap between the supply and demand of mobile bandwidth.

Candidate technologies being considered by the industry to achieve high capacity wireless systems include Small Cells, increased spectral efficiency through more complex modulation formats (including MIMO, Massive MIMO, etc.), and mm-wave frequencies, which offer large amounts of licensed and unlicensed spectrum.

The aforementioned techniques come with their own technical challenges – including the need for extensive high-capacity backhaul networks. Fiber-based infrastructure solutions can help alleviate many of the technical and deployment challenges faced by current and future wireless systems. To begin with, fiber offers enormously large bandwidth, which could be exploited to significantly increase the performance of wireless systems or to simplify their deployment and management complexity. The large fiber bandwidth can be used to integrate distribution systems for both analog and digital signals. Furthermore, analog Radio-over-Fiber transmission can be utilized as a powerful protocol-agnostic platform for distributing cost-effectively signals of multiple wireless standards.

This paper investigates a wide-range of technical challenges and proposes solutions for RoF-based distribution systems capable of supporting advanced wireless technologies including MIMO and mm-waves. We experimentally demonstrate the efficacy of simple and practical RoF system techniques and methods for realizing ultra high-capacity systems supporting > 70 Gb/s wireless data transmission over several meters wireless distance.

9387-11, Session 6

Waveform over fiber: DSP-aided coherent fiber-wireless transmission using millimeter and terahertz waves
(Invited Paper)

Atsushi Kanno, Pham Tien Dat, Toshiaki Kuri, Iwao Hosako, Tetsuya Kawanishi, National Institute of Information and Communications Technology (Japan); Yuki Yoshida, Ken'ichi Kitayama, Osaka Univ. (Japan)

A great disaster such as an earthquake can easily destroy a communication network because current networks are based on optical fiber technology. When the fiber is cut, all communication links, including mobile communication links, are broken. Wireless communication technology is a good candidate for establishing protection links in a fiber network. However, the capacity of conventional wireless communication is 10 times smaller than that of optical fiber communication. Therefore, high-speed and high-capacity wireless communication technologies are in high demand.

Millimeter-wave and terahertz-wave radio technologies are promising candidates for high-speed links that have capacities greater than 10 Gb/s because of their broad available bandwidths. In fact, in the 60-GHz band, 7-Gb/s wireless local access network technology has already been standardized and is commercially available. Effective media conversion with digital signal processing (DSP) is a key issue for realizing high-capacity radio links. However, to obtain greater capacity, the power consumption and processing latency of the DSP during media conversion must be drastically increased.

Radio-over-fiber (RoF)-based fiber-wireless link technology is a potential solution for achieving greater capacity with moderate power consumption. Recent DSP-assisted optical communication technology—called “digital coherent technology”—can exclude the DSP during media conversion. The coherent optical transmitter generates a radio-friendly signal, and the DSP compensates for transmission impairments at the receiver. In the present paper, we discuss the principle, demonstration, and application of waveform-over-fiber technology, which is based on coherent fiber-wireless transmission technology empowered by DSP-aided optical communication technology.

9387-12, Session 6

Laser-phase-fluctuation-insensitive offset-frequency-spaced two-tone optical coherent detection scheme with digital-signal-processing technique for radio-over-fiber systems

Toshiaki Kuri, Takahide Sakamoto, Tetsuya Kawanishi, National Institute of Information and Communications Technology (Japan)

We have proposed a laser-phase-fluctuation-insensitive optical coherent detection scheme assisted by a digital signal processing (DSP) technique for radio-over-fiber (RoF) systems. In this system, a “two-tone” local light is used for an individual optical coherent detection of both the carrier and the modulated components of RoF signal, where a frequency separation of two-

**Conference 9387:
 Broadband Access Communication Technologies IX**

tone local light is the same as that of RoF signal. To distinguish the carrier and the modulated components in the process of optical coherent detection, they have to be separated in the optical domain. In this paper, we proposed a new optical coherent detection scheme with an "offset-frequency-spaced two-tone" local light, which is also in principle insensitive to the laser phase fluctuation and is assisted by the DSP technique. In the proposed scheme, it is not required to separate the carrier and the modulated components in the optical domain because they can be easily separated in the electrical domain after the photodetection. Therefore, the system configuration is expected to be simpler than that in the previous scheme. First, we explain the principle of our new proposal and experimentally demonstrate the data recovery. Then, the influence of the frequency detuning between photo-detected modulated and unmodulated signals is discussed. Moreover, the transmission performance with an error vector magnitude (EVM) is also evaluated for the optical coherent detection of a 10-Gbaud quadrature-phase-shift-keying RoF signal after a 20-km-long standard single-mode fiber transmission. As a result, it is shown that the EVM of less than 12.4 %rms is achieved.

9387-13, Session 7

Wavelength shift tolerance of a heterodyne detection scheme for cost-efficient DWDM-PON / 60 GHz wireless integration *(Invited Paper)*

Maria C. R. Medeiros, Univ. de Coimbra (Portugal); Manoj P. Thakur, Spiros Mikroulis, John E. Mitchell, Univ. College London (United Kingdom)

Radio-over-fiber systems employing remote antenna units (RAUs) based on coherent optical heterodyne detection of two, phase-uncorrelated lasers and envelope detection have been demonstrated recently [1-3]. By using two uncorrelated lasers, this system concept allows simple implementations that can be further simplified, if thermally uncooled lasers are used. Although such asynchronous receiver designs are mildly affected by the laser phase noise a limiting affect is that they suffer from the wavelength drift that occurs between the two uncooled lasers. In addition, there are performance penalties due to high laser linewidth when complex modulation formats are used for transmission. In this work, we compare the performance of envelope detector based heterodyne and homodyne receivers, using OOK and multilevel modulation formats.

1. A. Stöhr, O. Cojucari, F. van Dijk, G. Carpintero, T. Tekin, S. Formont, I. Flammia, V. Rymanov, B. Khani, and R. Chuenchom, "Robust 71-76 GHz Radio-over-Fiber Wireless Link with High-Dynamic Range Photonic Assisted Transmitter and Laser Phase-Noise Insensitive SBD Receiver," in Optical Fiber Communication Conference, OSA Technical Digest (online) (Optical Society of America, 2014), M2D.4.
2. A. H. M. R. Islam, M. Bakaul, A. Nirmalathas, and G. E. Town, "Simplification of millimeter-wave radio-over-fiber system employing heterodyning of uncorrelated optical carriers and self-homodyning of RF signal at the receiver," *Opt. Express* 20, 5707-5724 (2012).
3. M. P. Thakur, S. Mikroulis, C. C. Renaud, J. E. Mitchell, and A. Stöhr, "DWDM-PON/mm-Wave Wireless Converged Next Generation Access Topology using Coherent Heterodyne Detection," in International Conference on Transparent Optical Networks, (IEEE, Graz, Austria, 2014).

9387-14, Session 7

All-optical virtual private network system in OFDM based long-reach PON using RSOA re-modulation technique

Chang-hun Kim, Sang-Min Jung, Soo-Min Kang, Sang-Kook Han, Yonsei Univ. (Korea, Republic of)

We propose an all optical inter-ONU communication system in an orthogonal frequency division multiplexing (OFDM) long reach PON (LR-PON). In the optical access network field, technologies based on fundamental upstream (U/S) and downstream (D/S) have been actively researched to accommodate explosion of data capacity. However, data transmission among the end users which is arisen from cloud computing, file-sharing and interactive game takes a large weight inside of internet traffic. Moreover, this traffic is predicted to increase more if Internet of Things (IoT) services are activated. In a conventional PON, inter-ONU communication data is transmitted through ONU-OLT-ONU via U/S and D/S carriers. It leads to waste of bandwidth and energy due to O-E-O conversion in the OLT and round-trip propagation between OLT and remote node (RN). Also, it causes inevitable load to the OLT for electrical buffer, scheduling and routing. The energy inefficiency for inter-ONU communication becomes more critical in a LR-PON which has been researched as an effort to reduce CAPEX and OPEX through metro-access consolidation.

In the proposed system, the inter-ONU data is separated from conventional U/S and re-modulated on the D/S carrier by using RSOA in the ONUs to avoid bandwidth consumption of U/S and D/S unlike in previously reported system. Moreover, the transmitted inter-ONU data is re-directed to the ONUs by wavelength selective reflector device in the RN without passing through the OLT. Experimental demonstration for the inter-ONU communication system in an OFDM based LR-PON has been verified.

9387-15, Session 7

Visible CWDM system design for Multi-Gbit/s transmission over SI-POF

Carmen Vázquez García, Plinio Jesús Pinzón Castillo, Isabel A. Pérez Garcilópez, Univ. Carlos III de Madrid (Spain)

Primarily due to the 'do-it-yourself' installation, easy maintenance and high bending tolerance, large core step index (SI) plastic optical fibers (POF) are considered more suitable than 50 mm core diameter multimode glass fibers or perfluorinated plastic optical fibers in some applications such as home networking. It is shown to be impossible to achieve more than 2 Gbit/s for 50 m single-core SI-POF using eye-safe VCSEL transmitters. In order to increase the data rates of Multi-Gbit/s links based on SI-POF, different modulation scenes have been proposed by different authors. Another option can be to use multiple optical carriers in a single POF for parallel transmission of communication channels over the same fiber. As the channels are broadband and far away in comparison to long haul optical communication, they are referred as course wavelength division multiplexing (CWDM) systems. Some designs to reach data rates of 10.7 Gbit/s in 25 m, with 4 channels and using NRZ modulation, have been developed using this approach, but those rates are reached by off line processing.

Commercial systems with SI-POF able to provide data rates around 1 Gbit/s over 50 m are already in the market. Designs to test the potential of real Multi-Gbit/s transmission systems using commercial products will be reported. Special care in designing low insertion loss multiplexers and demultiplexers will be carried out.

9387-16, Session 7

A colorless remote node for metro-access converged optical network

Simiao Xiao, Zhensen Gao, Kaibin Zhang, Alcatel-Lucent Shanghai Bell Co. Ltd. (China)

Metro-access network is a newly emerged network which combines the traditional separated metro network and access network together into a converged system. It serves more users in a larger geographical area, meanwhile maintaining a simplified network hierarchy which inherits the low cost, large bandwidth, and high reliability of PON. In this paper, a novel colorless interconnecting node (RN) with single specification for both xPON and 10G-PON subscribers in the metro-access converged optical network is

**Conference 9387:
 Broadband Access Communication Technologies IX**

proposed. Massive subscribers could be supported due to the high spectrum utilization efficiency.

N access-trees are assembled into one metro-ring through N "colorless" RNs. To avoid traffic jamming, N arbitrary wavelengths are allocated to N RNs in the metro-ring, modulated with the corresponding DS traffic. Two additional public wavelengths without modulation are shared by all RNs with the normal DS wavelengths of xPON and 10G-PON. At each RN, the DS traffic is converted from one of the N arbitrary wavelengths in the metro-ring to the two public wavelengths through a downstream wavelength convertor (DWC), then transmits to the subscribers of the local access-tree. Whereas the US traffic from the subscribers is converted from the normal US wavelength to the same dedicated wavelength in the metro part through an upstream wavelength convertor (UWC). That is, a single wavelength in the metro-ring firstly carries the DS traffic to one dedicated RN, and then re-carries the US traffic back after the RN. The DWC and UWC are based on the XGM effect of a SOA.

9387-18, Session 7

Secure bidirectional transmission in a WDM-PON architecture employing RSOA-based remodulation scheme

Anindya S. Das, Ardhendu S. Patra, Sidho-Kanho-Birsha Univ. (India)

WDM-PON is widely accepted network technology due to its high bandwidth and secure transmission capability. Injection locking technique and direct modulation scheme is used to reduce the cost of the PON configuration. Remodulation scheme is another scheme which is popularized for making low cost upstream transmission in network architecture. In this paper a full duplex WDM-PON architecture has been developed for transmitting Ethernet services over long haul SMF by using injection locking, direct modulation, remodulation and error correcting schemes. Fabry-Perot laser diode has been used as the light source which is injected by the ASE source and force to oscillate at the wavelength of 1552.49 nm with detuning of 0.12 nm. RSOA has been used at the user end for reusing and remodulation of the lightwave for the upstream transmission. The message signal with word length of (211-1) is encoded by the RS (255, 251) encoder at the source end and decoded by the RS (255, 251) decoder at the receiver end. RS (255, 251) is preferred due to its high coding rate of 0.984 with low redundancy of 1.59 and coding gain of 6.92 dB. Introduction of RS (255, 251) codec in the configuration has improved the performance as the proposed architecture is able to transmit 10 Gbps data rate over 20 km SMF in upstream while its conventional counterpart transmits 10 Gbps upto 10 km without using RS codec. The system is suitable for the XGPON services such as converging of IPTV and HDTV, triple play services, etc.

9387-17, Session 8

**Next-generation resilient access networks
 (Invited Paper)**

Katsumi Iwatsuki, Tohoku Univ. (Japan); Katsutoshi Tsukamoto, Osaka Institute of Technology (Japan)

After the East Japan Great Earthquake, the construction of resilient network has been strongly required. On the other hand, the technical convergence with wired and wireless plays an important role to achieve the next generation access networks beyond bandwidth of current optical access. In this presentation, we will talk about next generation resilient networks, handling the download of huge data, images, and videos, as well as to upload of a large number of sensor data, any time and anywhere.

9387-19, Session 8

An approach to resilient wireless communication systems research for massive disasters (Invited Paper)

Kiyoshi Hamaguchi, National Institute of Information and Communications Technology (Japan)

Wireless systems, which do not depend on physical networks of wires, play an important role in developing resilient telecommunication networks. We built a wireless mesh network test bed to demonstrate disaster-resistant telecommunication technologies, and we conducted open experiments in March 2013. An overview of the system and experimental results including recent experiments are briefly reported.

9387-21, Session 8

STBC AF relay for unmanned aircraft system (Invited Paper)

Fumiyuki Adachi, Hiroyuki Miyazaki, Chikara Endo, Tohoku Univ. (Japan)

Our society is heavily relying on modern communications network infrastructure. In a large scale disaster, however, many areas may lose communications services and become isolated. Right after the Great East Japan Earthquake 2011, we initiated several projects to develop disaster-resilient communications networks. Among them is unmanned aircraft system (UAS). UAS is able to quickly extend the communication services to isolated areas. A group of UAs can be used as relay nodes to connect an isolated area with normal (not damaged) area. In this paper, STBC amplify-and-forward (AF) relay is presented for UAS. A group of UAs forms single frequency network (SFN) for STBC AF relay. STBC AF relay achieves large spatial diversity gain and can improve the relay communication quality. After describing the STBC AF relay algorithm and system design, some computer simulation results are presented.

9387-22, Session 8

Hybrid optical fiber-wireless sensor and communication networks for environmental monitoring and disaster prevention

Ferney O. Amaya Fernández, Leonardo Betancur-Agudelo, Univ. Pontificia Bolivariana (Colombia); Idelfonso Tafur Monroy, DTU Fotonik (Denmark)

Climate change is producing ecological impact around the world negatively affecting the environment. Technological support may be used for disaster prevention and disaster reduction employing a remote sensing monitoring system for flood control, drought combat and mountainside displacement detection. We propose a hybrid optical and wireless sensor network for disaster prevention. Low cost fiber optic sensors take advantage of different effects of propagation through the optical fiber, offering low power consumption and coverage in extended geographic areas. A hybrid wireless mess passive optical network (PON) collects the sensor information. The wireless mess network (WMN) allows highly reconfigurable and self-healing capabilities, and the PON offers coverage and low latency. The proposed architecture network is presented. Performance simulation results and experimental results are included.

9387-31, Session PWed

Radio-over-fiber transport system employing free-space optical communication scheme with parabolic reflector

Anindya S. Das, Ardhendu S. Patra, Sidho-Kanho-Birsha Univ. (India)

Radio-over-fiber transport system is an attractive solution to increase capacity and mobility of communication system. WDM and the optical add-drop multiplexing (OADM) techniques have simplified ROF architecture and optical free space transmission scheme is used to provide high speed and high security to the ROF configuration. In this paper we have proposed and demonstrated a bidirectional ROF transport system in combination with optical free space transmission schemes based on WDM, external light injection and optical add-drop multiplexing techniques. A diverging lens at the fiber end and a parabolic reflector at the receiver end are designed to employ optical free space transmission scheme in the configuration which transmits data-stream of 1-10 Gbps at 12.5 GHz. Two DFB-LDs are used as light source and externally injection locked at 1543.98 nm (?1) and 1549.97 nm (?2). There are two base stations named BS1 and BS2. BS1 deals with ?1 for OADM1 of an insertion loss of 4.2 dB and >40 dB isolation. BS2 deals with ?2 for OADM2 of same property. High channel isolation offers good add drop ability and prevent the crosstalk. At a free space transmission distance of 10m the BER is around 10⁻⁴ without using preamplifier; with preamplifier the BER reached down to 10⁻⁹. Huge improvement of 10⁴ orders is obtained as push-pull amplifier and adaptive filter are used simultaneously. Excellent BER values and impressive eye diagrams for both down/uplink have shown that our proposed system is convenient and suitable for 80 km optical and 10 m free space transmission.

9387-32, Session PWed

Ultra-broadband GaInNAs semiconductor optical amplifier incorporating N compositional fluctuations for the next generation passive optical network

Xiao Sun, Qingjiang Chang, Alcatel-Lucent Shanghai Bell Co. Ltd. (China)

Analysis of the broadband gain of a GaInNAs single Quantum Well (QW) Semiconductor Optical Amplifier (SOA) is developed considering the tuneability of the gain in detail. The SOA is analyzed as a single device multi-wavelength channel amplifier in a Wavelength-Division-Multiplexing (WDM) network. The N fluctuations in GaInNAs QW material cause a random distribution of sizes in the resulting QDs-like fluctuations resulting in a distribution of the QD-like ground state energies. The gain model includes the quantum well material gain derived using a Band Anti-Crossing (BAC) model and includes the gain of Quantum Dot (QD)-like fluctuations in the conduction band minimum according to Sugawara model. The total GaInNAs material gain is broadened by adding the gain of the QD-like fluctuations and the QW confined level. The QW and QD gain depends on the carrier density in the relevant states so a rate equation model is developed to calculate the electron concentration in the QW and QD states. Simultaneous amplification of two optical signals is analyzed, one at the peak of the QW gain and one at the peak of the QD distribution gain and the linear and non-linear regions are established. In addition, multi-channel signal amplification, appropriate for WDM applications, has been modelled across the frequency range of the QW and the QD-like fluctuations and no wavelength degradation between the channels was observed demonstrating the potential of dilute nitride QW as multi-wavelength SOAs at optical communications wavelengths.

9387-34, Session PWed

Software design of segment optical transmitter for indoor free-space optical networks

Jan Latal, Jan Vitasek, Petr Koudelka, Petr Siska, Andrej Liner, Lukas Hajek, Ale? Vanderka, Vladimír Va?inek, V?B-Technical Univ. of Ostrava (Czech Republic); Michal Lucki, Czech Technical Univ. in Prague (Czech Republic)

During recent years the rapid development in optical networks occurs. This includes not only fiber optical networks but also the free space optical networks. The free space optical networks can be divided on indoor and outdoor. The indoor free space optical networks are experiencing dramatic progress in the last years allowed by newest IEEE norm 802.15.7, which enabled development of different types of transceivers, receivers, modulation formats, etc. The team of authors is dealing with software design of segment optical transceiver for indoor free space optical network based on the multi mode optical fiber 50/125 or 62.5/125 μm . Simulated data are then evaluated from the point of view of optical intensity uniform distribution and space spot light size radiating from segment optical transceiver.

9387-35, Session PWed

Analysis of an optical wireless transceiver using subcarrier intensity modulation in indoor visible light communications

Petr Koudelka, Andrej Liner, Radek Martinek, Jan Latal, Petr Siska, Stanislav Kepak, Vladimír Va?inek, V?B-Technical Univ. of Ostrava (Czech Republic)

Indoor optical wireless communications (OWC) links offer several advantages in terms of data rate, power efficiency, low transceiver complexity, security issues and unregulated bandwidths. Visible light communications (VLC) is a promising solution for high speed data transmission in indoor applications. VLC systems, which provide both illumination and communication over visible or hybrid visible/infrared LEDs, are presented as the most important representative of future indoor OWC. Intensity modulation with direct detection (IM/DD), LED-based OWC systems are widely used due to their simplicity. Subcarrier intensity modulation (SIM) is an attractive technology for future OWC systems. The first proposals subcarrier intensity modulation for OWC applications and the error rate performance of differential phase-shift keying (DPSK) and M-ary phase-shift keying (MPSK) in lognormal channels study. Besides PSK modulation, quadrature amplitude modulation (QAM) has also gained attention for SIM in OWC. The main advantage of QAM is its high spectral efficiency since a 2^N QAM offers N times the spectral efficiency offered by BPSK systems. The article discusses the analysis of an optical wireless transceiver using subcarrier intensity modulation in indoor visible light communications. Optical wireless transceiver has been designed for modulation element (SMD LED matrix 3 ? 3) and the overall design of the light will be composed of several modulation elements. Simulations and real measurements both in the dark room without the presence of parasitic ambient radiation and under the real conditions are performed on the basis of the proposed optical wireless transceiver. The bit error rate performance of subcarrierary M-ary phase-shift keying and QAM frequency-shift keying modulated systems using the same frequency domain approach was also analyzed. Measurements were performed on a warm white LED, cool white LED, blue LED (chip only, without the luminophor) and a white LED with the filter.

9387-36, Session PWed

Software design of optical link for indoor wireless optical communication network used LEDs as source visible light communication

Andrej Liner, Martin Papes, Jakub Jaros, Petr Koudelka, Jan Latal, Jan Vitasek, Lukas Hajek, Vladimír Vaříněk, V?B-Technical Univ. of Ostrava (Czech Republic)

Nowadays, the conventional light sources are replaced progressively evolving LED (Light Emitting Diode) for their deficient properties. This technology recorded dynamic growth mainly due to effective research in increasing power density and choice the color shade on good color rendering CRI (Color Rendering Index). This extending the zone of used LEDs. Development of lighting technology by means of white power LEDs provided impulse to the idea of the development of optical wireless data networks based on optical radiation in the visible region of the spectrum VLC (Visible Light Communications). In the last years being recorded a turnover of research from transmission of information via optical fiber to the transmission of information through wireless networks. At the same time the concept of information transmission by indirect sight between transmitter and receiver NLOS (Non Line of Sight) is changing. Line of research focuses mainly on the direct line of sight LOS (Line of Sight). This is due to the development of the semiconductor lighting through the white power LED. This is connected with the idea of using them as a transmitter for communication purposes. This article deals with software design of optical link for indoor wireless optical network in LightTools software. Optimal optical source was designed for communication using LED as the first. For the proposed type of LEDs sources were used different shapes and distances distribution between LEDs in a single cell at the designed optical transmitter. Furthermore, the article focuses on the formation of a homogeneous distribution of optical power in the room.

9387-37, Session PWed

Secure transmission of static and dynamic images via chaotic encryption in acousto-optic hybrid feedback with profiled light beams

Monish R. Chatterjee, Fares S. Almeahmadi, Univ. of Dayton (United States)

It is known that the chaos wave resulting from driving an acousto-optic device under first-order feedback into its chaotic regime may be used as a carrier which may be modulated by an information signal applied through the bias circuit for the RF driver in the feedback loop [1,2]. The resulting encrypted signals exhibit reasonable parameter (encryption keys) tolerance in terms of non-recovery of the output signal for "slave" Bragg cell time delay, feedback gain or bias voltage mismatch in excess of $\pm 10\%$ [2]. While this indicates acceptable robustness with effective tolerance threshold (combining the three keys) of about 0.1%, the results (using uniform input light beams) have been far less satisfactory for the case of static images, with discernable filtered outputs persisting for much higher tolerances [3]. Recently, it has been observed that the use of profiled optical beams leads to a substantial increase in both the number and extent of passbands in the chaotic system [4]. Using profiled beam propagation, the first-order scattered profile is derived numerically using a transfer function formalism. Using the stored scattered profile data, the closed-loop system is examined for encryption using both static images as well as low-bandwidth video signals (within a few Mb/s). The results, presented here, show considerably improved quality of signal retrieval as well as much lower parameter tolerance (around $\pm 0.1\%$ per key), attesting to the promise of greater information security.

1. M. Al-Saedi and M.R. Chatterjee, "Examination of the nonlinear dynamics

of a chaotic acousto-optic Bragg modulator with feedback under signal encryption and decryption," *Opt. Eng.* 51(1), 018003 (2012).

2. M.R. Chatterjee and M. Al-Saedi, "Examination of chaotic signal encryption and recovery for secure communication using hybrid acousto-optic feedback," *Opt. Eng.* 50(5), 055002-16 (2011).

3. M.R. Chatterjee and A. Kundur, "Information encryption and retrieval in mid-RF range using acousto-optic chaos," *Proc. SPIE* 8406, 840608 (2012).

4. F.S. Almeahmadi and M.R. Chatterjee, "Numerical examination of the nonlinear dynamics of a hybrid acousto-optic Bragg cell with positive feedback under profiled beam propagation," *JOSA B* 31(4), 833-841 (2014).

9387-23, Session 9

Organic semiconductors for visible light communication (*Invited Paper*)

Ifor D. W. Samuel, Pavlos Manousiadis, Univ. of St. Andrews (United Kingdom); Hyunhae Chun, Sujun Rajbhandari, Univ. of Oxford (United Kingdom); Jonathan D. McKendry, Univ. of Strathclyde (United Kingdom); Shuyu Zhang, Univ. of St. Andrews (United Kingdom); Dobrosław Tsonev, The Univ. of Edinburgh (United Kingdom); Dimali C. V. Amarasinghe, Univ. of St. Andrews (United Kingdom); Martin D. Dawson, Univ. of Strathclyde (United Kingdom); Harald Haas, The Univ. of Edinburgh (United Kingdom); Dominic C. O'Brien, Univ. of Oxford (United Kingdom); Graham A. Turnbull, Univ. of St. Andrews (United Kingdom)

Organic semiconductors are of growing importance for displays and lighting, and an emerging solar cell technology. They combine simple fabrication with scope to tune their electronic and optical properties by changing the chemical structure. Of particular relevance to visible light communication is the fact that they combine strong absorption, high fluorescence quantum yield and short radiative lifetime. This makes them attractive materials for colour conversion. The inorganic phosphors typically used to make white light from blue Gallium nitride LEDs have long excited state lifetimes that severely limit the bandwidth of data transmission. We show that the short radiative lifetime of conjugated polymers makes them attractive materials to overcome this limitation. The copolymer super-yellow was used in combination with a gallium nitride micro-LED to generate white light. This enabled data transmission at 1.68 Gb/s over a distance of 3 cm, and 840 Mb/s over a distance of 2 m. These are the fastest results so far reported for a single white-source visible light communication system.

9387-24, Session 9

Three dimensional indoor positioning based on visible light with Gaussian mixture sigma-point particle filter technique

Wenjun Gu, Weizhi Zhang, The Pennsylvania State Univ. (United States); Jin Wang, China Univ. of Geosciences (China); Mohammadreza Aminikashani, Mohsen Kavehrad, The Pennsylvania State Univ. (United States)

Over the past decade, location based services (LBS) has found its wide applications in indoor environments, such as large shopping malls, hospitals, warehouses, airports, etc. Current technologies provide wide choices of available solutions, which include Radio-Frequency Identification (RFID), Ultra wideband (UWB), wireless local area network (WLAN) and Bluetooth. With the rapid development of LED technology, visible light communication (VLC) also brings a practical approach to LBS. As visible light has a better

**Conference 9387:
 Broadband Access Communication Technologies IX**

immunity against multipath effect than radio waves, high positioning accuracy is achieved. LEDs are utilized both for illumination and positioning purposes to realize relatively lower infrastructure cost. In this paper, an indoor positioning system using VLC is proposed, with LEDs as transmitters and photo-diodes as receivers. The algorithm for the system is based on received-signal-strength (RSS) information collected from photo-diodes and trilateration techniques. By appropriately making use of the characteristics of receiver's movement and the property of trilateration, the estimation on 3-D coordinates is attained. Filtering technique is applied to enable the tracking capability of the algorithm, and higher accuracy is reached than raw measurements. Gaussian mixture Sigma-point particle filter (GM-SPPF) is proposed for this 3-D system, which introduces the notation of Gaussian Mixture Model (GMM). The number of particles in the filter is reduced by approximating the probability distribution with Gaussian components.

9387-25, Session 9

Integrated multiple-input multiple-output visible light communications systems: recent progress and results

Dominic C. O'Brien, Univ. of Oxford (United Kingdom); Harald Haas, The Univ. of Edinburgh (United Kingdom); Sujan Rajbhandari, Hyunchoe Chun, Grahame E. Faulkner, Univ. of Oxford (United Kingdom); Katherine Cameron, Aravind Jalajakumari, Robert K. Henderson, Dobroslav Tsonev, Muhammad Ijaz, Zhe Chen, The Univ. of Edinburgh (United Kingdom); Enyuan Xie, Jonathan D. McKendry, Johannes Herrnsdorf, Erdan Gu, Martin D. Dawson, Univ. of Strathclyde (United Kingdom)

Solid state lighting systems typically use multiple LED die within a single lamp, and multiple lamps within a coverage space. This infrastructure forms the transmitters for Visible Light Communications (VLC), and the availability of low-cost detector arrays offers the possibility of building Multiple Input Multiple Output (MIMO) transmission systems. The need to provide sufficient illumination for occupation leads to a high signal to noise ratio (SNR) channel, and the LED characteristics usually limit the modulation bandwidth of the VLC channel. MIMO therefore offers an efficient way to use this high SNR low bandwidth channel and achieve potentially linear capacity growth, by splitting the power available and using different techniques to provide parallel data streams.

There are several different approaches to achieving this, including line of sight imaging systems, diffuse systems and lower complexity spatial modulation techniques.

Several of these are being investigated as part of a UK government funded research programme, 'Ultra Parallel Visible Light Communications' (UPVLC). In this paper we present a brief review of the area and report results from the programme. Subsystems that use Gallium Nitride micro-LEDs as transmitters and CMOS based receivers have been developed, and these are being used in a number of MIMO demonstrations. Preliminary experiments are currently underway, and results from these will be reported. The scalability of these approaches, and future directions will also be discussed.

9387-26, Session 9

Novel channel models for visible light communications (Invited Paper)

Farshad Miramirkhani, Murat Uysal, Ozyegin Univ. (Turkey); Erdal Panayirci, Kadir Has Univ. (Turkey)

Abstract- In this paper, we investigate channel modeling for visible light communications (VLC) using non-sequential ray tracing simulation tools. We create three dimensional realistic simulation environments to depict indoor scenarios specifying the geometry of the environment, the objects

inside, the reflection characteristics of the surface materials as well as the characteristics of the transmitter and receivers, i.e., white LED sources and photodiodes. We further impose illumination levels as suggested by the international lighting authorities. Ray tracing simulations yield the received optical power and the delay of direct/indirect rays which are then used to obtain the channel impulse response (CIR) and channel transfer function (CTF). Following this methodology, we obtain CIR/CTFs for a number of configurations including empty/furnished rectangular rooms with different sizes and wall materials (i.e., plaster, plastic, wooden, brick) assuming both deployment of single and multiple LED transmitters. We further quantify multipath channel parameters such as delay spread, channel DC gain and coherence bandwidth for each configuration and provide insights into the effects of indoor environment parameters (i.e., size, wall coating, etc) and transmitter specifications (i.e., single vs multiple transmitters, array type, their location, etc) on the channel.

9387-20, Session 10

The performance of space shift keying for free-space optical communications over turbulent channels

Mohamed R. Abaza, Raed Mesleh, Univ. of Tabuk (Saudi Arabia); Ali Mansour, ENSTA Bretagne (France); El-Had M. Aggoune, Univ. of Tabuk (Saudi Arabia)

This paper evaluates the performance of space shift keying (SSK) free-space optical communication (FSO) over moderate and strong turbulent channels. It has been shown previously that repetition codes (RCs) using intensity modulation with direct detection techniques are superior to SSK system for a spectral efficiency of 1 bit/s/Hz. It is shown in this study that SSK outperforms RCs using M-ary pulse amplitude modulation for spectral efficiencies of 3 bits/s/Hz or larger. Analytical expressions for the bit error rate for the SSK system under study are derived and extensive simulation results corroborate the correctness of the conducted analysis.

9387-27, Session 10

Turn on the lights! Leveraging visible light for communications and positioning (Invited Paper)

Steve Hranilovic, McMaster Univ. (Canada)

The need for ubiquitous broadband connectivity is continually growing, however, radio spectrum is increasingly scarce and limited by interference. In addition, the energy efficiency of many radio transmitters is low and most input energy is converted to heat. A widely overlooked resource for positioning and broadband access is optical wireless communication reusing existing illumination installations. As many of the 14 billion incandescent bulbs in use worldwide are converted to energy efficient LED lighting, a unique opportunity exists to augment them with visible light communications (VLC) and visible light positioning (VLP). VLC- and VLP- enabled LED lighting is not only energy efficient but enables a host of new use cases such as location-aware ubiquitous high-speed wireless communication links.

This talk presents the recent work of the Free-space Optical Communication Algorithms Laboratory (FOCAL) at McMaster University in Hamilton, Canada in developing novel signalling and indoor localization techniques using illumination devices. Developments in the signalling design for VLC systems will be presented along with several prototype VLC communication systems. Novel approaches to the integration VLC networks with power line communications (PLC) are discussed. The role of visible light communications and ranging for automotive safety will also be highlighted. Several approaches to indoor positioning using illumination devices and simple smartphone-based receivers will be presented. Finally, a vision for VLC and VLP technologies will be presented along with our ongoing research directions.

9387-28, Session 10

Visible light communication links using organic semiconductors

Shuyu Zhang, Univ. of St. Andrews (United Kingdom); Dobroslav Tsonev, Stefan Videv, The Univ. of Edinburgh (United Kingdom); Sanjay Ghosh, Pavlos Manousiadis, Muhammad T. Sajjad, Dimali C. V. Amarasinghe, Guohua Xie, Univ. of St. Andrews (United Kingdom); Sujan Rajbhandari, Hyunchoe Chun, Grahame E. Faulkner, Univ. of Oxford (United Kingdom); Clara Orofino-Pena, Diego Cortizo-Lacalle, Alexander L. Kanibolotsky, Peter J. Skabara, Univ. of Strathclyde (United Kingdom); Dominic C. O'Brien, Univ. of Oxford (United Kingdom); Harald Haas, The Univ. of Edinburgh (United Kingdom); Graham A. Turnbull, Ifor D. W. Samuel, Univ. of St. Andrews (United Kingdom)

Visible light communications (VLC), which provide both illumination and high speed data links, have made remarkable progress using nitride semiconductor light sources.[1] The conventional phosphors used in LED lighting to achieve white illumination are, however, not suitable for fast modulation due to their long luminescence lifetime and therefore limit the data-rates for white VLC. Organic semiconductor materials have much shorter radiative lifetimes, therefore the data-rates achieved are much faster than conventional LED phosphors.

As well as their use as novel colour converters for hybrid LEDs, organic optoelectronic devices, such as organic LEDs and solar cells, have potential for VLC. Organic optoelectronics have unique properties of solution processability, compatibility with flexible substrates and with large-scale printing technology. Here we report two transmitter-receiver systems, one using an organic LED as the transmitter and the other using a PTB7:PC71BM organic solar cell as a receiver. The former VLC link achieved over 23 Mb/s and the latter achieved over 40 Mb/s. Using the organic solar cell we explore the potential for dual mode operation as a data receiver with energy harvesting.

We also report the development of directional-emission sources for VLC, using both organic LEDs and hybrid LEDs with imprinted photonic nanostructures.[2, 3] The photonic nanostructures are used to extract waveguide modes or substrate modes in an organic LED or fast colour converter layer into a directional beam.

[1] D. Tsonev, C. Hyunchoe, S. Rajbhandari, J. J. D. McKendry, S. Videv, E. Gu, M. Haji, S. Watson, A. E. Kelly, G. Faulkner, M. D. Dawson, H. Haas and D. O'Brien, *Photonics Technology Letters*, IEEE 26 (7), 637-640 (2014).

[2] S. Zhang, G. A. Turnbull and I. D. W. Samuel, *Appl Phys Lett* 103 (21), 213302 (2013).

[3] S. Zhang, G. A. Turnbull and I. D. W. Samuel, *Adv Opt Mater* 2 (4), 343-347 (2014).

9387-29, Session 10

Modulation bandwidth enhancement of white-LED-based visible light communications using electrical equalizations

Do-Hoon Kwon, Se-Hoon Yang, Sang-Kook Han, Yonsei Univ. (Korea, Republic of)

Utilizing the modulation capability of LEDs, there have been many studies about convergence technology to combine illumination and communication. The visible light communication (VLC) system has several advantages such as high security, immunity to RF interference and lower additional cost than comparing to LEDs just for illumination. However, modulation bandwidth of

LEDs is not enough for various wireless communication systems. Since the commercial LEDs are designed only for lighting systems; we need an effort to enhance the modulation characteristics of LEDs. When the area of LED is increased, internal junction capacitance of LED is also increased depending on the area of LEDs and then the RC delay time of LED is increased. As a result, the modulation bandwidth of LEDs is limited by large RC delay time. In addition, frequency response of commercial white LED is degraded by the slow response time of the used yellow phosphor. Thus, modulation bandwidth of VLC system is limited to several MHz which is not enough to accommodate high data rate transmission. In this paper, we designed equalization circuit using RLC component for compensating the white LEDs frequency response. Also, we used blue filtering to improve frequency response of white LEDs, which is degraded by yellow phosphorescent component. Power loss by optical filtering and distance is compensated by convex lens. Consequently, we extend the modulation bandwidth of VLC system from 3 MHz to more than 150 MHz, and it allows OOK-NRZ data transmission up to 300 Mbps at 1.5 m.

9387-30, Session 10

Differential pulse amplitude modulation for multiple-input single-output OWVLC

Se-Hoon Yang, Do-Hoon Kwon, Sung-Jin Kim, Yong-Hwan Son, Sang-Kook Han, Yonsei Univ. (Korea, Republic of)

White light-emitting diodes (LEDs) are widely used for lighting due to their energy efficiency, eco-friendly, and small size than previously light sources such as incandescent, fluorescent bulbs and so on. Optical wireless visible light communication (OWVLC) based on LED merges lighting and communications in applications such as indoor lighting, traffic signals, vehicles, and underwater communications because LED can be easily modulated. However, physical bandwidth of LED is limited about several MHz by slow time constant of the phosphor and characteristics of device. Therefore, using the simplest modulation format which is non-return-zero on-off-keying (NRZ-OOK), the data rate reaches only to dozens Mbit/s. Thus, to improve the transmission capacity, optical filtering and pre-, post-equalizer are adapted. Also, high-speed wireless connectivity is implemented using spectrally efficient modulation methods: orthogonal frequency division multiplexing (OFDM) or discrete multi-tone (DMT). However, these modulation methods need additional digital signal processing such as FFT and IFFT, thus complexity of transmitter and receiver is increasing.

To reduce the complexity of transmitter and receiver, we proposed a novel modulation scheme which is named differential pulse amplitude modulation. The proposed modulation scheme transmits different NRZ-OOK signals with same amplitude and unit time delay using each LED chip, respectively. The 'N' parallel signals from LEDs are overlapped and directly detected at optical receiver. Received signal is demodulated by power difference between unit time slots. The proposed scheme can overcome the bandwidth limitation of LEDs and data rate can be improved according to number of LEDs without complex digital signal processing.

Conference 9388: Optical Metro Networks and Short-Haul Systems VII

Tuesday - Thursday 10-12 February 2015

Part of Proceedings of SPIE Vol. 9388 Optical Metro Networks and Short-Haul Systems VII

9388-1, Session 2

MIMO signal processing in mode-division multiplexing systems (*Invited Paper*)

Sercan O. Arik, Daulet Askarov, Joseph M. Kahn, Stanford Univ. (United States)

As single-mode fiber systems approach fundamental capacity limits, continued traffic growth motivates the use of mode-division multiplexing (MDM) in multi-mode fiber (MMF). The D propagating modes of an MMF constitute parallel data transmission channels for D?D multi-input multi-output (MIMO) transmission. As optical signals propagate in an MMF, signals propagating in different modes are intermixed by mode coupling and distorted by modal dispersion (MD). An MDM receiver must employ adaptive MIMO signal processing to undo these effects, while tracking fast channel changes. In this talk, MIMO channel properties and their implications for the performance and scalability of adaptive MIMO signal processing techniques are reviewed. The computational complexity of MIMO equalization is potentially high because of the equalizer D?D matrix structure and the long group delay (GD) spread from MD. Various GD spread management techniques, including optimized fiber design, group delay compensation, and strong mode coupling, are reviewed. For low complexity implementation of MIMO equalization, adaptive frequency-domain equalization (FDE) is proposed. Two algorithms for adaptive FDE implementation, least-mean squares and recursive least squares, are described. Corresponding computational complexities are analyzed. Simulations are performed to assess impacts of link parameters on performance and adaptation speed. Scalability of the techniques for high D is discussed. Overall, it is demonstrated that with careful system design and judicious choice of signal processing architectures, it is possible to overcome MIMO signal processing challenges.

9388-2, Session 2

Adaptive multidimensional modulation and multiplexing for next generation optical networks (*Invited Paper*)

Milorad Cvijetic, College of Optical Sciences, The Univ. of Arizona (United States)

It is well known that the Internet traffic has been growing exponentially, with no indication that such trend will change. In addition to wireline connectivity of end-users, the wireless connectivity through (4G+) mobile networks is also becoming an integral part of the optical networking. All this together require very high aggregate bandwidth, and its arbitrary, elastic and dynamic allocation to end-users. The overall information capacity in optical transmission systems can be enhanced by employment of advanced modulation, multiplexing and coding schemes, as well as the advanced detection schemes. In parallel, novel networking concepts with the griddles and elastic bandwidth allocation are needed to increase the network dynamics and flexibility. In this invited paper we provide an overview of these techniques and concepts, which have been or may be used in the next generation high-speed optical network.

9388-3, Session 5

Coherent receiver architectures for secure key distribution using faint optical multilevel signals (*Invited Paper*)

Sebastian Kleis, Reinhold Herschel, Christian G. Schäffer, Helmut-Schmidt Univ. (Germany)

Optical multilevel signals for QKD are evaluated in terms of security and key generation rate when they are used with post-selection. Potential receiver architectures are analyzed from a quantum-mechanical point of view and compared regarding these parameters as well as implementation complexity. Based on that, a coherent state QKD system is proposed.

9388-4, Session 5

Sliceable transponders for metro-access transmission links (*Invited Paper*)

Christoph Wagner, Peter Madsen, Technical Univ. of Denmark (Denmark); Sandis Spolitis, Riga Technical Univ. (Latvia); Juan Jose J. Vegas Olmos, Idelfonso Tafur Monroy, Technical Univ. of Denmark (Denmark)

Internet traffic from end users grows faster than ever. Main reasons for the increasing demand of the end users are, for example, e-health systems, video conferences and cloud computing. Network operators face several challenges in design, deployment and maintenance, and have to cope with the increased bandwidth demand. Usual solutions for network upgrades are cost intensive, like using more wavelengths or wider bandwidth electronics and optical equipment. These solutions may not fit for cost sensitive networks, like Metro- and Access networks. Furthermore, future optical access networks are required to be flexible and capable to change the provided bandwidth on customer's request.

This paper presents a solution for upgrading optical access networks by reusing existing electronics or optical equipment: sliceable transponders using signal spectrum slicing and stitching back method after direct detection. This technique allows transmission of wide bandwidth signals from the service provider (OLT - optical line terminal) to the end user (ONU - optical network unit) over an optical distribution network (ODN) via low bandwidth equipment.

We demonstrate simulation and experimental results of sliceable transponders for intensity modulated optical access networks for duobinary modulation format. Signal detection uses low complexity direct detection. Signal slicing scalability also shown by varying the number of transmitted slices. Examined ODNs are single mode fiber (SMF), dispersion shifted fiber (DSF) and non-zero dispersion shifted fiber (NZ-DSF) with lengths up to 40 km. For all examined ODNs a post- forward error correction (FEC) error free transmission is achieved.

9388-5, Session 5

Comprehensive photonics-electronics convergent simulation and its application to high-speed electronic circuit integration on a Si/Ge photonic chip (*Invited Paper*)

Kotaro Takeda, Kentaro Honda, Tsutomu Takeya, Kota Okazaki, Tatsurou Hiraki, Tai Tsuchizawa, Hidetaka Nishi,

**Conference 9388:
Optical Metro Networks and Short-Haul Systems VII**

Rai Kou, Hiroshi Fukuda, Mitsuo Usui, Hideyuki Nosaka, Tsuyoshi Yamamoto, Koji Yamada, Nippon Telegraph and Telephone Corp. (Japan)

We developed a design technique that uses an equivalent circuit of an optical circuit in an electric circuit simulator. The technique unifies the optical and electrical design process in the electric circuit simulator, thereby eliminating the separation in the design of a photonics and electronics convergence system. We can calculate small signal response, transient response, and bit error rate of actual devices by using this technique. To confirm the feasibility of this new technique, we made an equivalent circuit of a four-channel WDM receiver as an example. The receiver includes a photodiode, ring filter and transimpedance amplifier. An optical input and output are converted into an electrical input and output to construct the equivalent circuit of optical circuits. The equivalent circuit of the photodiode and the ring filter emulate the optical responses of actual devices as electrical responses in the electrical circuit. In addition, the simulated eye pattern and bit error rate of the whole integrated equivalent circuit agree well with the measurement results for the integrated four-channel WDM receiver. These results indicate the validity of the new design technique.

9388-6, Session 5

Wavelength-tunable filter utilizing non-cyclic arrayed waveguide grating to create colorless, directionless, contentionless ROADMs

Masaki Niwa, Shoichi Takashina, Yojiro Mori, Hiroshi Hasegawa, Ken-ichi Sato, Nagoya Univ. (Japan); Toshio Watanabe, NTT Photonics Labs. (Japan)

With the rise of Internet traffic, reconfigurable optical add-drop multiplexers (ROADMs) are widely adopted by present networks. Current ROADMs, however, allow only static operation. To realize future dynamic optical network services and to minimize any human intervention in network operation, the optical signal add/drop part should have C/D/C (colorless/directionless/contentionless) capabilities. This is possible with matrix switches or a combination of splitter-switch and tunable filters. The scale of the matrix switch increases with the square of the number of supported channels, and hence, the matrix-switch-based architecture is not suitable for creating future large-scale ROADMs. In contrast, the number of splitter ports, switches, or tunable filters increases linearly with the needed drop channels, and hence the tunable-filter-based architecture will support the ever-increasing traffic in the future.

So far, we have succeeded in fabricating a compact tunable filter that consists of multi-stage cyclic arrayed waveguide gratings (AWGs) and switches by using planar-lightwave-circuit (PLC) technologies. However, this multi-stage configuration suffers from large insertion loss. Moreover, power-consuming temperature control is necessary since it is difficult to make cyclic AWGs athermal.

We propose here novel tunable-filter architecture that sandwiches a single-stage, non-cyclic, and athermal AWG between small switches. With this switch-AWG-switch arrangement, the tunable filter attains low loss, low-power consumption, and compactness. A prototype is monolithically fabricated with PLC technologies and excellent filtering performance is experimentally confirmed for multiple modulation formats.

9388-22, Session PWed

Optical-electrical hybrid signal equalizer for ultra-high-speed transmission

Shinya Maruyama, Aoyama Gakuin Univ. (Japan) and National Institute of Information and Communications Technology (Japan); Kazunari Tomishige, Aoyama Gakuin

Univ. (Japan); Atsushi Kanno, Tetsuya Kawanishi, National Institute of Information and Communications Technology (Japan); Hideyuki Sotobayashi, Aoyama Gakuin Univ. (Japan)

We propose an optical-electrical hybrid signal equalizer to improve the optical signal-to-noise ratio (OSNR) required for a bit error rate (BER) at a high symbol rate. High-speed modulation technology is indispensable for achieving a direct increase in the capacity of an optical transmission link. However, as the symbol rate increases, signal quality degrades drastically because of poor frequency response of devices. This issue requires the implementation of equalization to improve the frequency response at a transceiver. Nowadays, digital signal processing (DSP) technology can compensate these impairments by digital equalization, but ultra high-speed DSP consumes large energy. An optical equalization by passive components can also equalize the signal degradation. Power consumption by the optical equalizer (OEQ) can be lower than that by the DSP, however, the OEQ can perform coarse equalization because of its preciseness of the configuration. The hybrid equalizer consists of two-stage equalization: coarse compensation by the OEQ, and fine compensation by the electrical equalization. In the paper, the OEQ, which is consisted of two optical delay-line interferometers, is utilized as an optical high pass filter, and a 40-tap digital finite impulse response filter adapted by constant modulus algorithm (CMA) is implemented in the DSP. We demonstrated and evaluated the hybrid equalizer with degraded 40-Gbaud quadrature-phase-shift-keying (QPSK) signal experimentally by using the BER and constellation maps. The observed OSNR at a BER of 1×10^{-3} is improved 7 dB, and 6 dB in back-to-back and 10-km optical fiber transmission conditions, respectively.

9388-23, Session PWed

A novel optical path routing network that combines coarse granularity optical multicast with fine granularity add/drop and block

Mauro M. Soares, Yojiro Mori, Hiroshi Hasegawa, Ken-ichi Sato, Nagoya Univ. (Japan)

A novel optical path routing mechanism based on coarse granularity optical multicast and fine granularity add/drop & block is proposed. An optical cross-connect node hosting the proposed function can be devised cost-effectively by using a coarse granularity optical cross-connect and 1×2 wavelength selective switches for fine granular operations. The coarse granularity optical cross-connect consists of ultra-compact PLC-based waveband selective switches (WBSS) and optical couplers that are bridged to form a broadcast-and-select configuration. Routing is performed by groups of wavelengths, each of which is called a grouped routing entity (GRE). The coarse granular routing defines virtual pipes, called GRE pipes, to/from which any wavelength paths in a pipe can be added/dropped. A preliminary version of the routing scheme that provides neither coarse granularity multicast nor fine granularity blocks was proposed by us and presented at OFC2012, where we verified that the node hardware scale is significantly reduced while the number of optical fibers required is almost the same as the conventional fine granularity routing networks under the so-called static network design. In dynamic network operation scenarios, the lack of routing flexibility greatly increases the fiber number. Therefore, we also developed a novel routing method to enhance routing flexibility with no substantial increment in node hardware complexity. With the novel path/GRE routing and wavelength/GRE index assignment algorithm, we numerically verify the improved routing performance over preliminary GRE-based networks, and the significant hardware scale reduction relative to conventional fine granularity routing networks.

9388-24, Session PWed

FPGA implementation of high-performance QC-LDPC decoder for optical communications

Ding Zou, Ivan B. Djordjevic, The Univ. of Arizona (United States)

Forward error correction (FEC) has been recognized as one of the key technologies enabling the next-generation high-speed fiber optical communications. Thanks to the high-speed analog-to-digital converter (ADC), soft-decision FEC (SD-FEC) achieving large net coding gain (NCG) becomes possible. Specifically, quasi-cyclic (QC) low-density parity-check (LDPC) code is preferred due to its high performance and low implementation complexity. However, most LDPC codes suffer from the error-floor phenomenon. To solve the problem, either an outer FEC code such as Reed-Solomon (RS) code or the post-processing method (PPM) has to be adopted with 11.3 dB NCG achieved at bit error rate (BER) down to 10^{-15} [1,2], resulting in extra complexity and decoding latency. Most recently, LDPC convolutional code achieving 11.5dB NCG without outer FEC code and PPM has been reported [3]. In this paper, we present our designed QC LDPC code based on pairwise balanced design with length around 34,000, column weight 3, row weight 15 and girth 10. By FPGA emulation, we have demonstrated that the designed QC LDPC code can achieve close to 12 dB NCG exhibiting no error floor at BER down to 10^{-15} and thus require no outer code or PPM. Another contribution of the work is that the designed LDPC code has column weight 3 instead of 4 as reported in literature. Hence, implementation complexity and decoding latency can be reduced. To be efficient, we have implemented a layered LDPC decoding algorithm, in which 4-bit soft-decision information is used to mitigate the routing congestion and reduce the memory usage.

[1]. Y. Miyata, et al., "Efficient FEC for optical communications using concatenated codes to combat error-floor," OFC2008, OTuE4.

[2]. D. Chang, et al., "FPGA verification of a single QC-LDPC code for 100Gb/s optical systems without error floor down to BER of 10^{-15} ," OFC2011, OTuN2.

[3]. D. Chang, et al., "LDPC convolutional codes using layered decoding algorithm for high speed coherent optical transmission," OFC2012, OW1H4.

9388-25, Session PWed

High performance broadband photodetector and its array for optical communication

 Jeremy Bregman, Banpil Photonics, Inc. (United States);
 Robert Olah, Banpil Photonics, Inc. (United States); Achyut
 K. Dutta, Banpil Photonics, Inc. (United States)

Device-level reduction of dark current is critical for improving the Signal to Noise ratio and dynamic range of III-V based optical components. We report on low-noise, back-illuminated p-i-n photodetector and its arrays with high spectral response for short wave infrared (1.0 - 2.5 μm) optical communication and also optical interconnects applications at 1.3 μm and 1.55 μm wavelengths. The photodetector is based on planar structure fabricated from InP having a lattice-matched InGaAs-absorber layer, and it is designed specifically for high sensitivity and low dark current (nA/sq. cm) at room temperature by minimizing leakage current. Electrical and optical performance of both individual diodes and small-pixel array test structures will be presented in the conference paper.

9388-26, Session PWed

RFoG deployment into the next-generation networks

 Petr Siska, Tomáš Hlavinka, Petr Koudelka, Jan Latal, Jan
 Vitasek, Lukas Hajek, Radek Poboril, VŠB-Technical Univ. of
 Ostrava (Czech Republic)

This paper is dealing with problems and possibilities of RFoG (Radio Frequency over Glass) technology deployment into the new generation optical access networks. Passive optical networks (PON) offer, except high bit rate, also a very wide range of applicability for various traffic data services. These services can be combined with different transmission technologies. The one of the most important needs upon these networks is also their backward compatibility with older analog technologies. The experimental part is devoted to broadcasting of RFoG through the designed PON networks and experimental measurements, using objective methods. The conclusion of this article is focused on the evaluation of individual measurements and considering of the feasibility of RFoG technology deployment in practical utilization.

9388-7, Session 6

All-optical implementation of signal processing functions (Invited Paper)

 Amirhossein Mohajerin Ariaei, Morteza Ziyadi, Mohammad
 R. Chitgarha, Alan E. Willner, The Univ. of Southern
 California (United States)

Recent advances in all-optical implementation of signal processing functions are discussed. Signal processing using nonlinear-optics has been of great interest due to its inherent ultrafast THz bandwidth and its potentially phase-preserving nature. Many important functions can be implemented using various forms of photonic nonlinear interactions. Bit rate tunable all-optical noise mitigation of 20-Gbaud QPSK signals and optical channel deaggregation of 30-Gbaud QPSK signals are recent applications of nonlinear optical signal processing. In addition, optical tapped-delay-line (TDL) as a key building block in digital signal processing is discussed. In an optical TDL an incoming data stream is tapped at different time intervals, given complex optical weights, and then coherently added together. A TDL can be configured to perform many important functions, including a tunable optical finite-impulse response (FIR) filtering, equalization, optical pulse shaping, bit-depth and sample rate tunable optical digital to analog converter (DAC), discrete Fourier transform, and one (1-D) and two dimensional (2-D) optical correlations. The recent results of optical Nyquist generation of 32-Gbaud QPSK signals utilizing coherent optical comb fingers and nonlinear wave mixing is presented. In addition, 1-D optical comb-based correlator of 20-Gbaud QPSK, and 2-D optical correlator of 20-Gbaud QPSK signals are discussed. Moreover, a 2-stage continuously tunable optical TDL in which $N+M$ pump lasers produce $N \times M$ taps is discussed as a technique to increase the number of taps in tapped delay line. The result of a 32-taps optical TDL correlator is presented to search multiple patterns among 20-Gbaud QPSK symbols utilizing nonlinearities and coherent comb source.

9388-8, Session 6

Laser characterization with advanced digital signal processing

 Molly Piels, Idelfonso Tafur Monroy, Darko Zibar, DTU
 Fotonik (Denmark)

The relentless growth of datacenter traffic is driving research toward lasers and detectors with lower power consumption. Accurate component characterization is necessary in order to move in this direction, as good device models are needed in order to improve upon existing component

**Conference 9388:
Optical Metro Networks and Short-Haul Systems VII**

designs as well as to design optimal filters for digital links. For lasers in particular, phase noise spectra and relative intensity noise (RIN) spectra both yield useful information about the internal device dynamics, while RIN can in some cases limit link performance. Unfortunately, it is often very difficult to characterize low power consumption lasers because the output power can be on the order of nano- or microwatts. In this talk, we will discuss our recent research employing a coherent receiver in conjunction with Bayesian filtering to completely characterize lasers with low output power. Optimized phase and amplitude tracking algorithms can be used to generate accurate noise spectra. Traditionally, rate equation coefficients have been determined by fitting curves to these spectra, however, we will show that rate equation models can also be constructed using maximum likelihood estimation, which produces more accurate results.

9388-9, Session 6

Digital signal processing approaches for semiconductor phase noise tolerant coherent transmission systems (*Invited Paper*)

Miguel Iglesias Olmedo, KTH Royal Institute of Technology (Sweden); Xiaodan Pang, Acreo Swedish ICT AB (Sweden); Richard Schatz, KTH Royal Institute of Technology (Sweden); Darko Zibar, Idelfonso Tafur Monroy, Technical Univ. of Denmark (Denmark); Gunnar Jacobsen, Acreo Swedish ICT AB (Sweden) and KTH Royal Institute of Technology (Sweden); Sergei Popov, KTH Royal Institute of Technology (Sweden)

Cloud services have already revolutionized the way modern societies interact, yet this is just the beginning of a much bigger data communication revolution. Smart-grid, smart-city and autonomous transportation are feasible near-term solutions to reduce global energy consumption and therefore our environmental footprint. These approaches rely on enormous amounts of data being sensed and transported throughout the city, alongside next generation broadband services, compromising the ability of current metropolitan area networks to cope up with bandwidth demands. Pushing coherent technologies towards the end-user could effectively tackle the problem, but the strong requirements on laser linewidth make them rely on costly external cavity lasers, rendering the transceiver economically unviable for metro-access scenarios. Semiconductor lasers on the other hand, are generally more cost-effective, energy efficient, and easy to integrate, at the expense of higher linewidths due to carrier induced frequency noise. Consequently, realizing cost-competitive coherent data-links on the range of 100-500-km based on semiconductor lasers has become a timely research question.

In this paper, we discuss about digital signal processing approaches that can enable coherent links based on semiconductor lasers. Firstly, we show that the laser 3-dB linewidth fails to estimate system performance in this particular case, and explore different alternatives. Secondly, we experimentally study on the impact of carrier induced frequency noise on system performance for 56-GBaud DP-QPSK and 28-GBaud DP-16QAM using a decision directed phase lock loop algorithm. We conclude that there is a delicate trade-off between modulation order and baudrate, where equalization enhanced phase noise plays an important role.

9388-10, Session 6

Advanced digital signal processing for high-speed access networks (*Invited Paper*)

Anna Tatarczak, Jose Estaran, Miguel Iglesias Olmedo, Jesper B. Jensen, Juan Jose J. Vegas Olmos, Idelfonso

Tafur Monroy, DTU Fotonik (Denmark)

Digital signal processing (DSP) has established itself as key-enabler for high capacity coherent transmission technology in metro and long-haul systems. With the emerging demand for high-speed optical access network and the evolution towards front/back haul wireless transport over to optical fibers, we are witnessing increasing interest towards using digital signal processing (DSP) assisted transmission in such systems too, with the aim of achieving capacities towards 100 Gbps. In this talk we review advances in DSP for supporting several transmission systems that employ both direct as coherent detection. We present results for systems using direct detection with multi-band carrierless amplitude phase modulation (multi-CAP), discrete multitone (DMT), and multilevel pulse amplitude m-PAM, partial response and spectrum sliceable transmission among others. Coherent detection systems using vertical surface emitting lasers (VCSELs) are of major interest. We consider a coherent transmission scheme using VCSELs with frequency chirp management. We consider also latest advances from the research community on OFDM based access, modulation-level multiplexing, ultra-dense coherent access networks, among others.

9388-11, Session 7

100Gbps transmission with CFP coherent transceiver with power-optimized DSP (*Invited Paper*)

Hiroshi Onaka, Photonics Electronics Technology Research Association (Japan)

Pluggable coherent transceivers are expected in order to achieve WDM links between data centers and metro access networks. In order to realize the pluggable digital coherent transceiver, as well as miniaturization of the optical devices, drastic power reduction of the DSP ASIC is required. We have successfully developed a low- power DSP ASIC, an InP DP-IQ modulator module, and a compact integrated coherent receiver (ICR) module.

Functional optimization of DSP ASIC with regard to power consumption has been realized with selectable FEC and CD compensation options to cope with their trade-offs on performance. The single DSP ASIC can be used in different types of applications, spanning from short-range of 100 km or less to long-distance of more than 2,000 km.

In order to shrink the footprint, we employed an InP-based modulator in the transceiver. The DC V_{pi} is around 1.9 V with a bias voltage of less than 10 V, corresponding to a V_{pi} of less than 2.5 V for 32 Gbaud. The DC extinction ratios are better than 20 dB. The size of the module body is 12 mm × 39 mm × 6.5 mm excluding the nodes and tabs.

We measured the transmission performance of coherent CFP transceiver for OTU4 G-FEC mode with 70 km SMF, OTU4 E-FEC mode with 560 km SMF, and OTU4V SD-FEC+E-FEC mode with 840 km SMF. We confirmed stable real-time transmission for each operation modes. The CFP transceiver power in OTU4V SD-FEC+E-FEC mode was about 32 W.

9388-12, Session 7

20-Gb/s QPSK transmission over 10-km-long holey fiber using a wavelength tunable quantum dot light source in O-band

Akihiro Murano, Aoyama Gakuin Univ. (Japan) and National Institute of Information and Communications Technology (Japan); Fumiya Yagi, Aoyama Gakuin Univ. (Japan); Naokatsu Yamamoto, Atsushi Kanno, National Institute of Information and Communications Technology (Japan); Tetsuya Kawanishi, National Institute of Information and

**Conference 9388:
 Optical Metro Networks and Short-Haul Systems VII**

Communications Technology (Japan) and Aoyama Gakuin Univ. (Japan); Hideyuki Sotobayashi, Aoyama Gakuin Univ. (Japan)

The C band (1530-1565 nm, 4.39-THz bandwidth) and L band (1565-1625 nm, 71-THz bandwidth) have been utilized in conventional photonic transport networks. Pioneering and developing advanced transport technology in the new wavebands helps realize more higher capacity transport network. A novel functional waveband such as T band (Thousand-band: 1.000-1.260 nm, 61.9-THz) and O band (1.260-1.360 nm, 17.5-THz) is promising for increase of the capacity of the transport system. We have successfully demonstrated 20-Gb/s quadrature phase-shift keying (QPSK) signal over single-mode holey fiber in the wavelengths of the optical carriers were tuned between 1276-1304 nm (5.04-THz optical frequency range wider than a conventional C band). In the paper, we employed a newly developed tunable-wavelength quantum dot (QD) laser. By properties of the single InAs/InGaAs QD optical gain chip formed with sandwiched sub-nano separator technique in the O band, the QD light source realizes a stable, compact and high-performance wavelength tunable light source. The experimental results show bit error rates (BERs) within a forward error correction limit of $2^{10^{-3}}$. Carrier phase and IQ data recovery is implemented by an off-line processing digital signal processing in an optical intradyne receiver optimized for the O-band system. The signal can be adaptively equalized by a finite impulse response filter with a tap length of 20 by Constant Modulus Algorithm, and also be equalized using phase noise estimation and compensation in the same manner as the C-band system. The WDM transmission with T band and O band will realize the high-capacity photonic transport systems.

9388-13, Session 7

Optical performance monitoring for dynamic and flexible photonic networks
(Invited Paper)

Shoichiro Oda, Fujitsu Ltd. (Japan); Jeng-Yuan Yang, Youichi Akasaka, Olga Vassilieva, Fujitsu Network Communications Inc. (United States); Tomohiro Yamauchi, Fujitsu Labs., Ltd. (Japan); Yasuhiko Aoki, Fujitsu Ltd. (Japan); Motoyoshi Sekiya, Fujitsu Labs. of America, Inc. (United States); Jens C. Rasmussen, Fujitsu Labs., Ltd. (Japan)

Optical performance monitoring (OPM) is considered as an important tool in order to operate and manage dynamic, flexible, and thus complex photonic networks. In this presentation, firstly we review recent study on OPM and discuss its possible applications such as failure diagnosis of transmitter (Tx), receiver (Rx), and other transport equipment, optimization of system reach design, and so on. We then propose a novel in-band OSNR monitor, consisting of an optical bandpass filter, a photo detector, and a signal processor. In the method, the OSNR is monitored by the optical powers measured at central frequency of a subcarrier and in-between subcarriers. Since the proposed monitor might be realized by the same hardware implementation as an optical channel monitor (OCM), this is potentially integrated with an OCM in low-cost. Experimental evaluation showed the maximum error of monitored OSNR was 0.6 dB without WSS and 1.4dB after 15-cascaded WSSs. Finally, we also propose a BER monitor, which is realized by the same hardware configuration as the above in-band OSNR monitor. The BER in the method is estimated by monitoring OSNR including nonlinear noise as noise source and taking the imperfection of Tx, Rx, and other equipment into account. We experimentally evaluated the performance and showed the error of monitored Q-factor was within +/- 0.7 dB after 3000 km transmission. Sufficient monitoring accuracy and the capability of low-cost implementation suggest that the proposed monitors might be expected to be one of the promising technologies for enabling dynamic and flexible photonic networks.

9388-14, Session 7

Optimized signal constellations for ultra-high-speed optical transport
(Invited Paper)

Shaoliang Zhang, NEC Labs. America, Inc. (United States); Tao Liu, Yequn Zhang, The Univ. of Arizona (United States); Fatih Yaman, NEC Labs. America, Inc. (United States); Ivan B. Djordjevic, The Univ. of Arizona (United States); Ting Wang, NEC Labs. America (United States)

Recently, coded modulation has been studied to further improve the receiver sensitivity rather than going with the standard modulation formats, like QAM. The joint optimization of coding and modulation formats would provide significant receiver sensitivity improvement due to the increased Hamming distance of codes. By applying Arimoto-Blahut algorithm to maximize mutual information, optimized coded-modulation has been found out together with optimized bit-mapping rule. In simulation, at coded BER of 10^{-6} , optimized coded-8QAM outperforms standard 8-QAM by 0.2dB with natural mapping and 0.85dB with optimized mapping; whilst optimized coded-16QAM outperforms standard 16-QAM by 1.1 dB with optimized mapping. The improvement is found to be larger as modulation formats goes higher. In experiment, with the same LDPC codewords transmitted, the FEC limit achieved by using optimal coded-8QAM is 4.05 dB at 20% overhead whereas 4.6 dB for regular 8QAM, amounting to -0.55 dB improvement in terms of pre-FEC limit when utilizing optimal nonbinary LDPC-coded-8QAM due to the joint coded-modulation involving bit mapping, coding and modulation format.

Optimal coded-8QAM modulation has been further verified in our recent experiment, where 40Tb/s transmission capacity over 6787km is demonstrated by transmitting 200G per wavelength thanks to the better receiver sensitivity of the optimal coded modulation. The largest capacity-distance product per repeater over submarine distances is achieved by increasing the span length to 121 km while using EDFA amplification only.

9388-15, Session 7

Investigation of fiber dispersion impairment in 400GbE discrete multi-tone system for reach enhancement up to 40 km

Ryo Okabe, Toshiki Tanaka, Masato Nishihara, Yutaka Kai, Tomoo Takahara, Fujitsu Labs., Ltd. (Japan); Hao Chen, Weizhen Yan, Zhenning Tao, Fujitsu Research and Development Center Co., Ltd. (China); Jens C. Rasmussen, Fujitsu Labs., Ltd. (Japan)

Demands to increase the capacity of optical communication systems have been increasing continuously due to the widespread use of broadband mobile communication systems and cloud services. Digital coherent technology has been introduced in 100-Gb/s long haul systems in response to these demands, and the development of coherent 400-Gb/s and 1-Tb/s systems has started. The demands are growing similarly in shorter reach applications such as access networks. 100-Gb/s Ethernet (100GbE) systems based on 4 x 25-Gbps technology have been commercialized and the task force group for 400GbE standardization up to 10-km SMF has already started. Furthermore, there is a strong demand for reach enhancement up to around 40 km.

We propose discrete multi-tone (DMT) technology using a simple configuration to achieve high capacity at low cost. We believe 4 x 100-Gb/s technology is the best possible candidate for 400GbE. DMT technology is an orthogonal frequency division multiplexing (OFDM) based modulation format. DMT signals are modulated into the intensity domain of lightwaves. Cost-effective devices such as directly modulated laser (DML) and

**Conference 9388:
 Optical Metro Networks and Short-Haul Systems VII**

direct detectors are available for DMT technology. We experimentally demonstrated 400-Gb/s DMT transmission using four channels of DMLs on LAN-WDM in 1300-nm region without dispersion compensation. However, fiber dispersion impairment cannot be ignored in tens of km transmission. Interplay between fiber dispersion and the frequency chirp of transmitters degrades transmission characteristics. We investigated the fiber dispersion impairment in a 400GbE (4 x 116.1-Gb/s) DMT system up to 40-km through experiments and numerical simulations.

9388-16, Session 7

Realization of real-time 100G 16QAM OFDM signal detection *(Invited Paper)*

Fan Li, Xin Xiao, Jianjun Yu, ZTE USA (United States)

We review our recent research progresses on real-time OFDM transmission and reception. At first, we successfully demonstrated real-time one band 64-ary quadrature amplitude modulation (64QAM) orthogonal frequency division multiplexing (OFDM) transmission and reception with a line rate of 50Gbps with direct modulation and direct detection. Then, the system capacity was enhanced to 100Gbps by transmission dual optical carrier direct modulated 50Gbps 16QAM-OFDM at the same time. At the receiver, two set receivers are used to get these two 50Gbps 16QAM-OFDM with direct detection. As the chromatic dispersion in the fiber transmission leads to the frequency fading after direct detection, the transmission distance for 100Gbps OFDM with direct detection is extremely short (~only 20km LEAF under SD-FEC limit of 2¹⁰-2). At last, we successfully demonstrated the transmission and reception of real-time 100Gbps single-band coherent optical dual polarization (DP)-16QAM-OFDM signal with coherent detection for the first time. The transmission distance in standard single mode fiber (SSMF) can be extended to more than 100km without electrical dispersion compensation (EDC). The measured bit-error-ratio (BER) for 100Gbps single-band coherent optical DP-16QAM-OFDM signal after 200-km SSMF without EDC is less than HD-FEC limitation of 3.8¹⁰-3. The computation complexities of acquisition of timing metric and frequency offset metric are simplified in the real-time reception by only concerning the sign bit of every sample to avoid multiplication operations. Single band discrete Fourier transform-spread (DFT-spread) which covers all payload subcarriers is applied to reduce the Peak to Average Power Ratio (PAPR) of OFDM signal and overcome the high frequency attenuation. The intra-symbol frequency-domain averaging (ISFA) algorithm is applied to improve the accuracy of channel estimation.

9388-17, Session 8

Design of a stateless low-latency router architecture for green software-defined networking *(Invited Paper)*

Silvia Saldaña Cercós, Technical Univ. of Denmark (Denmark); Ramon M. Ramos, Ana C. Ewald Eller, Federal Univ. of Espírito Santo (Brazil); Magnos Martinello, Moisés R. N. Ribeiro, UFES (Brazil); Anna V. Manolova Fagertun, Idelfonso Tafur Monroy, Technical Univ. of Denmark (Denmark)

Software defined networking (SDN) has the potential to reshape today's Internet architecture. SDN main characteristic is to provide with a control plane detached from the data plane, facilitating intelligent network management (which resides in a centralized controller). SDN also eases evolution, since software evolves independent on the hardware, opening new doors for research and innovation.

However, considering the adoption of this new technology for transport networks raises three important questions: 1) what is the role of SDN in core networks? 2) What is SDN impact on the overall power consumption? And 3) how is network performance in terms of latency affected?

There are emerging hardware limitations to use OpenFlow (i.e. the most successful SDN implementation so far) in core networks. We propose an alternative flexible core network-fabric model named KeyFlow, which replaces table lookup in the forwarding engine by elementary operations relying on a residue number system.

This new approach provides with a design for stateless core routers, which do not have flow tables. This allows mitigating requirements for internal hardware such as the ternary content-addressable memories (TCAMs) which are power-demanding. By implementing KeyFlow core network fabrics 53.7% power savings are achieved. For completeness a comprehensive data plane power consumption analysis of an OpenFlow 1.0 switch broken down into its design modules is presented. Additionally, on an emulated scenario, KeyFlow can achieve above 50% reduction in the round trip time (RTT) compared to a standard OpenFlow 1.0 switch offering a core fabric service closer to deterministic circuit switching technologies.

9388-18, Session 8

Energy-efficient p^m-ary signaling for ultra-high-speed optical transport *(Invited Paper)*

Ivan B. Djordjevic, Tao Liu, The Univ. of Arizona (United States)

The future optical transport networks will be affected by limited bandwidth of information infrastructure, high power consumption, and heterogeneity of network segments. As a solution to all these problems, the multidimensional signaling has been proposed recently. In multidimensional signaling, all available degrees of freedoms have been used for conveyance information over spatial domain multiplexing (SDM) schemes. In electrical domain discrete-time basis functions (such as Slepian sequences) have been used. In optical domain, both polarization states and spatial modes have been used.

In this paper, we follow a different strategy. Instead of conventional binary and 2^m-ary signaling (m is an integer larger than or equal to 1) we propose to use the nonbinary p^m-ary signaling instead, where p is a prime larger than 2. With p^m-ary signaling we can improve the spectral of conventional 2^m-ary schemes by log₂(p) times for the same bandwidth occupancy. At the same time the energy efficiency of p^m-ary signaling scheme is much better than that of 2^m-ary signaling scheme based on binary representation of data. We further study the energy-efficient coded modulation for p^m-ary signaling. The energy-efficient signal constellation design for p^m-ary signaling will be discussed as well. We will demonstrate that with the proposed p^m-ary signaling in combination with energy-efficient signal constellation design, spectral-multiplexing, and polarization-division multiplexing, we can achieve beyond 1 Pb/s serial optical transport without a need for introduction of spatial-division multiplexing.

9388-19, Session 8

Toward green next-generation passive optical networks

Anand Srivastava, Indian Institute of Technology Mandi (India)

Energy efficiency has become an increasingly important aspect of designing access networks, due to both increased concerns for global warming and increased network costs related to energy consumption. Comparing access, metro, and core, the access constitutes a substantial part of the per subscriber network energy consumption and is regarded as the bottleneck for increased network energy efficiency. One of the main opportunities for reducing network energy consumption lies in efficiency improvements of the customer premises equipment. Access networks in general are designed for low utilization while supporting high peak access rates. The combination of large contribution to overall network power consumption and low utilization implies large potential for CPE power saving modes where functionality is

**Conference 9388:
 Optical Metro Networks and Short-Haul Systems VII**

powered off during periods of idleness.

Next-generation passive optical network, which is considered one of the most promising optical access networks, has notably matured in the past few years and is envisioned to massively evolve in the near future. This trend will increase the power requirements of NG-PON and make it no longer coveted. This invited paper will first provide a comprehensive survey of the previously reported studies on tackling this problem. A novel solution framework is then introduced, which aims to explore the maximum design dimensions and achieve the best possible power saving while maintaining the QoS requirements for each type of service.

9388-20, Session 8

Machine learning techniques in optical fibre communication networks

Darko Zibar, DTU Fotonik (Denmark); Luis Carvalho, CpqD (Brazil); Molly Piels, DTU Fotonik (Denmark); Julio Diniz, Carolina Francisangelis, Jose Estaran, Neil Guerreiro Gonzalez, Julio C. R. F. de Oliveira, CpqD (Brazil); Idelfonso Tafur Monroy, DTU Fotonik (Denmark)

In this invited paper, we will link powerful methods used in machine learning to the future challenges in optical communication. Machine learning is an area of intelligent signal processing which uses advanced statistical and probabilistic methods to identify, learn, and track patterns about the underlying system from measured/observed data. We intend to use methods from machine learning to identify, learn, and dynamically track optical fibre channel parameters, such as amplitude and phase noise, and self and cross phase modulation induced nonlinear phase noise. This knowledge can then be used to design methods to counteract interaction between nonlinearities and noise, and thereby maximize the capacity. It will also be demonstrated how machine learning techniques are used to perform characterization of low-output-power nanophotonic devices.

For dynamic tracking of optical fibre channel impairments and nanophotonic device characterization we will apply Bayesian filtering methods. State-of-the-art non-linear optimal filtering methods such as sequential importance sampling particle filter and extended Kalman filter with maximum likelihood parameter estimation. Bayesian filtering are used to produce an accurate estimate of the state (amplitude, phase and nonlinear phase noise), in maximum a posteriori sense, of a time-varying system based on observed data. It will be shown experimentally that Bayesian filtering offers a large advantage in terms of tracking of amplitude and phase noise as well as nonlinear phase noise compared to traditional approaches. This will be experimentally demonstrated for up to 64-Quadrature Amplitude Modulated polarization multiplexed optical signals.

Conference 9389: Next-Generation Optical Communication: Components, Sub-Systems, and Systems IV

Tuesday - Thursday 10-12 February 2015

Part of Proceedings of SPIE Vol. 9389 Next-Generation Optical Communication: Components, Sub-Systems, and Systems IV

9389-1, Session 1

SDM technologies for flexible networks (Invited Paper)

Dimitra E. Simeonidou, Univ. of Bristol (United Kingdom)

No Abstract Available.

9389-2, Session 2

Key technologies for energy and spectral efficient flexible optical networks (Invited Paper)

Satoshi Shimizu, National Institute of Information and Communications Technology (Japan); Gabriella Cincotti, Univ. degli Studi di Roma Tre (Italy); Naoya Wada, National Institute of Information and Communications Technology (Japan)

In future optical networks, versatile functionalities will be required for the optical network subsystems to fully utilize the spectral resources with low energy consumption. The key technologies are the spectral efficient MUX/DEMUX technique and flexible control of optical channels with high frequency granularity. An orthogonal frequency division multiplexing (OFDM) and Nyquist wavelength division multiplexing (N-WDM) are the most promising candidates of spectral efficient multiplexing techniques, and all-optical (AO) processing is expected to reduce the energy consumption. In an AO-OFDM systems, discrete Fourier transform (DFT) and inverse DFT (IDFT) are performed in optical domain by specially designed arrayed waveguide gratings (AWGs). In our experiment, 12.5 GHz spaced AO-OFDM system has been successfully demonstrated with no guard interval. In N-WDM systems, the Nyquist signal is generated by using carrier-suppressed return-to-zero (CS-RZ) signal and optical Nyquist filtering, which is achieved with two flat-top AWWs and optical interleaver, and the 25 Gbaud signals are successfully multiplexed in the experiment. Although both AO-OFDM and N-WDM can achieve the highest spectral efficiency, N-WDM is more suitable for flexible optical networks. This is because the N-WDM channels have less spectral overlap with the other channels than AO-OFDM, owing to its rectangular shaped compact spectrum. Therefore, N-WDM channel can be easily multiplexed and demultiplexed by optical filters. At an optical network node, channel defragmentation is indispensable technology to flexibly control the optical channels. We have experimentally demonstrated a format independent optical channel defragmentation with N-WDM signal. We believe these technologies are promising for future flexible optical networks.

9389-3, Session 5

Multicore erbium-doped fiber amplifiers (Invited Paper)

Kazi S. Abedin, Thierry F. Taunay, John M. Fini, Lalitkumar Bansal, Man F. Yan, Benyuan Zhu, Eric M. Monberg, David J. DiGiovanni, OFS Labs. (United States)

Space division multiplexing (SDM) has drawn enormous amount of

interests lately as a potential means for enhancing the capacity of optical transmission systems. Optical transmission at the bit rates of over 1pb/s has been demonstrated by using multicore (MC) and few-mode fibers. To overcome the loss in SDM transmission systems, and to repeat data transmission over multiple spans, one would need to amplify signals carried by all the SDM channels simultaneously.

Among the various forms of SDM amplifier developed so far, which includes bundled, multi-element and MC, EDFAs based on multicore are particularly attractive due to its compactness, lower cost, and reduced power consumption. With suitable design, it also becomes possible to connect passive MC fiber directly to the MC EDFAs without using fan-in and fan-out devices.

MC-EDFAs can be mainly divided into two different categories depending on pumping methods, which are core-and cladding-pumping. Pumping each core of a MC amplifier separately using single mode pumps, while involving higher cost, has the advantage of allowing independent control of gain in each core by adjustment of pump power. Cladding pumping, on the other hand, requires fewer optical components, and has the potential to use low-cost, energy efficient multimode diodes. In this paper, we report on the recent development of core and cladding-pumped MC-EDFAs. We will show different ways of pumping MC-EDF using single and multimode multimode laser diodes, and will present the amplification, noise properties and power conversion efficiencies of such MC-EDFAs.

9389-4, Session 5

Multicore fiber-based mode multiplexer/demultiplexer (Invited Paper)

Yusuke Sasaki, Hitoshi Uemura, Katsuhiro Takenaga, Fujikura Ltd. (Japan); Shoko Nishimoto, Takui Uematsu, Hokkaido Univ. (Japan); Koji Omichi, Ryuichiro Goto, Shoichiro Matsuo, Fujikura Ltd. (Japan); Kunimasa Saitoh, Hokkaido Univ. (Japan)

Space-division multiplexing using multicore fiber (MCF) and few-mode fibers (FMF) is expected as a new advanced technology to improve transmission capacity drastically. Mode multiplexer/demultiplexer (MUX/DEMUX) is essential to realize transmission systems over FMFs. Many types of MUX/DEMUX have been proposed so far: free space optics with phase plate, photonic lantern using 3D waveguide and fused fiber mode coupler. A fused fiber mode coupler is expected to have low-insertion-loss characteristics. Precise alignment of small-cladding fiber is required to obtain fine performances.

In this paper, we propose MCF based mode MUX/DEMUX which can overcome the alignment issue. In addition to low-insertion-loss of fiber-based device, a MCF based MUX/DEMUX has several advantages, such as easy fabrication by using fiber shaping mode of a commercially available arc fusion splicer, and flexible controllability of operation wavelength by changing the elongation ratio of a MCF. Design concept and fabrication results of MCF based mode MUX/DEMUX for two-mode operation (LP01 and LP11) (2M-MUX/DEMUX) is presented. 2M-MUX/DEMUX has a two-LP-mode center core and a single-mode outer core. Fabricated 2M-MUX/DEMUXs for C-band or L-band by using the same MCF with different elongation ratio demonstrates coupling efficiency over 90% over the each band. Finally, a MCF based mode MUX/DEMUX for three-mode operation (LP01, LP11a and LP11b) (3M-MUX/DEMUX) with FanIn/FanOut device is presented. A MCF for the 3M-MUX/DEMUX has a two-LP-mode center core and orthogonally arranged two outer cores. Selective excitation of LP01, LP11a and LP11b modes depending on input ports is experimentally demonstrated.

**Conference 9389: Next-Generation Optical Communication:
 Components, Sub-Systems, and Systems IV**

9389-5, Session 5

Spatial mode rotator based on mechanically-induced twist and bending in few-mode fibers

Dawei Yu, Songnian Fu, Ming Tang, Huazhong Univ. of Science and Technology (China); Perry Ping Shum, Nanyang Technological Univ. (Singapore); Deming Liu, Huazhong Univ. of Science and Technology (China)

Recently, few-mode fiber (FMF) based mode division multiplexing (MDM) transmission together with multi-input multi-output (MIMO) signal processing technique is ideal candidate to solve future single mode fiber (SMF) capacity crunch. Most existing mode division multiplexers/demultiplexers (MMUX/DEMUX) have a specific mode orientation for high-order non-circular symmetric mode. Taking the phase plate based DEMMUX as example and converting LP₁₁ mode to fundamental LP₀₁ mode, we need optimize input mode orientation the same as the phase pattern of phase plate. In this submission, we propose and experimentally demonstrate a spatial mode rotator based on mechanically induced twisting and bending in a step-index FMF. We theoretically find that the mode coupling strength between vector modes with similar propagation constants is determined by the FMF bending and twisting. When the input LP₁₁ mode cluster including TE₀₁, HE₂₁, HE₂₁, and TM₀₁ mode are properly perturbed, the output optical field is superposed as LP₁₁ mode with a rotation. Therefore, the proposed spatial mode rotator is composed of three FMF coils with a radius of 16 mm, while the number of each coil is 2, 1, and 2, respectively. Consequently, we are able to rotate the LP₁₁ mode with arbitrary angle within 360° range using the same configuration of conventional polarization controller (PC). The insertion loss of proposed spatial mode rotator is less than 0.82 dB when the operation wavelength varies from 1540 nm to 1560nm. In particular, from the measured mode profile, there exists little crosstalk between LP₀₁ mode and LP₁₁ mode during mode rotation operation.

9389-6, Session 5

Integration approaches for space-division multiplexing using parallelism of free space

Guifang Li, CREOL, The College of Optics and Photonics, Univ. of Central Florida (United States); Jian Zhao, Ningbo Zhao, Tianjin Univ. (China)

Space-division multiplexing (SDM) is currently a focus of research in optical communication. As a means to increase transport capacity, SDM will only be commercially viable if it provides cost per bit saving compared to multiple parallel single-mode systems which are mature today. One of the often-mentioned cost-saving areas is transceiver integration. However, large-scale integrated transceivers based in planar lightwave circuits (PLC) are applicable to both SDM and parallel systems. Other integration methods such as few-mode amplifiers would not lead to order-of-magnitude savings for SDM. Therefore, high levels of integration that is unique to SDM must be employed to provide cost saving expect to make SDM successful. This paper presents examples of receiver and amplifier integration using parallelism in free-space to provide sharing of components in SDM. They include bulk amplifiers and bulk WDM-SDM receivers.

9389-7, Session 6

Photonic analog-to-digital conversion with emphasis on parallel-configuration-free aspect (Invited Paper)

Tsuyoshi Konishi, Makoto Hasegawa, Tomotaka Nagashima,

Osaka Univ. (Japan)

High performance A/D Conversion (ADC) is a key interface technology between real world and advanced digital technology and various photonic approaches have pursued to realize for it so far. In particular, very low jitter characteristic comes from optical sampling is the main driving force for photonic ADC and is expected to drastically improve a jitter issue and realize a high speed ADC. Since, inherently, bandwidth of analog signal in real world is much broader than that of digital technology, serial-to-parallel conversion is definitely essential. Since, however, parallel configuration causes different issues of power consumption as well as clock skew and cost, it is expected to develop photonic approaches for subsequent processing of successful optical sampling with keeping a system as parallel-configuration-free as possible. One of our strategies is used WDM scheme for conversion itself. As well known, WDM-MUXed data keep a parallel form in spectral domain although data propagate through a single line. It means that we can treat parallel data in a single line without increasing the number of devices. Since the matured optical sampling technique ensures high-speed operation, the remaining issue is resolution expansion of optical quantization. To avoid the above issues due to parallel configuration, we have also proposed one of approaches for optical quantization and demonstrated its performance with connecting several optical coding schemes. Here, the state of the arts in our works will be introduced.

9389-8, Session 6

The optical capacitor: Processing signals with an extended broad-band mode cavity

Sébastien Loranger, Mathieu Gagné, Raman Kashyap, Ecole Polytechnique de Montréal (Canada)

Fabry-Perot resonators or interferometers (FPI) have existed for a long time and act as light accumulators. We present here a novel cavity, recently demonstrated [1], in which the wavelength dependency of a mode is eliminated by the use of chirped grating reflectors. With the appropriate conditions, which will be discussed here, chirped gratings can induce a linear phase shift capable of canceling the wavelength dependency of phase in a cavity round-trip. The result is a very broad-band resonating mode of several nm wide, but which still preserves the same energy accumulation as any other optical cavity. Since there is no free-spectral range to match, there is no restriction on the repetition frequency of the input signal and no need to match a signal's wavelength with picometer precision to a specific cavity mode. With such a capacitive nature, analog to an RC electrical circuit, this cavity can act simultaneously as a passive low-pass filter (in transmission) and as a high-pass filter (in reflection) as a wavelength independent component. Signal processing simulation and experimental result will be presented to show this filtering property of the broad-band mode cavity (BBMC).

[1] S. Loranger, M. Gagné, and R. Kashyap, "Capacitors go optical: wavelength independent broadband mode cavity," Optics Express, vol. 22, pp. 14253-14262, 2014/06/16 2014.

9389-9, Session 6

Six mode multi-plane light converter for mode-selective spatial multiplexing

Pu Jian, Guillaume Labroille, Bertrand Denolle, CAILabs (France); Philippe Genevaux, Alcatel-Lucent Bell Labs. (France); Nicolas Barré, Olivier Pinel, Jean-François Morizur, CAILabs (France)

We report a six mode spatial multiplexer with high efficiency and high mode selectivity, using the technique of Multi-Plane Light Conversion (MPLC). By a succession of spatial phase profiles and optical Fourier transforms, six separated input beams can be converted into any set of six orthogonal spatial modes. When addressing the individual eigenmodes of

**Conference 9389: Next-Generation Optical Communication:
Components, Sub-Systems, and Systems IV**

a few-mode fiber, this conversion performs mode selective multiplexing, or demultiplexing when used in the reverse direction. The characterization of this mode multiplexer / demultiplexer is performed both in free space and after injection in a few-mode fiber. We demonstrate the multiplexing of the first six modes of a few-mode fiber, with a total insertion loss below 5 dB in the fiber and a mode-to-mode selectivity greater than 18 dB over a broad wavelength range from 1530 to 1565 nm. Furthermore, this device can address any spatial mode profile of any few-mode fiber with high fidelity: the average fidelity of the produced modes with the theoretical modes of a fiber is of 78%. Therefore the total insertion loss can be easily reduced with improvements on optical coatings. This mode multiplexer / demultiplexer proves to be fully compatible with a wavelength- and space-division multiplexed optical transmission line.

9389-10, Session 7
Roles of spectral and spatial aggregation in optical network scaling *(Invited Paper)*

Sercan O. Arik, Stanford Univ. (United States); Keang-Po Ho, Silicon Image, Inc. (United States); Joseph M. Kahn, Stanford Univ. (United States)

As bit rates of routed data streams exceed the throughput of single channels, spectral and spatial traffic aggregation become essential for optical network scaling. We give an overview of spectral and spatial aggregation techniques. We show how they reduce network complexity: by increasing spectral efficiency to decrease the number of fibers, and by increasing switching granularity to decrease the number of switching elements. To quantify the complexity reduction, we analyze the number of switches required in a colorless, directionless, contentionless reconfigurable optical add-drop multiplexer architecture. We discuss two potential drawbacks of aggregation: reduced routing power and increased switching element size.

9389-11, Session 7
Densely packed NxN wavelength cross-connect switch module

Hisato Uetsuka, Masao Tachikura, Hitoshi Kawashima, National Institute of Advanced Industrial Science and Technology (Japan); Kazuhiko Ikeda, AIST (Japan); Keisuke Sorimoto, Hiroyuki Tsuda, Keio Univ. (Japan); Keiichi Sasaki, Yuto Yamashita, Kitanihon Electric Cable Corp. (Japan)

A 5x5 wavelength cross-connect switch (WXC) with densely integrated MEMS mirrors is proposed and demonstrated.

5246 mirrors integrated on a chip are driven by comb-actuators to achieve well-controlled seesaw-like movement.

The MEMS chip having an interposer is die-bonded onto the ceramic package. The ceramic package having a BGA on back facet is soldered onto the daughter board.

The module has a 100GHz channel spacing compatible with the ITU-grid, a low loss (8-10dB), a low PDL (-0.5dB) and compactness (220(W) x 270(L) x 90(H) mm³).

Also, recent experimental results on NxN WXC with LCOS will be presented.

9389-12, Session 7
Ultra-stable optical amplifier technologies for dynamic optical switching networks

Masaki Shiraiwa, National Institute of Information and

Communications Technology (Japan); K. S. Tsang, Ray Man, Amonics Ltd. (Hong Kong, China); Benjamin J. Puttnam, Yoshinari Awaji, Naoya Wada, National Institute of Information and Communications Technology (Japan)

High-capacity fiber-optic communications and networks are the promising technologies which can satisfy people's continuously growing demands on bandwidth.

Optical circuit switching (OCS) technology, such as the wavelength-switching-based OCS technology is widely deployed already nowadays. However, with the limited number of transceivers equipped at each optical node and other constraints, the number of lightpaths which can be established and employed simultaneously in an optical network is restricted. The wavelength resource in some fiber links among one optical network cannot be fully employed. This reduces the efficiency of utilization of wavelength resource. Comparing to OSC, dynamic optical switching such as optical packet switching (OPS) is of higher efficiency in terms of wavelength resource utilization. It has the large potential to fully take advantage of the wavelength resource on fiber-links and be shared by large number of users simultaneously.

Amplifiers for dynamic optical switching employ a feedback loop to mitigate power-level-drift which degrades the performance of dynamic optical networks. However, the feedback loop would introduce extra power-level-drift. When using the optical feedback, this extra power-level-drift will lead to the relaxation oscillations.

We propose and demonstrate a novel scheme for suppressing the whole power-level-drift and the relaxation oscillations. This scheme can be utilized in optical amplifiers even if the optical feedback is employed.

9389-13, Session 8
High symbol rate coherent transmission systems for data rates above 400 Gb/s *(Invited Paper)*

Gregory Raybon, Alcatel-Lucent (United States); Sebastian Randel, Andrew Adamiecki, Alcatel-Lucent Bell Labs. (United States); Peter J. Winzer, Alcatel-Lucent (United States)

As 100 Gb/s optical interfaces are being installed today in many areas of the network, Terabit/s interfaces appear more closely on the horizon. Terabit/s systems are typically based on multiple optical carriers, with a 7-subcarrier commercial demonstration to realize a 1.4-Tb/s interface recently reported in a field demonstration[1]. In research experiments, Terabit/s interfaces range from 24 subcarriers at 12.5 GBd to 2 subcarriers at 80 GBd, enabled by advanced quadrature amplitude modulation (QAM) and digital coherent detection[2,3,4,5]. Single carrier demonstrations have only been reported using optical time division multiplexing to get to a Terabit/s[6]. OTDM has never gain acceptance as a technology choice for commercialization and therefore Terabit/s systems are expected to be realized through a series of other technology choices. Clearly, trade-offs in electronic, electro-optic, and optical transmitter and receiver complexity, optical signal-to-noise ratio (OSNR) requirements, optical and electrical bandwidths, and spectral efficiency need to be considered when comparing the various approaches to find the most promising commercial solution. Here, we review the generation, transmission and detection of high symbol rate systems from 72 to 107 GBd designed to reach the maximum bit rate with a minimum number of subcarriers. Specifically, we describe systems based on high-speed electronic multiplexing and optical modulation using QPSK or 16-QAM to achieve single-carrier line rates from 320 to 856 Gb/s[5,7,8]. In addition, we review a system using a high-speed DAC to achieve 864 Gb/s, using 72 GBd 64-QAM[9].

**Conference 9389: Next-Generation Optical Communication:
Components, Sub-Systems, and Systems IV**

9389-14, Session 8

Investigation of receiver constraints on the transmission performance of 1 Tbps WDM-Nyquist and CO-OFDM signals

Hraghi Abir, Mourad Menif, SUP'COM (Tunisia)

In order to meet the evolutionary growth of the internet demand, research efforts are oriented to the exploration and development of 1 Tbps enabled transmission systems. There are two techniques, which are multicarrier techniques such as Wavelength Division Multiplexing-Nyquist (WDM-Nyquist) and Coherent Orthogonal Frequency Division Multiplexing (CO-OFDM), can be used to achieve 1 Tbps transmission capacity. However, the performance of CO-OFDM technique is limited by the implementation receiver constraints for example, the speed of the Analogue-to-Digital Converters (number of Samples per Symbol (SpS)) and the analogue receiver bandwidth compared to the WDM-Nyquist system.

In this work, we implement an Optical Flat Comb Source generating a coherent super-channel operating at 1 Tbps using WDM-Nyquist and CO-OFDM approaches. We evaluate through simulation the performance of two techniques for generating Dual Polarization-Quadrature Amplitude Modulation based on 16 (DP-16QAM).

We first study the required number of Samples per Symbol used in the Analogue-to-Digital Converters (ADCs) in the CO-OFDM and WDM-Nyquist systems in back-to-back scenarios in terms of Optical Signal-to-Noise Ratio (OSNR) and over long-haul dispersion compensated links using Standard Single Mode Fiber (SSMF). We find that CO-OFDM requires 6 SpS to achieve the performance of WDM-Nyquist system in terms of OSNR. However, the CO-OFDM system needs more than 6 SpS to achieve the same distances as WDM-Nyquist.

We also study the impact of the input power level in terms of OSNR for CO-OFDM and WDM-Nyquist systems in order to evaluate the robustness of both systems to the nonlinear effects.

9389-15, Session 8

Advanced unrepeatered systems using novel Raman amplification schemes
(Invited Paper)

Do-Il Chang, Wayne Pelouch, Sergey Burtsev, Philippe Perrier, Herve Fevrier, Xtera Communications, Inc. (United States)

Unrepeatered transmission systems provide a cost-effective solution to transmit high capacity channels in submarine networks to communicate between coastal population centers or in terrestrial networks to connect remote areas where service access is difficult. The main goal of unrepeatered systems has traditionally been to achieve the longest reach, however, increasing traffic demands now require unrepeatered systems to support both longer reach and higher transport capacity. As a result, transmission rate of unrepeatered systems has quickly moved from 10 Gb/s to 40 Gb/s or 100 Gb/s. This paper reviews the key basic technologies, with a specific focus on Raman amplification, required for long-reach, high-capacity unrepeatered optical transmission systems. We will discuss novel Raman amplification schemes, enhanced remote optically pumped amplifiers (ROPA), ultra-low loss / large effective area fibers, and coherent transmission with advanced modulation format and high FEC coding gain. We will also report recent experimental demonstrations that show how these technologies have been combined to achieve industry's leading capacity and reach transmission.

9389-16, Session 8

Parallel and simultaneous spatial mode conversion using photorefractive crystal for photonic cross-connect

Yanfeng Zhao, Atsushi Okamoto, Tomohiro Maeda, Yuki Hirasaki, Akihisa Tomita, Hokkaido Univ. (Japan); Masatoshi Bunsen, Fukuoka Univ. (Japan)

In this paper, we present a new technology for photonic cross-connect (PXC) in the spatial mode region for the realization of advanced and flexible optical transmission of spatial modes. The PXC is a kind of all-optical devices to switch high-speed optical signals for mode-division multiplexing (MDM) network and it can perform signal labeling in the spatial mode region similar to current photonic switching in the wavelength region. In addition, parallel and simultaneous mode conversion can be realized using multiplexed holograms in a photorefractive crystal.

In our experiment, during the recording process, a rewritable hologram is recorded in the photorefractive crystal (LiNbO₃) through the interference between the signal beam with certain input mode and the reference beam with the phase distribution of the desired output mode. Signal beams are generated by computer generated hologram (CGH) using a spatial light modulator (SLM) instead of an optical fiber, and reference beams are generated by phase only modulation using another SLM. Subsequently, during the converting process, the input signal beam is converted into the desired output mode through the holographic diffraction in the crystal and light propagation by an optical lens. By using phase code multiplexing method, parallel mode conversion can be realized. We performed an experiment on parallel mode conversion of two different conversion pairs. Signal beams and reference beams intersected in the photorefractive crystal with an angle of 18.43°. The intensity distributions of converted modes were observed by CCD camera set on the Fourier plane. We confirmed that the parallel mode conversions of LP01 to LP11 and LP21 to LP51 were successfully performed.

9389-17, Session 9

Nonlinear compensation technologies for future optical communication systems
(Invited Paper)

Tomofumi Oyama, Fujitsu Labs., Ltd. (Japan); Takeshi Hoshida, Hisao Nakashima, Fujitsu Ltd. (Japan); Shoichiro Oda, Tomohiro Yamauchi, Takahito Tanimura, Fujitsu Labs., Ltd. (Japan); Liang Dou, Ying Zhao, Zhenning Tao, Fujitsu Research and Development Center Co., Ltd. (China); Jens C. Rasmussen, Fujitsu Ltd. (Japan)

Digital nonlinear compensation techniques have been thought to be keys to realize further spectrally efficient optical fiber communication systems. The most critical issue of the digital nonlinear compensation algorithms has been their computational complexity, or gate count of digital signal processing circuit. Among several approaches, digital nonlinear compensation algorithms based on perturbation analysis are attractive in terms of the hardware efficiency because the algorithms can compensate the accumulated nonlinear noise over all transmission spans with only one stage. In this paper, we discuss three approaches to sophisticate the perturbation nonlinear compensation. First, we illustrate a perturbation-based post-equalization method to improve the robustness to transceiver device imperfections. We next propose and numerically evaluate a symbol degeneration method to extend the perturbation nonlinear compensation methods to higher-order QAM without increasing the computational complexity. Finally, we discuss a sub-band processing of perturbation nonlinear compensation for further computational complexity reduction. By combining the perturbation method with Nyquist frequency division multiplexing, the computational complexity of perturbation calculation

**Conference 9389: Next-Generation Optical Communication:
 Components, Sub-Systems, and Systems IV**

is reduced by a factor of more than 10 for 3000-km single-channel transmission of 128 Gbit/s dual-polarization QPSK with only 0.1 dB performance degradation.

9389-18, Session 9

Optical OFDM signal generation using integrated-optic multiplexer based on optical IFFT

Koichi Takiguchi, Takaaki Miwa, Ritsumeikan Univ. (Japan)

Optical orthogonal frequency division multiplexing (OFDM), which generates and transmits subcarrier channels that are orthogonal to each other, is being vigorously pursued because of its high spectral efficiency. Optical OFDM is applicable for highly-functional optical networks including an elastic network as well as point-to-point transmission. It is important to develop optical devices, which can process an OFDM signal directly in the optical domain, to overcome the electrical processing speed limit and reduce the power consumption. We demonstrate an integrated-optic device for multiplexing an OFDM signal (OFDM multiplexer) based on optical inverse fast Fourier transform (IFFT). The silica waveguide-based multiplexer with the refractive index difference of 1.1% is composed of four inputs followed by mutually connected directional couplers, an array of delay lines, and a combiner. Four signals modulated with different sequences of data are fed into the multiplexer, and an optical OFDM signal is generated through the IFFT process directly in the optical domain. We report the configuration, operating principle, and experimental results to indicate that the multiplexer operates properly. The size and loss of multiplexer were 18 mm x 38 mm and 2.4 dB, respectively. We successfully generated 40 and 80 Gbit/s OFDM signals with the multiplexer, whose temporal waveforms were noise-like and had high peak-to-average power ratio. The spectral deviation of 40 and 80 Gbit/s OFDM signals was 1.4 and 3.4 dB, respectively. This is the first experimental demonstration of OFDM signal generation by utilizing an integrated-optic multiplexer, which is advantageous over bulk and fiber Bragg grating-based multiplexers as regarding size and stability.

9389-19, Session 9

DSP-based optical modulation technique for long-haul transmission (*Invited Paper*)

Tsuyoshi Yoshida, Takashi Sugihara, Kenichi Uto, Mitsubishi Electric Corp. (Japan)

Nonlinear inter-symbol interference (ISI) from fiber nonlinearity and equalization enhanced phase noise (EPPN) limit the system capacity and distance on long-haul coherent optical transmission. These nonlinear ISI creates so fast perturbation, so its characterization and compensation is difficult. However, there is a possibility to cancel the fast perturbation by introducing the particular correlation among plural signal sets at the transmitter and analyzing them at the receiver with digital signal processing.

In this paper, we propose the techniques to cancel the fast perturbation from fiber nonlinearity and EPPN for polarization multiplexed quaternary phase-shift keying based signals and investigate the performance improvement by numerical simulation.

Fiber nonlinearity cancellation is based on dual phase-conjugate twin-wave scheme. We allocate two sets of phase-conjugate signal pair over orthogonal polarizations in a carrier. Perturbation from fiber nonlinearity can be partially cancelled by superimposing each pair of phase-conjugate signals without spectral efficiency reduction. The improvement is 1.2 dB over 5000 km standard single-mode fiber link.

EPPN cancellation is based on laser phase noise compensation. To avoid EPPN at receiver, local oscillator (LO) phase noise has to be compensated before chromatic dispersion (CD) equalization. Herein we introduce delay difference between orthogonal polarizations only at transmitter. Then the delay time for peak cross-correlation of phase noise in orthogonal

polarizations becomes different between transmitter and LO lasers. By analyzing the cross-correlation difference of those, transmitter and LO lasers phase noise can be separately identified. The improvement is 0.5 dB at CD of 200,000 ps/nm and laser linewidth of 500 kHz.

9389-20, Session 9

Offset-16QAM-based coherent WDM with multi-carrier group detection

Meng Xiang, Songnian Fu, Ming Tang, Huazhong Univ. of Science and Technology (China); Perry Ping Shum, Nanyang Technological Univ. (Singapore); Deming Liu, Huazhong Univ. of Science and Technology (China)

Recently, offset-QAM based coherent WDM (CoWDM) has been proposed to build up spectrally-efficient multi-carrier superchannels. Compared with Nyquist wavelength division multiplexing (N-WDM) and orthogonal frequency division multiplexing (OFDM), offset-QAM based CoWDM can relax the stringent transmitter-side requirements for spectrum shaping and achieve significant transmission performance improvement. In order to efficiently utilize the sampling rate of commercially available analog-to-digital converter (ADC) and decrease the receiver-side implementation complexity, multi-carrier group detection scheme is investigated in offset-QAM based CoWDM where multiple carriers are simultaneously detected with single coherent receiver, followed by carrier separation in the digital domain through the 4-point discrete Fourier transform (DFT) method at the baseband. Here, we demonstrate a transmission of five-carrier 100 Gb/s polarization-multiplexed offset-16QAM signal with 12.5 GHz channel spacing. Through 3-carrier group detection, the sampling rate per-carrier is reduced to 1.33 times symbol rate in terms of 50 GS/s ADC and there is only 0.35 dB required OSNR penalty at BER=10⁻³ compared with conventional one-by-one coherent detection. Meanwhile, good tolerance of coherent receiver analog bandwidth is secured and receiver bandwidth is reduced to 8 GHz. Moreover, 0.5 dB required OSNR penalty at BER=10⁻³ is obtained given 18 GHz ADC bandwidth. Besides, we find that side carriers suffer from severer performance degradation than the central carrier with limited ADC resolution and only 0.08 dB and 0.2 dB required OSNR penalty at BER=10⁻³ are secured with 6 bits ADC resolution for central carrier and side carriers, respectively.

9389-28, Session PWed

Photodiodes integration on a suspended ridge structure VOA using 2-step flip-chip bonding method

Seon Hoon Kim, Tae Un Kim, Hyun Chul Ki, Doo-Gun Kim, Hwe Jong Kim, Jung Woon Lim, Dong Yeol Lee, Korea Photonics Technology Institute (Korea, Republic of); Chul Hee Park, Wooriro Optical Telecom Co. Ltd. (Korea, Republic of)

We have demonstrated a variable optical attenuator (VOA) integrated with 4 monitor photodiodes (mPDs), based on silica-on-silicon planar light-wave circuit (PLC) and flip-chip bonding technologies. VOA is actuated with electrical power through thermo-optic effect. The suspended narrow ridge structure was applied to reduce the power consumption. It achieves the attenuation of 30dB in open loop operation with the power consumption of below 30W. Conventional methods have used chip-by-chip bonding method. These methods are found that it is difficult to obtain high bonding strength, because the solder interconnections re-melt during repeated bonding steps. To overcome this problem, we have applied two-step flip-chip bonding method using passive alignment to perform high density multi-chip integration on a VOA with eutectic AuSn solder bumps. Two-step flip-chip bonding method consists of a chip-by-chip pre-bonding step and a simultaneous single re-flow step. The align marks between the chip and

**Conference 9389: Next-Generation Optical Communication:
 Components, Sub-Systems, and Systems IV**

the VOA surface are matched and the assembly were pre-bonded below the melting temperature of the AuSn solder. The subsequent reflow step brings the bonding temperature above the melting temperature applying no external pressure. Also, die shear tests were conducted to evaluate mechanical reliability between the solder bump and the mPD chip pads. The average bonding strength of the two-step flip-chip bonding method was about 90gf.

9389-29, Session PWed

Ageing of fiber optical devices

Vladimír Vaříněk, Petr Siska, Lukáš Bednarek, Jan Látal, Petr Koudelka, Ondřej Marcinka, VŠB-Technical Univ. of Ostrava (Czech Republic)

Knowledge of fiber devices ageing is one of necessary conditions for successful applications of fiber communication systems into hard environmental surrounding and for application of fiber sensors. This paper deals with finding of typical ageing markers during the process of accelerated ageing.

9389-21, Session 10

Photonics technologies for orbital angular momentum multiplexing data transmission in short-haul systems (Invited Paper)

Mario A. Usuga Castaneda, Karsten Rottwitt, Idelfonso Tafur Monroy, Technical Univ. of Denmark (Denmark)

The Orbital Angular Momentum (OAM) of light is a wonderful property that starts to be recognized by the optical communications community as a viable candidate for a future capacity increase due to the fact that OAM modes form a suitable base for Mode Division Multiplexing (MDM). OAM was initially studied in a free space scenario but since very recently, the transmission of vortex beams through optical fiber has started to play an important role.

In this work we present an overview of our recent advancements in the study of OAM technology that both illustrate the potential of OAM in the context of short range communication and present novel solutions for the generation, transmission and evaluation of OAM modes.

We present 3 key cases of study: an OAM converter which exhibits a simple solution to the problem of fiber based OAM generation. The case of "OAM Enhanced transmission", where the transmission performance of a standard multimode short link is improved by employing OAM modes is also presented and finally, we show the case of an Interferometric based modal characterization technique that will serve as an efficient diagnostic tool.

We also discuss specific challenges and opportunities, both from system and devices points of view in such scenario and describe the foreseen steps needed towards a fully fiber-integrated optical system. We conclude with a discussion about specific areas where this technology has immediate applications and can have a high impact today

9389-22, Session 10

Rapid measurement of the fiber's transmission matrix

Robert Brüning, Daniel Flamm, Friedrich-Schiller-Univ. Jena (Germany); Sandile S. Ngcobo, Council for Scientific and Industrial Research (South Africa); Andrew Forbes, CSIR National Laser Ctr. (South Africa); Michael Duparré, Friedrich-Schiller-Univ. Jena (Germany)

Mode division multiplexing (MDM) is a promising solution to increase the data capacity in optical fiber communication systems, which are currently reaching their limits imposed by nonlinear effects. To use this additional degree of freedom the impact of the fiber on the mode signals is an important issue to improve MDM strategies. We present a modal resolved characterization scheme for optical multi mode fibers, which combines two holographic procedures for selective fiber-mode excitation and complete fiber-mode analysis. This enables the construction of the fiber's transmission matrix by directly measuring the response of a selectively excited mode in terms of the entire guided mode spectrum. Hence, all mode depending properties like inter-modal crosstalk or mode depending loss are fully characterized and included in the matrix representation. This facilitates the investigation of underlying physical effects. Since the transmission matrix represents the transfer function of the fiber, it can also be used for the realization of signal correction schemes, e.g. to reconstruct the input signal from a distorted output signal or for pre-compensation of the input signal to receive an unperturbed output signal, respectively. In our scheme the amount of measurements, which is needed to determine the transmission matrix, is proportional to the number of guided modes. This rapid characterization is enabled by the application of a spatial multiplexing technique for the modal decomposition, which allows to measure the whole modal response of the fiber at once.

9389-24, Session 10

Determination of the physical fiber modes

Robert Brüning, Daniel Flamm, Luise Lukas, Julian Lenz, Michael Duparré, Friedrich-Schiller-Univ. Jena (Germany)

The description of systems in terms of their eigenfunctions, the so called modes, is a fundamental concepts used in many fields of physics. Modes are solutions of the eigenvalue equation which describes the underlying physical system. Particularly in optics the concept of modes is very successful for the description of arbitrary paraxial light beams. Depending on the symmetry of the system, the possibility of degenerated modes occurs. For example, in cylinder symmetric systems, e.g. optical fibers for telecommunication, modes can be found which are degenerated regarding the sign of their azimuthal order. Since these modes cannot be discriminated by their propagation properties, in an ideal (no disturbed) system each arbitrary superposition of these modes can be used to form a new equivalent set of degenerated modes. In a real system sometimes this degeneracy can be broken even by slight external perturbations. As a consequence, in such perturbed system well defined non-degenerated modes exist, having different physical (propagation) properties. In the context of mode division multiplexing in optical fibers, this effect leads to crosstalk between mode channels assumed as degenerated, if the chosen mode set is not the real physical one. Based on the measurement of the transmission matrix of the perturbed fiber, we present a scheme to prove this degeneracy breaking, and to find physical non-degenerated modes of the perturbed system.

9389-25, Session 11

Coherent detection in self-homodyne systems with single and multi-core transmission (Invited Paper)

Ruben S. Luis, Benjamin J. Puttnam, Jose M. D. Mendinueta, National Institute of Information and Communications Technology (Japan); Ali Shahpari, Zoran Vujicic, Instituto de Telecomunicacoes (Portugal); Werner Klaus, Jun Sakaguchi, Yoshinari Awaji, National Institute of Information and Communications Technology (Japan); Antonio Teixeira, Instituto de Telecomunicacoes (Portugal); Naoya Wada, Tetsuya Kawanishi, Atsushi Kanno, National Institute of Information and Communications Technology (Japan)

Conference 9389: Next-Generation Optical Communication: Components, Sub-Systems, and Systems IV

This work reviews the latest advancements in coherent self-homodyne detection (SHD) using signals with polarization- or space-multiplexed pilot tones (PTs) originating from the same light source, towards the implementation of low-cost coherent receivers. The coherency between signals and PTs drastically reduces laser linewidth requirements, enabling the use of high-order modulation formats with low-cost DFB lasers. In this work, we revise the application of SHD in high-capacity space-division multiplexed links using multi-core fibers, outlining optical signal-to-noise ratio, skew and phase noise requirements of such systems. Furthermore, we evaluate the application of SHD for the implementation of laser-less optical network units in passive optical networks, as well as recent developments in digital SHD techniques.

9389-26, Session 11

Adaptation of AMO-FBMC-OQAM in optical access network for accommodating asynchronous multiple access in OFDM-based uplink transmission

Sun-Young Jung, Sang-Min Jung, Sang-Kook Han, Yonsei Univ. (Korea, Republic of)

Exponentially expanding various applications in company with proliferation of mobile devices make mobile traffic exploded annually. For future access network, bandwidth efficient and asynchronous signals converged transmission technique is required in optical network to meet a huge bandwidth demand, while integrating various services and satisfying multiple access in perceived network resource.

Orthogonal frequency division multiplexing (OFDM) is highly bandwidth efficient parallel transmission technique based on orthogonal subcarriers. OFDM has been widely studied in wired-/wireless communication and became a Long term evolution (LTE) standard. Consequently, OFDM also has been actively researched in optical network. However, OFDM is vulnerable frequency and phase offset essentially because of its sinc-shaped side lobes, therefore tight synchronism is necessary to maintain orthogonality. Moreover, redundant cyclic prefix (CP) is required in dispersive channel. Additionally, side lobes act as interference among users in multiple access. Thus, it practically hinders from supporting integration of various services and multiple access based on OFDM optical transmission

In this paper, adaptively modulated optical filter bank multicarrier system with offset QAM (AMO-FBMC-OQAM) is introduced and experimentally investigated in uplink optical transmission to relax multiple access interference (MAI), while improving bandwidth efficiency. Side lobes are effectively suppressed by using FBMC, therefore the system becomes robust to path difference and imbalance among optical network units (ONUs), which increase bandwidth efficiency by reducing redundancy. In comparison with OFDM, a signal performance and an efficiency of frequency utilization are improved in the same experimental condition. It enables optical network to effectively support heterogeneous services and multiple access.

9389-27, Session 11

Individually-n-addressable GaN-based micro-LED arrays for high-speed visible light communications at over 1 m

Enyuan Xie, Jonathan D. McKendry, Ricardo Ferreira, Johannes Herrnsdorf, Univ. of Strathclyde (United Kingdom); Sujan Rajbhandari, Hyunhae Chun, Grahame E. Faulkner, Univ. of Oxford (United Kingdom); Erdan Gu, Univ. of Strathclyde (United Kingdom); Dominic C. O'Brien, Univ. of Oxford (United Kingdom); Martin D. Dawson, Univ. of Strathclyde (United Kingdom)

GaN-based micro-light-emitting diodes (μ LEDs) can be driven at high

current densities, enabling significantly higher modulation bandwidths than conventional broad-area LEDs. Thus, μ LEDs are attractive candidates for high-speed visible light communications (VLC). However, the low optical power of a single μ LED limits the data-transmission distance and signal-to-noise ratio. Moreover, conventional GaN-based μ LED arrays are individually controlled through their p-type contacts. When integrating the LEDs with driver electronics, this configuration restricts the LED driver to be based on P-Metal-Oxide-Semiconductor (PMOS) transistors with lower carrier mobility and larger area than their N-type equivalents. Here, we demonstrate the design and fabrication of novel μ LED arrays targeting VLC links at ≥ 1 Gb/s over ≥ 1 m using both ganging (same data for all μ LEDs) and multiple input multiple output (MIMO, an independent data stream per μ LED) approaches. A key development is that each μ LED is individually addressed by its own n-type contact. This reversed configuration enables these arrays to be compatible with NMOS transistor-based drivers for faster modulation. Arrays fabricated with 450 nm emission wavelength show promising performance. At 8.0 kA/cm² DC operation current density, the optical power and electrical-to-electrical modulation bandwidth of a single μ LED with 24 μ m diameter are 1.2 mW and 110 MHz. For a 39 μ m-diameter μ LED, we obtain 3.6 mW and 125 MHz at the same DC current density. These values fulfil the design targets for an integrated system employing either ganging or MIMO operation. Initial results have demonstrated 920 Mb/s transmitted over 1 m free space using 4 MIMO channels.

Conference 9390: Next-Generation Optical Networks for Data Centers and Short-Reach Links II

Tuesday - Wednesday 10-11 February 2015

Part of Proceedings of SPIE Vol. 9390 Next-Generation Optical Networks for Data Centers and Short-Reach Links II

9390-1, Session 1

High-speed silicon photonics links over LX multimode fibers *(Invited Paper)*

Hai-Feng Liu, Intel Corp. (United States); Scott R. Bickham, Corning Incorporated (United States)

Silicon photonics, with the capability of offering scalable high bandwidth optical links at low cost, is poised to make significant impacts to the emerging mega data centers where more interconnects at higher data rates over longer reach are needed to accommodate the exponential data growth. While VCSEL based optical links at 850 nm have been traditionally used for such interconnects, it has become challenging to extend the reach beyond 100m as the data rate reaches 25 Gb/s due to the combined chromatic dispersion and modal dispersion. This presentation reviews the recent joint work by Intel and Corning that addresses the needs for extended interconnect reach in data centers. In particular, we demonstrate the transmission of 25 Gb/s signals from silicon photonics transceivers over 820m of Clear-Curve LX multimode fiber that was designed to have low modal dispersion at 1310nm. This reach is approximately 8x longer than 25Gb/s VCSEL based transceivers can offer over OM4 fibers.

9390-2, Session 1

Novel devices for low-power silicon-photonics-based optical links *(Invited Paper)*

Philippe P. Absil, IMEC (Belgium)

Silicon photonics technology has emerged in the past years in commercial products integrating the device building blocks demonstrated in the years 1990's and 2000's. However the ever growing demand for bandwidth at reduced power consumption in data centers require to develop novel electro-optical components beyond the established technology capable of operating at high data rate and very low power consumption towards sub-pJ/bit data links. In this paper we will first review the state of the art silicon photonics technology and its limits for low-power operation. We will then discuss our recent progress to go beyond the current limits. First we will discuss the micro-ring based modulators and approach to realize the required thermal control. Second we will present our recent progress made in alternative modulators based on a silicon photonics platform aiming at significantly reducing the optical devices power consumption. In particular we will discuss hybrid modulators combining silicon photonics technology and other materials that have significantly better electro-optical characteristics while being compatible with CMOS fabrication lines. We will also discuss opportunities to improve the efficiency of the germanium-on-silicon photo-detectors.

9390-3, Session 3

Should optical links be parallel or serial? *(Invited Paper)*

Karen Liu, Kaiam Corp. (United States)

A micromachined structure provides "mechanical lithography" which shrinks large displacements to small displacements. By this means, the >10 microns tolerances readily achievable by low-cost automatable assembly steps can be used for the submicron types of positioning accuracy needed for

single-mode optics packaging. This method has been published previously. This paper explores the implications of removing single-mode packaging from the constant tension between increasing total capacity with parallel channels and increasing per channel speed through device improvement. Fundamental arguments based on power consumption, device size, and complexity are used to project cost scaling scenarios for parallel and serial approaches

9390-4, Session 3

Optical technologies for >25 Gb/s short-reach high-bandwidth interconnects *(Invited Paper)*

Mitchell H. Fields, Avago Technologies Ltd. (United States)

Across many application areas, the need for high-bandwidth short-reach interconnects continues to grow. In data centers, it is driven by the ever improving compute power of servers and the demands that puts on the switching network. In routing and transport, the demand for increased bandwidth capacity per slot and the need to move data within and between systems precludes the use of electrical interconnects. In this presentation, technologies that address these requirements are discussed including the latest advancements in 850nm VCSELs, options for other VCSEL wavelengths, the impact of MMF properties (including EMB at various wavelengths) on reach, novel devices for SMF applications, and advanced modulation schemes.

9390-5, Session 3

50-Gb/s vertical illumination APD for 400GbE *(Invited Paper)*

Masahiro Nada, Nippon Telegraph and Telephone Corp. (Japan)

This talk will present about a high-performance InAlAs avalanche photodiode (APD) with vertical illumination structure for 50-Gbit/s applications. The vertical-illumination structure we employed is advantageous in large optical tolerance, and thus enables easy optical coupling compared with a waveguide-type structures. Although the vertical illumination structure generally has a disadvantage in both responsivity and bandwidth, our fabricated APD exhibits a high responsivity of 0.69 A/W with a large 3-dB bandwidth of over 30 GHz at a multiplication factor (M) of 4.6, thanks to an unique hybrid absorption layer of p-doped/undoped InGaAs and a thin InAlAs avalanche layer obtaining a large gain-bandwidth product of 270 GHz. Furthermore, an optical receiver assembling the APD together with trans-impedance amplifier (TIA) successfully demonstrates 50-Gbit/s error-free operation for the first time. The receiver sensitivity of -10.8 dBm at a BER of 10⁻¹² is obtained against non-return-to-zero optical input signals at a wavelength of 1310 nm. In this operating condition, the power consumption of the APD receiver module is less than 500 mW, and more than 98 % of the power is consumed by the TIA. Based on the results, the obtained minimum receiver sensitivity will be enough for 20-km transmission at 50 Gbit/s when we assume a launch power of 0 dBm and transmission loss in the optical fiber of 0.5 dB/km. These results indicate our APD is promising for the systems with serial baud rate of 50 Gbit/s such as 400-Gbit/s Ethernet systems.

**Conference 9390: Next-Generation Optical Networks
 for Data Centers and Short-Reach Links II**

9390-6, Session 3

Recent advances in high-data-rate optical transceivers *(Invited Paper)*

Julie A. Sheridan Eng, Finisar Corp. (United States)

This paper reviews the state-of-the-art in 100G optical modules, with a focus on datacom and client interfaces. The migration of 100G form factors from CFP to QSFP28 will be reviewed. Parallel multi-mode VCSEL-based technologies for 100G will also be reviewed, including what advances are needed in VCSELs, integrated circuits, and packaging to support increasing bandwidth densities. In addition, multi-channel single-mode optical modules, such as those supporting the 100G BASE LR4 standard, will be reviewed. Different transmitter sources including directly-modulated lasers and silicon photonics will be compared in power, performance, cost, and size. Finally, extension of both single-mode and multi-mode technology to 400G client and datacom modules will be reviewed, including higher data rate VCSELs, modulators, and the use of advanced modulation formats such as PAM, DMT, and others.

9390-7, Session 3

A global standardization trend for high-speed client and line-side transceivers *(Invited Paper)*

Hideki Isono, Fujitsu Ltd. (Japan)

Seeing the recent vast data increase in information society, IT society will move into the new era of Zettabyte in a few years. Under these circumstances, high-speed and high-capacity optical communication systems have been deployed in the industry. Especially high speed optical transceivers are key devices to realize high-speed systems, and the practical development is accelerated. In order to develop these leading edge products timely, the global standard criteria are strongly required in the industry. Based on these backgrounds, the forum standardization bodies such as OIF/PLL-WG/IEEE802.3 are energetically creating the de-facto standards. With regard to 100G/400G standardization activities, IEEE802.3 leads the client side, and OIF PLL-WG leads the line side, and both of which play important roles in the industry. In the previous Photonics West conferences, the activities of these standardization bodies till 2013 were reported. In 2014, the discussions of 400G client side transceiver projects have made some progress in IEEE802.3, whose baseline technologies are about to be fixed. Also 100G transceiver projects for metro applications in the line side, whose target profile is CFP2 form factor, have been discussed in OIF PLL-WG. In this paper, these high-end standardization topics are introduced and the future products direction is also discussed from the technical point of view. In order to realize these small form factor and cost effective transceivers, the device integration technologies, the low power device/electrical circuit technologies, and the development of high speed electrical interface such as 25G/50G are key factors.

9390-8, Session 4

High-speed bidirectional dual-core fiber transmission system for high-density short-reach optical interconnects *(Invited Paper)*

Ying Geng, Shenping Li, Ming-Jun Li, Clifford G. Sutton, Corning Incorporated (United States); Robert McCollum, L-3 Communications (United States); Randy L. McClure, Corning Incorporated (United States); Alexander V. Koklyushkin, Corning Incorporated (Russian Federation); Karen I. Matthews, James P. Luther, Douglas L. Butler, Corning Incorporated (United States)

Multicore fiber (MCF) is promising for high density optical interconnect applications to reduce the size and to improve manageability and scalability of transmission systems. In this paper, a complete single mode dual-core fiber system for short-reach optical interconnects is fabricated and tested for high-speed data transmission. It includes dual-core fibers capable of bidirectional data transmission, dual-core simplex LC connectors, and fan-outs. The transmission system offers simplified bidirectional traffic engineering with integrated bi-directional transceivers and compact system design, utilizing simplex dual-core LC connectors that use half the space while increasing the bandwidth density by two. The fiber has two cores that are compatible with the standard single mode fiber and conforms to the industry standard outer diameter of 125 μm . Overall this reduces operational complexity by reducing the size and number of fibers, cables and connectors. Measured OTDR Loss for both cores was 0.34 dB/km at 1310 nm, and 0.19 dB/km at 1550 nm. Crosstalk for a piece of 5.8 km long dual-core fiber was measured to be below -75 dB at 1310 nm, and below -40 dB at 1550 nm. Both free-space optics fan-outs and tapered-fiber-coupler based MCF fan-outs were evaluated for the transmission system. Error-free and penalty-free 25 Gb/s bidirectional transmission performance was demonstrated for a length of 200 meters using the complete all-fiber-based system including connectors and fan-outs. This single mode dual-core fiber transmission system adds complementary value to systems where additional increases in bandwidth density can come from wavelength division multiplexing and multiple bits per symbol.

9390-9, Session 5

Multi-core fiber technology for highly-reliable optical network in access areas *(Invited Paper)*

Kenichi Tanaka, Yong Lee, Etsuko Nomoto, Hitachi, Ltd. (Japan)

A failure recovery system utilizing multi-core fiber (MCF) link with field programmable gate array (FPGA)-based optical switch (SW) units was developed for achieving high capacity and highly reliable optical networks in access areas. In this presentation, we proposed a novel MCF link based on a multi-ring structure for robust optical networks. As components of the MCF link, a fan-in/-out module for connecting a MCF and single-mode fibers by free-space-based coupling and a connector with a prototype SC-type physical-contact were developed in pursuit of versatility, enabling us to connect SW units by just one fiber. Hence we can construct a network that abounds with capacity, scalability, flexibility and reliability. Moreover a switching algorithm implemented on FPGA in the SW unit was established according to five high-functioning processes capable of coping with complicated multiple link failure, thereby managing the MCF link suitably. To verify the operation of the proposed MCF link, we demonstrated automatic impairment-aware optical path switching when a multi-failure occurred in the MCF link based on a multi-ring structure. We can perform path recovery by switching operation within a short period of time, 7.4 msec, which is sufficiently less than that required by ITU-T. The selection of a protecting path as a substitute for the failure working path was also optimized for low loss transmission. These results indicate that the proposed MCF link is useful for network design that simultaneously ensures high capacity and reliability with respect to transmission in optical networks for future access areas.

9390-10, Session 5

Recent advances in indium phosphide based transceivers for 100G and 200G DWDM transmission *(Invited Paper)*

Robert Blum, Oclaro, Inc. (United States)

Coherent pluggable interfaces are now becoming reality thanks to a combination of recent progress in digital signal processing, photonic integration, and innovative packaging technologies. This paper will discuss

Conference 9390: Next-Generation Optical Networks for Data Centers and Short-Reach Links II

how advances in tunable lasers, indium phosphide based modulators and receivers are enabling new pluggable form factors with low power dissipation and cost/performance metrics that are ideal for datacenter, metro and regional applications. We will review the various form factors under consideration, discuss what performance trade-offs need to be considered in 100G and 200G DWDM transmission applications and how these solutions can be scaled to 400G and beyond.

The recent progress at the transceiver level has been made possible, in large part, by advances in several areas of photonic integration at the optical chip level and by new packaging concepts. Examples discussed in this paper include the following: (i) full-band tunable lasers with high power, narrow linewidth and low phase noise that can be used both as the transmission laser and act as a local oscillator in coherent applications; (ii) InP I&Q modulators with low electrical drive power, low insertion loss, low chirp and high extinction ratio for both linear and limiting drive applications; (iii) dual-polarization intradyne receivers with chip bandwidth above 32GHz and chip responsivity of 0.15 A/W, incorporating 90° optical hybrids and balanced waveguide photo-detectors, coupled to trans-impedance amplifiers which provide the electrical outputs for subsequent digital signal processing of the incoming signals.

9390-11, Session 5

850nm single mode VCSEL-based 25Gx16 transmitter/receiver boards for parallel signal transmission over 600m of multimode fiber

Joerg-Reinhardt Kropp, George Schaefer, Vitaly A. Shchukin, Nikolay N. Ledentsov, VI Systems GmbH (Germany); Jarek P. Turkiewicz, Warsaw Univ. of Technology (Poland); Bo Wu, Shaofeng Qiu, Yanan Ma, Zhiyong Feng, Huawei Technologies Co., Ltd. (China)

We report on parallel optical links based on single mode (SM) 850 nm vertical cavity surface-emitting lasers (VCSELs). SM VCSEL arrays were used as transmitters and PIN PD arrays were applied as photodetectors. Multi-channel driver and amplifier arrays were assembled on specially developed transmitter (Tx) and receiver (Rx) boards suited for 16- parallel channels. Optical components were coupled to multimode fiber (MMF) ribbon connectors with the following fan-out to separate channels. Advanced SM VCSEL design offered series resistances and voltages compatible to standard VCSEL driver electronics while allowing >35dB side mode suppression ratio. No noticeable eye diagram deterioration has been observed after the signal transmission over 600m of OM4 MMF at 25 Gigabits per second (Gb/s). Optical transmission over OM3 fiber at 25Gb/s led to error free operation at >300m distances.

9390-12, Session 6

High-speed integrated photonic devices for telecommunication applications (Invited Paper)

Alexandre P. Freitas, Giovanni B. Farias, Fellipe G. Peternella, Yesica R. R. Bustamante, Julio C. R. F. de Oliveira, CpqD (Brazil)

Silicon photonics has been widely researched as a potential technology for the next generation of optical devices due to its high integration capabilities. After presenting the first Brazilian high speed integrated 100G-DPQPSK transmitter, this paper brings the improvements added in the second layout, with lower insertion loss, better bias control combined with an integrated DC-Block to avoid any current flow due to the bias applied in the pn junction of the modulator arms. There is also an improvement in the TWMZ layout with better impedance match.

In addition, it is presented the development of a fast variable optical attenuator (FVOA) based on pin junction with response time lower than 5ps and an optical attenuation range of more than 30dB. For the FVOA, it was considered a 300nm thickness silicon layer with 2 doping levels. Besides the active regions, there was also the development of an inverted taper designed to reduce the PDL between the light polarization components

9390-13, Session 6

OAM-enhanced transmission for multimode short-range links

Anna Tatarczak, Technical Univ. of Denmark (Denmark); Mario A. Usuga Castaneda, Idelfonso Tafur Monroy, DTU Fotonik (Denmark)

Overcoming the spatial and optical bandwidth limitations in the data centers' short-range links is the timely quest of the telecom operators. This stimulates the search for increased capacity single lane solutions that use cost effective 850 nm MMF technologies as well as already employed fibers.

In this submission we propose, experimentally demonstrate, and evaluate a high capacity multimode (MM) transmission link, which is based on orbital angular momentum (OAM) modes. Previously, such OAM modes have been used in communications as a mean to obtain higher data rates through mode division multiplexing (MDM). This solution requires the design and use of special fibers to minimize modal crosstalk and therefore limits its applicability in several scenarios, especially those requiring the use of standard fibers.

The simple scheme that we propose here uses OAM modes to increase capacity and reach without recurring to MDM or special fibers: we first excite an OAM mode and couple it to a 50m, 100m and 200m MM fibers. The transmission performance is evaluated in terms of bit error rate at the FEC limit of 10⁻⁴ in the 850 nm and 879 nm bands. We compare an OAM mode and a standard optical single mode under the same launch and received optical power conditions.

The proposed OAM based solution is a promising candidate for the high capacity data centers interconnects and short range links that employ the existing multimode fiber infrastructure.

9390-14, Session 6

Monolithic integration of high-bandwidth waveguide-coupled Ge photodiode in a photonic BiCMOS process (Invited Paper)

Stefan Lischke, Dieter Knoll, Lars Zimmermann, IHP GmbH (Germany)

Monolithic integration of photonic functionality in the frontend-of-line (FEOL) of an advanced microelectronics technology is a key step towards future communication applications. This combines photonic components such as waveguides, couplers, modulators, and photo detectors with high-speed electronics plus shortest possible interconnects crucial for high-speed performance. Integration of photonics into CMOS FEOL is therefore in development for quite some time reaching 90nm node recently [1]. However, an alternative to CMOS is high-performance BiCMOS, offering significant advantages for integrated photonics-electronics applications with regard to cost and RF performance.

We already presented results of FEOL integration of photonic components in a high-performance SiGe:C BiCMOS baseline to establish a novel, photonic BiCMOS process. Process cornerstone is a local-SOI approach which allows us to fabricate SOI-based, thus low-loss photonic components in a bulk BiCMOS environment [2]. A monolithically integrated 10Gbit/sec Silicon modulator with driver was shown here

[3]. A monolithically integrated 25Gbps receiver was presented in [4], consisting of 200GHz bipolar transistors and CMOS devices, low-loss

**Conference 9390: Next-Generation Optical Networks
 for Data Centers and Short-Reach Links II**

waveguides, couplers, and high-speed Ge photo diodes showing 3-dB bandwidth of 35GHz, internal responsivity of more than 0.6A/W at $\lambda = 1.55\mu\text{m}$, and $\sim 50\text{nA}$ dark current at 1V. However, the BiCMOS-given thermal steps cause a significant smearing of the Germanium photo diodes doping profile, limiting the photo diode performance. Therefore, we introduced implantation of non-doping elements to overcome such limiting factors, resulting in photo diode bandwidths of more than 50GHz even under the effect of thermal steps necessary when the diodes are integrated in a high performance BiCMOS process.

[1] S. Assefa et al., "A 90nm CMOS Integrated Nano-Photonics Technology for 25Gbps WDM Optical Communications Applications," in Technical Digest of International Electron Devices Meeting (IEDM) (IEEE 2012), pp. 809-811.

[2] D. Knoll et al., "Substrate Design and Thermal Budget Tuning for Integration of Photonic Components in a High-Performance SiGe:C BiCMOS Process," ECS Transactions, 50, 9, pp. 297-303 (2012).

[3] L. Zimmermann et al., "Monolithically Integrated 10Gbit/sec Silicon Modulator with Driver in 0.25 μm SiGe:C BiCMOS," in European Conference and Exhibition on Optical Communication (ECOC), We.3.1, London (2013)

[4] D. Knoll et al., "Monolithically Integrated 25Gbit/sec Receiver for 1.55 μm in Photonic BiCMOS Technology," in Conference Optical Fiber Communication (OFC), Th4C.4, San Francisco (2014).

9390-15, Session 6
Function transformable photonic integrated circuits: Alternative approach toward compact monolithic integration for data center applications

Benjamin B. Dingel, Nasfine Photonics, Inc. (United States)

No Abstract Available

9390-17, Session 7
Athermal silicon optical interposers operating up to 125 degrees celsius (Invited Paper)

Yutaka Urino, Nobuaki Hatori, Kenji Mizutani, Tatsuya Usuki, Junichi Fujikata, Koji Yamada, Photonics Electronics Technology Research Association (Japan); Tsuyoshi Horikawa, National Institute of Advanced Industrial Science and Technology (Japan); Takahiro Nakamura, Photonics Electronics Technology Research Association (Japan); Yasuhiko Arakawa, The Univ. of Tokyo (Japan)

We have previously proposed a photonics-electronics convergence system to solve the bandwidth bottleneck among LSIs and demonstrated silicon optical interposers fully integrated with optical components, achieving a high bandwidth density of 30 Tbps/cm² at room temperature. For practical applications in inter-chip interconnects, interposers should be usable under high temperature and rapid temperature change so that they can cope with the heat generated by mounted LSIs. We designed and fabricated athermal silicon optical interposers integrated with temperature-insensitive components on a silicon substrate. An arrayed laser diode (LD) chip was flip-chip bonded to the substrate. Each LD has multi quantum dot layers with a 1.3- μm lasing wavelength. The output power was higher than 10 mW per channel up to 100 degrees celsius. Silicon optical modulator and germanium photo detector (PD) arrays were monolithically integrated on the substrate. The modulators were structured as symmetric Mach-Zehnder interferometers, which were inherently temperature insensitive. The phase shifters composed of PIN diodes were stable against temperature with constant bias currents. The PD photo current was also temperature insensitive and the photo-to-dark current ratio was higher than 30 dB up to

100 degrees celsius. We achieved error-free data links at 20 Gbps and high bandwidth density of 19 Tbps/cm² operating from 25 to 125 degrees celsius with the interposers without bias adjustments for the LDs, modulators, and PDs. Since maximum junction temperatures in most of LSIs will have been below 125 degrees celsius now and in the future, the interposers are tolerant of heat generated by LSIs, and suitable for inter-chip interconnects.

9390-18, Session 7
Micron-scale silicon photonics for WDM optical links (Invited Paper)

Dazeng Feng, Mellanox Technologies, Inc. (United States)

Silicon Photonics has become one of the most promising technologies to address connectivity bottlenecks in data center and optical networks. We have focused on the development of a manufacturable micron-scale silicon photonics platform to demonstrate the practical realization of this technology for WDM optical links. In this paper, we will review the latest progress in the development of key photonic components such as hybrid lasers, WDM multiplexers, electro-absorption modulators, and germanium detectors. We will also review recent advances in the development of highly integrated 4x25 Gbit/s WDM transceiver circuits and discuss the path to Tbit/s WDM transceivers.

9390-19, Session 7
Integrated silicon photonic WDM cross-connect chip (Invited Paper)

Young-Kai Chen, Po Dong, Lawrence L. Buhl, David T. Neilson, Jeffrey H. Sinsky, Alcatel-Lucent Bell Labs. (United States)

It is desirable to implement a compact cross-connect building block with low latency, re-configurability and scalability to construct a high capacity data switch. The performance of electronic cross-connect switch is limited by the power consumption, timing skews and latency. Photonic cross connects promise high throughput and scalability with fast channel data rate and low latency. Traditional photonic switches have been implemented in MEMS and LCOS technologies. These free-space photonic switching technologies require combination of bulky micro-optics to transfer high speed optical data among dozens of fiber ports. Recently several efforts have been explored to implement compact photonic switches on the highly integrated silicon substrates based on planar lightwave circuits (PLC), silicon Mach-Zehnder switches and nano-MEMS MZ switches.

In this talk, we will survey the current cross connect technologies and present our compact chip-scale cross connect switch circuits implemented using silicon photonics technology. This chip can provide a reconfigurable 10x10 non-blocking switch function as well as a broadcasting network at a channel data rate of 10 Gb/s. This chip-scale platform promises an even larger throughput and higher channel data rate.